ORGANOMETALLICS

Volume 5, Number 2, February 1986

Carbonyl Adducts of Dichlorotetrakis(dimethylamido)ditungsten and Insertion of Carbon Monoxide into a Tungsten–Amido Bond

Kazi J. Ahmed and Malcolm H. Chisholm*

Department of Chemistry, Indiana University, Bloomington, Indiana 47405

Received June 13, 1985

Addition of carbon monoxide (1 equiv) to 1,2-$W_2Cl_2(NMe_2)_4$ in toluene/pyridine solutions yields a monocarbonyl compound $W_2(NMe_2)_4Cl_2(py)_2(CO)$ (I) as a golden brown microcrystalline precipitate. This reacts in toluene solution with *i*-PrOH to give, by stepwise alkoxide for amide exchange, $W_2(NMe_2)_3(O\text{-}i\text{-}Pr)Cl_2(py)_2(CO)$ (II) and $W_2(NMe_2)_2(O\text{-}i\text{-}Pr)_2Cl_2(py)_2(CO)$ (III). The compounds I, II, and III show ν(CO) in the range 1700–1750 cm^{-1}, which, though typical of a μ-CO function, are not formulated as such but rather as terminal W–CO groups on the basis of the relative intensities of the satellites due to coupling to ^{183}W ($I = {}^1/_2$, 14.5% natural abundance). The chemical shifts for the carbonyl, ca. 250 ppm relative to Me_4Si and the magnitude of $J_{^{183}W-^{13}C}$, ca. 230 Hz, taken together with the low values for ν(CO) suggest a dominant contribution from the valence bond description, W=C=O. On the basis of NMR spectral data structures for I, II, and III are proposed on the basis of confacial bioctahedral geometries (py)$(NMe_2)_{4-x}(O\text{-}i\text{-}Pr)_xW(\mu\text{-}NMe_2)_2(\mu\text{-}Cl)WCl(CO)(py)$, where x = 0, 1, and 2, respectively. Compound I reacts further with CO in toluene to give IV which is formualted as a carbonyl–carbamoyl compound, $W_2(NMe_2)_3(CONMe_2)Cl_2(py)_2(CO)$. Addition of ^{13}CO to I containing natural abundance ^{13}CO indicates the formation of $W_2(NMe_2)_3(^{13}CONMe)Cl_2(py)_2(CO)$. Addition of PMe_2Ph to IV gives substitution of only one pyridine ligand yielding V which on the basis of NMR and IR spectral data is shown to exist as two isomers in solutions. The compounds IV and V are proposed to be related to I by insertion of CO into an amide bond at the tungsten not bearing the terminal CO ligand. These findings are compared to previous studies involving the addition of CO to $M_2(OR)_6$ compounds (M = Mo and W).

Introduction

The dimetal hexaalkoxides of molybdenum and tungsten have been found to react with carbon monoxide to give a variety of products depending upon the metal, the steric properties of the alkoxide, the relative amount of CO to $M_2(OR)_6$, and the reaction condition.[1] The initially formed compounds are carbonyl adducts of type **1**[2,3] or **2**.[3,4]

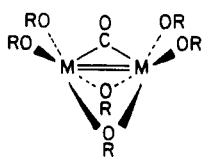

1, M = Mo or W; R = *t*-Bu

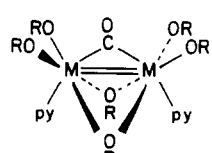

2, M = Mo or W; R = *i*-Pr or CH_2-*t*-Bu

These compounds have remarkably low values of ν(CO) for neutral molecules, ca. 1650 cm^{-1} for M = Mo and ca. 1560 cm^{-1} for M = W. In part the low ν(CO) values reflect the fact that these compounds are inorganic analogues of cyclopropenones and have significant contributions from the ionic resonance forms shown in **3a** and **3b**.

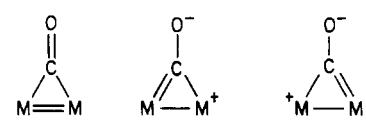

3 3a 3b

The markedly lower values of ν(CO) for the tungsten compounds (relative to molybdenum) are a reflection of the greater π-back-bonding (reducing) ability of tungsten in its middle oxidation states.[5] A consideration of the ionic

(1) Chisholm, M. H.; Hoffman, D. M; Huffman, J. C. *Chem. Soc. Rev.* **1985**, *14*, 69.
(2) Chisholm, M. H.; Cotton, F. A.; Extine, M. W.; Kelly, R. L. *J. Am. Chem. Soc.* **1979**, *101*, 7645.
(3) Chisholm, M. H.; Hoffman, D. M.; Huffman, J. C. *Organometallics* **1985**, *4*, 986.
(4) Chisholm, M. H.; Huffman, J. C.; Leonelli, J.; Rothwell, I. P. *J. Am. Chem. Soc.* **1982**, *104*, 7030.

0276-7333/86/2305-0185$01.50/0

resonance forms **3a** and **3b** leads to the expectation that the metal center should be susceptible to nucleophilic attack while the oxygen atom should behave as a nucleophile. This is indeed the case and $W_2(O\text{-}i\text{-}Pr)_6(py)_2(CO)$ dimerizes in solution to give $W_4(CO)_2(O\text{-}i\text{-}Pr)_{12}(py)_2$ and free pyridine.[3,6] Similarly addition of *i*-PrOH to $W_2(O\text{-}t\text{-}Bu)_6(\mu\text{-}CO)$ leads to $W_4(CO)_2(O\text{-}i\text{-}Pr)_{12}$.[3] In both these tetranuclear compounds there are planar $[W_2(\mu\text{-}CO)]_2$ units that have essentially W–W and C–O single bonds while the W–C bond distances (1.95 Å) are indicative of considerable multiple bond order. Again the central core can be viewed in terms of valence bond descriptions resulting from the combination of **3a** and **3b** to give **4a** and **4b**.

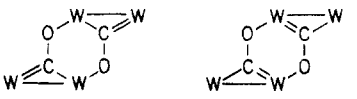

4a **4b**

We have suggested that these reactions of alkoxide-supported reduced metal centers may provide models for the initial steps of the reaction involving carbon monoxide on a reduced metal oxide surface leading ultimately to C–O bond cleavage to generate carbide and oxide ligands.

In the presence of excess carbon monoxide the reactions follow a different course leading to a disproportionation of the $(M{\equiv}M)^{6+}$ center to M(0) and metal alkoxides. The form of M(0) is $M(CO)_6$ while the nature of the oxidized metal alkoxides is again dependent upon the metal and the specific alkoxide ligand.[1] These reactions involve transfer and terminal–bridge scrambling of CO and OR groups. Intermediates along such a reaction path are understandable by consideration of the isolated species $Mo_2(O\text{-}i\text{-}Pr)_8(CO)_2$[7] and $W_2(O\text{-}i\text{-}Pr)_6(CO)_4$.[8] The latter compound may be viewed as a $W(O\text{-}i\text{-}Pr)_6$ molecule lightly ligated to a $W(CO)_4$ fragment through the agency of a pair of alkoxide ligands.

With this background, we turned our attention to reactions of carbon monoxide with $(M{\equiv}M)^{6+}$ centers (M = Mo, W) containing other ligands. Rather interestingly $M_2(NMe_2)_6$ compounds are much less reactive toward carbon monoxide and no simple 1:1 CO/M_2 adducts have as yet been detected or isolated.[9] However, substitution of two NMe_2 groups by Cl ligands greatly enhances the uptake of CO by the dimetal center. We describe here reactions involving 1,2-$W_2Cl_2(NMe_2)_4$[10] with 1 and 2 equiv of carbon monoxide.

Results and Discussion

Syntheses. Addition of carbon monoxide (1 equiv), by the use of a gas-tight syringe, to a toluene solution of $W_2Cl_2(NMe_2)_4$ in the presence of pyridine (3–4 equiv) yields a golden brown microcrystalline precipitate, $W_2Cl_2(NMe_2)_4(py)_2(CO)$ (I) which starts to form within 15 min. Compound I does not appear stable in toluene solution at room temperature, and this impeded our efforts to grow crystals suitable for single-crystal X-ray studies. Compound I reacts in toluene with *i*-PrOH to give two successive replacements of NMe_2 ligands by O-*i*-Pr ligands according to the reaction shown in eq 1.

Table I. Selected Spectroscopic Data for the New Carbonyl Ditungsten Compounds

compound	$\delta(^{13}CO)$	$\nu(CO)$, cm^{-1}	J_{WC}, Hz	I,[e] %
$W_2Cl_2(NMe_2)_4(CO)(py)_2$ (I)	257.6	1725 1695[a] 1730[b]	225	7
$W_2Cl_2(NMe_2)_3(O\text{-}i\text{-}Pr)(CO)(py)_2$ (II)	262.4	1750	234	9
$W_2Cl_2(NMe_2)_2(O\text{-}i\text{-}Pr)_2(CO)(py)_2$ (III)	251.4	1715	228	8
$W_2Cl_2(NMe_2)_3(C(O)MNe_2)(CO)(py)_2$ (IV)	258.8[c]	1725 1690[a] 1725[b]	239	9
	224.4[d]	1595 1570[a] 1590[b]	83.5	7
$W_2Cl_2(MNe_2)_3(C(O)NMe_2)(CO)(PMe_2Ph)(py)$ (V) (two isomers)	258.1[c] 257.2[c]	1725 1685 1695[a] 1660[a]	228	7
	224.2[d] 223.9[d]	1595 1575[a]	85	8

[a] ^{13}CO. [b] Solution value in toluene. [c] ^{13}CO group. [d] $^{13}CONMe_2$ group. [e] Intensity of each satellite peak due to ^{183}W natural abundance = 14.5%).

(i) $W_2Cl_2(NMe_2)_4(py)_2(CO) \xrightarrow[\text{toluene, 25 °C, 10 min}]{+i\text{-PrOH}} W_2Cl_2(NMe_2)_3(O\text{-}i\text{-}Pr)(py)_2(CO) + HNMe_2$ (1)
II

(ii) II $\xrightarrow[\text{toluene}]{i\text{-PrOH, 25 °C, 1 h}} W_2Cl_2(NMe_2)_2(O\text{-}i\text{-}Pr)_2(py)_2(CO) + HNMe_2$
III

The alcoholyses reactions shown in eq 1 were undertaken with the hope of obtaining crystalline products suitable for single-crystal X-ray studies in order to provide unequivocal identification of the terminal W–CO moiety (see later).

Compounds II and III are stable in solution, but repeated attempts to grow crystals suitable for X-ray studies always resulted in twinned crystals.

Compound I reacts with carbon monoxide (1 equiv) to give $W_2Cl_2(NMe_2)_3(CONMe_2)(py)_2(CO)$ (IV) which can be prepared directly from $W_2Cl_2(NMe_2)_4$ and CO (2 equiv), eq 2, allowing for the initially formed suspension of I in toluene to dissolve as it reacts further.

(i) $W_2Cl_2(NMe_2)_4 + 2py + CO \xrightarrow[\text{toluene}]{\text{15 min, 25 °C}} W_2Cl_2(NMe_2)_4(py)_2(CO)$ (2)
I

(ii)

$I + CO \xrightarrow[\text{toluene}]{\text{3 h, 25 °C}} W_2Cl_2(NMe_2)_3(CONMe_2)(py)_2(CO)$
IV

Compound IV is deep red and gives microcrystalline samples upon crystallization from toluene–hexane solutions. IV reacts in toluene with PMe_2Ph (1 equiv) to give $W_2Cl_2(NMe_2)_3(CONMe_2)(py)(PMe_2Ph)(CO)$ (V) which is obtained as a purple microcrystalline solid from toluene–hexane solutions. Formation of V is essentially quantitative according to eq 3, and, rather interestingly, a further addition of PMe_2Ph does not lead to a replacement of the last molecule of pyridine of ligation.

Crystalline samples of IV and V also proved unsatisfactory for single-crystal X-ray studies.

(5) A similar effect is seen in $\nu(NO)$ in compounds of formula $[M(OR)_3(NO)]_2$ where M = Cr, Mo, W: Bradley, D. C.; Newing, C. W.; Chisholm, M. H.; Kelly, R. L.; Haitko, D. A.; Little, D.; Cotton, F. A.; Fanwick, P. E. *Inorg. Chem.* **1980**, *19*, 3010.
(6) Cotton, F. A.; Schwotzer, W. *J. Am. Chem. Soc.* **1983**, *105*, 4955.
(7) Chisholm, M. H.; Huffman, J. C.; Kelly, R. L. *J. Am. Chem. Soc.* **1979**, *101*, 7615.
(8) Cotton, F. A.; Schwotzer, W. *J. Am. Chem. Soc.* **1983**, *105*, 5639.
(9) Ahmed, K. J; Chisholm, M. H., unpublished results.
(10) Akiyama, M.; Chisholm, M. H.; Cotton, F. A.; Extine, M. W.; Murillo, C. A. *Inorg. Chem.* **1977**, *16*, 2407.

$$\text{IV} + PMe_2Ph \xrightarrow[\text{toluene, } 1^1/_2 \text{ h}]{25\ ^\circ C} W_2Cl_2(NMe_2)_3(CONMe_2)(py)(PMe_2Ph)(CO) + py \quad (3)$$
V

Physicochemical and Spectroscopic Properties. The new compounds I–V are all air-sensitive crystalline solids, soluble in aromatic hydrocarbon solvents. Elemental analyses are given in the Experimental Section along with infrared and NMR data. Selected spectroscopic data are summarized in Table I.

Structural Assignments. W–CO. Compounds I, II, and III show ν(CO) in the range 1700–1750 cm^{-1} and δ-(^{13}CO) ca. 260 downfield from Me_4Si with coupling to ^{183}W ($I = {}^1/_2$, 14.5% natural abundance) of ca. 230 Hz. The integrated signals of the satellites due to coupling to ^{183}W establish that the CO ligand is bound to only one tungsten. Thus we rule out the presence of the $W_2(\mu$-CO) moiety which was previously seen in the chemistry of the 1:1 CO adducts with $M_2(OR)_6$ compounds.[1] It should be noted that since these compounds have been synthesized using *ca.* 90% ^{13}CO the satellite signal intensities can be established with a good deal of precision.

W–CONMe$_2$. The addition of ^{13}CO to $W_2Cl_2(NMe_2)_4$-$(py)_2(CO)$ leads to IV having the labeled carbamoyl ligand: $W_2Cl_2(NMe_2)_3(^{13}CONMe_2)(py)_2(CO)$. Conversely, the addition of CO (natural abundance) to the ^{13}CO-labeled I yields $W_2Cl_2(NMe_2)_3(CONMe_2)(py)_2(^{13}CO)$. The evidence for the carbamoyl ligand can be summarized: (i) the low ν(CO) value of ca. 1600 cm^{-1} is typical of a η^1-$CONMe_2$ ligand,[11] (ii) the magnitude of $J_{^{183}W-^{13}C}$ ca. 85 Hz is typical of a $C_{sp^2} - {}^{183}W$ coupling constant[12] and both the chemical shift and $J_{^{183}W-^{13}C}$ values are inconsistent with a $W_2(\mu$-CO) group;[1] (iii) the appearance of two NMe_2 signals in the ^1H NMR in 1:1 ratio which show $^3J_{^{13}C-H}$ ca. 4 Hz in the labeled ligand $^{13}CONMe_2$. The appearance of two NMe signals presumably reflects restricted rotation about the C–N bond due to contributions from the VB description.

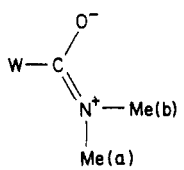

Evidence for a Confacial Bioctahedron. The gross structural features of the molecules can be accommodated with a common template having the following features:

1. There is no molecular plane of symmetry for any of the compounds.

2. There is in each compound, and in V for each isomer present in solution, a pair of bridging NMe_2 groups. These give rise to four NMe signals in the ratio 1:1:1:1. In compounds I and II, there are also terminal NMe_2 groups. These undergo temperature-dependent M–N bond rotations which can be frozen out at low temperatures on the ^1H NMR time scale but are rapid at room temperature.[13] In IV and V, the terminal NMe_2 groups show restricted rotation around W–N bonds at room temperature, presumably due to greater Me_2N-to-W π-bonding.

3. The conversion of I to II and II to III involves the successive substitution of terminal NMe_2 groups at one tungsten center. The first substitution is followed by a slower one because of enhanced Me_2N-to-W π-bonding in II relative to I.[14] The relatively small change in ν(CO) upon substitution of NMe_2 groups by O-*i*-Pr groups support the notion that the amido and alkoxy groups concerned are on the tungsten atom not bearing the carbonyl ligand.

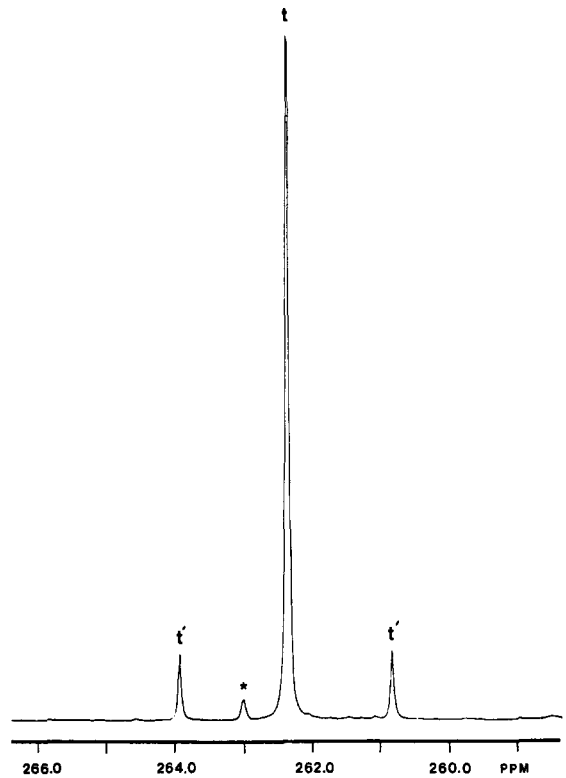

Figure 1. $^{13}C\{^1H\}NMR$ spectrum of $W_2Cl_2(NMe_2)_3(O$-*i*-$Pr)(^{13}CO)(py)_2$, where ^{13}C represents 92.5 atom % ^{13}C, in benzene-d_6 recorded at 21 °C and 74.8 MHz, shown at scale expansion in the region 266.2–258.1 ppm. Signals denoted by t and t′ correspond to $^{18x}W-^{13}CO$ and $^{183}W-^{13}CO$, respectively. The asterisk represents the resonance due to either a minor isomer or an impurity.

4. At least three pieces of experimental evidence indicate that the CO and $CONMe_2$ moieties in IV and V are on different tungsten atoms. (i) In the PMe_2Ph-containing compound V, only the terminal carbonyl ligand shows coupling to ^{31}P and the magnitude of $^1J_{^{13}P-^{13}C}$ is consistent with a *cis*-$(PMe_2Ph)W(CO)$ arrangement. (ii) The ^{13}C-labeled compound IV $W_2Cl_2(NMe_2)_3(^{13}CONMe_2)(py)_2$-$(^{13}CO)$ does not show any $^{13}C-{}^{13}C$ coupling. Had the $^{13}CONMe_2$ and ^{13}CO ligands been at the same metal center then such a coupling should have been apparent. (iii) In the formation of the carbamoyl compound IV, it is the second molecule of added carbon monoxide that forms the carbamoyl ligand and the W–CO group is not scrambled in this reaction.

All of the above can be accommodated about a common structural template involving a confacial bioctahedron. Compound I is formulated as $(py)(NMe_2)_2W(\mu$-Cl)$(\mu$-$NMe_2)_2W(Cl)(py)(CO)$. Note the carbonyl ligand is bonded to a tungsten atom having only a terminal chloride and pyridine ligand. The reaction between I and *i*-PrOH yields first II, $(py)(i$-PrO$)(Me_2N)W(\mu$-Cl$)(\mu$-$NMe_2)_2WCl$-$(py)(CO)$, and then III, $(py)(i$-PrO$)_2W(\mu$-Cl$)(\mu$-$NMe_2)_2WCl(py)(CO)$. The reaction between I and CO

(11) Angelici, R. J. *Acc. Chem. Res.* **1972**, *5*, 335 and references therein.
(12) For an extensive listing of $^1J_{^{183}W-^{13}C}$ see: Chisholm, M. H.; Folting, K.; Hoffman, D. M.; Huffman, J. C. *J. Am. Chem. Soc.* **1984**, *106*, 6794.
(13) These suggestions have analogies with observed solid-state structures and solution behaviors of $W_2Cl_n(NMe_2)_{6-n}(py)_2(\mu$-$C_2R_2)$ compounds where n = 2, 3, and 4. Ahmed, K. J.; Chisholm, M. H.; Huffman, J. C. *J. Chem. Soc. Chem. Commun.* **1985**, 151, and results to be published.
(14) This is typical of alcoholysis reactions involving 1,2-$M_2R_2(NMe_2)_4$ compounds. Tatz, R. J. Indiana University, Bloomington, Indiana, Ph.D. Thesis, 1984.

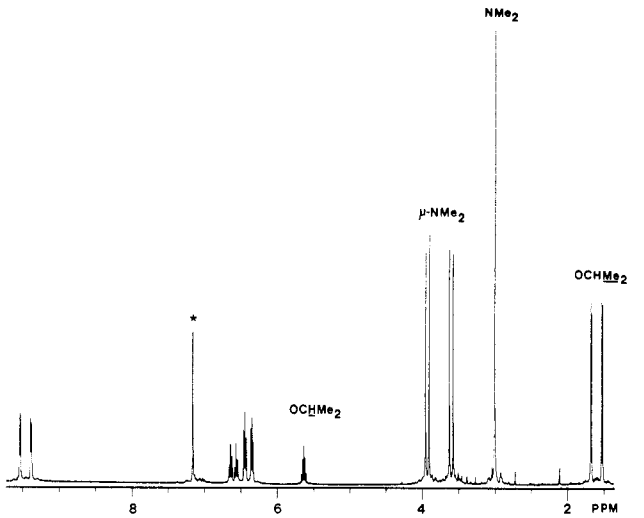

Figure 2. ^{1}H NMR spectrum of $W_2Cl_2(NMe_2)_3$(O-*i*-Pr)(CO)(py)$_2$ in benzene-d_6 recorded at 21 °C and 360 MHz. Signal denoted by the asterisk is due to the protio impurity of the solvent. Resonances between 6.3 and 9.6 ppm are due to the coordinated pyridine ligands.

proceeds to give IV, (py)(Me_2N)(Me_2N(O)C)W(μ-Cl)(μ-NMe_2)$_2$WCl(py)(CO), which upon reaction with PMe_2Ph gives (py)(Me_2N)(Me_2N(O)C)W(μ-Cl)(μ-NMe_2)$_2$WCl(CO)(PMe_2Ph) (V).

It is possible to envisage more than one isomer for compounds I–V, even with the specific grouping of terminal and bridging ligands given above. However only for compound V do we observe two isomers. If isomers are present in solution for the other compounds, their concentration is very small relative to the major isomer. For example, the ^{13}C NMR spectrum of the ^{13}CO-labeled compound II, in the carbonyl region, is shown in Figure 1. The central W–^{13}CO signal is flanked by satellites due to coupling to ^{183}W, and only a very small signal at 263 ppm provides possible evidence of another isomer. The ^{1}H NMR spectrum of II in toluene-d_8 is shown in Figure 2. In the region between 3 and 4 ppm four singlets of equal intensity are assigned to the bridging NMe_2 methyls; however, the terminal NMe_2 resonance at ca. 3 ppm is indicative of rapid W–N bond rotation. There is only one methyne resonance for the O-*i*-Pr ligand, but there are two sets of doublets for the O-*i*-Pr methyl groups which are diastereotopic. The 6–10 ppm range of the spectrum contains the ^{1}H NMR resonances of two different types of pyridine ligands.

This situation is contrasted with the spectral data for V. The ^{13}C NMR spectrum for the ^{13}C-labeled compound (py)(Me_2N)(Me_2N(O)^{13}C)W(μ-Cl)(μ-NMe_2)$_2$W(Cl)(PMe_2Ph)(^{13}CO) is shown in the W–^{13}CO and W–^{13}C(O)NMe_2 region in Figure 3. The downfield signals at ca. 258 ppm arising from the W–CO moiety reveal the presence of two such groups in the approximate ratio 3:4. Each W–CO signal shows coupling to ^{31}P and ^{183}W. A parallel situation is revealed in the W–^{13}C(O)NMe_2 portion of the spectrum except that coupling to ^{31}P is not observed. In the proton NMR spectrum there are 16 NMe signals: one set of eight lines of equal intensity standing in the integral ratio ca. 3:4 to another set of eight lines. Similarly the pyridine resonances reveal two py ligands.

Concluding Remarks

Addition of CO to $W_2Cl_2(NMe_2)_4$ in the presence of pyridine gives rise to first a 1:1 CO adduct and then to insertion of CO into a W–NMe_2 ligand. The latter is a rare example of a CO insertion into a transition metal–nitrogen

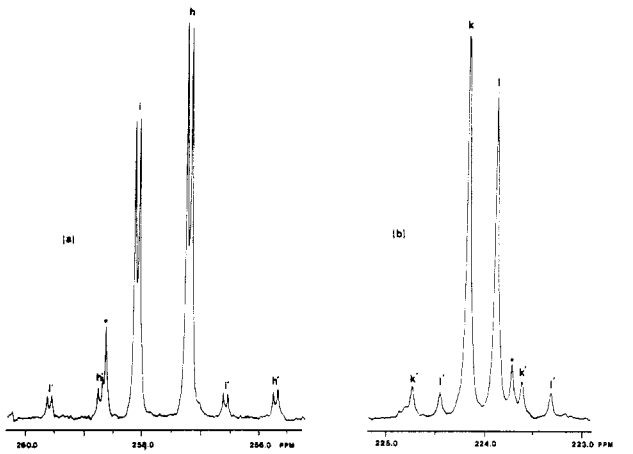

Figure 3. ^{13}C{^{1}H}NMR spectrum of $W_2Cl_2(NMe_2)_3$-(^{13}CONMe_2)(^{13}CO)(PMe_2Ph)(py) in its two isomeric forms, recorded in methylene-d_2 chloride at 21 °C and 74.8 MHz. Signals due to ^{18x}W–^{13}CO (h and i) showing coupling to the coordinated phosphine ligand. Signals labeled h′ and i′ are due to ^{183}W–^{13}CO. (b) The region of the spectrum representing the ^{13}CONMe_2 ligand showing no coupling to the coordinated phosphine. Signals represented by k and l are due to ^{18x}W–^{13}CONMe_2, whereas k′ and l′ denote ^{183}W–^{13}CONMe_2.

bond.[15] The 1:1 CO adduct contains a terminal W–CO function and not a W_2 (μ-CO) group, which contrasts to earlier findings involving 1:1 CO adducts of $W_2(OR)_6$ compounds. The CO ligand shows unusually low values for ν(CO) in compounds I, II, and III, and the chemical shifts and magnitude of the ^{13}C–^{183}W coupling contants are comparable to those seen for terminal alkylidyne groups: W≡CR.[12,16] These results may be rationalized by the presence of extensive W-to-CO π*-back-bonding in the compounds described in this paper, wherein a valance bond description of W=C=O or W^+≡C—O^- is being approached. For electron-counting purposes the d^3–d^3 dimer may be partitioned as d^2–d^4 with the CO ligand bound to the "soft" d^4 center (the one that also binds the phosphine in V) as shown in the diagram.

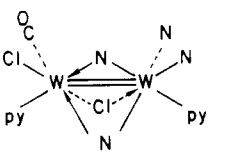

N = NMe_2; py = NC_5H_5

The CO insertion occurs at the other tungsten center (d^2) which is relatively "hard" and does not readily exchange pyridine for PMe_2Ph. Regretably we have been unable to back these claims by single-crystal X-ray crystallographic studies though the spectroscopic data provide a solid basis for the claims presented.

Further studies are in progress.

Experimental Section

All operations were carried out in dry and oxygen-free solvents and atmospheres (N_2). $W_2Cl_2(NMe_2)_4$ was prepared according to literature methods.[10] Carbon monoxide was purchased from Matheson and was used without any further purification. The 90% ^{13}C-labeled carbon monoxide was obtained from MSD and

(15) Carbamoyl ligands are more commonly generated by attack of an amine on a coordinated CO ligand (see ref 11) though CO insertion into actinide–amide bonds (Th and U) has been well established to give M-η^2-C(O)NMe_2 moieties: Fagan, P. J.; Manriquez, J. M.; Vollmer, S. H.; Day, C. S.; Day, V. W.; Marks, T. J. *J. Am. Chem. Soc.* **1981**, *103*, 2206.

(16) Mann, B. E.; Taylor, B. F. "^{13}C NMR Data for Organometallic Compounds"; Academic Press: New York, 1981.

was stored in glass containers over activated charcoal. Nicolet 360, Varian XL-300, and Varian XL-100 NMR instruments were used to obtain ^1H, ^{13}C, and ^{31}P NMR spectra, respectively. A Perkin-Elmer 283 infrared spectrometer was used to record IR spectra. Solid-state spectra were obtained from Nujol mulls between KBr plates while toluene solutions were used to obtain solution IR spectra.

$W_2Cl_2(NMe_2)_4(CO)(py)_2$ (I). $W_2Cl_2(NMe_2)_4$ (0.49 g, 0.8 mmol) was suspended in toluene (3 mL) and pyridine (3 equiv) was added. The solution was cooled to 0 °C in an ice bath. Carbon monoxide (1 equiv) was added by a gas-tight syringe (provided with a lock), and the gas was transferred to the syringe with the help of a calibrated vacuum manifold. The solution was stirred at 0 °C for $^3/_4$ h by which time a golden brown precipitate had formed and was collected by filtration, washed with toluene (5 mL), and dried under vacuum. The sample was spectroscopically pure, and no effort was made for any further purification; yield 0.45 g (73%). Anal. Calcd for $W_2Cl_2N_6C_{19}H_{34}O$: C, 28.5; H, 4.2; N, 10.5; Cl, 8.8. Found: C, 28.3; H, 4.5; N, 10.1; Cl, 8.5.

IR spectral data (major bands) from Nujol mulls: 2805 (s), 2760 (s), *1725* (vs), 1600 (w), 1595 (w), 1485 (m), 1322 (m), 957 (s), 945 (s), 930 (s), 765 (m), 755 (m), 705 (m), 695 (m) cm^{-1}.

^1H NMR spectral data (from benzene-d_6 solution at 22 °C, chemical shift values (δ) relative to Me_4Si): 3.13 (s, 6 H, NMe_2); 3.55 (s, 3 H, NMe_2); 3.56 (s, 6 H, NMe_2); 3.64 (s, 3 H, NMe_2); 3.73 (s, 3 H, NMe_2); 3.98 (s, 3 H, NMe_2); 6.35, 6.60, 9.50 (m, 10 H, NC_5H_5).

$W_2Cl_2(NMe_2)_3(O\text{-}i\text{-}Pr)(CO)(py)_2$ (II). $W_2Cl_2(NMe_2)_4(CO)(py)_2$ (0.39 g, 0.49 mmol) was suspended in toluene (4 mL) and cooled to 0 °C. *i*-PrOH (1 equiv) was added very slowly via a microliter syringe with constant stirring of the reaction mixture. Reaction was complete in 10 min after which the color became greenish brown. The volatile components of the reaction mixture were removed under vacuum, and the solid residue was redissolved in hot toluene (5 mL), which was let cool slowly to room temperature. Microcrystalline $W_2Cl_2(NMe_2)_3(O\text{-}i\text{-}Pr)(CO)(py)_2$ was removed after 2 days by filtration; total crystallized yield 0.23 g (58%). Anal. Calcd for $W_2Cl_2N_5C_{20}H_{35}O_2$: C, 29.4; H, 4.3; N, 8.6; Cl, 8.7. Found: C, 29.6; H, 4.3; N, 8.4; Cl, 8.6.

IR spectral data (major bands) from Nujol mulls: 2760 (w), *1750* (vs), 1600 (m), 1480 (m), 1130 (m), 1104 (s), 980 (s), 935 (s), 920 (s), 752 (s), 690 (s) cm^{-1}.

^1H NMR spectral data (obtained from benzene-d_6 solution at 22 °C, δ values relative to Me_4Si): 1.51 (d, J = 7.2 Hz, 3 H, $OCH(CH_3)_2$); 1.66 (d, J = 6.1 Hz, 3 H, $OCH(CH_3)_2$; 2.99 (s, 6 H, $N(CH_3)_2$); 3.57 (s, 3 H, $N(CH_3)_2$); 3.62 (s, 3 H, $N(CH_3)_2$); 3.90 (s, 3 H, $N(CH_3)_2$; 3.95 (s, 3 H, $N(CH_3)_2$; 5.63 (septet, J = 6.1 Hz, 1 H, $OCH(CH_3)_2$); 6.39, 6.59, 9.47 (m, 10 H, NC_5H_5).

$W_2Cl_2(NMe_2)_2(O\text{-}i\text{-}Pr)_2(CO)(py)_2$ (III). $W_2Cl_2(NMe_2)_4(CO)(py)_2$ (0.72 g, 0.9 mmol) was suspended in toluene, and *i*-PrOH (2 equiv) was added via a microliter syringe. The reaction mixture was stirred at room temperature for 1 h after which the solution turned brown. Microcrystalline $W_2Cl_2(NMe_2)_2(O\text{-}i\text{-}Pr)_2(CO)(py)_2$ was obtained by slow diffusion of hexane into the toluene solution, and the solids were separated by filtration; yield 0.42 g (51%). Anal. Calcd for $W_2Cl_2N_4C_{21}H_{36}O_3$: C, 30.4; H, 4.3; N, 6.7; Cl, 8.5. Found: C, 30.3; H, 4.4; N, 6.7; Cl, 8.6.

IR spectral data (major bands) from Nujol mull: 2760 (w), *1715* (vs), 1600 (m), 1480 (m), 1130 (m), 1104 (s), 980 (s), 935 (s), 920 (s), 752 (s), 690 (s) cm^{-1}. ^1H NMR spectral data (from toluene-d_8 solution at 55 °C, δ values relative to Me_4Si): 0.99 (d, J = 7.1 Hz, 3 H, $OCH(CH_3)_2$); 1.12 (d, J = 7.0 Hz, 3 H, $OCH(CH_3)_2$); 1.59 (d, J = 6.5 Hz, 3 H, $OCH(CH_3)_2$); 1.60 (d, J = 6.4 Hz, 3 H, $OCH(CH_3)_2$); 3.65 (s, 3 H, $N(CH_3)_2$); 3.85 (s, 3 H, $N(CH_3)_2$); 3.99 (s, 3 H, $N(CH_3)_2$); 4.10 (s, 3 H, $N(CH_3)_2$; 4.56 (septet, J = 6.5 Hz, 1 H, $OCH(CH_3)_2$);[17] 6.40, 6.52, 9.99 (br m, 10 H, NC_5H_5).

$W_2Cl_2(NMe_2)_3(C(O)NMe_2)(CO)(py)_2$ (IV). $W_2Cl_2(NMe_2)_4$ (0.52 g, 0.85 mmol) was suspended in toluene (5 mL), and pyridine (3 equiv) was added. The mixture was contained in a Schlenk flask provided with a 5-mm neck which was stoppered with a septum. Carbon monoxide (2.5 equiv) was transferred via a gas-tight syringe, and the reaction mixture was stirred at room temperature. A golden brown precipitate of $W_2Cl_2(NMe_2)_4(CO)(py)_2$ started to appear within 15 min. Upon continued stirring, the precipitate redissolved, and after about 3 h, the solution turned dark red. The volatile components from the mixture were removed under vacuum, and the solid residue was redissolved in toluene (3 mL). Dark red microcrystals of $W_2Cl_2(NMe_2)_3(C(O)NMe_2)(CO)(py)_2$ were obtained upon slow diffusion of hexane into the solution and were collected by filtration; total crystallized yield 0.47 g (69%). Anal. Calcd for $W_2Cl_2N_6C_{20}H_{34}O_2$: C, 28.9; H, 4.1; N, 10.1; Cl, 8.6. Found: C, 29.0; H, 4.0; N, 10.0; Cl, 8.7.

IR spectral data (major bands) from Nujol mulls: 2765 (w), *1725* (vs), 1600 (m), 1595 (br, m), 1481 (m), 1362 (m), 962 (m), 928 (m), 751 (m), 760 (m), 698 (m), 650 (m) cm^{-1}.

^1H NMR spectral data (obtained from toluene-d_8 solution, δ values relative to Me_4Si): 2.75 (s, 3 H, $N(CH_3)_2$); 3.00 (s, 3 H, $N(CH_3)_2$); 3.23 (s, 3 H, $N(CH_3)_2$); 3.31 (s, 3 H, $N(CH_3)_2$; 3.39 (s, 3 H, $N(CH_3)_2$); 3.44 (s, 3 H, $N(CH_3)_2$); 3.83 (s, 3 H, $N(CH_3)_2$); 3.86 (s, 3 H, $N(CH_3)_2$), 6.42, 6.62, 9.59 (m, 10 H, NC_5H_5).

$W_2Cl_2(NMe_2)_3(^{13}C(O)NMe_2)(^{13}CO)(py)_2$. Similar procedures were followed employing ^{13}CO. Satisfactory elemental analysis was obtained.

^1H NMR spectral data (from toluene-d_8 solution, δ) 2.75 (d, J = 3.2 Hz, 3 H, $C(O)N(CH_3)_2$); 3.00 (d, J = 3.5 Hz, 3 H, $C(O)N(CH_3)_2$); the rest of the spectral assignment is the same as in IV.

$W_2Cl_2(NMe_2)_3(C(O)NMe_2)(CO)(PMe_2Ph)(py)$ (V). The bis(pyridine) adduct $W_2Cl_2(NMe_2)_3(C(O)NMe_2)(CO)(py)_2$ (0.45 g, 0.54 mmol) was dissolved in toluene (4 mL), and PMe_2Ph (1.5 equiv) was added via a microliter syringe. The solution was initially warmed in a warm water bath (ca. 50 °C) and stirred for 10 min, after which stirring was continued at room temperature for 2 h. The resulting purple microcrystalline solids were isolated by filtration, washed with toluene (5 mL), and dried under vaccum. This compound can be recrystallized by cooling a saturated CH_2Cl_2 solution from room temperature to −15 °C for 4 days, resulting in purple needles of $W_2Cl_2(NMe_2)_3(C(O)NMe_2)(CO)(PMe_2Ph)(py)$. Total recrystallized yield: 0.28 g (57%). Anal. Calcd for $W_2Cl_2N_5C_{23}H_{40}O_2P$: C, 31.1; H, 4.5; N, 7.9; Cl, 8.0. Found: C, 31.2; H, 4.4; N, 7.8; Cl, 8.1.

IR spectral data (major bands) from Nujol mulls: 2760 (w), 1725 (vs), 1685 (vs), 1600 (m), 1595 (br, s), 1488 (m), 1350 (s), 1225 (m), 1125 (m), 950 (s), 930 (s), 911 (s), 760 (m), 751 (s), 700 (s), 650 (m) cm^{-1}.

^1H NMR spectral data (obtained from toluene-d_8 solution at 22 °C, δ values relative to Me_4Si) (two isomers): 1.25 (d, J = 5.1 Hz, $P(CH_3)_2Ph$); 1.27 (d, J = 5.1 Hz, $P(CH_3)_2Ph$); 1.48 (d, J = 6.9 Hz, $P(CH_3)_2Ph$); 1.52 (d, J = 6.5 Hz, $P(CH_3)_2Ph$); 2.69 (s, $N(CH_3)_2$); 2.73 (s, $N(CH_3)_2$); 2.90 (s, $N(CH_3)_2$); 2.91 (s, $N(CH_3)_2$); 2.98 (s, $N(CH_3)_2$); 3.02 (s, $N(CH_3)_2$); 3.03 (s, $N(CH_3)_2$); 3.13 (s, $N(CH_3)_2$); 3.15 (s, $N(CH_3)_2$); 3.39 (s, $N(CH_3)_2$); 3.43 (s, $N(CH_3)_2$); 3.51 (s, $N(CH_3)_2$); 3.60 (s, $N(CH_3)_2$); 3.61 (s, $N(CH_3)_2$); 3.82 (s, $N(CH_3)_2$); 4.38 (s, $N(CH_3)_2$); 6.29, 6.55, 6.70, 8.67, 8.80, 9.86, 9.98 (m, NC_5H_5); 6.95, 7.51 (m, PMe_2Ph).

Acknowledgment. We thank the National Science Foundation for financial support and Dr. John Huffman for his repeated attempts to select crystals suitable for single-crystal X-ray studies.

Registry No. I, 99495-95-1; II, 99495-96-2; III, 99495-97-3; IV, 99495-98-4; V, 99496-02-3; $W_2Cl_2(NMe_2)_3(O\text{-}i\text{-}Pr)(^{13}CO)(py)_2$, 99495-99-5; $W_2Cl_2(NMe_2)_3(^{13}CONMe_2)(^{13}CO)(PMe_2Ph)(py)$, 99496-00-1; $W_2Cl_2(NMe_2)_3(^{13}C(O)NMe_2)(^{13}CO)(py)_2$, 99496-01-2; $W_2Cl_2(NMe_2)_3(^{13}CONMe_2)(py)_2(CO)$, 99496-03-4; $W_2Cl_2(NMe_2)_4(^{13}CO)(py)_2$, 99496-04-5; $W_2Cl_2(NMe_2)_3(CONMe_2)(py)_2(^{13}CO)$, 99496-05-6; $W_2Cl_2(NMe_2)_4$, 63301-81-5; CO, 630-08-0; W, 7440-33-7; N_2, 7727-37-9.

(17) The other $OCHMe_2$ methyne resonance is probably obscured by the μ-NMe_2 methyl resonances.

Oxidative Addition Reactions of Dicarbonyl-[1,1,1-tris((diphenylphosphino)methyl)ethane]ruthenium(0). Elimination of Ketene from an Acetylmetal Compound

Sven I. Hommeltoft and Michael C. Baird*

Department of Chemistry, Queen's University, Kingston, Canada K7L 3N6

Received June 4, 1985

Oxidative addition reactions of the title compound ($Ru(CO)_2$(triphos)) with halogens, anhydrous hydrogen chloride, and several alkyl halides yield the series of complexes $[RuX(CO)_2(triphos)]^+$ (X = halide), $[RuH(CO)_2(triphos)]^+$, and $[RuR(CO)_2(triphos)]^+$ (R = Me, Et, $PhCH_2$, allyl). Most of the compounds appear to exhibit "normal" chemical properties but the hydride is surprisingly acidic, possibly because the hydride ligand is forced into an unusual (for it) coordination position, trans to a phosphorus atom, which would lie high in the trans influence series. While oxidative addition of acetyl chloride *appears* to give the acetyl complex $[Ru(COMe)(CO)_2(triphos)]^+$, the latter is unstable and eliminates ketene to form the above-mentioned hydride complex. The unusual instability of the acetyl complex is perhaps also to be attributed in part to the high trans influence and pronounced trans bond weakening properties of tertiary phosphines.

Oxidative addition reactions of protonic acids and alkyl halides to low-valent metal compounds to form metal hydride and alkyl compounds (eq 1) constitute two of the

$$ML_n + HX\ (RX) \rightarrow MHXL_n\ (MRXL_n) \qquad (1)$$

R = alkyl, aryl, acyl; X = halide

principal methods of forming metal–hydrogen and metal–carbon bonds, and thus are reactions of general significance and prime importance in the synthesis of organotransition metal compounds.[1-3] The reactions are also key features of many catalytically important processes and have been much studied mechanistically.[2,3]

Although bis(phosphine) compounds of the type $M(CO)_3(PPh_3)_2$ (M = Ru, Os) were among the earliest low-valent metal systems for which oxidative addition reactions were investigated,[4] it is surprising to note that very little has actually been reported of the oxidative additions of, for instance, hydrogen halides and alkyl halides to ruthenium(0) compounds.[5] Indeed, formation of compounds of the type $RuRX(CO)_2L_2$ (L = tertiary phosphine) is best accomplished by routes other than reactions of alkyl halides with the ruthenium(0) compounds $Ru(CO)_3L_2$.[6] Ruthenium(0) compounds containing three monodentate or one tridentate phosphine seem rather more reactive toward electrophilic reagents,[5,7,8] either because of the greater electron-donating ability of phosphorus over carbon monoxide or, possibly, because of lability of one of the phosphines. However, again little has been reported.

This paper deals with oxidative addition reactions of the ruthenium(0) compound $Ru(CO)_2[MeC(CH_2PPh_2)_3]$ (I)[7] with halogens, protonic acids and alkyl, allyl, and acyl halides. The reactions are of interest because the chelating ligand, henceforth triphos, preferentially assumes three 90° "bite angles",[9] and very comfortably caps a triangular face of an octahedron. Thus octahedral complexes of triphos of necessity assume facial stereochemistries and may be expected to provide useful points of contrast and comparison with complexes which assume meridional structures, for instance of the tridentate ligands $PhP(CH_2CH_2CH_2PR_2)_2$,[8] or containing three monodentate phosphines.[6] All three of the remaining coordination sites of a facial, octahedral MP_3 type of complex are trans to a phosphorus atom, while only two such sites are trans to phosphorus in a meridional structure. Therefore, as phosphorus donors lie high in the trans influence series,[10] one can anticipate greater reactivity in a facial series of complexes.

We describe herein an extensive series of alkyl- and hydridoruthenium complexes, all containing triphos and hence of facial geometry. A subsequent paper will describe the synthesis and resolution of the chiral products of substitution of one of the carbonyl groups. Aspects of the work have appeared in preliminary communications.[11]

Experimental Section

All reactions were carried out under purified nitrogen; the solvents used were dried using standard procedures. Infrared spectra (Table I) were run on a Beckman IR 4240 and Brucker IFS 85 FTIR spectrometers and ^1H, $^{13}C\{^1H\}$, and $^{31}P\{^1H\}$ NMR spectra (Tables II–IV, respectively) on a Bruker AM 400 NMR spectrometer. Elemental analyses were determined by Canadian Microanalytical Services, Vancouver, and are listed in Table I.

The compound $Ru(CO)_2$(triphos) (I) was prepared from $Ru(CO)_3(PPh_3)_2$ by a published procedure.[7] The compounds $[RuX(CO)_2(triphos)]PF_6$ (X = Cl (II), Br (III)) and $RuX_2(CO)$(triphos) (X = Cl (IV), Br (V)) were prepared essentially as in the literature.[7]

$RuI_2(CO)$(triphos) (VI). A solution of iodine in methylene chloride was added dropwise to a solution of I (2.33 g, 3.0 mmol) in 30 mL of methylene chloride until the color faded to yellow and began to darken again. The solution was refluxed for 18 h,

(1) Collman, J. P.; Hegedus, L. S. "Principles and Applications of Organotransition Metal Complexes"; University Science Books: Mill Valley, CA, 1980.
(2) Lukehart, C. M. "Fundamental Transition Metal Organometallic Chemistry"; Brooks/Cole Publishing Co.: Monterey, 1985.
(3) Atwood, J. D. "Inorganic and Organometallic Reaction Mechanism"; Brooks/Cole Publishing Co.: Monterey, 1985.
(4) Collman, P. P.; Roper, W. R. *Adv. Organomet. Chem.* **1968**, *7*, 53.
(5) Seddon, E. A.; Seddon, K. R. "The Chemistry of Ruthenium"; Elsevier: Amsterdam, 1984; Chapter 11.
(6) Barnard, C. F. J.; Daniels, J. A.; Mawby, R. J. *J. Chem. Soc., Dalton Trans.* **1976**, 961.
(7) Siegl, W. O.; Lapporte, S. J.; Collman, J. P. *Inorg. Chem.* **1973**, *12*, 674.
(8) Letts, J. B.; Mazanec, T. J.; Meek, D. W. *Organometallics* **1983**, *2*, 695 and references therein.
(9) (a) Mason, R.; Williams, G. A. *Aust. J. Chem.* **1981**, *34*, 471. (b) Ghilardi, C. A.; Midollini, S.; Sacconi, L. *J. Organomet. Chem.* **1980**, *186*, 279. (c) Bianchini, C.; Mealli, C.; Meli, A.; Orlandini, A.; Sacconi, L. *Inorg. Chem.* **1980**, *19*, 2968. (d) Di Vaira, M.; Sacconi, L. *Angew. Chem., Int. Ed. Engl.* **1982**, *21*, 330.
(10) Appleton, T. G.; Clark, H. C.; Manzer, L. E. *Coord. Chem. Rev.* **1973**, *10*, 335.
(11) (a) Hommeltoft, S. I.; Cameron, A. D.; Shackelton, T. A.; Fraser, M. E.; Fortier, S.; Baird, M. C. *J. Organomet. Chem.* **1985**, *282*, C17. (b) Hommeltoft, S. I.; Baird, M. C. *J. Am. Chem. Soc.* **1985**, *107*, 2548.

0276-7333/86/2305-0190$01.50/0

Table I. Analytical and Infrared Data

compd	anal. data found (calcd) C	H	$\nu_{CO}(CH_2Cl_2)$,
$Ru(CO)_2$(triphos) (I)[7]			1941 (s), 1858 (s)
$[RuCl(CO)_2$(triphos)$]PF_6$ (II)[7]			2089 (vs), 2049 (vs)
$[RuBr(CO)_2$(triphos)$]PF_6$ (III)[7]			2085 (vs), 2045 (vs)
$RuCl_2(CO)$(triphos) (IV)[7]			2024 (s)
$RuI_2(CO)$(triphos) (VI)	51.06 (50.07)	3.94 (3.90)	2007 (s)
$[RuI(CO)_2$(triphos)$]PF_6$ (VII)	*a*	*a*	2078 (vs), 2040 (s)
$[RuH(CO)_2$(triphos)$]PF_6$ (VIII)	55.87 (55.67)	4.53 (4.35)	2057 (vs), 2010 (s)[b]
$[RuMe(CO)_2$(triphos)$]PF_6$ (IX)	55.89 (56.12)	4.42 (4.49)	2054 (vs), 2007 (s)
$[RuEt(CO)_2$(triphos)$]PF_6$ (X)	56.00 (56.55)	4.60 (4.64)	2049 (vs), 2001 (s)
$[Ru(CH_2Ph)(CO)_2$(triphos)$]PF_6$ (XI)	58.75 (59.00)	4.61 (4.55)	2054 (vs), 2008 (s)
$Ru(\eta^1\text{-}C_3H_5)(CO)_2$(triphos)$]PF_6$ (XII)	54.01 (57.09)[a]	4.39 (4.58)	2054 (vs), 2008 (s)[c]
$Ru(\eta^3\text{-}C_3H_5)(CO)$(triphos)$]PF_6$ (XIII)	57.24 (57.51)	4.75 (4.72)	2003 (s)

[a] Compound could not be purified. See text. [b] ν_{RuH} = 1951 cm^{-1} (w). [c] $\nu_{C=C}$ = 1615 cm^{-1} (w).

Table II. ^1H NMR Data (δ, Internal Me_4Si)

compd	triphos Me ($^4J_{PH}$, Hz)	triphos CH_2 group(s)	triphos Ph	other
I[a]	1.52	2.27 (6 H, m)	6.8–7.4	
II[b]	1.90 (q, 3)	2.66 (2 H, m), 2.75 (2 H, d, J = 10 Hz), 2.81 (2 H, m)	6.8–8.0	
III[b]	1.90 (br, s)	2.66 (2 H, m), 2.78 (2 H, d, J = 10 Hz), 2.85 (2 H, m)	6.9–7.7	
IV[a]	1.55 (q, 3)	2.37 (2 H, m), 2.46 (2 H, m), 2.53 (2 H, d, J = 9 Hz)	6.8–8.0	
VI[a]	1.49 (q, 3)	2.38 (2 H, dd, J = 6, 15 Hz), 2.55–2.65 (4 H, m)	6.9–8.0	
VII[a]	1.90 (q, 3)	2.59 (2 H, m) 2.82 (2 H, br d, J = 10 Hz), 2.88 (2 H, m)	6.9–8.0	
VIII[a]	1.80 (q, 3)	2.42–2.52 (4 H, m), 2.68 (2 H, d, J = 9)	6.6–7.6	–6.70 (1 H, dt, J = 64, 15 Hz)
IX[a]	1.76 (q, 3)	2.5–2.7 (6 H, m)	7.0–7.6	0.30 (3 H, td, J = 5.3, 3.1 Hz)
X[a]	1.77 (q, 3)	2.4–2.7 (6 H, m)	6.9–7.7	1.23 (2 H, m), 1.58 (3 H, q, 7)
XI[a]	1.80 (q, 3)	2.5–2.65 (4 H, m), 2.8–2.9 (2 H, m)	6.9–7.6	2.89 (2 H, m, benzyl CH_2)[c]
XII[a]	1.78 (q, 3)	2.58–2.70 (4 H, m), 2.76 (2 H, m)	7.0–7.7	2.15 (2 H, m), 4.76 (1 H, m), 4.98 (1 H, br d, J = 6.5 Hz), 6.46 (1 H, m)
XIII[a]	1.79 (q, 3)	2.39 (2 H, br d, J = 9 Hz), 2.6–2.9 (m)[d]	6.4–7.6	2.6–2.9 (m)[d]

[a] In CD_2Cl_2. [b] In $CDCl_3$. [c] Note overlap between benzyl and triphos methylene resonances. [d] Note extensive overlap between alkyl and triphos resonances.

Table III. $^{13}C\{H\}$ NMR Data (CD_2Cl_2, δ, Internal Me_4Si)

compd	triphos resonances C	Me	CH_2	Ph	CO	other
I	38.4 (m)[a]	39.0 (m)[a]	35.5 (m)	128–140	221.8 (m)	
II	38.0 (br s)	37.7 (q)[b]	32.7 (1 C, m)	127–134	191.2 (m)	
			30.7 (2 C, m)			
III	37.8 (br s)	37.6 (q)[b]	32.2 (1 C, m)	128–135	191.1 (m)	
			31.1 (2 C, m)			
IV	38.1 (br s)	38.5 (q)[b]	34.8 (2 C, m)	127–139	197.6 (m)	
			31.7 (1 C, m)			
VII	37.6 (m)[a]	37.6 (m)[a]	31.0 (3 C, m)	127–135	191.2	
VIII	38.0 (m)[a]	38.1 (m)[a]	32.0 (1 C, m)	127–135	196.9 (m)	
			31.5 (2 C, m)			
IX	37.6 (m)	38.4 (q)[b]	33.1 (2 C, m)	129–136	198.4 (m)	–13.0 (MeRu, dt, J = 33, 6 Hz)
			30.1 (1 C, m)			
X	37.5 (br s)	38.5 (q)[b]	33.5 (2 C, m)	129–136	199.6 (m)	5.6 (CH_2Ru, br d, J = 34 Hz)
			30.3 (1 C, m)			21.8 (Me, s)
XI	37.3 (m)	38.3 (q)[b]	33.6 (2 C, m)	151, 124–135	198.7 (m)	14.9 (CH_2Ru, dt, J = 32, ~4 Hz)
			29.5 (1 C, m)			
XII	37.4 (br s)	38.2 (q)[b]	33.2 (2 C, m)	128–136	198.7 (m)	15.2 (CH_2Ru, dt, J = 32, 5 Hz)
			29.9 (1 C, m)			107.8 (=CH_2, d, J = 4 Hz), 147.3 (=CH, br s)
XIII	37.7 (m)	38.3 (q)[b]	34.9 (1 C, m)	128–137	201.5 (m)	46.6 (=CH_2, m), 95.4 (CH, s)
			33.5 (2 C, m)			

[a] Resonances overlap considerably. [b] Apparent coupling 9–10 Hz.

after which the yellow precipitate was collected, washed with methylene chloride, and dried in vacuo; yield 2.1 g (71%). If, instead of refluxing, the solvent was removed at room temperature, there was obtained a yellow precipitate which appeared (IR, NMR) to be $[RuI(CO)_2$(triphos)$]I$ (VII), contaminated with a little VI. Compound VII readily converted to VI on attempted purification and hence was not analyzed.

$[RuH(CO)_2$(triphos)$]PF_6$ (VIII). Anhydrous HCl was bubbled briefly through a solution of I in methylene chloride. The orange color faded immediately, and IR and NMR spectroscopy showed that conversion of I to VIII was complete. The cationic hydride complex was better prepared by treating I with acetyl chloride (see below).

$[RuMe(CO)_2$(triphos)$]PF_6$ (IX). I (3.86 g, 4.9-mmol) in 40 mL of methylene chloride was treated with 1.0 mL of methyl iodide (16 mmol). The solution was stirred at room temperature for 30 min, at which time the orange color had faded and the iodide salt was precipitated with hexane. Treatment of 1.1 g (1.1 mmol) of the latter with 0.4 g of sodium hexafluorophosphate (2.3 mmol) in 40 mL of ethanol yielded a white precipitate of IX which was collected, washed with ethanol and ethyl ether, and dried in vacuo at 80 °C; yield 1.1 g (96% yield).

Table IV. $^{31}P\{^1H\}$NMR Data[a]

compd	δ_P(trans to CO)	δ_P (trans to X, R)	J_{PP}, Hz
I	27.5 (fluxional)		
II	−1.7 (2 P, d)	26.6 (1 P, t)	32
III	−3.0 (2 P, d)	26.3 (1 P, t)	31
IV	−7.2 (1 P, t)	28.6 (2 P, d)	40
VI	−15.5 (1 P, t)	25.1 (2 P, d)	38
VII	−4.1 (2 P, d)	20.5 (1 P, t)	31
VIII[b]	18.4 (2 P, d)	7.3 (1 P, t)	29
IX	10.6 (2 P, d)	3.4 (1 P, t)	30
X	9.6 (2 P, d)	0.3 (1 P, t)	29
XI	8.3 (2 P, d)	0.7 (1 P, t)	30
XII	9.4 (2 P, d)	2.1 (1 P, t)	30
XIII	15.3 (1 P, t)	19.2 (2 P, d)	44

[a] In CD_2Cl_2. [b] In $CDCl_3$.

[RuEt(CO)$_2$(triphos)]PF$_6$ (X). Ethyl iodide (0.5 mL, 6.3 mmol) was added to 1.06 g (1.4 mmol) of I in 20 mL of methylene chloride, and the solution was stirred at room temperature for 5 h. The solvent was removed under reduced pressure, and the residue was taken up in ethanol. A small amount of yellow VI was removed by filtration, but IR spectroscopy showed that the solution still contained some VII. To remove the latter, 0.01 g of Me_3NO was added to the solution of the mixture in methylene chloride. An IR spectrum now showed that all of the monoiodo complex had been converted to VI. The solvent was again removed, the residue was dissolved in ethanol, some more VI was removed by filtration (for a total of 0.55 g, 40% yield), and metathesis with sodium hexafluorophosphate was carried out as for IX to give 0.29 g of pure X (22% yield), dried at room temperature.

[Ru(CH$_2$Ph)(CO)$_2$(triphos)]PF$_6$ (XI). Benzyl bromide (0.5 mL, 4.2 mmol) was added to 1.32 g (1.7 mmol) of I in 20 mL of methylene chloride. The solution was stirred for 10 min, and the product was worked up as for IX; yield 1.19 g (74% yield).

[Ru(η^1-C$_3$H$_5$)(CO)$_2$(triphos)]PF$_6$ (XII). Allyl bromide (0.20 mL, 2.3 mmol) was added to 1.61 g (2.1 mmol) of I in 20 mL of methylene chloride, and the solution was stirred for 30 min. The reaction was worked up as above to give about 1.6 g of crude XII contaminated with a little of the bromo complex. All attempts at purification failed, and the compound was characterized spectroscopically and by conversion to the η^3-allyl derivative XIII (see below).

[Ru(η^3-C$_3$H$_5$)(CO)(triphos)]PF$_6$ (XIII). To a solution of crude XII (0.7 g, 0.7 mmol) in 39 mL of methylene chloride was added 0.10 g (1.3 mmol) of Me_3NO. After 5 min, an IR spectrum showed that total conversion of XII to XIII had occurred. Recrystallization from acetone/ethanol yielded pure XIII (0.24 g, 35% yield).

Reaction of I with Acetyl Chloride. In a typical experiment, 2.58 g (3.3 mmol) of I was mixed with 2.5 mL of freshly distilled, dried[12] acetyl chloride in a flame-dried flask. The mixture was refluxed while a stream of nitrogen carried gaseous products into a liquid-nitrogen trap. After 35 min, the reaction mixture had faded in color and had turned into a paste. It was cooled and dissolved in 5 mL of methylene chloride, and an oil was precipitated by the addition of heptane. The oil was crystallized from methylene chloride/heptane and identified spectroscopically as the hydride obtained on the addition of anhydrous HCl to I (see above) yield 3.0 g (quantitative). As the chloride compound was contaminated with methylene chloride, it was converted to the hexafluorophosphate salt for purposes of elemental analyses.

The contents of the cold trap were identified as a mixture of ketene and acetyl chloride by several separate experiments. In the first, the contents of the trap were dissolved in a minimum of acetyl chloride and an IR spectrum was run as quickly as possible. The spectrum showed bands at 2140 and 1805 cm^{-1}, attributable to ketene[13] and acetyl chloride, respectively. A drop of ethanol resulted in the immediate disappearance only of the band at 2140 cm^{-1} and in the appearance of a band at 1735 cm^{-1} attributed to ethyl acetate. In a second experiment the contents of the trap were dissolved in $CDCl_3$ and a ^{13}C NMR spectrum run at −60 °C demonstrated the presence of ketene (193.7 (s), 2.70 ppm (t, J(CH) = 177 Hz)[14]) and acetyl chloride. About 40 μL of D_2O were then added to the NMR sample, which was held at room temperature for 4 h. At this time, the ^1H NMR spectrum revealed the presence of CH_2DCOOD (1:1:1 triplet at 2.09 ppm (J(HD) = 2.12 Hz))[15,16] and CH_3COOD (2.10 ppm (s)). The two species were also identified by characteristic methyl resonances in the $^{13}C(^1H)$ NMR spectrum as well (1:1:1 triplet at 20.24 ppm (J(CD) = 19.9 Hz), singlet at 20.4 ppm).

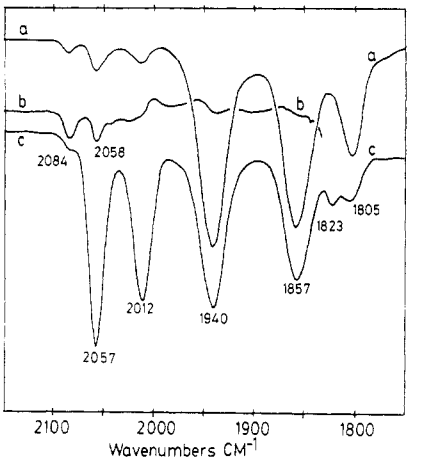

Figure 1. IR study of the reaction of a 1:1 mixture of acetyl chloride and I: (a) spectrum after 40 min, (c) spectrum after 20 h, (b) as (c) but bands of I and the hydride subtracted.

In a similar experiment, a 2:1 mixture of CH_3COCl and CD_3COCl was reacted, and the ruthenium deuteride complex was recognized in the ^2D NMR spectrum as a broadened doublet at −7.05 ppm (J(DP) = 11 Hz). Careful integration of the ^1H NMR spectrum of the same mixture showed that the hydride/deuteride ratio was about 6:1, consistent with a kinetic isotope effect of about 3.0. The ketene–acetyl chloride mixture in the cold trap was converted to acetic acid by the addition of water, and the isotope content of the acetic acid was determined by mass spectroscopy to give kinetic isotope effects of 3.9 and 2.5 on two samples. Thus the kinetic isotope effect of the ketene-forming reaction is about 3.0 ± 1.

The reaction of I with acetyl chloride was also followed by FTIR spectroscopy. A solution of 0.32 g (0.41 mmol) of I in 5 mL of methylene chloride was treated with 40 μL (0.57 mmol) of acetyl chloride. IR spectra were taken periodically as shown in Figure 1, where spectra at 40 min (a) and 20 h (c) are illustrated. Figure 1b shows the spectrum after 20 h with the carbonyl bands of Ru(CO)$_2$(triphos) and [RuH(CO)$_2$(triphos)]Cl subtracted.

Miscellaneous Reactions. Dissolution of I in chloroform resulted in almost quantitative conversion to II and IV within 15 min (IR), while reaction of I with (1-bromoethyl)benzene in methylene chloride gave predominantly III within 1 h rather than the anticipated benzylic ruthenium compound. Treatment of a benzene solution of I with 600 atm of hydrogen at room temperature for 4 days, followed by removal of the solvent under reduced pressure, yielded only unreacted I (IR).

Results and Discussion

The ruthenium(0) complex Ru(CO)$_2$(triphos) (I) was prepared as described in the literature.[7] It is a bright yellow, air-sensitive compound with two carbonyl stretching bands but only a single ^{31}P resonance. As I is expected to be trigonal bipyramidal in structure, with mutually cis carbonyl groups and nonequivalent phosphorus atoms, it is probably fluxional. The ^1H and $^{13}C(^1H)$

(12) Vogel, A. I. "Practical Organic Chemistry", 3rd ed.; Longmans: London, 1964; p 367.
(13) Arendale, W. F.; Fletcher, W. H. *J. Chem. Phys.* **1957**, *26*, 793.
(14) Firl, J.; Runge, W. *Z. Naturforsch., B: Anorg. Chem., Org. Chem.* **1974**, *29B*, 393.
(15) Trivedi, J. P. *J. Inst. Chem. (India)* **1977**, *49*, 237.
(16) Caminati, W.; Scappini, F.; Corbelli, G. *J. Mol. Spectrosc.* **1979**, *75*, 327.

NMR spectra were in accord with this conclusion; no change in the ^{31}P NMR spectrum was observed down to −90 °C.

As pointed out previously,[7] the low frequencies of the carbonyl stretching bands (1941, 1858 cm^{-1}) suggest that the metal atom of I is rather electron rich. Accordingly it is not surprising to find that I undergoes oxidative addition reactions with a variety of electrophilic reagents. Addition of halogens is instantaneous, the initially formed products being of the stoichiometry $[RuX(CO)_2(triphos)]X$. A second, slower step involves displacement of a carbonyl group by halide ion to give the neutral species $RuX_2(CO)(triphos)$. Both types of complexes have been reported previously.[7] While the suggestion has been made that the high reactivity of I toward electrophiles is a result of dissociation of one of the phosphorus atoms to give a coordinatively unsaturated, 16-electron intermediate,[7] this hypothesis now seems unlikely. We have carried out the chlorination reaction in the presence of excess chlorine, under conditions where a free phosphine moiety would be expected to be readily attacked by chlorine.[17] As no such reaction was observed, phosphine dissociation is quite unlikely.

Addition of anhydrous HCl to a methylene chloride solution of I results in instantaneous decolorization of the solution and formation of the new hydride $[RuH(CO)_2(triphos)]Cl$, ultimately isolated analytically pure from the reaction of I with acetyl chloride as the hexafluorophosphate salt VIII (see below). The assignment of a weak band at 1951 cm^{-1} in the IR spectrum to ν(RuH) was confirmed by observation of a band at 1403 cm^{-1} in the IR spectrum of the corresponding deuteride (ratio 1.39). The hydride resonance of VIII was observed (methylene chloride solution) as a double triplet centered at −6.70 ppm, the coupling to the trans phosphorus being 64 Hz, that to the two cis phosphorus atoms being 15 Hz. The ^2D NMR spectrum exhibited a broadened doublet at about −7.0 ppm, the coupling to the trans phosphorus atom being 11 Hz. These spectroscopic properties are typical for ruthenium(II) hydride complexes.[18]

Although VIII exhibits no hydridic properties chemically, being stable for at least 8 h in a methylene chloride solution saturated with anhydrous HCl, it is slightly acidic. Thus an IR study showed that it is partially deprotonated (to reform I) on treatment with diethylamine in methylene chloride, the reaction being reversed on partial evaporation of the solution followed by addition of more solvent. The hydride is also deprotonated by a suspension of potassium carbonate in tetrahydrofuran, a reaction which is reversed on the addition of acetic acid. Thus VIII exhibits an acid strength approximately comparable with that of acetic acid.

The latter conclusion is somewhat surprising for a platinum metal hydride complex containing a tridentate phosphine and may be a result in part of the cationic nature of VIII. However, the hydride ligand of this compound is also trans to a phosphorus atom. Thus, as phosphorus donors normally lie high in the trans influence series,[10] the hydrogen may be bonded relatively weakly to the ruthenium atom and dissociation as a proton may be facilitated. While the hypothesis that a phosphorus donor might labilize a trans hydride ligand as a proton rather than as a hydride seems counterintuitive, we can think of no other explanation for our observations and feel that the idea is at least worthy of consideration. There are few data in the literature which are relevant to the point, but we note that the compound *cis*-$[IrH(CO)(dppe)_2]^{2+}$ (dppe = 1,2-bis(diphenylphosphino)ethane) is a much stronger acid than is its trans isomer.[19] As the former contains a hydride ligand trans to phosphorus while the latter contains a hydride trans to carbon monoxide, the trend would appear to substantiate our hypothesis concerning the importance of the trans ligand on the acid strength of a platinum metal hydride.

Addition of methyl iodide to I proceeds essentially quantitatively at room temperature within 1 min. The methylruthenium product, isolated analytically pure as the hexafluorophosphate salt (IX), is stable to air oxidation, to substitution reactions by halides and hydride abstraction by triphenylcarbenium ion at room temperature. It is also inert to carbon monoxide over 15 h at 90 °C (270 atm) consistent with the apparent instability of the acetyl analogue (see below). The spectroscopic properties of IX were consistent with its formulation, most particularly the ruthenium–methyl resonance in the ^1H NMR spectrum at 0.3 ppm, a double triplet. Both the chemical shift and the coupling constant to the cis phosphorus atoms (5.3 Hz) are consistent with literature data for similar compounds.[6] It is interesting to note that the coupling constant to the trans phosphorus atom (3.1 Hz) is smaller than is the cis coupling constant. The ruthenium-methyl resonance in the $^{13}C\{^1H\}$ NMR spectrum was observed at −13.0 ppm, the cis and trans couplings to phosphorus being 6 and 33 Hz, respectively.

Addition of ethyl iodide to I to give the ethylruthenium complex $[RuEt(CO)_2(triphos)]I$ proceeds approximately 4 orders of magnitude more slowly than does the reaction of methyl iodide and gave a mixture of products which included the iodo complexes $[RuI(CO)_2(triphos)]I$ (VII) and $RuI_2(CO)(triphos)$ (VI). Removal of the iodo complexes was effected by dissolving the crude reaction mixture in ethanol and treating it with a small amount of trimethylamine *N*-oxide; VII was converted smoothly to VI, which is insoluble in ethanol. Reaction with the more electron-rich ethyl compound was much slower,[20] and thus this complex remained and could readily be precipitated as the hexafluorophosphate salt X.

Consistent with the electron-rich nature of the ruthenium atom of this compound, the methylene proton and carbon resonances both lie to higher field than do the methyl resonances. Although most spin–spin couplings to phosphorus by the methylene resonances could not be resolved, the trans J(PC) is approximately 34 Hz, very similar to the corresponding coupling of the methyl carbon of IX.

Benzyl bromide adds very smoothly to I, giving the benzyl compound (isolated as the hexafluorophosphate salt XI) in near quantitative yield. While the benzylic proton resonance was largely obscured by triphos methylene resonances, the corresponding carbon resonance was observed at 14.9 ppm, the cis and trans couplings to phosphorus being 32 and 4 Hz, respectively. Also possibly characteristic of a metal–benzyl compound is the low field chemical shift of the ipso carbon atom (151 ppm).[21] An attempt to add 1-(bromoethyl)benzene to I resulted in a mixture of products, predominantly the bromo complexes $[RuBr(CO)_2(triphos)]Br$ (III) and $RuBr_2(CO)(triphos)$ (V).

(17) Emeleus, H. J.; Miller, J. M. *J. Inorg. Nucl. Chem.* **1966**, *28*, 662.
(18) Reference 5, pp 547, 551.
(19) Lilga, M. A.; Ibers, J. A. *Inorg. Chem.* **1984**, *23*, 3538.
(20) Koelle, U. *J. Organomet. Chem.* **1977**, *133*, 53.
(21) See, for example: (a) Orlova, T. Y.; Petrovskii, P. V.; Setkina, V. N.; Kursanov, D. N. *J. Organomet. Chem.* **1974**, *67*, C23. (b) Todd, L. J.; Wilkinson, J. R. *J. Organomet. Chem.* **1974**, *80*, C31. (c) Bied-Charreton, C.; Septe, B.; Gaudemer, A. *Org. Magn. Reson.* **1975**, *7*, 116. (d) Chisholm, M. H.; Clark, H. C.; Manzer, L. E.; Stothers, J. B.; Ward, J. E. *J. Am. Chem. Soc.* **1975**, *97*, 721.

Allyl bromide adds readily to I to give the allyl complex $[Ru(\eta^1\text{-}C_3H_5)(CO)_2(triphos)]Br$ contaminated with a small amount of the bromo complex III. Purification of the compound proved to be surprisingly difficult, and the carbon/hydrogen analyses of the hexafluorophosphate salt XII were low. The allyl compound was therefore characterized spectroscopically and by conversion to the η^3-allyl analogue XIII, which could be obtained analytically pure (see below). The IR spectrum of XII exhibited a weak absorption at 1615 cm^{-1}; this disappeared on conversion to XIII and thus may be assigned to $\nu(C{=}C)$. The ^1H NMR spectrum of XII exhibited resonances at 2.15 (m, 2 H, α-CH_2), 6.46 (m, 1 H, β-CH), 4.76 (double triplet, J = 9.5, 2.0 Hz, 1 H, γ-CH), and 4.98 ppm (br d, J = 16.5 Hz, 1 H, γ-CH), while the $^{13}C\{^1H\}$ NMR spectrum exhibited resonances at 15.2 (double triplet, $J(trans\text{-}CP)$ = 32 Hz, $J(cis\text{-}CP)$ = 15.2 Hz), 147.3 (s), and 107.8 ppm (d, $J(CP)$ = 4 Hz), attributed to C_1, C_2, and C_3, respectively. The ^1H NMR spectrum is certainly consistent with the η^1-formulation, while the ^{13}C NMR data compare well with data in the literature[22] for similar compounds. We note long-range coupling of 4 Hz between C_3 and one phosphorus atom.

Compound XIII is readily obtained on treatment of XII with trimethylamine *N*-oxide and exhibits only a single carbonyl stretching band in its IR spectrum. The η^3-allyl group can be identified by its ^{13}C resonances at 46.6 (m) and 95.4 (s) ppm, attributed to the CH_2 and CH groups, respectively.[23] Allyl resonances in the ^1H NMR spectrum are unfortunately obscured by triphos resonances.

As we have not carried out kinetics studies on the alkyl halide oxidative addition reactions discussed above, we do not have any direct evidence with respect to mechanism(s) of the reactions. However, we note that the large apparent decrease in rate of addition on going from methyl to ethyl iodide has precedent in the literature and is consistent with either a mechanism involving nucleophilic displacement of iodide by the electron rich metal atom or a mechanism involving radical intermediates.[24] The observation of halo complexes among the products of most of the oxidative addition reactions of the alkyl, benzyl, and allyl halides, however, strongly suggests the importance a radical process as a reaction route in at least some cases.[25] The almost exclusive formation of the chloro complexes $[RuCl(CO)_2(triphos)]Cl$ and $RuCl_2(CO)(triphos)$ on dissolution of I in chloroform is also consistent with radical processes.

The reaction of acetyl chloride with I was slow and did not give the expected acetyl complex $[Ru(COMe)(CO)_2(triphos)]Cl$ (XIV) but rather the hydride complex $[RuH(CO)_2(triphos)]Cl$ in good yield. Indeed, it was material prepared in this way which first resulted in the isolation of analytically pure VIII. Reaction of acetyl-d_3 chloride gave the corresponding ruthenium deuteride, confirming the source of the hydride (deuteride) ligand and suggesting the following stoichiometry for reaction 2.

$$I + MeCOCl \rightarrow [RuH(CO)_2(triphos)]Cl + CH_2{=}C{=}O \quad (2)$$

As outlined in detail in the Experimental Section, the presence of ketene was demonstrated in several ways, including direct spectroscopic observation and derivatization.

Several mechanisms for the ketene elimination seem at first glance to be feasible. Direct dehydrohalogenation of acetyl chloride by I, a weak base, is one possibility, as ketenes can be prepared by treatment of acid halides by amines.[26] This route seems unlikely, however, as many metal acyl compounds have been prepared by reactions involving, for instance, metal carbonylate anions or low-valent metal compounds with acid halides.[27] There appear to be no reports of metal hydride formation from such reactions, and thus it is difficult to understand why I should uniquely deprotonate acetyl chloride.

Alternatively we considered the possibility that the acetyl complex XIV does form but that it is somehow unstable with respect to ketene elimination. Accordingly we carried out an FTIR study in which equimolar amounts of I and acetyl chloride were allowed to react in methylene chloride at room temperature (see Experimental Section for details). Initially there appeared a weak shoulder on the high-frequency side of the 2057 cm^{-1} band of the hydride product, but the weak band did not grow in intensity and was soon totally obscured. Subtraction of the spectrum of the hydride complex, however, revealed two very weak bands at 2085 and approximately 2056 cm^{-1}. These are at frequencies higher than the corresponding bands of the hydride complex (2057, 2010 cm^{-1}), and, as the acetyl group is more electronegative than is hydrogen, it is reasonable to assign the weak bands to XIV. No band corresponding to the acetyl carbonyl stretching mode could be assigned because such a band would be very weak and would be in the region obscured by ketene byproducts; no effort was made to identify the latter. Attempts to monitor the reaction using ^1H NMR spectroscopy were unsuccessful as resonances of triphos and ketene completely obscured the region of interest.

As XIV appears to be formed in a low, steady-state concentration, it seemed likely that its decomposition would be rate determining. Accordingly we carried out competition experiments in which I was reacted with mixtures of acetyl chloride and acetyl-d_3 chloride. A kinetic isotope effect of 3 ± 1 was found; this, although not very precise, is certainly a primary kinetic isotope effect and is consistent with the rate-determining step in the ketene formation involving C–H bond breaking.[28] Very similar kinetic isotope effects have been observed for hydride-forming, olefin elimination reactions from metal alkyl compounds,[29] and it seems reasonable to consider a similar elimination from XIV, i.e., eq 3. Indeed, a recent report

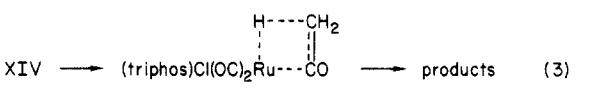

(3)

of an acetyl compound in which the methyl group is inclined toward the metal atom such that there is a very short metal–hydrogen distance[30] provides a possible model

(22) (a) Ciapenelli, D. J.; Cotton, F. A.; Kruczynski, L. *J. Organomet. Chem.* **1972**, *42*, 159. (b) Bassett, J.-M.; Green, M.; Howard, J. A. K.; Stone, F. G. A. *J. Chem. Soc., Chem. Commun.* **1977**, 853. (c) Oudeman, A.; Sorensen, T. S. *J. Organomet. Chem.* **1978**, *156*, 259.

(23) Mann, B. E.; Taylor, B. F. "^{13}C NMR Data for Organometallic Compounds"; Academic Press: New York, 1981; Table 2.11.

(24) Reference 3, Chapter 5.

(25) Labinger, J. A.; Osborn, J. A.; Coville, N. J. *Inorg. Chem.* **1980**, *19*, 3236 and references therein.

(26) Ward, R. S. In "The Chemistry of Ketenes, Allenes and Related Compounds"; Patai, S., Ed.; Wiley: New York, 1980; Part 1, p 223.

(27) (a) McCleverty, J. A.; Wilkinson, G. *J. Chem. Soc.* **1963**, 4096. (b) Coffield, T. H.; Kozikowski, J.; Closson, R. D. *J. Org. Chem.* **1957**, *22*, 598. (c) Hieber, W.; Braun, G.; Beck, W. *Chem. Ber.* **1960**, *93*, 901. (d) King, R. B. *J. Am. Chem. Soc.* **1963**, *85*, 1918. (e) Cook, C. D.; Jauhal, G. S. *Can. J. Chem.* **1967**, *45*, 301. (f) Bennet, M. A.; Charles, R.; Mitchell, T. R. B. *J. Am. Chem. Soc.* **1978**, *100*, 2737.

(28) Melander, L.; Saunders, W. H. "Reaction Rates of Isotopic Molecules"; Wiley: New York, 1980; p 157.

(29) (a) Ikariya, T.; Yamamoto, A. *J. Organomet. Chem.* **1976**, *120*, 257. (b) Evans, J.; Schwartz, J.; Urquhart, P. W. *J. Organomet. Chem.* **1974**, *81*, C37. (c) Ozawa, F.; Ito, T.; Yamamoto, A. *J. Am. Chem. Soc.* **1980**, *102*, 6457.

(30) Carmona, E.; Sanchez, L.; Marin, J. M.; Poveda, M. L.; Atwood, J. L.; Priester, R. D.; Rogers, R. D. *J. Am. Chem. Soc.* **1984**, *106*, 3214.

for the type of interaction which would be necessary. However, such an elimination reaction would require a vacant site on the ruthenium atom, a perhaps unlikely occurrence. We note that the ethyl complex X is very stable with respect to ethylene dissociation, suggesting that hydride migration from a β-carbon atom to ruthenium may not be facile.

An alternative mechanism finds possible precedent in the oft observed elimination of carbon dioxide from metallocarboxylic acids (hydroxycarbonyls),[31] i.e., eq 4.

$$L_nMCOOH \rightarrow L_nMH + CO_2 \quad (4)$$

Ketene is isoelectronic with carbon dioxide, and we have observed the extremely facile conversion of $[Ru(COOH)(CO)_2(triphos)]^+$ to $[RuH(CO)_2(triphos)]^+$.[32] While the mechanism of reactions of the type (4) are currently a controversial topic, *proton* dissociation may be involved,[31] followed first by dissociation of carbon dioxide and then by protonation of the metal. While this hypothesis is attractive because it does not require a vacant site on the metal, there are no precedents for acetyl compounds having the required acidity. In fact we note that meridional tris(phosphine)acetylruthenium complexes are quite robust,[33] in apparent contrast to the situation with the triphos system. We have already noted above, however, that a coordinated hydride trans to phosphorus can be labilized sufficiently that it becomes very acidic, and it may be that an acetyl group in a similar situation is also labilized in an unusual manner.

Although the elimination of ketenes from acyl complexes has not been reported previously, there have been two reports of the reverse reaction, the "insertions" of ketenes into metal–hydrogen bonds,[34] i.e., eq 5 and 6. While the

$$HMn(CO)_5 + CH_2{=}C{=}O \rightarrow MeCOMn(CO)_5 \quad (5)$$

$$HCo(CO)_4 + RR'C{=}C{=}O \rightarrow RR'CHCOCo(CO)_4 \quad (6)$$

$$R, R' = H, Me, Et$$

mechanism of these reactions is not known, we have found that similar "insertion" reactions of metal hydrides with conjugated dienes involve hydrogen atom abstraction from the metal by the diene to form metal and substituted allyl radicals. Geminate recombination of the intermediate radical pair, evidenced by observation of CIDNP effects, results in metal–carbon bond formation,[35] i.e., eq 7.

$$HMn(CO)_5 + CH_2{=}CHCH{=}CH_2 \rightarrow [MeCH{=}CHCH_2{\cdot},{\cdot}Mn(CO)_5] \rightarrow MeCH{=}CHCH_2Mn(CO)_5 \quad (7)$$

Similar processes may be involved in the corresponding ketene "insertion" and, invoking the principle of microscopic reversibility, in the ketene elimination reaction reported here. Research into the matter continues.

General Comments on the IR and NMR Spectra. The IR spectra of the dicarbonyl complexes exhibit two carbonyl stretching bands, of which the higher frequency band (symmetric stretch) is always of slightly greater intensity. The intensity ratios of most compounds are such that the bond angles between pairs of carbonyl groups are approximately 75–80°.[36] The monocarbonyl compounds, of course, exhibit only a single carbonyl stretching mode.

The methyl protons of the triphos always appear as slightly broadened quartets in the ^1H NMR spectra, a result of spin–spin coupling to the three phosphorus atoms. The observed broadening is probably a result of the nonequivalence of the phosphorus atoms, although the quartet patterns seem to be largely independent of the nature of the remaining ligands. Interestingly, the chemical shifts of the methyl groups exhibit greater dependence on the nature of the counterion than on the nature of the other ligands. There is an upfield shift of about 0.2 ppm on replacement of halide ion by hexafluorophosphate for several of the complex cations, suggesting that ion pairing in solution occurs at the "backside" of the coordinated triphos.

The $^{13}C\{^1H\}$ NMR resonances of the triphos carbon atoms were assigned largely on the basis of the spin–spin coupling patterns to the phosphorus atoms. Both the methyl and the quaternary carbon atoms appeared as quartets, and distinction was made in the case of the methyl complex $[RuMe(CO)_2(triphos)]^+$ by means of the SEFT (spin–echo Fourier transform) pulse sequence.[37] The similarity of the coupling patterns of these two resonances in the methyl and the other compounds formed the basis for the assignments of Table III. The methylene carbon resonances were very complicated, both because of long-(25–30 Hz) and short-range (4–5 Hz) coupling to phosphorus and because of the two possible methylene carbon environments for each compound. The carbonyl carbon resonances were complicated for much the same reasons; detailed elucidation and rationalization of the spectra, complete with determinations of the absolute signs of the carbon–phosphorus coupling constants, will be published elsewhere.

The $^{31}P\{^1H\}$ NMR spectra generally exhibit a doublet (2 P) and a triplet (1 P), consistent with the formulations. The chemical shifts are strongly dependent on the nature of the ligand trans to phosphorus, with there being a roughly inverse relationship between the phosphorus chemical shifts and the positions of the trans ligands in the trans influence series.[10] Thus methyl and hydride cause a trans phosphorus atom to resonate upfield relative to a phosphorus trans to carbon monoxide, while a phosphorus trans to halide resonates downfield relative to a phosphorus trans to carbon monoxide. This type of correlation has been noted previously.[38]

Acknowledgment. We thank the Natural Sciences and Engineering Research Council, Queen's University, and the NATO Science Fellowship Program for financial support, Johnson Matthey Ltd., and the International Nickel Co. of Canada for loans of ruthenium chloride.

Registry No. I, 37843-33-7; II, 37843-37-1; III, 99299-45-3; IV, 37843-35-9; V, 37843-38-2; VI, 99299-46-4; VII·PF_6, 99299-48-6; VII·I, 99299-61-3; VIII·PF_6, 99341-39-6; VIII·Cl, 95123-22-1; IX·PF_6, 99299-50-0; IX·I, 99299-59-9; X·PF_6, 99299-52-2; X·I, 99299-60-2; XI, 99299-54-4; XII·PF_6, 99299-56-6; XII·Br, 99299-62-4; XIII, 99299-58-8; MeI, 74-88-4; EtI, 75-03-6; $PhCH_2Br$, 100-39-0; C_3H_5Br, 106-95-6; $CHCl_3$ CH_3COCl, 75-36-5; $CHCl_3$, 67-66-3; (1-bromoethyl)benzene, 585-71-7.

(31) Lilga, M. A.; Ibers, J. A. *Organometallics* **1985**, *4*, 590 and references therein.
(32) Hommeltoft, S. I.; Baird, M. C., unpublished results.
(33) Barnard, C. F. J.; Daniels, A. J.; Mawby, R. J. *J. Chem. Soc., Dalton Trans.* **1979**, 1331.
(34) (a) Lindner, E.; Berke, H. *Z. Naturforsch., A* **1974**, *29A*, 275. (b) Ungváry, F. *J. Chem. Soc., Chem. Commun.* **1984**, 824.
(35) Thomas, M. J.; Shackleton, T. A.; Wright, S. C.; Colpa, J. P.; Baird, M. C., submitted for publication.
(36) Cotton, F. A.; Wilkinson, G. "Advanced Inorganic Chemistry", 4th ed.; Wiley-Interscience: New York, 1980; pp 1073–1076.
(37) Benn, R.; Gunther, H. *Angew Chem., Int. Ed. Engl.* **1983**, *22*, 350.
(38) (a) Meek, D. W.; Mazanec, T. J. *Acc. Chem. Res.* **1981**, *14*, 266. (b) Pregosin, P. S.; Kunz, R. W. "^{31}P and ^{13}C NMR of Transition Metal Phosphine Complexes"; Spinger-Verlag: New York, 1979.

Reactions of a Cationic Bridging Methylidyne Complex with Activated Alkenes

Charles P. Casey,* Mark A. Gohdes, and Mark W. Meszaros

McElvain Laboratories of Organic Chemistry, Department of Chemistry, University of Wisconsin—Madison, Madison, Wisconsin 53706

Received June 13, 1985

Reaction of $[(C_5H_5)_2(CO)_2Fe_2(\mu\text{-}CO)(\mu\text{-}CH)]^+PF_6^-$ (1) with allyltriphenyltin or allyltrimethylsilane produced $(C_5H_5)_2(CO)_2Fe_2(\mu\text{-}CO)(\mu\text{-}CHCH_2CH{=}CH_2)$ (2) in 34% and 51% yields. The trisubstituted allylsilane 4-(trimethylsilyl)-2-methyl-2-butene reacted with 1 to produce $[(C_5H_5)_2(CO)_2Fe_2(\mu\text{-}CO)(\mu\text{-}CC(CH_3)_2CH_2CH_2Si(CH_3)_3)]^+PF_6^-$ (3) in 54% yield. The reaction of 1 with 2-(dimethylphenylsilyl)propene (4) gave a mixture of products which was deprotonated by trimethylamine to produce $(C_5H_5)_2(CO)_2Fe_2(\mu\text{-}CO)[\mu\text{-}C{=}CHCH(CH_3)Si(CH_3)_2C_6H_5]$ (5). The reaction of 1 with the enol silyl ether $CH_2{=}C(C_6H_5)(OSi(CH_3)_3)$ (6) produced $(C_5H_5)_2(CO)_2Fe_2(\mu\text{-}CO)(\mu\text{-}CHCH_2C(O)C_6H_5)$ in 34% yield. 1 also reacted with vinyl acetate to give $[(C_5H_5)_2(CO)_2Fe_2(\mu\text{-}CO)(trans\text{-}\mu\text{-}\eta^1,\eta^2\text{-}CH{=}CHCH_2OC(O)CH_3)]^+PF_6^-$ (8) in 71% yield and small amounts of $(C_5H_5)_2(CO)_2Fe_2(\mu\text{-}CO)(\mu\text{-}CHCH_2CH(OC(O)CH_3)_2)$ (9).

Introduction

The bridging methylidyne complex 1 reacts with simple alkenes by two different pathways. For ethylene and most monosubstituted alkenes, 1 adds its C–H bond across the carbon–carbon double bond to form μ-alkylidyne complexes in a reaction we have named hydrocarbation.[1] For some alkenes such as 1-methylcyclohexene, *trans*-stilbene, and 1,1-diphenylethylene which are more sterically crowded and are capable of forming stabilized carbocation intermediates, we have observed the formation of bridging alkenyl complexes.[2] The alkenyl complexes are proposed to arise from electrophilic addition of 1 to the alkene to produce a carbocation that then undergoes a 1,2-hydride or alkyl migration to produce a bridging alkenyl complex.

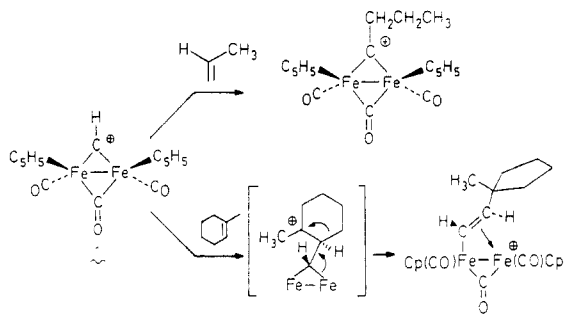

Here we report the reaction of methylidyne complex 1 with functionalized alkenes bearing silicon, tin, and oxygen substituents capable of stabilizing cationic intermediates.

Results and Discussion

Reactions of 1 with an Allylstannane and Allylsilanes. Allyltriphenyltin is very reactive toward electrophiles.[3] Reaction of methylidyne complex 1 with allyltriphenyltin occurred rapidly at −78 °C as indicated by a color change from red to dark red. The neutral bridging but-3-enylidene complex 2 was isolated in 34% yield after chromatography to remove tin compounds. The structure of 2 was established by spectroscopy. The proton on the bridging alkylidene carbon gives rise to a triplet (J = 8.2 Hz) at δ 11.6 in the ^{1}H NMR. 2 is the product resulting from transfer of the allyl group to the methylidyne carbon.

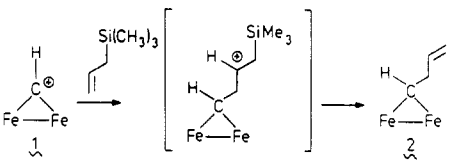

Allyltrimethylsilane also reacts with 1 to produce the same bridging but-3-enylidene complex 2. This is the preferred method for synthesis of 2 because of the higher yield obtained (51%) and because 2 can be purified without resorting to column chromatography.

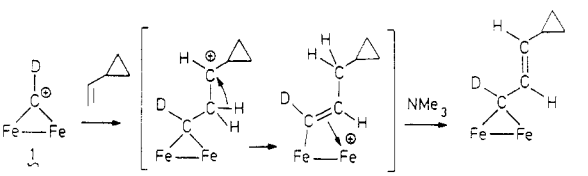

Ordinarily monosubstituted alkenes react with 1 to add the C–H bond across the carbon–carbon double bond of the alkene in a hydrocarbation reaction.[1,2] The only nonheteroatom-substituted alkene to react with 1 by an electrophilic addition pathway is vinylcyclopropane.[4] This is undoubtedly related to the high stability of the cyclopropylcarbinyl cation intermediate. Carbocations are also greatly stabilized by β-tin or β-silicon substituents.[5] The formation of 2 is proposed to occur via electrophilic attack of 1 on the terminal allyl carbon to give a carbocation stabilized by the β-group IV (14)[9] atom. Nucleophilic attack at tin or silicon then produces 2.

A different reaction pathway was seen in the reaction of 1 with the trisubstituted allylsilane 4-(trimethylsilyl)-2-methyl-2-butene. C–H addition across the carbon–carbon double bond produced the cationic bridging alkylidyne complex 3 in 54% yield. In this case, the trimethylsilyl group was retained in the product. The bridging carbyne carbon of 3 gives rise to a characteristically far downfield ^{13}C resonance at δ 522.9. The closest analogy to this reaction is the addition of 1 to tetramethylethylene.[1] In both these cases, even though a tertiary cation or a β-silyl-stabilized cation is a possible

(1) Casey, C. P.; Fagan, P. J. *J. Am. Chem. Soc.* **1982**, *104*, 4950.
(2) Casey, C. P.; Fagan, P. J.; Miles, W. H.; Marder, S. R. *J. Mol. Catal.* **1983**, *21*, 173.
(3) (a) Pereyre, M.; Quintard, J. *Pure Appl. Chem.* **1981**, *53*, 2401. (b) Mangravite, J. *J. Organomet. Chemistry Libr.* **1979**, *7*, 45.
(4) Casey, C. P.; Gohdes, M. A.; Meszaros, M. W., unpublished observations.
(5) (a) Chan, T. H.; Fleming, I. *Synthesis* **1979**, *79*, 761–786. (b) Wierschke, S. G.; Chandrasekhar, J.; Jorgensen, W. L. *J. Am. Chem. Soc.* **1985**, *107*, 1496–1500.

0276-7333/86/2305-0196$01.50/0

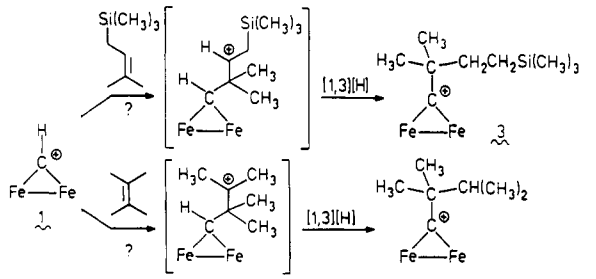

intermediate, only the formal product of C–H addition was observed. In these two cases, we cannot exclude the possibility that a cationic intermediate is formed which then undergoes a 1,3-hydride shift to produce the observed products. The regiochemistry seen in the formation of **3** indicates that electrophilic attack occurs to generate an electropositive center at a secondary carbon β to silicon rather than at the tertiary carbon. Similar regioselectivity is seen in the reaction of 4-(trimethylsilyl)-2-methyl-2-butene with other electrophilic reagents.[5a]

Reaction of 1 with a Vinylsilane. The reaction of methylidyne complex **1** with 2-(dimethylphenylsilyl)-propene (**4**) gave a deep red solution which was treated with trimethylamine. A 3:1 mixture of diastereomeric μ-alkenylidene complexes **5a**/**5b** was obtained in 56% yield after column chromatography. The structure of these μ-alkenylidene complexes was readily determined by ^1H and ^{13}C NMR. For **5a**, the vinyl hydrogen appears as a doublet at δ 7.03. Four well-resolved resonances for the nonequivalent Cp rings on the two diastereomers were observed as were four resonances for the diastereotopic silyl methyl groups of the two diastereomers.

The regiochemistry of the addition of **1** to vinylsilane **4** is the opposite to that normally seen for electrophilic additions to vinylsilanes.[5] Normally, the silicon substituent directs the electrophile to the carbon bound to the silicon since this leads to a cation strongly stabilized by a β-silicon substituent. In the present case, the steric factors favoring addition to the least substituted carbon of **4** are apparently greater than the difference in energy between the normally observed β-silicon-stabilized cation and the secondary α-silicon substituted cation seen here.

When the cationic products of the reaction of **1** and **4** were isolated directly by evaporation of solvent and crystallization from acetone–ether, a complex mixture of materials was seen by ^1H NMR. Interestingly, two doublets were seen at δ 11.96 (J = 12 Hz) and 11.49 (J = 11 Hz) which indicate the likely presence of two diastereomers of the bridging vinyl complex B. When the isolated bridging alkenylidene complexes **5a** and **5b** were treated with $HBF_4{\cdot}Et_2O$, the ^1H NMR spectrum was again very complex but the signals attributed to the bridging vinyl complex B were again observed. Our tentative interpretation is that the mixture of cationic materials consists of two diastereomers of B and μ-alkylidyne complex A which are in equilibrium. Deprotonation with trimethylamine produces the μ-alkenylidene complexes **5a** and **5b**; when **5a** and **5b** are reprotonated, an equilibrium mixture of A and B is obtained.

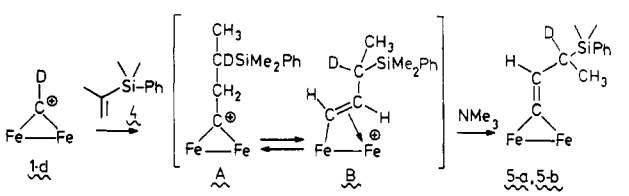

Previously we have documented the equilibration of alkylidyne and μ-alkenyl complexes.[2,6] The equilibration of A and B is apparently much faster than for the μ-pentylidyne to μ-pent-1-enyl rearrangement. The silicon substituent in A is β to the developing positive carbon center in B and may accelerate the rearrangement.

There are two possible ways that the equilibrating mixture of A and B might be formed. Hydrocarbation might initially produce A which then equilibrates with B. Alternatively, B might be the initially formed product of an electrophilic addition followed by a 1,2-hydride shift. To distinguish between the possibilities, the reaction of **1**-*d* with **4** was carried out and the deprotonated μ-alkenylidene product **5** was examined by ^1H NMR. The absence of the resonance of δ 2.5 indicates the presence of a $-CD(CH_3)Si(CH_3)_2C_6H_5$ unit. Similarly, the presence of this unit leads to singlets at δ 7.0 for C=C*H*CD and at δ 1.3 and 1.2 for the $CDCH_3Si$ group of the two diastereomers of **5**. This labeling experiment establishes that a net 1,2 addition of the C–H bond of **1** across the carbon–carbon double bond initially produces A which then equilibrates with the bridging vinyl complex B.

Reaction of 1 with an Enol Silyl Ether and Vinyl Acetate. Enol silyl ethers are electron-rich alkenes that are readily attacked by electrophiles. Reaction of **1** with the trimethylsilyl enol ether of acetophenone, **6**, gave the bridging 3-oxo-3-phenylpropylidene complex **7** in 34% yield. The proton on the bridging carbene carbon of **7** appears as a triplet at δ 11.65 in the ^1H NMR spectrum. The aryl ketone gives rise to a band at 1672 cm^{-1} in the infrared spectrum. The formation of **7** is best explained by electrophilic addition of **1** to the vinyl ether to give an oxygen-stabilized carbocation intermediate. Loss of the trimethylsilyl group to a nucleophilic species produces the observed ketone product **7**.

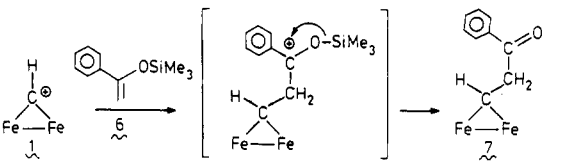

Reaction of **1** with vinyl acetate gave the cationic bridging alkenyl complex **8** in 71% yield. The protons on the bridging alkenyl group appear as a broad doublet (J = 10 Hz) at δ 12.3 and a multiplet at δ 3.6 in the ^1H NMR. In addition small variable yields of the neutral diacetate complex **9** were observed.

The formation of **8** can be explained by electrophilic addition of **1** to vinyl acetate to give an oxygen stabilized carbocation intermediate. A 1,2-hydride migration leads to formation of the bridging vinyl complex **8**. Reaction of the intermediate with an acetate donor leads to **9**. In the

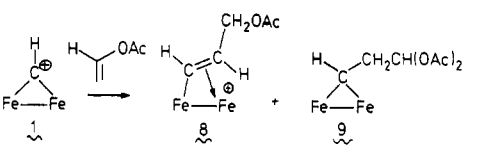

enol silyl ether reaction, the facile loss of the trimethylsilyl group led to formation of ketone **7** in a reaction that was faster than a 1,2-hydride shift. For vinyl acetate, the loss of an acylium species to give an aldehyde is much too slow to compete with a 1,2-hydride shift.

Experimental Section

General Data ^1H NMR spectra were obtained on a Brucker

(6) Casey, C. P.; Marder, S. R.; Fagan, P. J. *J. Am. Chem. Soc.* **1983**, *105*, 7197.

WP270 spectrometer. ^{13}C NMR spectra of samples containing 0.07 M $Cr(acac)_3$ as a shiftless relaxation reagent were obtained on a JEOL FX200 spectrometer at 50.1 MHz or Bruker AM500 spectrometer at 126 MHz. CD_3NO_2 was dried over P_2O_5 and acetone-d_6 was dried over molecular sieves or B_2O_3. IR spectra were recorded on a Beckman 4230 infrared spectrometer calibrated with polystyrene film. Mass spectra were obtained on an AIE-MS-902 or Kratos MS-80 mass spectrometer. Elemental analysis were performed by Galbraith Microanalytical Labs.

Air-sensitive compounds were handled by using standard Schlenk procedures and glovebox manipulations. Diethyl ether, THF, and hexane, were distilled from purple solutions of sodium and benzophenone. CH_2Cl_2 was distilled from CaH_2 and acetone was dried over molecular sieves or B_2O_3.

$[(C_5H_5)_2(CO)_2Fe_2(\mu\text{-}CO)(\mu\text{-}CHCH_2CH{=}CH_2)]$ (2) from Allyltriphenyltin. Methylene chloride (25 mL) was condensed onto solid allyltriphenyltin[7] (0.220 g, 0.56 mmol) and **1** (0.195 g, 0.40 mmol) at −78 °C. The reaction mixture was warmed to ambient temperature, and solvent was evaporated under vacuum. The residue was extracted with diethyl ether (15 mL). The ether extract was filtered, evaporated, and dried under vacuum. Column chromatography (alumina, 1:1 CH_2Cl_2/hexane) was employed to separate excess allyltriphenyltin and gave pure orange-red crystalline **2** (0.045 g, 34%).

$[(C_5H_5)_2(CO)_2Fe_2(\mu\text{-}CO)(\mu\text{-}CHCH_2CH{=}CH_2)]$ (2) from Allyltrimethylsilane. Allyltrimethylsilane (0.092 atm, 234 mL, 0.753 mmol, Aldrich) was condensed into a stirred slurry of **1** (0.182 g, 0.38 mmol) in CH_2Cl_2 (25 mL) at −78 °C, and the reaction mixture was warmed to ambient temperature. Solvent was evaporated under vacuum, and the residue was extracted with diethyl ether (15 mL). The ether extract was filtered and evaporated to give orange-red crystalline **2** (0.073 g, 51%): ^1H NMR (acetone-d_6, 200 MHz) δ 11.63 (t, J = 8.2 Hz, μ-CH), 6.34 (ddt, J = 17.0, 9.2, 7.2 Hz, =CH), 5.11 (dq, J = 17, 1 Hz, =C*H*H), 5.0 (dq, J = 9.2, 1 Hz, =CH*H*), 3.70 (ddt, J = 8.2, 7.2, 1 Hz, CH_2); ^{13}C NMR (acetone-d_6) δ 272.8 (μ-CO), 215.5 (CO), 174.5 (d, J = 136 Hz, μ-C), 143.5 (d, J = 150 Hz, =CH), 112.8 (t, J = 155 Hz, $=CH_2$), 88.3 (d, J = 180 Hz, C_5H_5), 61.1 (t, J = 126 Hz, CH_2); IR (CH_2Cl_2) 1979 (s), 1940 (w), 1778 (m), 1640 (w) cm^{-1}; HRMS calcd for $C_{17}H_{16}Fe_2O_3$ 379.9793, found 379.9798.

$[(C_5H_5)_2(CO)_2Fe_2(\mu\text{-}CO)(\mu\text{-}CC(CH_3)_2CH_2CH_2Si(CH_3)_3)]^+PF_6^-$ (3). 4-(Trimethylsilyl)-2-methyl-2-butene (0.075 mL, 0.056 g, 0.40 mmol, Petrarch) was injected into a stirred suspension of **1** (0.150 g, 0.31 mmol) in CH_2Cl_2 (25 mL) at −78 °C. The residue was dissolved in acetone (5 mL) and filtered. The addition of diethyl ether (15 mL) led to precipitation of light orange-red crystalline **3** (0.104 g, 54%): ^1H NMR (acetone-d_6, 270 MHz) δ 5.79 (s, 10 H, C_5H_5) 2.23 (AA′XX′, J_{H^3} = 10, 14 Hz, J_{H^2} = 4 Hz, C*H*$_2$CH$_2$Si), 1.88 (s, 6 H, CH_3), 0.87 (AA′XX′, J_{H^3} = 10, 14 Hz, J_{H^2} = 4 Hz, CH_2CH_2Si), 0.06 (s, 9 H, $SiCH_3$); ^{13}C NMR (CD_3NO_2) δ 522.9 (μ-C), 252.5 (μ-CO), 208.3 (CO), 93.6 (d, J = 183.5 Hz, C_5H_5), 79.0 (μ-C*C*) 40.3 (t, J = 127.3 Hz, *C*H$_2$CH$_2$Si), 29.3 (q, J = 134.8 Hz, C(*C*H$_3$)$_2$), 12.5 (t, J = 120.7 Hz, CH_2Si), −1.9 (q, J = 120.5 Hz, Si(*C*H$_3$)$_3$); IR (CH_2Cl_2) 2021 (s), 2002 (w), 1855 (m) cm^{-1}.

Anal. Calcd for $C_{22}H_{29}F_6Fe_2O_3PSi$: C, 42.20; H, 4.67. Found: C, 42.21; H, 4.48.

Dimethylphenylprop-2-enylsilane (4). Chlorodimethylphenylsilane (9.70 mL, 58.6 mmol, Petrarch) and the Grignard reagent prepared from 2-bromopropene (10.3 mL, 116 mmol) and magnesium turnings (1.89 g, 78 mmol) in THF (130 mL) were refluxed overnight. The reaction mixture was quenched with a saturated aqueous solution of NH_4Cl (80 mL) and the organic layer separated. The aqueous layer was neutralized and extracted with THF (7 mL). The combined organic layers were dried ($MgSO_4$) and vacuum distilled to give **4** as a clear liquid (5.65 g, 55%): bp 35 °C (0.1 mm); ^1H NMR ($CDCl_3$, 270 MHz) δ 7.65 (m, 2 H), 7.45 (m, 3 H), 5.78 (dq, J = 3.6, 1.5 Hz, =C*H*H), 5.45 (dq, J = 3.6, 1.2 Hz, =CH*H*), 1.93 (dd, J = 1.5, 1.2 Hz, CH_3), 0.48 (s, 6 H, $SiCH_3$); ^{13}C NMR ($CDCl_3$) δ 146.1, 138.0 (ipso C_6H_5, SiC=), 133.9 (d, J = 158 Hz, *o*- or *m*-C_6H_5), 128.9 (d, J = 158 Hz, *p*-C_6H_5), 127.7 (d, J = 155 Hz, *o*- or *m*-C_6H_5), 126.5 (t, J = 152 Hz, $=CH_2$), 22.5 (q, J = 126 Hz, CH_3), −3.5 (q, J = 121 Hz, $SiCH_3$); IR (neat) 1620 (m), 1430 (s); 1255 (s), 1130 (s), 960 (m) cm^{-1}; HRMS calcd for $C_{11}H_{16}Si$ 176.1017, found 176.1018.

$(C_5H_5)_2(CO)_2Fe_2(\mu\text{-}CO)(\mu\text{-}C{=}CHCH(CH_3)Si(CH_3)_2C_6H_5)$ (5). **4** (0.220 mL, 0.179 g, 1.01 mmol) was injected into a stirred suspension of **1** (0.372 g, 0.77 mmol) in CH_2Cl_2 (25 mL) at −78 °C, and the reaction mixture was warmed to ambient temperature. After 45 min, trimethylamine (0.66 atm, 235 mL, 6.27 mmol) was condensed into the reaction mixture at −78 °C. The solvent was evaporated under vacuum at ambient temperature. The residue was extracted with diethyl ether (15 mL). The ether extract was filtered, evaporated, and column chromatographed (alumina, 1:1 CH_2Cl_2/hexane) to give deep red crystals of **5** (0.220 g, 56%) as a 2:1 mixture of two diastereomers: ^1H NMR (acetone-d_6, 200 MHz) major isomer, δ 7.8–7.3 (m, 5 H, C_6H_5), 7.03 (d, J = 11.0 Hz, =CH), 4.86, 4.64 (10 H, C_5H_5), 2.51 (dq, J = 11.0, 7.2 Hz, CHSi), 1.18 (d, J = 7.2 Hz, CH_3), 0.50, 0.49 (s, $Si(CH_3)_2$), minor isomer, δ 4.98, 4.88 (10 H, C_5H_5), 1.33 (d, J = 7.2 Hz, CH_3), 0.33, 0.25 (s, $Si(CH_3)_2$); ^{13}C NMR (CD_3NO_2) major isomer, δ 274.4, 265.5 (μ-C, μ-CO), 213.9 (CO), 143.9 (d, J = 148 Hz, =CH), 140.8 (s, ipso-C_6H_5), 135.7, 130.3, 129.0 (three d, J = 156 Hz, C_6H_5), 89.1, 88.3 (two d, J = 179 Hz, C_5H_5), 32.5 (d, J = 121 Hz, CH), 17.9 (q, J = 125 Hz, CH_3), −4.5 (q, J = 113 Hz, $Si(CH_3)_2$), minor isomer, δ 266.3, 89.5, 18.5, −3.0; IR (CH_2Cl_2) 1991 (s), 1954 (w), 1785 (m), 1594 (w) cm^{-1}; HRMS calcd for $C_{25}H_{26}Fe_2O_3Si$ 514.0342, found 514.0349.

Similarly, reaction of a solution of **4** (40 μL, 0.25 mmol) with 1-*d* (90 mg, 0.186 mmol) followed by addition of NMe_3 (0.66 atm, 235 mL, 6.27 mmol) gave **5a**-*d* and **5b**-*d* (47 mg, 49%): ^1H NMR (acetone-d_6, 270 MHz) major isomer, δ 7.8–7.3 (m, C_6H_5), 7.03 (s, =CH), 4.86, 4.64 (C_5H_5), 1.33 (s, CH_3), 0.50, 0.49 (s, $Si(CH_3)_2$), minor isomer, δ 4.97, 4.88 (C_5H_5), 1.33 (s, CH_3), 0.34, 0.27 (s, $Si(CH_3)_2$); $^2H\{^1H\}$ NMR (acetone) δ 2.45.

$[(C_5H_5)_2(CO)_2Fe_2(\mu\text{-}CO)(\mu\text{-}CHCH_2COC_6H_5)]$ (7). **6**[8] (0.069 mL, 0.065 g, 0.33 mmol) was injected into a stirred suspension of **1** (0.108 g, 0.22 mmol) in CH_2Cl_2 (25 mL) at −78 °C. The reaction mixture was warmed to ambient temperature, and solvent was evaporated under vacuum. The residue was extracted with diethyl ether (15 mL). The ether extract was filtered, evaporated, and column chromatographed (alumina, 1:1 CH_2Cl_2/hexane) to give dark red crystals of **7** (0.045 g, 34%): ^1H NMR (acetone-d_6, 200 MHz) δ 11.65 (t, J = 8.2 Hz, μ-CH), 8.23–7.50 (m, 5 H, C_6H_5), 4.83 (s, 10 H, C_5H_5), 4.75 (d, J = 8.2 Hz, CH_2); ^{13}C NMR (CD_3NO_2) δ 274.7 (μ-CO), 214.9 (CO), 201.2 (COPh), 164.8 (d, J = 135 Hz, μ-CH), 138.9 (ipso-C_6H_5), 134.0 (d, J = 165 Hz, C_6H_5), 130.0 (d, J = 155 Hz, C_6H_5), 88.9 (d, J = 179 Hz, C_5H_5), 65.0 (t, J = 132 Hz, CH_2); IR (CH_2Cl_2) 1970 (s), 1932 (w), 1770 (m), 1672 (w) cm^{-1}; HRMS calcd for M − CO $C_{21}H_{18}Fe_2O_3$ 429.9949, found 429.9938.

$[(C_5H_5)_2(CO)_2Fe_2(\mu\text{-}CO)(\mu\text{-}trans\text{-}\eta^1,\eta^2\text{-}CH{=}CHCH_2OC(O)CH_3)]^+PF_6^-$ (8) and $(C_5H_5)_2(CO)_2Fe_2(\mu\text{-}CO)[\mu\text{-}CHCH_2CH(OC(O)CH_3)_2]$ (9). Vinyl acetate (0.06 atm, 235 mL, 0.54 mmol, Aldrich) was condensed into a stirred suspension of **1** (0.198 g, 0.41 mmol) in CH_2Cl_2 (70 mL) at −78 °C. The reaction mixture was concentrated to 10 mL by evaporation of solvent at −10 °C under vacuum. Addition of 20 mL of diethyl ether at −10 °C gave a dark brown precipitate and a red solution. **8** (0.165 g, 71%) was isolated as a dark brown solid by filtration. The ether solution was evaporated, and the residue was column chromatographed (alumina, 1:1 CH_2Cl_2/hexane) to give **9** (0.010 g, 5%) as an orange-red oil.

8: ^1H NMR (acetone-d_6) δ 12.3 (d, J = 10 Hz, μ-CH), 5.73 (s, C_5H_5), 4.7 (m, CH_2), 3.6 (m, =CHR), 2.13 (s, CH_3); ^{13}C NMR (CD_3NO_2) δ 237.4 (μ-CO), 211.8 (CO), 176.6 (CO_2), 171.9 (μ-CH=), 91.3 (C_5H_5), 87.2 (=CHR), 69.7 (CH_2), 20.7 (CH_3); IR (KBr) 2020 (s), 1854 (m), 1746 (w) cm^{-1}.

Anal. Calcd for $C_{18}H_{17}F_6Fe_2O_5P$: C, 37.93; H, 3.01. Found: C, 38.07; H, 3.17.

(7) Seyferth, D.; Weiner, M. A. "Organic Syntheses", Wiley: New York, 1973; Coll. Vol. 5, p 452.

(8) Krüger, C. R.; Rochow, E. G. *J. Organomet. Chem.* **1963**, *1*, 476.

(9) In this paper the periodic group notation is in accord with recent actions by IUPAC and ACS nomenclature committees. A and B notation is eliminated because of wide confusion. Groups IA and IIA become groups 1 and 2. The d-transition elements comprise groups 3 through 12, and the p-block elements comprise groups 13 through 18. (Note that the former Roman number designation is preserved in the last digit of the new numbering: e.g., III → 3 and 13.)

9: ^{1}H NMR (acetone-d_6) δ 11.40 (t, J = 8.3 Hz, μ-CH), 7.16 (t, J = 5.4 Hz, $CH(OAc)_2$), 4.87 (s, C_5H_5), 3.47 (dd, J = 8.3, 5.4 Hz, CH_2), 2.13 (s, CH_3); ^{13}C NMR (acetone-d_6, 126 MHz, −40 °C) δ 272.1 (μ-CO), 213.9 (CO), 169.4 (CO_2), 161.3 (μ-CHR), 92.2 ($CH(OAc)_2$), 88.2 (C_5H_5), 57.6 (CH_2), 20.8 (CH_3); IR (CH_2Cl_2) 1981 (s), 1944 (w), 1779 (m), 1761 (m) cm^{-1}; HRMS calcd for $C_{20}H_{20}O_7Fe_2$ 483.9901, found 483.9901.

Acknowledgment. Support from the National Science Foundation is gratefully acknowledged.

Conversion of Diiron Bridging Alkenyl Complexes to Monoiron Alkenyl Compounds and to Alkenes

Charles P. Casey,* Seth R. Marder, Robert E. Colborn, and Patricia A. Goodson

Department of Chemistry, University of Wisconsin, Madison, Wisconsin 53706

Received July 11, 1985

The reaction of the diiron μ-pentenyl complex $[(C_5H_5)_2(CO)_2Fe_2(\mu\text{-}CO)(\mu\text{-}\eta^1,\eta^2\text{-}(E)\text{-}CH{=}CHCH_2CH_2CH_3)]^+PF_6^-$ (**5**) with CH_3CN produces the monoiron pentenyl compound $(C_5H_5)(CO)_2Fe\text{-}((E)\text{-}CH{=}CHCH_2CH_2CH_3)$ (**10**) in 67% yield. Similarly, the μ-vinyl complex $[(C_5H_5)_2(CO)_2Fe_2(\mu\text{-}CO)(\mu\text{-}\eta^1,\eta^2\text{-}CH{=}CH_2)]^+PF_6^-$ (**8b**) reacts with CH_3CN to produce $(C_5H_5)(CO)_2FeCH{=}CH_2$ (**9**) in 58% yield and $(C_5H_5)(CO)Fe(CH_3CN)_2^+PF_6^-$ (**11**) in 54% yield. The kinetics of the reactions of **5** and of **8b** with CH_3CN are first order in both diiron complex and CH_3CN. The 100-fold larger second-order rate constant for unsubstituted μ-vinyl complex **8b** relative to μ-pentenyl complex **5** can best be explained by rate-determining attack of CH_3CN on the μ-alkenyl complexes. μ-Alkenyl diiron complexes **5** and **8b** were also converted to monoiron alkenyl compounds **10** (56% yield) and **9** (61% yield) by treatment with NaI and CO in acetone. Complete cleavage of the μ-alkenyl group from iron was achieved by treatment with LiI, CO, and HBF_4; with these conditions, 1-pentene was obtained from **5** in 72% yield and $CH_2{=}CHCH(C_6H_4\text{-}p\text{-}CH_3)_2$ (**20**) was obtained in 48% yield from $[(C_5H_5)_2(CO)_2Fe_2(\mu\text{-}CO)(\mu\text{-}\eta^1,\eta^2\text{-}(E)\text{-}CH{=}CHCH(C_6H_4\text{-}p\text{-}CH_3)_2)]^+PF_6^-$ (**18**).

Introduction

The reactions of the diiron methylidyne complex $[(C_5H_5)_2(CO)_2Fe_2(\mu\text{-}CO)(\mu\text{-}CH)]^+PF_6^-$ (**1**)[1] with certain alkenes such as 1-methylcyclohexene and *trans*-stilbene yield new μ-alkenyl complexes **2** and **3**, respectively. These reactions proceed via initial electrophilic attack of **1** on the carbon–carbon double bond followed by carbocation rearrangement.[2]

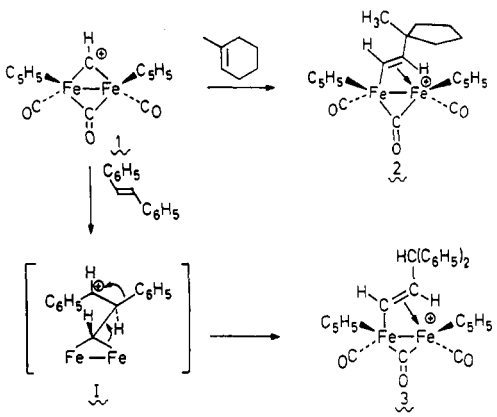

Most monosubstituted alkenes however react via a hydrocarbation[3] pathway in which the C–H bond of **1** is added across the carbon–carbon double bond of the alkene. For example, **1** reacts with 1-butene to yield the pentylidyne complex $[(C_5H_5)_2(CO)_2Fe_2(\mu\text{-}CO)(\mu\text{-}C(CH_2)_3CH_3)]^+PF_6^-$ (**4**).[4] Upon heating at 88 °C in the solid state, alkylidyne complexes such as **4** cleanly rearrange to μ-alkenyl complexes such as $[(C_5H_5)_2(CO)_2Fe_2(\mu\text{-}CO)(\mu\text{-}\eta^1,\eta^2\text{-}(E)\text{-}CH{=}CHCH_2CH_2CH_3)]^+PF_6^-$ (**5**).[5] Several 1,2-dialkyl-substituted alkenes such as cyclohexene react with **1** via hydrocarbation[6] to give alkylidyne complexes **6** which then equilibrate with the related μ-alkenyl complexes **7**.

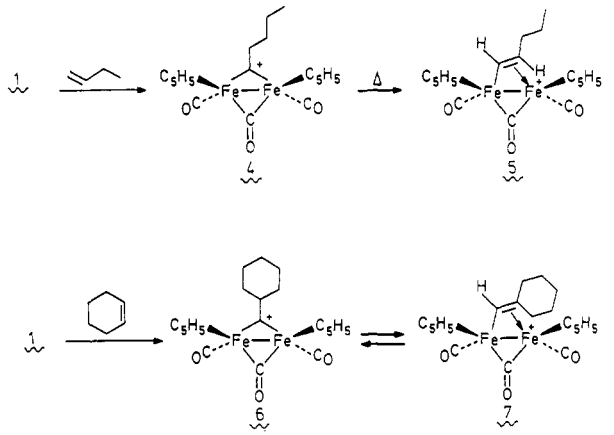

The reaction of **1** with most alkenes can lead to μ-alkenyl complexes either directly or indirectly via isomerization. Therefore, it became important to examine the chemistry of μ-alkenyl complexes with the aim of releasing the organic moiety in a synthetically useful manner. Many new dinuclear complexes with bridging organic groups have been synthesized by reaction of metal carbene,[7] carbyne,[8]

(1) Casey, C. P.; Fagan, P. J.; Miles, W. H. *J. Am. Chem. Soc.* **1982**, *104*, 1134.
(2) Casey, C. P.; Fagan, P. F.; Miles, W. H.; Marder, S. R. *J. Mol. Catal.* **1983**, *21*, 193.
(3) Casey, C. P.; Fagan, P. J. *J. Am. Che. Soc.* **1982**, *104*, 4950.
(4) Casey, C. P.; Fagan, P. J.; Meszaros, M. W.; Bly, R. K.; Marder, S. R.; Austin, E. A. *J. Am. Chem. Soc.*, manuscript in preparation.
(5) Casey, C. P.; Marder, S. R.; Adams, B. R. *J. Am. Chem. Soc.*, submitted for publication.
(6) Casey, C. P.; Meszaros, M. W.; Marder, S. R.; Fagan, P. J. *J. Am. Chem. Soc.* **1984**, *106*, 3680.

0276-7333/86/2305-0199$01.50/0

9: ^{1}H NMR (acetone-d_6) δ 11.40 (t, J = 8.3 Hz, μ-CH), 7.16 (t, J = 5.4 Hz, $CH(OAc)_2$), 4.87 (s, C_5H_5), 3.47 (dd, J = 8.3, 5.4 Hz, CH_2), 2.13 (s, CH_3); ^{13}C NMR (acetone-d_6, 126 MHz, −40 °C) δ 272.1 (μ-CO), 213.9 (CO), 169.4 (CO_2), 161.3 (μ-CHR), 92.2 ($CH(OAc)_2$), 88.2 (C_5H_5), 57.6 (CH_2), 20.8 (CH_3); IR (CH_2Cl_2) 1981 (s), 1944 (w), 1779 (m), 1761 (m) cm^{-1}; HRMS calcd for $C_{20}H_{20}O_7Fe_2$ 483.9901, found 483.9901.

Acknowledgment. Support from the National Science Foundation is gratefully acknowledged.

Conversion of Diiron Bridging Alkenyl Complexes to Monoiron Alkenyl Compounds and to Alkenes

Charles P. Casey,* Seth R. Marder, Robert E. Colborn, and Patricia A. Goodson

Department of Chemistry, University of Wisconsin, Madison, Wisconsin 53706

Received July 11, 1985

The reaction of the diiron μ-pentenyl complex $[(C_5H_5)_2(CO)_2Fe_2(\mu\text{-}CO)(\mu\text{-}\eta^1,\eta^2\text{-}(E)\text{-}CH{=}CHCH_2CH_2CH_3)]^+PF_6^-$ (**5**) with CH_3CN produces the monoiron pentenyl compound $(C_5H_5)(CO)_2Fe\text{-}((E)\text{-}CH{=}CHCH_2CH_2CH_3)$ (**10**) in 67% yield. Similarly, the μ-vinyl complex $[(C_5H_5)_2(CO)_2Fe_2(\mu\text{-}CO)(\mu\text{-}\eta^1,\eta^2\text{-}CH{=}CH_2)]^+PF_6^-$ (**8b**) reacts with CH_3CN to produce $(C_5H_5)(CO)_2FeCH{=}CH_2$ (**9**) in 58% yield and $(C_5H_5)(CO)Fe(CH_3CN)_2^+PF_6^-$ (**11**) in 54% yield. The kinetics of the reactions of **5** and of **8b** with CH_3CN are first order in both diiron complex and CH_3CN. The 100-fold larger second-order rate constant for unsubstituted μ-vinyl complex **8b** relative to μ-pentenyl complex **5** can best be explained by rate-determining attack of CH_3CN on the μ-alkenyl complexes. μ-Alkenyl diiron complexes **5** and **8b** were also converted to monoiron alkenyl compounds **10** (56% yield) and **9** (61% yield) by treatment with NaI and CO in acetone. Complete cleavage of the μ-alkenyl group from iron was achieved by treatment with LiI, CO, and HBF_4; with these conditions, 1-pentene was obtained from **5** in 72% yield and $CH_2{=}CHCH(C_6H_4\text{-}p\text{-}CH_3)_2$ (**20**) was obtained in 48% yield from $[(C_5H_5)_2(CO)_2Fe_2(\mu\text{-}CO)(\mu\text{-}\eta^1,\eta^2\text{-}(E)\text{-}CH{=}CHCH(C_6H_4\text{-}p\text{-}CH_3)_2)]^+PF_6^-$ (**18**).

Introduction

The reactions of the diiron methylidyne complex $[(C_5H_5)_2(CO)_2Fe_2(\mu\text{-}CO)(\mu\text{-}CH)]^+PF_6^-$ (**1**)[1] with certain alkenes such as 1-methylcyclohexene and *trans*-stilbene yield new μ-alkenyl complexes **2** and **3**, respectively. These reactions proceed via initial electrophilic attack of **1** on the carbon–carbon double bond followed by carbocation rearrangement.[2]

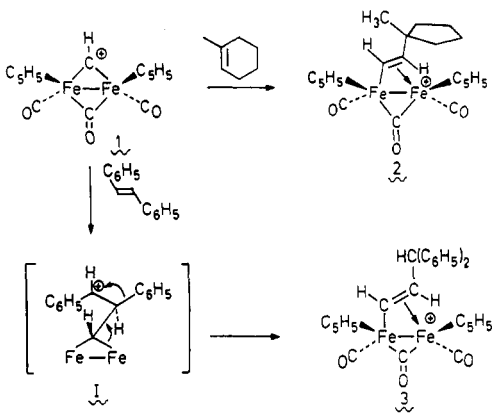

Most monosubstituted alkenes however react via a hydrocarbation[3] pathway in which the C–H bond of **1** is added across the carbon–carbon double bond of the alkene. For example, **1** reacts with 1-butene to yield the pentylidyne complex $[(C_5H_5)_2(CO)_2Fe_2(\mu\text{-}CO)(\mu\text{-}C(CH_2)_3CH_3)]^+PF_6^-$ (**4**).[4] Upon heating at 88 °C in the solid state, alkylidyne complexes such as **4** cleanly rearrange to μ-alkenyl complexes such as $[(C_5H_5)_2(CO)_2Fe_2(\mu\text{-}CO)(\mu\text{-}\eta^1,\eta^2\text{-}(E)\text{-}CH{=}CHCH_2CH_2CH_3)]^+PF_6^-$ (**5**).[5] Several 1,2-dialkyl-substituted alkenes such as cyclohexene react with **1** via hydrocarbation[6] to give alkylidyne complexes **6** which then equilibrate with the related μ-alkenyl complexes **7**.

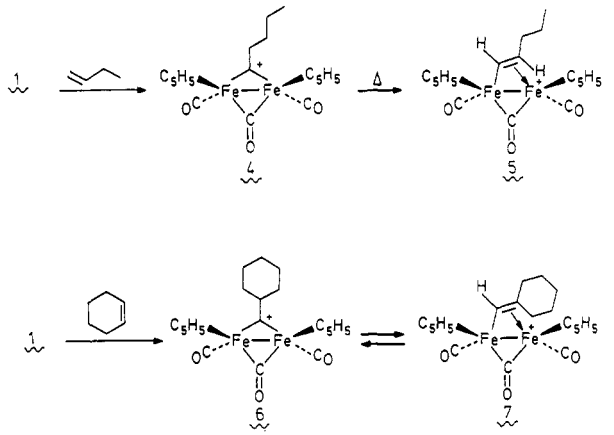

The reaction of **1** with most alkenes can lead to μ-alkenyl complexes either directly or indirectly via isomerization. Therefore, it became important to examine the chemistry of μ-alkenyl complexes with the aim of releasing the organic moiety in a synthetically useful manner. Many new dinuclear complexes with bridging organic groups have been synthesized by reaction of metal carbene,[7] carbyne,[8]

(1) Casey, C. P.; Fagan, P. J.; Miles, W. H. *J. Am. Chem. Soc.* **1982**, *104*, 1134.
(2) Casey, C. P.; Fagan, P. F.; Miles, W. H.; Marder, S. R. *J. Mol. Catal.* **1983**, *21*, 193.
(3) Casey, C. P.; Fagan, P. J. *J. Am. Che. Soc.* **1982**, *104*, 4950.
(4) Casey, C. P.; Fagan, P. J.; Meszaros, M. W.; Bly, R. K.; Marder, S. R.; Austin, E. A. *J. Am. Chem. Soc.*, manuscript in preparation.
(5) Casey, C. P.; Marder, S. R.; Adams, B. R. *J. Am. Chem. Soc.*, submitted for publication.
(6) Casey, C. P.; Meszaros, M. W.; Marder, S. R.; Fagan, P. J. *J. Am. Chem. Soc.* **1984**, *106*, 3680.

0276-7333/86/2305-0199$01.50/0

vinylidene,[9] and vinyl[10] complexes with coordinatively unsaturated organometallic compounds. However, little attention has been devoted to systematically fragmenting dinuclear bridging hydrocarbyl complexes into mononuclear complexes under mild conditions.

Since coordinated alkenes can be displaced from mononuclear iron–alkene complexes by various nucleophiles under mild conditions, we considered using a similar approach on the dinuclear μ-alkenyl system. Pettit's group reported that the vinyl complex $[(C_5H_5)_2(CO)_2Fe_2(\mu\text{-}CO)(\mu\text{-}\eta^1,\eta^2\text{-}CH{=}CH_2)]^+BF_4^-$ (**8a**), reacts with CD_3CN to give a solution with ^1H NMR resonances at δ 7.13 (dd, J = 12.0, 7.0 Hz), 5.80 (dd, J = 7.0, 2.0 Hz), 5.53 (dd, J = 12.0, 2.0 Hz) assigned to vinylic protons and resonances at δ 4.88 and 4.83 assigned to cyclopentadienyl protons. They suggested that CD_3CN displaced the coordinated vinyl moiety to give structure II.[11] However, the reported

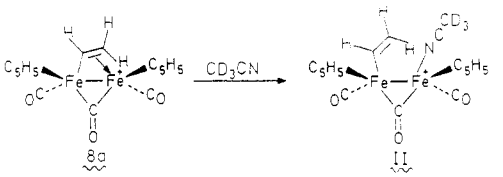

IR spectrum of the solution obtained by dissolving **8a** in CH_3CN has bands at 2040, 2002, and 1960 cm^{-1}; a low-energy bridging CO band expected for II was conspicuously absent. This suggests that the product of the reaction of **8a** with CH_3CN might not be II. Instead, CD_3CN may have caused the μ-alkenyl complex **8** to fragment to a mononuclear $(C_5H_5)Fe(CO)_2CH{=}CH_2$ complex, **9**,[12] and some solvated iron complex. Here we report the results of our investigation of the reactions of diiron μ-alkenyl complexes with CH_3CN and other nucleophilic ligands.

Results

Conversion of Diiron μ-Alkenyl Complexes to Iron Alkenyl Complexes with CH_3CN. The μ-pentenyl complex **5** was stirred in CH_3CN under N_2 at 35 °C for 2.5 days. Then most of the CH_3CN was evaporated under vacuum. Extraction of the residue with hexane and chromatography of the hexane solution gave the monoiron pentenyl complex $(C_5H_5)(CO)_2Fe((E)\text{-}CH{=}CHCH_2CH_2CH_3)$ (**10**) in 67% yield.

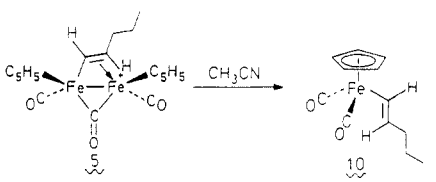

The structure of **10** was established spectroscopically. In the ^1H NMR (C_6D_6) spectrum, the vinylic protons of **10** give rise to resonances at δ 6.40 (d, J = 15.1 Hz) and 5.82 (dt, J = 15.1, 6.7 Hz); the cyclopentadienyl protons appear at δ 4.06. The shifts of the vinyl protons in **10** are substantially different from the shifts of the vinyl protons in the dinuclear complex **5**, in which the vinyl group is complexed to an iron atom. In μ-pentenyl complex **5**, the vinyl protons appear at δ 12.10 (d, J = 10.3 Hz) and 3.62 (m) in $(CD_3)_2CO$. The infrared spectrum of **10** has bands at 2007 (s) and 1960 (s) cm^{-1} in hexane and is similar to the spectra of other iron alkenyl complexes.[12,13]

Attempts to shorten reaction times for the conversion of **5** to **10** by heating the CH_3CN solution to 50 °C yielded substantial amounts of $(C_5H_5)_2Fe$. Because of the thermal instability and air sensitivity of **10**, we have never obtained a highly pure (≥95%) sample.

When the μ-vinyl complex $[(C_5H_5)_2(CO)_2Fe_2(\mu\text{-}CO)(\mu\text{-}\eta^1,\eta^2\text{-}CH{=}CH_2)]^+PF_6^-$ (**8b**) was stirred in CH_3CN, complete conversion to **9** was observed in 1.5 h as indicated by infrared spectroscopy. After workup, **9** was isolated in 58% yield. The major ether insoluble product from the reaction was $(C_5H_5)(CO)Fe(CH_3CN)_2^+PF_6^-$ (**11**)[14] which was isolated in 54% crude yield (contaminated with a small amount of $(C_5H_5)_2Fe$).

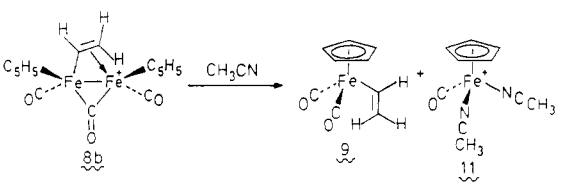

When a mixture of **6** and **7**, obtained from the reaction of **1** with cyclohexene, was reacted with CD_3CN in an NMR tube, conversion to the alkenylidene complex $(C_5H_5)_2(CO)_2Fe_2(\mu\text{-}CO)(\mu\text{-}C{=}\overline{CCH_2CH_2CH_2CH_2CH_2})$ (**12**) was observed by ^1H NMR. Small amounts of several unidentified products were present as evidenced by resonances in the cyclopentadienyl region. There were no singlets in the δ 5.8–8.0 region where the vinyl proton of $(C_5H_5)(CO)_2FeCH{=}\overline{CCH_2CH_2CH_2CH_2CH_2}$ (**13**) would have been expected to appear (5% detection limit).

Kinetics of the Conversion of μ-Alkenyl Complexes to Iron Alkenyl Complexes. Qualitatively, the reaction of the unsubstituted μ-vinyl complex **8b** with CH_3CN was much faster than the reaction of the monosubstituted μ-pentenyl complex **5** with CH_3CN.

If the reaction proceeded via unimolecular dissociation of the complexed alkene followed by rapid trapping of the vacant coordination site with CH_3CN, the substituted μ-alkenyl complex **5** would have been expected to react faster than **8**, since substituted alkenes are normally less tightly bound to metals than unsubstituted alkenes. On the other hand, if CH_3CN displaces the complexed alkenyl ligand in the slow step, the more crowded μ-pentenyl complex **5** should react slower than the unsubstituted vinyl complex **8b**. Even though associative processes are uncommon for 18-electron complexes, we suspected that an unusual associative mechanism was operative in this case.

To determine whether the conversion of μ-alkenyl complexes to iron–alkenyl complexes was proceeding by an associative or dissociative pathway, their rates of conversion were measured as a function of CH_3CN concentration.

The visible spectrum of unsubstituted μ-vinyl complex **8b** exhibits an absorption maximum at 557 nm ($\epsilon \geq 554$ cm^{-1} M^{-1}, see Experimental Section) in CH_3CN, whereas the product reaction mixture has almost no absorbance in this region. When the reaction of **8b** with CH_3CN was

(7) Awang, M. R.; Jeffery, J. C.; Stone, F. G. A. *J. Chem. Soc., Dalton Trans.* **1983**, *2091*.
(8) Ashworth, T. V.; Chetcuti, M. J.; Farugia, L. j.; Howard, J. A. K.; Jeffery, J. T.; Mills, R.; Pain, G. N.; Stone, F. G. A.; Woodward, P. In "Reactivity of Metal-Metal Bonds"; Chisholm, M. H., editor; American Chemical Society: Washington, D.C., 1981; *ACS Symp. Ser.*, No. 155, pp 299–313 and references therein.
(9) Antoneva, A. B.; Kolobova, N. E.; Petrovsky, P. V.; Lokshin, B. V.; Obezyuk, N. S. *J. Organomet. Chem.* **1977**, *137*, *55* and references therein.
(10) Nesmeyanov, A. N.; Rybinskaya, M. I.; Rybin, L. V.; Kaganovich, V. S.; Petrovskii, P. V. *J. Organomet. Chem.* **1971**, *31*, 257.
(11) Kao, S. C.; Lu, P. P. Y.; Pettit, R. *Organometallics* **1982**, *1*, 911.
(12) King, R. B.; Bisnette, M. B. *J. Organomet. Chem.* **1964**, *2*, 15.
(13) Miles, W. H. Ph. D. Dissertation, University of Wisconsin–Madison, 1984.
(14) Catheline, D.; Austruc, D. *J. Orgnomet. Chem.* **1984**, *272*, 417.

Table I. Disappearance of 8b in CH_3CN/CH_3NO_2 Monitored at 557 nm at 26.0 ± 0.5 °C

concn[a] of CH_3CN, M	$10^4\ k_{obsd}$,[b,c] s^{-1}	$10^5\ k_2$,[d] $M^{-1}\ s^{-1}$
1.74	0.67 ± 0.02	3.86
4.79	1.40 ± 0.01	2.92
9.57	2.70 ± 0.01	2.82
19.15	5.44 ± 0.02	2.84

[a] The remainder of the solvent was CH_3NO_2. [b] Slope from ln $[A_0 - A_t]/[A_0 - A_\infty]$ vs. time plot of data. [c] ± average deviation. [d] $k_2 = k_{obsd}/[CH_3CN]$.

Table II. Disappearance of 5 in CD_3CN/CD_3NO_2 Monitored by ^1H NMR Spectroscopy at 24.6 ± 0.2 °C

concn[a] of CH_3CN, M	$10^6\ k_{obsd}$,[b,c] s^{-1}	$10^7\ k^2$,[d] $M^{-1}\ s^{-1}$
9.57	2.76 ± 0.08	2.88
19.15	5.05 ± 0.10	2.64

[a] The remainder of the solvent was CD_3NO_2. [b] Slope from −ln [mol % of 5] vs. time plot of data. [c] ± average deviation. [d] $k_2 = k_{obsd}/[CH_3CN]$.

monitored by visible spectroscopy, the disappearance of the absorption at 557 nm was pseudo first order to greater than 4 half-lives. The disappearance of **8b** as a function of time was monitored at 560 nm for several CH_3CN concentrations in CH_3NO_2. CH_3NO_2 was chosen as the cosolvent because its dielectric constant (38.6) is very similar to the dielectric consant of CH_3CN (36.2).

Results of various runs with CH_3CN concentrations ranging from 1.74 to 19.15 M in CH_3NO_2 are summarized in Table I. As the CH_3CN concentration was increased, the value of k_{obsd} increased but little variation of the second-order rate constant k_2 ($k_{obsd} = k_2[CH_3CN]$) was observed. This establishes that the rate of reaction is first order in both CH_3CN and μ-vinyl complex **8b**.

The μ-pentenyl complex **5** also has an absorption maximum in the visible region at 564 nm (ϵ 813 $cm^{-1}\ M^{-1}$). However, the reaction of **5** with CH_3CN could not easily be monitored by following the disappearance of this band with time, since the reaction of **5** with CH_3CN is very slow and secondary reactions possibly arising from small amounts of air leaking into the system gave variable results. To circumvent these problems, the progress of the reaction was monitored by ^1H NMR spectroscopy in sealed tubes using CD_3CN and 1:1 CD_3CN/CD_3NO_2. In both cases the reactions were monitored to over 1 half-life. Results from these runs are summarized in Table II. A pseudo-first-order disappearance of μ-pentenyl complex **5** was observed. As before, the pseudo-first-order rate constant was directly proportional to the CD_3CN concentration. In agreement with our initial qualitative observation that **8b** is more reactive than **5** with CH_3CN, the second-order rate constant for the reaction of **8b** with CH_3CN is approximately 100 times larger than the second-order rate constant for the reaction of **5** with CH_3CN.

Conversion of Diiron μ-Alkenyl Complexes to Iron Alkenyl Complexes with NaI and CO. The reaction of μ-pentenyl complex **5** with CH_3CN is a very slow reaction requiring 2–3 days for completion and, when carried out at higher temperature, substantial decomposition occurred. The mixture of **6** and **7** reacts with CD_3CN to form the alkenylidene complex **12**[15] due to loss of the highly acidic methine proton from **6**. As a result of these limitations, improved procedures for the conversion of μ-alkenyl complexes to mononuclear alkenyl complexes were sought.

Since alkenes are easily displaced from $[(C_5H_5)(CO)_2Fe(alkene)]^+$ with I^-,[13] the reaction of μ-alkenyl complexes with I^- under an atmosphere of CO was examined with the hope of isolating mononuclear alkenyl complexes and $C_5H_5(CO)_2FeI$ (**14**). In the reaction of **5** with CO in methylene chloride, no reaction was observed by IR during 24 h at 80 °C. However, **5** reacts cleanly with CO and NaI in acetone at ambient temperature to give **10** in 56% yield and **14** in 62% yield. Under the same conditions, the μ-vinyl complex **8b** gives **9** (61%) and **14** (67%). The major advantage of the CO and I^- cleavage over CH_3CN cleavage is that the reaction is faster; it is complete within 2.5 h even with the sterically conjested μ-pentenyl complex **5**.

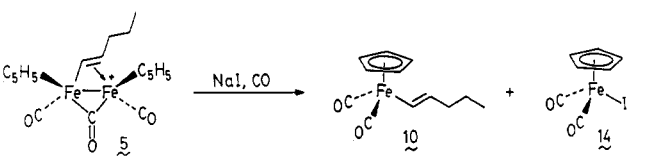

The NaI and CO reaction conditions provide a slightly basic medium and deprotonation of alkenyl complexes or of alkylidyne complexes in equilibrium with alkenyl complexes can interfere with formation of monoiron alkenyl complexes. When the equilibrating mixture of μ-alkylidyne complex $[(C_5H_5)_2(CO)_2Fe_2(\mu\text{-}CO)(\mu\text{-}C\overline{CHCH_2CH_2CH_2C}H_2)]^+PF_6^-$ (**15**) and μ-alkenyl complex $[(C_5H_5)_2(CO)_2Fe_2(\mu\text{-}CO)(\mu\text{-}\eta^1,\eta^2\text{-}CH{=}\overline{CCH_2CH_2CH_2CH_2}))]PF_6^-$ (**16**) (obtained from reaction of **1** with cyclopentene) was reacted with CO and NaI in acetone, the major product identified by ^1H NMR was the μ-alkenylidene complex $(C_5H_5)_2(CO)_2Fe_2(\mu\text{-}CO)(\mu\text{-}C{=}CCH_2CH_2CH_2CH_2)$ (**17**).[15] Although some **14** was formed, none of the desired monoiron alkenyl complex was observed. Similarly, when $[(C_5H_5)_2(CO)_2Fe_2(\mu\text{-}CO)(\mu\text{-}\eta^1,\eta^2\text{-}(E)\text{-}CH{=}CHCH(C_6H_4\text{-}p\text{-}CH_3)_2]^+PF_6^-$[17] (**18**) (obtained from reaction of **1** with $CH_2{=}C(C_6H_4\text{-}p\text{-}CH_3)_2$) was subjected to the same cleavage conditions, deprotonation occurred to give $(C_5H_5)_2(CO)_2Fe_2(\mu\text{-}CO)[\mu\text{-}CHCH{=}C(C_6H_4\text{-}p\text{-}CH_3)_2]$ in 59% yield.

To circumvent the deprotonation problem, the reactions were run in the presence of acid, excess I^-, and CO. In addition, we anticipated that the mononuclear alkenyl complexes might react with acid in situ to form alkenes.

Reaction of μ-pentenyl complex **5** with LiI, CO, and $HBF_4{\cdot}Et_2O$ gave 1-pentene in 72% yield (by GC) and **14** in 48% yield. Similarly, the μ-alkenyl complex **18** reacts to form $CH_2{=}CHCH(C_6H_4\text{-}p\text{-}CH_3)_2$ (**20**) in 48% yield after chromatography. However, when the mixture of **6** and **7** was treated with LiI, CO, and acid in CD_3CN, a peak in the ^1H NMR at δ 5.05 (assigned to **14**) appeared, but no resonances attributable to methylenecyclohexane were seen. In a control experiment, methylenecyclohexane was destroyed by either $HBF_4{\cdot}Et_2O$ or by HI in CH_3CN.

Discussion

Kinetic studies indicate that both **5** and **8b** react with CH_3CN by an associative mechanism. The initial reaction with CH_3CN must be slow relative to a subsequent fragmentation reaction since no intermediates in the conversion of μ-alkenyl complexes to mononuclear alkenyl complexes were observed by ^1H NMR or IR spectroscopy. The approximately 100-fold faster rate for the reaction of the unsubstituted μ-vinyl complex **8b** relative to that of the

(15) Marder, S. R. Ph.D. Dissertation, University of Wisconsin–Madison, 1985.

(16) Nesmeyanov, A. N.; Leshcheva, I. F.; Polovanyuk, I. V.; Ustynyuk, Y. A.; Makarova, L. G. *J. Organomet. Chem.* **1972**, *37*, 159.

(17) Casey, C. P.; Meszaros, M. W.; Fagan, P. J.; Bly, R. K.; Colborn, R. E. *J. Am. Chem. Soc.*, manuscript in preparation.

Scheme I

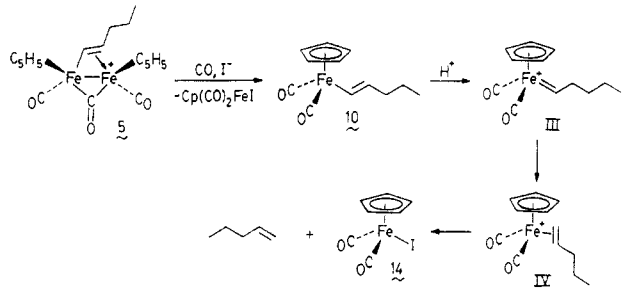

substituted μ-pentenyl complex **5** is best understood as a steric effect which slows attack of CH_3CN on the more substituted complex **5**.

We propose that these reactions proceed by rate-determining attack of CH_3CN which displaces the coordinated alkenyl group and generates an intermediate, II (this is the same structure that Pettit suggested for the final product of the reaction). This intermediate then undergoes either spontaneous or CH_3CN induced cleavage to give the mononuclear alkenyl complex and $(C_5H_5)Fe(CO)(CH_3CN)_2^+$ (**11**).

Monoiron alkenyl complexes can also be prepared by reaction of diiron μ-alkenyl complexes with I^- and CO. While this method is more rapid (for example, the conversion of **5** to **10** requires 3 days for completion with CH_3CN, but only 2.5 h with CO and I^-), deprotonation was a problem for some diiron μ-alkenyl complexes such as **18**.

When the diiron μ-alkenyl complexes were treated with I^-, CO, and H^+, fragmentation did not stop at the monoiron alkenyl stage. Instead, complete cleavage of the μ-alkenyl group to a free alkene was observed. The mechanism proposed is shown in Scheme I. Reaction with CO and I^- is proposed to generate the monoiron alkenyl complex **10** and 1 equiv of **14**. Electrophilic attack of H^+ on the β-carbon of **10** could produce the iron alkylidene complex III. A subsequent 1,2-hydride shift would give the iron alkene complex IV. Finally, I^- displaces the free alkene and generates a second equivalent of **14**.

These acidic cleavage conditions not only overcome the deprotonation problem encountered when CO and I^- alone were used but also provide a clean one-step conversion of the bridging alkenyl ligand to an alkene. Whereas **18** is deprotonated by I^- and CO to give the diiron alkylidene complex **19**, treatment with H^+, CO, and I^- leads to an alkene, presumably via acid cleavage of an intermediate monoiron alkenyl compound. However, this reaction is still not general. For example, attempted cleavage of the mixture of **6** and **7** to methylenecyclohexane failed since methylenecyclohexane is not stable under these highly acidic reaction conditions.

Experimental Section

General Data. ^1H NMR spectra were recorded on a Bruker WH 270, WP 270, or WP 200 spectrometer. ^{13}C NMR spectra were recorded on a JEOL FX 200 spectrometer operating at 50.1 MHz. CD_2Cl_2 was dried over P_2O_5; acetone-d_6 was dried over molecular sieves or B_2O_3; CD_3NO_2 was dried over CaH_2; CD_3CN was dried over P_2O_5 or CaH_2; benzene-d_6 was distilled from purple solutions of sodium and benzophenone. NMR samples were prepared and sealed on a vacuum line and centrifuged prior to analysis. IR spectra were recorded on a Beckman 4230 infrared spectrometer calibrated with polystyrene film. Visible spectra were recorded on a Cary Model 118 UV–visible spectrometer. Kinetics monitored by visible spectroscopy were run on a Gilford Model 222 spectrometer equipped with a Haake constant temperature bath. Mass spectra were obtained on an AEI-MS-902 or a KRATOS-MS-80 mass spectrometer. Air-sensitive compounds were handled by using standard vacuum line procedures, Schlenk procedures and glovebox manipulations. CH_3CN was distilled from P_2O_5 or CaH_2; CH_3NO_2 was distilled from CaH_2; hexane was distilled from purple solutions of sodium, benzophenone, and tetraglyme; CH_2Cl_2 was distilled from P_2O_5; acetone was distilled from B_2O_3. NaI and LiI were pulverized and then heated under vacuum prior to use. Gas chromatographic analyses were performed on a Varian Aerograph 2400.

$(C_5H_5)(CO)_2FeCH{=}CHCH_2CH_2CH_3$ (10). **5**[5] (118 mg, 0.22 mmol) was stirred in CH_3CN (20 mL) for 48 h at 35 °C. Most of the CH_3CN was evaporated under vacuum. The remaining solid was extracted with hexane which was passed through a short plug of activity III alumina. Evaporation of solvent under vacuum afforded **10** as a yellow oil (36.4 mg, 67%): ^1H NMR (270 MHz, C_6D_6) δ 6.40 (d, J = 15.1 Hz, 1 H), 5.82 (dt, J = 15.1, 7 Hz, 1 H), 4.06 (s, 5 H), 2.32 (q, J = 7 Hz, 2 H), 1.47 (pentet, J = 7 Hz, 2 H), 0.98 (t, J = 7 Hz, 3 H); $^{13}C\{^1H\}$ NMR (50.1 MHz, C_6D_6) δ 216.8 (CO), 145.7, 124.0 (*C*H=*C*H), 85.4 (C_5H_5), 41.7 (*C*HCH_2), 23.8 (CH_2CH_3), 13.8 (CH_3); IR (hexane) 2007 (s), 1960 (s) cm^{-1}; mass spectrum calcd for $C_{12}H_{14}FeO_2$ m/e 246.0339, found m/e 246.0344.

Reaction of 5 with CO and I^-. **5** (90 mg, 0.18 mmol), NaI (31 mg, 0.20 mmol), and CO (0.56 atm) were stirred in acetone for 1 h at 0 °C and 1.5 h at ambient temperature to give after chromatography **10** (25 mg, 56%) and **14**[16] (34 mg, 68%).

Reaction of 8b with CH_3CN. **8b**[11] (0.980 g, 1.97 mmol) was stirred in 20 mL of CH_3CN at 35 °C for 2 h. The solution was concentrated to 5 mL under vacuum. The solution was extracted with hexane (5 × 15 mL) and the combined hexane layers were passed through an alumina plug (1 × 8 cm). After solvent was evaporated on a rotary evaporator at ambient temperature, **9** remained as a yellow oil (0.233 g, 58%): ^1H NMR (200 MHz, CD_2Cl_2) δ 7.13 (dd, J = 17, 9 Hz, 1 H), 5.86 (dd, J = 9, 1 Hz, 1 H), 5.39 (dd, J = 17, 1 Hz, 1 H), 4.84 (s, 5 H). $^{13}C\{^1H\}$ NMR (50.1 MHz, CD_2Cl_2): δ 216.5 (CO), 140.7, 130.5 (*C*H=*C*H_2), 86.1 (C_5H_5); IR (CH_3CN) 2011 (s), 1957 (s) cm^{-1}.

The hexane-insoluble fraction from above was dried under high vacuum for 2 h and was recrystallized by dissolution in CH_3CN (15 mL), filtration, and precipitation with $(C_2H_5)_2O$ (20 mL) yielding **11** (0.400 g, 54%): ^1H NMR (200 MHz, acetone-d_6) δ 5.01 (s, 5 H), 2.47 (s, 6 H); $^{13}C\{^1H\}$ NMR (50.1 MHz, $(CD_3)_2CO$, 10 °C, 0.07 M $Cr(acac)_3$) δ 214.6 (CO), 133.8 (CN), 79.5 (C_5H_5)8 2.0 (cH_3); IR (CH_2Cl_2) 2000 cm^{-1}.

Reaction of 8b with CO and I^-. A solution of **8b** (200 mg, 0.40 mmol) and NaI (66 mg, 0.44 mmol) in 8 mL of acetone under 0.74 atm of CO was stirred at −78 °C for 10 min and at ambient temperature for 1 h. Solvent was evaporated, and the residue was dissolved in Et_2O and chromatographed (alumina with hexane) to give **9** (50 mg, 61%) as a yellow oil contaminated with a small amount of ferrocene. Elution with hexane/ether gave purple-black **14** (82 mg, 67%).

Reaction of 6 and 7 with CD_3CN. A 1.4:1 mixture of **6**/**7**[5] (~5 mg) was dissolved in CD_3CN (0.3 mL) and monitored by ^1H NMR spectroscopy. After 5 min a spectrum was taken, which showed **6** and **7** as indicated by the cyclopentadienyl resonances at δ 5.36 and 5.31. Alkylidene complex **12** was also present as indicated by a resonance at δ 4.93 for the cyclopentadienyl rings. The ratio of **6**:**7**:**12** was 1.4:1.0:0.9. After 20 min the ratio was 1.4:1.0:1.5; after 25 h the ratio was 1.3:1.0:3.6. After 27 h several impurities were present (~25%); however, the major organometallic species present was **12**.

Kinetics by Visible Spectroscopy. In a preliminary experiment, **8b**[11] (6.0 mg, 0.012 mmol) was dissolved in CH_3CN (10.0 mL) and a visible spectrum was recorded within 2 min. The absorption maximum at 557 nm had A = 0.67. Since there were roughly 2 min of reaction time (~15% reaction) prior to acquisition of the spectrum, the minimum value for ϵ is 554 cm^{-1} M^{-1}.

For kinetic runs, ~1.0 mM solutions of **8b** in CH_3CN/CH_3NO_2 were syringed into argon-purged cuvettes through a septum cap. Under a flush of argon, the septum cap was replaced with a Teflon plug.

Kinetics by ^1H NMR Spectroscopy. μ-Pentenyl complex **5**[5] (~2 mg) was dissolved in CD_3CN or a 1:1 mixture of CD_3CN/CD_3NO_2 in an NMR tube. The tubes were sealed under vacuum and maintained at 24.6 °C by using a constant temperature bath. The reaction was periodically monitored by ^1H NMR spectroscopy, using the integrated intensities of the vinyl,

cyclopentadienyl, and methyl protons as a measure of the extent of reaction. For both the 19.15 M CH_3CN and 9.56 M CH_3CN concentrations, the reactions were monitored to over 1 half-life.

Reaction of 5 with LiI, HBF_4·Et_2O, and CO. 5 (12 mg, 0.022 mmol), LiI (12) mg, 0.085 mmol), HBF_4·Et_2O (4.2 μL, 5.4 mg, 0.033 mmol), and CD_2Cl_2 (0.5 mL) were sealed in an NMR tube under 1 atm of CO. The slow reaction at 35 °C was monitored by ^1H NMR for 10 days. The volatile components were vacuum transferred into a flask containing the internal GC standard *n*-hexane (2.8 μL, 0.8 mg). The yield of 1-pentene was determined to be 72% by analytical gas chromatography (10% SE-30, 25 °C). Et_2O extraction of the black residue in the NMR tube gave 14 (6.3 mg, 48%).

Reaction of 18 with LiI, HBF_4·Et_2O, and CO. 18 (436 mg, 0.63 mmol), LiI (210 mg, 1.57 mmol), HBF_4·Et_2O (0.156 mL, 202 mg, 1.25 mmol), and CH_3CN (12.5 mL) were heated at 50 °C under 1 atm of CO for 8 h. Solvent was evaporated under vacuum, and the residue was extracted with hexane. Preparative TLC (silica gel/hexane) gave **20** (62 mg, 48%) as a colorless oil: ^1H NMR (200 MHz, acetone-d_6) δ 7.10 (s, 8 H), 6.33 (ddd, J = 7.3, 10.1, 17.2 Hz, 1 H), 5.15 (dm, J = 10.1 Hz, 1 H), 4.97 (dm, J = 17.2 Hz, 1 H), 4.68 (d, J = 7.3 Hz, 1 H), 2.26 (s, 6 H); $^{13}C\{^1H\}$ NMR (50.1 MHz, CD_3CN) δ 21.1 (CH_3), 51.1 (methine CH), 116.1 (= CH_2), 129.2, 130.0 (ortho, meta), 136.8, 142.0, 142.2 (ipso, para, CH=); mass spectrum calcd for $C_{17}H_{18}$ m/e 222.1404, found m/e 222.1409.

Acknowledgment. Support from the Department of Energy Division of Basic Energy Science and the National Science Foundation is gratefully acknowledged.

Synthesis, Catalytic Activity, and Attempt at the Resolution of an Homometallic Chiral Cobalt Cluster, $(\mu_3\text{-}CH_3C)Co_3(CO)_7(\mu\text{-}Ph_2PCH_2P(CH_3)_2)$

Jacqueline Collin, Christine Jossart, and Gilbert Balavoine*

UA-CNRS No. 255, Institut de Chimie Moléculaire d'Orsay, Université Paris-Sud, 91405 Orsay Cedex, France

Received April 10, 1985

The unsymmetrically substituted chelating 1,1-diphosphine $Ph_2PCH_2P(CH_3)_2$ reacts with the cluster $(\mu_3\text{-}CH_3C)Co_3(CO)_9$ to give the chiral cluster $(\mu_3\text{-}CH_3C)Co_3(CO)_7(Ph_2PCH_2P(CH_3)_2)$ as a racemic mixture. A method of resolving this cluster is studied. Substitution of a carbonyl by an asymmetric monophosphine yields the cluster $(\mu_3\text{-}CH_3C)Co_3(CO)_6(Ph_2PCH_2P(CH_3)_2)L^*$. The two expected diastereoisomers are characterized by NMR and HPLC, and no epimerization process is detected. Under CO pressure the monophosphine is selectively replaced to give back $(\mu_3\text{-}CH_3C)Co_3(CO)_7(Ph_2PCH_2P(CH_3)_2)$ but racemization of the cluster frame occurs under these conditions. The use of this cluster as a catalyst for styrene hydroformylation is discussed.

Introduction

Clusters are known to be efficient catalyst precursors for different types of reactions: hydrogenation, hydroformylation, cyclopropanation.[1] However, the precise nature of reactive species is still unknown. In some instances complete recovery of the starting cluster compound has been reported.[2] However, definitive experimentation that demonstrates that cluster fragmentation and reformation do not account for formation of the active catalyst has yet to appear. That is until now, no definitive proof has been presented that demonstrates that the cluster itself is a catalytic intermediate.

Criteria for identifying transition metal cluster catalyzed reactions have been reviewed,[3a,b] however, the simplest way of resolving the problem was pointed out some years ago:[3c] observation of asymmetric induction in a reaction catalyzed by a chiral cluster, the chirality of which comes from the cluster frame (excluding a chiral ligand), would demonstrate that the active species is of necessity a cluster.

Chart I

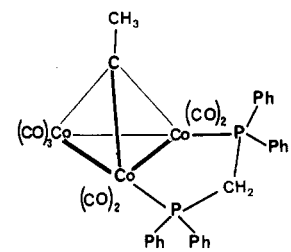

To our knowledge, only a few examples, all of them heteronuclear, of optically active chiral clusters have been published.[4-6] Photoinitiated hydrosilylation in the presence of a racemic cluster has been described by Pittman.[7] Using a resolved cluster as the catalyst, he was unable to observe any asymmetric induction. Moreover, at the end of the reaction the cluster recovered was completely ra-

(1) (a) Cho, B. R.; Laine, R. M. *J. Mol. Catal.* **1982**, *15*, 383. (b) Frediani, P.; Matteoli, U.; Bianchi, M.; Piacenti, F.; Menchi, G. *J. Organomet. Chem.* **1978**, *150*, 273. Bianchi, M.; Matteoli, U.; Menchi, G.; Frediani, P.; Pratesi, S.; Piancenti, F.; Botteghi, C. *J. Organomet. Chem.* **1980**, *198*, 73. (c) Chini, P.; Martinengo, S.; Garlaschelli, G. *J. Chem. Soc., Chem. Commun.* **1972**, 709. (d) Doyle, M. P.; Tamblyn, W. H.; Buhro, W. E.; Dorow, R. L. *Tetrahedron Lett.* **1981**, *22*, 1783. (e) Muetterties, E. L.; Krause, M. J. *Angew. Chem., Int. Ed. Engl.* **1983**, *22*, 135.

(2) Pittman, C. U., Jr.; Wilemon, M. W.; Wilson, W. D.; Ryan, R. C. *Angew. Chem., Int. Ed. Engl.* **1980**, *19*, 478.

(3) (a) Laine, R. M. *J. Mol. Catal.* **1982**, *14*, 137. (b) Balavoine, G.; Dang, T.; Eskenazi, C.; Kagan, H. B. *J. Mol. Catal.* **1980**, *7*, 531. (c) Norton, J. R. "Fundamental Research in Homogeneous Catalysis"; Tsutsui, Ed.; Plenum Press: New York, 1977.

(4) Richter, F.; Vahrenkamp, H. *Angew. Chem., Int. Ed. Engl.* **1980**, *19*, 65. Richter, F.; Vahrenkamp, H. *Chem. Ber.* **1982**, *115*, 3224, 3243.

(5) (a) Beurich, H.; Vahrenkamp, H. *Angew. Chem., Int. Ed. Engl.* **1981**, *20*, 98. (b) Muller, M.; Vahrenkamp, H. *Chem. Ber.* **1983**, *116*, 2748.

(6) Mahe, C.; Patin, H.; Le Marouille, J. Y.; Benoit, A. *Organometallics* **1983**, *2*, 1051.

(7) Pittman, C. U., Jr.; Richmond, M. G.; Ma'mun Absi-Halabi; Beurich, H.; Richter, F.; Vahrenkamp, H. *Angew. Chem., Int. Ed. Engl.* **1982**, *21*, 786.

0276-7333/86/2305-0203$01.50/0

cyclopentadienyl, and methyl protons as a measure of the extent of reaction. For both the 19.15 M CH_3CN and 9.56 M CH_3CN concentrations, the reactions were monitored to over 1 half-life.

Reaction of 5 with LiI, HBF_4·Et_2O, and CO. 5 (12 mg, 0.022 mmol), LiI (12) mg, 0.085 mmol), HBF_4·Et_2O (4.2 μL, 5.4 mg, 0.033 mmol), and CD_2Cl_2 (0.5 mL) were sealed in an NMR tube under 1 atm of CO. The slow reaction at 35 °C was monitored by ^1H NMR for 10 days. The volatile components were vacuum transferred into a flask containing the internal GC standard *n*-hexane (2.8 μL, 0.8 mg). The yield of 1-pentene was determined to be 72% by analytical gas chromatography (10% SE-30, 25 °C). Et_2O extraction of the black residue in the NMR tube gave 14 (6.3 mg, 48%).

Reaction of 18 with LiI, HBF_4·Et_2O, and CO. 18 (436 mg, 0.63 mmol), LiI (210 mg, 1.57 mmol), HBF_4·Et_2O (0.156 mL, 202 mg, 1.25 mmol), and CH_3CN (12.5 mL) were heated at 50 °C under 1 atm of CO for 8 h. Solvent was evaporated under vacuum, and the residue was extracted with hexane. Preparative TLC (silica gel/hexane) gave **20** (62 mg, 48%) as a colorless oil: ^1H NMR (200 MHz, acetone-d_6) δ 7.10 (s, 8 H), 6.33 (ddd, J = 7.3, 10.1, 17.2 Hz, 1 H), 5.15 (dm, J = 10.1 Hz, 1 H), 4.97 (dm, J = 17.2 Hz, 1 H), 4.68 (d, J = 7.3 Hz, 1 H), 2.26 (s, 6 H); $^{13}C\{^1H\}$ NMR (50.1 MHz, CD_3CN) δ 21.1 (CH_3), 51.1 (methine CH), 116.1 (= CH_2), 129.2, 130.0 (ortho, meta), 136.8, 142.0, 142.2 (ipso, para, CH=); mass spectrum calcd for $C_{17}H_{18}$ m/e 222.1404, found m/e 222.1409.

Acknowledgment. Support from the Department of Energy Division of Basic Energy Science and the National Science Foundation is gratefully acknowledged.

Synthesis, Catalytic Activity, and Attempt at the Resolution of an Homometallic Chiral Cobalt Cluster, $(\mu_3\text{-}CH_3C)Co_3(CO)_7(\mu\text{-}Ph_2PCH_2P(CH_3)_2)$

Jacqueline Collin, Christine Jossart, and Gilbert Balavoine*

UA-CNRS No. 255, Institut de Chimie Moléculaire d'Orsay, Université Paris-Sud, 91405 Orsay Cedex, France

Received April 10, 1985

The unsymmetrically substituted chelating 1,1-diphosphine $Ph_2PCH_2P(CH_3)_2$ reacts with the cluster $(\mu_3\text{-}CH_3C)Co_3(CO)_9$ to give the chiral cluster $(\mu_3\text{-}CH_3C)Co_3(CO)_7(Ph_2PCH_2P(CH_3)_2)$ as a racemic mixture. A method of resolving this cluster is studied. Substitution of a carbonyl by an asymmetric monophosphine yields the cluster $(\mu_3\text{-}CH_3C)Co_3(CO)_6(Ph_2PCH_2P(CH_3)_2)L^*$. The two expected diastereoisomers are characterized by NMR and HPLC, and no epimerization process is detected. Under CO pressure the monophosphine is selectively replaced to give back $(\mu_3\text{-}CH_3C)Co_3(CO)_7(Ph_2PCH_2P(CH_3)_2)$ but racemization of the cluster frame occurs under these conditions. The use of this cluster as a catalyst for styrene hydroformylation is discussed.

Introduction

Clusters are known to be efficient catalyst precursors for different types of reactions: hydrogenation, hydroformylation, cyclopropanation.[1] However, the precise nature of reactive species is still unknown. In some instances complete recovery of the starting cluster compound has been reported.[2] However, definitive experimentation that demonstrates that cluster fragmentation and reformation do not account for formation of the active catalyst has yet to appear. That is until now, no definitive proof has been presented that demonstrates that the cluster itself is a catalytic intermediate.

Criteria for identifying transition metal cluster catalyzed reactions have been reviewed,[3a,b] however, the simplest way of resolving the problem was pointed out some years ago:[3c] observation of asymmetric induction in a reaction catalyzed by a chiral cluster, the chirality of which comes from the cluster frame (excluding a chiral ligand), would demonstrate that the active species is of necessity a cluster.

Chart I

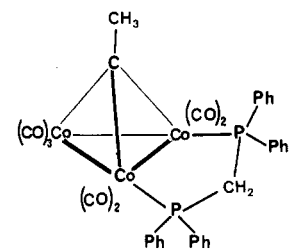

To our knowledge, only a few examples, all of them heteronuclear, of optically active chiral clusters have been published.[4-6] Photoinitiated hydrosilylation in the presence of a racemic cluster has been described by Pittman.[7] Using a resolved cluster as the catalyst, he was unable to observe any asymmetric induction. Moreover, at the end of the reaction the cluster recovered was completely ra-

(1) (a) Cho, B. R.; Laine, R. M. *J. Mol. Catal.* **1982**, *15*, 383. (b) Frediani, P.; Matteoli, U.; Bianchi, M.; Piacenti, F.; Menchi, G. *J. Organomet. Chem.* **1978**, *150*, 273. Bianchi, M.; Matteoli, U.; Menchi, G.; Frediani, P.; Pratesi, S.; Piancenti, F.; Botteghi, C. *J. Organomet. Chem.* **1980**, *198*, 73. (c) Chini, P.; Martinengo, S.; Garlaschelli, G. *J. Chem. Soc., Chem. Commun.* **1972**, 709. (d) Doyle, M. P.; Tamblyn, W. H.; Buhro, W. E.; Dorow, R. L. *Tetrahedron Lett.* **1981**, *22*, 1783. (e) Muetterties, E. L.; Krause, M. J. *Angew. Chem., Int. Ed. Engl.* **1983**, *22*, 135.

(2) Pittman, C. U., Jr.; Wilemon, M. W.; Wilson, W. D.; Ryan, R. C. *Angew. Chem., Int. Ed. Engl.* **1980**, *19*, 478.

(3) (a) Laine, R. M. *J. Mol. Catal.* **1982**, *14*, 137. (b) Balavoine, G.; Dang, T.; Eskenazi, C.; Kagan, H. B. *J. Mol. Catal.* **1980**, *7*, 531. (c) Norton, J. R. "Fundamental Research in Homogeneous Catalysis"; Tsutsui, Ed.; Plenum Press: New York, 1977.

(4) Richter, F.; Vahrenkamp, H. *Angew. Chem., Int. Ed. Engl.* **1980**, *19*, 65. Richter, F.; Vahrenkamp, H. *Chem. Ber.* **1982**, *115*, 3224, 3243.

(5) (a) Beurich, H.; Vahrenkamp, H. *Angew. Chem., Int. Ed. Engl.* **1981**, *20*, 98. (b) Muller, M.; Vahrenkamp, H. *Chem. Ber.* **1983**, *116*, 2748.

(6) Mahe, C.; Patin, H.; Le Marouille, J. Y.; Benoit, A. *Organometallics* **1983**, *2*, 1051.

(7) Pittman, C. U., Jr.; Richmond, M. G.; Ma'mun Absi-Halabi; Beurich, H.; Richter, F.; Vahrenkamp, H. *Angew. Chem., Int. Ed. Engl.* **1982**, *21*, 786.

0276-7333/86/2305-0203$01.50/0

cemized. Thus, this work failed to prove catalysis by intact clusters.

Our goal in the work reported here was to synthesize an homometallic chiral cluster that could be easily resolved and act as a catalyst. It seemed to us that the best approach was to generate an homometallic chiral cluster in which all the metal centers could act as catalysts rather than a mixed chiral cluster such as those described by Vahrenkamp.[4,5] We have already performed the synthesis and X-ray structure determination of the $(\mu_3\text{-}CH_3C)Co_3(CO)_7$(dppm) cluster shown in Chart I,[8] which contains the bidentate bridging ligand bis(diphenylphosphino)methane (dppm). This cluster acts as a catalyst for olefin hydroformylation, as does $(\mu_3\text{-}PhC)Co_3(CO)_9$.[9]

Substitution of an unsymmetrically substituted 1,1-diphosphine for dppm should lead to a chiral cluster. The use of a bidentate phosphine ligand for the synthesis of a chiral cluster is important from several points of view. A bidentate phosphine ligand will stabilize the cluster and serve as a better ligand by comparison with the imino or thioamido or formamido ligands used by Patin[10] and Deeming[11] in the synthesis of chiral clusters. It is well-known that phosphines have desirable effects on the activity and selectivity of catalysts.

In addition, further substitution with a chiral agent such as a monophosphine could be used to resolve the cluster. The monophosphine should be more labile than the bidentate phosphine and removed by CO. Such a resolution is not readily possible in the case of the cluster $(\mu_3\text{-}Cl_3C)Co_3(CO)_7(P(OC_6H_4\text{-}p\text{-}CH_3)_3P(OCH_3)_2Ph)$ reported by Bruce during the course of our work.[12]

We present here the synthesis of a racemic mixture of the cluster $(\mu_3\text{-}CH_3C)Co_3(CO)_7(Ph_2PCH_2P(CH_3)_2)$ and the related clusters $(\mu_3\text{-}CH_3C)Co_3(CO)_6((Ph_2PCH_2P(CH_3)_2)L^*$ obtained by substitution of a carbonyl ligand with a chiral phosphine L*. The isomerism and the stability of these compounds are discussed, and their catalytic activity for styrene hydroformylation is studied. The separation of the diastereomer clusters followed by selective decoordination of the chiral phosphine are performed leading to a racemized cluster.

Experimental Section

All reactions were carried out under nitrogen atmosphere and solvents deoxygenated before use. THF was distilled from benzophenone–sodium. (*R*)-(+)-PAMP (methylphenyl-*o*-anisylphosphine) and (*R*)-(+)-CAMP (methylcyclohexyl-*o*-anisylphosphine) were prepared according to the Knowles procedure.[13] (*S*)-(+)-(2-Methylbutyldiphenylphosphine) was purchased from Strem Chemicals.

Synthesis of the Diphosphine $(CH_3)_2PCH_2PPh_2$. To a suspension of Ph_2PCH_2Li (5.13 mmol) in pentane, prepared by the method of Peterson,[14] was added 5 mL of THF. The resulting solution then was added slowly at room temperature to a mixture of 530 mg (5.49 mmol) of Me_2PCl in 8 mL of THF. Decoloration of the anion was observed. After 2 h the mixture was treated with water and extracted with dichloromethane and the extracts were dried over magnesium sulfate. The product obtained after concentration of the extracts was chromatographed on silica and eluted by a mixture of ether/pentane (1:9). A 439-mg (33% yield) sample of diphosphine were obtained (NMR data were identical with those already published).[15]

Synthesis of Clusters. 1 $[(\mu_3\text{-}CH_3C)(Co_3(CO)_7\text{-}(Ph_2PCH_2P(CH_3)_2)]$. To a solution of 1 g (2.19 mmol) of $(\mu_3\text{-}(CH_3C)Co_3(CO)_9$ (prepared by a published method[16]) in 15 mL of benzene was added slowly 0.57 g (2.19 mmol) of $Ph_2PCH_2P\text{-}(CH_3)_2$ in 10 mL of benzene. Gaseous evolution was observed, and the mixture turned darker. After 2 h the solution was concentrated and chromatographed on a silica column. The product was eluted first with pentane/dichloromethane (70:30) as a purple band and separated from a second brown band. After recrystallization from pentane/ether (2:1) the product was obtained as purple crystals (1.06 g, yield 73%; mp 164 °C). Anal. Calcd: C, 43.66; H, 3.21; Co, 26.78; P, 9.38. Found: C, 43.91; H, 3.30; Co, 25.78; P, 9.25. The mass spectrum was recorded by using a chemical ionization technique on a Ribermag R 10-10 spectrometer (M + 1, *m/e* 661). ^{13}C NMR spectrum (recorded on a Cameca 250-MHz spectrometer at −40 °C; ppm): apical C, 288; CO, 204.9, 204.8, 204.7, 204.6, 204.5, 204.4, 204.2; CH_3-C, 45.2; CH_2, 44.2 (J_{PC} = 21.4 Hz.

2a $[(\mu_3\text{-}CH_3C)Co_3(CO)_6(Ph_2PCH_2P(CH_3)_2)PPh_2(CH_3)]$. A solution of 100 mg (0.15 mmol) of cluster 1 and 30 mg (0.15 mmol) of $PPh_2(CH_3)$ in benzene (10 mL) was heated at 60 °C for 16 h. After concentration, the solution was chromatographed on a silica column. A black band was eluted with pentane/dichloromethane (80:20). The crude product was recrystallized from ether/pentane (1:2) to give 50 mg (40% yield) of black crystals (mp 115 °C).

2b $[(\mu_3\text{-}CH_3C)Co_3(CO)_6(Ph_2PCH_2(CH_3)_2(CH_3PPh(o\text{-}anisyl))]$. A solution of 214 mg (0.32 mmol) of $(\mu_3\text{-}CH_3C)Co_3\text{-}(CO)_7(Ph_2PCH_2P(CH_3)_2)$ and 80 mg (0.35 mmol) of (*R*)-(+)-phenylanisylmethylphosphine [(*R*)-(+)-PAMP] in benzene (10 mL) was heated at 60 °C for 2 h. After concentration, the solution was chromatographed on a silica column. Two bands were separated with a mixture of pentane/dichloromethane (60:40). The first was red and contained the starting material 1, the second, black, contained cluster **2b**. The crude product was recrystallized from ether/pentane (1:2) at 0 °C to give 172 mg of black crystals (yield 62%; mp 168 °C). Anal. Calcd: C, 51.53; H, 4.21; Co, 20.50; P, 10.77. Found: C, 51.29; H, 4.09; Co, 21.09; P, 10.94.

2c $[(\mu_3\text{-}CH_3C)Co_3(CO)_6(Ph_2PCH_2P(CH_3)_2)(CH_3P(o\text{-}anisyl)cyclohexyl)]$. A solution of 218 mg (0.33 mmol) of cluster 1 and 78 mg (0.33 mmol) of (*R*)-(+)-cyclohexylanisylmethylphosphine [(*R*)-(+)-CAMP] in benzene (20 mL) was heated at 60 °C for 3 h. After concentration the solution was chromatographed on a silica column. Elution with pentane/dichloromethane (1:1) gave a single black band. The crude product was crystallized from pentane at −20 °C to give 157 mg of black crystals (55% yield; mp 155 °C dec). Anal. Calcd: C, 51.17; H, 4.87; P, 10.70. Found: C, 51.25; H, 5.02; P, 10.74.

2d $[(\mu_3\text{-}CH_3C)Co_3(CO)_6(Ph_2PCH_2P(CH_3)_2)(CH_3CH(C_2H_5)\text{-}CH_2PPh_2)]$. A solution of 140 mg (0.21 mmol) of cluster 1 and 59 mg (0.23 mol) of (*S*)-(+)-2-methylbutyldiphenylphosphine in benzene (8 mL) was heated at 60 °C for 4 h. After concentration, the solution was chromatographed on a silica column. With ether as solvent, a black band eluted first, followed by a purple band. The black product was crystallized from pentane/ether (2:1) at 0 °C to give 107 mg of black crystals (57% yield: mp 126 °C). Anal. Calcd: C, 54.06; H, 4.76; P, 10.46. Found: C, 54.28; H, 5.02; P, 10.37.

HPLC. A Zorbax ODS (inverse-phase column (25 × 5 mm) was used for the HPLC chromatographic studies. Quantities injected for each analysis were approximately 10 μL of solution containing 1 mg of cluster for 1 mL of dichloromethane. The products were eluted with mixtures of methanol and water containing different amounts of water (10% for cluster **2d**, 15% for **2b** and **2c**, 20% for 1 and **2a**). The pump was a Du Pont 8800 type, and the flow rate used was 1.3–1.6 mL/min. One peak was

(8) Balavoine, G.; Collin, J.; Bonnet, J. J.; Lavigne, G. *J. Organomet. Chem.* **1985**, *280*, 429.
(9) Ryan, R. C.; Pittman, C. U., Jr.; Connor, J. P. O. *J. Am. Chem. Soc.* **1977**, *99*, 1986.
(10) (a) Patin, H.; Mignani, G.; Mahé, C.; Le Marouille, J. Y.; Benoit, A.; Grandjean, D.; Levesque, G. *J. Organomet. Chem.* **1981**, *208*, C39. (b) Benoit, A.; Darchen, A.; Le Marouille, J. Y.; Mahé, C.; Patin, H. *Organometallics* **1983**, *2*, 555.
(11) Arce, A. J.; Deeming, A. J. *J. Chem. Soc., Chem. Commun.* **1980**, 1102.
(12) Bruce, M. I.; Matisons, J. G.; Nicholson, B. K.; Williams, M. L. *J. Organomet. Chem.* **1982**, *236*, C57.
(13) (a) Knowles, W. S.; Sabacky, M. J.; Vineyard, B. D. *Adv. Chem. Ser.* **1974**, *No. 132*, 274. (b) Knowles, W. S. U.S. Patent, 4 005 127, 1977; *Chem. Abstr.* **1977**, *86*, 190463.
(14) Peterson, D. J. *J. Organomet. Chem.* **1967**, *8*, 199.
(15) Harsch, H. M.; Schmidbaur, H. *Z. Naturforsch. B: Anorg. Chem., Org. Chem.* **1977**, *32B*, 762.
(16) Seyferth, D.; Hallgren, J. E.; Hung, P. L. K. *J. Organomet. Chem.* **1973**, *50*, 265.

observed for cluster **1**, and two peaks were observed for cluster **2**. The best separation was obtained for compound **2c**.

For the preparative separation of cluster **2c**, the same type of column (Zorbax ODS, inverse phase, 25 × 9.6 mm) was used with the same eluant and injections of 50 μL of a solution containing 20 mg of cluster in 2 mL of methanol. Retention times of the two diastereoisomers were 45 min for A′ and 47 min for A″, and the two fractions were collected manually. For each injection the two fractions were diluted with about 12 mL of solvent and evaporated to dryness under vacuum just after elution to limit decomposition of the cluster (which is very rapid in these dilutions and cannot be avoided). After purification of each diastereoisomer on a silica column, 9.8 mg of A′ and 5.8 mg of A″ were obtained.

Transformation of Cluster 2b into Cluster 1. A solution of 82 mg (0.095 mmol) of **2b** in benzene was added to a 250-mL magnetically stirred autoclave under argon. The autoclave was pressurized with 20 bars of carbon monoxide. Overnight, at room temperature, the solution turned red. This solution was concentrated and chromatographed on an alumina column. With a mixture of pentane/ether (1:1) the PAMP was eluted first, followed by a purple band containing 57 mg (91% yield) of cluster **1**.

Hydroformylation. All the hydroformylations were carried out in a 250-mL stainless-steel autoclave. Reactions were run with solutions of 0.06 mmol of catalyst, 20 mL of toluene, and 1.82 g (17.5 mmol) of styrene. This corresponds to a 292:1 styrene/cluster ratio. The solution containing the cluster and styrene in toluene was pressurized at room temperature at 80 bars with a mixture of hydrogen/carbon monoxide (1:1) and then heated with an oil bath.

The yields of 3-phenylpropanal and 2-phenylpropanal were based upon the initial quantity of styrene. They were determined by analytical GLC on a 3-m OV 225 column using an internal standard.

Results and Discussion

Synthesis of the 1,1-Diphosphine $Ph_2PCH_2P(CH_3)_2$. Two different synthetic routes to the diphosphine $Ph_2PCH_2P(CH_3)_2$ were explored: reaction of the lithiated anion of trimethylphosphine with diphenylchlorophosphine[15] and reduction by sodium of the disulfide $(CH_3)_2(S)PCH_2P(S)Ph_2$ obtained by a published method.[17] Both methods gave poor yields in our hands. Additionally, we found that reaction of the lithiated anion of methyldiphenylphosphine (obtained by the Peterson method)[14] with dimethylchlorophosphine gave the 1,1-diphosphine in 33% yield.[18]

$$Ph_2PCH_2Li + (CH_3)_2PCl \xrightarrow[THF]{\text{room temp}} PH_2PCH_2P(CH_3)_2$$

Synthesis of Clusters 1 and 2. The very air-sensitive diphosphine $(CH_3)_2PCH_2PPh_2$ reacts at room temperature in benzene under argon with the cluster $(\mu_3\text{-}CH_3C)Co_3(CO)_9$ to give cluster **1**.

$$(CH_3)_2PCH_2PPh_2 + (CH_3C)Co_3(CO)_9 \xrightarrow[\text{room temp}]{C_6H_6} (CH_3C)Co_3(CO)_7(Ph_2PCH_2P(CH_3)_2) + 2CO$$

Spectroscopic data (Table I) and analysis are in agreement with the structure in which the ligand bridges two cobalt atoms. In the NMR spectrum nonequivalence of the protons of the methylene group[19] as in $(\mu_3\text{-}CH_3C)Co_3(CO)_7$(dppm) supports the hypothesis that the two phosphorus atoms coordinate to two different metal centers. The IR spectrum, which shows no bridging carbonyls,

Table I. Spectroscopic Data of Clusters 1 and 2

			^1H NMR[b]				
			$Ph_2PCH_2PMe_2$				
	L	ν(C=O)[a]	δ(Me apical)	δ(CH_2)	δ(Me_1) (J_{31P1H})	δ(Me_2)[c] (J_{31P1H})	L, δ(J_{31P1H})
1		2055 (s)–2000 (s)	3.65 (s)	3.5–2.9 (m) (12 peaks)	1.4 (d) (10)	1.2 (d) (10)	
2a	Ph_2PMe	2015 (sh) 1980 (s)–1965 (s)	3.55 (s)	2.9–2.3 (m)	0.97 (d) (8)	0.70 (d) (8)	Me, 2.9 (d) (7)
2b	PAMP	2060 (sh)–2020 (sh) 1980 (s)–1960 (s)	3.23 (s) 3.18 (s)	2.63 (m)	0.96 (d of d) (9)	0.70 (t) (9)	OMe, 3.55 (s) 3.51 (s) Me, 1.92 (d) (7), 1.88 (d) (7)
2c	CAMP	2060 (sh)–2010 (sh) 1970 (s)–1950 (s)	3.59 (s) 3.46 (s)	2.78 (m)–2.56 (m)	1.09 (t)	0.94 (d)–0.65 (d)	OMe, 3.68 (s) 3.60 (s) cyclohexyl, 1.37 (m) Me, 1.79 (d of d)
	A′		3.46 (s)	2.77 (m)–2.65 (m)	1.07 (9)	0.94 (9)	3.60 (s) 1.51 (m) 1.72 (dm)
	A″		3.59 (s)	2.83 (m)–2.62 (m)	1.11 (9)	0.65 (9)	3.68 (s) 1.48 (m) 1.69 (d) (7)
2d	MeC*(Et)HCH_2PPh_2	2010 (sh) 1975 (s)–1955 (s)	3.18 (s) 3.15 (s)	2.8–2 (m)	0.9 (m)	0.6 (m)	CH_2(P), 2.5 H, 2.5, 1.3 $CH_2(CH_2CH_3)$ Me, 0.9

[a] ν(C=O), cm^{-1}; solvent CH_2Cl_2; Perkin-Elmer 457. [b] δ (J, Hz); solvent C_6D_6 except **1** ($CDCl_3$): d, doublet; m, multiplet; t, triplet. Perkin-Elmer R 32 except for compound **2b**, Varian (XL 100) and **2c**, Cameca (250 MHz). [c] Determination of which group is Me_1 and which is Me_2 has not been made.

(17) Wheatland, D. A.; Clapp, C. H.; Waldron, R. W. *Inorg. Chem.* **1972**, *11*, 2340.

(18) The synthesis of a similar diphosphine, using the same methods, was reported in the course of manuscript preparation: Wolf, T. E.; Klemann, L. P. *Organometallics* **1982**, *1*, 1667.

(19) If the two protons of the methylene group were equivalent, a doublet of doublet should be observed; in the spectrum twelve peaks are separated (maximum sixteen).

Chart II

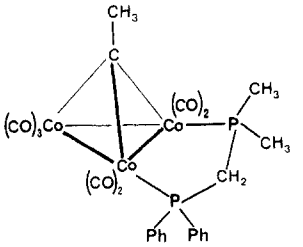

1

and the analogy with the compound $(\mu_3\text{-}CH_3C)Co_3(CO)_7$-(dppm), whose structure we have described elsewhere,[8] provide strong support for the structure in Chart II, where the two phosphorus atoms are in pseudoequatorial positions.

This cluster is chiral although it is obtained as a racemic mixture. We have never observed spontaneous resolution in any manipulation resulting in crystallization. The nonequivalence of the two methyl groups of the ligand in the NMR spectrum reveals the nonreversible coordination of the phosphine. That is to say, there should be no racemization of cluster 1 in solution at room temperature on the NMR time scale.

When compound 1 is heated in benzene with a monophosphine, a third carbonyl group is replaced by the phosphine and clusters **2a–d** are obtained. The IR and NMR data are reported in Table I.

$$\underset{\mathbf{1}}{(CH_3C)Co_3(CO)_7((CH_3)_2PCH_2PPh_2)} + L \xrightarrow[C_6H_6]{60\ ^\circ C} (CH_3C)Co_3(CO)_6(Ph_2PCH_2P(CH_3)_2)L$$

2a, L = $Ph_2P(CH_3)$
2b, L = PAMP
2c, L = CAMP
2d, L = $CH_3CH(C_2H_5)CH_2PPh_2$

Isomerism of Cluster 2. Monosubstitution of a carbonyl group of the cluster 1 can lead to three isomers A, B, and C according to the site of the reaction (Chart III).

With PCH_3Ph_2 a single product is obtained. Presumably, for electronic and steric reasons, the formation of isomer A is favored. In the NMR spectrum of cluster **2a** the methyl group of the monophosphine is coupled with only one phosphorus atom, another reason to prefer structure A. In compounds **2b–d**, which contain a chiral phosphine, there are two centers of chirality. If the monophosphine could coordinate to any of the three cobalt atoms, three pairs of diastereoisomers (one for each of the three structures A, B, and C) would result. The two diastereoisomers A_1 and A_2 corresponding to structure A are shown in Chart IV.

In the clusters **2b–d** the ^1H NMR signals of the methyl group located on the apical carbon are doublets. This

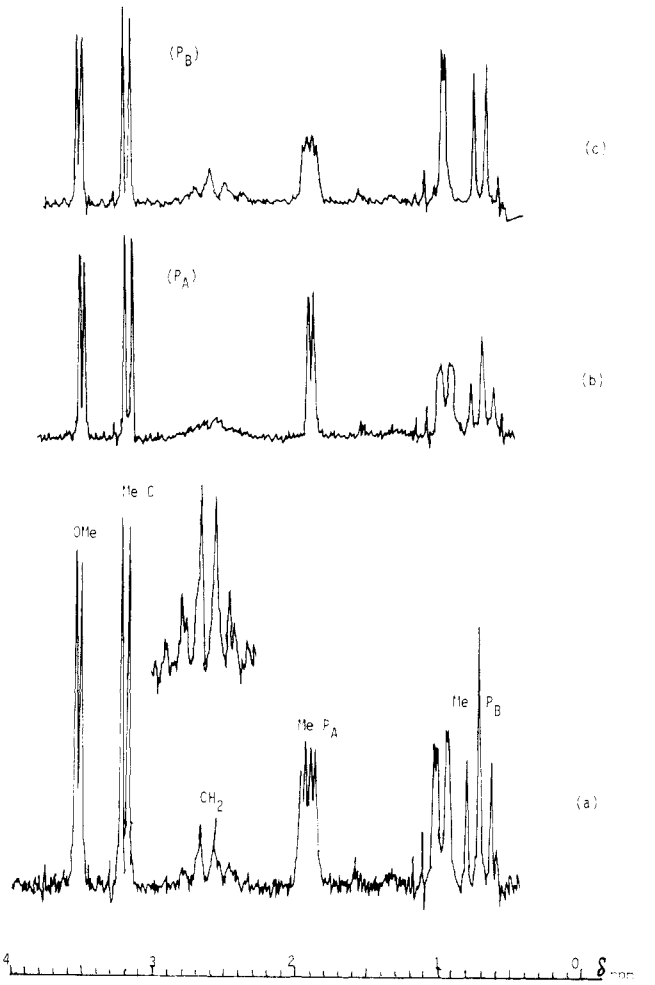

Figure 1. ^1H NMR spectrum of $(\mu_3\text{-}CCH_3)Co_3(CO)_6(P_AMePh$-(anisyl))$(Me_2P_BCH_2PPh_2)$: (a) without phosphorus decoupling; (b) with P_A decoupling; (c) with P_B decoupling.

difference between compounds 1 and **2a** is evidence for the occurrence of two cluster diastereoisomers.

Similarly, the signals due to the methyl substituents of the *o*-anisyl group in clusters **2b,c** are doublets. From phosphorus decoupling in the NMR spectrum of cluster **2b** (Figure 1) we can attribute the origin of the doublet to two diastereoisomers and not to coupling with one phosphorus of the monophosphine or of the diphosphine.

On HPLC of either pure **2b**, **2c**, or **2d** two peaks are eluted, which we consider to be definitive evidence for the existence of two diastereoisomeric forms for each cluster.

Stability of Cluster 2. Keeping in mind the aim of resolving cluster 1, for separation to be possible, cluster 2 must not epimerize in solution. We know already that clusters **2a–d** do not epimerize through the HPLC separation because two peaks are observed. When cluster **2b** was heated at 60 °C for 2 h in benzene in an NMR tube, no coalescence of signals was observed. So neither deg-

Chart III

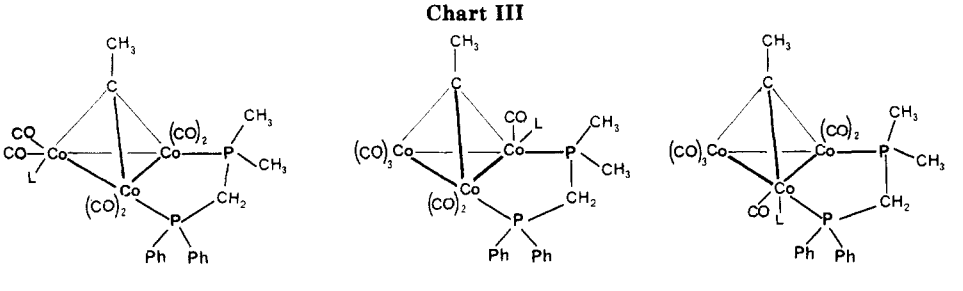

A B C

Chart IV

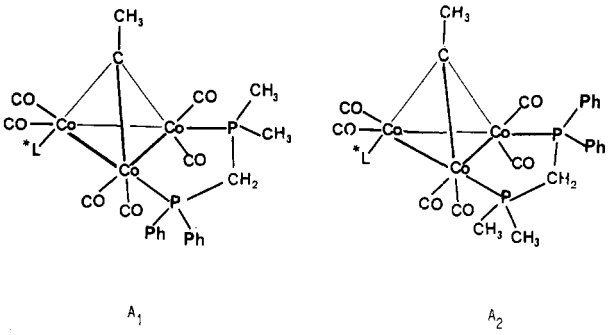

radation of the compound nor interconversion of the two diastereoisomers (on the NMR time scale) was detected. Under these conditions the cluster remains intact.

This result is somewhat different from those published by Jaouen and coworkers.[20] They studied the molecule $(\mu_3\text{-}(CH_3)_2CHO_2CO)Co_3(CO)_7(Ph_2PCH_2CH_2AsPh_2)$ and found a dynamic phenomenon: the diastereotopy of the two methyl groups is observed only at low temperature. However, in this case racemization could occur by decoordination and recoordination of the As ligand, which is not as tightly bound as a phosphine. Alternatively, the six-membered chelate ring could adopt a chiral conformation, at low temperature. For the molecules we have studied, we can assess from the NMR and HPLC data that the clusters coordinated by three phosphorus atoms do not epimerize. This is not surprising because the presence of the monophosphine should stabilize the cluster and make an epimerization process more difficult, occurring by coordination and decoordination of the diphosphine. Also, as we noted previously, in the clusters **2** as in the cluster **1**, the diphosphine is always tightly bound to two cobalt atoms, as shown by the nonequivalence of the methyl groups and of the protons of the methylene group of the phosphine. Another process of racemization could be to break the Co_2–Co_3 and Co_2–C apical bonds (Co_1 is the cobalt atom ligated by three carbonyls, and Co_2 and Co_3 are the two cobalt atoms ligated by the diphosphine) and to rotate the Co_1–C apical bond with respect to the Co_2–Co_3 bond. This mechanism postulated by Jaouen[20] should not operate in this case, due to the steric hindrance and the rigidity of the five-membered ring.[21]

Separation of the Diastereoisomers of Cluster 2c. All attempts to separate the two diastereoisomers by column chromatography on silica or alumina or by crystallization have failed as did a kinetic resolution of cluster **1** (with (*R*)-(+)-PAMP or with (*R*)-(+)-CAMP). For the three clusters **2b**, **2c**, and **2d**, the two diastereoisomers can be separated by analytical reverse-phase HPLC. The best separation is obtained for cluster **2c**. The products corresponding to the two peaks (A′ and A″ according to the order of elution) are separated and isolated by the use of a semipreparative reverse-phase HPLC column (9.6 mm diameter, 25 cm long), with injections of about 0.5–1 mg of cluster. The separation is quite effective: each product A′ and A″ injected independently on the HPLC column in the same conditions shows a purity of 95%. The dilution of the solutions recovered at the end of the HPLC ($MeOH/H_2O$, 85:15) are very high (about 10^{-5}), and under these conditions decomposition of the cluster is rapid even if the solutions are concentrated just after the elution. So the two products A′ and A″ must be purified on silica columns. NMR spectra of the two products A′ and A″ (Table I) are different, and the signals correspond to those obtained for cluster **2c**.

Table II. Optical Rotatory Dispersion of Diastereoisomers of Cluster 2c: $(\alpha)_\lambda$ (MeOH, deg)

	λ, nm			
	589	578	546	436
isomer A′ (*c* 0.98 mg/mL)	−460 (40)	−430 (40)	−220 (30)	+200 (30)
isomer A″ (*c* 0.58 mg/mL)	−790 (90)	−860 (90)	−960 (100)	−1570 (140)

Scheme I. Racemization of Cluster 1 in the Transformation 2c → 1

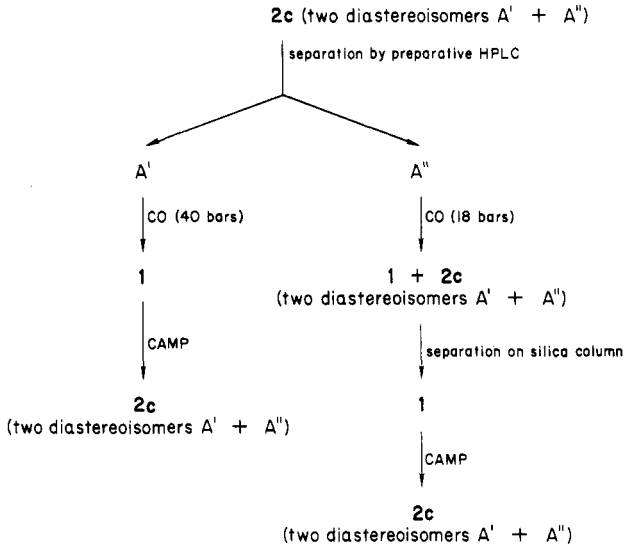

Optical rotations were measured in methanol for A′ and A″ (Table II). HPLC appears to be an efficient technique for the separation of the diastereoisomers of cluster **2c**.

Transformation of Cluster 2 into Cluster 1 (cf. Scheme I). We have investigated the selective decoordination of the chiral monophosphine (*R*)-(+)-CAMP or (*R*)-(+)-PAMP from clusters **2b** and **2c**. After a night at room temperature under a 20-bar pressure of carbon monoxide, **2b** and **2c** give back cluster **1** in quantitative yield. The diphosphine is not labilized. After the sepa-

$$(CH_3C)Co_3(CO)_6(Ph_2PCH_2P(CH_3)_2)L^* \xrightarrow{CO}$$
2b, L* = PAMP
2c, L* = CAMP
$$(CH_3C)Co_3(CO)_7(Ph_2PCH_2P(CH_3)_2) + L^*$$
1

ration of the diastereoisomers A′ and A″ of cluster **2c** we tried to decoordinate under these conditions the (*R*)-(+)-CAMP on each isomer and to measure the enantiomeric purity of each enantiomer of cluster **1** obtained. These clusters are dark purple, and their optical rotations are difficult to measure with precision, so each cluster is reacted once again with (*R*)-(+)-CAMP. The ratio of the two diastereoisomers obtained in each case determined by HPLC analysis must be the same as the ratio of the enantiomers of cluster **1** and give the value of the enantiomeric purity.

Cluster **1** obtained from product A′ shows no optical rotation, and after recoordination with (*R*)-(+)-CAMP the mixture of diastereoisomers A′ and A″ in 50:50 ratio is recovered. Racemization of the cluster frame has occurred during the process of substitution of the monophosphine by carbon monoxide (A′ → **1**) and/or during the recoordination of the monophosphine (**1** → **2c**). Product A″ reacts with carbon monoxide under a lower pressure (18

(20) Jaouen, G.; Marinetti, A.; Saillard, J. Y.; Sayer, B. G.; McGlinchey, M. J. *Organometallics* **1982**, *1*, 225.
(21) Hanson, B. E.; Mancini, J. S. *Organometallics* **1983**, *2*, 126.

Table III. Hydroformylation of Styrene[a]

no.	cluster	T, °C (autoclave)	total yield, %	% PhC(CH3)HCHO	reactn time
1	$MeCCo_3(CO)_9$	97	38	0.6	64 h
2	1	72	0		
3	1	104	9	0.44	16 h at 72 °C + 24 h at 104 °C
4	1	105	23	0.52	67 h
5	1	143	13	0.28	16 h
6	**2a**	89	10.5	0.51	16 h

[a] Reaction conditions: 40 mg of catalyst for 18 mmol of *olefin*; solvent toluene; P_{H_2+CO} = 80 bars. [b] No decomposition of cluster 1. [c] Cluster 1 is recovered at the end of the reaction.

bars) and a mixture of clusters **1** and **2c** (A′ and A″) is recovered at the end of the reaction. Reaction of (*R*)-(+)-CAMP with cluster **1** shows racemization of the cluster starting from A″ as it occurred from A′ (Scheme I).

There are two possibilities to explain the racemization of the cluster frame during the ligand exchange depicted in Scheme I: a process by ligand exchange, which needs the vacancy of two sites of coordination at the same time; a process by cleavage of cluster bonds as described above according to the Jaouen proposal. A decoordination of only one of the two phosphorus atoms of the diphosphine ligand would decrease the rigidity of the frame and permit the racemization of the cluster which is not observed under other conditions.

Our results do not allow us to distinguish between these two mechanisms, and it is impossible to tell in which step of Scheme I (treatment of the diastereoisomer A′ or A″ with CO or the conversion of the resulting **1** back to **2c**) racemization occurs, or whether **1** itself racemizes at a rate not detectable on the NMR time scale.

Hydroformylation. The results of the hydroformylation of styrene by $(\mu_3\text{-}CH_3C)Co_3(CO)_9$ and by clusters **1** and **2b** are given in Table III. $(\mu_3\text{-}CH_3C)Co_3(CO)_9$ and cluster **1** catalyze the hydroformylation reaction under similar conditions. With the diphosphine ligand, decomposition of the cluster is slower. Cluster **2b** catalyzes hydroformylation of styrene at a lower temperature than cluster **1**. Simultaneously (*R*)-(+)-PAMP is decoordinated and at the end of the reaction cluster **1** is obtained. In all experiments a significant amount of the branched aldehyde is obtained.[22]

Unfortunately, this activity cannot be used for detecting any optical induction induced by the cluster frame. Even the use of isomer A′ or A″ without decoordination of the (*R*)-(+)-CAMP in a hydroformylation reaction would be hopeless as partial racemization of A″ under 18 bars of CO and at room temperature has been observed.

Conclusion

We have synthesized the chiral cluster **1**, $(\mu_3\text{-}CH_3C)Co_3(CO)_7(Ph_2PCH_2P(CH_3)_2)$, as a racemic mixture and studied a method of resolving the cluster using a phosphine as the chiral resolving agent. Substitution of a carbonyl ligand of cluster **1** by chiral monophosphines provides new diastereoisomeric clusters which have been characterized. The absence of epimerization allows their separation. This is performed on a preparative scale. Although reaction under CO pressure gives a selective decoordination of monophosphine and leaves the diphosphine ligand on the cluster, these conditions cause racemization. We cannot succeed in the complete resolution of cluster **1**. We have access to the two enantiomers of the chiral frame of an homometallic chiral cluster, but we cannot be rid of the auxilliary chiral ligand. Nevertheless, it is the first example, to our knowledge, of such a separation. In the future it should be possible to compare the catalytic activity of the two diastereoisomers A′ and A″ for reactions (excluding carbonylation) as the stability of the frame in absence of CO has been established.

Acknowledgment. We are indebted to Professor H. Kagan for many fruitful discussions throughout the course of this work and to Dr. R. Laine for his helpful comments. We express our gratitude to Dr. J. C. Poulin for his assistance in the HPLC work and thank W. Knowles for a gift of (*R*)-(+)-methylphenyl-*o*-anisylphosphine oxide and (*R*)-(+)-methylcyclohexyl-*o*-anisylphosphine oxide. We also wish to acknowledge CNRS for financial support.

Registry No. **1**, 99299-63-5; **2a**, 99299-64-6; **2b**-A_1, 99299-65-7; **2b**-A_2, 99341-40-9; **2e**-A_1, 99299-66-8; **2c**-A_2, 99341-41-0; **2d**-A_1, 99299-67-9; **2d**-A_2, 99341-42-1; (*R*)-(+)-PAMP, 35144-01-5; (*R*)-(+)-CAMP, 52885-02-6; (*S*)-(+)-$CH_3CH(C_2H_5)CH_2PPh_2$, 53531-21-8; $(CH_3)_2PCH_2PPh_2$, 62263-64-3; Ph_2PCH_2Li, 62263-69-8; Me_2PCl, 811-62-1; $(\mu_3\text{-}(CH_3C)CO_3(CO)_9$, 13682-04-7; $PPh_2(CH_3)$, 1486-28-8; styrene, 100-42-5; 3-phenylpropanal, 104-53-0; 2-phenylpropanal, 93-53-8.

(22) There is also formation of ethylbenzene which reveals the hydrogenation reaction of styrene is concurrent to hydroformylation.

Kinetic Investigation of the Cleavage of *n*-Butyryl- or Isobutyrylcobalt Tetracarbonyl with Hydridocobalt Tetracarbonyl or Dihydrogen

István Kovács, Ferenc Ungváry, and László Markó*

Institute of Organic Chemistry, University of Veszprém, Veszprém, Hungary, 8201

Received March 11, 1985

The acylcobalt tetracarbonyls *n*-$C_3H_7C(O)Co(CO)_4$ (1) and *i*-$C_3H_7C(O)Co(CO)_4$ (2) react with H_2 or $HCo(CO)_4$ to yield *n*-butyraldehyde and isobutyraldehyde, respectively. The reactions, which are part of the catalytic cycle in the industrially important hydroformylation of propene, go over the corresponding acylcobalt tricarbonyls as intermediates formed by CO loss. Radical pathways of aldehyde formation may be excluded. Although the rate constants of the reactions with $HCo(CO)_4$ are at 25 °C 24–34 times larger than those with H_2, under the conditions of catalytic hydroformylation (>100 °C and >100 bar H_2 + CO) the reaction with H_2 is mainly responsible for aldehyde formation because of its stronger temperature dependence and the large concentration of H_2.

Introduction

The cleavage of acylcobalt carbonyls by $HCo(CO)_4$ or by H_2 is regarded as the ultimate step of aldehyde formation in hydroformylation:[1]

$$RC(O)Co(CO)_4 + HCo(CO)_4 \rightarrow RCHO + Co_2(CO)_8 \quad (1)$$

$$RC(O)Co(CO)_4 + H_2 \rightarrow RCHO + HCo(CO)_4 \quad (2)$$

Conflicting reports have appeared in recent years regarding the relative importance of reactions 1 and 2 under catalytic conditions (>100 °C, >100 bar H_2 + CO). On the basis of high-pressure IR studies Alemdaroglu et al. claimed reaction 1 to be the principal route of aldehyde formation,[2] whereas Mirbach provided evidence for the predominant role of reaction 2.[3]

There is also some dispute over the mechanism of these reactions. In the case of R = EtO we have shown that the rate of ethyl formate formation is first order in $EtOC(O)Co(CO)_4$, first order in H_2 or $HCo(CO)_4$, and negative first order in CO. Most probably the bimolecular reaction between coordinatively unsaturated $EtOC(O)Co(CO)_3$ and the reducing agent is involved in the rate-determining step.[4] Similar kinetics were found for the cleavage of $EtOC(O)CH_2Co(CO)_4$ with H_2 or with $HCo(CO)_4$.[5] For R = *n*-C_5H_{11} in reaction 1, however, it has been reported that contrary to earlier findings[6] the rate of aldehyde formation was not affected by CO and the reaction may be radical in character.[7]

Recently one of use developed a new way for the preparation of pure *n*-butyrylcobalt tetracarbonyl (1) and isobutyrylcobalt tetracarbonyl (2) by the fast and quantitative reaction of $HCo(CO)_4$ at −79 °C with ethylketene and dimethylketene, respectively.[8] Both complexes are believed to be intermediates in the commercially important propene hydroformylation. Using these model substances, we now studied the kinetics of their reductive cleavage by H_2 and $HCo(CO)_4$ in order to obtain information about the relative importance of reactions 1 and 2 and about their mechanism.

Results

n-Butyraldehyde and isobutyraldehyde were formed in quantitative reactions from *n*-butyrylcobalt tetracarbonyl (1) and isobutyrylcobalt tetracarbonyl (2), respectively, using either $HCo(CO)_4$ or H_2 under 0.5–3-bar total pressure of CO or CO + H_2 mixtures at 20–45 °C in *n*-heptane solution according to the stoichiometries of eq 3–6.

$$\underset{\mathbf{1}}{n\text{-}PrC(O)Co(CO)_4} + HCo(CO)_4 \xrightarrow{r_3} n\text{-}PrCHO + Co_2(CO)_8 \quad (3)$$

$$\underset{\mathbf{2}}{i\text{-}PrC(O)Co(CO)_4} + HCo(CO)_4 \xrightarrow{r_4} i\text{-}PrCHO + Co_2(CO)_8 \quad (4)$$

$$2\,n\text{-}PrC(O)Co(CO)_4 + H_2 \xrightarrow{r_5} 2\,n\text{-}PrCHO + Co_2(CO)_8 \quad (5)$$

$$2\,i\text{-}PrC(O)Co(CO)_4 + H_2 \xrightarrow{r_6} 2\,i\text{-}PrCHO + Co_2(CO)_8 \quad (6)$$

The initial rates of these reactions could be measured by infrared spectroscopy following the decrease of acyl complex concentration and by the increase of product concentration. From the results of the kinetic measurements at 25 °C (Figure 1 and Table I), reaction rates first order in 1 or 2, approximately first order in $HCo(CO)_4$ or H_2, and approximately negative first order in CO were calculated. Both reductions showed a strong temperature dependence (Figure 2) and became faster by using $DCo(CO)_4$ and D_2 instead of $HCo(CO)_4$ and H_2, respectively (Table II).

At low concentrations of H_2 ($p_{H_2} \sim 1$ bar) no $HCo(CO)_4$ could be detected as an intermediate in reactions 5 and 6 by IR. At higher concentrations of H_2 (p_{H_2} = 50–80 bar), however, considerable amounts of $HCo(CO)_4$ accompanied the aldehyde product. Under the same conditions no $HCo(CO)_4$ could be detected in a blank experiment starting from $Co_2(CO)_8$ alone (Table III). These experiments show that aldehyde formation with H_2 occurs in two steps over

(1) Pino, P.; Piacenti, F.; Bianchi, M. "Organic Syntheses via Metal Carbonyls"; Wender, I., Pino, P., eds.; Wiley: New York, 1977; Vol. 2, pp 43–135.
(2) Alemdaroglu, N. H.; Penninger, J. L. M.; Oltay, E. *Monatsh. Chem.* **1976**, *107*, 1153.
(3) Mirbach, M. F. *J. Organomet. Chem.* **1984**, *265*, 205.
(4) Ungváry, F.; Markó, L. *Organometallics* **1983**, *2*, 1608.
(5) Hoff, C. D.; Ungváry, F.; King, R. B.; Markó, L. *J. Am. Chem. Soc.* **1985**, *107*, 666.
(6) (a) Breslow, D. S.; Heck, R. F. *Chem. Ind. (London)* **1960**, 467. (b) Heck, R. F.; Breslow, D. S. *J. Am. Chem. Soc.* **1961**, *83*, 4023.
(7) Azran, J.; Orchin, M. *Organometallics* **1984**, *3*, 197.
(8) Ungváry, F. *J. Chem. Soc., Chem. Commun.* **1984**, 824.
(9) (a) Cook, M. W.; Hanson, D. N.; Alder, B. J. *J. Chem. Phys.* **1957**, *26*, 748. (b) Lachowicz, S. K.; Newitt, D. M.; Weale, K. E. *Trans. Faraday Soc.* **1955**, *51*, 1198.
(10) (a) Gjaldbaek, J. C. *Acta Chem. Scand.* **1952**, *6*, 623. (b) Ungváry, F. *J. Organomet. Chem.* **1972**, *36*, 363.

0276-7333/86/2305-0209$01.50/0

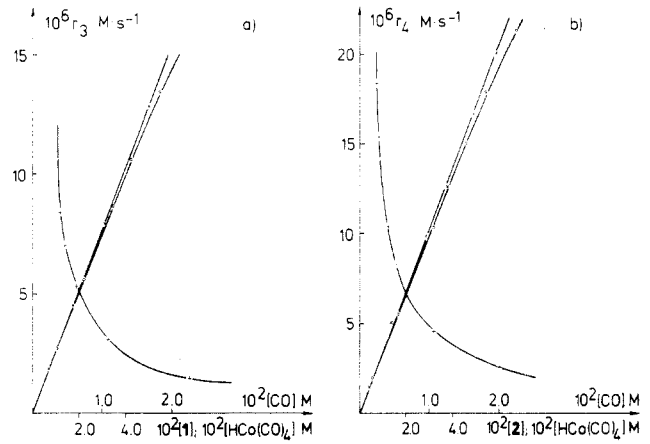

Figure 1. Influence of concentrations of initial rates of *n*-butyrylcobalt tetracarbonyl (**1**; r_3) and isobutyrylcobalt tetracarbonyl (**2**; r_4) consumption (eq 3 and 4) at 25 °C in *n*-heptane solution. a: ○, experiments at constant [**1**] = 0.0122 M and [CO] = 0.0108 M; ×, experiments at constant [HCo(CO)$_4$] = 0.0122 M and [CO] = 0.0108 M; +, experiments at constant [**1**] = [HCo(CO)$_4$] = 0.0122 M. b: ○, experiments at constant [**2**] = 0.0122 M and [CO] = 0.0108 M; ×, experiments at constant [HCo(CO)$_4$] = 0.0122 M and [CO] = 0.0108 M; +, experiments at constant [**2**] = [HCo(CO)$_4$] = 0.0122 M.

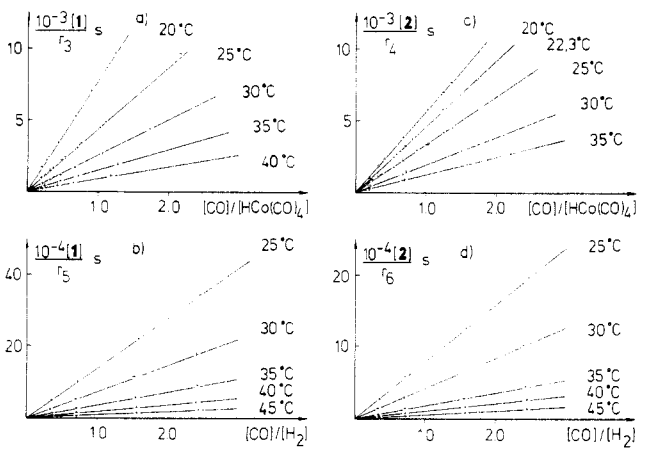

Figure 2. Kinetic data of reactions 3–6 in *n*-heptane at different temperatures plotted as [RC(O)Co(CO)$_4$]/r vs. [CO]/[H–X]: a, R = *n*-C$_3$H$_7$, X = Co(CO)$_4$; b, R = *n*-C$_3$H$_7$, X = H; c, R = *i*-C$_3$H$_7$, X = Co(CO)$_4$; d, R = *i*-C$_3$H$_7$, X = H.

reaction 2 followed by reaction 1, and at sufficiently high H_2 concentrations reaction 2 may become faster than reaction 1. The observed rates r_5 and r_6 are therefore at low H_2 concentrations twice as high as those of the primary reactions represented by eq 5a and 6a, respectively.

$$n\text{-PrC(O)Co(CO)}_4 + \text{H}_2 \xrightarrow{r_5'} n\text{-PrCHO} + \text{HCo(CO)}_4 \quad (5a)$$

$$i\text{-PrC(O)Co(CO)}_4 + \text{H}_2 \xrightarrow{r_6'} i\text{-PrCHO} + \text{HCo(CO)}_4 \quad (6a)$$

The data in Table III show that CO exerts its negative influence on the rates of reactions 5 and 6 not only around atmospheric pressure but also at high pressures as well.

By adding Ph_3P to solutions of **1** and **2** in *n*-heptane, 1 mol of CO was released and the Ph_3P derivatives of the acyls were formed (eq 7 and 8).

$$1 + \text{Ph}_3\text{P} \xrightarrow{r_7} n\text{-PrC(O)Co(CO)}_3(\text{PPh}_3) + \text{CO} \quad (7)$$

$$2 + \text{Ph}_3\text{P} \xrightarrow{r_8} i\text{-PrC(O)Co(CO)}_3(\text{PPh}_3) + \text{CO} \quad (8)$$

The rate of CO evolution in reactions 7 and 8 at 5–25 °C was first order in **1** and **2** and was dependent of both

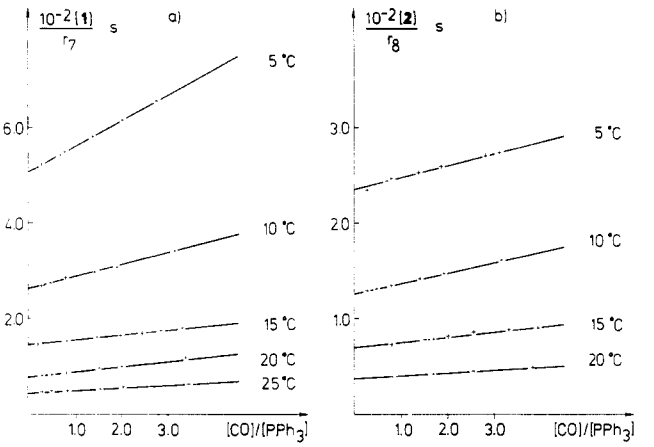

Figure 3. Kinetic data of reactions 7 and 8 in *n*-heptane at different temperatures plotted as [RC(O)Co(CO)$_4$]/r vs. [CO]/[Ph$_3$P]: a, R = *n*-C$_3$H$_7$; b, R = *i*-C$_3$H$_7$.

Scheme I

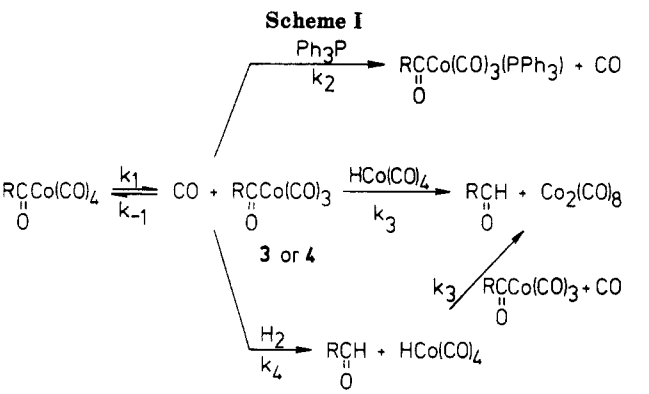

R = $CH_3(CH_2)_2$ in **1** and **3**
R = $(CH_3)_2CH$ in **2** and **4**

Ph_3P and CO concentration in a complex way (Table IV and Figure 3).[11] Kinetic data in Table IV show that Ph_3P had a slightly positive and CO had a slightly negative effect on the rates of reactions 7 and 8.

The observed negative effect of CO on the rates of reactions 3–8 can be rationalized by assuming the formation of an acylcobalt tricarbonyl in small concentrations followed by its reaction with either Ph_3P, $HCo(CO)_4$, or H_2 in competition with CO (Scheme I)

The kinetic measurements yielded linear plots of [acyl]/$r_{3,4}$ vs. [CO]/[HCo(CO)$_4$], [acyl]/$r_{5,6}'$ vs. [CO]/[H$_2$] (Figure 2), and [acyl]/$r_{7,8}$ vs. [CO]/[Ph$_3$P] (Figure 3) according to the expected rate laws for Scheme I using steady-state approximation for the acylcobalt tricarbonyl intermediate (eq 9–11). The rate constants k_{-1}/k_1k_2,

$$[\text{RC(O)Co(CO)}_4]/r_{7,8} = k_{-1}[\text{CO}]/k_1k_2[\text{Ph}_3\text{P}] + 1/k_1 \quad (9)$$

$$[\text{RC(O)Co(CO)}_4]/r_{3,4} = k_{-1}[\text{CO}]/k_1k_3[\text{HCo(CO)}_4] + 1/k_1 \quad (10)$$

$$[\text{RC(O)Co(CO)}_4]/r_{5,6}' = k_{-1}[\text{CO}]/k_1k_4[\text{H}_2] + 1/k_1 \quad (11)$$

k_{-1}/k_1k_3, k_{-1}/k_1k_4, and $1/k_1$ for Scheme I could be therefore

(11) Constant first-order rates, independent of phosphine concentration, have been found for the substitution of CO by Ph_3P for a great number of acylcobalt tetracarbonyls in diethyl ether solution. The rate constants of these reactions were regarded as a measure of the rate of CO dissociation from the acylcobalt tetracarbonyl.[12]

(12) Heck, R. F. *J. Am. Chem. Soc.* **1963**, *85*, 651.

Table I

a. Kinetic Data for Reactions of 1 and 2 with $HCo(CO)_4$ (Eq 3 and 4) at 25 °C in *n*-Heptane Solutions

10^2[1], M	10^2[2], M	10^2[3], M	10^2[CO],[a] M	$10^6 r_3$,[b] M·s^{-1}	$10^6 r_4$,[b] M·s^{-1}
0.74		1.22	1.08	1.91	
1.76		1.22	1.08	4.53	
3.10		1.22	1.08	7.95	
5.12		1.22	1.08	12.84	
1.22		1.07	1.08	2.75	
1.22		2.21	1.08	5.62	
1.22		3.46	1.08	8.70	
1.22		4.26	1.08	10.65	
1.22		5.48	1.08	13.47	
1.22		1.22	0.40	8.40	
1.22		1.22	0.47	7.04	
1.22		1.22	0.63	5.35	
1.22		1.22	1.07	3.14	
1.22		1.22	2.25	1.49	
	0.43	1.22	1.08		1.47
	1.34	1.22	1.08		5.06
	2.86	1.22	1.08		9.83
	3.72	1.22	1.08		12.59
	4.86	1.22	1.08		14.35
	5.89	1.22	1.08		20.08
	1.22	0.61	1.08		2.08
	1.22	1.64	1.08		5.53
	1.22	3.15	1.08		10.35
	1.22	4.56	1.08		15.05
	1.22	5.44	1.08		17.90
	1.22	6.75	1.08		21.40
	1.22	1.22	0.24		18.41
	1.22	1.22	0.28		15.43
	1.22	1.22	0.42		10.41
	1.22	1.22	0.53		8.37
	1.22	1.22	1.07		4.61
	1.22	1.22	2.00		2.56

b. Kinetic Data for Reactions of 1 and 2 with H_2 (Eq 5 and 6) at 25 °C in *n*-Heptane Solutions

10^2[1], M	10^2[2], M	10^3[H_2],[c] M	10^3[CO],[a] M	$10^7 r_5$,[b] M·s^{-1}	$10^7 r_6$,[b] M·s^{-1}
1.37		2.14	5.29	0.80	
1.18		2.60	4.10	1.08	
0.57		3.28	2.38	1.13	
1.35		3.28	2.38	2.68	
2.14		3.28	2.38	4.23	
1.21		3.70	1.30	4.93	
	1.29	2.15	5.32		1.30
	1.19	2.61	4.12		1.88
	2.41	2.15	5.32		2.43
	2.35	2.61	4.12		3.71
	3.84	2.15	5.32		3.87
	1.31	3.25	2.36		4.50
	3.50	2.59	4.12		5.53
	4.05	2.59	4.08		6.40
	4.96	3.25	4.08		7.83
	1.27	1.29	0.45		8.99
	1.27	3.76	1.29		9.00

[a] Calculated from p_{CO} and the solubility of CO in *n*-heptane.[10] [b] Initial rates measured by IR. [c] Calculated from p_{H_2} and the solubility of H_2 in *n*-heptane.[9]

Table II. Kinetic Isotope Effects on the Initial Rates of the Reactions 3–6 at 25 °C in *n*-Heptane Solutions

10^2[1], M	10^2[2], M	10^2[$HCo(CO)_4$], M	10^3[H_2],[a] M	10^3[CO],[b] M	$10^7 r_3$, M·s^{-1}	$10^7 r_4$, M·s^{-1}	$10^7 r_5$, M·s^{-1}	$10^7 r_6$, M·s^{-1}
1.21		1.07		10.8	27.2			
1.00		0.68[c]		10.7	17.9			
	1.34	1.11		10.7		46.0		
	0.98	1.14[c]		10.7		50.1		
1.21			3.70	1.30			4.9	
1.89			3.92[d]	1.07			10.4	
	1.27		3.76	1.29				9.0
	1.44		3.92[d]	1.07				14.4

[a] Calculated from p_{H_2} (or p_{D_2}) and the solubility of H_2 (or D_2) in *n*-heptane.[9] [b] Calculated from p_{CO} and the solubility of CO in *n*-heptane.[10] [c] $DCo(CO)_4$. [d] D_2.

derived from the kinetic data as the slopes and the intercepts of Figures 2 and 3 and are collected in Tables V and VI. It should be noted here, that the numbers compiled in Tables V and VI were calculated by regression analysis of the measured values and not evaluated from Figures 2 and 3.

The acyl complexes **1** and **2** are stable in hydrocarbon solution at room temperature under an atmospheric

Table III. Effect of CO and H_2 on the Conversion of 1 or 2 into $HCo(CO)_4$, $Co_2(CO)_8$, and the Corresponding *n*-Butyraldehyde or Isobutyraldehyde under Pressure at 45 °C (Initial Concentrations [1] = [2] = 0.015 M)

p_{CO}, bar	p_{H_2}, bar	time, min	convn of 1, %	convn of 2, %	$[HCo(CO)_4]/[Co_2(CO)_8]$
1	80	10			0.00[a]
1	80	10	68		0.94
1	80	10		>95	0.62
10	50	10		38	
10	50	15		63	1.63
10	50	20		76	
10	50	35		87	
14	50	25	39		1.92
20	50	15		36	
20	50	25	25		1.78
60	50	15		12	
60	50	30		25	0.77
66	50	25	8		
120	50	15		6	
100	50	30		14	
120	50	25	4		

[a] Experiment started with $[Co_2(CO)_8]$ = 0.015 M, without 1 or 2.

Table IV. Initial Rates of CO Substitution in 1 and 2 by Ph_3P at Various Conditions in *n*-Heptane Solution

temp, °C	10^3[1], M	10^3[2], M	$10^2[Ph_3P]$, M	10^3[CO],[a] M	$10^6 r_7$, M·s^{-1}	$10^6 r_8$, M·s^{-1}
5	4.53		3.33	9.17	8.7	
5	4.53		1.20	9.18	8.3	
5	4.53		0.67	9.18	7.8	
5	4.53		0.45	9.18	7.4	
5	4.53		0.67	4.54	8.4	
5	4.53		0.67	18.4	6.9	
5		4.53	3.33	9.17		19.4
5		4.53	1.20	9.27		18.4
5		4.53	0.67	9.27		18.0
5		4.53	0.50	9.27		17.6
5		4.53	0.30	9.27		16.6
5		4.53	0.67	4.66		18.6
5		4.53	0.67	18.7		16.8
15	4.53		0.30	9.89	14.3	
15	2.47		0.35	9.93	25.5	
15	4.53		0.40	9.75	27.0	
15	4.53		0.50	9.85	27.8	
15	0.90		0.67	9.85	5.6	
15	1.81		0.67	9.86	11.5	
15	4.53		0.67	9.89	28.3	
15	9.04		0.67	9.86	57.6	
15	4.53		1.20	9.88	29.8	
15	4.52		5.00	9.88	31.2	
15		2.46	0.25	9.92		27.3
15		5.00	0.30	9.94		56.8
15		2.46	0.39	9.92		29.6
15		5.00	0.50	9.94		58.7
15		1.00	0.67	9.93		12.4
15		5.00	0.67	9.82		25.8
15		10.0	0.67	9.84		129
15		2.46	0.59	9.92		31.5
15		2.00	0.67	9.82		25.8
15		2.46	1.25	9.92		33.7

[a] Calculated from p_{CO} and the solubility of CO in *n*-heptane.[10].

pressure of CO. Decomposition leading to $Co_2(CO)_8$, CO, propene, traces of propane, and the corresponding butyraldehydes[13] occurs only above 50 °C[15] at a rate convenient to measure by IR and gas evolution (Table VII). Under 80 bar CO no change of the acyl concentration or structure could be detected by IR in 1 h at 80 °C. In hydrocarbon solutions we never observed the isomerization of unreacted acyls during any of our experiments.[16]

Discussion

The Mechanism of Cleavage. The inhibiting effect of CO on the reactions of 1 and 2 with $HCo(CO)_4$, H_2, or Ph_3P suggests a tricarbonyl complex as intermediate formed by CO dissociation from the corresponding acylcobalt tetracarbonyl. This intermediate may react either with CO reforming the tetracarbonyl complex or with other reagents such as Ph_3P, $HCo(CO)_4$, and H_2 leading to the

(13) Slow disproportionation of the products from the reaction of butyryl halides and $NaCo(CO)_4$ in ether at room temperature into propene and a mixture of *n*-butyraldehyde and isobutyraldehyde have been reported.[14]

(14) Rupilius, W.; Orchin, M. *J. Org. Chem.* **1972**, *37*, 936.

(15) Pyrolysis of in situ formed propionylcobalt tetracarbonyl at 170 °C yielding 50% ethene, propionaldehyde, and a little ethane has been reported.[6b]

(16) Extensive isomerization of 1 and 2 during their formation from the corresponding acyl halide and $KCo(CO)_4$ at 25 °C in ether has been reported.[17] The conclusion was based on the formation of isomeric carboxylic acid *n*-propyl esters after decomposing the acyl complexes with I_2 + *n*-propyl alcohol.

(17) (a) Takegami, Y.; Yokokawa, C.; Watanabe, Y.; Okuda, Y. *Bull. Chem. Soc. Jpn.* **1964**, *37*, 181. (b) Takegami, Y.; Yokokawa, C.; Watanabe, Y.; Masada, H.; Okuda, Y. *Bull. Chem. Soc. Jpn.* **1965**, *38*, 787.

Table V. Rate Constants[a] for Reactions 3–8 at Various Temperatures

temp, °C	compd	k_{-1}/k_1k_2, s	$1/k_1$, s	k_{-1}/k_1k_3, s	$1/k_1$, s	k_{-1}/k_1k_4, s	$1/k_1$, s
5	1	54 ± 1	506 ± 2				
10	1	25 ± 2	261 ± 3				
15	1	10 ± 1	143 ± 2				
20	1	11 ± 0.2	77 ± 0.3	7673 ± 8	82 ± 5		
25	1	5 ± 0.3	43 ± 0.5	4332 ± 16	51 ± 2	139186 ± 48	68 ± 32
25	1			4637[b]		133044[c]	
30	1			2464 ± 9	31 ± 8	73316 ± 36	29 ± 26
35	1			1440 ± 11	19 ± 9	36396 ± 12	20 ± 8
40	1			875 ± 9	12 ± 6	17420 ± 8	10 ± 5
45	1					8712 ± 2	6 ± 1
5	2	13 ± 2	233 ± 4				
10	2	11 ± 0.4	126 ± 1				
15	2	5 ± 1	69 ± 3				
20	2	3 ± 0.5	37 ± 1	5625 ± 5	47 ± 5		
25	2			3297 ± 4	27 ± 4	80286 ± 2	28 ± 1
25	2			2018[b]		71920[c]	
30	2			1913 ± 6	17 ± 6	42416 ± 8	18 ± 6
35	2			1208 ± 3	10 ± 4	18852 ± 2	11 ± 2
40	2					10848 ± 8	7 ± 3
45	2					5382 ± 2	5 ± 1

[a] Deviations represent 95% confidence level. [b] From experiments using $DCo(CO)_4$. [c] From experiments using D_2.

Table VI. Temperature Dependence of the Rate Constants and the Calculated Thermodynamic Parameters[a]

compd	temp range, °C		$\Delta H^{\ddagger}_{25\,°C}$, kcal·mol^{-1}	$\Delta S^{\ddagger}_{25\,°C}$, eu
1	5–45	$\log k_1 = (13.22 \pm 0.08) - (4427 \pm 23)/T$	19.6 ± 0.1	0.1 ± 0.4
2	5–45	$\log k_1 = (13.20 \pm 0.21) - (4330 \pm 60)/T$	19.2 ± 0.3	0.0 ± 1
1	5–25	$\log k_1k_2/k_{-1} = (12.37 \pm 2.11) - (3901 \pm 608)/T$	17.2 ± 2.8	−3.8 ± 9.7
2	5–20	$\log k_1k_2/k_{-1} = (12.02 \pm 2.24) - (3669 \pm 640)/T$	16.2 ± 2.9	−5.4 ± 10.3
1	20–40	$\log k_1k_3/k_{-1} = (10.92 \pm 0.25) - (4337 \pm 78)/T$	19.2 ± 0.4	−10.5 ± 1.2
2	20–35	$\log k_1k_3/k_{-1} = (6.94 \pm 3.79) - (3121 \pm 356)/T$	13.7 ± 1.6	−53.8 ± 42
1	25–45	$\log k_1k_4/k_{-1} = (14.10 \pm 1.34) - (5740 \pm 417)/T$	25.7 ± 1.9	4.1 ± 6.2
2	25–45	$\log k_1k_4/k_{-1} = (13.78 \pm 1.56) - (5570 \pm 480)/T$	26.4 ± 2.2	2.7 ± 11.2

[a] Deviations represent 95% confidence level; k_1 (s^{-1}); k_1k_2/k_{-1} (s^{-1}); k_1k_3/k_{-1} (s^{-1}); k_1k_4/k_{-1} (s^{-1}); T = temperature in Kelvin.

Table VII. Initial Rate of Decomposition (r) of 1 and 2 under CO at 750 mmHg Total Pressure in *n*-Octane Solution ([1] = 0.0137 M; [2] = 0.0147 M)

	10^6r, M·s^{-1}	
temp, °C	1	2
60	0.82	1.1
70	5.3	7.3
80	31	48
80	0.0[a]	0.0[a]

[a] Under 80 bar CO.

products according to Scheme I. The reasonable agreement of the rate constant k_1 in these reactions (Table V) derived from the kinetic measurements assuming steady-state concentrations for **3** or **4** supports this assumption. The equilibria leading to **3** and **4** are certainly far on the side of the tetracarbonyls because the IR spectra of **1** or **2** did not show the presence of tricarbonyls in detectable concentrations in the absence of Ph_3P, $HCo(CO)_4$, H_2, and CO even at 45 °C.

The formation of propene and butyraldehydes as main products by thermal decomposition of **1** or **2** above 50 °C does also not support in the case of **1** and **2** the suggestion[18] and the results published for *n*-hexanoylcobalt tetracarbonyl[7] according to which aldehyde formation should be preceded by homolytic dissociation of the Co–acyl bond. The acyl radicals would in the absence of an appropriate reagent decarbonylate to the corresponding alkyl radicals which in turn would lead to a 1:1 mixture of alkene and alkane by disproportionation together with radical combination products. At 80 °C the decomposition of **1** and **2**, however, yielded nearly 50% aldehyde, 49% propene, and only 1% propane. This is in accord with the results of the high-temperature (170 °C) decomposition of propionylcobalt tetracarbonyl[6b] and the disproportionation of acylcobalt tetracarbonyls under N_2 at room temperature.[14] Apparently the spontaneous thermal reaction of acylcobalt tetracarbonyls is the reverse of their formation from alkenes, $HCo(CO)_4$, and CO (eq 12) and the formation of aldehyde and $Co_2(CO)_8$ during this decomposition is due to the secondary reaction between the acyl complexes and $HCo(CO)_4$ (eq 13).

$$RCH_2CH_2C(O)Co(CO)_4 \xrightarrow{\Delta} RCH{=}CH_2 + HCo(CO)_4 + CO \quad (12)$$

$$RCH_2CH_2C(O)Co(CO)_4 + HCo(CO)_4 \rightarrow RCH_2CH_2CHO + Co_2(CO)_8 \quad (13)$$

The inhibiting effect of CO on the reaction of **1** or **2** with H_2 could be observed up till 120 bar (Table III), suggesting that the mechanism of cleavage does not change even under the conditions of high-pressure catalytic hydroformylation. As to our opinion a radical mechanism of aldehyde formation may be therefore ruled out as an alternative for the hydroformylation of aliphatic olefins with unsubstituted cobalt carbonyls as catalysts.

Such a mechanism remains a distinctive possibility, however, for the Shell process which uses phosphine-substituted cobalt carbonyls as catalysts.[19] It has been shown that phosphine substitution favors the radical pathway in the case of acylmanganese carbonyl complexes because of disfavoring CO loss and enhancing steric destabilization.[20] A similar effect may be reasonably expected for analogous cobalt complexes.

(18) Halpern, J. *Pure Appl. Chem.* **1979**, *51*, 2171.

(19) Slaugh, L. H.; Mullineaux, R. D. *J. Organomet. Chem.* **1968**, *13*, 469.

(20) Nappa, M. J.; Santi, R.; Halpern, J. *Organometallics* **1985**, *4*, 34.

Table VIII. Comparison of Rate Constants for 25 °C

	1	2
k_1, s^{-1}	0.0233	0.0468
k_1k_2/k_{-1}, s^{-1}	0.19	0.51
$10^5k_1k_3/k_{-1}$, s^{-1}	23.3	29.5
	27.4[a]	49.5[a]
$10^5k_1k_4/k_{-1}$, s^{-1}	0.69	1.21
	0.75[b]	1.39[b]
k_2/k_{-1}	8.2	11
k_3/k_{-1}	0.010	0.0063
k_4/k_{-1}	0.00030	0.00026
k_3/k_3^a	0.85	0.60
k_4/k_4^b	0.92	0.87
k_3/k_4	34	24

[a] With $DCo(CO)_4$. [b] With D_2.

Dihydrogen vs. $HCo(CO)_4$ as a Reductant. As can be seen from the k_3/k_4 values in Table VIII, $HCo(CO)_4$ is at 25 °C 34 or 24 times more reactive than H_2 against 1 or 2, respectively. The higher reactivity of $HCo(CO)_4$ seems to be general for alkyl- or acylcobalt carbonyls under such conditions: the same ratio was found to be 12 in the case of $EtOC(O)Co(CO)_4$[4] and 130 with $EtOC(O)CH_2Co(CO)_4$.[5]

In drawing conclusions from these data with regard to the relative role of H_2 or $HCo(CO)_4$ under conditions of catalytic hydroformylation two important differences have to be considered. First, under the high pressures used in the catalytic process the concentration of H_2 in the reaction mixture will be about 2 orders of magnitude higher than that of $HCo(CO)_4$.[3] Second, due to the significantly larger enthalpies of activation for the reactions with H_2 (see Table VI), at the temperatures necessary for the catalytic process (>100 °C) the relative reactivity of H_2 will be much nearer to that of $HCo(CO)_4$ or even surpass it. Thus, for example, extrapolating the k_3/k_4 values to 80 °C, we obtain 6.2 for complex 1 and 1.2 for complex 2.

It can be stated therefore that mainly H_2 will be responsible for aldehyde formation from acylcobalt carbonyls under the industrial conditions of hydroformylation and the reaction with $HCo(CO)_4$ will only play a minor role. This conclusion is in agreement with the most recent measurements performed under catalytic conditions[3] and confirms the original proposal of Heck[6] put forward 25 years ago.

The inverse isotope effects obtained with D_2 and $DCo(CO)_4$ (Table VIII) are presumably of thermodynamic origin. We suggest that in both cases adducts are formed as primary products from the acylcobalt tricarbonyls 3 or 4 and the reductants in equilibrium reactions and that these adducts are more stable with the deuterium-containing species than with the hydrogen-containing analogues. Accordingly we propose the fine mechanisms (14) and (15) for steps 3 and 4 of Scheme I. Reversible ad-

$$RC(O)Co(CO)_3 + H_2 \rightleftharpoons RC(O)CoH_2(CO)_3 \xrightarrow{CO} RCHO + HCo(CO)_4 \quad (14)$$

$$RC(O)Co(CO)_3 + HCo(CO)_4 \rightleftharpoons RC(O)Co(CO)_3 \xrightarrow{CO} \begin{matrix} RC(O)Co(CO)_3 \\ | \\ H \\ | \\ Co(CO)_4 \end{matrix} \rightarrow RCHO + Co_2(CO)_8 \quad (15)$$

dition of H_2 or D_2 to coordinatively unsaturated transition-metal complexes is well documented;[21a] H- (or D-) bridged structures are also well-known[21b] and have been already invoked also as intermediates in similar reactions.[22]

Experimental Section

General Techniques. Infrared spectra were recorded on a Carl Zeiss Jena IR 75 spectrophotometer using a thermostated KBr cuvette. Analysis of the volatile compounds was performed on an analytical Hewlett-Packard Model 5830A gas chromatograph or on a Chromatron GCHF 18.3-1 gas chromatograph. All manipulations involving air-sensitive organometallic compounds were carried out by using anaerobic techniques.[23]

Materials. Hydrocarbon solvents were dried on sodium wire and were distilled under a CO atmosphere. Stock solutions of $HCo(CO)_4$ (0.6 M) were prepared in *n*-heptane from $Co_2(CO)_8$, DMF, and concentrated HCl.[24] $DCo(CO)_4$ was prepared from $HCo(CO)_4$ solutions by hydrogen and deuterium exchange with a 50-fold molar excess of D_2O.[25] Isotopic purity was >95% as calculated from mass spectrometric measurements of its decomposition products. The concentration of $HCo(CO)_4$ and $DCo(CO)_4$ solutions were determined by 0.1 N alkaline titration at 0 °C under CO. *n*-Butyrylcobalt tetracarbonyl (1) and isobutyrylcobalt tetracarbonyl (2) were prepared by the published method[8] from $HCo(CO)_4$ and ethylketene or dimethylketene, respectively. Stock solutions of the acylcobalt tetracarbonyls (0.2 M) in *n*-heptane were used in the kinetic experiments.

Kinetic runs using $HCo(CO)_4$ were performed under CO in a thermostated (±0.05 °C) reaction vessel connected to a 5-L buffer flask in order to maintain the pressure constant (0.2–3 bar). The actual total pressure was determined in millimeters of Hg by using an open mercury manometer measuring the pressure difference between the atmosphere and the reaction vessel. The reaction was started by injecting 0.6 M solutions of $HCo(CO)_4$ in *n*-heptane into vigorously stirred solutions of the acyl complexes in *n*-heptane. The change of IR spectra was followed from samples withdrawn by a gas-tight syringe and filled through a three-way Hamilton valve and Teflon tubing into the 0.11- or 0.25-mm KBr cuvette. [Absorbancies (*n*-heptane): 2116 ($\epsilon_M(HCo(CO)_4)$ 330 ± 10),[26] 2105 (ϵ_M(1) 1420),[27] 2104 (ϵ_M(2) 1490),[27] 1857 ($\epsilon_M(Co_2(CO)_8)$ 1735),[28] 1735 ($\epsilon_M(CH_3CH_2CH_2CHO)$ 208), 1742 ($\epsilon_M((CH_3)_2CHCHO)$ 228), 1717 (ϵ_M(1) 418),[27] 1737 (ϵ_M(2) 500),[27] 1699 cm^{-1} (ϵ_M(2) 370 cm^2 $mmol^{-1}$).[27]]

Reduction of 1 and 2 with H_2. In the kinetic runs H_2 + CO mixtures were used and the reactions were started by injecting 0.2 M solutions of the acyl complex in *n*-heptane into vigorously stirred *n*-heptane under a constant pressure between 0.2 and 3 bar. The composition of the gas mixture was checked by gas chromatography (3 m, Porapack Q, 25 °C, 5 mL/min of Ar, TCD). The change of IR spectra was followed as described above.

Reduction of 1 and 2 with H_2 under 80-Bar Pressure. The 5-mL samples of 0.015 M solutions of 1 or 2 in *n*-heptane were placed at room temperature under CO in a 20-mL stainless-steel rocking autoclave and pressurized to 80 bar with H_2. After 10-min agitation at 45 °C the autoclave was cooled to +5 °C and IR spectra were taken immediately after the pressure was released by using a cold (+5 °C) CaF_2 IR cell. The spectrum showed 68% conversion of 1 into *n*-butyraldehyde and $HCo(CO)_4$ + $Co_2(CO)_8$ in a 1:1.06 molar ratio. In the case of 2, 95% conversion into isobutyraldehyde and a 1:1.93 ratio of $HCo(CO)_4$ to $Co_2(CO)_8$ was found. In blank experiments using a 0.015 M solution of $Co_2(CO)_8$ in *n*-heptane no detectable amount of $HCo(CO)_4$ could be found by IR analysis, after 10-min agitation at 45 °C under 80 bar H_2. The same technique was used in experiments performed under p_{H_2} = 50 bar and p_{CO} = 10–120 bar pressures.

Decomposition of 1 and 2 under atmospheric pressure of CO was followed by using the gasometric apparatus and IR technique

(21) (a) Schunn, R. A. In "Transition Metal Hydrides"; Muetterties, E. L., Ed.; Marcel Dekker: New York, 1971; Vol. 1, p 210. (b) Frenz, B. A.; Ibers, J. A. *Ibid.*, p 60.

(22) Jones, W. D.; Bergman, R. G. *J. Am. Chem. Soc.* **1979**, *101*, 5447.

(23) (a) Thomas, G. *Chem.-Ztg., Chem. Appar.* **1961**, *85*, 567. (b) Shriver, D. F. "The Manipulation of Air-Sensitive Compounds"; R. E. Krieger Publishing Co.: Malabar, FL 1982.

(24) Kirch, L.; Orchin, M. *J. Am. Chem. Soc.* **1958**, *80*, 4428.

(25) Roos, L. Ph.D. Dissertation, University of Cincinnati, Cincinnati, OH, 1965; p 81.

(26) Tannenbaum, R. Dissertation ETH Zurich No. 6970, 1980, p 36.

(27) Ungváry, F. *J. Organomet. Chem.*, to be submitted for publication.

(28) Reference 26, p 31.

described before. The rate of gas evolution corresponded to the rate of acyl decomposition between 50 and 80 °C. During the decomposition of 1 or 2, isomerization of the acyl compounds did not occur. The composition of the reaction mixture was checked by IR with the ν(CO) bands of terminal CO ligands as a control of concentration and the acyl ν(CO) bands as a control of structure.

The organic products of decomposition were investigated in experiments performed at 80 °C and 1-h reaction time in sealed 20-mL ampules with 2-mL samples of 0.02 M solutions of 1 and 2 in *n*-octane containing *n*-pentane as internal reference for quantitative GC analysis (3 m, *n*-octane/Porasil C, 50 °C, 15 mL/min of Ar, FID). The decompositions yielded 45–48% propene, 1% propane, and 37% *n*-butyraldehyde (if starting from 1) or 45% isobutyraldehyde (if starting from 2).

Stability of 1 and 2 at 80 °C under CO Pressure. The 5-mL samples of 0.014 M solutions of 1 or 2 in *n*-heptane were placed at room temperature under CO in a 20-mL stainless-steel rocking autoclave and pressurized to 80 bar with CO. After 1-h agitation at 80 °C, the IR spectra of the reaction mixtures at room temperature showed within 1% accuracy unchanged concentrations of the acyl complexes as measured at 2105 cm^{-1}. No traces of isomerized acylcobalt tetracarbonyl could be recognized in the characteristic organic ν(CO) range of 1 and 2.

Reaction of Ph_3P with 1 and 2 was performed in the gasometric apparatus described above and started by injecting the acyl stock solutions into solutions containing known amounts of Ph_3P. In all kinetic experiments initial rates were calculated from graphical plots below 15% conversion.

Registry No. 1, 38722-67-7; 2, 38784-32-6; $HCo(CO)_4$, 16842-03-8; Hz, 1333-74-0; CO, 630-08-0; *n*-PrCHO, 123-72-8; *i*-PrCHO, 78-84-2; $Co2(CO)_8$, 10210-68-1; *n*-$PrC(O)Co(CO)_3(PPh_3)$, 34151-25-2; *i*-$PrC(O)Co(CO)_3(PPh_3)$, 99495-72-4; PPh_3, 603-35-0; propene, 115-07-1.

Rhodium(III)-to-Rhodium(I) Alkyl Transfer: A Rhodium Macrocycle Which Is Both Nucleophile and Leaving Group

James P. Collman,* John I. Brauman, and Alex M. Madonik

Department of Chemistry, Stanford University, Stanford, California 94305

Received February 12, 1985

The rhodium(I) macrocycles $Rh^I(BPDOBF_2)$ (**1a**) and $Rh^I(PPDOBF_2)$ (**1b**) are strong nucleophiles toward alkyl halides and may also be alkylated by their rhodium(III) alkyl halide adducts $R'-Rh^{III}(BPDOBF_2)-X$ and $R'-Rh^{III}(PPDOBF_2)-X$ (**2a** and **2b**), respectively. In the latter process, **1a,b** act as both nucleophile and leaving group. We have studied the kinetics of alkyl exchange between, e.g., **1a** and **2b** by ^1H NMR and the rate constants are $(5.8 \pm 0.5) \times 10^{-3}$ M^{-1} s^{-1} for methyl exchange (R' = Me, X = I) and $(6.4 \pm 1.0) \times 10^{-2}$ M^{-1} s^{-1} for benzyl exchange (R' = $PhCH_2$, X = Cl). Other alkyl groups do not participate in this reaction. These data are consistent with rhodium(I) attack at carbon; the process may be viewed as a carbon-bridged two-electron transfer. Halide-bridged electron transfer is implied in the much faster exchange ($k > 0.5$ M^{-1} s^{-1}) between **1a,b** and their rhodium(III) dichloride derivatives **3a** and **3b**.

Introduction

Low-valent transition-metal complexes exhibit nucleophilic behavior in many of their oxidative-addition reactions with alkyl halides, leading to the formation of metal–carbon bonds via an S_N2-like process.[1] The ability of metal centers to function as leaving groups is less widely recognized, despite scattered reports.[2] These include several examples of essentially degenerate nucleophilic reactions in which the same type of metal center serves as both nucleophile and leaving group[2a,b,c,e] (eq 1). The

$$M_1^n + R'-M_2^{n+2} \rightleftharpoons R'-M_1^{n+2} + M_2^n \quad (1)$$

latter reactions result in the transfer of an alkyl group from one metal center to another and may be viewed as carbon-bridged inner-sphere two-electron-transfer processes.[3] When the two centers are distinguished by a minor ligand modification, these exchange reactions are nearly thermoneutral, and their study should throw light on the kinetic factors which control two-electron processes that make and break metal–carbon bonds.[4]

We encountered a novel example of the process represented by eq 1 in the course of our studies on the oxidative addition of alkyl halides to a Rh(I) macrocycle.[1,5] We

(1) Collman, J. P.; Brauman, J. I; Madonik, A. M. *Organometallics*, following paper in this issue.

(2) (a) Johnson, R. W.; Pearson, R. G. *J. Chem. Soc., Chem. Commun.* **1970**, 986–987. (b) Dodd, D.; Johnson, M. D. *J. Chem. Soc., Chem. Commun.* **1971**, 1371–1372. (c) Mestroni, G.; Cocevar, C.; Costa, G. *Gazz. Chim. Ital.* **1973**, *103*, 273–285. (d) Schrauzer, G. N.; Stadlbauer, E. A. *Bioinorg. Chem.* **1974**, *3*, 353–366. Stadlbauer, E. A.; Holland, R. J.; Lamm, F. P.; Schrauzer, G. N. *Bioinorg. Chem.* **1974**, *4*, 67–77. (e) Dodd, D.; Johnson, M. D.; Lockman, B. L. *J. Am. Chem. Soc.* **1977**, *99*, 3664–3673.

(3) Reviews of inner-sphere electron transfer: (a) Taube, H. "Electron Transfer Reactions of Complex Ions in Solution"; Academic Press: New York, 1970. (b) Linck, R. G. *Surv. Prog. Chem.* **1976**, *7*, 89–147. (c) Sutin, N. "Inorganic Biochemistry"; Eichhorn, G. L., Ed.; Elsevier: New York, 1974; Chapter 7.

(4) Several groups have undertaken the analysis of "intrinsic" kinetic barriers to nucleophilic reactions in which the Marcus theory[4a] of electron transfer is applied to reactivity data for methyl transfer in the gas phase[4b–d] or in solution.[4e] Endicott's group has made an extensive analysis of the analogous S_H2 mechanism implicated in methyl and halide transfer between Co(II) and Co(III) macrocycles.[4f–h] (See also ref 4i.) (a) Marcus, R. A. *Annu. Rev. Phys. Chem.* **1964**, *15*, 155–196. (b) Shaik, S. S.; Pross, A. *J. Am. Chem. Soc.* **1982**, *104*, 2708–2719. (c) Wolfe, S.; Mitchell, D. J.; Schlegel, H. B. *J. Am. Chem. Soc.* **1981**, *103*, 7694–7696. (d) Pellerite, M. J.; Brauman, J. I. *J. Am. Chem. Soc.* **1983**, *105*, 2672–2680. Pellerite, M. J.; Brauman, J. I. *J. Am. Chem. Soc.* **1980**, *102*, 5993–5999. (e) Albery, W. J.; Kreevoy, M. M. *Adv. Phys. Org. Chem.* **1978**, *16*, 87–157. (f) Endicott, J. F.; Wong, C.-L.; Ciskowski, J. M.; Balakrishnan, K. P. *J. Am. Chem. Soc.* **1980**, *102*, 2100–2103. (g) Endicott, J. F.; Balakrishnan, K. P.; Wong, C.-L. *J. Am. Chem. Soc.* **1980**, *102*, 5519–5526. (h) Durham, B.; Endicott, J. F.; Wong, C.-L.; Rillema, D. P. *J. Am. Chem. Soc.* **1979**, *101*, 847–857. (i) Johnson, M. D. *Acc. Chem. Res.* **1983**, *16*, 343–349.

(5) Preliminary report: Collman, J. P.; MacLaury, M. R. *J. Am. Chem. Soc.* **1974**, *96*, 3019–3020. We have since adopted a modified nomenclature for the macrocyclic ligands: $(PPDOBF_2)$ = [difluoro[*N,N'*-bis(3-pentanon-2-ylidene)-1,3-diaminopropane)dioximato]borate], and $(BPDOBF_2)$ = [difluoro[*N,N'*-bis(3-butanon-2-ylidene)-1,3-diaminopropane)-dioximato]borate]. Other abbreviations: PPN^+ = bis(triphenylphosphoranediyl)nitrogen(1+) ion.

0276-7333/86/2305-0215$01.50/0

Rhodium(III)-to-rhodium(I) alkyl transfer: a rhodium macrocycle which is both nucleophile and leaving group

James P. Collman, John I. Brauman, and Alex M. Madonik

Organometallics, **1986**, 5 (2), 215-218• DOI: 10.1021/om00133a007 • Publication Date (Web): 01 May 2002

described before. The rate of gas evolution corresponded to the rate of acyl decomposition between 50 and 80 °C. During the decomposition of 1 or 2, isomerization of the acyl compounds did not occur. The composition of the reaction mixture was checked by IR with the ν(CO) bands of terminal CO ligands as a control of concentration and the acyl ν(CO) bands as a control of structure.

The organic products of decomposition were investigated in experiments performed at 80 °C and 1-h reaction time in sealed 20-mL ampules with 2-mL samples of 0.02 M solutions of 1 and 2 in *n*-octane containing *n*-pentane as internal reference for quantitative GC analysis (3 m, *n*-octane/Porasil C, 50 °C, 15 mL/min of Ar, FID). The decompositions yielded 45–48% propene, 1% propane, and 37% *n*-butyraldehyde (if starting from 1) or 45% isobutyraldehyde (if starting from 2).

Stability of 1 and 2 at 80 °C under CO Pressure. The 5-mL samples of 0.014 M solutions of 1 or 2 in *n*-heptane were placed at room temperature under CO in a 20-mL stainless-steel rocking autoclave and pressurized to 80 bar with CO. After 1-h agitation at 80 °C, the IR spectra of the reaction mixtures at room temperature showed within 1% accuracy unchanged concentrations of the acyl complexes as measured at 2105 cm^{-1}. No traces of isomerized acylcobalt tetracarbonyl could be recognized in the characteristic organic ν(CO) range of 1 and 2.

Reaction of Ph_3P with 1 and 2 was performed in the gasometric apparatus described above and started by injecting the acyl stock solutions into solutions containing known amounts of Ph_3P. In all kinetic experiments initial rates were calculated from graphical plots below 15% conversion.

Registry No. 1, 38722-67-7; 2, 38784-32-6; $HCo(CO)_4$, 16842-03-8; Hz, 1333-74-0; CO, 630-08-0; *n*-PrCHO, 123-72-8; *i*-PrCHO, 78-84-2; $Co2(CO)_8$, 10210-68-1; *n*-$PrC(O)Co(CO)_3(PPh_3)$, 34151-25-2; *i*-$PrC(O)Co(CO)_3(PPh_3)$, 99495-72-4; PPh_3, 603-35-0; propene, 115-07-1.

Rhodium(III)-to-Rhodium(I) Alkyl Transfer: A Rhodium Macrocycle Which Is Both Nucleophile and Leaving Group

James P. Collman,* John I. Brauman, and Alex M. Madonik

Department of Chemistry, Stanford University, Stanford, California 94305

Received February 12, 1985

The rhodium(I) macrocycles $Rh^I(BPDOBF_2)$ (**1a**) and $Rh^I(PPDOBF_2)$ (**1b**) are strong nucleophiles toward alkyl halides and may also be alkylated by their rhodium(III) alkyl halide adducts $R'-Rh^{III}(BPDOBF_2)-X$ and $R'-Rh^{III}(PPDOBF_2)-X$ (**2a** and **2b**), respectively. In the latter process, **1a,b** act as both nucleophile and leaving group. We have studied the kinetics of alkyl exchange between, e.g., **1a** and **2b** by ^1H NMR and the rate constants are $(5.8 \pm 0.5) \times 10^{-3}$ M^{-1} s^{-1} for methyl exchange (R' = Me, X = I) and $(6.4 \pm 1.0) \times 10^{-2}$ M^{-1} s^{-1} for benzyl exchange (R' = $PhCH_2$, X = Cl). Other alkyl groups do not participate in this reaction. These data are consistent with rhodium(I) attack at carbon; the process may be viewed as a carbon-bridged two-electron transfer. Halide-bridged electron transfer is implied in the much faster exchange ($k > 0.5$ M^{-1} s^{-1}) between **1a,b** and their rhodium(III) dichloride derivatives **3a** and **3b**.

Introduction

Low-valent transition-metal complexes exhibit nucleophilic behavior in many of their oxidative-addition reactions with alkyl halides, leading to the formation of metal–carbon bonds via an S_N2-like process.[1] The ability of metal centers to function as leaving groups is less widely recognized, despite scattered reports.[2] These include several examples of essentially degenerate nucleophilic reactions in which the same type of metal center serves as both nucleophile and leaving group[2a,b,c,e] (eq 1). The

$$M_1^n + R'-M_2^{n+2} \rightleftharpoons R'-M_1^{n+2} + M_2^n \quad (1)$$

latter reactions result in the transfer of an alkyl group from one metal center to another and may be viewed as carbon-bridged inner-sphere two-electron-transfer processes.[3] When the two centers are distinguished by a minor ligand modification, these exchange reactions are nearly thermoneutral, and their study should throw light on the kinetic factors which control two-electron processes that make and break metal–carbon bonds.[4]

We encountered a novel example of the process represented by eq 1 in the course of our studies on the oxidative addition of alkyl halides to a Rh(I) macrocycle.[1,5] We

(1) Collman, J. P.; Brauman, J. I; Madonik, A. M. *Organometallics*, following paper in this issue.

(2) (a) Johnson, R. W.; Pearson, R. G. *J. Chem. Soc., Chem. Commun.* **1970**, 986–987. (b) Dodd, D.; Johnson, M. D. *J. Chem. Soc., Chem. Commun.* **1971**, 1371–1372. (c) Mestroni, G.; Cocevar, C.; Costa, G. *Gazz. Chim. Ital.* **1973**, *103*, 273–285. (d) Schrauzer, G. N.; Stadlbauer, E. A. *Bioinorg. Chem.* **1974**, *3*, 353–366. Stadlbauer, E. A.; Holland, R. J.; Lamm, F. P.; Schrauzer, G. N. *Bioinorg. Chem.* **1974**, *4*, 67–77. (e) Dodd, D.; Johnson, M. D.; Lockman, B. L. *J. Am. Chem. Soc.* **1977**, *99*, 3664–3673.

(3) Reviews of inner-sphere electron transfer: (a) Taube, H. "Electron Transfer Reactions of Complex Ions in Solution"; Academic Press: New York, 1970. (b) Linck, R. G. *Surv. Prog. Chem.* **1976**, *7*, 89–147. (c) Sutin, N. "Inorganic Biochemistry"; Eichhorn, G. L., Ed.; Elsevier: New York, 1974; Chapter 7.

(4) Several groups have undertaken the analysis of "intrinsic" kinetic barriers to nucleophilic reactions in which the Marcus theory[4a] of electron transfer is applied to reactivity data for methyl transfer in the gas phase[4b-d] or in solution.[4e] Endicott's group has made an extensive analysis of the analogous S_H2 mechanism implicated in methyl and halide transfer between Co(II) and Co(III) macrocycles.[4f-h] (See also ref 4i.) (a) Marcus, R. A. *Annu. Rev. Phys. Chem.* **1964**, *15*, 155–196. (b) Shaik, S. S.; Pross, A. *J. Am. Chem. Soc.* **1982**, *104*, 2708–2719. (c) Wolfe, S.; Mitchell, D. J.; Schlegel, H. B. *J. Am. Chem. Soc.* **1981**, *103*, 7694–7696. (d) Pellerite, M. J.; Brauman, J. I. *J. Am. Chem. Soc.* **1983**, *105*, 2672–2680. Pellerite, M. J.; Brauman, J. I. *J. Am. Chem. Soc.* **1980**, *102*, 5993–5999. (e) Albery, W. J.; Kreevoy, M. M. *Adv. Phys. Org. Chem.* **1978**, *16*, 87–157. (f) Endicott, J. F.; Wong, C.-L.; Ciskowski, J. M.; Balakrishnan, K. P. *J. Am. Chem. Soc.* **1980**, *102*, 2100–2103. (g) Endicott, J. F.; Balakrishnan, K. P.; Wong, C.-L. *J. Am. Chem. Soc.* **1980**, *102*, 5519–5526. (h) Durham, B.; Endicott, J. F.; Wong, C.-L.; Rillema, D. P. *J. Am. Chem. Soc.* **1979**, *101*, 847–857. (i) Johnson, M. D. *Acc. Chem. Res.* **1983**, *16*, 343–349.

(5) Preliminary report: Collman, J. P.; MacLaury, M. R. *J. Am. Chem. Soc.* **1974**, *96*, 3019–3020. We have since adopted a modified nomenclature for the macrocyclic ligands: $(PPDOBF_2)$ = [difluoro[*N,N'*-bis(3-pentanon-2-ylidene)-1,3-diaminopropane)dioximato]borate], and $(BPDOBF_2)$ = [difluoro[*N,N'*-bis(3-butanon-2-ylidene)-1,3-diaminopropane)-dioximato]borate]. Other abbreviations: PPN^+ = bis(triphenylphosphoranediyl)nitrogen(1+) ion.

0276-7333/86/2305-0215$01.50/0

report here a kinetic study of this reaction, using two similar macrocyclic ligands which can be differentiated by ^1H NMR. The process is quite sensitive to steric bulk in the alkyl group to be transferred; nonetheless, in some cases alkyl exchange proceeds at a rate competitive with alkylation of Rh(I) by the corresponding halide (eq 2 and 3).

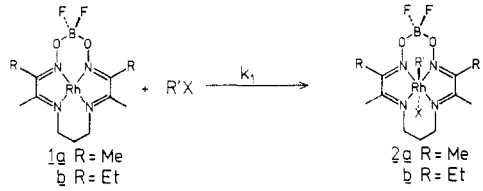

(2)

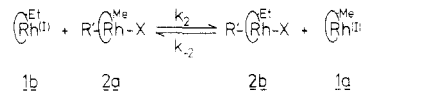

(3)

A much faster Rh(I)–Rh(III) exchange process, possibly involving a chloride-bridged transition state, was also observed (eq 4).

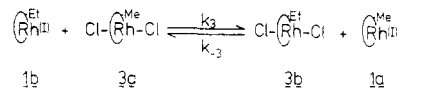

(4)

Experimental Section

The preparation of the Rh complexes has been described, as has the purification of solvents.[1] Inert-atmosphere techniques were required for all experiments because of the oxygen sensitivity of the Rh(I) complexes. NMR spectra were recorded on a Varian XL-100 instrument equipped with a Nicolet Technology data system.[6] Inorganic salts and benzyl chloride were purified according to the recommendations of Perrin, Armarego, and Perrin.[7] PPN^+Cl^- (Alfa) was recrystallized from ethanol and dried under vacuum. TLC analyses used silica gel plates supplied by Analtech, Inc., eluting with 30% $MeCN/CH_2Cl_2$.

Kinetics

Stock solutions of the Rh(I) reagents in CD_3CN (10 or 20 mM) were prepared in the glovebox, where weighing errors resulted in uncertainties of ±5–10% in their concentrations. Rh(III) compounds were weighed precisely before transfer to the glovebox. The Rh(I) solution (0.5 mL, 0.005 or 0.01 mmol of Rh(I)) was measured with a volumetric pipette or syringe, stirred with the Rh(III) (1.0 equiv) compound to dissolve it, and the mixture filtered into an NMR sample tube, which was capped with a rubber septum. Reacting samples were transferred to the probe of the spectrometer (at 28.5 °C), and sequential spectra were acquired automatically using the kinetic routine provided by Nicolet. At the minimum concentration used, 10 mM in each of the reacting species, reasonable signal-to-noise ratio was achieved in a 16-transient spectrum which took slightly under 1 min to acquire. Reactions having rate constants significantly greater than 0.1 M^{-1} s^{-1} could not be studied by this technique.

Kinetic data were obtained by separately integrating the distinct ethyl group triplets of the Rh(I) and Rh(III) species bearing the ($PPDOBF_2$) ligand. The ratios of the integrated signals were used as input for the kinetic analysis.[8] Attempts to use an internal standard (cyclohexane) for comparison of integrals gave erratic results, probably owing to the large differences in peak widths and relaxation times. We believe the peak ratios are reliable measures of [product]/[reactant], since rate constants were unchanged by variations in the pulse width and time delays used to acquire the spectra.

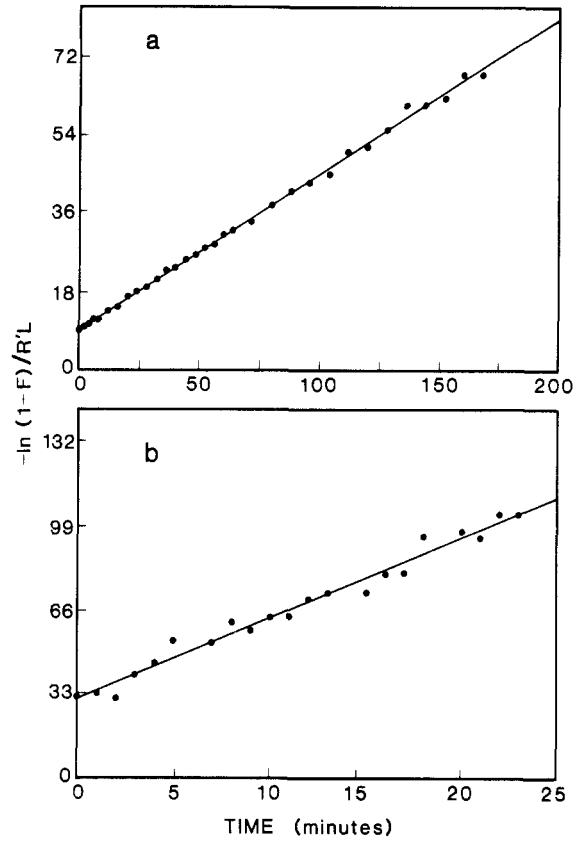

Figure 1. Least-squares plots of NMR kinetic data for the alkyl exchange reaction (at 28.5 °C in CD_3CN solution).[8] (a) Methyl exchange between **1b** and **2a** (R′ = Me, X = I), each at 20 mM. (b) Benzyl exchange between **1a** and **2b** (R′ = $PhCH_2$, X = Cl), each at 10 mM.

Results

The facility of alkyl exchange is extremely sensitive to the structure of the alkyl group R′. Thus, reaction is fastest for R′ = benzyl; methyl transfer also proceeds at a moderate rate at room temperature. Contrary to our preliminary report,[5] we could find no evidence for the exchange of bulkier R′ groups such as *n*-butyl or isopropyl, even over periods of several hours at 70 °C (in CD_3CN, with Rh(I) and Rh(III) complexes each at 20 mM). A 1-phenylethyl complex and an acetyl complex were also unreactive toward the Rh(I) reagent.

(6) NMR data are reported relative to internal Me_4Si; they were calibrated relative to the residual solvent peak at δ 1.93 for CD_3CN.

(7) Perrin, D.O.; Armarego, W. L. F.; Perrin, D. R. "Purification of Laboratory Compounds"; (Pergamon Press: New York, Oxford, 1966.

(8) The exchange reaction of eq 3 can be treated according to the kinetic scheme used for isotope exchange,[8a] provided that the equilibrium constant is equal to one ($k_2 = k_{-2}$): $\ln(1 - F) = RLt$, where R = the constant rate of exchange, $k_2[Rh'(I)]_0[Rh(III)]_0$, $L = (1/[Rh'(I)]_0 + 1/[Rh(III)]_0$, and F = the "fraction of exchange"; $([Rh'(III)]_t([Rh'(I)]_0) + [Rh(III)]_0)/([Rh'(I)]_0[Rh(III)]_0) = L[Rh'(III)]_t$. (Rh and Rh′ represent the two distinct macrocycles.) Since the NMR kinetic data were in the form of a ratio (Q = [product]/[reactant] = [Rh′(III)]/[Rh′(I)]), they were converted to concentration data using the known initial concentrations: $[Rh'(III)] = [Rh'(I)]_0Q/(Q + 1)$. The initial concentrations of both Rh and Rh′ are required to compute the input for the lease-squares analysis. If one was not known with sufficient accuracy, it could be calculated from the other in conjunction with the observed equilibrium ratio $Q_{infinity} = [Rh(III)]_0/[Rh'(I)]_0$. In practice, the value of $Q_{infinity}$ was sometimes varied slightly in order to obtain the best possible least-squares fit to the data. In Figure 1, $-(\log(1 - F))/(R'L)$ is plotted against time, and the slope is equal to the rate constant k ($R' = [Rh'(I)]_0[Rh(III)]_0$). (a) McKay, H. A. C. "Principles of Radiochemistry"; Butterworths: London, 1971; p 296. (b) Wilkins, R. G. "The Study of Kinetics and Transition Metal Complexes" Allyn and Bacon: Boston, 1975; p 152 ff.

Table I. Kinetic Data for Rh(I)–Rh(III) Alkyl Exchange[c]

Rh(I),[d] mM	R	Rh(III), mM		Na^+Y^-, mM	Q_{inf}[e]	10^3 k, M^{-1} s^{-1}	R[f]
14[b]	Me	20[a]	I		1.40	5.6 ± 0.11	0.997
20[b]	Me	20[a]	I		1.02	5.7 ± 0.10	0.995
22[b]	Me	20[a]	I		0.89	6.1 ± 0.10	0.997
20[b]	Me	20[a]	I		1.00	5.9 ± 0.14	0.994
29[b]	Me	20[a]	I		0.68	4.4 ± 0.04	0.999
18[b]	Me	20[a]	I		1.12	6.7 ± 0.07	0.999
19[b]	Me	20[a]	I		1.04	6.0 ± 0.05	0.999
15[a]	Bz	10[b]	Cl		1.49	66 ± 5.1	0.944
12[a]	Bz	10[b]	Cl		1.15	66 ± 5.5	0.942
11[a]	Bz	10[b]	Cl		1.11	60 ± 3.5	0.964
16[a]	Me	20[b]	BF_4		0.80	49 ± 2.1	0.991
11[a]	Me	10[b]	BF_4		1.09	34 ± 2.5	0.990
9[a]	Me	20[b]	I	I 200	0.45	5.0 ± 0.13	0.993
15[b]	Me	20[a]	I	I 200	1.35	6.0 ± 0.17	0.988
12[a]	Me	20[b]	I	I 200	0.58	2.2 ± 0.02	0.999
21[a]	Me	20[b]	I	ClO_4 200	1.07	9.0 ± 0.16	0.996

[a] Ligand = ($BPDOBF_2$). [b] Ligand = ($PPDOBF_2$). [c] Reactions at 28.5 °C in CD_3CN. [d] Calculated from the initial concentration of the Rh(III) complex using Q_{inf}[8]. [e] Product/reactant ratio at t = infinity, after adjustment to give the best least-squares fit. [f] Correlation coefficient.

The Rh(III)–alkyl derivatives of the two macrocyclic ligands ($PPDOBF_2$) and ($BPDOBF_2$) could be readily distinguished by TLC analysis. However, the progress of these exchange reactions was most conveniently followed by ^1H NMR. The equilibrium constants are equal to 1.0 within the uncertainties of the experiments (±5% in the product/reactant ratio). They exhibit straightforward second-order behavior, with a rate constant of (5.8 ± 0.5) × 10^{-3} M^{-1} s^{-1} for methyl exchange (eq 3, R′ = Me, X = I) and (6.4 ± 1.0) × 10^{-2} M^{-1} s^{-1} for benzyl exchange (eq 3, R′ = Bz, X = Cl). Representative kinetic data are plotted in Figure 1. (Zero time corresponds to the first spectrum acquired after transfer of the reacting sample to the spectrometer probe, so the plots do not intercept the origin at t = 0). The benzyl exchange reaction was almost too fast to study by this method, hence the greater uncertainty in its rate constant. Kinetic data are listed in Table I for all runs. The dependence of the Rh(I)–Rh(III) exchange rates on the structure of the alkyl group implies Rh(I) attack at the carbon bound to Rh(III) in the crucial step leading to group transfer (see below).

Methyl exchange was also studied by using the cationic methyl donor **4**, and it was found to be 8–10 times faster than with the neutral methyl iodide adduct (**2a** or **2b**, R′ = Me, X = I). The neutral and cationic methyl complexes exhibit distinct ^1H NMR spectra which do not broaden or merge in the presence of one another. By this NMR criterion, the neutral complex does not dissociate appreciably at concentrations as low as 5 mM in CD_3CN. Addition of sodium iodide to solutions of the neutral complex does cause slight shifts in its NMR spectrum, and the presence of NaI may retard Rh(I)–Rh(III) exchange somewhat (sodium perchlorate appears to have the opposite effect). Our data on these points are inconclusive, but given the implied low dissociation constant for coordinated iodide, it seems unlikely that formation of a five-coordinate intermediate precedes methyl transfer in the reactions of the neutral complex.

The chloride exchange reaction of eq 4 was found to be much more rapid than alkyl exchange. The presence of all four species at equilibrium was confirmed by quenching the reaction with benzyl chloride and identifying the two dichloride derivatives and the two benzyl chloride adducts by TLC. The equilibrium was completely established by the time an NMR sample could be transferred from the glovebox to the spectrometer (CD_3CN solution, Rh(I) and Rh(III) species each at 10 mM). This result indicates that the rate constant is greater than 0.5 M^{-1} s^{-1}. However, no significant broadening of the Rh(I) or Rh(III) ligand resonances was observed, which requires that the rate constant be less than 100 M^{-1} s^{-1}.[8b] Addition of a fivefold excess of PPN^+Cl^- did not appreciably retard this reaction.

Discussion

The normal second-order kinetics of the exchange reactions and the higher rate of benzyl vs. methyl transfer are consistent with nucleophilic attack at carbon. The Rh(I) macrocycle can be assigned a "leaving group ability" on a par with that of chloride, since benzyl chloride alkylates Rh(I) at a rate similar to that for the benzyl–Rh(III) complex.[1] No alkyl group more bulky than benzyl or methyl participates in this reaction. This result strongly suggests that attack at carbon is crucial to alkyl transfer. This reactivity sequence (benzyl > methyl ≫ *n*-butyl, isopropyl) is entirely consistent with our studies on the nucleophilic behavior or Rh(I) complex (1) toward alkyl halides.[1] The faster rate of methyl transfer from the cationic methyl–Rh(III) complex **4** compared to the neutral methyl iodide adduct (eq 2, R′ = Me, X = I) is also consistent with Rh(I) attack at an electrophilic center. If Rh(I)–Rh(III) exchange were initiated by Rh(I) attack on the coordinated halide (or on rhodium itself at the vacant axial coordination site of a cationic alkyl–Rh(III) intermediate), there would be no reason for dramatic reactivity differences among the various alkyl groups. Furthermore, such a mode of attack would generate an anionic alkyl–Rh(I) species, an energetically unfavorable intermediate (eq 5).

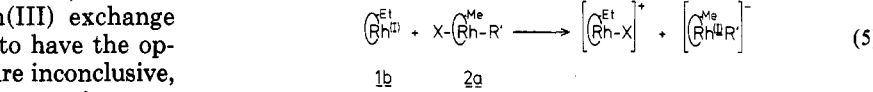

(5)

1b **2a**

Where Rh(I)–Rh(III) exchange actually does take place via Rh(I) attack on coordinated halide (eq 4), the process is much faster than alkyl-mediated exchange. The presumed mechanism involves formal transfer of Cl^+ to Rh(I), in which case the new Rh(I) complex is associated with an energetically reasonable chloride anion.

Macrocyclic alkyl–Co(III) complexes participate in exchange reactions with both Co(I) and Co(II) macrocycles.[2b,d,e,4g,9] The finding of second-order kinetics and

(9) (a) van den Bergen, A.; West, B. O. *J. Chem. Soc., Chem. Commun.* **1971**, 52–53. van den Bergen, A.; West, B. O. *J. Organomet. Chem.* **1974**, *64*, 125–134. (b) Chrzastowski, J. Z.; Cooksey, C. J.; Johnson, M. D.; Lockman, B. L.; Steggles, P. N. *J. Am. Chem. Soc.* **1975**, *97*, 932–934.

inversion of configuration at carbon supports S_N2 and S_H2 mechanisms for the reactions involving Co(I)[2b,e] and Co(II)[2e,4g,9b], respectively. In either case, alkyl transfer is much more facile than in the rhodium system. Given the structural similarities among these macrocyclic complexes, this rate difference can best be accounted for by the higher metal–carbon bond strength in the case of rhodium (c.f. ref 4g). Furthermore, methyl transfer to Rh(I) complex **1b** from methyl–Co(III) complex **5** proceeds quantitatively on mixing.[10] Thus, the cobalt macrocycle appears to be

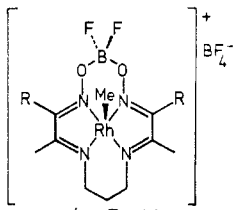

4a R = Me
b R = Et

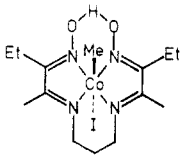

5

a better leaving group than the rhodium macrocycle, presumably owing to the difference in metal–carbon bond strengths. However, the "intrinsic" kinetic barriers for S_N2-like processes involving Co(I/III) and Rh(I/III) macrocycles cannot yet be ascertained precisely, as no activation parameters or overall free energy changes (for transfers between the two different metals) have been determined.

(10) Collman, J. P.; Finke, R. G.; Sobatka, P. A., unpublished observations. Prepartion of cobalt complexes: Finke, R. G.; Smith, B. L.; McKenna, W. A.; Christian, P. A. *Inorg. Chem.* **1981**, *20*, 687–693.

The greater efficiency of chloride-bridged vs. methyl-bridged metal–metal exchange reactions has also been noted for Co(II)–Co(III) exchange.[4f,g,h] Endicott et al.[4f] attribute this acceleration to the greater electron affinity of the chlorine radical compared to the methyl radical, leading to more favorable bonding in the transition state. The millionfold rate difference observed by these authors can be compared to the result for Rh(I)–Rh(III) exchange, where the factor is no more than 10^5. This smaller acceleration probably results from the requirements of the two-electron transfer. Furthermore, the observed lability[1] of coordinated halides in the Rh(III) complexes may reduce their efficiency as bridging ligands.

Summary

The scope of the Rh(III)–Rh(I) transfer reaction (eq 3) has been defined, and kinetic measurements confirm its S_N2-like nature. It is considerably slower than related Co(I)–Co(III) exchange reactions, probably owing to the difference in carbon–metal bond energies. Alkyl transfer from Co(III) to RhIII) is quantitative. Further comparisons within a given triad, combined with the measurement of activation parameters for "degenerate" exchange reactions, should serve to characterize the "intrinsic" barriers to the formation and cleavage of metal–carbon bonds via two-electron processes.

Acknowledgment. This work was supported by the NSF Grant CHE78-09443. Alex M. Madonik was the recipient of an NSF graduate fellowship.

Registry No. **1a**, 41707-60-2; **1b**, 53335-25-4; **2a** (R′ = Me, X = I), 99355-04-1; **2b** (R′ = Bz, X = Cl), 99355-15-4; **3a**, 99355-03-0; **4b**, 99355-24-5; **5**, 57255-98-8.

Reactions of a Rhodium(I) Macrocycle with Organic Dihalides: Oxidative-Addition and β-Elimination Pathways

James P. Collman,* John I. Brauman, and Alex M. Madonik

Department of Chemistry, Stanford University, Stanford, California 94305

Received March 18, 1985

The reduction of organic dihalides by low-valent metal species may occur via several mechanisms. We have examined the reactions of a macrocyclic rhodium(I) supernucleophile, **1**, with a variety of vicinal and 1,3-dihalide substrates. Unlike typical one electron reductants, **1** does not induce elimination of 1,3-dihalopropanes to give olefins or cyclopropanes; rather, normal alkyl–Rh(III) oxidative-addition products are isolated. (When the two halides are identical, the expected statistical mixture of "mono" and "bis" adducts is obtained, although reaction in the presence of undissolved **1** can skew the result in favor of the "bis" adducts.) In contrast, the reaction of **1** with vicinal dibromides invariably gives olefins and the Rh(III) dibromide, the only partial exception being 1,2-dibromoethane, from which a "bis" adduct is formed in ca. 50% yield. Reduction rates are comparable to those found for the oxidative addition of monofunctional alkyl bromides to **1**, except in the case of *trans*-1,2-dibromocyclohexane, whose reduction to cyclohexene occurs on mixing with **1** (the cis isomer is reduced at least 10^5 times more slowly, although it still reacts about 10 times faster than bromocyclohexane). The olefinic products probably result from decomposition of Rh(III)–β-bromoalkyl intermediates, except in the case of *trans*-1,2-dibromocyclohexane, where a concerted elimination process is proposed.

Introduction

The reduction of organic dihalides by metals is a well-known route to olefins[1] and cycloalkanes.[1a,2] Competing one- and two-electron processes frequently limit the stereospecificity of olefin formation by this route, especially from simple vicinal dihaloalkanes. In contrast, iodide-promoted elimination is highly stereospecific.[3] More re-

(1) (a) House, H. O. "Modern Synthetic Reactions", 2nd ed.; W. A. Benjamin: Menlo Park, CA, 1972; p 220 ff. (b) Singleton, D. M.; Kochi, J. K. *J. Am. Chem. Soc.* **1967**, *89*, 6547–6555 and references therein.

(2) Kochi, J. K.; Singleton, D. M. *J. Org. Chem.* **1968**, *33*, 1027–1034 and references therein.

0276-7333/86/2305-0218$01.50/0

inversion of configuration at carbon supports S_N2 and S_H2 mechanisms for the reactions involving Co(I)[2b,e] and Co(II)[2e,4g,9b], respectively. In either case, alkyl transfer is much more facile than in the rhodium system. Given the structural similarities among these macrocyclic complexes, this rate difference can best be accounted for by the higher metal–carbon bond strength in the case of rhodium (c.f. ref 4g). Furthermore, methyl transfer to Rh(I) complex **1b** from methyl-Co(III) complex **5** proceeds quantitatively on mixing.[10] Thus, the cobalt macrocycle appears to be

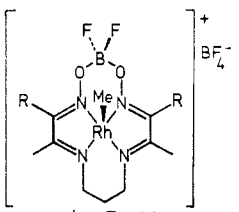

4a R = Me
b R = Et

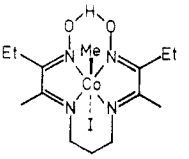

5

a better leaving group than the rhodium macrocycle, presumably owing to the difference in metal–carbon bond strengths. However, the "intrinsic" kinetic barriers for S_N2-like processes involving Co(I/III) and Rh(I/III) macrocycles cannot yet be ascertained precisely, as no activation parameters or overall free energy changes (for transfers between the two different metals) have been determined.

(10) Collman, J. P.; Finke, R. G.; Sobatka, P. A., unpublished observations. Prepartion of cobalt complexes: Finke, R. G.; Smith, B. L.; McKenna, W. A.; Christian, P. A. *Inorg. Chem.* **1981**, *20*, 687–693.

The greater efficiency of chloride-bridged vs. methyl-bridged metal–metal exchange reactions has also been noted for Co(II)–Co(III) exchange.[4f,g,h] Endicott et al.[4f] attribute this acceleration to the greater electron affinity of the chlorine radical compared to the methyl radical, leading to more favorable bonding in the transition state. The millionfold rate difference observed by these authors can be compared to the result for Rh(I)–Rh(III) exchange, where the factor is no more than 10^5. This smaller acceleration probably results from the requirements of the two-electron transfer. Furthermore, the observed lability[1] of coordinated halides in the Rh(III) complexes may reduce their efficiency as bridging ligands.

Summary

The scope of the Rh(III)–Rh(I) transfer reaction (eq 3) has been defined, and kinetic measurements confirm its S_N2-like nature. It is considerably slower than related Co(I)–Co(III) exchange reactions, probably owing to the difference in carbon–metal bond energies. Alkyl transfer from Co(III) to RhIII) is quantitative. Further comparisons within a given triad, combined with the measurement of activation parameters for "degenerate" exchange reactions, should serve to characterize the "intrinsic" barriers to the formation and cleavage of metal–carbon bonds via two-electron processes.

Acknowledgment. This work was supported by the NSF Grant CHE78-09443. Alex M. Madonik was the recipient of an NSF graduate fellowship.

Registry No. **1a**, 41707-60-2; **1b**, 53335-25-4; **2a** (R′ = Me, X = I), 99355-04-1; **2b** (R′ = Bz, X = Cl), 99355-15-4; **3a**, 99355-03-0; **4b**, 99355-24-5; **5**, 57255-98-8.

Reactions of a Rhodium(I) Macrocycle with Organic Dihalides: Oxidative-Addition and β-Elimination Pathways

James P. Collman,* John I. Brauman, and Alex M. Madonik

Department of Chemistry, Stanford University, Stanford, California 94305

Received March 18, 1985

The reduction of organic dihalides by low-valent metal species may occur via several mechanisms. We have examined the reactions of a macrocyclic rhodium(I) supernucleophile, **1**, with a variety of vicinal and 1,3-dihalide substrates. Unlike typical one electron reductants, **1** does not induce elimination of 1,3-dihalopropanes to give olefins or cyclopropanes; rather, normal alkyl–Rh(III) oxidative-addition products are isolated. (When the two halides are identical, the expected statistical mixture of "mono" and "bis" adducts is obtained, although reaction in the presence of undissolved **1** can skew the result in favor of the "bis" adducts.) In contrast, the reaction of **1** with vicinal dibromides invariably gives olefins and the Rh(III) dibromide, the only partial exception being 1,2-dibromoethane, from which a "bis" adduct is formed in ca. 50% yield. Reduction rates are comparable to those found for the oxidative addition of monofunctional alkyl bromides to **1**, except in the case of *trans*-1,2-dibromocyclohexane, whose reduction to cyclohexene occurs on mixing with **1** (the cis isomer is reduced at least 10^5 times more slowly, although it still reacts about 10 times faster than bromocyclohexane). The olefinic products probably result from decomposition of Rh(III)–β-bromoalkyl intermediates, except in the case of *trans*-1,2-dibromocyclohexane, where a concerted elimination process is proposed.

Introduction

The reduction of organic dihalides by metals is a well-known route to olefins[1] and cycloalkanes.[1a,2] Competing one- and two-electron processes frequently limit the stereospecificity of olefin formation by this route, especially from simple vicinal dihaloalkanes. In contrast, iodide-promoted elimination is highly stereospecific.[3] More re-

(1) (a) House, H. O. "Modern Synthetic Reactions", 2nd ed.; W. A. Benjamin: Menlo Park, CA, 1972; p 220 ff. (b) Singleton, D. M.; Kochi, J. K. *J. Am. Chem. Soc.* **1967**, *89*, 6547–6555 and references therein.

(2) Kochi, J. K.; Singleton, D. M. *J. Org. Chem.* **1968**, *33*, 1027–1034 and references therein.

0276-7333/86/2305-0218$01.50/0

cent studies have focused on soluble transition-metal species as reductants.[1b,2,4] The modest stereoselectivity exhibited by the one-electron reductant Cr(II) is attributed to stabilization of radical intermediates by "neighboring group" interactions and to the formation of transient metal–alkyl species.[4a,b] These reagents also reduce monohalides, but at much lower rates—further evidence for "neighboring group" effects in reactions with the dihalides.

We have previously examined the oxidative addition[5] of a wide range of alkyl halides to $Rh^{I}(PPDOBF_2)$[6,7] (**1**) and find that this Rh(I) macrocycle behaves as a supernucleophile,[8] giving Rh(III)–alkyl adducts according to eq 1. Its reactions with α,ω-dihalides were also studied in

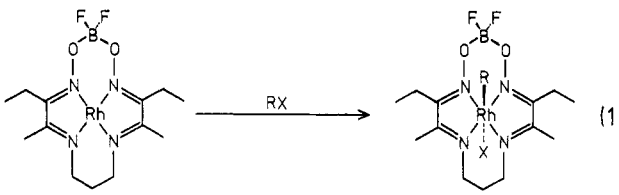

1 **2**

order to probe for radical pathways. The principal products were again found to be Rh(III)–alkyl adducts; moreover, in many cases only the "bis" adduct was isolated, seemingly the result of "neighboring group" activation of the second halide.[7a] We have since examined these reactions under a variety of conditions to determine what factors dictate the ratio of "mono" and "bis" adducts. In general, the so-called "neighboring group" effect was found to be an artifact of reactions carried out in the presence of incompletely dissolved Rh(I) complex. However, certain vicinal dibromides do display enhanced reactivity toward **1**, although in most cases the products are olefins and $Rh^{III}(PPDOBF_2)(Br)_2$. In this paper, we discuss the mechanism(s) of $Rh^{I}(PPDOBF_2)$ oxidative additions in light of these results.

Results[9]

Reactions with 1,3-Dihalopropanes. We investigated the reactivity of **1** with a spectrum of 1,3-disubstituted propanes **3a–f**. No propene or cyclopropane could be detected by ^1H NMR when reactions were carried out in acetone-d_6 or acetonitrile-d_3 ([Rh(I)] = 20 mM, 1 equiv of **3a–e**). With X ≠ Y (**3c–f**), we found only "mono" adducts, as determined by TLC analysis of the reaction mixtures and isolation of the products. For X = Y (**3a,b**), we found that the previously reported "bis" adducts[7a] are formed in conjunction with about half as much of the "mono" compound, when the reactions are carried out in THF or DME with 50% excess of substrate.

Table I. Product Yields in the Reaction of 1 with 1,3-Dibromopropane (2a)

	concn, mM		% yields[b]	
solvent/temp,[c] °C	1[a]	3a	4 ("mono")	5 ("bis")
DME/28–30	30	45	28	66
DME/28–30	30	45	22	75
DME/28–30	30	45	60	42
DME/28–30	30	45	61	40
DME/reflux	30	45	25	57
DME/reflux	30	180	55	35
DME/28–30	15	22.5	55	40
DME/28–30	15	22.5	58	37
acetone/28	30	45	91	9
acetone/28	30	45	92	13
MeCN/28–30	30	45	92	7

[a] Concentration assuming complete dissolution of the Rh(I) reagent. [b] Yields by UV–visible assay after chromatographic separation (accurate to within ±5%). [c] The ambient temperature of the inert-atmosphere box was 28–30 °C.

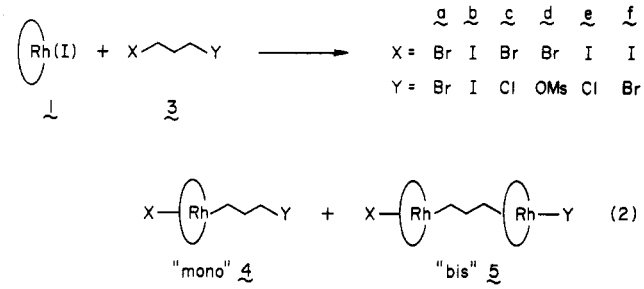

The yields of the two products **4** and **5** were studied in detail in the case of 1,3-dibromopropane (**3a**) (Table I). Increasing the substrate excess to sixfold approximately reverses the proportion of "mono" and "bis" adducts. However, we also noted disconcerting variations in the product ratios in supposedly identical experiments. Furthermore, when MeCN or acetone is substituted for the ethereal solvents, the "bis" to "mono" ratio declines to 1:9. Diluting the reactions in ethereal solvents also leads to decreased yields of the "bis" adduct. The solubility of the Rh(I) reagent was one factor that had not been carefully examined, and we found that it depends strongly on the solvent. In MeCN, the solubility of **1** is no less than 40 mg/mL (100 mM), while for acetone the figure is 8–10 mg/mL. Its solubility in THF is much less, approximately 2 mg/mL, and in DME it is lower still, little more than 1 mg/mL. Since preparative reactions had been conducted with 10 mg of **1** per mL, reactions in the ethereal solvents could not have been homogeneous. The deep purple color of the Rh(I) complex in solution is deceptive, as it conceals any undissolved material suspended in the reaction mixture.

Vicinal Dibromides: 1,2-Dibromoethane. We reexamined the addition of this substrate to **1** by ^1H NMR and TLC and found a roughly 1:1 mixture of a poorly soluble Rh(III)–alkyl species and the Rh(III) dibromide **8**, accompanied by a significant quantity of ethylene. The Rh(III)–alkyl compound proved difficult to characterize, but treatment with $AgBF_4$ precipitated AgBr and left a more soluble BF_4^- salt, which ^1H NMR showed to be derived from the "bis" adduct **7** consistent with earlier findings[7a] and elemental analysis of **7**.

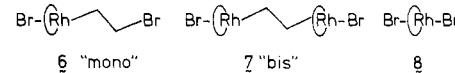

6 "mono" **7** "bis" **8**

(3) Stevens, C. L.; Valicenti, J. A. *J. Am. Chem. Soc.* **1965**, *87*, 838–842 and references therein.

(4) (a) Kray, W. C., Jr.; Castro, C. E. *J. Am. Chem. Soc.* **1964**, *86*, 4603–4608. (b) Kochi, J. K.; Singleton, D. M. *J. Am. Chem. Soc.* **1968**, *90*, 1582–1589. (c) Chock, P. B.; Halpern, J. *J. Am. Chem. Soc.* **1969**, *91*, 582–588. (d) Wegner, P. A.; Delaney, M. S. *Inorg. Chem.* **1976**, *15*, 1918–1921.

(5) Collman, J. P.; Roper, W. R. "Reviews of Oxidative-Addition"; *Adv. Organomet. Chem.* **1968**, *7*, 53–94. Stille, J. K.; Lau, K. S. Y. *Acc. Chem. Res.* **1977**, *10*, 434–442.

(6) This ligand, [difluoro[*N,N'*-bis(3-pentanon-2-ylidene)-1,3-diaminopropane)dioximato]borate], is also known in the literature as $[C_2(DO)(DOBF_2)_{pn}]$.

(7) (a) Collman, J. P.; MacLaury, M. R. *J. Am. Chem. Soc.* **1974**, *96*, 3019–3020. (b) Collman, J. P.; Brauman, J. I.; Madonik, A. M. *Organometallics*, preceding paper in this issue.

(8) Schrauzer, G. N.; Deutsch, E. *J. Am. Chem. Soc.* **1969**, *91*, 3341–3350.

(9) Abbreviations: DME = 1,2-dimethoxyethane; EtOH = ethanol; MeCN = acetonitrile; THF = tetrahydrofuran.

1,2-Dibromopropane. The only products identified by ^1H NMR in the reaction of this substrate with 1 were propene and the Rh(III) dibromide 8 (which was also isolated and analyzed). The reaction rate was similar to that for 1,2-dibromoethane.

1,2-Dibromocyclohexane. A startling observation was the extremely rapid reaction between 1 and *trans*-1,2-dibromocyclohexane, resulting in elimination to form cyclohexene and dibromide 8 (which was isolated and analyzed). The reaction was complete on mixing, so the rate constant could not be less than about 10 M^{-1} s^{-1} (i.e., considerably faster than the addition of 1-iodobutane to 1[7b]). Reaction with *cis*-1,2-dibromocyclohexane gave the same products but required a period of days for completion. A rate constant of approximately 2.5×10^{-4} M^{-1} s^{-1} (acetonitrile-d_3, 28.5 °C, statistical factor of 2) was deduced for this reaction from a series of ^1H NMR spectra recorded over this time.

Kinetic Data

Rh(I) disappearance was monitored by UV–visible spectroscopy in the presence of a large excess of the substrate, as described elsewhere.[7b] The reactions are second order, first order in both Rh(I) and alkyl halide. The rate constants for addition to 1 are, for 1,2-dibromoethane,[7a] 4.6×10^{-2} M^{-1} s^{-1} (THF, 25 ± 2 °C, statistical factor of 2), and for 1,3-dibromopropane, $(3.5 \pm 0.1) \times 10^{-2}$ M^{-1} s^{-1} (30.5 ± 2 °C, THF, statistical factor of 2). For comparison, the rate of addition of 1-bromobutane to 1 is $(1.67 \pm 0.05) \times 10^{-2}$ M^{-1} s^{-1} (THF, 30.5 ± 2 °C).[7b]

Discussion

Reactions with 1,3-Dihalopropanes. The absence of elimination products in these reactions is strong evidence in support of a two-electron, S_N2-like mechanism for oxidative addition to 1 (see ref 7b for details of our kinetic and mechanistic studies). Furthermore, the unexceptional rates of these reactions (when compared to reactions of 1 with simple alkyl halides), is in striking contrast to the large accelerations (25–50 times) observed in the case of one-electron reductants such as Cr(II)[2] and Co(II).[4c]

The formation of surprisingly high proportions of "bis" adducts (eq 2) was encountered at the outset of this investigation.[7a] We have since shown that this so-called "neighboring group" effect is a phenomenon resulting from reaction in the presence of undissolved Rh(I) complex.[10] When the concentration of 1 is adjusted so as to ensure its complete dissolution, the expected "mono" adducts predominate. Since all kinetic experiments were conducted in this more dilute regime (with a large excess of substrate), a simple 1:1 stoichiometry holds. The rate constant for 1,3-dibromopropane has been divided by a statistical factor of 2 (owing to the presence of two equivalent leaving groups). If formation of the "bis" adduct were predominant, a factor of 4 would be necessary, owing to the change in stoichiometry.[7a]

Vicinal Dibromides. Since the reduction of vicinal dibromides to olefins can occur by either one- or two-electron mechanisms, kinetic and stereochemical information is necessary in order to distinguish among the possibilities. One plausible route to olefins is via a normal oxidative-addition reaction, followed by decomposition of the "mono" adduct (such as 6) to the olefin and Rh^{III}(PPDOBF$_2$)(Br)$_2$. No "mono" adducts could be isolated, and Kochi[11] states that no stable β-bromoalkyl metal complexes are known. Kinetic data for the reaction of 1,2-dibromoethane are consistent with a normal oxidative-addition process. While the deceleration typical of nucleophilic reactions with vicinal dibromides[12] is absent, the rate differences between this substrate and 1,3-dibromopropane or 1-bromobutane are minimal compared to those observed with, for example, $Cr^{II}(en)_2^{2+}$, a powerful one-electron reductant.[2]

Formation of the "bis" adduct 7 from 1,2-dibromoethane is unlikely to occur via an electron-transfer mechanism; more reasonable is trapping of the "mono" adduct 6 by Rh^I(PPDOBF$_2$) in a second S_N2-like process. Thus, oxidative addition must compete successfully with the decomposition of 6. That it is able to do so may reflect an activating influence of the adjacent Rh(III) macrocycle on the β-bromo group. The failure of other vicinal dibromides to give "bis" adducts is not at all surprising, since secondary bromides add to 1 some 500 times slower than primary ones.[7b]

Turning to *cis*- and *trans*-1,2-dibromocyclohexane, each of these substrates reacts with 1 faster than does bromocyclohexane ($(1.25 \pm 0.25) \times 10^{-5}$ M^{-1} s^{-1}, THF, 30.5 ± 2 °C).[7b] For the trans dibromide, the accleration is on the order of 10^6-fold, which is unprecedented either in Cr(II) reductions (where the acceleration is roughly 1500 times)[1b] or in iodide-induced elimination (which is actually somewhat slower than nucleophilic substitution in bromocyclohexane).[13a] Iodide-promoted elimination is well-known to require a *trans* diaxial conformation,[3] and the trans dibromide is a particularly favorable substrate for the process because it actually prefers the diaxial conformation in solution.[14] However, the trans diaxial geometry is also the most favorable one for bromine atom abstraction, owing to "neighboring group" stabilization of the free radical intermediate.[1b,4a,b] A proper choice of mechanism for the Rh(I)-induced elimination can only be made after examination of the results with other substrates.

The rate difference between the cis and trans dibromide is also very large, approaching a factor of 10^5. Nonetheless, the cis compound still reacts some 20 times faster than bromocyclohexane. If one allows for the difference in solvent polarity between MeCN and THF, this rate ratio is reduced to ten.[7b] While vicinal dibromides are normally poor substrates for nucleophilic attack at carbon,[12] we have noted a modest acceleration in the reaction of 1 with 1,2-dibromoethane, relative to other 1-bromoalkanes. Thus, *cis*-1,2-dibromocyclohexane could add to 1 more rapidly than does bromocyclohexane. Furthermore, bromocyclohexane prefers an equatorial conformation in solution, inhibiting nucleophilic displacement, while one of the bromine atoms in the cis dibromide is obliged to occupy an axial position in either of the possible chair conformations. Displacement of bromide by the Rh(I) macrocycle in an S_N2-like process would convert the cis dibromide to a trans-substituted cyclohexane, favoring subsequent concerted elimination. Thus, a two-step, two-electron pathway appears feasible for the Rh(I)-in-

(10) A similar phenomenon may explain the formation of "bis" adducts in the reaction of Co(I) macrocycle vitamin B_{12a} with α,ω-dihalides: Smith, E. L.; Mervyn, L.; Muggleton, P. W.; Johnson, A. W.; Shaw, N. *Ann. N.Y. Acad. Sci.* **1964**, *112*, 565–574.

(11) Kochi, J. K. "Organometallic Mechanisms and Catalysis"; Academic Press: New York, San Francisco, London, 1978; p 176 ff. Note that the data quoted in the table on p 176 for Rh^IPPDOBF$_2$ are actually 10^3k; this factor of 10^3 was omitted.

(12) Streitweiser, A., Jr. "Solvolytic Displacement Reactions"; McGraw-Hill: New York, 1962; p 17.

(13) (a) Goering, H. L.; Espy, H. H. *J. Am. Chem. Soc.* **1955**, *77*, 5023–5026. (b) Goering, H. L.; Sims, L. L. *J. Am. Chem. Soc.* **1955**, *77*, 3465–3469.

(14) Bender, P.; Flowers, D. L.; Goering, H. L. *J. Am. Chem. Soc.* **1955**, *77*, 3463–3465.

Table II. R-Rh^{III}(PPDOBF$_2$)-X "Mono" Adducts 4a-f

R	X	equiv used	solv	reaction time	reaction temp	yield, %	spectral data	formula	anal.
$Br(CH_2)_3$	Br	1.5X	DME	45	reflux	15[c]	δ 1.17 (m, 4 H),[b] 3.22 (br t, J = 6.3 Hz, 2 H)	$C_{16}H_{28}BBr_2F_2N_2O_2Rh$	C, H, N, Br
$I(CH_2)_3$	I	1.5X	THF	5	room	31[c]	δ 1.16 (m, 4 H),[b] 2.81 (m, 2 H)	$C_{16}H_{28}BF_2I_2N_4O_2Rh$	C, H, N, I[d]
$CH_3SO_3(CH_2)_3$	Br	1.5X	THF	90	reflux	88	ν(SO) 1340 (s), 1180 (s) cm^{-1} δ 1.16 (m, 2 H)8 1.5–1.8 (m, 2 H), 2.90 (s, 3 H), 3.98 (m, 2 H)[b]	$C_{17}H_{31}BBrF_2N_4O_2RhS$	C, H, N, Br,[e] S
$Cl(CH_2)_3$	Br	1.5X	THF	5	reflux	88	δ 1.16 (m, 4 H),[f] 3.3 (m, 2 H)	$C_{16}H_{28}BBrClF_2N_4O_2Rh$	C, H, N, Br, Cl
$Cl(CH_2)_3$	I	1.5X	THF	45	room	44	δ 1.12 (m, 4 H), 3.29 (br t, J = 6.5 Hz, 2 H)[g]	$C_{16}H_{28}BClF_2IN_4O_2Rh$	C, H, N, Cl, I
$Br(CH_2)_3$	I	2X	THF	15	room	80	δ 0.9 (m, 2 H), 1.16 (m, 2 H), 3.22 (br t, 2 H)[b]	$C_{16}H_{28}BBrF_2IN_4O_2Rh$	C, H, N, Br, I

[a] All analyses were within ±0.4% of the calculated values unless otherwise noted. [b] NMR spectrum in CD_2Cl_2. [c] The major product under these conditions is the "bis" adduct. [d] I: calcd, 35.52; found, 34.87. [e] Br: calcd, 12.58; found, 13.99. [f] NMR spectrum in $CDCl_3$. [g] NMR spectrum in acetone-d_6.

duced elimination from the cis dibromide.

Returning to the trans isomer, the large trans/cis rate ratio observed here is also inconsistent with a one-electron pathway (for Cr(II) the ratio is only 150).[1b] In contrast, the corresponding ratio for iodide-induced elimination is[3] at least 322. The Rh(I) macrocycle is quite sensitive to steric hindrance, so it is not surprising that attack at bromine is much more facile than attack at carbon.[7b] It remains necessary to account for the comparative lack of activation in reactions of acyclic substrates such as 1,2-dibromoethane. Accelerations of 1000-fold are observed with typical one-electron reductants,[2,4c] relative to their reactions with monobromoalkanes. Iodide-induced elimination, on the other hand, is essentially an E2 process[13a] and as such should be comparatively slow in 1,2-dibromoethane, relative to the more highly substituted 1,2-dibromocyclohexane. Indeed, the iodide-promoted elimination of 1,2-dibromoethane is relatively inefficient, requiring a higher temperature than the corresponding reaction of either 1,2-dibromocyclohexane.[15] For 1,2-dibromoethane, then, the oxidative-addition pathway predominates, leading to either the "bis" adduct **7** or to elimination via the "mono" adduct **6**.

In summary, the reactions of **1** with organic dibromides are best explained in terms of two-electron mechanisms and thus represent a straightforward extension of the chemistry observed with monobromides. This Rh(I) complex resembles conventional nucleophiles except for the modest "neighboring group" accelerations observed in its reactions with 1,3-dibromopropane and 1,2-dibromoethane. Formation of a "bis" adduct from the latter substrate is not well understood but may involve "neighboring group" activation of bromine by the Rh(III) macrocycle in an intermediate β-bromoalkyl adduct (**6**).

Experimental Section

Materials and Methods. Techniques for the synthesis and manipulation of highly oxygen-sensitive **1** are described elsewhere,[7b] along with details of the kinetics procedure used to study its oxidative-addition reactions.

UV–visible spectra were recorded on a Cary 219 spectrometer using 1- and 10-mm quartz flow cells supplied by Hellma Cells. Infrared spectra were recorded on a Beckman Acculab spectrometer. ^{1}H NMR spectra were recorded at 100 MHz on a Varian XL-100 instrument equipped with a Nicolet Technology pulse generator and data system.[16] Elemental analyses were performed by the Stanford Microanalytical Laboratory.

The solubility of Rh^I(PPDOBF$_2$) in various solvents was determined by saturating a small volume of the solvent with excess reagent, filtering the solution, and removing a carefully measured volume via syringe. The solvent was then removed under vacuum and the sample diluted to a known volume in THF for assay by UV–visible spectroscopy (λ_{max} 560 nm (ε 21 500)).

Substrates for Oxidative-Addition Reactions. Commercially available substrates were purified by passage over activity I neutral alumina, followed by three cycles of freeze–pump–thaw degassing and storage in dark bottles over copper turnings in the glovebox. The mesylate **3d** of 3-bromo-1-propanol was obtained by the method of Crossland and Servis.[17]

While *trans*-1,2-dibromocyclohexane was commercially available (Aldrich), the cis isomer was prepared by photochemical hydrobromination[13b] of 1-bromocyclohexene.[3] It was recrystallized from pentane at −78 °C and then distilled (bp 83–85 °C (5 torr) (lit.[13b] 50.5–51.5 °C (0.13 torr))). Gas chromatography (10% OV-101, 150 °C) indicated that less than 1% of the trans isomer was present.

1,3-Diiodopropane (3b). Treatment of 1,3-dichloropropane (Aldrich) with NaI (2.1 equiv) in dry acetone at reflux overnight provided (after filtration, evaporation of the solvent, and distillation) the diiodide in 67% yield (bp 109–113 °C (20 torr) (lit.[18] 110 °C (19 torr))).

1-Chloro-3-iodopropane (3e). A solution of 1,3-dichloropropane and 1 equiv of NaI in dry acetone was stirred and heated under reflux overnight. Following filtration and removal of the solvent, distillation gave the desired product in 36% yield (bp 86–88.5 °C (45 torr) (lit.[19] 60.8 °C (15 torr))).

1-Bromo-3-iodopropane (3f). This compound has been prepared by allowing 1,3-dibromopropane to react with 1 equiv of NaI in solution.[4c] Accordingly, 100 mmol of the dibromide (Aldrich, 20.2 g) and NaI (Baker, 100 mmol, 15.0 g) in 100 mL of dry acetone were stirred and heated under reflux overnight. Filtration and removal of the solvent, followed by distillation provided an impure product boiling at 82–97 °C (24 torr), which was redistilled to give 5.34 g (21%) of product, bp 86–94 °C (25 torr). Gas chromatography (10% OV-101, 85 °C) showed that it contained less than 10% each of 1,3-dibromo- and 1,3-diiodopropane: ^{1}H NMR ($CDCl_3$) δ 2.33 (d of t, J = 7 Hz, 2 H) 3.30

(15) Urata, Y.; Bunya, K.; Kakihana, H. *Nippon Kagaku Zasshi* **1969**, *82*, 1403–1406 (*Chem. Abstr.* **1969**, *59*, 3753). While it remains true that iodide ion reacts more rapidly with bromocyclohexane than with either of the 1,2-dibromocyclohexanes,[13a] the relative rates of the substitution and elimination processes are undoubtedly influenced by their respective free energy changes. In the case of **1**, formation of a Rh(III)–carbon bond (via nuclophilic displacement) is a small driving force compared to the formation of a carbon–carbon double bond and the reduction of the second bromine to bromide ion (in the elimination process). Thus, elimination is probably much more favorable thermodynamically in the case of Rh(I) than in the case of iodide. However, this driving force is only manifested in the case of the trans dibromide, where concerted elimination generates a transition state resembling the final products.

(16) All ^{1}H NMR data are reported relative to internal Me_4Si and were calibrated relative to the residual solvent peak: CD_2HCN, δ 1.93; $CHDCl_2$, δ 5.27; CD_2HCOCD_3, δ 2.05; $CHCl_3$, δ 7.25.

(17) Crossland, R. G.; Servis, K. L. *J. Org. Chem.* **1970**, *35*, 3195–3196.

(18) "Handbook of Chemistry and Physics", 46th ed.; CRC Press: Cleveland, OH, 1965.

(19) "Dictionary of Organic Compounds", Oxford University Press: New York, Oxford, 1965; p 641.

(t, J = 7 Hz, 2 H), 3.51 (t, J = 7 Hz, 2 H).

Oxidative-Addition Products. Typical synthetic reactions used 0.25–0.50 mmol of the Rh(I) reagent and a 1.5-fold excess of the alkylating agent in 8 mL of solvent (light was excluded). When necessary the reaction mixture was heated under reflux until the purple color of the Rh(I) complex had disappeared. After a purity check by TLC[20a] (eluting with acetone or 30% $MeCN/CH_2Cl_2$) the adducts were usually recrystallized from CH_2Cl_2/EtOH. All adducts were characterized by IR and ^1H NMR spectroscopy and by analysis. (Except where otherwise noted, analyses for the elements listed agreed with the calculated values to within ±0.4%). Their IR spectra exhibit bands assigned to ligand stretching modes (KBr pellet): ν(CN) 1605 (m), 1530 (m), ν(BO) 1170 (s), 820 (s), ν(BF) 1000 (s), ν(NO) 1120 (s) cm^{-1}. The macrocyclic ligand also exhibits a relatively unvarying set of ^1H NMR resonances: δ 1.08 (t, J = 7.6 Hz, 6 H), 2.15 (m, 2 H), 2.30 (t, J = 1.2 Hz, 6 H), 2.76 and 2.78 (q, J = 7.6 Hz, 4 H total), 3.7–4.3 (br m, 4 H). See Table II for specific reaction conditions and further characterization of the "mono" adducts derived from **3a–f**.

***trans,trans*-(Br)Rh(PPDOBF$_2$)(CH$_2$)$_3$Rh(PPDOBF$_2$)(Br) (5a) and *trans*-(Br(CH$_2$)$_3$)Rh(PPDOBF$_2$)(Br) (4a).** A slurry of **1** (200 mg, 0.48 mmol) in 8 mL of DME was stirred under reflux and treated with 1,3-dibromopropane (**3a**, 0.72 mmol, 145 mg). After 45 min a large amount of flocculent yellow precipitate had appeared. It was collected on a glass frit and washed with EtOH, followed by recrystallization from CH_2Cl_2/EtOH to give the "bis" adduct. TLC analysis of the original filtrate showed that it contained a second species (the "mono" adduct), which could be isolated in 15% yield (45 mg) following recrystallization from CH_2Cl_2. The "bis" adduct accounted for the balance of the Rh(I) reagent. For the "mono" adduct: UV–vis (acetone) λ_{max} 362 nm (ϵ 4700); see Table II. For the "bis" adduct: UV–vis (acetone) λ_{max} 372 nm (ϵ 9560); ^1H NMR (CD_2Cl_2) δ 0.44 (m, 2 H), 0.88 (m, 4 H), 1.15 (t, J = 7.5 Hz, 12 H), 2.31 (s, 12 H), 2.55 and 2.97 (q, J = 7.5 Hz, 8 H total), 3.5–4.2 (br m, 8 H). Anal. ($C_{29}H_{50}B_2Br_2F_4N_8O_4Rh_2$) C, H, N, Br.

The yields of "mono" and "bis" adducts were quantified according to the following typical procedure: A mixture of **1** (100 mg, 0.24 mmol) and 1,3-dibromopropane (0.36 mmol, 73 mg) in 8 mL of THF was stirred under reflux for 0.5 h. The solvent was evaporated and the residue redissolved in CH_2Cl_2 and absorbed onto a small portion of silica gel[20b] by removal of the solvent. The silica gel was applied to the top of a wet silica gel column (acetone), and the Rh complexes were eluted with acetone. Two bands were collected, concentrated, and diluted to 50 mL with acetone. Each solution was further diluted 4:1 before measurement of its UV–vis absorption in a 1-mm cell. The leading band ("mono" adduct) exhibited an absorption of 0.15 at 362 nm, corresponding to 0.8 mmol of product (33%). The yield of "bis" adduct was 66% according to its absorption (0.30) measured at 372 nm (corresponding to 0.08 mmol of product, hence 0.16 mmol of Rh(I) reagent). The two adducts were subsequently recrystallized from CH_2Cl_2/EtOH: "mono", 29 mg (20%); "bis", 69 mg (55%).

***trans,trans*-(I)Rh(PPDOBF$_2$)((CH$_2$)$_3$)Rh(PPDOBF$_2$)(I) (5b) and *trans*-(I(CH$_2$)$_3$)Rh(PPDOBF$_2$)(I) (4b).** The substrate 1,3-diiodopropane (**3b**, 0.72 mmol, 210 mg) was added to a stirred slurry of **1** in 8 mL of THF. After 5 min at room temperature an orange precipitate was collected on a glass frit (186 mg). It proved to be the "bis" adduct (69%). The "mono" adduct was recovered from the filtrate by addition of EtOH and reduction of the volume (87 mg, 31%). Both compounds could be recrystallized from CH_2Cl_2/EtOH. For the "mono" adduct, see Table II. For the "bis" adduct: ^1H NMR (CD_2Cl_2) δ 0.30 (m, 2 H), 0.88 (m, 4 H), 1.12 (t, J = 7.5 Hz, 12 H), 2.27 (s, 12 H), 2.40 (m, 2 H), 2.5–3.1 (m, 8 H), 3.5–3.8 (br m, 4 H), 4.1–4.4 (br m, 4 H). Anal. ($C_{29}H_{50}B_2F_4I_2N_8O_4Rh$) C, H, N. Anal. I: calcd, 22.36; found, 21.80.

***trans,trans*-(Br)Rh(PPDOBF$_2$)(CH$_2$)Rh(PPDOBF$_2$)(Br) (7).** An NMR sample tube was charged with 0.5 mL of a 20 mM solution of **1** (0.01 mmol) in CD_3CN and capped with a rubber septum. Two equivalents of 1,2-dibromoethane (0.02 mmol, 1.7 μL) were added via syringe. The purple color of **1** faded within 10 min. The ^1H NMR spectrum revealed the presence of excess substrate (δ 3.76 (s)) and ethylene (δ 5.42 (s)) as well as two distinct Rh(III) species. One of these was clearly the Rh(III) dibromide **8** previously described.[7b] The other species exhibited the following ^1H signals: δ 1.1 (t), 2.3 (s), 2.6–2.9 (m), 3.5–4.1 (br m).

A preparative scale experiment involving 105 mg of Rh^I(PPDOBF$_2$) (0.25 mmol) and 10 equiv of 1,2-dibromoethane (2.50 mmol, 470 mg) in MeCN (5 mL) at room temperature also generated two species, according to TLC analysis. One of these precipitated from the reaction mixture, and its solubility was so poor that no ^1H NMR spectrum could be obtained. Treatment of 6 mg of this solid with 4 mg of $AgBF_4$ in 0.5 mL of CD_3CN produced an orange solution which was filtered (to remove AgBr) and examined by ^1H NMR. The "bis" adduct was identified on the basis of the following spectral data: δ 0.84 (d, J = 1.25 Hz, 4 H), 1.10 (t, J = 7.6 Hz, 12 H), 2.15 (m, 4 H), 2.39 (s, 12 H), 2.75 and 2.78 (q, J = 7.6 Hz, 8 H total), 3.5–4.2 (br m, 8 H). The doublet at δ 0.84 is diagnostic of a methylene group bound to ^{103}Rh (spin $^1/_2$). Anal. ($C_{28}H_{48}B_2Br_2F_4N_8O_4Rh$) H, N, Br. Anal. C: calcd. 32.84; found, 32.39.

Reaction of 1 with *cis*- and *trans*-1,2-Dibromocyclohexane. The Rh(III) dibromide **8** was the only product isolated when Rh^I(PPDOBF$_2$) was allowed to react with *trans*-1,2-dibromocyclohexane. The reaction was complete on mixing. An NMR scale experiment using 2 equiv of this substrate (0.02 mmol, 2.7 μL) and 0.5 mL of the stock Rh(I) solution (20 mM in CD_3CN) generated exclusively **8** as the Rh-containing product. A weak olefinic resonance at δ 5.65 was attributed to cyclohexene.

A similar ^1H NMR experiment using *cis*-1,2-dibromocyclohexane (0.01 mmol, 113 μL) as the substrate required about a week for complete reaction. The relative amounts of Rh(I) and Rh(II) were monitored by ^1H NMR, and the progress of the reaction was as follows: 18 h, 33% complete; 44 h, 60% complete; 72 h, 90% complete. The only species remaining after 1 week were the Rh(III) dibromide and cyclohexene, as the spectrum was identical with that obtained in the experiment with the trans isomer.

Acknowledgment. This work was supported by the NSF Grant CHE78-09443. Alex M. Madonik was the recipient of an NSF graduate fellowship.

Registry No. **1**, 53335-25-4; **3a**, 109-64-8; **3b**, 627-31-6; **3c**, 109-70-6; **3d**, 35432-34-9; **3e**, 6940-76-7; **3f**, 22306-36-1; **4a**, 99494-93-6; **4b**, 99494-94-7; **4c**, 99494-95-8; **4d**, 99494-96-9; **4e**, 99494-97-0; **4f**, 99494-98-1; **5a**, 99494-99-2; **5b**, 99495-00-8; **7**, 99495-01-9; **8**, 99355-26-7; 1,2-dibromoethane, 106-93-4; 1,2-dibromopropane, 78-75-1; propene, 115-07-1; ethylene, 74-85-1; *trans*-1,2-dibromocyclohexane, 7429-37-0; cyclohexane, 110-83-8; *cis*-1,2-dibromocyclohexane, 19246-38-9.

(20) (a) Silica gel plates for analytical TLC (250 μm thickness) were purchased from Analtech, Inc. (b) Silica gel (60–200 mesh, type 62) was supplied by W. R. Grace and activated at 80 °C.

(3-Chloro-2-methylenecycloalkyl)palladium Chloride Dimers: Preparation, Conformation, and Fluxional Behavior

William A. Donaldson

Department of Chemistry, Marquette University, Milwaukee, Wisconsin 53233

Received June 13, 1985

The title compounds are prepared in nearly quantitative yields by the reaction of Ω-methylenebicyclo[*n*.1.0]alkanes with bis(acetonitrile)palladium chloride. The C3 configuration and ring conformation of the (3-chloro-2-methylenecycloalkyl)palladium chloride dimers are assigned from their ^1H and ^{13}C NMR spectra. The chloropalladation of *exo*-3-methylenetricyclo[3.2.1.$0^{2,4}$]octane provides positive evidence for the addition of Cl to the sterically less hindered face of the methylenecyclopropane precursor. The kinetic products of the proposed cis-chloropalladation mechanism may undergo $\eta^3 \rightarrow \eta^1 \rightarrow \eta^3$ isomerization at the unsubstituted allyl terminus to afford the thermodynamically stable isomers. Allylic strain is shown to be an important factor in the relative stability of the (1-substituted 3-chloro-2-methylenecycloheptyl)palladium chloride $\eta^3 \rightarrow \eta^1 \rightarrow \eta^3$ diastereomers. Preparation of the title compounds with ring size ≥9 allows assessment of the factors involved in syn–anti isomerization at the endocyclic terminus of exocyclic π-allyl complexes. For the medium to large ring complexes the results indicate that ring strain, torsional strain, and transannular nonbonding repulsions greatly contribute to the relative stabilities of the syn and anti isomers.

Introduction

The catalytic and stoichiometric utilization of π-allyl palladium complexes in organic synthesis has become important due to the great regio- and stereoselectivity which these reagents can provide.[1] As well, the π-allyl system (**1**, eq 1) has been of interest in the study of fluxional

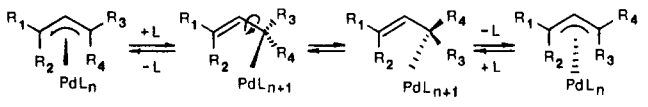

(1)

organometallic molecules.[2] The syn and anti positions of **1** may undergo exchange, in the presence of donor ligands, via an $\eta^3 \rightarrow \eta^1 \rightarrow \eta^3$ mechanism in which the metal atom is rearranged to the opposite face of the allyl ligand.[3]

Generally, terminal substituents on *acyclic* π-allyls tend to occupy syn positions.[4,5] *Surprisingly*, the cyclododecylpalladium chloride dimer, an inseparable mixture of *cyclic* π-allyls **2a**, **2b**, and **2c** (5:4:1 ratio, eq 2),[6] has been

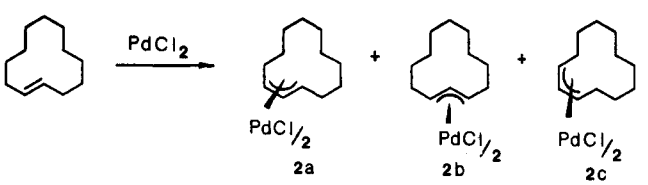

(2)

cited frequently[4,5] as an example of this positional preference. Only two exocyclic (π-allyl)palladium complexes

Chart I

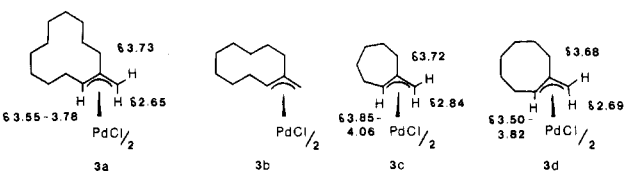

with ring size large enough to permit syn–anti isomerization have been reported; the (2-methylenecyclododecyl)-[6] and the (2-methylenecyclodecyl)palladium chloride dimers[7] (**3a** and **3b**, Chart I). Neither structure was unambiguously determined, and ^1H NMR spectral data are only available for compound **3a**.[6] Comparison of the chemical shifts of the allyl protons of **3a** with those of the (2-methylenecycloheptyl)- and (2-methylenecyclooctyl)palladium chloride dimers[8] (**3c** and **3d**) indicates that the (2-methylenecyclododecyl)palladium complex may have the syn orientation in solution.

Certain palladium allyls are resistant to $\eta^3 \rightarrow \eta^1 \rightarrow \eta^3$ isomerization, with the metal bound only to the sterically less hindered face of the allyl (e.g., **4a** and **4b**).[9] In fact,

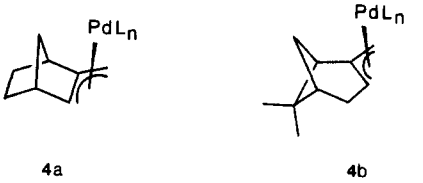

the inability of the cyclic π-allyls **5a**, **5b**, and **5c** (Scheme I) to undergo syn–anti isomerization under favorable conditions (0.05 equiv of PPh_3, C_6H_6, reflux, 8 h) was important to the mechanistic arguments for their formation.[10a] Thus, **5a** was assigned exclusively as the kinetic product from the chloropalladation of *cis*-9-methylene-

(1) Trost, B. M.; Verhoeven, T. R. "Comprehensive Organometallic Chemistry"; Pergamon Press: New York, 1982, Chapter 57, Vol. 8, pp 799–938.
(2) Tsutsui, M.; Courtney, A. *Adv. Organomet. Chem.* **1977**, *16*, 241–282.
(3) Faller, J. W.; Thomsen, M. E.; Mattina, M. J. *J. Am. Chem. Soc.* **1971**, *93*, 2642–53 and references therin.
(4) Maitlis, P. M. "The Organic Chemistry of Palladium"; Academic Press: New York, 1971; Vol. 1, pp 175–252.
(5) Maitlis, P. M.; Espinet, P.; Russell, M. J. H. "Comprehensive Organometallic Chemistry"; Pergamon Press: New York, 1982; Chapter 37.8, Vol. 6, pp 385–446.
(6) Hüttel, R.; Dietl, H. *Chem. Ber.* **1965**, *78*, 1753–60.
(7) Hüttel, R. *Synthesis* **1970**, 225–55.
(8) Hüttel, R.; Dietl, H.; Christ, H. *Chem. Ber.* **1964**, *97*, 2037–45.
(9) (a) Godleski, S. A.; Gudlach, K. B.; Ho, H. Y.; Keinan, E.; Frolow, F. *Organometallics* **1984**, *3*, 21–8. (b) Trost, B. M.; Strege, P. E.; Weber, L.; Fullerton, T. J.; Dietsche, T. J. *J. Am. Chem. Soc.* **1978**, *100*, 3407–15.
(10) (a) Albright, T. A.; Clemens, P. R.; Hughes, R. P.; Hunton, D. E.; Margerum, L. D. *J. Am. Chem. Soc.* **1982**, *104*, 5369–79. (b) Clemens, P. R.; Hughes, R. P.; Margerum, L. D. *Ibid.* **1981**, *103*, 2428–30. (c) Hughes, R. P.; Day, C. S. *Organometallics* **1982**, *1*, 1221–5.

0276-7333/86/2305-0223$01.50/0

Scheme I

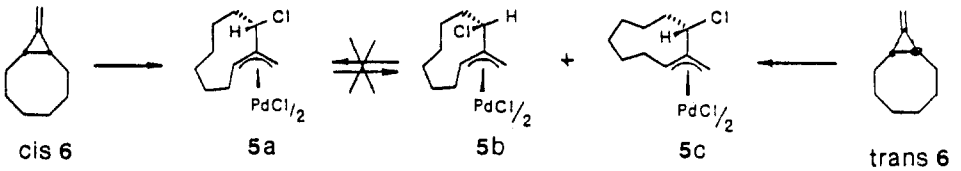

bicyclo[6.1.0]nonane (*cis*-**6**) while **5b** and **5c** were found to be the kinetic products from the chloropalladation of *trans*-**6**. Hughes et al. have used these results to support the proposed suprafacial addition of Pd–Cl to a disrotatory-out opening of the cyclopropane ring.[10] These authors also found no evidence for an intermediate containing carbonium ion character.

Recently, we have been reinvestigating the chloropalladation mechanism in nucleophilic solvents. *In contrast to Hughes*,[10] we have found evidence for the involvement of an intermediate with carbonium ion character in the ring opening of 1-phenyl-7-methylenebicyclo[4.1.0]heptane.[11] In addition, we are investigating the reactivity of the novel, ring-homologated (3-chloro-2-methylenecycloalkyl)palladium chloride dimers[12] (**7**, eq 3)

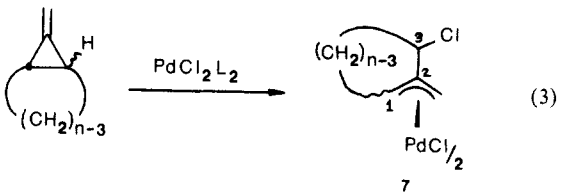

(3)

7

and their application to organic synthesis. Compounds of the general structure **7** react as "1,3 doubly activated"[13] palladium allyls, although this reactivity is in part dependent on the configuration at C3.[12a] Therefore, it was desirable to prepare a series of (3-chloro-2-methylenecycloalkyl)palladium complexes **7** (n = 6–9, 11, 13, 16) to gain configurational and conformational insight which might aid in understanding their reactivity.[14] Furthermore, compounds **7** (n = 9, 11, 13, 16) should present the opportunity to investigate, for the first time, the effects of ring size on the syn–anti isomerization of exocyclic π-allyl palladium complexes.

Results

All of the π-allyls described in this paper are racemic mixtures of enantiomers. For simplicity only one enantiomer is diagrammed.

(3-Chloro-2-methylenecycloheptyl)palladium chloride dimer (**8**) was prepared from 7-methylenebicyclo[4.1.0]-heptane (**9**) and $PdCl_2(CH_3CN)_2$ (**10**), as previously described[10a] (spectral data, Tables I and II). A sample of **8** was quantitatively recovered after being heated at reflux in CH_3CN (24 h).

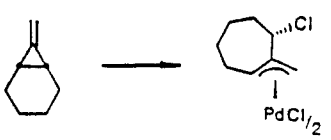

9 **8**

The reaction of *exo*-3-methylenetricyclo[3.2.1.0^{2,4}]octane (**11**) with **10** (CH_2Cl_2, 23 °C, 15 min) afforded a nearly quantitative yield of a single product, **12**, as a pale yellow

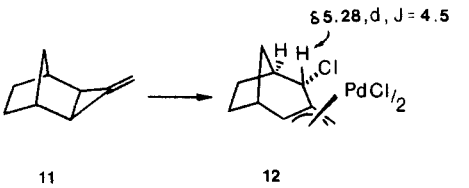

11 **12**

solid. The assignment of a π-allyl structure is consistent with the ^1H and $^{13}C\{^1H\}$ NMR spectral data (Tables I and II). The configuration at C3 (Cl-endo) was assigned on the basis of the 4.5-Hz coupling between the C3 and C4 protons. This coupling constant may be compared with the coupling constants for the C4 protons of *endo*- and *exo*-4-hydroxy-3-methylbicyclo[3.2.1]oct-2-ene (**13a** and **13b**,

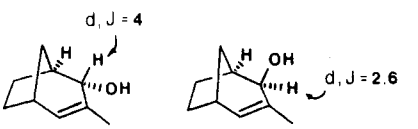

13a **13b**

4 and 2.6 Hz, respectively).[15] The Pd atom is presumably bound to the less hindered exo face of the allyl, as is the case for (2-methylenenorbonyl)palladium complexes (**4a**).[9a] A sample of **12** was recovered unchanged after being heated at reflux in CH_3CN (24 h).

The chloropalladation of 1-methyl-7-methylenebicyclo[4.1.0]heptane (**14**) (**10**, CH_2Cl_2, 23 °C, 15 min) afforded a crystalline yellow solid (99% yield). The ^1H NMR spectrum of the crude product indicated that it consisted of a 10:1:6 mixture of isomers **15a**, **15b**, and **16**. A pure

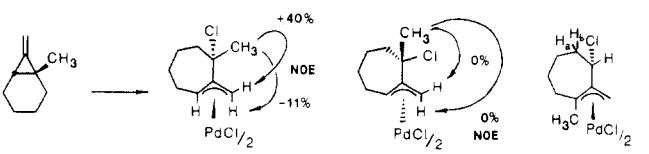

14 **15a** **15b** **16**

sample (by ^1H NMR spectroscopy) of the major isomer **15a** was obtained by fractional crystallization (CH_2Cl_2/hexanes). An enriched sample of **16** (~80%) was obtained by evaporation of the mother liquors. The pure compound **15a** isomerized to afford an 8:1 mixture of diastereomers **15a** and **15b** after 5 days in $CDCl_3$ solution. Heating either the initial mixture of **15a**, **15b**, and **16** or pure **15a** at reflux in CH_3CN for 24 h gave an 8:1:2 mixture of **15a**, **15b**, and **16** with 98% mass recovery.

The structural assignment for **16** is based on ^1H NMR spectral data (Table I). The singlet at δ 1.28 (3 H) indicates that the methyl group occupies an anti position on the allyl.[10a] The configuration at C3 (Cl-ax, H-eq) is assigned from the vicinal coupling of H_a and H_b to C*H*Cl (2.4 and 7.5 Hz).[11]

The skeletal structures of the two diastereomers **15a** and **15b** were established on the basis of their ^1H NMR spectral

(11) Donaldson, W. A. *J. Organomet. Chem.* **1984**, *269*, C25–C28.
(12) (a) Donaldson, W. A.; Taylor, B. S. *Tetrahedron Lett.* **1985**, 4163–6. (b) Donaldson, W. A.; Grief, V. J.; Gruetzmacher, J. A., manuscript in preparation.
(13) The reactivity of potential 1,1-diactivated π-allyls has recently been described: Lu, K.; Huang, Y. *J. Organomet. Chem.* **1984**, *268*, 185–190; Trost, B. M.; Vercauteren, J. *Tetrahedron Lett.* **1985**, 131–4.
(14) The consequences of ring conformation on the reactivity of macrocycles has been recently reported: Still, W. C.; Ealynker, I. *Tetrahedron* **1981**, *37*, 3981–96.
(15) Brun, P.; Waegell, B. *Tetrahedron* **1976**, 1125–35.

Table I. ^{1}H NMR Data for (3-Chloro-2-methylenecycloalkyl)palladium Chloride Dimers[a]

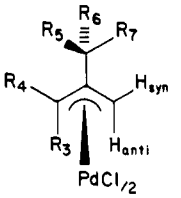

compd	H_{syn}	H_{anti}	R_3	R_4	R_5	R_6	R_7
8[b]	3.78 (s)	2.83 (s)	3.87 (dd), J = 6.0, 1.0	2.5–1.2 (m)	2.5–1.2 (m)	Cl	4.68 (dd), J = 5.5, 1.5
12[c]	3.96 (s)	2.84 (s)	4.04 (m)	2.6–1.2 (m)	5.28 (d), J = 4.5	2.6–1.2 (m)	Cl
15a[c]	3.97 (s)	2.67 (s)	3.75 (dd), J = 6.1, 2.5	2.4–1.4 (m)	2.4–1.4 (m)	Cl	1.83 (s)
15b[c]	4.37 (s)	2.64 (s)	3.71 (n)	2.4–1.4 (br m)	2.4–1.4 (br m)	1.78 (s)	Cl
16[d]	3.89 (d), J = 1.7	3.38 (d), J = 1.7	1.28 (s)	2.4–1.5 (m)	2.4–1.5 (m)	Cl	4.77 (dd), J = 7.5, 2.4
18a[e]	3.84 (d), J = 1.5	2.74 (d), J = 1.5	4.24 (br s)	2.5 (m, 1 H) 2.2–1.4 (m, 5 H)	2.5 (m, 1 H) 2.2–1.4 (m, 5 H)	4.82 (t), J = 6.1	Cl
18a[e,f]	3.52 (s)	2.19 (s)	3.44 (br s)	2.1–1.0 (m, 6 H)	2.1–1.0 (m, 6 H)	4.14 (t), J = 6.1	Cl
18b[e]	3.93 (s)	2.66 (s)	4.24 (br s)	2.2 (m, 1 H) 2.1–1.4 (m, 5 H)	2.2 (m, 1 H) 2.1–1.4 (m, 5 H)	Cl	4.62 (t), J = 6.1
18b[e,f]	3.68 (s)	2.05 (s)	3.44 (br s)	2.0–1.0 (m, 5 H) 0.8 (m, 1 H)	2.0–1.0 (m, 5 H) 0.8 (m, 1 H)	Cl	3.82 (t), J = 6.1
20[c]	4.19 (s)	2.52 (s)	3.58 (dd), J = 10.8, 5.4	2.4–1.2 (m)	4.96 (dd), J = 12.2, 5.4	2.4–1.2 (m)	Cl
5a[b]	4.36 (s)	3.12 (s)	2.5–1.1 (m)	4.33 (dd), J = 10, 3	4.22 (dd), J = 12, 5	2.5–1.1 (m)	Cl
5b[b]	3.84 (s)	3.20 (s)	2.3–1.2 (m)	4.80 (dd), J = 12, 3	Cl	2.3–1.2 (m)	4.67 (t), J = 3
5c[b]	4.07 (s)	2.54 (s)	3.72 (dd), J = 11, 6	2.3–1.2 (m)	4.98 (dd), J = 11, 5	2.3–1.2 (m)	Cl
22a[c]	4.33 (s)	3.21 (s)	2.1–1.0 (m)	4.41 (dd), J = 11.0, 3.0	4.25 (dd), J = 11.5, 3.5	2.2–1.0 (m)	Cl
22b[c]	3.86 (s)	3.33 (s)	2.2–1.0 (m)	4.84 (dd), J = 11.5, 3.0	Cl	2.2–1.0 (m)	4.51 (dd), J = 7.0, 4.0
22c[c]	3.98 (s)	2.58 (s)	3.74 (dd), J = 10.5, 4.5	2.2–1.0 (m)	4.64 (t), J = 7.0	2.2–1.0 (m)	Cl
24a[c]	4.29 (s)	3.10 (s)	2.2–1.0 (m)	4.35 (dd), J = 10, 4	4.24 (dd), J = 11, 4	2.2–1.0 (m)	Cl
24b[c]	3.78 (s)	3.18 (s)	2.2–1.0 (m)	4.86 (dd), J = 11, 4	Cl	2.2–1.0 (m)	4.54 (t), J = 4
24c[c]	4.06 (s)	2.52 (s)	3.62 (t), J = 7	2.1–1.0 (m)	4.73 (dd), J = 9, 4	2.1–1.0 (m)	Cl
26a[e]	4.26 (s)	3.17 (s)	2.0–1.1 (br m)	4.35 (m)	4.28 (t), J = 7	2.0–1.1 (br m)	Cl
26b[e]	3.83 (s)	3.25 (s)	2.0–1.1 (br m)	4.95 (br d), J = 12	Cl	2.0–1.1 (br m)	4.51 (dd), J = 7, 2
26c[d]	4.07 (s)	2.52 (s)	3.63 (t), J = 6.6	2.0–1.0 (br m)	4.67 (dd), J = 7.6, 4.1	2.0–1.1 (br m)	Cl
26d[e]	3.93 (s)	2.76 (s)	3.72 (t), J = 6	2.0–1.1 (br m)	Cl	2.2–1.1 (br m)	4.48 (m)

[a] In ppm downfield from $SiMe_4$ (multiplicities: s = singlet, d = doublet, t = triplet, m = multiplet, dd = doublet of doublets, br = broad); J values in hertz; $CDCl_3$ solution unless otherwise noted. [b] 270 MHz.[10a] [c] 200 MHz. [d] 60 MHz. [e] 300 MHz. [f] C_6H_6 solution.

Table II. $^{13}C\{^1H\}$ NMR Data (15 MHz) for (3-Chloro-2-methylenecycloalkyl)palladium Chloride Dimers (7)[a]

compd	C_1	C_2	C_3	$C_{methylene}$	other
8	83.93	125.20	61.89	61.00	36.77, 29.67, 27.56, 24.56
12	86.88	121.26	62.49	60.55	41.23, 37.57, 37.33, 30.39, 23.33
15a	84.13	128.89	70.38	58.12	44.69, 32.64, 29.72, 26.79, 26.23
18a	82.02	121.38	57.72	54.92	32.15, 24.97, 18.07
18b	82.83	124.19	55.12	54.19	33.33, 26.22, 18.07
20	80.51	125.11	57.01	54.95	42.00, 29.02, 28.33, 26.58, 25.73
5a	77.79	124.95	63.43	54.42	40.26, 30.96, 28.24, 24.92, 23.29, 20.61
5c	82.01	125.88	56.81	53.57	41.19, 30.56, 27.80, 27.72, 24.31, 22.93
26c	81.49	126.24	57.66	54.87	39.77, 29.01, 28.28, 27.47, 27.23, 26.66, 26.21, 25.69, 25.48, 25.32

[a] In ppm downfield from $SiMe_4$; $CDCl_3$ solution; carbon numbering refers to drawing of **7** in text.

data (Table I). Singlets at δ 1.83 (**15a**) and δ 1.78 (**15b**) indicate that the methyl groups in both **15a** and **15b** are attached to the ring at C3.[10a] Additional NMR data facilitated the C3 configurational assignment of compound **15a**. Difference ^{1}H NOE spectra (270 MHz, Argon purged $CDCl_3$ solution) provided the following enhancements: between CH_3, by irradiation at δ 1.83, and H_{syn} (+40%) and H_{anti} (−11%); and between H_{syn}, by irradiation at δ 3.97, and H_{anti} (+39%) and H_{allyl} (−30%). These enhancements are characteristic of the "linear three-spin effect",[16] indicating that the methyl group of **15a** is equatorial. Notably, irradiation of the CH_3 signal of diastereomer **15b** (at δ 1.78) produced no detectable NOE enhancements, as is also expected for the CH_3 axial configuration of **15b**.[16]

(16) Noggle, J. H.; Schirmer, R. E. "The Nuclear Overhouser Effect"; Academic Press: New York, 1971; pp 59–69.

Scheme II. Chloropalladation Products and Equilibrium Compositions

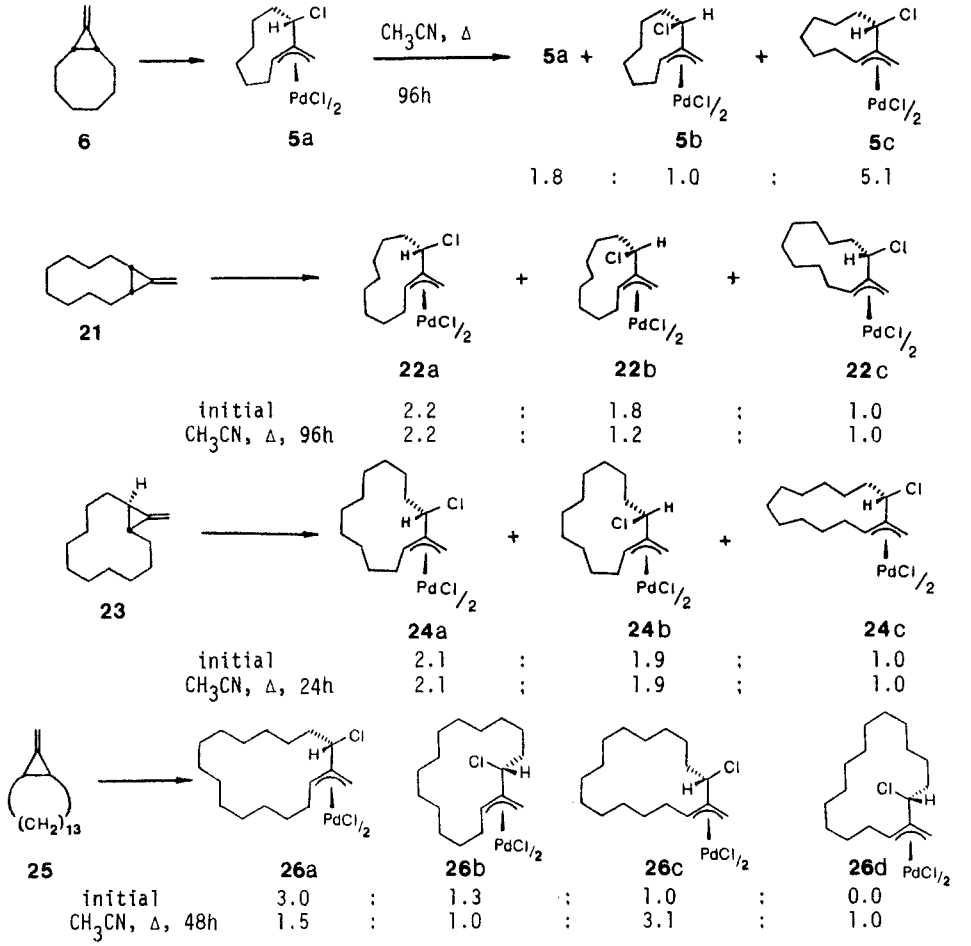

The reaction of 6-methylenebicyclo[3.1.0]hexane (**17**) with **10** (CH_2Cl_2, 23 °C, 15 min) afforded a gummy yellow solid, after evaporation of the solvent. The ^1H NMR spectrum of the crude product indicated a mixture of two π-allyls in roughly a 2.4:1 ratio. Crystallization of the crude mixture (CH_2Cl_2/hexanes) gave a pale yellow solid (85% yield). The crystalline sample contained the two diastereomeric π-allyls **18a** and **18b** in 2.5:1 ratio. Attempts to separate the two compounds by chromatography or fractional crystallization were unsuccessful. The ratio of **18a**:**18b** was unchanged in C_6D_6 solution or after being heated at reflux in CH_3CN (24 h).

The skeletal structures of the two products were established by comparison of their 300-MHz ^1H NMR spectra with that obtained for complex **8**. Assignment of the C3 configuration for diasteromers **18a** and **18b** is not possible from their ^3J_H coupling data; both C*H*Cl resonance signals appear as triplets. In the absence of any convincing spectral arguments, complex **18a** is arbitrarily assigned the Cl pseudoequatorial configuration and **18b** the Cl pseudoaxial configuration (^{13}C NMR data, Table II).

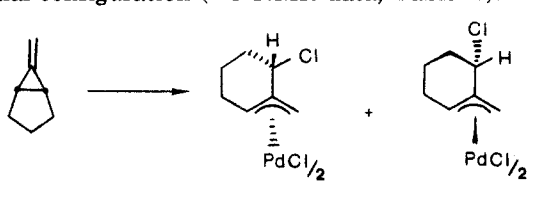

17 18a 18b

The chloropalladation of *cis*-9-methylenebicyclo[6.1.0]nonane (**6**) (**10**, CH_2Cl_2, 23 °C, 30 min) gave **5a** as the only product in nearly quantitative yield, as has been previously reported.[10a] Heating a sample of **5a** at reflux in CH_3CN (96 h) afforded a mixture of the known compounds **5a**, **5b**, and **5c** (1.8:1.0:5.1 by ^1H NMR integration, 99%, Scheme II). Recrystallization of the mixture (CH_2Cl_2/hexanes) afforded the known **5c** as a pure compound (^{13}C NMR data, Table II). Heating **5c** at reflux in CH_3CN (96 h) quantitatively yielded a mixture of **5a**, **5b**, and **5c** (1.8:1.0:5.1).

The chloropalladation of 8-methylenebicyclo[5.1.0]octane (**19**) (**10**, CH_2Cl_2, 23 °C, 15 min) quantitatively afforded a single yellow crystalline product. The product is assigned the structure **20** based on comparison of its ^1H and ^{13}C NMR spectra (Tables I and II) with the spectral data of the known compound **5c** (a one-carbon homologue, vide supra). In addition, the configuration of **20** at C3 (H-ax, Cl-eq) is assigned from the 5.4- and 12.2-Hz coupling of the C3 proton, the large coupling due to an ~180° dihedral angle to H_a.

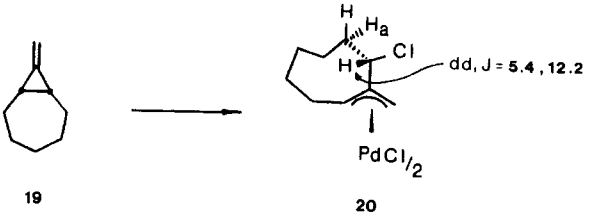

19 20

The reaction of *cis*-11-methylenebicyclo[8.1.0]undecane (**21**) with **10** (CH_2Cl_2, 23 °C, 15 min) gave a nearly quantitative yield of a mixture of three isomeric π-allyls, **22a**, **22b**, and **22c** (2.2:1.8:1.0, Scheme II). Recrystallization of the mixture (CH_2Cl_2/hexanes) afforded an enriched sample of **22a** (**22a**:**22b**:**22c**; 6.0:1.2:1.0). A sample of the recrystallized mixture isomerized into a 4.0:3.0:1.0 mixture of **22a**, **22b**, and **22c** in solution ($CDCl_3$, 10 h, 23 °C).

Scheme III

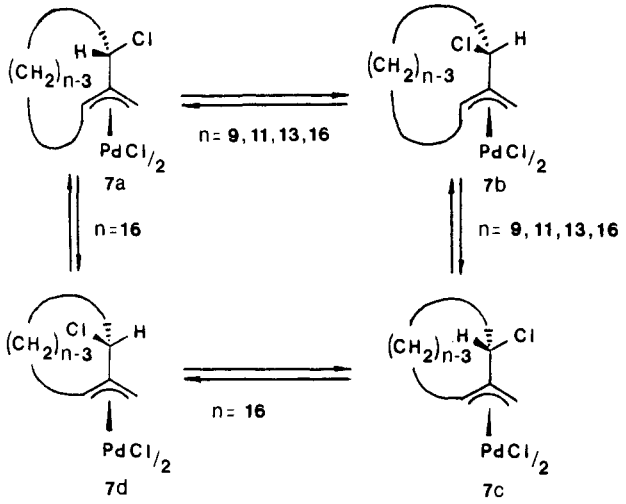

Heating either the initial mixture or the recrystallized mixture at reflux in CH_3CN (96 h) resulted in complete mass recovery of a 2.2:1.2:1.0 mixture of **22a**, **22b**, and **22c**.

The reaction of *trans*-13-methylenebicyclo[10.1.0]tridecane (**23**) with **10** (CH_2Cl_2, 23 °C, 30 min) gave a quantitative yield of a mixture of three isomeric π-allyls, **24a**, **24b**, and **24c** (2.1:1.9:1.0, Scheme II). Fractional crystallization of the mixture resulted in a sample enriched in **24c** (**24a**/**24b**/**24c** = 1.0:1.0:1.4). Twice recrystallization of the mother liquors gave a sample containing only **24a** and **24b** (1.5:1.0). Upon heating to reflux in CH_3CN (24 h) both enriched samples afforded the same equilibrium mixture (**24a**/**24b**/**24c** = 2.1:1.9:1.0, Scheme II).

The chloropalladation of 16-methylenebicyclo[13.1.0]-hexadecane (**25**) (**10**, CH_2Cl_2, 23 °C, 30 min) quantitatively afforded a mixture of three isomeric π-allyls, **26a**, **26b**, and **26c** (3.0:1.3:1.0, Scheme II). Fractional crystallization of the mixture (CH_2Cl_2/hexanes) yielded a single yellow crystalline isomer, **26c**. Heating either the initial mixture or isolated **26c** in CH_3CN (48 h) resulted in formation of a mixture of **26a**, **26b**, and **26c** and a fourth isomer tentatively assigned as **26d** (1.5:1.0:3.3:1.0). Isomer **26d** was identified only in the equilibrium mixture.

The structural assignments for compounds **22a–c**, **24a–c**, and **26a–d** were made in the following manner. The ^1H NMR spectral data for **22a**, **24a**, and **26a** can be compared with the data for the Pd–allyl complex **5a**, whose structure has been assigned by NMR and X-ray analysis.[10c] The chemical shifts for H_{syn}, H_{anti}, H_{allyl} (R4, Table I), and C*H*Cl of complexes **22a**, **24a**, and **26a** are similar to those of **5a** (within ±0.1 ppm). Thus, they can all be assigned the same general structure **7a** (Scheme III). The structural assignments for **22b**, **24b**, and **26b** can be made by comparison of their ^1H NMR spectral data with the known compound **5b**. It should be noted that the resonance signals for the C1 protons of complexes **5b**, **22b**, **24b**, and **26b** (R4, Table I, $\sim\delta$ 4.8–4.9) appear shifted downfield of the signals for the C1 protons of **5c**, **22c**, **24c**, **26c**, and **26d** ($\sim\delta$ 3.6–3.7). This indicates that the C1 allylic protons of general structure **7b** must occupy the syn position while the C1 allylic protons of structure **7c** must occupy the anti position (Scheme II).[17] If the C1 allylic proton of **7b** is in a syn position, then the configuration at C3 must be the opposite of that of general structure **7a**, in order that the two structures are not the same. Complexes **22c**, **24c**, and **26c** were assigned the general structure **7c** (Scheme III)

(17) The anti hydrogens of a Pd–allyl complex are significantly closer to the metal and are thus more shielded than the syn hydrogens.[4]

Scheme IV

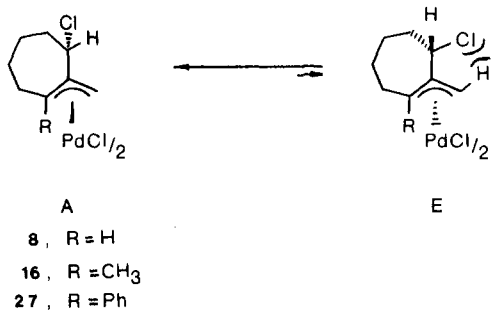

by comparison of their ^1H NMR spectral data with that obtained for compounds **5c** and **20** (vide supra). The structural assignment for **26c** is further supported by comparison of its ^{13}C NMR spectral data with that obtained for **5c** and **20** (Table II). Finally compound **26d** was assigned the only other possible combination of C1 and C3 configurations in order to be different from isomer **26c**.

Discussion

The chloropalladation of 7-methylenebicyclo[4.1.0]heptane (**9**) is believed to occur via initial complexation of $PdCl_2$ to the less hindered face of the olefin, followed by cis addition of Pd–Cl to the cyclopropane ring opening in a disrotatory-in fashion. The initially formed π-allyl 8′, which was not observed by NMR monitoring, undergoes extremely rapid $\eta^3 \rightarrow \eta^1 \rightarrow \eta^3$ isomerization to afford the more thermodynamically stable diastereomer/conformer **8** (eq 4). Although the isolated product reflects apparent

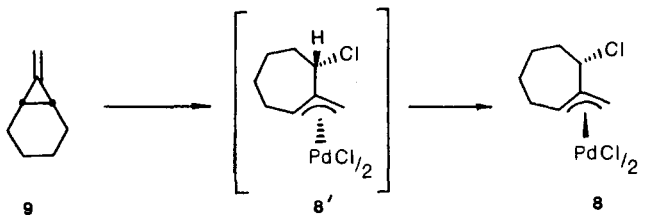

(4)

"trans-chloropalladation", the above mechanism was proposed in order to be consistent with the suprafacial addition of Pd–Cl which is oberved for the reaction of *cis*- and *trans*-9-methylenebicyclo[6.1.0]nonane with palladium chloride.[10a]

In fact, complexes **8**, **15a**, **16**, **20**, and **27**[11] all appear to be the products of trans addition of Pd–Cl to the corresponding methylenecyclopropane precursors. However, evidence to support the dis-in–cis-addition mechanism may be found in the chloropalladation of *exo*-3-methylenetricyclo[3.2.1.$0^{2,4}$]octane (**11**). The product **12** was assigned the Cl-endo configuration on the basis of NMR spectral analysis. Although the structure of this complex also represents apparent trans addition, the configuration at C3 indicates addition of Cl to the less hindered face of the methylenecyclopropane. This is the face which should preferentially coordinate to $PdCl_2$ in the initial step of the mechanism. After cis addition, facile $\eta^3 \rightarrow \eta^1 \rightarrow \eta^3$ isomerization would transfer the Pd atom to the less hindered face of the resultant allyl. In addition, complexes **18a** and **15b**, which are assigned the Cl-equatorial configuration, are the products from cis-chloropalladation without subsequent isomerization.

If the cis-chloropalladation–isomerization mechanism is valid, then complexes **8**, **16**, **20**, and **27** must be considerably more thermodynamically stable than their corresponding $\eta^3 \rightarrow \eta^1 \rightarrow \eta^3$ diastereomers. The factors contributing to this thermodynamic stability deserve some comment. The thermodynamically stable structure for the

Scheme V

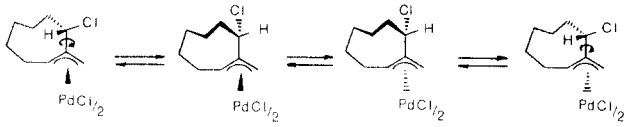

20 28 29 30

three (1-substituted 3-chloro-2-methylenecycloheptyl)-palladium complexes (**8**, **16**, and **27**) all have the Cl-axial configuration (A, Scheme IV). The higher energy of the Cl-equatorial diastereomer (E, Scheme IV) with respect to A can be attributed to the allylic strain[18] between the equatorial Cl atom and the methylene protons in structure E which is not present in the Cl-axial diasteromer A. Both diastereomers of the (3-chloro-3-methyl-2-methylenecycloheptyl)palladium complex (**15a** and **15b**) are present at equilibrium (8:1 ratio, 120 h, 23 °C, $CDCl_3$). These two diastereomers should be closer in relative energy due to the contributions of allylic strain between methyl and methylene in **15a** and between Cl and methylene in **15b**.

Although the C3 configuration of **18a** and **18b** cannot be definitively assigned, it is important to note that both diastereomers are present in the product mixture. Calculations indicate that there is greater conformational mobility in the cyclohexene ring than the cycloheptene ring.[19] The less rigid cyclohexene ring can distort to relieve allylic strain between pseudoaxial and pseudoequatorial conformers better than can the rigid cycloheptene ring. Thus allylic strain should contribute less to the relative stabilities of the diastereomers of (3-chloro-2-methylenecyclohexyl)palladium complexes (**18a** and **18b**). This is demonstrated by the 2.5:1 ratio of **18a** and **18b** in solution.

Complex **20** has the same C3 configuration as complex 8; however, the cyclooctyl ring adopts a different ring conformation (Cl-ax). Molecular models indicate that **20** is the lowest energy structure of the two conformers of each of the two syn diastereomers (**20**, **28**, **29**, and **30**, Scheme V). Conformers **28** and **29** will be higher in energy than **20** and **30**, respectively, due to the steric interactions between the cyclooctyl ring and the palladium metal. In addition, diastereomer **28** will be higher in energy with respect to diastereomer **20** due to the unfavorable transannular interactions of the chloride atom. In fact nearly all of the syn isomers of the complexes **7** ($n \geq 8$) adopt this conformation and C-3 configuration (vide infra).

In our hands, chloropalladation of *cis*-**6** gave only **5a** as was previously reported.[10a] The π-allyl complexes **5a**, **5b**, and **5c** were also reported to be resistant to interconversion via the $\eta^3 \rightarrow \eta^1 \rightarrow \eta^3$ mechanism (C_6H_6, 0.05 equiv of PPh_3, 80 °C, 8 h). The authors speculated that the considerable reorganization of the organic ring which must be involved in the rearrangement would be sufficient to preclude isomerization.[10a] Our results show that **5a**, **5b**, and **5c** *do indeed* isomerize, albeit under more vigorous reaction conditions (96 h, 82 °C, CH_3CN solution). These conditions indicate a higher barrier to $\eta^3 \rightarrow \eta^1 \rightarrow \eta^3$ isomerization for the cyclononyl system (**7**, $n = 9$) than for the larger ring systems (**7**, $n = 11$, 13, 16).[22] In fact, a sample enriched in **22a** rearranges to a mixture of **22a** and **22b**, via isomerization at the exocyclic terminus, under extremely mild conditions ($CDCl_3$ 23 °C, 10 h). However, it should be noted that syn–anti isomerization at the endocyclic terminus of **22b** and **22c** requires more vigorous conditions (CH_3CN, reflux), as would be expected.[3]

Table III. Syn-Anti (Cis-Trans) Equilibrium Mixtures

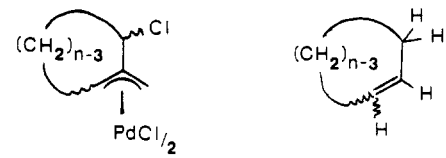

	7	31
n	7 (syn:anti)[a]	31 (cis:trans)
9	1.82	232[b]
11	0.29	0.4[b]
13	0.25	0.66[c]
16	1.64	*d*

[a] [(**7c** + **7d**):(**7a** + **7b**)] at 82 °C; CH_3CN solution. [b] Equilibrium at 100.4 °C; CH_3CO_2H solution.[25] [c] Reference 26. [d] Ratio was not established from the trace cyclohexadecene found in the products of hydroboration–oxidation of 1,9-cyclohexadecadiene.[27]

Syn–anti equilibrium mixtures can be obtained for the larger ring complexes (**7**, $n = 9$, 11, 13, 16), in refluxing CH_3CN (82 °C). These mixtures are shown to be the equilibrium mixtures by approach from either extreme. The ratio of syn to anti isomers at equilibrium [(**7c** + **7d**):(**7a** + **7b**)], a reflection of their relative thermodynamic stabilities, is dependent on ring size. The cyclononyl and cyclohexadecyl systems (**7**, $n = 9$ and 16, respectively) have a syn:anti ratio of ~2 while the cycloundecyl and cyclotridecyl systems (**7**, $n = 11$ and 13, respectively) have a syn:anti ratio of ~0.3–0.25 (Table III). The latter two cases are in contrast to the expectation[4,5] that the syn isomers will be more stable than the anti isomers. The equilibrium constants for the *cis:trans* cyclic olefins (**31**, $n = 9$, 11, 13) also appear in Table III. The rough direction of the syn:anti equilbria for **7** parallels that of the cis:trans equilibria for **31**. The molecular interactions intrinsic to the relative thermodynamic stability of cis and trans cyclic olefins (i.e., ring strain, torsional strain, and transannular interactions)[23] are undoubtedly important considerations in the relative thermodynamic stability of the syn and anti isomers of cyclic π-allyls, as well. The X-ray structure of the anti cyclononyl π-allyl complex **5a** (acac derivative)[10c] reveals the rigidity and strain in this particular ring conformation. On the other hand, the syn isomer **5c** is relatively flexible and should be better able to minimize the transannular interactions and imperfect C–H staggering. In contrast to **5a**, the anti cycloundecyl and cyclotridecyl isomers are relatively flexible and transannular interactions should be best minimized in the anti isomers (**23a,b** and **25a,b**) rather than their corresponding syn isomers (**23c** and **25c**, respectively). Transannular nonbonded repulsions are much less significant in very large rings.[24] This

(18) Allylic $A^{(1,2)}$ strain is defined as the steric interactions between sufficiently large C2 and C3 substituents on a cyclohexene ring which results in the C3-axial conformer being energetically favored. Allylic $A^{(1,3)}$ strain is defined as the steric repulsions in 2-substituted methylenecyclohexanes which result in an energetic preference for the C2-axial conformer. $A^{(1,3)}$ strain is believed to involve greater repulsion than 1,3-diaxial repulsions in the cyclohexane system.[19] The definition of $A^{(1,2)}$ strain might also be extended to the cycloheptene ring system, in which the chair conformation is predicted[20] to be lower in energy than the boat. In fact, allylic strain may be greater in the cycloheptene ring due to the decreased conformational mobility of the cycloheptene ring with respect to the cyclohexene ring.[21]

(19) Johnson, F. *Chem. Rev.* **1968**, 375–413.

(20) Favini, G.; Buemi, G.; Raimondi, M. *J. Mol. Struct.* **1968**, *2*, 137.

(21) Glazer, E. S.; Knorr, R.; Ganter, C.; Roberts, J. O. *J. Am. Chem. Soc.* **1972**, *94*, 6026–32.

(22) Theoretical calculations indicate a lower barrier to conformational interconversion for cycloundecane (3.5 kcal/mol) compared to cyclononane (8.6 kcal/mol): Dale, J. *Acta. Chem. Scand.* **1973**, 1130–48.

(23) Eliel E. L.; Allinger, N. L.; Angyal, S. L.; Morrison, G. A. "Conformational Analysis"; American Chemical Society: Washington, D. C., 1981; pp 213–223.

(24) Anet, F. A. L.; Cheng, A. K. *J. Am. Chem. Soc.* **1975**, *97*, 2420–4.

is exemplified by the presence of an isomer of general structure **7d** only in the equilibrium of (3-chloro-2-methylenecyclohexadecyl)palladium chloride dimers (**26**). Apparently, transannular repulsions of the Cl atom in the syn conformation and C3 configuration of structure **7d** (Scheme II) are large enough to preclude this isomeric structure for all but the very large ring systems (i.e., **7**, n = 16). The decreased transannular interactions inherent in the large 16-membered ring is also reflected in an increase of the syn–anti ratio of the exocyclic π-allyls, at equilibrium.

In light of our results, it is indeed surprising that the cyclododecylpalladium chloride dimer mixture (**2a**, **2b**, and **2c**) is cited[4,5] as an example of the *acyclic* syn preference. The predominance of the syn,anti isomer **2a** and the syn,syn isomer **2b** over the anti,anti isomer **2c** in the mixture might be more realistically attributed to the lower energy of **2a** and **2b** due to the relief of transannular nonbonding interactions and imperfect staggering present in structure **2c**.

Summary

(3-Chloro-2-methylenecycloalkyl)palladium chloride dimers may be prepared in excellent yields from the corresponding Ω-methylenebicyclo[n.1.0]alkanes. Since the precursor methylenebicycloalkanes may be prepared from the corresponding cyclic olefins, these reactions constitute a formal ring homologation methodology. The chloropalladation of *exo*-3-methylenetricyclo[3.2.1.0^{2,4}]octane clearly proceeds via addition of Cl to the less hindered face of the cyclopropane ring, as had been previously speculated.[10a] In general, the kinetic products undergo rapid $\eta^3 \rightarrow \eta^1 \rightarrow \eta^3$ isomerization to afford the thermodynamically stable diastereomers. The exception is the cyclononyl ring system. The syn–anti isomers of the medium to large ring π-allyl complexes (**7**, n = 9, 11, 13, 16) exist in an equilibrium. Our results indicate that the relative stabilities of the cyclic syn–anti isomers depends on ring strain, torsional strain, and transannular interactions. With this conformational information in hand, the reactivity of the product (3-chloro-2-methylenecycloalkyl)-palladium complexes will be reported in due course.

Experimental Section

General Data. All IR spectra were recorded on a Perkin-Elmer 700 or 337 spectrophotometer and calibrated against the 1601-cm^{-1} peak of polystyrene. All 60-MHz ^{1}H NMR and 15-MHz ^{13}C{^{1}H} NMR spectra were recorded on either a Varian EM360L or a JEOL FX60Q spectrometer; chemical shifts are reported in parts per million downfield from tetramethylsilane, and couplings are reported in hertz. All 200-MHz ^{1}H NMR spectra were recorded on a Varian XL200 spectrometer at Wesleyan University, and all 300-MHz ^{1}H NMR spectra were recorded on a General Electric QE-300 spectrometer. Microanalysis were sent to Midwest Microlab, Ltd., Indianapolis, IN. Melting points were obtained by using a Mel-Temp melting point apparatus and are uncorrected.

All reactions were run under an atmosphere of nitrogen. Spectrograde solvents were used without further purification except for diethyl ether, which was distilled from sodium benzophenone ketyl.

7-Methylenebicyclo[4.1.0]heptane (**9**), *cis*-9-methylenebicyclo[6.1.0]nonane (**6**), and 6-methylenebicyclo[3.1.0]hexane (**17**)[28] were prepared by the literature procedure.[29] The following compounds were prepared in a similar fashion (unoptimized yields, except for **23**).

***exo*-3-Methylenetricyclo[3.2.1.0^{2,4}]octane (11)**: 5%; bp 44 °C (19 mmHg); IR (neat, cm^{-1}) 3090 m, 2950 s, 2890 s, 1760 m, 1450 m, 1300 m, 880 s; ^{1}H NMR ($CDCl_3$) δ 5.2 (t, J = 1.3, 2 H, C=CH_2), 2.4 (br s, 1 H), 1.6–0.8 (m, 9 H) [lit.[30] IR (neat, cm^{-1}) 3060, 2950, 2870, 1763, 1450, 1295, 880; ^{1}H NMR (CCl_4) δ 5.13 (t, J = 1.3), 2.35 (m), 1.65–1.27 (m), 1.48 (H_2, H_4), 0.85 (AB_q, J = 9.5)].

1-Methyl-7-methylenebicyclo[4.1.0]heptane (14): 33%; bp 29–30 °C (19 mmHg); IR (neat, cm^{-1}) 3080 m, 2950 s, 1440 m, 880 s; ^{1}H NMR ($CDCl_3$) δ 5.3 (d, J = 2.4, 2 H, C=CH_2), 2.2–1.1 (m, 9 H, CH_2), 1.15 (s, 3 H, CH_3); ^{13}C{^{1}H} NMR ($CDCl_3$) δ 148.48 (*C*=CH_2), 91.91 (C=*C*H_2), 29.5, 25.81, 23.33, 21.83, 21.63, 20.45, 18.55. Anal. Calcd for C_9H_{14}: C, 88.45; H, 11.55. Found: C, 88.01; H, 11.95.

8-Methylenebicyclo[5.1.0]octane (19): 9%; bp 54 °C (19 mmHg); IR (neat, cm^{-1}) 3075 m, 2940 s, 2860 s, 1740 w, 1430 s, 1180 m, 1170 m, 1030 m, 895 s, 805 m; ^{1}H NMR ($CDCl_3$) δ 5.28 (s, 2 H, C=CH_2), 2.0–0.8 (m, 12 H, CH_2) [lit.[31] bp 50–52 °C (8 mmHg); ^{1}H NMR (CCl_4) δ 5.22 (s, 2 H, C=CH_2), 1.1–2.2 (12 H)].

***trans*-13-Methylenebicyclo[10.1.0]tridecane (23)**: 81% (based on consumed *trans*-cyclododecene); bp 51–56 °C (0.10 mmHg); IR (neat, cm^{-1}) 3080 m, 2940 s, 1750 w, 1440 s, 1350 m, 1330 m, 1145 m, 975 m, 885 s, 725 m; 200-MHz ^{1}H NMR ($CDCl_3$) δ 5.25 (t, 2 H, C=CH_2), 2.00 (t, J = 10, 2 H), 1.8–1.1 (m, 18 H), 0.92 (m, 2 H, cyclopropyl H); ^{13}C{^{1}H} NMR ($CDCl_3$) δ 144.35 (*C*=CH_2), 100.32 (C=*C*H_2), 31.00, 27.80, 27.11, 24.31, 23.46, 21.30. Anal. Calcd for $C_{14}H_{24}$: C, 87.42; H, 12.58. Found: C 87.12; H, 12.79.

16-Methylenebicyclo[13.1.0]hexadecane (25): 11%; bp 68–72 °C (0.07 mmHg); IR (neat, cm^{-1}) 3100 w, 2960 s, 2890 s, 1760 w, 1460 m, 980 w, 885 m; ^{1}H NMR ($CDCl_3$) δ 5.28 (br s, $^1/_2W$ = 3 Hz, 2 H, C=CH_2), 1.68 (m, 2 H), 1.34 (br s, $^1/_2W$ = 4.5 Hz, 24 H), 1.00 (br s, 2 H). Anal. Calcd for $C_{17}H_{30}$: C, 87.10; H, 12.90. Found: C, 86.97; H, 13.01.

***cis*-11-Methylenebicyclo[8.1.0]undecane (21)** was prepared in a manner similar to *trans*-9-methylenebicyclo[6.1.0]nonane:[10a] 56% (based on consumed *cis*-cyclodecene); bp 70 °C (0.3 mmHg, Kugelrohr distillation); IR (neat, cm^{-1}) 3100 w, 2950 s, 2890 s, 1740 w, 1445 m, 1355 w, 1140 w, 880 s, 710 m; ^{1}H NMR ($CDCl_3$) δ 5.29 (br s, W = 3.1 Hz, 2 H, C=CH_2), 2.2–0.9 (m, 18 H, CH_2); ^{13}C{^{1}H} NMR ($CDCl_3$) δ 141.38 (*C*=CH_2), 100.76 (C=*C*H_2), 28.69, 26.54, 23.78, 21.75, 20.45. Anal. Calcd for $C_{12}H_{20}$: C, 87.73; H, 12.27. Found: C, 87.42; H, 12.47.

General Procedure for Chloropalladation of Methylenecyclopropanes. To a solution of $PdCl_2(CH_3CN)_2$ (1–5 mmol) in CH_2Cl_2 (~50 mL) was added, in one portion, a solution of the methylenecyclopropane (1 molar equiv) in CH_2Cl_2 (~10 mL). The red-orange solution rapidly turned pale yellow, and the solution was allowed to stir an additional 15–30 min. The solvent was removed under reduced pressure and the product dried under high vacuum. The following methylenecyclopropanes were allowed to react according to this general procedure:

Chloropalladation of 9. The product was identified by NMR spectroscopy[10a] (Tables I and II) as only consisting of **8** (98% yield). A sample of **8** (0.20 g, 0.38 mmol) was heated to reflux in CH_3CN (25 mL) for 24 h. The solution was allowed to cool and the solvent removed first under reduced pressure and finally under high vacuum to afford **8** (0.20 g, 0.77 mmol, 100%).

Chloropalladation of 11. The product **12** was identified by NMR spectroscopy (Tables I and II) (98% yield). Crystallization from CH_2Cl_2/hexanes afforded an analytically pure sample, mp 168 °C dec. Anal. Calcd for $[C_9H_{12}Cl_2Pd]_2$: C, 36.34; H, 4.07. Found: C, 36.60; H, 4.26. A sample of **12** (0.05 g, 0.08 mmol) was heated to reflux in CH_3CN (50 mL) for 24 h. Removed of the solvent under reduced pressure quantitatively afforded **12** (0.05 g).

Chloropalladation of 14. The product was identified by NMR spectroscopy (Tables I and II) as consisting of **15a**, **15b**, and **16** (10:1:6 ratio, 99%). Fractional crystallization of the mixture

(25) Cope, A. C.; Moore, P. T.; Moore, W. R. *J. Am. Chem. Soc.* **1959**, *71*, 3153.
(26) Joshi, G. C.; Devaprabhakara, D. *J. Organomet. Chem.* **1968**, *15*, 497–9.
(27) Wideman, L. G. *J. Org.* Chem. **1968**, *33*, 4541–3.
(28) This sample contained ~40% **17** with the remainder as other C_7H_{10} isomers.
(29) Arora, S.; Binger, P. *Synthesis* **1974**, 801–3.
(30) Miller, R. D.; Dolce, D. L. *Tetrahedron Lett.* **1973**, 4403–6.
(31) Solomon, R. G.; Sinha, A.; Solomon, M. F. *J. Am. Chem. Soc.* **1978**, *100*, 520–6.

afforded pure **15a** as a pale yellow solid, (mp 160–165 °C dec). Anal. Calcd for $[C_9H_{14}Cl_2Pd]_2$: C, 36.09; H, 4.71. Found: C, 35.91; H, 4.83. Heating a sample of the original product mixture or pure **15a** at reflux in CH_3CN (50 mL) for 24 h afforded a mixture of **15a**/**15b**/**16** (8:1:2 ratio, 98%).

Chloropalladation of 17. The product was filtered through a small silica gel column (CH_2Cl_2) and crystallized from CH_2Cl_2/hexanes (−10 °C) to afford a pale yellow solid which was identified by NMR spectroscopy (Tables I and II) as consisting of **18a** and **18b** (2.5:1 ratio, 85%), mp 159 °C. Anal. Calcd for $[C_7H_{10}Cl_2Pd]_2$: C, 30.97; H, 3.71. Found: C, 30.70; H, 3.80. A sample of the mixture (0.04 g, 0.07 mmol) was heated to reflux in CH_3CN (10 mL) for 24 h. The solution was cooled and the solvent removed to afford the initial mixture (0.04 g, 100%).

Chloropalladation of 6. The product was identified by NMR spectroscopy[10a] as **5a** (99% yield). A sample of **5a** (0.31 g, 0.49 mmol) was heated to reflux in CH_3CN (50 mL, 96 h). Removal of the solvent under reduced pressure afforded a mixture identified as consisting of **5a**, **5b**, and **5c** (1.8:1.0:5.1) by ^1H NMR spectroscopy[10a] (0.31 g, 100%). Fractional recrystallization of the mixture afforded a pure sample of **5c** (0.11 g). This sample was heated to reflux in CH_3CN (50 mL) for 96 h. Removal of the solvent under reduced pressure lead to a mixture of **5a**, **5b**, and **5c** (1.8:1.0:5.1; 0.11 g, 100%).

Chloropalladation of 19. The product **20** was identified by NMR spectroscopy (Tables I and II) (99% yield). Crystallization from CH_2Cl_2/hexanes afforded an analytically pure sample, mp 160 °C dec. Anal. Calcd for $[C_9H_{14}Cl_2Pd]_2$: C, 36.09; H, 4.71. Found: C, 36.23; H, 4.95.

Chloropalladation of 21. The product was identified by NMR spectroscopy (Table I) as consisting of **22a**, **22b**, and **22c** (2.2:1.8:1.0, 98%), mp 80–90 °C. Anal. Calcd for $[C_{12}H_{20}Cl_2Pd]_2$: C, 42.19; H, 5.90. Found: C, 42.38; H, 6.13. A sample of the initial mixture (0.13 g, 0.19 mmols) was heated to reflux in CH_3CN (25 mL) for 96 h. Removal of the solvent under reduced pressure afforded a mixture of **22a**, **22b**, and **22c** (2.1:1.2:1.0, 0.13 g, 100%).

Chloropalladation of 23. The product was identified by NMR spectroscopy (Table I) as consisting of a mixture of **24a**, **24b**, and **24c** (2.1:1.9:1.0, 99%), mp 180–185 °C dec. Anal. Calcd for $[C_{14}H_{24}Cl_2Pd]_2$: C, 45.37; H, 6.53. Found: C, 45.25; H, 6.74. Fractional crystallization of the mixture from CH_2Cl_2/hexanes afforded a solid consisting of **24a**, **24b**, and **24c** (1.0:1.0:1.4 by ^1H NMR integration). Recrystallization of the resultant mother liquors from CH_2Cl_2/hexanes afforded a sample of **24a** and **24b** (1.5:1.0 by ^1H NMR integration). Upon heating to reflux in CH_3CN (50 mL) both samples were quantitatively converted into a mixture of **24a**, **24b**, and **24c** (2.1:1.9:1.0).

Chloropalladation of 25. The product was identified by NMR spectroscopy (Table I) as consisting of **26a**, **26b**, and **26c** (3.0:1.3:1.0, 98%). Fractional crystallization of the mixture from CH_2Cl_2/hexanes afforded a pure sample of **26c** (Table II), mp 185–190 °C dec. Anal. Calcd for $[C_{17}H_{30}Cl_2Pd]_2$: C, 49.59; H, 7.34. Found: C, 49.60; H, 7.54. Heating either a sample of the initial mixture or of pure **26c** to reflux in CH_3CN (25 mL) for 48 h quantitatively afforded a mixture of **26a**, **26b**, **26c**, and **26d** (1.5:1.0:3.3:1.0).

Acknowledgment. The author wishes to acknowledge the donors of the Petroleum Research Fund, administered by the American Chemical Society, Marquette University, and Wesleyan University (Connecticut) for financial support of this research. The Varian XL200 NMR spectrometer used in this research was financed by the National Science Foundation (CHE-7908593), the Dreyfus Foundation, and Wesleyan University. The author wishes to thank Ms. Barbara Taylor for the preparation of compound **20**, and Dr. Suzanne Wehrli (University of Wisconsin—Milwaukee) for obtaining the ^1H NOE difference spectra of compounds **15a** and **15b**.

The Nature of the Low-Lying Excited States of Bridged Rhodium(I) and Iridium(I) Binuclear Complexes

M. Inga S. Kenney and John W. Kenney, III

Department of Physical Sciences-Chemistry, Eastern New Mexico University, Portales, New Mexico 88130

Glenn A. Crosby*

Department of Chemistry, Washington State University, Pullman, Washington 99164

Received December 4, 1984

Electronic absorption and luminescence measurements on the four binuclear systems $[Rh(CO)Cl(dppm)]_2$, $[Rh(CO)Cl(dam)]_2$, $[Ir(CO)Cl(dppm)]_2$, and $[Ir(CO)Cl(dam)]_2$ [dppm = bis(diphenylphosphino)methane and dam = bis(diphenylarsino)methane] are reported at room temperature and 77 K. These d^8 rhodium(I) and iridium(I) molecules exhibit temperature-dependent low- and high-energy luminescences that are interpreted as the phosphorescences and the fluorescences arising from the metal-centered $np_z \rightarrow (n-1)d_{z^2}$ transition (n = 6 for Ir and 5 for Rh).

Introduction

Numerous studies[1-10] have focused on the synthesis, structure, and chemistry of bridged binuclear rhodium(I) complexes. Interest in these intensely colored molecules with square-planar-metal coordination geometry stems from their capacity to bind biologically and catalytically important small molecules (e.g., CO, CO_2, H_2O, HC≡CR, H^+) and from their ability to serve as catalysts. More recently,[9,11-13] attention has been directed toward the iridium(I) analogues of these rhodium systems. Spectroscopic studies have concentrated on structural elucidation

(1) Mague, J. T.; Mitchener, J. P. *Inorg. Chem.* **1969**, *8*, 119.
(2) Mague, J. T. *Inorg. Chem.* **1969**, *8*, 1975.
(3) Balch, A. L. *J. Am. Chem. Soc.* **1976**, *98*, 8049.
(4) Sanger, A. R. *J. Chem. Soc., Dalton Trans.* **1977**, 120.
(5) Balch, A. L.; Tulyathan, B. *Inorg. Chem.* **1977**, *16*, 2840.
(6) Cowie, M.; Dwight, S. K. *Inorg. Chem.* **1980**, *19*, 209.
(7) Cowie, M.; Dwight, S. K. *Inorg. Chem.* **1980**, *19*, 2500.
(8) Kubiak, C. P.; Eisenberg, R. *Inorg. Chem.* **1980**, *19*, 2726.
(9) Mague, J. T.; DeVries, S. H. *Inorg. Chem.* **1980**, *19*, 3743.
(10) Kubiak, C. P.; Woodcock, C.; Eisenberg, R. *Inorg. Chem.* **1982**, *21*, 2119.
(11) Sanger, A. R. *J. Chem. Soc., Dalton Trans.* **1977**, 1971.
(12) Sutherland, B. R.; Cowie, M. *Inorg. Chem.* **1984**, *23*, 2324.
(13) Marshall, J. L.; Stobart, S. R.; Gray, H. B. *J. Am. Chem. Soc.* **1984**, *106*, 3027.

0276-7333/86/2305-0230$01.50/0

afforded pure **15a** as a pale yellow solid, (mp 160–165 °C dec). Anal. Calcd for $[C_9H_{14}Cl_2Pd]_2$: C, 36.09; H, 4.71. Found: C, 35.91; H, 4.83. Heating a sample of the original product mixture or pure **15a** at reflux in CH_3CN (50 mL) for 24 h afforded a mixture of **15a**/**15b**/**16** (8:1:2 ratio, 98%).

Chloropalladation of 17. The product was filtered through a small silica gel column (CH_2Cl_2) and crystallized from CH_2Cl_2/hexanes (−10 °C) to afford a pale yellow solid which was identified by NMR spectroscopy (Tables I and II) as consisting of **18a** and **18b** (2.5:1 ratio, 85%), mp 159 °C. Anal. Calcd for $[C_7H_{10}Cl_2Pd]_2$: C, 30.97; H, 3.71. Found: C, 30.70; H, 3.80. A sample of the mixture (0.04 g, 0.07 mmol) was heated to reflux in CH_3CN (10 mL) for 24 h. The solution was cooled and the solvent removed to afford the initial mixture (0.04 g, 100%).

Chloropalladation of 6. The product was identified by NMR spectroscopy[10a] as **5a** (99% yield). A sample of **5a** (0.31 g, 0.49 mmol) was heated to reflux in CH_3CN (50 mL, 96 h). Removal of the solvent under reduced pressure afforded a mixture identified as consisting of **5a**, **5b**, and **5c** (1.8:1.0:5.1) by ^1H NMR spectroscopy[10a] (0.31 g, 100%). Fractional recrystallization of the mixture afforded a pure sample of **5c** (0.11 g). This sample was heated to reflux in CH_3CN (50 mL) for 96 h. Removal of the solvent under reduced pressure lead to a mixture of **5a**, **5b**, and **5c** (1.8:1.0:5.1; 0.11 g, 100%).

Chloropalladation of 19. The product **20** was identified by NMR spectroscopy (Tables I and II) (99% yield). Crystallization from CH_2Cl_2/hexanes afforded an analytically pure sample, mp 160 °C dec. Anal. Calcd for $[C_9H_{14}Cl_2Pd]_2$: C, 36.09; H, 4.71. Found: C, 36.23; H, 4.95.

Chloropalladation of 21. The product was identified by NMR spectroscopy (Table I) as consisting of **22a**, **22b**, and **22c** (2.2:1.8:1.0, 98%), mp 80–90 °C. Anal. Calcd for $[C_{12}H_{20}Cl_2Pd]_2$: C, 42.19; H, 5.90. Found: C, 42.38; H, 6.13. A sample of the initial mixture (0.13 g, 0.19 mmols) was heated to reflux in CH_3CN (25 mL) for 96 h. Removal of the solvent under reduced pressure afforded a mixture of **22a**, **22b**, and **22c** (2.1:1.2:1.0, 0.13 g, 100%).

Chloropalladation of 23. The product was identified by NMR spectroscopy (Table I) as consisting of a mixture of **24a**, **24b**, and **24c** (2.1:1.9:1.0, 99%), mp 180–185 °C dec. Anal. Calcd for $[C_{14}H_{24}Cl_2Pd]_2$: C, 45.37; H, 6.53. Found: C, 45.25; H, 6.74. Fractional crystallization of the mixture from CH_2Cl_2/hexanes afforded a solid consisting of **24a**, **24b**, and **24c** (1.0:1.0:1.4 by ^1H NMR integration). Recrystallization of the resultant mother liquors from CH_2Cl_2/hexanes afforded a sample of **24a** and **24b** (1.5:1.0 by ^1H NMR integration). Upon heating to reflux in CH_3CN (50 mL) both samples were quantitatively converted into a mixture of **24a**, **24b**, and **24c** (2.1:1.9:1.0).

Chloropalladation of 25. The product was identified by NMR spectroscopy (Table I) as consisting of **26a**, **26b**, and **26c** (3.0:1.3:1.0, 98%). Fractional crystallization of the mixture from CH_2Cl_2/hexanes afforded a pure sample of **26c** (Table II), mp 185–190 °C dec. Anal. Calcd for $[C_{17}H_{30}Cl_2Pd]_2$: C, 49.59; H, 7.34. Found: C, 49.60; H, 7.54. Heating either a sample of the initial mixture or of pure **26c** to reflux in CH_3CN (25 mL) for 48 h quantitatively afforded a mixture of **26a**, **26b**, **26c**, and **26d** (1.5:1.0:3.3:1.0).

Acknowledgment. The author wishes to acknowledge the donors of the Petroleum Research Fund, administered by the American Chemical Society, Marquette University, and Wesleyan University (Connecticut) for financial support of this research. The Varian XL200 NMR spectrometer used in this research was financed by the National Science Foundation (CHE-7908593), the Dreyfus Foundation, and Wesleyan University. The author wishes to thank Ms. Barbara Taylor for the preparation of compound **20**, and Dr. Suzanne Wehrli (University of Wisconsin—Milwaukee) for obtaining the ^1H NOE difference spectra of compounds **15a** and **15b**.

The Nature of the Low-Lying Excited States of Bridged Rhodium(I) and Iridium(I) Binuclear Complexes

M. Inga S. Kenney and John W. Kenney, III

Department of Physical Sciences-Chemistry, Eastern New Mexico University, Portales, New Mexico 88130

Glenn A. Crosby*

Department of Chemistry, Washington State University, Pullman, Washington 99164

Received December 4, 1984

Electronic absorption and luminescence measurements on the four binuclear systems $[Rh(CO)Cl(dppm)]_2$, $[Rh(CO)Cl(dam)]_2$, $[Ir(CO)Cl(dppm)]_2$, and $[Ir(CO)Cl(dam)]_2$ [dppm = bis(diphenylphosphino)methane and dam = bis(diphenylarsino)methane] are reported at room temperature and 77 K. These d^8 rhodium(I) and iridium(I) molecules exhibit temperature-dependent low- and high-energy luminescences that are interpreted as the phosphorescences and the fluorescences arising from the metal-centered $np_z \rightarrow (n-1)d_{z^2}$ transition (n = 6 for Ir and 5 for Rh).

Introduction

Numerous studies[1-10] have focused on the synthesis, structure, and chemistry of bridged binuclear rhodium(I) complexes. Interest in these intensely colored molecules with square-planar-metal coordination geometry stems from their capacity to bind biologically and catalytically important small molecules (e.g., CO, CO_2, H_2O, HC≡CR, H^+) and from their ability to serve as catalysts. More recently,[9,11-13] attention has been directed toward the iridium(I) analogues of these rhodium systems. Spectroscopic studies have concentrated on structural elucidation

(1) Mague, J. T.; Mitchener, J. P. *Inorg. Chem.* **1969**, *8*, 119.
(2) Mague, J. T. *Inorg. Chem.* **1969**, *8*, 1975.
(3) Balch, A. L. *J. Am. Chem. Soc.* **1976**, *98*, 8049.
(4) Sanger, A. R. *J. Chem. Soc., Dalton Trans.* **1977**, 120.
(5) Balch, A. L.; Tulyathan, B. *Inorg. Chem.* **1977**, *16*, 2840.
(6) Cowie, M.; Dwight, S. K. *Inorg. Chem.* **1980**, *19*, 209.
(7) Cowie, M.; Dwight, S. K. *Inorg. Chem.* **1980**, *19*, 2500.
(8) Kubiak, C. P.; Eisenberg, R. *Inorg. Chem.* **1980**, *19*, 2726.
(9) Mague, J. T.; DeVries, S. H. *Inorg. Chem.* **1980**, *19*, 3743.
(10) Kubiak, C. P.; Woodcock, C.; Eisenberg, R. *Inorg. Chem.* **1982**, *21*, 2119.
(11) Sanger, A. R. *J. Chem. Soc., Dalton Trans.* **1977**, 1971.
(12) Sutherland, B. R.; Cowie, M. *Inorg. Chem.* **1984**, *23*, 2324.
(13) Marshall, J. L.; Stobart, S. R.; Gray, H. B. *J. Am. Chem. Soc.* **1984**, *106*, 3027.

0276-7333/86/2305-0230$01.50/0

via IR and NMR. Almost all of the electronic spectroscopic data on these systems are derived from solution absorption measurements at room temperature.

This work addresses the temperature-dependent electronic absorption and luminescence behavior of two $4d^8$ rhodium(I) molecules, $[Rh(CO)Cl(dppm)]_2$ and $[Rh(CO)Cl(dam)]_2$, and their $5d^8$ iridium(I) analogues, $[Ir(CO)Cl(dppm)]_2$ and $[Ir(CO)Cl(dam)]_2$ [dppm = bis(diphenylphosphino)methane and dam = bis(diphenylarsino)methane]. All four systems are assumed to have the trans[14] structure I.[2,7,9,12]

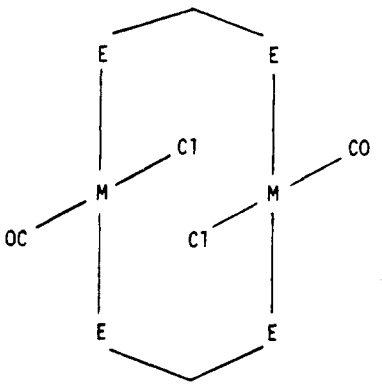

I

M = Rh, Ir

E = P, As

These spectroscopic results comprise the first reported luminescence measurements and electronic assignments on "face-to-face" bridged iridium species and the first on these particular rhodium(I) complexes. They complement the recent report of Marshall et al. on the $[Ir(\mu\text{-pz})(COD)]_2$ (pz = pyrazolyl, COD = 1,5-cyclooctadiene) system that has an open structure and lower symmetry.[13]

Experimental Section

Standard Schlenk techniques and dry deoxygenated solvents were employed in all preparations. All subsequent manipulations involving iridium products were carried out by using Schlenk or glovebag techniques. Bis(diphenylphosphino)methane, bis(diphenylarsino)methane, and bis(μ-chloro)bis(1,5-cyclooctadiene)diiridium(I) dimer, $[Ir(COD)Cl]_2$, were obtained from Strem Chemicals, Inc. Tetracarbonylbis(μ-chloro)dirhodium(I), $[Rh(CO)_2Cl]_2$, was obtained from Aldrich Chemical Co. Bis(μ-chloro)dicarbonyltetrakis(cyclooctene)diiridium(I), $[Ir(CO)Cl(c\text{-octene})_2]_2$, was obtained from Alfa Products. Matheson UHP grade CO was employed. $[Rh(CO)Cl(dppm)]_2$ and $[Rh(CO)Cl(dam)]_2$ were synthesized according to the procedure given by Mague and Mitchener.[1]

Preparation of $[Ir(CO)Cl(dppm)]_2$. The following modification of Sanger's method was used in this synthesis.[4] The reaction mixture $[Ir(COD)Cl]_2$ and dppm in distilled benzene purged by CO bubbling was stirred for several days at room temperature and then was refluxed under a CO atmosphere. The mixture turned dark purple when hot, changed to orange when warm, and turned light yellow when cold. The cool mixture was filtered under Ar atmosphere, washed with benzene and ether, and vacuum dried. The precipitate turned to a peach color while drying. The compound was then heated to 82 °C while still under vacuum. A bright red-violet microcrystalline product resulted. Anal. Calcd: C, 48.79; H, 3.46; P, 9.68. Found: C, 48.01; H, 3.50; P, 9.02.

(14) The trans (i.e., C_{2h}) geometry of the rhodium dimers has been confirmed by X-ray crystallography; the geometry of the iridium dimers has not been determined conclusively although current evidence suggests a trans assignment.

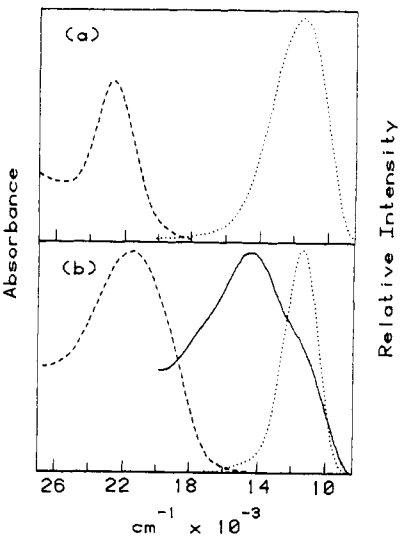

Figure 1. Absorption and emission spectra of bridged rhodium binuclear complexes: (a) $[Rh(CO)Cl(dppm)]_2$; (b) $[Rh(CO)Cl(dam)]_2$. Absorption in CH_2Cl_2 at room temperature (---); emission from polycrystalline powder at room temperature (—) and at 77 K (···). For molecular extinction coefficients, see ref 3, Table II.

Preparation of $[Ir(CO)Cl(dam)]_2$. A sample of 0.22 g (0.466 mmol) of dam in 35 mL of distilled spectroscopic grade acetone was purged by vigorous Ar bubbling for about 10 min. To this clear solution was added 0.20 g (0.210 mmol) of $[Ir(CO)Cl(c\text{-octene})_2]_2$, a green-yellow powder, in small amounts. The solution turned purple on addition of the metal complex and a deep purple precipitate formed. The precipitate was filtered under an Ar atmosphere, washed with acetone and diethyl ether, and dried under vacuum. A bright purple-pink air-sensitive precipitate was recovered. Anal. Calcd: C, 42.90; H, 3.05. Found: C, 42.07; H, 3.21.

Spectroscopic Measurements. The CH_2Cl_2 used in spectroscopic measurements was purified by washing with water and sodium carbonate solution, drying over calcium chloride, and fractionally distilling. Absorption spectra were obtained in CH_2Cl_2 at room temperature on a Cary 219 spectrophotometer. Solid-state KBr pellet absorption spectra were also recorded. Luminescence spectra were measured on a custom-built prism spectrophotometer employing a cooled red-sensitive photomultiplier tube with dc detection and computer data acquisition. Samples were excited with the beam of a 200-W Hg arc lamp. The exciting light was passed through a $CuSO_4$ solution filter and Corning 7-60 and 7-37 filters and then directed to the sample through an array of quartz lenses.

Luminescence lifetimes were measured with a computer-controlled Biomation 6500 waveform recorder connected to the output of a cooled red-sensitive photomultiplier tube wired for fast response. The sample was excited with the filtered 337-nm line of a Molectron UV 22 pulsed nitrogen laser. The emitted light was focused through a KNO_2 solution filter onto the entrance slit of a Spex Minimate monochromator tuned within the emission band envelope. For all luminescence and luminescence lifetime studies, microcrystalline powders of the samples were placed between quartz disks sealed with indium gaskets. Iridium samples were prepared for study under an Ar atmosphere. Spectroscopic studies at 77 K were carried out in quartz optical Dewars.

Results

Shown in Figure 1 are the absorption and emission spectra for $[Rh(CO)Cl(dppm)]_2$ and $[Rh(CO)Cl(dam)]_2$. No room-temperature emission was observed from $[Rh(CO)Cl(dppm)]_2$. Absorption and emission spectra for $[Ir(CO)Cl(dppm)]_2$ and $[Ir(CO)Cl(dam)]_2$ are displayed in Figure 2. Listed in Table I are absorption maxima, emission maxima, and decay times measured at 77 K.

Each of the four complexes displays a well-defined low-energy absorption band (see Figures 1 and 2). Bridging

Table I. Photophysical Properties of Rhodium(I) and Iridium(I) Binuclear Molecules at Room Temperature (RT) and 77 K

complex	absorpn $\bar{\nu}_{max}$, cm^{-1}		fluorescence	phosphorescence	
	CH_2Cl_2	KBr[a]	$\bar{\nu}_{max}$,[b] cm^{-1}	$\bar{\nu}_{max}$,[b] cm^{-1}	τ, μs
$[Rh(CO)Cl(dppm)]_2$					
77 K		22 000		11 400	
RT	22 600	21 900			
$[Rh(CO)Cl(dam)]_2$					
77 K		21 200	14 700 (sh)	11 200	~1
RT	21 500	21 800	14 300 (vb)	11 100 (sh)	
$[Ir(CO)Cl(dppm)]_2$					
77 K		18 900	16 300 (w)	11 700	~2
RT	19 300	19 200	15 000 (sh)	11 800	
$[Ir(CO)Cl(dam)]_2$					
77 K		19 300	16 900	12 900	~3
RT	18 800	19 200	16 600 (sh)	12 800	
assignt	$^1A_g \rightarrow {}^1B_u$ $1b_u \rightarrow 2a_g$		$^1B_u \rightarrow {}^1A_g$ $2a_g \rightarrow 1b_u$	$^3B_u \rightarrow {}^1A_g$ $2a_g \rightarrow 1b_u$	

[a] Pellet. [b] sh = shoulder; vb = very broad; w = wide.

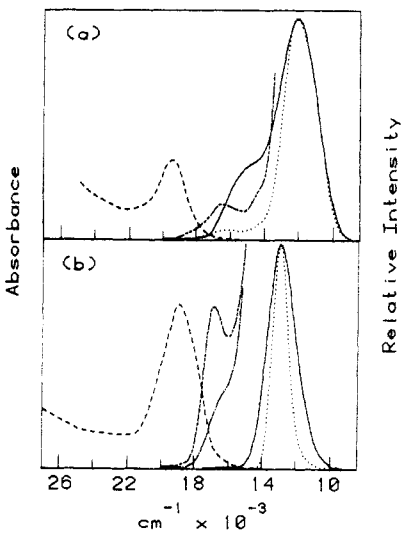

Figure 2. Absorption and emission spectra of bridged iridium binuclear complexes: (a) $[Ir(CO)Cl(dppm)]_2$; (b) $[Ir(CO)Cl(dam)]_2$. Absorption in CH_2Cl_2 at room temperature (- - -); emission from polycrystalline powder at room temperature (—) and at 77 K (···). Expanded sensitivity of room temperature emission (-·) and of 77 K emission (- - -).

ligand choice does not significantly affect the band maximum for a given metal [i.e., Rh(I), dppm, 22 600 cm^{-1}, dam, 21 500 cm^{-1}; Ir(I), dppm, 19 300 cm^{-1}, dam, 18 800 cm^{-1}]. These room-temperature CH_2Cl_2 solution absorption maxima are very close to the corresponding room-temperature and 77 K KBr pellet absorption maxima for all four systems (see Table I). The molecules do exhibit absorption bands at higher energy but they are not addressed in this study. Scans on the low-energy side of the principal low-energy absorption band revealed no measurable features for any of the four species.

At 77 K the rhodium complexes displayed low-energy emission bands maximizing at 11 400 cm^{-1} (dppm) and 11 200 cm^{-1} (dam), each with a long tail at higher energy. Neither of the rhodium molecules showed a distinctive band at higher energy when the ordinate was expanded. $[Rh(CO)Cl(dppm)]_2$ was not observed to emit light in the polycrystalline state at room temperature. At room temperature, $[Rh(CO)Cl(dam)]_2$ exhibited a broad high-energy band at 14 300 cm^{-1} with a less intense lower energy shoulder at 11 100 cm^{-1}.

At 77 K the iridium complexes displayed low-energy emission bands at 11 700 cm^{-1} (dppm) and 12 900 cm^{-1} (dam) each with weaker well-resolved bands at higher energy. These higher bands maximized at 16 300 cm^{-1} (dppm) and 16 900 cm^{-1} (dam). For $[Ir(CO)Cl(dppm)]_2$ at 77 K an additional small shoulder appeared at 14 200 cm^{-1}, between the low- and high-energy bands. The luminescence of the iridium species at room temperature was characterized by a low-energy band with a less intense higher energy shoulder. For both iridium molecules the low-energy band was broader at room temperature than at 77 K and the strength of the emission much diminished. Generally, the emission maxima at room temperature were not shifted greatly (400 cm^{-1}) from the emission maxima at 77 K with the exception of the high-energy band of $[Ir(CO)Cl(dppm)]_2$, whose room-temperature maximum was moved about 1300 cm^{-1} to the red from the maximum at 77 K.

The molecules containing the dppm-bridging ligand, $[Rh(CO)Cl(dppm)]_2$ and $[Ir(CO)Cl(dppm)]_2$, displayed much broader low-energy luminescence bands, about 1300 cm^{-1} broader (fwhm), than those of the analogous dam-bridged species, $[Rh(CO)Cl(dam)]_2$ and $[Ir(CO)Cl(dam)]_2$. Within the group, $[Ir(CO)Cl(dam)]_2$ luminesced with the greatest intensity, $[Ir(CO)Cl(dppm)]_2$ and $[Rh(CO)Cl(dam)]_2$ luminesced with an approximately equal intensity although with much less intensity than $[Ir(CO)Cl(dam)]_2$, and $[Rh(CO)Cl(dppm)]_2$ was a very weak emitter. The lower energy emission bands of the rhodium and iridium molecules exhibit lifetimes in the microsecond range at 77 K with some nonexponential behavior (see Table I). The lifetimes of the higher energy emission bands at 77 K fell below the detection limit of our apparatus (20 ns).

Discussion

All available experimental evidence for these systems, i.e., lifetime data, temperature dependence of emission, relative positions of emission, and absorption bands, is consistent with the assignment of the higher energy luminescence as a fluorescence and the lower energy emission as a phosphorescence. The evidence is most conclusive for $[Rh(CO)Cl(dam)]_2$ (Figure 1b) since the principal absorption band overlaps the tail of the higher energy luminescence band, indicating that the absorption and the fluorescence have the same excited state parentage. The lower energy luminescence of $[Rh(CO)Cl(dam)]_2$ is a comparatively weak shoulder at room temperature but dominates at 77 K. If a phosphorescence assignment is made for this band, then the diminished emission intensity at higher temperature is easily rationalized as temperature-dependent phosphorescence quenching. The enhancement of the higher energy luminescence band relative to the lower energy one as temperature increases provides additional evidence for assigning the former to a fluorescence.

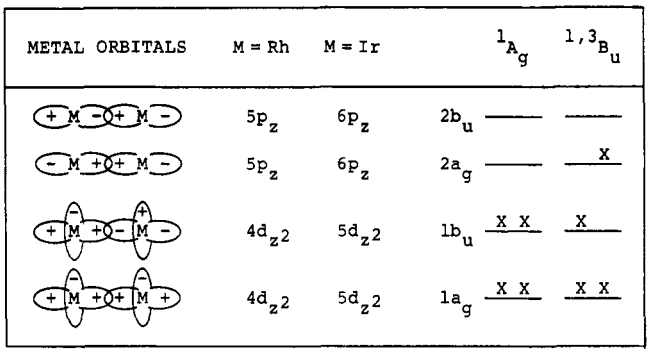

Figure 3. Proposed valence orbitals and states for bridged rhodium(I) and iridium(I) binuclear complexes. States are classified according to C_{2h} (x) where the M–M axis is the z axis (see text).

Finally, these assignments are supported by the short lifetime of the higher energy luminescence (<20 ns) and the longer lifetime (1 μs) of the lower energy luminescence at the reference temperature of 77 K. Although no band was resolved, the long high-energy tail on the 77 K emission spectrum of $[Rh(CO)Cl(dppm)]_2$ (Figure 1a) suggests a weak unresolved fluorescence tail on the phosphorescence maximum analogous to what is seen for $[Rh(CO)Cl(dam)]_2$ at 77 K. Unfortunately, no room-temperature emission spectra could be obtained from this weakly emitting system to confirm the existence of fluorescence.

The two iridium complexes exhibit somewhat different temperature-dependent luminescence behavior from that of their rhodium analogues. The low-energy emission band predominates both at room temperature and at 77 K. For $[Ir(CO)Cl(dam)]_2$, the higher energy luminescence is very weak at both 77 K and room temperature. If it is postulated that the intersystem crossing rate is enhanced by the larger spin–orbit-coupling constant introduced by the substitution of rhodium for iridium, then a phosphorescence/fluorescence assignment is reasonable for the lower/higher energy luminescence band. The dominance of phosphorescence is completely analogous to the behavior of the $[Pt_2H_8P_8O_{20}]^{4-}$ ion.[15] The position of the weak higher energy luminescence and its overlap with the corresponding absorption band are also consistent with a fluorescence assignment to the former. Spin–orbit coupling may also account for the presence of the intermediate energy shoulder present in the 77 K luminescence spectrum of $[Ir(CO)Cl(dppm)]_2$. A higher sample temperature could favor a transition to the ground-state singlet from a higher energy component of the lowest spin–orbit coupled triplet term or perhaps from a higher triplet.

The orbitals, configurations, and states relevant to the analysis of the low-energy electronic transitions in these systems are shown in Figure 3. To facilitate comparisons between these d^8 binuclear systems and d^8 binuclear complexes with D_{4h}[16] and D_{2h}[17] symmetry, a right-handed coordinate system is chosen for these C_{2h} binuclears that preserves the z axis as the metal–metal axis. Within this convention, the x axis becomes the principle C_{2h} symmetry axis. The normal C_{2h} character table, defined with respect to a z principal symmetry axis, is easily converted to the desired C_{2h} (x) character table by the coordinate permutation $x \rightarrow y$, $y \rightarrow z$, and $z \rightarrow x$.

The ground-state metal–metal bond order of these C_{2h} binuclear species is formally zero; a bond order of 1.0 is predicted for the lowest excited singlet and triplet terms. The well-resolved low-energy absorption observed in all of these systems is assigned to $^1A_g \rightarrow {}^1B_u$ (C_{2h}). The fluorescence and phosphorescence transition assignments are $^1B_u \rightarrow {}^1A_g$ and $^3B_u \rightarrow {}^1A_g$, respectively.

Within this electronic model for these C_{2h} binuclear systems the three spin–orbit coupled states arising from the triplet manifold (B_u, $2A_u$) are all dipole allowed. Thus, no significant increase in the phosphorescence lifetime of any of these systems is expected as the temperature is lowered. This predicted behavior contrasts with the observed temperature-dependent behavior of the phosphorescence lifetime of D_{4h} and D_{2h} binuclears.[15,17] In the latter systems, the dramatic increase in the phosphorescence lifetime as the temperature decreased was attributed to the preferential population of a low-lying dipole forbidden component of the spin–orbit coupled triplet manifold. No symmetry-forbidden triplet component is predicted for these C_{2h} systems.

Several previous workers[4,6,10,18] have assigned the low-energy absorptions of rhodium(I) dam- and dppm-bridged molecules to metal-to-ligand charge-transfer transitions primarily because of their high intensities; however, they seem to be better characterized by the metal-centered assignments adopted by Fordyce and Crosby that also accommodate intensely allowed transitions in the visible region of the spectrum.[17] In both the Ir(I) and Rh(I) species under study, the position of the low-energy absorption maximum is not greatly affected by replacement of dppm with dam, by change of environment from solid state to solution, or by change of temperature. This experimental evidence is consistent with metal-centered orbital assignments. The evident similarities within the two rhodium luminescence spectra and the two iridium luminescence spectra also suggest metal-centered transitions. Differences between the electronic spectra of the rhodium and iridium systems could become manifest at temperatures well below 77 K. We predict that the phosphorescence lifetimes of both rhodium species will remain in the microsecond range even to very low temperatures, unlike the more symmetric species (D_{2h}) studied earlier;[17] whereas we expect substantial increases in the phosphorescence decay times of the iridium species well above 10 K if the cis configuration (C_{2v}) is present. If the complexes possess a trans configuration (C_{2h}), as we have implicitly assumed above and as preliminary data seem to indicate,[12] then no dramatic lengthening of the lifetime, as $T \rightarrow 0$ K, is expected. Temperature-dependent studies on these and other analogous molecules are planned.

Finally, we comment specifically on the role of spin–orbit coupling in these systems. Because of the incorporation of heavy-metal ions in the structures one would, in analogy with numerous other complexes of rhodium, iridium, and ruthenium, expect no fluorescence at all and enormous triplet splittings (>10^3 cm^{-1}). That fluorescence occurs and the spin–orbit splittings of the lowest triplet levels are small (<50 cm^{-1}) is a consequence of the near cylindrical symmetry of the metal-centered molecular orbitals with respect to the binuclear axis.[17] To first order the lowest excited singlet and triplet states involve no nodes about the metal–metal axis; thus no orbital magnetism is generated about this axis and, to first order, the spin–orbit coupling vanishes. The spectroscopic consequence of this circumstance is that these heavy-metal binuclear species behave more like organic systems than their mononuclear

(15) Fordyce, W. A.; Brummer, J. G.; Crosby, G. A. *J. Am. Chem. Soc.* **1981**, *103*, 7061.
(16) Mann, K. R.; Gordon, J. G.; Gray, H. B. *J. Am. Chem. Soc.* **1975**, *97*, 3553.
(17) Fordyce, W. A.; Crosby, G. A. *J. Am. Chem. Soc.* **1982**, *104*, 985.
(18) Balch, A. L.; Labadie, J. W.; Delker, G. *Inorg. Chem.* **1979**, *18*, 1224.

analogues.

Acknowledgment. This research has been supported by the National Science Foundation Grants CHE-8119060 and CHE-8421282 at Washington State University and by the New Mexico Research Bond Fund at Eastern New Mexico University.

Registry No. $[Ir(CO)Cl(dppm)]_2$, 99511-21-4; $[Ir(COD)Cl]_2$, 12112-67-3; $[Ir(CO)Cl(dam)]_2$, 99511-22-5; $[Ir(CO)Cl(cot)_2]_2$, 51812-37-4; $[Ph(CO)Cl(dam)]_2$, 99511-23-6; $[Ph(CO)Cl(dppm)]_2$, 99511-24-7.

Palladium-Catalyzed Additions of Amines to Conjugated Dienes: Alteration of Behavior of (Triphenylphosphine)palladium Catalysts with Amine Hydroiodide Salts

Robert W. Armbruster, Michael M. Morgan, James L. Schmidt, Chun Man Lau, Rose M. Riley, Daniel L. Zabrowski, and Harold A. Dieck*

Department of Chemistry, Saint Louis University, Saint Louis, Missouri 63103

Received June 24, 1985

When amine hydroiodide salts are present, (triphenylphosphine)palladium catalyst systems are capable of effecting the addition of primary and secondary amines to certain conjugated dienes. The generality and mechanistic aspects of these reactions were investigated.

Introduction

We have found that amine hydroiodide salts are capable of altering the behavior of (triphenylphosphine)palladium catalyst systems in reactions of amines with conjugated dienes. Such reactions produce 1:1 adducts which, in the case of 1,3-butadiene, isoprene, and 2,3-dimethyl-1,3-butadiene, consist primarily of products resulting from a 1,4-addition of the N–H moiety across the diene system. These addition products are obtained in fair to good yields with only traces of 1,2-addition products and octadienyl amines (1:2 adducts) being formed. Literature reports of similar systems using (triphenylphosphine)palladium catalysts without the amine hydroiodide salt indicate that octadienylamines are the major products.[1,2] Octadienylamines are also the major products in reactions employing phosphonite[3,4] and 1,5-cyclooctadienyl ligands.[5]

Other reports indicate that when a diphosphine ligand, e.g., 1,2-bis(diphenylphosphino)ethane, is substituted for triphenylphosphine (no amine hydroiodide salt), 1:1 adducts are obtained,[6,7] but in some cases the products consist of considerable quantities of 1,2-addition products. Another group has had some success in obtaining 1:1 adducts using a palladium acetoacetate–tributylphosphine–triethyl aluminum catalyst system, but reports that octadienylamines are the major products in reactions using 1,3-butadiene or isoprene.[8]

In this paper we report the results of our studies concerned with the generality and mechanistic aspects of these reactions incorporating the amine hydroiodide salts and offer an explanation for the poor or nonexistent yields of 1,2-addition products.

Results and Discussion

The results of some of our experiments involving reactions of equimolar amounts of amines and dienes using a catalyst precursor system of palladium acetate, triphenylphosphine, and triethylammonium iodide in quantities of 1, 2, and 10 mol %, respectively, are listed in Table I. No 1:1 adducts were obtained if any one of these substances were excluded. The minimum quantity of amine salt needed for optimum conditions (rate and yield) seems to differ for each reaction although we found no noticeable improvement when more than 10 mol % was used. The reaction of diethylamine with isoprene seems to proceed as well with 3 mol % amine salt as with 10 mol % salt, but the rates are slower when quantities less than 3 mol % are used. Similar results were obtained by using other amine hydroiodide salts. Successful results are also possible using reduced catalyst quantities as evidenced by the reaction of isoprene with diethylamine using 0.2 mol % palladium acetate, 0.4 mol % triphenylphosphine, and 1.0 mol % triethylammonium iodide which resulted in 52% isolated yield of a mixture of *N*-(2-methyl-2-buten-

(1) (a) Takahashi, S.; Shibano, T.; Hagihara, N. *Bull. Chem. Soc. Jpn.* **1968**, *41*, 454. (b) Shryne, T. M. U.S. Patent 3 530 187, 1970; *Chem. Abstr.* **1970**, *73*, 930615. (c) Walker, W. E.; Manyik, R. M.; Adkins, K. E.; Farmer, M. L. *Tetrahedron Lett.* **1970**, *43*, 3817. (d) Hata, T.; Takahashi, K.; Miyaki, A. Japan 72 25 045, 1972; *Chem. Abstr.* **1972**, *77*, 101117. (e) Watanabe, H.; Nagai, A.; Saito, M.; Tanaka, H.; Nagai, Y. *Asaki Garasu Kogyo Gijutsu Shoreikai* **1981**, *38*, 111; *Chem. Abstr.* **1982**, *97*, 181653. (f) Keim, W.; Roeper, M.; Schieren, M. *J. Mol. Catal.* **1983**, *20*, 139.

(2) (a) Mitsuyasu, T.; Hara, M.; Tsuji, J. *J. Chem. Soc. D* **1971**, 1345. (b) Tsuji, J. Japan 75 22 014, 1975; *Chem. Abstr.* **1975**, *84*, 16736.

(3) (a) Hobbs, C. F.; McMackins, D. E. U.S. Patent 4 100 194, 1978; *Chem. Abstr.* **1979**, *90*, 22297. (b) Hobbs, C. F.; McMackins, D. E. U.S. Patent 4 130 590, 1978; *Chem. Abstr.* **1979**, *90*, 137247.

(4) (a) Hobbs, C. F.; McMackins, D. E. U.S. Patent 4 100 196, 1978; *Chem. Abstr.* **1979**, *90*, 5894. (b) Keim, W.; Kurtz, K. R.; Roeper, M. *J. Mol. Catal.* **1983**, *20*, 129.

(5) Stone, F. G. A.; Green, M.; Scholes, G.; Spencer, J. L. U.S. Patent 4 104 471, 1978; *Chem. Abstr.* **1979**, *90*, 87479.

(6) (a) Takahashi, K.; Miyake, A.; Hata, G. *Bull. Chem. Soc. Jpn.* **1972**, *45*, 1183. (b) Takahashi, K.; Hata, T. and Miyake, A. Japan 70 25 321, 1972; *Chem. Abstr.* **1972**, *77*, 101114.

(7) Hobbs, C. F.; McMackins, D. E. U.S. Patent 4 129 901, 1978; *Chem. Abstr.* **1979**, *90*, 54459. U.S. Patent 4 204 997, 1980; *Chem. Abstr.* **1980**, *93*, 185742.

(8) Dzhemilev, U. M.; Yakupova, A. Z.; Minsker, S. K.; Tolstikov, G. A. *J. Org. Chem. USSR, Engl. Transl.* **1979**, *15*, 104.

0276-7333/86/2305-0234$01.50/0

analogues.

Acknowledgment. This research has been supported by the National Science Foundation Grants CHE-8119060 and CHE-8421282 at Washington State University and by the New Mexico Research Bond Fund at Eastern New Mexico University.

Registry No. $[Ir(CO)Cl(dppm)]_2$, 99511-21-4; $[Ir(COD)Cl]_2$, 12112-67-3; $[Ir(CO)Cl(dam)]_2$, 99511-22-5; $[Ir(CO)Cl(cot)_2]_2$, 51812-37-4; $[Ph(CO)Cl(dam)]_2$, 99511-23-6; $[Ph(CO)Cl(dppm)]_2$, 99511-24-7.

Palladium-Catalyzed Additions of Amines to Conjugated Dienes: Alteration of Behavior of (Triphenylphosphine)palladium Catalysts with Amine Hydroiodide Salts

Robert W. Armbruster, Michael M. Morgan, James L. Schmidt, Chun Man Lau, Rose M. Riley, Daniel L. Zabrowski, and Harold A. Dieck*

Department of Chemistry, Saint Louis University, Saint Louis, Missouri 63103

Received June 24, 1985

When amine hydroiodide salts are present, (triphenylphosphine)palladium catalyst systems are capable of effecting the addition of primary and secondary amines to certain conjugated dienes. The generality and mechanistic aspects of these reactions were investigated.

Introduction

We have found that amine hydroiodide salts are capable of altering the behavior of (triphenylphosphine)palladium catalyst systems in reactions of amines with conjugated dienes. Such reactions produce 1:1 adducts which, in the case of 1,3-butadiene, isoprene, and 2,3-dimethyl-1,3-butadiene, consist primarily of products resulting from a 1,4-addition of the N–H moiety across the diene system. These addition products are obtained in fair to good yields with only traces of 1,2-addition products and octadienyl amines (1:2 adducts) being formed. Literature reports of similar systems using (triphenylphosphine)palladium catalysts without the amine hydroiodide salt indicate that octadienylamines are the major products.[1,2] Octadienylamines are also the major products in reactions employing phosphonite[3,4] and 1,5-cyclooctadienyl ligands.[5]

Other reports indicate that when a diphosphine ligand, e.g., 1,2-bis(diphenylphosphino)ethane, is substituted for triphenylphosphine (no amine hydroiodide salt), 1:1 adducts are obtained,[6,7] but in some cases the products consist of considerable quantities of 1,2-addition products. Another group has had some success in obtaining 1:1 adducts using a palladium acetoacetate–tributylphosphine–triethyl aluminum catalyst system, but reports that octadienylamines are the major products in reactions using 1,3-butadiene or isoprene.[8]

In this paper we report the results of our studies concerned with the generality and mechanistic aspects of these reactions incorporating the amine hydroiodide salts and offer an explanation for the poor or nonexistent yields of 1,2-addition products.

Results and Discussion

The results of some of our experiments involving reactions of equimolar amounts of amines and dienes using a catalyst precursor system of palladium acetate, triphenylphosphine, and triethylammonium iodide in quantities of 1, 2, and 10 mol %, respectively, are listed in Table I. No 1:1 adducts were obtained if any one of these substances were excluded. The minimum quantity of amine salt needed for optimum conditions (rate and yield) seems to differ for each reaction although we found no noticeable improvement when more than 10 mol % was used. The reaction of diethylamine with isoprene seems to proceed as well with 3 mol % amine salt as with 10 mol % salt, but the rates are slower when quantities less than 3 mol % are used. Similar results were obtained by using other amine hydroiodide salts. Successful results are also possible using reduced catalyst quantities as evidenced by the reaction of isoprene with diethylamine using 0.2 mol % palladium acetate, 0.4 mol % triphenylphosphine, and 1.0 mol % triethylammonium iodide which resulted in 52% isolated yield of a mixture of *N*-(2-methyl-2-buten-

(1) (a) Takahashi, S.; Shibano, T.; Hagihara, N. *Bull. Chem. Soc. Jpn.* **1968**, *41*, 454. (b) Shryne, T. M. U.S. Patent 3 530 187, 1970; *Chem. Abstr.* **1970**, *73*, 930615. (c) Walker, W. E.; Manyik, R. M.; Adkins, K. E.; Farmer, M. L. *Tetrahedron Lett.* **1970**, *43*, 3817. (d) Hata, T.; Takahashi, K.; Miyaki, A. Japan 72 25 045, 1972; *Chem. Abstr.* **1972**, *77*, 101117. (e) Watanabe, H.; Nagai, A.; Saito, M.; Tanaka, H.; Nagai, Y. *Asaki Garasu Kogyo Gijutsu Shoreikai* **1981**, *38*, 111; *Chem. Abstr.* **1982**, *97*, 181653. (f) Keim, W.; Roeper, M.; Schieren, M. *J. Mol. Catal.* **1983**, *20*, 139.

(2) (a) Mitsuyasu, T.; Hara, M.; Tsuji, J. *J. Chem. Soc. D* **1971**, 1345. (b) Tsuji, J. Japan 75 22 014, 1975; *Chem. Abstr.* **1975**, *84*, 16736.

(3) (a) Hobbs, C. F.; McMackins, D. E. U.S. Patent 4 100 194, 1978; *Chem. Abstr.* **1979**, *90*, 22297. (b) Hobbs, C. F.; McMackins, D. E. U.S. Patent 4 130 590, 1978; *Chem. Abstr.* **1979**, *90*, 137247.

(4) (a) Hobbs, C. F.; McMackins, D. E. U.S. Patent 4 100 196, 1978; *Chem. Abstr.* **1979**, *90*, 5894. (b) Keim, W.; Kurtz, K. R.; Roeper, M. *J. Mol. Catal.* **1983**, *20*, 129.

(5) Stone, F. G. A.; Green, M.; Scholes, G.; Spencer, J. L. U.S. Patent 4 104 471, 1978; *Chem. Abstr.* **1979**, *90*, 87479.

(6) (a) Takahashi, K.; Miyake, A.; Hata, G. *Bull. Chem. Soc. Jpn.* **1972**, *45*, 1183. (b) Takahashi, K.; Hata, T. and Miyake, A. Japan 70 25 321, 1972; *Chem. Abstr.* **1972**, *77*, 101114.

(7) Hobbs, C. F.; McMackins, D. E. U.S. Patent 4 129 901, 1978; *Chem. Abstr.* **1979**, *90*, 54459. U.S. Patent 4 204 997, 1980; *Chem. Abstr.* **1980**, *93*, 185742.

(8) Dzhemilev, U. M.; Yakupova, A. Z.; Minsker, S. K.; Tolstikov, G. A. *J. Org. Chem. USSR, Engl. Transl.* **1979**, *15*, 104.

0276-7333/86/2305-0234$01.50/0

Table I. Addition Reactions of Amines to Conjugated Dienes[a]

diene	amine	reaction temp, °C	reaction time, h	products	% yield[b]
isoprene	diethylamine	100–105	12	*N*-(2-methyl-2-buten-1-yl)-*N*,*N*-diethylamine, I	(25)
				N-(3-methyl-2-buten-1-yl)-*N*,*N*-diethylamine, II	(51)
1,3-butadiene	diethylamine	100–105	12	*N*-(2-buten-1-yl)-*N*,*N*-diethylamine	45
1,3-butadiene	*p*-toluidine	100–105	52	*N*-(1-buten-3-yl)-*p*-toluidine, III	0 (8)
				N-(2-buten-1-yl)-*p*-toluidine, IV	40 (66)
2,3-dimethyl-1,3-butadiene	diethylamine	100–105	43	*N*-(2,3-dimethyl-2-buten-1-yl)-*N*,*N*-diethylamine, V	67
2,3-dimethyl-1,3-butadiene	*n*-butylamine	100–105	170	*N*-(2,3-dimethyl-2-buten-1-yl)-*N*-butylamine	21 (32)
2,3-dimethyl-1,3-butadiene	piperidine	100–105	48	*N*-(2,3-dimethyl-2-buten-1-yl)piperidine	61
1,3-cyclohexadiene	diethylamine	115–120	25	*N*-(2-cyclohexenyl)-*N*,*N*-diethylamine	37
1,3-hexadiene[c]	aniline	100–105	18	*N*-(3-hexen-2-yl)aniline, VI	(45)
				N-(2-hexen-4-yl)aniline, VII	(4.5)
2,4-hexadiene[c]	aniline	125–130	18	VI	(30)
				VII	(2.5)

[a] Unless otherwise noted, reactions used 1:1 molar ratios of dienes and amines with 1 mol % $Pd(OAc)_2$, 2 mol % Ph_3P and 10 mol % $Et_3NH^+I^-$. [b] Isolated yields. Yields in parentheses were determined by GLC. [c] 5 mol % $Pd(OAc)_2$, 10 mol % Ph_3P, 10 mol % $Et_3NH^+I^-$.

1-yl)-*N*,*N*-diethylamine (I) and *N*-(3-methyl-2-buten-1-yl)-*N*,*N*-diethylamine (II) in an approximate ratio of 1:2 (115 °C, 24 h).

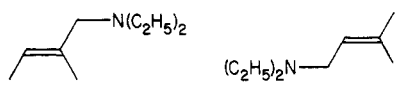

I II

Poorer yields and slower reaction rates resulted when amine hydrobromide salts were used. The reaction between diethylamine and isoprene in the presence of triethylammonium iodide yielded 25% I and 51% II. However, in the presence of triethylammonium bromide only 14% I and 30% II were formed (12 h). No change in yield occurred upon extending the reaction time. Only traces of the 1:1 products were observed in reactions using amine hydrochloride salts.

Parallel results were obtained by using 1,2-bis(diphenylphosphino)ethane as the activating ligand, e.g., substituting 1 mol % of this ligand for triphenylphosphine gave 9% I and 50% II in the reaction of diethylamine and isoprene (100 °C, 54 h) and 81% *N*-(2,3-dimethyl-2-buten-1-yl)-*N*,*N*-diethylamine (V) in the reaction of diethylamine with 2,3-dimethyl-1,3-butadiene (100 °C, 43 h). However, poor yields (less than 5%) were obtained when either tri-*o*-tolylphosphine or triphenylarsine was used.

The reaction of *p*-toluidine and 1,3-butadiene resulted in predominately 1,4-addition product, 66% *N*-(2-buten-1-yl)-*p*-toluidine (IV) and 8% *N*-(1-buten-3-yl)-*p*-toluidine (III). This reaction was investigated for comparison with the results reported for the 1,2-bis(diphenylphosphino)-ethane catalyst system in which the major product resulted from 1,2-addition (32% III, 8% IV).[6]

One major limitation of the reactions reported herein appears to relate to steric properties of the dienes. Although terminal dienes appear to undergo this addition reaction quite readily, reaction of aniline with 2,4-hexadiene is extremely sluggish compared to its reaction with 1,3-hexadiene. Furthermore, no amine products were obtained in reactions of diethylamine or piperidine with 1,4-diphenyl-1,3-butadiene or 1-phenyl-3-methyl-1,3-butadiene. A reaction of diethylamine and 1,3,5-cycloheptatriene was also unsuccessful.

A mechanism consistent with experimental evidence is depicted in Scheme I. This involves the in situ reduction of the palladium (II) catalyst precursor to a palladium(0) species. Reaction of this complex with HI from the amine hydroiodide salt forms an hydridopalladium iodide species, "H–Pd–I", which acts as the true catalyst. Addition to the diene forms a (π-allyl)palladium complex which then undergoes nucleophilic attack by the amine to form the amine addition product and regenerate the hydridopalladium iodide catalyst.

Scheme I

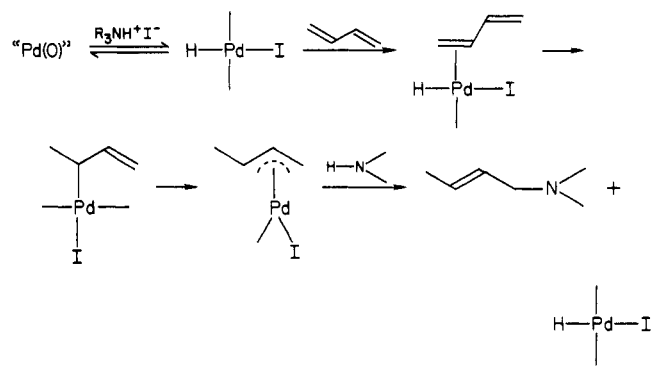

Support for this mechanism comes in part from the following observations. Tetrakis(triphenylphosphine)-palladium(0) may also be used as a catalyst precursor in these reactions.[9] This is consistent with the proposed initial in situ reduction of the palladium(II) precursor to a palladium(0) species. Also, tetraethylammonium iodide and tetraethylammonium bromide fail to serve as suitable substitutes for the amine hydroiodide salt indicating the necessity of a source of HI.

Further support comes from experiments where the ammonium salts were generated in situ. Diethylamine (11 mmol), isoprene (10 mmol), palladium acetate (0.1 mmol), and triphenylphosphine (0.2 mmol) were combined, 1.0 mmol of concentrated acid was added, and the reaction mixtures were heated at 100–150 °C (21 h). The following yields (GLC, based on isoprene) were obtained for the indicated acid: hydriodic acid, 16% I and 53% II; hydrobromic acid, 10% I and 18% II; hydrochloric acid, 6% I and 8% II. Very poor yields of I (less than 4%) and no II were formed with acetic, sulfuric, or phosphoric acid. The poor results with sulfuric and phosphoric acids indicate that an hydridopalladium iodide species and not an hydridopalladium cationic species ("H–Pd^+") is the necessary catalyst for these reactions.

The results of the reactions of aniline with 1,3- and 2,4-hexadiene provide evidence for a (π-allyl)palladium intermediate. Addition of the hydridopalladium iodide to either diene should form the same (π-allyl)palladium complex which after attack by the amine would yield the

(9) A reaction of equimolar amounts isoprene and triethylamine using 1 mol % $(Ph_3P)_4Pd$ and 10 mol % $Et_3NH^+I^-$ (100 °C, 15 h) yielded 14% I and 46% II (GLC).

same distribution of products, *N*-(3-hexen-2-yl)aniline (VI) and *N*-(2-hexen-4-yl)aniline (VII). The reaction with 1,3-hexadiene produced 45% VI and 4.5% VII while the reaction using 2,4-hexadiene produced 30% VI and 2.5% VII. The slight difference in the ratios of VI to VII from the two reactions could be due to some reaction of the amine with the initially formed σ-palladium complexes.[10]

Products from the reactions of butadiene and isoprene are believed to consist primarily of the *E* isomer resulting from reaction of the "H–Pd–I" species with the predominant *s-trans* conformation of the diene. As support for this, the product from the reaction of diethylamine and 1,3-butadiene was determined to consist primarily of the *E* isomer (with traces of the *Z* isomer) by comparison of its NMR spectrum with those for the pure *E* and *Z* isomers reported in the literature.[11]

Although successful examples of reactions employing primary and secondary aliphatic amines and the aromatic amines aniline and *p*-toluidine were obtained, no significant quantities of amine products were observed for reactions of ammonia with 1,3-butadiene, isoprene, 2,3-dimethyl-1,3-butadiene, or 1,3-cyclohexadiene. This is in contrast to reports that ammonia does react with dienes when amine hydroiodide salts are not included in the catalyst system.[2,7] This apparent failure of ammonia to participate in the reactions that include the amine hydroiodide salts suggests that the (π-allyl)palladium complexes in these reactions resemble the π-allyl complexes formed in the reactions of allyl acetates with palladium(0) species (which also do not react with ammonia[12]) more so than those presumed to be formred in the reactions involving dienes with no amine hydroiodide salt added. Although Scheme I shows this intermediate as a (π-allyl)palladium iodide, it is indeed possible that this is actually a bis(triphenylphosphine)(π-allyl palladium cation as the work of Trost[13] and Godleski[14] indicates to be the case in reactions in which the intermediate is generated from allyl acetates.

The fact that 1,2-addition products either are not observed or are obtained in poor yields in reactions involving 1,3-butadiene, isoprene, or 2,3-dimethyl-1,3-butadiene may be explained by the presence of equilibrium processes in which these products are converted to 1,4-addition products. To determine if such a transformation can occur under the reaction conditions, pure *N*-(1-buten-3-yl)-*p*-toluidine (III) in a solution of triethylamine to which catalytic quantities of palladium acetate, triphenylphosphine, and triethylammonium iodide had been added was heated at 100 °C. After 9 h, greater than 85% conversion (GLC) to the 1,4-addition product *N*-(2-buten-1-yl)-*p*-toluidine (IV) had not occurred. As a control, solutions of III with each of the three catalyst precursor ingredients alone and in combination with only one of the other ingredients were also heated at 100 °C. No isomerization occurred after 6 days.

This isomerization could occur by reaction of a 1,2-addition product with the original amine hydroiodide salt to form an allylammonium salt which could then serve as a suitable precursor for the regeneration of a (π-allyl-palladium species by reaction with a palladium(0) complex which is in equilibrium with the "H–Pd–I" species.

Trost has shown that (π-allyl)palladium complexes can be generated by reactions of allylamines with palladium(0) catalysts in the presence of an acid.[15] Also, Hirao has shown that quaternary allylammonium salts react with (phosphine)palladium(0) catalysts to generate (π-allyl)-palladium species.[16] Furthermore, the palladium-catalyzed positional isomerization of allylamines has been reported, but reaction conditions were not given and no mechanism was proposed.[17]

Further evidence for the existence of such equilibrium processes comes from studies of reactions of diethylamine with isoprene. Prolonged heating of the reaction mixture described in Table I (1 mol % palladium acetate and 2 mol % triphenylphosphine) resulted in little change in the distribution of the products I and II. However, when the quatities of palladium acetate and triphenylphosphine were increased to 1.5 and 3.0 mol %, respectively (10 mol % triethylammonium iodide), the yields (GLC) of I and II after 8 h were 19% and 56%, respectively, but after 28 h had changed to 38% I and 38% II. In another experiment in which only 1 mol % palladium acetate was used but the quantity of triphenylphosphine was increased to 4 mol %, the yields of I and II were 12% and 53%, respectively, after 15 h but had changed to 30% I and 37% II after 84 h. We believe that in the latter two cases, (triphenylphosphine)palladium species are present in the reaction mixture for a greater length of time and are therefore available to continue the equilibrium processes which cause isomerization of products. The fact that II is initially formed in greater yield is consistent with the contention that the allyl moieties of the (π-allyl)palladium intermediates may be interpreted as having cationic properties.[16] Thus the (π-allyl)palladium intermediate that would lead to II, having tertiary carbonium ion character, is more stable than that which reacts with amine to form I. Since both I and II have a trisubstituted double bond, they should be of about the same stability and equilibrium processes can lead to nearly equivalent quantities of the two compounds.

Experimental Section

General Comments. All chemicals were used as obtained from commercial sources without further purification. Elemental analyses were obtained from Galbraith Laboratories, Knoxville, TN. Proton NMR spectra were obtained by using a Varian EM-360A NMR spectrometer. GLC yield determinations were obtained by using a Perkin-Elmer Model 900 gas chromatograph (SE-30) with a Cole-Palmer Model 8384-32 recorder with electronic integrator. For preparative GLC purifications, an F&M Model 720 gas chromatograph (SE-52) was used.

Triethylammonium iodide was prepared by bubbling hydrogen iodide gas into a solution of triethylamine in ether followed by removal of solvent and unreacted amine under reduced pressure.

General Procedure for the Palladium-Catalyzed Addition Reactions of Amines with Conjugated Dienes. (a) Preparative Scale Reactions. The amine (100 mmol), conjugated diene (100 mmol), palladium acetate (1.0 mmol), triphenylphosphine (2.0 mmol), and triethylammonium iodide (10 mmol) were placed in a thick-wall Pyrex reaction bottle containing a magnetic stirring bar. The bottle was flushed briefly with nitrogen and then closed with a neoprene gasket and crown cap. For reactions using 1,3-butadiene, all the reactants but the butadiene were added, the bottle was then flushed with nitrogen, closed, cooled to −78 °C, and evacuated and then the butadiene added

(10) Åkermark, B.; Åkermark, G.; Hegedus, L. S.; Zetterburg, K. *J. Am. Chem. Soc.* **1981**, *103*, 3037.
(11) Narita, T.; Inai, N.; Tsurata, T. *Bull. Chem. Soc. Jpn.* **1973**, *46*, 1242.
(12) Trost, B. M.; Keinan, E. *J. Org. Chem.* **1979**, *44*, 3451.
(13) Trost, B. M.; Fullerton, T. J. *J. Am. Chem. Soc.* **1973**, *95*, 292. (b) Trost, B. M.; Weber, L.; Strege, P. E.; Fullerton, T. J.; Dietsche, T. J. *J. Am. Chem. Soc.* **1978**, *100*, 3416.
(14) Godleski, S. A.; Gundlach, K. B.; Ho, H. Y.; Keinan, E.; Frolow, F. *Organometallics* **1984**, *3*, 21.
(15) Trost, B. M.; Keinan, E. *J. Org. Chem.* **1980**, *45*, 2741.
(16) Hirao, T.; Yamada, N.; Ohshiro, Y.; Agawa, T. *J. Organomet. Chem.* **1982**, *236*, 409.
(17) Bäckvall, J.-E.; Nordberg, R. E.; Zetterburg, K.; Akermark, B. *Organometallics* **1983**, *2*, 1625.

to the preweighed bottle. The reaction mixture was heated with stirring at the indicated temperature (Table I) until the reaction appeared to be complete as determined by GLC (based on the size of the reactant and product peaks). The amine addition product(s) was (were) then obtained by distillation of the reaction mixture. Samples of pure compounds for elemental analyses, NMR spectra, and GLC yield determinations were obtained by either preparative GLC or from center fractions taken during distillation.

(b) Reactions in Which Yield Was Determined by GLC. Suitable internal standards were identified (*o*-xylene or naphthalene) and sensitivity coefficients determined. Reactions generally incorporated from one-twentieth to one-fifth the quantities of amine, diene, and catalyst precursor as used in the preparative reactions. The vessel used in these reactions was either a thick-wall Pyrex tube with a neoprene stopper and crown cap or a Fischer-Porter tube. The reactants plus a known quantity of internal standard were combined, and the tube was closed and heated with magnetic stirring at the indicated temperature (Table I). Yields were determined by GLC at various reaction times by direct injection of aliquots of the reaction mixture.

***N*-(2-Methyl-2-buten-1-yl)-*N*,*N*-diethylamine (I)**: NMR ($CDCl_3$) δ 0.98 (t, J = 7 Hz, 6 H), 1.61 (d, J = 6 Hz, 3 H), 1.65 (s, 3 H), 2.42 (q, J = 7 Hz, 4 H), 2.88 (s, 2 H), 5.38 (q, J = 6 Hz, 1 H). Anal. Calcd: C, 76.60; H, 13.48; N, 9.93. Found: C, 76.55; H, 13.30; N, 9.74.

***N*-(3-Methyl-2-buten-1-yl)-*N*,*N*-diethylamine (II)**: NMR ($CDCl_3$) δ 1.02 (t, J = 7 Hz, 6 H), 1.67 (s, 3 H), 1.73 (s, 3 H), 2.53 (q, J = 7 Hz, 4 H), 3.05 (d, J = 6 Hz, 2 H), 5.28 (t, J = 6 Hz, 1 H); bp (I and II, mixture) 62–64 °C (15 mmHg) [lit.[17] bp(II) 45–47 °C (10 mmHg)]. Anal. Calcd: C, 76.60; H, 13.48; N, 9.93. Found: C, 76.92; H, 13.65; N, 9.42.

***N*-(2-Buten-1-yl)-*N*,*N*-diethylamine**: NMR[18] (neat) δ 0.90 (t, J = 7 Hz, 6 H), 1.56 (d, J = 3 Hz, 3 H), 2.35 (q, J = 7 Hz, 4 H), 2.90 (d, J = 4 Hz, 2 H), 5.44 (m, 2 H); bp 111–112 °C [lit.[6a] 57–58 °C (42 mmHg)]. Anal. Calcd: C, 75.52; H, 13.47; N, 11.01. Found: C, 75.81; H, 13.44; N, 10.75.

***N*-(1-Buten-3-yl)-*p*-toluidine (III)**: NMR ($CDCl_3$) δ 1.13 (d, J = 6 Hz, 3 H), 2.17 (s, 3 H), 3.20 (s, 1 H), 3.77 (m, 1 H), 4.83–5.23 (m, 2 H), 5.38–5.93 (m, 1 H), 6.33 (d, J = 8 Hz, 2 H), 6.80 (d, J = 8 Hz, 2 H).

***N*-(2-Buten-1-yl)-*p*-toluidine (IV)**: NMR ($CDCl_3$) δ 1.60 (d, J = 3 Hz, 3 H), 2.10 (s, 3 H), 3.27 (s, 1 H), 3.57 (d, J = 3 Hz, 2 H), 5.50 (m, 2 H), 6.40 (d, J = 8 Hz, 2 H), 6.83 (d, J = 8 Hz, 2 H); bp 260 °C (lit.[6a] 260 °C). Samples of III and IV (purified by preparative GLC) were also obtained by an alternate synthesis from the reaction of *p*-toluidine and 3-chloro-1-butene.

(18) Trost, B. M. *Acc. Chem. Res.* **1980**, *13*, 385.

***N*-(2,3-Dimethyl-2-buten-1-yl)-*N*,*N*-diethylamine (V)**: NMR (neat) δ 0.96 (t, J = 7 Hz, 6 H), 1.66 (s, 9 H), 2.37 (q, J = 7 Hz, 4 H), 2.89 (s, 2 H); bp 50 °C (12 mmHg) [lit.[19] 63.5–64 °C (16 mmHg)]. Anal. Calcd: C, 77.35; H, 13.63; N, 9.02. Found: C, 77.48; H, 13.46; N, 9.16.

***N*-(2,3-Dimethyl-2-buten-1-yl)-*N*-butylamine**: NMR ($CDCl_3$) δ 4.73 (s, 2 H), 0.45–3.38 with significant absorptions at 1.13, 1.65, 2.32, 3.12 (m, 19 H). Anal. Calcd: C, 77.35; H, 13.63. Found: C, 77.25; H, 13.97.

***N*-(2,3-Dimethyl-2-buten-1-yl)piperidine**: NMR ($CDCl_3$) δ 1.42 (m, 6 H); 1.67 (s, 9 H), 2.22 (m, 4 H), 2.73 (s, 2 H); bp 105 °C (28 mmHg) [lit.[19] 53.5–54 °C (2 mmHg)]. Anal. Calcd: C, 78.98; H, 12.65; N, 8.37. Found: C, 79.13; H, 12.49;, N, 8.23.

***N*-(2-Cyclohexenyl)-*N*,*N*-diethylamine**: NMR (neat) δ 0.88 (t, J = 7 Hz, 6 H), 1.10–2.00 (m, 6 H), 2.30 (q, J = 7 Hz, 4 H), 3.20 (m, 1 H), 5.48 (t, 2 H); bp 60 °C (14 mmHg). Anal. Calcd: C, 78.36; H, 12.49; N, 9.14. Found: C, 78.22; H, 12.33; N, 9.16.

***N*-(3-Hexen-2-yl)aniline (VI)**: NMR ($CDCl_3$) δ 1.13 (d, J = 6 Hz, 3 H), 1.62 (t, J = 3 Hz, 3 H), 2.13 (d, J = 3 Hz, 2 H), 3.02 (s, 1 H), 3.37 (q, J = 6 Hz, 1 H), 5.38 (m, 2 H), 6.45 (m, 3 H), 7.10 (m, 2 H). Anal. Calcd: C, 82.23; H, 9.78; N, 7.99. Found: C, 82.14; H, 9.72; N, 8.03.

***N*-(2-Hexen-4-yl)aniline (VII)**: NMR ($CDCl_3$) δ 0.97 (t, J = 7 Hz, 3 H), 1.63 (s, 1 H), 2.02 (m, 2 H), 3.20 (m, 4 H), 5.48 (m, 2 H), 6.58 (m, 3 H), 7.13 (m, 2 H). Anal. Calcd: C, 82.23; H, 9.78; N, 7.99. Found: C,82.24, H, 9.60; N, 8.02. A ca. 10:1 mixture of VI and VII was reacted with hot alkaline $KMnO_4$ followed by acidification and extraction with ether. GLC analysis (Carbowax-20M) of the organic phase showed the presence of propionic and acetic acids in a ratio of ca. 10:1.

Isomerization of *N*-(1-Buten-3-yl)-*p*-toluidine (III) to *N*-(2-Buten-1-yl)-*p*-toluidine (IV). A solution of 0.602 g (3.73 mmol) of III, 0.0224 g (0.1 mmol) of palladium acetate, 0.0524 g (0.2 mmol) of triphenylphosphine, 0.478 g (3.73 mmol) of naphthalene (used as the internal standard) in 1.0 mL of triethylamine was prepared in a thick-wall Pyrex reaction tube. A 0.229-g (1.0-mmol) sample of triethylammonium iodide was added and the tube closed and heated at 100–105 °C. After 9 h, GLC analysis of the reaction mixture (SE-30) indicated that ca. 86% of III had isomerized to IV.

Acknowledgment. Support for undergraduate research participants (R.M.R. and D.L.Z.; summer, 1980) from the National Science Foundation is gratefully appreciated.

(19) Martirosyan, G. T.; Grigoryan, E. A. *Izv. Akad. Nauk Arm. SSR, Khim. Nauki* **1963**, *16*, 31; *Chem. Abstr.* **1963**, *59*, 6354d.

(20) Martirosyan, G. T.; Grigoryan, E. A.; Babayan, A. T. *Izv. Akad. Nauk Arm. SSR, Khim. Nauki* **1965**, *18*, 161; *Chem. Abstr.* **1965**, *63*, 14686b.

Acylation and Alkylation of (η^1-Acryloyl)tetracarbonylferrates. Formation of (η^3:η^1-Allylacyl)iron Complexes by the Carbonylation of α,β-Unsaturated Carbene Ligands

Take-aki Mitsudo, Atsushi Ishihara, Mamoru Kadokura, and Yoshihisa Watanabe*

Department of Hydrocarbon Chemistry, Faculty of Engineering, Kyoto University, Sakyo-Ku, Kyoto 606, Japan

Received May 29, 1985

(η^1-Acryloyl)tetracarbonylferrates **2a–d** reacted with acyl halides **3a–c** or ethyl fluorosulfonate in THF at 20 °C to give (η^3:η^1-allylacyl)tricarbonyliron complexes **5a–h** in moderate yield. (1-*syn*-(Benzoyloxy)-3-*syn*-phenyl-η^3:η^1-allylacyl)tricarbonyliron (**5a**) reacted with nonacarbonyldiiron in diethyl ether at 35 °C to give a binuclear α,β-unsaturated alkylidene complex, (μ-1-(η^1-benzoyloxy)-3-*syn*-phenyl-η^3:η^1-allyl)hexacarbonyldiiron(*Fe–Fe*) (**7**) in 72% yield. Thermolysis of **5a** in toluene at 105 °C for 1 h gave **7** in 78% yield. The formation of **5** or **7** could be explained by assuming the formation of a mononuclear η^1-vinylcarbene complex or a η^3-vinylcarbene complex as a reaction intermediate, respectively.

Introduction

Since the discovery of the first carbene–transition-metal complex by E. O. Fischer in 1964,[1] the chemistry of the carbon–metal multiple bond has undergone rapid development.[2] Recently, much attention has been focused on α,β-unsaturated carbene complexes **1**[3-7] which are key

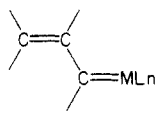

1

compounds in several important organic syntheses such as the Doetz reaction[2,8] or polymerization of acetylenes induced by a metal–carbene complex.[9] On the other hand, carbonylation of a carbene carbon of a transition-metal–carbene complex affording a ketene complex (eq 1) has turned out to be a novel and versatile method for the construction of carbon skeletons.[10-13] This reaction has often been pointed out to be a key step of carbon–carbon bond formation in the hydrogenation of carbon monoxide to oxygenated compounds.[14-16]

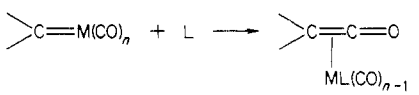

(1)

Scheme I

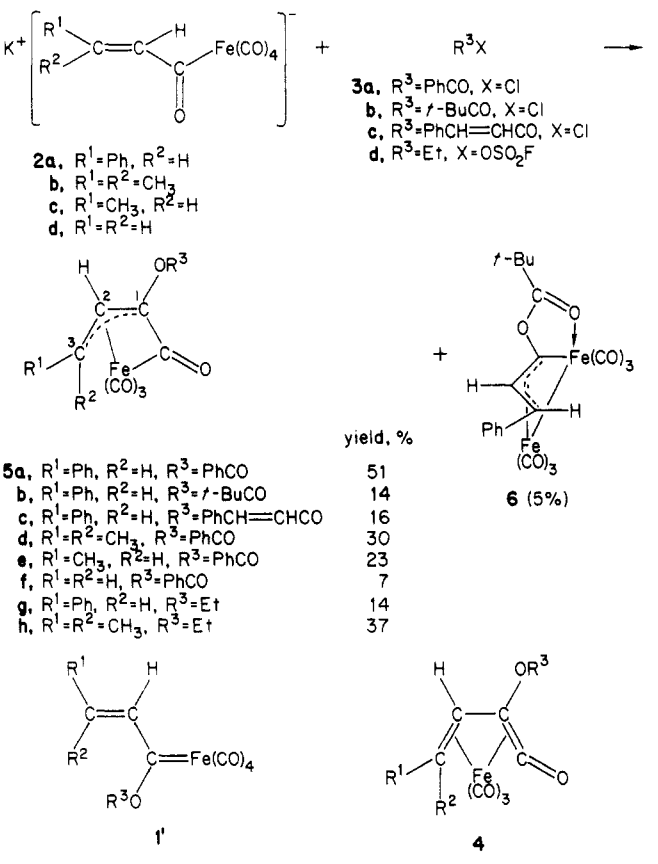

In the course of our study of α,β-unsaturated carbene–metal complexes,[17] we attempted to prepare a (η^1-vinylcarbene)iron complex (**1′**) by alkylation or acylation of an α,β-unsaturated acylferrate. An expected (η^1-vinylcarbene)iron complex (**1′**) was not isolated, but (η^4-vinylketene)tricarbonyliron **4** or alternatively (η^3:η^1-allylacyl)-tricarbonyliron **5** (vide infra) derived by the carbonylation of the carbene carbon in a η^1-vinylcarbene complex (**1′**) was isolated (Scheme I). We now report this novel method

(1) Fischer, E. O.; Maarsboel, A. *Angew. Chem.* **1964**, 76, 645; *Angew. Chem., Int. Ed. Engl.* **1964**, *3*, 580.
(2) For review, e.g. Doetz, K. H.; Fischer, H.; Hofmann, P.; Kreissl, F. R.; Schubert, U.; Weiss, K. "Transition Metal Carbene Complexes"; Verlag Chemie: Weinheim, 1983.
(3) Casey, C. P.; Brunsvold, W. R. *Inorg. Chem.* **1977**, *16*, 2, 391.
(4) Doetz, K. H. *Chem. Ber.* **1977**, *110*, 78.
(5) Casey, C. P.; Boggs, R. A.; Anderson, R. L. *J. Am. Chem. Soc.* **1972**, *94*, 8947. Rudler-Chauvin, M.; Rudler, H. *J. Organomet. Chem.* **1981**, *212*, 203. Casey, C. P.; Polichnowski, S. W.; Shusterman, A. J.; Jones, C. R. *J. Am. Chem. Soc.* **1979**, *101*, 7282.
(6) Doetz, K. H.; Pruskil, I. *J. Organomet. Chem.* **1977**, *132*, 115.
(7) Kuo, G.-H.; Helquist, P.; Kerber, R. C. *Organometallics* **1984**, *3*, 806. Casey, C. P.; Miles, W. H. *Organometallics* **1984**, *3*, 808. Casey, C. P.; Miles, H. M.; Tukada, H. *J. Am. Chem. Soc.* **1985**, *107*, 2924.
(8) E.g.: Doetz, K. H. ref 2, p 210. Doetz, K. H.; Kuhn, W. *J. Organomet. Chem.* **1983**, *252*, C78. Wulff, W. D.; Chan, K. S.; Tang, P. C. *J. Org. Chem.* **1984**, *49*, 2293. Tang, P. C.; Wulff, W. D. *J. Am. Chem. Soc.* **1984**, *106*, 1132. Wulff, W. D.; Yang, D. C. *J. Am. Chem. Soc.* **1984**, *106*, 7565.
(9) Katz, T. J.; Lee, S. J. *J. Am. Chem. Soc.* **1980**, *102*, 424.
(10) Mitsudo, T.; Sasaki, T.; Watanabe, Y.; Takegami, Y.; Nisigaki, S.; Nakatsu, K. *J. Chem. Soc., Chem. Commun.* **1978**, 252.
(11) Herrmann, W. A.; Plank, J. *Angew. Chem.* **1978**, *90*, 555; *Angew. Chem., Int. Ed. Engl.* **1978**, *17*, 525.
(12) Semmelhack, M. F.; Tamura, R.; Schnatter, W.; Springer, J. *J. Am. Chem. Soc.* **1984**, *106*, 5363.
(13) Doerer, B.; Fischer, E. O. *Chem. Ber.* **1974**, *107*, 2683.
(14) Stevens, A. E.; Beauchamp, J. L. *J. Am. Chem. Soc.* **1978**, *100*, 2584.
(15) Muetterties, E. L.; Stein, J. *Chem. Rev.* **1979**, *79*, 479.
(16) Henrici-Olive, G.; Olive, S. *Angew. Chem., Int. Ed. Engl.* **1975**, *15*, 136–141.
(17) Mitsudo, T.; Ogino, Y.; Komiya, Y.; Watanabe, H.; Watanabe, Y. *Organometallics* **1983**, *2*, 1202 and references cited therein.

0276-7333/86/2305-0238$01.50/0

Table I. Infrared Spectral Data (cm^{-1})[a]

complex	metal carbonyl	ν(C=O) of acyl	ester	others	medium
5a	2078 vs, 2022 vs, 2008 vs, 1989 vs	1753 vs	1732 s		KBr disk
	2070 vs, 2016 vs, 2006 vs	1780 vs	1752 s		hexane
5b	2070 vs, 2016 vs, 1995 vs	1767 vs	1747 s		KBr disk
5c	2065 vs, 2015 vs, 2000 vs, 1985 vs	1755 vs	1735 s	1630 (C=C)	KBr disk
5d	2060 vs, 2006 vs, 2000 vs, 1981 vs	1753 s	1736 vs		KBr disk
5e	2064 vs, 2058 vs, 2010 vs, 1993 vs	1763 vs	1738 s		KBr disk
5f	2070 vs, 2017 vs, 2004 vs, 1995 vs	1775 vs	1736 s		KBr disk
5g	2055 vs, 1990 br	1745 s			KBr disk
5h	2064 vs, 1983 vs, 1970 vs	1728 vs			KBr disk
12	2075 vs, 2020 vs, 2000 vs, br	1740 vs, br	1720 vs		KBr disk
6	2058 vs, 2024 vs, 2014 vs, 2000 vs, 1979 vs, 1966 m, 1948 s, 1941 s		1607 m		KBr disk
	2068 vs, 2022 vs, 2000 vs, 1981 vs, 1956 m		1618 w		pentane
7	2064 vs, 2025 vs, 2018 vs, 2008 vs, 1997 vs, 1981 vs, 1962 vs, 1941 vs, 1933 vs, 1927 vs		1611 s		KBr disk
	2068 vs, 2043 vs, 2022 vs, 2000 vs, 1981 vs, 1960 s		1617 m		hexane
8	2060 vs, 1998 vs, 1985 vs	1736 s			pentane
9	2045 s, 1973 vs				pentane
10[b]	2012 s, 2004 s, 1902 vs, br, 1890 vs, br, 1869 vs	1551 m (C=O)	1622 w (C=C)		KBr disk
	2010 s, 1898 vs, br	1549 m (C=O)	1617 w (C=C)		CH_2Cl_2

[a] Abbreviations: vs = very strong; s = strong; m = medium; w = weak; br = broad. [b] Assignment of absorptions is shown in parentheses.

for the preparation of (η^3:η^1-allylacyl)tricarbonyliron complexes and their reactivities.

Results and Discussion

Reaction of (η^1-Acryloyl)tetracarbonylferrates 2a–d with Acyl Halides 3a–c or with Ethyl Fluorosulfonate (3d). Potassium tetracarbonyl(η^1-cinnamoyl)ferrate (**2a**; 10 mmol), prepared in situ from $K_2Fe(CO)_4$ and cinnamoyl chloride, reacted with benzoyl chloride in tetrahydrofuran (THF) at 20 °C for 13 h to give yellow crystals of (1-*syn*-(benzoyloxy)-3-*syn*-phenyl-η^3:η^1-allylacyl)tricarbonyliron (**5a**) in 51% yield (Scheme I) as the sole isolable product (a structure of **5a** will be discussed below). HPLC analysis of the reaction solution showed that the reaction is rather selective, and four small peaks due to complexes other than **5a** were detected. Neither styryl phenyl ketone nor benzoyl styryl ketone was detected by GLC..

Acylation of **2a**, potassium tetracarbonyl(η^1-3-methyl-2-butenoyl)- (**2b**), tetracarbonyl(η^1-(*E*)-2-butenoyl)- (**2c**), or tetracarbonyl(η^1-acryloyl)ferrate (**2d**) with benzoyl chloride (**3a**), 2,2-dimethylpropanoyl chloride (**3b**), or cinnamoyl chloride (**3c**) also gave **5a–f**. The yields of the products are summarized in the Scheme I.

In the reaction of **2a** with an acyl halide (**3b**), an (η^3:η^1-allyl)diiron(*Fe–Fe*) complex (**6**) was also isolated in 5% yield (Scheme I). In other reactions, only a trace (less than 1%) of such a complex was detected by spectroscopy.

Complex **5c** was obtained by the reaction of $K_2Fe(CO)_4$ with cinnamoyl chloride in diethyl ether.

Potassium cinnamoylferrate (**2a**) reacted with ethyl fluorosulfonate in dichloromethane at 20 °C for 1.5 h to give yellow crystals of tricarbonyl(1-*syn*-ethoxy-3-*syn*-phenyl-η^3:η^1-allylacyl)iron (**5g**) in 14% yield. The ethylation of (3-methyl-2-butenoyl)ferrate (**2b**) also gave the corresponding η^3:η^1-allylacyl complex **5h** in 37% yield. The bis(triphenylphosphine)nitrogen(1+) (PPN) salts of **2a**[18] and **2b** also reacted with 2 molar equiv of ethyl fluorosulfonate to give **5g** and **5h** in 21 and 37% yield, respectively.

All products were isolated by column chromatography on silica gel in an atmosphere of argon. The isolated yields of **5a–f** were rather low, partly because of the decomposition of the complexes during chromatography on silica gel at room temperature. The yields of the products were not affected by other solvents such as hexamethylphosphoric triamide (HMPA) and the atmosphere of carbon monoxide or argon during the reaction. Analytical data and IR, ^1H NMR, and ^{13}C NMR spectral data of the products were summarized in Tables I–IV.

Structures of 5a–h and Their Spectral Data. The structures of **5a–h** were confirmed on the basis of their spectral data and their reactivities (vide infra).

First, the structure of **5f**, which has the simplest structure, was reasonably deduced to be (1-*syn*-(benzoyloxy)-η^3:η^1-allylacyl)tricarbonyliron[19] by comparing its spectral data with those of **12** (spectral data of **12** are also cited in Tables I–III) and **13**.[10] These complexes have been prepared by the reaction of (η^3-vinylcarbene)iron **11** with carbon monoxide or triphenylphosphine (eq 2). The

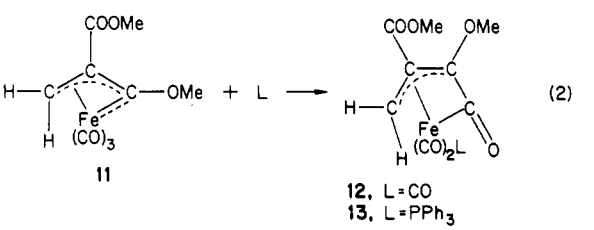

(2)

structure of **13** has been determined by an X-ray analysis.[10] Taking into account the substituent effects of methyl, phenyl, and ethoxy groups, **5a–e** and **5g–h** were also inferred to be analogues of **5f**.

The IR spectra of **5a–f** in KBr disks (Table I) exhibited three or four strong absorptions due to terminal ν (C≡O) vibrations[20] in the 1981–2078 cm^{-1} region and to ν(C=O) of acyl groups in 1753–1775 cm^{-1} as well as ν(C=O) of esters in the 1732–1747 cm^{-1} regions. When the ν(C=O) vibrations of the acyls of **5f**, **5e**, and **5d** are compared, the substituent effect of the methyl group at C(3) (see Scheme

(18) The PPN salt of **2a**, **10**, was isolated (see Experimental Section and Tables I–IV).

(19) (η^3:η^1-Allylacyl)tricarbonyliron complex is alternatively represented as tricarbonyl(η^4-vinylketene)iron **4**. The X-ray analysis of **13** showed that the former representation is preferable.

(20) In hexane **5a** had three absorptions of terminal ν(C≡O) (Table I). The discrepancies in the ν(C≡O) in solution compared to KBr disk is due to the effect of solid state, which was also observed in complex **13**: Mitsudo, T.; Sasaki, T.; Takegami, Y.; Watanabe, Y., unpublished work.

Table II. Hydrogen NMR Spectral Data (δ, Relative to $SiMe_4$, J (Hz))[a]

	olefinic protons[e]		
	H^1	H^2	others
5a	3.19 (d, 9.2, 1 H)	6.99 (d, 9.2, 1 H)	7.25–8.15 (m, 10 H, Ph)
5b	3.08 (d, 9.2, 1 H)	6.85 (d, 9.2, 1 H)	1.29 (s, 9 H, *t*-Bu), 7.24–7.48 (m, 5 H, Ph)
5c	3.16 (d, 9.2, 1 H)	6.94 (d, 9.2, 1 H)	7.84 (d, 16.1, 1 H), 6.94 (d, 16.0, 1 H) 7.25–7.62 (m, 10 H, Ph)
5d		6.32 (s, 1 H)	1.30 (s, 3 H, Me), 2.04 (s, 3 H, Me) 7.37–8.21 (m, 5 H, Ph)
5e	2.19 (dq, 8.4, 6.2, 1 H)	6.31 (d, 8.4, 1 H)	1.87 (d, 6.2, 3 H, Me), 7.37–8.10 (m, 5 H, Ph)
5f	1.25 (dd, 8.8, 2.4, 1 H)	6.43 (dd, 8.8, 7.4, 1 H)	2.61 (dd, 2.4, 7.4, 1 H, H^3) 7.45–8.17 (m, 5 H, Ph)
5g	2.92 (d, 8.8, 1 H)	6.47 (d, 8.8, 1 H)	3.89 (m, 2 H, CH_2), 1.34 (t, 7.1, 3 H, CH_3) 7.24–7.60 (m, 5 H, Ph)
5h		5.84 (s, 1 H)	1.18 (s, 3 H, Me), 1.94 (s, 3 H, Me) 3.84 (m, 2 H, CH_2), 1.30 (t, 3 H, CH_3)
12	0.87 (d, 2.9, 1 H, H^1) 2.92 (d, 2.9, 1 H, H^3)		3.95 (s, 3 H, CO_2Me), 3.84 (s, 3 H, OMe)
6	3.25 (d, 9.4, 1 H)	6.67 (d, 9.4, 1 H)	1.28 (s, 9 H, *t*-Bu), 7.24–7.35 (m, 5 H, Ph)
7	3.32 (d, 9.5, 1 H)	6.81 (d, 9.5, 1 H)	7.25–8.14 (m, 10 H, Ph)
8[b]	2.23 (d, 1.8, 1 H, H^1) 5.84 (d, 5.1, 1 H, H^3)	2.25 (d, 1.8, 1 H, H^2) 5.08 (d, 5.1, 1 H, H^4)	2.25 (br, 3 H, Me), 7.37–7.84 (m, 5 H, Ph)
8[c]	1.87 (dd, 1.8, 1.8, 1 H, H^1) 5.82 (d, 5.1, 1 H, H_3)	2.22 (m, 1.8, 1 H, H^2) 4.44 (d, 5.1, 1 H, H^4)	1.68 (s, 3 H, Me), 6.96–7.94 (m, 5 H, Ph)
9	−0.07 (dd, 1.0, 2.6, 1 H, H^1) 5.26 (dm, 6.0, 1 H, H^3)	1.59 (dd, 2.0, 2.6, 1 H, H^2) 3.03 (d, 6.0, 1 H, H^4)	3.58 (qd, 7.0, 0.6, 2 H, CH_2) 1.21 (t, 7.0, 1 H, CH_3), 2.16 (s, 3 H, Me)
10[d]	6.68 (d, 15.7, 1 H)	7.22 (d, 15.7, 1 H)	7.17–7.52 (m, 35 H, Ph and PPN)

[a] At 24.0 °C. Abbreviations: s = singlet; d = doublet; q = quartet; m = multiplet. Solvent $CDCl_3$ (except for **8** and **10**). [b] Solvent $CDCl_3$. [c] Solvent benzene-d_6. [d] Solvent CD_2Cl_2. [e] Olefinic protons

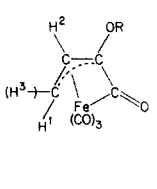

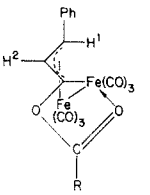

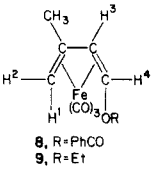

8, R=PhCO
9, R=Et

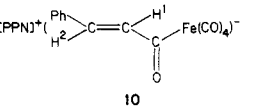

10

I) of the allyl group on the ν(C=O) vibrations can be estimated. When a syn proton of **5f** is substituted by a methyl group, the ν(C=O) vibration in **5e** is shifted to a lower wavenumber by 12 cm^{-1} and the further substitution of the anti proton by another methyl group caused a further 10-cm^{-1} shift to a lower wavenumber. This effect would be explained by the electron donation of the methyl groups which may enhance the larger π-back-donation from the iron to the acyl carbonyl. The IR spectra of **5g** and **5h** in KBr disks showed strong absorptions due to terminal ν(C≡O) vibrations in the 1970–2064 cm^{-1} region and to ν(C=O) vibrations of the acyl group at 1745 and 1728 cm^{-1}, respectively, which are shifted to lower wavenumbers than those of **5a–f** because of the substituent effect of an electron-donating alkoxy group on the C^1 carbon of the allyl group (see Table I). The ^1H NMR signals of **5a–h** exhibited the H^1 protons at high field (δ 1.25–3.19) and signals of the H^2 protons at low field (δ 5.84–6.99) (see Table II). The ^{13}C NMR spectra of **5a–h** exhibited C^3 signals at 31–73 ppm, C^2 signals at 86–101 ppm, C^1 signals at 81–96 ppm, and characteristic signals of the acyl carbon (FeC=O) at 228–235 ppm (see Table III). These NMR spectra showed the presence of a (η^3:η^1-allylacyl)-Fe^{II} system. In conclusion, elemental analyses, molecular weights (Table IV), and all spectral data for **5a–h** were fully consistent with the structure of (η^3:η^1-allylacyl)$Fe(CO)_3$.

In complexes **5a**, **5b**, **5c**, **5e**, and **5g**, the position of the substituents at the C^3 carbon was determined by their ^1H NMR spectra. In complex **5f** the coupling constants of the protons of the coordinated olefins $J_{H^1-H^2}$(trans) and $J_{H^2-H^3}$ (cis) (see the footnotes in Table II) were 8.8 and 7.4 Hz, respectively. Thus the coupling constants of 8.4–9.2 Hz in **5a**, **5b**, **5c**, **5e**, and **5g** show that the olefinic protons are

Scheme II

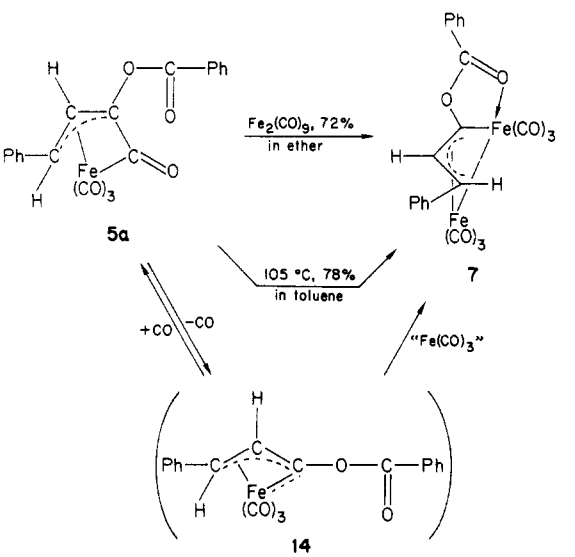

trans and the methyl or the phenyl group is at the syn position; i.e., the stereochemistry of the starting α,β-unsaturated acyl halides are retained in the products.

Mechanisms of the Formation of 5a–h. The formation of **5a–5h** by the reaction of **2** with **3** may be rationalized as follows. The acylation or alkylation of **2** occurs at the oxygen atom of the acyl group giving unstable η^1-vinylcarbene complexes (**1′**) (Scheme I). The intramolecular carbonylation of the carbene carbon of **1′** and the coordination of the olefinic group to the vacant site would afford the η^4-vinylketene or η^3:η^1-allylacyl complexes **5** (eq 3). Formation of η^3-vinylcarbene complexes **14** (Scheme

Table III. Carbon-13 NMR Spectral Data (δ, $SiMe_4$, Internal Reference, $J(^{13}C-H)$ (Hz))[a]

	olefinic or allylic carbons[d]						
	C^1	C^2	C^3	FeC=O	C=O	FeCO	others[c]
5a	82.3 (s)	93.6 (d, 168.0)	54.0 (d, 164.1)	227.9 (d, 7.8)	163.5 (s)	206.2 (s)	126.9 (d), 127.9 (d), 128.7 (d), 129.3 (d), 130.2 (d), 134.3 (d), 137.4 (s, Ph)
5b	82.0 (s)	93.2 (d, 168.0)	53.5 (d, 164.1)	228.4 (d, 9.8)	175.6 (s)	206.2 (s)	26.8 (q, 127.6 $OC(CH_3)_3$) 39.8 (s, $OC(CH_3)_3$) 126.9 (d), 127.7 (d), 129.2 (d), 137.5 (s Ph)
5c	81.9 (s)	93.4 (d, 168.0)	53.9 (d, 164.1)	228.1 (d, 7.8)	163.5 (s)	206.1 (s)	148.1 (d, 154.3, OCCH=CHPh) 115.2 (d, 164.1, OCCH=CHPh) 126.7 (d), 127.6 (d), 128.3 (d), 128.9 (d), 129.1 (d), 131.1 (d), 133.5 (s), 137.0 (s, Ph)
5d	82.6 (s)	101.0 (d, 168.0)	73.4 (s)	229.5 (d, 9.8)	163.8 (s)	207.0 (s)	28.0 (q, 129.7, Me) 30.9 (q, 127.0, Me) 128.2 (s), 128.6 (d), 130.1 (d), 134.1 (d, Ph)
5e	82.0 (s)	99.5 (d, 168.0)	51.8 (d, 166.0)	228.1 (d, 9.8)	163.6 (s)	206.8 (s)	19.6 (q, 128.9, Me) 128.0 (s), 128.6 (d), 130.1 (d), 134.2 (d, Ph)
5f	85.6 (s)	96.5 (d, 170.9)	31.3 (t, 162.3)	228.6 (br)	162.5 (s)	206.0 (s)	128.0 (s), 128.7 (d), 130.4 (d), 134.5 (d, Ph)
5g	96.1 (s)	86.1 (d, 164.1)	50.9 (d, 164.1)	235.0 (d, 7.8)		207.2 (s)	65.6 (tq, 145.5, 3.9, CH_2) 14.8 (q, 127.6, CH_3) 126.7 (d), 127.2 (d), 129.0 (d), 138.5 (s, Ph)
5h	95.0 (s)	93.5 (d, 164.1)	67.2 (s)	235.0 (d, 7.8)		207.1 (s)	27.4 (q, 128.3, Me) 30.1 (q, 127.0, Me) 63.9 (t, 145.5, CH_2) 13.7 (q, 127.0, CH_3)
12	102.6 (s)	91.7 (s)	20.0 (dd, 167.2, 162.9)	233.5 (s)	166.1 (s)	206.6 (s)	52.9 (q, 147.9, CO_2Me) 58.0 (q, 147.9, OMe)
6	204.3 (s)	88.1 (d, 162.1)	60.5 (d, 160.2)		189.7 (s)	210.6 (s) 211.5 (s)	26.7 (q, 129.6, $OC(CH_3)_3$) 38.6 (s, $OC(CH_3)_3$) 126.5 (d), 126.8 (d), 128.8 (d), 140.0 (s, Ph)
7	203.4 (s)	88.3 (d, 163.6)	60.7 (d, 163.6)		176.4 (s)	210.6 (s) 211.3 (s)	124.9 (s), 126.4 (d), 126.7 (d), 128.8 (d), 129.0 (d), 130.4 (d), 135.2 (d), 139.9 (s, Ph)
8	45.8 (t, 160.2)	112.0 (s)	74.2 (d, 175.8)	85.5 (dd, 184.6, 6.8, C^4)	165.9 (s)	209.3 (s)	23.8 (q, 129.9, Me) 128.4 (d), 129.3 (d), 133.0 (d) (Ph)
10[b]	127.2 (m, OCCH=CHPh)	142.0 (dd, 158.2, 5.9, OCCH=CHPh)		262.1 (s, OCCH=CHPh)		220.7 (s) 220.2 (s)	125.1 (s), 127.9 (d), 128.2 (d), 128.4 (d), 128.6 (d), 129.5 (d), 129.7 (d), 130.0 (d), 132.2 (d), 132.4 (d), 132.6 (d), 134.0 (d), 137.5 (s) (Ph and PPN)

[a] At 24 °C. Abbreviations: s = singlet; d = doublet; t = triplet; q = quartet; br = broad. Solvent: $CDCl_3$ (except for **10**). [b] Solvent: CD_2Cl_2. Assignment of signals are in the parentheses. [c] Assignment of signals in parentheses. [d] Olefinic or allylic carbons.

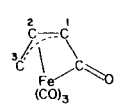

5a-h

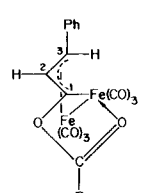

6 or **7**

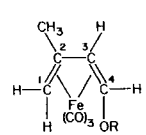

8, R=PhCO

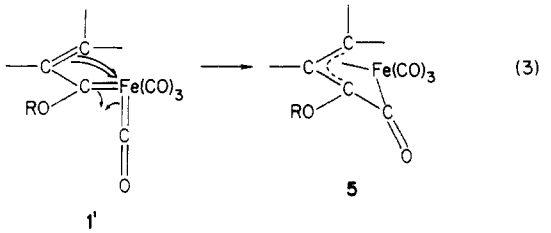

(3)

II) as reaction intermediates instead of η^1-vinylcarbene complexes 1′ should be noted. Although this route is unlikely because a release of carbon monoxide from the metal is required for the formation of **14** and a carbene carbon of **14** must be carbonylated by a released carbon monoxide in the atmosphere, it cannot be ruled out completely.

Attempts to isolate the intermediates, η^1-vinylcarbene complexes (1′), and to detect them by ^{13}C NMR at low temperature were unsuccessful. It seems that the rate of the rearrangement or the isomerization of 1′ to **5** is fast.

Although the carbonylation of (η-cyclopentadienyl)(diphenylcarbene)manganese to the diphenylketene complex required a high pressure of carbon monoxide (35 °C, 650 atm),[11] the carbonylation of the η^1-vinylcarbene ligand in 1′ occurred under mild reaction conditions.

The present results should shed some light on the mechanism of the following reactions in which the carbonylation of a carbene–metal species is often proposed to be a key step of the carbon–carbon bond-forming reactions; (1) the transition-metal-catalyzed reduction of carbon monoxide to oxygen-containing products;[14-16] (2) the Doetz reaction including an annelation reaction by acetylene, carbon monoxide, and an arylcarbene moiety on a transition metal.[8,21]

Reaction of 5a with $Fe_2(CO)_9$ and Thermal Reactions of 5a, 5d, and 5h. A η^3:η^1-allylacyl complex (**5a**) readily reacted with 2 molar equiv of $Fe_2(CO)_9$ in diethyl ether at 35 °C under argon to give **7** in 72% yield (Scheme II). Thermolysis of **5a** at 105 °C in toluene for 1 h also gave **7** under either carbon monoxide or argon atmosphere in 78% yield (based on 2 equiv of **5a**) (Scheme II).

Analytical data and IR and ^1H and ^{13}C NMR spectral data of **7** are also summarized in Tables I–IV. The spectral data for **7** clearly showed that **7** is an analogue of **6**. The structures of **6** and **7** were deduced to be hexacarbonyl(μ-1-η^1-*syn*-(benzyloxy)-η^3:η^1-allyl)diiron(Fe-Fe) by comparing the spectral data of these complexes with those of complex **15**[22] prepared by the reaction of tricarbonyl(η^3-vinylcarbene)iron **16**[23-25] with $Fe_2(CO)_9$ (eq 4). The

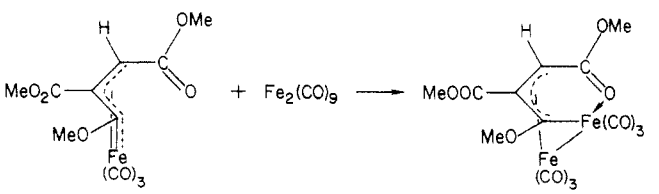

(4)

structure of **15** has been determined by X-ray analysis.[22]

The spectral data of **6** and **7** were also in good agreement with those of other known binuclear vinylcarbene complexes.[26,27]

The IR spectra of **6** and **7** in solution (Table I) exhibited six or five absorptions of terminal ν(C≡O) in the 1956–2068 cm^{-1} region and ν(C═O) of an ester coordinated to the iron atom at 1617 or 1618 cm^{-1}. The ^1H NMR signal of the H^1 proton at high field (**7**, δ 3.32 (d, 9.5, 1 H); **6**, δ 3.25 (d, 9.4, 1 H)) and those of the H^2 proton at low field (**7**, δ 6.81 (d, 9.5, 1 H); **6**, δ 6.67 (d, 9.4, 1 H)) (see Table II) showed the presence of an olefin coordinated to an iron atom. The ^{13}C NMR spectrum of **7** is also in complete agreement with that of **6**. The low field shift of the C^3 and C^2 carbon and the high field shift of the C^1 carbon of **6** or **7** compared with those of **15**[22] (for **15**, 221.2 (C^1), 82.0 (C^2), 38.4 (C^3) ppm) are due to the substituent effects at the respective carbon. ^{13}C NMR signals at 176.4 and 189.7 ppm in **7** and **6**, respectively, also showed the coordination of the ester group to an iron atom. Taking into account these facts, substituent effects and molecular weights (Table IV), **6** and **7** were inferred to be derivatives of **15**. In **6** and **7**, since the ester group is attached to C^1 of the allyl group, the ester group coordinates to the iron from the opposite side, compared with **15**, to satisfy the 18-electron rule.

When **5d** or **5h** is heated in toluene at 103 °C, (η^4-1,3-butadiene)tricarbonyliron complex **8** or **9** is obtained in good yields (eq 5). The intramolecular hydrogen transfer

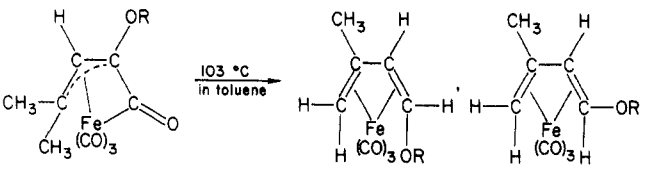

(5)

reaction of a (3,3-dimethyl-η^3:η^1-allylacyl)iron complex has been reported.[28] In our reaction only one of the isomers was isolated; only **8** and **9** were isolatd and **8′** and **9′** were not detected. This result also confirms the structures of complexes **5a–h**.

Mechanisms of the Formation of 6 and 7. Taking into account the reactions of mononuclear tricarbonyl(η^3-vinylcarbene)iron **16** with $Fe_2(CO)_9$ affording **15** (eq 4), the present reaction could be explained by assuming the formation of a reactive mononuclear η^3-vinylcarbene complex (**14**) derived by the decarbonylation of a η^3:η^1-allylacyl complex (**5**) (Scheme II).[29] Complex **7** would be formed by the coordination of **14** to the $Fe(CO)_3$ moiety as a "bidentate ligand" through the carbon–iron double bond and the carbonyl group of the ester in a similar manner to the reaction of complex **16** with $Fe_2(CO)_9$.[22] In the thermolysis of **5a**, **7** would be formed via **14** in a similar manner. However, in this case a source of a $Fe(CO)_3$ moiety is another molecule of **5a** instead of $Fe_2(CO)_9$. The fate of the half of the organic ligand of **5a** was ambiguous. Complex **6** was also formed similarly. It is well-known that the reaction of a (η^3-vinylcarbene)iron complex with Fe_2-

(21) Doetz, K. H.; Dietz, R. *Chem. Ber.* **1978**, *111*, 2517 and references cited therein.
(22) Mitsudo, T.; Watanabe, H.; Watanabe, K.; Watanabe, Y. *Organometallics* **1982**, *1*, 612.
(23) Mitsudo, T.; Nakanishi, H.; Inubushi, T.; Morishima, I.; Watanabe, Y.; Takegami, Y. *J. Chem. Soc., Chem. Commun.* **1976**, 416.
(24) Nakatsu, K.; Mitsudo, T.; Nakanishi, H.; Watanabe, Y.; Takegami, Y. *Chem. Lett.* **1977**, 1447.
(25) Mitsudo, T.; Watanabe, Y.; Nakanishi, H.; Morishima, I.; Inubushi, T.; Takegami, Y. *J. Chem. Soc., Dalton Trans.* **1978**, 1298.
(26) Dyke, A. F. *J. Chem. Soc., Chem. Commun.* **1980**, 803.
(27) Elsenstadt, A.; Efraty, A. *Organometallics* **1982**, *1*, 1100.
(28) Frank-Neumann, M.; Dietrich-Buchecker, C.; Knemiss, A. *Tetrahedron Lett.* **1981**, *22*, 2307.
(29) The decarbonylation of a (η^3:η^1-allylacyl)iron complex to a η^3-vinylcarbene complex has been reasonably assumed in several reactions. Mitsudo, T.; Watanabe, H.; Sasaki, T.; Watanabe, Y.; Takegami, Y.; Kafuku, K.; Kinoshita, K.; Nakatsu, K. *J. Chem. Soc., Chem. Commun.* **1981**, 22.

Table IV. Analytical Data

complex	color	mol wt[a] calcd	mol wt[a] found	mp, °C	C calcd	C found	H calcd	H found	N calcd	N found
5a	yellow	404.2	384	102 dec	59.44	59.61	2.99	2.89		
5b	yellow	384.2	353	87 dec	56.28	56.26	4.20	4.22		
5c	yellow	430.2	414	126 dec	61.42	61.21	3.28	3.26		
5d	yellow	356.1	347	64	53.96	53.98	3.40	3.32		
5e	yellow	342.1	328	92 dec	52.67	52.65	2.95	2.86		
5g	yellow	328.1	319	96 dec	54.91	54.89	3.69	3.62		
5h	yellow	280.1	290	43	47.18	46.98	4.32	4.37		
6	reddish brown			110 dec	48.43	48.53	3.25	3.15		
7	reddish brown	518.2	473	169 dec	51.41	51.14	2.33	2.35		
10	orange			120 dec	70.26	69.74	4.45	4.27	1.67	1.64

[a] Cryoscopic in benzene.

$(CO)_9$ gives either a "ferrole" derivative (**17**) by the reaction of **11** with $Fe_2(CO)_9$ (eq 6) or a (η^3:η^1-allyl)diiron(*Fe–Fe*)

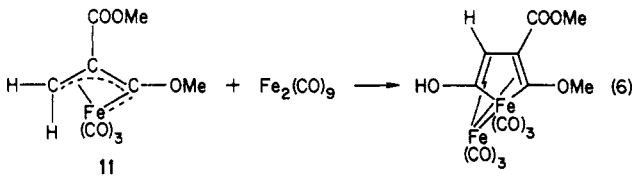

system (**15**) (eq 4).[22] If the η^3-vinylcarbene complex is able to coordinate as a "bidentate ligand" to a $Fe(CO)_3$ moiety, (η^3:η^1-allyl)diiron complexes would be formed and otherwise a "ferrole" complex is formed. In the reactions of **5a** with $Fe_2(CO)_9$ to **7**, thermolysis of **5a**, and the reaction of **2a** with **3b** to **6**, since the decarbonylated intermediate, the η^3-vinylcarbene complex **14**, has an acyloxy group on a carbene carbon, it can coordinate to $Fe(CO)_3$ as a "bidentate ligand" giving the (η^3:η^1-allyl)diiron(*Fe–Fe*) complex (Scheme II).

Concluding Remarks

The reactions of acryloyltetracarbonylferrates with acyl halides or ethyl fluorosulfonate gave (η^3:η^1-allylacyl)iron complexes. This is, to our knowledge, the first example of the carbonylation of η^1-vinylcarbene ligands affording the corresponding η^3:η^1-allylacyl complexes. Although several η^1-vinylcarbene complexes of chromium,[3] molybdenum,[4] tungsten,[5] manganese,[6] or iron[7] are known, intramolecular carbonylation reaction to a stable η^3:η^1-allylacyl or vinylketene complex has not been reported.[30]

Acylation of η^1-acyl ferrates by acyl halides is well-known to give ketones or α-diketones.[31,32] Sawa and his coworkers proposed that the formation of ketone proceeds by thermolysis of the (acyloxy)carbene complex derived by the acylation of the oxygen atom of acyltetracarbonylferrates.[31] However, there has been no evidence for the formation of the carbene complex. The present results showed that the acylation or alkylation of an α,β-unsaturated acylferrate gives (η^3:η^1-allylacyl)iron complexes and that the η^1-vinylcarbene complexes are formed by O-acylation or by O-alkylation of the oxygen atom of the acyl ferrate.[33] Several methods to prepare (η^3:η^1-allylacyl)iron complexes have been reported: reactions of cyclopropenes with nonacarbonyldiiron,[28,34,35] reactions of (η^3-vinylcarbene)iron complexes with carbon monoxide or triphenylphosphine,[10] and reactions of allyl halides with nonacarbonyldiiron.[36] The present reaction provides a novel and facile method for the preparation of the (η^3:η^1-allylacyl)iron complexes.

The reaction of the η^3:η^1-allylacyl complex **5a** with $Fe_2(CO)_9$ or thermolysis of **5a** gave a binuclear α,β-unsaturated alkylidene complex, (η^3:η^1-allyl)diiron(*Fe–Fe*). Although several (η^3:η^1-allyl)dimetal(*M–M*) complexes, the derivatives of **6** or **7** have been reported,[26,27,35,37] there have been only few examples derived from a mononuclear carbene complex.[17,22]

Experimental Section

Unless indicated otherwise, all experiment were performed in an atmosphere of argon. Infrared spectra were recorded on a Nicolet Model 5 MX Fourier transform infrared spectrophotometer, ^1H NMR spectra on a JEOL JNM-FX-100 spectrometer, and ^{13}C NMR spectra on a JEOL JNM-FX-100 spectrometer at 25.05 MHz. Elemental analyses were performed at the Micro Analytical Center of Kyoto University. Solvents were dried by published techniques and were distilled in an atmosphere of argon before use. $K_2Fe(CO)_4$ were prepared by the methods described in the literature.[38]

Reaction of Cinnamoyltetracarbonylferrate (2a) with Benzoyl Chloride (3a). To a suspension of $K_2Fe(CO)_4$ (2.5 g, 10 mmol) in tetrahydrofuran (30 mL) was added a solution of cinnamoyl chloride (1.7 g, 10 mmol) in tetrahydrofuran (6 mL), and the mixture was stirred at 20 °C in an atmosphere of carbon monoxide for 2.5 h to give a deep brown solution of **2a**. To this solution was added 1.4 g (10 mmol) of benzoyl chloride **3a** at 0 °C, and the mixture was stirred at 20 °C for 13 h. The solvent was distilled in vacuo, and the residue was extracted with five 10-mL portions of diethyl ether. After the evaporation of solvent, the residue was chromatographed on silica gel (Merk 0.063–0.200 mm, deactivated by 5% of water, eluent benzene–hexane (1:1))

(30) An η^4-vinylketene chromium complex is proposed in the Doetz reaction: Doetz, K. H.; Sturm, W. *J. Organomet. Chem.* **1985**, *285*, 205.
(31) E.g.: Sawa, Y.; Ryang, M.; Tsutsumi, S. *J. Org. Chem.* **1970**, *35*, 4183.
(32) Collman, J. P. *Acc. Chem. Res.* **1975**, *8*, 342.
(33) O-Acylation of acylpentacarbonyltungstenate gave the corresponding (acyloxy)carbene complexes: Fischer, E. O.; Selmayr, T.; Kreissl, F. R. *Chem. Ber.* **1977**, *110*, 2947.
(34) King, R. B. *Inorg. Chem.* **1963**, *2*, 642.
(35) Dettlaf, G.; Behrens, U.; Weiss, E. *Chem. Ber.* **1978**, *111*, 3019.
(36) Hill, A. E.; Hoffmann, H. M. *J. Chem. Soc., Chem. Commun.* **1972**, 574.
(37) E.g.: Rodrique, P. L.; Meersschi, M. V.; Piret, P. *Acta Crystallogr., Sect. B: Struct. Crystallogr. Cryst. Chem.* **1969**, *B25*, 519. Levisalles, J.; Rose-Munch, F.; Rudler, H.; Daran, J.-C.; Dromzee, Y.; Jennin, Y.; Ades, D.; Fontanille, N. *J. Chem. Soc., Chem. Commun.* **1981**, 152, 1055. Levisalles, J.; Rudler, H.; Dahan, F.; Jennin, Y. *J. Organomet. Chem.* **1980**, *188*, 193. Barker, G. K.; Carroll, W. E.; Green, M.; Welch, A. J. *J. Chem. Soc., Chem. Commun.* **1980**, 1071. Aumann, R.; Averback, H.; Kruger, C. *Chem. Ber.* **1975**, *108*, 3336. Jeffreys, J. A. D.; Willis, C. M.; Robertson, I. C.; Ferguson, G.; Sim, J. G. *J. Chem. Soc., Dalton Trans.* **1973**, 749. Hong, P.; Aoki, K.; Yamazaki, H. *J. Organomet. Chem.* **1978**, *150*, 279. Johnson, B. F. G.; Kelland, J. M.; Lewis, J.; Mann, A. L.; Raithby, P. R. *J. Chem. Soc., Chem. Commun.* **1980**, 547. Messerle, L.; Curtis, M. D. *J. Am. Chem. Soc.* **1980**, *102*, 7789. Dyke, A. F.; Guerchais, J. E.; Knox, S. A. R.; Roue, J.; Short, R. L.; Tayler, G. E.; Woodward, P. *J. Chem. Soc., Chem. Commun.* **1981**, 537.
(38) Gladysz, J. A.; Tam, W. *J. Org. Chem.* **1978**, *43*, 2279.

and recrystallization of the obtained yellow-brown solid from diethyl ether–*n*-hexane gave yellow crystals of **5a** (2.1 g, yield 51%).

This reaction was also performed under an atmosphere of argon instead of carbon monoxide to give **5a** in a yield of 43%.

Reaction of 2a with 2,2-Dimethylpropanoyl Chloride (3b). To a solution of **2a** (10 mmol) in tetrahydrofuran (30 mL) (see above) was added 1.2 g (10 mmol) of 2,2-dimethlpropanoyl chloride (**3b**) at 0 °C, and the mixture was stirred at 25 °C for 4 h. After the solvent was distilled in vacuo, the residue was extracted with five 10-mL portions of diethyl ether. Evaporation of the solvent gave a dark brown solid which was chromatographed on silica gel. Concentration of the first red-brown fraction (eluent *n*-hexane–benzene (2:1)) and recrystallization from diethyl ether–*n*-hexane gave reddish brown crystals of **6** (0.13 g, yield 5.2%). Evaporation of the solvent of the next yellow-brown fraction (eluent *n*-hexane–benzene (1:1)) gave yellow solid, and recrystallization of which from diethyl ether–*n*-hexane gave yellow crystals of **5b** (0.54 g, yield 14%).

Reaction of 2a with Cinnamoyl Chloride (3c) in Diethyl Ether. To a suspension of $K_2Fe(CO)_4$ (2.5 mmol) in diethyl ether (15 mL) was added a solution of cinnamoyl chloride (**3c**; 0.83 g, 5 mmol), and the mixture was stirred at 20 °C for 2.5 h under an atmosphere of carbon monoxide. After the solvent was distilled off in vacuo, the residue was extracted with five 10-mL portions of diethyl ether. The solvent was evaporated, and the residual oil was chromatographed on silica gel (eluent benzene). Pale brown fraction was collected, and the solvent was evaporated to give yellow solid; recrystallization from diethyl ether–*n*-hexane gave yellow crystals of **5c** (0.17 g, yield 16%).

Reaction of (3-Methyl-2-butenoyl)tetracarbonylferrate (2b) with Benzoyl Chloride (3a). To a suspension of $K_2Fe(CO)_4$ (5 mmol) in tetrahydrofuran (30 mL) was added 0.59 g (5 mmol) of 3-methyl-2-butenoyl chloride, and the mixture was stirred for 3.0 h at 20 °C under a carbon monoxide atmosphere to give the dark brown solution of **2b**. To this solution was added 0.70 g (5.0 mmol) of benzoyl chloride (**3a**) at 0 °C, and the mixture was stirred at 20 °C for 4.0 h. The work up as described above gave yellow crystals of **5d** (0.53 g, yield 30%).

Reaction of (*E*)-2-Butenoyltetracarbonoylferrate (2c) with Benzoyl Chloride (3a). To a suspension of $K_2Fe(CO)_4$ (5 mmol) in tetrahydrofuran (15 mL) was added 0.52 g (5 mmol) of (*E*)-2-butenoyl chloride, and the mixture was stirred for 3.5 h at 20 °C under an atmosphere of carbon monoxide to give a brown solution of **2c**. To this solution was added 0.70 g (5.0 mmol) of benzoyl chloride (**3a**) at 0 °C, and the mixture was stirred at 20 °C for 12 h. The workup as described above gave yellow crystals of **5e** (0.39 g, yield 23%).

Reaction of Acryloyltetracarbonylferrate (2d) with Benzoyl Chloride (3a). After an addition of acryloyl chloride (0.45 g, 5 mmol) to a suspension of $K_2Fe(CO)_4$ (5 mmol) in tetrahydrofuran (15 mL), the mixture was stirred for 4.0 h at 20 °C under carbon monoxide to give a brown solution of **2d**. To this solution was added 0.70 g (5 mmol) of benzoyl chloride (**3a**) at 0 °C, and the mixture was stirred at 20 °C for 14 h. The workup as described above gave yellow crystals of raw **5f** (0.12 g, 7.4%). Although spectral data apparently showed that **5f** is the analogue of **5a–e** and **5g**, an analytically pure sample could not be obtained.

Reaction of Cinnamoyltetracarbonylferrate (2a) with Ethyl Fluorosulfonate (3d). To **2a** (2.5 mmol) (cf. the reaction of **2a** with **3a**) in CH_2Cl_2 (10 mL) was added $EtOSO_2F$ (0.53 mL, 5 mmol) at −78 °C, and then the solution was stirred at 20 °C for 1.5 h. The solvent was distilled in vacuo, and the residue was extracted with diethyl ether. After the evaporation of the solvent, the residual oil was chromatographed on silica gel (eluent benzene) and recrystallization from diethyl ether–*n*-hexane gave yellow crystals of **5g** (0.12 g, yield 14%).

The PPN salt of **2a** (5 mmol) also reacted with 2 equiv of $EtOSO_2F$ to give **5g** (yield 21%).

Reaction of 2b with Ethyl Fluorosulfonate. To a solution of **2b** (5 mmol) in tetrahydrofuran (15 mL) (cf. the reaction of **1b** with **2a**) was added 1.06 mL (10 mmol) of $EtOSO_2F$ at −78 °C, and the mixture was stirred and was warmed slowly to 28 °C over ca. 20 h. The solvent was distilled in vacuo, and the residue was extracted with four 10-mL portions of *n*-pentane. After the evaporation of the solvent, the residual oil was chromatographed on silica gel (eluent *n*-hexane–benzene (1:1)) and recrystallization from *n*-pentane gave yellow crystals of **5h** (0.52 g, yield 37%).

Reaction of 5a with $Fe_2(CO)_9$. To a suspension of $Fe_2(CO)_9$ (0.23 g, 0.64 mmol) in 20 mL of diethyl ether was added 0.13 g (0.32 mmol) of **5a**, and the mixture was stirred at 35 °C for 3 h. After the solvent was distilled in vacuo, the residue was chromatographed on silica gel (eluent *n*-hexane–benzene (2:1)) to give reddish brown crystals of **7** (0.12 g, yield 72%).

Thermal Reaction of 5a. The solution of **5a** (0.092 g, 0.23 mmol) in toluene (10 mL) was stirred under an atmosphere of argon and was heated at 105 °C for 1 h. After the solvent was distilled in vacuo, the residue was chromatographed on silica gel (eluent *n*-hexane–benzene (2:1)) to give reddish brown crystals of **7** (0.046 g, yield 78%, based on 2 equiv of **5a**).

Thermal Reaction of 5d and 5h. The solution of **5d** (0.17 g, 0.48 mmol) in toluene (20 mL) was heated at 103 °C under an atmosphere of argon for 4.5 h. After the solvent was distilled in vacuo, the residue was chromatographed on silica gel (eluent *n*-hexane–benzene (2:1)) to give a pale yellow oil of **8** (0.075 g, yield 47%).

Thermolysis of **5h** (0.13 g, 0.46 mmol) was performed in a similar procedure to give a pale yellow oil of **9** (0.081 g, yield 70%).

Although analytically pure samples of **8** and **9** were not obtained, the structures of them were confirmed by their spectral data shown in Tables I–III.

Synthesis of the PPN Salt of 1a by a Reaction of $Fe(CO)_5$ with (*E*)-PhCH=CHLi. To a solution of $Fe(CO)_5$ (2.1 g, 10 mmol) in diethyl ether (30 mL) was added dropwise (*E*)-PhCH=CHLi (80 mmol, solvent ether) at −78 °C under argon. The solution was warmed to 0 °C over ca. 15 h. The solution was concentrated to 50 cm^3, and a solution of bis(triphenylphosphine)nitrogen(1+) chloride (5.7 g, 10 mmol) in CH_2Cl_2 (50 mL) was added at 0 °C. After the solvent was distilled off in vacuo, the residue was extracted with 50 mL of CH_2Cl_2–ether (1:10) and filtered. To the filtrate was added excess amount of diethyl ether to give orange crystals of **10** (3.1 g, yield 37%).

Registry No. **2a**, 99457-44-0; **2b**, 99457-45-1; **2b** (PPN salt), 99457-62-2; **2c**, 99457-46-2; **2d**, 99528-50-4; **3a**, 98-88-4; **3b**, 3282-30-2; **3c**, 102-92-1; **3d**, 371-69-7; **5a**, 99457-47-3; **5b**, 99457-48-4; **5c**, 99457-49-5; **5d**, 99457-50-8; **5e**, 99457-51-9; **5f**, 99457-52-0; **5g**, 99457-53-1; **5h**, 99457-54-2; **6**, 99457-55-3; **7**, 99457-56-4; **8** (isomer 1), 99457-57-5; **8** (isomer 2), 99528-51-5; **9** (isomer 1), 99457-58-6; **9** (isomer 2), 99529-35-8; **10**, 99457-60-0; **12**, 67507-17-9; $K_2Fe(CO)_4$, 16182-63-1; $Fe_2(CO)_9$, 15321-51-4; $Fe(CO)_5$, 13463-40-6; (*E*)-PhCH=CHLi, 6160-69-6; 3-methyl-2-butenoyl chloride, 3350-78-5; (*E*)-2-butenoyl chloride, 625-35-4; acryloyl chloride, 814-68-6; carbon monoxide, 630-08-0.

An Examination of the Unsaturation in the Clusters $Fe_4(CO)_{11}(\mu_4\text{-}PR)_2$

Tilman Jaeger,[1a] Silvio Aime,*[1b] and Heinrich Vahrenkamp*[1a]

Institut für Anorganische und Analytische Chemie der Universität, D-7800 Freiburg, Germany, and Istituto di Chimica Generale ed Inorganica della Università, I-10125 Torino, Italy

Received May 29, 1985

The clusters $Fe_4(CO)_{11}(PR)_2$ (1, R = *t*-Bu, Ph, Tol) were investigated chemically and NMR spectroscopically. They easily add one ligand L (CO, $P(OMe)_3$, *t*-BuNC) to form $Fe_4(CO)_{11}L(PR)_2$ (**2**, **3**). Subsequent CO elimination under vacuum forms the new unsaturated clusters $Fe_4(CO)_{10}L(PR)_2$ (**4**). Further addition–elimination cycles allow the introduction of a total of four $P(OMe)_3$ and three *t*-BuNC ligands. The products with two, three, and four $P(OMe)_3$ and with three *t*-BuNC ligands can only be obtained in the unsaturated form. ^1H and ^{13}C NMR spectroscopy reveals the high fluxionality of the CO and *t*-BuNC ligands in these compounds. ^1H, ^{13}C, and ^{31}P NMR data of the unsaturated clusters can be interpreted in terms of an "aromatic ring current" in the Fe_4 system. Crystal structure determinations of $Fe_4(CO)_{11}[P(OMe)_3](PTol)_2$ [**3b**, triclinic, $P\bar{1}$, a = 1300.0 (2) pm, b = 1506.9 (3) pm, c = 944.5 (2) pm, α = 100.65 (1)°, β = 107.35 (1)°, γ = 84.43 (1)°, V = 1.7339 (3) nm^3, Z = 2] and $Fe_4(CO)_{10}[P(OMe)_3](PTol)_2$ [**4b**, orthorhombic, $P2_12_12_1$, a = 1289.0 (8) pm, b = 1478.5 (4) pm, c = 1819.7 (3) pm, V = 3.4678 (8) nm^3, Z = 4] reveal the difficulty of locating a Fe–Fe double bond in the unsaturated systems and the steric strain in the ligand sphere of the saturated systems.

Introduction

Cluster unsaturation is one of the simple conditions for the investigation of the cluster-surface analogy. The number of stable unsaturated organometallic clusters is, however, relatively small; and, with the exception of $H_2Os_3(CO)_{10}$, few studies on the nature of the unsaturation have been made.[2-4] In simplest terms, the chemical consequences of cluster unsaturation should be related to the chemistry of multiple bonds in general. But the disputable nature of metal–metal multiple bonds in clusters[5] and the hidden unsaturation due to donor–acceptor metal–metal bonds[6] cause a more diversified picture which still lacks systematization. In the course of our cluster construction studies we found a group of tetrairon clusters $Fe_4(CO)_{11}(PR)_2$ (**1**)[7] which according to the 18-electron rule lack two electrons. The unsaturation of these compounds was obvious from the ease of CO addition. The location of a Fe–Fe double bond proved to be difficult since Fe–Fe bond lengths (244–269 pm) are not significantly different and the shortest Fe–Fe bond is CO bridged. A delocalized 2π situation in the planar tetrairon ring could therefore not be excluded.

In order to better understand the unsaturation in the clusters **1**, we undertook a chemical and NMR spectroscopic investigation. The aim was to learn about the double bond fluctuation or possible delocalization, the interconvertibility of saturated and unsaturated cluster forms when donor ligands have been introduced, and the isomerism and bonding situation in derivatives with more than one donor ligand. Parts of this work have been published as a communication.[8]

Experimental Section

All experimental techniques were as previously reported.[9] The clusters **1a** and **1c** were prepared according to the published procedure.[7] Reagents were obtained commercially, distilled under nitrogen before use, and applied as 0.5 M solutions in benzene. Chromatographic separations were done on silica gel (0.063–0.200 mm) which was dried for 6 h at 180 °C vacuum. All new compounds are characterized in Table I.

IR spectra were measured of cyclohexane solutions on a Perkin-Elmer 782 spectrometer. ^1H NMR spectra were obtained on an Varian T60 A spectrometer using $CDCl_3$ as a solvent and Me_4Si as internal standard. ^{13}C and ^{31}P NMR spectra were obtained on a JEOL GX 270/89 spectrometer operating at 67.9 and 109.4 MHz, respectively. The ^{13}C measurements were carried out on ^{13}CO-enriched (ca. 10%) samples which were prepared by exchange between the natural abundance $Fe_4(CO)_{11}(PR)_2$ samples and ^{13}CO (Monsanto, 90%) in *n*-hexane/$CHCl_3$ solutions contained in sealed vials (11 days at +30 °C). The variable-temperature ^{13}C spectra of **1a** and **2a** were recorded also at higher field (JEOL GX-400 operating at 100.6 MHz for ^{13}C).

Improved Preparation of $Fe_4(CO)_{11}(PPh)_2$ (1b). $Fe_2(CO)_6(PHPh)_2$[7] (0.62 g, 1.24 mmol) and $Fe_3(CO)_{12}$ (1.35 g, 2.68 mmol) in benzene (250 mL) were irradiated by a water-cooled 150-W high-pressure Hg lamp (type Hanau TQ 150 Z 3) immersed into the reaction vessel in which a circulating flow of the reactants was maintained. The reaction vessel was connected to a 500-mL flask, evacuated, and heated to 60 °C. After 3.5 h the solution was filtered and evaporated to dryness. The residue was subjected to flash chromatography (20 × 4 cm column, excess pressure 0.10–0.15 bar) with hexane. A green band of $Fe_3(CO)_{12}$ and an orange band of $Fe_3(CO)_9(PPh)_2$ were quickly eluted. Hexane/benzene (10:1) eluted **1b** as a dark brown band. Filtration and recrystallization from hexane/benzene (5:1) yielded 300 mg (32%) of **1b**.

Preparation of $Fe_4(CO)_{11}[P(OMe)_3](PPh)_2$ (3a). **1b** (90 mg, 0.12 mmol) in benzene (15 mL) was treated dropwise with $P(OMe)_3$ in benzene (0.5 M, 0.24 mL, 0.12 mmol). Immediate reaction was obvious from a color change from black to red. The solution was concentrated to 5 mL in a stream of CO, 10 mL of hexane was added, and **3a** was crystallized at −30 °C; yield 90 mg (86%).

Preparation of $Fe_4(CO)_{11}[P(OMe)_3](PTol)_2$ (3b): as above from **1c** (70 mg, 0.09 mmol) and $P(OMe)_3$ (0.18 mL, 0.09 mmol); yield 70 mg (86%).

(1) (a) Universität Freiburg. (b) Università di Torino.
(2) Cf. Johnson, B. F. G.; Lewis, J. *Adv. Inorg. Chem. Radiochem.* **1981**, *24*, 225.
(3) Cf. Vahrenkamp, H. *Adv. Organomet. Chem.* **1983**, *22*, 169.
(4) Muetterties, E. L.; Krause, M. J. *Angew. Chem.* **1983**, *95*, 135; *Angew. Chem., Int. Ed. Engl.* **1983**, *22*, 135.
(5) Granozzi, G.; Benoni, R.; Tondello, E.; Casarin, M.; Aime, S.; Osella, D. *Inorg. Chem.* **1983**, *22*, 3899.
(6) Mayr, A.; Ehrl, W.; Vahrenkamp, H. *Chem. Ber.* **1974**, *107*, 3860.
(7) Vahrenkamp, H.; Wucherer, E. J.; Wolters, D. *Chem. Ber.* **1983**, *116*, 1219.
(8) Vahrenkamp, H.; Wolters, D. *Organometallics* **1982**, *1*, 874.
(9) Müller, R.; Vahrenkamp, H. *Chem. Ber.* **1980**, *113*, 3517.

0276-7333/86/2305-0245$01.50/0

Table I. Characterization of New Compounds

no.	color	mp, °C	formula (mol wt)	anal. calcd (found) C	H	Fe
3a	red-black	>50 dec	$C_{26}H_{19}Fe_4O_{14}P_3$ (871.8)	35.82 (35.61)	2.20 (1.93)	25.63 (26.41)
3b	red-black	>60 dec	$C_{28}H_{23}Fe_4O_{14}P_3$ (899.8)	37.37 (37.57)	2.58 (2.43)	24.83 (24.51)
3c[a]	red-brown	>75 dec	$C_{28}H_{19}Fe_4NO_{11}P_2$ (830.8)	40.48 (39.77)	2.30 (1.78)	26.88 (26.54)
4a	black	118	$C_{25}H_{19}Fe_4O_{13}P_3$ (843.7)	35.58 (35.48)	2.26 (1.96)	26.47 (26.38)
4b	black	>90 dec	$C_{27}H_{23}Fe_4O_{13}P_3$ (871.8)	37.19 (37.19)	2.66 (2.58)	25.63 (25.76)
4c[a]	black	178	$C_{27}H_{19}Fe_4NO_{10}P_2$ (802.8)	40.39 (39.45)	2.38 (1.92)	27.82 (27.94)
6a[b]	black	>160 dec	$C_{27}H_{28}Fe_4O_{15}P_4$ (939.8)	34.51 (34.62)	3.00 (2.88)	23.77 (23.82)
6b	black	>120 dec	$C_{29}H_{32}Fe_4O_{15}P_4$ (967.9)	35.99 (36.18)	3.33 (3.30)	23.08 (21.82)
6c[a]	black	>155 dec	$C_{31}H_{28}Fe_4N_2O_9P_2$ (857.9)	43.40 (43.29)	3.28 (2.54)	26.03 (25.81)
6d[a]	black	118	$C_{29}H_{28}Fe_4NO_{12}P_3$ (898.8)	38.75 (38.83)	3.13 (3.03)	24.85 (25.03)
7a[c]	black	>130 dec	$C_{29}H_{37}Fe_4O_{17}P_5$ (1035.8)	33.63 (33.76)	3.60 (3.20)	21.56 (21.68)
7d[a,d]	black	>100 dec	$C_{31}H_{37}Fe_4NO_{14}P_4$ (994.9)	37.42 (37.70)	3.74 (3.84)	22.45 (22.38)
8a	black	122 dec	$C_{31}H_{46}Fe_4O_{19}P_6$ (1131.9)	32.89 (33.10)	4.00 (3.99)	19.73 (19.59)

[a] N analyses calcd (found): **3c**, 1.68 (1.60); **4c**, 1.74 (1.82); **6c**, 3.26 (2.90); **6d**, 1.55 (1.69); **7d**, 1.40 (1.54). [b] Mol wt 940 (FD-MS). [c] Mol wt 1036 (FD-MS). [d] Mol wt 995 (FD-MS).

Preparation of $Fe_4(CO)_{11}(t\text{-BuNC})(PPh)_2$ (3c). **1b** (100 mg, 0.13 mmol) in benzene (50 mL) was treated dropwise with *t*-BuNC in benzene (0.5 M, 0.26 mL, 0.13 mmol). The reaction was complete within a few minutes. After filtration the solvent was removed under vacuum and the residue recrystallized from *n*-pentane/dichloromethane (5:2) at −30 °C to yield 98 mg (88%) of **3c**.

Preparation of $Fe_4(CO)_{10}[P(OMe)_3](PPh)_2$ (4a). **3a** (150 mg, 0.17 mmol) in benzene (30 mL) in a 250-mL flask was evacuated and heated to 60 °C for 1 h while the color changed from red to black. After filtration the solvent was removed under vacuum and the residue recrystallized from hexane/benzene (4:1) at −30 °C to yield 130 mg (91%) of **4a**.

Preparation of $Fe_4(CO)_{10}[P(OMe)_3](PTol)_2$ (4b). **3b** (50 mg, 0.055 mmol) in benzene (10 mL) was treated as above to yield 45 mg (94%) of **4b**.

Preparation of $Fe_4(CO)_{10}(t\text{-BuNC})(PPh)_2$ (4c). **3c** (90 mg, 0.10 mmol) in benzene (25 mL) was treated as above to yield 57 mg (71%) of **4c**.

Conversions 4 → 3. Solutions of **4a**, **4b**, and **4c** (ca. 30 mg) in benzene (ca. 15 mL) were stirred under an atmosphere of CO for 1 day when IR and NMR evidence indicated complete conversion to **3a**, **3b**, and **3c**. The isolated yield of **3a** from **4a** (34 mg) after crystallization from hexane/benzene (5:1) at −30 °C was 28 mg (80%).

Preparation of $Fe_4(CO)_{10}(t\text{-BuNC})_2(PPh)_2$ (5c). **4c** (110 mg, 0.14 mmol) in benzene (50 mL) at 8–10 °C was treated dropwise with *t*-BuNC in benzene (0.5 M, 0.28 mL, 0.14 mmol) while the color changed from black to red. Evacuation to dryness and recrystallization from hexane/toluene (5:1) at −70 °C yielded 19 mg (18%) of **5c**. The low yield of the compound allowed only a spectroscopic identification.

Preparation of $Fe_4(CO)_9[P(OMe)_3]_2(PPh)_2$ (6a). **4a** (66 mg, 0.08 mmol) and $P(OMe)_3$ (0.5 M, 0.16 mL, 0.08 mmol) in benzene (25 mL) were heated to 60 °C for 1 h. After filtration and evaporation to dryness, the residue was recrystallized from hexane/benzene (4:1) at −30 °C to yield 65 mg (88%) of **6a**.

Preparation of $Fe_4(CO)_9[P(OMe)_3]_2(PTol)_2$ (6b). **1c** (70 mg, 0.09 mmol) and $P(OMe)_3$ (0.5 M, 0.36 mL, 0.18 mmol) in benzene (15 mL) were heated to 60 °C for 30 min. Filtration, evaporation to dryness, and recrystallization from hexane at −30 °C yielded 70 mg (80%) of **6b**.

Preparation of $Fe_4(CO)_9(t\text{-BuNC})_2(PPh)_2$ (6c). **4c** (260 mg, 0.32 mmol) in benzene (50 mL) was treated with *t*-BuNC in benzene (0.5 M, 0.64 mL, 0.32 mmol). The solution was stirred for 1.5 h at room temperature and for 1.5 h at 65 °C. After evaporation to dryness, the residue was chromatographed with hexane/benzene (5:1) over a 2 × 20 cm column. From the first black band after evaporation and recrystallization from *n*-pentane/toluene (5:1) at −30 °C 46 mg (16%) of **6c** was obtained.

Preparation of $Fe_4(CO)_9[P(OMe)_3](t\text{-BuNC})(PPh)_2$ (6d). **4c** (130 mg, 0.16 mmol) and $P(OMe)_3$ (0.5 M, 0.32 mL, 0.16 mmol) in benzene were stirred at room temperature for 1 h. The color of the solution turned from black to red. Upon concentration under vacuum the solution became black again. To complete the CO elimination, the remaining solution (40 mL) was heated to 60 °C for 1 h. Filtration, evaporation to dryness, and crystallization from *n*-pentane/dichlormethane (4:1) at −30 °C yielded 57 mg (40%) of **6d**.

Preparation of $Fe_4(CO)_8[P(OMe)_3]_3(PPh)_2$ (7a). **6a** (73 mg, 0.08 mmol) and $P(OMe)_3$ (0.5 M, 0.16 mL, 0.08 mmol) in benzene (40 mL) were heated at reflux for 1.5 h. Filtration, evaporation to dryness, and crystallization from hexane/dichloromethane (4:1) yielded 66 mg (82%) of **7a**.

Preparation of $Fe_4(CO)_8(t\text{-BuNC})_3(PPh)_2$ (7c). **6c** (28 mg, 0.03 mmol) and *t*-BuNC (0.5 M, 0.06 mL, 0.03 mmol) in benzene (25 mL) were heated at 60 °C for 1.5 h. After evaporation to dryness, the residue was chromatographed with hexane/benzene (5:1) over a 2 × 15 cm column. From the first dark brown band 15 mg (55%) of **7c** remained as an oily material which could not be purified by crystallization.

Preparation of $Fe_4(CO)_8[P(OMe)_3]_2(t\text{-BuNC})(PPh)_2$ (7d). **6d** (28 mg, 0.03 mmol) and $P(OMe)_3$ (0.5 M, 0.06 mL, 0.03 mmol) in benzene (40 mL) were heated at reflux for 3.5 h. Filtration, evaporation to dryness, and crystallization from *n*-pentane/dichloromethane (2:1) yielded 12 mg (39%) of **7d**.

Preparation of $Fe_4(CO)_7[P(OMe)_3]_4(PPh)_2$ (8a). **7a** (49 mg, 0.05 mmol) and $P(OMe)_3$ (0.5 M, 0.10 mL, 0.05 mmol) in benzene (25 mL) were refluxed for 6 h. After filtration and evaporation to dryness, the residue was recrystallized twice from hexane/dichloromethane (5:1), resulting in 27 mg (52%) of **8a**.

Crystal Structure Determinations. The quality of the crystals was checked by photographic methods. All crystal data and details of the structure solutions are given in Table II. The positions of the iron atoms were found from Patterson maps. Two successive Fourier cycles then revealed the positions of all other non-hydrogen atoms. The structures were refined by standard least-squares techniques using unit weights. The C_6H_4 units of the tolyl groups were treated as rigid bodies with C–C = 139.5 pm and C–H = 108 pm, only the positions of the rigid bodies and the thermal parameters of the C atoms being varied while the H atoms were assigned a common variable-temperature factor. All atoms except the aromatic C and H atoms were refined anisotropically. Tables III and IV list the atomic positions and $U(eq)$ or $U(ij)$ values. The supplementary material[8] contains, in addition, the anisotropic temperature factors, all bond lengths and angles, and the F_o/F_c lists.

Results and Discussion

Reactions. The unsaturation of the clusters **1** manifests itself in the easy CO addition to form the clusters **2**.[7] The latter, however, are not significantly more stable and are quantitatively reconverted to **1** under vacuum. The color change between black (**1**) and red (**2**) makes it easy to follow these reactions.[7]

It was now found that PX_3 and RNC ligands are added the same way. From reactions of **1b** and **1c** with $P(OMe)_3$ and *t*-BuNC the new saturated clusters **3** are obtained. Heating of these in vacuum converts them back to unsaturated clusters by elimination of CO. The resulting

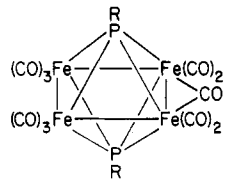

1a, R = *t*-Bu
b, R = Ph
c, R = Tol

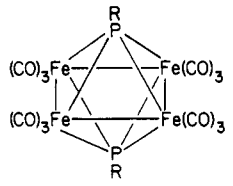

2a, R = *t*-Bu
b, R = Ph
c, R = Tol

clusters **4** can be called substitution derivatives of **1**, just as the clusters **3** are substitution derivatives of **2**. Reconversion of **4** to **3** occurs readily under a CO atmosphere. Again, the saturated compounds **3** are red and the unsaturated compounds **4** are black in solution.

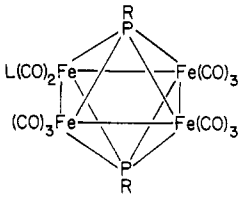

3a, R = Ph, L = $P(OMe)_3$
b, R = Tol, L = $P(OMe)_3$
c, R = Ph, L = *t*-BuNC

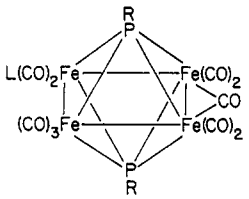

4a, R = Ph, L = $P(OMe)_3$
b, R = Tol, L = $P(OMe)_3$
c, R = Ph, L = *t*-BuNC

The next cycle of ligand additions should produce saturated clusters of the type $Fe_4(CO)_{10}L_2(PR)_2$ starting from **4**. However, only in the case of the bis(isocyanide) compound **5c**, which was not analytically pure, was the isolation of such a product possible. Heating of the reactants **4c** and *t*-BuNC caused the reaction to proceed directly to the unsaturated product **6c**. Likewise, a red, probably saturated intermediate could be observed but not isolated in the reaction between **4c** and $P(OMe)_3$ which led to the isolation of **6d**. The phosphite substituted clusters **4a** and **4b** did not react fast enough with further phosphite at room temperature which caused them to be directly converted to **6a** and **6b** upon heating. These conversions are net substitution reactions the addition/elimination nature of which is obvious.

$Fe_4(CO)_{10}(t\text{-BuNC})_2(PPh)_2$

5c

$Fe_4(CO)_9L_2(PR)_2$

6a, R = Ph, L = $P(OMe)_3$
b, R = Tol, L = $P(OMe)_3$
c, R = Ph, L = *t*-BuNC
d, R = Ph, L_2 = *t*-BuNC + $P(OMe)_3$

The introduction of a third and fourth donor ligand was only possible as a substitution reaction due to the more drastic reaction conditions required. The higher isocyanide derivatives of **1** seem to be progressively more unstable since **7c** could only be obtained impure and a tetraisocyanide compound was not accessible. The tris(phosphite)-substituted cluster **7a** is, however, moderately stable, the tetrakis(phosphite)-substituted cluster **8a** could be obtained under conditions close to decomposition, and the mixed phosphite–isocyanide derivative **7d** was accessible as well. Further reactions with these donor ligands could not be observed.

$Fe_4(CO)_8L_3(PPh)_2$

7a, L = $P(OMe)_3$
b, L = *t*-BuNC
c, L_3 = *t*-BuNC + $2P(OMe)_3$

$Fe_4(CO)_7[P(OMe)_3]_4(PPh)_2$

8a

Constitution and Isomerism of the Products. The identity and geometry of the compounds **1c**,[7] **3b**, and **4b** (see below) is confirmed by crystal structure analyses. In addition, the constitutions of one bis-substituted (**6a**) and two tris-substituted derivatives (**7a,d**) were established by FD-MS. The MS method failed on the tetrakis(phosphite) derivative **8a**. On the basis of the IR spectroscopic similarity within the groups of clusters and the correct intensity ratios in the ^1H NMR spectra (see Table V) all new clusters **3–8** can be considered as confirmed.

The IR spectra of the clusters, like their colors, allow a clear distinction between the saturated and the unsaturated compounds (cf. Table V). The presence of 11 terminal ligands around the tetrairon core goes along with one CO being in a bridge position. All unsaturated clusters show this by ν(CO) bands around 1800 cm^{-1}. As the number of donor ligands increases from **2** to **8**, so the general pattern of ν(CO) absorptions moves to lower wavenumbers. All isocyanide-substituted compounds here show the ν(CN) absorption. Its position (between 2130 and 2150 cm^{-1}) is hardly shifted with respect to the ν(CN) band of free *t*-BuNC (2135 cm^{-1}), as might be expected for compounds of metals in relatively low oxidation states.[10,11]

The ^1H NMR spectra of **3–8** (cf. Table V) give some insight into possible ligand arrangements. There is a large number of possible isomers for all new clusters. Extrapolating from the CO positions in **1** and **2** (and taking into account the molecular structures of **3b** and **4b**), the additional ligands can be axial or equatorial with respect to the tetrairon ring. They can be adjacent to or distant from the CO bridge (respectively the Fe–Fe double bond), and with more than one $P(OMe)_3$ or *t*-BuNC ligands these can be placed in gem, vic, cis, trans, ortho, and para positions. On this background most of the ^1H NMR spectra are surprisingly simple. They indicate that the clusters **3** and **4** exist as just one isomer. They allow the interpretation that the bis(isocyanide) compounds **5c** and **6c** either contain equivalent *t*-BuNC groups or are fluxional molecules. And they seem to prove the symmetrical configuration of **8a** with four equivalent phosphite ligands. The crystal structure determination of **4b** has located the $P(OMe)_3$ ligand nonadjacent to the CO bridge. This was taken into account in the formula drawing of all clusters **4**, whereas in the absence of further information no detailed ligand arrangements can be suggested for **5–8**.

Since two ligands L on one iron atom are unlikely and since axial/equatorial isomerism or the position of the CO bridge seem to be without effect in the clusters **3** and **4**, it is realistic to take into consideration only the possibility of ortho and para arrangements of the two L in the clusters **5** and **6**. Whereas no information relating to this can be obtained from the NMR spectra of **5c** and **6c** (see above), **6a** and **6b** seem to be mixtures of isomers. In the $P(OMe)_3$ region they show two signal groups marked A and B in Table V whose intensity ratio is approximately 2:1 in **6a** and 3:2 in **6b**. The same holds for the ^{31}P and ^{13}C resonances of **6a** (see below). If the signals marked A are assigned to the ortho isomer $P(OMe)_3$ on adjacent Fe atoms) and the signals marked B to the para isomer, then the relative abundances of A and B correspond roughly to the statistical chance of their formation: for the $P(OMe)_3$-substituted iron atoms in **4** there are two ortho iron atoms and one para iron atom. Just like the bis(isocyanide) derivatives **5c** and **6c** the mixed phosphite–isocyanide derivative **6d** does not give NMR evidence for isomerism. Again a possible explanation for this is fluxionality; and since the phosphite ligands seem to be firmly

(10) Treichel, P. M. *Adv. Organomet. Chem.* **1973**, *11*, 21.
(11) Adams, R. D.; Chodosh, D. F. *J. Am. Chem. Soc.* **1977**, *99*, 6544.
(12) Cf. Grant, S.; Newman, J.; Manning, A. R. *J. Organomet. Chem.* **1975**, *96*, C11. Adams, R. D.; Cotton, F. A. *J. Am. Chem. Soc.* **1973**, *95*, 6589, 6594.

Table II. Crystallographic Data for $Fe_4(CO)_{10}(P\text{-}p\text{-}Tol)_2 \cdot P(OMe)_3$ (4b) and $Fe_4(CO)_{11}(P\text{-}p\text{-}Tol)_2 \cdot P(OMe)_3$ (3b)

	4b	3b
mol formula	$C_{27}H_{23}Fe_4O_{13}P_3$	$C_{28}H_{23}Fe_4O_{14}P_3$
mol wt	871.8	899.8
cryst from	toluene/hexane (1:2)	benzene/hexane (1:2)
color	black	red
space group	$P2_12_12_1$	$P\bar{1}$
cell dimens (20 °C)		
a, pm	1289.0 (8)	1300.0 (2)
b, pm	1478.5 (4)	1506.9 (3)
c, pm	1819.7 (3)	944.5 (2)
α, deg	90	100.65 (1)
β, deg	90	107.35 (1)
γ, deg	90	84.43 (1)
V, nm^3	3.4678 (8)	1.7339 (3)
Z	4	2
d_{obsd}, g cm^{-3}	1.70	1.70
d_{calcd} g cm^{-3}	1.67	1.72
radiatn	Mo Kα	Mo Kα
monochromator	graphite	graphite
cryst dimens, mm	0.15 × 0.15 × 0.30	0.20 × 0.25 × 0.50
μ, cm^{-1}	17.5	16.8
absorptn correctn	none	none
diffractometer	Nonius CAD 4	Nonius CAD 4
data collection	ω–2θ	ω–2θ
2θ range	1–45	1–45
reflectns measd	2944	4832
obsd data, $I > 3\sigma(I)$	1782	3700
structure soln	Patterson/Fourier	Patterson/Fourier
programs	SHELX[a]	SHELX[a]
scattering factors	Cromer/Mann[b]	Cromer/Mann[b]
R(unit weights)	0.045	0.055
residual electron density (10^6e·pm^{-3})	+0.5/−0.4	+1.1/−0.9

[a] Distributed by G. M. Sheldrick, University of Göttingen, West Germany. [b] Cromer, D. T.; Mann, J. B. *Acta Crystallogr., Cryst. Phys., Diffr., Theor. Gen. Crystallogr.* **1968**, *A24*, 321.

bound, this must be due to isocyanide mobility. We have not been able so far to enrich or isolate the different isomers of the clusters **5** and **6**.

With the assumption of one PR_3 or RNC ligand per iron atom, the trisubstituted clusters **7a** and **7c** cannot form different isomers. This is borne out for **7a** by the exact 2:1 ratio of the NMR signals due to the $P(OMe)_3$ ligands. For **7c** there are two *t*-BuNC resonances of approximately 1:1 intensity which cannot be interpreted nor discussed at the moment since the compound is not analytically pure. The mixed derivative **7d** behaves like the bis(phosphite) derivatives **6a** and **6b** showing signal groups A and B with intensity ratio ca. 2:1 in the $P(OMe)_3$ and *t*-BuNC spectral regions. Again, mobility of the isocyanide ligand offers the simplest explanation for this.

Fluxionality and NMR Anisotropy. To gain some insight into the possible orientation of the ligands and the location of the CO bridge and the assumed Fe–Fe double bond in the unsaturated clusters, some of the clusters were also examined by ^{31}P and ^{13}C NMR spectroscopy. Table VI lists the results which for **6a** and **7a** confirm the isomeric situation discussed above.

It became obvious immediately from the ^{13}C NMR spectra in the CO region that the basic clusters **1** and **2** are highly fluxional. There is just one resonance which down to the lowest accessible temperatures (ca. −130 °C) and at the high field strength (400-MHz instrument) does not significantly broaden. This situation does not change significantly upon introduction of one to four $P(OMe)_3$ ligands. It has not been possible to observe more than one ^{13}CO resonance in **3a**, **4a**, **6aA**, **6aB**, **7a**, and **8a**. Although the phosphite ligands slow down the fluxional process as evidenced from the collapse of the ^{13}CO signals of **6aA** and **8a** around −110 °C, no "frozen out" situation could be reached. The room-temperature ^{13}CO signals show multiplets with J(C–P) coupling of ca. 6 Hz according to the number of phosphite ligands present. The coupling to the μ_4 phosphorus atoms seems to be negligible (<1 Hz). All this is simply interpreted by a facile scrambling of all CO ligands which also involves bridge–terminal interchange. No conclusions can be drawn with respect to the orientation or movement of the $P(OMe)_3$ ligands. But if there is a Fe–Fe double bond present which electron counting requires to be CO bridged, it has to fluctuate as fast as the CO ligands.

Besides the high fluxionality of the clusters the NMR anisotropy of the unsaturated ones is noticeable. This had been observed for the ^1H chemical shifts for the PR groups in **1** and **2**.[7] Of these, those for **2** are in a normal range whereas those for **1** show an upfield shift which is larger the closer the group R is to the tetrairon ring (maximum 2.36 ppm for R = Me[7]). This is now confirmed for all other NMR data (cf. Tables V and VI). The weighted average of the phenyl ^1H chemical shifts for the saturated compounds **2b**, **3a**, **3c**, and **5c** is 8.0 ppm whereas for the corresponding unsaturated compounds **1b**, **4a**, **4c**, and **6c** it is approximately 7.0 ppm, again representing a significant upfield shift. In fact, the phenyl NMR resonances were the simplest indication of the bonding type for all new clusters **3**–**8**. The ^{31}P chemical shifts for the μ_4-PR group follow the same trend, but 2 orders of magnitude larger: for the unsaturated clusters **1b**, **4a**, **6a**, and **7a** the PPh signals are in the 225–245 ppm range while for the saturated counterparts **2b** and **3a** they are in the 340–350 ppm range; the corresponding **1a**/**2a** pair shows the same shift difference. The nature of the anisotropy is such that the effective magnetic field is weakened above the center of the tetrairon ring in the unsaturated compounds. This is the same type of anisotropy as the ring current effect in aromatic compounds which at first glance is not unreasonable since the unsaturated tetrairon rings can be called 2π systems in the Hückel terminology.

Table III. Atomic Parameters for $Fe_4(CO)_{11}[P(OMe)_3](PTol)_2$ (3b)

atom	x	y	z	U(11)	U(22)	U(33)	U(12)	U(13)	U(23)	U(eq), Å²
Fe1	0.3059 (1)	0.3173 (1)	0.3710 (1)	0.0183 (6)	0.0243 (7)	0.0158 (6)	−0.0093 (5)	0.0005 (5)	0.0025 (5)	0.0200 (5)
Fe2	0.3143 (1)	0.1597 (1)	0.4740 (1)	0.0185 (6)	0.0208 (7)	0.0235 (7)	−0.0057 (5)	0.0012 (5)	0.0033 (5)	0.0217 (6)
Fe3	0.2527 (1)	0.4037 (1)	0.6140 (1)	0.0191 (7)	0.0235 (7)	0.0240 (7)	−0.0062 (5)	0.0041 (5)	−0.0008 (5)	0.0229 (6)
Fe4	0.3042 (1)	0.2549 (1)	0.7401 (1)	0.0233 (7)	0.0355 (8)	0.0195 (7)	−0.0067 (6)	0.0056 (5)	0.0067 (6)	0.0256 (6)
C11	0.3739 (8)	0.4162 (7)	0.3688 (9)	0.034 (6)	0.046 (7)	0.015 (5)	−0.013 (5)	−0.003 (4)	0.003 (4)	0.033 (5)
O11	0.4140 (7)	0.4774 (5)	0.3647 (8)	0.075 (6)	0.049 (5)	0.058 (5)	−0.043 (4)	0.013 (4)	0.013 (4)	0.059 (4)
C12	0.1875 (7)	0.3326 (6)	0.212 (1)	0.027 (5)	0.033 (6)	0.029 (6)	−0.013 (4)	0.000 (5)	0.008 (4)	0.030 (5)
O12	0.1199 (6)	0.3453 (5)	0.1097 (8)	0.040 (4)	0.071 (6)	0.041 (5)	−0.015 (4)	−0.021 (4)	0.018 (4)	0.056 (4)
C13	0.3826 (8)	0.2497 (6)	0.261 (1)	0.034 (6)	0.033 (6)	0.027 (5)	−0.003 (5)	0.006 (5)	0.006 (5)	0.032 (5)
O13	0.4345 (6)	0.2123 (5)	0.1884 (8)	0.065 (5)	0.058 (5)	0.046 (5)	0.004 (4)	0.031 (4)	0.003 (4)	0.054 (4)
C31	0.3548 (8)	0.4836 (7)	0.729 (1)	0.032 (5)	0.034 (6)	0.035 (6)	−0.015 (5)	0.006 (5)	−0.007 (5)	0.035 (5)
O31	0.4092 (6)	0.5383 (6)	0.8008 (9)	0.053 (5)	0.062 (5)	0.065 (5)	−0.033 (4)	0.011 (4)	−0.026 (5)	0.064 (4)
C32	0.1527 (8)	0.4312 (7)	0.712 (1)	0.033 (6)	0.035 (6)	0.047 (6)	−0.006 (5)	0.014 (5)	0.001 (5)	0.038 (5)
O32	0.0894 (7)	0.4494 (6)	0.775 (1)	0.050 (5)	0.087 (7)	0.080 (6)	0.003 (5)	0.042 (5)	0.006 (5)	0.068 (5)
C33	0.1899 (8)	0.4756 (6)	0.483 (1)	0.036 (6)	0.026 (5)	0.034 (6)	−0.006 (5)	0.004 (5)	−0.001 (5)	0.034 (5)
O33	0.1447 (7)	0.5243 (5)	0.4021 (9)	0.073 (6)	0.045 (5)	0.055 (5)	0.007 (4)	0.008 (4)	0.021 (4)	0.059 (4)
C41	0.4130 (9)	0.1817 (7)	0.828 (1)	0.042 (6)	0.051 (7)	0.027 (6)	−0.003 (5)	0.015 (5)	0.005 (5)	0.039 (5)
O41	0.4825 (7)	0.1365 (6)	0.8791 (9)	0.062 (6)	0.087 (7)	0.054 (5)	0.031 (5)	0.009 (4)	0.034 (5)	0.069 (5)
C42	0.1860 (8)	0.2134 (7)	0.768 (1)	0.042 (6)	0.058 (7)	0.029 (6)	−0.016 (5)	0.017 (5)	0.010 (5)	0.040 (5)
O42	0.1154 (7)	0.1884 (6)	0.7932 (9)	0.056 (5)	0.109 (8)	0.069 (6)	−0.034 (5)	0.027 (5)	0.024 (5)	0.073 (5)
C43	0.3285 (8)	0.3393 (7)	0.901 (1)	0.044 (6)	0.041 (6)	0.023 (6)	−0.008 (5)	0.011 (5)	0.005 (5)	0.035 (5)
O43	0.3463 (7)	0.3904 (6)	1.0101 (9)	0.082 (6)	0.066 (5)	0.032 (5)	−0.020 (5)	0.016 (4)	−0.001 (4)	0.060 (5)
P3	0.2300 (2)	0.0871 (2)	0.2533 (3)	0.032 (1)	0.024 (1)	0.034 (1)	−0.09 (1)	0.001 (1)	−0.002 (1)	0.032 (1)
O51	0.1433 (5)	0.1424 (4)	0.1481 (7)	0.044 (4)	0.030 (4)	0.044 (4)	−0.011 (3)	−0.015 (3)	0.002 (3)	0.045 (3)
C51	0.0367 (8)	0.1204 (8)	0.051 (1)	0.038 (6)	0.062 (8)	0.043 (6)	−0.020 (5)	−0.014 (5)	0.011 (6)	0.052 (6)
O52	0.1612 (6)	0.0006 (5)	0.2380 (8)	0.058 (5)	0.032 (4)	0.062 (5)	−0.023 (4)	−0.012 (4)	0.001 (4)	0.057 (4)
C52	0.209 (1)	−0.0853 (7)	0.273 (2)	0.11 (1)	0.020 (6)	0.082 (9)	−0.012 (6)	−0.034 (8)	0.013 (6)	0.082 (8)
O53	0.3146 (6)	0.0471 (5)	0.1628 (8)	0.052 (5)	0.063 (5)	0.048 (5)	−0.015 (4)	0.011 (4)	−0.027 (4)	0.059 (4)
C53	0.287 (1)	0.009 (1)	0.004 (1)	0.11 (1)	0.10 (1)	0.045 (8)	−0.016 (9)	0.022 (8)	−0.028 (8)	0.089 (9)
C21	0.4477 (8)	0.1147 (6)	0.472 (1)	0.034 (6)	0.016 (5)	0.034 (6)	−0.006 (4)	0.003 (4)	0.005 (4)	0.029 (5)
O21	0.5309 (6)	0.0857 (5)	0.4671 (9)	0.029 (4)	0.043 (5)	0.094 (6)	0.007 (4)	0.018 (4)	0.013 (4)	0.056 (4)
C23	0.2830 (8)	0.0777 (7)	0.562 (1)	0.041 (6)	0.031 (6)	0.038 (6)	−0.003 (5)	0.010 (5)	0.003 (5)	0.037 (5)
O23	0.2606 (7)	0.0225 (5)	0.6163 (9)	0.091 (6)	0.044 (5)	0.068 (6)	−0.022 (4)	0.037 (5)	0.018 (4)	0.062 (5)
P1	0.3968 (2)	0.2954 (2)	0.6016 (2)	0.017 (1)	0.027 (1)	0.018 (1)	−0.0059 (9)	0.0019 (9)	0.003 (1)	0.021 (1)
P2	0.1917 (2)	0.2690 (2)	0.4911 (3)	0.016 (1)	0.025 (1)	0.024 (1)	−0.0052 (9)	0.0030 (9)	0.004 (1)	0.022 (1)
C67	0.8814 (8)	0.3525 (9)	0.869 (1)	0.019 (6)	0.10 (1)	0.066 (8)	−0.030 (6)	−0.013 (5)	0.025 (7)	0.064 (7)
C77	−0.2954 (7)	0.2156 (8)	0.239 (1)	0.013 (5)	0.084 (9)	0.066 (8)	−0.021 (5)	0.005 (5)	−0.018 (7)	0.059 (6)

atom	x	y	z	U(11) or U(eq), Å²	atom	x	y	z	U(11) or U(eq), Å²
C61	0.5399 (3)	0.3133 (4)	0.6793 (6)	0.023 (2)	C71	0.0468 (3)	0.2530 (4)	0.4184 (7)	0.025 (2)
C62	0.5825 (3)	0.3422 (4)	0.8334 (6)	0.039 (2)	C72	−0.0229 (3)	0.3230 (4)	0.3628 (7)	0.035 (2)
C63	0.6927 (3)	0.3554 (4)	0.8944 (6)	0.046 (3)	C73	−0.1335 (3)	0.3105 (4)	0.3052 (7)	0.039 (2)
C64	0.7604 (3)	0.3398 (4)	0.8013 (6)	0.039 (2)	C74	−0.1744 (3)	0.2279 (4)	0.3032 (7)	0.038 (2)
C65	0.7178 (3)	0.3110 (4)	0.6472 (6)	0.036 (2)	C75	−0.1047 (3)	0.1578 (4)	0.3588 (7)	0.040 (2)
C66	0.6075 (3)	0.2977 (4)	0.5862 (6)	0.030 (2)	C76	0.0059 (3)	0.1704 (4)	0.4164 (7)	0.037 (2)
H62	0.5301 (3)	0.3542 (4)	0.9054 (6)	0.05 (1)	H72	0.0087 (3)	0.3870 (4)	0.3644 (7)	0.06 (2)
H63	0.7257 (3)	0.3778 (4)	1.0137 (6)	0.05 (1)	H73	−0.1874 (3)	0.3647 (4)	0.2622 (7)	0.06 (2)
H65	0.7701 (3)	0.2989 (4)	0.5752 (6)	0.05 (1)	H75	−0.1364 (3)	0.0939 (4)	0.3573 (7)	0.06 (2)
H66	0.5746 (3)	0.2754 (4)	0.4669 (6)	0.05 (1)	H76	0.0598 (3)	0.1161 (4)	0.4594 (7)	0.06 (2)

While the present data give no proof for the actual presence of a ring current, they can be consistently interpreted by its existence. Thus in the corresponding pairs **1a/2a**, **1b/2b**, and **3a/4a** the "outside" groups (^{13}CO, $^{31}P(OMe)_3$) show opposite shift effects as the "inside" groups ($^1H(R)$, ^{31}PR). In each case there is a downfield shift for the "outside" groups in the unsaturated clusters which for the ^{13}CO resonances is of the same order of magnitude as the ^{13}C shift for the methyl groups between toluene and methylcyclohexane. Even the NMR data for the distant groups show the expected effects, although on a smaller scale, cf. the ^{13}C data for the phenyl groups in **1b/2b**, the ^1H data for the tolyl CH_3 groups in **3b/4b**, the ^1H data for the $P(OMe)_3$ ligands in **3a/4a** and **3b/4b** and for the *t*-BuNC ligands in **3c/4c** and **5c/6c**. This anisotropy and the "ring current" effect may be related to the possible absence of a localized Fe–Fe double bond and to the fact that the tetrairon ring is planar in the unsaturated clusters and puckered in the saturated clusters. It should be borne in mind, however, that chemical shift anisotropies (though not as large as here) can simply be the result of a change in cluster geometry and that the ring current interpretation remains a hypothesis until further evidence is obtained.

As previously observed for the ^1H NMR spectra of $Fe_4(CO)_{11/12}(PCH_3)_2$,[7] there is evidence for strong P–P coupling. The ^{13}C NMR resonances of all compounds measured here show deceptively simple triplets for the aromatic carbon atoms (C-1, C_{ortho}, C_{para}). Although because of that it is not possible to obtain the values of $^nJ_{P-C}$ and $^{n+2}J_{P-C}$ (n = 1–3), it demonstrates that the ^{31}P nuclei are strongly coupled. A similar situation is often observed in trans-substituted mononuclear complexes, but in our case it has probably to be related also to the close proximity of the two phosphorus atoms as shown from the X-ray results.

Molecular Structures of 3b and 4b. Views of the compounds with hydrogen atoms omitted for clarity are given in Figures 1 and 2. Selected distances and angles are listed in Table VII. Both clusters which are representatives of the saturated and unsaturated class have distorted octahedral heavy-atom frameworks containing Fe_4 rings. Besides this they have in common a similar bonding situation around the phosphorus atoms including a rather short P–P contact, a similar range of Fe–P bond distances, the out-of-plane location of the $P(OMe)_3$ ligand, and a similar disposition of substituents about the phos-

Table IV. Atomic Parameters for $Fe_4(CO)_{10}[P(OMe)_3](PTol)_2$ (4b)

atom	x	y	z	U(11)	U(22)	U(33)	U(12)	U(13)	U(23)	U(eq), Å²
Fe1	0.2461 (2)	0.0136 (1)	0.1763 (1)	0.034 (1)	0.038 (1)	0.034 (1)	−0.002 (1)	0.002 (1)	0.001 (1)	0.035 (1)
Fe2	0.2524 (2)	0.1996 (1)	0.1842 (1)	0.032 (1)	0.036 (1)	0.033 (1)	0.000 (1)	0.001 (1)	0.003 (1)	0.033 (1)
Fe3	0.3137 (2)	0.0127 (2)	0.3134 (1)	0.036 (1)	0.044 (1)	0.038 (1)	0.000 (1)	0.000 (1)	0.009 (1)	0.039 (1)
Fe4	0.3168 (2)	0.1786 (2)	0.3226 (1)	0.043 (1)	0.045 (1)	0.035 (1)	−0.003 (1)	−0.003 (1)	−0.003 (1)	0.041 (1)
C11	0.311 (2)	0.002 (1)	0.088 (1)	0.05 (1)	0.05 (1)	0.05 (1)	0.00 (1)	−0.01 (1)	−0.01 (1)	0.05 (1)
O11	0.353 (1)	−0.006 (1)	0.0357 (7)	0.057 (9)	0.14 (1)	0.043 (8)	0.00 (1)	0.023 (7)	−0.017 (9)	0.08 (1)
C12	0.120 (2)	−0.019 (1)	0.1370 (9)	0.06 (1)	0.05 (1)	0.04 (1)	0.00 (1)	0.04 (1)	−0.004 (9)	0.05 (1)
O12	0.043 (1)	−0.042 (1)	0.1150 (8)	0.031 (7)	0.10 (1)	0.08 (1)	−0.022 (8)	−0.001 (7)	−0.009 (8)	0.07 (1)
C13	0.274 (1)	−0.099 (1)	0.208 (1)	0.05 (1)	0.06 (1)	0.06 (1)	−0.02 (1)	0.005 (9)	0.02 (1)	0.06 (1)
O13	0.284 (1)	−0.1743 (9)	0.2178 (7)	0.11 (1)	0.046 (8)	0.062 (9)	0.008 (9)	−0.001 (9)	0.010 (7)	0.07 (1)
C21	0.319 (1)	0.222 (1)	0.102 (1)	0.025 (9)	0.06 (1)	0.05 (1)	0.007 (9)	0.01 (1)	0.012 (9)	0.05 (1)
O21	0.366 (1)	0.237 (1)	0.0497 (7)	0.058 (9)	0.11 (1)	0.063 (9)	0.011 (9)	0.018 (8)	0.036 (9)	0.08 (1)
C23	0.275 (1)	0.309 (1)	0.2217 (9)	0.03 (1)	0.06 (1)	0.04 (1)	0.00 (1)	0.003 (9)	0.02 (1)	0.05 (1)
O23	0.286 (1)	0.3823 (8)	0.2366 (7)	0.09 (1)	0.037 (8)	0.076 (9)	−0.013 (8)	−0.016 (8)	−0.003 (7)	0.067 (9)
C31	0.432 (2)	−0.053 (1)	0.328 (1)	0.06 (1)	0.05 (1)	0.04 (1)	0.00 (1)	0.01 (1)	0.01 (1)	0.05 (1)
O31	0.503 (1)	−0.091 (1)	0.3377 (9)	0.050 (8)	0.11 (1)	0.10 (1)	0.03 (1)	0.005 (8)	0.03 (1)	0.09 (1)
C32	0.239 (2)	−0.066 (1)	0.366 (1)	0.06 (1)	0.05 (1)	0.04 (1)	0.01 (1)	−0.01 (1)	0.008 (9)	0.05 (1)
O32	0.193 (1)	−0.118 (1)	0.3979 (8)	0.07 (1)	0.07 (1)	0.08 (1)	−0.007 (9)	0.009 (9)	0.019 (8)	0.07 (1)
C41	0.433 (2)	0.242 (1)	0.344 (1)	0.06 (1)	0.06 (1)	0.04 (1)	−0.01 (1)	−0.01 (1)	0.00 (1)	0.06 (1)
O41	0.502 (1)	0.283 (1)	0.359 (1)	0.055 (9)	0.11 (1)	0.13 (1)	−0.04 (1)	−0.028 (9)	−0.02 (1)	0.10 (1)
C42	0.241 (2)	0.257 (1)	0.380 (1)	0.08 (2)	0.06 (1)	0.06 (1)	−0.02 (1)	−0.04 (1)	0.01 (1)	0.07 (1)
O42	0.196 (1)	0.306 (1)	0.4135 (9)	0.11 (1)	0.09 (1)	0.09 (1)	0.01 (1)	0.04 (1)	−0.06 (1)	0.10 (1)
C34	0.343 (1)	0.089 (1)	0.3980 (9)	0.04 (1)	0.06 (1)	0.05 (1)	0.00 (1)	−0.001 (9)	0.00 (1)	0.05 (1)
O34	0.366 (1)	0.085 (1)	0.4604 (7)	0.14 (1)	0.08 (1)	0.050 (8)	−0.02 (1)	−0.031 (9)	0.013 (8)	0.09 (1)
P1	0.1804 (3)	0.1035 (3)	0.2657 (2)	0.034 (2)	0.041 (2)	0.034 (2)	−0.005 (3)	0.003 (2)	0.000 (2)	0.036 (2)
P2	0.3749 (3)	0.1021 (3)	0.2194 (2)	0.030 (2)	0.042 (2)	0.040 (2)	0.000 (2)	0.002 (2)	0.008 (2)	0.037 (2)
P3	0.1087 (3)	0.2434 (3)	0.1333 (2)	0.035 (2)	0.038 (2)	0.038 (2)	−0.01 (2)	0.003 (2)	0.001 (2)	0.037 (2)
O51	0.0093 (7)	0.2665 (7)	0.1828 (6)	0.036 (6)	0.057 (7)	0.056 (7)	0.007 (5)	0.007 (6)	0.006 (7)	0.050 (6)
O52	0.1305 (8)	0.3310 (7)	0.0863 (6)	0.043 (7)	0.045 (7)	0.064 (7)	0.002 (6)	−0.001 (6)	0.015 (6)	0.051 (7)
O53	0.0483 (9)	0.1770 (8)	0.0799 (6)	0.043 (7)	0.067 (8)	0.042 (7)	0.005 (7)	−0.003 (6)	−0.002 (6)	0.051 (7)
C67	−0.255 (2)	0.105 (2)	0.402 (1)	0.05 (1)	0.24 (3)	0.11 (2)	0.01 (2)	0.05 (1)	0.04 (2)	0.13 (2)
C77	0.807 (1)	0.086 (2)	0.081 (1)	0.04 (1)	0.13 (2)	0.09 (1)	0.01 (1)	0.02 (1)	0.02 (2)	0.08 (1)
C51	0.013 (2)	0.327 (1)	0.244 (1)	0.08 (2)	0.07 (1)	0.05 (1)	0.02 (1)	0.01 (1)	−0.03 (1)	0.07 (1)
C52	0.049 (1)	0.378 (1)	0.0463 (9)	0.033 (9)	0.07 (1)	0.07 (1)	0.013 (9)	−0.017 (9)	0.03 (1)	0.06 (1)
C53	0.089 (2)	0.148 (1)	0.0102 (9)	0.08 (1)	0.09 (1)	0.04 (1)	0.02 (1)	0.00 (1)	−0.01 (1)	0.07 (1)

atom	x	y	z	U(11) or U(eq), Å²	atom	x	y	z	U(11) or U(eq), Å²
C61	0.0516 (6)	0.1004 (8)	0.3060 (5)	0.044 (4)	C71	0.5056 (6)	0.0974 (7)	0.1849 (5)	0.036 (3)
C62	0.0397 (6)	0.1166 (8)	0.3811 (5)	0.052 (5)	C72	0.5645 (6)	0.1761 (7)	0.1781 (5)	0.052 (4)
C63	−0.0592 (6)	0.1186 (8)	0.4121 (5)	0.072 (6)	C73	0.6628 (6)	0.1725 (7)	0.1461 (5)	0.053 (5)
C64	−0.1463 (6)	0.1044 (8)	0.3681 (5)	0.071 (5)	C74	0.7021 (6)	0.0903 (7)	0.1209 (5)	0.048 (4)
C65	−0.1345 (6)	0.0882 (8)	0.2930 (5)	0.066 (5)	C75	0.6431 (6)	0.0116 (7)	0.1277 (5)	0.053 (5)
C66	−0.0355 (6)	0.0862 (8)	0.2620 (5)	0.047 (4)	C76	0.5449 (6)	0.0152 (7)	0.1597 (5)	0.044 (4)
H62	0.1071 (6)	0.1276 (8)	0.4152 (5)	0.14 (4)	H72	0.5341 (6)	0.2398 (7)	0.1976 (5)	0.05 (2)
H63	−0.0684 (6)	0.1312 (8)	0.4702 (5)	0.14 (4)	H73	0.7085 (6)	0.2334 (7)	0.1409 (5)	0.05 (2)
H65	−0.2019 (6)	0.0772 (8)	0.2590 (5)	0.14 (4)	H75	0.6736 (6)	−0.0521 (7)	0.1082 (5)	0.05 (2)
H66	−0.0263 (6)	0.0736 (8)	0.2039 (5)	0.14 (4)	H76	0.4992 (6)	−0.0458 (7)	0.1649 (5)	0.05 (2)

phorus atoms. The 12 terminal ligands in **3b** and the 10 terminal plus one bridging ligands in **4b** give each iron atom a coordination number of 3 on the outside of the Fe_4P_2 octahedron. The difference between **3b** and **4b** can therefore be discussed with respect to the central Fe_4 core only.

There exist some analogues for the unsaturated cluster **4b** in the literature, viz., $Ru_4(CO)_{11}(PPh)_2$,[13] $Fe_4(CO)_{11}(NR)(ONR)$,[14] and $Fe_4(CO)_{11}(R_2C_2)_2$,[15] which are unsaturated as well as containing one CO bridge. The closest similarity exists between **4b** and the parent **1b**[7] with almost all comparable molecular parameters being similar within standard deviation limits and both molecules having one bridging and two semibridging CO ligands in the tetrairon plane. The Fe_4 ring planarity is close to ideal, all iron atoms in **4b** being within 2 pm of the common least-squares plane. Considering also the not too wide spread of Fe–Fe distances in **4b** (245–275 pm) the possibility for a ring current is given. The structural data do not allow a firm conclusion as to whether or not a Fe–Fe double bond exists in **1b** or **4b**. CO-bridged metal–metal bonds are in general shorter than unbridged ones, and this holds for saturated clusters with a similar geometry like $Fe_2Co_2(CO)_{11}(PPh)_2$[7] or $Co_4(CO)_{10}(PPh)_2$[16] where the maximum differences between bridged and unbridged metal–metal bonds are 21[7] and 18[16] pm and where the CO-bridged single bonds (251[7] and 252[16] pm) are not significantly longer than the "double bond" in **1b** (244 pm) or **4b** (246 pm). Since the geometry of the saturated cluster $Co_4(CO)_{11}(GeMe)_2$[17] is also very similar to that of **1b** or **4b**, we assume that the number of the ligands and the size of the Fe_4P_2 core are best adjusted to one another by the ligand arrangement found in all $M_4(CO)_{11}(\mu_4\text{-}L)_2$ clusters which in turn means that the unsaturation of **1b** or **4b** is not located in the CO-bridged Fe–Fe bonds. In this context it is worth mentioning that electron counting according to *Wade's* rules[18] which does not refer to bond orders gives the correct

(13) Field, J. S.; Haines, R. J.; Smit, D. N. *J. Organomet. Chem.* **1982**, *224*, C 49.
(14) Gervasio, G.; Rossetti, R.; Stanghellini, P. L. *J. Chem. Res., Synop.* **1979**, 334; *J. Chem. Res.*, Minip 3943.
(15) Sappa, E.; Tripicchio, A.; Tripicchio-Camellini, M. *J. Chem. Soc., Dalton Trans.* **1978**, 419.
(16) Ryan, R. C.; Pittman, C. U.; O'Connor, J. P.; Dahl, L. F. *J. Organomet. Chem.* **1980**, *193*, 247.
(17) Foster, S. P.; Mackay, K. M.; Nicholson, B. K. *J. Chem. Soc., Chem. Commun.* **1982**, 1156.
(18) Wade, K. *Adv. Inorg. Chem. Radiochem.* **1976**, *18*, 1.

Table V. IR and ^1H NMR Spectra of New Compounds

no.	ν(CO), cm^{-1}				δ(PR)	δ/J(L), Hz
3a	2060 m	2024 vs	2015 s	1991 s	7.67 (m, 6 H), 8.40 (m, 4 H)	3.50/11.1 (9 H)
3b	2060 w	2038 sh	2024 vs	2016 s	7.37 (m, 4 H), 8.17 (m, 4 H)	3.48/11.0 (9 H)
	1988 s	1980 sh	1955 w	1934 w	2.47 (s, 6 H)	
3c[a]	2055 w	2023 vs	2013 s	1993 m	7.78 (m, 6 H), 8.45 (m, 4 H)	1.20 (s, 9 H)
	1986 s	1973 w	1956 m			
4a	2062 m	2017 vs	1995 w	1979 w	7.18 (m, 6 H), 6.76 (m, 4 H)	3.66/11.1 (9 H)
	1968 sh	1952 w	1825 w			
4b	2050 w	2012 vs	1983 sh	1979 s	6.60 (m, 8 H)	3.57/11.0 (9 H)
	1968 sh	1823 w			2.15 (s, 6 H)	
4c[a]	2055 w	2025 sh	2019 vs	1991 s	7.21 (m, 6 H), 6.75 (m, 4 H)	1.23 (s, 9 H)
	1988 s	1947 s	1825 w			
5c[a]	2040 m	2022 m	2010 vs	1993 sh	7.70 (m, 6 H), 8.53 (m, 4 H)	1.16 (s, 18 H)
	1990 s	1982 s	1973 s	1941 m		
6a	2036 w	2018 sh	1998 vs	1979 s	7.10 (m, 10 H)	A 3.56/11.2 (18 H)[b]
	1969 s	1955 sh	1815 w	1790 w		B 3.50/11.2
6b	2038 w	2018 sh	2000 vs	1978 m	6.75 (m, 8 H)	A 3.53/11.0 (18 H)[b]
	1968 m	1812 w	1788 w		2.15 (s, 6 H)	B 3.48/11.0
6c[a]	2030 m	2001 vs	1995 vs	1982 s	7.13 (m, 6 H), 6.75 (m, 4 H)	1.25 (s, 18 H)
	1969 s	1961 s	1928 w	1808 w		
6d[a]	2030 m	2001 vs	1998 vs	1978 s	7.13 (m, 10 H)	3.61/11.6 (9 H)
	1965 s	1955 sh	1810 w			1.21 (s, 9 H)
7a	2033 m	1999 vs	1980 sh	1971 vs	7.03 (m, 10 H)	3.55/11.6 (9 H)
	1955 sh	1918 sh	1814 w	1788 w		3.50/11.2 (18 H)
7c[a]	2010 sh	2001 s	1995 s	1988 s	7.06 (m, 10 H)	1.26 s (27 H)[b]
	1978 s	1959 vs	1800 w			1.21 s
7d[a]	2035 sh	2015 s	2005 s	1988 s	6.96 (m, 10 H)	A 1.26 (s, 9 H), 3.54/11.6 (18 H)[b]
	1975 vs	1953 vs	1802 w	1780 w		B 1.16 3.47/11.6
8a	2010 m	1981 vs	1953 s	1938 s	6.96 (m, 10 H)	3.47/10.8 (36 H)
	1931 sh	1871 w	1778 w			

[a] ν(CN) absorptions (cm^{-1}): **3c**, 2141 w; **4c**, 2150 w; **5c**, 2130 m; **6c**, 2130 w; **6d**, 2142 w; **7c**, 2130 s; **7d**, 2135 m. [b] Intensity ratio see text.

Table VI. Room-Temperature ^{31}P and ^{13}C NMR Data

	$\delta(^{31}P)$ vs. H_3PO_4		$\delta(^{13}C)$ vs. Me_4Si	
no.	μ_4-PR	P(OMe)	CO	μ_4-PR
1a	320.9		215.9	*b*
1b	242.6		214.6	128–132
2a	445.8		210.9	*b*
2b	350.6		209.9	129–136
3a	340.0	158.9	211.5 (br)	128–137
4a	230.1	163.1	218.0 (d, J = 6.1 Hz)	128–133
6a[a] A	224.1	164.0	221.6 (t, J = 6.1 Hz)	
B	230.9	161.0	222.7 (t, J = 6.1 Hz)	127–135
7a	225.1 (2 P)	163.0 (2 P)	226.9 (q, J = 5.7 Hz)	126–136
		162.3 (1 P)		
8a	*b*	*b*	227.2 (quintet, J = 6.0 Hz)	*b*

[a] Intensity ratios see text. [b] Not measured.

count of seven skeletal electron pairs for a closo octahedral structure for all unsaturated Fe_4P_2 clusters described here.

The molecules of the saturated cluster **3b** differ from those of **4b** mainly in the puckering of the Fe_4 ring and the orientation of the terminal ligands: there is a folding angle of 163° along the Fe1–Fe4 line which means an average distance of 14 pm of all iron atoms from the common least-squares plane, and the iron atoms alternatively have one ligand above and two ligands below the tetrametal plane and vice versa. We think the reason for this is steric strain between the 12 terminal ligands which cannot be accommodated as in **4b**. The resulting distortion also makes the four Fe–P bonds of each RP group significantly different, but it does not cause a wide spread of the Fe–Fe bond lengths (267–271 pm). The average Fe–Fe bond length for **3b** (268 pm) is slightly longer than for **4b** (263 pm) as expected due to the higher number of ligands and skeletal electrons. Clusters with $E_2M_4(CO)_{12}$ compositions like **3b** have not been reported yet, but the interlocking of alternatively oriented $M(CO)_3$ units in clusters with ligand crowding is not uncommon; e.g., selected $[Ru(CO)_3]_4$ rings in $Ru_6C(CO)_{17}$[19] resemble the $[FeL_3]_4$ ring in **3b**. It is not unlikely that due to the steric strain clusters **2** or **3**, although having the "better" electron count, are not

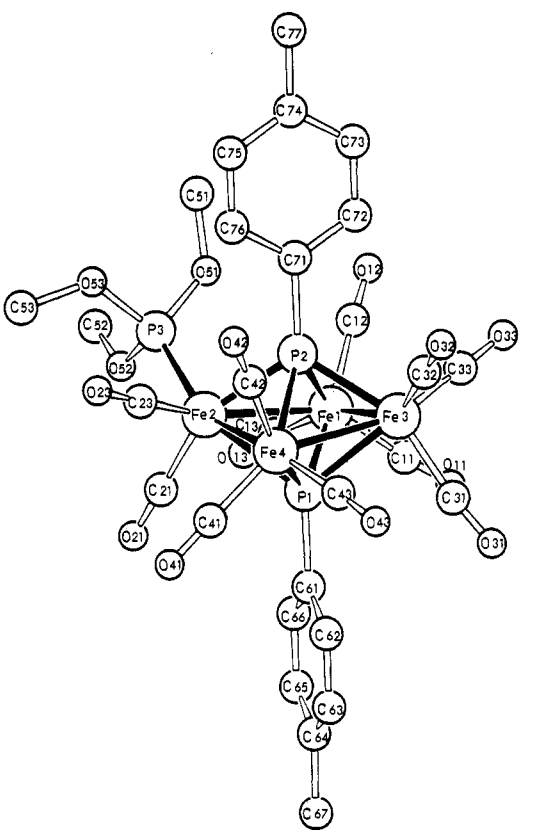

Figure 1. Molecular structure of $Fe_4(CO)_{11}[P(OMe)_3](PTol)_2$ (**3b**).

(19) Sirigu, A.; Bianchi, M.; Benedetti, E. *J. Chem. Soc., Chem. Commun.* **1969**, 596.

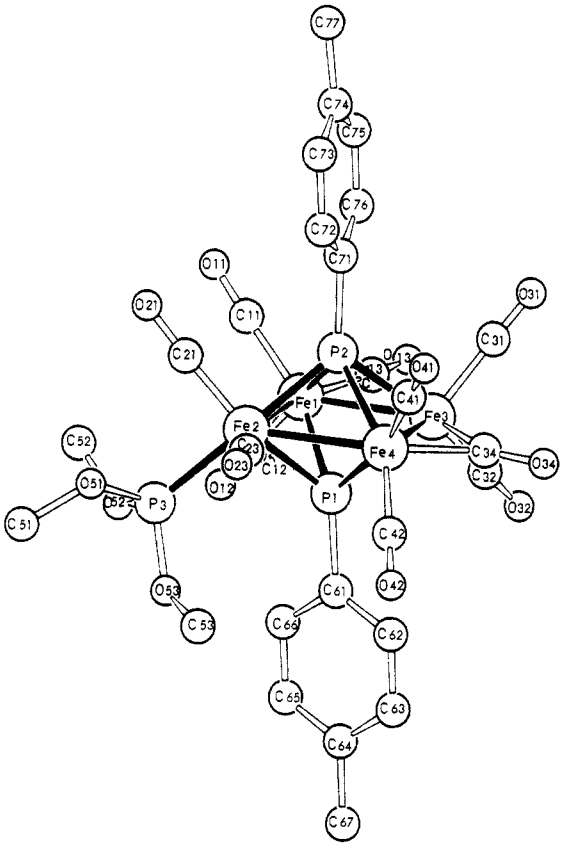

Figure 2. Molecular structure of $Fe_4(CO)_{10}[P(OMe)_3](PTol)_2$ (**4b**).

Table VII. Important Bond Lengths (pm) and Angles (deg) in 3b and 4b

	3b	4b
Fe1–Fe2	271.0 (2)	275.5 (3)
Fe1–Fe3	266.6 (2)	264.2 (3)
Fe2–Fe4	268.7 (2)	267.1 (3)
Fe3–Fe4	266.8 (2)	245.8 (3)
Fe1–P1	221.5 (2)	226.4 (5)
Fe2–P1	235.1 (2)	225.6 (5)
Fe3–P1	237.7 (2)	234.6 (5)
Fe4–P1	221.5 (3)	232.3 (5)
Fe1–P2	235.5 (2)	225.3 (5)
Fe2–P2	219.7 (2)	223.2 (5)
Fe3–P2	223.4 (2)	230.1 (5)
Fe4–P2	240.6 (2)	231.9 (5)
P1···P2	259.8 (3)	264.6 (8)
Fe–C_{term}	175–184 (1)	175–184 (2)
C_{term}–O_{term}	111–116 (1)	110–116 (2)
Fe2–P3	218.4 (2)	217.0 (5)
P1–Fe–P2	68.3–69.6 (1)	69.4–72.2 (2)
Fe1–P1–Fe4	117.2 (1)	108.5 (2)
Fe2–P1–Fe3	105.5 (1)	107.6 (2)
Fe1–P2–Fe4	105.2 (1)	109.1 (2)
Fe2–P2–Fe3	116.4 (1)	110.0 (2)
Fe–C_{term}–O_{term}	174–180 (1)	177–178 (2)
Fe1–C13–O13	175 (1)	168 (2)
Fe2–C23–O23	178 (1)	171 (2)

more stable than the unsaturated clusters **1** or **4**.

Conclusions

The improved synthesis of the starting cluster $Fe_4(CO)_{11}(PPh)_2$ (**1b**) has allowed a full series of ligand additions to this unsaturated system followed by increasingly facile CO eliminations. Saturated clusters $Fe_4(CO)_{11}L(PR)_2$ with L = $P(OMe)_3$ and *t*-BuNC and $Fe_4(CO)_{10}(t\text{-BuNC}))_2(PPh)_2$ were obtained whereas up to four $P(OMe)_3$ ligands and up to three *t*-BuNC ligands could be introduced to form the unsaturated clusters $Fe_4(CO)_{7+n}L_{4-n}$ with n = 0–3. Both types of clusters can be considered to have correct electron counts, the unsaturated ones according to Wade's rules, the saturated ones according to the 18-electron rule. They are both of comparable stability since the closed-shell electronic configuration is in favor of the saturated ones while the strain-free ligand arrangement is in favor of the unsaturated ones. This explains the easy interconversions between the Fe_4L_{11} and Fe_4L_{12} situations in the predominantly CO-substituted representatives **1–4**. As the number of donor ligands ($P(OMe)_3$ or *t*-BuNC) exceeds two the steric crowding seems to pass a critical limit causing only the unsaturated compounds to be stable in the series **6–8**.

Combined crystallographic and NMR spectroscopic investigations have not given an unambiguous answer to the question whether the unsaturation in $Fe_4(CO)_{11}(PR)_2$ and its derivatives is localized in a Fe–Fe double bond or delocalized over the tetrairon ring. The shortest Fe–Fe bond is CO bridged and not significantly shorter than comparable CO-bridged single bonds. The overall shrinkage of the Fe_4 core of the unsaturated clusters relative to the saturated ones is small. All clusters are highly fluxional down to temperatures below −100 °C. This reduces the number of observable isomers to one in most cases and to two in the compounds with two $P(OMe)_3$ ligands. Semibridging CO ligands adjacent to the bridging CO in the unsaturated clusters allow to visualize an easy pathway for CO migration. A fast movement of the bridging CO also implies a fast movement of the possible Fe–Fe double bond, and it is likely that ligand movement in the saturated clusters is accompanied by a "breathing" of the puckered tetrairon ring. Indications of the delocalized nature of the unsaturated clusters come from their NMR anisotropy. For all chemical shifts measured (^1H, ^{31}P, ^{13}C) the comparison between the corresponding saturated and unsaturated clusters is in accord with a ring current effect in the unsaturated compounds which can be called Hückel 2π systems. Since no theoretical treatment of such compounds has been done yet, the ring current phenomenon cannot be more than a working hypothesis at the moment.

Future developments with these types of compounds should bring about a better understanding of their bonding and some use of their reactivity. Our own contribution is planned to be in the application of more organic ligands and in the synthesis and investigation of corresponding Fe/Ru mixed-metal systems.

Acknowledgment. This work was supported by the Fonds der Chemischen Industrie and by the Rechenzentrum der Universität Freiburg. We thank Dr. K. Steinbach, University of Marburg, for mass spectra and Mrs. D. Wolters for technical assistance.

Registry No. **1a**, 81534-72-7; **1b**, 81534-73-8; **1c**, 81534-74-9; **2a**, 81478-18-4; **2b**, 81191-38-0; **2c**, 81447-26-9; **3a**, 81478-20-8; **3b**, 81478-19-5; **3c**, 99376-28-0; **4a**, 99376-29-1; **4b**, 81534-75-0; **4c**, 99376-30-4; **5c**, 99376-31-5; **6a** (isomer A), 99397-54-3; **6a** (isomer B), 99376-37-1; **6b** (isomer A), 99397-55-4; **6b** (isomer B), 99397-57-6; **6c**, 99376-32-6; **6d**, 99376-33-7; **7a**, 99397-56-5; **7c**, 99376-34-8; **7d**, 99376-35-9; **8a**, 99376-36-0; $Fe_2(CO)_6(PHPh)_2$, 39049-79-1; $Fe_3(CO)_{12}$, 17685-52-8.

Arylation of Enolate Anions with (η^6-Chlorobenzene)(η^5-cyclopentadienyl)iron(II) Hexafluorophosphate

Robert M. Moriarty* and Udai S. Gill

Department of Chemistry, University of Illinois at Chicago, Chicago, Illinois 60680

Received June 4, 1985

(η^6-Chlorobenzene)(η^5-cyclopentadienyl)iron(II) hexafluorophosphate undergoes nucleophilic displacement with enolate anions generated (K_2CO_3/DMF) from diethyl malonate, 2,4-pentanedione, dimedone, ethyl acetoacetate, benzoylacetone, (phenylsulfonyl)acetone, ethyl (phenylsulfonyl)acetate, and deoxybenzoin. The resulting product is the substituted (η^6-benzene)(η^5-cyclopentadienyl)iron(II) hexafluorophosphate. In the case of benzoylacetone deacylation occurs to yield the (η^5-cyclopentadienyl)iron(II) hexafluorophosphate of the deoxybenzoin. This pathway was demonstrated for the reaction of benzoylacetone with other (η^6-arene halide)(η^5-cyclopentadienyl)iron(II) hexafluorophosphates. Similarly, the reaction of 2,4-pentanedione and ethyl acetoacetate enolate anions with (η^6-*o*-dichlorobenzene)(η^5-cyclopentadienyl)iron(II) hexafluorophosphate gives directly the corresponding monocarbonyl complexes. The compounds prepared in this study were $C_6H_5CH(CO_2C_2H_5)_2FeCp^+PF_6^-$, $C_6H_5CH(COCH_3)_2FeCp^+PF_6^-$, C_6H_5(dimedonyl)$FeCp^+PF_6^-$, $C_6H_5CH(COCH_3)CO_2C_2H_5FeCp^+PF_6^-$, $C_6H_5CH(SO_2C_6H_5)COCH_3FeCp^+PF_6^-$, $C_6H_5CH(SO_2C_6H_5)CO_2C_2H_5FeCp^+PF_6^-$, $C_6H_5CH(COC_6H_5)C_6H_5FeCp^+PF_6^-$, $C_6H_5CH_2COC_6H_5FeCp^+PF_6^-$, *p*-$ClC_6H_4CH_2COC_6H_5FeCp^+PF_6^-$, *p*-$CH_3C_6H_4CH_2COC_6H_5FeCp^+PF_6^-$, *m*-$ClC_6H_4CH_2COC_6H_5FeCp^+PF_6^-$, *o*-$ClC_6H_4CH_2COCH_3FeCp^+PF_6^-$, *o*-$ClC_6H_4CH_2COC_6H_5FeCp^+PF_6^-$, and *o*-$ClC_6H_4CH_2CO_2C_2H_5FeCp^+PF_6^-$.

The arylation of β-dicarbonyl compounds is an important synthetic goal in organic chemistry. Recently two useful solutions to this problem have been provided. The first achieves α-arylation by means of reaction of an aryllead triacetate with a 1,3-dicarbonyl compound,[1] and the second uses either triphenylbismuth carbonate[2] or pentaphenylbismuth[3] to effect arylation. An earlier method used the reaction of enolate anions of β-dicarbonyl compounds with diaryliodonium salts.[4]

Our approach, reported herein, is based upon activation of aryl halides toward nucleophilic displacement by complexation with cyclopentadienyliron(II) ($CpFe^+$).

Activation toward S_NAr substitution of normally unreactive arene halides by complexation to a metal is well recognized for $Cr(CO)_3$, $Mn(CO)_3^+$, $(\eta^5\text{-}C_5H_5)Ru^+$ and $(\eta^5\text{-}C_5H_5)Fe^+$.[5-18] From a synthetic viewpoint formation of a C–C bond, i.e., via displacement of halide by a carbanion, is perhaps the most interesting variant of this process. Only in the case of tricarbonylchromium arene halides has this reaction become an important part of

Scheme I

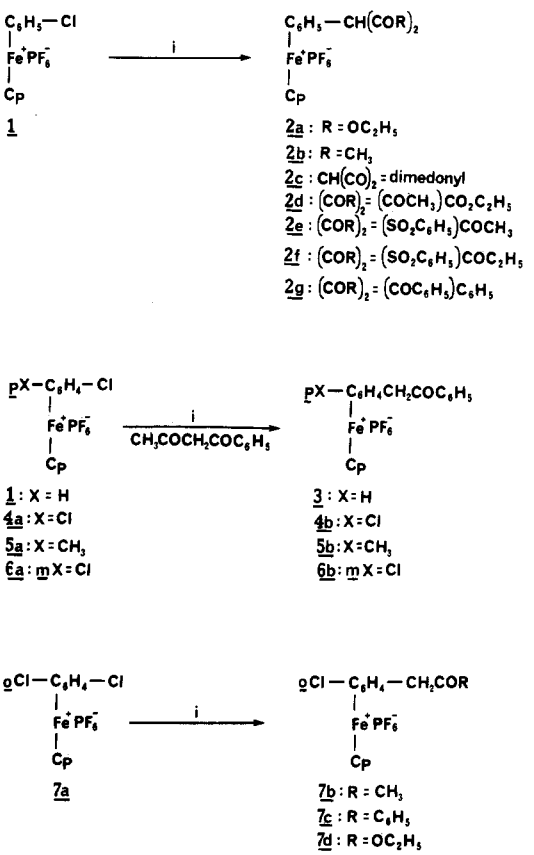

(1) Pinhey, J. T.; Rowe, B. A. *Aust. J. Chem.* **1979**, *32*, 1561; **1980**, *32*, 113. Pinhey, J. T.; Rowe, B. A. *Tetrahedron Lett.* **1980**, 965.
(2) Barton, D. H. R.; Lester, D. J.; Motherwell, W. B.; Barros Papoula, M. T. *J. Chem. Soc., Chem. Commun.* **1980**, 246.
(3) Barton, D. H. R.; Blazejewski, J. C.; Charpiot, B.; Lester, D. J.; Motherwell, W. B.; Barros Papoula, M. T. *J. Chem. Soc., Chem. Commun.* **1980**, 827.
(4) Beringer, F. M.; Forgione, P. S. *J. Org. Chem.* **1963**, *28*, 714 and references cited therein.
(5) Nicholls, B.; Whiting, M. C. *J. Org. Chem.* **1959**, *24*, 551.
(6) Semmelhack, M. F.; Hall, H. T. *J. Am. Chem. Soc.* **1974**, *96*, 7091.
(7) Semmelhack, M. F.; Clark, G. R.; Garcia, J. L.; Harrison, J. J.; Thebtararonth, Y.; Wulff, W.; Yamashita, A. *Tetrahedron* **1981**, *37*, 3959.
(8) Mahaffy, C. A. L.; Pauson, P. L. *J. Chem. Res., Synap.* **1979**, 128; *J. Chem. Res., Miniprint* **1979**, 1776.
(9) Pauson, P. L.; Segal, J. A. *J. Chem. Soc., Dalton. Trans.* **1975**, 1677.
(10) Bhasin, K. K.; Balkeen, W. G.; Pauson, P. L. *J. Organomet. Chem.* **1981**, *204*, C25.
(11) Nesmeyanov, A. N.; Vol'kenau, N. A.; Bolesova, I. N.; Shulpina, L. S. *Dokl. Acad. Nauk SSSR* **1980**, *254*, 1408.
(12) Nesmeyanov, A. N.; Vol'kenau, N. A.; Bolesova, I. N. *Dokl. Acad. Nauk SSSR* **1967**, *175*, 606.
(13) Nesmeyanov, A. N.; Vol'kenau, N. A.; Isaeva, I. S.; Bolesova, I. N. *Dokl. Acad. Nauk SSSR* **1968**, *183*, 834.
(14) Helling, J. F.; Hendrickson, W. A. *J. Organomet. Chem.* **1979**, *168*, 87.
(15) Lee, C. C.; Gill, U. S.; Igbal, M.; Azogu, C. I.; Sutherland, R. G. *J. Organomet. Chem.* **1982**, *231*, 151.
(16) Lee, C. C.; Azogu, C. I.; Chang, P. C.; Sutherland, R. G. *J. Organomet. Chem.* **1981**, *220*, 181.
(17) The order of reactivity of these organometallic arylhalide complexes for S_NAr substitution with methoxide in methanol is $(CO)_3Cr < (CO)_3Mo^+ \ll (Cp)Fe^+ < (CO)_3Mn^+$ (Knipe, A. C.; McGuiness, S. J.; Watts, W. E. *J. Chem. Soc., Perkin Trans. 2* **1981**, 193).
(18) Khand, I. U.; Pauson, P. L.; Watts, W. E. *J. Chem. Soc. C* **1969**, 2024.

0276-7333/86/2305-0253$01.50/0

Scheme II

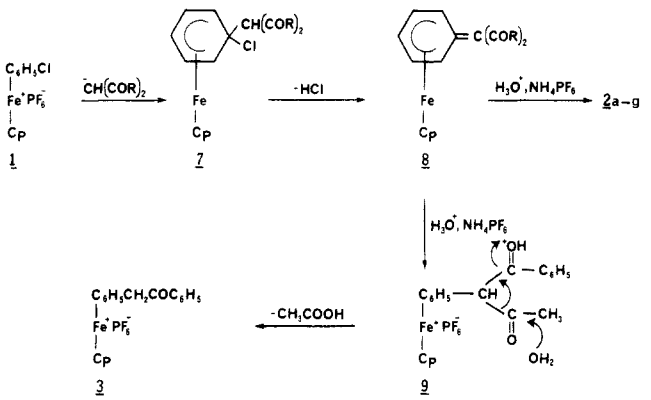

organic synthetic methodology.[5-7]

In the case of $CpFe^+$-complexed arene halides, simple heteroatom anions have been used in displacement reactions.[12,13,14,15,17] However, carbanions have not been employed as the nucleophile in these reactions. We report now the first examples of the use of enolate anions as nucleophiles in S_NAr reactions of (η^6-aryl halide)(η^5-cyclopentadienyl)iron(II) hexafluorophosphates, **1**, **4a**, **5a**, **6a**, and **7a**.

Results and Discussion

(η^6-Aryl halide)(η^5-cyclopentadienyl)iron(II) hexafluorophosphates (aryl halide = chlorobenzene (**1**), *p*-dichlorobenzene (**4a**), *p*-chlorotoluene (**5a**), *m*-dichlorobenzene (**6a**), or *o*-dichlorobenzene (**7a**) were prepared by the $AlCl_3$-catalyzed ligand exchange reaction of ferrocene and the appropriate aryl halide as previously described.[12,18] Hexafluorophosphate salts were isolated in yields of 40–60% in each case.

The active methylene compounds used in this study were diethyl malonate, 2,4-pentanedione, dimedone, ethyl acetoacetate, benzoylacetone, (phenylsulfonyl)acetone, ethyl (phenylsulfonyl)acetate, and deoxybenzoin (Scheme I). The yields of the various complexes **2a-g**, **3**, **4b**, **5b**, **6b**, and **7b-d** average around 70%, and the structures are based upon ^1H NMR, IR, and microanalytical data. The displacement reaction may be interpreted in terms of reversible (IPSO attack) with formation of **7** (Scheme II) followed by irreversible loss of hydrogen chloride to yield the highly conjugated system present in **8** (Scheme II). By contrast,[9,18] methide ion (from methyllithium) or other reactive carbanions[18,19] add irreversibly to the ring exclusively ortho to the chlorine atom to yield the corresponding (η^5-cyclohexadienyl)iron complexes.

Of course other pathways are available for the overall reaction, however, the ipso addition–displacement mechanism has the favorable feature of forming the extended conjugated system present in **8**.

In the case of $CH_3COCH_2COC_6H_5$, reaction with **1** and ring-substituted derivatives **4a**, **5a**, **6a**, and **7a** proceeds with deacylation. This reaction occurs under the same reaction conditions used for examples **1** → **2a–g**. The following pathway is suggested for the overall reactions **1** → **2a–g** as well as the deacylation examples **1** → **3**, **4a** → **4b**, **5a** → **5b**, **6a** → **6b**, and **7a** → **7c** (Scheme II). Deacylation of β-diketones to monoketones under stronger condition (i.e., higher temperatures) is well documented.[20]

Presumably in the present case the $CpFe^+$ unit further facilitates this process. It is interesting to note that in the reaction of (chlorobenzene)$FeCp^+PF_6^-$ (**1**) with enolate anions derived from 2,4-pentanedione and ethyl acetoacetate, the β-dicarbonyl system is preserved, i.e., **2b** and **2d** were obtained.

Reaction of 2,4-pentanedione and ethyl acetoacetate enolate anions with *o*-$ClC_6H_4ClFeCp^+PF_6^-$ (**7a**) under similar workup conditions gave directly the corresponding monocarbonyl complexes **7b** and **7d** derived from deacylation of the corresponding β-dicarbonyl complexes. The ^1H NMR spectrum of **7b**, **7c**, and **7d** complexes showed a typical AB pattern for methylene protons, $J_{AB} \sim 18$–20 Hz, while **3**, **4b**, **5b**, and **6b** complexes show only a single absorption peak for the benzylic methylene group.

Sutherland et al.[21] reported an example of nucleophilic substitution of the chlorine atom in *p*-$CH_3C_6H_4ClFeCp^+PF_6^-$ (**5a**) upon reaction with CpFe(fluorenyl). This example, likewise, fits into the scheme of extended conjugation for the anionic intermediate analogous to **8**, which upon protonation yields the final product.

Of course an important aspect of this overall synthetic utility is release of the desired organic ligand from the organometallic complex. Disengagement of the ligand in arene $FeCp^+$ complexes has been achieved using photolysis or by vacuum sublimation at 160–200 °C.[22,23] As an illustration of yields of the free ligand, in the present method of synthesis, the reaction of **1** with benzoylacetone gave a 65% yield of (η^6-deoxybenzoin)(η^5-cyclopentadienyl)iron hexafluorophosphate (**3**) which upon vacuum sublimation at 200 °C gave a 92% yield of deoxybenzoin. The overall yield of deoxybenzoin is 59% based on cation **1**. Similar vacuum sublimation of complex **7c** gave 92% yield of α-(*o*-chlorophenyl)acetophenone. The overall yield of α-(*o*-chlorophenyl)acetophenone is 74% based upon **7a**. Vacuum sublimation of complex **2c** gave a 53% yield of 5,5-dimethyl-2-phenylcyclohexane-1,3-dione. The overall yield is 44% based on cation **1**. This method of obtaining 5,5-dimethyl-2-phenylcyclohexane-1,3-dione is superior to that involving the reaction between dimedone and diphenyliodonium salt (bromide, chloride, or tosylate) in the presence of a strong base, i.e., sodium *tert*-butoxide (yields 8–22%).[4]

We conclude that reaction of enolate anions with aryl halide $FeCp^+PF_6^-$ complexes offers a useful way of attaching a $CH(COR)_2$ unit or, in cases of deacylation, $CH_2COC_6H_5$, $CH_2CO_2C_2H_5$, or CH_2COCH_3 units to an aromatic ring.

Experimental Section

All reactions were performed under nitrogen. DMF was dried over 4A molecular sieves. Melting points were determined with a Thomas-Hoover capillary melting point apparatus and are uncorrected. IR spectra were recorded on a Unicam SP1000 spectrometer. NMR spectra were recorded on a Varian A-60 or Varian EM-360 spectrometer. Microanalyses were performed by Microtech Labs, Skokie, IL.

(η^6-Arene halide)(η^5-cyclopentadienyl)iron(II) hexafluorophosphates (arene halide = chlorobenzene, *p*-dichlorobenzene, *p*-chlorotoluene, *o*-dichlorobenzene, and *m*-dichlorobenzene) were prepared by using published procedures.[12,18]

Diethyl malonate, 2,4-pentanedione, dimedone, ethyl acetoacetate, benzoylacetone, chloroacetone, ethyl chloroacetate,

(19) Astruc, D.; Hammon, J. R.; Roman, E.; Michaud, P. M. *J. Am. Chem. Soc.* **1981**, *103*, 7502.
(20) Krapcho, A. P. *Synthesis* **1982**, 805.
(21) Sutherland, R. G.; Steele, B. R.; Demchuk, K. J.; Lee, C. C. *J. Organomet. Chem.* **1979**, *181*, 411.
(22) Sutherland, R. G.; Pannekock, W. J.; Lee, C. C. *Can. J. Chem.* **1978**, *56*, 178.
(23) Astruc, D. *Tetrahedron* **1984**, *39* (24), 4027 and references cited therein.

benzenesulfinic acid sodium salt, deoxybenzoin, ferrocene, aluminum chloride, aluminum metal, chlorobenzene, *p*-dichlorobenzene, *p*-chlorotoluene, *o*-dichlorobenzene, and *m*-dichlorobenzene are commercially available (Aldrich).

General Procedure for Nucleophilic Substitution. Synthesis of $C_6H_5CH(CO_2C_2H_5)_2FeCp^+PF_6^-$ (2a) from 1. A mixture of (η^6-chlorobenzene)(η^5-cyclopentadienyl)iron(II) hexafluorophosphate (1) (756 mg, 2.0 mmol), K_2CO_3 (690 mg, 5.0 mmol), diethyl malonate (0.32 mL, 2.1 mmol), and DMF (10 mL) was stirred for 5–6 h at 25 °C under N_2. The red reaction mixture was filtered rapidly into a flask containing 10% HCl (10 mL). The reaction flask was washed with ethanol. The ethanol was removed in vacuo, and to the remaining yellow DMF solution was added 60–80 mL of H_2O containing NH_4PF_6 (326 mg, 2.0 mmol). The resulting yellow solid precipitate was collected, dried, and recrystallized from acetone–ethanol–ether to yield 776 mg (77%) of **2a** as a crystalline yellow solid: ^1H NMR (CD_3COCD_3) δ 6.53 (s, 5 H, aromatic), 5.23 (s, 5 H, Cp), 4.26 (q, 4 H, CH_2, $J \sim 7$ Hz), 1.43 (t, 6 H, CH_3, $J \sim 7$ Hz); IR (cm^{-1}, KBr) 1755 (CO); mp 105–107 °C.

Anal. Calcd for $C_{18}H_{21}O_4FePF_6$: C, 43.05; H, 4.22. Found: C, 43.41; H, 4.20.

Synthesis of $C_6H_5CH(COCH_3)_2FeCp^+PF_6^-$ (2b). The general procedure using 2,4-pentanedione at room temperature (4–5 h) gave a 50% yield of **2b** as a yellow solid after crystallization from acetone–ether: ^1H NMR (CD_3COCD_3) δ 6.56 (s, 5 H, aromatic), 5.13 (s, 5 H, Cp), 2.50 (s, 6 H, CH_3); IR (cm^{-1}, KBr) 1690 (CO); mp 155–162 °C.

Anal. Calcd for $C_{16}H_{17}O_2FePF_6$: C, 43.46; H, 3.87. Found: C, 43.18; H, 3.85.

Synthesis of $C_6H_5\overline{CHCOCH_2C(CH_3)_2CH_2CO}FeCp^+PF_6^-$ (2c). Complex **2c**, a yellow crystalline salt, was prepared in 83% yield after recrystallization from acetone–ether according to the procedure described for **2a** but with dimedone as enolate anion: ^1H NMR (CD_3COCD_3) δ 6.03–6.46 (m, 5 H, aromatic), 4.76 (s, 5 H, Cp), 2.46 (s, 4 H, CH_2), 1.13 (s, 6 H, CH_3); IR (cm^{-1}, Nujol) 1595 (CO); mp 186–191 °C.

Anal. Calcd for $C_{19}H_{21}O_2FePF_6$: C, 47.32; H, 4.39. Found: C, 48.15; H, 4.43.

Synthesis of $C_6H_5CH(COCH_3)CO_2C_2H_5FeCp^+PF_6^-$ (2d). Treatment of 1 with ethyl acetoacetate according to the general procedure gave (80%) of **2d** as a yellow crystalline solid: ^1H NMR (CD_3CN) δ 6.6 (s, 5 H, aromatic), 5.36 (s, 1 H, CH), 5.20 (s, 5 H, Cp), 4.43 (q, 2 H, CH_2, $J \approx 7$ Hz), 2.4 (s, 3 H, CH_3, $J \approx 7$ Hz); IR (cm^{-1}, KBr) 1730 (CO); mp 135–138 °C.

Anal. Calcd for $C_{17}H_{19}O_3FePF_6$: C, 43.24; H, 4.06. Found: C, 43.26; H, 4.20.

Synthesis of $C_6H_5CH(SO_2C_6H_5)COCH_3FeCp^+PF_6^-$ (2e). The reaction of 1-methyl-2-(phenylsulfonyl)ethanone[24] with 1 according to the general procedure for 8–10 h at room temperature gave 50% yield of **2e** as yellow solid after recrystallization from acetone–ether: ^1H NMR δ 7.5–8.0 (m, 5 H, uncomplexed aromatic), 6.33–6.90 (m, 5 H, complexed aromatic), 6.2 (s, 1 H, CH), 5.10 (s, 5 H, Cp), 2.73 (s, 3 H, CH_3); IR (cm^{-1}, KBr) 1720 (CO); mp 138–142 °C.

Anal. Calcd for $C_{20}H_{19}O_3SFePF_6$: C, 44.46; H, 3.54. Found: C, 44.25; H, 3.73.

Synthesis of $C_6H_5CH(SO_2C_6H_5)CO_2C_2H_5FeCp^+PF_6^-$ (2f). The reaction of ethyl (phenylsulfonyl) acetate[25] with 1 was carried out according to the general procedure for 8–10 h. The red reaction mixture was filtered quickly into a flask containing 10% HCl (10 mL). The reaction flask was washed with acetone. A solution of 334 mg (2.0 mmol) of NH_4PF_6 in 10 mL of H_2O was added. The acetone was removed in vacuo, and to the remaining mixture was added 50 ml of H_2O. The resulting yellow solid precipitated was collected, dried, and recrystallized from acetone–ether to yield 80% of **2f** as yellow plates: ^1H NMR (CD_3SOCD_3) δ 7.63–8.03 (m, 5 H, uncomplexed aromatic), 6.50–6.83 (m, 5 H, complexed aromatic), 6.2 (s, 1 H, CH), 5.13 (s, 5 H, Cp), 4.36 (q, 2 H, CH_2, $J \sim 7$ Hz), 1.26 (t, 3 H, CH_3, $J \sim 7$ Hz); IR (cm^{-1}, KBr) 1740 (CO); mp 211–212 °C.

Anal. Calcd for $C_{21}H_{21}O_4SFePF_6$: C, 44.23; H, 3.71. Found: C, 44.15; H, 3.85.

Synthesis of $C_6H_5CH(COC_6H_5)C_6H_5FeCp^+PF_6^-$ (2g). Complex **2g** was prepared as orange-brown crystals in 65% yield using the same procedure as that described for **2a** but with deoxybenzoin as a source of the enolate anion in an overnight reaction: ^1H NMR (CD_3COCD_3) δ 7.86–8.32 (m, 2 H), 7.3–7.86 (m, 8 H, uncomplexed aromatic), 5.9–6.63 (m, 5 H, complexed aromatic), 5.9–6.63 (s, 1 H, CH), 4.83 (s, 5 H, Cp); IR (cm^{-1}, KBr) 1680 (CO); mp 146–147 °C.

Anal. Calcd for $C_{25}H_{21}OFePF_6$: C, 55.78; H, 3.93. Found: C, 55.35; H, 4.09.

Synthesis of $C_6H_5CH_2COC_6H_5FeCp^+PF_6^-$ (3). The general procedure takes 4–5 h with benzoylacetone at room temperature and gave a 65% yield of **3** as yellow crystalline product after recrystallization from acetone–ether: ^1H NMR (CD_3COCD_3) δ 8.0–8.3 (m, 2 H), 7.6–7.86 (m, 3 H, aromatic), 6.3 (s, 5 H, complexed aromatic), 5.1 (s, 5 H, Cp), 4.6 (s, 2 H, CH_2); IR (cm^{-1}, KBr) 1680 (CO); mp 113–114 °C.

Anal. Calcd for $C_{19}H_{17}OFePF_6$: C, 49.37; H, 3.71. Found: C, 49.45; H, 3.81.

Synthesis of *p*-$ClC_6H_4CH_2COC_6H_5FeCp^+PF_6^-$ (4b) from 4a. The reaction between **4a** and benzoylacetone according to the general procedure gave **4b** in 70% yield, as a yellow crystalline solid after crystallization from acetone–ether: ^1H NMR (CD_3COCD_3) δ 8.0–8.33 (m, 2 H), 7.5–7.9 (m, 3 H, uncomplexed aromatic), 6.93 (d, 2 H), 6.63 (d, 2 H, complexed aromatic), 5.4 (s, 5 H, Cp), 4.83 (s, 2 H, CH_2); IR (cm^{-1}, KBr) 1670 (CO); mp 215–216 °C.

Anal. Calcd for $C_{19}H_{16}ClOFePF_6$: C, 45.95; H, 3.25. Found: C, 45.88; H, 3.20.

Synthesis of *p*-$CH_3C_6H_4CH_2COC_6H_5FeCp^+PF_6^-$ (5b) from 5a. Complex **5b** was prepared as a yellow solid in 65% yield using the general procedure from reaction of benzoylacetone upon **5a**: ^1H NMR (CD_3COCD_3) δ 8.0–8.3 (m, 2 H), 7.53–7.83 (m, 3 H, uncomplexed aromatic), 6.43 (s, 4 H, complexed aromatic), 5.2 (s, 5 H, Cp), 4.76 (s, 2 H, CH_2), 2.57 (s, 3 H, CH_3); IR (cm^{-1}, KBr) 1670 (CO); mp 209–210 °C.

Anal. Calcd for $C_{20}H_{19}OFePF_6$: C, 50.44; H, 4.02. Found: C, 50.34; H, 4.07.

Synthesis of *m*-$ClC_6H_4CH_2COC_6H_5FeCp^+PF_6^-$ (6b) from 6a. The reaction between **6a** and benzoylacetone according to general procedure yielded 70% of **6b** as yellow crystalline solid: ^1H NMR (CD_3COCD_3) δ 8.06–8.33 (m, 2 H), 7.53–7.83 (m, 3 H, uncomplexed aromatic), 6.43–7.03 (m, 4 H, complexed aromatic), 5.4 (s, 5 H, Cp), 4.88 (s, 2 H, CH_2); IR (cm^{-1}, KBr) 1680 (CO); mp 111–112 °C.

Anal. Calcd for $C_{19}H_{16}ClOFePF_6$: C, 45.95; H, 3.25. Found: C, 46.25; H, 3.16.

Synthesis of *o*-$ClC_6H_4CH_2COCH_3FeCp^+PF_6^-$ (7b) from 7a. Treatment of 2.0 mmol of **7a** with 2.05 mmol of 2,4-pentanedione according to general procedure gave 70–80% of **7b** as a yellow crystalline product after recrystallization from methylene chloride–ether: ^1H NMR (CD_3COCD_3) δ 6.83 (d, 1 H), 6.44–6.59 (m, 3 H, aromatic), 5.28 (s, 5 H, Cp), 4.68, 4.59, 4.39, 4.29 (AB, 2 H, CH_2, $J_{AB} \sim 20$ Hz), 2.34 (s, 3 H, CH_3); ^{13}C NMR (CD_3CN) δ 203.67 (CO), 109.07, 100.49, 90.33, 89.77, 88.58, 88.21 (aromatic), 80.20 (Cp), 47.69 (CH_2), 30.26 (CH_3); IR (cm^{-1}, KBr) 1690 (CO); mp 126–127 °C.

Anal. Calcd for $C_{14}H_{14}ClOFePF_6$: C, 38.69; H, 3.25; Cl, 8.17. Found: C, 38.57; H, 3.17; Cl, 8.37.

Synthesis of *o*-$ClC_6H_4CH_2COC_6H_5FeCp^+PF_6^-$ (7c) from 7a. The reaction between **7a** (2 mmol) and benzoylacetone (2.05 mmol) according to the general procedure gave a 68–75% yield of **7c** as yellow crystalline product after recrystallization from acetone–ether: ^1H NMR (CD_3COCD_3) δ 8.23 (d, 2 H), 7.56–7.8 (m, 3 H, uncomplexed aromatic), 6.9 (d, 1 H), 6.6–6.73 (m, 2 H), 6.46–6.56 (m, 1 H, complexed aromatic), 5.4 (s, 5 H, Cp), 4.9, 5.0, 5.26, 5.36 (AB, 2 H, CH_2, $J_{AB} \sim 20$ Hz); ^{13}C NMR (CD_3COCD_3) δ 195.27 (CO), 136.75, 134.85, 129.75, 129.15 (uncomplexed aromatic), 109.28, 101.04, 90.65, 89.68, 88.65, 88.24 (complexed aromatic), 80.21 (Cp), 43.98 (CH_2); IR (cm^{-1}, KBr) 1659 (CO); mp 178–179 °C.

Anal. Calcd for $C_{19}H_{16}ClOFePF_6$: C, 45.94; H, 3.24; Cl, 7.15. Found: C, 46.13; H, 3.32; Cl, 7.20.

(24) Crumbie, R. L.; Deol, B. S.; Nemorin, J. E.; Ridley, D. D. *Aust. J. Chem.* **1978**, *31*, 1965. Also: Tauares, D. F.; O'Sullivan, W. I.; Hauser, C. R. *J. Org. Chem.* **1962**, *27*, 1251.

(25) Huppatz, J. L. *Aust. J. Chem.* **1971**, *24*, 653.

Synthesis of o-$ClC_6H_4CH_2CO_2C_2H_5FeCp^+PF_6^-$ (7d) from 7a. The reaction of ethyl acetoacetate with **7a** according to the general procedure gave a 65–70% yield of **7d** as yellow crystalline product after recrystallization from methylene chloride–ether: ^1H NMR (CD_3COCD_3) δ 6.88 (d, 1 H), 6.59–6.68 (m, 2 H), 6.46–6.52 (m, 1 H, aromatic), 5.23 (s, 5 H, Cp), 4.14, 4.23, 4.32, 4.41 (AB, 2 H, CH_2, $J_{AB} \approx 18$ Hz), 4.19, (q, 2 H, CH_2, $J \approx 7$ Hz), 1.24, (t, 3 H, OCH_2CH_3, $J \approx 7$ Hz); ^{13}C NMR (CD_3COCD_3) δ 169.03 (CO), 109.01, 99.63, 90.37, 89.75, 88.77, 88.31 (complexed aromatic), 80.31 (Cp), 62.17 (CH_2), 38.83 (OCH_2), 14.35 (OCH_2CH_3); IR (cm^{-1}, KBr) 1745 (CO); mp 138–140 °C.

Anal. Calcd for $C_{15}H_{16}ClO_2FePF_6$: C, 38.77; H, 3.47; Cl, 7.64. Found: C, 38.56; H, 3.56; Cl, 7.59.

Decomplexation Reactions. A 1-mmol sample of each complex (**3**, **7c**, **2c**) was placed in a vacuum sublimator, dissolved in a minimum amount of methylene chloride, and dried to a thin film using a N_2 stream. The sample was heated by using an oil bath under vacuum (0.25 mm). After 2 h of heating at 200 °C, the material from the cold finger was removed by dissolution with chloroform. After removal of chloroform, the white residue was washed with hexane (2 × 5 mL) to remove the ferrocene formed during this process. The white solid can be redissolved in the minimum amount of ether and recrystallized with hexane.

Specifically, for the vacuum sublimation of 462 mg of **3**, the yield of deoxybenzoin was 178 mg (91%), mp 54–56 °C (lit.[26] 55–56 °C). Similarly from 496 mg of **7c**, the yield α-(o-chlorophenyl)acetophenone was 211 mg (92%): mp 67–69 °C; ^1H NMR (CD_3COCD_3) δ 8.05–8.2 (m, 3 H), 7.3–7.7 (m, 6 H, aromatic), 4.53 (s, 2 H, CH_2); IR (cm^{-1}, KBr) 1700 (CO).

Anal. Calcd for $C_{14}H_{11}ClO$: C, 72.87; H, 4.80. Found: C, 72.55; H, 4.80.

From 1 mmol of **2c**, the yield of 5,5-dimethyl-2-phenylcyclohexane-1,3-dione was 53%: mp 192 °C (lit.[27] 192–193 °C); ^1H NMR ($CDCl_3$) δ 7.1–7.6 (m, 5 H, aromatic), 6.45 (b s, 1 H, OH), 2.4 (s, 4 H, CH_2), 1.2 (s, 6 H, CH_3).

Acknowledgment. We thank the Office of Naval Research for support of this work under Contract N00014-83K-0306.

(26) Truce, W. E.; Abraham, D. J. *J. Org. Chem.* **1963**, *28*, 964.
(27) Neilands, O.; Vanags, G.; Gudriniece, E. *J. Gen. Chem. USSR (Engl. Transl.)* **1958**, *28*, 1201; *Chem. Abstr.* **1958**, *52*, 19988. Also: Beringer, F. M.; Forgione, P. S.; Yudis, M. D. *Tetrahedron* **1960**, *8*, 49.

Intra- and Intermolecular Rearrangements in Fp(η^1-allyl) and Fp(η^2-olefin) Complexes

J. Celebuski, G. Munro, and M. Rosenblum*

Department of Chemistry, Brandeis University, Waltham, Massachusetts 02254

Received May 13, 1985

(η^1-1-Bromoallyl)Fp **6** and (η^1-1-bromo-2-methallyl)Fp **9** [Fp = $C_5H_5Fe(CO)_2$] undergo substitution reactions by aryl-, vinyl-, and 2-methylcyclohexanone enolate zinc chloride to give rearranged condensation products **7a–d** and **10a–c**. Deuterium labeling studies have shown that these products can be accounted for in terms of a slow, rate-limiting rearrangement through a [1,3] sigmatropic shift of the Fp group. The resulting allylic bromide then undergoes rapid coupling by S_N2' displacement of bromide. Deuteration of (η^1-*cis*-1-bromoallyl)Fp with deuteriotriflic acid proceeds stereospecifically trans to the Fp–carbon σ-bond to give a single diastereomeric product **5**-*d*. On standing, this cation undergoes stereospecific rearrangement to (η^1-*trans*-1-deuterio-3-bromoallyl)Fp **5**-*d'* in equilibrium with **5**-*d*. A mechanism involving concerted intramolecular 1,3-migration of both Fp and Br groups has been proposed for this reaction. A similar transposition of these groups has been observed in the bromination of ethyl *trans*-4-Fp-crotonate (**15**).

Introduction

While [1,3] sigmatropic shifts are well-known for a number of σ-allyl derivatives of the main-group metals,[1,2] such behavior is less well documented for the corresponding transition-metal complexes. We recently provided evidence that the facile rearrangements observed in (η^1-allyl)Fp complexes [Fp = $C_5H_5Fe(CO)_2$]proceed by a radical chain S_H2' mechanism in which the chain-carrying species is the relatively stable 17-electron Fp· radical (eq 1).[2]

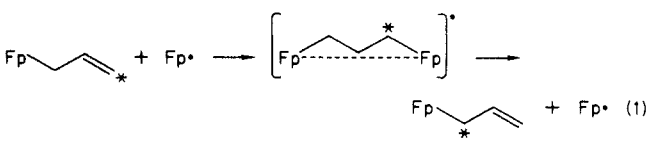

(1)

Nondegenerate [1,3] sigmatropic rearrangements of (η^1-allyl)Fp complexes have generally been observed to give

Scheme I

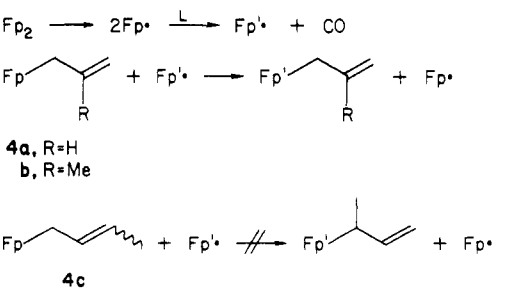

preferentially the product with the least substituted Fe–C bond, as would be expected for the relatively electropositive Fp radical.[3] This is illustrated by the formation of the 1-butenyl complex **3** on deprotonation of either the *cis*- or *trans*-2-butene complex **1**.[4] The initially formed

(1) Mann, B. E. In "Comprehensive Organometallic Chemistry"; Wilkinsonn, G., Ed.; Pergamon Press: Oxford, 1982; Vol. 3, Chapter 20.
(2) Rosenblum, M.; Waterman, P. *J. Organomet. Chem.* **1981**, *206*, 197.
(3) Symon, D. A.; Waddington, T. C. *J. Chem. Soc., Dalton Trans.* **1975**, 2140. Green, J. C. *Struct. Bonding (Berlin)* **1981**, *43*, 37.
(4) Cutler, A.; Ehentholt, D.; Giering, W. P.; Lennon, P.; Raghu, S.; Rosan, A.; Rosenblum, M.; Tancrede, J.; Wells, D. *J. Am. Chem. Soc.* **1976**, *98*, 3495.

0276-7333/86/2305-0256$01.50/0

Synthesis of o-$ClC_6H_4CH_2CO_2C_2H_5FeCp^+PF_6^-$ (7d) from 7a. The reaction of ethyl acetoacetate with **7a** according to the general procedure gave a 65–70% yield of **7d** as yellow crystalline product after recrystallization from methylene chloride–ether: ^1H NMR (CD_3COCD_3) δ 6.88 (d, 1 H), 6.59–6.68 (m, 2 H), 6.46–6.52 (m, 1 H, aromatic), 5.23 (s, 5 H, Cp), 4.14, 4.23, 4.32, 4.41 (AB, 2 H, CH_2, $J_{AB} \approx 18$ Hz), 4.19, (q, 2 H, CH_2, $J \approx 7$ Hz), 1.24, (t, 3 H, OCH_2CH_3, $J \approx 7$ Hz); ^{13}C NMR (CD_3COCD_3) δ 169.03 (CO), 109.01, 99.63, 90.37, 89.75, 88.77, 88.31 (complexed aromatic), 80.31 (Cp), 62.17 (CH_2), 38.83 (OCH_2), 14.35 (OCH_2CH_3); IR (cm^{-1}, KBr) 1745 (CO); mp 138–140 °C.

Anal. Calcd for $C_{15}H_{16}ClO_2FePF_6$: C, 38.77; H, 3.47; Cl, 7.64. Found: C, 38.56; H, 3.56; Cl, 7.59.

Decomplexation Reactions. A 1-mmol sample of each complex (**3**, **7c**, **2c**) was placed in a vacuum sublimator, dissolved in a minimum amount of methylene chloride, and dried to a thin film using a N_2 stream. The sample was heated by using an oil bath under vacuum (0.25 mm). After 2 h of heating at 200 °C, the material from the cold finger was removed by dissolution with chloroform. After removal of chloroform, the white residue was washed with hexane (2 × 5 mL) to remove the ferrocene formed during this process. The white solid can be redissolved in the minimum amount of ether and recrystallized with hexane.

Specifically, for the vacuum sublimation of 462 mg of **3**, the yield of deoxybenzoin was 178 mg (91%), mp 54–56 °C (lit.[26] 55–56 °C). Similarly from 496 mg of **7c**, the yield α-(o-chlorophenyl)acetophenone was 211 mg (92%): mp 67–69 °C; ^1H NMR (CD_3COCD_3) δ 8.05–8.2 (m, 3 H), 7.3–7.7 (m, 6 H, aromatic), 4.53 (s, 2 H, CH_2); IR (cm^{-1}, KBr) 1700 (CO).

Anal. Calcd for $C_{14}H_{11}ClO$: C, 72.87; H, 4.80. Found: C, 72.55; H, 4.80.

From 1 mmol of **2c**, the yield of 5,5-dimethyl-2-phenylcyclohexane-1,3-dione was 53%: mp 192 °C (lit.[27] 192–193 °C); ^1H NMR ($CDCl_3$) δ 7.1–7.6 (m, 5 H, aromatic), 6.45 (b s, 1 H, OH), 2.4 (s, 4 H, CH_2), 1.2 (s, 6 H, CH_3).

Acknowledgment. We thank the Office of Naval Research for support of this work under Contract N00014-83K-0306.

(26) Truce, W. E.; Abraham, D. J. *J. Org. Chem.* **1963**, *28*, 964.
(27) Neilands, O.; Vanags, G.; Gudriniece, E. *J. Gen. Chem. USSR (Engl. Transl.)* **1958**, *28*, 1201; *Chem. Abstr.* **1958**, *52*, 19988. Also: Beringer, F. M.; Forgione, P. S.; Yudis, M. D. *Tetrahedron* **1960**, *8*, 49.

Intra- and Intermolecular Rearrangements in Fp(η^1-allyl) and Fp(η^2-olefin) Complexes

J. Celebuski, G. Munro, and M. Rosenblum*

Department of Chemistry, Brandeis University, Waltham, Massachusetts 02254

Received May 13, 1985

(η^1-1-Bromoallyl)Fp **6** and (η^1-1-bromo-2-methallyl)Fp **9** [Fp = $C_5H_5Fe(CO)_2$] undergo substitution reactions by aryl-, vinyl-, and 2-methylcyclohexanone enolate zinc chloride to give rearranged condensation products **7a–d** and **10a–c**. Deuterium labeling studies have shown that these products can be accounted for in terms of a slow, rate-limiting rearrangement through a [1,3] sigmatropic shift of the Fp group. The resulting allylic bromide then undergoes rapid coupling by S_N2' displacement of bromide. Deuteration of (η^1-*cis*-1-bromoallyl)Fp with deuteriotriflic acid proceeds stereospecifically trans to the Fp–carbon σ-bond to give a single diastereomeric product **5**-*d*. On standing, this cation undergoes stereospecific rearrangement to (η^1-*trans*-1-deuterio-3-bromoallyl)Fp **5**-*d'* in equilibrium with **5**-*d*. A mechanism involving concerted intramolecular 1,3-migration of both Fp and Br groups has been proposed for this reaction. A similar transposition of these groups has been observed in the bromination of ethyl *trans*-4-Fp-crotonate (**15**).

Introduction

While [1,3] sigmatropic shifts are well-known for a number of σ-allyl derivatives of the main-group metals,[1,2] such behavior is less well documented for the corresponding transition-metal complexes. We recently provided evidence that the facile rearrangements observed in (η^1-allyl)Fp complexes [Fp = $C_5H_5Fe(CO)_2$]proceed by a radical chain S_H2' mechanism in which the chain-carrying species is the relatively stable 17-electron Fp· radical (eq 1).[2]

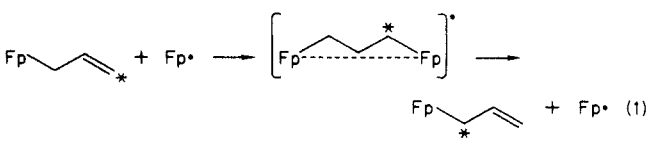

(1)

Nondegenerate [1,3] sigmatropic rearrangements of (η^1-allyl)Fp complexes have generally been observed to give

Scheme I

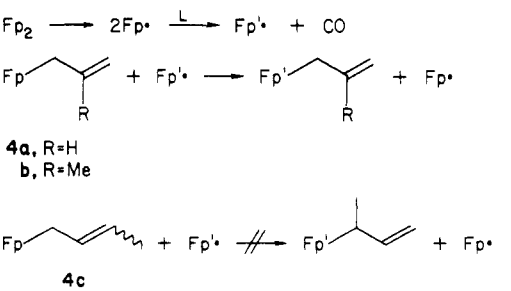

preferentially the product with the least substituted Fe–C bond, as would be expected for the relatively electropositive Fp radical.[3] This is illustrated by the formation of the 1-butenyl complex **3** on deprotonation of either the *cis*- or *trans*-2-butene complex **1**.[4] The initially formed

(1) Mann, B. E. In "Comprehensive Organometallic Chemistry"; Wilkinsonn, G., Ed.; Pergamon Press: Oxford, 1982; Vol. 3, Chapter 20.
(2) Rosenblum, M.; Waterman, P. *J. Organomet. Chem.* **1981**, *206*, 197.
(3) Symon, D. A.; Waddington, T. C. *J. Chem. Soc., Dalton Trans.* **1975**, 2140. Green, J. C. *Struct. Bonding (Berlin)* **1981**, *43*, 37.
(4) Cutler, A.; Ehentholt, D.; Giering, W. P.; Lennon, P.; Raghu, S.; Rosan, A.; Rosenblum, M.; Tancrede, J.; Wells, D. *J. Am. Chem. Soc.* **1976**, *98*, 3495.

0276-7333/86/2305-0256$01.50/0

methallyl complex **2** is not observed in these reactions since at room temperature its rearrangement is more rapid than its formation.

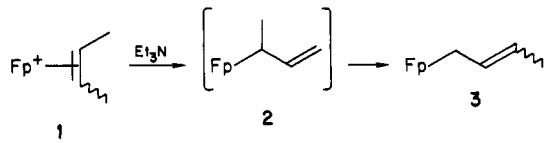

Similarly, the replacement of Fp by Fp′ (Fp′ = $C_5H_5Fe(CO)L$) in **4a,b** may readily be achieved by a radical chain process.[5] However, this reaction fails for the terminally substituted allyl complex **4** (Scheme I).

The above generalization appears to be a useful guide to the preferred structure and to the reactions of alkyl-substituted (η^1-allyl)Fp complexes, but some more recent observations with functionalized (η^1-allyl)Fp complexes now illustrate its limitations, with respect to the prediction of reaction products derived from such potentially tautomeric systems. Furthermore, we observed a new stereospecific rearrangement in Fp(η^2-bromoolefin) cations, which further illustrates the high mobility of the Fp group. These observations were made in the course of studies designed to extend the methods for elaborating the ligand in (η^1-allyl)Fp complexes and form the substance of this paper.

Results and Discussion

The most commonly employed means for elaborating simple (η^1-allyl)Fp complexes has been through electrophilic addition to these substances, followed by deprotonation of the resulting cationic olefin complex (eq 2).[7]

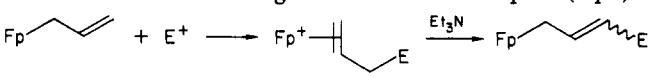

(2)

We sought to exploit the readily available 1-bromoallyl complex and its congeners as starting materials in Kumada type coupling[6] of **6**[8] with carbanionic reagents in the presence of nickel catalysts.

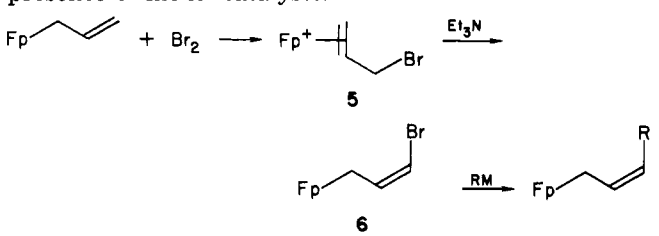

In the event, treatment of **6** with phenylzinc chloride in the presence of [1,3-bis(diphenylphosphino)propane]-nickel(II) chloride as catalyst gave **7a** rather than the expected coupling product **8**.

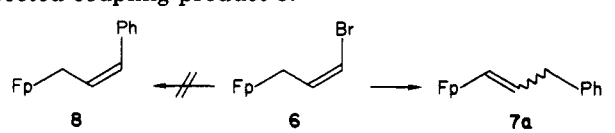

The unusual coupling product is obtained as a mixture of *Z* and *E* isomers (1:1), and its structural assignment is based on its ^1H NMR spectrum which shows a two-proton resonance at δ 3.4 compatible with structure **7a**, rather than near δ 2.0, as would be expected for structure **8**.

Table I

substr	nucleophile	product	yield, %
6	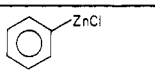	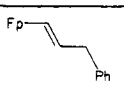 **7a**	93
6	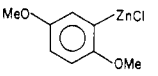	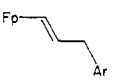 **7b**	24
6	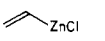	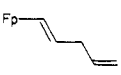 **7c**	73
6	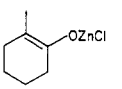	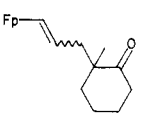 **7d**	100
6	MeZnCl	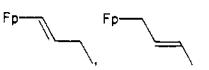 **7e** **7f**	75
7	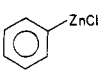	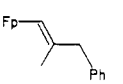 **10a**	61
9	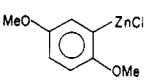	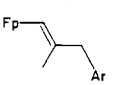 **10b**	24
9	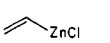	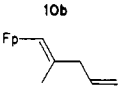 **10c**	69

The unexpected course of the reaction suggested that a process very different than the one anticipated had been followed and that the catalyst might not be essential. Indeed, this proved to be true, and the modest yield of **7a** obtained in the presence of catalyst could be improved to 93% in its absence.

Similarly conversion of (η^1-methallyl)Fp **4b** to a mixture of (*Z*)- and (*E*)-bromomethallyl isomers **9** followed by reaction with phenylzinc chloride gave **10a** as a mixture of geometrical isomers (*Z*/*E* = 3:1) in 61% yield.[9]

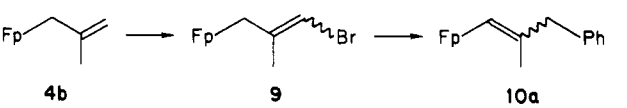

However, treatment of (2-bromo-2-butenyl)Fp (**11**) with phenylzinc chloride failed to yield any coupling product.

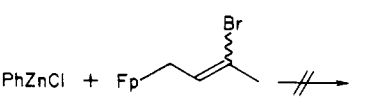

The coupling reaction appears to be a fairly general one for **6** and **9** with both aryl- and vinylzinc halides. Methylzinc chloride and the zinc salt of 2-methylcyclohexanone also couple with **6**, but allylzinc chloride failed to react with this complex. Table I provides a summary of condensations carried out with **6** and **9**. In general these reactions were run at room temperature in the presence of 2 equiv of the zinc reagent. Under these conditions, the

(5) Fabian, B. D.; Labinger, J. A. *J. Am. Chem. Soc.* **1979**, *101*, 2239. Labinger, J. A. *J. Organomet. Chem.* **1977**, *136*, C31.
(6) Rosenblum, M.; Waterman, P. S. *J. Organomet. Chem.* **1980**, *187*, 267.
(7) Cutler, D.; Ehntholdt, D.; Lennon, P.; Nicholas, K.; Marten, D. F.; Madhavarao, M.; Raghu, S.; Rosan, A.; Rosenblum, M. *J. Am. Chem. Soc.* **1975**, *97*, 3149.
(8) Kumada, M. *Pure Appl. Chem.* **1980**, *52*, 669.
(9) These may not represent kinetically determined ratios of product since the closely related $CpFe(PPh_3)(CO)$(vinyl) complexes have been shown undergo facile cis to trans isomerization on heating. Reger, D. L.; McElligott, P. J. *J. Am. Chem. Soc.* **1980**, *102*, 5923.

reaction is slow and requires 48 h for completion.

As a means of probing the mechanism of the coupling reaction, we sought to prepare complex **6** specifically deuterated at C-1. Unexpectedly, these experiments provided evidence for yet another rearrangement process, which like the coupling reaction itself owes its operation apparently to the high mobility of the Fp group.

Before proceeding to an account of these experiments, it is important to note, for the purpose of these discussions, that the diastereotopic methylene protons in **5**, the precursor to **6**, show very different chemical shifts at δ 3.67 and 4.53, possibly as a consequence of their spatial relationship to the complexed double bond.[10] These high- and low-field resonances may be assigned to H-3_S and H-3_R, respectively, from the observed coupling constants for each with H-2 (J = 9.6 and 3.9 Hz, respectively). The conformational preference[11] for the unsaturated chain in the complex, shown in structure **12**, is in turn based on exam-

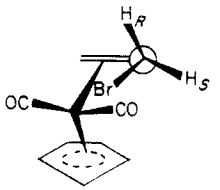

12

ination of the ^{13}C NMR spectra of a number of closely related 3-substituted Fp(η^2-propene) cations, which suggests that the halogen atom in **5** is oriented so as to interact equally with both of the diastereotopic carbonyl ligands.[7]

Deuteration of (η^1-*cis*-1-bromoallyl)Fp **6** with deuteriotriflic acid gave an 89% yield of labeled product **5**-*d*, isolated as the triflate salt by precipitation with ether. Proton NMR analysis showed a 50% incorporation of deuterium entirely by replacement of H-3_R. The protonation of **6** is consequently highly stereospecific as is the reverse process, which proceeds through the removal of H-3_R in **5** by triethylamine to give exclusively the *cis*-1-bromoallyl isomer **6**.[7]

On standing in acetone solution at −20 °C for several days, **5**-*d* undergoes stereospecific rearrangement to give *trans*-1-deuterio-3-bromoallyl complex **5**-*d*′ in equilibrium with **5**-*d*.

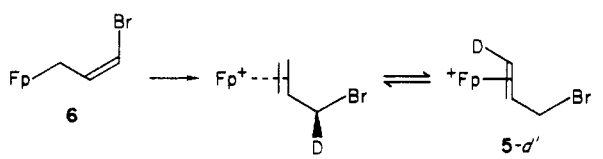

We suggest that the rearrangement proceeds through a concerted 1,3-migration of both the Fp and Br groups. Such a mechanism requires that rearrangement takes place through a higher energy conformation of **5** in which the C–Br bond is anti rather than syn to the Fp–olefin bond as depicted in **12**. Such a conformation allows charge delocalization in the transition state to be shared by both Fp and Br groups moving concertedly across opposite faces of the C_3 ligand. Moreover, such a mechanism accounts for the stereospecific transposition of deuterium label to give the *trans*-1-deuteriopropene complex **5**-*d*′ (eq 3).

The equilibration of **5**-*d* with **5**-*d*′ is accelerated on changing the gegen ion from $CF_3SO_3^-$ to PF_6^-, which may reflect a rate dependence on ion pair association in the salt.

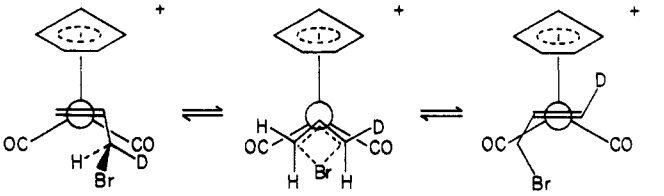

(3)

Thus, isomerization of the triflate salt is relatively slow at −20 °C, requiring several days for completion, but equilibration of the hexafluorophosphate salt is complete within 3 h at this temperature.

The stereospecific deuteration of **6** may be contrasted with the reaction of (η^1-1-phenylallyl)Fp, which has been observed to undergo nonstereospecific deuteration in the presence of CF_3COOD.[7]

Deprotonation of an equilibrated mixture of **5**-*d* and **5**-*d*′, as the PF_6 salt, with diisopropylethylamine at 0 °C gave (η^1-*cis*-1-bromoallyl)Fp with deuterium incorporation only at C-3 and little loss in total deuterium content, by NMR analysis.

The formation of **6**-*d* as the sole product of the reaction is consistent with stereospecific deprotonation, which would be expected to result in selective removal of deuterium from **5**-*d*. But the overall high retention of deuterium in the product requires that the rate of exchange of **5**-*d* and **5**-*d*′ be faster than the rate of deprotonation and that the primary isotope effect for the deprotonation reaction be relatively large.[12]

The parallel reactions of (η^1-methallyl)Fp **4b** form a striking contrast to those of the parent complex **4a**. While the sequence of bromination and deprotonation with the latter compound gives only the (*Z*)-bromoallyl derivative **6**, similar transformation of **4b** gives **9** as a 3.5:1 mixture of *Z*/*E* isomers.

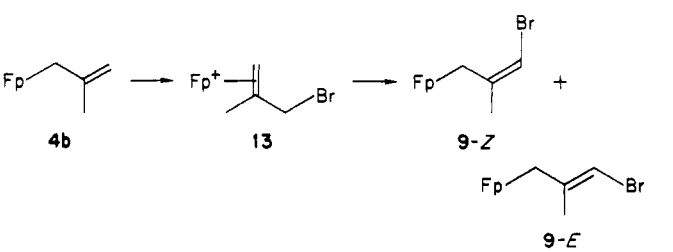

An examination of the proton NMR spectrum of the intermediate olefin complex **13** provides a rationale for this behavior. While the diastereotopic protons in **5** show disparate chemical shifts ($\Delta\delta$ = 0.9 ppm), those in **13** are nearly identical. We attribute this to destabilization of a conformation for **13** similar to that shown for **5** (structure **12**), due to steric interactions of the methyl substituent with cyclopentadienyl ring protons. Such interactions are relieved by rotation of the olefinic C–C bond axis out of a plane parallel to the cyclopentadienyl ring plane (Scheme II), with the consequence that both H_R and H_S may adopt a conformation, required for metal-assisted deprotonation,

(10) Jackman, L. M. "Nuclear Magnetic Resonance Spectroscopy", 2nd ed.; Pergammon Press: Oxford, 1900; pp 83–88.
(11) Faller, J. W.; Johnson, B. V. *J. Organomet. Chem.* **1975**, *88*, 101.
(12) Primary deuterium isotope ratios (k_H/k_D) as large as 7 have been observed in E2 reactions of 2-phenylethyl derivatives: Saunders, W. H.; Cockerill, A. F., "Mechanisms of Elimination Reactions"; Wiley: New York, 1973; 79. The primary isotope effect for proton loss from the phenonium ion generated by protonation of 1,3,5-trimethoxybenzene has the value of 9: Kresge, A. J.; Chiang, Y. *J. Am. Chem. Soc.* **1967**, *89*, 4411.

Scheme II

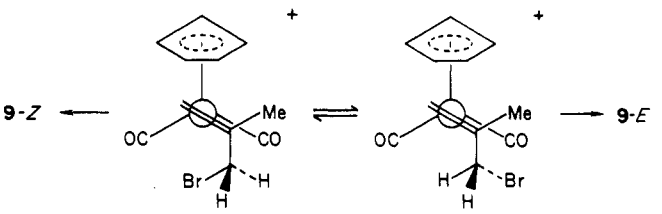

trans to the Fp–olefin bond. In these circumstances, loss of H_R yields the (*cis*-bromomethallyl)Fp complex **9**-*Z*, while loss of H_S gives the trans isomer **9**-*E*.

Deuteration of **9**-*Z*,*E* with CF_3SO_3D in methylene chloride at −78 °C, followed by gegen ion exchange with NH_4PF_6 gave **13**-*d* with 75% incorporation of deuterium.

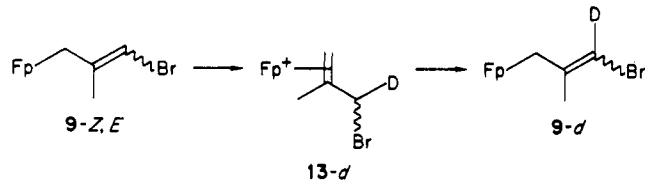

Proton NMR analysis of the product showed that all the deuterium was at C-3, in both diastereotopic positions. In contrast to **5**-*d*, no scrambling of the deuterium label was observed when solutions of **13**-*d* were left standing. It seems likely that the increased barrier to 1,3-transposition of bromine in **13**-*d* compared with **5**-*d* may be due in part to steric interactions of the methyl group at C-2 with the cyclopentadienyl ring in the transition state (eq 3). Moreover, the energy of the transition state compared with that for **5**-*d* would be expected to be further increased by the need for partial Fe–C bonding to a tertiary carbon center.

Deprotonation of **13**-*d* with diisopropylethylamine in methylene chloride at 0 °C gave **9**-*d* as a 2:1 mixture of *Z* and *E* isomers, with 60% incorporation of deuterium.

With specifically deuterated bromoallyl complexes **6**-*d* and **9**-*d* in hand, coupling of each with phenylzinc chloride was examined. These reactions gave products **7a**-*d* and **10a**-*d*, respectively, each of which corresponds to a 1,3-transposition of the Fp group in the course of the reaction.

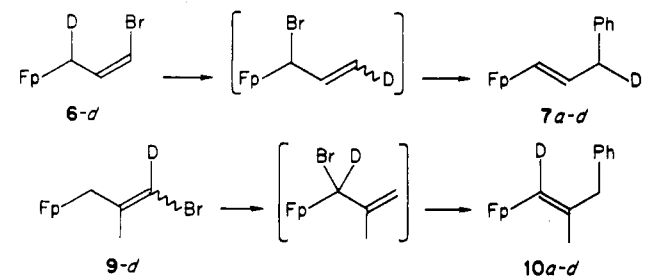

These results may be accounted for by a sequence involving radical induced isomerization of starting materials in a preequilibrium reaction, which results in the conversion of relatively unreactive vinyl halides to reactive allyl halides. Reaction of these with the organozinc reagents by an S_N2' process would be expected to take place rapidly. The relatively low overall rate of reaction may be attributed to a low concentration of the rearranged allylic halide intermediates in equilibrium with starting complexes, while the failure of the butenyl complex **11** to react is apparently due to increased retardation of the S_H2' processes by the methyl substituent.

Some earlier observations, made in the course of examining the reactions of Fp crotonate complexes, deserve comment at this point, since the rearrangements observed for these complexes appear to be closely related to the present results.

Fp(η^2-*trans*-ethyl-2-butenoate)BF_4 (**14**), prepared from the epoxide by reaction with NaFp followed by treatment with HBF_4-etherate, gave the sigmatropically transposed complex **15** on treatment with triethylamine. This latter substance reacted with bromine at −78 °C to give bromoallyl complex **17** rather than the anticipated isomeric complex **16**. It seems likely that **16** is initially formed in the bromination reaction, but undergoes rapid 1,3-rearrangement to **17**. The complex salt **17** was too unstable to characterize spectrally, but decomposition in solution yielded the free ligand **18**. Furthermore, deprotonation of the salt at low temperature gave the bromoester complex **19** as a mixture of *Z* and *E* isomers. These reactions serve

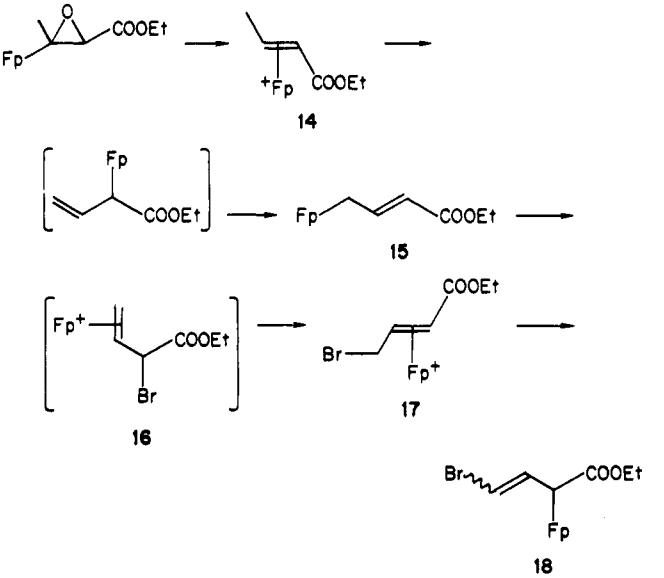

to illustrate the high mobility of the Fp substituent, in neutral (η^1-allyl)Fp complexes as well as in Fp(η^2-olefin) cations. However, the mechanisms by which these substances undergo rearrangement differ substantially. The allyl complexes rearrange by a radical chain S_H2' process, while the cationic bromoolefin complexes undergo 1,3-rearrangement through an ionic pathway involving concerted migration of halogen and the Fp group.

Experimental Section

All reactions and subsequent manipulations of organometallic compounds were performed under argon atmosphere. Solvents used, except for diethyl ether (ether) and tetrahydrofuran (THF), were deaerated by bubbling argon through the solvent. Ether and THF were freshly distilled immediately before use from Na–benzophenone ketyl solutions. Unless otherwise noted, reactions were run in Ar-filled rubber-septum capped flasks.

Infrared spectra were run on a Perkin-Elmer 457 or 683 spectrophotometer in CH_2Cl_2 solution at a concentration of roughly 20 mg/mL. Proton magnetic resonance spectra were obtained by using a 90-MHz Varian EM-390 spectrometer, a Varian XL-300 spectrometer (NSF GU 3852), or a homebuilt 500-MHz spectrometer (NIH GM 20168). Carbon-13 magnetic resonance spectra were determined at 22.64 MHz on a Bruker WH-90 spectrometer (NSF GU 3852, GP 37156) and were obtained with broad-band decoupling. Chemical shifts were referenced to the center line of $CDCl_3$ (76.9 ppm). Mass spectra were recorded on a Hewlett-Packard GC/MS system, Model 5985. Combustion analyses were performed by Galbraith Laboratories, Knoxville, TN.

Preparation of (*E*,*Z*)-1-Fp-3-phenylpropene (7a). To 285 mg (2.09 mmol) of $ZnCl_2$ was added 20 mL of THF. The solution was cooled to −78 °C, and 0.88 mL of commercial (Aldrich) PhLi (2.3 M in 70/30 cyclohexane/ether, 2.03 mmol) was rapidly added dropwise. Then, 289 mg (0.97 mmol) of **6**[7] in 25 mL of THF was

added via cannula. The dry ice bath was removed, and the reaction mixture was left to stir at ambient temperature for 48 h. The mixture was quenched with 50 mL of saturated aqueous $NaHCO_3$, and to the resultant two-phase system in a separatory funnel was added 100 mL of ether. The combined organic extracts were back-washed with 50 mL of saturated aqueous $NaHCO_3$, dried over $MgSO_4$, filtered, rotary evaporated to dryness, and then vacuum dried. The crude material obtained had a weight of 276 mg. This material was taken up as much as possible into petroleum ether and filtered through Celite on a glass wool plug. The solvent was stripped off, and the residue was vacuum dried to give 265 mg of product **7a** as a red oil (93%). The crude product was purified by preparative TLC on alumina plates (petroleum ether), but good elemental analyses could not be obtained since the product decomposed on brief storage: IR (CH_2Cl_2) ν_{max} 2004, 1951 (CO), 1599 (Ph) cm^{-1}; ^1H NMR (CS_2) δ 7.10 (br m, 5 H, Ph), 6.33 (dt, 1 H, J = 15.3, 1.4 Hz, H-1), 5.58 (dt, 1 H, J = 15.3, 6.2 Hz, H-2), 4.67, 4.70 (2s, 5 H, Cp), 3.40 (dd, 2 H, J = 6.2, 1.4 Hz, benzyl); ^{13}C NMR ($CDCl_3$) δ 40.5, H 45.1 (Z)- and (E)-CH_2Ph), 85.2, 85.5 (Cp) 122.6, 125.2, 125.9, 126.3, 126.9, 127.3, 127.6, 128.0, 128.1, 142.0, 142.9, 144.8, (Ph, vinyl) 215.7 (MCO); mass spectrum (70 eV), m/e (fragmentation, relative intensity) 294 (M, 1.6), 266 (M - CO, 10.6), 238 (M - 2CO, 71.1).

Preparation of (E,Z)-1-Fp-3-(2,5-dimethoxyphenyl)-propene (7b). To 290 mg (2.1 mmol) of p-dimethoxybenzene in ether at room temperature was added 1.21 mL of 2.6 M n-BuLi (3.15 mmol) in hexane. The mixture was stirred for 24 h at ambient temperature. The yellow solution of 1-lithio-2,5-dimethoxybenzene was added via cannula to solution prepared from 327 mg (2.4 mmol) of $ZnCl_2$ in THF and cooled to -78 °C. Then, 315.1 mg (1.05 mmol) of **6** in 10 mL of THF was added via cannula. The cold bath was removed, and the mixture was left to stir at ambient temperature for 46 h. Solid CO_2 was added, followed by 100 mL of saturated aqueous $NaHCO_3$. After the standard workup, 482 mg of crude material was isolated. Filtration of a petroleum ether solution of the crude product through Celite, followed by preparative TLC (1-mm alumina plate, petroleum ether eluent) gave 91 mg of **7b** (24%): IR (CH_2Cl_2) ν_{max} 2011, 1962 cm^{-1} (CO); ^1H NMR (CS_2) δ 7.0–6.0 (m, 4 H, H-1, aryl), 5.50 (dt, 1 H, J = 15.8, 7.0 Hz, vinyl), 4.78, 4.73, (2s, 5 H, Cp) 3.8–3.6 (4s, 6 H, OMe), 3.28 (d, 2 H, J = 7 Hz, benzyl); mass spectrum (20 eV), m/e (relative intensity) 354.2 (M, 1.3), 326.1 (M - CO, 7), 297.9 (M - 2CO, base). Anal. Calcd for $C_{18}H_{18}FeO_4$: C, 61.04; H, 5.12. Found: C, 60.87; H, 5.35.

Preparation of (E)-1-Fp-1,4-pentadiene (7c). To 327 mg (2.4 mmol) of vacuum dried $ZnCl_2$ in 15 mL of THF at -78 °C was added 2.32 mL of 1.0 M vinylmagnesium bromide (2.32 mmol) in THF via syringe. Immediately, a white precipitate formed. Then, 331 mg (1.11 mol) of **6** in 20 mL of THF was added via cannula. The cold bath was removed, and the suspension was stirred at room temperature for 48 h, whereupon the suspension clarified. After the standard workup, 269 mg of crude material was isolated. After extraction of this material with petroleum ether and Celite filtration of the resultant suspension, 196 mg (73%) of **7c** was isolated as a yellow oil. Combustion analysis was precluded by sample decomposition: IR (CH_2Cl_2): ν_{max} 2012, 1960 cm^{-1}. ^1H NMR (CS_2): δ 6.19 (dt, 1 H, J = 15.2, 1.0 Hz, H-1), 5.55 (m, 1 H, H-4), 5.17 (dt, 1 H, J = 15.2, 6.3 Hz, H-2), 4.9–4.6 (m, 2 H, H-5), 4.75 (s, 5 H, Cp), 2.80 (t, 2 H, CH_2).

Preparation of (E,Z)-1-Fp-3-(2-methyl-1-oxo-2-cyclohexyl)propene (7d). A solution of 419 mg (2.29 mmol) of 1-[(trimethylsilyl)oxy]-2-methylcyclohexene in 10 mL of THF was cooled to 0 °C, and 0.97 mL of 2.6 M n-BuLi (2.52 mmol) in hexane was added in five equal portions over 10 min. The reaction mixture was stirred at 0 °C for 1 h, and then 343 mg (2.52 mmol) of solid $ZnCl_2$ was added. Upon solution of the $ZnCl_2$, the mixture was cooled to -78 °C, and 370 mg (1.24 mmol) of **6** in 10 mL of THF was added via cannula to the organozinc reagent. The cold bath was removed, and the reaction mixture was left to stir at ambient temperature for 46 h. After standard workup and petroleum ether Celite filtration, 410 mg of a viscous yellow-red oil was obtained (100%). NMR analysis indicated a 1.92/1.0 ratio of the E/Z isomers. IR (CH_2Cl_2): ν_{max} 2010, 1960 (CO), 1703 (C=O) cm^{-1}. ^1H NMR (CS_2) δ 6.15 (dt, 0.66 H, J = 15.3, 1.0 Hz, FpCH trans), 5.73 (dt, 0.34 H, J = 6.8, 1.0 Hz, FpCH cis), 5.23 (dt, 1 H, J = 15.3, 8.2 Hz, vinyl), 4.80 (s, 1.7 H, Cp, cis), 4.73 (s, 3.3 H, Cp trans), 2.3–1.4 (br m, 10 H, CH_2), 0.94 (s, 3 H, Me). Anal. Calcd for $C_{17}H_{20}FeO_3$: C, 62.22; H, 6.14. Found: C, 62.47; H, 6.62.

Attempted Reaction of 6 with Allylzinc Chloride. To 226 mg (1.66 mmol) of vacuum dried $ZnCl_2$ in 10 mL of THF was added 0.83 mL of 2.0 M allylmagnesium chloride (1.66 mmol) in THF via syringe. Then, 226 mg (0.76 mmol) of **6** in 10 mL of THF was added to the solution via cannula. The cold bath was removed, and the mixture was stirred at ambient temperature for 48 h. After standard workup and filtration of the crude petroleum ether extract through Celite, 114 mg of the starting alkenyl bromide **6** was isolated (50% recovery).

Reaction of 6 with MeZnCl. Preparation of 7e,f. To 250 mg (1.83 mmol) of vacuum-dried $ZnCl_2$ in 20 mL of THF at -78 °C was added 1.37 mL of 1.30 M MeLi (1.78 mmol) in ether via syringe. Then, 254 mg (0.85 mmol) of **6** in 20 mL of THF was added to the MeZnCl solution via cannula. The cold bath was removed, and the mixture was stirred at ambient temperature for 48 h. After standard workup 145 mg of a yellow oil was obtained (75%). Proton NMR analysis showed a mixture of four Cp-containing materials. (Z)- and (E)-1-Fp-2-butene were identified as two of the four compounds by comparison with a spectrum of the authentic materials. The other two Cp containing materials were identified as (Z)- and (E)-Fp-1-butene from analysis of the NMR spectrum. ^1H NMR (CS_2): (1-Fp-2-butene), δ 5.8–4.8 (m, 2 H, vinyl), 4.67, 4.60 (2s, 5 H, Cp), 2.2–1.9 (m, 2 H, CH_2), 1.53 (d, 3 H, J = 7 Hz, Me); (1-Fp-1-butene), δ 6.3–6.0 (m, 1 H, FpCH), 5.7–5.4 (m, 1 H, vinyl), 4.78 4.70 (2s, 5 H, Cp), 2.2–1.9 (m, 2 H, CH_2), 0.9 (t, 3 H, J = 7 Hz, Me).

Preparation of (E,Z)-1-Fp-2-methyl-3-phenylpropene (10a). To 351 mg (2.57 mmol) of vacuum-dried $ZnCl_2$ was added 10 mL of THF. The solution was cooled to -78 °C, and 1.1 mL (2.54 mmol) of 2.3 M PhLi in 70/30 cyclohexane/ether was added via syringe. To the in situ generated PhZnCl was added 376 mg (1.21 mmol) of **9** in 15 mL of THF via cannula. The cold bath was removed, and the reaction mixture was left to stir for 42 h. After standard workup (see above), extraction of crude product with low-boiling petroleum ether, and filtration through Celite, 523 mg of red oil resulted. The oil was purified by preparative TLC (1 mm alumina plates, petroleum ether eluent) to give, upon extraction of the yellow band with ether, 230 mg of yellow oil (61%). This material like **7a** decomposed on standing briefly and could not be analyzed: IR (CH_2Cl_2) ν_{max} 2006, 1956 (CO), 1600 (Ph) cm^{-1}; ^1H NMR (CS_2) δ 7.04 (m, 5 H, Ph), 6.03 (s, 1 H, vinyl), 4.75, 4.73 (two s, 5 H Cp), 3.40 (s, 2 H, benzyl), 1.67, 1.53 (two s, 3 H, Me); ^{13}C NMR ($CDCl_3$) δ 21.8, 27.4 (E- and Z-CH_3), 44.4, 50.8 (Z- and E-CH_2Ph), 85.3, 85.5 (E- and Z-Cp), 117.8, 118.1, 122.7, 125.4, 125.8, 126.9, 127.1, 127.3, 127.6, 127.8, 128.0, 128.3, 128.5, 141.0, 141.2, 144.8, 145.9, 146.1 (Ph, vinyl), 216.0 (MCO).

Preparation of (E,Z)-1-Fp-2-methyl-3-(2,5-dimethoxyphenyl)propene (10b). To 290 mg (2.1 mmol) of p-dimethoxybenzene in ether at room temperature was added 1.21 mL of 2.6 M n-BuLi (3.15 mmol) in hexane. The mixture was stirred for 24 h at ambient temperature. To the yellow ether solution was added 30 mL of THF, followed by 327 mg (2.4 mmol) of $ZnCl_2$. The yellow solution turned colorless. The mixture was cooled to -78 °C, and 383 mg (1.23 mmol) of **9** in 15 mL of THF was added via cannula. The cold bath was removed, and the reaction mixture was stirred at ambient temperature for 48 h. Workup gave 110 mg of product (24%); NMR analysis indicated that the product was roughly an equal mixture of geometric isomers. IR (CH_2Cl_2): ν_{max} 2004, 1957 cm^{-1}. ^1H NMR (CS_2): δ 6.6–6.2 (m, 3 H, aryl), 5.93, 5.88 (2s, 1 H, vinyl), 4.70 (s, 5 H, Cp), 3.7–3.5 (3s, 6 H, OMe), 3.29 3.23 (2s, 2H, benzyl), 1.67, 1.47 (2s, 3 H, Me). Mass spectrum (70 eV); m/e (relative intensity) 368 (M, 0.4), 340 (M - CO, 4.5), 312 (M - 2CO, 61.6). Anal. Calcd for $C_{19}H_{20}FeO_4$: C, 61.98; H, 5.47. Found: C, 61.93; H, 5.63.

Preparation of 1-Fp-2-methyl-1,4-pentadiene (10c). To 406 mg (2.98 mmol) of vacuum-dried $ZnCl_2$ in 15 mL of THF at -78 °C was added 2.98 mL (2.98 mmol) of 1.0 M vinylmagnesium bromide in THF via syringe. Immediately, a white precipitate formed. Then, 463 mg (1.49 mmol) of **9** in 20 mL of THF was added via cannula. The cold bath was removed, and the suspension was stirred at room temperature for 48 h, whereupon the suspension clarified. After the standard aqueous bicarbonate workup, 363 mg of crude material was isolated. After extraction

of this material with petroleum ether and Celite and filtration of the resultant suspension, 266 mg (69%) of **10c** was isolated as a yellow oil. Combustion analysis was precluded by sample decomposition. IR (CH_2Cl_2): ν_{max} 2066, 1957 cm^{-1} (CO). ^1H NMR (CS_2): δ 5.90 (t, 1 H, J = 0.8 Hz, H-1), 5.71 (m, 1 H, H-4), 4.86–4.6 (m, 2 H, H-5), 4.75 (s, 5 H, Cp), 2.76 (dd, 2 H, j = 6.9, 0.8 Hz, H-3), 1.59 (s, 3 H, Me).

Preparation of Fp(η^2-3-bromo-2-methyl-1-propene)BF_4 (13). (Isobutenyl)Fp (**4b**; 2.19 g, 9.4 mmol) was taken up in 30 mL of CH_2Cl_2 and cooled to −78 °C. Bromine (0.49 mL, 9.0 mmol) was added dropwise. Reaction was continued at −78 °C for 45 min, and then 1.30 mL (9.0 mmol) of HBF_4·Et_2O was added. The cold bath was removed, and the solution was purged of HBr by a stream of argon. Ether was added to precipitate the product, which was filtered off, washed with ether, and dried in vacuo. The yield of crude product isolated as a yellow solid was 3.29 g (88%). The material slowly decomposes at room temperature. ^1H NMR (CD_3NO_2, 0 °C): δ 5.60 (s, 5 H, Cp), 5.17 (s, 1 H, CH=), 5.00 (q, 1 H, CH=), 4.06 (s, 2 H, CH_2Br) 1.90 (s, 3 H, CH_3).

Preparation of (*E*,*Z*)-3-Fp-1-bromo-2-methylpropene (9-*Z*,*E*). The salt **13** (3.24 g, 8.13 mmol) was stirred in 25 mL of CH_2Cl_2 and cooled to 0 °C. Diisopropylethylamine (1.42 mL, 8.2 mmol) was added dropwise, and the reaction mixture was stirred at 0° for 45 min. The reaction solution was allowed to come to room temperature, solvent was removed in vacuo, and the residue was extracted into petroleum ether. This was filtered through Celite. Removal of solvent left 2.06 g of product as a red oil (82%). ^{13}C NMR ($CDCl_3$): δ 2.20 ($FpCH_2$, *Z* isomer) 8.00 ($FpCH_2$, *E* isomer) 23.27 (CH_3), 84.56, 85.49 (Cp, *E* and *Z* isomers), 94.61, 94.73 (CHBr, *Z* and *E* isomers), 151.65 (CMe=), 216.80 (CO). The ratio of *Z*/E isomers, based on the relative intensities of $FpCH_2$ resonances, was calculated to be 3.5. ^1H NMR (CS_2): δ 1.77 (s, 3 H, CH_3) 2.03 (s, 2 H, CH_2Fp), 4.75, 4.60 (2 s, 5 H, Cp), 5.52 (q, CH=, *Z* isomer) 5.72 (m, CH=, E isomer).

Preparation of Deuterated Fp(η^2-3-bromo-1-propene)F_3CSO_3 (5-*d*). To a solution of 344 mg (1.15 mmol) of **6** in 25 mL of CH_2Cl_2 at −78 °C was added dropwise, via syringe 0.11 mL (1.26 mmol) of CF_3SO_3D, prepared from $(CF_3SO_2)_2O$ and D_2O at 60 °C for 3 h. The reaction mixture was stirred at −78 °C for 1 h, and ether was then added to precipitate the product. The salt was filtered off and washed with ether until the washings were colorless. The product was then air- and vacuum-dried to give 461 mg of **5-*d*** (89%). Proton NMR analysis of this material indicated a 50 ± 5% incorporation of deuterium by replacement of H_R exclusively (structure **12**) as indicated by the loss in intensity of the signal at δ 4.53. Extended reaction periods (6 days) at −20 °C led to the scrambling of the label to give a 1:1 mixture of **5-*d*** and **5-*d′*** as indicated by changes in integrations for methylene vinyl proton resonance at δ 4.12 and 3.83. ^1H NMR of freshly prepared material (acetone-d_6): δ 6.03 (s, 5 H, Cp), 5.5–5.4 (m, 1 H, CH=), 4.53 (dd, 0.5 H, J = 3.8, 9.9 Hz, H_R), 4.18 (d, 0.9 H, J = 8.2 Hz, CH_2=), 3.83 (d, 1.0 H, J = 14.4 Hz, CH_2=), 3.70 (t, 1.0 H, J = 9.9 Hz, H_S).

Preparation of Deuterated Fp(η^2-3-bromo-1-propene)PF_6 (5-d/5-*d′*). The 461 mg of triflate salt (0.99 mmol) was slurried into acetone and cooled to −78 °C, and then 465 mg (2.85 mmol) of solid NH_4PF_6 was added all at once. The cold bath was replaced with an ice water bath, and the slurry clarified. The acetone was stripped off on the rotary evaporator, and the residue was slurried into cold distilled water. The salt was filtered off and washed with cold water, and then the solid was taken up into acetone. Precipitation was effected with ether. Filtration and ether washing of the precipitate gave a 90% yield of yellow PF_6. NMR analysis established that the D label was located mostly at C-3. Upon leaving the NMR solution stand at −20 °C for 3 h, the deuterium label scrambled into the H-1c position such that the composition of **5-*d*/5-*d′*** in the mixture of the products was 50/50. There was a total of 45 ± 5% D in the molecule, by NMR integration, using the Cp resonance as internal standard. ^1H NMR (Acetone-d_6): freshly prepared material, δ 6.03 (s, 5 H, Cp), 5.6–5.3 (m, 1 H, methine), 4.57 (dd, 0.68 H, J = 9.9, 3.8 Hz, CHD), 4.19 (d, 0.89 H, J = 8.2 Z, *cis*-CH_2=), 4.0–3.5 (m, 2 H, *trans*-CH_2=, CHD); after 3 h, δ 6.03 (s, 5 H, Cp), 5.6–5.1 (m, 1 H, methine), 4.57, (dd, 0.78 H, J = 9.9, 3.8 Hz, CHD), 4.19 (d, 0.78 H, J = 8.2 Hz, *cis*-CH_2=), 3.89 (d, 1 H, J = 14.6 Hz, *trans*-CH_2=), 3.70 (t, 1 H, J = 9.9 Hz, CHD).

Preparation of 1-Bromo-3-deuterio-3-Fp-propene (6-*d*). A sample of 491 mg (1.1 mmol) of 50 ± 5% monodeuterated **5-*d*/5-*d′*** (by NMR integration) was slurried into 15 mL of CH_2Cl_2 and cooled to 0 °C. Diisopropylethylamine (0.19 mL, 1.1 mmol) was syringed dropwise into the suspension, and the reaction mixture was stirred at 0 °C for 50 min. The solvent was stripped off via rotary evaporation, and the residue was taken up into a minimal amount of CH_2Cl_2 and applied to a 1 mm alumina prep TLC plate. Elution with petroleum ether gave a yellow band which was extracted with ether to give 218 mg of the desired as a yellow oil, 50 ± 5% labeled, with the deuterium label exclusively located at C-3 of the complex. ^1H NMR (CS_2): δ 6.22 (m, 1 H, H-2), 5.70 (d, 1 H, J = 7.5 Hz, H-1), 4.77 (s, 5 H, Cp), 1.92 (br d, 1.40 H, J = 9 Hz, $FpCH_2$).

Preparation of (*E*)-1-Fp-3-deuterio-3-phenylpropene (7a-*d*). To 227.4 mg (1.67 mmol) of $ZnCl_2$ in 15 mL of THF at −78 °C was added 0.64 mL of 2.4 M PhLi (1.52 mmol) solution via syringe. To the in situ generated PhZnCl was added 217.7 mg (0.72 mmol) of 50% monodeuterated **6-*d*** in 10 mL of THF via cannula, and the cold bath was removed. The reaction mixture was left to stir at ambient temperature for 48 h. After standard workup and petroleum ether extraction and filtration procedure 98.9 mg of dark red oil was isolated. This was chromatographed on a 1 mm preparative TLC plate (alumina, petroleum ether) to give, upon ether extraction of the yellow band, filtration, and solvent removal, 68.9 mg (32%) of the title compound. Integration analysis of the proton NMR spectrum shows that the product was 45 ± 5% monodeuterated in the benzylic position. IR (CH_2Cl_2): ν_{max} 2012, 1961 (CO), 1600 (Ph) cm^{-1}. ^1H NMR (CS_2): δ 7.1–6.9 (m, 5 H, Ph), 6.31 br d, 1 H, J = 18 Hz, H-1), 5.7-5.2 (m, 1 H, H-2), 4.72 (s, 5 H, Cp), 3.31 (br d, 1.55 H, J = 7.4 Hz, benzyl).

Preparation of Fp(η^2-3-bromo-3-deuterio-2-methylpropene)PF_6(13-*d*). To 809.3 mg (2.60 mmol) of **9-*Z*,*E*** in 20 mL of CH_2Cl_2 at−78 °C was added 0.24 mL (2.8 mmol) of CF_3SO_3D dropwise via syringe. The reaction mixture was stirred at −78 °C for 1 h. Ether was added to precipitate the triflate salt at −78 °C. The solid was allowed to settle, and the supernatant was removed via careful cannulation. The solid remaining was slurried into acetone at −78 °C, and 1.37 g (8.4 mmol) of NH_4PF_6 was added. In a few minutes, the slurry clarified to a clear red solution. The acetone was then stripped off in an ice bath. The resultant solid was slurried into cold distilled water and filtered. After the air-stable solid was washed with cold distilled water and air-dried, the solid was taken up into acetone and precipitated with ether. The light yellow solid was filtered, washed with ether, and air- and vacuum-dried to give 604 mg of salt, 51% overall. Proton NMR analysis showed a deuterium content of 75% at the 3-position of the olefin. IR (CH_3CN): ν_{max} 2070, 2018 cm^{-1} (CO). ^1H NMR (CD_3NO_2): δ 5.54 (s, 5 H, (Cp), 5.32 (s, 1 H, vinyl), 4.95 (q, 1 H, J = 2 Hz, vinyl), 4.10 (br s, 1.25 H, methylene), 1.72 (br s, 3 H, Me).

Preparation of 1-Bromo-1-deuterio-2-methyl-3-Fp-propene (9-*d*). To a slurry of 204 mg (0.44 mmol) of **13-*d*** in 20 mL of CH_2Cl_2 at 0 °C was added 78 μL (57.5 mg, 0.44 mmol) of diisopropylethylamine via syringe. The suspension clarified in a few minutes to a red solution. The solvent was stripped off via rotary evaporation, and the residue was taken up into ether. The organic solution was filtered through Celite and stripped, and the residue was vacuum dried. This crude sample (137 mg) was chromatographed on a preparative TLC plate (petroleum ether, 1 mm alumina), and the yellow band was scraped and extracted with ether to give upon solvent removal 83 mg of a yellow oil, 60%. Proton NMR analysis indicated that the sample was 58 ± 5% monodeuterated, and the deuterium was at C-1. The ratio of *Z*/*E* isomers, based on analysis of the ^{13}C spectrum of the product, was 2.0. IR (CH_2Cl_2): ν_{max} 2006, 1952 cm^{-1} (CO). ^1H NMR (CS_2): *Z* isomer, δ 5.51 (q, 0.43 H, J = 1 Hz, vinyl), 4.78 (s, 5 H, Cp), 2.05 (s, 2.0 H, $FpCH_2$), 1.79 (br s, 3.0 H, Me); *E* isomer, δ 5.70 (br m, 0.40 H, vinyl), 4.59 (s, 5 H, Cp), 2.16 (s, 2.0 H, $FpCH_2$), 1.79 (br s, 3 H, Me).

Preparation of (*E*)-1-Fp-2-methyl-3-phenyl-1-deuteriopropene (10a-*d*). To 188 mg (1.38 mmol) of $ZnCl_2$ in 15 mL of THF at −78 °C was added 0.6 mL (1.31 mmol) of 2.2 M PhLi via syringe. Then, 204 mg (0.66 mmol) of 80 ± 5% monodeuterated **9-*d*** in 15 mL of THF was added via cannula to the PhZnCl

solution. The cold bath was removed, and the mixture was left to stir at ambient temperature for 48 h. After the standard aqueous bicarbonate workup, 198 mg of crude material was isolated. Preparative TLC (1 mm alumina plate, petroleum ether eluent) gave 120 mg of a light yellow oil, 60% yield from the alkenyl bromide. Proton NMR integration analysis showed that the sample was 77 ± 5% deuterated in the vinyl position. As in the case of nondeuterated analogue **9**, combustion analysis was precluded by the fact that the sample decomposed on standing. Mass spectral analysis shows that the sample has a 73% deuterium content, by comparison of the M - 2CO peak intensities in the mass spectrum of the product. IR (CH_2Cl_2): ν_{max} 2010, 1958 (CO), 1600 (Ph) cm^{-1}. ^1H NMR (CS_2): δ 7.2–7.0 (m, 5 H, Ph), 6.04 (br s, 0.23 H, vinyl), 4.74 (s, 5 H, Cp), 3.40 (s, 2 H, benzyl), 1.61 (s, 3 H, Me). Mass spectrum (20 eV); *m/e* (relative intensity) 308 (M, 8.4), 280 (M - CO, 36), 252 (M - 2CO, 100), 251 (m - 2CO, 36.8).

Preparation of (*E*)-Ethyl 4-Fp-2-butenoate (15). To a slurry of 1.16 g (3.08 mmol) of Fp(η^2-ethyl 2-butenoate)BF_4[4] in 15 mL of CH_2Cl_2 at −23 °C was added 0.43 mL (3.10 mmol) of NEt_3 dropwise. The slurry became a solution in 5 min. The solvent was stripped off, and the residue was extracted into petroleum ether as much as possible. The petroleum ether extracts were filtered through Celite, and solvent was removed by rotary evaporation and vacuum drying to give 810 mg of the product as a dark oil: 93%; ^1H NMR (CS_2) δ 7.05 (dt, 1 H, J = 15, 9.2 Hz, $FpCH_2CH$), 5.37 (dt, 1 H, J = 15, 0.5 Hz, RO_2CCH), 4.70 (s, 5 H, Cp), 3.96 (q, 2 H, J = 7 Hz, OCH_2), 1.98 (d, 2 H, J = 9.2 Hz, $FpCH_2$), 1.18 (t, 3 H, J = 7 Hz, MeO). Anal. Calcd for $C_{13}H_{14}FeO_4$: C, 53.82; H, 4.86. Found: C, 53.65; H, 5.02.

Preparation of Fp(η^2-(*E*)-ethyl 4-bromo-2-butenoate) (17). To 765 mg (2.64 mmol) of **15** in 15 mL of CH_2Cl_2 at −78 °C was added 0.15 mL (2.9 mmol) of Br_2 dropwise via syringe. The mixture was stirred at −78 °C for 45 min, and then 0.36 mL (2.64 mmol) of $HBF_4 \cdot Et_2O$, was added via syringe. The cold bath was removed, and the reaction mixture was agitated by a rapid stream of Ar to remove HBr. A precipitate began to form. Ether was added to finish precipitation, and the yellow salt was filtered off and washed with ether. After air- and vacuum-drying, 969.5 mg of yellow-orange solid was obtained, 80%.

Preparation of 3-(Ethoxycarbonyl)-3-Fp-1-bromopropene (18). A suspension of 965 mg (2.11 mmol) of **17** in 10 mL of CH_2Cl_2 was cooled to 0 °C. Then, 0.37 mL (2.11 mmol) of *i*-Pr_2NEt was added dropwise, and the reaction mixture was stirred at 0 °C for 10 min. During this time, the suspension claified. The solvent was tripped off, and the residue was extracted into petroleum ether as much as possible. The petroleum ether extracts were filtered through Celite in a Schlenk tube, and the extracts were rotary evaporated and vacuum dried to give 741 mg of red oil, 95%. Proton NMR analysis showed a *Z*/*E* ratio of 3.43/1.0. IR (CH_2Cl_2): ν_{max} 2017, 1976 (CO), 1682 (C=O) cm^{-1}. ^1H NMR (CS_2): δ 6.45 (dd, 0.77 H, J = 11, 7.3 Hz, vinyl-*Z*), 6.45–6.22 (m, 0.23 H, vinyl-*E*), 5.79 (d, 0.23 H, J = 14 Hz, CHBr-*E*), 5.58 (dd, 0.77 H, J = 7.3, 1 Hz, CHBr-*Z*), 4.76 (s, 3.9 H, Cp-*Z*), 4.64 (s, 1.1 H, Cp-*E*), 3.89 (q, 2 H, J = 7 Hz, $-OCH_2$), 3.31 (dd, 0.77 H, J = 11, 1.0 Hz, FpCH-*Z*), 2.82 (d, 0.22 H, J = 9.6 Hz, FpCH-*E*), 1.16 (t, 3 H, Me). Anal. Calcd for $C_{13}H_{13}BrFeO_4$: C, 42.32; H, 3.55. Found: C, 42.31; H, 3.67.

Decomposition of Complex 17. The crotonate salt **14** (1 g) was taken up in 8 mL of CH_2Cl_2 and cooled to −40 °C. Triethylamine (0.21 g) in 2 mL of CH_2Cl_2 was added dropwise, and stirring was continued for 30 min. Bromine (0.36 g) in 2 mL of CH_2Cl_2 was then added, and reaction was continued for an additional 20 min. The solution was then allowed to come to room temperature, during which time, the color of the solution changed from yellow to dark red, indicative of the formation of FpBr. Solvent was removed, and the residue was extracted with ether and filtered through Celite. The procedure was repeated by using light petroleum ether. Solvent was removed, and the residue was distilled in a Kugelrohr at 58 °C/2 min to give 0.33 g (83%) of product as a near colorless oil: NMR (CS_2) δ 6.95 (dt, 1 H, J = 8, 15 Hz, β-CH=), 6.0 (d, 1 H, J = 15 Hz, α-CH=), 4.16 (q, 2 H, OCH_2), 4.04 (d, 2 H, CH_2Br), 1.28 (t, 3 H, CH_3).

Preparation of 4-Fp-2-bromo-2-butene (11). To a −78 °C solution of 1.18 g (5.09 mmol) of 1-Fp-2-butene in 20 mL of CH_2Cl_2 was added 0.26 mL (5.1 mmol) of Br_2 via syringe. The reaction mixture was left to stir at −78 °C for 1 h and then diluted with 5 mL of acetone. Next, solid HN_4PF_6 (2.5 g, 5.3 mmol) was added all at once. The mixture was stirred vigorously for 10 min at −78 °C, and then the solvent was stripped off. The solid residue was slurried into cold distilled water and filtered. The filter cake was washed with water and air-dried. The resultant dark yellow solid was taken up into a minimal amount of acetone and precipitation effected with ether. The yellow solid was filtered off and washed with ether until the washings were clear. The solid was then air- and vacuum-dried. This gave 1.71 g of Fp(η^2-3-bromo-1-butene)PF_6 as a yellow solid, 74%. The sample decomposed upon dissolution in CD_3NO_2 for NMR analysis. Deprotonation of this material with DBU and flash chromatogrpahy on a silica gel column of the product (15/1 cyclohexane/EtOAc) gave a 20% overall yield of product. *i*-Pr_2NEt and NEt_3 were ineffective in deprotonating the salt. ^1H NMR (CS_2): δ 5.70 (tq, 1 H, J = 8.7, 1.5 Hz, vinyl), 4.73 (s, 5 H, Cp), 2.12 (d, 3 H, J = 1.5 Hz, Me), 1.99 (d, 2 H, J = 8.7 Hz, $FpCH_2$).

Acknowledgment. This research was supported by a grant from the National Science Foundation (CHE 8117510), which is gratefully acknowledged.

Structure and Reactivity Studies of Bis(cyclopentadienyl) Ytterbium and Yttrium Alkyl Complexes Including the X-ray Crystal Structure of $(C_5H_5)_2Yb(CH_3)(THF)$[1]

William J. Evans,*[2] Raul Dominguez, and Timothy P. Hanusa

Department of Chemistry, University of California at Irvine, Irvine, California 92717

Received May 20, 1985

$(C_5H_5)_2Yb(CH_3)(THF)$ crystallizes from THF under hexane diffusion in space group $P2_1/a$, with unit cell dimensions a = 14.518 (5) Å, b = 13.063 (7) Å, c = 8.141 (2) Å, β = 105.96 (2)°, U = 1484 Å^3, and D_{calcd} = 1.747 g cm^{-3} for Z = 4. Least-squares refinement on the basis of 1825 unique observed reflections converged to a final R = 0.035. The two ring centroids, the THF oxygen atom, and the methyl carbon describe a distorted tetrahedron. The average Yb–C(ring) distance is 2.60 (2) Å, the Yb–C(methyl) distance is 2.36 (1) Å, and the Yb–O(THF) distance is 2.31 (1) Å. Comparison of the Ln–C distances in $(C_5H_5)_2Yb(CH_3)(THF)$ and the $(C_5H_5)_2LuR(THF)$ complexes (R = t-C_4H_9, CH_2SiMe_3, C_6H_4Me-4) suggests trends in steric crowding whose effects on reactivity were experimentally examined in hydrogenolysis reactions. Over 20 systems were examined in which the metal, the alkyl group, and the ring substituent in the formulas $(C_5H_4R)_2LnR'(THF)$ and $[(C_5H_4R)_2LnR']_2$ (R = H, CH_3; Ln = Y, Er, Yb, Lu; R′ = CH_3, CH_2SiMe_3, t-C_4H_9) were varied as well as the solvent. Small changes in the size of the metal, the steric crowding caused by the alkyl group, and the solvent can have dramatic effects on reactivity. Using this new reactivity data, optimum conditions for isolating ytterbium hydrides were determined and the ytterbium analogues of $[(C_5H_5)_2LnH(THF)]_2$ and $\{[(C_5H_5)_2LnH]_3H\}\{Li(THF)_4\}$ were synthesized and characterized.

The first report in the literature of the hydrogenolysis of an organolanthanide metal alkyl complex to form a molecular organolanthanide hydride compound involved ytterbium[3] (eq 1). The reaction proceeded slowly and was

$$[(CH_3C_5H_4)_2Yb(\mu\text{-}CH_3)]_2 + 2H_2 \xrightarrow{\text{toluene}} 2CH_4 + 2[(CH_3C_5H_4)_2YbH] \quad (1)$$

complicated by the fact that the trivalent ytterbium hydride was unstable with respect to divalent ytterbium species (eq 2). To avoid the Ln(III) → Ln(II) decompo-

$$[(CH_3C_5H_4)_2YbH] \rightarrow (CH_3C_5H_4)_2Yb \quad (2)$$

sition, hydrogenolysis of alkyl complexes of Lu, Er, and Y, which do not have readily accessible divalent oxidation states, were examined and provided fully characterizable hydride complexes[4] (eq 3; R = CH_3, H; Ln = Lu, Er, Y).

$$2(C_5H_4R)_2Ln(t\text{-}C_4H_9)(THF) + 2H_2 \xrightarrow{\text{toluene}} [(C_5H_4R)_2Ln(\mu\text{-}H)(THF)]_2 + 2C_4H_{10} \quad (3)$$

In the presence of lithium salts, trimeric hydride complexes of formula $\{[(C_5H_5)_2Ln(\mu\text{-}H)]_2[(C_5H_5)_2Ln(\mu\text{-}X)](\mu_3\text{-}H)\}\{Li(THF)_4\}$ (X = H, Cl) were discovered.[5] Improved syntheses of both the dimers[6] and the trimers[7] have subsequently been developed.

In the course of studying the above hydride complexes, evidence for some general principles of organolanthanide and organoyttrium reactivity has accumulated. We have recently obtained an X-ray diffraction structure of a simple lanthanide methyl complex, $(C_5H_5)_2Yb(CH_3)(THF)$, which provides benchmark structural information useful in understanding the observed reactivity. In this report, we describe the structure of the ytterbium methyl compound and the hydrogenolysis of this complex to form isolable ytterbium(III) hydride complexes. In addition, we examine further the patterns of hydrogenolysis reactivity observed earlier by studying the reaction of several lanthanide and yttrium(III) alkyl complexes with hydrogen under a variety of conditions. These studies demonstrate how small differences in the size of the metal, the size of the alkyl group, and the solvent can change reactivity substantially.

Experimental Section

The complexes described below are extremely air- and moisture-sensitive. Therefore, all syntheses and subsequent manipulations of these compounds were conducted under nitrogen with the rigorous exclusion of air and water using Schlenk, vacuum line, and glovebox (Vacuum/Atmospheres HE-553 Dri-Lab) techniques.

Materials. Toluene and THF were distilled from potassium benzophenone ketyl. THF-d_8 and benzene-d_6 were vacuum transferred from potassium benzophenone ketyl. Anhydrous ytterbium and yttrium trichlorides were prepared from the hydrates (Research Chemicals, Phoenix, Az) by the method of Taylor and Carter.[8] Hydrogen (Matheson, prep grade) was purified by passage through an Alltech Oxytrap. Deuterium (Union Carbide, CP grade) was used as received. $LiCH_2SiMe_3$ was prepared according to the literature[9] from lithium shot and $ClCH_2SiMe_3$ (Aldrich). NaC_5H_4R (R = H, CH_3) and $[(C_5H_4R)_2LnCl]_2$ were prepared as previously described.[4] Methyllithium (1.5 M in Et_2O, Aldrich) was used in the preparation of $[(C_5H_4R)_2LnCH_3]_2$ (Ln = Y, Er, Yb, Lu) according to the literature.[6] Literature procedures were followed in the preparation of $(C_5H_5)_2Ln(CH_2SiMe_3)(THF)$[10] (Ln = Y, Yb) and $(CH_3C_5H_4)_2Ln(CMe_3)(THF)$[4,11] (Ln = Y, Lu).

(1) Part 8 of the series Organolanthanide and Organoyttrium Hydride Chemistry. Part 7: Evans, W. J.; Grate, J. W., Doedens, R. J. *J. Am. Chem. Soc.* **1985**, *107*, 1671–1679.
(2) Alfred P. Sloan Research Fellow.
(3) Zinnen, H. A.; Pluth, J. J.; Evans, W. J. *J. Chem. Soc., Chem. Commun.* **1980**, 810–812.
(4) Evans, W. J.; Meadows, J. H.; Wayda, A. L.; Hunter, W. E.; Atwood, J. L. *J. Am. Chem. Soc.* **1982**, *104*, 2008–2014.
(5) Evans, W. J.; Meadows, J. H.; Wayda, A. L.; Hunter, W. E.; Atwood, J. L. *J. Am. Chem. Soc.* **1982**, *104*, 2015–2017.
(6) Evans, W. J.; Meadows, J. H.; Hunter, W. E.; Atwood, J. L. *J. Am. Chem. Soc.* **1984**, *106*, 1291–1300.
(7) Evans, W. J.; Meadows, J. H.; Hanusa, T. P. *J. Am. Chem. Soc.* **1984**, *106*, 4454–4460.
(8) Taylor, M. D.; Carter, C. P. *J. Inorg. Nucl. Chem.* **1962**, *24*, 387–391.
(9) Collier, M. R.; Lappert, M. F.; Pearce, R. *J. Chem. Soc., Dalton Trans.* **1973**, 445–451.
(10) Schumann, H.; Genthe, W.; Bruncks, N.; Pickardt J. *Organometallics* **1982**, *1*, 1194–1200.
(11) Evans, W. J.; Wayda, A. L.; Hunter, W. E.; Atwood, J. L. *J. Chem. Soc., Chem. Commun.* **1981**, 292–293.

0276-7333/86/2305-0263$01.50/0

Physical Measurements. Infrared spectra were obtained as previously described.[4] ^1H NMR spectra were recorded by using a Bruker 250 spectrometer and were referenced to residual β-methylene protons in C_4D_8O (δ 1.72) or to residual aryl protons in C_6D_6 (δ 7.15). Gas chromatographic analyses were performed on a Hewlett-Packard 5830A thermal conductivity gas chromatograph equipped with a 6 ft. × $^1/_2$ in. column of 4A molecular sieves pulverized to 40/60 mesh. Complete elemental analyses were obtained from Analytische Laboratorien, Engelskirchen, Germany. Complexometric analyses were obtained as previously described.[12] GC/MS data were collected on a Finnigan 4000 mass spectrometer equipped with a gas inlet system.

$[(C_5H_5)_2YbCH_3]_2$. This modification of the original preparation of this compound[13] is included since slight variations in procedure can alter the purity of the product, particularly with respect to the presence of LiCl. In the glovebox, a 500-mL Schlenk flask was charged with $[(C_5H_5)_2YbCl]_2$ (3.135 g, 4.63 mmol), 75 mL of THF, and a magnetic stirring bar and attached to an addition funnel containing CH_3Li (7.8 mL of 1.5 M solution in Et_2O, 11.7 mmol). The apparatus was removed to a double manifold and the Schlenk flask cooled to −78 °C. The CH_3Li solution was added dropwise over 10 min, and the stirred solution was allowed to warm to room temperature overnight. The apparatus was returned to the glovebox, and the solvent was removed by rotary evaporation. The resulting orange oil was extracted with toluene (50 mL) and filtered. Removal of solvent from the filtrate gave an orange solid which was subsequently extracted with 50 mL of toluene heated to boiling. This solution was filtered hot and reduced in volume to ca. 10 mL by rotary evaporation. Hexane was layered over the toluene solution which was then cooled to −20 °C overnight. Bright orange crystals of $[(C_5H_5)_2YbCH_3]_2$ were isolated by filtration (1.01 g, 34%). Anal. Calcd for $YbC_{11}H_{13}$: Yb, 54.40; Li, 0.00; Cl, 0.00. Found: Yb, 54.3; Li, <0.01; Cl, <0.1. IR (KBr): 3110 (m), 3080 (m), 2890 (w), 1440 (m), 1270 (m), 1190 (m), 1010 (s), 935 (m), 880 (w), 790 (s), 775 (s) cm^{-1}.

Extraction of the crude reaction product with hot toluene as described above appears to be crucial for removing all LiCl.[6] We have extracted the crude product, i.e., the orange oil described above, with toluene at 32 °C, filtered the solution, reduced the solution to dryness, and repeated the entire ambient-temperature extraction process two more times only to find a product containing at least 0.24% Li (equivalent to 1:7 $Li/(C_5H_5)_2YbCH_3$). Centrifugation of these ambient-temperature toluene extracts removes some but not all lithium contaminants from these solutions.

$(C_5H_5)_2Yb(CH_3)(THF)$. Dissolution of $[(C_5H_5)_2YbCH_3]_2$ in THF gives an auburn-orange solution. Crystals of $(C_5H_5)_2Yb(CH_3)(THF)$ can be obtained from this solution by layering hexane on the THF and cooling to −20 °C for approximately 2 days. Orange plates suitable for X-ray diffraction were obtained in this way.

X-ray Crystallography of $(C_5H_5)_2Yb(CH_3)(THF)$. General procedures used in data collection and reduction have been previously described.[14] A single crystal measuring approximately 0.39 × 0.04 × 0.49 mm was sealed in a glass capillary under N_2 and mounted on a Syntex $P2_1$ diffractometer. Lattice parameters were determined at 24 °C from the angular settings of 15 computer-centered reflections with $5° < 2\theta < 22°$. Pertinent crystal and data collection parameters for the present study are given in Table I. Systematic absences ($0k0$, k odd; $h0l$, h odd) uniquely defined the monoclinic space group as $P2_1/a$ (nonstandard setting of $P2_1/c$, no.14). During the data measurement, the intensities of three standard reflections monitored every 100 reflections decreased linearly by 4%; the intensities of the data set were later corrected for the decay. An analytical absorption correction was applied, but corrections for extinction were not made. A combination of Patterson and difference Fourier techniques provided the locations of all non-hydrogen atoms, which were refined with anisotropic thermal paramaters using full-matrix least-squares methods. A total of seven hydrogen atoms, including the three belonging to the methyl group, were identified on a difference map. The rest were included in calculated positions (C–H = 0.95 Å); none were refined. The largest peak in a final difference map had a height of 1.66 e Å^{-3} and was 1.15 Å from the ytterbium atom; there were minima of 4.5 e Å^{-3} at 8.8 and 9.0 Å from the metal. Final fractional coordinates are given in Table II.

Table I. Crystal Data for $(C_5H_5)_2Yb(CH_3)(THF)$

formula	$C_{15}H_{21}OYb$
fw	390.37
space group	$P2_1/a$
a, Å	14.518 (5)
b, Å	13.063 (7)
c, Å	8.141 (2)
β, deg	105.96 (2)
V, Å^3	1484 (1)
Z	4
D_{calcd}, g/cm^{-3}	1.747
temp, °C	24
λ (Mo K$\bar{\alpha}$), Å	0.710 73; graphite monochromator
μ, cm^{-1}	62.7
min–max transmissn coeff	0.373–0.888
type of scan	θ–2θ
scan width, deg	−1.2 in 2θ from Kα_1 to +1.2 from Kα_2
scan speed, deg/min	2–12, variable
bkgd counting	evaluated from 96-step peak profile
data collecn range	$0° \le 2\theta \le 50°$
total unique data	2597
unique data with $I \ge 3.0\sigma(I)$	1825
no. of parameters	154
$R(F)$	0.035
$R_w(F)$	0.044
GOF	1.387
max Δ/σ in final cycle	0.02

Table II. Fractional Coordinates and Their Estimated Errors for $(C_5H_5)_2Yb(CH_3)(THF)$

atom	x	y	z
Yb	0.19972 (2)	0.40480 (3)	0.20518 (4)
O	0.3376 (4)	0.3941 (5)	0.4290 (7)
C(11)	0.1351 (12)	0.2274 (10)	0.2617 (29)
C(12)	0.1424 (9)	0.2757 (14)	0.4017 (19)
C(13)	0.0789 (14)	0.3514 (13)	0.3730 (25)
C(14)	0.0308 (8)	0.3494 (16)	0.2036 (31)
C(15)	0.0664 (20)	0.2671 (20)	0.1388 (19)
C(21)	0.3062 (9)	0.4757 (13)	0.0194 (14)
C(22)	0.3156 (11)	0.3718 (16)	0.0165 (18)
C(23)	0.2264 (13)	0.3319 (11)	−0.0753 (18)
C(24)	0.1661 (9)	0.4163 (12)	−0.1273 (13)
C(25)	0.2167 (8)	0.5018 (10)	−0.0668 (13)
C(32)	0.3514 (8)	0.4510 (12)	0.5877 (14)
C(33)	0.4427 (9)	0.4253 (14)	0.6894 (15)
C(34)	0.4700 (10)	0.3279 (14)	0.6318 (17)
C(35)	0.4107 (8)	0.3161 (9)	0.4520 (15)
C(41)	0.1614 (9)	0.5715 (9)	0.2776 (15)

$[(C_5H_5)_2YbH(THF)]_2$.[15] In a 250-mL flask equipped with a high vacuum Teflon stopcock and a Teflon stirring bar, $[(C_5H_5)_2YbCH_3]_2$ (0.351 g, 0.552 mmol) was dissolved in 30 mL of dimethoxyethane to yield a dark amber solution. The flask was attached to a vacuum line, cooled to −196 °C, and evacuated. Hydrogen was admitted to the flask, and the vessel was warmed to room temperature. When the hydrogen pressure was 1 atm, the flask was sealed. The solution was vigorously stirred for 24 h during which time the solution became paler and a fine orange powder was deposited. The solid was collected by filtration and washed with 10 mL of toluene followed by 10 mL of hexane giving

(12) Atwood, J. L.; Hunter, W. E.; Wayda, A. L.; Evans, W. J. *Inorg. Chem.* **1981**, *20*, 4115–4119.
(13) Ely, N. M.; Tsutsui, M. *Inorg. Chem.* **1975**, *14*, 2680–2687.
(14) Sams, D. B.; Doedens, R. J. *Inorg. Chem.* **1979**, *18*, 153–156.
(15) This complex is tentatively formulated as a dimer in analogy to the crystallographically characterized complexes $[(CH_3C_5H_4)_2LnH(THF)]_2$ (Ln = Er, Y)[4] and the complex $[(C_5H_5)_2YH(THF)]_2$ whose dimeric structure in solution was established by ^{89}Y–^1H coupling in the ^1H and ^{89}Y NMR spectra.[4,16] Proof of the dimeric nature of the ytterbium complex is difficult to obtain since the usual, isopiestic analysis[12] is not possible due to decomposition in solution, NMR spectroscopy of the paramagnetic complex is uninformative in this regard, and desolvation of the complex has precluded X-ray structure analysis.
(16) Evans, W. J.; Meadows, J. H.; Kostka, A. G.; Closs, G. L. *Organometallics* **1985**, *4*, 324–326.

an orange powder (0.226 g, 52%).[17] The DME-insoluble orange powder slowly dissolved in THF to give a yellow solution. Recrystallization by hexane diffusion into a saturated THF solution yielded small yellow plates of the THF adduct $[(C_5H_5)_2YbH(THF)]_2$.[15] Anal. Calcd for $YbC_{14}H_{19}O$: Yb, 46.01. Found: Yb, 45.70. ^1H NMR (THF-d_8): δ 0.4 (br s, $w_{1/2}$ = 50 Hz, C_5H_5). IR (KBr): 3090 (m), 2965 (m), 2880 (m), 1440 (m), 1350 (v br), 1060 (w), 1030 (sh), 1010 (s), 930 (m), 865 (s), 770 (sh), 770 (vs), 775 (s) cm^{-1}. Freshly recrystallized $[(C_5H_5)_2YbH(THF)]_2$ (0.074 g, 0.20 mmol of monomer) was decomposed with H_2O in a Toepler pump system to give H_2 (4.4 mL, 0.20 mmol) which was identified by GC.

$[(C_5H_5)_2YbD(THF)]_2$.[15] Following the procedure described above, $[(C_5H_5)_2YbCH_3]_2$ (112 mg, 0.18 mmol) was treated with D_2 to form the analogous deuteride in approximately 48% yield. The initial product of the hydrogenolysis was recrystallized from THF. IR (KBr): 3100 (m), 2950 (m), 2880 (m), 1440 (w), 1020 (sh w), 1010 (s), 920 (m br, sh), 870 (s), 770 (vs) cm^{-1}.

Decomposition of $[(C_5H_5)_2YbH(THF)]_2$. This ytterbium hydride complex desolvates readily in the glovebox (cf. the facile desolvation of $[(C_5H_5)_2LuH(THF)]_2$[4]) and decomposes in THF within 48 h to form $(C_5H_5)_2Yb(THF)$. This decomposition could be followed by ^1H NMR spectroscopy by monitoring the disappearance of the broad 0.4 ppm C_5H_5 resonance of the hydride complex and the growth of the 5.8 ppm C_5H_5 resonance of $(C_5H_5)_2Yb(THF)$.[18]

$\{[(C_5H_5)_2YbH]_3H\}\{Li(THF)_4\}$. (a) In a 250-mL flask equipped with a high vacuum Teflon stopcock and a Teflon stirring bar, a sample of $[(C_5H_5)_2YbCH_3]_2$ (0.765 g, 0.377 mmol) prepared without hot toluene extraction and containing a trace of LiCl (approximately 1:7 LiCl/Yb) was dissolved in a mixture of 45 mL of diethyl ether and 9 mL of hexane yielding a dark amber solution. The flask was attached to a vacuum line, cooled to −196 °C, and evacuated. An atmospheric pressure of H_2 was established as described above, and the vessel was sealed. The solution was stirred vigorously for 8 days over which time a yellow powder was slowly deposited. The solid was collected by filtration and was washed first with 10 mL of diethyl ether followed by 10 mL of hexane. A bright yellow powder (0.472 g, 65% based on a precursor formula of $[(C_5H_5)_2YbCH_3]_7LiCl$) was isolated. Recrystallization by hexane diffusion into THF yielded long transparent yellow needles. These crystals became opaque and brittle after 30 min under nitrogen presumably due to desolvation (cf. the ready desolvation of $\{[(C_5H_5)_2LuH]_3H\}\{Li(THF)_4\}$[5]). The IR spectrum of a freshly recrystallized sample indicated the presence of THF but the elemental analysis was consistent with a desolvated sample. Anal. Calcd for the desolvate $C_{30}H_{34}LiYb_3$: C, 39.13; H, 3.70; Li, 0.76; Yb, 56.41. Found: C, 38.71; H, 4.25; Li, 0.57; Yb, 55.70. IR (KBr): 3090 (w), 2960 (m), 2880 (m), 1440 (w), 1350 (m), 1210 (vs), 1120 (w), 1035 (m), 1010 (s), 880 (s), 770 (vs), 730 (m), 685 (m) cm^{-1}. ^1H NMR (THF-d_8): δ 23 (s, C_5H_5). Freshly recrystallized $\{[(C_5H_5)_2YbH]_3H\}\{Li(THF)_4\}$ (0.031 g, 0.026 mmol) was decomposed with H_2O in a Toepler pump system to give H_2 (2.49 mL, 0.111 mmol, 94%) identified by GC.

(b) In the glovebox, $[(C_5H_5)_2YbH(THF)]_2$ (100 mg, 0.13 mmol) was suspended in DME (10 mL) in an Erlenmeyer flask. Solid t-C_4H_9Li (7 mg, 0.109 mmol) was added to the solution causing a vigorous reaction to occur with formation of a yellow solid and a green solution. Toluene (10 mL) was added to the solution, and the yellow precipitate was isolated by filtration. Recrystallization by slow hexane diffusion into a saturated THF solution gave bright yellow plates of $\{[(C_5H_5)_2YbH]_3H\}\{Li(THF)_4\}$ (50 mg, 47%) identical with the hydride product described above by IR and ^1H NMR. The green solution was identified to contain $(C_5H_5)_2Yb(DME)$[19] by ^1H NMR spectroscopy.[11]

$\{[(C_5H_5)_2YbD]_3D\}\{Li(THF)_4\}$. In a manner analogous to (a) above, this substance was obtained as a yellow powder in 37% yield after 6 days under deuterium gas. It was recrystallized by hexane diffusion into a saturated THF solution. ^1H NMR (THF-d_8): δ 23 (s, C_5H_5). IR (KBr): 3090 (w), 2970 (m), 2950 (m), 2880 (m), 1440 (w), 1035 (m), 1010 (s), 965 (m), 880 (s), 850 (sh m), 775 (vs), 730 (s) cm^{-1}. The complex was also prepared by route b above in 40% yield.

Decomposition of $\{[(C_5H_5)_2YbH]_3H\}\{Li(THF)_4\}$. The decomposition of this hydride to $(C_5H_5)_2Yb(THF)$ in THF was also followed by ^1H NMR spectroscopy. The decomposition half-life was found to be approximately 50 days.

$(C_5H_5)_2Y[CH_2Si(CH_3)_3](THF)$. In a Schlenk flask equipped with a magnetic stirring bar, YCl_3 (6.493 g, 33.25 mmol) was suspended in 100 mL of THF. Over 5 min NaC_5H_5 (5.848 g, 66.439 mmol) was added. After being stirred for $^1/_2$ h, the solution was cooled to −78 °C, and $LiCH_2Si(CH_3)_3$ (3.146 g, 33.41 mmol) in 30 mL of hexane was added dropwise. The mixture was allowed to warm to room temperature over several hours and then filtered. Solvent was removed from the filtrate by rotary evaporation to give an oil. This oil was twice extracted with 50 mL of room-temperature toluene, filtered, and rotary evaporated to dryness. The pale yellow solid was recrystallized by diffusing hexane into a saturated toluene solution to yield large clear and colorless hexagonal prisms (3.321 g, 33% based on YCl_3). ^1H NMR (THF-d_8): δ 6.37 (s, C_5H_5), −0.05 (s, $CH_2Si(CH_3)_3$), −0.93 (d, $CH_2Si(CH_3)_3$, J = 3.2 Hz). ^1H NMR (benzene-d_6): δ 6.12 (s, C_5H_5) 3.00 (m, THF), 0.95 (m, THF), 0.42 (s, $CH_2Si(CH_3)_3$), −0.66 (d, J = 2.6 Hz, CH_2SiMe_3). IR (KBr): 3080 (w), 2940 (s), 2880 (m), 1440 (w), 1247 (m), 1233 (s), 1010 (s), 905 (m), 860 (s), 780 (vs), 770 (vs), 715 (w), 660 (w) cm^{-1}. Single crystals are orthorhombic with a = 17.39 (1) Å, b = 12.37 (4) Å, c = 9.23 (5) Å, and U = 1986 (2) Å^3 and are isomorphous with $(C_5H_5)_2Lu(CH_2SiMe_3)(THF)$.[10]

$(CH_3C_5H_4)_2Y[CH_2Si(CH_3)_3](THF)$. This substance is synthesized as described above. After the second toluene extraction, the product is isolated in 55% yield based on YCl_3. ^1H NMR (benzene-d_6): δ 6.00 (s, 8, $CH_3C_5H_4$), 3.03 (m, 4, THF), 2.15 (s, 7, $CH_3C_5H_4$), 0.97 (m, 4, THF), 0.45 (s, 9, $CH_2Si(CH_3)_3$), −0.75 (d, J = 3.4 Hz, CH_2SiMe_3). THF assignments were verified by exchanging the THF with THF-d_8 and retaking the spectrum. IR (KBr): 3090 (w), 2840 (m), 2880 (m), 1443 (m), 1387 (m), 1265 (m), 1020 (s), 830 (w), 820 (s), 760 (vs) cm^{-1}.

Hydrogenolysis Experiments. Procedure. The following standardized procedure was used in the hydrogenolysis studies of the $(C_5H_4R)_2LnX$ (R = H, CH_3; Ln = Y, Er, Yb, Lu; X = CH_3, $CH_2Si(CH_3)_3$, $C(CH_3)_3$) compounds. The yttrium or lanthanide alkyl precursor (50–100 mg) was dissolved in 10 mL of the desired solvent system and placed into a tube of approximate volume 90 mL fitted with a high vacuum greaseless stopcock and a stirring bar. The flask was connected to a vacuum line, cooled to −196 °C, and evacuated. Hydrogen was admitted to the flask, and the vessel was warmed to room temperature. When the hydrogen pressure was 1 atm, the flask was sealed and the solution was stirred. After the desired interval of reaction time, the solids were isolated by filtration and washed with 10 mL of hexane, dried, and weighed. For those cases in which solids were not deposited, IR and/or NMR spectroscopy was used to detect the presence of hydrides or decomposition products in the reaction solutions. The results are given in Table III.

Identification of Products. For reactions carried out in THF, the $[(C_5H_4R)_2LnH(THF)]_2$ products (R = H, CH_3; Ln = Y, Lu) were identified by their IR and ^1H NMR spectra.[4] $[(C_5H_5)_2ErH(THF)]_2$ was identified by IR spectroscopy.[4] For yttrium reactions run in DME, the presence of a dimeric hydride product was indicated by the characteristic broad ν_{Y-H} IR absorption in the 1300 cm^{-1} region of the powdery product. IR (KBr): 3100 (m), 2950 (m), 2890 (w), 2720 (w), 1470 (m), 1447 (m), 1310 (s br), 1175 (s), 1090 (m), 1040 (m), 1010 (m), 860 (m), 780 (s), 670 (m) cm^{-1}. The DME-insoluble products were then dissolved in THF to give a ^1H NMR spectrum characteristic of DME and $[(C_5H_5)_2Y(\mu\text{-}H)(L)]_2$ (L = THF or DME). The Y-H-Y triplet due to ^{89}Y-^1H coupling was observed in the usual region.[4] ^1H NMR (THF-d_8): δ 6.07 (s, 10, C_5H_5), 3.39 (s, 4, $(CH_3OCH_2)_2$), 3.23 (s, 6, $(CH_3OCH_2)_2$), 2.18 (t, J = 20 Hz, 1, Y-H-Y). Hydrogenolysis reactions in dioxane gave a white powdery product with a broad IR absorption in the 1300 cm^{-1} region. $[(C_5H_5)_2YH(dioxane)]_2$: IR (KBr) 3100 (m), 2970 (m), 2940 (m), 2870 (m), 2640 (w), 2620 (w), 1640 (w), 1460 (m), 1450 (m), 1300 (s), 1260 (s), 1120 (s), 1065 (s), 1010 (s), 970 (w), 890 (s), 880 (s), 850 (m), 820 (s), 770 (vs),

(17) This yield assumes that the product is a DME solvate, $[(C_5H_5)_2YbH(DME)]_2$, analogous to the yttrium system described later.

(18) Calderazzo, F.; Pappalardo, R.; Losi, S. *J. Inorg. Nucl. Chem.* **1966**, 28, 987–999.

(19) Deacon, G. B.; MacKinnon, P. I.; Hambley, T. W.; Taylor, J. C. *J. Organomet. Chem.* **1983**, *259*, 91–97.

Table III. Hydrogenolysis Results[a]

expt	substr[a]	solv	reactn time, h	% yield of hydride product[b]
1	$(Cp_2YCH_3)_2$	toluene	168	0
2	$(Cp_2YCH_3)_2$	toluene/THF = 10	40	85
3	$(Cp_2YCH_3)_2$	THF	39	60
4	$(Cp_2YCH_3)_2$	DME	24	80
5	$(Cp_2YCH_3)_2$	dioxane	24	30
6	$(Cp'_2YCH_3)_2$	hexane/THF = 10	34	85
7	$(Cp'_2YCH_3)_2$	THF	36	50
8	$Cp_2Y(CH_2SiMe_3)(THF)$	toluene	72	70
9	$Cp_2Y(CH_2SiMe_3)(THF)$	THF	120	50
10	$Cp_2Y(t\text{-Bu})(THF)$	toluene	24	70
11	$Cp_2Y(t\text{-Bu})(THF)$	THF	24	0
12	$(Cp_2ErCH_3)_2$	toluene/THF = 10	48	85
13	$(Cp_2ErCH_3)_2$	THF	24	55
14	$[Cp_2YbCH_3]_2$	toluene	72	0
15	$[Cp_2YbCH_3]_2$	THF	24	0
16	$[Cp_2YbCH_3]_2$	THF	336	20
17	$[Cp_2YbCH_3]_2$	DME	24	52
18	$Cp_2Yb(CH_2SiMe_3)(THF)$	THF	96	0
19	$Cp_2Yb(CH_2SiMe_3)(THF)$	DME	72	0
20	$(Cp_2LuCH_3)_2$	toluene	24	0
21	$(Cp_2LuCH_3)_2$	toluene/THF = 10	40	0
22	$(Cp_2LuCH_3)_2$	THF	24	6
23	$(Cp_2LuCH_3)_2$	DME	24	10

[a] Cp = C_5H_5; Cp′ = $CH_3C_5H_4$. [b] $[(C_5H_4R)_2LnH(ether)_n]_2$ (R = H, CH_3; Ln = Y, Er, Yb, Lu).

640 (s), 610 (s) cm^{-1}; ^1H NMR (THF-d_8) δ 5.92 (s, 10, C_5H_5), 3.61 (s, 10, dioxane), 2.05 (br m, H, a clean triplet was not resolved possibly due to exchange of THF for dioxane on the NMR time scale).

Characterization of Some Incomplete Reactions. $[(C_5H_5)_2LuCH_3]_2$ (70 mg, 0.109 mmol) in 10 mL of toluene was reacted with H_2 for 24 h as described above. No precipitated $[(C_5H_5)_2LuH(THF)]_2$ was observed in this time period. The transparent solution was reduced to dryness by rotary evaporation and the resulting solid identified as starting material by ^1H NMR spectroscopy. A reaction on the same scale was run in THF. The ^1H NMR spectrum of the product contained primarily starting materials plus resonances of $[(C_5H_5)_2LuH(THF)]_2$ accounting for an approximately 6% yield.

Hydrogenolysis of $[(C_5H_5)_2LuCH_3]_2$ (66 mg, 0.103 mmol) was also carried out for 24 h in 10 mL of DME. Addition of 20 mL of toluene generated a white precipitate which was collected by filtration, recrystallized from THF, and identified by ^1H NMR spectroscopy as $[(C_5H_5)_2LuH(THF)]_2$ (8 mg, 10%). The remaining solution was reduced to dryness and examined by ^1H NMR spectroscopy which revealed it to be composed of starting material.

Reaction of H_2 with $[(C_5H_5)_2YbCH_3]_2$ (90 mg, 0.142 mmol) in 10 mL of THF for 24 h did not change the appearance of the dark auburn solution. Rotary evaporation of the solution gave an orange solid which had the IR spectrum of the starting material.

Reaction of H_2 with $[(C_5H_5)_2YbCH_3]_2$ (136 mg, 0.214 mmol) in 10 mL of THF for 336 h formed a yellow precipitate (30 mg, 20%) and a purple solution. The precipitate was identified as $[(C_5H_5)_2YbH(THF)]_2$ by IR spectroscopy. The purple solution was reduced to dryness and identified as $(C_5H_5)_2Yb(THF)$ by IR and ^1H NMR spectroscopy.

Results and Discussion

Synthesis of $(C_5H_5)_2Yb(CH_3)(THF)$. A standard method for preparing bis(cyclopentadienyl) lanthanide methyl complexes is the ionic metathesis reaction shown in eq 4.[6,10,13,20,21] Separation of the LiCl byproduct can

$$[(C_5H_5)_2LnCl]_2 + 2CH_3Li \xrightarrow{THF} [(C_5H_5)_2Ln(CH_3)]_2 + 2LiCl \quad (4)$$

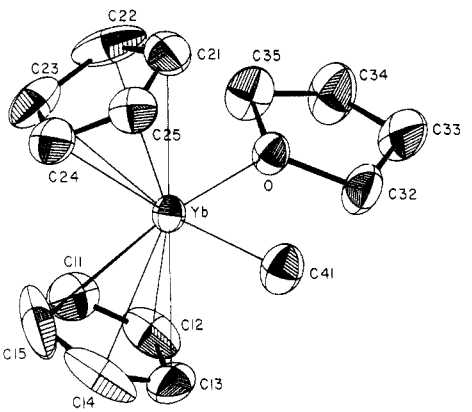

Figure 1. ORTEP view of $(C_5H_5)_2Yb(CH_3)(THF)$ with the atom-numbering scheme used in the tables. Thermal ellipsoids are drawn at the 35% probability level.

be achieved by removing the THF solvent, extracting the soluble methyl complex into toluene, and filtering off the insoluble LiCl. Although room-temperature extraction removes a large percentage of lithium as LiCl, some lithium is carried along into the toluene, possibly as an adduct such as $(C_5H_5)_2Ln(\mu\text{-}CH_3)(\mu\text{-}Cl)Li(THF)_x$, a structural type which has ample precedent in the literature.[22-28] In general, we find that even after three cycles of extracting with toluene at room temperature, filtering, removing the toluene, and reextracting with toluene, residual lithium may persist. We find it essential to extract the methyl product with hot toluene (or at least to heat the toluene extract solution) to remove all detectable lithium. Since for yt-

(20) Evans, W. J. In "The Chemistry of the Metal-Carbon Bond"; Hartley, F. R., Patai, S., Eds.; Wiley: New York, 1982; Chapter 12, pp 489–537.

(21) See also: Holton, J.; Lappert, M. F.; Ballard, D. G. H.; Pearce, R.; Atwood, J. L.; Hunter, W. E. *J. Chem. Soc., Dalton Trans.* **1979**, 54–61.

(22) Atwood, J. L.; Hunter, W. E.; Rogers, R. D.; Holton, J.; McMeeking, J.; Pearce, R.; Lappert, M. F. *J. Chem. Soc., Chem. Commun.* **1978**, 140–142.

(23) Wayda, A. L.; Evans, W. J. *Inorg. Chem.* **1980**, *19*, 2190–2191.

(24) Watson, P. L. *J. Chem. Soc., Chem. Commun.* **1980**, 652–653.

(25) Tilley, T. D.; Andersen, R. A. *Inorg. Chem.* **1981**, *20*, 3267–3270.

(26) Watson, P. L.; Whitney, J. F.; Harlow, R. L. *Inorg. Chem.* **1981**, *20*, 3271–3278.

(27) Lappert, M. F.; Singh, A.; Atwood, J. L.; Hunter, W. E. *J. Chem. Soc., Chem. Commun.* **1981**, 1191–1193.

(28) Schumann, H.; Lauke, H.; Hahn, E.; Heeg, M. J.; van der Helm, D. *Organometallics* **1985**, *4*, 321–324.

Table IV. Bond Distances (Å) in $(C_5H_5)_2Yb(CH_3)(THF)$

Yb	O	2.311 (6)
Yb	C(41)	2.362 (11)
Yb	C(11)	2.588 (12)
Yb	C(12)	2.613 (11)
Yb	C(13)	2.598 (11)
Yb	C(14)	2.553 (12)
Yb	C(15)	2.588 (13)
Yb	C(21)	2.612 (10)
Yb	C(22)	2.607 (11)
Yb	C(23)	2.600 (11)
Yb	C(24)	2.620 (10)
Yb	C(25)	2.621 (10)
Yb	cntrd 1	2.399
Yb	cntrd 2	2.336
C(11)	C(12)	1.281 (20)
C(11)	C(15)	1.310 (26)
C(12)	C(13)	1.328 (22)
C(13)	C(14)	1.364 (23)
C(14)	C(15)	1.360 (27)
C(21)	C(25)	1.340 (16)
C(21)	C(22)	1.365 (22)
C(22)	C(23)	1.405 (22)
C(23)	C(24)	1.399 (17)
C(24)	C(25)	1.353 (17)
C(32)	C(33)	1.397 (16)
C(32)	O	1.456 (12)
C(33)	C(34)	1.448 (21)
C(34)	C(35)	1.488 (15)
C(35)	O	1.446 (11)

terbium, $[(C_5H_4R)_2Yb(CH_3)]_2$ complexes (R = H, CH_3) can thermally decompose to divalent $(C_5H_4R)_2Yb$ compounds[3] or in the presence of THF to species such as $[(C_5H_4R)_2Yb(OCH{=}CH_2)]_2$,[29] the material in the final hot toluene extract must be recrystallized before use.

X-ray Crystal Structure of $(C_5H_5)_2Yb(CH_3)(THF)$ (I). Although a number of bis(cyclopentadienyl) organolanthanide and organoyttrium alkyl complexes have been crystallographically characterized, including $[(C_5H_5)_2Ln(\mu\text{-}CH_3)]_2$ (Ln = Yb, Y),[21] $(C_5H_5)_2Er(\mu\text{-}CH_3)_2Li(TMEDA)$[28] (TMEDA = $Me_2NCH_2CH_2NMe_2$), $(C_5H_5)_2Lu(t\text{-}C_4H_9)(THF)$[11] (II), $(C_5H_5)_2Lu(CH_2SiMe_3)(THF)$[10] (III), and $(C_5H_5)_2Lu(C_6H_4CH_3\text{-}4)(THF)$[10] (IV), no crystal studies of a simple solvated bis(cyclopentadienyl) methyl complex, $(C_5H_5)_2Ln(CH_3)(THF)$, have previously been reported.[30,31] Since the $(C_5H_5)_2Ln(CH_3)(THF)$ complexes are common precursors to a variety of organolanthanide complexes,[6,12,32-34] full characterization of this class was desirable.

Single crystals of $(C_5H_5)_2Yb(CH_3)(THF)$ (I), obtained by diffusing hexane into a THF solution at 0 °C, crystallize in space group $P2_1/a$. Figure 1 illustrates the molecular structure of I, and Table IV gives the important bond distances and angles. As in II, III, and IV, the two cyclopentadienyl ring centroids, the THF oxygen atom, and the alkyl carbon coordinate to the metal in I in a roughly tetrahedral fashion. The structure is typical of bent metallocene species which contain two additional ligands.[35,36]

Table V. Selected Bond Angles (deg) in $(C_5H_5)_2Yb(CH_3)(THF)$

O	Yb	C(41)	94.1 (3)
Yb	O	C(32)	123.2 (6)
Yb	O	C(35)	126.2 (6)
O	Yb	cntrd 1	99.2
O	Yb	cntrd 2	107.5
C(41)	Yb	cntrd 1	95.2
C(41)	Yb	cntrd 2	106.7
cntrd 1	Yb	cntrd 2	143.7
C(12)	C(11)	C(15)	110.1 (16)
C(11)	C(12)	C(13)	109.1 (14)
C(12)	C(13)	C(14)	107.5 (15)
C(15)	C(14)	C(13)	105.3 (15)
C(11)	C(15)	C(14)	107.9 (13)
C(25)	C(21)	C(22)	109.3 (12)
C(21)	C(22)	C(23)	107.2 (11)
C(24)	C(23)	C(22)	106.1 (13)
C(25)	C(24)	C(23)	108.0 (12)
C(21)	C(25)	C(24)	109.4 (12)
C(32)	C(33)	C(34)	108.6 (11)
C(33)	C(34)	C(35)	105.9 (11)
C(35)	O	C(32)	109.1 (8)

The orientation of the THF ring with respect to the cyclopentadienyl rings and methyl group can be described by some dihedral angles involving the best least-squares "plane" of the five atoms in the THF ring. The THF "plane" makes an 85° angle with the plane defined by the two cyclopentadienyl ring centroids and the ytterbium atom; i.e., it is almost perpendicular. The plane defined by the methyl carbon atom, ytterbium, and the THF oxygen atom also makes a near perpendicular (90.7°) angle with the centroid–Yb–centroid plane. The THF ring is tipped to avoid being coplanar with the methyl group as evidenced by the dihedral angle of 16.9° between the THF "plane" and the methyl carbon–Yb–THF oxygen plane.

The average ytterbium–cyclopentadienyl carbon distance, 2.60 (2) Å, is similar to that found in the ytterbium complexes $[(C_5H_5)_2Yb(\mu\text{-}CH_3)]_2$[21] (V), 2.613 (13) Å, and $[(CH_3C_5H_4)_2Yb(\mu\text{-}Cl)]_2$,[37] 2.585 (7) Å. Taking into account that trivalent ytterbium is 0.008[38]–0.01[39] Å larger than trivalent lutetium, the average Yb–C(η^5) distance in I is also very similar to those found in III, 2.61 (3) Å, and IV, 2.59 (3) Å. The analogous average in $(C_5H_5)_2Lu(t\text{-}C_4H_9)(THF)$, 2.63 (2) Å, is slightly larger as previously noted.[11] The ytterbium–oxygen (THF) distance in I, 2.31 (1) Å, is similar to the analogous metal–oxygen (THF) distance in II, 2.31 (2) Å, III, 2.288 (10) Å, and IV, 2.265 (28) Å.

The most interesting distance in the structure of I is the Yb–C methyl distance of 2.36 (1) Å. The ytterbium-bridging methyl carbon distances in $[(C_5H_5)_2Yb(\mu\text{-}CH_3)]_2$, 2.486 (17) and 2.536 (17) Å, are considerably longer as expected for a bridging alkyl compared to the identical terminal alkyl. The Yb–(μ-CH_3) distances in $(C_5H_5)_2Yb(\mu\text{-}CH_3)_2Al(CH_3)_2$,[40] 2.562 (18) and 2.609 (2) Å, are also longer as expected. The Er–, Ho–, and Lu–(μ-CH_3) dis-

(29) Evans, W. J.; Dominguez, R.; Hanusa, T. P., submitted for publication.

(30) The structure of the *pentamethylcyclopentadienyl* derivative $(C_5Me_5)_2Nd[CH(SiMe_3)_2]$ has been communicated: Mauermann, H.; Swepston, P. N.; Marks, T. J. *Organometallics* **1985**, *4*, 200–202.

(31) ORTEP plots of structures of the *pentamethylcyclopentadienyl* derivatives $(C_5Me_5)_2Yb(CH_3)(Et_2O)$ and $(C_5Me_5)_2Yb(CH_3)(THF)$ have been released, but details of the structural analysis have not been reported: Watson, P. L.; Herskovitz, T. *ACS Symp. Ser.* **1983**, *No. 212*, 459–479.

(32) Evans, W. J.; Wayda, A. L. *J. Organomet. Chem.* **1980**, *202*, C6–C8.

(33) Marks, T. J.; Ernst, R. D. In "Comprehensive Organometallic Chemistry"; Wilkinson, G., et al., Eds.; Pergamon Press: New York, 1982; Vol. 3, Chapter 21.

(34) Evans, W. J. *Adv. Organomet. Chem.* **1985**, *24*, 131–177.

(35) Lauher, J. W.; Hoffmann, R. *J. Am. Chem. Soc.* **1976**, *98*, 1729–1742 and references therein.

(36) The thermal parameters of the cyclopentadienyl carbons are relatively large, reflecting either a slight disorder or considerable thermal motion. Such libration of cyclopentadienyl rings is fairly common in organometallic complexes, as exemplifed in the structures of $(C_5H_5)_2M$ compounds. See: Sailer, P.;Dunitz, J. D. *Acta Crystallogr., Sect. B: Struct. Crystallogr. Cryst. Chem.* **1979**, *B35*, 1068–1074.

(37) Baker, E. C.; Brown, L. D.; Raymond, K. N. *Inorg. Chem.* **1975**, *14*, 1376.

(38) Shannon, R. D. *Acta Crystallogr., Sect. A: Cryst. Phys., Diffr., Theor. Gen. Crystallogr.* **1976**, *A32*, 751–767.

(39) Cotton, F. A.; Wilkinson, G. "Advanced Inorganic Chemistry", 4th ed.; Wiley: New York, 1980.

(40) Holton, J.; Lappert, M. F.; Ballard, D. G. H.; Pearce, R.; Atwood, J. L.; Hunter, W. E. *J. Chem. Soc., Dalton Trans.* **1979**, 45–53.

tances in $Er(\mu\text{-}CH_3)_6Li_3(TMEDA)_3$,[41] 2.57 (2) Å, $(C_5H_5)_2Er(\mu\text{-}CH_3)_2Li(TMEDA)$,[28] 2.458 (19) Å, $Ho(\mu\text{-}CH_3)_6Li_3(TMEDA)_3$,[42] 2.563 (18) Å, and $Lu(\mu\text{-}CH_3)_6Li_3(MeOCH_2CH_2OMe)_3$,[43] 2.53 (2) Å, are also longer when the differences in metallic radii are considered. The lutetium terminal alkyl carbon distances in III and IV, 2.376 (17) and 2.345 (39) Å, are similar to the Yb–C distance in I, but the Lu–C distance in II is considerably and significantly longer, 2.471 (2) Å.

The Yb–C distance in I provides for the first time a Ln–C distance for an unsubstituted terminal alkyl ligand of modest size in a late lanthanide $(C_5H_5)_2LnR(THF)$ complex. This distance allows one to characterize the relative amount of steric crowding in other terminal organolanthanide alkyl complexes. Evidently, the steric bulk of the CH_2SiMe_3 and C_6H_4-4-CH_3 ligands in III and IV is not so large at the carbon atom coordinated to lutetium as to prevent "normal" Lu–C bond lengths. In contrast, the Lu–C bond in $(C_5H_5)_2Lu(t\text{-}C_4H_9)(THF)$ is clearly long in comparison and suggests that this molecule is quite sterically crowded.

Analysis of the relative degree of steric crowding is quite important in organolanthanide chemistry, since steric effects influence the structure, stability, and reactivity of the complexes.[44-46] Comparison of $(C_5H_5)_2Yb(CH_3)(THF)$ with the lutetium analogue $(C_5H_5)_2Lu(CH_3)(THF)$[10] constitutes a clear example of how small changes in steric crowding can have large effects on stability. $(C_5H_5)_2Lu(CH_3)(THF)$ is reported to decompose below 20 °C,[10] whereas a room-temperature crystal structure of the ytterbium analogue was readily obtained. Although both compounds desolvate, the lutetium complex is much more susceptable to this decomposition reaction.[47] The main difference between the complexes of these metals, which are adjacent in the periodic table, is the 0.008[38]–0.01[39] Å difference in the size of the metal. This small change in radius causes the lutetium derivative to be slightly more sterically crowded. This may enhance the THF extrusion process and cause the decomposition to occur more readily. Consistent with this, both $[(C_5H_5)_2LuH(THF)]_2$ and $(CH_3C_5H_4)_2Lu(t\text{-}C_4H_9)(THF)$ are less stable than the analogous erbium or yttrium complexes.[4]

Hydrogenolysis Studies. We sought to examine the consequences in reactivity of the structural features discussed above. The hydrogenolysis reaction was chosen to probe Ln–C bond reactivity because the substrate is relatively small, the hydride products are well-characterized,[4,6] and our earlier studies showed a wide range of rates for this reaction.[4,6,34]

The structural data discussed above indicated that, for a given metal, $(C_5H_5)_2Ln(t\text{-}C_4H_9)(THF)$ complexes were significantly more crowded than $(C_5H_5)_2Ln(CH_2SiMe_3)(THF)$ or $(C_5H_5)_2Ln(CH_3)(THF)$ species. Consistent with the crystallographically established steric congestion in $(C_5H_5)_2Lu(t\text{-}C_4H_9)(THF)$ we have found that this species is rather unreactive to H_2 in THF solvent where it is likely to be fully solvated[6] (eq 5). In contrast, in toluene a rapid

$$(C_5H_5)_2Lu(t\text{-}C_4H_9)(THF) + H_2 \xrightarrow[\text{room temp}]{\text{THF}} \text{no reaction} \quad (6\ \text{h}) \tag{5}$$

hydrogenolysis is observed[6] (eq 3) to give the $[(C_5H_5)_2LuH(THF)]_2$ product in good yield.[4] The toluene reaction presumably differs from the THF reaction in that in toluene some dissociation of THF occurs to provide access to a highly reactive, sterically unsaturated species like $(C_5H_5)_2Lu(t\text{-}C_4H_9)$.[6] Consistent with these observations, we had found that the bridged dimer $[(CH_3C_5H_4)_2Yb(\mu\text{-}CH_3)]_2$ reacted slowly with hydrogen in toluene (eq 1)[3] but that $[(CH_3C_5H_4)_2Y(\mu\text{-}CH_3)]_2$ and $[(C_5H_5)_2Y(\mu\text{-}CH_3)]_2$ reacted rapidly in mixed 1:10 THF/alkane or 1:10 THF/arene solvents.[6] In these latter cases, the presence of the substoichiometric amounts of THF could effect a bridge cleavage leading to $(C_5H_5)_2Y(CH_3)(THF)$ and $(C_5H_5)_2YCH_3$, species more reactive than the doubly bridged dimer. Clearly, the solvent and degree of association of a complex can be as important as the size of the metal and the alkyl ligand.

To more fully examine the previously observed trends in Ln–C bond reactivity to hydrogenolysis, we have examined several alkyl complexes in a variety of solvents. The widest range of reactions has been carried out with yttrium complexes since ^1H NMR spectroscopy is particularly informative with this metal due to the $I = {}^1/_2$ nuclear spin of the metal.[16] The degree of association of organoyttrium complexes in solution can often be determined from the Y–H coupling patterns.[4,6] The reactivity of yttrium complexes is compared with those of Er, Yb, and Lu by using a more limited range of alkyls and solvents. A summary of these results is shown in Table III.

Alkyl Yttrium Complexes. The methyl carbon yttrium bond in dimeric $[(C_5H_5)_2YCH_3]_2$ fails to react with hydrogen in toluene under ambient conditions over a several day period as expected based on the ytterbium results (eq 1).[3] With a mixed solvent of 10:1 toluene/THF, hydrogenolysis is efficient as previously reported.[6] In the latter case, the $(C_5H_5)_2YCH_3$ complexes present would be expected to react with H_2, but the reactivity of the solvated $(C_5H_5)_2Y(CH_3)(THF)$ was less certain. Fully solvated $(C_5H_5)_2Lu(t\text{-}C_4H_9)(THF)$ in THF did not react with hydrogen (eq 4), but since the crystal structure of I indicated that $(C_5H_5)_2Ln(CH_3)(THF)$ complexes were less sterically crowded than $(C_5H_5)_2Lu(t\text{-}C_4H_9)(THF)$, reactivity of the solvated methyl species toward hydrogen was feasible. As shown in entry 3 of Table III $(C_5H_5)_2Y(CH_3)(THF)$ does react readily with H_2 in THF (eq 6) to form $[(C_5H_5)_2Y(\mu\text{-}H)(THF)]_2$[4] in good yield. DME is a better ethereal solvent than THF for the hydrogenolysis of a terminal Y–CH_3 bond, and dioxane is worse although the reaction still proceeds at a reasonable rate.

$$2(C_5H_5)_2Y(CH_3)(THF) + 2H_2 \xrightarrow{\text{THF}} [(C_5H_5)_2Y(\mu\text{-}H)(THF)]_2 + 2CH_4 \tag{6}$$

$(C_5H_5)_2Y(t\text{-}C_4H_9)(THF)$ readily undergoes hydrogenolysis in toluene, but in THF no hydride is generated over 24 h. The inertness of $(C_5H_5)_2Y(t\text{-}C_4H_9)(THF)$ compared to the reactivity of $(C_5H_5)_2Y(CH_3)(THF)$ in THF clearly demonstrates the importance of steric crowding in organolanthanide reactivity. Substitution of the larger t-C_4H_9 ligand for CH_3 drastically reduces reactivity. Substituting the CH_3 ligand with CH_2SiMe_3, which is large but not as sterically bulky around the Ln–C bond as the t-C_4H_9 ligand, does not stop the hydrogenolysis from occurring in

(41) Schumann, H.; Pickardt, J.; Bruncks, N. *Angew. Chem., Int. Ed. Engl.* **1981**, *20*, 120–121.
(42) Schumann, H.; Muller, J.; Bruncks, N.; Lauke, H.; Pickardt, J.; Schwarz, H.; Eckart, K. *Organometallics* **1984**, *3*, 69–74.
(43) Schumann, H.; Lauke, H.; Hahn, E.; Pickardt, J. *J. Organomet. Chem.* **1984**, *263*, 29–35.
(44) For a more extensive discussion of the consequences of steric crowding in organolanthanide chemistry, see ref 34 and 45.
(45) Evans, W. J.; Peterson, T. T.; Rausch, M. D.; Hunter, W. E.; Zhang, H.; Atwood, J. L. *Organometallics* **1985**, *4*, 554–559.
(46) Quantitative analysis of the steric crowding is under development: Xing-Fu, Li; Fischer, R. D. *Inorg. Chim. Acta* **1983**, *94*, 50–52.
(47) Freshly recrystallized clear crystals of $(C_5H_5)_2Lu(CH_3)(THF)$ start to become opaque within 10 min at room temperature and appear by ^1H NMR spectroscopy to lose about one-third of their solvated THF in this time period.

$(C_5H_5)_2YR(THF)$ complexes. This is consistent with the similar Ln–C bond distances in the $(C_5H_5)_2LnR(THF)$ complexes (R = CH_3, CH_2SiMe_3) and the fact that $(C_5H_5)_2Y(CH_2SiMe_3)(THF)$ is a monomer in both toluene and THF solution (by ^{89}Y–^1H splitting in the ^1H NMR spectra). Monomethylation of the cyclopentadienyl rings of the yttrium methyl complexes (entries 5 and 6) does not greatly affect the hydrogenolysis reactivity. In summary, for bis(cyclopentadienyl) yttrium alkyl complexes, reactivity to hydrogenolysis depends mainly on access to an unsolvated monomeric complex, $(C_5H_5)_2LnR$, or to a solvated species, $(C_5H_5)_2LnR(THF)$, in which R does not cause steric crowding close to the metal.

Alkyl Complexes of Erbium, Ytterbium, and Lutetium. Since Er^{3+} is almost identical in size with Y^{3+} (0.881 vs. 0.88 Å, respectively[39]), its chemistry is likely to be the same. Indeed, entries 12 and 13 show that the reactivity of $[(C_5H_5)_2ErCH_3]_2$ to hydrogenolysis in toluene/THF and in THF is very similar to that of the yttrium analogue. $[(C_5H_5)_2YbCH_3]_2$ and $[(C_5H_5)_2LuCH_3]_2$ in toluene are also similar to $[(C_5H_5)_2YCH_3]_2$; i.e., no reaction occurs with H_2. In THF, however, the reactivity of the ytterbium and lutetium complexes differs. Only small amounts of $[(C_5H_5)_2YbCH_3]_2$ and $[(C_5H_5)_2LuCH_3]_2$ undergo hydrogenolysis after 24 h under H_2 in THF. Neither reaction produces enough hydride to form a precipitate as is observed in the yttrium reactions. A 6% yield of $[(C_5H_5)_2LuH(THF)]_2$ can be detected by ^1H NMR spectroscopy after 24 h, and, after many days, the ytterbium reaction gives detectable amounts of $[(C_5H_5)_2YbH(THF)]_2$ as well as its decomposition product $(C_5H_5)_2Yb(THF)$. Hence, the reactivity of $(C_5H_5)_2Ln(CH_3)(THF)$ complexes differs substantially for Ln = Y and Er compared to Ln = Yb and Lu. If the observed difference in reactivity is due entirely to steric effects, it means that a change in metal radius as small as 0.022[39]–0.034[38] Å can greatly effect reactivity.

Dimethoxyethane, which was a better solvent for $[(C_5H_5)_2YCH_3]_2$ hydrogenolysis than THF (entries 3 and 4), is also a better solvent for the ytterbium and lutetium reactions (entries 17 and 23), although $[(C_5H_5)_2LuCH_3]_2$ still gives only a 10% yield of hydridic product. Comparison of the latter two reactions suggests that a radial difference of only 0.008[38]–0.01[39] Å can change significantly the yield of the hydrogenolysis reaction.

These data can be summarized with a few general statements. Bridged methyl dimers $[(C_5H_5)_2Ln(\mu\text{-}R)]_2$ in non-coordinating solvents are clearly the least reactive toward hydrogenolysis. The reactivity of fully solvated terminal alkyl complexes $(C_5H_5)_2LnR(THF)$ depends on the size of the alkyl group: R = CH_3 is more reactive than R = CH_2SiMe_3 which is more reactive than R = t-C_4H_9. Terminal alkyls on unsolvated, sterically unsaturated metal centers would be expected to be the most reactive.[7,33,48] In sterically crowded molecules, small changes in the radius of the metal can have significant effects on reactivity.

Organoytterbium Hydrides. The principles of hydrogenolysis reactivity outlined above indicate why the original hydrogenolysis of the bridged ytterbium dimer $[(CH_3C_5H_4)_2YbCH_3]_2$ (eq 1) was so slow. Clearly, there were better precursors and solvents for the formation of ytterbium hydrides. Moreover, a reasonably rapid reaction was necessary in the ytterbium case to minimize the amount of Yb^{3+}–H to Yb^{2+} decomposition. The initially observed trends in hydrogenolysis reactivity[4] suggested that $(C_5H_5)_2Yb(t\text{-}C_4H_9)(THF)$ (VI) in toluene was likely to be a better precursor to ytterbium hydride complexes than $[(C_5H_5)_2YbCH_3]_2$. Unfortunately, attempts to prepare VI from $[(C_5H_5)_2YbCl]_2$ and t-C_4H_9Li in THF gave the divalent reduction product $(C_5H_5)_2Yb$.[11] The reaction of $(C_5H_5)_2YbCl(THF)_{1.6}$ in toluene with t-C_4H_9Li in pentane has been reported to give VI, but the yield is only 15%.[10] The major product of that reaction again is $(C_5H_5)_2Yb$. Hence, VI is not accessible in high enough yield to be a viable precursor to ytterbium hydrides. The reaction of $[(C_5H_5)_2YbCH_3]_2$ in the presence of ethers was therefore studied. As shown in Table III, the $[(C_5H_5)_2YbCH_3]_2$/DME system has the necessary characteristics to allow isolation of an ytterbium hydride in a reasonably high yield and convenient time as described below.[49]

In DME, $[(C_5H_5)_2YbCH_3]_2$ reacts with H_2 in 24 h to give an orange precipitate. This product dissolves in THF and can be recrystallized from THF as yellow plates. Complexometric ytterbium analysis is consistent with the empirical formula $(C_5H_5)_2YbH(THF)$. The IR spectrum exhibited a broad absorption centered around approximately 1350 cm^{-1} in the region found for $\nu_{Ln\text{-}H}$ absorptions of other $[(C_5H_5)_2LnH(THF)]_2$ complexes.[4] The IR spectrum of the analogous complex prepared from D_2 lacked this 1350 cm^{-1} band and had new broad absorptions in the frequency range expected for an Yb–D absorption. Decomposition of the freshly recrystallized hydride complex with H_2O generated a quantitative yield of the expected amount of H_2. The instability of this hydride in solution precluded the usual isopiestic molecular weight determination, but this species is likely to be a dimer, $[(C_5H_5)_2YbH(THF)]_2$, like the Y, Er, and Lu analogues.[4,15] The complex desolvates readily in a glovebox atmosphere (as does $[(C_5H_5)_2LuH(THF)]_2$[4]), and X-ray diffraction analysis of solvated crystals has not yet been possible.

When $[(C_5H_5)_2Yb(CH_3)]_2$ was hydrogenolyzed in the presence of lithium salts, a different organoytterbium hydride complex was formed. With 5:1 Et_2O/hexane as a solvent, a yellow precipitate was obtained which contained lithium. Complete elemental analysis of this species suggested the formula $[(C_5H_5)_2LnH]_3H\{Li(THF)_4\}$ (cf. the Ln = Y,[7] Er,[51] and Lu[5] analogues, VII, VIII, and IX, respectively). The IR spectrum of this material contained a strong broad band at 1210 cm^{-1} compared to absorptions in the 1170–1205 cm^{-1} region for VII–IX. The analogous ytterbium complex prepared with D_2 lacks the 1210 cm^{-1} absorption and has an additional band at approximately 850 cm^{-1} (ratio = 1.4). Hydrolysis of a freshly recrystallized sample of this organoytterbium hydride gave 95% of the hydrogen expected from the trimer $\{[(C_5H_5)_2YbH]_3H\}\{Li(THF)_4\}$. This ytterbium hydride could also be prepared from $[(C_5H_5)_2YbH(THF)]_2$ described above and t-C_4H_9Li following the direct synthetic route recently developed for VII from $[(C_5H_5)_2YH(THF)]_2$.[7] Attempts to fully identify this complex by X-ray diffraction have been unsuccessful since crystals of this product have repeatedly desolvated

(48) Ample evidence for this is available from the reactivity of the $(C_5Me_5)_2Ln(\mu\text{-}Z)LnZ(C_5Me_5)_2$ complexes (Ln = Lu, Yb; Z = H, CH_3): Watson, P. L.; Parshall, G. W. *Acc. Chem. Res.* **1985**, *18*, 51–56 and references therein.

(49) The characterization of trivalent ytterbium cyclopentadienyl hydride complexes is somewhat more difficult than the analysis of other lanthanide or yttrium systems. In addition to the problem of Yb^{3+}–H to Yb^{2+} decomposition, Yb^{3+} has a room-temperature magnetic moment of 4.4–4.9 μ_B and is not likely to yield the definitive NMR evidence readily obtainable with the diamagnetic lutetium and yttrium systems. In general, it has proven difficult to obtain complete elemental analysis on solvated late lanthanide hydride complexes and those systems not accessible by NMR, e.g., the erbium systems, have usually been fully characterized only by X-ray crystallography.[4,5] The success of the latter approach, particularly with solvated species, depends on the stability of the crystals.[50]

(50) Four different crystal systems were tried before a refinable X-ray data set on a $[(C_5H_4R)_2Ln(\mu\text{-}H)(THF)]_2$ complex was obtained.[4]

(51) Evans, W. J.; Meadows, J. H., unpublished results.

and decomposed in the X-ray beam before a unit cell could be determined.

Decomposition Studies. Both of the trivalent ytterbium hydride complexes described above decompose to $(C_5H_5)_2Yb(THF)$.[3,52] Both decompositions can be followed by ^1H NMR spectroscopy by monitoring the disappearance of the paramagnetically broadened C_5H_5 absorption of the Yb^{3+} hydride and the growth of the 5.8 ppm resonance of the diamagnetic Yb^{2+} product. At room temperature the $[(C_5H_5)_2YbH(THF)]_2$ conversion to $(C_5H_5)_2Yb(THF)$ in THF is nearly complete in 48 h. In contrast, the anionic $\{[(C_5H_5)_2YbH]_3H\}\{Li(THF)_4\}$ has a half-life of almost 50 days in THF.

Conclusion

These studies indicate that the reactivity of bis(cyclopentadienyl) lanthanide and yttrium alkyl complexes is a sensitive function of the size of the metal, the size of the ligand, and the coordinating ability of the solvent. Three major classes of organolanthanide complexes can be differentiated on the basis of the relative size of the ligands and the metal: sterically unsaturated, sterically saturated, and sterically oversaturated.[34,45] Each class has its own distinctive type of reactivity. The results of this study on sterically saturated complexes show that *within a single class*, there can also be considerable variation in reactivity due to small changes in steric saturation and the degree of molecular association. Furthermore, the present results show that these factors can effect reactivity in different directions depending on the reaction considered. Hence, by increasing the steric saturation of a $(C_5H_5)_2Ln(CH_3)(THF)$ complex by changing from Ln = Y to Ln = Lu, reactivity toward hydrogen decreases. However, the same change in metal increases the reactivity to desolvation. In $(C_5H_5)_2YR(THF)$ complexes, increasing steric saturation by changing from R = CH_3 to R = t-C_4H_9 decreases reactivity toward hydrogen. In contrast for $(R'C_5H_4)_2Y(t\text{-}C_4H_9)(THF)$ complexes, increasing steric saturation by changing from R′ = H to R′ = CH_3 increases decomposition reactivity. A similar dichotomy exists in solvent effects. Addition of THF to $[(C_5H_5)_2LnCH_3]_2$ dimers increases reactivity to hydrogen, but the presence of THF diminishes the reactivity of $(C_5H_5)_2Ln(t\text{-}C_4H_9)(THF)$ complexes. All of these effects can be correlated with access to a terminal alkyl ligand on a sterically unsaturated metal center as the most reactive species. Clearly, there are several ways to finely manipulate the reactivity of organolanthanide alkyl complexes, providing a level of control unusual in organometallic chemistry. The fact that the lanthanide elements constitute the largest series of metals with similar chemistry but a gradually changing radial size makes these metals ideal for this sterically based variation of reactivity.[53]

Acknowledgment. For support of this research, we thank the Division of Basic Energy Sciences of the Department of Energy. We also thank the Alfred P. Sloan Foundation and the University of California, Irvine Faculty Mentor Program, for fellowships (to W.J.E. and R.D., respectively). We thank Professor R. J. Doedens for his help and advice with the crystal structure determination.

Supplementary Material Available: Tables of thermal parameters, structure factor amplitudes, and least-squares planes (10 pages). Ordering information is given on any current masthead page.

(52) The decomposition of the trivalent ytterbium complex $[(C_5Me_5)_2Yb(DME)][PF_6]$ by KH has been reported.[24]

(53) Evans, W. J.; Engerer, S. C.; Piliero, P. A.; Wayda, A. L. In "Fundamental Research in Homogeneous Catalysis"; Tsutsui, M., Ed.; Plenum Press: New York, 1979; Vol. 3, pp 941–952.

Characterization of the Anion $[(\eta^5\text{-}C_5H_5)_3U^{III}\text{-}n\text{-}C_4H_9]^-$. Synthesis and Crystal Structure of Tricyclopentadienyl-*n*-butyluranium(III) Lithium Cryptate: $[(C_5H_5)_3UC_4H_9]^-[LiC_{14}H_{28}N_2O_4]^+$

Lucile Arnaudet, Pierrette Charpin, Gérard Folcher,* Monique Lance, Martine Nierlich, and Daniel Vigner

SCM-CEA-IRDI, 91191 GIF Sur Yvette Cédex, France

Received March 19, 1985

The anion $[(\eta^5\text{-}C_5H_5)_3U^{III}\text{-}n\text{-}C_4H_9]^-$ forms with lithium inserted in a macrocycle a solid crystalline compound of stoichiometry 1/1. $[Cp_3UC_4H_9]^-[Li\text{-}2.1.1]^+$ crystallizes in the centrosymmetric monoclinic space group $P2_1/n$ (no. 14) with a = 8.873 (6) Å, b = 26.594 (8) Å, c = 14.175 (3) Å, β = 93.01 (3)°, and Z = 4. The structure was refined to R = 4.18% for 1890 reflections with θ = 2–20° and $I > 3\sigma(I)$. The two entities have no crystallography-imposed symmetry: the U^{III} anion is very similar to the neutral equivalent U^{IV} compound, with distances significantly smaller between uranium and its carbon neighbors.

Introduction

The organometallic chemistry of trivalent uranium offers a few examples of well-established compounds. The π-bonded ligands[1] like $C_5H_5^-$ (hereafter Cp^-) and $C_8H_8^{2-}$ stabilize the four oxidation state of uranium and render the reduction more difficult than in the case of simple hydrated ions. Strong reductants are required to achieve quantitative reduction, and consequently the resulting compounds are very reactive. For instance, the reduction of $(C_8H_8)_2U$ can be obtained only with lithium naphthalenide,[2] and the expected anion $(C_8H_8)_2U^-$ has not yet

(1) Marks, T. J.; Fischer, R. D. "Organometallics of f Elements"; D. Reidel Publishing Co.: Dordrecht, 1979; Chapter 1 and Chapter 2.

0276-7333/86/2305-0270$01.50/0

and decomposed in the X-ray beam before a unit cell could be determined.

Decomposition Studies. Both of the trivalent ytterbium hydride complexes described above decompose to $(C_5H_5)_2Yb(THF)$.[3,52] Both decompositions can be followed by ^1H NMR spectroscopy by monitoring the disappearance of the paramagnetically broadened C_5H_5 absorption of the Yb^{3+} hydride and the growth of the 5.8 ppm resonance of the diamagnetic Yb^{2+} product. At room temperature the $[(C_5H_5)_2YbH(THF)]_2$ conversion to $(C_5H_5)_2Yb(THF)$ in THF is nearly complete in 48 h. In contrast, the anionic $\{[(C_5H_5)_2YbH]_3H\}\{Li(THF)_4\}$ has a half-life of almost 50 days in THF.

Conclusion

These studies indicate that the reactivity of bis(cyclopentadienyl) lanthanide and yttrium alkyl complexes is a sensitive function of the size of the metal, the size of the ligand, and the coordinating ability of the solvent. Three major classes of organolanthanide complexes can be differentiated on the basis of the relative size of the ligands and the metal: sterically unsaturated, sterically saturated, and sterically oversaturated.[34,45] Each class has its own distinctive type of reactivity. The results of this study on sterically saturated complexes show that *within a single class*, there can also be considerable variation in reactivity due to small changes in steric saturation and the degree of molecular association. Furthermore, the present results show that these factors can effect reactivity in different directions depending on the reaction considered. Hence, by increasing the steric saturation of a $(C_5H_5)_2Ln(CH_3)(THF)$ complex by changing from Ln = Y to Ln = Lu, reactivity toward hydrogen decreases. However, the same change in metal increases the reactivity to desolvation. In $(C_5H_5)_2YR(THF)$ complexes, increasing steric saturation by changing from R = CH_3 to R = t-C_4H_9 decreases reactivity toward hydrogen. In contrast for $(R'C_5H_4)_2Y(t\text{-}C_4H_9)(THF)$ complexes, increasing steric saturation by changing from R′ = H to R′ = CH_3 increases decomposition reactivity. A similar dichotomy exists in solvent effects. Addition of THF to $[(C_5H_5)_2LnCH_3]_2$ dimers increases reactivity to hydrogen, but the presence of THF diminishes the reactivity of $(C_5H_5)_2Ln(t\text{-}C_4H_9)(THF)$ complexes. All of these effects can be correlated with access to a terminal alkyl ligand on a sterically unsaturated metal center as the most reactive species. Clearly, there are several ways to finely manipulate the reactivity of organolanthanide alkyl complexes, providing a level of control unusual in organometallic chemistry. The fact that the lanthanide elements constitute the largest series of metals with similar chemistry but a gradually changing radial size makes these metals ideal for this sterically based variation of reactivity.[53]

Acknowledgment. For support of this research, we thank the Division of Basic Energy Sciences of the Department of Energy. We also thank the Alfred P. Sloan Foundation and the University of California, Irvine Faculty Mentor Program, for fellowships (to W.J.E. and R.D., respectively). We thank Professor R. J. Doedens for his help and advice with the crystal structure determination.

Supplementary Material Available: Tables of thermal parameters, structure factor amplitudes, and least-squares planes (10 pages). Ordering information is given on any current masthead page.

(52) The decomposition of the trivalent ytterbium complex $[(C_5Me_5)_2Yb(DME)][PF_6]$ by KH has been reported.[24]

(53) Evans, W. J.; Engerer, S. C.; Piliero, P. A.; Wayda, A. L. In "Fundamental Research in Homogeneous Catalysis"; Tsutsui, M., Ed.; Plenum Press: New York, 1979; Vol. 3, pp 941–952.

Characterization of the Anion $[(\eta^5\text{-}C_5H_5)_3U^{III}\text{-}n\text{-}C_4H_9]^-$. Synthesis and Crystal Structure of Tricyclopentadienyl-*n*-butyluranium(III) Lithium Cryptate: $[(C_5H_5)_3UC_4H_9]^-[LiC_{14}H_{28}N_2O_4]^+$

Lucile Arnaudet, Pierrette Charpin, Gérard Folcher,* Monique Lance, Martine Nierlich, and Daniel Vigner

SCM-CEA-IRDI, 91191 GIF Sur Yvette Cédex, France

Received March 19, 1985

The anion $[(\eta^5\text{-}C_5H_5)_3U^{III}\text{-}n\text{-}C_4H_9]^-$ forms with lithium inserted in a macrocycle a solid crystalline compound of stoichiometry 1/1. $[Cp_3UC_4H_9]^-[Li\text{-}2.1.1]^+$ crystallizes in the centrosymmetric monoclinic space group $P2_1/n$ (no. 14) with a = 8.873 (6) Å, b = 26.594 (8) Å, c = 14.175 (3) Å, β = 93.01 (3)°, and Z = 4. The structure was refined to R = 4.18% for 1890 reflections with θ = 2–20° and $I > 3\sigma(I)$. The two entities have no crystallography-imposed symmetry: the U^{III} anion is very similar to the neutral equivalent U^{IV} compound, with distances significantly smaller between uranium and its carbon neighbors.

Introduction

The organometallic chemistry of trivalent uranium offers a few examples of well-established compounds. The π-bonded ligands[1] like $C_5H_5^-$ (hereafter Cp^-) and $C_8H_8^{2-}$ stabilize the four oxidation state of uranium and render the reduction more difficult than in the case of simple hydrated ions. Strong reductants are required to achieve quantitative reduction, and consequently the resulting compounds are very reactive. For instance, the reduction of $(C_8H_8)_2U$ can be obtained only with lithium naphthalenide,[2] and the expected anion $(C_8H_8)_2U^-$ has not yet

(1) Marks, T. J.; Fischer, R. D. "Organometallics of f Elements"; D. Reidel Publishing Co.: Dordrecht, 1979; Chapter 1 and Chapter 2.

0276-7333/86/2305-0270$01.50/0

Table I. ^1H NMR Spectra[a] of Cp_3UR^- at 25 °C

	Cp protons	R protons
$Cp_3UCH_3^-$	21.7 (s, 15)	101 (s, 3)
$CP_3UC_4H_9^-$	21.3 (s, 15)	98.5 (t, 2), 15.8 (m, 2), 14.0 (m, 2), 12.0 (t, 3)
$Cp_3UC_6H_5^-$	21.6 (s, 15)	−11.3 (d, 2), −5.2 (t, 2), −3.3 (t, 1)

[a] Positive chemical shifts, in ppm, are downfield from C_6H_6.

been isolated. In the case of cyclopentadienyl derivatives, only Cp_3U and its THF adduct have been well characterized.[3] With methyl-substituted cyclopentadienyl the structures of $[(C_5Me_5)_2UCl]_3$[4] and $(C_5Me_5)_3UH$ dmpe[5,6] have been published by T. Marks and co-workers.

On the other hand, it is noticeable that like $(C_8H_8)_2U$, cyclopentadienyluranium(IV) molecules seem to be reversibly reduced adding one electron to give a stable anion.[7] This trend can be questionable when one of the ligands is an alkyl group weakly bonded through the carbon atom to uranium. We have found[8] when alkyllithium is used as an electron donor that an unusual anionic species, Cp_3UR^-, can be prepared. The interesting high reactivity of this anion, which is able to activate dinitrogen,[9] likely due to the low stability of the σ uranium(III)–carbon bond, prompted us to isolate solid compounds in view of a crystallographic characterization.

Experimental Section

Preparation of Cp_3UR^-. The reduction of Cp_3UCl and Cp_3UR with strong chemical reductants like hydrides[10] and aluminohydrides[11] or photochemically[12] leads to Cp_3U and Cp_3U·THF or to an unsoluble dimer, $Cp_4U_2(C_5H_4)_2$. On the opposite end alkyllithium acting as a reducing and alkylating agent stabilizes the uranium–alkyl bond, as evidenced by NMR spectroscopy[8] of the compound in solution. The same result can also be achieved by electrochemistry.[13] Starting from Cp_3UCl the reaction is complicated by the formation of chlorine derivatives, the preparation of the anion requiring then alkyllithium in excess. An easier route starting from Cp_3UR should be preferred when Cp_3UR is available as a pure material, free from any LiCl.

All operations involving uranium compounds were carried out in a vacuum line using the Schlenk technique. THF was carefully distilled on $CuCl_2$ and then on sodium–benzophenone. UCl_4, Cp_3UCl, and $Cp_3UC_4H_9$ were prepared according to published procedures.[14]

Table II. Summary of Crystal Structure Data

(A) Crystal Data

formula: $C_{33}H_{52}O_4N_2LiU$	space group: $P2_1/n$
cryst system: monoclinic	V = 3348 Å^3
a = 8.873 (6) Å	Z = 4
b = 26.628 (8) Å	M_r = 785.76
c = 14.189 (3) Å	D_{calcd} = 1.559 M g^{-3}
β = 92.96 (3)°	μ(Mo Kα) = 46.31 cm^{-1}
	F(000) = 1564

max transmissn coeff = 99.98%
minimum transmissn coeff = 47.45%
average transmissn coeff = 78.55%

(B) Data Collection

radiatn:	Mo Kα (λ = 0.710 73 Å)
θ limits:	2–20° (limited by the decomposition of the crystal)
scan type:	$\omega/2\theta$
monochromator:	graphite
reflctns measd:	$0 < h < 8$, $-25 < k < 0$, $-13 < l < 13$.
reflctns collected:	3486 total, 2585 unique, 1890 data with $I < 3\sigma(I)$
standard reflctns:	three reflctns remeasd after each hour ($0\bar{7}\bar{6}$, 206, $2\bar{4}\bar{6}$); a decay was observed (22.1% in 31.8 h) and a correction made, based on the intensities of the standard reflctns
temp:	295 K
no. of variables	174

$Cp_3UC_4H_9^-$, Li^+·THF. To 2 mmol of $Cp_3UC_4H_9$ in 10 mL of THF was added 1 equiv of an hexane solution of LiC_4H_9. Gas evolution was observed: the hydrocarbon product characterized by gas chromatography was butane only. After a few minutes the solution was analyzed by NMR spectroscopy (Table I). The THF was vacuum distilled and a very unstable red-brown powder obtained.

$Cp_3UCH_3^-$, Li^+·THF. $Cp_3UC_4H_9$ (2 mmol) in 10 mL of THF was reacted with an ether solution of $LiCH_3$ (16%). Butane and small amounts of methane were detected by chromatography. The product in solution was characterized by NMR spectroscopy. A dark brown powder remained after the solvent was removed.

$Cp_3UC_6H_5^-$,Li^+·THF: the same procedure as above with C_6H_5Li (17%) in a benzene–ether mixture instead of CH_3Li.

Isolation of $[Cp_3U$-*n*-Bu$]^-[$Li-2.1.1$]^+$. Crystals suitable for X-ray analysis have been obtained by slow diffusion in a small volume of THF of two separate solutions of Cp_3U-*n*-BuLi and $C_{14}H_{28}N_2O_4$ (≡ 2.1.1) through porous sintered glass. After 20 days, brown crystals, extremely air and moisture sensitive, were collected on the vessel walls (elemental analysis of the compound has been given in ref 8). Similar experiments were attempted with Cp_3UMe^-, but the single crystals were not stable enough to be kept during the data collection without severe loss of intensity.

NMR Results. ^1H NMR measurements were carried out on a Bruker WH 60 spectrometer.

The shifts, mainly paramagnetic, are generally downfield like those for the analogous uranium(IV). All the signals are broader for U^{III}, as previously observed[11] and related to its expected longer electronic relaxation time.

The values presented in Table I are referred to C_6H_6 and measured positively downfield.

Collection of X-ray Diffraction Data. A dark brown badly formed single crystal of approximate dimensions 500 × 350 × 190 μm was introduced into a thin-walled Lindeman glass tube in an inert-atmosphere drybox. The capillary was temporarily sealed with wax and later flame-sealed. (Note that crystals are very air sensitive and form an amorphous powder within a few hours of exposure to air.) The capillary was mounted on an Enraf-Nonius CAD4 automatic diffractometer. Cell parameters were obtained by a least-squares refinement of the setting angles of 25 reflections with θ between 8° and 12°. Information on data collection appears

(2) Billiau, F.; Folcher, G.; Marquet-Ellis, H.; Rigny, P.; Saito, E. *J. Am. Chem. Soc.* **1981**, *103*, 5603.
(3) Kanellakopoulos, B.; Fischer, E. O.; Dornberger, E. D.; Baumgärtner, B. F. *J. Organomet. Chem.* **1970**, *24*, 507.
(4) Manriquez, J.; Fagan, J.; Marks, T. J. *J. Am. Chem. Soc.* **1979**, *101*, 5075.
(5) Edwards, P. G.; Fagan, P. J.; Marks, T. J.; Day, V. W. *J. Am. Chem. Soc.* **1982**, *104*, 86.
(6) Fagan, P. J.; Manriquez, J. M.; Marks, T. J.; Day, C. S.; Wollmer, S. H.; Day, V. W. *Organometallics* **1982**, *1*, 170.
(7) (a) Mugnier, Y.; Dormond, A.; Laviron, E. *J. Chem. Soc., Chem. Commun.* **1982**, 258. (b) Finke, R. G.; Gaughan, G.; Voegeli, R. *J. Organomet. Chem.* **1982**, *229*, 179.
(8) Arnaudet, L.; Folcher, G.; Marquet-Ellis, H.; Klähne, E.; Yünlü, K.; Fischer, R. D. *Organometallics* **1983**, *2*, 344.
(9) Arnaudet, L.; Brunet, F.; Folcher, G.; Saito, E. *C.R. Acad. Sci., Ser. 2* **1983**, *296*, 431.
(10) Eller, G.; Moody, C. *Inorg. Chim. Acta* **1980**, *44*, L155.
(11) Marquet-Ellis, H.; Folcher, G. *J. Organomet. Chem.* **1977**, *131*, 257.
(12) (a) Klähne, E.; Folcher, G.; Gianotti, C., Marquet-Ellis, H.; Fisher, R. D. *J. Organomet. Chem.* **1980**, *201*, 399. (b) Kalina, D. G. "The Photogeneration, Characterization, and Reactivity of Low-Valent Uranium and Thorium Organometallics", Thesis, Evanston, IL, 1981.
(13) Arnaudet, L.; Folcher, G.; Mugnier, Y.; Laviron, E., to be submitted for publication.
(14) (a) UCl_4 from UO_3 and C_3Cl_6: Hermann, J. A. "Inorganic Synthesis", Vol. V. (b) Cp_3UCl by reacting UCl_4 with TlCp: Reynold, L. T.; Wilkinson, G. *J. Inorg. Nucl. Chem.* **1956**, *2*, 246. (c) Cp_3UR from Cp_3UCl and RLi: Marks, T. J.; Seyam, A. M.; Kolb, J. R. *J. Am. Chem. Soc.* **1973**, *95*, 5529.

Table III. Atomic Coordinates and Isotropic or Equivalent Isotropic Thermal Parameters for Non-Hydrogen Atoms

	x	y	z	B, Å²
U	0.1488 (1)	−0.10553 (5)	0.2076 (1)	2.82 (2)[a]
C(20)	0.345 (2)	−0.024 (1)	0.259 (1)	5.3 (7)
C(21)	0.355 (3)	−0.030 (1)	0.160 (2)	5.3 (7)
C(22)	0.225 (3)	−0.017 (1)	0.109 (2)	5.3 (7)
C(23)	0.128 (3)	−0.000 (1)	0.172 (2)	5.3 (7)
C(24)	0.191 (3)	−0.004 (1)	0.262 (2)	5.3 (7)
C(30)	0.404 (3)	−0.144 (1)	0.307 (2)	4.9 (7)
C(31)	0.287 (3)	−0.179 (1)	0.330 (2)	4.9 (7)
C(32)	0.248 (3)	−0.204 (1)	0.249 (2)	4.9 (7)
C(33)	0.339 (3)	−0.188 (1)	0.172 (2)	4.9 (7)
C(34)	0.431 (3)	−0.154 (1)	0.212 (2)	4.9 (7)
C(40)	−0.046 (3)	−0.099 (1)	0.045 (2)	3.6 (1.5)
C(41)	−0.142 (4)	−0.096 (1)	0.118 (2)	3.6 (1.5)
C(42)	−0.152 (4)	−0.141 (1)	0.161 (2)	3.6 (1.5)
C(43)	−0.063 (4)	−0.171 (1)	0.113 (2)	3.6 (1.5)
C(44)	0.003 (4)	−0.147 (1)	0.045 (2)	3.6 (1.5)
C(45)	−0.092 (9)	−0.086 (3)	0.065 (5)	3.8 (1.6)
C(46)	−0.155 (8)	−0.117 (3)	0.150 (5)	3.8 (1.6)
C(47)	−0.092 (8)	−0.167 (3)	0.147 (5)	3.8 (1.6)
C(48)	0.011 (8)	−0.171 (3)	0.077 (5)	3.8 (1.6)
C(49)	0.014 (9)	−0.121 (3)	0.024 (5)	3.8 (1.6)
C(50)	0.022 (3)	−0.101 (1)	0.365 (2)	4.8 (6)
C(51)	−0.112 (4)	−0.067 (1)	0.376 (2)	6.1 (8)
C(52)	−0.189 (4)	−0.068 (1)	0.471 (2)	6.9 (9)
C(53)	−0.318 (4)	−0.034 (1)	0.479 (2)	7.5 (9)
Li	0.127 (5)	0.334 (1)	0.704 (3)	4.0 (9)
O(3)	0.303 (2)	0.2825(8)	0.743 (1)	5.5 (5)
O(6)	0.126 (2)	0.2847(7)	0.588 (1)	4.6 (4)
O(11)	0.199 (2)	0.4052(7)	0.659 (1)	4.2 (4)
O(16)	−0.045 (2)	0.3260(7)	0.812 (1)	4.2 (4)
N(1)	0.244 (2)	0.3672(9)	0.844 (2)	4.4 (5)
N(2)	−0.081 (2)	0.3575(8)	0.625 (1)	3.5 (5)
C(1)	0.361 (4)	0.332 (1)	0.875 (2)	6.2 (8)
C(2)	0.425 (3)	0.304 (1)	0.797 (2)	5.1 (7)
C(4)	0.339 (4)	0.255 (1)	0.664 (2)	7.0 (1)
C(5)	0.204 (4)	0.239 (1)	0.610 (2)	6.7 (9)
C(7)	−0.027 (4)	0.275 (1)	0.558 (2)	5.9 (8)
C(8)	−0.093 (3)	0.326 (1)	0.536 (2)	5.7 (8)
C(9)	0.310 (3)	0.416 (1)	0.816 (2)	4.3 (7)
C(10)	0.212 (3)	0.439 (1)	0.739 (2)	4.1 (7)
C(12)	0.095 (4)	0.421 (1)	0.586 (2)	5.6 (8)
C(13)	−0.068 (3)	0.409 (1)	0.605 (2)	4.7 (7)
C(14)	0.129 (3)	0.376 (1)	0.912 (2)	4.7 (7)
C(15)	0.020 (3)	0.334 (1)	0.906 (2)	5.0 (7)
C(17)	−0.171 (4)	0.358 (1)	0.787 (2)	5.7 (7)
C(18)	−0.210 (3)	0.348 (1)	0.685 (2)	4.5 (7)

[a] $B_{eq} = {}^4/_3(a^2\beta_{11} + b^2\beta_{22} + c^2\beta_{33} + ac(\cos\beta)\beta_{13})$.

in Table II. An empirical absorption correction was applied.[15] After correction for Lorentz and polarization effects, 1890 data with $I > 3\sigma(I)$ were used in structure solution and refinement.

Solution and Refinement of the Structure. The U atom was located from a Patterson map, and the remaining non-hydrogen atoms were located from subsequent least-squares refinements and difference Fourier syntheses (33 C, 4 O, 2 N, Li). In the final difference Fourier map five residual peaks have been observed near one η^5-C_5H_5 (C(40)···C(44)), showing an occupation disorder for this cyclopentadienyl; then alternate positions (C(45)···C(49)) were introduced in the least-squares refinement with occupation factors fixed from their relative intensities, respectively 0.66 for the main cycle 3A and 0.33 for the other cycle 3B. In addition, the five carbons on each η^5-C_5H_5 were constrained to have the same isotropic thermal parameter. H atoms were included in the refinement at calculated positions on the basis of sp^2 and sp^3 geometries with d(C–H) = 0.95 Å and fixed isotropic temperature factors equal to 5 Å²: they were not refined but constrained to ride their C atoms. The structure converged with $R = 4.18\%$ and $R_w = 5.6\%$. All calculations were performed on a PDP 11/23 Plus computer using the Enraf-Nonius Structure Determination Package.[16] Analytical scattering factors for neutral atoms[17] were corrected for both the $\Delta f'$ and $\Delta f''$ components of anomalous dispersion ($\Delta f'_U = -10.673$, $\Delta f''_U = 9.654$). The U atom only was refined with anisotropic thermal parameters. The final difference Fourier synthesis showed no peaks greater than 0.5 e Å⁻³.

Final positional parameters are given in Table III; lists of structure factors, anisotropic thermal parameters, and H atoms coordinates are deposited as supplementary material.

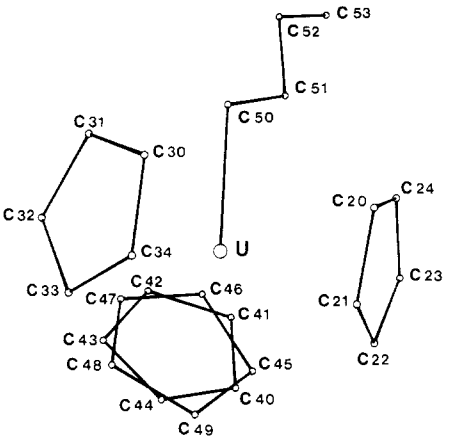

Figure 1. ORTEP II[21] drawing of the anion $[Cp_3U\text{-}n\text{-}Bu]^-$.

Table IV. Inner U Coordination Sphere Bond Lengths (Å) with Esd's: $[Cp_3U\text{-}n\text{-}Bu]^-$

	σ-Bond		
U–C(50)	2.557 (9)		
	Ring 1		
U–C(20)	2.859 (11)	U–C(23)	2.849 (11)
U–C(21)	2.826 (12)	U–C(24)	2.826 (13)
U–C(22)	2.833 (11)		
	Ring 2		
U–C(30)	2.803 (10)	U–C(33)	2.829 (11)
U–C(31)	2.848 (11)	U–C(34)	2.822 (10)
U–C(32)	2.815 (11)		
	Ring 3A		
U–C(40)	2.81 (2)	U–C(43)	2.85 (2)
U–C(41)	2.83 (2)	U–C(44)	2.81 (2)
U–C(42)	2.87 (2)		
	Ring 3B		
U–C(45)	2.91 (4)	U–C(48)	2.77 (3)
U–C(46)	2.79 (4)	U–C(49)	2.83 (3)
U–C(47)	2.79 (4)		

Results and Discussion

The crystal structure consists of discrete $[Cp_3U\text{-}n\text{-}Bu]^-$ and $[Li\text{-}2.1.1]^+$ ions.

$[Cp_3U\text{-}n\text{-}Bu]^-$ Anion. The structure of this anion with atom numbering is shown in Figure 1. Important bond lengths and angles are reported in Table IV for the U inner coordination sphere, and in Table V for σ-bonded and η^5-cyclopentadienyl groups.

The ionic species contains no crystallographically imposed symmetry. The U atom lies at the center of a distorted tetrahedron with three π-bonded η^5-cyclopentadienyl and one σ-bonded n-butyl groups. The four distances, U–centroid of Cp and U–C(50)(n-butyl), are almost the same: 2.578 (8), 2.564 (8), 2.595 (12), and 2.557 (9) Å (Table VI). The distortion refers to the angles: the centroid–U–centroid angles are all greater than the ideal

(15) North, A. C. T.; Phillips, D. C.; Mathews, F. S. *Acta Crystallogr., Sect. A: Cryst. Phys., Diffr., Theor. Gen. Crystallogr.* **1968**, *A24*, 351.

(16) Frenz, B. A. "Structure Determination Package"; College Station, TX, and Enraf-Nonius: Delft, Holland, 1983.

(17) "International Tables for X-Ray Crystallography"; Kynoch Press: Birmingham, England 1974; Vol. IV, Tables 2-2B and 2.3.1.

Table V. Bond Lengths (Å) and Angles (deg) for the η^5-Cyclopentadienyl and σ-Bonded Groups

		σ-Bonded Group	
C(50)–C(51)	1.51 (1)	U–C(50)–C(51)	120 (1)
C(51)–C(52)	1.53 (2)	C(50)–C(51)–C(52)	117 (1)
C(52)–C(53)	1.48 (2)	C(51)–C(52)–C(53)	116 (1)
		Ring 1	
C(20)–C(21)	1.42 (1)	C(24)–C(20)–C(21)	100 (1)
C(21)–C(22)	1.37 (1)	C(20)–C(21)–C(22)	113 (1)
C(22)–C(23)	1.34 (1)	C(21)–C(22)–C(23)	106 (1)
C(23)–C(24)	1.38 (1)	C(22)–C(23)–C(24)	110 (1)
C(24)–C(20)	1.47 (1)	C(23)–C(24)–C(20)	109 (1)
		Ring 2	
C(30)–C(31)	1.44 (1)	C(34)–C(30)–C(31)	105 (1)
C(31)–C(32)	1.36 (1)	C(30)–C(31)–C(32)	106 (1)
C(32)–C(33)	1.45 (1)	C(31)–C(32)–C(33)	111 (1)
C(33)–C(34)	1.32 (1)	C(32)–C(33)–C(34)	104 (1)
C(34)–C(30)	1.40 (1)	C(33)–C(34)–C(30)	114 (1)
		Ring 3A	
C(40)–C(41)	1.37 (3)	C(44)–C(40)–C(41)	105 (2)
C(41)–C(42)	1.34 (2)	C(40)–C(41)–C(42)	111 (1)
C(42)–C(43)	1.34 (3)	C(41)–C(42)–C(43)	104 (1)
C(43)–C(44)	1.32 (2)	C(42)–C(43)–C(44)	112 (2)
C(44)–C(40)	1.35 (3)	C(43)–C(44)–C(40)	108 (2)
		Ring 3B	
C(45)–C(46)	1.59 (5)	C(49)–C(45)–C(46)	103 (2)
C(46)–C(47)	1.45 (5)	C(45)–C(46)–C(47)	108 (3)
C(47)–C(48)	1.39 (4)	C(46)–C(47)–C(48)	111 (3)
C(48)–C(49)	1.52 (4)	C(47)–C(48)–C(49)	109 (3)
C(49)–C(45)	1.46 (4)	C(48)–C(49)–C(45)	109 (2)

Table VI. Comparative Bond Lengths (Å) and Angles (deg) in $(\eta^5\text{-}C_5H_5)_3U(n\text{-}C_4H_9)$

	$U^{III}(C_5H_5)_3(n\text{-}C_4H_9)$	$U^{IV}(C_5H_5)_3(n\text{-}C_4H_9)$[18]
U–C(σ-bonded)	2.557 (9)	2.426 (23)
U–1[a]	2.578 (8)	2.470
U–2	2.564 (8)	2.474
U–3	2.595 (12)	2.494
C–U–1	101 (1)	98.2
C–U–2	97 (1)	102.3
C–U–3	100 (1)	100.7
1–U–2	117 (1)	118.1
1–U–3	117 (1)	116.5
2–U–3	118 (1)	115.8
U–C(π-bonded)[b]		
ring 1	2.839 (5)	2.728 (12)
ring 2	2.823 (5)	2.738 (15)
ring 3A	2.834 (7)	2.747 (14)
ring 3B	2.820 (16)	

[a] 1 is the centroid of the cyclopentadienyl ring 1 etc. [b] Average values and related standard deviation calculated with the formulas $d_{av} = \sum_i d_i/\sigma_i^2/\sum_i 1/\sigma_i^2$ and $\sigma_{av} = (1/\sum_i 1/\sigma_i^2)^{1/2}$ where d_i is the individual distances U–C and σ_i their standard deviations.[23]

tetrahedral values ($\langle 117° \rangle$), whereas the centroid–U–*n*-Bu angles range from 97° to 101°. These angular distortions can be seen as a consequence of the steric hindrance of the Cp ligands and have also been reported in Cp_3U^{IV} compounds: Cp_3U-*n*-Bu[18] and Cp_3UCl.[19]

The Cp rings have the usual planar geometry: the C atoms of each Cp are within 0.01 Å of the best least-squares planes. The average C–C distances have correct values for cycles 1 and 2 (1.40 (1) and 1.39 (1) Å) but are somewhat too large or too small and unprecise for cycles 3A and 3B,

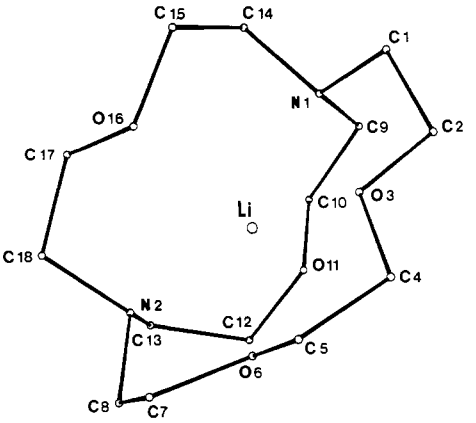

Figure 2. ORTEP II drawing of the cation $[Li\text{-}2.1.1]^+$.

Table VII. Inner Li Coordination Sphere Bond Lengths (Å) and Angles (deg) with Esd's: $[Li\text{-}2.1.1]^+$

		Bond Lengths	
Li–N(1)	2.37 (2)	N(1)–N(2)	4.134 (8)
Li–N(2)	2.20 (2)	O(11)–O(16)	3.780 (7)
Li–O(3)	2.13 (2)	N(1)–O(11)	2.816 (11)
Li–O(6)	2.10 (2)	N(1)–O(16)	2.800 (11)
Li–O(11)	2.12 (2)	N(2)–O(11)	2.809 (10)
Li–O(16)	2.22 (2)	N(21)–O(16)	2.783 (11)
		Bond Angles	
N(1)–Li–O(11)	77.6 (6)	N(1)–Li–O(3)	74.9 (6)
N(1)–Li–O(16)	75.2 (6)	O(3)–Li–O(6)	77.1 (6)
O(11)–Li–N(2)	81.2 (6)	O(6)–Li–O(16)	120.4 (8)
N(2)–Li–O(16)	78.0 (6)		

the disordered position of the third Cp ring (1.34 (3) and 1.48 (4) Å).

The conformation of the butyl ligand is trans, the internal rotation angles about the C(50)–C(51) and C(51)–C(52) bonds being 176 (2)° and 179 (2)°, respectively. The value of U–C(50)–C(51), 120 (1)°, and the C–C–C bond angles are significantly larger than the ideal tetrahedral value. The C–C distances are equal within the standard deviations (Table V).

In Table VI, the geometric parameters of $[Cp_3U^{III}\text{-}n\text{-}Bu]^-$ are compared with the distances and angles found in Cp_3U^{IV}-*n*-Bu.[18] The structure of the anion $[Cp_3U^{III}\text{-}n\text{-}Bu]^-$ on a whole is identical with the structure of Cp_3U^{IV}-*n*-Bu, U^{IV} being simply replaced by U^{III}. However, the differences observed in all the U–C distances exactly corresponds to the difference between U^{IV} and U^{III} ionic radii (0.1 Å).[20] The unusual geometry of the butyl ligand in Cp_3U^{IV}-*n*-Bu, i.e., the large value of the U–C_α–C_β angle (128.5°), the decrease of the C–C–C bond angles, and the increase of the C–C–C bond lengths from C_α to C_δ are not observed in Cp_3U^{III}-*n*-Bu^-.

$[Li\text{-}2.1.1]^+$ Cation. An ORTEP[21] drawing of the Li^+ cation, inserted in the bicyclic ligand with atom labeling scheme, is presented in Figure 2. Important bond distances and angles are listed in Table VII.

The complex cation has already been structurally characterized by Moras and Weiss[22] in the compound $[Li\text{-}2.1.1]^+[I]^-$. The structure of the cation is nearly the same in both complexes but the diad axis does not exist

(18) Perego, G.; Cesari, M.; Farina, F.; Lugli, G. *Acta Crystallogr., Sect. B: Struct. Crystallogr. Cryst. Chem.* **1976**, *B32*, 3034.
(19) Wong, C. H.; Yen, T. M.; Lee, T. Y. *Acta Crystallogr.* **1965**, *18*, 340.
(20) Shannon, R. D. *Acta Crystallogr., Sect. A: Cryst. Phys., Diffr., Theor Gen. Crystallogr.* **1976**, *A32*, 751.
(21) Johnson, C. K. ORTEP II, Report ORNL-5138; Oak Ridge National Laboratory: Oak Ridge: TN, 1976.
(22) Moras, D.; Weiss, R. *Acta Crystallogr., Sect. B: Struct. Crystallogr. Cryst. Chem.* **1973**, *B29*, 400.
(23) "Tables of Interatomic Distances and Configurations in Molecules and Ions"; The Chemical Society: London 1965.

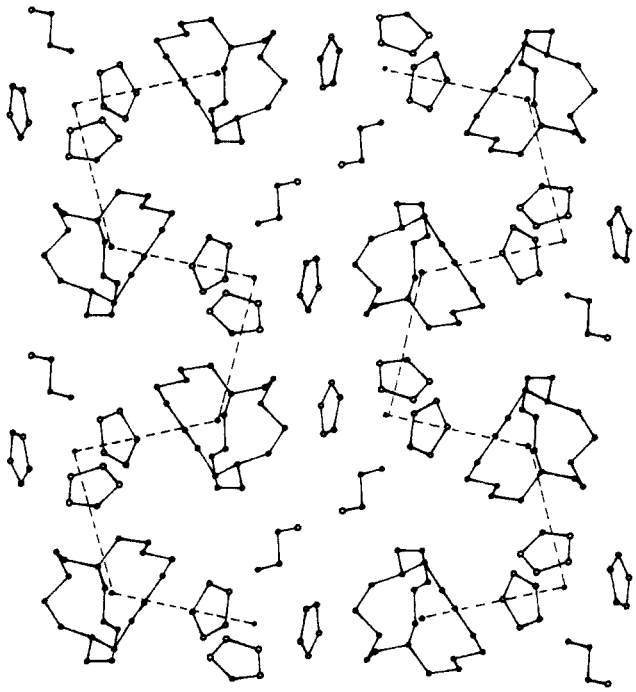

Figure 3. ORTEP II view of the packing along [100] (dashed lines through U–Li nearest neighbors).

in the present compound. The two N atoms participate in the coordination of the Li atom owing to an endo–endo conformation of the bicyclic ligand. The Li atom lies at the center of a highly distorted octahedron, a skew-parallelogram bipyramid, made of the four O atoms and the two N atoms of the cryptand. The four atoms N(1), N(2), O(11), and O(16), oxygen atoms from the two shortest chains, are coplanar within 0.02 Å while the Li atom is displaced out of this plane by 1.01 (5) Å toward O(3) and O(6) (oxygens of the long chain). O(3) and O(6) are on the same side of this plane at 2.67 (2) and 2.66 (2) Å, respectively, and form with N(1) and N(2) an approximate plane (±0.15 Å) containing Li, nearly orthogonal (92°) to the N(1)–N(2)–O(11)–O(16) plane.

The crystal packing is shown in Figure 3. No critical intermolecular distance is observed since all the C···C contacts are greater than 3.8 Å. However, this shortest intramolecular distances are observed between the α-carbon of butyl and some carbon atoms of Cp1 and Cp2 (3.2 and 3.4 Å), which may explain the relative freedom of the third Cp. Though the structure can be considered as a three-dimensional network with a marked ionic character, there exist shorter distances between metallic atoms U and Li (6.69 (1) and 6.48 (2) Å) in the [10$\bar{1}$] direction compared to other lying from 8.39 (2) to 8.89 (2) Å, which define chains of alternating anions and cations.

Registry No. $[Cp_3U\text{-}n\text{-}Bu]^-[Li\text{-}2.1.1]^+$, 99476-34-3; $Cp_3UC_4Hg^-,Li^+$, 83999-88-6; $Cp_3UCH_3^-,Li^+$, 82762-08-1; $Cp_3UC_6H_5^-,Li^+$, 99476-32-1; $Cp_3UC_4H_9$, 37298-84-3; LiC_4H_9, 109-72-8; $LiCH_3$, 917-54-4; LiC_6H_5, 591-51-6; U, 7440-61-1; C, 7440-44-0.

Supplementary Material Available: Tables of observed and calculated structure factors, refined temperature factors, and positional parameters (18 pages). Ordering information is given on any current masthead page.

Syntheses, Structures, and Solid-State ^{13}C NMR of Two η^6-Arene Uranium(IV) Complexes, $[U(C_6Me_6)Cl_2(\mu\text{-}Cl)_3UCl_2(C_6Me_6)]AlCl_4$ and $U(C_6Me_6)Cl_2(\mu\text{-}Cl)_3UCl_2(\mu\text{-}Cl)_3UCl_2(C_6Me_6)$

Gordon C. Campbell, F. Albert Cotton,* James F. Haw, and Willi Schwotzer

Department of Chemistry and Laboratory for Molecular Structure and Bonding, Texas A&M University, College Station, Texas 77843

Received May 29, 1985

Two complexes of U(IV) with hexamethylbenzene as an η^6-ligand have been prepared and structurally characterized. $[U(C_6Me_6)Cl_2(\mu\text{-}Cl)_3U(C_6Me_6)Cl_2]AlCl_4$ (1) crystallizes in the monoclinic space group $P2_1/c$ with a = 15.028 (4) Å, b = 8.716 (3) Å, c = 29.180 (11) Å, β = 93.70 (2)°, V = 3814 (4) Å^3, and Z = 4. The complex cation consists of an face-sharing bioctahedron with the η^6-C_6Me_6 moiety occupying one octahedral coordination site. $\{[UCl_2(C_6Me_6)]_2UCl_8\}$ (2) is a molecular trinuclear complex. It crystallizes in the monoclinic space group $P2_1/c$ with a = 17.171 (4) Å, b = 13.484 (3) Å, c = 17.279 (4) Å, β = 102.74 (2)°, V = 3902 (3) Å^3, and Z = 4. The molecules consist of two terminal octahedrally coordinated uranium atoms, each of which is bonded to a hexamethylbenzene. Each is sharing a trigonal $(\mu\text{-}Cl)_3$ face with the central uranium atom which has a square-antiprismatic coordination sphere of chlorine atoms. This leads to a symmetrical bent chain of uranium atoms with a U···U···U angle of 142.2° and a U···U distance of 4.033 (3) Å. Comparable bonds in both compounds are of equal length in a statistical sense, viz., U–Cl (bridge) = 2.75 [8], U–Cl (terminal) = 2.55 [2], and U–C(ring) = 2.93 [3] Å. Compound 2, which can be prepared in large quantities, was also subjected to a solid state ^{13}C NMR study. It has a temperature-dependent spectrum with chemical shifts (at −53 °C) of 3.7 (CH_3) and −39.3 ppm (aromatic). At room temperature the two signals coincide at 8 ppm.

Introduction

Despite many examples of organometallic compounds of f-block elements with π-donor ligands the nature of the bonding interaction is still controversial. Most authors who have addressed this problem in the past appear to believe that the covalent contribution to the interaction between the organic π-system and the uranium atom is of limited importance, and an entirely ionic model for cyclopentadienyl (Cp) and cyclooctatetraenyl (COT) complexes was suggested based on the results of Hückel calculations[1,2]

(1) Tatsumi, K.; Hoffmann, R. *Inorg. Chem.* **1984**, *23*, 1633.

0276-7333/86/2305-0274$01.50/0

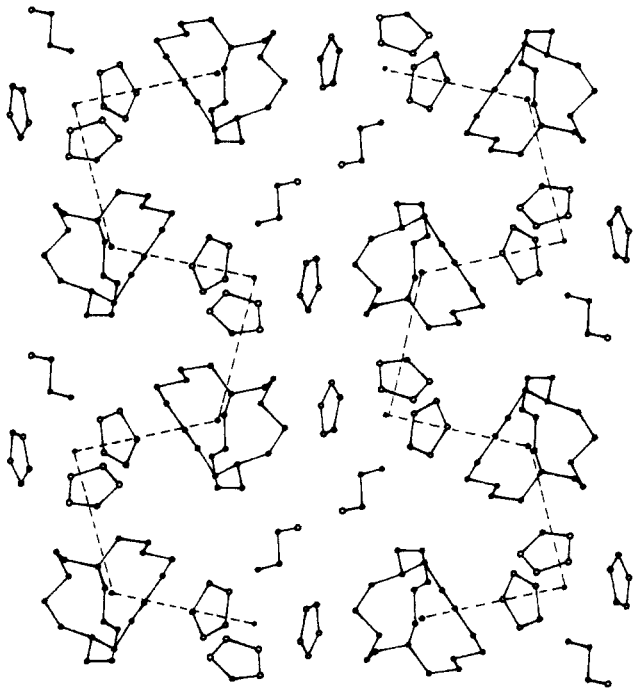

Figure 3. ORTEP II view of the packing along [100] (dashed lines through U–Li nearest neighbors).

in the present compound. The two N atoms participate in the coordination of the Li atom owing to an endo–endo conformation of the bicyclic ligand. The Li atom lies at the center of a highly distorted octahedron, a skew-parallelogram bipyramid, made of the four O atoms and the two N atoms of the cryptand. The four atoms N(1), N(2), O(11), and O(16), oxygen atoms from the two shortest chains, are coplanar within 0.02 Å while the Li atom is displaced out of this plane by 1.01 (5) Å toward O(3) and O(6) (oxygens of the long chain). O(3) and O(6) are on the same side of this plane at 2.67 (2) and 2.66 (2) Å, respectively, and form with N(1) and N(2) an approximate plane (±0.15 Å) containing Li, nearly orthogonal (92°) to the N(1)–N(2)–O(11)–O(16) plane.

The crystal packing is shown in Figure 3. No critical intermolecular distance is observed since all the C···C contacts are greater than 3.8 Å. However, this shortest intramolecular distances are observed between the α-carbon of butyl and some carbon atoms of Cp1 and Cp2 (3.2 and 3.4 Å), which may explain the relative freedom of the third Cp. Though the structure can be considered as a three-dimensional network with a marked ionic character, there exist shorter distances between metallic atoms U and Li (6.69 (1) and 6.48 (2) Å) in the [10$\bar{1}$] direction compared to other lying from 8.39 (2) to 8.89 (2) Å, which define chains of alternating anions and cations.

Registry No. $[Cp_3U\text{-}n\text{-}Bu]^-[Li\text{-}2.1.1]^+$, 99476-34-3; $Cp_3UC_4Hg^-,Li^+$, 83999-88-6; $Cp_3UCH_3^-,Li^+$, 82762-08-1; $Cp_3UC_6H_5^-,Li^+$, 99476-32-1; $Cp_3UC_4H_9$, 37298-84-3; LiC_4H_9, 109-72-8; $LiCH_3$, 917-54-4; LiC_6H_5, 591-51-6; U, 7440-61-1; C, 7440-44-0.

Supplementary Material Available: Tables of observed and calculated structure factors, refined temperature factors, and positional parameters (18 pages). Ordering information is given on any current masthead page.

Syntheses, Structures, and Solid-State ^{13}C NMR of Two η^6-Arene Uranium(IV) Complexes, $[U(C_6Me_6)Cl_2(\mu\text{-}Cl)_3UCl_2(C_6Me_6)]AlCl_4$ and $U(C_6Me_6)Cl_2(\mu\text{-}Cl)_3UCl_2(\mu\text{-}Cl)_3UCl_2(C_6Me_6)$

Gordon C. Campbell, F. Albert Cotton,* James F. Haw, and Willi Schwotzer

Department of Chemistry and Laboratory for Molecular Structure and Bonding, Texas A&M University, College Station, Texas 77843

Received May 29, 1985

Two complexes of U(IV) with hexamethylbenzene as an η^6-ligand have been prepared and structurally characterized. $[U(C_6Me_6)Cl_2(\mu\text{-}Cl)_3U(C_6Me_6)Cl_2]AlCl_4$ (1) crystallizes in the monoclinic space group $P2_1/c$ with a = 15.028 (4) Å, b = 8.716 (3) Å, c = 29.180 (11) Å, β = 93.70 (2)°, V = 3814 (4) Å^3, and Z = 4. The complex cation consists of an face-sharing bioctahedron with the η^6-C_6Me_6 moiety occupying one octahedral coordination site. $\{[UCl_2(C_6Me_6)]_2UCl_8\}$ (2) is a molecular trinuclear complex. It crystallizes in the monoclinic space group $P2_1/c$ with a = 17.171 (4) Å, b = 13.484 (3) Å, c = 17.279 (4) Å, β = 102.74 (2)°, V = 3902 (3) Å^3, and Z = 4. The molecules consist of two terminal octahedrally coordinated uranium atoms, each of which is bonded to a hexamethylbenzene. Each is sharing a trigonal $(\mu\text{-}Cl)_3$ face with the central uranium atom which has a square-antiprismatic coordination sphere of chlorine atoms. This leads to a symmetrical bent chain of uranium atoms with a U···U···U angle of 142.2° and a U···U distance of 4.033 (3) Å. Comparable bonds in both compounds are of equal length in a statistical sense, viz., U–Cl (bridge) = 2.75 [8], U–Cl (terminal) = 2.55 [2], and U–C(ring) = 2.93 [3] Å. Compound 2, which can be prepared in large quantities, was also subjected to a solid state ^{13}C NMR study. It has a temperature-dependent spectrum with chemical shifts (at −53 °C) of 3.7 (CH_3) and −39.3 ppm (aromatic). At room temperature the two signals coincide at 8 ppm.

Introduction

Despite many examples of organometallic compounds of f-block elements with π-donor ligands the nature of the bonding interaction is still controversial. Most authors who have addressed this problem in the past appear to believe that the covalent contribution to the interaction between the organic π-system and the uranium atom is of limited importance, and an entirely ionic model for cyclopentadienyl (Cp) and cyclooctatetraenyl (COT) complexes was suggested based on the results of Hückel calculations[1,2]

(1) Tatsumi, K.; Hoffmann, R. *Inorg. Chem.* **1984**, *23*, 1633.

0276-7333/86/2305-0274$01.50/0

and a comparison of metric properties.[3] Perhaps the strongest support for an ionic description stems from the conspicuous absence, with one exception, of π-complexes with neutral or cationic π-ligands. There is, on the other side, evidence that an f-orbital contribution to ligand bonding is not to be neglected.[4]

It appeared to us that further experimental and theoretical work pertinent to the above question had to involve nonanionic π-ligands.[5] In such complexes, for which there is only one example, $U(\eta^6\text{-}C_6H_6)(AlCl_4)_3$, on record[6] the π-ligand cannot be bonded by an ionic interaction and, consequently, there must be an appreciable amount of covalency.

In this paper we report the syntheses of two such complexes: $[(\eta^6\text{-}C_6Me_6)UCl_2(\mu\text{-}Cl)_3UCl_2(\eta^6\text{-}C_6Me_6)](AlCl_4)$ (1) and $[(\eta^6\text{-}C_6Me_6)UCl_2(\mu\text{-}Cl)_3UCl_2(\mu\text{-}Cl)_3UCl_2(\eta^6\text{-}C_6Me_6)]$ (2). Both compounds were isolated as crystalline solids and were stable enough to permit X-ray data collection at room temperature over several days. However, we found that the choice of solvents suitable either as reaction media or for spectroscopic studies was a very limited one, as the arene is easily displaced by even weak σ-donors. Because our options for characterization of the products were thus very restricted, we decided to turn an apparent disadvantage into an advantage by using these compounds to probe the applicability of solid-state NMR for structural problems involving paramagnetic actinide compounds.

Experimental Section

All operations were performed in a dry and anaerobic atmosphere of argon. UCl_4 was prepared from UO_3 by published procedures.[7] $AlCl_3$ was sublimed immediately prior to use. Hexamethylbenzene (hmb) was of commercial origin (Kodak) and used as received. Solvents were distilled under argon from appropriate drying agents.

Preparation of $U_2Cl_7(C_6Me_6)_2AlCl_4$. Weighed amounts of UCl_4 (380 mg, 1 mmol), hmb (200 mg, 1.2 mmol), and $AlCl_3$ (500 mg) were placed in a Schlenk flask. Hexane (20 mL) was added and the suspension boiled under reflux for 12 h. During this time the appearance and color changed and a yellow greenish precipitate deposited at the walls of the Schlenk flask close to the solvent boundary. The slightly turbid hexane solution was decanted and 20 mL of CH_2Cl_2 added. Part of the solid dissolved to form a yellowish solution. Addition of zinc powder afforded a deep red solution within 2 h. It was filtered through Celite and layered with hexane. Well-defined crystals of 1 grew at the interlayer boundary within 36 h while an amorphous red precipitate, which has not been identified, was deposited at the bottom of the flask over a period of 1 week; yield 384 mg (63%).

Preparation of $U_3Cl_{12}(C_6Me_6)_2$. A mixture of 3.8 g of UCl_4, 2 g of hmb, and 1 g of $AlCl_3$ in 50 mL of hexane was boiled under reflux for 18 h. The solvent was then decanted and the residue extracted with 50 mL of CH_2Cl_2. A first crop of green crystals (1.8 g), which deposited upon standing at room temperature overnight, was isolated by filtration. A second crop of 0.6 g was isolated after the solution was kept at 5 °C for 72 h. More of 2 was deposited at −20 °C but was contaminated with a reddish precipitate. The isolated yield of pure (coarsely crystalline) product for the NMR study was 2.4 g. Once deposited, the compound is no longer soluble in CH_2Cl_2, and it dissolves in THF or acetonitrile only with decomposition to the corresponding UCl_4 solvates.

X-ray Crystallography. Because of their moderate air sensitivity the pale green plates of 1 as well as the dark-green prisms of 2 were mounted inside Lindemann capillaries. In each case a series of crystals was surveyed and the specimen chosen for data collection was a good diffractor of X-rays with a minimal anisotropy of absorption, as evaluated by an azimuthal scan of a reflection with an Eulerian χ angle close to 90°.

Structure 1. All geometric and intensity data were taken by a CAD-4 automated four-circle diffractometer equipped with monochromated Mo Kα radiation.

The crystal orientation matrix and unit cell parameters were derived from a least-squares fit to the goniometer settings of 25 accurately located reflections in the range of $15° \leq 2\theta \leq 31°$. Data scans which employed an ω motion were made in the range of $5° \leq 2\theta \leq 45°$. The intensity data were corrected for Lorentz and polarization effects before structure factors were derived. An empirical absorption correction (μ(Mo Kα) = 88.6 cm^{-1}) was based on azimuthal scans of nine reflections near $\chi = 90°$. In all there were 2408 unique reflections with $F_o^2 \geq 3\sigma(F_o^2)$. Systematically absent reflections uniquely identified the spacegroup as $P2_1/c$.

The position of the two uranium atoms in the crystallographic asymmetric unit were derived from a three-dimensional Patterson map. The remainder of the structure was located and refined, without difficulties, by an alternating sequence of least-squares cycles and difference maps. The last cycle gave residuals of $R = 0.048$ ($R_w = 0.053$) with a quality of fit of 1.389 for the fit of 343 variables to 2408 observations.

Structure 2. All data were obtained from a Syntex P$\bar{1}$ automated four-circle diffractometer. The lattice vectors were identified by application of the automatic indexing routine to the positions of 15 reflections taken from a rotation photograph and located and centered by the diffractometer. Axial photographs confirmed the unit-cell dimensions and the monoclinic symmetry. The crystal orientation matrix and the unit cell were refined by a least-squares fit to the goniometer positions of 15 accurately located reflections in the range of $6° \leq 2\theta \leq 30°$. Intensity data were collected by the ω-scan technique in the range $5° \leq 2\theta \leq 45°$. The scan speed was variable in the range of 2–24°/min. The intensity data were corrected for Lorentz and polarization effects before structure factors were derived. An empirical absorption correction (μ(Mo Kα) = 126.25 cm^{-1}) was based on azimuthal scans of nine reflections near $\chi = 90°$. Systematically absent reflections uniquely identified the space group as $P2_1/c$. A trial structure consisting of the three uranium atoms was obtained by direct methods (MULTAN). Iterative application of least-squares refinement and difference Fourier maps led to the development of the entire structure. All but one non-hydrogen atom (C(2)) were refined with anisotropic displacement parameters; the latter refined with a satisfactory isotropic displacement parameter. The last cycle gave residuals of $R = 0.043$ ($R_w = 0.053$) with a quality of fit of 0.958 for the fit of 347 parameters to 2807 observations with $F_o^2 \geq 3\sigma(F_o^2)$.

Many data pertaining to data collection and refinement are summarized in Table I.[8] Fractional coordinates for 1 and 2 are listed in Tables II and III, respectively.

Tables IV and V summarize important bond lengths and angles for 1 and 2, respectively.

Solid-State NMR. Spectra of 2 were recorded at several temperatures on a Chemagnetics M100S NMR spectrometer at a ^{13}C frequency of 25.02 MHz. Cross polarization and magic-angle spinning were used.

Results and Discussion

Chemical Reactions. Among the relatively few examples of metal–metal bonding between very early transition metals (Ti, Zr) are the trinuclear organometallic clusters formed under reductive Friedel–Crafts conditions.[9] In an

(2) Pyykkö, P.; Lohr, L. L., Jr. *Inorg. Chem.* **1981**, *20*, 1950.
(3) Raymond, K. N.; Eigenbrot, C. W., Jr. *Acc. Chem. Res.* **1980**, *13*, 283.
(4) (a) Rösch, N.; Streitwieser, A. *J. Organomet. Chem.* **1978**, *145*, 195. (b) Veal, B. W.; Law, D. T. In "Lanthanide and Actinide Chemistry and Spectroscopy": Edelstein, N. M., Ed.; American Chemical Society: Washington, D.C., 1980; *ACS Symp. Ser. No. 131*. (c) Denning, R. G.; Norris, T. O. W.; Shom, I. G.; Snellgrove, T. R.; Woodwark, D. R. *Ibid.* **1980**, *No. 131*, 313–330.
(5) Cotton, F. A.; Schwotzer, W. *Organometallics* **1985**, *4*, 942.
(6) Cesari, M.; Pedretti, U.; Zazetta, A.; Lugli, G.; Marconi, W. *Inorg. Chim. Acta* **1971**, *5*, 439.
(7) Herman, T. A.; Suttle, J. F. *Inorg. Synth.* **1957**, *5*, 143.
(8) Crystallographic calculations were done with VAXSDP software on the VAX-11/780 computer at the Department of Chemistry, Texas A&M University.
(9) Fischer, E. O.; Wawersik, T. *J. Organomet. Chem.* **1966**, *5*, 559.

Table I. Crystallographic Data

formula	$U_2Cl_{11}AlC_{24}H_{36}$	$U_3Cl_{12}C_{24}H_{36}$
fw	1217.6	1464.1
space group	$P2_1/c$	$P2_1/c$
systematic absences	$h0l$, $l = 2n + 1$; $0k0$, $k = 2n + 1$	$h0l$, $l = 2n + 1$; $0k0$, $k = 2n + 1$
a, Å	15.028 (4)	17.171 (4)
b, Å	8.716 (3)	13.484 (3)
c, Å	29.180 (11)	17.279 (4)
β, deg	93.70 (2)	102.74 (2)
V, Å^3	3814 (4)	3902 (3)
Z	4	4
d_{calcd}, g/cm^3	2.12	2.49
cryst size, mm	0.2 × 0.2 × 0.1	0.3 × 0.2 × 0.2
μ(Mo Kα), cm^{-1}	88.60	126.25
data collectn instrument	Enraf-Nonius CAD-4	Syntex P$\bar{1}$
radiatn (monochromated in incident beam)	Mo Kα	Mo Kα
orientatn reflctns, no., range (2θ)	25, $15 < 2\theta < 31$	15, $16 < 2\theta < 30$
temp, °C	25	5
scan method	ω scan	ω scan
data col range 2θ, deg	$5 < 2\theta < 45$	$5 < 2\theta < 45$
no. of unique data, total with $F_o^2 > 3\sigma(F_o^2)$	2408	2807
no. of parameters refined	343	347
trans factors, max, min (exptl)	1.0, 0.73	1.0, 0.82
R^a	0.048	0.043
$R_w{}^b$	0.053	0.053
quality of fit indicator^c	1.309	0.958
largest shift/esd, final cycle	0.31	0.08
largest peak, e/Å^3	1.5, 1.4 (around U1, U2)	0.79

^{a} $R = \Sigma \| F_o| - |F_c| / \Sigma |F_o|$. ^{b} $R_w = [\Sigma w(|F_o| - |F_c|)^2 / \Sigma w|F_o|^2]^{1/2}$; $w = 1/\sigma^2(|F_o|)$. ^{c} Quality of fit = $[\Sigma w(|F_o| - |F_c|)^2/(N_{obsd} - N_{parmeters})]^{1/2}$.

Table II. Positional and Thermal Parameters and Their Estimated Standard Deviations for $U_2Cl_{11}AlC_{24}H_{36}$[a]

atom	x	y	z	B, Å^2
U1	0.28098 (6)	0.0517 (1)	0.02409 (3)	3.32 (2)
U2	0.33840 (6)	0.1421 (1)	0.15475 (3)	3.72 (2)
Cl1	0.8011 (4)	0.7043 (7)	0.4072 (2)	4.4 (2)
Cl2	0.6765 (4)	0.3841 (7)	0.3960 (2)	4.8 (2)
Cl3	0.5866 (4)	0.7045 (7)	0.4285 (2)	4.4 (2)
Cl4	0.6145 (4)	0.3612 (8)	0.5084 (2)	5.2 (2)
Cl5	0.8524 (4)	0.3783 (8)	0.4800 (3)	5.6 (2)
Cl6	0.6351 (5)	0.9257 (9)	0.3342 (3)	7.2 (2)
Cl7	0.5036 (4)	0.5669 (9)	0.3197 (2)	6.4 (2)
Cl8	0.1268 (5)	0.766 (1)	0.2988 (3)	8.4 (2)
Cl9	0.9478 (6)	0.380 (1)	0.0979 (3)	8.9 (3)
Cl10	0.7381 (6)	0.479 (1)	0.1274 (3)	11.1 (3)
Cl11	0.9211 (8)	0.647 (1)	0.1824 (4)	13.8 (4)
Al1	0.8708 (6)	0.445 (1)	0.1522 (3)	6.2 (2)
C1	0.756 (2)	0.859 (3)	0.5139 (8)	4.7 (6)
C2	0.674 (2)	0.821 (3)	0.5316 (8)	4.5 (6)
C3	0.671 (1)	0.687 (2)	0.5616 (8)	3.8 (5)
C4	0.752 (2)	0.600 (3)	0.5730 (8)	4.5 (6)
C5	0.834 (2)	0.652 (3)	0.5565 (9)	5.5 (7)
C6	0.834 (2)	0.775 (3)	0.5232 (8)	4.5 (6)
C7	0.758 (2)	1.000 (3)	0.485 (1)	7.8 (9)
C8	0.590 (2)	0.922 (3)	0.524 (1)	7.5 (8)
C9	0.586 (2)	0.651 (3)	0.5846 (9)	6.5 (7)
C10	0.752 (2)	0.467 (3)	0.6066 (9)	7.6 (8)
C11	0.920 (2)	0.573 (4)	0.573 (1)	9.0 (9)
C12	0.922 (2)	0.823 (3)	0.505 (1)	7.6 (9)
C13	0.774 (1)	0.420 (3)	0.2973 (8)	3.8 (6)
C14	0.696 (2)	0.435 (3)	0.2696 (8)	5.4 (7)
C15	0.671 (1)	0.581 (3)	0.2504 (8)	4.7 (6)
C16	0.730 (2)	0.710 (3)	0.2562 (8)	4.8 (7)
C17	0.807 (2)	0.698 (3)	0.2864 (7)	4.8 (6)
C18	0.830 (2)	0.552 (3)	0.3040 (8)	5.4 (7)
C19	0.804 (2)	0.264 (3)	0.3151 (9)	6.2 (7)
C20	0.633 (2)	0.299 (3)	0.261 (1)	8.8 (9)
C21	0.588 (2)	0.594 (4)	0.2164 (9)	8.4 (9)
C22	0.709 (2)	0.858 (3)	0.230 (1)	9 (1)
C23	0.867 (2)	0.839 (3)	0.294 (1)	8.2 (9)
C24	0.920 (2)	0.534 (3)	0.3304 (8)	5.7 (7)

[a] Anisotropically refined atoms are given in the form of the isotropic equivalent thermal parameter defined as $^4/_3[a^2\beta_{11} + b^2\beta_{22} + c^2\beta_{33} + ab(\cos\gamma)\beta_{12} + ac(\cos\beta)\beta_{13} + bc(\cos\alpha)\beta_{23}]$.

Table III. Positional and Thermal Parameters and Their Estimated Standard Deviations $U_3Cl_{12}C_{24}H_{36}$[a]

atom	x	y	z	B, Å^2
U1	0.18196 (5)	0.27943 (7)	0.44100 (5)	2.92 (2)
U2	0.22146 (5)	0.52907 (7)	0.32673 (5)	2.78 (2)
U3	0.37833 (5)	0.65674 (7)	0.21490 (5)	2.66 (2)
Cl1	0.2974 (4)	0.1575 (6)	0.4589 (4)	5.2 (2)
Cl2	0.1947 (4)	0.3046 (6)	0.5893 (4)	5.5 (2)
Cl3	0.2021 (3)	0.3211 (4)	0.2936 (3)	3.2 (1)
Cl4	0.1060 (3)	0.4525 (5)	0.4129 (4)	4.1 (1)
Cl5	0.3006 (3)	0.4213 (5)	0.4585 (3)	3.5 (1)
Cl6	0.0916 (4)	0.5283 (5)	0.2228 (4)	4.1 (1)
Cl7	0.1942 (5)	0.6710 (6)	0.4118 (4)	5.7 (2)
Cl8	0.2994 (4)	0.4780 (5)	0.2078 (4)	3.9 (1)
Cl9	0.3804 (4)	0.6005 (5)	0.3670 (3)	4.2 (1)
Cl10	0.2308 (4)	0.7019 (5)	0.2288 (4)	4.2 (2)
Cl11	0.4978 (4)	0.5496 (5)	0.2093 (6)	7.2 (2)
Cl12	0.3286 (6)	0.6577 (6)	0.0661 (4)	7.1 (2)
C1	0.433 (2)	0.848 (2)	0.164 (1)	4.4 (6)
C2	0.375 (1)	0.871 (2)	0.207 (1)	2.9 (5)*
C3	0.391 (1)	0.851 (2)	0.289 (1)	4.2 (6)
C4	0.460 (1)	0.807 (2)	0.327 (1)	3.8 (6)
C5	0.516 (1)	0.781 (2)	0.280 (2)	4.4 (6)
C6	0.501 (1)	0.798 (2)	0.198 (2)	4.0 (6)
C7	0.420 (2)	0.880 (2)	0.076 (1)	9 (1)
C8	0.296 (2)	0.929 (2)	0.167 (2)	9 (1)
C9	0.335 (2)	0.892 (3)	0.340 (2)	9.7 (9)
C10	0.490 (3)	0.804 (2)	0.418 (2)	9 (1)
C11	0.598 (2)	0.734 (3)	0.326 (2)	8 (1)
C12	0.566 (1)	0.778 (3)	0.150 (2)	7.3 (8)
C13	0.111 (1)	0.083 (2)	0.390 (1)	4.0 (6)
C14	0.096 (1)	0.099 (2)	0.467 (1)	4.4 (6)
C15	0.044 (2)	0.173 (2)	0.480 (1)	4.3 (6)
C16	0.009 (1)	0.238 (2)	0.417 (2)	4.7 (6)
C17	0.025 (1)	0.227 (2)	0.337 (1)	4.4 (6)
C18	0.076 (1)	0.148 (2)	0.327 (1)	3.4 (5)
C19	0.155 (2)	−0.009 (2)	0.374 (2)	6.9 (9)
C20	0.135 (2)	0.032 (2)	0.538 (2)	7.5 (9)
C21	0.019 (2)	0.185 (3)	0.557 (2)	8 (1)
C22	−0.054 (2)	0.316 (3)	0.427 (2)	8 (1)
C23	−0.017 (2)	0.294 (2)	0.269 (2)	6.2 (7)
C24	0.089 (2)	0.121 (2)	0.243 (1)	6.2 (7)

[a] Anisotropically refined atoms are given in the form of the isotropic equivalent thermal parameter defined as $^4/_3[a^2\beta_{11} + b^2\beta_{22} + c^2\beta_{33} + ab(\cos\gamma)\beta_{12} + ac(\cos\beta)\beta_{13} + bc(\cos\alpha)\beta_{23}]$.

Table IV. Selected Bond Distances (Å) and Angles (deg) for $U_2Cl_{11}AlC_{24}H_{36}$[a]

(a) Bond Lengths

U1	U2	3.934 (1)	U1	C4	2.88 (2)	U2	C14	2.92 (3)
U1	Cl1	2.763 (6)	U1	C5	2.96 (2)	U2	C15	2.83 (2)
U1	Cl2	2.791 (6)	U1	C6	2.89 (2)	U2	C16	2.91 (2)
U1	Cl3	2.701 (6)	U2	Cl1	2.732 (6)	U2	C17	2.91 (2)
U1	Cl4	2.513 (7)	U2	Cl2	2.694 (6)	U2	C18	2.98 (3)
U1	Cl5	2.507 (6)	U2	Cl3	2.796 (6)	Cl8	Al1	2.119 (13)
U1	C1	2.94 (2)	U2	Cl6	2.521 (7)	Cl9	Al1	2.100 (13)
U1	C2	2.96 (2)	U2	Cl7	2.529 (6)	Cl10	Al1	2.098 (12)
U1	C3	2.90 (2)	U2	C13	2.98 (2)	Cl11	Al1	2.089 (14)

(b) Bond Angles

Cl1	U1	Cl2	74.6 (2)	Cl1	U2	Cl2	76.6 (2)	U1	Cl1	U2	91.4 (2)
Cl1	U1	Cl3	74.9 (2)	Cl1	U2	Cl3	73.9 (2)	U1	Cl2	U2	91.6 (2)
Cl1	U1	Cl4	155.7 (2)	Cl1	U2	Cl6	89.9 (2)	U1	Cl3	U2	91.4 (2)
Cl1	U1	Cl5	86.1 (2)	Cl1	U2	Cl7	155.8 (2)	Cl8	Al1	Cl9	103.8 (5)
Cl2	U1	Cl3	73.1 (2)	Cl2	U2	Cl3	73.1 (2)	Cl8	Al1	Cl10	108.2 (5)
Cl2	U1	Cl4	81.6 (2)	Cl2	U2	Cl6	153.6 (2)	Cl8	Al1	Cl11	110.4 (5)
Cl2	U1	Cl5	82.2 (2)	Cl2	U2	Cl7	89.4 (2)	Cl9	Al1	Cl10	109.6 (5)
Cl3	U1	Cl4	93.5 (2)	Cl3	U2	Cl6	81.5 (2)	Cl9	Al1	Cl11	110.2 (6)
Cl3	U1	Cl5	151.9 (2)	Cl3	U2	Cl7	83.3 (2)	Cl10	Al1	Cl11	109.6 (6)
Cl4	U1	Cl5	95.8 (2)	Cl6	U2	Cl7	94.5 (3)				

[a] Numbers in parentheses are estimated standard deviations in the least significant digits.

attempt to mimic their chemistry we originally reacted UCl_4, $AlCl_3$, hmb, and aluminum in a melt reaction. Although a reaction appeared to have occurred, we were unable to isolate uranium–arene complexes. The crude reaction mixture was insoluble in all but coordinating solvents from which we were able to isolate only the UCl_4 solvates.[10] We then decided to perform the reaction in two steps: electrophilic addition of the UCl_4–$AlCl_3$ complex in an inert solvent followed by reduction in a more polar but noncoordinating solvent. We realized that the choice of solvent for the first step was a limited one, indeed. Solvents with σ-donor capability will directly compete with the π-ligand, halohydrocarbons in the presence of $AlCl_3$ are electrophiles in their own right, and aromatic hydrocarbons will compete with hmb by mass action. We thus chose hexane in which the arylation of UCl_4 was completed in less than 12 h.

That the proposed reduction of the U(IV)–arene complex is yet to be achieved was obvious after successful structural characterization of **1**. We then considered the possibility that **1** might be isolated directly from a CH_2Cl_2 extract of the reaction mixture. At the same time we reduced the amount of the Friedel–Crafts catalyst, $AlCl_3$, from a massive excess to a near-stoichiometric quantity. While this did not, in fact, provide a way to prepare **1**, it leads reproducibly to a structurally related trinuclear U(IV) complex, **2**, which is unprecedented. In contrast to **1**, which is difficult to isolate in pure form and large quantities, compound **2** is obtained in decent yields without contamination by slow crystallization from CH_2Cl_2.

Structures. Crystals of **1** consist of an ordered array of dinuclear complex cations and $AlCl_4$ anions. Compound **2** is a trinuclear molecular complex. Perspective drawings are shown in Figures 1 and 2 for compounds **1** and **2**, respectively.

The complex cation $\{[U(C_6Me_6)Cl_2]_2(\mu\text{-}Cl)_3\}^+$ is conveniently described in terms of a face-sharing bioctahedron with the C_6Me_6 molecule occupying one ligand site. Important bond distances are U–Cl (bridge) = 2.75 [5] Å, U–Cl (terminal) = 2.58 [1] Å, and U–C (ring) = 2.92 [4] Å. The U···U distance is 3.937 (1) Å. The coordination of the uranium is discussed below in comparison with structure **2**. The $AlCl_4$ anion is, within the error of the experiment, tetrahedral with average Al–Cl bond lengths of 2.10 [5] Å.

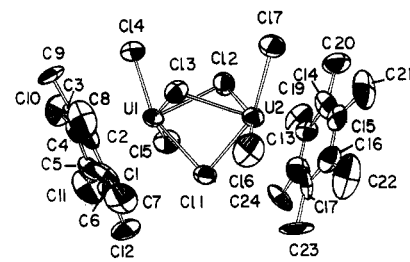

Figure 1. An ORTEP drawing of the $\{[U(C_6Me_6)Cl_2]_2(\mu\text{-}Cl)_3\}^+$ cation, giving the atom labeling scheme. All atoms are represented by their ellipsoids of thermal vibration at the 40% probability level.

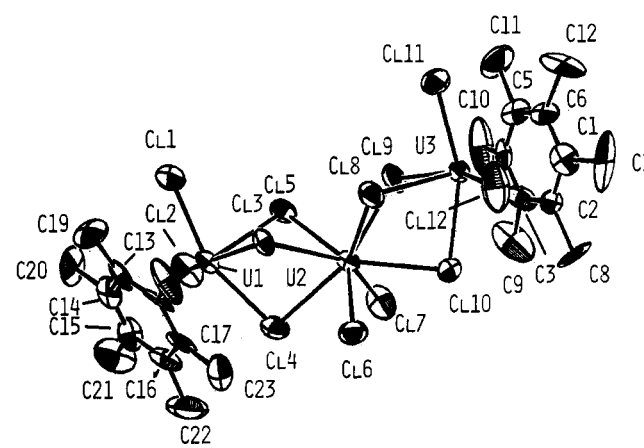

Figure 2. An ORTEP drawing of the $[(C_6Me_6)UCl_2(\mu\text{-}Cl)_3UCl_2(\mu\text{-}Cl)_3UCl_2(C_6Me_6)]$ molecule with the atom labeling scheme.

Complex **2** can be derived from **1** by formal insertion of a UCl_5^- subunit into the $(\mu\text{-}Cl)_3$ bridge. The central uranium atom is thus eight-coordinate, and we can describe the coordination polyhedron as a square antiprism (SAP) with Cl(3), Cl(5), Cl(9), Cl(8) and Cl(4), Cl(7), Cl(10), Cl(6) defining the squares.[11] The distortion from the ideal SAP metric[12] stems from the significant differences in bond

(10) Cotton, F. A.; Marler, D. O.; Schwotzer, W. *Acta Crystallogr. Sect. C: Cryst. Struct. Commun.* **1984**, *C40*, 1186.

(11) A description as a kinked bicapped bigonal prism is also conceivable but we found that the distortions from the idealized geometry are more severe.

Table V. Table of Bond Distances (Å) and Bond Angles (deg) in $U_3Cl_{12}C_{24}H_{36}$

(a) Bond Distances

U1	U2	4.035 (1)	U1	C18	2.96 (2)	U3	Cl9	2.728 (6)
U1	Cl1	2.541 (7)	U2	U3	4.031 (1)	U3	Cl10	2.667 (7)
U1	Cl2	2.546 (7)	U2	Cl3	2.867 (6)	U3	Cl11	2.529 (8)
U1	Cl3	2.703 (6)	U2	Cl4	2.918 (7)	U3	Cl12	2.523 (7)
U1	Cl4	2.666 (7)	U2	Cl5	2.789 (6)	U3	C1	2.94 (3)
U1	Cl5	2.762 (6)	U2	Cl6	2.535 (5)	U3	C2	2.89 (2)
U1	C13	2.97 (2)	U2	Cl7	2.519 (8)	U3	C3	2.90 (3)
U1	C14	2.93 (3)	U2	Cl8	2.775 (7)	U3	C4	2.94 (2)
U1	C15	2.97 (3)	U2	Cl9	2.833 (6)	U3	C5	2.92 (2)
U1	C16	2.96 (2)	U2	Cl10	2.905 (7)	U3	C6	2.90 (2)
U1	C17	2.97 (2)	U3	Cl8	2.755 (6)			

(b) Bond Angles

Cl1	U1	Cl2	94.2 (2)	Cl4	U2	Cl5	70.3 (2)	Cl8	U2	Cl9	70.8 (2)
Cl1	U1	Cl3	89.4 (2)	Cl4	U2	Cl6	76.7 (2)	Cl8	U2	Cl10	70.7 (2)
Cl1	U1	Cl4	157.8 (2)	Cl4	U2	Cl7	74.7 (2)	Cl9	U2	Cl10	72.3 (2)
Cl1	U1	Cl5	84.1 (2)	Cl4	U2	Cl8	141.5 (2)	Cl8	U3	Cl9	72.6 (2)
Cl2	U1	Cl3	156.9 (2)	Cl4	U2	Cl9	136.1 (2)	Cl8	U3	Cl10	74.7 (2)
Cl2	U1	Cl4	89.8 (2)	Cl4	U2	Cl10	135.4 (2)	Cl8	U3	Cl11	83.9 (2)
Cl2	U1	Cl5	84.2 (2)	Cl5	U2	Cl6	140.4 (2)	Cl8	U3	Cl12	84.7 (2)
Cl3	U1	Cl4	78.8 (2)	Cl5	U2	Cl7	92.2 (2)	Cl9	U3	Cl10	77.8 (2)
Cl3	U1	Cl5	73.4 (2)	Cl5	U2	Cl8	104.4 (2)	Cl9	U3	Cl11	92.3 (3)
Cl4	U1	Cl5	74.5 (2)	Cl5	U2	Cl9	73.0 (2)	Cl9	U3	Cl12	155.8 (3)
U1	U2	U3	142.47 (3)	Cl5	U2	Cl10	144.5 (2)	Cl10	U3	Cl11	158.2 (2)
Cl3	U2	Cl4	72.2 (2)	Cl6	U2	Cl7	99.7 (2)	Cl10	U3	Cl12	88.6 (3)
Cl3	U2	Cl5	70.6 (2)	Cl6	U2	Cl8	88.1 (2)	Cl11	U3	Cl12	93.4 (3)
Cl3	U2	Cl6	79.0 (2)	Cl6	U2	Cl9	145.5 (2)	U1	Cl4	U2	92.4 (2)
Cl3	U2	Cl7	146.2 (2)	Cl6	U2	Cl10	75.1 (2)	U1	Cl5	U2	93.3 (2)
Cl3	U2	Cl8	70.3 (2)	Cl7	U2	Cl8	143.4 (2)	U2	Cl8	U3	93.6 (2)
Cl3	U2	Cl9	116.4 (2)	Cl7	U2	Cl9	83.8 (2)	U2	Cl9	U3	92.9 (2)
Cl3	U2	Cl10	133.4 (2)	Cl7	U2	Cl10	76.8 (2)	U2	Cl10	U3	92.6 (2)

[a] Numbers in parentheses are estimated standard deviations in the least significant digits.

lengths for the bridging and the terminal chlorides. Consequently the deviations from the best plane including chlorides 3, 5, 9, and 8 (all bridging) are less than 0.1 Å while those of 4, 7, 10, and 6 are all 0.26 Å. The dihedral angle between the best planes is 2.2°. Each terminal octahedral uranium atom and the central square-antiprismatic one are then mutually sharing a trigonal face which leads to a bent arrangement of the three uranium atoms with an angle of 142.4° and an average U···U distance of 4.033 [3] Å. Other important averaged distances are U–Cl (terminal) = 2.53 [1] Å, U–Cl (bridge) = 2.78 [8] Å, and U–C (ring) = 2.94 [3] Å.

The coordination of the uranium atoms bonded to hmb deserves special attention. Both U atoms in **1** and the terminal U atoms in **2** have a distorted octahedral coordination with the hmb molecules occupying one site. There are two sources of distortion: First, hmb is a rather bulky ligand and, second, three of the five remaining chloride ligands are tied together as they constitute a μ_3 bridge. Consequently we find the U atom displaced from the meridinal plane defined by the four chlorides cis to the hmb ligand. This deviation, which is easily seen in the ORTEP drawing, is on the average 0.53 Å in **1** and 0.48 Å in **2**, while deviations of the Cl from the respective mean planes are less than 0.02 Å. No statistically significant deviations from planarity for the hmb moieties is seen in either structure. All aromatic carbon atoms are planar with none of the sums of bond angles deviating more than 1° from the theoretical value of 360°.

Turning our attention now to the U–C distances we find, in comparison with previously published data (Table VI), that the U–C bond lengths observed in **1** and **2** are among the longest on record. While it is understood that there is no simple correlation between bond length and bond strength, this observation concurs with our experience that the hmb ligands are easily displaced.

Table VI. Comparison of U(IV)–C π-Bond Lengths

compd	U–C(mean), Å	ref
$(C_8H_8)_2U$	2.65	18
$[(CH_3)_4C_8H_4]_2U$	2.66	19
$Cp_3U(C{\equiv}CPh)$	2.68	20
$CpU(2\text{-}Me\text{-}C_3H_4)_3$	2.79 (Cp), 2.66 (term), 2.80 (centr)	21
$U[(Cp)_2CH_2]Cl_2(bpy)$	2.72	22
$(Cp)_4U$	2.81	23
$[U(\eta^3\text{-}C_3H_5)_2(O\text{-}i\text{-}Pr)_2]_2$	2.68	24
$U[(CH_3)_5C_5]_2\{\eta^2\text{-}CO[N\text{-}(CH_3)_2]\}_2$	2.78	25
$Cp_2U[O_2C_2CHP(Me)_2(C_6H_5)\text{-}Fe_2Cp_2(CO)_2]_2$	2.89	26
$U(\eta^6\text{-}C_6H_6)(AlCl_4)_3$	2.91	6
$\{[U(\eta^6\text{-}C_6Me_6)Cl_2]_2(\eta\text{-}Cl)_3\}\text{-}AlCl_4$	2.92	this work
$\{[UCl_2(C_6Me_6)]_2UCl_5\}$	2.94	this work

Bonding. The nature of the bond between π-donor ligands and the actinide centers has attracted a great deal of attention. On the theoretical side it appears that extended Hückel analysis and relativistically parameterized extended Hückel calculations consistently evaluate the interaction between Cp^- and U^{4+} as well as between COT^{2-} and U^{4+} as being almost exclusively ionic.[1,2] This view received support from an attempt to derive the ionic nature of these bonds from the metric properties of the compounds.[3] SCF-Xα scattered-wave MO studies on uranocene and thorocene, on the other hand, suggested a considerable amount of covalency in these compounds.[4a]

Quite obviously, an ionic bonding model cannot be invoked for the two complexes presented here. Consistent with the high Lewis acidity of UCl_4 and the electron-rich character of C_6Me_6 the bonding can be visualized as a dative interaction of the arene with UCl_4. The composition

(12) (a) Hoard, J. L.; Silverton, J. V. *Inorg. Chem.* **1963**, *2*, 235. (b) Blight, D. G.; Kepert, D. L. *Theor. Chim. Acta* **1968**, *11*, 51. (c) Kepert, D. *J. Chem. Soc.* **1965**, 4736.

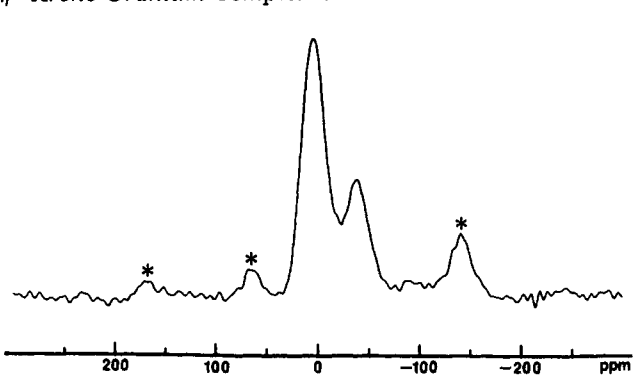

Figure 3. CP/MAS ^{13}C NMR spectrum $[(C_6Me_6)UCl_2(\mu\text{-}Cl)_3UCl_2(\mu\text{-}Cl)_3UCl_2(C_6Me_6)]$ at −53 °C. Spinning sidebands are labeled with asterisks.

of the metal acceptor orbitals is unknown. It cannot be considered surprising that both **1** and **2** are easily decomposed by efficient σ-donors such as pyridine or THF even though they are quite stable in a thermodynamic sense.

It is our experience that the above complexes are by no means isolated examples as we have observed (though not yet characterized) Friedel–Crafts type reactions of UCl_4 with other π-systems including pyrene and perilene. It was interesting to learn in a recent report about a Th–Ni interaction, i.e., a dative bond between a nucleophilic transition metal with Th(IV).[13]

Solid-State ^{13}C NMR. The insolubility of the title compounds in nondestructive solvents aroused our interest in solid-state analytical techniques other than X-ray crystallography. NMR spectroscopy, which is such a powerful tool in solution chemistry, came to mind, although we were concerned about possible difficulties related to the paramagnetism of U(IV). Spectra with good signal to noise ratios and with reasonable line widths were obtained in relatively short times (typically 45 min). At room temperature a single resonance, accompanied by the spinning sidebands, was detected at 8.0 ppm, i.e., 9.4 ppm upfield from the methyl resonance of solid hmb. It was tempting to assign this signal to the methyl groups of the complexed hmb and to rationalize the apparent absence of resonances due to the aromatic carbons in terms of broadening of the lines below detection level by paramagnetic relaxation. However, a careful evaluation of the intensity of the spinning sidebands and the powder pattern (obtained in a CP/MAS experiment without sample spinning) suggested an alternative (and correct) interpretation: the signal at 8.0 ppm consists of a superposition of two signals with almost identical isotropic chemical shift but different chemical shift anisotropies. In order to verify this interpretation, we recorded a set of spectra at temperatures between −105 °C and +23 °C.[14] It is well-known from solution NMR studies that chemical shifts of paramagnetic compounds are temperature dependent.[15] This temperature dependence is in a first approximation a Curie–Weiss behavior, possibly modified by temperature-dependent conformational changes or the presence of low-lying excited states. Important for our purpose is that the temperature shift increments will depend on the nature of the individual nuclei; i.e., the shifts of chemically different nuclei will be affected differently by temperature changes. This is exactly our observation, and a representative spectrum at −53 °C is shown in Figure 3 while a composite drawing of the variable-temperature experiment was deposited with the supplementary material. While the chemical shift of the methyl groups is hardly affected at all ($\Delta\delta$ = 4.7 ppm), the aromatic signal (identified by the larger size of the spinning sidebands due to the inherently larger chemical shift anisotropy) is shifted by 47.7 ppm.

Even with the fortuitous coincidence of the methyl and the aromatic signals resolved the spectrum still is deceptively simple. Inspection of the solid-state structure reveals virtual C_{2v} symmetry and nonequivalence of the carbons within the ring. There are two possible explanations for the observed signal averaging. It is conceivable that the chemical shift differences between the individual sites are obscured by the relatively broad lines. Alternatively, fast rotation (on the time scale of the experiment) of the hmb rings will lead to signal averaging. Dynamic processes of this type in the solid state are not unprecedented.[16]

A detailed study of the temperature dependence of this and other uranium organometallics is presently in progress and will be reported separately. We note that this represents the first CP/MAS ^{13}C NMR study of organoactinide compounds and that there is only one report of a solid-state NMR study of a paramagnetic compound on record.[17] It is our impression that solid-state ^{13}C is widely applicable to organoactinides and thus represents a valuable tool for the synthetic chemist.

Acknowledgment. We thank the Robert A. Welch Foundation (F.A.C.) and the Center for Energy and Mineral Resources at Texas A&M University (J.F.H.) for financial support.

Registry No. 1, 99496-10-3; 2, 99496-11-4; hmb, 87-85-4; $AlCl_3$, 7446-70-0; UCl_4, 10026-10-5.

Supplementary Material Available: Two tables of observed and calculated structure factors, two tables of anisotropic displacement parameters, complete tables of bond lengths and bond angles, and a composite drawing of the CP/MAS ^{13}C NMR spectra between −74 °C and 23 °C (40 pages). Ordering information is given on any current masthead page.

(13) Ritchey, J. M.; Zoznlin, A. J.; Wrobleski, D. A.; Ryan, R. R.; Wasserman, H. J.; Moody, D. C.; Paine, R. T. *J. Am. Chem. Soc.* **1985**, *107*, 501.

(14) An attempt to acquire the spectrum at temperatures above ambient ended when the deldrin rotor in which the sample was packed shattered.

(15) Luke, W. D.; Streitwieser, A., Jr. *ACS Symp. Ser.* **1980**, *No. 131*, 93.

(16) Fyfe, C. A. "Solid State NMR For Chemists"; C.F.C. Press: Guelph, 1984; pp 412–419.

(17) Chacko, V. P.; Ganapathy, S.; Bryant, R. G. *J. Am. Chem. Soc.* **1983**, *105*, 5491.

(18) Zalkin, A.; Raymond, K. N. *J. Am. Chem. Soc.* **1969**, *91*, 5667.

(19) Hogson, K. O.; Raymond, K. N. *Inorg. Chem.* **1973**, *12*, 458.

(20) Atwood, J. L.; Hains, C. F.; Tsutsui, M.; Gebala, A. E. *J. Chem. Soc., Chem. Commun.* **1973**, 453.

(21) Day, V. W.; Ernst, R. D. Cited In "Comprehensive Organometallic Chemistry"; Wilkinson, G.; Stone, F. G. A.; Abel, E. W., Eds.; Pergamon Press: Oxford, 1982; Vol. 3, p 240.

(22) Secaur, C. A.; Day, V. W.; Ernst, R. D.; Kennelly, W. J.; Marks, T. J. *J. Am. Chem. Soc.* **1976**, *98*, 3713.

(23) Burns, J. H. *J. Organomet. Chem.* **1974**, *69*, 225.

(24) Brunelli, M.; Perego, G.; Lugli, G.; Mazzei, A. *J. Chem. Soc., Dalton Trans.* **1979**, 861.

(25) Fagan, P. J.; Manriquez, J. M.; Vollmer, S. H.; Secaur Day, C.; Day, V. W.; Marks, T. J. *J. Am. Chem. Soc.* **1981**, *103*, 2206.

(26) Cramer, R. E.; Higa, K. T.; Pruskin, S. L. Gilje, J. W. *J. Am. Chem. Soc.* **1983**, *105*, 6749.

The Chemistry of (Fulvalene)dimolybdenum Hexacarbonyl: A Rigidly Held Dinuclear Transition-Metal Complex

James S. Drage and K. Peter C. Vollhardt*

Department of Chemistry, University of California, Berkeley, and the Materials and Molecular Research Division, Lawrence Berkeley Laboratory, Berkeley, California 94720

Received August 13, 1985

The X-ray structure of (fulvalene)dimolybdenum hexacarbonyl [$FvMo_2(CO)_6$] has been determined. Thermal, photolytic, and chemical treatment failed to yield the metal–metal triply bonded complex $FvMo_2(CO)_4$, either because it was not formed or because of its instability; this result may have been caused by excessive bond strain in the fulvalene ligand. Photolysis of $FvMo_2(CO)_6$ in the presence of alkynes afforded mono- and bis(alkyne) complexes $FvMo_2(CO)_4(RC{\equiv}CR)$ and $FvMo_2(CO)_3(RC{\equiv}CR)_2$. Spectroscopic evidence indicated that the former bears as a ligand a μ-η^2-alkyne and that this ligand partially moved about the Mo–Mo bond in a rapid fluxional process: $\Delta G^{\ddagger} = 15 \pm 0.5$ kcal mol^{-1}. The bis(alkyne) systems contained uncoupled alkynes as determined by an X-ray diffraction study of one complex. This result is unusual in light of the frequent occurrence of alkyne coupling at a dinuclear center. Reduction of $FvMo_2(CO)_6$ with Na–Hg or $LiBEt_3H$ furnished the dianion $FvMo_2(CO)_6^{2-}$. The latter reacted with protic acids and haloalkanes to give the respective dihydride $FvMo_2(CO)_6H_2$ and dialkyl complexes $FvMo_2(CO)_6R_2$ (R = CH_3, CH_2Ph, CH_2OCH_3). At 20 °C the dihydride eliminated H_2 with formation of $FvMo_2(CO)_6$. Treatment of $FvMo_2(CO)_6(CH_2OCH_3)_2$ with $HBF_4{\cdot}(Et_2O)$ at −20 °C (CD_2Cl_2) produced $FvMo_2(CO)_6(CH_2OCH_3)(=CH_2)^+$, as determined by ^1H NMR spectroscopy. Warming to 0 °C gave the carbene-coupling product $FvMo_2(CO)_6(C_2H_4)^{2+}$. The bis(carbene) $FvMo_2(CO)_6(=CH_2)_2^{2+}$ was not detected. The dianion $FvMo_2(CO)_6^{2-}$ reacted with $I(CH_2)_3I$ to give a metal–metal bonded 1-oxacyclopent-2-ylidene complex. An X-ray diffraction analysis showed that the Fischer-type carbene ligand was terminally bound. This complex exhibited fluxional behavior which may involve a bridging carbene species ($\Delta G^{\ddagger} = 18 \pm 0.5$ kcal mol^{-1}). Thermolysis (100 °C) led to efficient generation of propene and $FvMo_2(CO)_6$ by a novel pathway.

Organometallic compounds containing two transition metals, typically referred to as "dinuclear" complexes, have been intensively studied in recent years.[1] These materials have been regarded with considerable interest in part because they have been proposed as models for the interaction of organic molecules with metal surfaces. Dinuclear complexes are also attractive as potential catalysts for synthetic organic transformations.[1d] One of the rationales for the study of these systems is the anticipation that their chemical behavior may differ significantly from that of analogous mononuclear complexes.[1c] A common hypothesis is that concerted or cooperative interaction of two metal centers with a substrate might lead to transformations which do not occur when only one metal is involved.[1] The validity of this idea has not been demonstrated unambiguously, for there have been few closely related mono- and dinuclear complexes suitable for comparison.

Synthetically, a wide variety of ligands has been employed in order to anchor two metals in close proximity. The most common classes include diphosphines,[2] diarsines,[2] ortho-metalated arylphosphines,[3] phosphido,[4] arsido,[5] alkoxido,[6] alkyl sulfido,[6] carbonate,[7] and pyrazolate anions.[8] Linkage of two dissimilar metals has been achieved by using heterodifunctional ligands, cyclopentadienylphosphido dianions being recent examples.[9]

Most of the neutral ligands, such as diphosphines, suffer the disadvantage of forming relatively weak bonds to transition metals, with the result that bridged compounds have limited thermal stability. In contrast, ligands which contain cyclopentadienyl (Cp) rings should form more robust connections to dinuclear metal systems. Typical dissociation enthalpies of trialkylphosphine–metal bonds fall in the range of 30–40 kcal mol^{-1}, whereas η^5-cyclopentadienyl metal bond energies have been estimated to vary between 60 and 70 kcal mol^{-1}.[10] In a few cases, two Cp rings connected by methylene[11] or dimethylsilene[12] units have been employed as bridging ligands. Thus far, none of these compounds has exhibited reactivities significantly different from those of the analogous cyclopentadienyl complexes.

Strong divergence from the chemistry of Cp metal dimers might exist in dinuclear complexes in which the

(1) (a) Muetterties, E. L.; Rhodin, R. N.; Band, E.; Brucker, C. F.; Pretzer, W. R. *Chem. Rev.* **1979**, *79*, 91. (b) Bruce, M. I. *J. Organomet. Chem.* **1983**, *242*, 147. (c) Bergman, R. G. *Acc. Chem. Res.* **1980**, *13*, 113. (d) Schore, N. E.; Ilenda, C. S.; White, M. A.; Bryndza, H. E.; Matturro, M. G.; Bergman, R. G. *J. Am. Chem. Soc.* **1984**, *106*, 7451 and the references therein.

(2) Maitlis, P. M.; Espinet, P.; Russell, M. J. H. In "Comprehensive Organometallic Chemistry"; Wilkinson, G., Stone, F. G. A., Abel, E., Eds.; Pergamon Press: New York, 1982; Vol. 6, p 268.

(3) Arnold, D. P.; Bennett, M. A.; McLaughlin, G. M.; Robertson, G. B.; Whittaker, M. J. *J. Chem. Soc., Chem. Commun.* **1983**, 32.

(4) (a) Puddephatt, R. J.; Thompson, P. J. *J. Organomet. Chem.* **1976**, *117*, 395. (b) Ebsworth, E. A. V.; Ferrier, H. M.; Henner, B. J. L.; Ranking, D. W. H.; Reed, J. F. S.; Robertson, H. E.; Whiteloch, J. D. *Angew. Chem., Int. Ed. Engl.* **1977**, *16*, 482.

(5) Richter, U.; Vahrenkamp, H. *J. Chem. Res., Synop.* **1977**, 156.

(6) (a) Kopf, H.; Rathlein, K. H. *Angew. Chem., Int. Ed. Engl.* **1969**, *8*, 980. (b) Braterman, P. S.; Wilson, V. A.; Joshi, K. K. *J. Chem. Soc. A* **1971**, 191.

(7) Hughes, R. P. In "Comprehensive Organometallic Chemistry"; Wilkinson, G., Stone, F. G. A., Abel, E., Eds.; Pergamon Press: New York, 1982; Vol. 5, p 277.

(8) Weiss, J. C.; Beck, W. *Chem. Ber.* **1972**, *105*, 3203.

(9) Casey, C. P.; Bullock, R. M.; Nief, F. *J. Am. Chem. Soc.* **1983**, *105*, 7574 and references therein.

(10) Connor, J. A. *Top. Curr. Chem.* **1976**, *71*, 71.

(11) (a) Bryndza, H. E.; Bergman, R. G. *J. Am. Chem. Soc.* **1979**, *101*, 4766. (b) Mueller-Westerhoff, U. T.; Nazzal, A.; Tanner, M. *J. Organomet. Chem.* **1982**, *236*, C41.

(12) (a) Day, V. W.; Thompson, M. R.; Nelson, G. O.; Wright, M. E. *Organometallics* **1983**, *2*, 494. (b) Nelson, G. O.; Wright, M. E. *Ibid.* **1982**, *1*, 565. (c) Nelson, G. O.; Wright, M. E. *J. Organomet. Chem.* **1982**, *239*, 353. (d) Wegner, P. A.; Uski, V. A.; Kiester, R. P.; Dabestani, S.; Day, V. W. *J. Am. Chem. Soc.* **1977**, *99*, 4846. (e) Weaver, J.; Woodward, P. *J. Chem. Soc., Dalton Trans.* **1973**, 1439. (f) Wright, M. E.; Mezza, T. M.; Nelson, G. O.; Armstrong, N. E.; Day, V. W.; Thompson, M. R. *Organometallics* **1983**, *2*, 1711.

0276-7333/86/2305-0280$01.50/0

Table I. Correlation of Metal-Metal Distance with the Dihedral Angle θ (deg)

entry	compd	M-M, Å	θ	ref
1	$(\eta^5:\eta^5\text{-}C_{10}H_8)_2Fe_2$	3.984	2.6	20c
2	$(\eta^5:\eta^5\text{-}C_{10}H_8)_2V(NCCH_3)_2^{2+}$	3.329	13.6	20b
3	$(\eta^5:\eta^5\text{-}C_{10}H_8)Mo_2(CO)_6$	3.371	15.3	this work
4	$(\eta^5:\eta^5\text{-}C_{10}H_8)W_2(CO)_6$	3.347	16.1	20d
5	$(\eta^5:\eta^5\text{-}C_{10}H_8)(\eta^5\text{-}C_5H_5)_2Mo_2H_3^+$	3.227	17.5	20a
6	$(\eta^5:\eta^5\text{-}C_{10}H_8)(\eta^5\text{-}C_5H_5)_2MoH(OH)^{2+}$	3.053	18.1	20e
7	$(\eta^5:\eta^5\text{-}C_{10}H_8)Ru_2(CO)_4$	2.821	28.5	16
8	$(\eta^5:\eta^5\text{-}C_{10}H_8)Ru_2(CO)_2(\mu\text{-}CO)(\mu\text{-}\eta^2\text{-}C_2H_2)$	2.719	31.6	18a

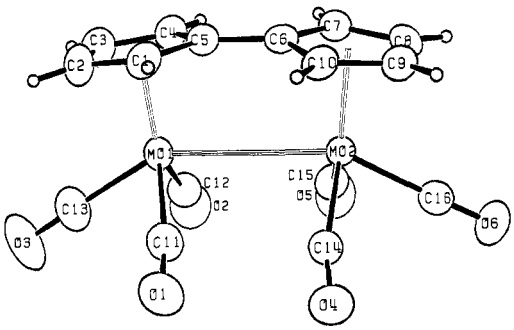

Figure 1. ORTEP drawing of 1 with labeling scheme. View is from the "side" of the molecule. The ellipsoids are scaled to represent the 50% probability surface. Hydrogen atoms, where shown, are given as arbitrary small spheres, and are labeled according to the carbon to which they are attached.

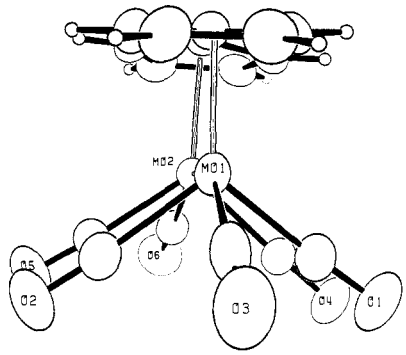

Figure 2. "End"-view of 1. The ellipsoids are scaled to represent the 50% probability surface.

metals are bridged by two joined Cps as in the fulvalene ligand, shown in generalized form in A. In the absence

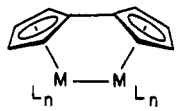

A

of a metal–metal bond, the fulvalene should hold the metal centers relatively closely together and thereby enforce stronger interactions between them. It may also be expected that novel reactivity in these compounds could arise from a bending distortion of the π-ligand in metal–metal bonded systems. Indeed, the intermetal distance in a planar $\eta^5:\eta^5$-bridging fulvalene complex has been estimated to be about 4.0 Å,[13] whereas most M–M bonds are less than 3.5 Å. Strain energy resulting from this distortion may cause the metal–metal bonds to be weaker and more reactive as compared to those of the Cp analogues. Fulvalene might also exert novel electronic effects on its environment. The metal atoms in fulvalene complexes should be more electron-rich compared to the metals in Cp metal dimers.[14] In addition, fulvalene should provide electronic communication between the two metal centers regardless of whether there is a metal–metal bond or not. Electrochemical evidence for this phenomenon has already been observed in a dirhodium system.[15] We have recently reported a new entry into the class of "half-sandwich" fulvalene systems based on the discovery that dihydrofulvalene is relatively stable when pure and can therefore be reacted with metal carbonyls at elevated temperatures to give a number of fulvalene dimetal carbonyls,[16] including $(\eta^5:\eta^5\text{-}C_{10}H_8)(CO)_6Mo_2$ (1).[17] In this paper we describe the chemistry of 1 and compare it with that of $(\eta^5\text{-}C_5H_5)_2Mo_2(CO)_6$, which differs in its reactivity both quantitatively and qualitatively.[18] In the subsequent discussion the fulvalene ligand will be abbreviated Fv.

Results and Discussion

X-ray Structural Analysis of $FvMo_2(CO)_6$ (1). In order to ascertain the surmised presence of strain in 1, an X-ray structural investigation was performed.[19] Figures 1 and 2 show two views of the molecule, clearly confirming the molecular structure. As in other fulvalene dimetal systems which have been characterized in this way (Table I), the metals are nearly symmetrically bound to all five Cp carbons. The bonds linking the two Cps in 1 and other systems vary only slightly (1.43–1.47 Å). Perhaps the most interesting feature with respect to structure-activity relationships is the enforced bend of the fulvalene ligands from planarity because of the metal–metal bond.

The bend angle θ (the "dihedral angle" between the two Cp planes) generally increases with decreasing metal–metal bond length (Table I),[21] as might be expected. Similar to the tungsten analogue of 1,[20d] for which a "stretched" metal–metal bond was invoked, the Mo–Mo distance (3.371 Å) in 1 is unusually long compared with models, such as $(CpMo)_2(CO)_6$[22] (3.235 Å) or (η^{10}-dihydroheptalene)dimolybdenum hexacarbonyl (3.193 Å),[23] boding well for unusual chemistry. The bond distances and angles in the molecule are given in Table II.

(13) Smart, J. C.; Curtis, C. J. *J. Am. Chem. Soc.* **1977**, *99*, 3518.
(14) For an MO diagram of fulvalene see: Streitwieser, A., Jr.; Brauman, J. I. "Supplemental Tables of Molecular Orbital Calculations"; Pergamon Press: London, 1965; Vol. I, p 87.
(15) Connelly, N. G.; Lucy, A. R.; Payne, J. D.; Galas, A. M. R.; Geiger, W. E. *J. Chem. Soc., Dalton Trans.* **1983**, 1879.
(16) Vollhardt, K. P. C.; Weidman, T. W. *Organometallics* **1984**, *3*, 82; *J. Am. Chem. Soc.* **1983**, *105*, 1676.
(17) Smart, J. C.; Curtis, C. *Inorg. Chem.* **1977**, *16*, 1788.
(18) Preliminary reports of some of the aspects of this work have appeared: (a) Drage, J. S.; Tilset, M.; Vollhardt, K. P. C.; Weidman, T. W. *Organometallics* **1984**, *3*, 812. (b) Drage, J. S.; Vollhardt, K. P. C. *Ibid.* **1985**, *4*, 191.
(19) We thank M. Tilset for providing crystals suitable for X-ray diffraction.
(20) (a) Bashkin, J.; Green, M. L. H.; Poveda, M. L.; Prout, K. *J. Chem. Soc., Dalton Trans.* **1982**, 2485. (b) Smart, J. C.; Pinsky, B. L.; Frederich, M. F.; Day, V. W. *J. Am. Chem. Soc.* **1979**, *101*, 4371. (c) Churchill, M. R.; Wormald, J. *Inorg. Chem.* **1969**, *8*, 1970. (d) Abrahamson, H. B.; Heeg, M. J. *Inorg. Chem.* **1984**, *23*, 2281. (e) Cooper, N. J.; Green, M. L. H.; Couldwell, C.; Prout, K. *J. Chem. Soc., Chem. Commun.* **1977**, 145.
(21) Guggenberger, L. J.; Tebbe, F. N. *J. Am. Chem. Soc.* **1976**, *98*, 4137.
(22) Adams, R. D.; Collins, D. M.; Cotton, F. A. *Inorg. Chem.* **1974**, *13*, 1086.
(23) Lindley, P. F.; Mills, O. S. *J. Chem. Soc. A* **1969**, 1286.

Photoinduced Reactions of 1. As mentioned earlier, an investigation of the chemistry of $FvMo_2(CO)_6$ (1) was initiated with the intent of discovering new processes distinct from those seen for $Cp_2Mo_2(CO)_6$. In light of the extensive and varied transformations observed for the metal–metal triple-bonded complex $Cp_2Mo_2(CO)_4$,[24] we sought the preparation of the fulvalene analog $FvMo_2(CO)_4$ by both photochemical[25-27] and thermal means. It was of interest whether a (presumably higher strained) triple-bonded dinuclear system bridged by the fulvalene ligand was accessible. On the basis of the reactivity of $Cp_2Mo_2(CO)_4$ in the presence of ligands,[28,29] we anticipated an equal plethora of reactions with 1. $Cp_2Mo_2(CO)_4$ can be prepared in high yield by heating $Cp_2Mo_2(CO)_6$ in boiling *m*-xylene.[28a,29d] In contrast, we found that $FvMo_2(CO)_6$ (1) possessed remarkable thermal stability. Heating it in toluene to 110 °C or in triglyme to 216 °C for several days lead only to slight decomposition. Flash vacuum pyrolysis at 550 °C (10^{-3} torr) gave only starting material (55% yield) and intractable decomposition materials at the site of sublimation and in the hot zone of the pyrolysis tube. Higher temperature pyrolyses were not carried out.

Turning to irradiative techniques,[28a] we attempted the photochemical synthesis of $FvMo_2(CO)_4$ from 1. The UV–visible spectrum of 1 in THF shows absorptions at 378 and 558 nm which are assigned to $\sigma \rightarrow \sigma^*$ and $d\pi \rightarrow \sigma^*$ excitations associated with metal–metal bonding and metal nonbonding electrons.[18] The $Cp_2Mo_2(CO)_6$ complex in THF exhibits the corresponding transitions at 388 and 512 nm.[25] Irradiation of 1 in THF (0.001 M, 20 °C) with 250-, 300-, or 350-nm light led within an hour to extensive decomposition to intractable materials. After 5 h in bright sunshine the same result was observed. Purging the solution with N_2 during irradiation in order to expel carbon monoxide accelerated the decomposition. Photolysis with 300-nm light at −30 °C gave roughly the same rate of decomposition as at 20 °C. Attempts to detect any photogenerated intermediates by use of IR or ^1H NMR spectroscopy were unsuccessful. In all cases only residual starting material was observed. Treatment of 1 with trimethylamine oxide[30] did not give any new characterizable products.

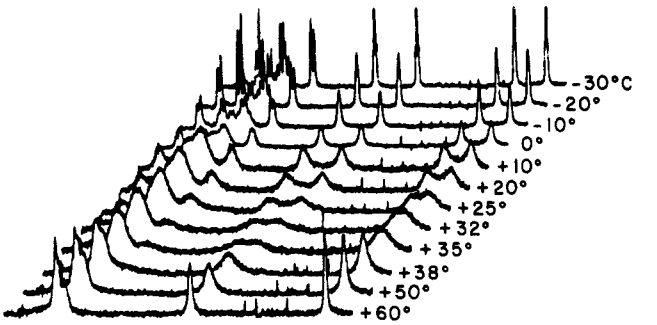

Figure 3. Dynamic ^1H NMR behavior of diphenylethyne complex 3 between −20 and +60 °C. Coalescence of the two low field fulvalene signals occurred at +35 °C.

The failure to generate $FvMo_2(CO)_4$ was attributed to steric constraints associated with the fulvalene ligand. Considering that the triple bond in $Cp_2Mo_2(CO)_4$ is 2.448 Å long,[27g] the fulvalene ligand in $FvMo_2(CO)_4$ would be severely strained. In the photolysis of 1 it is not known whether $FvMo_2(CO)_4$ was produced with subsequent decomposition, or if some other unstable species was formed.

The hexacarbonyl 1 was then irradiated in the presence of various ligands with the expectation that the latter would attack a transiently photogenerated fulvalene complex, possibly $FvMo_2(CO)_4$. Reagents such as phosphines [PPh_3, $P(OMe)_3$], hexamethylbenzene, and cyclooctatetraene did not react at all, whereas acetonitrile, pyridine, 2,2′-bipyridine, thiophenol, and diphenyl disulfide gave only intractable undefined materials. However, alkynes were found to smoothly displace CO ligands from 1 to form mono- and bis(alkyne) complexes. For example, photolysis (300 nm) in the presence of 10 equiv of dimethyl ethynedicarboxylate in THF at 20 °C with a slow N_2 purge caused a gradual color change from the purple of 1 to orange-red. After 5 h about 90% of the starting material had disappeared, and two new compounds were present which were subsequently formulated as $FvMo_2(CO)_4(RCCR)$ and $FvMo_2(CO)_3(RCCR)_2$. These products were cleanly separated by chromatography.

The first product isolated from this reaction was the mono(alkyne) 2 (orange crystals, mp 164–165 °C dec, 14% yield). The C, H analysis and mass spectrum (M^+ at *m/e*

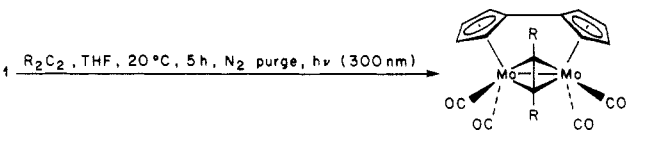

574) were consistent with a fulvalene dimolybdenum complex containing four CO ligands and one alkyne. The ^1H NMR spectrum showed four broad multiplets at δ 6.00, 5.58, 4.54, and 4.27 (2 H each) for the fulvalene ligand hydrogens and two broad singlets at δ 3.85 and 3.36 (3 H each) for the ester methyl groups. The broadness of each peak was due to a fluxional process (vide infra). In the

(24) Davis, R.; Kane-Maguire, L. A. P. In "Comprehensive Organometallic Chemistry"; Wilkinson, G., Stone, F. G. A., Abel, E. W., Eds.; Pergamon Press: New York, 1982; Vol. 3, p 1149.
(25) Geoffroy, G. L.; Wrighton, M. S. "Organometallic Photochemistry"; Academic Press: New York, 1979; Chapter 2.
(26) Stiegman, A. E.; Tyler, D. R. *Acc. Chem. Res.* **1984**, *17*, 61.
(27) (a) Wrighton, M. S.; Ginley, D. S. *J. Am. Chem. Soc.* **1975**, *97*, 4246. (b) Laine, R. M.; Ford, P. C. *Inorg. Chem.* **1977**, *16*, 388. (c) Hughey J. L., IV; Bock, C. R.; Meyer, T. J. *J. Am. Chem. Soc.* **1975**, *97*, 4440. (d) Mahmoud, K. A.; Rest, A. J.; Alt, H. G. *J. Organomet. Chem.* **1983**, *246*, C37. (e) Hooker, R. H.; Mahmoud, K. A.; Rest, A. J. *Ibid.* **1983**, *254*, C25. (f) Haines, R. J.; Nyholm, R. S.; Stiddard, M. H. B. *J. Chem. Soc. A* **1968**, 43. (g) Klinger, R.; Butler, W.; Curtis, M. D. *J. Am. Chem. Soc.* **1975**, *97*, 3535. (h) Stiegman, A. E.; Tyler, D. R. *J. Am. Chem. Soc.* **1982**, *104*, 2944. (i) Stiegman, A. E.; Stieglitz, M.; Tyler, D. R. *Ibid.* **1983**, *105*, 6032. (j) Ginley, D. S.; Wrighton, M. S. *Ibid.* **1975**, *97*, 3533. (k) Hackett, P.; O'Neil, P. S.; Manning, A. R. *J. Chem. Soc., Dalton Trans.* **1974**, 1625. (l) Goldman, A. S.; Tyler, D. R. *J. Am. Chem. Soc.* **1984**, *106*, 4066.
(28) (a) Ginley, D. S.; Bock, C. R.; Wrighton, M. S. *Inorg. Chim. Acta* **1977**, *23*, 85. (b) Bailey, W. I., Jr.; Chisholm, M. H.; Cotton, F. A.; Rankel, L. A. *J. Am. Chem. Soc.* **1978**, *100*, 5764. (c) For comparison, the Mo–Mo distance in $Cp_2Mo_2(CO)_6$ is 3.235 Å, see ref 22.
(29) (a) Knox, S. A. R.; Stansfield, R. F. D.; Stone, F. G. A.; Winter, M. J.; Woodward, P. *J. Chem. Soc., Chem. Commun.* **1978**, 221; *J. Chem. Soc., Dalton Trans.* **1982**, 173. (b) Boileau, A. M.; Orpen, A. G.; Stansfield, R. F. D.; Woodward, P. *Ibid.* **1982**, 187. (c) Beck, J. A.; Knox, S. A. R.; Stansfield, R. F. D.; Stone, F. G. A.; Winter, M. J.; Woodward, P. *Ibid.* **1982**, 195. (d) Curtis, M. D.; Klingler, R. J. *J. Organomet. Chem.* **1978**, *161*, 23. (e) Adams, R. D.; Katahira, D. A.; Yang, L. *Organometallics* **1982**, *1*, 231. (f) Brunner, H.; Buchner, H.; Wachter, J. *J. Organomet. Chem.* **1983**, *244*, 247. (g) Alper, H.; Petrignani, J.; Einstein, F. W. B.; Willis, A. C. *J. Am. Chem. Soc.* **1983**, *105*, 1701. (h) Brunner, H.; Wachter, J.; Wintergerst, H. *J. Organomet. Chem.* **1982**, *235*, 77 and references therein. (i) Alper, H.; Einstein, F. W. B.; Nagai, R.; Petrignani, J.; Willis, A. C. *Organometallics* **1983**, *2*, 1291. (j) Alper, H.; Einstein, F. W. B.; Petrignani, J.; Willis, A. C. *Ibid.* **1983**, *2*, 1422 and references therein. (k) Endrich, K.; Korswagen, R.; Zahn, T.; Ziegler, M. L. *Angew. Chem., Int. Ed. Engl.* **1982**, *21*, 919. (l) Green, M.; Orpen, A. G.; Schaverien, C. J.; Williams, I. D. *J. Chem. Soc., Chem. Commun.* **1983**, 181. (m) Herrmann, W. A.; Ihl, G. *J. Organomet. Chem.* **1983**, *251*, C1. (n) Messerle, L.; Curtis, M. D. *J. Am. Chem. Soc.* **1980**, *102*, 7789; **1982**, *104*, 889.
(30) Shvo, Y.; Hazum, E. *J. Chem. Soc., Chem. Commun.* **1975**, 829.

Table II. Selected Bond Distances (Å) and Angles (deg) in 1[a,b]

Intramolecular Distances

atom 1	atom 2	dist	atom 1	atom 2	dist	atom 1	atom 2	dist
Mo1	Mo2	3.371 (1)	Cp1	Cp2	3.835 (0)	C5	C1	1.429 (3)
Mo1	C1	2.333 (2)	C11	C1	3.253 (3)	C1	C2	1.403 (3)
Mo1	C2	2.311 (2)	C11	C12	3.158 (3)	C2	C3	1.426 (3)
Mo1	C3	2.322 (2)	C11	C13	2.493 (3)	C3	C4	1.393 (3)
Mo1	C4	2.330 (2)	C11	C14	2.870 (3)	C4	C5	1.428 (3)
Mo1	C5	2.333 (2)	C12	C4	3.226 (3)	C5	C6	1.442 (2)
Mo1	Cp1	1.990 (1)	C12	C13	2.495 (3)	C6	C7	1.422 (3)
Mo2	C6	2.344 (2)	C12	C15	2.876 (3)	C7	C8	1.417 (3)
Mo2	C7	2.336 (2)	C13	C2	2.954 (3)	C8	C9	1.419 (3)
Mo2	C8	2.306 (2)	C13	C3	3.042 (3)	C9	C10	1.408 (3)
Mo2	C9	2.326 (2)	C14	C10	3.279 (3)	C10	C6	1.429 (3)
Mo2	C10	2.334 (2)	C14	C15	3.122 (3)	C1	H1	0.86 (2)
Mo2	Cp2	1.992 (1)	C14	C16	2.534 (3)	C2	H2	0.92 (2)
Mo1	C11	1.992 (2)	C15	C7	3.239 (3)	C3	H3	0.97 (2)
Mo1	C12	1.984 (2)	C15	C16	2.505 (3)	C4	H4	0.98 (2)
Mo1	C13	1.965 (2)	C16	C8	2.910 (3)	C7	H7	0.96 (2)
Mo2	C14	1.987 (2)	C16	C9	3.020 (3)	C8	H8	0.85 (2)
Mo2	C15	1.990 (2)				C9	H9	0.90 (2)
Mo2	C16	1.962 (2)				C10	H10	0.92 (2)
C11	O1	1.136 (2)						
C12	O2	1.153 (3)						
C13	O3	1.150 (3)						
C14	O4	1.143 (3)						
C15	O5	1.142 (3)						
C16	O6	1.157 (2)						

Intramolecular Angles[b]

atom 1	atom 2	atom 3	angle	atom 1	atom 2	atom 3	angle
Mo2	Mo1	C11	80.97 (6)	Mo2	Mo1	C11	80.97 (6)
Mo2	Mo1	C12	84.83 (6)	Mo2	Mo1	C12	84.83 (6)
Mo2	Mo1	C13	148.58 (7)	Mo2	Mo1	C13	148.58 (7)
Mo2	Mo1	Cp1	97.03	Mo2	Mo1	Cp1	97.03
C11	Mo1	C12	105.16 (9)	C11	Mo1	C12	105.16 (9)
C11	Mo1	C13	78.10 (8)	C11	Mo1	C13	78.10 (8)
C12	Mo1	C13	78.40 (8)	C12	Mo1	C13	78.40 (8)
Cp1	Mo1	C11	128.25	Cp1	Mo1	C11	128.25
Cp1	Mo1	C12	126.29	Cp1	Mo1	C12	126.29
Cp1	Mo1	C13	114.32	Cp1	Mo1	C13	114.32
Mo1	Mo2	C14	84.38 (5)	Mo1	Mo2	C14	84.38 (5)
Mo1	Mo2	C15	80.78 (5)	Mo1	Mo2	C15	80.78 (5)
Mo1	Mo2	C16	150.32 (5)	Mo1	Mo2	C16	150.32 (5)
Mo1	Mo2	Cp2	96.27	Mo1	Mo2	Cp2	96.27
C14	Mo2	C15	103.45 (9)	C14	Mo2	C15	103.45 (9)
C14	Mo2	C16	79.84 (7)	C14	Mo2	C16	79.84 (7)
C15	Mo2	C16	78.68 (8)	C15	Mo2	C16	78.68 (8)
Cp2	Mo2	C14	128.50	Cp2	Mo2	C14	128.50
Cp2	Mo2	C15	127.60	Cp2	Mo2	C15	127.60
Cp2	Mo2	C16	113.24	Cp2	Mo2	C16	113.24
Mo1	C11	O1	172.26 (18)	Mo1	C11	O1	172.26 (18)
Mo1	C12	O2	170.72 (18)	Mo1	C12	O2	170.72 (18)
Mo1	C13	O3	178.26 (20)	Mo1	C13	O3	178.26 (20)
Mo2	C14	O4	171.90 (16)	Mo2	C14	O4	171.90 (16)
Mo2	C15	O5	171.09 (17)	Mo2	C15	O5	171.09 (17)
Mo2	C16	O6	177.24 (16)	Mo2	C16	O6	177.24 (16)
C5	C1	C2	107.67 (18)	C5	C1	C2	107.67 (18)
C1	C2	C3	108.37 (18)	C1	C2	C3	108.37 (18)
C2	C3	C4	108.24 (18)	C2	C3	C4	108.24 (18)
C3	C4	C5	108.23 (17)	C3	C4	C5	108.23 (17)
C1	C5	C4	107.48 (16)	C1	C5	C4	107.48 (16)
C1	C5	C6	126.32 (16)	C1	C5	C6	126.32 (16)
C4	C5	C6	125.53 (16)	C4	C5	C6	125.53 (16)
C5	C6	C7	125.55 (16)	C5	C6	C7	125.55 (16)
C5	C6	C10	125.80 (16)	C5	C6	C10	125.80 (16)
C7	C6	C10	107.98 (15)	C7	C6	C10	107.98 (15)
C6	C7	C8	107.63 (18)	C6	C7	C8	107.63 (18)
C7	C8	C9	108.23 (19)	C7	C8	C9	108.23 (19)
C8	C9	C10	108.33 (18)	C8	C9	C10	108.33 (18)
C9	C10	C6	107.79 (17)	C9	C10	C6	107.79 (17)
Cp1	C5	C6	172.54	Cp1	C5	C6	172.54
C5	C6	Cp2	172.79	C5	C6	Cp2	172.79

Torsional Angles (deg)

atom 1	atom 2	atom 3	atom 4	angle	atom 1	atom 2	atom 3	atom 4	angle
Cp1	Mo1	Mo2	Cp2	4.9	C1	C5	C6	C10	4.2
C13	Mo1	Mo2	C16	14.7	C4	C5	C6	C7	4.3
C11	Mo1	Mo2	C14	5.4	C1	C5	C6	C7	173.7
C12	Mo1	Mo2	C15	3.7	C4	C5	C6	C10	−165.2

[a] In this and all subsequent tables the esds of all parameters are given in parentheses, right-justified to the least significant digit(s) quoted. [b] Cp1 and Cp2 are the centroids of the rings of the fulvalene ligand.

IR spectrum (KBr disk) there were four terminal CO (2010, 1970, 1945, 1920 cm^{-1}) and three ester carbonyl bands (1735, 1705, 1675 cm^{-1}). Altogether the ^1H NMR and IR data indicated a structure of C_s symmetry. The structure proposed for **2** has a four-electron-donating μ-η^2-alkyne ligand which is symmetrically aligned with respect to both metals and perpendicular to the Mo–Mo bond. The alkyne leans toward one side of the fulvalene ligand while carbonyls occupy the opposite side. This structure is consistent with the symmetry exhibited in the IR and NMR spectra, it fulfills the 18-valence-electron requirement of each metal, and it is similar to mono(alkyne) complexes **4** derived from $Cp_2Mo_2(CO)_4$.[28b]

A compound structurally related to **2** was isolated from the photolysis of **1** with diphenylethyne (300 nm, THF, 20 °C, N_2 purge, 10 h). As in the previous case, a mono- and a bis(alkyne) compound were produced. The first fraction from chromatography contained the mono(alkyne) **3** (bright orange crystals, mp 162 °C dec, 8.8% yield). The C, H analysis and mass spectrum (M^+ at m/e 610) indicated a tetracarbonyl mono(alkyne) complex. As for the dimethyl ethynedicarboxylate species **2**, the ^1H NMR spectrum showed four broad multiplets for the fulvalene protons (δ 5.96, 5.54, 4.43, 4.13) and the IR spectrum revealed four terminal CO signals (1987, 1955, 1916, 1900 cm^{-1}).

Complexes **2** and **3** exhibited dynamic ^1H NMR spectra indicating the occurrence of a fluxional process similar to that reported for $Cp_2Mo_2(CO)_4(RCCR)$ **4**.[28b] A variable-temperature study of the diphenylethyne derivative **3** demonstrated coalescence of the four sharp fulvalene multiplets seen at −30 °C into two broad signals at +60 °C (Figure 3). The coalescence temperature of +35 °C was used to calculate the activation free energy: $\Delta G^{\ddagger}$ = 15.0 ± 0.5 kcal mol^{-1}. This fluxional behavior may have been due to rapid interconversion of the species **3a** and **3b**, in which the alkyne slides from one to the other side

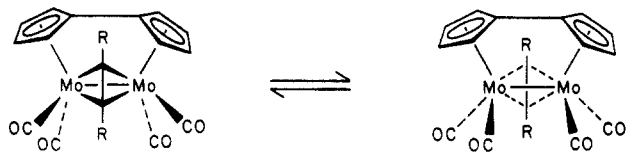

3a **3b**

of the fulvalene ligand in a sort of pendular motion. A slight movement of the carbonyl ligands would occur simultaneously.

For comparison, Cotton's[28b] work on the fluxional behavior of the complexes **4** should be discussed. Variable-temperature ^{13}C NMR data revealed a very low-energy process (rapid at −132 °C) which was thought to involve site exchanges between CO ligands b and c and between a and d. Apparently, there was no intermetal transfer of CO ligands even at +80 °C. In a higher energy process (rapid at −70 °C) the two enantiomeric forms **4c** and **4d** were thought to be in equilibrium ($\Delta G^{\ddagger}$ = 9.9 ± 0.2 kcal mol^{-1}). This interconversion was believed to arise through a combination of the low-energy process with rotation of

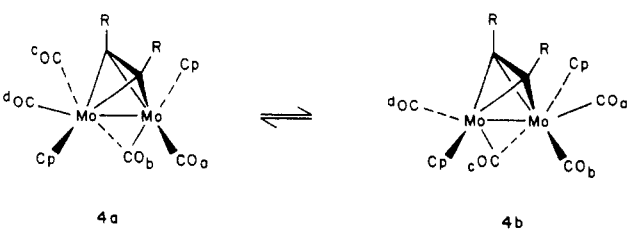

4a **4b**

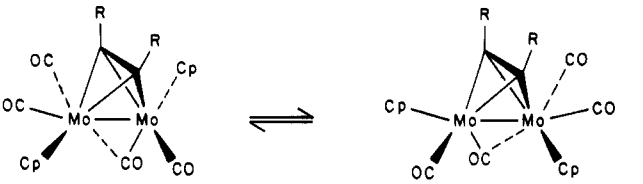

4c **4d**

the terminal CO and η^5-C_5H_5 ligands about the Mo–Mo bond, requiring more energy. The rotation was postulated to occur without rearrangement of the Mo_2C_2 core. In one respect this fluxional behavior is similar to that of the fulvalene complexes. One can envision the alkyne ligand being stationary in space while the fulvalene moves from one side of the alkyne to the other via a rotation about the Mo–Mo bond.

The parent mono(alkyne) complex **5** was obtained by irradiation (300 nm) of **1** exposed to a slow stream of ethyne. In less than 5 min the reaction was complete, and after chromatography the only product isolated was **5** (red crystals, mp 154–155 °C dec, 27% yield). The mass spectrum (M^+ at m/e 458) and C, H analysis were in accord with a monoethyne tetracarbonyl formulation. Whereas the IR spectrum, in which there were four terminal CO bands (1991, 1959, 1909, 1889 cm^{-1}), indicated C_s symmetry, the ^1H NMR spectrum was consistent with a C_{2v} structure. There were two broadened multiplets for the fulvalene protons (4 H each) at δ 5.60 and 4.38 and a slightly broad singlet (2 H) at δ 3.30 for the ethyne protons. Presumably the ^1H NMR data represented the average structure of the two rapidly interconverting species of the type **3a,b**.

The photochemical formation of **5** occurred without generation of the bis(alkyne) complexes also observed for the reactions of diphenylethyne and dimethyl ethynedicarboxylate. Thus, in addition to **3** the bis(alkyne) species **6**, $FvMo_2(CO)_3(PhCCPh)_2$, was also isolated (dark orange crystals, mp 179 °C dec, 23.6% yield). The C, H analysis was consistent with a dimolybdenum fulvalene complex containing two PhC≡CPh ligands and either three or four carbonyls. The parent ion in the mass spectrum (direct inlet) was not observed; instead the highest peak was at m/e 610. The latter was assigned to the $FvMo_2(CO)_4$-$(PhC{\equiv}CPh)^+$ ion, which must have been derived from loss of one alkyne and addition of a CO ligand. In the IR spectrum there were three terminal CO stretching signals at 1960, 1935, and 1890 cm^{-1}, and in the ^1H NMR spectrum there was a complicated pattern of phenyl protons (20 H total) and eight fulvalene multiplets (1 H each) at δ 6.45, 5.79, 5.68, 5.59, 5.38, 5.13, 4.74, and 4.69. These data clearly indicated that **6** had a totally asymmetric structure. Unlike the mono(alkyne) complexes, there was no indication of a fluxional process in the ^1H NMR spectrum (−60 to +100 °C).

Similarly, photolysis of **1** with dimethyl ethynedicarboxylate gave **2** and bis(alkyne) complex **7**, the latter as the major product (red crystals, mp 161–162 °C dec, 67% yield). The C, H analysis and the mass spectrum of **7** were in accord with the $FvMo_2(CO)_3(CH_3O_2CC{\equiv}CCO_2CH_3)_2$ formulation. The IR and ^1H NMR spectral data, especially the latter, suggested that it was isostructural to **6**. In the IR spectrum there were three terminal CO (2042, 2002, 1944 cm^{-1}) and three ester carbonyl stretching bands (1706, 1691, 1678 cm^{-1}). Again, the ^1H NMR spectrum reflected a total lack of symmetry. Eight fulvalene multiplets were observed at δ 6.04, 5.87, 5.57, 5.51 (2 H), 5.08, 4.79, and 4.72; there were also methyl singlets at δ 3.82, 3.68, 3.57, and 3.50.

Table III. Bond Distances (Å) and Angles (deg) in 7 (Esds in Parentheses)

Intramolecular Distances

atom 1	atom 2	dist	atom 1	atom 2	dist	atom 1	atom 2	dist
C1	C2	1.417 (5)	C15	O3	1.305 (4)	Mo1	C1	2.337 (3)
C2	C3	1.408 (5)	O3	C16	1.442 (4)	Mo1	C2	2.403 (3)
C3	C4	1.420 (5)	C22	O7	1.442 (5)	Mo1	C3	2.379 (3)
C4	C5	1.421 (4)	O7	C21	1.330 (4)	Mo1	C4	2.295 (3)
C5	C1	1.415 (5)	C21	O8	1.194 (4)	Mo1	C5	2.308 (3)
C5	C6	1.453 (5)	C21	C20	1.460 (5)	Mo2	C23	2.024 (4)
C6	C7	1.427 (5)	C20	C19	1.265 (4)	C23	O9	1.136 (4)
C7	C8	1.402 (5)	C19	C18	1.465 (4)	Mo2	C24	1.986 (4)
C8	C9	1.418 (5)	C18	O6	1.193 (4)	C24	O10	1.142 (4)
C9	C10	1.415 (5)	C18	O5	1.332 (4)	Mo2	C14	2.180 (3)
C10	C6	1.436 (5)	O5	C17	1.439 (4)	Mo2	C13	2.157 (3)
C11	O1	1.444 (4)	Mo1	C25	2.027 (4)	Mo2	C6	2.279 (3)
O1	C12	1.339 (4)	C25	O11	1.131 (4)	Mo2	C7	2.338 (3)
C12	O2	1.200 (4)	Mo1	C19	2.186 (3)	Mo2	C8	2.366 (3)
C12	C13	1.462 (4)	Mo1	C20	2.161 (3)	Mo2	C9	2.325 (3)
C13	C14	1.374 (4)	Mo1	C14	2.175 (3)	Mo2	C10	2.267 (3)
C14	C15	1.473 (4)	Mo1	C13	2.134 (3)	Mo1	Mo2	2.906 (1)
C15	O4	1.187 (4)						

Intramolecular Angles

atom 1	atom 2	atom 3	angle	atom 1	atom 2	atom 3	angle
C1	C2	C3	108.5 (3)	O5	C18	C19	110.4 (3)
C2	C3	C4	107.6 (3)	C18	C19	C20	141.8 (3)
C3	C4	C5	108.3 (3)	C19	C20	C21	145.3 (3)
C4	C5	C1	107.5 (3)	C20	C21	O8	124.3 (3)
C5	C1	C2	108.0 (3)	C20	C21	O7	111.1 (3)
C6	C7	C8	108.6 (3)	O7	C21	O8	124.6 (3)
C7	C8	C9	108.1 (3)	C21	O7	C22	115.8 (3)
C8	C9	C10	108.5 (3)	C23	Mo2	C24	90.25 (14)
C9	C10	C6	107.5 (3)	C24	Mo2	C14	78.94 (13)
C10	C6	C7	107.2 (3)	C14	Mo2	C13	36.94 (11)
C4	C5	C6	126.1 (3)	C13	Mo2	C23	85.85 (12)
C1	C5	C6	124.7 (3)	Mo2	C14	C13	70.63 (17)
C10	C6	C5	126.3 (3)	C14	C13	Mo2	72.42 (18)
C7	C6	C5	124.6 (3)	C25	Mo1	C19	77.46 (13)
C11	O1	C12	116.4 (3)	C19	Mo1	C20	33.83 (11)
O1	C12	O2	123.3 (3)	C20	Mo1	C13	83.15 (11)
O1	C12	C13	111.5 (3)	C13	Mo1	C14	37.18 (11)
O2	C12	C13	125.2 (3)	C14	Mo1	C25	75.21 (12)
C12	C13	C14	131.1 (3)	C14	Mo1	C19	90.04 (11)
C13	C14	C15	134.6 (3)	Mo1	C19	C20	71.97 (20)
C14	C15	O4	124.8 (3)	Mo1	C20	C19	74.20 (21)
C14	C15	O3	112.5 (3)	Mo1	C14	C13	69.81 (18)
O4	C15	O3	122.7 (3)	Mo1	C13	C14	73.02 (18)
C15	O3	C16	118.5 (3)	C24	Mo2	Mo1	97.11 (10)
C17	O5	C18	116.5 (3)	C23	Mo2	Mo1	130.43 (9)
O6	C18	O5	123.7 (3)	C25	Mo1	Mo2	87.22 (10)
O6	C18	C19	125.9 (3)				

Torsional Angles (deg)

atom 1	atom 2	atom 3	atom 4	angle	atom 1	atom 2	atom 3	atom 4	angle
C4	C5	C6	C10	2.1	C25	Mo1	Mo2	C24	4.4
C4	C5	C6	C7	164.4	H2	C2	C3	H3	0.7
C1	C5	C6	C7	1.3	C5	C4	C3	C2	1.4
C1	C5	C6	C10	-161.0	C10	C9	C8	C7	0.6
C13	C14	C19	C20	15.7	C15	C14	C13	C12	-5.9
C19	C20	C13	C14	17.1	C18	C19	C20	C21	9.0

Initially, it was thought that these complexes were of metallacyclic structure, in analogy to the "alkyne-stitching" chemistry observed for $Cp_2Mo_2(CO)_6$.[29a-c] However, the spectroscopic evidence was sufficiently ambiguous to warrant an X-ray diffraction study.

A single crystal of complex **7** was obtained by slow diffusion of hexane vapor into an acetone solution of **1**. The ORTEP drawing of the structure determined from the diffraction study[31] is shown in Figure 4, and the bond lengths, bond angles, and torsional angles are listed in Table III.

It was surprising to find that there are no bonding interactions between the two alkyne ligands. One alkyne bridges the two metals nearly symmetrically with its alkyne C–C bond almost perpendicular to the Mo–Mo axis. The bridging alkyne is also tipped over to one side of the fulvalene ligand as in the proposed structures for the mono(alkyne) complexes **2**, **3**, and **5**. The elongated C–C alkyne bond (1.374 Å) and the obtuse angles C12–C13–C14 (131.1°) and C13–C14–C15 (134.6°) are typical of what are thought to be four-electron-donating μ-η^2-alkyne ligands.[32] The terminal alkyne is best described as a two-electron

(31) Details will be reported in: Bularzik, J.; Kourtakis, K.; Nitschke, J.; Tötsch, W. *Acta Crystallogr., Sect. C: Cryst. Struct. Commun.* submitted for publication.

(32) (a) Cotton, F. A.; Jamerson, J. D.; Stults, B. R. *J. Am. Chem. Soc.* **1976**, *98*, 1774. (b) Sly, W. G. *Ibid.* **1959**, *81*, 18. (c) Bailey, W. I., Jr.; Chisholm, M. H.; Cotton, F. A.; Rankel, L. A. *Ibid.* **1978**, *100*, 5764.

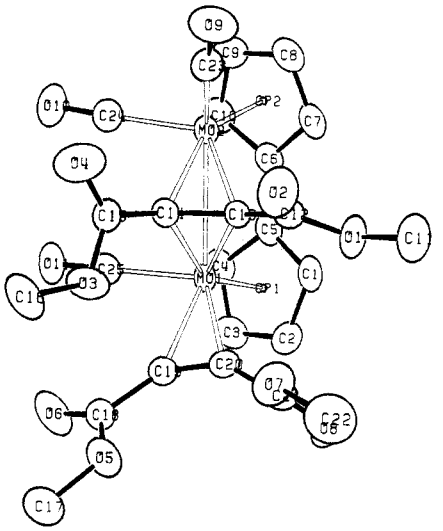

Figure 4. ORTEP drawing of 7 with labeling scheme. The ellipsoids are scaled to represent the 50% probability surface.

donor, as indicated by a short alkyne C–C bond (1.265 Å) and the bond angles C18–C19–C20 (141.8°) and C19–C20–C21 (145.3°).[33] The Mo–Mo single bond (2.906 Å) is shorter by 0.05–0.08 Å than the Mo–Mo bonds in $Cp_2Mo_2(CO)_4(RCCR)$.[28b,c] This effect may have been caused by the bridging fulvalene. Another peculiar feature is that the bridging and terminal alkynes are quite close to each other. This is evident from the carbon–metal bond distances and the positioning of the terminal next to the bridging alkyne.

The structure of 7 was unexpected considering the ubiquitous occurrence of alkyne coupling within the coordination sphere of dinuclear complexes.[29a-c,34] Indeed, there are very few examples of uncoupled alkynes in such an environment.[35]

Several unsuccessful attempts were made to induce coupling of the alkyne ligands in 6 and 7. Heating of these compounds in toluene at 110 °C gave the corresponding tetracarbonyl complexes 2 and 3 in moderate yields, in addition to some intractable decomposed material. Substantial amounts of the free alkynes were observed in the ^1H NMR spectra of the reaction mixtures. Heating of 6 and 7 with added alkynes did not give new products. Irradiation (250 and 300 nm) in the presence of excess dimethyl ethynedicarboxylate in THF at room temperature also had no effect. It is difficult to find a rationale for this curious departure from the chemistry of the analogous η^5-cyclopentadienyl compounds. Perhaps a bridging metallacycle[29a-c] requires a relatively short metal–metal distance, which might be prevented in 6 and 7 by the resulting strain energy in the fulvalene ligand.

Formation of the bis(alkyne) complexes most likely proceeds via photochemical dissociation of CO from the mono(alkyne) compounds. Irradiation (300 nm) of 2 in the presence of diphenylethyne afforded 6 in high yield, whereas this transformation did not occur thermally. The mechanism probably involves a simple photodissociation of CO, followed by entry of the second alkyne. The route by which the mono(alkyne) complexes are formed is unclear. In view of the work on the $Cp_2Mo_2(CO)_6$ system,[25-27] a triplet diradical devoid of a metal–metal bond might be the first intermediate. This species could lose two CO ligands to form a tetracarbonyl diradical which might subsequently convert to $FvMo_2(CO)_4$. Either species could react with alkynes to yield the observed products. Direct photochemical conversion of 1 to $FvMo_2(CO)_4$ is also a possibility.

Finally, the results presented in this section should be compared to data obtained in the photochemical reactions of $FvW_2(CO)_6$ with alkynes. Here single and double alkyne photosubstitution was observed[18a] in the presence of diphenylethyne to afford the complexes 8 (16% yield) and 9 (18% yield). The spectroscopic data indicated that the

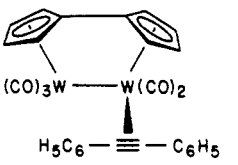

8

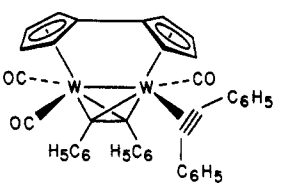

9

latter product may have the same structure as the dimolybdenum monoalkyne complexes mentioned above. However, 8 exhibited IR and ^1H NMR spectra which were more in accord with a structure involving a terminal, unsymmetrically bound alkyne. No change was observed in the ^1H NMR spectrum up to 70 °C. Again, this chemistry differed from that of the analogous $Cp_2W_2(CO)_6$.[36]

Reduction of 1 to (η^5:η^5-Fulvalene)dimolybdenum Dianion 10. Our attention next turned to the reductive cleavage of the metal–metal bond. Preliminary electrochemical work[37] revealed chemically reversible two-electron reductions at –0.77 V (vs. NHE), appreciably more facile than the corresponding process in $Cp_2Mo_2(CO)_6$ ($E°$ = –0.92 V).[38] This result suggested that a dianion should be accessible from 1 and provide a useful starting material for further functionalization. Indeed, the reported procedure[39] for preparing $Na[Cp(CO)_3Mo]$ from $Cp_2Mo_2(CO)_6$ and sodium amalgam was applied to the synthesis of the dianion $FvMo_2(CO)_6^{2-}$ (10). Exposure of a dilute THF solution of 1 to excess sodium amalgam (1% Na w/w) for 2–3 h caused the solution to change from the deep purple of 1 to the yellow of 10. Compound 10 is rapidly air-oxidized to 1. The dilithium salt $Li_2[FvMo_2(CO)_6]$ was more conveniently prepared by dropwise addition of about 2.5 equiv of lithium triethylborohydride[40] (Super Hydride) to a THF solution of 1 at 0 °C.

The disodium salt was characterized by IR spectroscopy and by its reaction with iodomethane which afforded the known[17] dimethyl compound $FvMo_2(CO)_6(CH_3)_2$ (vide infra). Infrared carbonyl stretching bands were observed at 1890, 1790, and 1740 cm^{-1}. These low-energy absorptions are typical of metal carbonyl anions in which there is

(33) (a) Davies, G. R.; Hewerston, W.; Mais, R. H. B.; Owston, P. G.; Patel, C. G. *J. Chem. Soc. A* **1970**, 1873. (b) Ittel, S. D.; Ibers, J. A. *Adv. Organomet. Chem.* **1976**, *14*, 55.

(34) (a) Dickson, R. S.; Fraser, P. J. *Adv. Organomet. Chem.* **1974**, *12*, 323. (b) Mays, M. J.; Prest, D. W.; Raithlay, P. R. *J. Chem. Soc., Dalton Trans.* **1981**, 771. (c) Green, M.; Norman, N. C.; Orpen, A. G. *J. Am. Chem. Soc.* **1981**, *103*, 1269. (d) Wilke, G. *Pure Appl. Chem.* **1978**, *50*, 677.

(35) (a) Davidson, J. L. *J. Chem. Soc., Dalton Trans.* **1983**, 1667. (b) Cotton, F. A.; Schwotzer, W.; Shamshoum, E. S. *Organometallics* **1983**, *2*, 1167. (c) Boag, N. M.; Green, M.; Howard, J. A. K.; Spencer, J. L.; Stansfield, R. F. D.; Thomas, M. D. O.; Stone, F. G. A.; Woodward, P. *J. Chem. Soc., Dalton Trans.* **1980**, 2182.

(36) Finnimore, S. R.; Knox, S. A. R.; Taylor, G. E. *J. Chem. Soc., Chem. Commun.* **1980**, 411.

(37) Moulton, R.; Weidman, T. W.; Vollhardt, K. P. C.; Bard, A. J., submitted for publication.

(38) Dessy, R. E.; Weissman, P. M.; Pohl, R. L. *J. Am. Chem. Soc.* **1966**, *88*, 5117.

(39) Piper, T. S.; Wilkinson, G. *J. Inorg. Nucl. Chem.* **1956**, *3*, 104. See also: King, R. B.; Fronzaglia, A. *J. Am. Chem. Soc.* **1966**, *88*, 709.

(40) (a) Gladysz, J. A.; Williams, G. M.; Tam, W. T.; Johnson, D. L.; Parker, D. W.; Selover, J. C. *Inorg. Chem.* **1979**, *18*, 553. (b) Tam, W.; Marsi, M.; Gladysz, J. A. *Ibid.* **1983**, *22*, 1413.

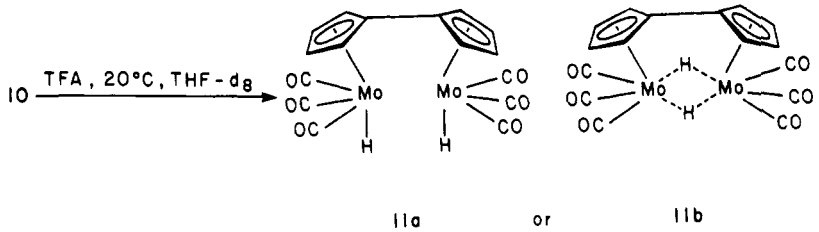

11a or 11b

strong electron back-donation from the metal to the carbonyl ligands. The ^{1}H NMR resonances in THF-d_8 appeared at δ 5.21 and 4.76 in the form of AA'MM' patterns (4 H each). As expected for a dianionic structure, these chemical shifts were upfield from those of the dialkyl and dihydride derivatives (vide infra).

Dihydride Complex $FvMo_2(CO)_6H_2$ Prepared from $FvMo_2(CO)_6^{2-}$. The dilithium salt $Li_2[FvMo_2(CO)_6]$ was protonated instantaneously by treatment with trifluoroacetic acid (TFA) in THF-d_8 at 20 °C. The IR and ^{1}H NMR spectra of the resulting dark yellow solution were consistent with the expected dihydride structure **11**. In the infrared spectrum there were three terminal carbonyl stretching absorptions at 2020, 1929, and 1902 cm^{-1} which were indicative of C_s symmetry about each metal atom. A metal–hydride stretching band could not be observed, either because it was too weak or because it was obscured by the carbonyl signals. The Mo–H absorption could also not be detected for $Cp(CO)_3MoH$.[39] Two AA'MM' ^{1}H NMR (THF-d_8) resonances were seen at δ 6.15 and 5.59 (4 H each) in addition to a singlet for the hydride proton at δ −5.43 (2 H). In comparison, the hydride singlet for $Cp(CO)_3MoH$ appears at δ −5.70 (toluene).[39] The syn conformation drawn for **11a** is not known to be correct; alternative structures such as an anti form or the bridging dihydride **11b** must also be considered. The highly air- and heat-sensitive **11** proved to be too unstable for complete purification.

The fulvalene dihydride **11** was envisioned to undergo a facile intramolecular elimination of dihydrogen, and the mechanism of such a reaction was of interest as a model for desorption of H_2 from metal surfaces.[41] Thus, in a rigorously deoxygenated THF solution, **11** cleanly extruded dihydrogen at 20 °C over a period of less than 24 h. This reaction was not affected by ambient light. The metal–metal bonded complex **1** was isolated in quantitative yield, and dihydrogen was detected by mass spectroscopy. The $Cp(CO)_3MoH$[39] analogue of **11** also thermally decomposed in THF solution to $Cp_2Mo_2(CO)_6$ and dihydrogen; but, in contrast, this process required heating to 110 °C to proceed at the same rate. It is possible that the acceleration of dihydrogen elimination from **11** was a result of catalysis by impurities present in the reaction mixture. An alternative explanation is that the reaction follows an entropically favorable intramolecular pathway. One possibility is a dinuclear reductive elimination of dihydrogen, although this type of transformation is virtually unknown in the literature.[42] Recent theoretical work[43] has established that such a process occurring via a planar four-center transiton state would be symmetry forbidden. However, if the M–H bonds are twisted relative to each other, then such a restriction might be lifted. Whether or not dihydrogen extrusion is intramolecular can in principle be determined by carrying out a crossover experiment starting from a mixture of $FvMo_2(CO)_6H_2$ (**11**) and $FvMo_2(CO)_6D_2$ (**11-d_2**). However, this experiment was anticipated to be complicated by unavoidable traces of protic and deuterated acids in the respective solutions of **11** and **11-d_2**; it was thought that these acids would cause rapid H/D exchange.[44] This expectation was confirmed when a small quantity of TFA-d_1, added to a THF-d_8 solution of **11** at 20 °C, led to immediate partial incorporation of deuterium as indicated by a relatively diminished ^{1}H NMR hydride resonance. Current efforts to unveil the mechanistic details of H_2 extrusion from fulvalene dimetallic hydrides center on the more stable and purifiable ditungsten species.[45]

Table IV. ^{1}H NMR and IR Data of Dialkyl Complexes $FvMo_2(CO)_6R_2$

compd	^{1}H NMR (acetone-d_6), δ	IR (KBr), cm^{-1}
$FvMo_2(CO)_6(CH_3)_2$ (**12**)	5.78 (m, 4 H), 5.42 (m, 4 H), 0.26 (s, 6 H)	2010, 1965, 1925
$FvMo_2(CO)_6(CH_2Ph)_2$ (**13**)	7.45 (m, 4 H), 7.30 (m, 6 H), 5.93 (m, 4 H), 5.49 (m, 4 H), 2.78 (s, 4 H)	2010, 1950, 1920
$FvMo_2(CO)_6(CH_2OCH_3)_2$ (**14**)	5.56 (m, 4 H), 5.35 (m, 4 H), 4.47 (s, 4 H), 3.25 (s, 6 H)[a]	2010, 1935, 1910

[a] CD_2Cl_2 solvent.

Dialkyl and Carbene Complexes $FvMo_2(CO)_6R_2$ Prepared from $FvMo_2(CO)_6^{2-}$. Addition of primary alkyl, allyl, and benzyl halides to $Cp(CO)_3Mo^-$ anion has been known to afford the corresponding metal alkyl compounds $Cp(CO)_3MR$ in high yields.[39] Not surprisingly, treatment of $Li_2[FvMo_2(CO)_6]$ with various haloalkanes produced the alkylated complexes $FvMo_2(CO)_6R_2$. The ^{1}H NMR and IR spectral data of the three dialkyl complexes prepared (Table IV) are consistent with their expected structures based on the comparison with $Cp(CO)_3MR$,[39,46] although their actual conformations are not known.

In analogy to the methyl complex $Cp(CO)_3MoCH_3$,[22] $FvMo_2(CO)_6(CH_3)_2$ (**12**) was observed to decompose photochemically in THF or benzene to yield **1** (62% yield) and large quantities of methane (detected by mass spectroscopy). Photolysis of the deuteriomethyl complex **12-d_6** in C_6D_6 producted mostly CD_3H. Similarly, Rausch[47] found that irradiation of $Cp(CO)_3MoCD_3$ in C_6D_6 generated predominantly CD_3H. It was proposed that the departing

(41) (a) Susuki, K. *J. Less-Common Met.* **1983**, *89*, 183. (b) Paal, Z.; Menon, P. G. *Catal. Rev.-Sci. Eng.* **1983**, *25*, 229. (c) Saillard, J.-Y.; Hoffmann, R. *J. Am. Chem. Soc.* **1984**, *106*, 2006. (d) For other homogeneous models, see: Mueller-Westerhoff, U. T.; Nazzal, A. *J. Am. Chem. Soc.* **1984**, *106*, 5381. Waleh, A.; Loew, G. H.; Mueller-Westerhoff, U. T. *Inorg. Chem.* **1984**, *23*, 2859. Moore, M. F.; Wilson, S. R.; Hendrickson, D. N.; Mueller-Westerhoff, U. T. *Ibid.* **1984**, *23*, 2918.

(42) Bitterwolf, T. E.; Ling, A. C. *J. Organomet. Chem.* **1973**, *57*, C15.

(43) Trinquier, G.; Hoffmann, R. *Organometallics* **1984**, *3*, 370.

(44) See: Gaus, P. L.; Kao, S. C.; Darensbourg, M. Y.; Arndt, L. W. *J. Am. Chem. Soc.* **1984**, *106*, 4752.

(45) Tilset, M.; Vollhardt, K. P. C., unpublished results.

(46) Green, M. L. H.; Ishaq, M.; Whiteley, R. N. *J. Chem. Soc. A* **1967**, 1508.

(47) Rausch, M. D.; Gismondi, T. E.; Alt, H. G.; Schwarzle, J. A. *Z. Naturforsch., B: Anorg. Chem., Org. Chem.* **1977**, *32B*, 998.

Scheme I

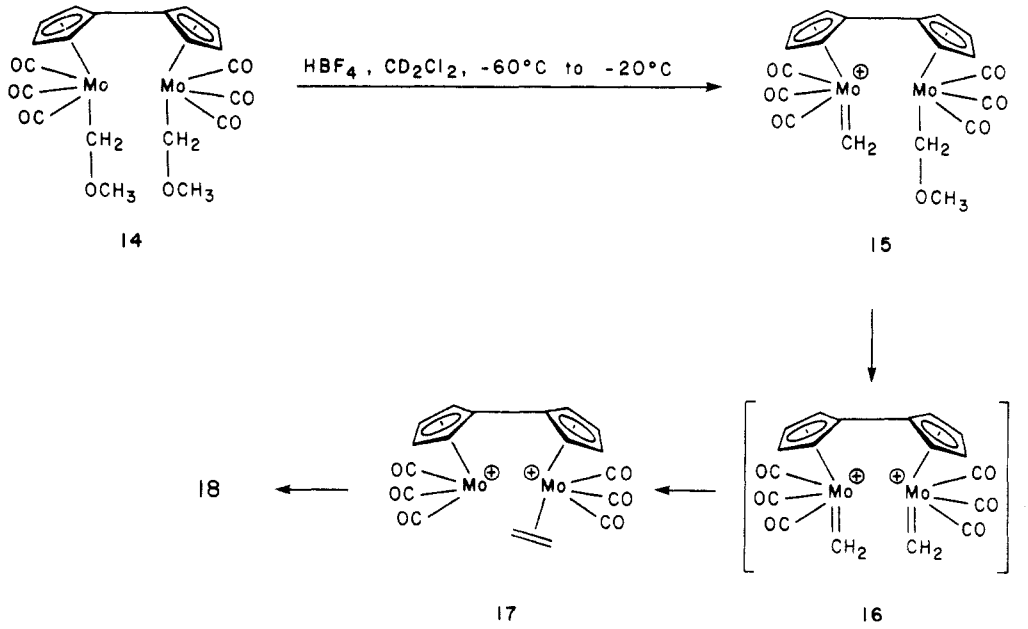

methyl group abstracted hydrogen from the cyclopentadienyl ring in a concerted manner. It is also possible that some type of Cp or Fv photodegradation product was the source of the fourth hydrogen for methane. The isotopic selectivity is puzzling, and the mechanism of these reactions remains obscure.

The dialkylated fulvalene complexes **12–14** were briefly examined as potential precursors to dinuclear bis(alkylidene) compounds. There has been considerable interest in the generation of CpM carbenes.[46,48] With relevance to our system, it had been noted earlier that treatment of $Cp(CO)_3MoCH_2OCH_3$ with hydrochloric acid afforded the chloromethyl complex $Cp(CO)_3MoCH_2Cl$ which was though to have been formed via the alkylidene species $Cp(CO)_3Mo{=}CH_2^+$.[46] Addition of trityl cation to $Cp(CO)_2(PPh_3)MoCH_3$ generated the phosphine-stabilized carbene $Cp(CO)_2(PPh_3)Mo{=}CH_2^+$ which was detected by ^1H NMR spectroscopy at −90 °C.[48e] This species decomposed at −70 °C to the alkylidene coupling products $Cp(CO)_2(PPh_3)Mo(C_2H_4)^+$ and $Cp(CO)_2(PPh_3)Mo^+$. Fulvalene bis(alkylidene) complexes were expected to undergo even more effective intramolecular alkylidene coupling reactions as a result of the enforced proximity of the two metal centers. This type of process can be viewed as a potential model for a dinuclear pathway by which alkylidene moieties bound to metal surfaces might couple to form alkenes.[49,50]

Our initial attempts to prepare bis(alkylidene) complexes were unsuccessful. As determined by ^1H NMR spectroscopy, the dimethyl derivative **12** did not react with $Ph_3C^+BF_4^-$ in CD_2Cl_2 even after heating to 60 °C for 12 h. Complex **13** disappeared immediately in the presence of trityl cation at −80 °C to yield a complex mixture of products, none of which could be identified.

Modest success was found in the protonation of the methoxymethyl compound **14**. Treatment with an excess of tetrafluoroboric acid dimethyl etherate in CD_2Cl_2 at −80 °C produced an immediate color change from yellow to deep red. The latter was apparently caused by an intensely colored minor product because ^1H NMR signals assignable only to starting material were observed. Warming of the solution from −60 to −20 °C caused the gradual disappearance of **14** and formation of a new complex which, based on its ^1H NMR spectrum, was thought to be the cationic mono(alkylidene) **15** (Scheme I). This species exhibited four fulvalene multiplets at δ 6.20, 6.03, 5.67, and 5.59 (2 H each), singlets at 4.80 (2 H) and 3.71 (3 H) for the methylene and methyl groups, and a singlet at 15.92 (2 H) assignable to the alkylidene hydrogens. The chemical shift of the latter resonance was very close to that of the alkylidene signal in $Cp(CO)_2(PPh_3)Mo{=}CH_2^+$ (δ 15.4, CD_2Cl_2, −90 °C).[48e] The observation of the remainder of the hydrogens at relatively larger chemical shifts was consistent with the positive charge present in **15**. Moreover, the lifted degeneracy of the Cp absorptions was in agreement with the unsymmetrical structure proposed.

As the temperature of the solution containing **15** was raised between −30 and 0 °C the peaks due to **15** diminished with concomitant emergence of a new set of signals which were indicative of the presence of structure **17**. Four new fulvalene proton resonances were observed at δ 6.38, 6.17, 5.73, and 5.42 (2 H each). As expected for a dication, this set was shifted to lower field compared to the corresponding peaks for **15**. A singlet at δ 3.78 (4 H) was assigned to the ethene ligand protons. For comparison, the corresponding signal in $Cp(CO)_2(PPh_3)Mo(C_2H_4)^+$ appears slightly upfield at δ 3.53 (CD_2Cl_2, +20 °C).[48e] This chemical shift difference is reasonable considering the relatively strong electron-donating ability of triphenylphosphine. Ethene slowly dissociated from **17** at 20 °C over the course of 2 days; an unknown organometallic product **18** precipitated from the solution. The ethene produced was analyzed by gas chromatography.

We interpret the above ^1H NMR evidence as being indicative of the occurrence of a novel carbene coupling reaction via the pathway outlined in the scheme. The ^1H NMR data do not exclude the possibility that alkylidene coupling was an intermolecular process. Regardless of the mechanism, the overall transformation of **14** to the ethene complex is qualitatively similar to that observed in the mononuclear phosphine analogue. The greater stability of **15** can perhaps be attributed to the more extensive

(48) (a) Mahmoud, K. A.; Rest, A. J.; Alt, H. G. *J. Chem. Soc., Chem. Commun.* **1983**, 1011. (b) Jolly, P. W.; Pettit, R. *J. Am. Chem. Soc.* **1966**, *88*, 5044. (c) Brookhart, M.; Nelson, G. O. *Ibid.* **1977**, *99*, 6099. (d) Bodnar, T. W.; Cutler, A. R. *Ibid.* **1983**, *105*, 5926. (e) Kegley, S. E.; Brookhart, M.; Husk, G. R. *Organometallics* **1982**, *1*, 760.

(49) Gault, F. G. *Adv. Catal.* **1981**, *30*, 1.

(50) For a theoretical appreciation of carbene–carbene coupling, see: Wilker, C. N.; Hoffmann, R.; Eisenstein, O. *Nouv. J. Chim.* **1983**, *7*, 535.

Scheme II

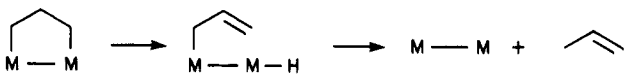

delocalization of the positive charge and the better electron-donating capability of fulvalene when compared to the Cp ligand.

Reactions of $FvMo_2(CO)_6^{2-}$ with Dihaloalkanes. Formation and Structural Characterization of Fischer-Type Carbene Complexes. The facile alkylations giving rise to **12–14** suggested that it might be possible to synthesize the novel dimetallacycles of the type B by the reaction of **10** with dihaloalkanes. These promised to be unique because they are structurally in between μ-α,α-alkanediyl complexes of the form L_xM-$(CH_2)_n$-ML_x (C) and bona fide dimetallacycles of the type D. Such

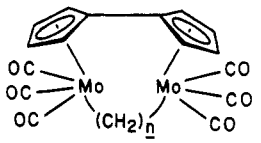

B

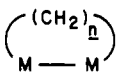

D

compounds have attracted attention[51] because of their structural resemblance to proposed intermediates in a variety of metal surface-catalyzed reactions. For example, when $n = 3$ both C and D have been observed to produce cyclopropane and/or propene.[51f-h] A favored mechanism for these hydrocarbon extrusions has been β-hydrogen elimination followed by bimetallic reductive elimination (e.g., Scheme II, E → F → G). Because several of the systems in the literature had been prepared in a similar manner, we anticipated ready access to analogues B by double alkylation. Interestingly, addition of dihaloalkanes to $Li_2[FvMo_2(CO)_6]$ failed to yield bridged complexes. Treatment of a solution of the dianion at −78 °C in THF with diiodomethane or 1,2-diiodoethane caused instantaneous oxidation of **1**, a process which was not investigated further. Exposure of the dianion to 1,2-dibromoethane gave the same result. The analogous tosylates $CH_2(OTs)_2$ and $TsOCH_2CH_2OTs$ were also exposed in this way but no reaction occurred even at 65 °C. After 10 h at this temperature the dianion had decomposed.

In contrast, the reaction between **10** and 1,3-diiodopropane proceeded smoothly (Scheme III). Surprisingly, the product was not **19**, but the Fischer-type carbene complex **20**, isolated after column chromatography (red crystals, mp 202–203 °C dec, 90% yield). Mass spectral (M^+ at m/e 530) and C, H analytical data were consistent with the expected molecular formula. The ^1H NMR spectrum (250 MHz, C_6D_6) was in accord with the presence of a 1-oxacyclopent-2-ylidene ligand which was terminally bound to one metal atom and aligned with the Mo–Mo bond. Four nonequivalent fulvalene proton signals were observed at δ 5.14, 4.47, 4.00, and 3.57. In addition, there were three peaks at δ 3.61 (t, J = 7.2 Hz, 2 H), 3.30 (t, J = 7.6 Hz, 2 H), and 1.03 (tt, J = 7.6, 7.2 Hz, 2 H). The low field triplet was assigned to the methylene protons α to the oxygen because of the electronegativity of the heteroatom. This assignment is also consistent with that of the corresponding quartet found in $(CO)_9Mn_2[=CCH_3(OCH_2CH_3)]$.[51i] The proton-decoupled ^{13}C NMR spectrum (45 MHz, C_6D_6) was also in agreement with structure **20**. Signals due to six nonequivalent fulvalene carbons (δ 97.4, 94.0, 89.4, 85.9, 85.5, 83.3) and three different methylene carbons (δ 80.0, 56.2, 23.1) were observed. A peak at δ 231.6 was assigned to the fluxional terminal carbonyl ligands. The carbene carbon resonance could not be detected.

Confirmation of the structure of **20** was achieved by an X-ray diffraction study. Figure 5 shows two ORTEP drawings of **20**. Table V lists the intramolecular atomic distances, angles, and torsional angles. The analysis revealed a terminally bound 1-oxacyclopent-2-ylidene ligand which is envelope-shaped and nearly coplanar with the Mo–Mo bond. The carbonyl ligands are slightly staggered to relieve steric congestion, resulting in a twisted fulvalene ligand. The Mo1–Mo2 separation of 3.266 Å is consistent with the presence of a metal–metal single bond.[28c] The C21–O6 distance of 1.325 Å indicates that there is partial double bond character between the carbene carbon and the oxygen atom. This bonding feature is common among Fischer carbene complexes.[52]

The analogous 1-oxacyclohex-2-ylidene complex **21** was prepared in very low yield from the reaction of **10** with 1.5 equiv of 1,4-diiodobutane. Column chromatography of the reaction mixture afforded the product (red crystals, mp 187–188 °C dec, 7% yield) which exhibited ^1H NMR and IR spectral features very similar to those of **20**. In the ^1H NMR spectrum there were four fulvalene peaks at δ 5.08, 4.44, 4.04, and 3.55 (2 H each) and four methylene signals at δ 3.47 (t, J = 6.1 Hz, 2 H), 3.24 (t, J = 6.9 Hz, 2 H), 1.26 (apparent quintet, J = 6.3 Hz, 2 H), and 1.04 (apparent quintet, J = 6.3 Hz, 2 H). Five terminal carbonyl stretching bands were observed at 2018, 1987, 1962, 1928, and 1908 cm^{-1}. The mass spectrum (M^+ at m/e 544) was also consistent with the assigned structure. A very low mass balance in this reaction accompanied the poor yield. After 24 h at room temperature the reaction mixture contained a large amount of insoluble material. Infrared spectroscopy indicated the presence of the carbene product and no other metal carbonyl species, including $Li_2[FvMo_2(CO)_6]$. The cause of decomposition in this reaction was not investigated, nor was an attempt made to increase the yield of **21**. In contrast to the formation of these Fischer-type carbenes, we have found that treatment of

Scheme III

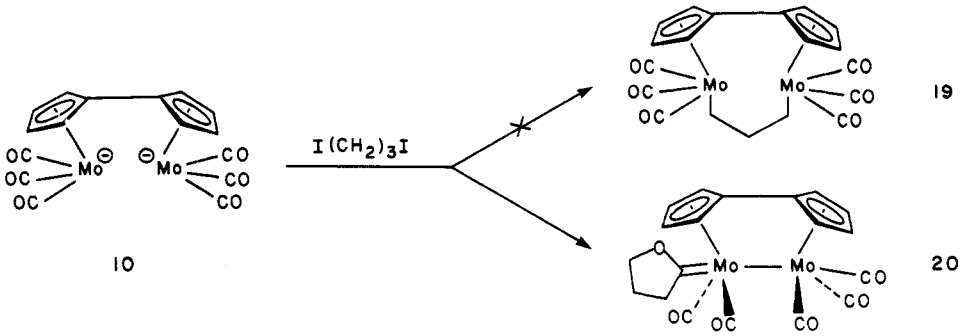

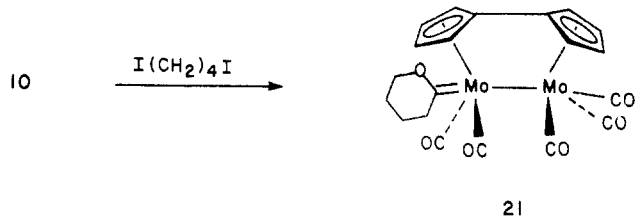

21

$FvW_2(CO)_6^{2-}$ with 1,3-diiodopropane gives only the dialkylated unbridged product $FvW_2(CO)_6(CH_2CH_2CH_2I)_2$.[45]

The formation of oxaalkylidenes has been observed previously in the attempted generation of alkanediyl complexes from certain metal anions,[51i,j,k,l,m] including CpMo.[51i,j] Adapting the mechanisms proposed for these systems to ours generates the mechanistic picture presented in Scheme IV en route to **20**.

The initially formed monoalkylated species H probably undergoes CO insertion to give the coordinatively unsaturated acyl species I. Intramolecular attack on the open coordination site by the remaining anionic metal leads to the metal–metal bonded enolate J. This intermediate can be readily envisaged to cyclize to yield the product.

Dynamic ^{1}H NMR Behavior of 20. ^{1}H NMR spectra of the Fischer-type carbene **20** acquired between 40 and 110 °C revealed a gradual broadening of the four fulvalene resonances (Figure 6). It was curious that while the fulvalene proton resonances broadened with increasing temperature the signals for the Fischer carbene methylene protons remained sharp. To explain this finding, a mechanism can be invoked in which the 1-oxacyclopent-2-ylidene ligand is supposed to remain intact while moving from one metal to the other. This process involves as a crucial intermediate the bridging carbene K (Scheme V).

Further evidence for this pathway was obtained by application of ^{1}H NMR magnetization (spin saturation) transfer techniques.[53] Interpretation of the results of this work required the assumption that the two lowest field fulvalene resonances were either both due to α and α' or to β and β' protons. The spectra obtained from these experiments clearly demonstrated magnetization transfer between the two lowest field fulvalene resonances. Figure 7 shows, for example, that irradiation of the signal at δ 5.14 causes a 50% decrease in the intensity of the peak at δ 4.47. Accordingly, irradiation of the latter signal produces a 50% diminution of the signal at δ 5.14. No other peaks in the spectrum were affected in these experiments. Similar results were obtained for the two highest field fulvalene resonances. In contrast to these observations, there was no magnetization transfer seen when any of the Fischer carbene methylene protons were irradiated.

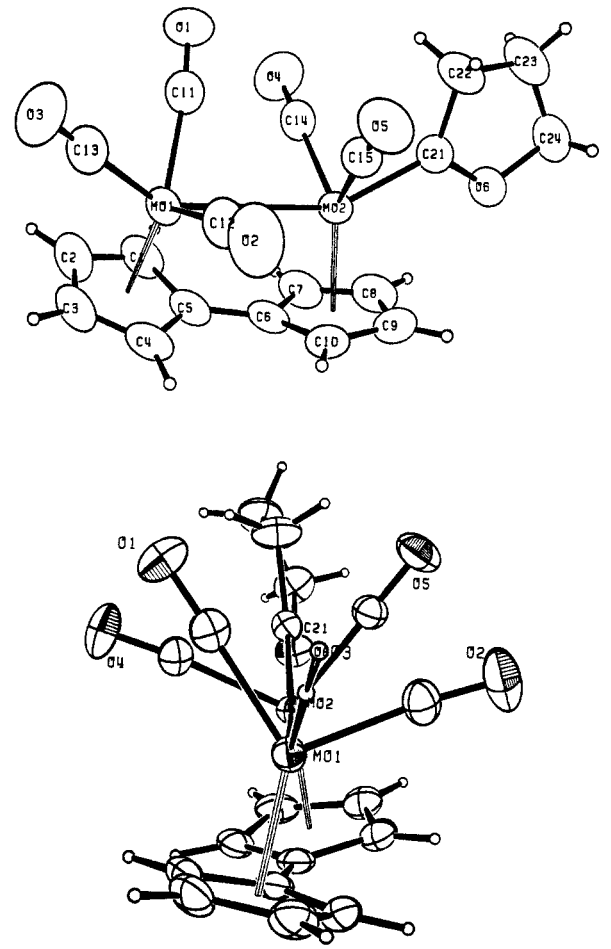

Figure 5. ORTEP drawings of **20**. The top drawing shows the view perpendicular to the Mo–Mo bond and the labeling scheme. Ellipsoids are scaled to represent the 50% probability surface. The bottom drawing depicts the view down the Mo–Mo axis. C13 and O3 have been reduced in size for clarity. Ellipsoids are scaled to represent the 30% probability surface.

Scheme IV

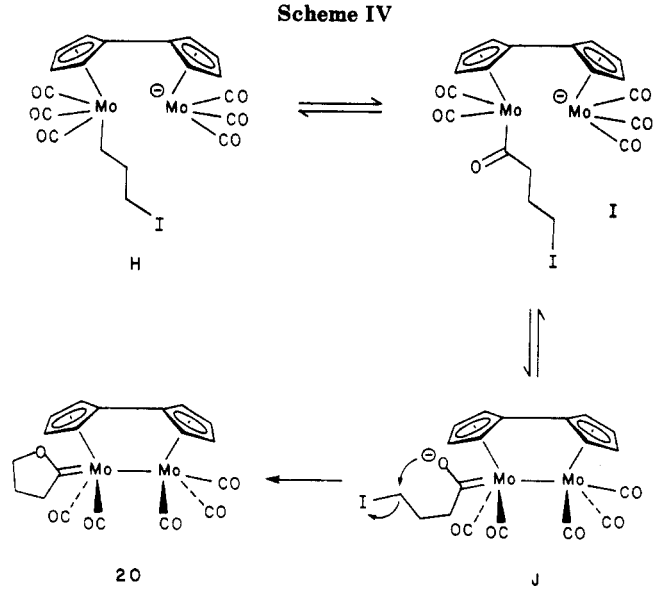

Additional support for the proposed mechanism involving a bridging carbene species K was found in a deuterium labeling experiment. The acidic methylene protons α to the carbene carbon were replaced by deuterium through exposure of **20** to sodium methoxide in a

(51) (a) Lin, Y. C.; Calabrese, J. C.; Wreford, S. S. *J. Am. Chem. Soc.* **1983**, *105*, 1679. (b) Olgemöller, B.; Beck, W. *Chem. Ber.* **1981**, *114*, 867. (c) Kaminsky, W.; Kopf, J.; Sinn, H.; Vollmer, H. *Angew. Chem., Int. Ed. Engl.* **1976**, *15*, 629. (d) Bennett, J. J.; Mathieu, R.; Poilblanc, R.; Ibers, J. A. *J. Am. Chem. Soc.* **1976**, *98*, 2357. (e) King, R. B. *Inorg. Chem.* **1963**, *2*, 531. (f) Cooke, M.; Farrow, N. J.; Knox, S. A. R. *J. Organomet. Chem.* **1981**, *222*, C21; *J. Chem. Soc., Dalton Trans.* **1983**, 2435. (g) Koa, S. C.; Theil, C. H.; Pettit, R. *Organometallics* **1983**, *2*, 914. (h) Theopold, K. H.; Bergman, R. G. *J. Am. Chem. Soc.* **1980**, *102*, 5694. (i) Bailey, N. A.; Chell, P. L.; Mukhopadhyay, A.; Tabbron, H. E.; Winter, M. J. *J. Chem. Soc., Chem. Commun.* **1982**, 215. (j) Bailey, N. A.; Chell, P. L.; Manuel, C. P.; Mukhopadhyay, A.; Rodgers, D.; Tabbron, E.; Winter, M. J. *J. Chem. Soc., Dalton Trans.* **1983**, 2397. (k) Cotton, F. A.; Lukehart, C. M. *J. Am. Chem. Soc.* **1971**, *93*, 2672; **1973**, *95*, 3552. (l) Casey, C. P. *J. Chem. Soc., Chem. Commun.* **1970**, 1220. (m) Casey, C. P.; Cyr, C. R.; Anderson, R. L.; Morten, D. F. *J. Am. Chem. Soc.* **1975**, *97*, 3053. (n) Casey, C. P.; Anderson, R. L. *Ibid.* **1971**, *93*, 3554. (o) For a review, see: Moss, J. R.; Scott, L. G. *Coord. Chem. Rev.* **1984**, *60*, 171.

(52) (a) Dötz, K. H.; Fischer, H.; Hofmann, P.; Kreissl, F. R.; Schubert, U.; Weiss, K. "Transition Metal Carbene Complexes"; Verlag Chemie: Weinheim, 1983. (b) Fischer, E. O. *Adv. Organomet. Chem.* **1976**, *14*, 1.

(53) (a) Faller, J. W. In "Determination of Organic Structures by Physical Methods"; Zuckerman, H., Ed.; Academic Press: New York, 1973; Chapter 2. (b) Benn, R.; Rufinska, A.; Schroth, G. *J. Organomet. Chem.* **1981**, *217*, 91.

Table V. Selected Bond Distances (Å) and Angles (deg) in 20[a]

Intramolecular Distances

atom 1	atom 2	dist	atom 1	atom 2	dist	atom 1	atom 2	dist
Mo1	Mo2	3.266 (1)	Mo2	C9	2.336 (2)	C11	O1	1.145 (3)
Mo1	C1	2.344 (2)	Mo2	C10	2.340 (2)	C12	O2	1.155 (3)
Mo1	C2	2.342 (2)	Mo2	Cp2	1.995	C13	O3	1.148 (2)
Mo1	C3	2.315 (2)	Mo2	C14	1.965 (2)	C14	O4	1.154 (2)
Mo1	C4	2.322 (2)	Mo2	C15	1.982 (2)	C15	O5	1.143 (2)
Mo1	C5	2.326 (2)	Mo2	C21	2.053 (2)	C5	C1	1.415 (3)
Mo1	Cp1	2.000	C21	C22	1.500 (3)	C1	C2	1.398 (3)
Mo1	C11	1.996 (2)	C22	C23	1.514 (3)	C2	C3	1.401 (3)
Mo1	C12	1.960 (2)	C23	C24	1.469 (3)	C3	C4	1.392 (3)
Mo1	C13	1.966 (2)	C24	O6	1.463 (3)	C4	C5	1.419 (3)
Mo2	C6	2.319 (2)	O6	C21	1.325 (2)	C5	C6	1.463 (3)
Mo2	C7	2.327 (2)				C6	C7	1.412 (3)
Mo2	C8	2.321 (2)				C7	C8	1.387 (3)
						C8	C9	1.426 (3)
						C9	C10	1.408 (3)
						C10	C6	1.425 (3)

Intramolecular Angles

atom 1	atom 2	atom 3	angle	atom 1	atom 2	atom 3	angle
Mo2	Mo1	C11	76.80 (6)	C5	C1	C2	107.50 (19)
Mo2	Mo1	C12	80.16 (6)	C1	C2	C3	108.90 (20)
Mo2	Mo1	C13	144.41 (6)	C2	C3	C4	107.95 (20)
Mo2	Mo1	Cp1	96.39	C3	C4	C5	108.26 (20)
C11	Mo1	C12	101.55 (9)	C1	C5	C4	107.36 (19)
C11	Mo1	C13	77.91 (8)	C1	C5	C6	126.09 (19)
C11	Mo1	Cp1	133.44	C4	C5	C6	125.90 (20)
C12	Mo1	C13	80.83 (8)	C5	C6	C7	125.05 (20)
C12	Mo1	Cp1	122.91	C5	C6	C10	126.15 (19)
C13	Mo1	Cp1	119.19	C10	C6	C7	107.65 (19)
Mo1	Mo2	C14	83.68 (5)	C6	C7	C8	108.53 (20)
Mo1	Mo2	C15	79.20 (6)	C7	C8	C9	108.52 (20)
Mo1	Mo2	C21	149.84 (5)	C8	C9	C10	107.51 (20)
Mo1	Mo2	Cp2	98.01	C9	C10	C6	107.78 (19)
C14	Mo2	C15	100.31 (8)	Mo2	C21	O6	123.76 (14)
C14	Mo2	C21	80.97 (8)	Mo2	C21	C22	128.84 (15)
C14	Mo2	Cp2	124.67	O6	C21	C22	107.40 (17)
C15	Mo2	C21	78.24 (8)	C21	C22	C23	105.65 (19)
C15	Mo2	Cp2	134.55	C22	C23	C24	102.65 (19)
C21	Mo2	Cp2	112.07	C23	C24	O6	105.47 (18)
Mo1	C11	O1	172.88 (18)	C24	O6	C21	112.24 (16)
Mo1	C12	O2	173.01 (19)				
Mo1	C13	O3	178.68 (20)				
Mo2	C14	O4	172.64 (18)				
Mo2	C15	O5	174.07 (18)				

Torsion Angles (deg)

atom 1	atom 2	atom 3	atom 4	angle	atom 1	atom 2	atom 3	atom 4	angle
Cp1	Mo1	Mo2	Cp2	-21.1	C14	Mo2	C21	O6	-123.1
C13	Mo1	Mo2	C21	-16.2	Cp2	Mo2	C21	O6	0.7
C12	Mo1	Mo2	C15	-32.7	O6	C21	C22	C23	13.2
C11	Mo1	Mo2	C14	-30.1	C21	C22	C23	C24	-23.4
C1	C5	C6	C10	150.8	C22	C23	C24	O6	24.9
C4	C5	C6	C7	175.0	C23	C24	O6	C21	-18.5
C15	Mo2	C21	O6	134.3	C24	O6	C21	C22	3.0

[a] Cp1 and Cp2 are the centroids of the two five-carbon fulvalene rings.

Scheme V

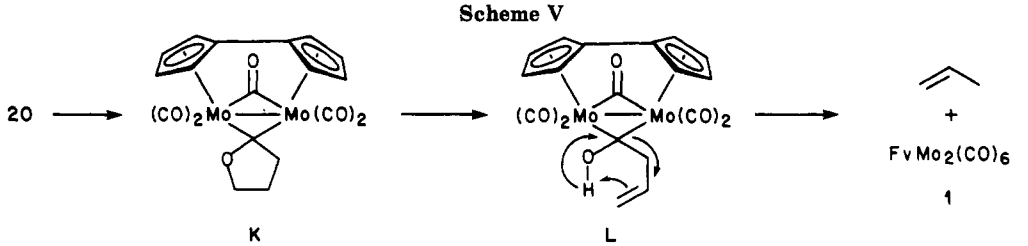

CH_3OD/THF solution.[54] When **20**-d_2 was heated at 100 °C for about an hour, the deuterium label was found to be entirely in the original position. This result clearly indicated that it was not a rearrangement of the carbene ligand itself, perhaps through a metallacycle of the type B, which was responsible for the fluxional behavior observed.

The magnetization transfer technique was also used to determine the rate and activation free energy of the pro-

(54) Kreiter, C. G. *Angew. Chem., Int. Ed. Engl.* **1968**, *7*, 390.

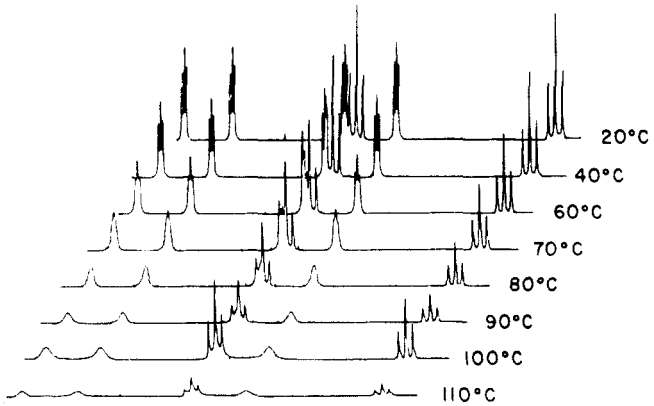

Figure 6. Dynamic ^1H NMR behavior of Fischer carbene complex **20** between 20 °C and 110 °C (250 MHz, acetone-d_6). In order to present a clearer drawing, the spectra have been attenuated with increasing temperature. The spectral behavior shown is completely reversible. This experiment was also carried out in toluene-d_8 with identical results.

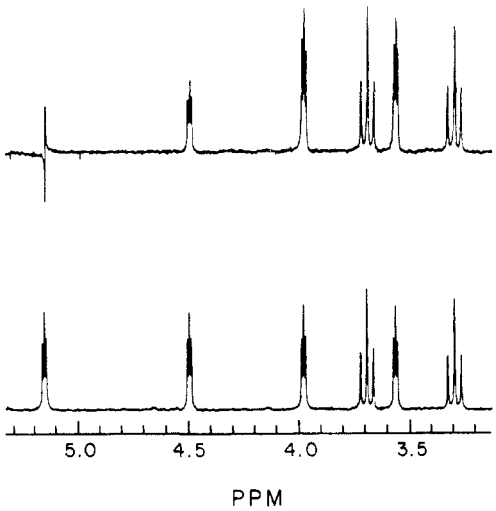

Figure 7. Magnetization transfer in **20** between the low-field fulvalene proton signals at δ 5.14 and 4.47 is shown in the upper spectrum. Irradiation of the peak at δ 5.14 produced a 50% decrease in the intensity of the signal at δ 4.47. The normal spectrum is shown below. Both experiments were carried out at 20 °C, 250 MHz, in toluene-d_8.

cess. The first-order rate constant k at 20 °C was 0.22 s^{-1} and $\Delta G^{\ddagger}$ = 18 ± 0.5 kcal mol^{-1}.

While there have been other reports in which bridging to terminal carbene interconversions have been postulated,[29n,55] the 1-oxacyclopent-2-ylidene **20** is the only known system for which the carbene starts and ends this process from a terminal position. Moreover, it is the only Fischer-type carbene reported to undergo either type of transformation.[52]

Thermal Extrusion of Propene from 20. The most surprising feature of the Fischer-type carbene complex **20** is that it thermolyzes at 100 °C in benzene or toluene to yield hexacarbonyl **1** and propene, both in 80% yield. The elimination of propene proceeded with a half-life of about 12 h at 100 °C. In addition to **20** and propene, some intractable decomposition material was produced. Propene was detected by ^1H NMR spectroscopy (sealed tube experiments) and quantitatively analyzed by gas chromatography. No cyclopropane and only a trace of ethene were detected.

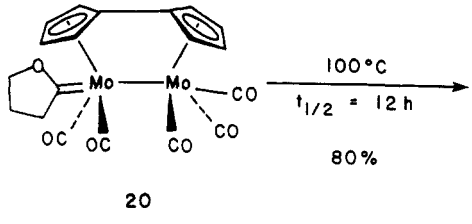

20

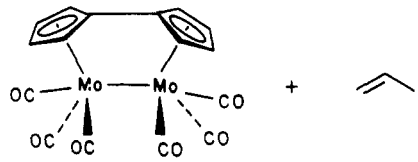

1

It is remarkable that other oxacyclopentylidene complexes do not extrude propene on thermolysis but rather form carbene dimers of 2,3-dihydrofuran. For example, Casey[56] reported that thermolysis of a mononuclear pentacarbonyl chromium oxacyclopentylidene at 120 °C gave mostly the carbene dimer and some 2,3-dihydrofuran in addition to $Cr(CO)_6$, but no propene. In the case of a known dimanganese system, $Mn_2(CO)_{10}(CH_2)_3$,[51l] we have found that heating results only in $Mn_2(CO)_{10}$ and 2,3-dihydrofuran. None of these systems appears to proceed through the intermediacy of the free carbene, since it gives additional products not observed;[57] cyclobutanone, 2,3-dihydrofuran, ethene, and some cyclopropane were detected, but not propene. Our observations may, however, be related to the thermal extrusion of ethene from ethoxycarbene complexes,[58] although mechanistic evidence is lacking.

Kinetic measurements of the thermolysis of **20** were attempted by using ^1H NMR and UV–visible spectroscopy. Unfortunately, line broadening of the NMR signals due to insoluble decomposition products caused peak integrations to be highly inaccurate, and thus the rate determinations were irreproducible. Application of UV–visible spectroscopy was unsuccessful because the principal absorptions of **20** and **1** are sufficiently close that accurate measurements of changes in concentrations were not possible. A rough indication that propene elimination followed a unimolecular pathway (at least with respect to the rate-determining step) was found by carrying out the thermolysis at different concentrations. Within an error margin of ±10%, there was no noticeable difference in half-life when the initial concentration of starting material was decreased from 0.020 to 0.002 M (sealed NMR tube experiments).

A series of labeling experiments in which deuterium was placed in each of the methylene sites of the carbene ligand provided valuable information about the mode of propene extrusion. Syntheses of the labeled starting materials were carried out as follows. Base-catalyzed H/D exchange as described earlier provided **20**-d_2 containing deuterium at C-3. Next **20**-d_2 labeled at C-4 was prepared by treating $Li_2[FvMo_2(CO)_6]$ with $ICH_2CD_2CH_2I$.[58] Last, **20**-d_1 labeled at C-5 was formed by first exposing excess $Ph_3C^+BF_4^-$ to **20** in THF, followed by addition of $LiAlD_4$. The latter

(55) (a) Dyke, A. F.; Knox, S. A. R.; Mead, K. A.; Woodward, P. *J. Chem. Soc., Chem. Commun.* **1981**, 861. (b) Theopold, K. H.; Bergman, R. G. *J. Am. Chem. Soc.* **1983**, *105*, 464. (c) Laws, W. J.; Puddephatt, R. J. *J. Chem. Soc., Chem. Commun.* **1983**, 1020.

(56) Casey, C. P.; Anderson, R. L. *J. Chem. Soc., Chem. Commun.* **1975**, 895.

(57) Foster, A. M.; Agosta, W. C. *J. Am. Chem. Soc.* **1972**, *94*, 5777.

(58) (a) Schubert, U.; Hörnig, H.; Erdmann, K.-U.; Weiss, K. *J. Chem. Soc., Chem. Commun.* **1984**, 13. (b) Schubert, U.; Hörnig, H. *J. Organomet. Chem.* **1984**, *273*, C11. We thank Professor Schubert for providing us with unpublished information on his systems.

(59) For the preparation of $ICH_2CD_2CH_2I$ see: Theopold, K. H. Ph.D. Thesis, University of California, Berkeley, 1982.

Scheme VI

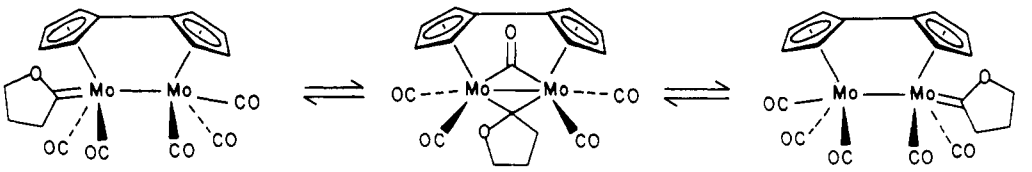

K

process presumably occurred via hydride abstraction by $Ph_3C^+BF_4^-$ to form the oxonium cation **22** to be subsequently reduced with deuteride. Hydride abstraction of this type has apparently never been described before for Fischer carbene complexes.[52]

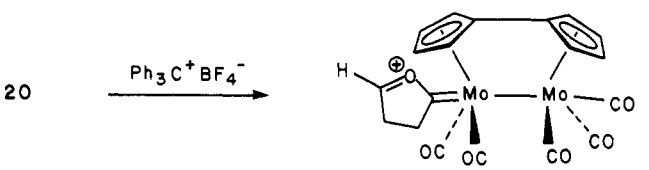

22

Thermolysis of each of these labeled materials clearly showed that a hydrogen atom was transferred from C-4 to C-5 during propene extrusion. Heating C-3 labeled **20**-d_2 to 100 °C in toluene-d_8 gave propene-*1,1*-d_2 as indicated by ^{1}H NMR resonances at δ 5.70 (q, J = 6.4 Hz, 1 H) and 1.57 (d, J = 6.4 Hz, 3 H). For comparison, the ^{1}H NMR spectrum of propene-d_0 exhibited a signal at δ 5.70 (m, 1 H) assignable to the internal olefinic proton, two multiplets centered at δ 4.83 (m, 2 H) due to the terminal olefinic protons, and a methyl peak at δ 1.57 (dt, J = 6.4, 1.6 Hz, 3 H). In the other experiments **20**-d_2 labeled at C-4 furnished propene-*2,3*-d_2 [^{1}H NMR δ 4.90 (m, 1 H), 4.79 (m, 1 H), 1.57 (m, 2 H)], and **20**-d_1 labeled at C-5 resulted in propene-*3*-d_1 [^{1}H NMR δ 5.70 (m, 1 H), 4.83 (m, 2 H), 1.57 (m, 2 H)]. There were no noticeable deuterium isotope effects on the rate of thermolysis of any of the labeled complexes and no observable deuterium scrambling on the time scale of the experiment.

Scheme VI depicts a possible (but not required) mechanistic rationale for the results of these labeling studies. This pathway involves initial conversion of **20** to the bridged carbene K which was earlier postulated from dynamic NMR studies to be in rapid equilibrium with **20** at the temperatures required for propene extrusion. A hydrogen atom at C-4 in K could then transfer to the carbene oxygen yielding the hydroxy allyl carbene L. The latter species would then undergo a retroene reaction to furnish 1 and propene. An analogous mechanism involving only terminal carbene intermediates is also possible. Yet a more direct route to propene extrusion can be envisioned in which a hydrogen at the C-4 carbon of **20** migrates directly to C-5 in a concerted process. Other mechanisms can be devised which are more circuitous. However, we find the pathway outlined in Scheme V to be most appealing for the following reasons. First, the conversion of K to L has some organic analogy in lactone pyrolyses.[60] Although γ-butyrolactones analogous to **20** are stable, the metal might somehow facilitate fragmentation. The behavior of Fischer carbene complexes has been found to be similar to that of esters and lactones in other respects as well.[52] In addition, the nonoccurrence of propene elimination in mononuclear oxacyclopentylidene species may be an indication that bridged intermediates similar to K are required in this process. It has been shown that electron-withdrawing ligands raise the energy of bridging carbenes in dinuclear systems.[61] This finding would explain the absence of propene extrusion in $Mn_2(CO)_{10}(CH_2)_3$ which is relatively electron deficient compared to the fulvalene complex **20**. Finally, the last step involving the decomposition of L has excellent precedence in the analogous fragmentation of β,γ-unsaturated acids.[62]

It is intriguing to speculate on the potential intermediacy of oxacyclopentylidene species similar to **20** and/or K in other propene-forming reactions. As mentioned earlier, dimetallacyclopentane complexes D have been used as starting materials or have been invoked as intermediates, in thermally induced reactions leading to propene (Scheme II). Could it be that these systems (all of which curiously contain CO ligands) transform somehow to 1-oxacyclopent-2-ylidene intermediates en route to eliminating propene? And, is it possible that such carbene moieties are involved in propene formation on metal surfaces exposed to CO and H_2? Such a process would begin with reduction of CO to surface-bound methylene units which could subsequently oligomerize to a bridging structure analogous to D. The latter would then combine with CO to form an oxacyclopentylidene species capable of releasing propene.

Conclusion

A study of ligand substitution reactions of $FvMo_2(CO)_6$ (1) under thermal and photolytic conditions did not furnish the metal–metal triple-bonded complex $FvMo_2(CO)_4$ either because it was not formed or because of its instability. This departure from the chemistry of $Cp_2Mo_2(CO)_6$ is possibly a result of excessive bond strain in the fulvalene ligand. Nevertheless, photochemically induced alkyne substitution reactions were observed starting from $FvMo_2(CO)_6$. While the structure and NMR fluxional behavior of the mono(alkyne) systems were similar to those in the corresponding Cp compounds, we found that this was not the case for bis(alkyne) fulvalenes. Whereas Cp bis(alkyne) complexes contain coupled ligands, their fulvalene counterparts maintain the latter intact. These results are unusual in light of the rare nonoccurrence of alkyne coupling at a dinuclear center.

We postulated that dialkyl and dihydride fulvalene complexes $FvMo_2(CO)_6R_2$ (R = H, alkyl) might exhibit unique reactivity by virtue of the proximity of the metal atoms and the special electronic properties of the fulvalene ligand. Instead, the behavior of these compounds appeared to be very similar, at least qualitatively, to that of the mononuclear analogues $Cp(CO)_3MoR$. Nevertheless, some quantitative differences were observed, such as the greater rate of H_2 elimination from the dihydride **11** as compared to $Cp(CO)_3MoH$. This observation could be attributed to the occurrence of a more favorable intramolecular pathway in the fulvalene case. In addition, we obtained evidence that a fulvalene bis(carbene) had undergone a rapid

(60) Bailey, W. J.; Bird, C. N. *J. Org. Chem.* **1977**, *42*, 3895.

(61) (a) Herrmann, W. A. *Adv. Organomet. Chem.* **1982**, *20*, 159. (b) Shaik, S.; Hoffmann, R.; Fisel, C. R.; Sumerville, R. H. *J. Am. Chem. Soc.* **1980**, *102*, 4555.

(62) Bigley, D. B. *J. Chem. Soc.* **1964**, 3897.

carbene-coupling reaction, in analogy to the mononuclear complex $Cp(CO)_2(PPh_3)Mo{=}CH_2^+$. The stability of the cationic mono(carbene) **15** was consistent with our prediction that fulvalene should be more electron donating and more capable of charge delocalization than the Cp ligand.

Our attempts to prepare bridged dialkylated compounds led to the Fischer-type carbene complex **20**. We anticipated that the presence of two metals in this system might lead to unusual reactivity, and in two instances this has been true. First, the NMR fluxional behavior **20** most likely involved an intermetal transfer of the carbene ligand via the bridging species K. Secondly, complex **20** underwent an unprecedented thermal extrusion of propene. Although the mechanism is not well understood, the presence of two metal centers might be important. Labeling studies clearly ruled out the involvement of the bridged species **19**. This finding suggested that propene extrusion from dimetallacyclopentane complexes might occur via oxacyclopentylidene intermediates and that the latter may play a role in propene formation in other systems.

Experimental Section

General Data. Melting points are uncorrected. ^1H NMR spectra were recorded on the UCB 200-, 250-, and 300-MHz instruments equipped with Cryomagnets Inc. magnets and Nicolet Model 1180 and 1280 data collection systems. ^1H NMR data are reported as follows: chemical shift in parts per million referenced to residual solvent proton resonance (multiplicity, coupling constant(s) in hertz, number of protons). Infrared spectra were obtained on a Perkin-Elmer 681 instrument, and all absorptions are expressed in wavenumbers (cm^{-1}). Low-resolution mass spectra were acquired on AEI-MS12 or Finnigan 4000 instruments by the Mass Spectral Service at the University of California, Berkeley. Mass spectral data are listed as m/e (intensity as a percent of base peak). Elemental analyses were performed by the Microanalytical Laboratory of the University of California, Berkeley. Photochemical experiments were carried out with a Rayonet Photochemical Reactor.

Tetrahydrofuran was distilled from sodium benzophenone ketyl prior to use. All reagents and starting materials obtained from commercial sources were used without further purification.

Crystal Structure of 1. (For references and footnotes relevant to this and the discussion of the structure of **20**, see ref 43–52 in: Hersh, W. H.; Hollander, F. J.; Bergman, R. G. *J. Am. Chem. Soc.* **1983**, *105*, 5834). Tabular very dark red crystals of the compound were obtained by ether vapor diffusion into a solution of **1** in CH_2Cl_2. Fragments cleaved from some of these crystals were mounted on glass fibers by using polycyanoacrylate cement. Preliminary precession photographs indicated triclinic Laue symmetry and yielded preliminary cell dimensions.

The crystal used for data collection was then transferred to an Enraf-Nonius CAD-4 diffractometer and centered in the beam. Automatic peak search and indexing procedures yielded a triclinic reduced primitive cell. Inspection of the Niggli values revealed the absence of conventional cells of higher symmetry. The final cell and specific data collection parameters are given in Table VI.

The 1995 unique raw intensity data were converted to structure factor amplitudes and their esds by correction for scan speed, background, and Lorentz and polarization effects. No correction for crystal decomposition was necessary. Inspection of the azimuthal scan data showed a variation $I_{min}/I_{max} = 0.847$ for the average curve. An empirical correction for absorption, based on the azimuthal scan data, was applied to the intensities.

The structure was solved by Patterson methods and refined via standard least-squares and Fourier techniques. The assumption that the space group was centric $P\bar{1}$ was confirmed by the successful solution and refinement of the structure. In a difference Fourier map which was calculated following refinement of molybdenum atoms with anisotropic thermal parameters, peaks corresponding to the expected positions of all of the hydrogen atoms were found. Hydrogens were included in the structure factor calculations and refined with isotropic thermal parameters. A secondary extinction parameter was refined in the final cycles of least squares. Two data, the (001) and the (1-3-7), had weighted residuals an order of magnitude larger than any others and were removed from the data set.

The final residuals for 250 variables refined against the 1927 data for which $F^2 > 3\sigma(F^2)$ were $R = 1.73\%$, $wR = 3.24\%$, and GOF = 1.933. The R value for all 1995 data was 1.82%.

The quantity minimized by the least squares program was $\sum w(|F_o| - |F_c|)^2$, where w is the weight of a given observation. The p factor, used to reduce the weight of intense reflections, was set to 0.03 throughout the refinement. The analytical forms of the scattering factor tables for the neutral atoms were used, and all non-hydrogen scattering factors were corrected for both the real and imaginary components of anomalous dispersion.

Inspection of the residuals ordered in ranges of $(\sin\theta)/\lambda$, $|F_o|$, and parity and value of the individual indexes showed the absence of unusual features or trends. The largest peak in the final difference Fourier map had an electron density of 0.28 e/Å^3, and all of the top peaks were located near one of the molybdenum atoms.

The positional and thermal parameters of the refined atoms and a listing of the values of F_o and F_c are available as supplementary material.

$FvMo_2(CO)_4(CH_3O_2CC{\equiv}CCO_2CH_3)$ (2) and $FvMo_2(CO)_3(CH_3O_2CC{\equiv}CCO_2CH_3)_2$ (7). $FvMo_2(CO)_6$ (1; 100 mg, 0.20 mmol) and dimethyl ethynedicarboxylate (290 mg, 2.0 mmol) were dissolved in THF (80 mL) in a 30 cm × 2.5 cm Pyrex test tube. The latter was sealed at the top with a rubber septum. For 20 min the solution was flushed with N_2. Then, with continued N_2 flushing, it was irradiated with 300-nm light at room temperature for 5 h. The resulting dark brown mixture was filtered through alumina, and the solvent was removed by rotary evaporation to give a brown oil. The latter was chromatographed on alumina by using pentane–acetone mixtures. The first product eluted was red crystalline **2** (mp 164–165 °C dec; 16 mg, 14%): ^1H NMR (250 MHz, acetone-d_6) δ 6.00 (m, 2 H), 5.58 (m, 2 H), 4.54 (m, 2 H), 4.27 (m, 2 H), 3.85 (s, 3 H), 3.36 (s, 3 H); IR (KBr) 2010, 1970, 1945, 1920, 1735, 1705, 1675 cm^{-1}; MS, m/e (relative intensity) 574 (M^+, 27), 518 (61), 490 (28), 462 (5), 432 (54), 404 (82), 376 (42), 344 (100). Anal. Calcd for $C_{20}H_{14}Mo_2O_8$: C, 41.83; H, 2.46. Found: C, 41.99; H, 2.44.

The second product eluted was orange crystalline **7** (mp 161–162 °C dec; 92 mg, 67%): ^1H NMR (250 MHz, acetone-d_6) δ 6.04 (m, 1 H), 5.87 (m, 1 H), 5.57 (m, 1 H), 5.51 (m, 2 H), 5.08 (m, 1 H), 4.79 (m, 1 H), 4.72 (m, 1 H), 3.82 (s, 3 H), 3.68 (s, 3 H), 3.57 (s, 3 H), 3.50 (s, 3 H); IR (KBr) 2042, 2002, 1944, 1706, 1691, 1678 cm^{-1}; MS, m/e (relative intensity) 688 (M^+, 0.06), 660 (0.59), 632 (0.10), 604 (1), 57 (100). Anal. Calcd for $C_{25}H_{20}Mo_2O_{11}$: C, 43.62; H, 2.93. Found: C, 43.80; H, 2.90.

$FvMo_2(CO)_4(PhC{\equiv}CPh)$ (3) and $FvMo_2(CO)_3(PhC{\equiv}CPh)_2$ (6). $FvMo_2(CO)_6$ (1; 50 mg, 0.10 mmol) and dipphenylethyne (91 mg, 0.51 mmol) were brought to reaction, and the resulting mixture was processed as in the preparation of **2** and **7**. The first product eluted was orange crystalline **3** (mp 162 °C dec; 5.4 mg, 8.8%): ^1H NMR (200 MHz, acetone-d_6) δ 7.50 (m, 1 H), 7.33–6.90 (m, 8 H), 6.76 (m, 1 H), 5.96 (m, 2 H), 5.54 (m, 2 H), 4.43 (m, 2 H), 4.13 (m, 2 H); IR (KBr) 1987, 1955, 1916, 1900 cm^{-1}; MS, m/e (relative intensity) 610 (M^+, 3), 554 (7), 498 (63), 178 (60), 57 (100). Anal. Calcd for $C_{28}H_{18}Mo_2O_4$: C, 55.10; H, 2.97. Found: C, 55.17; H, 3.11.

The second product eluted was dark orange crystalline **6** (mp 179 °C dec; 17.9 mg, 24%): ^1H NMR (250 MHz, acetone-d_6) δ 7.44–6.92 (m, 17 H), 6.75 (m, 3 H), 6.45 (m, 1 H), 5.79 (m, 1 H), 5.68 (m, 1 H), 5.59 (m, 1 H), 5.38 (m, 1 H), 5.13 (m, 1 H), 4.74 (m, 1 H), 4.69 (m, 1 H); IR (KBr) 1960, 1935, 1890 cm^{-1}; MS (chemical ionization), m/e (relative intensity) 610 ($M^+ - Ph_2C_2$, + CO, 36), 582 (13), 554 (4), 526 (1), 178 (100). Anal. Calcd for $C_{41}H_{28}Mo_2O_3$: C, 64.74; H, 3.60. Found: C, 64.54; H, 3.81.

$FvMo_2(CO)_4(HC{\equiv}CH)$ (5). A THF solution (90 mL) of $FvMo_2(CO)_6$ (1; 50 mg, 0.10 mmol) in a 30 cm × 2.5 cm Pyrex test tube was flushed with ethyne while being irradiated (300 nm). After 5 min the color had changed from purple to brownish orange. The solution was filtered through alumina, and the solvent was removed by rotary evaporation. The resulting solid was chro-

Table VI. Crystal and Data Collection Parameters for 1 and 20

	$C_{16}H_{10}Mo_2O_6$ (1)	$C_{19}H_{16}Mo_2O_6$ (20)
Crystal Parameters at 25 °C[a]		
a, Å	6.7721 (10)	8.2680 (12)
b, Å	9.6610 (12)	9.4957 (10)
c, Å	12.4911 (19)	12.5989 (10)
α, deg	76.101 (11)	110.290 (7)
β, deg	84.461 (12)	93.937 (9)
γ, deg	74.876 (11)	92.049 (10)
V, Å^3	765.3 (2)	923.7 (4)
space group	$P\bar{1}$	$P\bar{1}$
M_r, amu	488.12	530.20
Z	2	2
d(calcd), g cm^{-3}	2.12	1.906
μ(calcd), cm^{-1}	16.29	13.57
size, mm	0.18 × 0.27 × 0.40	0.10 × 0.22 × 0.32
Data Measurement Parameters		
diffractometer	Enraf-Nonius CAD-4	
radiatn	Mo Kα ($\bar{\lambda}$ = 0.710 73 Å)	
monochromator	highly oriented graphite ($2\theta_m$ = 12.2°)	
detector	crystal scintillation counter, with pulse height analyzer	
aperture-crystal dist, mm	173	
vertical aperture, mm	3.0	
horizonal aperture, mm	2 + 1.0 tan θ, variable	
reflectns measured	$+h,\pm k,\pm l$	
2θ range	3–45°	
scan type	θ–2θ	
scan speed (θ), deg/min	0.60–6.7	
scan width ($\Delta\theta$)	0.5 + 0.347 tan θ	
bkgd	0.25 ($\Delta\theta$) at each end of the scan	
unique reflctns	1995	2411
intensity standards[b]	$21\bar{7}$, 434, $2\bar{5}\bar{2}$	053, $2\bar{3}8$, $4\bar{2}\bar{5}$
orientation[c]	3 reflections were checked after every 250 measurements	

[a] Unit cell parameters and their esds were derived by a least-squares fit to the setting angles of the unresolved Mo Kα components of 24 reflections with 2θ between 27° and 30° for **1** and 24° and 28° for **20**. [b] Measured every 2 h of X-ray exposure time. Over the period of data collection no decay in intensity was observed, for both **1** and **20**. [c] Crystal orientation was redetermined if any of the reflections were offset from their predicted position by more than 0.1°. Reorientation during data collection was carried out once for **1** and not needed for **20**.

matographed on alumina with hexane to give red-orange crystalline **5** (mp 154–155 °C; 12.6 mg, 27%): ^{1}H NMR (200 MHz, acetone-d_6) δ 5.60 (m, 4 H), 4.38 (m, 4 H), 3.30 (s, 2 H); IR (KBr) 1991, 1959, 1909, 1889 cm^{-1}; MS, m/e (relative intensity) 458 (M^+, 17), 430 (17), 402 (28), 374 (26), 346 (99), 344 (100). Anal. Calcd for $C_{16}H_{10}Mo_2O_4$: C, 41.95; H, 2.20. Found: C, 42.22; H, 2.23.

Kinetic Measurements of the ^{1}H NMR Fluxional Behavior of $FvMo_2(CO)_4(PhC{\equiv}CPh)$ (3). An acetone-d_6 solution of **3** (5 mg) in an NMR tube was degassed by three freeze–pump–thaw cycles; the tube was then sealed under vacuum. ^{1}H NMR (200 MHz, acetone-d_6) spectra were obtained between −30 and +60 °C. As shown in Figure 3 coalescence of the two low-field fulvalene signals occurred at +35 °C. The coalescence temperature T_c was used to determine the rate constant and free energy of activation $\Delta G^\ddagger$ for the fluxional process. Assuming that the latter was unimolecular, the rate constant at the coalescence temperature k_c was calculated from

$$k_c = \pi\Delta\nu/\sqrt{2}$$

in which $\Delta\nu$ is the frequency difference in hertz between the two resonances at a slow exchange temperature.[63] The two lowest field fulvalene peaks were assumed to be either a pair of exchanging α or β protons. The rate constant k_c determined in this way was used in the expression

$$\Delta G^\ddagger = 2.3RT_c(10.32 + \log T_c/k_c)$$

For $\Delta G^\ddagger$ at the coalescence temperature T_c = +35 °C, k_c = 187 s^{-1} and $\Delta G^\ddagger$ = 15.0 ± 0.5 kcal mol^{-1}.

$Na_2[FvMo_2(CO)_6]$. A flask containing $FvMo_2(CO)_6$ (1; 50 mg, 0.10 mmol) and Na–Hg (1 g, 1% Na w/w), stoppered with a rubber septum, was flushed for 5 min with N_2. THF (5 mL was subsequently added. After the solution was stirred for 2–3 h at 20 °C, the color of the solution had changed from purple to yellow. Filtration through Celite in an N_2 atmosphere glovebox gave a bright yellow homogeneous solution of the air-sensitive dianion. A sample of this solution was transferred to an infrared liquid cell, which was then tightly sealed; IR (THF) 1890, 1790, 1740 cm^{-1}.

$Li_2[FvMo_2(CO)_6]$. A 1 M solution of lithium triethylborohydride in THF (0.2k mL, 0.25 mmol) was added dropwise to a solution of $FvMo_2(CO)_6$ (1; 50 mg, 0.10 mmol) in THF (5 mL) at 0 °C. During the addition period of 1 min the solution gradually changed from purple to yellow. The presence of triethylborane in these solutions did not affect the chemistry of the dianion. However, in initial experiments the Et_3B was removed under high vacuum along with the solvent, and fresh THF was subsequently added.

In an N_2 atmosphere glovebox, a sample of the air-sensitive dianion in THF was transferred to an infrared liquid cell, and the latter was tightly closed; IR (THF) 1900, 1806, 1782, 1716 cm^{-1}.

In a separate experiment, the solvent was removed at low pressure (10^{-4} torr) and THF-d_8 (0.5 mL) vacuum transferred into the reaction vessel. In an N_2 atmosphere glovebox the solution was transferred into an NMR tube which was subsequently sealed under vacuum; ^{1}H NMR (300 MHz, THF-d_8) δ 5.21 (m, 4 H), 4.76 (m, 4 H).

$FvMo_2(CO)_6H_2$ (11). A 5-mL THF solution of **10** (here and in subsequent experiments the lithium salt of **10** was used) was prepared from $FvMo_2(CO)_6$ (1; 50 mg, 0.10 mmol). Trifluoroacetic acid (19 μL, 0.25 mmol) was added at 20 °C. the color changed immediately from bright to brownish yellow. In an N_2 atmosphere glovebox a sample of the solution containing the highly air-sensitive **11** was transferred to an infrared liquid cell; IR (THF) 2020, 1929, 1902 cm^{-1}.

In a separate experiment, a THF-d_8 solution (0.5 mL) of **10** [prepared from **1** (5 mg, 0.01 mmol)] was taken into an N_2 atmosphere glovebox. The solution was treated with trifluoroacetic acid (2 μL, 0.025 mmol) and then transferred to an NMR tube which was attached to a 14/20 outer joint. The tube was sealed under high vacuum; ^{1}H NMR (300 MHz, THF-d_8) δ 6.15 (m, 4 H), 5.59 (m, 4 H), −5.43 (s, 2 H).

Dihydrogen Elimination from $FvMo_2(CO)_6H_2$ (11). A solution of **11** in THF (5 mL) was prepared from **1** (5 mg, 0.01 mmol). In an N_2 atmosphere glovebox the mixture was transferred to a flask fitted with a 14/20 outer joint and a Teflon vacuum needle valve and degassed by three freeze–pump–thaw cycles. After 24 h at 20 °C the color had changed from yellow to purple. The flask was connected through the 14/20 joint to a mass spectrometer; with the solution frozen at −196 °C, the Teflon valve was opened to allow the most volatile gases to enter the instrument. Dihydrogen was the only species detected. The solution was thawed, and the solvent was removed by rotary evaporation. Filtration of the residue through alumina using acetone afforded $FvMo_2(CO)_6$ (1; 50 mg, 100%). For comparison, a pure sample of $(\eta^5\text{-}C_5H_5)(CO)_3MoH$[39] (25 mg, 0.10 mmol) in oxygen-free THF (5 mL) was stable indefinitely at 20 °C. Heating to 110 °C over several hours gave decomposition to $(\eta^5\text{-}C_5H_5)_2Mo_2(CO)_6$.

Addition of Trifluoroacetic Acid-d_1 to $FvMo_2(CO)_6H_2$ (11). A solution of **11** in THF-d_8 (0.5 mL) was prepared from **1** (5 mg, 0.01 mL) as described above. In an N_2 atmosphere glovebox, the mixture was treated with trifluoroacetic acid-d_1 (0.5 μL, 0.006 mmol) and then transferred into an NMR tube which was attached to a 14/20 outer joint. The tube was sealed under a vacuum. An ^{1}H NMR spectrum showed that the hydride resonance was approximately 30% smaller than normal as determined by integration against the fulvalene signals.

$FvMo_2(CO)_6(CH_3)_2$ (12). A solution of **10** was prepared from **1** (50 mg, 0.10 mmol). At room temperature it was treated with

(63) Lambert, J. B.; Shurvell, H. F.; Verbit, L.; Cooks, R. G.; Stout, G. H. "Organic Structure Analysis"; MacMillan: New York, 1976; p 116.

methyl iodide (13 μL, 0.20 mmol). After 1 h the solvent was removed by vacuum transfer. Chromatography of the residue (alumina, pentane) and subsequent recrystallization from diethyl ether and pentane afforded yellow crystalline **12** (mp 181–182 °C dec; 47 mg, 90%); ^{1}H NMR (200 MHz, acetone-d_6) δ 5.78 (m, 4 H), 5.42 (m, 4 H), 0.26 (s, 6 H); IR (KBr) 2010, 1965, 1925, cm^{-1}. These data are nearly identical with those reported by Smart.[17]

$FvMo_2(CO)_6(CH_2Ph)_2$ (13). A THF solution (5 mL) of **10** was prepared from **1** (50 mg, 0.10 mmol). Benzyl bromide (35 μL, 0.30 mmol) was added at room temperature. After 1 h the solvent was removed by rotary evaporation, and the residue was chromatographed (alumina, pentane). Recrystallization of the resulting yellow solid from diethyl ether and pentane gave **13** (mp 200 °C dec; 50.4 mg, 79%): ^{1}H NMR δ 7.45 (m, 4 H), 7.30 (m, 6 H), 5.93 (m, 4 H), 5.49 (m, 4 H), 2.78 (s, 4 H); IR (KBr) 2010, 1950, 1020 cm^{-1}; MS, m/e (relative intensity) 638 (M^+, 0.7), 348 (100). Anal. Calcd for $C_{30}H_{22}Mo_2O_6$: C, 56.44; H, 3.48. Found: C, 56.92; H, 3.58.

$FvMo_2(CO)_6(CH_2OCH_3)_2$ (14). A THF solution (5 mL) of **10** was prepared from **1** (100 mg, 0.20 mmol). Chloromethyl methyl ether (60 μL, 0.80 mmol) was added at room temperature. After 1 h the volatile components were removed by vacuum transfer. Chromatography of the residue (alumina, pentane) and recrystallization from pentane and acetone gave **14** (mp 146–147 °C dec; 100 mg, 87%): ^{1}H NMR (200 MHz, CD_2Cl_2) δ 5.56 (m, 4 H), 5.35 (m, 4 H), 4.47 (s, 4 H), 3.35 (s, 6 H); IR (KBr) 2010, 1935, 1910 cm^{-1}; MS, m/e (relative intensity) 579 (M^+ + 1, 1.4), 75 (100). Anal. Calcd for $C_{20}H_{18}Mo_2O_8$: C, 41.54; H, 3.13. Found: C, 41.36; H, 3.39.

Photolysis of $FvMo_2(CO)_6(CH_3)_2$ (12). An oxygen-free THF or benzene solution (20 mL) of **12** (21 mg, 0.040 mmol) was transferred to a Pyrex flask fitted with a 14/20 outer joint and a Teflon vacuum needle valve. With the valve open the solution was flushed with He gas for 1 h. The valve was closed, and the mixture was irradiated (300 nm) for 2.5 h at room temperature. The flask was connected to a mass spectrometer via the 14/20 outer joint. While the solution was maintained at −78 °C, the Teflon valve was opened to allow gaseous components to enter the instrument. The most intense peak appeared at m/e 16 for methane. Solvent removal from the reaction mixture by rotary evaporation gave a brown residue. Chromatography of the latter (alumina, acetone) afforded $FvMo_2(CO)_6$ (**1**; 12 mg, 62%).

Photolysis of $FvMo_2(CO)_6(CD_3)_2$ (12-d_6) in C_6D_6. Deuterated complex **12**-d_6 was prepared in the same manner as **12** except that CD_3I was used. Photolysis in C_6D_6 (99.8% isotopic purity) was carried out by the procedure described above. The major volatile product was CD_3H; MS, m/e (relative intensity) 20 (1.3), 19 (100), 18 (20), 17 (11), 16 (0.1).

Reaction of $FvMo_2(CO)_6(CH_2OCH_3)_2$ (14) with Tetrafluoroboric Acid Dimethyl Etherate. A solution of **14** (15 mg, 0.026 mmol) in CD_2Cl_2 (0.5 mL, distilled from P_2O_5) was degassed by three freeze–pump–thaw cycles. In an N_2 atmosphere glovebox it was transferred to an NMR tube fitted with a 14/20 outer joint. The tube was stoppered with a rubber septum. With the NMR tube cooled in liquid N_2, a solution of tetrafluoroboric acid dimethyl etherate (28 mg, 0.20 mL) in dry degassed CD_2Cl_2 (0.2 mL) was added by syringe. The tube was sealed under vacuum and transferred to a −78 °C bath. As the reactants mixed, the color changed from brownish yellow to deep red. ^{1}H NMR (200 MHz, CD_2Cl_2) spectra were then acquired between −60 and +20 °C. **15**: δ 15.92 (s, 2 H), 6.20 (m, 2 H), 6.03 (m, 2 H), 5.67 (m, 2 H), 5.59 (m, 2 H), 4.80 (s, 2 H), 3.71 (s, 3 H). **17**: δ 6.38 (m, 2 H), 6.17 (m, 2 H), 5.73 (m, 2 H), 5.42 (m, 2 H), 3.78 (s, 4 H). A red-orange solid precipitated after 2 days at 20 °C. Removal of the solvent by rotary evaporation gave **18** (mp 266–267 °C dec; 14 mg): ^{1}H NMR (250 MHz, acetone-d_6) δ 6.22 (m, 4 H), 5.27 (m, 4 H); IR (KBr) 2010, 1940, 1900 cm^{-1}.

(1-Oxacyclopent-2-ylidene)$FvMo_2(CO)_5$ (20). A THF solution of **10** was prepared from $FvMo_2(CO)_6$ (**1**; 50 mg, 0.10 mmol) and 1,3-diiodopropane (44 mg, 0.15 mmol) in THF (3 mL) added at 20 °C. After 5 h the color had changed from yellow to red. Removal of the solvent by rotary evaporation and chromatography (alumina, acetone–pentane) afforded red crystalline **20** (mp 202–203 °C dec; 48 mg, 90%): ^{1}H NMR (200 MHz, C_6D_6) δ 5.14 (m, 2 H), 4.47 (m, 2 H), 4.00 (m, 2 H), 3.61 (t, J = 7.2 Hz, 2 H), 3.57 (m, 2 H), 3.30 (t, J = 7.6 Hz, 2 H), 1.03 (tt, J = 7.6, 7.2 Hz, 2 H); ^{13}C NMR (45 MHz, C_6D_6) δ 231.6, 97.4, 94.0, 89.4, 85.9, 85.5, 83.3, 80.0, 56.2, 23.1; IR (KBr) 1981, 1916, 1905, 1884, 1849 cm^{-1}; MS, m/e (relative intensity) 530 (M^+, 4), 502 (9), 474 (1), 446 (13), 418 (6), 390 (18), 362 (3), 43 (100). Anal. Calcd for $C_{19}H_{14}Mo_2O_6$: C, 43.04; H, 2.66. Found: C, 43.73; H, 2.84.

X-ray Diffraction Analysis of 20. Large clear red-orange prismatic crystals of the compound were obtained by pentane vapor diffusion into a solution of **20** in acetone. Fragments cleaved from the tips of some of these crystals were mounted on glass fibers by using polycyanoacrylate cement. Preliminary precession photographs indicated triclinic Laue symmetry and yielded approximate reciprocal cell dimensions.

The crystal used for data collection was then transferred to an Enraf-Nonius CAD-4 diffractometer and centered in the beam. Automatic peak search and indexing procedures yielded a triclinic reduced primitive cell. Inspection of the Niggli values revealed the absence of conventional cells of higher symmetry. The final cell and specific data collection parameters are given in Table VI.

The 2411 unique raw intensity data were converted to structure factor amplitudes and their esds by correction for scan speed, background, and Lorentz and polarization effects. No correction for crystal decay was necessary. Inspection of the azimuthal scan data showed a variation I_{min}/I_{max} = 0.87 for the average curve. An absorption correction based on the measured shape and size of the crystal and a 16 × 10 × 6 Gaussian grid of internal points was applied to the data (T_{max} = 0.876, T_{min} = 0.768).

The structure was solved by Patterson methods and refined via standard least-squares and Fourier techniques. The assumption that the space group was the centric $P\bar{1}$ was confirmed by the successful solution and refinement of the structure. The chemical identity of C21 and O6, in the unexpected C_4H_6O ring ligand, was determined by comparison of thermal parameters and residuals for trial structures refined with isotropic thermal parameters. These identities were confirmed by the location of all hydrogen atoms in the structure on a subsequent difference Fourier map. No peaks were observed near O6. Hydrogen atoms were included in the structure factor calculations, but their parameters were not refined in least squares.

The final residuals for 245 variables refined against the 2263 data for which $F^2 > 3\sigma(F^2)$ were R = 1.77%, wR = 3.27%, and GOF = 2.08. The R value for all 2411 data was 1.97%.

The quantity minimized by the least-squares program was $\sum w(|F_o| - |F_c|)^2$, where w is the weight of a given observation. The p factor, used to reduce the weight of intense reflections, was set to 0.025 throughout the refinement. The analytical forms of the scattering factor tables for the neutral atoms were used, and all non-hydrogen scattering factors were corrected for both the real and imaginary components of anomalous dispersion.

Inspection of the residuals ordered in ranges of $(\sin\theta)/\lambda$, $|F_o|$, and parity and value of the individual indexes showed the absence of unusual features or trends. Examination of the high-intensity, low-angle data just prior to the final cycles of least squares revealed indications of secondary extinction. An isotropic extinction parameter was included in the last cycles of refinement.

The largest peak in the final difference Fourier map had an electron density of 0.25 e/Å^3.

The positional and thermal parameters of the refined atoms and a listing of the values of F_o and F_c are available as supplementary material.

(1-Oxacyclohex-2-ylidene)$FvMo_2(CO)_5$ (21). A THF solution of **10** was prepared from $FvMo_2(CO)_6$ (**1**; 300 mg, 0.615 mmol) and 1,4-diiodobutane (97 μL, 0.738 mmol) added by syringe to the reaction mixture at 20 °C. After 1 day the color had turned dark brownish red, and there was a large amount of insoluble material. In an N_2 atmosphere glovebox a sample of the solution was transferred to an infrared liquid cell, which was then closed tightly. The IR spectrum indicated the presence of only **21**. Solvent removal from the reaction mixture by rotary evaporation and chromatography (alumina, acetone–pentane) afforded red crystalline **21** (mp 187–188 °C dec; 29 mg, 7%): ^{1}H NMR (300 MHz, C_6D_6) δ 5.08 (m, 2 H), 4.44 (m, 2 H), 4.04 (m, 2 H), 3.55 (m, 2 H), 3.47 (t, J = 6.1 Hz, 2 H), 3.24 (t, J = 6.9 Hz, 2 H), 1.26 (apparent quintet, J = 6.3 Hz, 2 H), 1.04 (apparent quintet, J = 6.3 Hz, 2 H); IR (THF) 2018, 1987, 1962, 1928, 1908 cm^{-1}; MS, m/e (relative intensity) 544 (M^+, 2), 5.16 (17), 488 (3), 460 (7),

432 (10), 404 (10), 376 (5), 43 (100).

Magnetization Transfer Experiments Applied to 20. A solution of **20** (5 mg) in toluene-d_8 (0.5 mL) was transferred to an NMR tube fitted with a 14/20 joint. The solution was degassed by three freeze–pump–thaw cycles, and then the tube was sealed under vacuum. Samples prepared in this way were used to acquire the variable-temperature spectra (Figure 6) and to carry out the magnetization transfer experiments. The latter employed the presaturation pulse sequence: D3; D4; P2; DE; AT; D5. During D3, a selective decoupling pulse was activated for a variable period of time. The decoupler was turned off at D4, and then the normal sequence for proton observation began. A standard proton pulse P2 was followed by a short delay DE, and then by the acquisition time AT, a final delay D5 was also included.

The theory of magnetization transfer and the methods for calculating rate constants have been discussed elsewhere.[53] In practical terms, magnetization transfer can occur between two exchanging sites A and B; thus, irradiation of the latter will cause a decrease in the intensity of A. When B has been irradiated for a time, t, the magnetization of A, $M^A(t)$, can be defined as the intensity of A expressed as a fraction of the normal intensity of A. The intensities are measured by integrating the signal for A against another signal which is not involved in the exchange process. In the experiments on **20** the fulvalene peak at δ 5.14 was irradiated for a time, t, and the diminished area of the fulvalene peak at δ 4.47 was integrated against the signal at δ 4.00. Measurements were carried out in this way at 20 °C for 15 different values of t. By methods described in the literature,[53] these data were applied to the calculation of a first-order rate constant; at 20 °C $k = 0.22\ s^{-1}$ and $\Delta G^{\ddagger} = 18 \pm 0.5$ kcal mol^{-1}.

Two control experiments were performed to support the results of this study. The selective decoupling frequency used in D3 of the pulse sequence was moved to a point downfield from the peak at δ 5.14 where no signals appear. The frequency difference between this point and the peak at δ 5.14 was the same as that between the latter signal and the peak at δ 4.47. Irradiation at this downfield position did not affect the intensity of the peak at δ 5.14. Thus, there was no artificial saturation of the resonance at δ 4.47 when the peak at δ 5.14 was irradiated. In addition, it was necessary to show that nuclear Overhauser effects were not modifying the intensity of the observed signals. Lowering of the sample temperature should decrease the rate of proton site exchange, but it should not change the degree of NOE enhancement. Thus, at −20 °C all four fulvalene signals were irradiated in succession. In each case there was no change in the intensity of the other signals. Evidently no NOE processes were occurring at −20 °C, and presumably also not at 20 °C.

Thermal Extrusion of Propenes from 20. A solution of **20** (53 mg, 0.10 mmol) in 20 mL of benzene or toluene was added to a flask equipped with a 14/20 outer joint and a Teflon vacuum needle valve. The solution was degassed by three freeze–pump–thaw cycles, and the flask was immersed in a 100 °C oil bath. After 24 h all of the volatile contents were vacuum transferred to a flask fitted with a side-arm stopcock. Gas chromatographic (20% SE30 on Chromosorb WHP, 10 ft × $^1/_4$ in.) analysis of the solution showed the presence of only one major component, which was assigned to propene based on its retention time. To verify this finding, a sample of propene was condensed into the reaction mixture. The GC peak for the major reaction product was found to coincide precisely with the propene peak. The only other gaseous product of the reaction was a trace of ethene which was identified in the same way as propene. Cyclopropane was not detected. In a separate experiment, isobutane (0.10 mmol) was condensed into the reaction mixture in order to provide an internal standard for quantitative analysis of the gaseous products. By comparing the integrated GC peaks for propene and isobutane, the yield of propene was found to be 80%. A correction was applied for the different detector response factors of propene and isobutane.

Chromatography (alumina, acetone) of the nonvolatile material gave $FvMo_2(CO)_6$ (1; 40 mg, 80%) as the only product.

Half-Life of the Thermal Extrusion of Propene from 20. Complex **20** (5.0 mg, 0.010 mmol) and ferrocene (2 mg, 0.010 mmol), which was employed as an internal standard, were dissolved in toluene-d_8 (0.50 mL). The solution (0.020 M) was transferred to an NMR tube attached to a 14/20 outer joint. After it had been degassed by three freeze–pump–thaw cycles, the tube was sealed under vacuum. In an oil bath the tube was heated to 100 °C, and periodically removed and cooled to 20 °C prior to analysis by ^{1}H NMR spectroscopy. The disappearance of **20** proceeded with a half-life of about 12 h.

In a nearly identical experiment, a 0.002 M solution of **20** was heated to 100 °C, and the half-life for disappearance of starting material was found to be about 12 h as in the previous case.

Deuteration of 20 at C-3. Sodium methoxide (1 mg, 0.02 mmol) was added to a solution of **20** (52 mg, 0.10 mmol) in THF (7 mL) and CH_3OD (3 mL). After 5 min the solution was filtered through a short column of alumina which had been partially deactivated with D_2O. The product was eluted with THF. Removal of the solvent by rotary evaporation gave red crystalline **20**-d_2 (52 mg, 100%); ^{1}H NMR (200 MHz, toluene-d_8) δ 5.15 (m, 2 H), 4.49 (m, 2 H), 3.97 (m, 2 H), 3.69 (t, J = 7.2 Hz, 2 H), 3.55 (m, 2 H), 1.10 (t, J = 7.2 Hz, 2 H). Deuterium incorporation in the C-3 position was >98%.

Deuteration of 20 at C-4. A THF solution (5 mL) of **10** prepared from **1** (50 mg, 0.10 mmol) was treated with $ICH_2CD_2CH_2I$[59] (45 mg, 0.15 mmol) as described for the synthesis of **20**. Solvent removal by rotary evaporation and chromatography (alumina, acetone) afforded **20**-d_2 labeled at C-4 (47 mg, 90%); ^{1}H NMR (250 MHz, C_6D_6) δ 5.14 (m, 2 H), 4.47 (m, 2 H), 4.00 (m, 2 H), 3.61 (s, 2 H), 3.57 (m, 2 H), 3.30 (s, 2 H).

Deuteration of 20 at C-5. A THF solution (10 mL) of $Ph_3C^+BF_4^-$ (62 mg, 0.19 mmol) was slowly added to a THF solution (10 mL) of **20** (50 mg, 0.094 mmol) at −78 °C. As the reaction mixture warmed to room temperature the color changed from red to a dark brownish red. Next, a THF solution (5 mL) of $LiAlD_4$ (8 mg, 0.19 mmol) was added to the reaction mixture at −78 °C. The mixture was allowed to warm to 20 °C, and then the solvent was removed by rotary evaporation. Chromatography of the crude product (alumina, acetone–pentane) gave **20**-d_1 labeled at C-5 (16 mg, 32%); ^{1}H NMR (250 MHz, C_6D_6) δ 5.14 (m, 2 H), 4.47 (m, 2 H), 4.00 (m, 2 H), 3.61 (t, J = 7.2 Hz, 1 H), 3.57 (m, 2 H), 3.30 (t, J = 7.6 Hz, 2 H)8 1.03 (dt, J = 7.6, 7.2 Hz, 2 H).

Thermolysis of 20-d_2 Labeled at C-3. A degassed toluene-d_8 solution of **20**-d_2 labeled at C-3 (5 mg, 0.010 mmol) was heated in a sealed ^{1}H NMR tube for 24 h at 100 °C. The NMR tube was placed in a long cylindrical vessel which was fitted with a 14/20 outer joint at the top and a Teflon vacuum needle valve in the middle. The NMR tube was positioned in such a way that it would be broken by an inward movement of the needle valve. With this arrangement in place, the vessel was fitted to a vacuum line through the 14/20 joint. Under high vacuum the NMR tube was broken, and the volatile contents were allowed to condense into another NMR tube which was attached to the vacuum line and cooled in liquid N_2. The tube was then sealed with a flame. Propene-*1,1*-d_2 was the only product observed; ^{1}H NMR (200 MHz, toluene-d_8) δ 5.70 (q, J = 6.4 Hz, 1 H), 1.57 (d, J = 6.4 Hz, 3 H).

Thermolysis of 20-d_2 Labeled at C-4. Thermolysis of **20**-d_2 labeled at C-4 was carried out in the same manner as described above. At 100 °C the reaction was complete within 24 h. Propene-*2,3*-d_2 was the only volatile product; ^{1}H NMR (200 MHz, toluene-d_8) δ 4.90 (m, 1 H), 4.79 (m, 1 H), 1.57 (m, 2 H).

Thermolysis of 20-d_2 Labeled at C-5. Thermolysis of **20**-d_1 labeled at C-5 was carried out in the same manner as described above. Propene-*3*-d_1 was the only volatile product observed; ^{1}H NMR (200 MHz, toluene-d_8) δ 5.70 (m, 1 H), 4.83 (m, 2 H), 1.57 (m, 2 H).

Acknowledgment. This work was supported by the Director, Office of Energy Research, Office of Basic Energy Sciences, Chemical Sciences Division of the U.S. Department of Energy, under Contract DE-AC03-76SF 00098. The crystal structure analyses of **1** and **20** were carried out by Dr. F. J. Hollander, U. C. Berkeley X-ray Crystallographic Facility. K.P.C.V. was a Camille and Henry Dreyfus Teacher-Scholar (1978–1983).

Supplementary Material Available: Tables of positional and thermal parameters and the values for F_o and F_c for **1** and **20** (33 pages). Ordering information is given on any current masthead page.

Syntheses and NMR Spectra of Ruthenium(II) η^5-Dienyl η^6-Arene Compounds. The Crystal and Molecular Structure of Ruthenium(II) η^5-Cyclooctadienyl η^6-*p*-Toluenesulfonate, $Ru(\eta^5\text{-}C_8H_{11})(\eta^6\text{-}C_7H_7SO_3)$

Monika Stebler-Röthlisberger, Albrecht Salzer,[1a] Hans Beat Bürgi,[1b] and Andreas Ludi*

Institut für Anorganische Chemie, Universität Bern, CH-3000 Bern 9, Switzerland

Received May 21, 1985

A series of mixed-sandwich compounds $[Ru^{II}(\eta^5\text{-dienyl})(\eta^6\text{-arene})]^+$ have been prepared in high yield by reacting the tosylate or triflate salt of $[Ru(H_2O)_6]^{2+}$ in ethanol with the corresponding diene in the presence of a suitable arene. Air-stable crystalline yellow compounds have been isolated for dienyl = cyclooctadienyl, $C_8H_{11}^-$, 2,4-dimethylpentadienyl, $C_7H_{11}^-$, and pentamethylcyclopentadienyl, $C_{10}H_{15}^-$, and arene = *p*-toluenesulfonate (tos), benzene, mesitylene, and hexamethylbenzene. The overall molecular geometry of a combination of a η^5-dienyl and η^6-arene fragment agrees with ^1H and ^{13}C NMR spectroscopic data and is verified by the single-crystal X-ray structure of $Ru(C_8H_{11})(tos)$. The compound crystallizes in the monoclinic space group *Cc* with $a = 16.733$ (3) Å, $b = 7.149$ (2) Å, $c = 14.692$ (2) Å, $\beta = 127.38$ (2)°, and $Z = 4$. The structure was refined to 2.0% for 1494 reflections with $F_o > 3\sigma(F_o)$. The neutral molecule has the arene plane of tos at a distance of 1.74 Å and the dienyl plane at 1.534 Å from the ruthenium center. The dihedral angle is 12.4°. Average distances are Ru–C = 2.185 (10) and 2.239 (13) Å and C–C = 1.414 (6) and 1.409 (2) Å for the dienyl and arene fragments, respectively.

Introduction

The impressive progress in organoruthenium chemistry has been achieved by using essentially one single starting reagent, the commercially available "$RuCl_3 \cdot xH_2O$".[2] The seemingly simple standard reagent, however, has some considerable disadvantages: (i) Composition and hence oxidation state of the ruthenium center are not well-defined but may vary from batch to batch. (ii) Since the vast majority of organoruthenium compounds contain either Ru(II) or Ru(0), a reducing step has to be included in the preparative reaction. This is accomplished by adding Zn powder or by employing the organic ligand itself as the reductant. (iii) The inertness of the Ru–Cl bond very often leads to products retaining one or more chloride ligands which are rather difficult to remove. These three properties of "$RuCl_3 \cdot xH_2O$" may act in a cooperative manner to produce the variable and sometimes disappointingly low yields in synthetic organoruthenium chemistry.

Ruthenium complexes containing the ligands cyclooctadiene (COD) or cyclooctatriene (COT) and mixed species with COD or COT and an arene ligand have been studied extensively.[3,4] They are attractive model compounds for studying allylic C–H bond activation processes owing to their facile formation of dienyl species.[4,5] Moreover, the reduced mixed complex $Ru^0COD(arene)$ acts as a hydrogenation catalyst.[6] The molecular structure of the C_8H_{11} moiety of these compounds usually is described as a combination of a η^2- and η^3-bonding mode.[3] Spectroscopic studies are indicative of η^5 bonding in one of the $RuC_{16}H_{22}$ isomers.[5]

Our recent study of the hexaaqua ions of ruthenium opens novel and surprisingly simple and efficient preparative routes for a variety of compounds.[7] The moderate substitution lability of $[Ru(H_2O)_6]^{2+}$ [7c] coupled with the well-known stabilizing effect of typical π-acids for low-spin d^6 ruthenium(II) prompted us to develop syntheses of organometallic compounds using solid $[Ru(H_2O)_6]^{2+}$ salts as starting reagents. Owing to their solubility in convenient nonaqueous solvents the *p*-toluenesulfonate (tosylate, tos) and trifluoromethanesulfonate (triflate, tfl) salts[7b] are best suited for this task. This paper reports the results of our study of the reaction of $[Ru(H_2O)_6]^{2+}$ with dienes in the presence of an arene. Whereas simple acyclic dienes such as 1,3-butadiene polymerize methylated and cyclic dienes, e.g., 2,4-dimethylpentadiene, 1,3-COD, 1,5-COD, and pentamethylcyclopentadiene produce well-defined compounds consisting of an anionic η^5-ligand and a η^6-arene moiety.

Experimental Section

A. Preparation and Characterization of Compounds. All the mixed sandwich-type compounds (cf. Table I) described in this paper are prepared by using either $[Ru(H_2O)_6](tos)_2$ or $[Ru(H_2O)_6](tfl)_2$[7b] in ethanolic solution or in tetrahydrofuran. A mixture of the diene and the arene is added, and the reaction mixture is stirred for several hours at room temperature in a Ar atmosphere. Cooling to −18 °C or concentration by evaporation and addition of ether produces the crude solid compound. Alternatively, the reaction mixture is evaporated to yield an oil which is redissolved in water and extracted with *n*-hexane. Addition of a stoichiometric amount of NH_4PF_6 to the concentrated aqueous phase affords the crude product. Recrystallization of the crude

(1) (a) Institut für Anorganische Chemie, Universität Zürich. (b) Laboratorium für Kristallographie, Universtiät Bern.

(2) (a) Bennett, M. A.; Bruce, M. I.; Matheson, T. W. In "Comprehensive Organometallic Chemistry"; Wilkinson, G., Ed.; Pergamon Press: Oxford, 1982; Vol. 4, pp 691. (b) Seddon, E. A.; Seddon, K. R. "The Chemistry of Ruthenium"; Elsevier: Amsterdam, 1984.

(3) Pertici, P.; Vitulli, G.; Paci, M.; Porri, L. *J. Chem. Soc., Dalton Trans.* **1980**, 1961. Pertici, P.; Vitulli, G.; Lazzaroni, R.; Salvadori, P.; Barili, P. L. *Ibid.* **1982**, 1019.

(4) Bennett, M. A.; Matheson, T. W.; Robertson, G. B.; Smith, A. K.; Tucker, P. A. *Inorg. Chem.* **1981**, *20*, 2353.

(5) Itoh, K.; Nagashima, H.; Ohshima, T.; Oshima, N.; Nishiyama, H. *J. Organomet. Chem.* **1984**, *272*, 179.

(6) Pertici, P.; Vitulli, G.; Bigelli, C.; Lazzaroni, R. *J. Organomet. Chem.* **1984**, *275*, 113.

(7) (a) Bernhard, P.; Lehmann, H.; Ludi, A. *J. Chem. Soc., Chem. Commun.* **1981**, 1216. (b) Bernhard, P.; Bürgi, H. B.; Hauser, J.; Lehmann, H.; Ludi, A. *Inorg. Chem.* **1982**, *21*, 3936. (c) Bernhard, P.; Helm, L.; Rapaport, I.; Ludi, A.; Merbach, A. E. *J. Chem. Soc., Chem. Commun.* **1984**, 302. (d) Bailey, O.; Beck, U.; Stebler, M.; Ludi, A. "Proceedings of the 2nd International Conference on the Chemistry of the Platinum Group Metals, Edinburgh, 1984.

0276-7333/86/2305-0298$01.50/0

Table I. Analytical Data for Ru(η^5-dienyl)(η^6-arene)$^+$ [a]

	C	H	Ru	S	F	P
$Ru(C_8H_{11})(tos)$	47.5	4.75	26.6	8.4		
	47.4	4.75	25.3	8.05		
$Ru(C_8H_{11})(C_6H_6)(tfl)$	41.3	3.94	23.2	7.36	13.1	
	41.3	4.0	22.4	7.5	13.4	
$Ru(C_8H_{11})(mes)PF_6$	43.1	4.9	21.4		24.1	6.5
	43.1	5.0	20.6		24.7	7.6
$Ru(C_8H_{11})(C_6Me_6)PF_6$	46.6	5.7	19.6		22.1	6.0
	46.5	5.7	18.0		21.8	6.0
$Ru(C_7H_{11})(tos)$	45.8	4.9	27.5	8.7		
	45.8	5.1	26.6	8.6		
$Ru(C_7H_{11})(C_6H_6)PF_6$	37.2	4.1	24.1		27.2	
	37.3	4.1	23.1		27	
$Ru(C_7H_{11})(mes)PF_6$	41.7	5.0	21.9		24.7	
	41.7	5.1	20.2		24.6	
$Ru(C_7H_{11})(C_6Me_6)PF_6$	45.3	5.8	20.1		22.6	
	45.3	5.9	19.8		22.2	
$Ru(C_{10}H_{15})(tos)$	50.1	5.4	24.8	7.9		
	50.1	5.5	23.9	7.8		
$Ru(C_{10}H_{15})(C_6H_6)(tfl)$	44.1	4.5	21.8	6.9	12.3	
	44.0	4.5	21.0	6.9	12.3	
$Ru(C_{10}H_{15})(mes)PF_6$	45.5	5.4	20.2		22.7	
	45.6	5.4	19.1		22.4	
$Ru(C_{10}H_{15})(C_6Me_6)PF_6$	48.6	6.1	18.6		21.0	
	46.8	5.7	18.2		21.6	

[a] Upper line = calculated; lower line = found; $C_8H_{11}^-$ = η^5-cyclooctadienyl; mes = mesitylene, 1,3,5-trimethylbenzene; C_7H_{11} = η^5-2,4-dimethylpentadienyl; $C_{10}H_{15}^-$ = η^5-pentamethylcyclopentadienyl.

Table II. Crystal Data, Intensity Collection, and Refinement Procedures for Ru(C_8H_{11})(tos)

formula	$RuC_{15}H_{18}O_3S$
fw	379.2
T, °C	22
space group	Cc
a, Å	16.733 (3)
b, Å	7.149 (2)
c, Å	14.692 (2)
β, deg	127.38 (2)
V, Å^3	1396.6
Z	4
D_{measd}, g cm^{-3}	1.78 (2)
D_{calcd}, g cm^{-3}	1.804
cryst dimens, mm	0.05 × 0.2 × 0.25
linear abs coeff, cm^{-1}	12.5
2θ limits, deg	1–54
scan width, deg	0.85 + 0.4 tan θ
no. of unique refl measd	1520
no. of unique refl with $F_o > 3\sigma(F_o)$	1494
no. of parameters	182
R, %	2.0
R_w, %	2.7
goodness of fit	2.07
final shift/error	<0.01

solids from water yield air-stable, light yellow crystals. The synthesis of Ru(η^5-C_8H_{11})(η^6-tos) as a specific example is described in detail.

Ru(η^5-C_8H_{11})(η^6-tos). A 2.2-g sample of $[Ru(H_2O)_6](tos)_2$ (4 mmol) is dissolved in 120 mL of Ar-saturated absolute ethanol. A 4.8-mL (40 mmol) sample of freshly distilled Ar-saturated 1,3-cyclooctadiene is added dropwise while stirring. The color of the solution changes from pink to bright yellow. Stirring at room temperature is continued for 6 h. Cooling to −18 °C produces a microcrystalline solid, which is filtered and recrystallized from water; yield 85%.

Microanalyses were carried out by CIBA-GEIGY, Basel; Ru was determined spectrophotometrically.[8] The analytical results are collected in Table I.

^{1}H NMR spectra were recorded on Varian XL 200 and Bruker WP 400 instruments and ^{13}C NMR spectra on Varian XL 100 and XL 200 instruments.

(8) Marshall, E. D.; Rickard, R. R. *Anal. Chem.* **1950**, *22*, 795. Woodhead, J. L.; Fletcher, J. M. *J. Chem. Soc.* **1961**, 5039.

Table III. Atomic Coordinates and B Values for Ru(C_8H_{11})(tos)[a]

atom	x	y	z	B, Å^2
Ru	0.000	0.04599 (3)	0.250	1.621 (4)
S	0.19904 (6)	0.2541 (1)	0.25068 (7)	2.56 (2)
O1	0.2781 (2)	0.1666 (5)	0.3581 (3)	3.54 (8)
O2	0.2171 (2)	0.2490 (6)	0.1671 (2)	4.56 (7)
O3	0.1696 (3)	0.4334 (4)	0.2650 (4)	4.6 (1)
C1	0.0927 (2)	0.1027 (6)	0.1912 (3)	1.96 (6)
C2	−0.0056 (2)	0.1712 (5)	0.1088 (3)	2.21 (7)
C3	−0.0879 (3)	0.0493 (5)	0.0610 (3)	2.39 (9)
C4	−0.0759 (2)	−0.1414 (6)	0.0917 (3)	2.50 (8)
C5	0.0233 (2)	−0.2067 (5)	0.1752 (3)	2.41 (7)
C6	0.1060 (2)	−0.0859 (6)	0.2249 (3)	2.19 (7)
C7	−0.1655 (3)	−0.2693 (8)	0.0385 (4)	4.3 (1)
C8	0.1155 (3)	0.1280 (8)	0.4298 (3)	3.25 (9)
C9	0.0611 (3)	−0.0279 (6)	0.4241 (3)	3.0 (1)
C10	−0.0462 (3)	−0.0371 (5)	0.3556 (3)	2.93 (9)
C11	−0.1153 (2)	0.0915 (7)	0.2710 (3)	2.62 (8)
C12	−0.0924 (3)	0.2672 (3)	0.2490 (3)	2.85 (8)
C13	−0.0509 (4)	0.4345 (6)	0.3255 (4)	4.1 (1)
C14	0.0259 (3)	0.3977 (8)	0.4509 (3)	4.1 (1)
C15	0.1210 (4)	0.3212 (9)	0.4748 (4)	4.9 (1)

[a] Anisotropically refined atoms are given in the form of the isotropic equivalent thermal parameter defined as $(^4/_3)$ $[a^2B(1,1) + b^2B(2,2) + c^2B(3,3) + ab(\cos\gamma)[B(1,2) + ac(\cos\beta B(1,3) + bc(\cos\alpha)B(2,3)]$; numbering scheme is given on Table IV.

B. Collection and Reduction of Diffraction Data. Lattice parameters for Ru(C_8H_{11})(tos) were determined by least-squares optimization of 14 accurately centered reflections in the θ range between 11.4 and 17.0° using graphite-monochromatized Mo Kα radiation (λ = 0.71069 Å) and a CAD-4 diffractometer (Table II). The conditions for intensity collection (zigzag mode, h, −17 to +17, k, 0 to 9, l, 0 to 18) and details of the refinement procedures are also summarized in Table II. Three check reflections recorded every 180 min did not show any systematic intensity fluctuations. Lorentz–polarization but no absorption correction was applied, the estimated transmission factors being between 0.78 and 0.9. Neutral-atom scattering factors including anomalous dispersion for the non-hydrogen atoms were used.[9] All calculations employed the structure determination package (SDP, version 18) of En-

(9) Cromer, D. T.; Waber, J. T. "International Tables for X-Ray Crystallography"; Kynoch Press: Birmingham, England, 1974; Vol. IV, Table 2.2B.

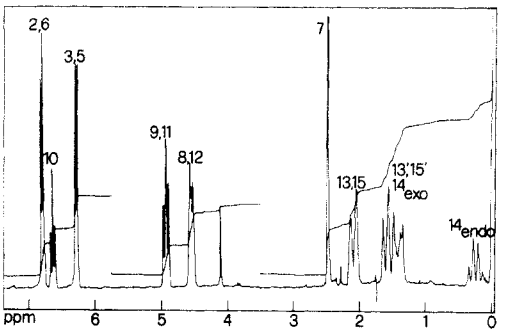

Figure 1. The proton NMR spectrum of $Ru(C_8H_{11})(tos)$ (numbering scheme: cf. Table IV).

raf-Nonius on a PDP 11/34. ORTEP drawings were made by using the XRAY 76 program system on a IBM 3033.

C. Solution and Refinement of the Structure. The structure of $Ru(C_8H_{11})(tos)$ was solved by a straightforward application of Patterson and Fourier methods. The least-squares refinement minimized the function $\sum w(|F_o| - |F_c|)^2$ with $w = 4F_o^2/[(\sigma(I))^2 + (pI)^2]$, $p = 0.02$. An isotropic extinction correction, $F_c/(1 + gI_c)$ ($g = 1.187 \times 10^{-6}$), was introduced after the anisotropic refinement of all of the non-hydrogen atoms. Hydrogen positions were included in the final stages of the refinement process with a fixed C–H distance of 0.95 Å and $B = 5.0$ Å. A final ΔF map showed chemically insignificant residual electron density of about 0.8 e/Å^3 in the vicinity of Ru and less than 0.5 e/Å^3 elsewhere. Atomic coordinates are given in Table III. Listings of structure factors, thermal parameters, hydrogen positions, and least-squares planes are available as supplementary material.

Results

A. ^{1}H and ^{13}C NMR Spectra. The proton and ^{13}C NMR data of the various compounds present the same overall pattern diagnostic of a mixed η^5, η^6-coordination geometry. For each of the four series of complexes Ru(η^5-dienyl)(η^6-arene) with arene = tos, C_6H_6, mesitylene, and hexamethylbenzene and dienyl = cyclooctadienyl, 2,4-dimethylpentadienyl, and pentamethylcyclopentadienyl (cf. Table I) the proton and ^{13}C resonances for the two π-bonded organic molecular fragments show only a very weak mutual dependence.

^{1}H and ^{13}C NMR spectra for the conventional arene ligands benzene, mesitylene, and hexamethylbenzene occurring in our compounds match those of other ruthenium arene complexes[4] and do not require further comment. The corresponding data for two specific species containing tosylate as a η^6-ligand are presented in Table IV. Obviously, NMR data alone are not sufficient to furnish unambiguous evidence for tosylate in a η^6-arrangement. The combination of analytical data, reduction potentials (cf. Discussion) in comparison with those of other ruthenium(II) compounds, and the NMR results together with a rigorous application of the 18-electron rule provides sufficient experimental evidence to conclusively assign the

Table IV. ^{1}H and ^{13}C NMR Spectra (ppm) for $Ru(C_8H_{11})(tos)$ and $Ru(C_7H_{11})(tos)$

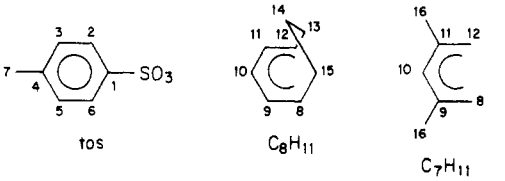

	$Ru(C_8H_{11})(tos)$		$Ru(C_7H_{11})(tos)$	
atom	^{1}H[a]	^{13}C[a]	^{1}H[b]	^{13}C[c]
10	6.63 (t, 6 Hz)	92.5	6.23; s	101.3
9, 11	4.94 (m)	86.0		112.0
8, 12	4.57 (m)	63.8	exo 3.70 (d, 5 Hz) endo 1.24 (d, 5 Hz)	55.8
13, 15	2.1 (m), 1.58 (m)	29.0		
14	exo 1.37 (m) endo 0.24 (m)	19.7		
16			2.11 (s)	27.5
1		unobsd		
2, 6	6.80 (d, 6 Hz)	93.4	6.48 (d, 7 Hz)	90.9
3, 5	6.30 (d, 6 Hz)	109.3	6.12 (d, 7 Hz)	
4		117.7		110.2
7	2.48 (s)	19.5	2.39; s	21.5

[a] Varian XL-200; 22 °C; CF_3COOD. Me_4Si. [b] Bruker AM 400; 22 °C; D_2O; TMSP. [c] Varian XL-100; 22 °C; D_2O; TMSP.

general molecular structure. The most important direct illustration of this bonding arrangement is produced, of course, by the X-ray structure analysis (see next section).

NMR data for the η^5-dienyl ligands are summarized in Table IV. Resolvable multiplets show coupling constants of 5–7 Hz for proton–proton coupling. The observed integrals are fully compatible with the assignments given in Table IV. To a first approximation the ligands cyclooctadienyl and 2,4-dimethylpentadienyl can be considered to contain a mirror plane passing through C10 and the midpoint between C8 and C12. Atoms 8 and 12, 9 and 11, 13 and 15 are thus considered to be equivalent. It is important to note, however, that this equivalence does not imply a corresponding symmetry for the complete molecule. The molecular structure as determined by X-ray crystallography exhibits a staggered conformation. Dynamic behavior in solution may produce the pseudosymmetry reflected in the NMR spectra. The ^{1}H and ^{13}C NMR spectra fully support the assignment of a η^5-dienyl coordination to both molecules. Chemical shift data as well as the integrals (Figure 1) definitely rule out a $\eta^2 + \eta^2$ bonding mode of a neutral cyclooctadiene or pentadiene molecule. One proton of $Ru(C_8H_{11})(arene)$ exhibits an extreme high-field shift to 0.02–0.34 ppm. Looking at the general structure of the cyclooctadienyl ligand (Table IV, Figure 2), we notice that one of the hydrogen atoms attached to C14 lies above the plane defined by the carbon atoms forming Ru–C bonds (C8–C12). This endo proton

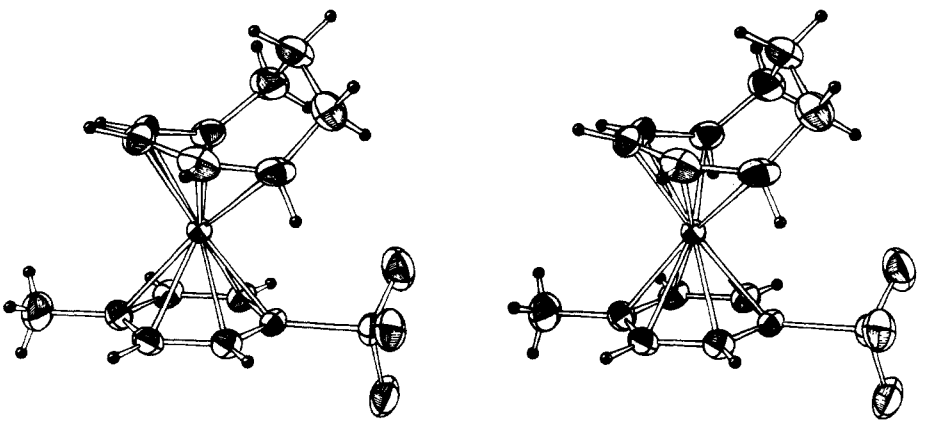

Figure 2. Stereoscopic view of the $Ru(C_8H_{11})(tos)$ molecule.

Table V. Interatomic Distances (Å) and Angles (deg) for $Ru(C_8H_{11})(tos)$[a]

	Bond Distances		
Ru–Cl	2.224 (3)	Ru–C8	2.204 (3)
Ru–C2	2.209 (3)	Ru–C9	2.166 (4)
Ru–C3	2.217 (4)	Ru–C10	2.194 (3)
Ru–C4	2.287 (3)	Ru–C11	2.156 (4)
Ru–C5	2.268 (3)	Ru–C12	2.206 (3)
Ru–C6	2.229 (3)		
C1–C2	1.412 (4)	C8–C9	1.408 (6)
C1–C6	1.406 (5)	C9–C10	1.431 (6)
C2–Cr	1.405 (5)	C10–C11	1.408 (6)
C3–C4	1.412 (5)	C11–C12	1.407 (5)
C4–C5	1.416 (4)	C12–C13	1.493 (4)
C5–C6	1.403 (4)	C13–C14	1.496 (7)
C4–C7	1.508 (4)	C14–C15	1.509 (6)
C1–S	1.792 (3)	C15–C8	1.510 (6)
S–O1	1.448 (3)		
S–O2	1.433 (3)		
S–O3	1.433 (3)		
	Bond Angles		
C1–C2–C3	119.5 (3)	C9–C8–C15	128.0 (4)
C2–C3–C4	122.2 (3)	C8–C9–C10	124.6 (3)
C3–C4–C5	117.4 (3)	C9–C10–C11	126.7 (3)
C4–C5–C6	121.0 (3)	C10–C11–C12	126.4 (3)
C5–C6–C1	120.8 (3)	C11–C12–C13	127.5 (3)
C6–C1–C2	119.2 (3)	C12–C13–C14	116.4 (2)
C3–C4–C7	121.2 (3)	C13–C14–C15	110.3 (3)
C6–C1–S	120.6 (2)	C8–C15–C14	117.0 (3)
C1–S–O1	104.5 (2)		
O1–S–O2	113.3 (2)		

[a] See Table IV for numbering scheme.

thus sits above the π-electron density of the η^5-dienyl group, reasonably explaining the observed significant high-field shift. Signals for the methyl protons of pentamethylcyclopentadienyl show up as singlets between 1.9 and 2.1 ppm for the various combinations with an arene ligand.

B. The Molecular Structure of $Ru(C_8H_{11})(tos)$. The crystal structure of $Ru(C_8H_{11})(tos)$ consists of neutral sandwich molecules with an η^5-$C_8H_{11}^-$ and an η^6-tos^- moiety. The sandwiches are stacked parallel to the *c* axis. If both ligands are considered as six-electron donors and the metal center as a d^6 Ru(II) ion, the title complex obeys the 18-electron rule. The relative arrangement of the two ligands (Figure 2) is best described by the angle between the two planes Ru, C1, C4 and Ru, C10, C14, respectively (cf. Table IV for the numbering scheme). An angle of 0° corresponds to an eclipsed conformation, i.e., a mirror symmetric molecule if the oxygen atoms of the SO_3 group are excluded from consideration. The actual angle is 30.9°, very close to the staggered conformation. Owing to the lack of structural data for analogous compounds, we are not in a position to discuss the observed conformation in terms of electronic effects or in terms of the steric influence exerted by the SO_3 group. The dihedral angle between the two ligand planes of the molecular sandwich is 12.4°, the opened side of the molecule coinciding approximately with the methyl group of the arene (C7).

The interatomic distances and angles collected in Table V demonstrate together with Figure 2 the η^6-coordination for tosylate. To our knowledge $Ru(C_8H_{11})(tos)$ represents the first reported example where the η^6-coordination of tosylate is demonstrated by an X-ray crystal structure. Infrared and NMR data have been used to postulate this bonding mode for tosylate in $RuH(tos)(PPh_3)_2$·THF.[10] A similar example where a fragment of a normally noncoordinating counterion acts as a π-acid has been described for the system Ru^{II}–BPh_4^-.[11] The average Ru–C distance is 2.239 (13) Å, the average C–C distance is 1.409 (1) Å, and the distance between Ru and the center of the ring is 1.740 Å. The benzene ring retains its planar geometry, no carbon atom deviates more than 0.01 Å (C6) from the least-squares plane. The two substituents are nicely coplanar with the ring, the deviations from the plane being only 0.005 and 0.060 Å for the methyl carbon C7 and S, respectively. The small shifts correspond to a bending away from the metal center.

Slightly larger deviations from planarity occur for the C_8H_{11} fragment, where the dienyl plane is defined by C8, C9, C10, C11, and C12. The largest deviation from the plane, 0.043 (5) Å, is observed for C10. The average Ru–C and C–C distances for the η^5-ligand are 2.185 (10) and 1.414 (6) Å, respectively. As in similar compounds (vide infra) the two terminal (C8, C12) and the central (C10) Ru–C bonds are longer than those in between. The metal to plane distance is 1.534 Å. The bond angles at the relevant carbon atoms within the η^5-fragment correspond to a somewhat opened ring. With an average angle of 125.9 (7)° the nonbonded distance C8–C12 is longer than C9–C11, 2.988 (10) vs. 2.539 (11) Å. An interesting structural detail concerns the endo hydrogen atom on C14 which lies above the delocalized π-electron density of the octadienyl ligand. The implication of this special position on the ^1H NMR spectrum has been referred to in the previous section. Closely related distances and angles (Ru–C = 2.226 (24) Å, C–C = 1.412 (3) Å, C–C–C = 127.2 (10)°) for the Ru–η^5-C_8H_{11} moiety have been reported in a recent preliminary communication on $[Ru(\eta^5\text{-}C_8H_{11})(PMe_2Ph)_3]PF_6$.[12] The longer Ru–C distances in the half-sandwich compound may be attributed to the stronger σ-donor properties of the phosphine ligands.

Structurally related compounds comprise, of course, ruthenocene[13] and $Ru(\eta^5\text{-indenyl})_2$[14] together with the pentachloropentadienyl[15] and 2,3,4-trimethylpentadienyl[16] species. The last example, forming an "open ruthenocene", is a particularly suitable point of reference for the discussion of our compound. Complete structural information on corresponding mixed ruthenium(II) sandwich compounds, on the other hand, is rather scarce. Examples are represented by $Ru(C_7H_7)(C_7H_9)$[17] and $Ru(C_8H_9)(mesitylene)^+$.[4] 1,5-COD is easily deprotonated and rearranged to a 1–3:5–6-η-C_8H_{11} anionic species[5,11] combining a η^2-monoene and a η^3-allylic group. This arrangement definitely can be ruled out for $Ru(C_8H_{11})(tos)$, where the structural data comply with a genuine η^5-geometry of the cyclooctadienyl ligand.

With the emphasis on the η^5-moiety of $Ru(C_8H_{11})(tos)$ salient structural features for several similar organoruthenium compounds are collected in Table VI for the purpose of comparison. The rather close range of the geometrical properties for various ligands is clearly indicative of the intimate relationship among these "open ruthenocenes". In particular, the narrow clustering of

(10) Cole-Hamilton, D. J.; Young, R. J.; Wilkinson, G. *J. Chem. Soc., Dalton Trans.* **1976**, 1995.
(11) Ashworth, T. V.; Nolte, M. J.; Reimann, R. H.; Singleton, E. *J. Chem. Soc., Chem. Commun.* **1977**, *937*.
(12) Ashworth, T. V.; Chalmers, A. A.; Liles, D. C.; Meintjies, E.; Oosthuizen, H. E.; Singleton, E. *J. Organomet. Chem.* **1985**, *284*, C19.
(13) (a) Hardgrove, G. L.; Templeton, D. H. *Acta Crystallogr.* **1959**, *12*, 28. (b) Haaland, A.; Nilsson, J. E. *Acta Chem. Scand.* **1968**, *22*, 2653. (c) Seiler, P.; Dunitz, J. D. *Acta Crystallogr., Sect. B: Struct. Crystallogr. Cryst. Chem.* **1980**, *B36*, 2946.
(14) Webb, N. C.; Marsh, R. E. *Acta Crystallogr.* **1967**, *22*, 382.
(15) Brown, F. L.; Hedberg, F. L.; Rosenberg, H. *J. Chem. Soc., Chem. Commun.* **1972**, 5.
(16) Stahl, L.; Ernst, R. D. *Organometallics* **1983**, *2*, 1229.
(17) Schmid, H.; Ziegler, M. L. *Chem. Ber.* **1976**, *109*, 125.

Table VI. Structural Properties of the Ru(η^5-Dienyl) Unit in Ruthenium Sandwich Compounds

	ruthenocene[b]	$Ru(TMP)_2$[c]	$Ru(C_7H_7)(C_7H_9)$[d]	$[Ru(C_8H_9)(mes)]^+$[e]	$Ru(C_8H_{11})(tos)$[f]
Ru–C,[a] Å	2.191 (3)	2.188 (12)	2.187 (9), 2.201 (9)	2.166 (12)	2.185 (10)
C–C,[a] Å	1.441 (4)	1.428 (10)	1.426 (7), 1.422 (5)	1.400 (15)	1.414 (6)
∠CCC,[a] deg	107.7 (15)	122.5 (7)	122.9 (4), 123.4 (20)	125.7 (12)	125.9 (7)
largest deviation of C from least-squares plane, Å		0.053	0.036, 0.066	0.07	0.043
Ru–center of η^5-plane, Å	1.84	1.582	1.595, 1.609	1.54	1.534
dihedral angle between ligand planes, deg	0	18.2	16.9	6.1	12.4
conformation	eclipsed	~eclipsed	~eclipsed	~eclipsed	staggered

[a] average distances and angles; $\sigma(\text{average}) = [\sum^m(\bar{x} - x_i)^2/m(m-1)]^{1/2}$ [b] Reference 13. [c] TMP = 2,3,4-trimethylpentadienyl.[16] [d] Reference 17. [e] mes = mesitylene.[4] [f] This work.

Ru–C, C–C, and Ru–plane distances around 2.19, 1.42, and 1.57 Å, respectively, shows that these data are distinctive features for this class of organoruthenium compounds.

Discussion

1,3-Dienes readily react with $[Ru(H_2O)_6]^{2+}$ in ethanol in the presence of an aromatic molecule according to the general reaction scheme (1). Substituents R are crucial

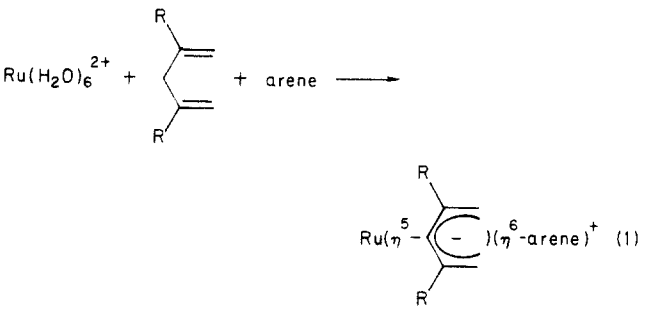

(1)

in the case of acyclic dienes to prevent polymerization which rapidly proceeds for 1,3-butadiene. The mixed-sandwich compounds of ruthenium(II) containing a η^5-dienyl and a η^6-arene fragment are obtained under very mild reaction conditions, e.g., room temperature. Generally, rather satisfactory yields in the 50–90% range are achieved. Whereas the preparative reaction has to be carried out under argon the final products are air-stable and usually can be recrystallized from aqueous solution. The drastic stabilizing effect of the π-bonded organic ligands on Ru(II) is clearly illustrated by the reduction potentials of various complexes.[18] For the hexaaquaruthenium(II/III) couple a value of 0.21 V (vs. NHE) is reported.[7a] In the potential range from −1.5 to +1.5 V (vs. NHE, solvents CH_2Cl_2 and 0.5 M H_2SO_4), we could not observe a wave in the cyclic voltammetry corresponding to a reduction or oxidation for one of the mixed η^5,η^6-compounds.

The efficiency of triflate or tosylate salts of $[Ru(H_2O)_6]^{2+}$ as starting reagents in synthetic procedures is also illustrated by employing cyclopentadiene as the diene and by omitting the arene altogether in the above equation. The reaction proceeds even at 0 °C to produce crystalline ruthenocene with a yield of 80% and the pentamethyl analogue with a yield of 55%, for the latter a yield superior to previously published procedures.[19]

In the case of cyclooctadiene identical products are obtained with both isomers, 1,3-COD and 1,5-COD. When the reaction is monitored in the NMR spectrometer, an isomerization of the 1,5 to the 1,3 form is observed prior to the reaction with the ruthenium aqua ion. With use of the general reaction procedure, the final products invariably are a combination of the η^5-dienyl ligand and a η^6-arene moiety.

The tosylate anion is one of the convenient "hard" innocent counterions specifically employed in preparative chemistry owing to its reluctance to enter the first coordination shell of a transition-metal ion. For that reason it could be applied with success to isolate crystalline salts of the ruthenium aqua ions.[7b] It is thus quite remarkable how smoothly this inert and generally noninterfering anion adapts to the function of a "soft" η^6-ligand within an organometallic molecule.

It is obvious from the general reaction stoichiometry that a C–H cleavage must occur to produce the dienyl anion from the original diene. We assume a disproportionation reaction of the diene to be a crucial step since we observed the formation of cyclooctene in the reaction mixture. In conclusion we notice that the very facile deprotonation of a diene is a characteristic property of the reaction $Ru(H_2O)_6^{2+}$ + diene, the nature of the final product depending on the particular choice of the diolefin. Cyclopentadienes produce in very good yield ruthenocene and its derivatives; 1,3- or 1,4-cyclohexadienes afford the interesting link between classical coordination complexes and ruthenium organic compounds, $Ru(\eta^6\text{-}C_6H_6)(H_2O)_3^{2+}$.[7d] Cyclooctadienes in the presence of an arene produce the mixed species $Ru(\eta^5\text{-}C_8H_{11})(\eta^6\text{-arene})^+$. Without an aromatic partner the ion $Ru(\eta^5\text{-}C_8H_{11})(\eta^6\text{-cyclooctatriene})^+$ is obtained. The 18-electron rule is fulfilled regardless of the starting combination of dienes. No detailed information can be given so far concerning a plausible reaction mechanism. We assume the first step to be a substitution of one water ligand by one of the olefinic bonds of the diene with the subsequent rearrangement of the organic molecule and further replacements of the water molecules.

In conclusion, we notice that a considerable variety of ruthenium dienyl compounds can be prepared by a remarkably facile route from the aqua ion. All of these reactions proceed under very mild conditions with encouraging yields generally in the 50–90% range. Solid $Ru(H_2O)_6^{2+}$ salts thus compare favorably with "$RuCl_3 \cdot xH_2O$", the standard starting reagent which often leads to low and badly reproducible yields. A disadvantage of the reported syntheses, however, is the preparation of $Ru(H_2O)_6^{2+}$ involving the distillation of the highly toxic RuO_4.[7b]

Acknowledgment. We thank CIBA-GEIGY AG, Basel, for the microanalyses, Dr. P. Bigler for some NMR measurements and helpful discussions, and one of the reviewers for bringing ref 12 to our attention. This work was supported by the Swiss National Science Foundation (Grant No. 2.209–0.81).

Supplementary Material Available: Listings of observed and calculated structure factors, anisotropic thermal parameters, hydrogen positions, and least-squares planes (10 pages). Ordering information is given on any current masthead page.

(18) Lehmann, H.; Schenk, K. J.; Chapuis, G.; Ludi, A. *J. Am. Chem. Soc.* **1979**, *101*, 6197.
(19) (a) Koelle, U.; Salzer, A. *J. Organomet. Chem.* **1983**, *243*, C27. Tilley, T. D.; Grubbs, R. H.; Bercaw, J. E. *Organometallics* **1984**, *3*, 274.

Synthesis and Characterization of Mixed-Ligand Cyclopentadienyl–Pyrazolylborate Complexes of Ruthenium

Amy M. McNair, David C. Boyd, and Kent R. Mann*

Department of Chemistry, University of Minnesota, Minneapolis, Minnesota 55455

Received May 20, 1985

Neutral compounds of Ru(II) that contain a cyclopentadienyl and a pyrazolylborate ligand were synthesized from $[CpRu(CH_3CN)_3]PF_6$ and $[Cp^*Ru(CH_3CN)_3]PF_6$ (Cp^- = η^5-cyclopentadienyl; Cp^{*-} = η^5-pentamethylcyclopentadienyl). $[CpRu(HBpz_3)]$, $[CpRuHB(3,5\text{-}Me_2pz)_3]$, $[CpRuBpz_4]$, and $[Cp^*Ru(HBpz_3)]$ were characterized spectroscopically. An X-ray crystallographic study of $[CpRu(HBpz_3)]$ was completed. $CpRu(HBpz_3)$ crystallizes in the $P2_1/m$ space group with $Z = 2$, $V = 749.8$ Å^3, $a = 9.0854$ (4) Å, $b = 10.074$ (4) Å, $c = 8.195$ (2) Å, and $\beta = 91.50$ (3)°. Full-matrix least-squares refinement (112 variables, 2290 reflections) converged to give R and R_w values of 0.043 and 0.052, respectively. The structure consists of discrete (η^5-Cp)Ru($HBpz_3$) units with Ru–C bonds of 2.153 (3) Å and Ru–N bonds of 2.128 (3) Å. Electrochemical measurements for the series of compounds were carried out for comparison with ferrocene and ruthenocene. The compounds exhibit a quasi-reversible, one-electron oxidation that falls in the range 0.145–0.463 V vs. Ag/AgCl. Oxidation of $CpRuHB(3,5\text{-}Me_2pz)_3$ with $AgPF_6$ allowed the isolation of $[CpRuHB(3,5\text{-}Me_2pz)_3]PF_6$. The thermal reactivity of these compounds allowed the synthesis of the new complexes $[CpRuHB(3,5\text{-}Me_2pz)_3(CO)]$, $[CpRuBpz_4(CO)]$, and $[Cp_2Ru_2(CO)_2Bpz_4]PF_6$ that exhibit bidentate coordination of pyrazolylborate ligands to ruthenium. While the CpRu pyrazolylborate complexes are formally similar to ruthenocene, the replacement of cyclopentadienyl with a pyrazolylborate ligand significantly alters the chemistry of these new compounds.

Introduction

Since the discovery in 1966 of the pyrazolylborate ligands by Trofimenko,[1] an extensive transition-metal chemistry that utilizes these ligands has emerged. Most of the studies have been with first-row transition metals[2–6] or molybdenum. An initial attraction of the tridentate pyrazolylborate ligands was their apparent similarity in coordination and electronic structure to the cyclopentadienyl ligand. Much of the chemistry developed with these ligands has involved compounds whose cyclopentadienyl analogues were well established. Despite these similarities, there were for many years no reports of mixed-ligand complexes containing a pyrazolylborate ligand and an arene or cyclopentadienyl ligand.[3,4] To date, only a limited number of cyclopentadienyl pyrazolylborate compounds and no neutral ferrocene analogue have been reported.[7,8] Previous attempts, as well as our own attempt (vide infra) to synthesize the mixed-ligand iron compound, were unsuccessful.

We previously reported the successful use of the compounds $[CpRu(CH_3CN)_3]PF_6$ and $[Cp^*Ru(CH_3CN)_3]PF_6$ in a variety of synthetic reactions to introduce the $CpRu^{II}$ moiety into new complexes.[9–11] These compounds proved viable reagents for the synthesis of the pyrazolylborate–cyclopentadienyl mixed-ligand analogues of ruthenocene. We report here the synthesis, characterization, and reaction chemistry of neutral mixed-ligand compounds of Ru(II) that contain cyclopentadienyl or pentamethylcyclopentadienyl and a pyrazolylborate ligand. The following pyrazolylborate-containing compounds were prepared: $[CpRuHBpz_3]$, $[CpRuHB(3,5\text{-}Me_2pz)_3]$, $[CpRuBPz_4]$, and $[Cp^*RuHB(3,5\text{-}Me_2pz)_3]$, where Cp^- = cyclopentadienyl anion, Cp^{*-} = pentamethylcyclopentadienyl anion, $HBpz_3^-$ = hydrotris(1-pyrazolyl)borate, $HB(3,5\text{-}Me_2pz)_3^-$ = hydrotris(3,5-dimethyl-1-pyrazolyl)borate, and BPz_4^- = tetrakis(1-pyrazolyl)borate.

Experimental Section

General Considerations. All synthetic procedures were carried out under an inert N_2 atmosphere. Solvents used were of spectroscopic grade and were used without further purification. Potassium pyrazolylborates were purchased from Columbia Organic Chemicals Co. ^{1}H NMR spectra were recorded on a Varian Associates CFT 20 NMR spectrometer equipped with a 79.5-MHz proton accessory. Chemical shifts, δ, are relative to Me_4Si. The high-field ^{1}H NMR spectra and all ^{31}P NMR spectra were recorded on a Nicolet NT 300-MHz instrument. The ^{31}P spectra are reported in units of δ and are referenced to a 85% orthophosphoric acid external standard. IR spectra were recorded on a Perkin-Elmer 297. UV–vis spectra were recorded on a Hewlett-Packard 8450A diode array spectrophotometer. Elemental analyses were performed by MHW laboratories except for $[Cp^*RuHBpz_3]$ and $[CpRuHB(pz(CH_3)_2)_3]PF_1$ which were analyzed by Galbraith Laboratories. The syntheses of the starting materials $[CpRu(CH_3CN)_3]PF_6$ and $[Cp^*Ru(CH_3CN)_3]PF_6$ have been previously reported.[9]

Synthesis of Compounds. $[CpRuHBpz_3]$. A solution of 48.4 mg (0.192 mmol) of $KHBpz_3$ in approximately 20 mL of acetonitrile was purged with nitrogen. To this solution was added 86.5 mg (0.199 mmol) of $[CpRu(CH_3CN)_3]PF_6$. The solution was refluxed for 1.5 h, and the solvent was then removed by rotary evaporation. The resultant residue was extracted into diethyl ether and filtered through a Milli-pore filter. The solvent was removed to yield 60.3 mg of pure $[CpRuHBpz_3]$ as a yellow microcrystalline product (83% yield based on $KHBpz_3$): mp 244–246 °C with decomposition; ^{1}H NMR δ 4.271 (s, Cp, 5 H), 6.146 (d of d, H^4, 3 H, J = 2.11 Hz), 7.629 (d, H^3, 3 H, J = 2.26 Hz), 8.123 (d, H^5, 3 H, J = 1.56 Hz). Anal. Calcd for $C_{14}H_{15}N_6RuB$: C, 44.35; H, 3.99; N, 22.16. Found: C, 44.47; H, 4.19; N, 22.24.

(1) Trofimenko, S. *J. Am. Chem. Soc.* **1966**, *88*, 1842.
(2) Trofimenko, S. *J. Am. Chem. Soc.* **1967**, *89*, 3904.
(3) Trofimenko, S. *J. Am. Chem. Soc.* **1969**, *91*, 588.
(4) Trofimenko, S. *Acc. Chem. Res.* **1971**, *4*, 17.
(5) Trofimenko, S. *Chem. Rev.* **1972**, *72*, 497.
(6) Shaver, A. *Organomet. Chem. Rev.* **1977**, *3*, 157.
(7) O'Sullivan, D. J.; Lalor, F. J. *J. Organomet. Chem.* **1973**, *57*, C58.
(8) Manzer, L. E. *J. Organomet. Chem.* **1975**, *102*, 167.
(9) Gill, T. P.; Mann, K. R. *Organometallics* **1982**, *1*, 485.
(10) McNair, A. M.; Schrenk, J. L.; Mann, K. R. *Inorg. Chem.* **1984**, *23*, 2633.
(11) $[Cp^*Ru(CH_3CN)_3]PF_6$ is synthesized by photolysis of $[Cp^*Ru(\eta^6\text{-}C_6H_6)]PF_6$ in acetonitrile. $[Cp^*Ru(\eta^6\text{-}C_6H_6)]PF_6$ is obtained in low yield following the procedure of Zelonka and Baird, substituting LiCp* for TlCp. Work to improve this procedure is currently in progress in our laboratory.
(12) The spectral assignments of the pyrazolylborate ligands are based on those of: Trofimenko, S. *J. Am. Chem. Soc.* **1967**, *89*, 3170.

0276-7333/86/2305-0303$01.50/0

[CpRuBpz$_4$]. [CpRu(CH$_3$CN)$_3$]PF$_6$ (78.9 mg, 0.182 mmol) was added to a solution of KBpz$_4$ (57.7 mg, 0.181 mmol) in 20 mL of acetonitrile under nitrogen. The solution was refluxed for 2 h, and the solvent was removed. The resultant residue was dissolved in diethyl ether and the excess [CpRu(CH$_3$CN)$_3$]PF$_6$ and KPF$_6$ were filtered off with a Milli-pore filter. After evaporation of the solvent, 65.2 mg of dark yellow [CpRuBpz$_4$] was recovered (81% yield based on KBpz$_4$): mp 244–246 °C with decomposition; ^{1}H NMR δ 4.346 (s, CP, 5 H), 6.180 (unresolved d of d, bound H^4, 3 H), 6.587 (unresolved d of d, unbound H^4, 1 H), 7.638 (d, bound H^3, 3 H, J = 2.41 Hz), 7.861 (apparent s, unbound H^5, 1 H), 8.025 (d, unbound H^3, 1 H, J = 2.29 Hz), 8.256 (d, bound H^5, 3 H, J = 0.98 Hz). Anal. Calcd for C$_{17}$H$_{17}$N$_8$RuB: C, 45.86; H, 3.85; N, 25.17. Found: C, 45.74; H, 4.00; N, 25.00.

[CpRuHB(3,5-Me$_2$pz)$_3$]. A solution of 48.4 mg (0.192 mmol) of KHB(3,5-Me$_2$pz)$_3$ in approximately 20 mL of acetonitrile was prepared and degassed by bubbling nitrogen through the sample for 20 min. To this solution was added 86.5 mg (0.199 mmol) of [CpRu(CH$_3$CN)$_3$]$^+$, and the solution was refluxed for 1.5 h. The solvent was removed and the product extracted into diethyl ether and filtered by using a Milli-pore filter to remove unreacted starting material and KPF$_6$. After the solvent was removed, 60.3 mg of bright yellow [CpRuHB(3,5-Me$_2$pz)$_3$] was recovered (82.8% yield based on KHB(3,5-Me$_2$pz)$_3$): mp 259–261 °C; ^{1}H NMR δ 4.571 (s, Cp, 5 H); 5.758 (s, H^4, 3 H), 2.366 (s, CH$_3$, 9 H), 2.276 (s, CH$_3$, 9 H). Anal. Calcd for C$_{20}$H$_{27}$N$_6$RuB: C, 51.85; H, 5.87; N, 18.14. Found: C, 51.97; H, 5.96; N, 18.33.

[Cp*RuHBpz$_3$]. A 67.0-mg (0.172-mmol) sample of [Cp*Ru(C$_6$H$_6$)]PF$_6$ was photolyzed in degassed acetonitrile for 25 h to convert it to [Cp*Ru(CH$_3$CN)$_3$]PF$_6$. The acetonitrile was removed under vacuum and the product washed with ether. To this product was added a degassed acetonitrile solution containing 36.0 mg (0.143 mmol) of KHBpz$_3$. The mixture was allowed to react at room temperature overnight. After the reaction was judged complete, the solvent was again removed and the product extracted into ether while a nitrogen atmosphere was maintained. After removal of the ether, 42.1 mg (64% yield) of [Cp*RuHBpz$_3$] was recovered as a yellow powder: ^{1}H NMR δ 8.07 (d, H, 3 H), 7.65 (d, H, 3 H), 6.24 (d of d, H, 3 H), 1.73 (s, Cp*, 15 H). Anal. Calcd for C$_{19}$H$_{25}$N$_6$RuB: C, 50.79; H, 5.61; N, 18.70. Found: C, 50.78; H, 5.53; N, 18.53.

[CpRuHB(3,5-Me$_2$pz)$_3$]PF$_6$. A solution of 98.6 mg (0.218 mmol) of [CpRuHB(3,5-Me$_2$pz)$_3$] in 20 mL of acetonitrile was bubbled with dry N$_2$ for 30 min. An acetonitrile solution of 51.8 mg (0.205 mmol) of AgPF$_6$ in 10 mL was added by cannula to this solution. The solution changed color immediately from yellow to deep burgundy and a fine white precipitate of AgCl formed. The solution was left to stir for approximately 30 min and was then filtered under nitrogen through a Milli-pore filter attached to a degassed syringe. The resultant solution was pumped to dryness on a vacuum line. The solid was washed repeatedly with ether to remove the excess [CpRuHB(3,5-Me$_2$pz)$_3$]. The red solid was redissolved in acetonitrile and the solution filtered again, and then the solvent was removed in the same manner as before. The product was isolated under nitrogen to yield 68.9 mg (55.3% yield) of maroon [CpRuHB(3,5-Me$_2$pz)$_3$]PF$_6$. Anal. Calcd for C$_{20}$H$_{27}$N$_6$RuBPF$_6$: C, 39.49; H, 4.47; N, 13.81. Found: C, 39.32; H, 4.58; N, 13.69.

[CpRuHB(3,5-Me$_2$pz)$_3$(CO)]. A sample of 55.9 mg (0.121 mmol) was dissolved in 30 mL of acetonitrile, and CO was bubbled through the solution for 1.5 h. During this time the color of the solution changed from deep golden yellow to pale yellow. The solution was rotovapped to dryness, and 52.0 mg (88% yield) of pale yellow [CpRuHB(3,5-Me$_2$pz)$_3$(CO)] was recovered: ^{1}H NMR δ 4.573 (s, Cp, 5 H), 6.000 (s, bound H^4, 1 H), 5.728 (s, unbound H^4, 1 H), 2.410 (s, bound CH$_3$, 6 H), 2.227 (s, bound CH$_3$, 6 H), 2.135 (s, unbound CH$_3$, 3 H), 1.393 (s, unbound CH$_3$, 3 H); IR data (fluorolube mull) $\bar{\nu}$(CO) 1940, 1955 cm^{-1}, $\bar{\nu}$(B–H) 2490 cm^{-1}. Anal. Calcd for C$_{19}$H$_{25}$N$_6$BRu: C, 50.70; H, 5.61; N, 18.70. Found: C, 50.78; H, 5.53; N, 18.53.

[CpRu(Bpz$_4$)(CO)]. This compound was prepared in the same manner as above with 20 mg of [CpRuBpz$_4$] used, and 19.0 mg of the product was formed (89% yield): ^{1}H NMR δ 4.73 (s, Cp, 5 H), 7.87 (d, bound pz, 2 H), 7.71 (d, unbound pz, 1 H), 7.65 (d, unbound pz, 1 H), 7.15 (d, bound pz, 2 H), 6.77 (d, unbound pz, 1 H), 6.59 (d, unbound pz, 1 H), 6.40 (d of d, bound pz, 2 H), 6.35 (d of d, unbound pz$_4$, 1 H), 6.24 (d of d, unbound pz, 1 H); IR data $\bar{\nu}$(CO) 1950, 1963 cm^{-1}.

[(Cp)$_2$(CO)$_2$Ru$_2$Bpz$_4$]PF$_6$. To a degassed flask containing 57.4 mg (0.121 mmol) of [CpRuBpz$_4$(CO)] and 49.5 mg (0.118 mmol) of [CpRu(CH$_3$CN)$_2$(CO)]PF$_6$ was added approximately 30 mL of degassed ClCH$_2$CH$_2$Cl. While the solution was gently refluxed for 17 h, its color changed from golden yellow to brown yellow. After removal of the solvent, the brown oil was washed repeatedly with ether to remove excess [CpRuBpz$_4$(CO)]. The oil was then eluted through a short alumina column with methylene chloride to yield a bright yellow solution. The solvent volume was reduced, and a yellow powder was isolated after the addition of ether. A yield of 80.3 mg of [(Cp)$_2$(CO)$_2$Ru$_2$Bpz$_4$]PF$_6$ was obtained (84% based on [CpRu(CH$_3$CN)$_2$(CO)]PF$_6$): ^{1}H NMR δ 5.315 (s, Cp, 10 H), 8.142 (d, pz, 2 H), 8.013 (d, pz, 2 H), 7.817 (d, pz, 2 H), 7.119 (d, pz, 2 H), 6.644 (d of d, pz, 2 H), 6.542 (d, of d, pz, 2 H); IR data $\bar{\nu}$(CO) 1975 cm^{-1}. Anal. Calcd for C$_{24}$H$_{22}$N$_8$O$_2$Ru$_2$BPF$_6$: C, 35.48; H, 2.73; N, 13.79. Found: C, 36.45; H, 3.23; N, 13.76.

[CpRuHBpz$_3$(P(OCH$_3$)$_3$)] and [CpRuHB(3,5-Me$_2$pz)$_3$(P(OCH$_3$)$_3$)]. These two compounds were prepared by reaction of the parent pyrazolylborate compounds, [CpRuHBpz$_3$] and [CpRuHB(3,5-Me$_2$pz)$_3$], respectively, with an excess of P(OCH$_3$)$_3$ in either acetonitrile or methylene chloride. The solutions changed in color from a deep golden yellow to pale yellow. These compounds were isolated as oily solids contaminated with excess phosphite which could not be removed.

[CpRuHBpz$_3$(P(OCH$_3$)$_3$)]: ^{1}H NMR δ 4.18 (d, Cp, 5 H, J = 0.9 Hz), 8.00 (d, bound pz, 2 H), 7.78 (d, bound pz, 2 H), 7.41 (d, unbound pz, 1 H), 6.53 (d, unbound pz, 1 H), 6.39 (d of d, bound pz, 2 H), 6.14 (d of d, unbound pz, 1 H), 3.18 (d, P(OCH$_3$)$_3$, 9 H, J = 11.2 Hz); ^{31}P NMR δ 159.228 (s).

[CpRuHB(3,5-Me$_2$pz)$_3$(P(OCH$_3$)$_3$)]: ^{1}H NMR δ 4.16 (d, Cp, 5 H, J = 1.2 Hz), 5.98 (s, bound pz, 2 H), 5.62 (s, unbound pz, 1 H), 2.39 (s, bound CH$_3$, 6 H), 2.19 (s, bound CH$_3$, 6 H), 2.10 (s, unbound CH$_3$, 3 H), 1.32 (s, unbound CH$_3$, 3 H), 3.18 (d, P(OCH$_3$)$_3$, 9 H, J = 10.6 Hz); ^{31}P NMR δ 153.373 (s).

Attempted Synthesis of [CpRuH$_2$Bpz$_2$(P(OCH$_3$)$_3$)]. Reaction of [CpRu(CH$_3$CN)$_2$(P(OCH$_3$)$_3$)]PF$_6$ with slightly more than 1 equiv of KH$_2$Bpz$_2$ under nitrogen resulted in the expected appearance of finely divided KPF$_6$ and a gold colored solution. All attempts to isolate a product from these solutions failed.

Attempted Synthesis of [CpFeHBpz$_3$] and [CpFeHB(3,5-Me$_2$pz)$_3$]. Three unsuccessful attempts were made to synthesize mixed pyrazolylborate–cyclopentadienyl compounds of iron. Two attempts followed the general reaction scheme which successfully produced the ruthenium species. Samples of [CpFe(η^6-toluene)PF$_6$ were photolyzed at −40 °C to produce purple [CpFe(CH$_3$CN)$_3$]PF$_6$. A cold solution (−40 °C) of either KHBpz$_3$ or KHB(3,5-Me$_2$pz)$_3$ was then added with stirring. In both instances, when the solution was allowed to slowly warm, the color of the solution changed from purple to brown and an insoluble pink precipitate formed before reaching room temperature. In the third attempt, photolysis of the [CpFe(η^6-toluene]PF$_6$ at low temperature in the presence of KHB(3,5-Me$_2$pz)$_3$ gave results similar to the two previous attempts. Analysis of the materials formed in all of these reactions reveals them to be ferrocene and the known bis(pyrazolylborato)iron species.

Electrochemical Measurements. All electrochemical experiments were performed with a BAS 100 electrochemical analyzer. Electrochemical measurements were performed at 20 ± 2 °C with a normal three-electrode configuration consisting of a highly polished glassy-carbon-disk working electrode and a Ag/AgCl reference electrode containing 1.0 M KCl. The working compartment of the electrochemical cell was separated from the reference compartment by a modified Luggin capillary. All three compartments contained a 0.1 M solution of the supporting electrolyte. Bulk electrolyses were performed by substituting a Pt mesh electrode for the glassy carbon electrode in the cell outlined above. The acetonitrile, dichloromethane (Burdick and Jackson), and supporting electrolyte tetrabutylammonium hexafluorophosphate (TBAH) were used without further purification.

Electrolyte solutions were prepared and stored over 80–200 mesh activated alumina (Fisher Scientific Co.) prior to use in the experiments. In all cases working solutions were prepared by recording background cyclic voltammograms of 30.0 mL of the electrolyte solution before addition of the depolarizer. The

Table I. Crystal Data and Collection Parameters

compound	[CpRuHBpz$_3$]
formula	$C_{14}H_{15}N_6BRu$
fw	379.212
space group	$p2_1/m$, no. 11
a, Å	9.085 (4)
b, Å	10.074 (4)
c, Å	8.195 (2)
β, deg	91.50 (3)
V, Å^3	749.8 (10)
Z	2
d(calcd), gcm^{-3}	1.680
cryst size, mm	0.25 × 0.30 × 0.20
μ, cm^{-1}	10.292
radian (graphite monochromated)	Mo (λ = 0.710 73 Å)
scan type	ω–2θ
collectn range	2θ = 0-64
no. of unique data	2878
no. of data for $F^2 > \sigma(F^2)$	2290
P	0.05
no. of variables	112
R	0.043
R_w	0.052

working compartment of the cell was bubbled with solvent-saturated argon to dearate the solution.

Magnetic Susceptibility Measurements. Magnetic susceptibility measurements were performed on a solid sample of [CpRuHB(3,5-Me$_2$pz)$_3$]PF$_6$ using the Faraday method. HgCo(SCN)$_4$ was used as a calibrant with a $\chi_g = 16.28 \times 10^{-6}$/g at 24 °C. Weight changes were measured at two different field strengths for both the oxidized material [CpRuHB(3,5-Me$_2$pz)$_3$]PF$_6$ and the unoxidized parent compound [CpRuHB(3,5-Me$_2$pz)$_3$]. The values of χ_m obtained for the unoxidized material were then used as the diamagnetic correction after additional corrections for the PF_6^- anion. The χ_m for [CpRuHB(3,5-Me$_2$pz)$_3$] was found to be -166.2×10^{-6} cgs/mol. The χ_m^{corr} for the oxidized [CpRuHB(3,5-Me$_2$pz)$_3$]PF$_6$ was $+1565 \times 10^{-6}$ cgs/mol giving μ_{eff}(24 °C) = 1.95 μ_B.

Photochemical Equipment. All photochemical experiments were carried out under a nitrogen atmosphere using a modified medium-pressure mercury vapor street lamp as the light source. All experiments which were monitored by ^{1}H NMR were carried out in standard glass NMR tubes equipped with serum stoppers. Dark reaction blanks were run concurrently with the photochemical experiments to correct for possible thermal reactions.

Collection and Reduction of the Crystallographic Data. Crystals of [CpRuHBpz$_3$] were obtained by evaporation of a saturated hot ethanol solution of the compound over a period of 2 days. The crystal selected was a well-formed prism of approximate dimensions 0.25 × 0.30 × 0.20 mm. The automatic peak searching, centering, and indexing routines available on the Enraf-Nonius SDP-CAD4 automatic diffractometer[13] were used to find and center the reflections which were used to define the unit cell constants. The space group $P2_1/m$ was assigned by examining the data for systematic absences and was subsequently successfully employed in solving and refining the structure. Crystal data are given in Table I. The calculated density, for Z = 2, is 1.680 g cm^{-3}. A total of 2878 independent reflections were collected in the scan range 2θ = 0–64° with use of graphite-monochromatized Mo Kα radiation by employing the ω–2θ technique. Crystal decomposition was monitored by three check reflections collected every 75 reflections. A linear correction was made for the 4% decrease observed for the check reflections during data collection. After data processing and reduction,[14] 2290 reflections for which $F_o^2 > \sigma(F_o^2)$ were used in the structure solution and refinement. An empirical correction was made for absorption (μ = 10.292 cm^{-1}).

Table II. Positional Parameters and Their Estimated Standard Deviations

atom	x	y	z
Ru	0.02610 (4)	0.250	0.15467 (4)
N1A	0.1314 (4)	0.250	−0.0733 (5)
N2A	0.2816 (4)	0.250	−0.0809 (5)
C3A	0.3189 (6)	0.250	−0.2389 (7)
C4A	0.1946 (7)	0.250	−0.3351 (7)
C5A	0.0799 (6)	0.250	−0.2263 (6)
N1B	0.1930 (3)	0.1114 (3)	0.2264 (3)
N2B	0.3345 (3)	0.1273 (3)	0.1787 (4)
C3B	0.4202 (4)	0.0352 (4)	0.2521 (5)
C4B	0.3355 (4)	−0.0432 (4)	0.3479 (5)
C5B	0.1937 (4)	0.0084 (3)	0.3281 (4)
B	0.3749 (5)	0.250	0.0767 (8)
C1P	−0.1394 (6)	0.250	0.3407 (8)
C2P	−0.1581 (4)	0.1374 (5)	0.2392 (5)
C3P	−0.1858 (4)	0.1769 (5)	0.0747 (5)
C4P	−0.191 (2)	0.2550	0.047 (3)
C5P	−0.173 (1)	0.137 (2)	0.148 (2)
C6P	−0.145 (1)	0.177 (2)	0.313 (2)

The structure was solved from the three-dimensional Patterson function which allowed placement of the Ru atom. Fourier and difference Fourier analyses in conjunction with cycles of least-squares refinement[15] allowed the placement of the remaining atoms, excluding the hydrogens.

The cyclopentadienyl ring was found to be disordered with respect to a 180° rotation about the plane normal. The additional atoms were placed at their idealized positions with fixed isotropic temperature factors. The ring carbons were then refined to yield 76%–24% occupancy factors. Then the occupancy factors were fixed and all the 76% ring carbons were refined anisotropically. The 24% ring carbon parameters were readjusted to be those directly related to the 76% carbon parameters. Only the 76% occupied carbons are used in discussions about the structure in the text.

Full-matrix least-squares refinement (112 variables) utilized anisotropic temperature factors for Ru, C, N, and B. The hydrogens were placed at idealized positions with B = 5.0 Å^2. Convergence occurred to give R and R_w of 0.043 and 0.052, respectively. Scattering factors were from Cromer and Waber;[16] the effects of anomalous dispersion were included.[17] The error

(13) All calculations were carried out on PDP 8A and 11/34 computers using the Enraf-Nonius CAD 4-SDP programs. The crystallographic computing package is described in the following references. Frenz, B. A. "The Enraf-Nonius CAD 4 SDP-A Real Time System for Concurrent X-Ray Data Collection and Crystal Structure Determination", In "Computing in Crystallography", Schenk, H.; Olthof-Hazekamp, R.; van Koningsveld, H.; Bassi, G. C., Eds.; Delft University Press: Delft, Holland, 1978; pp 64–71 and In "CAD 4 SDP Users Manual"; Enraf-Nonius: Delft, Holland, 1978.

(14) The intensity data were processed as described in the "CAD 4 and SDP Users Manual"; Enraf-Nonius: Delft, Holland, 1978. The net intensity **I** is given as

$$I = (K/\mathrm{NPT})\,(C - 2B)$$

where K = 20.1166 × (attenuator factor), NPI = ratio of fastest possible scan rate to scan rate for the measurement, C = total count, and B = total background count. The standard deviation in the net intensity is given by

$$\sigma^2(I) = (K/\mathrm{NPI})[C + 4B + (pI)^2]$$

where p is a factor used to downweight intense reflections. The observed structure factor amplitude F_o is given by

$$F_o = (I/Lp)^{1/2}$$

where Lp = Lorentz and polarization factors. The $\sigma(I)$'s were converted to the estimated errors in the relative structure factors $\sigma(F_o)$:

$$(F_o) = \tfrac{1}{2}\,\sigma(I)/IF_o$$

(15) The function minimized was $\omega(|F_o| - |F_c|)^2$ where $\omega = 1/\sigma^2(F_o)$. The unweighted and weighted residuals are defined as follows:

$$R = (\Sigma||F_o| - |F_c||)/\Sigma|F_o|$$

$$R = [(\Sigma\omega(|F_o| - |F_c|))^2/(\Sigma|F_o|)^2]^{1/2}$$

The error in an observation of unit weight is

$$[\Sigma\omega(|F_o| - |F_c|)^2/(\mathrm{NO} - \mathrm{NV})]^{1/2}$$

where NO and NV are the number of observations and variables, respectively.

(16) Cromer, D. T.; Waber, J. T. "International Tables for X-ray Crystallography"; Kynoch Press: Birmingham, England, 1974; Vol. IV, Table 2.2.4. Cromer, D. T. *Ibid.*, Table 2.3.1.

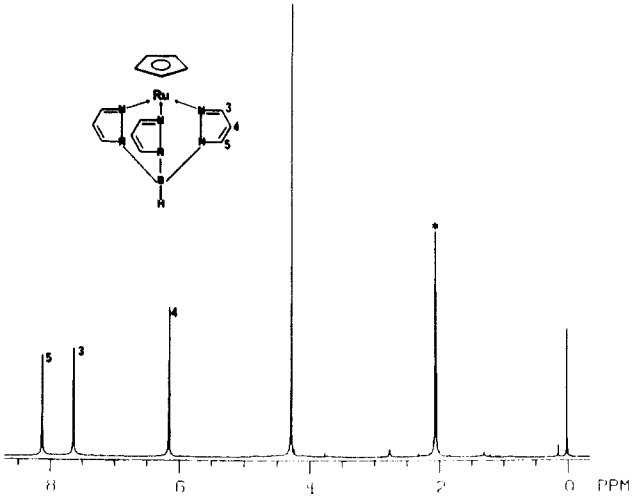

Figure 1. 300-MHz ^1H NMR spectrum of [CpRuHBpz$_3$] in acetone-d_6. The peak marked with the asterisk is due to the solvent.

in an observation of unit weight was 1.40 with the use of a value of 0.05 for p in the $\sigma(I)$ equation. A final difference Fourier map revealed three peaks of 1.2–1.4 e/Å^3 about 1 Å from the ruthenium atom. Table II contains the final positional and thermal parameters. A list of final calculated and observed structure factors is available.

Results and Discussion

Synthesis and Characterization. Although all attempts to synthesize polypyrazolylborate derivatives of the CpFe$^+$ moiety met with failure, the Ru analogues were readily available. The reaction of the potassium salts KHBpz$_3$, KHB(3,5-Me$_2$pz)$_3$, and KBpz$_4$, with [CpRu(CH$_3$CN)$_3$]PF$_6$ in refluxing acetonitrile led to the replacement of the acetonitrile ligands with the nitrogen donor polypyrazolylborates in high yield. The resulting neutral ruthenium(II) compounds [CpRuHBpz$_3$], [CpRuHB(3,5-Me$_2$pz)$_3$], and [CpRuBpz$_4$] were all air-stable, ether-soluble, yellow microcrystalline compounds as obtained from the reaction mixtures. The compound [Cp*RuHBpz$_3$] is synthesized by combining KHBpz$_3$ and [Cp*Ru(CH$_3$CN)$_3$]PF$_6$ in CH$_3$CN under a nitrogen atmosphere at room temperature for 24 h. This compond is moderately air sensitive both in the solid state and in solution and was handled under nitrogen. All attempts to synthesize [Cp*RuHB(3,5-Me$_2$pz)$_3$] were unsuccessful. Presumably, steric interactions between the methyl substituents of the cyclopentadienyl ring and those on the pyrazolyl rings destabilize either the final product or a reaction intermediate. The structures of these compounds (1–4) as determined by spectroscopic data and an X-ray crystal structure are diagrammed below, with the numbering scheme which will be used. The ^1H NMR spectra of these compounds are consistent with the presence of an η^5-Cp$^-$ ligand and a tridentate pyrazolylborate ligand. The ^1H NMR of [CpRuHBpz$_3$] is shown in Figure 1. It exhibits a sharp singlet at 4.271 ppm that is assigned to the η^5-cyclopentadienyl ring. Three other sets of peaks appear in the spectrum: a doublet at 8.123 ppm (J = 1.56 Hz), a doublet at 7.629 ppm (J = 2.26 Hz), and a overlapping doublet of doublets at 6.146 ppm (J = 2.11 Hz). These peaks are characteristic of the aromatic protons of the three equivalent coordinated pyrazolyl groups. The overlapping doublet of doublets is assigned to the proton bound to the H^4 carbon on the pyrazolyl group. It is more

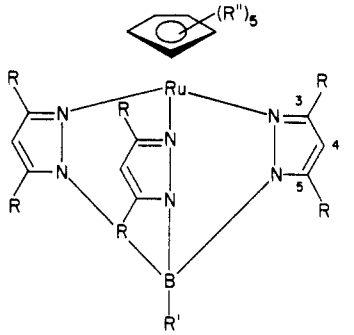

1, R=R'=R"=H
2, R=CH$_3$; R'=R"=H
3, R=R"=H; R=pz
4, R=R'=H; R"=CH$_3$

difficult to assign the H^3 and H^5 peaks. However, Trofimenko[4] observed in a study of the proton NMR spectrum of the free ligand that the peak with the larger coupling constant was consistently the most sensitive to changes in solvent and to metal binding. He concluded that this signal was due to H^3, the proton closest to the N site of binding. Adopting this assignment, the doublet at 7.629 ppm is due to the H^3 and the 8.123 ppm resonance to H^5. The ^1H NMR spectrum of [CpRuBpz$_4$] shows a similar pattern of two doublets and one pseudotriplet assignable to the three bound pyrazolyl rings and three additional signals assignable to the three protons of the unbound pyrazolyl ring. At room temperature, this compound does not undergo any fluxional interchange of the pyrazolyl groups. The pyrazolyl region of the ^1H NMR spectrum of [CpRuHB(3,5-Me$_2$pz)$_3$] is much simpler due to the presence of methyl groups at the 3- and 5-positions of the pyrazolyl rings. The single proton at the 4-position gives rise to a singlet at 5.758 ppm. The two methyl resonances occur at 2.366 and 2.276 ppm and cannot be unambiguously assigned. The ^1H NMR spectrum of [Cp*RuHBpz$_3$] is similar in all respects to the non-methylated analogue with the exception of a resonance at 1.73 ppm due to the pentamethylcyclopentadienyl ring.

All of the neutral compounds are yellow in color and exhibit a single feature in the electronic spectrum. The electronic spectrum consists of a broad shoulder varying with pyrazolylborate between 367 and 393 nm on the low-energy side of an intense UV absorption.

IR spectra of [CpRuHBpz$_3$] and [CpRuHB(3,5-Me$_2$pz)$_3$] exhibit stretches at 2508 and 2510 cm^{-1}, respectively, that are attributable to the B–H stretching mode. These bands appear at about 60 cm^{-1} higher than the corresponding band in the free ligand, in good agreement with data observed in other coordinated pyrazolylborates complexes.[18-20]

The yellow, prismatic crystals of [CpRuHBpz$_3$] obtained from the slow evaporation of a hot ethanol solution, were subjected to an X-ray structural analysis. The crystal conforms to $P2_1/m$ symmetry with Z = 2. An ORTEP view of the molecule is shown in Figure 2 with the atomic numbering scheme. The final atomic parameters are given in Table II. Table III contains selected bond lengths and bond angles. There is a mirror plane in the molecule which bisects the Cp ring and contains the Ru, B, and one of the pyrazolyl rings; however, the HBpz$_3$ ligand retains nearly perfect C_{3v} local symmetry at the Ru(II) center. The

(17) Cromer, D. T.; Ibers, J. A. "International Tables for X-ray Crystallography"; Kynoch Press: Birmingham, England, 1974; Vol. IV.

(18) Mcleverty, J. A.; Seddon, D.; Bailey, N.; Walker, N. W. *J. Chem. Soc., Dalton Trans.* **1976**, 898.
(19) May, S.; Reinsalu, P.; Powell, J. *Inorg. Chem.* **1980**, *19*, 1582.
(20) Thompson, J. S.; Harlow, R. L.; Whitney, J. F. *J. Am. Chem. Soc.* **1983**, *105*, 3522.

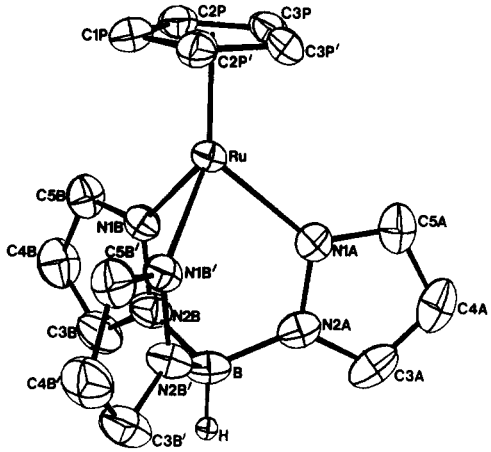

Figure 2. ORTEP drawing of [CpRuHBpz$_3$] showing labeling scheme.

Table III. Selected Interatomic Distances (Å) and Angles (deg) with Their Estimated Standard Deviations

	Bond Distances		
Ru–N1A	2.120 (3)	N1A–C5A	1.325 (5)
Ru–N1B	2.132 (2)	C4A–C5A	1.389 (7)
Ru–C1P	2.168 (3)	C3A–C4A	1.360 (7)
Ru–C2P	2.151 (3)	C3A–N2A	1.346 (6)
Ru–C3P	2.147 (3)	N2B–B	1.542 (4)
Ru–centroid	1.777 (3)	N1B–N2B	1.362 (3)
C1P–C2P	1.414 (5)	N1B–C5B	1.331 (4)
C2P–C3P	1.424 (5)	C4B–C5B	1.394 (4)
C3P–C3P′	1.473 (9)	C3B–C4B	1.365 (5)
N2A–B	1.525 (6)	C3B–N2B	1.343 (4)
N1A–N2A	1.368 (5)		
	Bond Angles		
N1A–Ru–N1B	84.8 (1)	C5A–C4A–C3A	104.7 (4)
Ru–N1A–N2A	120.9 (3)	C4A–C3A–N2A	109.4 (4)
Ru–N1B–N2B	120.9 (2)	C3A–N2A–N1A	108.6 (4)
N1A–Ru–centroid	128.7 (3)	N2A–N1A–C5A	106.6 (4)
N1B–Ru–centroid	130.0 (3)	B–N2B–N1B	119.3 (2)
C1P–C2P–C3P	110.4 (4)	B–N2B–C3B	130.8 (3)
C2P–C1P–C2P′	106.7 (4)	N1B–C5B–C4B	110.7 (3)
C2P–C3P–C3P′	106.3 (4)	C5B–C4B–C3B	104.5 (3)
B–N2A–N1A	119.6 (3)	C4B–C3B–N2B	109.1 (3)
B–N2A–C3A	131.7 (4)	C3B–N2B–N1B	109.3 (3)
N1A–C5A–C4A	110.8 (4)	N2B–N1B–C5B	106.4 (2)

overall coordination geometry at the ruthenium atom can best be described as a "piano stool". The central ruthenium atom is bound directly to the three nitrogens [N1A, N1B, N1B′] of the planar pyrazolyl rings, with an average Ru–N bond distance of 2.128 (3) Å. The bite angle of the HBpz$_3$ ligand produces an average N–Ru–N angle of 83.8°, only slightly distorted from 90°. Additionally, the ruthenium atom is bound to the cyclopentadienyl ring with Ru–C bond distances that range from 2.147 (3) Å to 2.168 (3) Å and a Cp ring centroid to Ru atom distance of 1.777 Å, in good agreement with other Ru cyclopentadienyl compounds. The average C–C distances in the planar Cp ring is 1.43 Å.

The boron atom exhibits pseudotetrahedral symmetry with an average N–B–N angle of 107.4°. As a consequence of the short average B–N bond distances of 1.536 (6) Å the N1–N2 bond vectors are tilted slightly toward the B and are not parallel to the ruthenium–boron axis. Overall, the observed solid-state structure of [CpRuHBpz$_3$] is in excellent agreement with spectroscopic observations of the compound in solution and is consistent with other crystal structures of pyrazolylborate-containing compounds.[21,22]

(21) Restivo, R. J.; Ferguson, G.; O'Sullivan, D. J.; Lalor, F. J. *Inorg. Chem.* **1975**, *14*, 3046.

Table IV

couple	$E^{\circ\prime}$(CH$_3$CN)[a]	$E^{\circ\prime}$(CH$_2$Cl$_2$)[a]
[CpRuHBpz$_3$]$^{+/0}$	+0.353	+0.390
[CpRuHB(3,5-Me$_2$pz)$_3$]$^{+/0}$	+0.323	+0.336
[CpRuBpz$_4$]$^{+/0}$	+0.413	+0.463
[Cp*RuHBpz$_3$]$^{+/0}$	+0.145	+0.153

[a] Values in volts; scan rate = 100 mV/s.

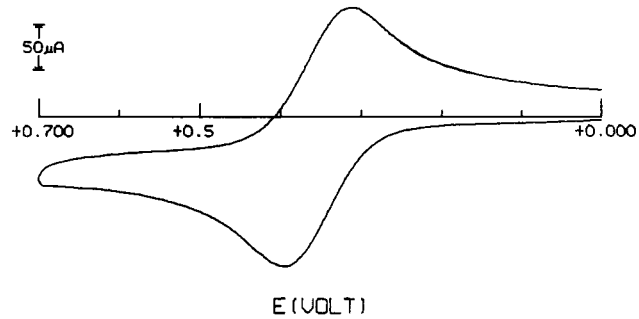

Figure 3. Cyclic voltammogram exhibited by a 1.0 mM solution of [CpRuHB(pz)$_3$] in 0.1 M TBAH/CH$_3$CN. The scan rate is 100 mV/s.

Electrochemistry. To the extent that tridentate pyrazolylborate ligands are cyclopentadienyl anion substitutes, the electrochemistry of the CpRu pyrazolylborate compounds might be expected to be similar to ruthenocene. However, the cyclic voltammograms and general electrochemical behavior of these compounds are different from ruthenocene and more nearly resemble the behavior of ferrocene. The comparison of the electrochemical response of the compounds in this study with that observed for ruthenocene requires a brief review of ruthenocene electrochemistry.

The electrochemical studies of ruthenocene that have been reported are apparently quite dependent on the electrode material and the medium. At a dropping mercury electrode (DME) ruthenocene exhibits a one-electron irreversible oxidation and yields a mercury adduct as a product.[23-25] At a Pt electrode, oxidation of RuCp$_2$ proceeds via an apparent two-electron process.[24,26,27] At a glassy carbon electrode the cyclic voltammogram also exhibits a two-electron process. In acetonitrile/TBAH solutions, an irreversible anodic two-electron wave is observed at +0.84 V. A cathodic wave at +0.35 V corresponds to the reduction of the EC products. In methylene chloride solutions the CV is slightly more reversible, with the anodic wave at +1.00 V and the corresponding cathodic peak at +0.66 V. This difference may be due to the coordination of acetonitrile ligands to the oxidized form. The high degree of irreversibility exhibited by the oxidation in methylene chloride solutions that contain Cl$^-$ is consistent with strong, irreversible ligand binding in the oxidized form.[28]

The Table IV the $E^{\circ\prime}$ values of [CpRuHBpz$_3$], [CpRuHB(3,5-Me$_2$pz)$_3$], [CpRuBpz$_4$], and [Cp*RuHBpz$_3$] measured in acetonitrile/TBAH and methylene chloride/TBAH are listed. The cyclic voltammogram of

(22) Restivo, R. J.; Ferguson, G. *J. Chem. Soc., Chem. Commun.* **1973**, 847.
(23) Page, J. A.; Wilkinson, G. *J. Am. Chem. Soc.* **1952**, *74*, 6149.
(24) Gubin, S. P.; Smirnova, S. A.; Denisovich, L. I.; Lubovich, A. A. *J. Organomet. Chem.* **1971**, *30*, 243.
(25) Hendrickson, D. N.; Sohn, Y. S.; Morrison, W. H.; Gray, H. B. *Inorg. Chem.* **1972**, 11, 808.
(26) Kuwana, T.; Bublitz, D. E.; Hoh, G. *J. Am. Chem. Soc.* **1960**, *82*, 5811.
(27) Denisovich, L. I.; Zakurin, N. V.; Bezrukova, A. A.; Gubin, S. P. *J. Organomet. Chem.* **1974**, *81*, 207.
(28) Bohling, D. A. Thesis, University of Minnesota, 1984.

[CpRuHBpz$_3$] in acetonitrile/TBAH is shown in Figure 3. A quasi-reversible, one-electron anodic wave is apparent at +0.393 V. The return cathodic wave occurs at +0.314 V with $E_{p,a} - E_{p,c}$ = 79 mV at 100 mV/s (ΔE_p for an electrochemically reversible system is 59 mV). The separation of these two waves is dependent on the scan rate, with facter scan rates resulting in a larger separation and slower scan rates producing a smaller ΔE_p (ΔE_p = 64 mV when the scan rate is 20 mV/s). In methylene chloride solutions this feature is less reversible and appears at more positive potentials. The $E^{\circ\prime}$ in methylene chloride solution is +0.390 V with a peak separation of 120 mV at 20 mV/s. The greater irreversibility in methylene chloride and the positive shift in position of the one electron feature where found to be general characteristics of all of the compounds studied. The shift in the position of the wave is likely due to the ability of acetonitrile, with its higher dielectric constant, to better solvate charged species. The result is net stabilization of the oxidized species and a shift to more negative potentials. The quasi-reversible one-electron wave is only slightly sensitive to variations in the pyrazolylborate ligand. The variations with Cp substituent changes are larger. The $E^{\circ\prime}$ for [Cp*RuHBpz$_3$] is shifted to more negative potentials, reflecting either stabilization of the metal in the oxidized form or the destabilization of the reduced form by the electron-rich pentamethylcyclopentadienyl ligand. The one-electron wave observed for these compounds is similar to that observed for ferrocene and stands in contrast to the two-electron electrochemical process reported for ruthenocene at glassy carbon electrodes under these conditions. While much of the chemistry of cyclopentadienyl compounds can be repeated with the pyrazolylborate compounds, our results indicate significant differences in the electronic nature of these two ligands.

The cyclic voltammograms of [CpRuHBpz$_3$], [CpRuHB(3,5-Me$_2$pz)$_3$], [CpRuBpz$_4$], and [Cp*RuHBpz$_3$] in acetonitrile solutions each show a second feature near the positive potential solvent limit. This anodic wave is an irreversible two-electron process at approximately +1.6 V for the cyclopentadienyl compounds and +1.5 V for the pentamethylcyclopentadienyl complex. A cathodic wave results from the reduction of the EC product at approximately +0.7 and +0.4 V for the Cp and Cp* compounds, respectively. We believe this wave is due to oxidation of pyrazolylborate ligand. Oxidation of the free ligands occurs in the potential range +1.18 to +1.95 V.

Bulk electrolyses were performed on all the compounds to ensure the one-electron nature of the main feature in the CV. Bulk electrolyses were carried out with a Pt mesh electrode poised at potentials either between the first one-electron wave and the second two-electron wave (acetonitrile solutions) or between the first wave and the positive potential solvent limit (methylene chloride solutions). Changes in current and charge were monitored as a function of time. In all cases, coulometry indicated that one mole of electrons per mole of complex was passed within experimental error. The bulk electrolyses of [CpRuBpz$_4$] and [CpRuHB(3,5-Me$_2$pz)$_3$] produced red-orange solutions which, when scanned first in a cathodic direction, produced a cyclic voltammogram identical with the starting material. Either no changes in coordination occur upon electrolysis, or they are rapid and reversible on the CV time scale. When exposed to air, both solutions turned green and showed significant changes in the CV. The original wave decreased in size and shifted to lower potential as a new pair of quasi-reversible waves appeared. When the transformation was complete, a final scan of the [CpRuHB(3,5-Me$_2$pz)$_3$] solution was taken. Upon a positive potential scan, an anodic wave at $E^{\circ\prime}$ = +0.282 V corresponding to the reduced complex is present. Additionally, a wave at +0.997 V corresponding to an unknown product is also present. While the exact nature of the transformation to the green product is unknown, we speculate that it involves reaction(s) of the one-electron oxidation product with water. It is interesting to note that solutions of [Cp*RuHBpz$_3$] oxidized by moist air immediately develop a similar green color. Future studies will be needed to ascertain the nature of these green species.

The apparent stability in the absence of water of solutions of the red oxidized Ru(III) analogues of the original Ru(II) compounds, suggested that we attempt the chemical synthesis and isolation of an oxidized compound. Treatment of [CpRuHB(3,5-Me$_2$pz)$_3$] with slightly less than 1 equiv of $AgPF_6$ in acetonitrile yielded a brick red product with an elemental analysis consistent with its formulation as the one-electron oxidized Ru(III) compound [CpRuHB(3,5-Me$_2$pz)$_3$]PF_6. The cyclic voltammogram of the product was identical with that obtained after bulk electrolysis of the neutral compound. The measured magnetic moment of the red product is 1.95 μ_B, in good agreement with other low-spin d^5 Ru(III) complexes.[29]

Chemical Reactivity Studies. A cursory investigation of the photochemistry and thermal chemistry of [CpRuHBpz$_3$] was initiated. A 0.1 mM sample of the compound was photolyzed in acetonitrile solution with approximately 3 equiv of added trimethyl phosphite and monitored by ^{1}H NMR. No photochemical reactivity was observed after 139 h of irradiation. Under identical conditions, a dark control reaction also yielded no reaction. But in the dark, in the presence of a large excess of trimethyl phosphite, the golden color of [CpRuHBpz$_3$] and [(CpRuHB(3,5-Me$_2$pz)$_3$] in acetonitrile or methylene chloride fades to pale yellow. After removal of the solvent and most of the excess phosphite, slightly impure oils were isolated. Proton NMR spectra of both products reveal significant changes. In the spectra of both compounds, the cyclopentadienyl resonance ion appears as a sharp doublet (J = 1 Hz), consistent with the coordination of one P(OCH$_3$)$_3$ to the ruthenium. The doublet assignable to the coordinated phosphite appears at 3.18 ppm in both compounds, 0.33 ppm upfield from the free ligand. To accommodate the phosphite ligand in the Ru(II) coordination core the pyrazolylborates adopt a bidentate binding mode forming the complexes [CpRuHBpz$_3$(P(OCH$_3$)$_3$)] and [CpRu(HB(3,5-Me$_2$pz)$_3$)(P(OCH$_3$)$_3$)]. Bidentate pyrazolylborate binding is consistent with the appearance in the ^{1}H spectra of two sets of pyrazolyl resonances with an intensity ratio of 2:1 for the HBpz$_3^-$ compound. The pyrazolyl region of [CpRuHBpz$_3$(P(OCH$_3$)$_3$)] consists of two doublets and one doublet of doublets that are not significantly shifted from the parent complex and another set nearly identical in appearance but of half the intensity. This second set of peaks is consistent with a "dangling" pyrazolyl ring having NMR shifts similar to the free ligand. The ^{1}H NMR spectrum of [CpRu(HB(3,5-Me$_2$pz)$_3$)(P(OCH$_3$)$_3$)] in the pyrazolyl region consists of two sets of aromatic singlets and two methyl resonances assignable to two bound and one "dangling" pyrazolyl rings. These compounds exhibit the first examples of bidentate binding of a tris- or tetrakis(pyrazolyl)borate to ruthenium. Surprisingly, attempts to synthesize for comparison [CpRuH$_2$Bpz$_2$(P(OCH$_3$)$_3$)], a complex where the pyrazolylborate ligand must be bidentate were unsuccessful.

(29) Figgis, B. N.; Lewis, J. *Prog. Inorg. Chem.* **1964**, *6*, 37.

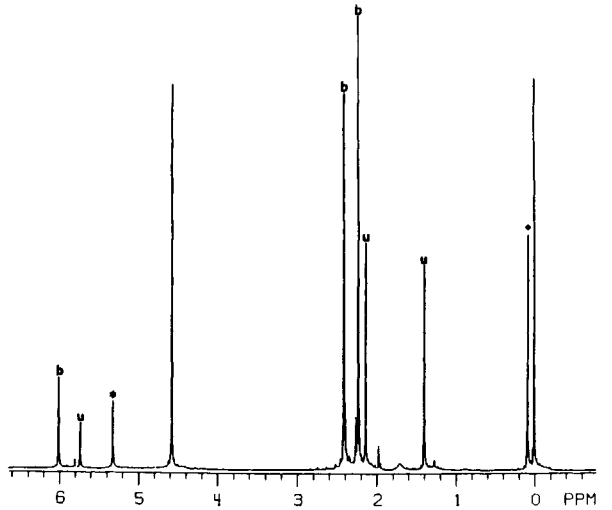

Figure 4. ^{1}H NMR spectrum of [CpRu(HB(3,5-Me_2pz)$_3$)(CO)] in CD_2Cl_2. Peaks labeled b are those assigned to the pyrazolyl rings bound directly to ruthenium. Peaks labeled u are assigned to the uncoordinated pyrazolyl ring. The peaks marked with an asterisk and a diamond are due to the solvent and silicone grease, respectively.

However, displacement of one pyrazolyl ring from the tris- or tetrakis(pyrazolyl)borate complexes also occurs when carbon monoxide is the entering ligand. When CO is bubbled through solutions of [CpRuHB(3,5-Me_2pz)$_3$] or [CpRuBpz$_3$)] for approximately 2 h, the solution color again fades to a pale yellow. The elemental analysis of the product isolated from the reaction of CO with [CpRuHB-(3,5-Me_2pz)$_3$] agrees well with its formulation as [CpRuHB(3,5-Me_2pz)$_3$(CO)]. The pyrazolyl ring region of the ^{1}H NMR spectra of both [CpRu(HB(3,5-Me_2pz)$_3$(CO)] and [CpRuBpz$_4$(CO)] are again consistent with the bidentate binding of the pyrazolylborate to the ruthenium in these compounds. The spectrum of [CpRu(HB(3,5-Me_2pz)$_3$)(CO)], shown in Figure 4, is almost identical to the corresponding P(OCH$_3$)$_3$ adduct, with resonances assignable to two bound pyrazolyl rings and one dangling ring. In the complex [CpRuBpz$_4$(CO)], with two pyrazolyl rings bound to the ruthenium and two not bound, *three* sets of resonances are apparent. One set, of relative intensity 2, is due to the two bound pyrazolyl rings, while the other two *distinct* sets of resonances of intensity 1 are due to two nonequivalent, dangling pyrazolyl rings.

IR spectra of the $\bar{\nu}$(CO) region of the CO adducts were recorded. Two $\bar{\nu}$(CO) stretches appear in the Nujol mull spectra of both [CpRu(HB(3,5-Me_2pz)$_3$)(CO)] and [CpRuBpz$_4$(CO)] at 1940 and 1955 cm^{-1} and at 1950 and 1963 cm^{-1}, respectively. IR spectra of the compounds (dichloromethane solutions) exhibit a single very broad CO stretch. The widths at half height are more than 35 cm^{-1}, suggesting that the two peaks observed in the mull spectra are still present (the width at half-height of the peaks in the mull spectra range from 25 to 35 cm^{-1}). At face value, these results appear to contradict the formulation of the compounds as mono CO adducts; however, in the only other systems where bidentate binding of pyrazolylborate ligands with dangling pyrazolyl groups has been reported, similar observations were made.[6,30] The two complexes [(Bpz$_4$)(Cp)(CO)$_2$Mo] and [(HBpz$_3$)(Cp)(CO)$_2$Mo] each exhibit a total of *four* CO stretches in the IR which are sensitive to changes in solvent and media. In this previously studied case, conformational isomerism was invoked to explain the doubling of the $\bar{\nu}$(CO) bands. Similar considerations successfully explain our results as well.

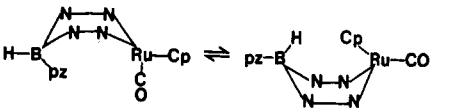

Figure 5. Possible structures for the conformational isomers of [CpRu(HB(3,5-Me_2pz)$_3$)(CO)].

Molecular models of [CpRu(HB(3,5-Me_2pz)$_3$)(CO)] and [CpRuBpz$_4$(CO)] indicate that the six-member ring containing the bidentate pyrazolylborate and the ruthenium is forced into a shallow boat configuration by the pyrazolyl rings. With two different substituents (cyclopentadienyl and CO) on the ruthenium, the process which interconverts the two six-member-ring boat forms simultaneously interconverts two different conformational isomers as shown in Figure 5. Each isomer places the CO ligand in a unique environment. Because the IR time scale is short compared with the interconversion rate, the CO stretch of each isomer is observed. This explanation requires that the cyclopentadienyl ligand exhibit two different environments, but on the longer time scale of the NMR experiment the boat to boat interconversion occurs fast enough to average the cyclopentadienyl environments. Geometric isomers of [CpRu(HB(3,5-Me_2pz)$_3$)(CO)] are possible as well, but are not observed.

The compound [CpRuBpz$_4$(CO)] with two dangling pyrazolyl rings was used as a ligand to synthesize a binuclear complex. Reaction of [CpRuBpz$_4$(CO)] with [CpRu(CH$_3$CN)$_2$(CO)]PF$_6$ results in the displacement of both acetonitrile ligands to form [Cp$_2$Ru$_2$(CO)$_2$Bpz$_4$]PF$_6$. A single cyclopentadienyl resonance, in the ^{1}H NMR spectrum of the compound, indicates that both rings are equivalent at room temperature. The six resonances of equal intensity that are assignable to the pyrazolyl ring protons indicate two different environments for the four rings. These data are consistent with a binuclear structure in which each ruthenium atom is bound to a cyclopentadienyl ligand and a CO and the tetrakis(1-pyrazolyl)borate bridges the two metals in a bidentate manner. The $\bar{\nu}$(CO) stretch in the IR spectrum of this compound is extremely broad in both Nujol mulls and acetone solutions. At this time, we are not able to unambiguously attribute the broadness of the $\bar{\nu}$(CO) band to the conformational isomerization processes observed in the monomeric compounds. A brief electrochemical study of this compound was initiated to ascertain the extent of interaction between the ruthenium centers in this compound. The cyclic voltammogram of this compound exhibits a single irreversible oxidation at 1.57 V and shows no evidence of a significant metal–metal interaction.

Conclusions. We have demonstrated that new mixed-ligand compounds containing a cyclopentadienyl or pentamethylcyclopentadienyl ligand and various pyrazolylborate ligands can be synthesized starting with [CpRu(CH$_3$CN)$_3$]PF$_6$ and [Cp*Ru(CH$_3$CN)$_3$]PF$_6$, respectively. The neutral species [CpRuHBpz$_3$], [CpRuHB-(3,5-Me_2pz)$_3$], [CpRuBpz$_4$], and [Cp*RuHBpz$_3$)] are well-crystallized substances and have been characterized by spectroscopic means. The X-ray crystal structure of [CpRuHBpz$_3$] demonstrates that the complex contains an η^5-cyclopentadienyl ring and a tridentate HB(pz)$_3^-$ ligand in good agreement with other compounds of this type. The cyclic voltammograms of these compounds consist of a one-electron quasi-reversible wave. Chemical oxidation of [CpRuHB(3,5-Me_2pz)$_3$] allowed the isolation of the Ru(III) analogue of the parent compound.

The reaction chemistry of the neutral compounds was examined. None of the new complexes are photoactive

(30) Calderon, J. L.; Cotton, F. A.; Shaver, A. *J. Organomet. Chem.* **1972**, *37*, 127.

under standard reaction conditions. However, at room temperature the ligation of one pyrazolyl ring may be replaced with a $P(OCH_3)_3$ or a CO ligand to form novel compounds in which the pyrazolylborate ligand binds in a bidentate manner. At room temperature the CO adducts $[CpRuHB(3,5\text{-}Me_2pz)_3(CO)]$ and $[CpRuBpz_4(CO)]$ exhibit conformational isomerism on the IR time scale that is averaged on the NMR time scale. The reaction of $[CpRuBpz_4(CO)]$ and $[CpRu(CH_3CN)_2CO]PF_6$ allowed the isolation of a new binuclear ruthenium complex, $[Cp_2Ru_2(CO)_2Bpz_4]PF_6$.

Acknowledgment. We wish to thank Professor J. D. Britton for his expert assistance in the X-ray structure determination. A.M.M. acknowledges a Louise T. Dosdall Fellowship in science. The X-ray diffractometer was purchased in part through funds provided by the National Science Foundation Grant CHE 77-28505. We thank the Engelhard Minerals and Chemicals Corp. for a generous loan of $RuCl_3 \cdot 3H_2O$. This work was supported by the Department of Energy Grant DOE/DE-ACO2-83ER13103.

Supplementary Material Available: Listings of thermal parameters, hydrogen atom positions, and observed and calculated structure factors (12 pages). Ordering information is given on any current masthead page.

Oxidative Addition Mechanisms of a Four-Coordinate Rhodium(I) Macrocycle

James P. Collman,* John I. Brauman, and Alex M. Madonik

Department of Chemistry, Stanford University, Stanford, California 94305

Received February 13, 1985

Oxidative addition of a wide range of alkyl halides (RX) to the four-coordinate Rh(I) macrocyclic complex **5b** yields six-coordinate Rh(III)–alkyl adducts. The reactions exhibit second-order kinetics (first order in substrate and Rh(I) complex) for all substrates except hindered alkyl iodides, and the reactivity trends (X = I > Br > OTs > Cl; R = methyl > primary > secondary > tertiary [no reaction]) are consistent with a nucleophilic, S_N2-like mechanism. The observed activation parameters and rate variation with solvent polarity also support this interpretation. Complex **5b** is the most reactive neutral nucleophile which has been isolated (k = 2000 M^{-1} s^{-1} for iodomethane at 25 °C in tetrahydrofuran); it exhibits unusually high sensitivity to steric hindrance and leaving-group polarizability, characteristics it shares with other metal-centered nucleophiles. The shift to a one-electron mechanism in reactions with hindered iodides (2,2-dimethyl-1-iodopropane, 3,3-dimethyl-1-iodobutane, and 2-iodopropane) is signaled by their departure from second-order kinetics and by their unexpectedly high rates; even 1-iodoadamantane forms an adduct. Furthermore, scrambling of stereochemistry is observed in the addition of *erythro*-3,3-dimethyl-1-iodobutane-*1,2-d*$_2$. While a radical chain mechanism is implicated by these kinetic results, any free radical intermediates must be very short-lived, as no rearrangement was detected in the reaction of 6-iodo-1-heptene. It seems likely that electron transfer from the Rh(I) reagent leads to the formation of radical pairs, most of which collapse to product without escaping the solvent cage.

Introduction

The oxidative addition of alkyl halides to low-valent transition-metal centers has been intensively studied,[1] particularly as it is the most general method of forming metal–carbon σ bonds. Nonetheless, fundamental questions remain about the detailed mechanism of the reactions. Early work distinguished between the one-electron change observed at odd-electron centers such as the pentacyanocobalt(II) anion[2] and the apparent two-electron process involved in additions to even-electron centers, such as Vaska's iridium(I) complex.[3] Chock and Halpern[3a] proposed a nucleophilic mechanism for the addition of methyl iodide to Vaska's complex, with attack by the metal center at carbon leading to an S_N2-like transition state. They contrasted this behavior to that of dioxygen and dihydrogen, which form cis adducts with Vaska's complex by a concerted, three-center process.

The rate laws and activation parameters for the addition of methyl iodide to Vaska's complex[3a,4] and a variety of other d^8 metal complexes[5-7] were shown to support the proposed nucleophilic mechanism. The relative rates of addition for other alkyl halides were found to reflect the expected influences of steric hindrance and leaving-group reactivity.[7] More basic phosphines were found to enhance to nucleophilicity of a metal center,[8-10] although increasing steric bulk in the ligands can mask these effects.[7a,9]

Attempts to demonstrate the expected inversion of configuration at carbon resulting from these oxidative additions led to conflicting reports[11-13] and ultimately to the recognition of a competing, radical-chain mechanism

(1) Stille, J. K.; Lau, K. S. Y. *Acc. Chem. Res.* **1977**, *10*, 434.
(2) (a) Halpern, J.; Maher, J. P. *J. Am. Chem. Soc.* **1965**, *87*, 5361. (b) Chock, P. B.; Halpern, J. *J. Am. Chem. Soc.* **1969**, *91*, 582.
(3) (a) Chock, P. B.; Halpern, J. *J. Am. Chem. Soc.* **1966**, *88*, 3511. (b) Vaska, L. *Acc. Chem. Res.* **1976**, *9*, 175.
(4) Stieger, H.; Kelm, H. *J. Phys. Chem.* **1973**, *77*, 290.
(5) Douek, I. C.; Wilkinson, G. *J. Chem. Soc. A* **1969**, 2604.
(6) Uguagliati, P.; Palazzi, A.; Deganello, G.; Belluco, U. *Inorg. Chem.* **1970**, *9*, 724.
(7) (a) Hart-Davis, A. J.; Graham, W. A. G. *Inorg. Chem.* **1970**, *9*, 2658. (b) Hart-Davis, A. J.; Graham, W. A. G. *Inorg. Chem.* **1971**, *10*, 1653.
(8) Ugo, R.; Pasini, A.; Fusi, A.; Cenini, S. *J. Am. Chem. Soc.* **1972**, *94*, 7364.
(9) Kubota, M.; Kiefer, G. W.; Ishikawa, R. M.; Bencala, K. E. *Inorg. Chim. Acta* **1973**, *7*, 195.
(10) Thompson, W. H.; Sears, C. T., Jr. *Inorg. Chem.* **1977**, *16*, 769.
(11) Pearson, R. G.; Muir, W. R. *J. Am. Chem. Soc.* **1970**, *92*, 5519.
(12) Labinger, J. A.; Braus, R. J.; Dolphin, D.; Osborn, J. A. *J. Chem. Soc., Chem. Commun.* **1970**, 612.
(13) Jensen, F. R.; Knickel, B. *J. Am. Chem. Soc.* **1971**, *93*, 6339.

0276-7333/86/2305-0310$01.50/0

(Me)(I)Rh(BPDOBF$_2$), 99355-04-1; ((CH$_3$)$_2$CH)(Br)Rh(BPDOBF$_2$), 99355-05-2; (Me)(Br)Rh(PPDOBF$_2$), 99355-06-3; (Me)(Cl)Rh(PPDOBF$_2$), 99355-07-4; (*t*-C$_4$H$_9$)(I)Rh(PPDOBF$_2$), 99355-08-5; (*t*-C$_4$H$_9$)(Br)Rh(PPDOBF$_2$), 99355-09-6; (*t*-C$_4$H$_9$)(Cl)Rh(PPDOBF$_2$), 99355-10-9; (*t*-C$_4$H$_9$)(OTs)Rh(PPDOBF$_2$), 99355-11-0; ((CH$_3$)$_2$CH)(I)Rh(PPDOBF$_2$), 99355-12-1; ((CH$_3$)$_2$CH)(Br)Rh(PPDOBF$_2$), 99355-13-2; (Bz)(Br)Rh(PPDOBF$_2$), 99355-14-3; (Bz)(Cl)Rh(PPDOBF$_2$), 99355-15-4; (*c*-(C$_3$H$_5$)CH$_2$)(I)Rh(PPDOBF$_2$), 99355-16-5; ((CH$_3$)$_3$CCH$_2$)(I)Rh(PPDOBF$_2$), 99355-17-6; (B)(I)Rh(PPDOBF$_2$) (B = 1-adamantyl), 99355-18-7; ((CH$_3$)$_3$C(CH$_2$)$_2$)(I)Rh(PPDOBF$_2$), 99355-19-8; ((CH$_3$)$_3$C(CH$_2$)$_2$)(Br)Rh(PPDOBF$_2$), 99355-20-1; (MeCO)(Cl)Rh(PPDOBF$_2$), 99355-21-2; (Bz)(SCN)Rh(PPDOBF$_2$), 99355-22-3; (*c*-C$_6$H$_{11}$)(Br)Rh(PPDOBF$_2$), 99355-25-6; (Br$_2$)Rh(PPDOBF$_2$), 99355-27-8; ((CH$_3$)$_3$CCHDCHD)(I)Rh(PPDOBF$_2$), 99355-28-9; RhCl$_3$, 10049-07-7; MeI, 74-88-4; (CH$_3$)$_2$CHBr, 75-26-3; MeBr, 74-83-9; MeCl, 74-87-3; *t*-C$_4$H$_9$I, 558-17-8; *t*-C$_4$H$_9$Br, 507-19-7; *t*-C$_4$H$_9$Cl, 507-20-0; *t*-C$_4$H$_9$OTS, 4664-57-7; (CH$_3$)$_2$CHI, 75-30-9; BzBr, 100-39-0; BzCl, 100-44-7; *c*-(C$_3$H$_5$)CH$_2$I, 33574-02-6; (CH$_3$)$_3$CCH$_2$I, 15501-33-4; BI (B = 1-adamantyl), 768-93-4; (CH$_3$)$_3$C(CH$_2$)$_2$I, 15672-88-5; (CH$_3$)$_3$C(CH$_2$)$_2$Br, 1647-23-0; MeCOCl, 75-36-5; BzSCN, 3012-37-1; 1-bromobutane, 109-65-9; bromocyclohexane, 108-85-0; 1-bromoadamantane, 768-90-1; 1-chlorobutane, 109-69-3; 2-methyl-2-phenyl-1-propanol, 100-86-7; 2-methyl-2-phenyl-1-propanol tosylate, 21816-03-5; 1-iodobutane, 542-69-8; *n*-butyl tosylate, 778-28-9.

Supplementary Material Available: A table of analytical data (5 pages). Ordering information is given an any current masthead page.

Arylnickel(III) Species Containing NO_3, NO_2, and NCS Ligands. ESR Data and the X-ray Crystal Structure of Hexacoordinate (Pyridine)bis(isothiocyanato)-[*o*,*o*′-bis{(dimethylamino)methyl}phenyl]nickel(III)

David M. Grove, Gerard van Koten,* Wilhelmus P. Mul, Adolphus A. H. van der Zeijden, and Jos Terheijden

Anorganisch Chemisch Laboratorium, University of Amsterdam, Nieuwe Achtergracht 166, 1018 WV Amsterdam, The Netherlands

Martin C. Zoutberg and Casper H. Stam

Laboratorium voor Kristallografie, University of Amsterdam, Nieuwe Achtergracht 166, 1018 WV Amsterdam, The Netherlands

Received March 20, 1985

A method for the interconversion of the five-coordinated Ni(III) species [Ni{C$_6$H$_3$(CH$_2$NMe$_2$)$_2$-*o*,*o*′}X$_2$] (X = Cl, Br, I) and its application to the synthesis of the new species with X = NO_3 and NO_2 are described. For X = NCS the same route leads to the formation of species in which the Ni(III) center is hexacoordinate and ESR data are reported. For one derivative, [Ni{C$_6$H$_3$(CH$_2$NMe$_2$)$_2$-*o*,*o*′}(NCS)$_2$(C$_5$H$_5$N)] (**5b**), the molecular geometry has been established by X-ray crystallographic methods. Crystals of **5b**, C$_{19}$H$_{24}$NiN$_5$S$_2$, are orthorhombic with a = 13.146 (2), b = 16.101 (4) Å, c = 10.064 (1) Å, V = 2122 (1) Å^3, and Z = 4. Refinement included 1308 reflections leading to a final R value of 0.058. The structure of **5b** consists of a hexacoordinate Ni(III) center which is directly σ-bonded to the phenyl carbon of the C$_6$H$_3$(CH$_2$NMe$_2$)$_2$-*o*,*o*′ ligand (Ni(III)–C = 1.900 (9) Å). The Ni center is further bonded to five nitrogen donor ligands: to two mutually trans N-bonded NCS ligands (1.965 (6) Å), to two trans NMe$_2$ ligands (2.207 (6) Å), and to the pyridine N atom which is trans to the C donor site (2.057 (8) Å). On the basis of these structural data and in combination with the ESR data with $g_\parallel > g_\perp$, it is concluded that the unpaired electron resides in the $d_{x^2-y^2}$ orbital.

Introduction

In the last few years it has become increasingly apparent that nickel plays an important role in certain biological systems, e.g., the hydrogenases,[1] and this has emphasized the relevance of studies concerning the range and stabilty of the less common Ni(I) and Ni(III) oxidation states.[2] Those inorganic coordination complexes of trivalent (d^7) nickel are paramagnetic, and in the majority of examples known stabilization of this oxidation state is accomplished by the use of N donor ligands of a polydentate or macrocyclic nature.[3-5]

Recently, with use of the terdentate anionic N,N′,C ligand C$_6$H$_3$(CH$_2$NMe$_2$)$_2$-*o*,*o*′ we prepared the novel square-pyramidal arylnickel(III) species [Ni{C$_6$H$_3$(CH$_2$NMe$_2$)$_2$-*o*,*o*′}X$_2$] (X = Cl, Br, I) (**1a–c**), which were the first reported true Ni(III) organometallics.[6] The presence of a C–Ni(III) σ-bond makes these compounds also interesting models for the arylnickel(III) intermediates postulated to be key intermediates in the nickel-catalyzed cross-coupling reactions of alkyl Grignards with aryl halides.[7]

(1) (a) Thompson, A. J. *Nature (London)* **1982**, *298*, 602 and references therein. (b) Albracht, S. P. J.; van der Zwaan, J. W.; Fontijn, R. D. *Biochim. Biophys. Acta* **1984**, *766*, 245–258 and references therein.
(2) (a) Nag, K.; Chakravorty, A. *Coord. Chem. Rev.* **1980**, *33*, 87–147. (b) Haines, R. I.; McAuley, A. *Coord. Chem. Rev.* **1981**, *39*, 77–119.
(3) Jacobs, S. A.; Magerum, D. W. *Inorg. Chem.* **1984**, *23*, 1195–1201.
(4) Lati, J.; Koresh, J.; Meijerstein, D. *Chem. Phys. Lett.* **1975**, *33*, 286–288.
(5) Bencini, A.; Fabrizzi, L.; Poggi, A. *Inorg. Chem.* **1981**, *20*, 2544–2549.
(6) Grove, D. M.; van Koten, G.; Zoet, R.; Murrall, N. W.; Welch, A. J. *J. Am. Chem. Soc.* **1983**, *105*, 1379–1380.
(7) Smith, G.; Kochi, J. K. *J. Organomet. Chem.* **1980**, *198*, 199–214. Negishi, E. *Acc. Chem. Res.* **1982**, *15*, 340–348.

0276-7333/86/2305-0322$01.50/0

In this paper the results of an extension of this study are reported and the synthesis of analogues of 1 with X = NO_3 and NO_2 outlined. More importantly we describe the first examples of a new class of Ni(III) species of general formula [Ni{$C_6H_3(CH_2NMe_2)_2$-*o*,*o*'}$(NCS)_2$(solvent)] which are shown to contain hexacoordinate nickel(III) in a tetragonally compressed octahedral environment.

Experimental Section

All reactions were performed with freshly distilled solvents. ^1H NMR spectra were recorded on a Bruker WM-250 spectrometer, and chemical shifts are relative to tetramethylsilane (0 ppm). IR spectra (KBr disks) were recorded on a Perkin-Elmer 283 spectrometer. ESR spectra were obtained from glasses (diglyme, CH_2Cl_2) or powdered solids contained in 5-mm i.d. quartz tubes using a Bruker ER 200D-MR X-band spectrometer with **g** tensors referenced to DPPTH (2.002).

[Ni^{II}{$C_6H_3(CH_2NMe_2)_2$-*o*,*o*'}(NCS)] (3). To a stirred solution of [Ni{$C_6H_3(CH_2NMe_2)_2$-*o*,*o*'}Br][8] (300 mg, 0.91 mmol) in H_2O (30 mL) was added $AgBF_4$ (195 mg, 1.00 mmol), and after 15 min AgBr was removed by filtration. To the resulting yellow-brown solution of [Ni{$C_6H_3(CH_2NMe_2)_2$-*o*,*o*'}(H_2O)][BF_4][8] was added excess NH_4NCS (500 mg, 6.6 mmol), and after 15 min the brown-green solution was evaporated to dryness in vacuo. Extraction with CH_2Cl_2 and recrystallization from CH_2Cl_2/pentane yielded pure olive green **3**. Anal. Calcd for $C_{13}H_{19}N_3SNi$: C, 50.68; H, 6.22; N, 13.64; S, 10.41. Found: C, 50.66; H, 6.22; N, 13.70; S, 10.37.

[Ni^{III}{$C_6H_3(CH_2NMe_2)_2$-*o*,*o*'}$(NCS)_2(H_2O)$] (5a). To a stirred solution of [Ni{$C_6H_3(CH_2NMe_2)_2$-*o*,*o*'}Br_2][6] (145 mg, 0.35 mmol) in acetone (20 mL) was added $AgBF_4$ (153 mg, 0.79 mmol). After 5 min AgBr was removed by filtration and an excess of NH_4NCS (1.73 mg, 2.28 mmol) was added to the brownish solution. The solvent was then removed in vacuo from the resulting dark green solution to yield a thick green oil. Attempts to crystallize this oil failed; yield 96 mg (~70%).

[Ni^{III}{$C_6H_3(CH_2NMe_2)_2$-*o*,*o*'}X_2] (X = NO_3 (1d), NO_2 (1e)). To a stirred solution of [Ni{$C_6H_3(CH_2NMe_2)_2$-*o*,*o*'}Br_2][8] (200 mg, 0.49 mmol) in acetone (20 mL) was added 2.1 equiv of $AgBF_4$. After 5 min the precipitated AgBr was removed by filtration and an excess of NaX (5 equiv) was added to the brownish solution. After 15 min the solvent was removed in vacuo and the product was extracted with CH_2Cl_2. Recrystallization from CH_2Cl_2/toluene (1:1) afforded pure **1d** (yellow-brown) and **1e** (dark green) in greater than 70% yield. Anal. Calcd for $C_{12}H_{19}N_4O_6Ni$ (**1d**): C, 38.53; H, 5.12; N, 14.98. Found: C, 39.04; H, 5.13; N, 14.50. Calcd for $C_{12}H_{19}N_4O_4Ni$ (**1e**): C, 42.14; H, 5.60; N, 16.38. Found: C, 42.14; H, 5.61; N, 16.25.

The products could also be obtained by either oxidation of the analogous Ni^{II} species with an excess of AgX in water or the use of $AgNO_3$ or $AgNO_2$ in a 1/>2 molar ratio. After filtration of Ag^0 and AgX precipitates workup of the filtrates was carried out as described above.

[Ni^{III}{$C_6H_3(CH_2NMe_2)_2$-*o*,*o*'}$(NCS)_2$(py)] (5b). On addition of 1 mL of pyridine to the solution of **5a** described above small dark green crystals were formed. Recrystallization from pyridine/CH_2Cl_2/toluene yielded the title compound. Anal. Calcd for $C_{18}H_{24}N_4SNi$ (**5b**): C, 51.25; H, 5.43; N, 15.73; S, 14.40. Found: C, 51.14; H, 5.44; N, 15.69; S, 14.27.

Structure Determination and Refinement: X-ray Data Collection. Dark green, almost black, crystals of **5b** were obtained as well-formed plates by slow evaporation of a saturated solution of **5b** in pyridine/CH_2Cl_2/toluene (1:3:4), and one of suitable dimension was chosen and glued on top of a glass fiber. Unit-cell dimensions were derived from a least-squares fit of the setting angles for 18 reflections ($30 < 2\theta < 45$). The crystal data and details of data collection and structure refinement are summarized in Table I. A total of 3137 reflections were measured on a Nonius CAD4 diffractometer and of these 1829 were below the $2.5\sigma(I)$ level and were treated as unobserved. An empirical absorption correction has been applied.

The structure was solved by means of the heavy-atom method using standard Patterson and Fourier techniques and subsequently refined by means of anisotropic block-diagonal least-squares calculations. The molecules were found to be situated on crystallographic binary axes with a $^1/_2$ molecule in the asymmetric unit. The H atoms were introduced at their calculated positions and not refined. The final R value for 1308 observed reflections was 0.058 (R_w = 0.101). A weighting scheme $w = 1/(2.7 + F_o + 0.037F_o^2)$ was applied, and the anomalous dispersion of Ni taken into account.

Computations were carried out with the X-RAY 76 system[9] using ref 10 for atomic scattering factors and the anomalous

Table I. Crystal Data and Details of the Structure Determination

A. Crystal Data	
formula	$C_{19}H_{24}NiN_5S_2$
mol wt	445.25
space group	*Pnab* (nonstandard *Pbcn*, no. 60)
cryst system	orthorhombic
a, Å	13.146 (2)
b, Å	16.101 (4)
c, Å	10.064 (1)
V, Å^3	2130 (2)
Z	4
D_{calcd}, g cm^{-3}	1.39
$F(000)$	932
μ(Mo Kα), cm^{-1}	11.2
cryst size, mm	0.23 × 0.18 × 0.13
B. Data Collection	
radiation	Mo Kα λ = 0.71 069 Å
T, K	301
θ_{min}, θ_{max}	1.10, 30.0
max time/refln, min	3
ref refln	402
total refln data	3501
total unique reflns	3501
obsd data	1308 ($I > 2.5\sigma(I)$)
C. Refinement	
no. of refined parameters	350
weighting scheme	$A + F + BF^2 + CF^2$
final R values	$R(F)$ = 0.058, $R_w(F)$ = 0.101

Table II. Final Values of the Atomic Coordinates (Esd's)

atom	x/a	y/b	z/c
Ni	0.2500 (0)	0.1507 (1)	0.0000 (0)
C(1)	0.2500 (0)	0.0327 (6)	0.0000 (0)
C(2)	0.1975 (6)	−0.0067 (4)	0.1014 (7)
C(3)	0.1984 (7)	−0.0937(5)	0.0998 (9)
C(4)	0.2500 (0)	−0.1349 (6)	0.0000 (0)
C(5)	0.1485 (6)	0.0472 (5)	0.2031 (8)
C(6)	0.1190 (7)	0.1931 (6)	0.2464 (9)
C(7)	0.0243 (7)	0.1239 (5)	0.0772 (9)
C(8)	0.3197 (6)	0.3221 (5)	0.0685 (8)
C(9)	0.3219 (7)	0.4087 (5)	0.0701 (9)
C(10)	0.2500 (0)	0.4532 (6)	0.0000 (0)
C(11)	0.3869 (5)	0.1329 (4)	0.2516 (7)
N(1)	0.1243 (4)	0.1295 (4)	0.1414 (6)
N(2)	0.2500 (0)	0.2785 (5)	0.0000 (0)
N(3)	0.3413 (5)	0.1470 (4)	0.1545 (6)
S	0.4518 (2)	0.1153 (2)	0.3831 (2)
H(3)	0.1543	−0.1219	0.1574
H(4)	0.2500	−0.1995	0.0000
H(51)	0.0859	0.0269	0.2445
H(52)	0.2023	0.0470	0.2680
H(61)	0.0772	0.1816	0.2986
H(62)	0.1902	0.2037	0.2942
H(63)	0.0894	0.2473	0.2059
H(71)	−0.0279	0.1060	0.1369
H(72)	0.0031	0.1751	0.0239
H(73)	0.0315	0.0900	0.0044
H(8)	0.3726	0.2809	0.1137
H(9)	0.3807	0.4368	0.1180
H(10)	0.2500	0.5027	0.0000

(8) Grove, D. M.; van Koten, G.; Ubbels, H. J. C.; Zoet, R.; Spek, A. L. *Organometallics* **1984**, *3*, 1003–1009.

(9) Steward, J. M. "The X-ray 76 System", Technical Report TR-466, Computer Science Center, University of Maryland, College Park, MD.

Scheme I

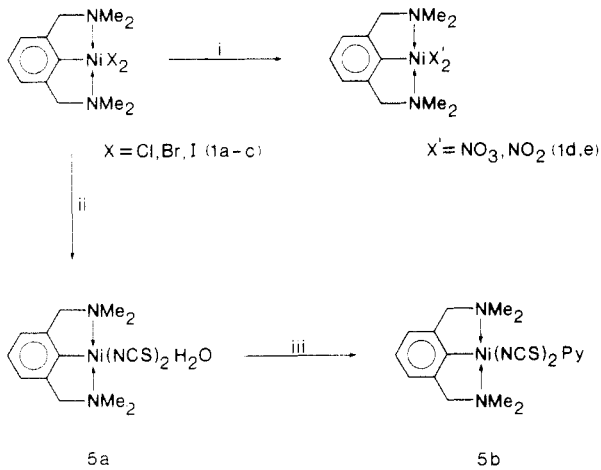

[a] i, Ag^+, acetone, -AgX, MX' (X' = NO_2, NO_3, M = Li, Na, K); ii, Ag^+, acetone, -AgX, NH_4NCS excess; iii, pyridine, CH_2Cl_2/acetone/toluene.

dispersion correction. The final values of the refined parameters are given in Table II.

Results and Discussion

The synthetic results for the various arylnickel(III) species are outlined in Scheme I.

A. Synthesis of NO_3 and NO_2 Species. A previous publication described the synthesis of a variety of [Ni^{II}-{$C_6H_3(CH_2NMe_2)_2$-*o,o'*}X] species,[8] and for the chloro, bromo, and iodo derivatives the use of oxidizing agents to yield the corresponding Ni(III) species **1a–c** has been communicated.[8] In further studies it has now been found that with use of one of these arylnickel(III) species as starting material the overall ligand substitution sequence shown in Scheme I (eq i) is a route of great potential for the ready interconvention of **1a–c** and the preparation of further related arylnickel(III) species. In particular with this method the new five-coordinate arylnickel(III) complexes [Ni{$C_6H_3(CH_2NMe_2)_2$-*o,o'*}$(NO_3)_2$] (**1d**) and [Ni-{$C_6H_3(CH_2NMe_2)_2$-*o,o'*}$(NO_2)_2$] (**1e**) have been synthesized.[11]

In synthetic route i the addition of 2 equiv of Ag(I) (BF_4^- or $CF_3SO_3^-$ anion) leads to quantitative precipitation of 2 equiv of AgX which may be filtered off to leave a clear brown solution of the solvated Ni(III) species [Ni{C_6H_3-$(CH_2NMe_2)_2$-*o,o'*}(solvent)$_n$]$^{2+}$ (**2**) (solvent = acetone or H_2O). Treatment of **2** in situ with an excess of a new anion, X^- (Li^+, Na^+, or K^+ cation) generates an unchanged [Ni-{$C_6H_3(CH_2NMe_2)_2$-*o,o'*}X_2] species that can be isolated by evaporation of the mixture to dryness in vacuo followed by extraction with CH_2Cl_2 or toluene.

B. Synthesis of NCS Species. Our interest in N donor ligands and the successful synthesis of **1d** and **1e** containing polyatomic anions (as well as of the Ni(II) derivatives [Ni{$C_6H_3(CH_2NMe_2)_2$-*o,o'*}X] (X = NO_3, NO_2)) led us to consider syntheses of the NCS analogues [Ni^{II}-{$C_6H_3(CH_2NMe_2)_2$-*o,o'*}(NCS)] (**3**) and [Ni^{III}-{C_6H_3-$(CH_2NMe_2)_2$-*o,o'*}$(NCS)_2$] (**4**). The synthesis of **3**,[12] which

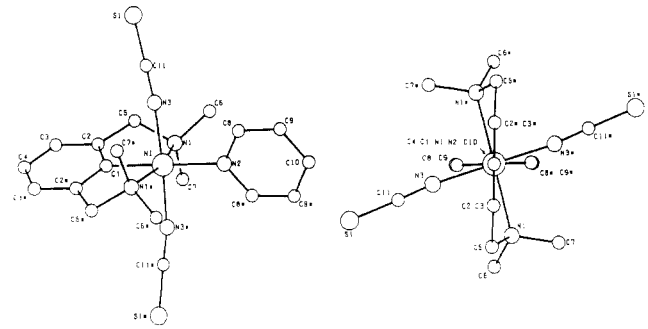

a b

Figure 1. (a) Pluto drawing of [Ni{$C_6H_3(CH_2NMe_2)_2$-*o,o'*}-$(NCS)_2$(py)] (**5b**). (b) Projection along the C(1)–Ni–N(2) axis showing the relative positions of the aryl and pyridine planes with respect to the N(3)–Ni–N(3*) axis.

Table III. Relevant Bond Distances (Å) and Bond Angles (deg) of [Ni{$C_6H_3(CH_2NMe_2)_2$-*o,o'*}$(NCS)_2$(py)] (5b)

Bond Distances			
Ni-C(1)	1.900 (9)	C(5)-N(1)	1.497 (10)
Ni-N(1)	2.207 (6)	C(6)-N(1)	1.474 (11)
Ni-N(2)	2.057 (8)	C(7)-N(1)	1.468 (11)
Ni-N(3)	1.965 (6)	C(8)-N(2)	1.344 (9)
C(1)-C(2)	1.385 (8)	C(8)-C(9)	1.396 (11)
C(2)-C(3)	1.401 (10)	C(9)-C(10)	1.380 (10)
C(2)-C(5)	1.489 (11)	C(11)-N(3)	1.169 (9)
C(3)-C(4)	1.382 (10)	C(11)-S(1)	1.600 (7)
Bond Angles			
C(1)-Ni-N(1)	81.1 (1)	C(2)-C(5)-N(1)	108.8 (6)
C(1)-Ni-N(2)	180.0 (0)	Ni-N(1)-C(5)	104.2 (4)
C(1)-Ni-N(3)	88.2 (2)	Ni-N(1)-C(6)	113.0 (5)
N(1)-Ni-N(2)	98.9 (1)	Ni-N(1)-C(7)	113.4 (5)
N(1)-Ni-N(3)	86.7 (2)	C(5)-N(1)-C(6)	109.1 (6)
N(1)-Ni-N(3*)	92.8 (2)	C(5)-N(1)-C(7)	108.6 (6)
N(2)-Ni-N(3)	91.8 (2)	C(6)-N(1)-C(7)	108.4 (6)
Ni-C(1)-C(2)	117.3 (4)	Ni-N(2)-C(8)	121.5 (4)
C(2)-C(1)-C(2*)	125.5 (8)	C(8)-N(2)-C(8*)	117.0 (7)
C(1)-C(2)-C(3)	116.5 (7)	N(2)-C(8)-C(9)	122.9 (8)
C(1)-C(2)-C(5)	117.1 (6)	C(8)-C(9)-C(10)	119.9 (8)
C(3)-C(2)-C(5)	126.5 (7)	C(9)-C(10)-C(9*)	117.4 (8)
C(2)-C(3)-C(4)	119.5 (8)	Ni-N(3)-C(11)	168.7 (5)
C(3)-C(4)-C(3*)	122.6 (8)	N(3)-C(11)-S(1)	178.3 (6)

is a diamagnetic species, has been achieved according to the reaction of eq 1. However, attempting to prepare **4**

$$[Ni^{II}\{C_6H_3(CH_2NMe_2)_2\text{-}o,o'\}Br] \xrightarrow[\text{b. } NH_4NCS \text{ excess}]{\text{a. } Ag^+} [Ni^{II}\{C_6H_3(CH_2NMe_2)_2\text{-}o,o'\}NCS] \quad (1)$$

3

by the sequence of route ii in Scheme I (using $AgBF_4$ and NH_4NCS) resulted in the isolation of a CH_2Cl_2 and acetone-soluble thick green oil presumed to be **5a**. Treatment of a solution of **5a** in CH_2Cl_2/toluene with excess pyridine provided dark green poorly soluble crystals of **5b**. Elemental microanalytical data for **5b** were consistent with a Ni{$C_6H_3(CH_2NMe_2)_2$-*o,o'*}$(NCS)_2$(py) stoichiometry, and this information taken together with the fundamental differences between ESR spectra of **1a–e** and those of **5a** and **5b** (vide infra) prompted a crystallographic study of the latter complex. Although this study (see below) confirmed that the pyridine was coordinated to the Ni(III) center in the solid state, there is good reason to believe that in CH_2Cl_2 solution **5b** is in equilibrium with [Ni{C_6H_3-$(CH_2NMe_2)_2$-*o,o'*}$(NCS)_2$] (**4**)[13] and free pyridine. The comparability of the IR (ν_{CN}), UV, and ESR spectra of **5a**

(10) "International Tables for X-ray Crystallography"; Kynoch Press: Birmingham, England 1974; Vol. IV.

(11) Compounds **1d** and **1e** have ESR data similar to those of **1a–c** and can also be synthesized directly from the reaction of **1a–c** in acetone/H_2O mixture with excess $AgNO_3$ and $AgNO_2$, respectively. Full synthetic and spectroscopic data for **1a–e** will be published.

(12) **3**: olive-green solid; air stable; ^1H NMR (30 °C, C_6D_6, δ) 7.0 (m, 3, C_6H_3), 2.83 (s, 4, CH_2), 2.05 (s, 12, NMe_2); IR (KBr) ν_{NCS} 2090 cm^{-1}; Anal. Found (Calcd) for $C_{13}H_{19}NiN_2S$: C, 50.7 (50.7); H, 6.2 (6.2); N, 13.7 (13.6); S, 10.4 (10.4).

(13) A brown extremely hygroscopic powder (most likely **4**) obtained by heating **5b** in vacuo at 120 °C is now under investigation.

and **5b** (vide infra) strongly suggests that **5a** is [Ni^{III}-{$C_6H_3(CH_2NMe_2)_2$-*o,o'*}$(NCS)_2(H_2O)$] though it should be noted that full characterization of this species is not yet complete.

C. Description of the Structure of [Ni{C_6H_3-$(CH_2NMe_2)_2$-*o,o'*}$(NCS)_2$(py)] (5b). The molecular geometry along with the adopted numbering scheme is shown in Figure 1, and relevant bond distances and angles are given in Table III. In **5b**, the Ni(III) center is hexacoordinate, the metal being bonded to two mutually trans N-bonded NCS ligands, the N,N',C-coordinated $C_6H_3(CH_2NMe_2)_2$-*o,o'* ligand (with the two hard N donors of the CH_2NMe_2 side arms coordinating trans to each other), and a pyridine molecule trans to C(1) of the terdentate system. The only significant distortion from a true octahedral geometry lies in the N(1)–Ni–N(1*) angle of 162.2 (2)° resulting from the constraints of the two five-membered NiNCCC(1) chelate rings. The latter rings show the "twofold axis" type puckering found in complexes of $C_6H_3(CH_2NMe_2)_2$-*o,o'* bonded to four- and six-coordinate metal centers.[14]

The bonding of the NCS ligands to the Ni center via the N atoms is to be expected for a "hard" Ni(III) center and both Ni–N distances of 1.965 (6) Å, and the slight bending of these anions (away from the pyridine), Ni–N(3)–C(11) = 168.7 (5)°, is not exceptional (cf. data in ref 15). It is difficult to conclude whether these distances are shorter or longer then expected (vide infra) in the absence of data for comparison. The bond distances and angles within the NCS anion are typical those expected for σ-N-bonded isothiocyanate ligands.[16]

The plane of the aryl ring and the pyridine molecule are mutually perpendicular but, as seen in a projection along the C(1)–Ni–N(2) axis (Figure 1b), are rotated about 70 and 20°, respectively, out of the coordination plane defined by C(1), N(3), N(3*), N(2), and Ni. This staggered arrangement would on steric grounds alone appear to be appropriate. The bond distances of the aryl group (Ni–C(1) = 1.900 (9) Å) and the pyridine (Ni–N(2) = 2.057 (8) Å) to the nickel are within the range expected for such bonds, and again the present data do not allow conclusions as to the shortening or/and lengthening effects as a result of the electronic features of the bonding (vide infra).

One geometrical feature, which is, however, worthy of comment, is the Ni–N(1) [and Ni–N(1*)] distances of 2.207 (6) Å for the amine bonding of the terdentate ligand. This Ni–N bond can be considered to be long when compared to the corresponding distance in either the Ni(II) species [Ni{$C_6H_3(CH_2NMe_2)_2$-*o,o'*}(O_2CH)] [1.975 (2) Å (mean)][8] or the Ni(III) species [Ni{$C_6H_3(CH_2NMe_2)_2$-*o,o'*}I_2] [2.044 (4) Å (mean)].[6] The significance of the elongation of these Ni–N(amine) bonds with respect to the location of the unpaired electron in this species is discussed below in combination with the spectroscopic data.

D. Spectroscopic Data for 5a and 5b. Compounds **5a** and **5b** have a distinctive bright green color, and a solution of **5a** (CH_2Cl_2 or acetone) retains this color. The bright green color obviously corresponds to the particular hexacoordinate structural type identified in the crystal

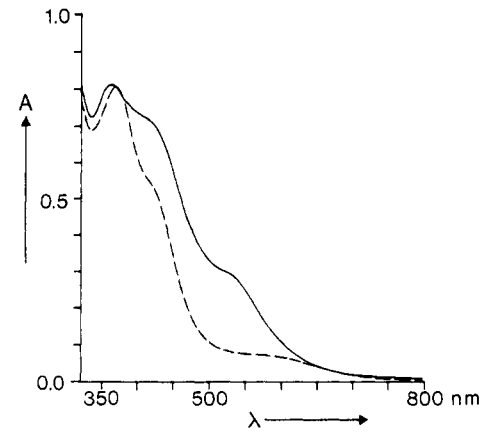

Figure 2. UV/vis spectra of **5b** (0.27×10^{-3} M) in CH_2Cl_2 without (full line) and with added pyridine (dotted line).

structure of **5b**. However, a solution of **5b** in CH_2Cl_2 at room temperature is, surprisingly, brownish in color, and the expected green color is only obtained either on cooling the solution (ca. −30 °C) or on the addition of a small excess of free pyridine. These observations suggest the following solution equilibrium: **5b** (green) ⇄ **4** (brown) + pyridine. This dissociation behavior is clearly reflected in the UV/vis spectra of **5b** (CH_2Cl_2) with and without added pyridine; see Figure 2. IR data for **5a** and **5b** (KBr) show the presence of only one ν_{CN} (2083 and 2083 cm^{-1}, respectively) consistent with the presence of a trans disposition of two coordinated NCS units. This data is comparable to the ν_{CN} value of 2089 cm^{-1} observed for **3**.

Probably the most informative data regarding the similarity of **5a** and **5b** is that of their very distinctive ESR spectra. The spectrum of **5a** (diglyme glass, 139 K) is shown in Figure 3, and it may be described to a first approximation as axial with $g_\parallel > g_\perp$ ($g_{zz} > g_{xx} \approx g_{yy}$; g_{zz} = 2.27 and $g_{xx}/g_{yy} \simeq 2.08$). The latter tensors are clearly broadened, and a second derivative spectrum (Figure 3b) resolves hyperfine splitting (8–9 lines) that can be attributed to coupling of an unpaired electron with four N atoms (a_N = 11 G). The spectrum of **5b** (solid, 143 K) gives tensor values of g_{zz} = 2.26 and $g_{xx}/g_{yy} \simeq 2.10$, but the lower solubility of this species has precluded good quality second derivative data.

For both **5a** and **5b** $\langle g \rangle > 2.14$, indicating that these species are low-spin d^7 situations in which the unpaired electron is associated primarily with the nickel ion. For **5b**, and hence by analogy for **5a** also, these ESR spectra arise from a Ni(III) ion in a distorted octahedral environment. For this d^7 ion Figure 4 shows a simplified energy level diagram for an octahedron (Figure 4b) with the most commonly tetragonal distortions arising from extension of two axial bonds (Figure 4a) and the rare situation in which there is extension of four coplanar bonds (Figure 4c), cf. ref 3. For a low-spin d^7 ion these two distortions give rise to a situation in which the unpaired electron is in either the d_{z^2} or $d_{x^2-y^2}$ orbital.[17] The former situation is commonly found with Co(II) and Ni(III), and, in theory[18] and practice,[19] this leads to ESR spectra in which $g_{xx}, g_{yy} > g_{zz}$. Sharp superhyperfine splitting on g_{zz}

(14) (a) Grove, D. M.; van Koten, G.; Louwen, J. N.; Noltes, J. G.; Spek, A. L.; Ubbels, H. J. C. *J. Am. Chem. Soc.* **1982**, *104*, 6609–6616. (b) Grove, D. M.; van Koten, G.; Spek, A. L. *J. Am. Chem. Soc.* **1982**, *104*, 4285–4286. (c) Terheijden, J.; van Koten, G.; de Booijs, J. L.; Ubbels, H. J. C.; Stam, C. H. *Organometallics* **1983**, *2*, 1882–1883. (d) van Koten, G.; Jastrzebski, J. T. B. H.; Noltes, J. G.; Spek, A. L.; Schoone, J. C.; *J. Organomet. Chem.* **1978**, *148*, 233–245.

(15) MacDougall, J. J.; Nelson, J. H.; Babich, M. W.; Fuller, C. C.; Jacobson, R. A. *Inorg. Chim. Acta* **1978**, *27*, 201–208.

(16) Norbury, A. H. *Adv. Inorg. Chem. Radiochem.* **1975**, *17*, 231–386.

(17) Orgel, L. E. "An Introduction to Transition-Metal Chemistry Ligand Field Theory"; Methuen: London, 1963; pp 53–68; Goodman, A.; Raynor, J. B. *Adv. Inorg. Chem. Radiochem.* **1970**, *13*, 135–162.

(18) Maki, A. H.; Edelstein, N.; Davidson, A.; Holm, R. H. *J. Am. Chem. Soc.* **1964**, *86*, 4580–4587.

(19) Good illustrative examples of ESR spectra for low-spin d^7 Ni(III) complexes in which the unpaired electron is in the d_{z^2} orbital are given by: Lappin, A. G.; Murray, C. K.; Magerum, D. W. *Inorg. Chem.* **1978**, *17*, 1630–1634.

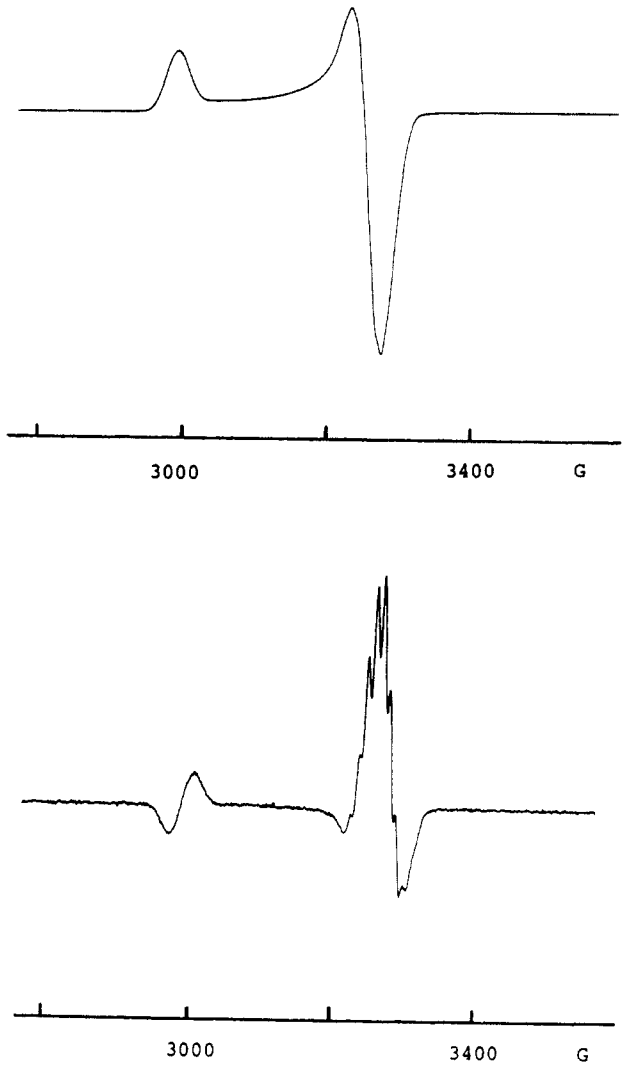

Figure 3. ESR spectrum **5a** in diglyme glass at 139 K (top) and its second derivative (below).

has been found for the z axis halogen donor X in square-pyramidal [Ni{$C_6H_3(CH_2NMe_2)_2$-o,o'}X$_2$][6,20] (X = Cl, Br, or I). Clearly this is not the situation pertaining in **5a** and **5b** and the unexpected d^2_{xy}, d^2_{xz}, d^2_{yz}, $d^1_{x^2-y^2}$, $d^0_{z^2}$ configuration must be considered as likely. A similar situation has recently been described for a series of bis(dipeptide)nickel(III) complexes which long-lived species in neutral solution are generated by oxidation of the corresponding nickel(II) complexes.[3]

(20) In square-pyramidal [Co{$C_6H_3(CH_2NMe_2)_2$-o,o'}X(pyridine)] $g_x,g_y > g_z$ with an eight-line pattern with A_z^{Co} = 70 G and a superhyperfine splitting of the z axis N pyridine atom of 9 G: van der Zeijden A. A. H.; van Koten, G., to be submitted for publication.

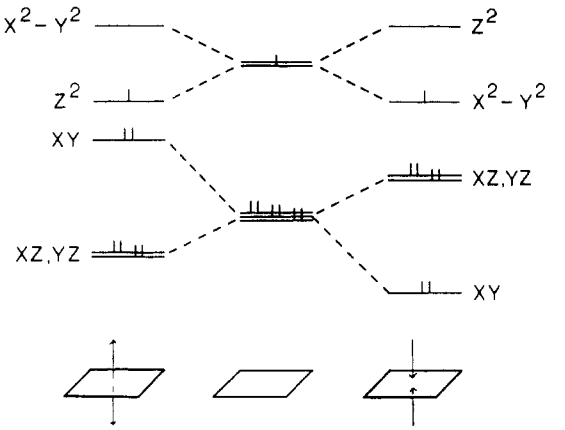

Figure 4. Schematic orbital schemes for various d^7 Ni(III) coordination geometries.

The different ligating groups present in **5b** make positive identification of geometric distortions fairly difficult and hence correlation of g with the molecular axis system somewhat tentative. Certainly discrimination of the x and y axes in the absence of further information is not possible. However, the long Ni–N(1) distance of the amino ligand suggests this bond to be closely associated with either the x or y axis. Furthermore, since the multiplicity of $g_{xx}g_{yy}$ in the ESR spectrum of **5a** is indicative of superhyperfine splitting from four N atoms ($a_N \simeq 11$ G), we conclude that the Ni–N(3)(isothiocyanate) bonds define the other axis of the x,y pair. This definition of the axis system has the z axis then running through the C(1)–Ni–N(pyridine) bonds (see Figure 1a), which assignment is supported by the absence of any coupling of the unpaired electron with the z axis ligands. It must be noted that since the ESR spectra point to a compressed tetragonal octahedral geometry for **5a** and **5b**, it is the bonds along the z axis that are shortened in these compounds; i.e., obviously the C(1)–Ni and Ni–N(py) distances are shorter than would be anticipated in the absence of this electronic effect. Further studies are clearly needed to assess this.

Registry No. **1b**, 84520-52-5; **1d**, 99532-40-8; **1e**, 99532-41-9; **3**, 99532-38-4; **5a**, 99532-39-5; **5b**, 99532-42-0; [Ni{$C_6H_3(CH_2NMe_2)_2$-o,o'}Br], 84500-93-6.

Supplementary Material Available: Tables of positional and thermal parameters for all atoms and their esd's in parentheses and observed and calculated structure factors as well as a stereo ORTEP plot (20% probability elipsoids) of (pyridine)bis(isothiocyanato)[o,o'-bis{(dimethylamino)methyl}-phenyl]nickel(III) (8 pages). Ordering information is given on any current masthead page.

Metal Atom Synthesis of Metallaboron Clusters. 8. Synthesis of New Cobalt, Iron, and Nickel Clusters Derived from 2,6-$C_2B_7H_{11}$. Structural Characterization of 2-[η^6-$C_6(CH_3)_3H_3$]Fe-1,6-$C_2B_7H_9$, 6-[η^6-$C_6(CH_3)_3H_3$]Fe-9,10-$C_2B_7H_{11}$, and 5,7,8-$(CH_3)_3$-11,7,8,10-[η^3-$C_4(CH_3)_4H$]$NiC_3B_7H_7$

James J. Briguglio and Larry G. Sneddon*

Department of Chemistry and the Laboratory for Research on the Structure of Matter, University of Pennsylvania, Philadelphia, Pennsylvania 19104

Received June 14, 1985

The reactions of thermally generated cobalt, iron, or nickel atoms with the *nido*-carborane 2,6-$C_2B_7H_{11}$ and either cyclopentadiene, toluene, mesitylene, or 2-butyne were explored and found to yield a number of unique metallacarborane clusters. Reaction of the carborane with cobalt atoms and cyclopentadiene gave two new cobaltacarborane clusters 2-(η-C_5H_5)Co-1,4-$C_2B_7H_9$ (I) and 4-(η-C_5H_5)Co-2,3-$C_2B_7H_{13}$ (II) along with the known compounds 2-(η-C_5H_5)Co-6,9-$C_2B_7H_9$ and 8-(η-C_5H_5)Co-6,7-$C_2B_7H_{11}$. Reaction of 2,6-$C_2B_7H_{11}$ with iron atoms and toluene gave the closo η^6-arene complexes 2-(η^6-$CH_3C_6H_5$)Fe-6,9-$C_2B_7H_9$ (III) and 2-(η^6-$CH_3C_6H_5$)Fe-1,6-$C_2B_7H_9$ (IV) while reaction with mesitylene gave both closo, 2-[η^6-$(CH_3)_3C_6H_3$]Fe-1,6-$C_2B_7H_9$ (V), and nido, 6-[η^6-$(CH_3)_3C_6H_3$]Fe-9,10-$C_2B_7H_{11}$ (VI), complexes. The structures of V and VI were confirmed by single-crystal X-ray crystallographic studies. Crystal data for V: space group $P2_1/m$; $Z = 2$; $a = 8.179$ (4) Å, $b = 10.952$ (3) Å, $c = 8.949$ (5) Å; $\beta = 114.65$ (3)°; $V = 728.6$ Å^3. The structure was refined to a final $R = 0.042$ and $R_w = 0.049$ for the 1243 reflections that had $F_o^2 > 3\sigma(F_o^2)$. Crystal data for VI: space group $P2_12_12_1$; $Z = 4$; $a = 9.291$ (4) Å, $b = 11.688$ (6) Å, $c = 13.524$ (2) Å; $\beta = 90.02$ (3)°; $V = 1468.6$ Å^3. The structure was refined to a final $R = 0.056$ and $R_w = 0.055$ for the 1180 reflections having $F_o^2 > 3\sigma(F_o^2)$. The reaction of 2,6-$C_2B_7H_{11}$ with nickel atoms, toluene, and 2-butyne was found to produce the unique metallacarborane cluster 5,7,8-$(CH_3)_3$-11,7,8,10-[η^3-$C_4(CH_3)_4H$]$NiC_3B_7H_7$ (VII). A single-crystal X-ray study of the compound proved it to have a sandwich-type structure in which a nickel atom is bonded to both a η^3-cyclobutenyl group and a three-carbon carborane. Furthermore, the nickelacarborane cage has a slip distortion resulting in an open-cage geometry rather than the closo structure predicted by simple electron-counting rules. Crystal data for VII: space group $P2_1/n$; $Z = 4$; $a = 9.537$ (3) Å, $b = 13.892$ (5) Å, $c = 14.695$ (4) Å; $\beta = 106.83$ (2)°; $V = 1863.7$ Å^3. The structure was refined to a final $R = 0.072$ and $R_w = 0.065$ for the 1473 reflections that have $F_o^2 > 3\sigma(F_o^2)$.

Introduction

Work in our laboratory has shown that metal atom reaction techniques can be successfully applied to the synthesis of new types of polyhedral metallaboron compounds not attainable by using more conventional synthetic procedures. Much of our previous work has employed reactive small cage systems such as B_5H_9, B_6H_{10}, or *nido*-2,3-$(C_2H_5)_2C_2B_4H_6$ as reactants and has resulted in the production of a variety of new metallaborane,[1] -carborane,[1-4] and -thiaborane[5,6] clusters. Our recent work[7] reporting the synthesis of new types of (η^6-arene)ferraborane compounds, as well as the first example of a ferraoxaborane cluster, derived from decaborane(14) demonstrated that these techniques can also be used to generate new types of metallaboron clusters from higher boron cage systems. We are now further investigating such possibilities and report here the synthesis and structural characterization of a number of unique metal–boron clusters derived from the *nido*-carborane 2,6-$C_2B_7H_{11}$.[8]

Experimental Section

Materials and Procedures. Iron, cobalt, and nickel were obtained from Alfa Products/Ventron Division. Mesitylene and toluene were obtained from Baker Chemical Co. and MCB Inc. respectively. Cyclopentadiene was distilled from dicyclopentadiene. The carborane 2,6-$C_2B_7H_{11}$ was prepared by using the method of Plešek, Heřmánek, and Štibr.[9a,b] All other reagents were commercially obtained and used as received. Preparative thin-layer chromatography was conducted on 0.5 mm (20 × 20 cm) silica gel F-254 plates (Merck).

Boron-11 and proton Fourier transform NMR spectra at 32.1 and 100 MHz, respectively, were obtained on a JEOL PS-100 spectrometer equipped with the appropriate decoupling accessories. Proton NMR spectra, at 250 MHz, were obtained on a Bruker WH-250 Fourier transform spectrometer. Boron-11 and proton NMR spectra at 64.2 and 200 MHz, respectively, were obtained on an IBM WP200SY Fourier transform spectrometer. Boron-11 NMR spectra, at 115.5 MHz, were obtained on a Bruker WH-360 Fourier transform spectrometer located in the Mid-Atlantic Regional NMR Facility. All boron-11 chemical shifts

(1) Zimmerman, G. J.; Hall, L. W.; Sneddon, L. G. *Inorg. Chem.* **1980**, *19*, 3642–3650.
(2) Micciche, R. P.; Sneddon, L. G. *Organometallics* **1983**, *2*, 674–678.
(3) Micciche, R. P.; Briguglio, J. J.; Sneddon, L. G. *Organometallics* **1984**, *3*, 1396–1402.
(4) Briguglio, J. J.; Sneddon, L. G. *Organometallics* **1985**, *4*, 721–726.
(5) Zimmerman, G. J.; Sneddon, L. G. *J. Am. Chem. Soc.* **1981**, *103*, 1102–1111.
(6) Micciche, R. P.; Carroll, P. J.; Sneddon, L. G. *Organometallics* **1985**, *4*, 1619–1623.
(7) Micciche, R. P.; Briguglio, J. J.; Sneddon, L. G. *Inorg. Chem.* **1984**, *23*, 3992–3999.
(8) The compounds described herein have been numbered according to the recently proposed polyhedral cage nomenclature system. See: (a) Casey, J. B.; Evans, W. J.; Powell, W. H. *Inorg. Chem.* **1981**, *20*, 1333–1341. (b) Casey, J. B.; Evans, W. J.; Powell, W. H. *Inorg. Chem.* **1983**, *22*, 2228–2235. (c) *Ibid.* **1983**, *22*, 2236–2245.
(9) (a) Plešek, J.; Heřmánek, S.; Štibr, B. *Inorg. Synth.* **1983**, *22*, 231–234. (b) *Ibid.* **1983**, *22*, 237–239.

0276-7333/86/2305-0327$01.50/0

were referenced to $BF_3{\cdot}O(C_2H_5)_2$ (0.0 ppm) with a negative sign indicating an upfield shift. All proton chemical shifts were measured relative to internal residual benzene from the lock solvent (99.5% C_6D_6) and then referenced to Me_4Si (0.00 ppm).

The 2-D ^{11}B–^{11}B NMR spectra of 4-(η-C_5H_5)Co-2,3-$C_2B_7H_{13}$ (II) were obtained at 64.2 MHz (Bruker Aspect 2000A with DisNMR version 820601 software) using a ^{11}B shift correlated COSY experiment with N-type selection parameters. The sweep width in the F_2 direction was 10000 and that in the F_1 direction was 5000. A total of 128 increments with an increment size of 0.1 ms were collected, each slice having 512 F_2 data points. The data were zero filled once in the F_1 direction and subjected to 2-D FT transformation with sine-bell apodization in both domains.[10] A total of 160 scans were taken for each increment and the recycle time was 0.1 s.

High- and low-resolution mass spectra were obtained on a Hitachi Perkin-Elmer RMH-2 mass spectrometer and/or a VG Micromass 7070H mass spectrometer interfaced to a Kratos DS50S data system. Infrared spectra were obtained on a Perkin-Elmer 337 spectrophotometer. The melting points are uncorrected.

The metal atom apparatus employed in these studies was based on a design by Klabunde[11a] and is described elsewhere.[1,11b] The rotary metal atom apparatus used was purchased from Kontes (Model No. K-927550) and modified according to a design published by Ittel and Tolman.[12]

Reaction of Cobalt Vapor with C_5H_6 and 2,6-$C_2B_7H_{11}$. A solution of 1.0 g of 2,6-$C_2B_7H_{11}$ dissolved in 10 mL of cyclopentadiene was placed at the bottom of the static reactor. Cobalt vapor (~0.75 g) was cocondensed with 20 mL of C_5H_6. Following metal deposition, the matrix was warmed to room temperature and stirred for 1 h. The mixture was separated by TLC on silica gel using a 50% hexanes in benzene solution resulting in the isolation of the following new compounds: I, 2-(η-C_5H_5)Co-1,4-$C_2B_7H_9$, R_f 0.66, red, 2.0 mg, decomp mp 58 °C, mass measurement calcd for $^{12}C_7{}^1H_{14}{}^{11}B_7{}^{59}Co$ 234.1075, found 234.1094 (major fragment at m/e 124 ((η-C_5H_5)Co)); II, 4-(η-C_5H_5)Co-2,3-$C_2B_7H_{13}$, R_f 0.48, yellow, 7.9 mg, mp 146–149 °C; mass measurement calcd for $^{12}C_7{}^1H_{18}{}^{11}B_7{}^{59}Co$ 238.1387, found 238.1400 (major fragment at m/e 124 ((η-C_5H_5)Co)).

In addition, four known compounds were also isolated, two were characterized by their ^{11}B NMR and mass spectral data: 2-(η-C_5H_5)Co-6,9-$C_2B_7H_9$[13a] (10 mg) and 8-(η-C_5H_5)Co-6,7-$C_2B_7H_{11}$[13b] (5 mg). On the basis of high-resolution mass spectral data and color, the other two compounds (both isolated in <1-mg yields) are consistent with the following: 4,7-(η-C_5H_5)$_2$$Co_2$-2,3-$C_2B_7H_9$[14] and 2,3,5-($\eta$-$C_5H_5$)$_3$$Co_3$-1,7-$C_2B_7H_9$.[15]

Isomerization of 2-(η-C_5H_5)Co-1,4-$C_2B_7H_9$. A 10-mg sample of 2-(η-C_5H_5)Co-1,4-$C_2B_7H_9$ was heated at 70 °C for 12 h in a sealed Pyrex tube under vacuum. The resulting product was the red 2-(η-C_5H_5)Co-1,6-$C_2B_7H_9$ isomer identified by ^{11}B NMR.

Reaction of Iron with Toluene and 2,6-$C_2B_7H_{11}$. Approximately 1.5 g of iron was placed in an integral tungsten alumina crucible in the static reactor and iron vapor (~0.75 g) was generated by electrical heating (~8.0 V, ~60 A). At the bottom of the flask was placed 1.5 g of 2,6-$C_2B_7H_{11}$ along with 15 mL of toluene. The flask was evacuated and metal vapor condensed with 15 mL of toluene over a 1.5-h period onto the walls of the reactor, which was maintained at −196 °C. After metal deposition was completed, the matrix was warmed to −78 °C and stirred for 0.5 h. The solution was then allowed to warm to room temperature and stirred for an additional 1 h. Separation of the crude product mixture in a manner similar to that described above, using a 50% hexanes in benzene solution, resulted in three bands (R_f 0.98, 0.58, and 0.52).

An additional separation of band 2 using a 30% hexanes in benzene solution gave as the major products: III, 2-(η^6-$CH_3C_6H_5$)Fe-6,9-$C_2B_7H_9$, R_f 0.18, yellow, 7.1 mg, mass measurement calcd for $^{12}C_9{}^1H_{17}{}^{11}B_7{}^{56}Fe$ 258.1343, found 258.1333 (major fragment at m/e 148 ((η^6-$CH_3C_6H_5$)Fe)); IV, 2-(η^6-$CH_3C_6H_5$)Fe-1,6-$C_2B_7H_9$, R_f 0.13, red, 8.7 mg, decomp mp 154 °C, mass measurement calcd for $^{12}C_9{}^1H_{17}{}^{11}B_7{}^{56}Fe$ 258.1343, found 258.1333 (major fragment at m/e 148 ((η^6-$CH_3C_6H_5$)Fe)).

Isomerization of 2-(η^6-$CH_3C_6H_5$)Fe-6,9-$C_2B_7H_9$. A 5-mg sample of the 2-(η^6-$CH_3C_6H_5$)Fe-6,9-$C_2B_7H_9$ (yellow) was sealed in a Pyrex tube under vacuum and heated at 75 °C for 1 h. This produced a red compound which was identified by its spectral data as 2-(η^6-$CH_3C_6H_5$)Fe-1,6-$C_2B_7H_9$.

Reaction of Iron Vapor with Mesitylene and 2,6-$C_2B_7H_{11}$. A solution of 1 g of 2,6-$C_2B_7H_{11}$ in 200 mL of mesitylene was placed in the rotary metal atom reactor. After degassing, the solution was warmed to −40 °C and maintained at that temperature for the entire reaction. Iron vapor (~0.75 g) was condensed into the rotating solution over a 1-h period. Upon completion of metal deposition, the dark slurry was warmed to room temperature and stirred for an additional 0.5 h. Excess mesitylene was removed in vacuo, and the reactor flask was flushed with N_2(g). The remaining black residue was extracted with methylene chloride, filtered through a course frit, and concentrated. The crude product mixture was initially separated by TLC on silica gel by using benzene resulting in two bands (R_f 0.95 and 0.76). Further separation of band 2 using a 50% hexanes in benzene solution gave as the major products: V, 2-[η^6-$(CH_3)_3C_6H_3$]Fe-1,6-$C_2B_7H_9$, R_f 0.31, pink, 1.3 mg, mp 165–180 °C dec, mass measurement calcd for $^{12}C_{11}{}^1H_{21}{}^{11}B_7{}^{56}Fe$ 286.1658, found 286.1662 (major fragment at m/e 176 ([η^6-$(CH_3)_3C_6H_3$]Fe)); VI, 6-[η^6-$(CH_3)_3C_6H_3$]Fe-9,10-$C_2B_7H_{11}$, R_f 0.35, red, 3.2 mg, mp 134 °C, mass measurement calcd for $^{12}C_{11}{}^1H_{23}{}^{11}B_7{}^{56}Fe$ 288.1814, found 288.1765 (major fragment at m/e 176 ([η^6-$(CH_3)_3C_6H_3$]Fe)). An additional compound was isolated from the base line, using a methylene chloride solution, from the original separation in insufficient amounts (<1 mg) to allow complete characterization. However, high-resolution mass spectral data indicates the formula [η^6-$(CH_3)_3C_6H_3$]$FeC_2B_6H_8$: mass measurement calcd for $^{12}C_{11}{}^1H_{20}{}^{11}B_6{}^{56}Fe$ 274.1485, found 274.1497.

Reaction of Nickel with Toluene, 2,6-$C_2B_7H_{11}$, and 2-Butyne. A solution of 1.0 g of 2,6-$C_2B_7H_{11}$ dissolved in 10 mL of toluene was placed at the bottom of the static reactor. Nickel vapor (~0.75 g) was cocondensed with 20 mL of toluene and 10 mL of 2-butyne at −196 °C. After metal deposition was complete, the matrix was warmed to −78 °C and stirred for 0.5 h. The resulting slurry was then allowed to warm to room temperature and stirred for an additional 1 h. The black solution was filtered through a course frit, stirred with silica gel, and filtered again. Initial separation was obtained by a silica gel chromatography column using a 30% benzene in hexanes as the eluent. This resulted in the isolation of the compound VII: 5,7,8-$(CH_3)_3$-11,7,8,10-[η^3-$C_4(CH_3)_4H$]$NiC_3B_7H_7$, R_f 0.5, orange, 10.7 mg, mp 108 °C, mass measurement calcd for 332.2266, found 332.2291 (major fragment at m/e 109 ($C_4(CH_3)_4H$)). Also obtained in smaller amounts (1 mg) were [η^3-$C_4(CH_3)_4H$]Ni-(C_4H_9)-$(CH_3)_3C_3B_7H_6$, as suggested by spectral data and high-resolution mass spectrum, and [η^5-$C_5(CH_3)_5$]Ni-$(C_4H_9)C_2B_7H_9$, as suggested by high-resolution mass spectrum.

Crystallographic Data for 2-[η^6-$(CH_3)_3C_6H_3$]Fe-1,6-$C_2B_7H_9$ (V), 6-[η^6-$(CH_3)_3C_6H_3$]Fe-9,10-$C_2B_7H_{11}$ (VI), and 5,7,8-$(CH_3)_3$-11,7,8,10-[η^3-$C_4(CH_3)_4H$]$NiC_3B_7H_7$ (VII). Single crystals of V and VII were grown overnight by slow evaporation in air of methylene chloride/heptane solutions and a methylene chloride/hexane solution for compound VI. In each case, a suitable size crystal was mounted and transferred to the diffractometer. Refined cell dimensions and their standard deviations were obtained from least-squares refinement of 20–25 accurately centered reflections. See Table IV for crystal data.

Collection and Reduction of the Data. Diffraction data were collected at 295 K on an Enraf-Nonius four-circle CAD-4 (VII) diffractometer or a Picker FACS-I (V and VI) diffractometer employing Mo Kα radiation from a highly oriented graphite-crystal monochromator. The raw intensities were corrected for Lorentz

(10) Bax, A. "Two-Dimensional Nuclear Magnetic Resonance in Liquids"; Delft University Press: Delft, Holland, 1982.
(11) (a) Klabunde, K. J.; Efner, H. F. *Inorg. Chem.* **1975**, *14*, 789–791. (b) Freeman, M. B.; Hall, L. W.; Sneddon, L. G. *Inorg. Chem.* **1980**, *19*, 1132–1141.
(12) Ittel, S. D.; Tolman, C. A. *Organometallics* **1982**, *1*, 1432–1436.
(13) (a) Jones, C. J.; Francis, J. N.; Hawthorne, M. F. *J. Am. Chem. Soc.* **1972**, *94*, 8391–8399. (b) Callahan, K. P.; Lo, F. Y.; Strouse, C. E.; Sims, A. L.; Hawthorne, M. F. *Inorg. Chem.* **1974**, *13*, 2842–2847.
(14) (a) Plešek, J.; Štibr, B.; Heřmánek, S. *Chem. Ind. (London)* **1980**, *2*, 626–627. (b) Štibr, B.; Heřmánek, S.; Plešek, J.; Baše, K.; Zakharova, I. A. *Chem. Ind. (London)* **1980**, *11*, 468.
(15) Evans, W. J.; Hawthorne, M. F. *Inorg. Chem.* **1974**, *13*, 869–874.

Table I. ^{11}B NMR Data

compound	δ (J, Hz)	rel areas
2-(η-C_5H_5)Co-1,4-$C_2B_7H_9$ (I)[c]	27.5 (110)	1
	9.3 (169)	2
	5.6 (173)	2
	-13.6 (177)	2
4-(η-C_5H_5)Co-2,3-$C_2B_7H_{13}$ (II)[c]	13.1 (141)	1
	0.2 (148)	1
	-7.9 (148)	1
	-10.1 (148)	1
	-12.3 (133, 54)	1
	-18.7 (134)	1
	-32.5 (154)	1
2-(η^6-$CH_3C_6H_5$)Fe-6,9-$C_2B_7H_9$ (III)[b]	81.3 (148)	1
	-2.9 (155)	1
	-10.6 (146)	2
	-22.9 (167)	1
	-30.2 (148)	2
2-(η^6-$CH_3C_6H_5$)Fe-1,6-$C_2B_7H_9$ (IV)[b]	20.4 (180)	1
	-3.9 (143)	1
	-8.2 (153)	1
	-19.8 (153)	1
	-26.2 (107)	1
	-26.9 (156)	1
	-33.7 (153)	1
2-[η^6-$(CH_3)_3C_6H_3$]Fe-1,6-$C_2B_7H_9$ (V)[b]	20.2 (155)	1
	-4.5 (118)	1
	-7.8 (150)	1
	-19.5 (131)	1
	-25.1 (168)	1
	-26.6 (156)	1
	-33.1 (171)	1
6-[η^6-$(CH_3)_3C_6H_3$]Fe-9,10-$C_2B_7H_{11}$ (VI)[b]	24.7 (141)	1
	10.2 (150)	1
	8.8 (147)	1
	4.3 (137)	1
	1.9[d]	1
	-16.4 (110)	1
	-17.6 (146)	1
5,7,8-$(CH_3)_3$-11,7,8,10-[η^3-$C_4(CH_3)_4H$]-$NiC_3B_7H_7$ (VII)[b]	8.1 (158)	1
	-1.2 (150)	1
	-5.0	1
	-5.9 (184)	1
	-7.3 (161)	1
	-13.9 (167)	1
	-15.3 (159)	1

[a] All complexes were run in CH_2Cl_2 with internal C_6D_6 lock material. [b] ^{11}B NMR spectrum at 115.5 MHz. [c] ^{11}B NMR spectrum at 64.2 MHz. [d] Unresolved multiplet.

Table II. ^1H NMR Data

compound[a]	δ[b] (rel area)	assignt
I[c]	4.36 (5)	C_5H_5
II[c]	4.46 (5)	C_5H_5
	0.47 (1)	CH_e
	0.05 (1)	CH_a
	-1.89 (1)	CH_e
	-2.47 (1)	CH_a
	-3.12 (1)	B-H-B
	-17.50 (1)[e] (J_{BH} = 63 Hz)	Co-H-B
III[c]	4.78 (5)[e]	C_6H_5
	1.51 (3)	CH_3
IV[c]	4.63 (5)[e]	C_6H_5
	1.53 (3)	CH_3
V[c]	4.45 (3)	C_6H_3
	1.60 (9)	CH_3
VI[c]	4.66 (3)	C_6H_3
	1.78 (9)	CH_3
	-13.75 (1) (J_{BH} = 56 Hz)	Fe-H-B
	-18.45 (1) (J_{BH} = 61 Hz)	Fe-H-B
VII[d]	2.24 (3)	CH_3
	1.98 (3)	CH_3
	1.52 (3)	CH_3
	1.28 (3)	CH_3
	1.11 (3)	CH_3
	0.79 (3)	CH_3
	0.28 (3)	CH_3

[a] Complex run in C_6D_6. [b] Shift relative to $(CH_3)_4Si$ (positive sign indicates downfield shift). [c] ^1H NMR spectrum at 250 MHz. [d] ^1H NMR spectrum at 360 MHz. [e] Center for multiplet.

Table III. Infrared Data

compound[a,b]	IR absorptns, cm^{-1}
I	3100 (w), 2925 (vw), 2545 (s), 1425 (m), 1085 (w), 1060 (w), 1000 (w, br), 975 (w), 880 (w), 845 (s), 750 (w, br), 670 (sh), 620 (m, br)
II	3100 (s), 3025 (w), 2950 (w, br), 2505 (vs), 1401 (s), 1050 (br), 960 (w), 900 (sh), 855 (sh), 840 (m), 800 (sh), 780 (m), 730 (w), 670 (sh), 580 (w)
III	2505 (s), 1475 (m), 1400 (w), 1035 (w), 1010 (w), 950 (w), 920 (w), 835 (w)
IV	2503 (s), 1475 (w), 1400 (w), 1250 (w), 1090 (w), 1040 (w), 840 (w)
V	2580 (sh), 2540 (s), 1450 (w), 1390 (w), 1250 (w), 620 (w, br)
VI	2600 (sh), 2500 (m), 1650 (w), 1450 (w), 1399 (w), 990 (w), 890 (m), 810 (w, br), 620 (w, br)
VII	2925 (m), 2575 (sh), 2525 (s), 1450 (m), 1399 (m), 1350 (sh), 1301 (m), 1120 (w), 1080 (w), 1035 (w), 990 (w), 970 (w), 820 (w), 670 (w), 620 (w, br)

[a] KBR pellet. [b] Perkin-Elmer 337.

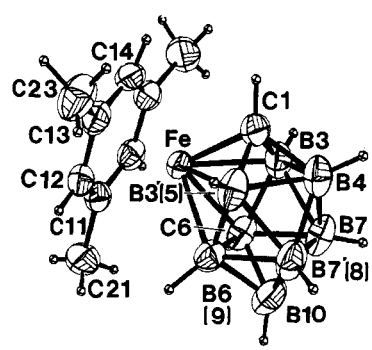

Figure 1. ORTEP drawing of 2-[η^6-$(CH_3)_3C_6H_3$]Fe-1,6-$C_2B_7H_9$ (V).

and polarization effects by using the Enraf-Nonius program START.

Solution and Refinement of the Structure. All calculations were performed on a PDP 11/60 computer using the Enraf-Nonius structure package.[16] The full-matrix least-squares refinement was based on F, and the function minimized was $\sum w(|F_o| - |F_c|)^2$. The weights (w) were taken as $(4F_o/\delta(F_o)^2)^2$, where $|F_o|$ and $|F_c|$ are the observed and calculated structure factor amplitudes. The atomic scattering factors for non-hydrogen atoms were taken from Cromer and Waber[17] and those for hydrogen from Stewart.[18] The effects of anomalous dispersion were included in F_c by using Cromer and Iber's values[19] for $\Delta f'$ and $\Delta f''$. Agreement factors are defined as $R = \sum||F_o| - |F_c||/\sum|F_o|$ and $R_w = (\sum w(|F_o| - |F_c|)^2/\sum w|F_o|^2)^{1/2}$.

Three-dimensional Patterson syntheses gave the coordinates of the metal atoms. Subsequent Fourier maps led to the location of the remaining heavy atoms. Anisotropic refinement followed by a difference Fourier synthesis resulted in the location of all hydrogen atoms in V and VI and the cage hydrogens in VII. The positions of the remaining cyclobutenyl hydrogen atoms in VII were calculated and included (but not refined) in the structure factor calculations. Final refinements included numerical absorption corrections along with anisotropic thermal parameters for non-hydrogen atoms and fixed isotropic thermal parameters for the hydrogen atoms.

Final positional parameters are given in Tables V, VI, and VII, Intramolecular bond distances and selected bond angles are

(16) Enraf-Nonius Inc., Garden City Park, NY.
(17) Cromer, D. T.; Waber, J. T. "International Tables for X-Ray Crystallography"; Kynoch Press: Birmingham, England, 1974; Vol. IV.
(18) Stewart, R. F.; Davidson, E. R.; Simpson, W. T. *J. Chem. Phys.* **1965**, *42*, 3175-3187.
(19) Cromer, D. T.; Ibers, J. A. "International Tables for X-Ray Crystallography"; Kynoch Press: Birmingham, England, 1974; Vol. IV.

Table IV. Data Collection and Structure Refinement Information

	V	VI	VII
space group	$P2_1/m$	$P2_12_12_1$	$P2_1/n$
a, Å	8.179 (4)	9.291 (4)	9.537 (3)
b, Å	10.952 (3)	11.688 (6)	13.892 (5)
c, Å	8.949 (5)	13.524 (2)	14.695 (4)
β, deg	114.65 (3)	90.02 (3)	106.82 (2)
V, Å^3	728.6	1468.6	1863.7
Z	2	4	4
ρ(calcd), g cm^{-3}	1.298	1.288	1.182
cryst dimens, mm	0.07 × 0.10 × 0.40	0.05 × 0.13 × 0.40	0.12 × 0.20 × 0.30
mol formula	$B_7C_{11}H_{21}Fe$	$B_7C_{11}H_{23}Fe$	$B_7C_{14}H_{29}Ni$
mol wt	284.8	286.8	331.8
λ(Mo Kα), Å	0.710 73	0.710 73	0.710 73
scanning range, deg	$4 < 2\theta < 55$	$4 < 2\theta < 55$	$0 < 2\theta < 55$
scan mode	θ–2θ	θ–2θ	ω–2θ
$\pm h,\pm k,\pm l$ collected	−9,−14,±10	+12,+15,+17	±12,+18,−19
no. of measd intensities	1827	1971	4629
unique reflctns $F_o^2 > 3\sigma(F_o^2)$	1243	1180	1473
no. of variables	97	172	227
abs coeff μ, cm^{-1}	10.09	10.01	10.33
transmissn coeff			
max, %	93.90	99.68	88.30
min, %	83.38	94.72	73.23
R	0.0419	0.0557	0.0722
R_w	0.0488	0.0546	0.0653

Table V. Positional Parameters and Their Estimated Standard Deviation for 2-[η^6-$(CH_3)_3C_6H_3$]Fe-1,6-$C_2B_7H_9$ (V)

atom	x	y	z
Fe	0.14871 (8)	0.250	0.39821 (7)
C11	−0.1252 (6)	0.250	0.2237 (5)
C12	−0.0400 (4)	0.3592 (3)	0.2170 (3)
C13	0.1220 (4)	0.3616 (4)	0.1983 (3)
C14	0.1990 (6)	0.250	0.1889 (5)
C21	−0.2971 (6)	0.250	0.2469 (6)
C23	0.2135 (5)	0.4811 (4)	0.1967 (4)
C1	0.4010 (6)	0.250	0.5487 (5)
B10	0.1174 (8)	0.250	0.7551 (7)
B3	0.3190 (5)	0.3669 (4)	0.5964 (5)
B4	0.4612 (8)	0.250	0.7417 (7)
B7	0.3010 (6)	0.3331 (4)	0.7888 (4)
C6 (B6)	0.1106 (5)	0.3292 (4)	0.5948 (4)
HB3	0.353 (3)	0.453 (3)	0.582 (3)
HC6	0.004 (4)	0.400 (4)	0.558 (4)
HB4	0.598 (5)	0.250	0.820 (5)
HB7	0.355 (4)	0.398 (3)	0.884 (3)
HB10	0.015 (6)	0.250	0.787 (5)
HC1	0.491 (7)	0.250	0.506 (6)
HC12	−0.088 (3)	0.424 (3)	0.225 (3)
HC14	0.315 (6)	0.250	0.195 (5)
H21A	−0.298 (4)	0.325 (3)	0.312 (4)
H21B	−0.376 (8)	0.250	0.167 (7)

Table VI. Positional Parameters and Their Estimated Standard Deviation for 6-[η^6-$(CH_3)_3C_6H_3$]Fe-9,10-$C_2B_7H_{11}$ (VI)

atom	x	y	z
Fe	0.0656 (1)	0.1496 (1)	0.20578 (8)
C15	−0.1284 (8)	0.2151 (7)	0.2640 (6)
C14	−0.0561 (8)	0.2998 (6)	0.2131 (6)
C13	−0.0084 (9)	0.2825 (7)	0.1153 (6)
C12	−0.0389 (9)	0.1766 (7)	0.0702 (5)
C11	−0.1095 (8)	0.0884 (7)	0.1198 (6)
C16	−0.1526 (7)	0.1085 (7)	0.2175 (6)
C25	−0.1733 (9)	0.2339 (8)	0.3690 (7)
C23	0.070 (1)	0.3734 (7)	0.0612 (6)
C21	−0.137 (1)	−0.0253 (8)	0.0721 (7)
C9	0.3422 (8)	−0.0410 (7)	0.2879 (8)
B5	0.1791 (9)	0.154 (1)	0.3422 (7)
B2	0.268 (1)	0.2266 (9)	0.2409 (7)
B7	0.272 (1)	0.122 (1)	0.1447 (7)
B3	0.4296 (9)	0.1483 (9)	0.2163 (6)
B1	0.374 (1)	0.1701 (9)	0.3396 (7)
B4	0.4717 (9)	0.050 (1)	0.3080 (9)
B8	0.3943 (9)	0.0092 (9)	0.1960 (8)
C10	0.3127 (9)	0.0384 (8)	0.3685 (7)
HB3	0.502 (8)	0.209 (6)	0.173 (5)
HC10	0.328 (8)	0.013 (6)	0.449 (5)
HB1	0.430 (9)	0.217 (5)	0.395 (5)
HBC8	0.422 (8)	−0.036 (5)	0.147 (5)
HB4	0.587 (8)	0.032 (5)	0.332 (4)
HB9	0.358 (7)	−0.100 (6)	0.297 (5)
HC14	−0.025 (8)	0.380 (5)	0.242 (5)
HC16	−0.171 (8)	0.045 (6)	0.254 (4)
HB2	0.288 (7)	0.320 (5)	0.234 (4)
HB7	0.294 (8)	0.146 (6)	0.064 (5)

presented in Tables VIII–XIII. Figures 1, 2, and 3 give ORTEP views of V, VI, and VII, respectively.

Listing of final thermal parameters, selected molecular planes, and observed and calculated structure factors are available as supplementary material.

Results and Discussion[8]

The *nido*-carborane 2,6-$C_2B_7H_{11}$ was first synthesized by Rietz and Schaeffer[20] in 1973; however, it has been only recently that a good high yield synthesis of this compound has become available.[9a,b] As a result, the transition-metal chemistry of this compound has been largely unexplored. In fact, while there are a number of known C_2B_7 metallacarboranes which have been obtained from either the *arachno*-carborane 6,8-$C_2B_7H_{13}$ or the *closo*-carborane 4,6-$C_2B_7H_9$, there appear to be only three complexes 4,7-(η-$C_5H_5)_2Co_2$-2,3-$C_2B_7H_9$,[14a] 9,9-$(PPh_3)_2$-9,3,6-

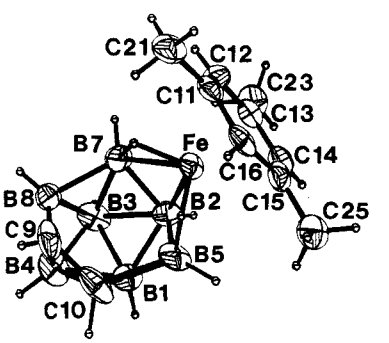

Figure 2. ORTEP drawing of 6-[η^6-$(CH_3)_3C_6H_3$]Fe-9,10-$C_2B_7H_{11}$ (VI).

(20) Rietz, R. R.; Schaeffer, R. *J. Am. Chem. Soc.* **1973**, *95*, 6254–6262.

Table VII. Positional Parameters and Their Estimated Standard Deviations for 5,7,8-$(CH_3)_3$-11,7,8,10-[η^3-$C_4(CH_3)_4H$]$NiC_3B_7H_7$ (VII)

atom	*x*	*y*	*z*
Ni	0.0947 (1)	0.38012 (9)	0.27705 (8)
C8	−0.1690 (9)	0.3529 (6)	0.1837 (6)
B9	−0.134 (1)	0.3628 (8)	0.3109 (6)
B2	0.043 (1)	0.2410 (8)	0.2074 (7)
C7	−0.0374 (8)	0.3299 (7)	0.1545 (6)
C10	0.0138 (9)	0.3261 (7)	0.3731 (5)
B4	−0.224 (1)	0.2631 (9)	0.2427 (8)
B3	−0.148 (1)	0.2346 (9)	0.1521 (8)
B6	0.068 (1)	0.2350 (8)	0.3380 (7)
B5	−0.111 (1)	0.2432 (8)	0.3537 (8)
B1	−0.080 (1)	0.1773 (8)	0.2604 (8)
C19	−0.026 (1)	0.3659 (7)	0.0601 (6)
C20	−0.282 (1)	0.4162 (7)	0.1245 (7)
C18	−0.166 (1)	0.1998 (8)	0.4387 (6)
C11	0.2072 (9)	0.4872 (7)	0.3582 (6)
C12	0.262 (1)	0.4524 (7)	0.2429 (6)
C13	0.1635 (9)	0.5120 (7)	0.2618 (6)
C14	0.350 (1)	0.4463 (8)	0.3480 (7)
C23	0.062 (1)	0.5868 (7)	0.2083 (8)
C24	0.424 (1)	0.3594 (9)	0.3933 (8)
C22	0.319 (1)	0.4355 (9)	0.1578 (7)
C21	0.180 (1)	0.5320 (8)	0.4421 (7)

Table VIII. Interatomic Distances (Å) for 2-[η^6-$(CH_3)_3C_6H_3$]Fe-1,6-$C_2B_7H_9$ (V)

Fe–C11	2.130 (4)	B10–B7	1.672 (7)
Fe–C12	2.087 (3)	B10–C6	1.657 (5)
Fe–C13	2.101 (3)	B10–B6	1.657 (4)
Fe–C14	2.078 (4)	B10–HB10	0.99 (4)
Fe–C1	1.938 (4)	B3–B4	1.850 (5)
Fe–B3	2.160 (3)	B3–B7	1.826 (5)
Fe–C6	2.098 (3)	B3–C6	1.748 (5)
Fe–B6	2.098 (0)	B3–B6	1.748 (4)
C11–C12	1.399 (4)	B3–HB3	1.01 (3)
C11–C21	1.504 (6)	B4–B7	1.785 (6)
C12–C13	1.403 (4)	B4–HB4	1.04 (4)
C13–C14	1.393 (3)	B7–C6	1.785 (5)
C13–C23	1.511 (4)	B7–B6	1.785 (3)
C1–B3	1.585 (5)	B7–HB7	1.06 (3)
C1–B4	1.586 (6)	C6–HC6	1.11 (3)
C1–HC1	0.96 (5)	B6–HB6	1.11 (3)

Table IX. Selected Interatomic Angles (deg) for 2-[η^6-$(CH_3)_3C_6H_3$]Fe-1,6-$C_2B_7H_9$ (V)

C11–C12–C13	122.2 (3)	Fe–C6–B10	123.1 (2)
C12–C13–C14	117.6 (3)	Fe–C6–B3	67.6 (2)
C12–C13–C23	120.9 (3)	Fe–C6–B7	116.8 (2)
C14–C13–C23	121.4 (3)	B10–C6–B3	115.8 (3)
Fe–C1–B3	74.9 (2)	B10–C6–B7	58.0 (3)
Fe–C1–B4	120.9 (3)	B3–C6–B7	62.2 (2)
B3–C1–B4	71.4 (2)	Fe–B6–B10	123.1 (1)
Fe–B3–C1	60.0 (2)	Fe–B6–B3	67.6 (1)
Fe–B3–B4	99.7 (2)	Fe–B6–B7	116.8 (1)
Fe–B3–B7	112.1 (2)	B10–B6–B3	115.8 (2)
Fe–B3–C6	63.9 (2)	B10–B6–B7	58.0 (2)
C1–B3–B4	54.4 (2)	B3–B6–B7	62.2 (2)
C1–B3–B7	107.5 (3)	B10–B7–B3	111.1 (3)
B4–B3–B7	58.1 (2)	B10–B7–B4	111.9 (3)
B4–B3–C6	99.7 (3)	B10–B7–C6	57.2 (2)
B7–B3–C6	59.9 (2)	B3–B7–B4	61.6 (2)
C1–B4–B3	54.3 (2)	B3–B7–C6	57.9 (2)
C1–B4–B7	109.4 (3)	B4–B7–C6	100.8 (3)
B3–B4–B7	60.3 (2)	B7–B10–B6	64.8 (2)

$PtC_2B_7H_{11}$,[14b] and 6,6-$(Et_3P)_2$-6,1,2-$CoC_2B_7H_9$,[21] which have been prepared directly from 2,6-$C_2B_7H_{11}$.

In the present study, the reactions of thermally generated cobalt, iron, or nickel atoms with *nido*-2,6-$C_2B_7H_{11}$

(21) Barker, G. K.; Garcia, M. P.; Green, M.; Pain, G. N.; Stone, F. G. A.; Jones, S. K. R.; Welch, A. J. *J. Chem. Soc., Chem. Commun.* **1981**, 652–653.

Table X. Interatomic Distances (Å) for 6-[η^6-$(CH_3)_3C_6H_3$]Fe-9,10-$C_2H_7H_{11}$ (VI)

Fe–C16	2.090 (6)	B1–B4	1.724 (12)
Fe–C15	2.111 (7)	B1–C10	1.686 (11)
Fe–C14	2.090 (6)	B2–B7	1.782 (11)
Fe–C13	2.094 (6)	B2–B3	1.793 (11)
Fe–C12	2.099 (6)	B2–B1	1.786 (11)
Fe–C11	2.124 (6)	B3–B1	1.765 (11)
Fe–B5	2.125 (7)	B3–B4	1.732 (11)
Fe–B2	2.134 (9)	B3–B8	1.682 (11)
Fe–B7	2.114 (8)	B4–B8	1.745 (11)
C11–C16	1.401 (9)	B4–C10	1.695 (10)
C11–C21	1.499 (9)	B5–B2	1.810 (11)
C12–C11	1.395 (8)	B5–B1	1.817 (10)
C13–C23	1.480 (8)	B5–C10	1.867 (11)
C13–C12	1.408 (8)	B7–B3	1.779 (10)
C14–C13	1.410 (8)	B7–B8	1.876 (11)
C15–C25	1.496 (9)	C9–B4	1.631 (10)
C15–C16	1.414 (9)	C9–B8	1.458 (11)
C15–C14	1.380 (8)	C9–C10	1.457 (10)

Table XI. Selected Interatomic Angles (deg) for 6-[η^6-$(CH_3)_3C_6H_3$]Fe-9,10-$C_2B_7H_{11}$ (VI)

B5–Fe–B2	50.3 (3)	B4–B3–B8	61.5 (5)
B5–Fe–B7	83.8 (3)	C9–B4–B3	98.5 (6)
B2–Fe–B7	49.6 (3)	C9–B4–B8	51.0 (5)
C16–C11–C21	120.4 (7)	C9–B4–C10	51.9 (4)
C12–C11–C21	121.9 (6)	B3–B4–B1	61.4 (5)
C12–C11–C16	117.7 (6)	B3–B4–B8	57.9 (5)
C13–C12–C11	122.4 (6)	B1–B4–C10	59.1 (5)
C14–C13–C12	118.0 (6)	Fe–B5–B2	65.1 (4)
C14–C13–C23	121.0 (6)	Fe–B5–C10	118.6 (5)
C12–C13–C23	121.0 (6)	B1–B5–C10	54.4 (4)
C15–C14–C13	121.2 (6)	Fe–B7–B2	65.8 (4)
C14–C15–C16	119.2 (6)	Fe–B7–B8	120.7 (5)
C14–C15–C25	120.2 (7)	B2–B7–B3	60.5 (5)
C16–C15–C25	120.5 (7)	B3–B7–B8	54.7 (4)
B5–B1–B2	60.3 (5)	C9–B8–B7	113.4 (5)
B5–B1–C10	64.3 (5)	C9–B8–B3	108.3 (6)
B3–B1–B4	59.5 (5)	C9–B8–B4	60.4 (5)
B4–B1–C10	59.6 (5)	B7–B8–B3	59.7 (4)
Fe–B2–B5	64.6 (4)	B2–B8–B4	60.7 (5)
Fe–B2–B7	64.6 (4)	B4–C9–B8	68.5 (6)
B5–B2–B1	60.7 (4)	B4–C9–C10	66.3 (5)
B7–B2–B3	59.7 (4)	B8–C9–C10	116.4 (6)
B3–B2–B1	59.1 (4)	C9–C10–B5	116.2 (6)
B2–B3–B7	59.8 (4)	C9–C10–B1	110.2 (6)
B2–B3–B1	60.2 (4)	C9–C10–B4	61.8 (5)
B7–B3–B8	65.6 (5)	B5–C10–B1	61.3 (4)
B1–B3–B4	59.1 (5)	B1–C10–B4	61.3 (5)

Table XII. Interatomic Distances (Å) for 5,7,8-$(CH_3)_3$-11,7,8,10-[η^3-$C_4(CH_3)_4H$]$NiC_3B_7H_7$ (VII)

Ni–B2	2.177 (9)	B3–HB3	1.12 (4)
Ni–B9	2.382 (11)	B4–B3	1.735 (11)
Ni–C7	2.001 (7)	B4–B5	1.697 (12)
Ni–C8	2.520 (7)	B4–B1	1.781 (13)
Ni–C10	1.944 (7)	B4–HB4	1.05 (4)
Ni–B6	2.251 (9)	B5–B1	1.745 (12)
Ni–C11	2.011 (7)	B5–C18	1.603 (9)
Ni–C12	2.071 (7)	B6–B5	1.792 (12)
Ni–C13	1.981 (7)	B6–B1	1.731 (12)
Ni–C14	2.532 (9)	B6–HB6	1.10 (4)
Ni–C24	3.124 (10)	C7–B3	1.687 (10)
C11–C13	1.399 (9)	C7–C19	1.510 (8)
C11–C14	1.526 (10)	C8–B9	1.806 (10)
C11–C21	1.471 (9)	C8–C7	1.473 (8)
C12–C13	1.345 (9)	C8–B4	1.688 (10)
C12–C14	1.533 (9)	C8–B3	1.734 (10)
C12–C22	1.514 (9)	C8–C20	1.467 (8)
C13–C23	1.481 (9)	B9–C10	1.527 (11)
C14–C24	1.456 (10)	B9–B4	1.778 (12)
B1–HB1	1.05 (5)	B9–B5	1.768 (11)
B2–C7	1.539 (10)	B9–HB9	1.09 (4)
B2–B3	1.767 (12)	C10–B6	1.513 (10)
B2–B6	1.865 (10)	C10–B5	1.623 (10)
B2–B1	1.811 (11)	C10–HC10	0.87 (4)
B2–HB2	1.08 (4)		
B3–B1	1.729 (12)		

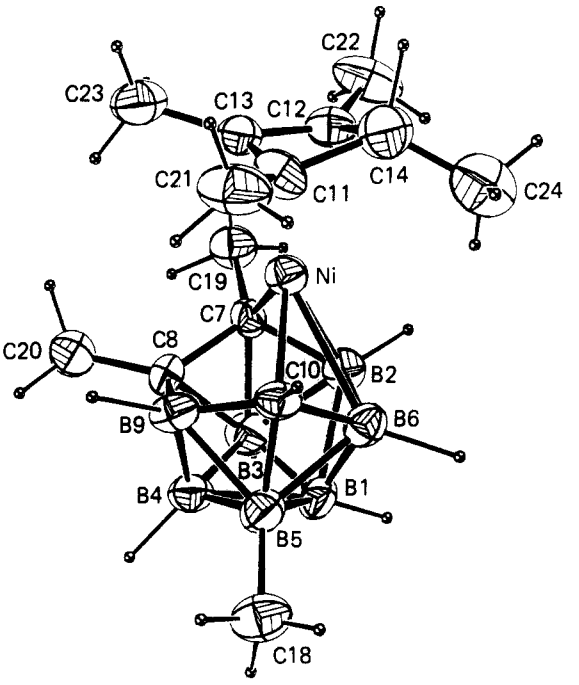

Figure 3. ORTEP drawing of 5,7,8-$(CH_3)_3$-11,7,8,10-[η^3-$C_4(CH_3)_4H$]$NiC_3B_7H_7$ (VII).

Table XIII. Selected Interatomic Angles (deg) for 5,7,8-$(CH_3)_3$-11,7,8,10-[η^3-$C_4(CH_3)_4H$]$NiC_3B_7H_7$ (VII)

B2-Ni-C7	43.0 (3)	C8-B3-C7	51.0 (4)
B2-Ni-B6	49.8 (3)	C8-B3-B4	58.2 (5)
C7-Ni-C10	103.9 (3)	B2-B3-C7	52.9 (4)
C10-Ni-B6	41.5 (3)	B2-B3-B1	62.4 (5)
C13-C11-C14	90.3 (6)	B4-B3-B1	61.9 (5)
C13-C11-C21	132.1 (8)	C8-B4-B9	62.7 (5)
C14-C11-C21	128.3 (8)	C8-B4-B3	60.9 (5)
C13-C12-C14	92.1 (7)	B9-B4-B5	61.1 (5)
C13-C12-C22	134.8 (8)	B3-B4-B1	58.9 (5)
C14-C12-C22	127.0 (8)	B5-B4-B1	60.2 (5)
C11-C13-C12	92.1 (7)	B9-B5-C10	53.3 (5)
C11-C13-C23	132.0 (8)	B9-B5-B4	61.7 (5)
C12-C13-C23	135.3 (8)	B9-B5-C18	126.7 (6)
C11-C14-C12	80.4 (6)	C10-B5-B6	52.3 (9)
C11-C14-C24	126.1 (8)	C10-B5-C18	121.2 (7)
C12-C14-C24	123.9 (8)	B4-B5-B1	62.3 (5)
B2-B1-B3	59.8 (5)	B4-B5-C18	123.5 (7)
B2-B1-B6	63.5 (5)	B6-B5-B1	58.6 (5)
B4-B1-B5	57.5 (5)	B6-B5-C18	127.8 (7)
B6-B1-B5	62.1 (5)	B1-B5-C18	125.7 (7)
Ni-B2-B6	67.2 (4)	Ni-B6-B2	63.0 (4)
C7-B2-B3	60.9 (5)	Ni-B6-C10	58.3 (4)
B3-B2-B1	57.8 (5)	B2-B6-B1	60.4 (5)
B6-B2-B1	56.2 (5)	B5-B6-B1	59.3 (5)
Ni-C7-C19	121.1 (5)	B3-C8-C20	122.1 (6)
C8-C7-B3	66.2 (4)	C8-B9-C10	117.2 (6)
C8-C7-C19	119.4 (6)	C8-B9-B4	56.2 (4)
B2-C7-B3	66.2 (5)	C10-B9-B5	58.5 (5)
B9-C8-C7	113.5 (6)	B4-B9-B5	57.2 (5)
B9-C8-B4	61.1 (4)	Ni-C10-B9	85.8 (4)
C7-C8-B3	62.9 (4)	Ni-C10-B6	80.2 (4)
C7-C8-C20	120.1 (6)	B9-C10-B5	68.2 (5)
B4-C8-B3	60.9 (5)	B6-C10-B5	69.6 (5)
B4-B8-C20	117.5 (6)		

and either cyclopentadiene, toluene, mesitylene, or 2-butyne were explored and found to yield a number of unique metallacarborane clusters. All the compounds reported are air and water stable, and their structures have been either confirmed by single-crystal X-ray studies or deduced from the spectroscopic data, as discussed below.

Cobaltacarboranes. The reaction of cobalt atoms with cyclopentadiene and 2,6-$C_2B_7H_{11}$ gave two new cobaltacarborane complexes 2-(η-C_5H_5)Co-1,4-$C_2B_7H_9$ (I) and 4-(η-C_5H_5)Co-2,3-$C_2B_7H_{13}$ (II) along with the known compounds 2-(η-C_5H_5)Co-6,9-$C_2B_7H_9$[13a] and 8-(η-C_5H_5)Co-6,7-$C_2B_7H_{11}$.[13b]

Table XIV. Boron-11 NMR Data for (η-C_5H_5)$CoC_2B_7H_9$ Isomers

compound	^{11}B NMR data δ	ref
2-(η-C_5H_5)Co-1,4-$C_2B_7H_9$	27.5 (1), 9.3 (2), 5.6 (2), −13.6 (2)	this work
2-(η-C_5H_5)Co-1,6-$C_2B_7H_9$	20.2 (1), −4.3 (1), −6.8 (1), −20.2 (1), −24.2 (1), −25.4 (1), −33.3 (1)	22
2-(η-C_5H_5)Co-1,10-$C_2B_7H_9$	5.2 (1), 1.6 (2), −18.0 (2), −19.2 (2)	22
2-(η-C_5H_5)Co-3,10-$C_2B_7H_9$	49.6 (1), −3.0 (1), −3.8 (1), −11.5 (1), −23.1 (1), −24.2 (1), −26.1 (1)	23
2-(η-C_5H_5)Co-6,9-$C_2B_7H_9$	79.3 (1), −3.0 (1), −11.7 (2), −24.8 (1), −29.3 (2)	13a
2-(η-C_5H_5)Co-1,7-$C_2B_7H_9$	17.0 (1), 13.3 (1), 3.9 (3), −5.0 (1), −37.4 (1)	13a, 25, 24

Scheme I

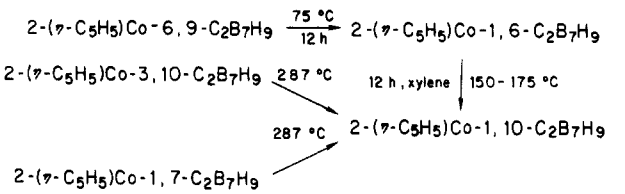

Compound I, 2-(η-C_5H_5)Co-1,4-$C_2B_7H_9$ (red), is, in fact, the sixth isomer of this cobaltacarborane complex to be reported. The 2-(η-C_5H_5)Co-1,6-$C_2B_7H_9$ (red),[22] 2-(η-C_5H_5)Co-1,10-$C_2B_7H_9$ (orange),[22] 2-(η-C_5H_5)Co-3,10-$C_2B_7H_9$ (yellow),[23] 2-(η-C_5H_5)Co-6,9-$C_2B_7H_9$ (yellow),[13a] and 2-(η-C_5H_5)Co-1,7-$C_2B_7H_9$ (yellow)[13a,22,24] isomers of this complex have previously been isolated, and their NMR data are presented in Table XIV for comparison with I. The ^{11}B NMR spectrum of I is inconsistent with any of the known isomers and the observed four resonances of intensity 1:2:2:2 indicate that the cage has mirror symmetry. The absence of a low-field peak in the ^{11}B NMR indicates that one carbon must occupy the four-coordinate 1-position adjacent to the cobalt atom in the cage system. The remaining carbon must then also be situated on the mirror plane, and since the 1,10-carbon isomer has already been reported, this means that I must be the 1,4-carbon isomer.

Skeletal rearrangements in the previously known isomers have been extensively studied[25] as outlined in Scheme I.

The rearrangements observed in these systems are consistent with the general trends observed[25] in metallacarborane isomerizations; that is, adjacent carbons separate with the carbons ultimately migrating to lower coordinate cage positions, which in this case are the four-coordinate 1,10-positions.

Compound I also undergoes isomerization reactions consistent with the above observations.

(22) George, T. A.; Hawthorne, M. F. *J. Am. Chem. Soc.* **1969**, *91*, 5475–5482.

(23) Evans, W. J.; Dunks, G. B.; Hawthorne, M. F. *J. Am. Chem. Soc.* **1973**, *95*, 4565–4574.

(24) It should be noted that Todd has recently questioned the closo structural assignment of this isomer and proposed on the basis of the similarity of its ^{11}B NMR spectrum with that of 2-(η-C_6H_6)Ru-5,6-$C_2B_7H_{11}$ that the compound is the nido-cage system 2-(η-C_5H_5)Co-5,6-$C_2B_7H_{11}$, see ref 35g.

(25) Dustin, D. F.; Evans, W. J.; Jones, C. J.; Wiersema, R. J.; Gong, H.; Chan, S.; Hawthorne, M. F. *J. Am. Chem. Soc.* **1974**, *96*, 3085–3090.

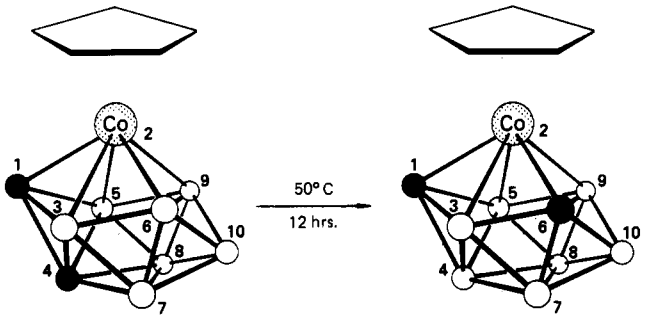

The adjacent carbon compound I can thus be essentially quantitatively converted to the 2-(η-C_5H_5)Co-1,6-$C_2B_7H_9$ isomer by heating at 70 °C in a sealed tube. It should also be noted that this rearrangement occurs slowly even at room temperature. Thus, samples of I stored for weeks have shown considerable isomerization as determined by ^{11}B NMR.

The second new compound isolated in the cobalt reaction was the *arachno*-metallacarborane 4-(η-C_5H_5)Co-2,3-$C_2B_7H_{13}$. The compound shows a mass spectral cutoff at m/e 238.1400 which is consistent with the proposed formula; however, both the parent and parent − 1 peaks are of low intensity, indicating the facile loss of two hydrogens upon ionization. A compound of this formula would be a n + 3 skeletal electron pair system (10 cage atoms, 13 skeletal electron pairs) and would be expected to adopt an arachno-type geometry. The spectroscopic data and the results[26] obtained from a partial X-ray structure, carried out on a twinned crystal, support the structure shown in Figure 4 which is consistent with this prediction.

As can be seen in the figure, the proposed structure is based on an icosahedron missing two vertices. Similar structures have either been proposed or confirmed for the isoelectronic compounds 2,3-$C_2B_8H_{14}$,[27] $B_{10}H_{14}^{2-}$,[28] $B_{10}H_{12}(SMe_2)_2$,[29] and 2,3,4-$SeC_2B_7H_{11}$.[30] The X-ray study clearly demonstrated that the compound adopts this type of geometry with the cobalt atom situated in the four-vertex position on the open face. Because of the twinned nature of the crystal, the structure could not be successfully refined beyond R = 0.36 and the positions of the carbon atoms could not be unambiguously determined. However, the NMR data discussed below strongly support the structure indicated in the figure.

The ^1H NMR spectrum shows, in addition to the η-C_5H_5 resonance at 4.45 ppm, four additional C–H resonances each of intensity one. These resonances are consistent with the presence of two different $-CH_2$ groups in the compound. These groups result in two sets of resonances (0.47 and 0.05 ppm and −1.89 and −2.47 ppm) with the upfield resonance in each set being assigned to the axial –CH and the downfield resonance to the equatorial –CH. Similar ^1H NMR spectra and assignments have been made for other carboranes containing $-CH_2$ groups including 2,3-$C_2B_8H_{14}$ (0.81 and −0.70 ppm),[27] 2,3-$C_2B_7H_{13}$ (0.77 and −0.10 ppm),[31] 4-CB_8H_{14} (0.10 and −1.75 ppm),[32] and 2,3,4-$SeC_2B_7H_{11}$ (1.80 and 1.68 ppm).[30] The boron-11 spin

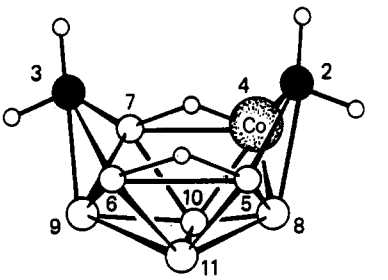

Figure 4. Proposed structure of 4-(η^5-C_5H_5)Co-2,3-$C_2B_7H_{13}$, (II). Terminal B–H hydrogens and the η^5-C_5H_5 group are not shown.

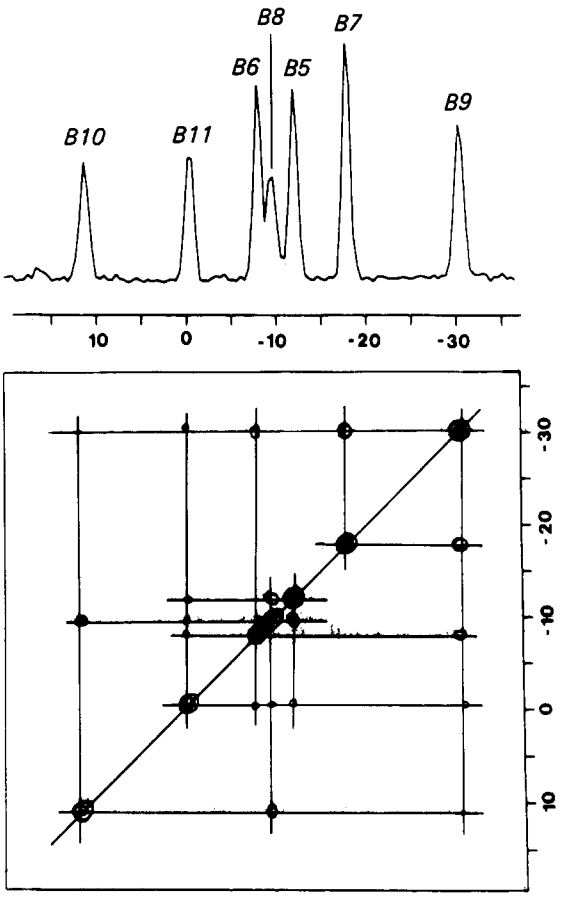

Figure 5. The 64.2-MHz 2-D ^{11}B–^{11}B NMR spectrum (proton-spin decoupled) of 4-(η-C_5H_5)Co-2,3-$C_2B_7H_{13}$ (II). The spectrum at the top is the normal 1-D ^{11}B proton-spin-decoupled spectrum.

decoupled ^1H NMR also clearly indicates the presence of a boron–boron bridging hydrogen (−3.12 ppm) and a boron–cobalt bridging hydrogen (−17.50 ppm), with the latter resonance showing a distinct quartet structure (J = 63 Hz) consistent with coupling to a single boron atom (B7).

The ^{11}B NMR spectrum at 115.5 MHz shows seven well-separated resonances with the doublet at −12.31 ppm showing an additional ~54 Hz coupling consistent with its assignment as the boron (B7) involved in the Co-H-B bridge. Additionally, the proposed structure is consistent with a 2-D NMR study of the molecule, the results of which are depicted in Figure 5.

Grimes has previously demonstrated[33] that J-correlated, two-dimensional ^{11}B–^{11}B NMR spectroscopy can be used for the direct determination of boron–boron connectivities in polyhedral boranes. Thus, in the plot shown in Figure 5 the peaks on the diagonal correspond to a one-dimensional proton-spin-decoupled ^{11}B NMR spectrum of the

(26) Briguglio, J. J.; Carroll, P. J.; Sneddon, L. G., unpublished results.
(27) (a) Štibr, B.; Plešek, J.; Heřmánek, S. *Chem. Ind. (London)* **1972**, 649. (b) Štibr, B.; Plešek, J.; Heřmánek, S. *Collect. Czech. Chem. Commun.* **1974**, *39*, 1805–1809.
(28) Kendall, D. S.; Lipscomb, W. N. *Inorg. Chem.* **1973**, *12*, 546–551.
(29) Knoth, W. H.; Muetterties, E. L. *J. Inorg. Nucl. Chem.* **1961**, *20*, 66–72.
(30) Friesen, G. D.; Barriola, A.; Todd, L. J. *Chem. Ind. (London)* **1978**, *19*, 631.
(31) Tebbe, F. N.; Garrett, P. M.; Hawthorne, M. F. *J. Am. Chem. Soc.* **1968**, *90*, 869–879.
(32) Štibr, B.; Baše, K.; Heřmánek, S.; Plešek, J. *J. Chem. Soc., Chem. Commun.* **1976**, 150–151.
(33) Venable, T. L.; Hutton, W. C.; Grimes, R. N. *J. Am. Chem. Soc.* **1984**, *106*, 29–37.

molecule, while the cross peaks arise from spin–spin coupling between connected ^{11}B nuclei. In the case of 4-(η-C_5H_5)Co-2,3-$C_2B_7H_{13}$ the observed cross peaks support the proposed structure, although it should be noted that not all predicted connectivities are observed. Thus, in agreement with the proposed structure, cross peaks are observed for B6–B9, B7–B9, B9–B10, B9–B11, B10–B8, B11–B8, B5–B11, and B5–B8. As expected based on previous observations,[33] no cross peak is observed between the hydrogen-bridged B5 and B6 borons. Surprisingly, no cross peaks are observed between B7–B10 and B10–B11 which must be connected in the proposed structure; however, Grimes has also observed several examples of missing cross peaks between connected borons and has discussed possible reasons for their absence.[33]

Ferracarboranes. Although the first (η-arene)metallacarborane was reported[34] in 1975, this area of metallaboron chemistry has been slow to develop because of the lack of general synthetic techniques needed to obtain these complexes. However, in recent years there has been increased interest in this area and a number of new routes to these complexes have now been reported.[35] Our work has demonstrated that metal vapor reactions can be used to generate both (η-arene)metallacarborane[2,3] and -borane clusters,[7] and, therefore, corresponding reactions with 2,6-$C_2B_7H_{11}$ were investigated.

It was found that the reaction of this carborane with iron atoms and either toluene or mesitylene gave new types of (η^6-arene)ferracarborane clusters. The reaction with toluene yielded the closo complexes 2-(η^6-$CH_3C_6H_5$)Fe-6,9-$C_2B_7H_9$ (III) and 2-(η^6-$CH_3C_6H_5$)Fe-1,6-$C_2B_7H_9$ (IV) while the reaction with mesitylene gave both closo, 2-[η^6-$(CH_3)_3C_6H_3$]Fe-1,6-$C_2B_7H_9$ (V), and nido, 6-[η^6-$(CH_3)_3C_6H_3$]Fe-9,10-$C_2B_7H_{11}$ (VI), complexes.

The ^{11}B NMR data for IV and V are similar to that obtained for the cobalt complex 2-(η-C_5H_5)Co-1,6-$C_2B_7H_9$, while that obtained for III is comparable to the 2-(η-C_5H_5)Co-6,9-$C_2B_7H_9$ isomer, strongly supporting their structural assignments. Likewise, in agreement with the cobaltacarborane isomerization reactions discussed above, it was observed that the 6,9-carbon isomer readily isomerized to the 1,6-carbon isomer.

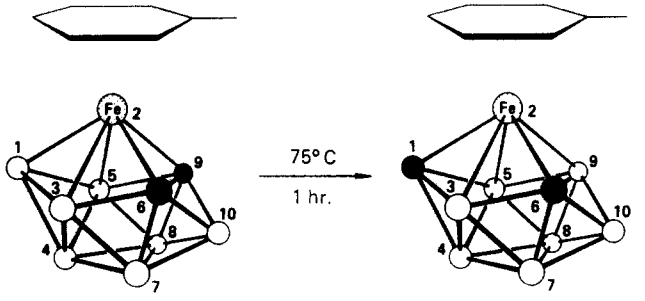

The structure of V was established by means of a single-crystal X-ray determination as depicted in the ORTEP diagram given in Figure 1. As predicted, the structure is composed of a closo bicapped square antiprism in which the iron and carbon atoms occupy adjacent five-coordinate positions in the antiprism.

The complex lies on a crystallographic mirror plane which contains the cage atoms Fe, Cl, B4, and B10 and the mesitylene carbons C14, C11, and C21. The atoms C6 and B6 are related by this mirror symmetry and are therefore disordered. The disorder was treated by using the average of the scattering factors of boron and carbon for these two atoms, and the corresponding bond distances involving either of these two atoms must, therefore, be considered average values. The remaining intracage distances and angles are consistent with those previously reported for isostructural metallacarborane clusters such as 1-(PPh_3)-2-H-2,2-(PPh_3)$_2$-2,10-$IrCB_8H_8$,[36] 2-H-2,2-(Et_3P)$_2$-2,1,6-$CoC_2B_7H_9$,[37] 2-H-2,2-(Et_3P)$_2$-2,1,6-$RhC_2B_7H_9$,[37] and 6,6-(Et_3P)$_2$-6,1,2-$CoC_2B_7H_9$.[21]

The iron to arene bonding appears normal with average iron–ring carbon (2.099 Å) and iron–ring plane (1.564 (5) Å) distances similar to those reported for other (η^6-arene)metallacarboranes[2,3,35] and -boranes.[7] Also consistent with previously reported structures, is the fact that the methyl groups and hydrogens attached to the η^6-arene ring are distorted out of the plane of the ring toward the metal atom. The reasons for this type of distortion in η^6-arene systems have previously been discussed.[38]

In addition to the closo complex V, the reaction with mesitylene also yielded the new *nido*-ferracarborane complex 6-[η^6-$(CH_3)_3C_6H_3$]Fe-9,10-$C_2B_7H_{11}$. This structure was confirmed by a single-crystal X-ray study as shown in the ORTEP drawing given in Figure 2. The cage structure is composed of a ten-vertex *nido*-decaborane(14)-type structure in which the iron atom occupies the 6-cage position and the carbon atoms the 9,10-cage positions on the open face of the polyhedron. In agreement with the proton NMR spectrum, which shows two separate proton resonances, each with quartet structure ($J \approx 60$ Hz), at positions characteristic of metal–boron bridging hydrogens, the structure is seen to have two different Fe–boron bridging protons. The iron to boron distances Fe–B2 = 2.134 (9) Å, Fe–B7 = 2.114 (8) Å, and Fe–B5 = 2.125 (7) Å and the iron to B2,B7,B5 plane distance of 1.531 (1) Å are normal, being similar to those reported for other ferracarborane and ferraborane complexes.[2,3,7,35] The iron to η^6-mesitylene distances in VI (average Fe–ring carbon = 2.101 Å, Fe–ring plane = 1.566 (1) Å) are similar to those observed above for V, and the plane of the mesitylene ring is found to be parallel (dihedral angle 1.6°) to the B2,B7,B5 plane. As noted above for V, in VI the methyl groups are again distorted out of the ring plane toward the iron atom.

Nickelacarboranes. The reaction of nickel atoms with 2,6-$C_2B_7H_{11}$, 2-butyne, and toluene resulted in the formation of only one product, VII, in sufficient amounts to allow complete characterization. The high-resolution mass spectrum showed a parent ion and fragmentation corresponding to the formula [η^3-$C_4(CH_3)_4H$]Ni$(CH_3)_3C_3B_7H_7$. The NMR data are also consistent with this structure. Thus, the ^1H NMR spectrum indicates the presence of seven methyl groups while the ^{11}B NMR spectrum showed six doublets and one singlet, indicating that one of the methyl groups is substituted on a boron atom and also that the complex lacks a plane of symmetry. A single-crystal X-ray structural determination confirmed the above interpretations and proved the compound to be 5,7,8-$(CH_3)_3$-11,7,8,10-[η^3-$C_4(CH_3)_4H$]Ni$C_3B_7H_7$ (VII) as can be seen in the ORTEP drawing presented in Figure 3.

(34) Salentine, C. G.; Hawthorne, M. F. *J. Am. Chem. Soc.* **1975**, *97*, 6382–6388.

(35) (a) Garcia, M. P.; Green, M.; Stone, F. G. A.; Somerville, R. G.; Welch, A. J. *J. Chem. Soc., Chem. Commun.* **1981**, 871–872. (b) Hanusa, T. P.; Huffman, J. C.; Todd, L. J. *Polyhedron* **1982**, *1*, 77–82. (c) Swisher, R. G.; Sinn, E.; Grimes, R. N. *Organometallics* **1983**, *2*, 506–514. (d) Swisher, R. G.; Sinn, E.; Butcher, R. J.; Grimes, R. N. *Organometallics* **1985**, *4*, 882–890. (e) Swisher, R. G.; Sinn, E.; Grimes, R. N. *Organometallics* **1985**, *4*, 890–895. (f) *Ibid.* **1985**, *4*, 896–901. (g) Hanusa, T. P.; Huffman, J. C.; Curtis, T. L.; Todd, L. J. *Inorg. Chem.* **1985**, *24*, 787–792.

(36) Alcock, N. W.; Taylor, J. G.; Wallbridge, M. G. H. *J. Chem. Soc., Chem. Commun.* **1983**, 1168–1169.

(37) Barker, G. K.; Garcia, M. P.; Green, M.; Stone, F. G. A.; Basset, J.-M.; Welch, A. J. *J. Chem. Soc., Chem. Commun.* **1981**, 653–655.

(38) Elian, M.; Chen, M. M. L.; Mingos, D. M. P.; Hoffmann, R. *Inorg. Chem.* **1976**, *15*, 1148–1155.

The structure can be described as a sandwich complex in which a nickel atom is bonded between a η^3-cyclobutenyl group and a three-carbon carborane cage. Several unique structural features are apparent. Firstly, the cage structure is seen to deviate from the geometry predicted based on simple electron-counting rules. Thus, if the $[\eta^3\text{-}C_4(CH_3)_4H]Ni$ group is considered a one-electron donor to skeletal bonding, the cluster would be a $n + 1$ skeletal electron pair system (11 cage atoms, 12 skeletal electron pairs) and would be expected to have a closo octadecahedral geometry. As can be seen in Figure 3 the complex does not have this closo structure, but appears to have an open five-membered face composed of Ni, C7, C8, B9, and C10. This structure is not, however, the normal open-cage structure adopted by 11-vertex nido complexes, such as $10,10'\text{-}Ni[B_{10}H_{12}]_2^{2-}$,[39] $[(C_2H_5)_4N^+][(C_2B_9H_{11})Co(C_2B_8H_{10}py)^-]$,[40] μ-2,7-$(SCSNEt_2)$-7-$(PMe_2Ph)PtB_{10}H_{11})$,[41] and $10\text{-}[(C_2H_5)_3P]_2Pt(H)\text{-}11\text{-}SB_9H_{10}$.[42] These nido structures are derivatives of an icosahedron, formed by removal of one vertex, and have planar or nearly planar five-membered open faces. The open face in VII is clearly nonplanar, and the structure might be described as intermediate between a closo and nido structure. Of particular interest are the Ni–C8, 2.520 (7) Å, and Ni-B9, 2.383 (11) Å, bond distances, which are significantly longer than the other Ni–cage distances, Ni–C7 = 2.001 (7) Å, Ni–B2 = 2.177 (9) Å, Ni–B6 = 2.251 (9) Å, and Ni–C10 = 1.944 (7) Å, but short enough to indicate some interaction. The nickel atom appears to have "slipped" to one side in a closo-type structure to form the open face. Such slip distortions in metallacarborane complexes containing d^8 metals have been widely observed. In fact, at least three other 11-vertex, 12 skeletal electron pair platinacarborane complexes, μ-4,8-$[(Me_3P)_2Pt]$-8,8-$[(Me_3P)_2]$-8,7,10-$PtC_2B_8H_{10}$,[43] 8,8-$[(Me_3P)_2]$-8,7,10-$PtC_2B_8H_{10}$,[44] and 9-H-9,10-$(Et_3P)_2$-9,7,8-$PtC_2B_8H_9$,[44] have been shown to adopt open-cage slipped structures similar to that observed for VII.

The origin of the slip distortions observed in platinaboranes and -carboranes containing bis(phosphine)-substituted metal atoms has been analyzed[45] in detail by Mingos using extended Hückel calculations. It was concluded that the nonconical nature of the $Pt(PR_3)_2$ group leads to unequal bonding capabilities of the platinum $5d_{xz}$ and $5d_{yz}$ orbitals with respect to the cage, resulting in anisotropic metal to cage bonding. An analysis of the bonding ability of the nonconical $[\eta^3\text{-}C_4(CH_3)_4H]Ni$ group would also be expected to reveal similar bonding differences between the nickel $3d_{xz}$ and $3d_{yz}$ orbitals and to account for the slip distortion observed in VII.

The carborane ligand contains three carbon framework atoms each of which are located on the open face at the 8,7- and 10-cage positions, respectively. The intracage boron–boron and boron–carbon distances are normal, and the carbon–carbon distance between the only adjacent carbons, C7–C8 = 1.473 (8) Å, is also in the range previously observed in larger cage carboranes. There are three exopolyhedral methyl groups, one each substituted on carbons C7 and C8 and one on B5. Consistent with this observation the B5–C18 bond distance of 1.603 (9) Å is found to be lengthened relative to the C8–C20, 1.467 (8) Å, and C7–C19, 1.510 (8) Å, bonds.

In addition to being bound to the carborane cage the nickel is also bonded in an η^3-fashion to a cyclobutenyl group, which apparently formed from the condensation of two 2-butyne molecules. This allylic mode of bonding is supported by the structural data which indicates that the nickel is bound to only three of the ring carbons with a nickel–ring plane distance of 1.783 (1) Å. The Ni–central carbon distance, Ni–C13 = 1.981 (7) Å, is slightly shorter than the other two Ni–carbon distances, Ni–C11 = 2.011 (7) Å and Ni–C12 = 2.071 (7) Å, as is commonly observed in η^3-allylic ligands.[46]

The tetrahedral ring carbon C14 is bent out of the C11–C12–C13 plane by 0.46 (1) Å away from the nickel and the long C14–Ni distance, 2.532 (9) Å, indicates little interaction. The distances and angles within the cyclobutenyl ring are similar to those observed in other (η^3-cyclobutenyl)metal complexes, such as $[\eta^3\text{-}(CH_3)_4C_4(C_5H_5)]Ni(\eta^5\text{-}C_5H_5)$[47] and $(\eta^3\text{-}(C_6H_5)_4C_4(OC_2H_5)]_2Pd_2Cl_2$.[48] In particular, the bond lengths between the carbons in the allylic system, C11–C13 = 1.399 (9) Å and C12–C13 = 1.345 (9) Å, are much shorter than the bonds to the tetrahedral carbon C14, C11–C14 = 1.526 (10) Å and C12–C14 = 1.533 (9) Å. The four bond angles in the cyclobutenyl ring, C11–C13–C12 = 92.1 (7)°, C13–C11–C14 = 90.3 (6)°, C13–C12–C14 = 92.1 (7)°, and C11–C14–C12 = 80.4 (6)°, are also consistent with those previously observed and indicate a high degree of strain in the ligand.

Attached to each of the four cyclobutenyl carbon atoms is a methyl group. The methyl groups attached to the allylic carbons C11, C13, and C12 are displaced slightly (0.28–0.15 Å) out of the C11–C13–C12 plane away from the nickel. The methyl on C14 is, perhaps surprisingly, endo to the nickel; however, the long Ni–C24 distance, 3.124 (10) Å, again indicates no interaction with the metal.

The formation of a complex such as VII in this reaction is indeed unusual and is deserving of further comment. The composition of VII corresponds to the reaction of the carborane with exactly three equivalents of 2-butyne and a nickel atom:

$$2,6\text{-}C_2B_7H_{11} + 3CH_3C{\equiv}CCH_3 + Ni \rightarrow [\eta^3\text{-}C_4(CH_3)_4H]Ni(CH_3)_3C_3B_7H_7$$

Obviously, extensive rearrangement and hydrogen-transfer reactions have occurred. Of perhaps most interest are the rearrangements which have resulted in the formation of three-carbon carborane cage. The fact that the cage contains two adjacent carbons, both substituted with methyl groups, indicates that one of the 2-butyne molecules was incorporated directly into the cage during the reactions. If there was no other reaction or rearrangement involved, this would have resulted in a four-carbon carborane; however, since the final product contains only three carbons in the cage framework, this means that one of the original cage carbons must have been hydrogenated, by perhaps the bridging hydrogens, and then expelled from the cage to give the methyl group attached to B5. This, in fact, appears to be the first report of such a transfor-

(39) Guggenberger, L. J. *J. Am. Chem. Soc.* **1972**, *94*, 114–119.
(40) Churchill, M. R.; Gold, K. *Inorg. Chem.* **1973**, *12*, 1157–1165.
(41) Beckett, M. A.; Greenwood, N. N.; Kennedy, J. A.; Thornton-Pett, M. *Polyhedron* **1985**, *4*, 505–511.
(42) Kane, A. R.; Guggenberger, L. J.; Muetterties, E. L. *J. Am. Chem. Soc.* **1970**, *92*, 2571–2572.
(43) (a) Barker, G. K.; Green, M.; Spencer, J. L.; Stone, F. G. A.; Taylor, B. F.; Welch, A. J. *J. Chem. Soc., Chem. Commun.* **1975**, 804–805. (b) Green, M.; Spencer, J. L.; Stone, F. G. A. *J. Chem. Soc. Dalton Trans.* **1979**, 1679–1686.
(44) Barker, G. K.; Green, M.; Stone, F. G. A.; Wolsey, W. C.; Welch, A. J. *J. Chem. Soc., Dalton Trans.* **1983**, 2063–2069.
(45) (a) Mingos, D. M. P. *J. Chem. Soc., Dalton Trans.* **1977**, 602–610. (b) Mingos, D. M. P.; Forsyth, M. I.; Welch, A. J. *J. Chem. Soc., Dalton Trans.* **1978**, 1363–1374. (c) Evans, D. G.; Mingos, D. M. P. *J. Organomet. Chem.* **1982**, *240*, 321–327.
(46) Kaduk, J. A.; Poulos, A. T.; Ibers, J. A. *J. Organomet. Chem.* **1977**, *127*, 245–260.
(47) Oberhansli, W. E.; Dahl, L. F. *Inorg. Chem.* **1965**, *4*, 150–157.
(48) Dahl, L. F.; Oberhansli, W. E. *Inorg. Chem.* **1965**, *4*, 629–637.

mation in either a carborane or a metallacarborane cluster.

A plausible, but clearly unproven, reaction sequence which is consistent with both the above cage rearrangements and with the formation of an $[\eta^3\text{-}C_4(CH_3)_4H]Ni$ group is outlined in eq 1–5.

$$Ni + CH_3C_6H_5 \rightarrow Ni(CH_3C_6H_5)_x \quad (1)$$

$$Ni(CH_3C_6H_5)_x + C_2B_7H_{11} \rightarrow \eta^1\text{-}C_2B_7H_{10}Ni^{II}(H)(CH_3C_6H_5) \quad (2)$$

$$\eta^1\text{-}C_2B_7H_{10}Ni^{II}(H)(CH_3C_6H_5) + 3MeC{\equiv}CMe \rightarrow \eta^1\text{-}C_2B_7H_{10}Ni^{II}(H)(\eta^2\text{-}C_2Me_2)_3 \quad (3)$$

$$\eta^1\text{-}C_2B_7H_{10}Ni^{II}(H)(\eta^2\text{-}C_2Me_2)_3 \rightarrow Me_2C_4B_7H_{10}Ni^{II}(H)(\eta^2\text{-}C_2Me_2)_2 \quad (4)$$

$$Me_2C_4B_7H_{10}Ni^{II}(H)(\eta^2\text{-}C_2Me_2)_2 \rightarrow Me_3C_3B_7H_7Ni^{II}(\eta^3\text{-}C_4Me_4H) \quad (5)$$

Thus, the initially formed toluene-solvated nickel atoms[49] (eq 1) could react via an oxidative-addition process to yield an 18e nickel hydride complex such as in eq 2. The toluene could be displaced by three 2-butyne molecules (eq 3), and then one of the alkynes could become incorporated into the cage as shown in eq 4. Cage rearrangement, as discussed above, coupled with dimerization and hydrogen transfer to the remaining two coordinated 2-butyne ligands would yield the final product (eq 5).

Again it must be emphasized that the above sequence is entirely speculative, but it is clear from the results described herein that the very highly reactive metal atoms, or the organometallic intermediates which are produced in these reactions, cannot only be used to produce traditional types of metallaboron complexes but also can cause dramatic and unprecedented rearrangements to yield new types of hybrid organometallic/metallaboron clusters.

Acknowledgment. We thank the National Science Foundation and the Army Research Office for the support of this research. We also thank Dr. George Furst and Dr. Pat Carroll for their assistance in performing NMR and X-ray crystallographic studies.

Registry No. I, 99531-65-4; II, 99496-28-3; III, 99496-29-4; IV, 99496-30-7; V, 99496-31-8; VI, 99510-58-4; VII, 99496-32-9; 2,6-$C_2B_7H_{11}$, 42319-46-0; 2-[η-C_5H_5)Co-6,9-$C_2B_7H_9$, 41348-07-6; 8-(η-C_5H_5)Co-6,7-$C_2B_7H_{11}$, 52760-69-7; 4,7-(η-$C_5H_5)_2Co_2$-2,3-$C_2B_7H_9$, 76046-88-3; 2,3,5-(η-$C_5H_5)_3Co_3$-1,7-$C_2B_7H_9$, 50803-51-5; 2-(η-C_5H_5)Co-1,6-$C_2B_7H_9$, 41348-11-2; Co, 7440-48-4; Fe, 7439-89-6; Ni, 7440-02-0; C_5H_6, 542-92-7; $CH_3C_6H_5$, 108-88-3; $(CH_3)_3C_6H_3$, 108-67-8; 2-butyne, 503-17-3.

Supplementary Material Available: Tables of general temperature factors, molecular planes, calculated hydrogen positions, and observed and calculated structure factors (40 pages). Ordering information is given on any current masthead page.

(49) Klabunde, K. J.; Efner, H. F.; Murdock, T. O.; Ropple, R. *J. Am. Chem. Soc.* **1976**, *98*, 1021–1023.

Reaction Chemistry of Some New Hybrid Phosphine Amide Complexes of Platinum(II) and Palladium(II). Isolation and X-ray Structure Determination of an Ortho-Metalated Platinum(II) Complex Derived from a Chelated Phosphine Amide Complex of Platinum(II)

David Hedden,[1a] D. Max Roundhill,*[1a] William C. Fultz,[1b] and Arnold L. Rheingold[1b]

Departments of Chemistry, Tulane University, New Orleans, Louisiana 70118, and University of Delaware, Newark, Delaware 19716

Received March 25, 1985

Refluxing the complex *trans*-$PtCl_2(o\text{-}Ph_2PC_6H_4NHC(O)Ph)_2$ in DMF/Et_3N gives the cyclometalated complex *cis*-$Pt(o\text{-}Ph_2PC_6H_4NC(O)C_6H_4)(o\text{-}Ph_2PC_6H_4NHC(O)Ph)$. The complex crystallizes in a triclinic $P\bar{1}$ space group with a = 12.038 (3) Å, b = 12.576 (5) Å, c = 16.220 (6) Å, α = 105.80 (3)°, β = 104.84 (3)°, and γ = 95.73 (3)°. The structure shows respective values of 2.063 (7) and 2.065 (8) Å for Pt–N(1) and Pt–C(3). The monodentate P-bonded PNH(CPhO) ligand shows a close "agostic" interaction of the type N–H···Pt. The hydrogen atom has been located at a distance of 2.318 (22) Å from Pt. The analogous palladium complex has been synthesized. The transfer of the ortho carbon hydrogen to the amido nitrogen has been confirmed by deuteration studies using $o\text{-}Ph_2PC_6H_4NHC(O)C_6D_5$. The "agostic" hydrogen atom undergoes H/D exchange with benzene, acetonitrile, or chloroform. These cyclometalated complexes add HCl to give *cis*-$MCl_2(o\text{-}Ph_2PC_6H_4NHC(O)Ph)_2$ (M = Pd, Pt). With CF_3CO_2H the reaction is reversible, and N-alkylation occurs with Me_2SO_4 to give $[Pd(o\text{-}Ph_2PC_6H_4N(Me)C(O)C_6H_4)(o\text{-}Ph_2PC_6H_4NHC(O)Ph)]SO_4Me$. These amido complexes are stable to water and acetic acid.

Recently we have synthesized two new amido phosphine compounds having an amido substituent bonded to the ortho position of a phenyl phosphine moiety. In particular these compounds are $o\text{-}Ph_2PC_6H_4NHC(O)Ph$ and $o\text{-}Ph_2PC_6H_4C(O)NHPh$. These ligands are shown in Figure 1. These compounds have been chosen for the synthesis of complexes in which the (M–P–N) chelate ring have the preferred five- and six-membered ring sizes. Following a preliminary communication,[2] the first paper in this series

(1) (a) Tulane University. (b) University of delaware.

(2) Hedden, D.; Roundhill, D. M.; Fultz, W. C.; Rheingold, A. R. *J. Am. Chem. Soc.* **1984**, *106*, 5014–5016.

0276-7333/86/2305-0336$01.50/0

mation in either a carborane or a metallacarborane cluster.

A plausible, but clearly unproven, reaction sequence which is consistent with both the above cage rearrangements and with the formation of an $[\eta^3\text{-}C_4(CH_3)_4H]Ni$ group is outlined in eq 1–5.

$$Ni + CH_3C_6H_5 \rightarrow Ni(CH_3C_6H_5)_x \quad (1)$$

$$Ni(CH_3C_6H_5)_x + C_2B_7H_{11} \rightarrow \eta^1\text{-}C_2B_7H_{10}Ni^{II}(H)(CH_3C_6H_5) \quad (2)$$

$$\eta^1\text{-}C_2B_7H_{10}Ni^{II}(H)(CH_3C_6H_5) + 3MeC{\equiv}CMe \rightarrow \eta^1\text{-}C_2B_7H_{10}Ni^{II}(H)(\eta^2\text{-}C_2Me_2)_3 \quad (3)$$

$$\eta^1\text{-}C_2B_7H_{10}Ni^{II}(H)(\eta^2\text{-}C_2Me_2)_3 \rightarrow Me_2C_4B_7H_{10}Ni^{II}(H)(\eta^2\text{-}C_2Me_2)_2 \quad (4)$$

$$Me_2C_4B_7H_{10}Ni^{II}(H)(\eta^2\text{-}C_2Me_2)_2 \rightarrow Me_3C_3B_7H_7Ni^{II}(\eta^3\text{-}C_4Me_4H) \quad (5)$$

Thus, the initially formed toluene-solvated nickel atoms[49] (eq 1) could react via an oxidative-addition process to yield an 18e nickel hydride complex such as in eq 2. The toluene could be displaced by three 2-butyne molecules (eq 3), and then one of the alkynes could become incorporated into the cage as shown in eq 4. Cage rearrangement, as discussed above, coupled with dimerization and hydrogen transfer to the remaining two coordinated 2-butyne ligands would yield the final product (eq 5).

Again it must be emphasized that the above sequence is entirely speculative, but it is clear from the results described herein that the very highly reactive metal atoms, or the organometallic intermediates which are produced in these reactions, cannot only be used to produce traditional types of metallaboron complexes but also can cause dramatic and unprecedented rearrangements to yield new types of hybrid organometallic/metallaboron clusters.

Acknowledgment. We thank the National Science Foundation and the Army Research Office for the support of this research. We also thank Dr. George Furst and Dr. Pat Carroll for their assistance in performing NMR and X-ray crystallographic studies.

Registry No. I, 99531-65-4; II, 99496-28-3; III, 99496-29-4; IV, 99496-30-7; V, 99496-31-8; VI, 99510-58-4; VII, 99496-32-9; 2,6-$C_2B_7H_{11}$, 42319-46-0; 2-[η-C_5H_5)Co-6,9-$C_2B_7H_9$, 41348-07-6; 8-(η-C_5H_5)Co-6,7-$C_2B_7H_{11}$, 52760-69-7; 4,7-(η-$C_5H_5)_2Co_2$-2,3-$C_2B_7H_9$, 76046-88-3; 2,3,5-(η-$C_5H_5)_3Co_3$-1,7-$C_2B_7H_9$, 50803-51-5; 2-(η-C_5H_5)Co-1,6-$C_2B_7H_9$, 41348-11-2; Co, 7440-48-4; Fe, 7439-89-6; Ni, 7440-02-0; C_5H_6, 542-92-7; $CH_3C_6H_5$, 108-88-3; $(CH_3)_3C_6H_3$, 108-67-8; 2-butyne, 503-17-3.

Supplementary Material Available: Tables of general temperature factors, molecular planes, calculated hydrogen positions, and observed and calculated structure factors (40 pages). Ordering information is given on any current masthead page.

(49) Klabunde, K. J.; Efner, H. F.; Murdock, T. O.; Ropple, R. *J. Am. Chem. Soc.* **1976**, *98*, 1021–1023.

Reaction Chemistry of Some New Hybrid Phosphine Amide Complexes of Platinum(II) and Palladium(II). Isolation and X-ray Structure Determination of an Ortho-Metalated Platinum(II) Complex Derived from a Chelated Phosphine Amide Complex of Platinum(II)

David Hedden,[1a] D. Max Roundhill,*[1a] William C. Fultz,[1b] and Arnold L. Rheingold[1b]

Departments of Chemistry, Tulane University, New Orleans, Louisiana 70118, and University of Delaware, Newark, Delaware 19716

Received March 25, 1985

Refluxing the complex *trans*-$PtCl_2(o\text{-}Ph_2PC_6H_4NHC(O)Ph)_2$ in DMF/Et_3N gives the cyclometalated complex *cis*-$Pt(o\text{-}Ph_2PC_6H_4NC(O)C_6H_4)(o\text{-}Ph_2PC_6H_4NHC(O)Ph)$. The complex crystallizes in a triclinic $P\bar{1}$ space group with a = 12.038 (3) Å, b = 12.576 (5) Å, c = 16.220 (6) Å, α = 105.80 (3)°, β = 104.84 (3)°, and γ = 95.73 (3)°. The structure shows respective values of 2.063 (7) and 2.065 (8) Å for Pt–N(1) and Pt–C(3). The monodentate P-bonded PNH(CPhO) ligand shows a close "agostic" interaction of the type N–H···Pt. The hydrogen atom has been located at a distance of 2.318 (22) Å from Pt. The analogous palladium complex has been synthesized. The transfer of the ortho carbon hydrogen to the amido nitrogen has been confirmed by deuteration studies using $o\text{-}Ph_2PC_6H_4NHC(O)C_6D_5$. The "agostic" hydrogen atom undergoes H/D exchange with benzene, acetonitrile, or chloroform. These cyclometalated complexes add HCl to give *cis*-$MCl_2(o\text{-}Ph_2PC_6H_4NHC(O)Ph)_2$ (M = Pd, Pt). With CF_3CO_2H the reaction is reversible, and N-alkylation occurs with Me_2SO_4 to give $[Pd(o\text{-}Ph_2PC_6H_4N(Me)C(O)C_6H_4)(o\text{-}Ph_2PC_6H_4NHC(O)Ph)]SO_4Me$. These amido complexes are stable to water and acetic acid.

Recently we have synthesized two new amido phosphine compounds having an amido substituent bonded to the ortho position of a phenyl phosphine moiety. In particular these compounds are $o\text{-}Ph_2PC_6H_4NHC(O)Ph$ and $o\text{-}Ph_2PC_6H_4C(O)NHPh$. These ligands are shown in Figure 1. These compounds have been chosen for the synthesis of complexes in which the (M–P–N) chelate ring have the preferred five- and six-membered ring sizes. Following a preliminary communication,[2] the first paper in this series

(1) (a) Tulane University. (b) University of delaware.

(2) Hedden, D.; Roundhill, D. M.; Fultz, W. C.; Rheingold, A. R. *J. Am. Chem. Soc.* **1984**, *106*, 5014–5016.

0276-7333/86/2305-0336$01.50/0

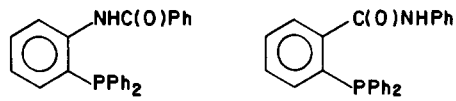

o-$Ph_2PC_6H_4NHC(O)Ph$ o-$Ph_2PC_6H_4C(O)NHPh$

Figure 1. Structures of o-$Ph_2PC_6H_4NHC(O)Ph$ and o-$Ph_2PC_6H_4C(O)NHPh$.

described the ligand synthesis and characterization, along with the preparation of a series of amide complexes of the type MCl_2L_2 (L = o-$Ph_2PC_6H_4NHC(O)Ph$, o-$Ph_2PC_6H_4C(O)NHPh$) and amido complexes ML_2 (L = o-$Ph_2PC_6H_4NC(O)Ph$, o-$Ph_2PC_6H_4C(O)NPh$).[3] In the complexes MCl_2L_2 the ligands L are bonded solely via phosphorus. Interconversion between these amide and amido complexes has been effected by the addition of strong base or the strong acid HCl.

These amido phosphine compounds have been prepared with a number of desired goals targeted. One such goal is to investigate the facility with which a hydrogen can be transferred from nitrogen either to an external base by deprotonation or to a metal by an intramolecular oxidative addition process. A second aim of this paper is an evaluation of the chemical reactivity of an amido ligand complexed to platinum(II) and palladium(II). Although amido complexes of the early transition elements are common, only relatively few complexes are known where such a ligand is coordinated to a platimum group metal,[4] and therefore their reaction chemistry is largely unexplored. This paper focuses on the proton-transfer reactions which can be observed between the free amides and the complexed amido ligands in these complexes and also on probing the chemical reactivity of an amido ligand coordinated to a platinum group element.

Finally we will present data which suggests that we have isolated a complex which provides the first example of a compound having an "agostic" interaction between a transition-metal center and a hydrogen atom bonded to a nitrogen atom of an amido functionality. The synthesis and reaction chemistry of these platinum and palladium complexes comprises a major portion of this article.

These new hybrid phosphine amide ligands o-$Ph_2PC_6H_4NHC(O)Ph$ and o-$Ph_2PC_6H_4C(O)NHPh$ coordinate to platinum(II) and palladium(II) in either a monodentate or a bidentate mode. In the former case coordination is via the phosphorus atom, while in the latter case both the phosphorus and secondary nitrogen atoms are coordinated. The various bonding modes and stereochemistries can be determined by a combination of $^{31}P\{^1H\}$ NMR, ^1H NMR, and IR spectroscopy. Coordination of a phosphine ligand to Pt(II) or Pd(II) usually results in a downfield shift of between 10 and 50 ppm in the ^{31}P NMR chemical shift. Structural characterization by IR spectroscopy uses changes in the frequencies of the amide I, II, and III bands to identify the mode of amide coordination. Complexation via oxygen will shift the amide I band to lower frequency, whereas coordination via amide nitrogen will increase the amide I frequency. Thirdly coordination via a nitrogen atom of the iminol tautomer will result in ν(CN) being found in the 1600–1650 cm^{-1} range and ν(CO) in the 1300–1400 cm^{-1} range. Coordination via an N-deprotonated amide causes a simplification of the IR spectrum since the ν(NH) and amide II bands disappear. Coordination of a secondary amide via nitrogen results in a downfield shift of the NH resonance in the ^1H NMR spectrum.[3]

Experimental Section

Many of the experimental details relevant to the synthesis and characterization of these new complexes have been described in the first paper in this series.[3] The details here are either additional or are specific to individual complexes. Far-infrared spectra were recorded on a Hitachi Perkin-Elmer FIS3 spectrophotometer. The 360-MHz ^1H NMR spectra of *cis*-Pt(o-$Ph_2PC_6H_4NC(O)C_6H_4$)(o-$Ph_2PC_6H_4NHC(O)Ph$) (**1**) was measured as a solution in $CDCl_3$ on a NTC-360 spectrometer at the Colorado State University Regional NMR Center. Conductivity measurements were carried out in a conductivity cell connected to an Industrial Instruments RC-16B2 conductivity bridge. All measurements were made at 25 ± 0.5 °C. The cell constant of 0.417 cm^{-1} was determined from the conductance of a 0.100 m aqueous KCl solution. Acetonitrile for synthetic uses and conductivity measurements was dried by refluxing over CaH_2 under a nitrogen atmosphere, and dichloromethane for conductivity measurements was dried by refluxing over P_2O_5 under nitrogen. Fresh samples of each were distilled immediately prior to use. The synthesis of the ligands and the following complexes have been described in our previous article:[3] *trans*-$PtCl_2$(o-$Ph_2PC_6H_4NHC(O)Ph)_2$ (**9**), $PdCl_2$(o-$Ph_2PC_6H_4NHC(O)Ph)_2$ (**10**), *trans*-Pt(o-$Ph_2PC_6H_4C(O)NPh)_2$ (**11**), *cis*-Pd(o-$Ph_2PC_6H_4C(O)NPh)_2$ (**12**), *cis*-Pd(o-$Ph_2PC_6H_4C(O)NPh)_2$ (**13**), *cis*-Pt(o-$Ph_2PC_6H_4NC(O)Ph)_2$ (**14**). Spectral simulations were made by using the LAOCOON III program.

***cis*-Pt(o-$Ph_2PC_6H_4NC(O)C_6H_4$)(o-$Ph_2PC_6H_4NHC(O)Ph$)·$C_6H_5CH_3$ (1).** Complex **9** (400 mg, 0.39 mmol) was suspended in a mixed DMF/Et_3N (19 mL/1 mL) solvent. The yellow suspension was stirred under reflux for 1 h and then allowed to cool. Addition of water (30 mL) precipitated a white solid. This complex was isolated by vacuum filtration and the solid washed successively with water (3 × 10 mL) and ethanol (3 × 5 mL). The solid was purified by recrystallization. Cooling a saturated boiling toluene solution to −10 °C gave the product as transparent cubic crystals, which were filtered and dried in vacuo. Filtrate concentration gave an additional 50 mg of the compound for a total yield of 347 mg (85%); mp >300 °C. Anal. Calcd for $C_{57}H_{46}N_2O_2P_2Pt$: C, 65.3; H, 4.42; N, 2.67; P, 5.91; Cl, 0.00. Found: C, 65.4; H, 4.38; N, 2.66; P, 6.02; Cl, <0.05. The analogous procedure in refluxing acetonitrile solvent can also be used to prepare the complex. The reaction times required were longer but the complex precipitated during the course of the reaction.

***cis*-Pt(o-$Ph_2PC_6H_4NC(O)Ph$)(o-$Ph_2PC_6H_4NHC(O)Ph$)Cl (2).** This complex has been identified as an intermediate in the synthesis of **1**. If **1** was prepared by refluxing **9** as a suspension in MeCN/Et_3N (19 mL/1 mL) solvent, a white precipitate was formed after 60–90 min. This precipitate was a mixture of **1** and **2**. Separation of **1** and **2** was achieved by preparative scale TLC. Elution with CH_2Cl_2 separated the two complexes, **2** being the least mobile band.

Pd(o-$Ph_2PC_6H_4NC(O)C_6H_4$)(o-$Ph_2PC_6H_4NHC(O)Ph$) (3). Complex **10** (266 mg, 0.28 mmol) and DABCO (250 mg, 2.2 mmol) were suspended in acetonitrile (20 mL). The suspension was stirred for 3 h, during which time the mixture remained heterogeneous as the yellow color discharged. The white precipitate was filtered, washed with acetone (4 × 50 mL), and dried in vacuo. Yield 240 mg (97%); mp 290–292 °C (yellows above 90 °C). Anal. Calcd for $C_{50}H_{38}N_2O_2P_2Pd$: C, 69.3; H, 4.41; P, 7.15. Found: C, 68.6; H, 4.66; P, 6.88. Recrystallization from chloroform by addition of diethyl ether gave the complex containing $^2/_3$ mol of chloroform in the lattice. Anal. Calcd for $C_{50.6}H_{38.6}Cl_2N_2O_2Pd$: C, 64.3; H, 4.11; N, 2.87. Found: C, 64.4; H, 4.34; N, 2.94.

Benzoyl-d_5 Chloride. Benzoic-d_5 acid (1.0 g, 8.2 mmol) and thionyl chloride (8.2 g, 68.0 mmol) were placed in a 25-mL one-neck round-bottom flask fitted with a calcium sulfate drying tube. The mixture was stirred for 5 days. Distillation at ambient pressure gave $SOCl_2$ (80 °C) followed by product (190 °C): yield 0.92 g (80%) of clear liquid.

(3) Hedden, D.; Roundhill, D. M. *Inorg. Chem.* **1985**, *24*, 4152–4158.
(4) Lappert, M. F.; Power, P. P.; Sanger, A. R.; Srivastava, R. C. "Metal and Metalloid Amides"; Ellis Horwood: Chichester, U.K., 1980; pp 488–493.
(5) Garrou, P. E. *Chem. Rev.* **1981**, *81*, 229–266.

o-(Diphenylphosphino)-N-benzoylaniline (o-$Ph_2PC_6H_4NHC(O)C_6D_5$). Using the method developed for o-$Ph_2PC_6H_4NHC(O)Ph$ using o-$Ph_2PC_6H_4NH_2$ (1.1 g, 0.4 mmol) and benzoyl-d_5 chloride (0.58 g, 0.4 mmol) gave crude product. The compound was purified by recrystallization from CH_2Cl_2/hexane: yield 0.75 g (50%); mp 104–105 °C.

***trans*-Pt($OCOCF_3$)$_2$(o-$Ph_2PC_6H_4C(O)NHPh$)$_2$ (4).** Complex **11** (200 mg, 0.21 mmol) was dissolved in dichloromethane (5 mL). Excess trifluoroacetic acid (0.5 mL) was added dropwise to the solution, causing it to change from a yellow-green to a pale yellow color. The solution was allowed to stand for 10 min, and then a hexane/diethyl ether (10:1) mixture was added dropwise to precipitate a pale yellow solid. The product was collected by vacuum filtration, washed with hexane (5 mL), and dried in vacuo; yield 195 mg (78%). Anal. Calcd for $C_{54}H_{40}F_6N_2O_2P_2Pt$: C, 54.8; H, 3.40; P, 5.23; F, 9.62. Found: C, 54.7; H, 3.61; P, 5.38; F, 9.33.

***cis*-[Pt(o-$Ph_2PC_6H_4C(O)NPh$)(o-$Ph_2PC_6H_4C(O)NHPh$)(CF_3CO_2H)]CF_3CO_2 (5).** A solution of **12** (100 mg, 0.11 mmol) in dichloromethane (5 mL) was treated with excess trifluoroacetic acid. After 10 min the pale yellow solution was filtered and the solvent removed to yield an oil. Stirring the oil for 12 h with diethyl ether caused it to solidify. The off-white powder was filtered, washed with diethyl ether, and dried in vacuo: yield 112 mg (90%); mp 144–146 °C (with decomp). Anal. Calcd for $C_{54}H_{40}F_6N_2O_6P_2Pt$: C, 54.8; H, 3.40; F, 9.63. Found: C, 54.0; H, 3.68; F, 9.47.

Pd($OCOCF_3$)$_2$(o-$Ph_2PC_6H_4NHC(O)Ph$)$_2$ (6). The complex Pd(o-$Ph_2PC_6H_4NC(O)Ph$)$_2$·0.5(C_2H_5)$_2$O (90 mg, 0.1 mmol) in acetone (10 mL) was treated with excess trifluoroacetic acid (0.2 mL). After 1 h the solution was filtered and then reduced in volume to ca. 2 mL. Dropwise addition of a mixture of hexane and diethyl ether (10:1 ratio; 20 mL) precipitated a yellow powder which was filtered, washed with hexane (10 mL), and dried in vacuo: yield 106 mg (93%); mp 184–186 °C. Anal. Calcd for $C_{54}H_{40}F_6N_2O_6P_2Pd$: C, 59.1; H, 3.67; F, 10.2. Found: C, 58.7; H, 3.81; F, 10.4.

Pd($OCOCF_3$)$_2$(o-$Ph_2PC_6H_4C(O)NHPh$)$_2$·2CF_3CO_2H (7). Complex **13** (100 mg, 0.11 mmol) in dichloromethane (5 mL) was treated with excess trifluoroacetic acid. The yellow solution immediately darkened. After 10 min the solution was filtered and then reduced in volume to ca. 2 mL. Addition of hexane (10 mL) precipitated a yellow oil which solidified upon standing (12 h). The bright yellow microcrystals were collected by filtration, washed with hexane (10 mL), and dried in vacuo; yield 125 mg (86%). Anal. Calcd for $C_{58}H_{40}F_{12}N_2O_2P_2Pd$: C, 52.6; H, 3.05; F, 17.2. Found: C, 52.1; H, 3.30; F, 17.6.

[Pd(o-$Ph_2PC_6H_4N(Me)C(O)C_6H_4$)(o-$Ph_2PC_6H_4NHC(O)Ph$)]$SO_4Me$ (8). A solution of compound **2** (210 mg, 0.24 mmol) in chloroform (20 mL) was treated with dimethyl sulfate (61 mg, 0.48 mmol). After 2 h the dark yellow solution was reduced in volume to ca. 4 mL. Addition of diethyl ether (20 mL) gave an oily yellow solid which solidified after 12 h at −10 °C. The complex was filtered and dried in vacuo: yield 190 mg (79%); mp 187–189 °C (with decomp.). Anal. Calcd for $C_{52}H_{46}N_2O_2P_2PdS$: C, 62.8; H, 4.66. Found: C, 62.6; H, 4.27.

X-ray Structural Determination. Crystals of complex **1** were obtained by recrystallization from $CHCl_3$ and mounted on a fine glass fiber. Preliminary photographic characterization showed the specimen to belong to the triclinic crystal system. The space group $P\bar{1}$ was assumed and later proven correct by the chemically reasonable and well-behaved solution and refinement of the structure. Table I provides crystal, data collection, and refinement parameters.

The location of the Pt atom was obtained from a sharpened Patterson projection and was used to locate the remaining non-hydrogen atoms by difference Fourier syntheses. A severely disordered, substoichiometric molecule of $CHCl_3$ (site occupancy ~20%) was located and refined. In the final cycles of refinement (blocked cascade), the non-hydrogen atoms except for the carbon atoms of the five terminal phenyl groups were refined with anisotropic temperature factors. Additionally, the same five phenyl groups were treated as rigid hexagons, d(C–C) = 1.395 Å. With the exception of H(2) which was located and refined, all hydrogen atom contributions were calculated in idealized locations (d(C–H) = 0.96 Å; U = 1.2U attached). Computer programs used in the data collection, data reduction, and refinement are contained in the P3 and SHELXTL (3.0) program libraries distributed by the Nicolet Corp., Madison, WI.

Table I. Crystal, Data Collection, and Refinement Parameters for *cis*-Pt(o-$Ph_2PC_6H_4NC(O)C_6H_4$)(o-$Ph_2PC_6H_4NHC(O)Ph$)

formula	$PtC_{45}H_{39}N_2O_2P_2$
cryst system, space group	triclinic, $P\bar{1}$
a, b, c, Å	12.038 (3), 12.576 (5), 16.220 (6)
α, β, γ, deg	105.80 (3), 104.84 (3), 95.75 (3)
V, Å^3	2245.6 (13)
Z	2
cryst size, mm	0.21 × 0.26 × 0.41
μ, cm^{-1}	32.9 (Mo Kα)
min, max, transm	0.566, 0.484
diffractometer	Nicolet R3
temperature, °C	23
correctns to data	Lp, absorption (ψ scan), decay
scan speed, deg min^{-1}	var 3.5–10
scan technique	$\theta/2\theta$
std reflns	3/197 (4% decay)
scan range, deg	$4 < 2\theta < 45$
data collected	$\pm h, \pm k, +l$
unique reflns	5632 (5858 collected)
unique reflns, $F_o > 3\sigma(F_o)$	5115
R (av redun data)	0.0126
R_F, R_{wF}, GOF[a]	0.0375, 0.0402, 1.626
g[b]	0.008
slope, normal prob plot	1.244
highest peak, final diff map, e Å^{-3}	1.03 (in $CHCl_3$)

[a] $R_F = \sum||\Delta|/\sum|F_o|$, $R_{wF} = \sum(|\Delta|w^{1/2})/\sum(|F_o|w^{1/2})$, and GOF = $[w(\Delta^2/(N_{obsd} - N_{par})]^{1/2}$, $\Delta = |F_o| - |F_o|$. [b] $w^{-1} = \sigma^2(F_o) + gF_o^2$.

In the final difference map the seven highest peaks in the range 0.81–1.03 e Å^{-3} were all associated with the disordered solvent molecule. These were followed by a diffuse and chemically meaningless background (<0.5 e Å^{-3}). Fractional atomic coordinates are provided in Table II. Additional supplementary material has been deposited with our preliminary communication.[2]

Results and Discussion

In the first paper of this series we have outlined in detail the spectroscopic methods used to characterize the products.[3] We briefly summarize the salient features again here in order to guide the reader through the chemistry reported in this paper. Coordination of a phosphine ligand to Pt(II) and Pd(II) result in a downfield shift of between 10 and 50 ppm in the ^{31}P NMR chemical shift, and for the Pt(II) complexes we can use ^1J(PtP) values to deduce stereochemistry. For the chelated phosphine amido complexes we also need to include ring shifts before we can interpret ^{31}P chemical shift values.

Complexes **9** and **10** can be readily prepared by the addition of 2 equiv of o-$Ph_2PC_6H_4NHC(O)Ph$ to MCl_4^{2-} (M = Pt, Pd) (eq 1).[3] Complex **9** does not react with

$$MCl_4^{2-} + 2o\text{-}Ph_2PC_6H_4NHC(O)Ph \rightarrow MCl_2(o\text{-}Ph_2PC_6H_4NHC(O)Ph)_2 + 2Cl^- \quad (1)$$

9, M = Pt
10, M = Pd

triethylamine or DABCO at ambient temperature, either as a suspension in DMF or acetonitrile or as a solution in chloroform. When, however, the suspension of **9** in triethylamine/acetonitrile is refluxed for 60–90 min, a yellow solution is formed, and *cis*-Pt(o-$Ph_2PC_6H_4NC(O)Ph)_2$ (**14**) can be isolated (eq 2). At these lower reflux temperatures this cis amido complex is the final product.

Intramolecular Ortho Metalation of a Benzoyl Group. When a suspension of **9** and triethylamine in

$$\textit{trans}\text{-}PtCl_2(o\text{-}Ph_2PC_6H_4NHC(O)Ph)_2 + 2Et_3N \rightarrow \underset{14}{\underset{9}{\textit{cis}\text{-}Pt(o\text{-}Ph_2PC_6H_4NC(O)Ph)_2}} + 2Et_3NHCl \quad (2)$$

DMF is refluxed, a clear solution is obtained. Addition of water precipitates complex 1 as a white powder (eq 3).

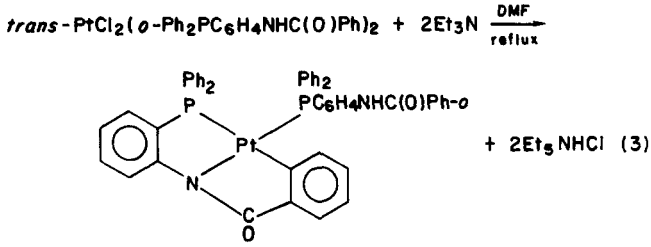

Complex 1 is slightly soluble in chloroform but insoluble in other organic solvents. The infrared spectrum (Nujol) shows absorptions characteristic of both a *o*-$Ph_2PC_6H_4NHC(O)Ph$ ligand (ν(NH) 3200, 3150 cm^{-1}; amide I, 1675 cm^{-1}, amide II, 1515 cm^{-1}, amide III, 1290 cm^{-1}) and a *o*-$Ph_2PC_6H_4NC(O)Ph$ ligand (amide I, 1620 cm^{-1}, amide III, 1320 cm^{-1}). The presence of a *o*-$Ph_2PC_6H_4NHC(O)Ph$ group is further supported by the observation of a resonance at δ 11.0 characteristic of a NH group.

The $^{31}P\{^1H\}$ NMR spectrum supports a structure with mutually cis phosphorus atoms coordinated to platinum(II) where the *o*-$Ph_2PC_6H_4NC(O)Ph$ ligand is bidentate and the *o*-$Ph_2PC_6H_4NHC(O)Ph$ is monodentate. The downfield resonance at δ 26.2 (P_A) is characteristic of a phosphine ligand in a five-membered ring[5] and is therefore assigned to *o*-$Ph_2PC_6H_4NC(O)Ph$. The upfield resonance at δ 2.4 (P_B) is due to the phosphorus of monodentate *o*-$Ph_2PC_6H_4NC(O)Ph$. The spectrum has been simulated for an AB pair flanked by satellites due to coupling with ^{195}Pt ($I = {}^1/_2$, 33.7% abundance). A value of 14 Hz for $^2J(PP)$ is found, which necessitates mutually cis phosphorus atoms. The magnitude of $^1J(PtP_B)$ at 3334 Hz is an expected value for a phosphine trans to an amido ligand which is low in the trans influence series.[4] The 1905-Hz coupling constant $^1J(PtP_A)$ is characteristic of a phosphine *trans* to a σ-alkyl or σ-aryl ligand bonded to platinum(II). The aryl ligand in the fourth coordination position about platinum is an ortho-metalated carbon of the benzoyl group. The low solubility of the complex in organic solvents precludes measurement of a $^{13}C\{^1H\}$ NMR spectrum, and the metalated structure has been confirmed by X-ray crystallography on a single crystal.

The coordination geometry about platinum is distorted planar with angles P(1)–Pt–P(2) = 100.6 (1)°, P(1)–Pt–N(1) = 83.7 (2)°, N(1)–Pt–C(3) = 81.2 (3)°, and P(2)–Pt–C(3) = 94.5 (3)° (Figure 2). The distances Pt–P(1) of 2.298 (2) Å and Pt–P(2) of 2.259 (2) Å are normal, the increased Pt–P(1) length being indicative of the higher trans influence of a σ-aryl ligand as compared to an amido ligand. The Pt–N(1) distance is 2.063 (7) Å which falls within the range of 2.02 (1)–2.09 (2) Å found for the small number of such complexes which have been structurally characterized.[6] Selected bond distances and angles are collected in Table III. The most interesting feature of the structure is the location of the amide group of the monodentate *o*-$Ph_2PC_6H_4NHC(O)Ph$ ligand. It is apparent from Figure 2 that this amido group lies close to the platinum center below the coordination plane. The hydrogen bonded to the amide nitrogen has been located on difference maps at a distance of 2.318 (22) Å from platinum (Figure 3). This Pt–H(2) distance is close to that which would be expected for a weak bonding interaction. Recently the term "agostic" has been used to discuss the various manifestations of covalent interactions between carbon–hydrogen groups and transition-metal centers in

Table II. Atomic Coordinates (×10⁴) and Temperature Factors (Å² × 10³)

atom	x	y	z	U_{iso}, Å²
Pt	1661.9 (2)	1851.5 (2)	2500.2 (2)	33 (0)[a]
P(1)	914 (2)	77 (2)	2459 (1)	35 (0)[a]
P(2)	3504 (2)	1659 (2)	2491 (1)	35 (0)[a]
N(1)	4 (5)	2145 (5)	2495 (4)	29 (3)[a]
N(2)	3535 (6)	2886 (6)	4480 (4)	53 (3)[a]
H(2)	2937 (17)	2697 (14)	4048 (13)	93 (8)
O(1)	−1131 (7)	3512 (7)	2476 (6)	96 (4)[a]
O(2)	4155 (7)	2988 (7)	5938 (5)	86 (4)[a]
C(1)	−185 (8)	3179 (8)	2499 (6)	57 (4)
C(2)	863 (8)	3936 (7)	2527 (6)	54 (4)[a]
C(3)	1899 (7)	3521 (6)	2553 (5)	42 (3)[a]
C(4)	2860 (9)	4247 (7)	2565 (6)	58 (4)[a]
C(5)	2797 (10)	5323 (8)	2572 (7)	78 (5)[a]
C(6)	1768 (11)	5710 (8)	2519 (8)	89 (5)[a]
C(7)	824 (10)	5024 (8)	2511 (7)	74 (5)[a]
C(8)	3357 (8)	2965 (7)	5286 (5)	55 (4)[a]
C(11)	−560 (6)	242 (7)	2475 (5)	42 (3)[a]
C(12)	−1343 (7)	−622 (8)	2509 (6)	51 (4)[a]
C(13)	−2422 (7)	−442 (9)	2582 (6)	65 (4)[a]
C(14)	−2726 (8)	572 (9)	2613 (6)	66 (5)[a]
C(15)	−1976 (7)	1443 (8)	2579 (6)	55 (4)[a]
C(16)	−855 (7)	1283 (7)	2509 (5)	43 (3)[a]
C(21)	2226 (5)	−1174 (4)	3417 (3)	45 (2)
C(22)	2668 (5)	−1482 (4)	4184 (3)	53 (2)
C(23)	2373 (5)	−1003 (4)	4963 (3)	61 (2)
C(24)	1636 (5)	−215 (4)	4976 (3)	61 (2)
C(25)	1193 (5)	94 (4)	4210 (3)	51 (2)
C(26)	1488 (5)	−385 (4)	3430 (3)	37 (2)
C(31)	825 (5)	−838 (4)	695 (4)	56 (2)
C(32)	628 (5)	−1700 (4)	−100 (4)	80 (3)
C(33)	328 (5)	2816 (4)	−144 (4)	93 (4)
C(34)	227 (5)	−3070 (4)	622 (4)	78 (3)
C(35)	424 (5)	−2208 (4)	1424 (4)	56 (2)
C(36)	724 (5)	−1092 (4)	1460 (4)	41 (2)
C(41)	4624 (5)	266 (4)	3401 (3)	46 (2)
C(42)	4984 (5)	−740 (4)	3457 (3)	55 (2)
C(43)	4690 (5)	−1674 (4)	2690 (3)	61 (2)
C(44)	4036 (5)	−1602 (4)	1869 (3)	55 (2)
C(45)	3675 (5)	−597 (4)	1813 (3)	45 (2)
C(46)	3969 (5)	337 (4)	2580 (3)	38 (2)
C(51)	4691 (4)	1379 (5)	1176 (4)	56 (2)
C(52)	4811 (4)	1395 (5)	347 (4)	67 (3)
C(53)	3957 (4)	1735 (5)	−237 (4)	76 (3)
C(54)	2983 (4)	2059 (5)	8 (4)	74 (3)
C(55)	2863 (4)	2043 (5)	838 (4)	54 (2)
C(56)	3717 (4)	1703 (5)	1422 (4)	41 (2)
C(61)	1357 (5)	3385 (5)	4726 (4)	57 (2)
C(62)	240 (5)	3462 (5)	4808 (4)	71 (3)
C(63)	−75 (5)	3192 (5)	5507 (4)	88 (3)
C(64)	727 (5)	2845 (5)	6122 (4)	92 (4)
C(65)	1843 (5)	2768 (5)	6040 (4)	80 (3)
C(66)	2159 (5)	3038 (5)	5341 (4)	49 (2)
C(71)	4675 (7)	2704 (6)	3408 (5)	41 (2)
C(72)	5701 (8)	3051 (7)	3240 (6)	56 (2)
C(73)	6658 (9)	3737 (8)	3948 (7)	70 (3)
C(74)	6602 (9)	4058 (9)	4780 (7)	70 (3)
C(75)	5577 (8)	3776 (8)	4973 (7)	59 (2)
C(76)	4597 (7)	3099 (7)	4285 (5)	45 (2)
C(99)[b]	7086 (32)	4826 (30)	1398 (25)	56 (9)
Cl(2)[b]	5907 (17)	4908 (17)	1816 (15)	151 (12)[a]
Cl(3)[b]	6946 (23)	4035 (22)	469 (16)	225 (15)[a]
Cl(4)[b]	7311 (36)	6209 (29)	1620 (17)	126 (16)[a]
Cl(5)[b]	7713 (22)	6093 (25)	1392 (16)	101 (12)[a]

[a] Equivalent isotropic U defined as one-third of the trace of the orthogonalized U_{ij} tensor. [b] Disordered solvent molecule.

(6) Fryzuk, M. D.; MacNeil, P. A.; Rettig, S. J.; Secco, A. S.; Trotter, J. *Organometallics* **1982**, *1*, 918–930. Zipprich, M.; Pritzkow, H.; Jarder, J. *Angew. Chem. Int. Ed. Engl.* **1976**, *15*, 225–226.

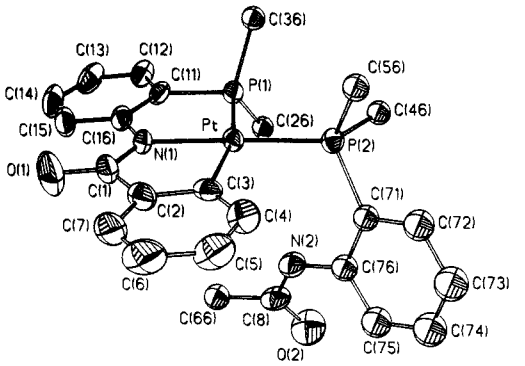

Figure 2. ORTEP diagram for *cis*-Pt(*o*-$Ph_2PC_6H_4NC(O)C_6H_4$)-(*o*-$Ph_2PC_6H_4NHC(O)Ph$) (1). Terminal phenyl groups shown as pivotal atom only.

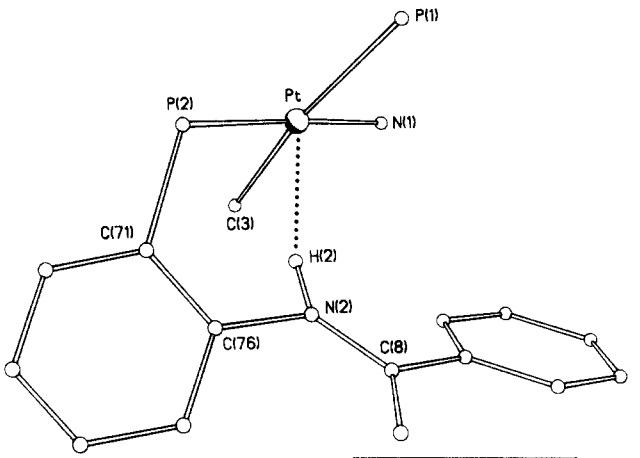

Figure 3. ORTEP diagram for *cis*-Pt(*o*-$Ph_2PC_6H_4NC(O)C_6H_4$)-(*o*-$Ph_2PC_6H_4NHC(O)Ph$) (1) showing the location of the "agostic" N–H···Pt bond.

Table III. Selected Bond Distances of Angles for *cis*-Pt(*o*-$Ph_2PC_6H_4NC(O)C_6H_4$)(*o*-$Ph_2PC_6H_4NHC(O)Ph$)

	(a) Bond Distances (Å)		
Pt–P(1)	2.298 (2)	N(1)–C(1)	1.342 (12)
Pt–P(2)	2.259 (2)	C1–O(1)	1.247 (13)
Pt–N(1)	2.063 (7)	C(1)–C(2)	1.485 (14)
Pt–C(3)	2.065 (8)	C(2)–C(3)	1.396 (14)
Pt–H(2)	2.318 (22)	P(2)–C(71)	1.848 (6)
P(1)–C(11)	1.814 (8)	C(71)–C(76)	1.405 (12)
C(11)–C(16)	1.382 (13)	C(76)–N(2)	1.411 (12)
C(16)–N(1)	1.431 (11)	N(2)–C(8)	1.357 (12)
H(2)–N(2)	1.04 (3)	C(8)–O(2)	1.225 (11)
	(b) Bond Angles (deg)		
P(1)–Pt–P(2)	100.6 (1)	N(1)–C(1)–O(1)	125.6 (9)
P(1)–Pt–N(1)	83.7 (2)	N(1)–C(1)–C(2)	113.4 (8)
P(1)–Pt–C(3)	164.8 (3)	C(1)–C(2)–C(3)	118.6 (8)
P(2)–Pt–N(1)	175.6 (2)	Pt–C(3)–C(2)	110.9 (6)
P(2)–Pt–C(3)	94.5 (3)	Pt–P(2)–C(71)	115.4 (3)
N1)–Pt–C(3)	81.2 (3)	C(46)–P(2)–C(56)	102.1 (3)
Pt–P(1)–C(11)	100.4 (3)	P(2)–C(11)–C(76)	122.4 (6)
C(26)–P(1)–C(36)	107.9 (3)	C(71)–C(76)–N(2)	121.4 (6)
P(1)–C(11)–C(16)	117.5 (6)	C(76)–N(2)–C(8)	128.8 (7)
C(11)–C(16)–N(1)	118.2 (8)	N(2)–C(8)–O(2)	121.5 (9)
C(16)–N(1)–C(1)	123.8 (7)	N(2)–C(8)–C(66)	116.8 (7)

organometallic compounds,[7] and we propose that complex 1 shows an "agostic" interaction of the type N–H···Pt. This

(7) Brookhart, M.; Green, M. L. H. *J. Organomet. Chem.* **1983**, *250*, 395–408. Eisenstein, O.; Jean, Y. *J. Am. Chem. Soc.* **1985**, *107*, 1177–1186. Brookhart, M.; Lukacs, A. *J. Am. Chem. Soc.* **1984**, *106*, 4161–4166. Ashworth, T. V.; Liles, D. C.; Singleton, E. *Organometallics* **1984**, *3*, 1851–1855. Rothwell, I. P. *Polyhedron* **1985**, *4*, 177–200.

Scheme I. Conversion of *trans*-$PtCl_2$(*o*-$Ph_2PC_6H_4NHC(O)Ph)_2$ into *cis*-Pt(*o*-$Ph_2PC_6H_4NC(O)C_6H_4$)(*o*-$Ph_2PC_6H_4NHC(O)Ph$) (1)

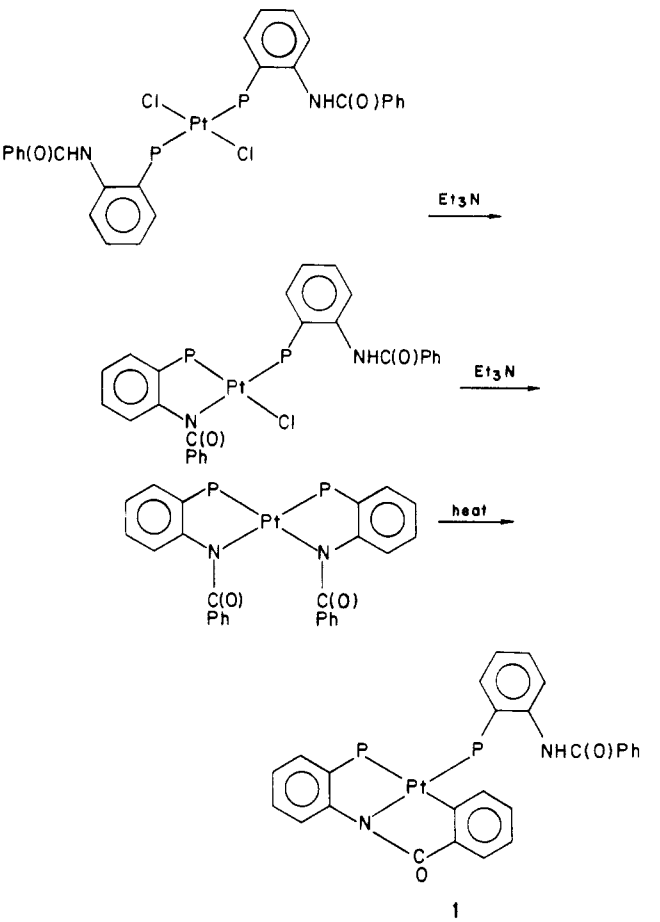

1

interaction is also identifiable in the solid-state infrared spectrum (Nujol mull) of 1 which shows the ν(NH) band at 3200 and 3150 cm^{-1}. This position represents a shift of 150–200 cm^{-1} to low frequency over the value of ν(NH) found in the free ligand (3350 cm^{-1}) or in the monodentate P-bonded complex **9** (3340 cm^{-1}).[3]

We have no conclusive proof that this "agostic" N–H···Pt interaction is present in chloroform solutions of the complex, although circumstantial evidence suggests that the solution structure is analogous. The ^1H NMR spectrum of complex 1 shows a resonance at δ 11.0 for NH, which represents a downfield shift of 2.3 ppm from that found in free *o*-$Ph_2PC_6H_4NHC(O)Ph$ and of 2.0 ppm from δ(NH) in **9**.[3] No coupling ^1J(PtH) is observed in the 360-MHz ^1H NMR spectrum of 1 at ambient temperature or at −50 °C. If there is any s character in the Pt–H bond we would expect to observe ^1J(PtH) coupling, unless, of course, the peaks are unobserved because of chemical shift anisotropy broadening.

Intramolecular Hydrogen Transfer. The cyclometalated complex 1 was initially discovered while attempting to prepare Pt(*o*-$Ph_2PC_6H_4NC(O)Ph)_2$. A plausible explanation for the formation of 1 from **9** is shown in Scheme I. The first step involves deprotonation of the free amide group followed by intramolecular amido substitution of a chloride ligand to give complex **2**. The substitution occurs with isomerization, which is unexpected since substitutions at platinum(II) typically occur with retention of stereochemistry. It is apparent that the intermediate **2** then undergoes a second analagous halide substitution reaction to give *cis*-Pt(*o*-$Ph_2PC_6H_4NC(O)Ph)_2$

(14). This second replacement occurs with stereochemical retention at platinum(II). The formation of the C-metalated complex 1 results from a subsequent thermal reaction of complex 14 induced by the high reaction temperatures produced in refluxing DMF.

The formation of 1 can be prevented by using lower reaction temperatures. Refluxing 9 with triethylamine as a suspension in acetonitrile solvent gives a mixture of 2 and 14 (^{31}P δ 9.5 (^1J(PtP) = 3241 Hz)) (eq 4).[3] The

$$\underset{\mathbf{9}}{trans\text{-}PtCl_2(o\text{-}Ph_2PC_6H_4NHC(O)Ph)_2} \xrightarrow[CH_3CN]{Et_3N} \underset{\mathbf{2}}{cis\text{-}Pt(o\text{-}Ph_2PC_6H_4NC(O)Ph)(o\text{-}Ph_2C_6H_4NHC(O)Ph)Cl} + \underset{\mathbf{14}}{cis\text{-}Pt(o\text{-}Ph_2PC_6H_4NC(O)Ph)_2} \quad (4)$$

percentage of complex 2 in the reaction mixture does not exceed 5%, and it is identified as *cis*-Pt(*o*-$Ph_2PC_6H_4NC$-(O)Ph)(*o*-$Ph_2PC_6H_4NHC(O)Ph)Cl$ by $^{31}P\{^1H\}$ NMR spectroscopy. Spectral simulation shows the observed spectrum to be an AB pair flanked by ^{195}Pt satellites. A value of 14 Hz for ^2J(PP) verifies a cis stereochemistry for the phosphines,[3] and the respective shift values of δ 23.7 (^1J-(PtP) = 3750 Hz and −4.9 (^1J(PtP) = 3073 Hz) confirm that one phosphorus is contained in a five-membered chelate ring, and the other one is P-bonded monodentate to platinum(II). The magnitudes of ^1J(PtP) indicate that each phosphine ligand is trans to a ligand of low trans influence (chloro and amido). At ambient temperatures the complexes 14 and 2 are indefinitely stable both in solution and the solid state. Refluxing complex 14, either alone or with 2, in chloroform, acetonitrile, toluene, or hexane solvent, gives 1 as the sole product even in the absence of added base. No intermediates have been observed in this final step. In the preliminary communication we have suggested that the reaction may involve an intermediate platinum(IV) hydride complex PtH(*o*-$Ph_2PC_6H_4NC(O)C_6H_4)(o\text{-}Ph_2PC_6H_4NC(O)Ph)$.[1] Such an intermediate is formed by oxidative addition of the C–H bond to platinum(II). Some support for this premise is found in the observation that ortho metalation is not observed under a high pressure of CO, where presumably the blocked fifth coordination position prevents the addition step at a coordinately unsaturated center.

Deuteration Experiments. The conversion of complex 14 into 1 via a platinum(IV) hydride intermediate involves intramolecular C–H addition to platinum(II) followed by N–H reductive elimination. Such a pathway transfers an ortho hydrogen on the benzoyl group of a complexed *o*-$Ph_2PC_6H_4NC(O)Ph$ group onto the coordinated nitrogen of the second *o*-$Ph_2PC_6H_4NC(O)Ph$ ligand to give monodentate P-bonded *o*-$Ph_2PC_6H_4NHC(O)Ph$. The ideal ligand to test this premise is *o*-$Ph_2PC_6H_4NHC(O)$-2,5-$C_6H_3D_2$, but in view of its synthetic inaccessibility in high yield, we have prepared *o*-$Ph_2PC_6H_4NHC(O)C_6D_5$ for the deuterium-transfer experiments. The complex *cis*-Pt(*o*-$Ph_2PC_6H_4NC(O)C_6D_5)_2$ has been prepared by initially synthesizing *trans*-$PtCl_2(o\text{-}Ph_2PC_6H_4NHC(O)C_6D_5)_2$ from the ligand and $PtCl_4^{2-}$ in acetonitrile solvent and then converting this intermediate to the product by a 5-day reaction with sodium *tert*-butoxide. Comparison of the $^{31}P\{^1H\}$ NMR and the IR spectra of the deuterated and nondeuterated compounds shows no changes except for an additional band due to ν(C–D) at 2290 cm^{-1} in *trans*-$PtCl_2(o\text{-}Ph_2PC_6H_4NHC(O)C_6D_5)_2$ and at 2275 cm^{-1} in *cis*-Pt(*o*-$Ph_2PC_6H_4NC(O)C_6D_5)_2$. Refluxing *cis*-Pt(*o*-$Ph_2PC_6H_4NC(O)C_6D_5)_2$ for 15 min in dry toluene gives a mixture of *cis*-Pt(*o*-$Ph_2PC_6H_4NC(O)C_6D_4)(o\text{-}Ph_2PC_6H_4NDC(O)C_6D_5)$ (**1a**) and *cis*-Pt(*o*-$Ph_2PC_6H_4NC(O)C_6D_4)(o\text{-}Ph_2PC_6H_4NHC(O)C_6D_5)$ (**1b**). Longer reaction times of approximately 1 h give only **1b**. Refluxing **1b** in C_6D_6 converts it into **1a** (eq 5). For

$$\underset{\mathbf{1b}}{cis\text{-}Pt(o\text{-}Ph_2PC_6H_4NC(O)C_6D_4)(o\text{-}Ph_2PC_6H_4NHC(O)C_6D_5)} \xrightarrow[\text{reflux}]{C_6D_6} \underset{\mathbf{1a}}{cis\text{-}Pt(o\text{-}Ph_2PC_6H_4NC(O)C_6D_4)(o\text{-}Ph_2PC_6H_4NDC(O)C_6D_5)} \quad (5)$$

complete **1b** we find ν(CD) at 2350 and 2310 cm^{-1} and ν(NH) at 3150 cm^{-1}. For compound **1a** we again find ν(CD) bands at 2350 and 2310 cm^{-1}, but now there are bands due to ν(ND) at 2260 and 2270 cm^{-1}. This experiment provides support for the premise that the cyclometalation reaction involves transfer of a hydrogen atom from the benzoyl phenyl ring to the complexed nitrogen of the second *o*-$Ph_2PC_6H_4NC(O)Ph$ ligand, followed by H/D exchange at nitrogen with the solvent. This mechanism results in one *o*-$Ph_2PC_6H_4NC(O)Ph$ group becoming an ortho-metalated tridentate ligand, and the other *o*-$Ph_2PC_6H_4NC(O)Ph$ moiety becoming a monodentate *o*-$Ph_2PC_6H_4NHC(O)Ph$ ligand. Although not fully proven, it is reasonable to assume that it is an ortho hydrogen which is transferred from the benzoyl group. No intermediates are observed, but our preferred pathway still involves oxidative addition of the C–H group followed by reductive elimination of the N–H moiety from a hydrido platinum(IV) intermediate. The observed scrambling of our H/D label from the solvent was completely unexpected. The exchange is subsequent to metalation since refluxing complex 1 in $CDCl_3$, C_6D_6, or CD_3CN solvent results in conversion of the N–H bond into N–D. This process can be reversed by refluxing N-deuterated product in toluene or CH_3CN solvent. Refluxing either the uncomplexed compound *o*-$Ph_2PC_6H_4NHC(O)Ph$ or complex **9** in CD_3CN for 24 h causes *no* H/D exchange. It appears therefore that the "agostic" N–H(D)···Pt interaction facilitates the H(D) atom to exchange with solvent, possibly by a weakening of the N–H(D) bond.

A second feature of this ortho-metalation reaction relates to the isotope effect for the conversion of 14 into the C-metalated complex 1. The hydrogen transfer to give 1 can be effected rapidly by refluxing 14 in benzene, acetonitrile, or chloroform, but even when *cis*-Pt(*o*-$Ph_2PC_6H_4NC$-$(O)C_6D_5)_2$ (deuterated 14) is refluxed up to 12 h in these lower boiling point solvents, there is no detectable ortho-metalated product. This result implies that there is a substantial kinetic isotope effect for the ortho-metalation reaction. Kinetic isotope effects (k_H/k_D) for cyclometalation reactions are often in the region of 6,[8] but no values are known for reductive elimination of N–H(D) step. Our overall hydrogen transfer reaction may indeed show a very high deuterium isotope effect if it occurs by a series of steps, each having a high k_H/K_D ratio. The major

(8) Diamond, S. E.; Mares, F. *J. Organomet. Chem.* **1977**, *142*, C55–C57.

Table IV. ^1H and $^{31}P\{^1H\}$ NMR Data for the New Complexes

complex	$\delta(^{31}P)$; J/Hz	$\delta(^1H)$
cis-Pt(*o*-$Ph_2PC_6H_4NC(O)C_6H_4$)(*o*-$Ph_2PC_6H_4NHC(O)Ph$) (1)	P_A, 26.2; P_B, 2.4; $^2J(PP)$ = 14; $^1J(PtP_A)$ = 1905; $^1J(PtP_B)$ = 3334	11.0 (NH)
cis-Pt(*o*-$Ph_2PC_6H_4NC(O)Ph$)(*o*-$Ph_2PC_6H_4NHC(O)Ph$)Cl (2)	P_A, 23.7; P_B, −4.9; $^2J(PP)$ = 14; $^1J(PtP_A)$ = 3750; $^1J(PtP_B)$ = 3073	
cis-Pd(*o*-$Ph_2PC_6H_4NC(O)C_6H_4$)(*o*-$Ph_2PC_6H_4NHC(O)Ph$) (3)	P_A, 23.1; P_B, 19.3; $^2J(PP)$ = 32	10.3 (NH)
trans-$Pt(OCOCF_3)_2$(*o*-$Ph_2PC_6H_4C(O)NHPh)_2$ (4)	7.2; $^1J(PtP)$ = 2760	11.8 (NH)
cis-[Pt(*o*-$Ph_2PC_6H_4C(O)NPh$)(*o*-$Ph_2PC_6H_4C(O)NHPh$)(CF_3CO_2H)]CF_3CO_2 (5)	P_A, 10.7; P_B, 2.1; $^2J(PP)$ = 11.6; $^1J(PtP_A)$ = 3120; $^1J(PtP_B)$ = 4150	9.4 (NH)
$Pd(OCOCF_3)_2$(*o*-$Ph_2PC_6H_4NHC(O)Ph)_2$ (6)	30.5 (br)	
$Pd(OCOCF_3)_2$(*o*-$Ph_2PC_6H_4C(O)NHPh)_2$·$2CF_3CO_2H$ (7)	37.8	11.8 br (OH + NH)
cis-[Pd(*o*-$Ph_2PC_6H_4N(Me)C(O)C_6H_4$)(*o*-$Ph_2PC_6H_4NHC(O)Ph$)]$MeSO_4$ (8)	P_A, 31.5; P_B, 30.8 (−55 °C)	

problem to quantifying this ratio is our observed H/D exchange between the "agostic" N–H group and the solvent. This feature creates difficulty in accurately measuring the kinetic ratio obtained in the metalation reaction.

The analogous ortho-metalated palladium(II) complex *cis*-Pd(*o*-$Ph_2PC_6H_4NC(O)C_6H_4$)(*o*-$Ph_2PC_6H_4NHC(O)Ph$) (**3**) can be prepared by reacting a suspension of **10** in acetonitrile with excess DABCO (eq 6). The yield is

$$\underset{\mathbf{10}}{PdCl_2(o\text{-}Ph_2PC_6H_4NHC(O)Ph)_2} \xrightarrow[CH_3CN]{DABCO} \underset{\mathbf{3}}{cis\text{-}Pd(o\text{-}Ph_2PC_6H_4NC(O)C_6H_4)(o\text{-}Ph_2C_6H_4NHC(O)Ph)} \quad (6)$$

quantitative. When triethylamine is used as base, the mixture must be heated to reflux to obtain **3**. The colorless complex is slightly soluble in $CHCl_3$ and CH_2Cl_2 but insoluble in other organic solvents. Crystals can be grown from a saturated $CHCl_3$ solution to which diethyl ether has been added. Spectral simulation of the ^{31}P NMR spectrum gives an AB pattern with $\delta(P_A)$ 23.1, $\delta(P_B)$ 19.3, and $^2J(PP)$ = 32 Hz. The ring shift for the phosphorus in a chelate is very small. In this palladium complex **3** we measure $\Delta(P_A–P_B)$ to be only 3.8 ppm whereas the platinum analogue **2** shows a 23.8 ppm difference.

The infrared spectrum of **3** as a Nujol mull shows absorptions characteristic of *o*-$Ph_2PC_6H_4NHC(O)Ph$ (ν(NH) 3240 cm^{-1}, amide I, 1675 cm^{-1}, amide II, 1510 cm^{-1}, amide III, 1295 cm^{-1}) and of *o*-$Ph_2PC_6H_4NC(O)Ph$ (amide I, 1610 cm^{-1}, amide III, 1340 cm^{-1}). Interaction of the amide hydrogen with palladium is indicated by the 100 cm^{-1} low frequency of ν(NH) as compared to free ligand and also by the downfield shift of the NH proton resonance by 1.5 ppm from free ligand to δ 10.3. Again the complex undergoes H/D exchange at the "agostic" NH with deuterated solvents such as C_6D_6, $CDCl_3$, and CD_3CN. No H/D exchange is found at the NH position of **10**, even after prolonged reflux.

The ortho-metalated palladium complex is more readily formed than the platinum analogue. Neither Pd(*o*-$Ph_2PC_6H_4NC(O)Ph)_2$[9] nor Pd(*o*-$Ph_2PC_6H_4NC(O)Ph$)(*o*-$Ph_2PC_6H_4NHC(O)Ph$)Cl can be formed from treating **10** with the base DABCO. The only observed product is the metalated complex **3**.

Chemical Reactivity of Chelated Amido Ligands to Brønsted Acids. Amido complexes of high-valent early-transition-metal ions are well-known. The compounds are stable thermodynamically, but chemically the complexes are moisture sensitive and react rapidly with water to give oxo and hydroxo complexes.[4] By contrast the amido complex **1** has been isolated by the addition of water to the reaction mixture, and the amido complexes **14**, **11**, **12**, and **13** are quite stable to hydrolysis. Nevertheless monomeric amido complexes have a nonbonded lone pair of electrons on the coordinated nitrogen, and we find that strong acids such as HCl will protonate these amido ligands at nitrogen.[3]

It is useful now for us to qualitatively investigate the reactivity of these monomeric amido complexes to Brønsted acids and electrophiles. In addition to using water and HCl as Brønsted acids, we have now added acetic and trifluoroacetic acids to these new amido complexes. These two acids span a wide range of strength, yet in each case the anionic ligand which may coordinate is a carboxylate group. All the amido complexes are resistant to attack by acetic acid. The amido complexes show no evidence of protonation by this reagent, and they can be recovered unchanged from the solutions. Trifluoroacetic acid, like HCl, is a sufficiently strong acid that protonation at nitrogen occurs, and the weakly coordinating amide ligand is replaced by a trifluoroacetate group. Reaction of excess trifluoroacetic acid with dichloromethane solutions of **11**, **12**, *cis*-Pd(*o*-$Ph_2PC_6H_4NC(O)Ph)_2$, and **13** gives respectively *trans*-$Pt(OCOCF_3)_2$(*o*-$Ph_2PC_6H_4C(O)NHPh)_2$, **4**, *cis*-[Pt(*o*-$Ph_2PC_6H_4C(O)NPh$)(*o*-$Ph_2PC_6H_4C(O)NHPh$)(CF_3CO_2H)]CF_3CO_2, **5**, $Pd(OCOCF_3)_2$(*o*-$Ph_2PC_6H_4NHC(O)Ph)_2$, **6**, and $Pd(OCOCF_3)_2$(*o*-$Ph_2PC_6H_4C(O)NHPh)_2$·$2CF_3CO_2H$, **7**. As with the analogous reaction with HCl,[3] this protonation reaction occurs with retention of stereochemistry. The pertinent $^{31}P\{^1H\}$, ^1H NMR, and IR data which confirm the structures of the compounds and the stereochemistries of the platinum complexes are as follows. **4**: δ_P 7.2 ($^1J(PtP)$ = 2760 Hz); δ_H 11.8; ν(NH) 3260 cm^{-1} (CH_3CN solvent), $\nu(OCOCF_3)$ 1790, 1745 cm^{-1}, amide I 1695 cm^{-1}. **5**: δ_{P_A} 10.7 ($^1J(PtP_A)$ = 3120 Hz), δ_{P_B} 2.1 ($^1J(PtP_B)$ = 4150 Hz, $^2J(P_AP_B)$ = 11.6 Hz), δ_H 9.4 (br); ν(NH) 3270 cm^{-1} (br), $\nu(OCOCF_3)$ 1790, 1745 cm^{-1} (*o*-$Ph_2PC_6H_4NHC(O)Ph$), 1610 cm^{-1} (*o*-$Ph_2PC_6H_4NC(O)Ph$), 1695 cm^{-1} for amide I (CH_3CN solvent). **6**: δ_P 30.5 (br); $\nu(OCOCF_3)$ 1775 cm^{-1} (br). **7**: δ_P

(9) Prepared from Pd_2(dibenzylideneacetone)$_3$ and *o*-$Ph_2PC_6H_4NHC(O)Ph$.

37.8; δ_H = 11.8 (br) (OH + N*H*); ν(NH) and ν(OH) 3250, 3210, 3160 cm^{-1}, $\nu(OCOCF_3)$ 1775 cm^{-1}. The NMR data are collected in Table IV.

For these complexes the observation of $\nu(OCOCF_3)$ bands in the 1750–1800 cm^{-1} region is diagnostic of monodentate O-bonded trifluoroacetate ligands. Hydrogen bonding between the acidic amide protons and either the trifluoroacetate or amide oxygens is indicated by the low-field resonance of the NH proton at δ 11.8, a downfield shift of 3 ppm from *o*-$Ph_2PC_6H_4C(O)NHPh$. The ν(NH) band is too broad to be observed in Nujol, but it is found in the region of 3250 cm^{-1} in acetonitrile solvent. Similarly the broad absorption bands characteristic of uncoordinated amide and the trifluoroacetate groups are very broad in the solid-state infrared spectrum, but in acetonitrile solvent the bands sharpen. For complex **4** the amide I and ν(CO) bands of the trifluoroacetate ligand can be identified at the respective positions of 1695, 1745, and 1790 cm^{-1}. The complex is a weak electrolyte in acetonitrile solvent. At high concentrations of the complex (0.7 mM) the solution conductivity Λ_M is 50 Ω^{-1} cm^2 mol^{-1}, but at low concentrations (0.034 mM) the value of Λ_M is 117 Ω^{-1} cm^2 mol^{-1}. This latter value approaches that characteristic of a 1:1 electrolyte.[10] These data show that a trifluoroacetate ligand undergoes replacement by acetonitrile. This equilibrium is shown in eq 7. The ionic complex **5** has

$$\textit{trans}\text{-Pt}(OCOCF_3)_2(o\text{-}Ph_2PC_6H_4C(O)NHPh)_2 + \underset{4}{} MeCN \rightarrow \textit{trans}\text{-}[Pt(OCOCF_3)(o\text{-}Ph_2PC_6H_4C(O)NHPh)_2MeCN]\text{-}CF_3CO_2 \quad (7)$$

an equivalent conductivity of 130 Ω^{-1} cm^2 mol^{-1}, in acetonitrile solvent which is that expected for a 1:1 electroyte. Complex **7** is slightly conducting, but the small value of 10.6 Ω^{-1} cm^2 mol^{-1} is likely due to the presence of trifluoroacetic acid.

The ortho-metalated complexes **1** and **3** present an interesting case for probing reactivities to Brønsted acids and electrophilic methylating agents. Two sites of attack at coordinated ligands are present in each molecule. It is plausible that protonation or electrophilic attack can occur at the coordinated phenyl carbon,[11] or at the amido nitrogen, or at both.

The ortho-metalated complexes **1** and **3** undergo protonation with HCl. In each case both the metal–aryl and metal–amido bonds undergo protolysis, and the respective products are *cis*-$PtCl_2$(*o*-$Ph_2PC_6H_4NHC(O)Ph)_2$ and **10** (eq 8). With trifluoroacetic acid, protonation of **1** and **3** again

$$\textit{cis}\text{-}\overline{M(o\text{-}Ph_2PC_6H_4NC(O)C_6H_4)}\text{-}(o\text{-}Ph_2PC_6H_4NHC(O)Ph) + 2HCl \rightarrow \textit{cis}\text{-}MCl_2(o\text{-}Ph_2PC_6H_4NHC(O)Ph)_2 \quad (8)$$

M = Pt, Pd

occurs, but now the reaction is reversible. In the presence of excess CF_3CO_2H both the Pt and Pd complexes give a single ^{31}P NMR resonance. For **1** this peak is at δ 9.8 (^1J(PtP) = 3241 Hz), and for **3** the resonance is at δ 38.4 ($\nu_{1/2}$ = 50 Hz). Neither product is isolable since addition of hexane to the solutions causes reversion back to **1** and **3**, respectively. We suggest that protonation occurs at the amido ligand to give [$\overline{M(o\text{-}Ph_2PC_6H_4N(H)C(O)C_6H_4)}$(*o*-$Ph_2PC_6H_4NHC(O)Ph)]^+$ (eq 9). This complex has both

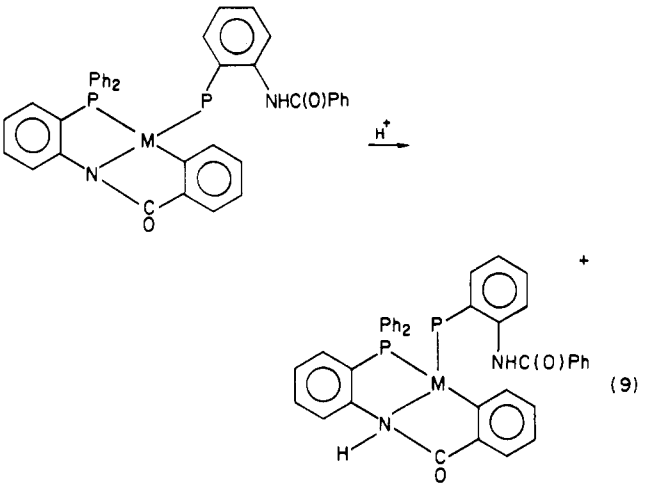

(9)

an internal and an external amide group, and coordination of each amide to M will cause the complex to be pentacoordinate and fluxional. Attempts to obtain satisfactory ^{31}P NMR spectra at low temperature were unsuccessful because of the solidification of trifluoroacetic acid. Alkylation of **3** also occurs at the amide nitrogen rather than at the coordinated aryl carbon atom. Complex **3** reacts with dimethyl sulfate in chloroform solvent to give [$\overline{Pd(o\text{-}Ph_2PC_6H_4N(Me)C(O)C_6H_4)}$(*o*-$Ph_2PC_6H_4NHC(O)Ph)]SO_4Me$ (**8**) (eq 10). This complex **8** now has a tertiary

$$\overline{Pd(o\text{-}Ph_2PC_6H_4NC(O)C_6H_4)}\text{-}(o\text{-}Ph_2PC_6H_4NHC(O)Ph) + Me_2SO_4 \rightarrow \overline{Pd(o\text{-}Ph_2PC_6H_4N(Me)C(O)C_6H_4)}\text{-}(o\text{-}Ph_2PC_6H_4NHC(O)Ph)]SO_4Me \quad (10)$$

amine coordinated to palladium(II), and since *N*-methyl heterolytic cleavage is much less facile than N–H deprotonation, this methylated product is stable in the solid state and can be isolated. The spectroscopic data are as follows: ν(NH) 3450 cm^{-1}, amide I 1610 cm^{-1}, ν(S=O) 1200 cm^{-1}. $^{31}P\{^1H\}$ shows δ 33.8 ($\nu_{1/2}$ = 10 Hz at 25 °C) which broadens on lowering the temperature. At −55 °C two peaks ($\nu_{1/2}$ = 5 Hz) are observed at δ 30.8 and 31.5. The exchange process can be explained again on the basis of a pentacoordinate intermediate.

Acknowledgment. We thank the Colorado State University Regional NMR Center, funded by National Science Foundation Grant CHE-820882, for the 360-MHz ^1H NMR spectrum. The University of Delaware received support from the National Science Foundation for the purchase of the diffractometer.

Supplementary Material Available: Tables of atomic coordinates, bond distances, bond angles, anisotropic temperature factors, and hydrogen atom coordinates for **1** (37 pages). Ordering information is given on any current masthead page.

(10) Geary, W. J. *Coord. Chem. Rev.* **1971**, *7*, 81–122.
(11) Hartley, F. R. In "Comprehensive Organometallic Chemistry"; Wilkinson, G., Ed.; Pergamon Press: Oxford, 1982; Vol. 6, pp 551–554.

A Platinum Cluster Complex Containing a Triply Bridging Carbonyl: The Synthesis and Structure of (μ_3-Carbonyl)tris[μ-bis(diphenylphosphino)methane]-*triangulo*-triplatinum(2+) Hexafluorophosphate

George Ferguson,*[1a] Brian R. Lloyd,[1b] and Richard J. Puddephatt*[1b]

Departments of Chemistry, University of Guelph, Guelph, Ontario, Canada N1G 2W1, and University of Western Ontario, London, Ontario, Canada N6A 5B7

Received June 24, 1985

Reaction of $[Pt(O_2CCF_3)_2(dppm)]$, dppm = $Ph_2PCH_2PPh_2$, with CO in aqueous methanol gives the cluster complex $[Pt_3(\mu_3\text{-}CO)(\mu\text{-}dppm)_3][CF_3CO_2]_2$ (1) which may be converted to the $[PF_6]^-$ salt **2**. The complexes **1** and **2** are the first complexes reported to contain the $Pt_3(\mu_3\text{-}CO)$ group and are significant as models for CO chemisorbed at a threefold site on a Pt surface. Complexes **1** and **2** were characterized by elemental analysis, IR, and ^1H, ^{31}P, and ^{195}Pt NMR and by X-ray crystallography (for **2**, as the acetone solvate). Crystals of $2\cdot C_3H_6O$ are triclinic, space group $P\bar{1}$, with $Z = 2$, $a = 14.090$ (2) Å, $b = 22.711$ (4) Å, $c = 13.637$ (4) Å, $\alpha = 103.43°$, $\beta = 99.52$ (2)°, and $\gamma = 106.72$ (1)°. The structure was solved by the heavy-atom method and refined by full-matrix least-squares calculations with anisotropic thermal parameters for the non-phenyl and non-solvate atoms. At convergence, $R = 0.035$ for 6234 reflections with $I > 3\sigma(I)$. The crystal structure contains discrete cations, anions, and acetone solvate molecules. The Pt atoms of the cation form a triangle with Pt–Pt = 2.613–2.650 (1) Å. The carbonyl ligand occupies a triply bridging site with Pt–C = 2.080–2.095 (9) Å. The atoms of the Pt_3P_6 moiety are only approximately coplanar; the Pt–P distances are in the range 2.262–2.304 (2) Å. The three Pt_2P_2C five-membered rings adopt envelope conformations with the CH_2 moiety at the flap.

Introduction

When carbon monoxide is adsorbed onto a Pt(111) surface, the on-top (terminal) sites are occupied first [ν(CO) ≈ 2110 cm^{-1}] but at higher coverage the twofold (μ_2) sites are preferred [ν(CO) = 1840–1875 cm^{-1}].[2] Recently it has been shown that threefold (μ_3) sites are also occupied at high coverage [ν(CO) = ca. 1810 cm^{-1}][2] and that the energy difference between the μ_2-CO and μ_3-CO groups is only 4 (±1) kJ mol^{-1}. From the analogy between surfaces and clusters,[3] it should therefore be possible to prepare cluster complexes containing $Pt_3(\mu_3\text{-}CO)$ units. However, even high nuclearity clusters such as $[Pt_{19}(CO)_{22}]^{4-}$ or $[Pt_{30}(CO)_{60}]^{2-}$ contain only terminal and μ_2-CO ligands.[3-5] We now report the first synthesis of a complex containing the $Pt_3(\mu_3\text{-}CO)$ group and its characterization by spectroscopic techniques and by X-ray crystallography as $[Pt_3(\mu_3\text{-}CO)(\mu\text{-}dppm)_3][PF_6]_2\cdot(CH_3)_2CO$, dppm = $Ph_2PCH_2PPh_2$.[6]

Results and Discussion

Reaction of $[Pt(O_2CCF_3)_2(dppm)]$ with carbon monoxide at 100 °C for 3 days in methanol–water solvent gave the complex $[Pt_3(\mu_3\text{-}CO)(\mu\text{-}dppm)_3][CF_3CO_2]_2$ (1) in 97% yield. This complex was formed in spectroscopically pure form, and it was readily converted to $[Pt_3(\mu_3\text{-}CO)(\mu\text{-}dppm)_3][PF_6]_2$ (**2**) by reaction in methanol with excess $NH_4[PF_6]$. Complex **2** was characterized crystallographically as its acetone solvate.

Description of the Structure of $2\cdot(CH_3)_2CO$. The structure contains discrete cations, anions and loosely entrapped acetone of solvation separated by normal distances. In the cation (Figure 1) the Pt atoms form a triangle with Pt–Pt distances 2.613 (1), 2.638 (1), and 2.650 (1) Å and Pt–Pt–Pt angles 59.23 (1), 60.17 (1), and 60.60 (1)° (see Table I). The carbonyl ligand occupies a triply bridging site, with Pt–C distances 2.080 (9), 2.089 (8), and 2.095 (9) Å and Pt–C–Pt angles 77.6–78.8(3)°. The Pt_3P_6 atoms are only approximately coplanar (the deviation of the P atoms from the Pt_3 plane are as follows: P11, –0.276 (2); P12, –0.013 (2); P21, –0.619 (2); P22, 0.154 (2); P31, –0.495 (2); P32, –0.069 (2) Å). The Pt–P distances are in the range 2.262 (2) to 2.304 (2) Å with a mean value of 2.282 Å. All three Pt_2P_2C rings adopt envelope conformations with the methylene carbon at the flap; two of the atoms, C(2) and C(3), are folded toward the bridging carbonyl and the other, C(4), is folded away. Presumably these conformational variations improve the packing of the ions. In the related palladium complex $[Pd_3(\mu_3\text{-}CO)(\mu\text{-}dppm)_3][CF_3CO_2]_2$, the corresponding Pd–Pd, Pd–C, and Pd–P distances are 2.576 (1)–2.610 (2) Å, 2.09 (1)–2.18 (1), and 2.296 (3)–2.340 (3) Å, respectively.[6] The structures are very similar, but, in the platinum complex, the metal–metal distances are slightly longer and the metal–phosphorus and metal–carbon distances are slightly shorter than in the palladium complex. The Pt–Pt distances in **2** are slightly shorter than the range of Pt–Pt distances of 2.672 (2)–2.790(7) Å found in platinum clusters such as $[Pt_3(\mu\text{-}SO_2)_3(PPh_3)_3]$, $[Pt_3(\mu\text{-}CO)_3(PCy_3)_4]$ (Cy = cyclohexyl), and $[Pt_4(\mu\text{-}CO)_5(PMe_2Ph)_4]$[7-10] but lie in the range

(1) (a) University of Guelph. (b) University of Western Ontario.
(2) Baro, A. M.; Ibach, H. *Surf. Sci.* **1981**, *103*, 248. Hayden, B. E.; Bradshaw, A. M. *Surf. Sci.* **1983**, *125*, 787.
(3) Muetterties, E. L.; Rhodin, T. N.; Band, E.; Brucker, C. F.; Pretzer, W. R. *Chem. Rev.* **1979**, *79*, 91.
(4) Clark, H. C.; Jain, V. K. *Coord. Chem. Rev.* **1984**, *55*, 151.
(5) Semitriply bridging carbonyls are observed in some heteronuclear clusters. Bender, R.; Braunstein, P.; Dusausoy, Y.; Protas, J. *J. Organomet. Chem.* **1979**, *172*, C51. Bender, R.; Braunstein, P.; Jud, J. M.; Dusausoy, Y. *Inorg. Chem.* **1984**, *23*, 4489.
(6) The synthesis of a related palladium complex, $[Pd_3(\mu_3\text{-}CO)(\mu\text{-}dppm)_3][CF_3CO_2]_2$, has been reported recently. Manojlović-Muir, Lj.; Muir, K. W.; Lloyd, B. R.; Puddephatt, R. J. *J. Chem. Soc., Chem. Commun.* **1983**, 1336. Lloyd, B. R.; Puddephatt, R. J. *Inorg. Chim. Acta* **1984**, *90*, L77. Manojlović-Muir, Lj.; Muir, K. W.; Lloyd, B. R.; Puddephatt, R. J. *J. Chem. Soc., Chem. Commun.* **1985**, 536.
(7) Moody, D. C.; Ryan, R. R. *Inorg. Chem.* **1977**, *16*, 1052.
(8) Albinati, A.; Carturan, G.; Musco, A. *Inorg. Chim. Acta* **1976**, *16*, L3.

0276-7333/86/2305-0344$01.50/0

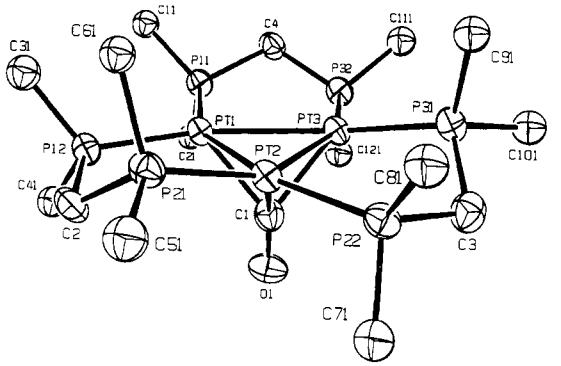

Figure 1. A view of the $[Pt_3(\mu\text{-CO})(\mu\text{-dppm})_3]^{2+}$ cation with the crystallographic numbering scheme. For clarity only the phenyl carbon bonded to each phosphorus atom is shown (phenyl ring atoms are numbered Cn1–Cn6 where n = 1–12).

of Pt–Pt bond lengths of 2.584 (2)–2.769 (1) Å found for diplatinum(I) complexes.[11,12] These observations are consistent with the formal oxidation state for platinum of $+^2/_3$ for complex **2** and with the presence of Pt–Pt single bonds in the cluster.

Spectroscopic Properties of 1 and 2. The carbonyl stretching frequencies of **1** and **2** were at 1750 and 1765 cm^{-1}, respectively, which may be compared to the value of ν(CO) of 1810 cm^{-1} for CO at a threefold site on Pt(111). It seems that back-bonding from platinum into π^* orbitals of CO is reasonably strong despite the 2+ charge on the cluster. The ν(CO) values for **1** and **2** were ~70 cm^{-1} to lower energy than those of the analogous palladium complexes; similar differences have been observed in other carbonyl complexes such as $[M_2Cl_2(\mu\text{-CO})(\mu\text{-dppm})_2]$, M = Pd or Pt.[13,14]

The $^1H\{^{31}P\}$ NMR spectra of **1** and **2** each contained an AB quartet for the $CH^AH^BP_2$ protons showing that there is no plane of symmetry containing the $Pt_3P_6C_3$ atoms of the $Pt_3(dppm)_3$ unit. This nonequivalence of the CH_2P_2 protons arises due to the presence of the μ_3-CO ligand on one side of the Pt_3 triangle.

The $^{31}P\{^1H\}$ NMR spectra of **1** and **2** each contained a singlet with very complex and incompletely resolved satellites due to coupling to ^{195}Pt, as shown in Figure 2a. The complexity arises in part from the superposition of resonances due to the Pt_3P_6 systems containing 0 (29% natural abundance), 1 (44%), 2 (23%), and 3 (4%) ^{195}Pt atoms. The spectra were insufficiently resolved to allow a full simulation, but the coupling constant ^1J(PtP) was easily obtained and partial simulation of the system containing one ^{195}Pt center showed that there is one large ^3J(PP) coupling of 170 Hz in **1** and 140 Hz in **2** [illustrated by i in Figure 2]. This large coupling is tentatively assigned as that between the nearly trans phosphorus atoms P(11)P(22), P(21)P(32), and P(12)P(31), defined in Figure 1. The long-range couplings ^2J(PtP) were too small to be resolved.

In the $^{195}Pt\{^1H\}$ NMR spectrum (Figure 2b) the most prominent feature is the triplet arising from the isotopomer containing a single ^{195}Pt atom, due to coupling to the two

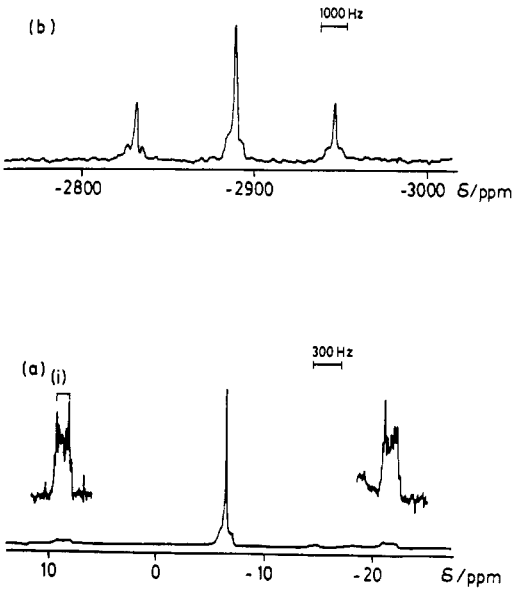

Figure 2. NMR spectra of complex **2**: (a) ^{31}P NMR spectrum (121.4 MHz). The inset shows the ^{195}Pt satellites at higher sensitivity and (i) shows the large J(PP) coupling (see the text). (b) ^{195}Pt NMR spectrum (64.3 MHz).

directly bound phosphorus atoms. Satellite spectra, arising from the isotopomer with two ^{195}Pt atoms, were also observed (Figure 2b) and allowed the coupling constant ^1J(PtPt) ≈ 540 Hz to be determined. The value is comparable to values found in other triangular Pt_3 clusters.[15,16]

Another feature of interest is the significant difference in the ^{31}P and ^{195}Pt chemical shifts between complexes **1** and **2**. A similar effect has been observed in the analogous palladium complexes,[6] and it is rationalized by assuming that in **1** a trifluoroacetate ion is weakly coordinated to platinum at the triply bridging site, which is vacant in complex **2**. Complex **1** may therefore be better characterized as $[Pt_3(O_2CCF_3)(\mu_3\text{-CO})(\mu\text{-dppm})_3][CF_3CO_2]$.

The spectroscopic data are clearly consistent with the structure of **2** being the same in solution as in the solid-state structure determined crystallographically (Figure 1).

Bonding in Complex 2. The bonding in complex cation **2** can be treated in several ways. First, it can be seen that each platinum atom is in oxidation state $+^2/_3$ and that, if the Pt–Pt bonds within the Pt_3 triangle are single two-electron bonds, each platinum atom has a 16-electron-valence shell. Secondly, the total number of valence electrons in the cluster is 42 and polyhedral skeletal electron pair theory predicts a "latitudinal" structure with a planar Pt_3P_6 skeleton.[17] The theoretical work is based on a neutral Pt_3L_6 cluster but, since the carbonyl ligand in **2** provides two electrons to make up for the 2+ charge on the cluster cation, the result is the same. In a latitudinal $[Pt_3L_6]^{2+}$ cluster the LUMO is expected to be an orbital of A_1 symmetry derived from a linear combination of the hybrid 6s $5d_z^2$ orbitals directed toward the center of the Pt_3 triangle.[17] If the CO ligand donates two electrons into this A_1 molecular orbital, it would be expected to occupy the symmetrical triply bridging coordination site as observed. It is possible, and only detailed MO calculations could

(9) Chatt, J.; Chini, P.; Dahl, L. F.; Vranka, R. G. *J. Am. Chem. Soc.* **1969**, *91*, 1574.
(10) Braunstein, P.; Jud, J.-M.; Dusausoy, Y.; Fischer, J., *Organometallics* **1983**, *2*, 1980.
(11) Manojlović-Muir, Lj.; Muir, K. W.; Solomun, T. *J. Organomet. Chem.* **1979**, *179*, 479.
(12) Manojlović-Muir, Lj.; Muir, K. W. *J. Organomet. Chem.* **1981**, *219*, 129.
(13) Balch, A. L.; Benner, L. S. *J. Am. Chem. Soc.* **1979**, *100*, 6099.
(14) Brown, M. P.; Puddephatt, R. J.; Rashidi, M.; Seddon, K. R. *J. Chem. Soc., Dalton Trans.* **1978**, 1540.
(15) Moor, A.; Pregosin, P. S.; Venanzi, L. M. *Inorg. Chim. Acta* **1981**, *48*, 153.
(16) Moor, A.; Pregosin, P. S.; Venanzi, L. M. *Inorg. Chim. Acta* **1981**, *48*, 153.
(17) Evans, D. G.; Mingos, D. M. P. *J. Organomet. Chem.* **1982**, *240*, 321. The planarity of the Pt_3L_6 skeleton is most simply rationalizing in terms of the isolobal analogy of PtL_2 and CH_2 fragments, so that planar Pt_3L_6 is isolobal with cyclopropane. Hoffmann, R. *Angew. Chem., Int. Ed. Engl.* **1982**, *21*, 711.

Table I. Selected Interatomic Distances and Angles

a. Bond Distances (Å)

atom 1	atom 2	dist	atom 1	atom 2	dist
Pt1	Pt2	2.638 (1)	P12	C31	1.807 (8)
Pt1	Pt3	2.650 (1)	P12	C41	1.807 (8)
Pt1	P11	2.304 (2)	P21	C2	1.848 (8)
Pt1	P12	2.284 (2)	P21	C51	1.804 (8)
Pt1	C1	2.095 (9)	P21	C61	1.813 (8)
Pt2	Pt3	2.613 (1)	P22	C3	1.858 (8)
Pt2	P21	2.277 (2)	P22	C71	1.789 (8)
Pt2	P22	2.271 (2)	P22	C81	1.792 (8)
Pt2	C1	2.089 (8)	P31	C3	1.823 (8)
Pt3	P31	2.294 (2)	P31	C91	1.814 (8)
Pt3	P32	2.262 (2)	P31	C101	1.817 (8)
Pt3	C1	2.080 (9)	P32	C4	1.832 (8)
P11	C4	1.843 (8)	P32	C111	1.803 (8)
P11	C11	1.807 (8)	P32	C121	1.812 (8)
P11	C21	1.811 (8)	O1	C1	1.154 (9)
P12	C2	1.835 (8)			

mean P–F = 1.570 (7) Å; mean aromatic C–C = 1.38 (1) Å

b. Bond Angles (deg)

atom 1	atom 2	atom 3	angle	atom 1	atom 2	atom 3	angle
Pt2	Pt1	Pt3	59.23 (1)	Pt2	Pt3	C1	51.3 (2)
Pt2	Pt1	P11	154.10 (5)	P31	Pt3	P32	113.28 (8)
Pt2	Pt1	P12	94.86 (5)	P31	Pt3	C1	121.4 (2)
Pt2	Pt1	C1	50.8 (2)	P32	Pt3	C1	115.3 (2)
Pt3	Pt1	P11	95.69 (5)	Pt1	P11	C4	109.5 (3)
Pt3	Pt1	P12	154.09 (6)	Pt1	P11	C11	119.3 (3)
Pt3	Pt1	C1	50.4 (2)	Pt1	P11	C21	113.1 (3)
P11	Pt1	P12	109.98 (8)	C4	P11	C11	103.6 (4)
P11	Pt1	C1	119.8 (2)	C4	P11	C21	105.9 (4)
P12	Pt1	C1	115.0 (2)	C11	P11	C21	104.4 (4)
Pt1	Pt2	Pt3	60.60 (1)	Pt1	P12	C2	111.6 (3)
Pt1	Pt2	P21	92.62 (5)	Pt1	P12	C31	121.1 (3)
Pt1	Pt2	P22	157.63 (5)	Pt1	P12	C41	108.7 (3)
Pt1	Pt2	C1	51.0 (2)	C2	P12	C31	103.6 (4)
Pt3	Pt2	P21	149.30 (6)	C2	P12	C41	105.1 (4)
Pt3	Pt2	P22	97.34 (5)	C31	P12	C41	105.6 (4)
Pt3	Pt2	C1	51.0 (2)	Pt2	P21	C2	107.6 (3)
P21	Pt2	P22	109.64 (8)	Pt2	P21	C51	119.8 (3)
P21	Pt2	C1	124.6 (2)	Pt2	P21	C61	111.1 (3)
P22	Pt2	C1	113.4 (2)	C2	P21	C51	105.2 (4)
Pt1	Pt3	Pt2	60.17 (1)	C2	P21	C61	106.0 (4)
Pt1	Pt3	P31	148.86 (5)	C51	P21	C61	106.2 (4)
Pt1	Pt3	P32	94.46 (5)	Pt2	P22	C3	109.4 (3)
Pt1	Pt3	C1	50.9 (2)	Pt2	P22	C71	109.1 (3)
Pt2	Pt3	P31	91.04 (5)	Pt2	P22	C81	120.9 (3)
Pt2	Pt3	P32	154.58 (5)	C3	P22	C71	104.51 (4)
C3	P22	C81	105.4 (4)	C4	P32	C121	106.9 (4)
C71	P22	C81	106.3 (4)	C111	P32	C121	106.2 (4)
Pt3	P31	C3	108.1 (3)	Pt1	C1	Pt2	78.2 (3)
Pt3	P31	C91	114.1 (3)	Pt1	C1	Pt3	78.8 (3)
Pt3	P31	C101	120.1 (3)	Pt1	C1	O1	131.8 (6)
C3	P31	C91	104.1 (4)	Pt2	C1	Pt3	77.6 (3)
C3	P31	C101	104.0 (4)	Pt2	C1	O1	133.1 (7)
C91	P31	C101	104.9 (4)	Pt3	C1	O1	134.9 (7)
Pt3	P32	C4	110.3 (3)	P12	C2	P21	109.0 (4)
Pt3	P32	C111	119.2 (3)	P22	C3	P31	110.0 (4)
Pt3	P32	C121	110.1 (3)	P11	C4	P32	112.8 (4)
C4	P32	C111	103.3 (4)				

settle this point, that the above argument is oversimplified, and it should be recognized that greater steric effects would be observed if the CO ligand adopted a μ_2-bridging position. However, we suggest that both steric and electronic effects probably favor the unique $Pt_3(\mu_3\text{-CO})$ linkage found experimentally for complex **2**.

Experimental Section

Infrared spectra were recorded as Nujol mulls using a Beckman Acculab 4 spectrometer. ^1H NMR and $^1H\{^{31}P\}$ NMR spectra were recorded on a Varian XL-100 NMR spectrometer. ^{31}P and ^{195}Pt NMR spectra were recorded on a Varian XL-300 NMR spectrometer. References were Me_4Si (^1H), $(MeO)_3PO$ (^{31}P), and aqueous $K_2[PtCl_4]$ (^{195}Pt).

Preparation of $[Pt(O_2CCF_3)_2(dppm)]$. $[PtCl_2(dppm)]$ (5.131 mmol) and $[AgO_2CCH_3]$ (10.244 mmol) were reacted in acetone (50 mL) in the presence of excess CF_3COOH (15 mL). The suspension was stirred for 0.5 h at room temperature under N_2, then heated briefly at 60 °C, and then allowed to cool for 1 h. The solution was then filtered, and the solvent was evaporated from the filtrate under vacuum to give an oil. The oil was then dissolved in acetone (50–100 mL), and excess pentane was added to precipitate a white crystalline solid: yield 92%; mp 200–210 °C dec; ^1H NMR $[(CD_3)_2CO]$ δ 5.00 [t, $^2J(PH)$ = 12, $^3J(PtH)$ = 88 Hz, CH_2P_2]; ^{31}P NMR $[(CD_3)_2CO]$ δ –67.7 [s, $^1J(PtP)$ = 3360 Hz]. Anal. Calcd for $[Pt(CF_3CO_2)_2(dppm)]$: C, 43.24; H, 2.75. Found: C, 43.00; H, 2.92.

Preparation of $[Pt_3(\mu_3\text{-CO})(\mu\text{-dppm})_3][CF_3CO_2]_2$. $[Pt(O_2CCF_3)_2(dppm)]$ (1.319 mmol) and CO (4 atm) were reacted

Table II. Positional Parameters and Their Estimated Standard Deviations[a]

atom	x	y	z	B, Å²	atom	x	y	z	B, Å²
Pt1	0.00260 (2)	0.26436 (2)	0.11090 (3)	2.166 (8)	C52	0.0610 (8)	0.1162 (5)	0.4012 (8)	4.5 (2)*
Pt2	0.14305 (2)	0.22463 (2)	0.20046 (3)	2.159 (8)	C53	0.0927 (9)	0.0800 (6)	0.4618 (9)	5.7 (3)*
Pt3	0.16857 (2)	0.26799 (2)	0.04172 (3)	2.168 (8)	C54	0.1723 (9)	0.1087 (6)	0.547 (1)	6.3 (3)*
P1	0.2588 (3)	0.5404 (2)	0.2445 (3)	5.37 (9)	C55	0.2204 (8)	0.1720 (5)	0.5768 (9)	5.5 (3)*
P2	0.7962 (3)	0.9755 (2)	0.1938 (3)	6.3 (1)	C56	0.1915 (8)	0.2102 (5)	0.5177 (8)	4.6 (3)*
P11	−0.0578 (2)	0.3181 (1)	0.0049 (2)	2.52 (6)	C61	0.1159 (6)	0.3095 (4)	0.4269 (6)	2.3 (2)*
P12	−0.1010 (2)	0.2438 (1)	0.2201 (2)	2.68 (6)	C62	0.0838 (7)	0.3224 (5)	0.5175 (8)	3.8 (2)*
P21	0.0809 (2)	0.2275 (1)	0.3447 (2)	2.53 (6)	C63	0.1114 (7)	0.3862 (5)	0.5781 (8)	4.4 (2)*
P22	0.2843 (2)	0.1951 (1)	0.2213 (2)	2.45 (6)	C64	0.1695 (8)	0.4350 (5)	0.5499 (8)	4.6 (2)*
P31	0.3361 (2)	0.2729 (1)	0.0738 (2)	2.61 (6)	C65	0.2012 (7)	0.4227 (5)	0.4611 (8)	4.2 (2)*
P32	0.1265 (2)	0.3126 (1)	−0.0836 (2)	2.58 (6)	C66	0.1738 (7)	0.3601 (4)	0.3980 (7)	3.2 (2)*
F11	0.2142 (6)	0.4647 (3)	0.2201 (6)	8.1 (2)	C71	0.2463 (6)	0.1114 (4)	0.2120 (7)	2.9 (2)*
F12	0.3178 (6)	0.5473 (3)	0.3584 (5)	7.7 (2)	C72	0.2644 (8)	0.0888 (5)	0.2966 (8)	4.6 (3)*
F13	0.3112 (7)	0.6141 (3)	0.2611 (6)	9.9 (3)	C73	0.2230 (8)	0.0217 (5)	0.2854 (9)	5.7 (3)*
F14	0.1991 (6)	0.5326 (4)	0.1317 (5)	8.5 (2)	C74	0.1634 (8)	−0.0186 (5)	0.1940 (9)	5.5 (3)*
F15	0.3543 (6)	0.5290 (4)	0.1995 (7)	9.8 (3)	C75	0.1439 (9)	0.0022 (6)	0.109 (1)	6.4 (3)*
F16	0.1685 (6)	0.5486 (5)	0.2857 (6)	11.8 (3)	C76	0.1830 (8)	0.0674 (5)	0.1192 (9)	5.2 (3)*
F21	0.7856 (7)	1.0376 (4)	0.2601 (8)	12.0 (3)	C81	0.3879 (6)	0.2355 (4)	0.3355 (7)	2.8 (2)*
F22	0.7107 (7)	0.9667 (5)	0.1003 (7)	12.0 (3)	C82	0.3868 (7)	0.2879 (5)	0.4094 (8)	4.2 (2)*
F23	0.8106 (6)	0.9129 (4)	0.1265 (7)	9.5 (3)	C83	0.4680 (8)	0.3196 (5)	0.4988 (8)	4.8 (3)*
F24	0.8854 (7)	0.9807 (4)	0.2850 (6)	11.9 (3)	C84	0.5452 (8)	0.2951 (6)	0.5129 (9)	5.5 (3)*
F25	0.7159 (7)	0.9332 (1)	0.2394 (6)	9.9 (8)	C85	0.5502 (9)	0.2461 (6)	0.4434 (9)	5.7 (3)*
F26	0.8764 (7)	1.0198 (4)	0.1506 (6)	9.5 (3)	C86	0.4694 (7)	0.2143 (5)	0.3509 (8)	4.2 (2)*
O1	0.0087 (5)	0.1374 (3)	−0.0072 (5)	3.6 (2)	C91	0.4204 (6)	0.3395 (4)	0.1846 (7)	2.7 (2)*
C2	−0.0603 (6)	0.1969 (4)	0.3010 (7)	3.1 (2)	C92	0.3838 (7)	0.3872 (5)	0.2294 (8)	3.8 (2)*
Co	0.3426 (6)	0.2015 (4)	0.1098 (7)	3.1 (2)	C93	0.4491 (8)	0.4377 (5)	0.3160 (9)	5.4 (3)*
C4	0.0466 (6)	0.3605 (4)	−0.0456 (7)	2.9 (2)	C94	0.5448 (9)	0.4386 (6)	0.3545 (9)	5.9 (3)*
C11	−0.1077 (6)	0.3799 (4)	0.0588 (7)	2.7 (2)*	C95	0.5815 (8)	0.3936 (5)	0.3105 (9)	5.3 (3)*
C12	−0.0424 (7)	0.4410 (5)	0.1150 (8)	4.2 (2)*	C96	0.5188 (7)	0.3422 (5)	0.2235 (8)	4.1 (2)*
C13	−0.0780 (8)	0.4874 (5)	0.1659 (9)	5.3 (3)*	C101	0.4034 (6)	0.2744 (4)	−0.0289 (7)	3.0 (2)*
C14	−0.1808 (8)	0.4720 (5)	0.1593 (8)	4.8 (3)*	C102	0.4649 (7)	0.3324 (5)	−0.0367 (8)	4.3 (2)*
C15	−0.2478 (8)	0.4122 (5)	0.1055 (9)	5.4 (3)*	C103	0.5150 (8)	0.3339 (5)	−0.1159 (9)	5.3 (3)*
C16	−0.2106 (7)	0.3658 (5)	0.0543 (8)	4.2 (2)*	C104	0.5024 (8)	0.2780 (5)	−0.1865 (9)	5.2 (3)*
C21	−0.1583 (6)	0.2647 (4)	−0.1084 (6)	2.5 (2)*	C105	0.4399 (8)	0.2204 (5)	−0.1832 (8)	4.8 (3)*
C22	−0.2026 (7)	0.2905 (5)	−0.1797 (7)	3.7 (2)*	C106	0.3897 (7)	0.2184 (5)	−0.1040 (8)	3.9 (2)*
C23	−0.2773 (8)	0.2496 (5)	−0.2673 (8)	4.8 (3)*	C111	0.2268 (6)	0.3675 (4)	−0.1181 (7)	3.0 (2)*
C24	−0.3085 (8)	0.1849 (5)	−0.2832 (9)	5.4 (3)*	C112	0.2867 (7)	0.4257 (5)	−0.0443 (8)	4.0 (2)*
C25	−0.2677 (8)	0.1590 (5)	−0.2143 (9)	5.5 (3)*	C113	0.3680 (8)	0.4677 (5)	−0.0673 (9)	5.1 (3)*
C26	−0.1907 (7)	0.1999 (5)	−0.1247 (7)	3.6 (2)*	C114	0.3898 (8)	0.4523 (5)	−0.1609 (9)	5.6 (3)*
C31	−0.1186 (6)	0.3086 (4)	0.3125 (7)	3.1 (2)*	C115	0.3342 (9)	0.3959 (6)	−0.2311 (9)	5.8 (3)*
C32	−0.1802 (7)	0.2957 (5)	0.3795 (8)	4.3 (2)*	C116	0.2509 (8)	0.3532 (5)	−0.2135 (8)	4.6 (3)*
C33	−0.1871 (8)	0.3466 (5)	0.4558 (9)	5.3 (3)*	C121	0.0520 (6)	0.2502 (4)	−0.2036 (7)	3.0 (2)*
C34	−0.1362 (8)	0.4075 (5)	0.4610 (8)	4.8 (3)*	C122	0.0617 (7)	0.1899 (5)	−0.2180 (8)	4.2 (2)*
C35	−0.0781 (8)	0.4208 (5)	0.3931 (8)	4.7 (3)*	C123	0.0018 (8)	0.1392 (6)	−0.3094 (9)	5.6 (3)*
Co6	−0.0670 (7)	0.3712 (4)	0.3191 (7)	3.4 (2)*	C124	−0.0623 (8)	0.1525 (6)	−0.3807 (9)	5.5 (3)*
C41	−0.2280 (6)	0.1931 (4)	0.1427 (7)	2.9 (2)*	C125	−0.0720 (8)	0.2099 (5)	−0.3680 (9)	5.1 (3)*
C42	−0.2474 (8)	0.1298 (5)	0.0920 (9)	5.1 (3)*	C126	−0.0132 (7)	0.2612 (4)	−0.2785 (7)	3.5 (2)*
C43	−0.3417 (9)	0.0906 (6)	0.022 (1)	6.6 (3)*	O(S1)	0.705 (1)	0.1391 (8)	0.415 (1)	18.9 (6)*
C44	−0.4141 (9)	0.1199 (6)	0.006 (1)	6.8 (3)*	C(S2)	0.636 (2)	0.081 (1)	0.373 (2)	21 (1)*
C45	−0.3968 (9)	0.1829 (6)	0.051 (1)	6.5 (3)*	C(S3)	0.563 (2)	0.067 (1)	0.271 (2)	16.1 (8)*
C46	−0.3024 (7)	0.2198 (5)	0.1228 (8)	4.3 (2)*	C(S4)	0.643 (2)	0.039 (1)	0.437 (2)	17.2 (9)*
C51	0.119 (7)	0.1818 (4)	0.4295 (7)	3.2 (2)*					

[a] Atoms with an asterisk were refined isotropically. Anisotropically refined atoms are given in the form of the isotropic equivalent thermal parameter defined as $(^4/_3)[a^2B(1,1) + b^2B(2,2) + c^2B(3,3) + ab(\cos\gamma)B(1,2) + ac(\cos\beta)B(1,3) + bc(\cos\alpha)B(2,3)]$.

in a Parr pressure reactor (300-mL capacity) using methanol (50 mL) and distilled water (4 mL), which had initially been purged with N_2, as solvent. The system was allowed to react for 71 h at 100 °C. At 15-h intervals, the pressure reactor was cooled and a fresh CO atmosphere was introduced. After this period the system was cooled to room temperature, the reactor was opened, and the solution was filtered. The solvent was evaporated from the filtrate under vacuum to give the crude product as an orange solid, yield 97.5%.

A sample was purified by recrystallization from an acetone–pentane solvent system and characterized by elemental analysis. IR: 1750 cm^{-1} [ν(CO)]. ^1H NMR {$(CD_3)_2CO$}: δ 5.85, 5.56 [m, $^2J(H^aH^b)$ = 14, $^3J(PtH^a)$ = 52, $^3J(PtH^b)$ = 16 Hz, $CH^aH^bP_2$]. ^{31}P NMR [$(CD_3)_2CO$]: δ −15.1 [s, $^1J(PtP)$ = 3720, $^3J(PP)$ = 170 Hz, ^{31}P]. ^{195}Pt NMR: δ −2685 [t, $^1J(PtP)$ = 3740, $^1J(PtPt) \approx$ 380 Hz]. Anal. Calcd for $[Pt_3(CO)(dppm)_3][CF_3CO_2]_2 \cdot (CH_3)_2CO$: C, 48.6; H, 3.5. Found: C, 49.0; H, 3.9.

Preparation and Crystal Structure Analysis of $[Pt_3(\mu_3\text{-}CO)(\mu\text{-}dppm)_3][PF_6]_2$. Crude $[Pt_3(\mu_3\text{-}CO)(\mu\text{-}dppm)_3][CF_3CO_2]_2$ (0.334 mmol) was reacted with excess $NH_4[PF_6]$ (8.190 mmol) in methanol (10 mL). Upon addition of the $NH_4[PF_6]$ solution a flocculent orange precipitate formed. This product was filtered, washed with methanol (1 mL), and dried in vacuo: yield 82%; mp 275–285 °C dec. Anal. Calcd for $[Pt_3(\mu_3\text{-}CO)(\mu\text{-}dppm)_3][PF_6]_2$: C, 44.39; H, 3.24. Found: C, 44.69; H, 3.52. Single crystals of the acetone solvate were grown as small red plates from acetone–pentane by slow diffusion: IR 1765 cm^{-1} [ν(CO)]. ^1H NMR [$(CD_3)_2CO$]: δ 6.26, 5.66 [m, $^2J(H^aH^b)$ = 14, $^3J(PtH^a)$ = 72, $^3J(PtH^b)$ = 14 Hz, $CH^aH^bP_2$]. ^{31}P NMR [CD_3CO]: δ −6.7 [s, $^1J(PtP)$ = 3710, $^3J(PP)$ = 140 Hz, ^{31}P]. ^{195}Pt NMR: δ −2893 [t, $^1J(PtP)$ = 3730, $^1J(PtPt)$ = 540 Hz].

For the X-ray data collection a small crystal was selected and coated with thin layers of epoxy resin; preliminary studies had shown that uncoated crystals decayed rapidly in the X-ray beam.

Crystal data (at 21 °C) for $[Pt_3(\mu\text{-}CO)(\mu\text{-}dppm)_3][PF_6]_2 \cdot (CH_3)_2CO$: $C_{79}H_{72}F_{12}O_2P_8Pt_3$; M_r = 2114.5, triclinic, a = 14.090 (2) Å, b = 22.711 (4) Å, c = 13.637 (4) Å; α = 103.43 (2)°, β = 99.52 (2)°, γ = 106.72 (1)°; U = 3937 (4) Å³; Z = 2, D_{calcd} = 1.784; $F(000)$ = 2048; Mo Kα radiation, λ = 0.710 69 Å; μ(Mo Kα) = 56.1 cm^{-1}; space group $P1$ or $P\bar{1}$; $P\bar{1}$ chosen and confirmed by the analysis.

Accurate cell dimensions and crystal orientation matrix were determined on a CAD4 diffractometer by a least-squares treatment of 25 reflections with θ in the range 10–15°. The intensities of reflections with h, −13 to +13, k, −21 to +21, and l, 0 to +13, with $2° < \theta < 20°$ were measured by the ω–2θ method using graphite-monochromatized Mo Kα radiation. The intensities of three reflections chosen as standards were monitored every 0.83 h and showed no evidence of crystal decay.

The intensities of 8060 reflections were measured of which 7318 were unique after averaging. Of these 6234 and $I > 3\sigma(I)$ and were used in the structure solution and refinement. Data were corrected[18] for Lorentz and polarization effects and later for absorption. The crystal used for the data collection measured 0.10 × 0.20 × 0.43 mm; the maximum and minimum values of the transmission coefficients are 0.601 and 0.311, respectively.

Structure Solution and Refinement. The coordinates of the three Pt atoms were deduced from a three-dimensional Patterson function computed with data which had not been corrected for absorption; the remaining non-hydrogen atoms of the cation and anions were located from neccessive rounds of structure factor and difference electron density maps. Initial isotropic full-matrix refinement of the atoms was followed by five cycles in which the non-phenyl atoms were allowed anisotropic vibration. A difference map computed at this stage showed clearly that acetone of solution had been entrapped in the crystal lattice; maxima consistent with many of the hydrogen atoms of the structure were also present. The composition of the unit cell having now been established, the data were corrected for absorption. In the final rounds of full-matrix calculations the solvate O and C atoms and the phenyl C atoms were allowed isotropic vibration, all other non-hydrogen atoms were allowed to vibrate anisotropically, and the 66 hydrogens of the cation were positioned on geometrical grounds (C–H = 0.95 Å) and included in the calculation (with an overall B_{iso} of 5.0 Å^2) but not refined. The acetone of solvation is very loosely held in the lattice (average B_{iso} for acetone atoms 18 Å^2), and no allowance was made for the six acetone hydrogens.

Refinement converged with $R = \sum||F_o| - |F_c||/\sum|F_o| = 0.035$ and $R_w = (\sum w(|F_o| - |F_c|)^2/\sum w|F_o|^2)^{1/2} = 0.046$ for the 6234 observed reflections; $R = 0.044$ for all reflections. The number of variables in the final rounds of refinement was 557, and the "goodness of fit" value was 1.50. The maximum shift/error ratios were 0.02 for the x coordinate of atom C93 and 0.01 for the B_{iso} parameter of atom C103. A final difference map computed at the end of the refinement calculations had three maxima greater than 0.3 e Å^{-3} (0.6–1.3 e Å^{-3}) near the Pt atoms but no chemically significant features. In the refinement calculations, scattering factors and anomalous dispersion corrections were taken from ref 19; the weighting scheme was of the form $w = 1/[\sigma^2(F_o) + 0.05(F_o^2)]$.

Principal dimensions for the structure are summarized in Table I. Table II lists the final fractional coordinates of the non-hydrogen atoms with their estimated standard deviations. Tables of all bond lengths and angles, thermal parameters, calculated hydrogen coordinates, and mean plane data and a structure factor listing are available as supplementary material.

Acknowledgment. Financial support from N.S.E.R.C. (Canada) to G.F. and R.J.P. is gratefully acknowledged.

Supplementary Material Available: Tables of all bond lengths and angles, thermal parameters, calculated hydrogen coordinates, and mean plane data and a listing of structure amplitudes (87 pages). Ordering information is given on any current masthead page.

(18) All calculations were made on a PDP-11/73 computer using the SDP-PLUS system, (B.A. Frenz and Associates, Inc., College Station, TX 77840, and Enraf-Nonius, Delft, Holland).

(19) "International Tables for X-ray Crystallography"; The Kynoch Press, Birmingham, England, 1974; Vol. IV.

Metallocyclic Palladium(II) Complexes Possessing Six- and Seven-Membered Rings:[1] Synthesis and Structural Characteristics

George R. Newkome,* Garry E. Kiefer, Yves A. Frere,[2a] Masayoshi Onishi,[2b] Vinod K. Gupta, and Frank R. Fronczek

Department of Chemistry, Louisiana State University, Baton Rouge, Louisiana 70803-1804

Received June 10, 1985

The syntheses of several new cyclometalated Pd(II) complexes, which contain either phenanthroline or bipyridine moieties, are described. These complexes achieve partial coordination to the metal core via an sp^3 carbon anionic bond(s) and form fused cyclic ring systems with overall cis geometry. The dipyridyl ethylenic and ketonic ligands undergo facile cyclometalation to generate the symmetric 5.7.5 and 5.6.5 complexes, respectively; in contrast, the potentially tetracoordinate 6.5.6 ligand systems available with phenanthroline and bipyridine yielded only a single C–Pd bond. The single-crystal X-ray structural analyses of selected complexes have afforded insight into the molecular features responsible for precluding generation of dual C–Pd bonds in the 6.5.6 system.

Introduction

Up to this point, our interest in metallocyclic palladium(II) complexes has been limited primarily to 2,2′-bipyridine- and 1,10-phenanthroline-based ligands capable of forming a cis 5.5.5-cumulated ring system.[3] These

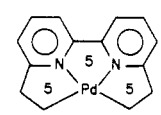

Cis 5·5·5 cumulated ring system

prototypes were designed specifically for the encapsulation of square-planar transition-metal ions and, with the exception of the phenanthroline derivatives, have demonstrated a propensity for generating very stable tetradentate complexes in which partial coordination is achieved via sp^3

(1) Chemistry of Heterocyclic Compounds series. Part 121.

(2) (a) On leave from Centre de Recherche sur les Macromolecules, Strasbourg, France, 1982–1983. (b) On leave from Nagasaki University, Nagasaki, Japan, 1982–1983.

(3) Newkome, G. R.; Puckett, W. E.; Kiefer, G. E.; Gupta, V. K.; Fronczek, F. R.; Pantaleo, D. C.; McClure, G. L.; Simpson, J. B. Deutsch, W. A. *Inorg. Chem.* **1985**, *24*, 811.

0276-7333/86/2305-0348$01.50/0

Accurate cell dimensions and crystal orientation matrix were determined on a CAD4 diffractometer by a least-squares treatment of 25 reflections with θ in the range 10–15°. The intensities of reflections with h, −13 to +13, k, −21 to +21, and l, 0 to +13, with $2° < \theta < 20°$ were measured by the ω–2θ method using graphite-monochromatized Mo Kα radiation. The intensities of three reflections chosen as standards were monitored every 0.83 h and showed no evidence of crystal decay.

The intensities of 8060 reflections were measured of which 7318 were unique after averaging. Of these 6234 and $I > 3\sigma(I)$ and were used in the structure solution and refinement. Data were corrected[18] for Lorentz and polarization effects and later for absorption. The crystal used for the data collection measured 0.10 × 0.20 × 0.43 mm; the maximum and minimum values of the transmission coefficients are 0.601 and 0.311, respectively.

Structure Solution and Refinement. The coordinates of the three Pt atoms were deduced from a three-dimensional Patterson function computed with data which had not been corrected for absorption; the remaining non-hydrogen atoms of the cation and anions were located from neccessive rounds of structure factor and difference electron density maps. Initial isotropic full-matrix refinement of the atoms was followed by five cycles in which the non-phenyl atoms were allowed anisotropic vibration. A difference map computed at this stage showed clearly that acetone of solution had been entrapped in the crystal lattice; maxima consistent with many of the hydrogen atoms of the structure were also present. The composition of the unit cell having now been established, the data were corrected for absorption. In the final rounds of full-matrix calculations the solvate O and C atoms and the phenyl C atoms were allowed isotropic vibration, all other non-hydrogen atoms were allowed to vibrate anisotropically, and the 66 hydrogens of the cation were positioned on geometrical grounds (C–H = 0.95 Å) and included in the calculation (with an overall B_{iso} of 5.0 Å^2) but not refined. The acetone of solvation is very loosely held in the lattice (average B_{iso} for acetone atoms 18 Å^2), and no allowance was made for the six acetone hydrogens.

Refinement converged with $R = \sum||F_o| - |F_c||/\sum|F_o| = 0.035$ and $R_w = (\sum w(|F_o| - |F_c|)^2/\sum w|F_o|^2)^{1/2} = 0.046$ for the 6234 observed reflections; $R = 0.044$ for all reflections. The number of variables in the final rounds of refinement was 557, and the "goodness of fit" value was 1.50. The maximum shift/error ratios were 0.02 for the x coordinate of atom C93 and 0.01 for the B_{iso} parameter of atom C103. A final difference map computed at the end of the refinement calculations had three maxima greater than 0.3 e Å^{-3} (0.6–1.3 e Å^{-3}) near the Pt atoms but no chemically significant features. In the refinement calculations, scattering factors and anomalous dispersion corrections were taken from ref 19; the weighting scheme was of the form $w = 1/[\sigma^2(F_o) + 0.05(F_o^2)]$.

Principal dimensions for the structure are summarized in Table I. Table II lists the final fractional coordinates of the non-hydrogen atoms with their estimated standard deviations. Tables of all bond lengths and angles, thermal parameters, calculated hydrogen coordinates, and mean plane data and a structure factor listing are available as supplementary material.

Acknowledgment. Financial support from N.S.E.R.C. (Canada) to G.F. and R.J.P. is gratefully acknowledged.

Supplementary Material Available: Tables of all bond lengths and angles, thermal parameters, calculated hydrogen coordinates, and mean plane data and a listing of structure amplitudes (87 pages). Ordering information is given on any current masthead page.

(18) All calculations were made on a PDP-11/73 computer using the SDP-PLUS system, (B.A. Frenz and Associates, Inc., College Station, TX 77840, and Enraf-Nonius, Delft, Holland).

(19) "International Tables for X-ray Crystallography"; The Kynoch Press, Birmingham, England, 1974; Vol. IV.

Metallocyclic Palladium(II) Complexes Possessing Six- and Seven-Membered Rings:[1] Synthesis and Structural Characteristics

George R. Newkome,* Garry E. Kiefer, Yves A. Frere,[2a] Masayoshi Onishi,[2b] Vinod K. Gupta, and Frank R. Fronczek

Department of Chemistry, Louisiana State University, Baton Rouge, Louisiana 70803-1804

Received June 10, 1985

The syntheses of several new cyclometalated Pd(II) complexes, which contain either phenanthroline or bipyridine moieties, are described. These complexes achieve partial coordination to the metal core via an sp^3 carbon anionic bond(s) and form fused cyclic ring systems with overall cis geometry. The dipyridyl ethylenic and ketonic ligands undergo facile cyclometalation to generate the symmetric 5.7.5 and 5.6.5 complexes, respectively; in contrast, the potentially tetracoordinate 6.5.6 ligand systems available with phenanthroline and bipyridine yielded only a single C–Pd bond. The single-crystal X-ray structural analyses of selected complexes have afforded insight into the molecular features responsible for precluding generation of dual C–Pd bonds in the 6.5.6 system.

Introduction

Up to this point, our interest in metallocyclic palladium(II) complexes has been limited primarily to 2,2′-bipyridine- and 1,10-phenanthroline-based ligands capable of forming a cis 5.5.5-cumulated ring system.[3] These

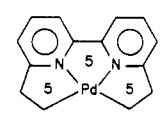

Cis 5·5·5 cumulated ring system

prototypes were designed specifically for the encapsulation of square-planar transition-metal ions and, with the exception of the phenanthroline derivatives, have demonstrated a propensity for generating very stable tetradentate complexes in which partial coordination is achieved via sp^3

(1) Chemistry of Heterocyclic Compounds series. Part 121.

(2) (a) On leave from Centre de Recherche sur les Macromolecules, Strasbourg, France, 1982–1983. (b) On leave from Nagasaki University, Nagasaki, Japan, 1982–1983.

(3) Newkome, G. R.; Puckett, W. E.; Kiefer, G. E.; Gupta, V. K.; Fronczek, F. R.; Pantaleo, D. C.; McClure, G. L.; Simpson, J. B. Deutsch, W. A. *Inorg. Chem.* **1985**, *24*, 811.

0276-7333/86/2305-0348$01.50/0

Scheme I

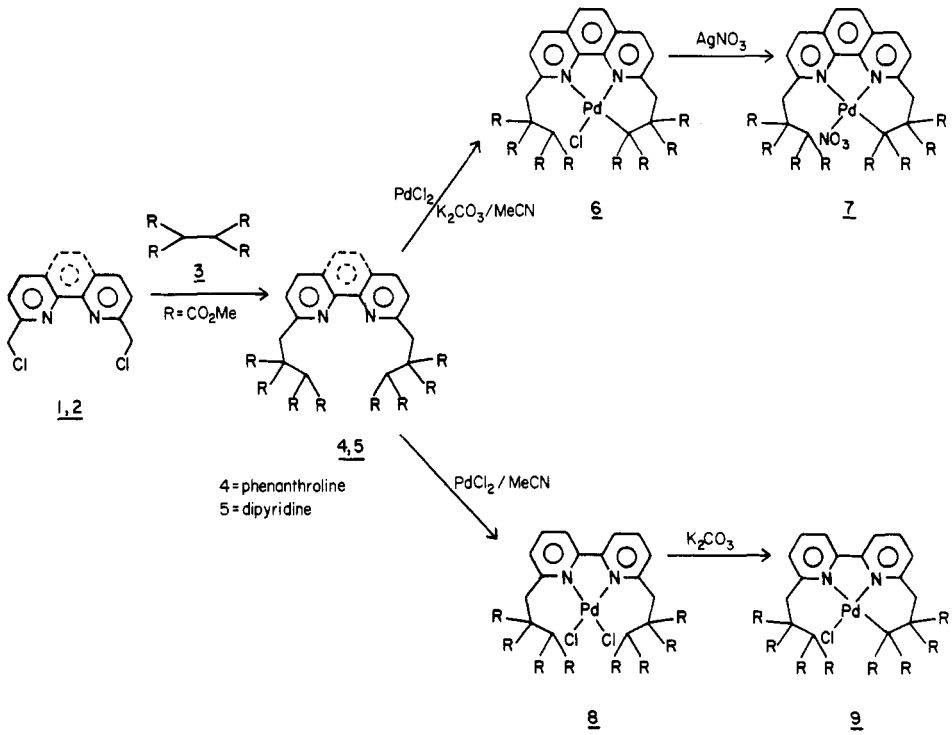

C–Pd bonds. The evidence suggests that the 5.5.5 bis C–Pd bonded phenanthroline complex *cannot* be prepared due to the rigidity imposed by the 5,6-bridge which prevents angular distortions necessary for C–Pd bonding to occur on *both* sides of the molecule. To overcome this problem, we envisioned a simple homologation of the 2,9-alkyl substituents, thereby introducing sufficient flexibility to promote the proper alignment required for C–Pd bond formation.

In order to incorporate a greater variety of metals into our general approach to cyclometalation, the syntheses of new ligands that can accommodate mutable coordination geometries have been deemed necessary. Thus, we herein report the preparation and preliminary complexation studies on several new ligands capable of forming bis C–Pd bonded complexes possessing 5.6.5-, 5.7.5-, and 6.5.6-fused tricyclic ring systems. Overall augmentation of the ligand bite has been accomplished via insertion of an ethano or carbonyl bridging unit between two pyridine rings.

Results and Discussion

1. Substituent Homologation. Synthesis of **4** was accomplished by generating the anion of 1,1,2,2-tetracarbomethoxyethane (**3**)[4] with NaH in THF followed by the addition of 2,9-bis(chloromethyl)-1,10-phenanthroline (**1**).[5] A more efficient method for the preparation of **5** proved to be our standard K_2CO_3/DMF procedure,[3] from which ligand **5** was isolated (>80%) without extensive chromatographic procedures and crystallized to afford an analytical sample. The ^1H NMR of **5** was surprising in that the nonequivalent methyl ester protons appear as a single spike at δ 3.73; however, upon formation of the $PdCl_2$ adduct **8**, the methyl groups demonstrate the anticipated disparate behavior with two distinct singlets (δ 3.60, 3.86) appearing. Hence, the syn conformation of adduct **8** has a pronounced influence upon the molecular environment on the NMR time scale.

Complexation of **4** proceeded smoothly by using $PdCl_2$ and anhydrous K_2CO_3 in CH_3CN (Scheme I), whereas the bipyridine analogue gave inconsistent yields of monometalated complex **9** and normally required longer reaction times. The addition of $AgNO_3$ did not facilitate biscyclometalation although production of the intermediary monometalated complex was accelerated. Further, chloride/nitrate ligand exchange to produce complex **7** was confirmed by NMR with a noticeable upfield shift of the methylene signals (δ 4.10 and 4.24) as well as an upfield shift ($\Delta\delta$ = 0.16) for the remaining methine proton. The nitrate ligand may, therefore, relieve some of the unfavorable steric interactions since the methylene and methine protons of **7** are, on the average, closer to the chemical shift of the free ligand than those observed in complex **6**.

The sluggish reactivity of **5** and low yields of the C-metalated bipyridine complex **9** are uncharacteristic in view of previous studies,[3,6] where cyclometalation occurred rapidly under identical conditions. These observations are best rationalized in terms of the stereochemical congestion introduced by multiple methoxycarbonyl substituents juxtaposed in the immediate vicinity of the coordination sphere. Thus, even initial formation of the N-bonded palladium adduct is retarded and decreased yields of the mono C–Pd bonded complex are a direct consequence.

2. Central Bishomologation. Ligand **16** was prepared in a fashion similar to that reported by Baker et al.[7] Thus, treatment of 1,2-bis(6-methyl-2-pyridyl)-1,2-ethylene (**10**) with peracetic acid gave di-*N*-oxide **11**, which underwent smooth rearrangement with acetic anhydride to afford diester **12**. Following transesterification with absolute EtOH and anhydrous K_2CO_3, the ethylene bridge was catalytically hydrogenated by using PtO_2 to give (60%) diol **14**. Reduction of the ethylene moiety at this stage precludes the possibility of acetate rearrangement to the

(4) Newkome, G. R.; Gupta, V. K.; Fronczek, F. R. *Acta Crystallogr., Sect. C: Cryst. Struct. Commun.* **1983**, *C39*, 113.
(5) Newkome, G. R.; Kiefer, G. E.; Puckett, W. E.; Vreeland, T. *J. Org. Chem.* **1983**, *48*, 5112.
(6) Puckett, W. E. Ph.D. dissertation, 1983.
(7) Baker, W.; Buggle, K. M.; McOmie, J. F.; Watkins, D. A. M. *J. Chem. Soc.* **1958**, 3594.

Scheme II

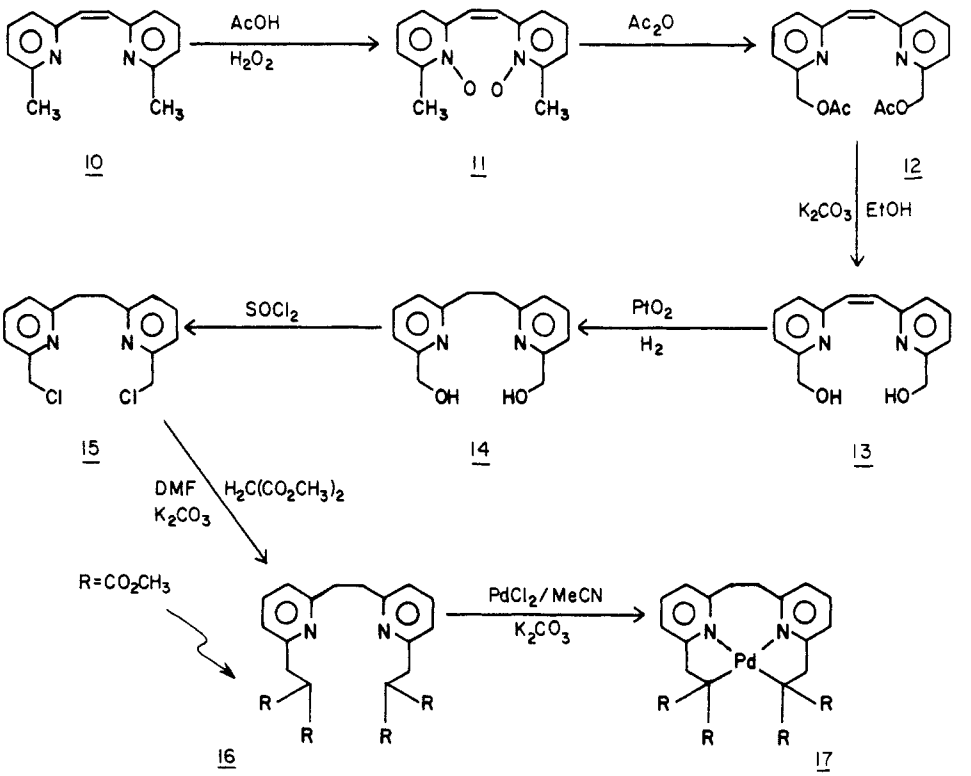

bridging methylene carbons. Subsequent treatment with $SOCl_2$ afforded **15**, which was immediately transformed into the desired **16** with dimethyl malonate and K_2CO_3 in DMF (Scheme II).

Preparation of the bis C–Pd bonded complex **17** was readily accomplished (85%) from **16** under standard conditions[3] ($PdCl_2/CH_3CN/K_2CO_3$). Unlike the phenanthroline and bipyridine models, cyclometalation was extremely rapid and complete within 1 h with *or* without added $AgNO_3$. Numerous attempts at isolating the monometalated species were fruitless owing to the facile C-metalation reaction. Notably, **17** was unusually resistant to typical chemical degradation as evidenced by its prolonged stability in aqueous alcoholic solutions; under similar conditions, the 5.5.5 bipyridine and phenanthroline 5.5 cyclopalladated complexes[3] showed signs of decomposition.

3. Central Monohomologation. Insertion of a ketonic moiety between the two pyridine rings (e.g., dipyridyl ketone) permitted minimal expansion of the ligand bite and access to a 5.6.5 tricyclic tetradentate complex. Ligand **21** was synthesized starting from 2-bromo-6-methylpyridine (**18**)[8] by initial lithium–halogen exchange (BuLi) in THF at low temperature (–90 °C), followed by a double addition–elimination of the organolithium intermediate on ethyl chloroformate.[9] The ketone **19** was transformed in moderate yield to the symmetrical bis[6-(bromomethyl)-2-pyridyl] ketone (**20**) under standard NBS conditions.[10] Treatment of **20** with diethyl malonate in DMF/K_2CO_3 gave (10% from **19**) the desired ligand **21** which was transformed into the bismetalated 5.6.5 complex **22** with $PdCl_2{\cdot}(C_6H_5CN)_2$ and NaOEt in dry THF (Scheme III). The reaction conditions were not optimized, and

Scheme III

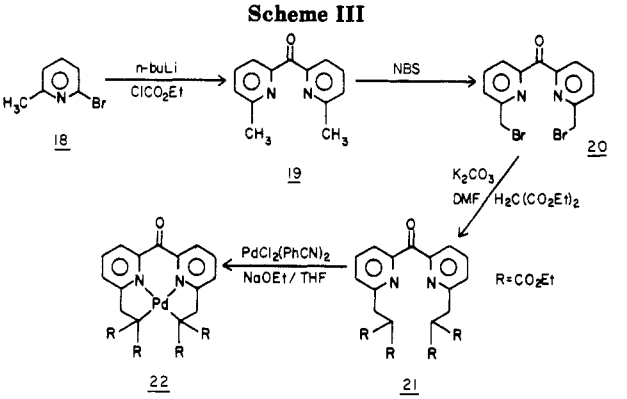

further synthetic modifications to the complexation procedure were not made due to our inability to increase the yields of the very unstable bromomethyl intermediate **20**.

Introduction of a carbonyl unit between the pyridine rings expands the ligand "bite" to a more favorable disposition but diminishes the initial N-ligandophilicity via electron withdrawal from the already electron-deficient rings. This choice still allows the convenience of a well-studied[11,12] ligand fragment within our tetradenate framework.

The expanded 5.6.5 geometry of **21** is well-suited for the preparation of the bismetalated complex, since this ring system is well documented with related tetraamine ligands.[13] This ring size combination may be preferred over our initial 5.5.5 system, which imposes considerable bond angle deformation of the central metal. The diminished N-electron density may reduce preliminary N-complexa-

(8) Newkome, G. R.; Puckett, W. E.; Kiefer, G. E.; Gupta, V. K.; Xia, Y.-J.; Coriel, M.; Hackney, M. A. *J. Org. Chem.* **1982**, *47*, 4116.
(9) Taylor, H. C. R. Ph.D. dissertation, 1983.
(10) (a) Offermann, W.; Vögtle, F. *J. Org. Chem.* **1979**, *44*, 710. (b) Newkome, G. R.; Kiefer, G. E.; Xia, Y. J.; Gupta, V. K. *Synthesis* **1984**, 676.
(11) Newkome, G. R.; Sauer, J. D.; McClure, G. L. *Tetrahedron Lett.* **1973**, 1599.
(12) Newkome, G. R.; Taylor, H. C. R.; Fronczek, F. R.; Delord, T. J.; Kohli, D. K. *J. Am. Chem. Soc.* **1981**, *103*, 7376.
(13) (a) Omae, I. *Chem. Rev.* **1979**, *79*, 287. (b) Ros, R.; Renaud, J.; Roulet, R. *J. Organomet. Chem.* **1974**, *77*, C4. (c) Holton, R. A. *J. Am. Chem. Soc.* **1977**, *99*, 8083. (d) Schwarzenbach, D.; Pinkerton, A.; Chapius, G.; Wenger, J.; Ros, R.; Roulet, R. *Inorg. Chim. Acta* **1977**, *25*, 255.

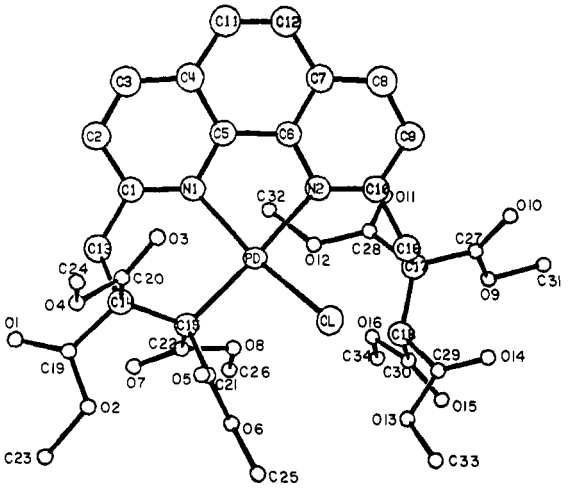

Figure 1. ORTEP drawing of 6.

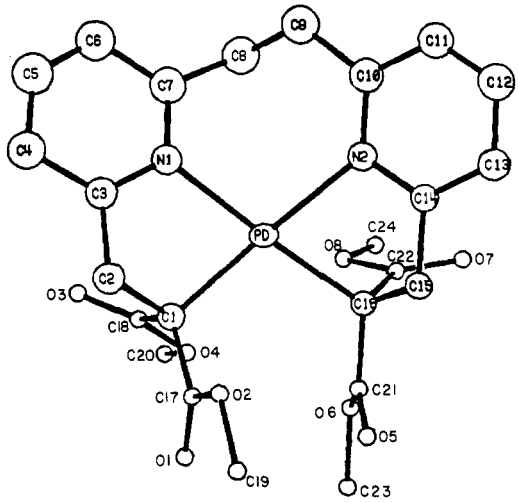

Figure 2. ORTEP drawing of 17.

tion when compared to 4 or 16 but does not prohibit formation of the C–Pd bonds.

The majority of the known cyclometalated complexes have exploited the five-membered metallocyclic ring structure.[6] The five-membered chelate ring has been shown to enhance the stability of organometallic complexes by virtue of the favorable bond angles formed with respect to the transition-metal coordination sphere. There are examples of six-membered chelate ring structures,[13] whereas larger metallocyclic ring systems are less common. Our previous report of a six-membered cyclopalladated trans complex (23) was the first example of a totally

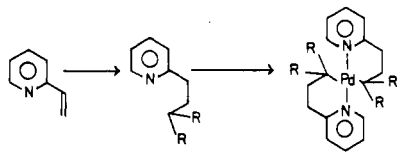

23

characterized, expanded chelate ring structure incorporating both the N-donor atom and an sp^3 C–Pd bond.[14] Similarly, the complexes reported herein are the first examples of cis geometry within fused tetradentate 6.5.6, 5.7.5, and 5.6.5 cumulated ring systems, which possess the equivalent bonding mode.

Although the "five-membered chelate ring theory"[15] is a useful and valid criterion for assessing the stability of latent transition-metal complexes, it should not be used as an exclusive guide for the design and synthesis of potential ligands. In fact, these five-membered chelates can actually become a hindrance to cyclometalation if other conformational restraints exist. Obviously, the probability of forming the C–Pd bond with excessively large chelate rings is remote; however, with judicious ligand design, it seems likely that the occurrence of cyclometalated complexes with six-, seven-, and possibly eight-membered chelate rings could become more frequent.

4. X-ray Structural Analysis. The structure of 6 is depicted in Figure 1. The Pd–N1 and Pd–N2 bond distances are 2.064 (5) and 2.153 (5) Å, respectively, which are surprisingly close to the average Pd–N bond length (2.064 Å) determined for the $PdCl_2$ adduct of 2,9-dimethyl-1,10-phenanthroline.[16] Thus, the relatively undistorted bond lengths are supportive of a complex, which is free of any geometrical constraints imposed via cyclometalation. In contrast, the previously reported complex 24[3] exhibits an unusually long Pd–N bond (2.225 Å) on the non C–Pd-bonded side, which is indicative of the increased strain inherent in the five-membered chelate ring

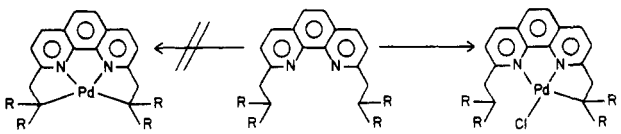

25 24

The symmetric arrangement of the ligating atoms around the palladium core in 6 is also supportive of the unperturbed bonding in the coordination sphere. Nonetheless, generation of the second C–Pd bond was not possible and can be attributed to the steric bulk of the ester groups. Close inspection of Figure 1 reveals that if the second C–Pd bond were to form, the terminal ester groups of the 2- and 9-alkyl substituents would overlap. Thus, it is clear that the steric requirements of the substituents on the methine carbon must be considerably reduced over the present case in order to permit formation of the bismetalated complex.

The structure of 17 is depicted in Figure 2. Bond angles in the Pd coordination sphere are considerably distorted from ideal (90%) with N1–Pd–Cl and N2–Pd–C16 being 79.7 and 78.3°, respectively, averaged over the two independent molecules of the asymmetric unit. In addition, the average N1–Pd–N2 angle in the seven-membered ring is 101.2°, which is noticeably larger than those observed in previous studies.[3] The pyridine rings are not coplanar with the dihedral angle between the best planes defining the two rings being 132.3° in one of the independent molecules, and 138.9° in the other. Table IV summarizes the bond lengths and angles in the immediate coordination sphere of 6 and 17 for comparative purposes.

Conclusion

The purpose of the work described herein was to determine the feasibility of synthesizing cyclopalladated complexes containing a variety of ring sizes with overall cis geometry. We have demonstrated that the six-membered chelate ring is not unique to trans complexes alone and can be incorporated into cis complexes which exhibit stability comparable to the five-membered analogues. In addition, variations in the ligand "bite" achieved via in-

(14) Newkome, G. R.; Puckett, W. E.; Gupta, V. K.; Fronczek, F. R. *Organometallics* **1983**, *2*, 1247.
(15) Matsuda, S.; Kikkawa, S.; Omae, I. *Kogyo Kagaku Zasshi* **1966**, *69*, 646 [*Chem. Abstr.* **1966**, *65*, 18612e].
(16) Newkome, G. R.; Gupta, V. K.; Kiefer, G. E.; Fronczek, F. R.; Xia, -Y.; Watkins, S. F. *Inorg. Chem.*, submitted for publication.

Table I. Coordinates for 6

atom	*x*	*y*	*z*	*B* or *B*(eq)*, Å²	atom	*x*	*y*	*z*	*B* or *B*(eq)*, Å²
Pd	0.49051 (8)	0.33696 (6)	0.24845 (6)	2.68 (2)*	C12	0.6711 (10)	0.6238 (8)	0.5646 (7)	4.2 (2)
Cl	0.4170 (3)	0.1755 (2)	0.2563 (2)	4.17 (7)*	C13	0.4096 (9)	0.4941 (7)	0.0953 (7)	3.4 (2)
O1	0.2637 (7)	0.4393 (5)	−0.0965 (5)	5.2 (2)*	C14	0.3192 (8)	0.3900 (7)	0.0600 (6)	3.0 (2)
O2	0.2241 (7)	0.2787 (5)	−0.0968 (4)	4.3 (2)*	C15	0.3930 (8)	0.3080 (7)	0.0972 (6)	2.8 (2)
O3	0.2231 (6)	0.4110 (6)	0.1839 (4)	4.8 (2)*	C16	0.7040 (9)	0.2293 (7)	0.4168 (7)	3.4 (2)
O4	0.0989 (6)	0.3912 (5)	0.0285 (5)	4.6 (2)*	C17	0.8324 (9)	0.2191 (7)	0.4006 (6)	3.2 (2)
O5	0.1934 (6)	0.2011 (5)	0.0670 (5)	4.2 (2)*	C18	0.7968 (9)	0.1423 (7)	0.3017 (6)	3.2 (2)
O6	0.3473 (6)	0.1362 (5)	0.0274 (5)	4.4 (2)*	C19	0.2675 (9)	0.3744 (7)	−0.0524 (7)	3.9 (2)
O7	0.4963 (6)	0.3287 (5)	−0.0193 (4)	4.2 (2)*	C20	0.2087 (9)	0.3964 (7)	0.1000 (7)	3.3 (2)
O8	0.5939 (6)	0.2658 (5)	0.1074 (4)	4.1 (2)*	C21	0.2993 (9)	0.2108 (7)	0.0652 (7)	3.4 (2)
O9	1.0159 (7)	0.1513 (5)	0.4629 (5)	5.0 (2)*	C22	0.4957 (9)	0.3018 (7)	0.0538 (6)	3.2 (2)
O10	0.9190 (7)	0.1964 (6)	0.5660 (5)	6.4 (2)*	C23	0.1923 (13)	0.2554 (10)	−0.2021 (8)	6.5 (4)*
O11	0.9987 (7)	0.3656 (6)	0.4553 (6)	5.8 (2)*	C24	−0.0080 (11)	0.3945 (10)	0.0604 (9)	6.5 (4)*
O12	0.8321 (6)	0.3501 (5)	0.3172 (5)	4.1 (2)*	C25	0.2672 (12)	0.0395 (8)	0.0010 (9)	6.5 (4)*
O13	0.6382 (7)	0.0070 (5)	0.2081 (5)	5.4 (2)*	C26	0.6957 (11)	0.2595 (9)	0.0700 (8)	5.7 (3)*
O14	0.7148 (7)	0.0136 (5)	0.3697 (5)	5.6 (2)*	C27	0.9254 (10)	0.1878 (7)	0.4863 (7)	4.2 (3)*
O15	0.9266 (7)	0.0313 (5)	0.2580 (5)	5.6 (2)*	C28	0.9007 (9)	0.3198 (7)	0.3946 (7)	3.7 (3)*
O16	0.9746 (6)	0.1924 (5)	0.2593 (5)	4.5 (2)*	C29	0.7134 (10)	0.0466 (7)	0.2997 (7)	4.0 (3)*
N1	0.5101 (7)	0.4889 (5)	0.2670 (5)	2.9 (2)	C30	0.9060 (10)	0.1139 (8)	0.2728 (7)	4.0 (3)*
N2	0.6226 (7)	0.3806 (5)	0.3973 (5)	2.9 (2)	C31	1.1156 (12)	0.1265 (10)	0.5404 (9)	7.2 (4)*
C1	0.4586 (8)	0.5400 (7)	0.2016 (6)	3.0 (2)	C32	0.8799 (12)	0.4494 (8)	0.3093 (9)	6.0 (4)*
C2	0.4533 (9)	0.6403 (7)	0.2305 (7)	3.9 (2)	C33	0.5486 (14)	−0.0833 (11)	0.1906 (11)	8.5 (5)*
C3	0.5016 (10)	0.6840 (8)	0.3273 (7)	4.3 (2)	C34	1.0829 (11)	0.1751 (10)	0.2329 (9)	6.5 (4)*
C4	0.5587 (9)	0.6343 (7)	0.3987 (7)	3.8 (2)	O1A	0.2556 (11)	0.8025 (9)	0.1401 (9)	11.3 (4)
C5	0.5630 (9)	0.5343 (7)	0.3659 (6)	3.1 (2)	C1A	0.1702 (16)	0.8163 (13)	0.1691 (12)	9.9 (5)
C6	0.6210 (9)	0.4775 (7)	0.4333 (6)	3.1 (2)	C2A	0.0830 (17)	0.8804 (14)	0.1357 (13)	10.6 (5)
C7	0.6808 (9)	0.5223 (7)	0.5338 (7)	3.5 (2)	C3A	0.1297 (19)	0.7238 (15)	0.2118 (14)	12.1 (6)
C8	0.7455 (10)	0.4679 (8)	0.5956 (8)	4.6 (2)	OC1B	0.4479 (22)	0.0265 (18)	0.4754 (19)	16.1 (9)
C9	0.7567 (10)	0.3746 (8)	0.5572 (7)	4.1 (2)	C2B[a]	0.5160 (30)	0.1069 (23)	0.5405 (22)	8.5 (9)
C10	0.6928 (9)	0.3322 (7)	0.4575 (7)	3.3 (2)	C3B[a]	0.3378 (39)	−0.0114 (32)	0.4003 (30)	12.9 (13)
C11	0.6128 (10)	0.6744 (8)	0.5017 (7)	4.5 (3)					

[a] Population = $^1/_2$.

Table II. Coordinates for 17

atom	*x*	*y*	*z*	*B* or *B*(eq)*, Å²	atom	*x*	*y*	*z*	*B* or *B*(eq)*, Å²
Pd	0.66659 (7)	0.49610 (4)	0.23321 (4)	3.60 (2)*	C15	0.6299 (8)	0.4826 (5)	0.4000 (5)	3.7 (2)
Pd′	0.38683 (6)	0.09243 (4)	0.22399 (4)	3.03 (1)*	C16	0.6624 (8)	0.5592 (5)	0.3585 (5)	3.4 (2)
O1	1.0660 (7)	0.6361 (4)	0.3171 (5)	6.7 (2)*	C17	0.9884 (9)	0.5674 (5)	0.2868 (5)	4.2 (2)
O2	1.0007 (6)	0.4963 (3)	0.3166 (3)	4.6 (1)	C18	0.8610 (9)	0.6227 (5)	0.1736 (5)	4.5 (2)
O3	0.8666 (8)	0.6240 (4)	0.1004 (4)	6.6 (2)*	C19	1.1162 (10)	0.5050 (6)	0.3857 (7)	6.2 (3)*
O4	0.8387 (6)	0.6896 (4)	0.2308 (4)	5.7 (1)	C20	0.8181 (11)	0.7652 (5)	0.2009 (7)	6.3 (3)*
O5	0.8822 (6)	0.6028 (4)	0.4558 (4)	5.4 (2)*	C21	0.7888 (8)	0.6217 (5)	0.4118 (5)	3.4 (2)
O6	0.7820 (6)	0.7038 (3)	0.4112 (3)	4.6 (1)	C22	0.5367 (8)	0.6041 (5)	0.3562 (5)	3.8 (2)
O7	0.4519 (6)	0.6017 (4)	0.4039 (4)	5.9 (2)*	C23	0.8968 (10)	0.7683 (6)	0.4616 (7)	6.4 (3)*
O8	0.5312 (6)	0.6501 (3)	0.2959 (3)	4.7 (1)	C24	0.4321 (10)	0.7081 (6)	0.3053 (6)	6.1 (3)*
O1′	−0.0165 (6)	−0.0280 (3)	0.2429 (4)	4.9 (2)*	C1′	0.1740 (8)	0.0314 (5)	0.1727 (5)	3.0 (2)
O2′	0.0588 (6)	0.1130 (3)	0.2715 (3)	4.2 (1)	C2′	0.1321 (8)	0.0825 (5)	0.1063 (5)	3.3 (2)
O3′	0.1686 (6)	−0.0851 (4)	0.0544 (3)	4.9 (2)*	C3′	0.2470 (8)	0.0960 (5)	0.0539 (5)	3.2 (2)
O4′	0.1935 (6)	−0.1089 (4)	0.1854 (4)	5.2 (1)	C4′	0.2246 (9)	0.0929 (5)	−0.0335 (5)	4.0 (2)
O5′	0.2070 (6)	0.0416 (4)	0.4054 (3)	5.1 (2)*	C5′	0.3393 (9)	0.0985 (5)	−0.0760 (5)	4.5 (2)
O6′	0.2924 (6)	−0.0766 (4)	0.3625 (4)	4.9 (1)	C6′	0.4745 (9)	0.1087 (5)	−0.0321 (5)	4.3 (2)
O7′	0.5274 (6)	−0.0534 (4)	0.2554 (4)	5.5 (2)*	C7′	0.4928 (8)	0.1152 (5)	0.0553 (5)	3.5 (2)
O8′	0.6195 (6)	0.0016 (3)	0.3907 (3)	4.7 (1)	C8′	0.6375 (9)	0.1329 (6)	0.1083 (5)	4.5 (2)*
N1	0.6539 (7)	0.4372 (4)	0.1041 (4)	4.8 (2)	C9′	0.6732 (10)	0.2265 (6)	0.1636 (6)	5.4 (2)*
N2	0.4826 (7)	0.4176 (4)	0.2657 (4)	4.3 (2)	C10′	0.6813 (8)	0.2331 (5)	0.2573 (5)	4.0 (2)
N1′	0.3802 (6)	0.1100 (4)	0.0971 (4)	3.2 (1)	C11′	0.7893 (9)	0.2968 (5)	0.3127 (5)	4.5 (2)
N2′	0.5849 (6)	0.1818 (4)	0.2888 (4)	3.5 (1)	C12′	0.7981 (9)	0.3045 (6)	0.3972 (6)	4.8 (2)
C1	0.8732 (8)	0.5462 (5)	0.2116 (5)	3.9 (2)	C13′	0.7041 (9)	0.2535 (6)	0.4303 (6)	4.7 (2)
C2	0.9029 (10)	0.4726 (6)	0.1431 (6)	5.2 (2)	C14′	0.5934 (8)	0.1915 (5)	0.3734 (5)	3.9 (2)
C3	0.7765 (10)	0.4355 (6)	0.0776 (6)	5.2 (2)	C15′	0.4821 (9)	0.1363 (5)	0.4050 (5)	4.3 (2)
C4	0.7880 (12)	0.4011 (7)	−0.0103 (7)	7.4 (3)	C16′	0.4182 (8)	0.0530 (5)	0.3388 (5)	3.4 (2)
C5	0.6583 (13)	0.3732 (8)	−0.0606 (8)	8.7 (3)	C17′	0.0645 (8)	0.0326 (5)	0.2328 (5)	3.1 (2)
C6	0.5354 (13)	0.3761 (8)	−0.0375 (8)	8.1 (3)	C18′	0.1776 (8)	−0.0587 (5)	0.1297 (5)	3.4 (2)
C7	0.5289 (11)	0.4121 (7)	0.0503 (7)	6.8 (3)	C19′	−0.0502 (10)	0.1186 (6)	0.3248 (6)	5.6 (3)*
C8	0.3932 (13)	0.4240 (7)	0.0846 (7)	8.9 (3)*	C20′	0.2077 (11)	−0.1955 (5)	0.1536 (7)	6.8 (3)*
C9	0.3313 (13)	0.3553 (8)	0.1231 (9)	9.9 (4)*	C21′	0.2939 (9)	0.0073 (5)	0.3714 (5)	4.0 (2)
C10	0.3648 (10)	0.3619 (6)	0.2159 (6)	5.9 (2)	C22′	0.5230 (8)	−0.0059 (5)	0.3207 (5)	3.6 (2)
C11	0.2775 (11)	0.3076 (6)	0.2548 (6)	6.2 (2)	C23′	0.1728 (11)	−0.1259 (6)	0.3884 (6)	6.4 (3)*
C12	0.3032 (11)	0.3066 (7)	0.3342 (7)	6.6 (3)	C24′	0.7169 (10)	−0.0574 (6)	0.3837 (6)	5.8 (3)*
C13	0.4195 (10)	0.3632 (6)	0.3859 (6)	5.2 (2)	O1W	−0.001 (2)	0.742 (1)	0.960 (1)	31 (1)*
C14	0.5055 (8)	0.4182 (5)	0.3482 (5)	3.9 (2)					

[a] Estimated standard deviations in the least significant digits are shown in parentheses

Table III. Crystal Data and Data Collection Parameters

	6	17
formula	$PdClC_{34}H_{35}N_2O_{16}\cdot1^1/_2C_3H_6O$	$PdC_{24}H_{26}N_2O_8\cdot^1/_2H_2O$
fw	927.6	585.9
cryst system	triclinic	triclinic
space group	$P\bar{1}$	$P\bar{1}$
a, Å	11.298 (2)	9.610 (2)
b, Å	13.932 (3)	16.182 (2)
c, Å	14.778 (5)	16.191 (2)
α, deg	99.06 (2)	101.53 (1)
β, deg	109.03 (2)	96.47 (1)
γ, deg	97.44 (2)	99.86 (1)
V, Å^3	2130 (2)	2402.3 (13)
d, g·cm^{-3}	1.491	1.620
Z, formulas/cell	2	4
temp, °C	28	26
μ(Mo Kα), cm^{-1}	5.6	8.1
crystal size, mm	0.20 × 0.24 × 0.44	0.16 × 0.48 × 0.52
color:	orange	yellow-orange
min relative transmissn, %	85.10	82.20
2θ limits, deg	2–43	2–40
scan rates, deg·min^{-1}	0.69–10	0.49–10
precision	$I \cong 25\sigma(I)$	$I \cong 25\sigma(I)$
max scan time, s	90	120
unique data	4883	4473
obsd data	2798	3811
variables	395	401
R	0.048	0.045
R_w	0.055	0.047
max residual, e Å^{-3}	0.61	0.69

Table IV. Bond Lengths (Å) and Angles (deg) in Complexes 6 and 17

6		17	
atoms	dist, Å	atoms	dist, Å
Pd–N1	2.064 (5)	Pd–N1	2.112 (5)
Pd–N2	2.153 (5)	Pd–N2	2.184 (5)
Pd–C15	2.090 (6)	Pd–C1	2.108 (5)
Pd–Cl	2.329 (2)	Pd–C16	2.090 (5)
6		**17**	
atoms	angle, deg	atoms	angle, deg
N1–Pd–N2	80.4 (2)	N1–Pd–N2	101.2 (2)
N1–Pd–C15	95.0 (2)	N1–Pd–C1	79.7 (2)
N1–Pd–Cl	159.3 (2)	N1–Pd–C16	170.8 (2)
N2–Pd–C15	168.4 (2)	N2–Pd–C1	165.3 (2)
N2–Pd–Cl	96.2 (1)	N2–Pd–C16	78.3 (2)
C15–Pd–Cl	91.8 (2)	C1–Pd–C16	103.1 (2)

sertion of bridging units between the heteroatom donors have proven very successful for increasing the degree of geometrical freedom in the resulting complexes. Further, incorporation of the carbonyl bridge has established that a diminished electron density on the heteroatom donor does not necessarily preclude generation of the cyclometalated species as evidenced by complex **22**.

Our previous work dealing with cyclometalated Pd(II) complexes has established the type of ligand best suited for square-planar geometry in which partial coordination is via an sp^3 carbon(s). Presently, we are interested in expanding this methodology to include a greater number of transition metals in various geometries. Thus, it has become necessary for us to explore new synthetic approaches to ligand design which will introduce an added degree of ligand flexibility as well as variations in the electronic character of heteroatom donors. The work described herein is representative of our initial efforts in this area which are ultimately directed toward the incorporation of two or more organometallic subunits into a macrocyclic framework. Presently we are investigating the syntheses of Pt(II), Rh(II), Rh(III), Ru(II), Ni(II), and Fe(II) complexes of these and other ligands to be reported later.

Experimental Section

All melting points were taken in capillary tubes with a Thomas-Hoover Uni-melt apparatus and are uncorrected. ^{1}H and ^{13}C NMR spectra were determined on an IBM-Bruker NR/80 spectrometer using $CDCl_3$ as solvent with Me_4Si as internal standard. Mass spectral (MS) data (70eV) were determined by Mr. D. A. Patterson on a Hewlett-Packard HP 5985 GC/mass spectrometer and reported herein as (assignment, relative intensity). Preparative thick-layer chromatography (ThLC) was performed on 20 × 40 cm glass plates coated with a 2-mm layer of Brinkmann silica gel PF-254-366. IR spectra were recorded on a Perkin-Elmer 621 grating infrared spectrophotometer. X-ray data were collected on an Enraf-Nonius CAD4 diffractometer equipped with Mo Kα radiation (λ = 0.710 73 Å) and a graphite monochromator, by ω–2θ scans of variable speed designed to measure all significant reflections with equal relative precision.

Crystal data and experimental details are listed in Table III. The crystal of **6** was sealed in a thin-walled glass capillary to prevent solvent loss. One hemisphere of data was collected for each crystal within the specified angular limits. Data reduction included corrections for background, Lorentz, and polarization effects, as well as an empirical absorption correction, based upon ψ scans of reflections near χ = 90°.

Structures were solved by heavy-atom methods, and refinement was conducted by full-matrix least squares upon F, with data for which $I > 1\sigma(I)$, using the Enraf-Nonius SDP programs.[17] Due to the rather low quality of the available crystals and resulting low resolution of the data, full anisotropic refinement was not possible. For **6**, only Pd, Cl, O, and methyl carbon were anisotropic, while all other non-hydrogen atoms were refined isotropically. For **17**, Pd, O, methyl carbon, and methylene carbon of the seven-membered ring were anisotropic, while other non-hydrogen atoms were isotropic. While the crystal of **6** contained one ordered solvent molecule (acetone) in a general position, a second acetone molecule was found disordered across a center, which lies approximately at the midpoint of the C=O bond in two half-populated orientations. Hydrogen atoms of the disordered acetone were ignored; all other hydrogen atoms were included as fixed contributions in calculated positions. Final R factors and residual electron densities are given in Table III; coordinates are given in Tables I and II.

(17) Frenz, B. A.; Okaya, Y. "Enraf-Nonius Structure Determination Package"; Enraf-Nonius: Delft, Holland, 1982.

1,2-Bis(6-methyl-2-pyridyl)ethylene Di-*N*-oxide (11). A mixture of 1,2-bis(6-methyl-2-pyridyl)ethylene[7] (mp 208–209 °C; 10 g, 48 mmol), 30% H_2O_2 (50 mL), and glacial AcOH (50 mL) was stirred at 90 °C for 4 h. Additional 30% H_2O_2 (50 mL) and glacial AcOH (25 mL) were added, and the solution was stirred at 90 °C for 12 h. The solution was cautiously concentrated, repeatedly diluted with water, and concentrated in vacuo. (*Note*: Explosions have been reported when 30% H_2O_2 was used. Proceed cautiously when concentrating any solutions containing peroxides. Use no less than four reaction volumes of water to dilute the mixture when following the procedure given here.) The resulting viscous liquid was neutralized with solid Na_2CO_3 and extracted with $CHCl_3$. The extract was dried and concentrated to give a crude product, which was crystallized from $EtOH/C_6H_6$ as white crystals: 75%; mp 245 °C dec; (lit.[7] mp 247–249 °C dec).

1,2-Bis[6-(acetoxymethyl)-2-pyridyl]ethylene (12). A solution of di-*N*-oxide **11** (10 g, 45 mmol) in distilled Ac_2O (100 mL) was refluxed for 30 min and then concentrated in vacuo. The resulting solid was dissolved in CH_2Cl_2, washed with dilute aqueous Na_2CO_3, dried over anhydrous $MgSO_4$, and reconcentrated in vacuo. The crude product was passed through a short silica gel column eluting with CH_2Cl_2. The eluant was concentrated and the product crystallized from a small volume of EtOH to give the diester, as white needles: 6.6 g (50%); mp 133–136 °C (lit.[7] mp 133–134 °C).

1,2-Bis[6-(hydroxymethyl)-2-pyridyl]ethylene (13). Step A. A suspension of 1,2-bis[6-(acetoxymethyl)-2-pyridyl]ethylene (10 g, 31 mmol) and anhydrous K_2CO_3 (14 g, 102 mmol) in absolute EtOH (200 mL) was stirred for 1 h. The mixture was filtered and concentrated in vacuo to give the enediol, which was crystallized from EtOH, as white needles: 7.1 g (95%); mp 138–140 °C (lit.[7] mp 142–144 °C).

Step B. 1,2-Bis[6-(hydroxymethyl)-2-pyridyl]ethylene (**13**) was catalytically reduced to give (27%) diol **14**: mp 155–157 °C (lit.[7] mp 157–159 °C).

1,2-Bis[6-(chloromethyl)-2-pyridyl]ethane (15). To freshly distilled[18] $SOCl_2$ (5 mL) precooled to 0 °C was added diol **14** (1.1 g, 4.5 mmol) in small portions under nitrogen. The solution was refluxed for 1 h and cooled and excess $SOCl_2$ removed in vacuo. The residue was neutralized with 10% aqueous Na_2CO_3 and then extracted with CH_2Cl_2 (5 × 50 mL). The combined organic extract was dried over anhydrous $MgSO_4$ and concentrated in vacuo to afford a light tan solid, which was crystallized from CH_2Cl_2/C_6H_{12} to give the dichloride, as white crystals: 1.2 g (95%); mp 100–101 °C; ^1H NMR δ 3.24 (s, CH_2CH_2, 4 H, 4.60 (s, CH_2Cl, 4 H), 7.05 (dd, 5-py*H*, J = 7.8, 1.2 Hz, 2 H), 7.15 (dd, 3-py*H*, J = 7.8, 1.2 Hz, 2 H), 7.50 (t, 4-py*H*, J = 7.8 Hz, 2 H); MS, m/e 280 (M^+, 1), 279 (2), 245 (22), 244 (*100*), 210 (20), 209 (41), 207 (60).

Bis(6-methyl-2-pyridyl) Ketone (19). To a solution of 2-bromo-6-methylpyridine (19 g, 0.11 mol) in THF (150 mL) cooled to −90 °C (petroleum ether–liquid nitrogen) under argon was added BuLi (0.1 mol, 2.4 M in hexane) dropwise. The resultant solution was stirred at −90 °C for 1 h, and then a solution of ethyl chloroformate (6 g, 0.05 mmol) in THF (15 mL) was added rapidly while the temperature was still maintained at <−80 °C. After stirring for 1.5 h at −80 °C, the reaction was quenched with MeOH (1.0 mL). The solvent was removed in vacuo and the residue extracted with $CHCl_3$, followed by washing with 10% aqueous $NaHCO_3$. The combined organic extract was dried over anhydrous $MgSO_4$, concentrated, and column chromatographed (silica) eluting with C_6H_{12}/EtOAc (1:1) to give **19** as colorless needles: 5.6 g (48%); mp 6 °C; bp 162–166 °C (2.8 mm); ^1H NMR δ 2.65 (s, CH_3, 6 H), 7.35 (dd, 5-py*H*, J = 7.7, 0.5 Hz, 2 H), 7.76 (t, 4-py*H*, J = 7.7 Hz, 2 H), 7.91 (dd, 3-py*H*, J = 7.7, 0.5 Hz, 2 H); IR ($CHCl_3$) 1681 (C=O) cm^{-1}; MS, m/e 212 (77), 183 (*100*). Anal. Calcd for $C_{13}H_{12}N_2O$: C, 73.56; H, 5.70; N, 13.20. Found: C, 73.40; H, 5.85; N, 13.25.

Bis[6-(bromomethyl)-2-pyridyl] Ketone (20). To a solution of **19** (2.0 g, 9.5 mmol) in anhydrous CCl_4 (200 mL) were added NBS (3.7 g, 20.8 mmol) and benzoyl peroxide (40 mg). The mixture was refluxed for 4 h under a nitrogen atmosphere while irradiating with a 100-W bulb. After cooling and filtration, the filtrate was washed with 10% aqueous Na_2CO_3, dried over anhydrous $MgSO_4$, and concentrated in vacuo to give a viscous residue, which was column chromatographed on silica gel eluting with $EtOAc/C_6H_{12}$ (1:1) to give dibromide **15**, as white crystals: 580 mg (17%); mp 102–103 °C dec; ^1H NMR δ 4.61 (s, CH_2, 4 H), 7.68 (dd, 5-py*H*, J = 7.7, 1.1 Hz, 2 H), 7.91 (t, 4-py*H*, J = 7.7 Hz, 2 H), 8.06 (dd, 3-py*H*, J = 7.7, 1.1 Hz, 2 H); IR ($CHCl_3$) 1686 (C=O) cm^{-1}; MS, m/e 372 (1), 370 (1), 368 (1), 291 (*100*), 280 (83), 210 (28). Anal. Calcd for $C_{13}H_{10}Br_2N_2O$: C, 42.19; H, 2.72; N, 7.57. Found: C, 41.96; H, 2.80; N, 7.46.

General Preparation of Ligands 5, 16, and 21. A mixture of the dialkyl malonate (4 equiv), the bis(halomethyl) compound (1 equiv),[5,8] and anhydrous K_2CO_3 (4 equiv) in distilled DMF (50 mL) was stirred at 25 °C for 24 h. The mixture was filtered and concentrated in vacuo to give an oil, which was passed through a short silica column eluting with CH_2Cl_2, and concentrated in vacuo and the product crystallized.

Dimethyl 2,2,2′,2′,3,3′-hexakis(methoxycarbonyl)[2,2′-bipyridine]-2,9-dibutanoate (5) as a white solid (CH_2Cl_2/C_6H_{12}): 90%; mp 218–220 °C dec; ^1H NMR δ 3.73 (s, CH_3, 24 H), 3.77 (s, pyCH_2, 4 H), 4.56 [s, $CH(CO_2Me)_2$, 2 H], 7.17 (dd, 5-py*H*, J = 7.6, 1.0 Hz, 2 H), 7.75 (t, 4-py*H*, J = 7.6 Hz, 2 H), 8.18 (dd, 3-py*H*, J = 7.6, 1.0 Hz, 2 H); ^{13}C NMR δ 40.15 (CH_2), 52.55 (CH_3), 52.84 (CH_3), 53.23 [$CH(CO_2Me)_2$], 58.14 [$C(CO_2Me)_2$], 119.24 (C3), 124.15 (C5), 137.42 (C4), 155.21 (C6), 156.14 (C2), 168.38 (C=O), 170.34 (C=O); IR (KBr) 2950, 1725 (C=O) cm^{-1}; MS, m/e 704 (1), 674 (3), 673 (8), 573 (16), 445 (25), 444 (*100*), 184 (94), 159 (42), 115 (45). Anal. Calcd for $C_{32}H_{36}N_2O_{16}$: C, 54.55; H, 5.15; N, 3.98. Found: C, 54.48; H, 5.05; N, 3.72.

1,2-Bis[6-(2,2-dicarbomethoxyethyl)-2-pyridyl]ethane (16) as white crystals (C_6H_{12}): 91%; mp 99–100 °C; ^1H NMR δ 3.12 (s, CH_2CH_2, 4 H), 3.39 (d, pyCH_2, J = 7.4 Hz, 4 H), 3.73 (s, CH_3, 12 H), 4.16 [t, $CH(CO_2CH_3)_2$, J = 7.4 Hz, 2 H], 6.88 (d, 5-py*H*, J = 7.8 Hz, 2 H), 6.97 (d, 3-py*H*, J = 7.8 Hz, 2 H), 7.43 (t, 4-py*H*, J = 7.8 Hz, 2 H); IR (KBr) 1715 (C=O) cm^{-1}; MS m/e 475 (2), 474 (8), 473 (36), 472 (M^+, *100*), 409 (39), 218 (38), 186 (86), 145 (35). Anal. Calcd for $C_{24}H_{28}N_2O_8$: C, 61.01; H, 5.97; N, 5.93. Found: C, 59.89; H, 5.93; N, 5.85.

Diethyl 2,2′-bis(ethoxycarbonyl)-2,2′-dicarbonylbis[pyridine]-6,6′-dipropanoate (21) was column chromatographed on silica gel eluting with C_6H_{12}/EtOAc (1:1) to give the tetraester, as a pale yellow oil: 53%; R_f 0.5; ^1H NMR δ 1.19 (t, CH_2CH_3, J = 7.1 Hz, 12 H), 3.47 (d, pyCH_2, J = 7.5 Hz, 4 H), 4.07 [t, $CH(CO_2Et)_2$, J = 7.5 Hz, 2 H], 4.11 (m, CH_2CH_3, 8 H), 7.41 (dd, 4-py*H*, J = 7.7, 1.2 Hz, 2 H), 7.79 (t, 4-py*H*, J = 7.7 Hz, 2 H), 7.89 (dd, 3-py*H*, J = 7.7, 1.2 Hz, 2 H); IR ($CHCl_3$) 1743 (C=O), 1729 (C=O), 1687 (C=O) cm^{-1}; MS, m/e 528 (75), 483 (32), 455 (35), 437 (53), 363 (*100*). Anal. Calcd for $C_{27}H_{32}N_2O_9$: C, 61.36; H, 6.10; N, 5.30. Found: C, 60.79; H, 6.23; N, 5.04.

Dimethyl 2,2,2′,2′,3,3′-Hexakis(methoxycarbonyl)[1,10-phenanthroline]-2,9-dibutanoate (4). To a refluxing mixture of anh. THF (100 mL) and NaH (168 mg, 50% dispersion in oil) was added tetraester **2** (950 mg, 3.6 mmol) in THF (20 mL). After 30 min, **3** (500 mg, 1.8 mmol) in THF (20 mL) was added in one portion. After 2 h at reflux, the reaction was quenched with MeOH and the mixture concentrated in vacuo to give a residue, which was passed through a short silica gel column (CH_2Cl_2). After concentration in vacuo, the product was crystallized from CH_2Cl_2/C_6H_{12}: 85%; mp 150–151 °C; ^1H NMR δ 3.55 (s, CH_3, 12 H), 3.78 (s, CH_3, 12 H), 3.90 (s, phenCH_2, 4 H), 4.92 [s, $CH(CO_2Me)_2$, 2 H], 7.66 (d, 3,8-phen*H*, J = 8.3 Hz, 2 H), 7.68 (s, 5,6-phen*H*, 2 H), 8.10 (d, 4,7-phen*H*, J = 8.3 Hz, 2 H); ^{13}C NMR δ 42.44 (CH_2), 52.40 (CH_3), 52.84 (CH_3), 53.30 [$CH(CO_2Me)_2$], 59.60 [$C(CO_2Me)_2$], 124.59 (C3,8), 126.10 (C5,6), 127.41 (C4a,b), 136.01 (C4,7), 145.49 (C10a,b), 157.25 (C2,9), 168.43 (C=O), 170.04 (C=O); IR (KBr) 1740, 1715 cm^{-1}; MS, m/e 728 (M^+, 1), 698 (2), 469 (28), 468 (*100*), 241 (25), 208 (70), 59 (26). Anal. Calcd for $C_{34}H_{36}N_2O_{16}$: C, 56.05; H, 4.98; N, 3.84. Found: C, 56.25; H, 5.20; N, 3.76.

Dichloro[dimethyl 2,2,2′,2′,3,3′-hexakis(methoxycarbonyl)(2,2′-bipyridine)-6,6′-dibutanoate]palladium(II) (8). To a CH_3CN solution (25 mL) of $PdCl_2$ (1 mmol) was added **4** (1 mmol) dissolved in CH_3CN (5 mL), and the mixture was then warmed to 50 °C for 2 h. After cooling and concentration in vacuo, the resultant product was dissolved in CH_2Cl_2, filtered, and reconcentrated in vacuo. The orange solid was characterized by

(18) Vogel, A. I. "Practical Organic Chemistry"; Longmans: London, 1973; p 189.

NMR and immediately used in subsequent cyclometalation reactions: ^{1}H NMR δ 3.60 (s, CH_3, 12 H), 3.86 (s, CH_3, 12 H), 4.32 (s, pyCH_2, 4 H), 4.64 [s, $CH(CO_2Me)_2$, 2 H], 7.52 (dd, 5-py*H*, J = 7.8, 1.4 Hz, 2 H), 7.88 (t, 4-py*H*, J = 7.8 Hz, 2 H), 8.10 (dd, 3-py*H*, J = 7.8, 1.4 Hz, 2 H).

General Preparation of Carbon–Palladium Bonded Complexes 6, 9, and 17. A mixture of Na_2PdCl_4 or $PdCl_2$ (1.5 equiv) and the ligand (1.0 equiv) in anhydrous CH_3CN (25 mL) was stirred for 1 h at 50 °C. Anhydrous K_2CO_3 (3.0 equiv) was added and the mixture stirred for 18 h at 50 °C. The heterogeneous mixture was filtered through Celite and concentrated and the crude product passed through a short silica gel column eluting with MeOAc. After concentration in vacuo, the complex was recrystallized.

Chloro{3-methoxy-2-(methoxycarbonyl)-1,1-bis(methoxycarbonyl)-1-[[9-[4-methoxy-3-(methoxycarbonyl)-2,2-bis(methoxycarbonyl)-4-oxobutyl][1,10-phenanthroline]-2-yl]methyl]-3-oxopropyl-*C,N,N*'}palladium (6) as orange crystals from acetone: 60%; mp 183–186 °C dec; ^{1}H NMR δ 3.66 (s, CH_3, 6 H), 3.70 (s, CH_3, 6 H), 3.73 (s, CH_3, 6 H), 3.77 (s, CH_3, 6 H), 4.22 (s, phenCH_2, 2 H), 4.55 [s, $CH(CO_2Me)_2$, 1 H], 4.78 (s, phenCH_2, 2 H), 7.59 (d, 8-phen*H*, J = 8.4 Hz, 1 H), 7.81, 7.83 (2s, 5,6-phen*H*, 2 H), 7.87 (d, 3-phen*H*, J = 8.4 Hz, 1 H), 8.27 (d, 7-phen*H*, J = 8.4 Hz, 1 H), 8.35 (d, 4-phen*H*, J = 8.4 Hz, 1 H); IR (CsI) 1720 (C=O) cm^{-1}. Anal. Calcd for $C_{34}H_{35}N_2O_{16}PdCl$: C, 46.96; H, 4.06; N, 3.22. Found: C, 46.37; H, 3.88; N, 2.94.

Chloro{3-methoxy-2-(methoxycarbonyl)-1,1-bis(methoxycarbonyl)-1-[[6-[4-methoxy-3-(methoxycarbonyl)-2,2-bis(methoxycarbonyl)-4-oxobutyl][2,2'-bipyridine]-6'-yl]methyl]-3-oxopropyl-*C,N,N*'}palladium (9) as orange crystals from CH_2Cl_2/C_6H_{12}: 20%; mp 240 °C dec; ^{1}H NMR δ 3.66 (s, CH_3, 6 H), 3.72 (s, CH_3, 6 H), 3.75 (s, CH_3, 6 H), 3.76 (s, CH_3, 6 H), 4.00 (s, phenCH_2, 2 H), 4.32 [s, $CH(CO_2Me)_2$, 1 H], 4.46 (s, phenCH_2, 2 H), 7.33 (dd, 5'-py*H*, J = 6.0, 3.0 Hz, 1 H), 7.67 (dd, 5-py*H*, J = 5.0, 1.0 Hz, 1 H), 7.92 (m, 4,4',3,3'-py*H*, 4 H); IR (CsI) 1722 (C=O) cm^{-1}; MS, m/e 674 (3), 673 (8), 645 (6), 587 (8), 573 (17), 527 (16), 495 (16), 445 (25), 444 (*100*). Anal. Calcd for $C_{32}H_{35}N_2O_{16}PdCl$: C, 45.46; H, 4.17; N, 3.31. Found: C, 45.23; H, 4.11; N, 3.40.

{[1,2-Bis(2-pyridyl)ethane]-6,6'-diylbis[1,1-bis(methoxycarbonyl)-2,1-ethanediyl]-*C,C',N,N*'}palladium (17) as yellow crystals from CH_2Cl_2/C_6H_{12}: 85%; mp 155–160 °C dec; ^{1}H NMR δ 3.11 (s, CH_2CH_2, 4 H), 3.48 (s, pyCH_2, 4 H), 3.66 (s, CH_3, 12 H), 6.94 (d, 5-py*H*, J = 7.5 Hz, 2 H), 7.23 (d, 3-py*H*, J = 7.5 Hz, 2 H), 7.61 (t, 4-py*H*, J = 7.5 Hz, 2 H); IR (CsI) 1725 (C=O) cm^{-1}; MS, m/e 580 (1), 578 (2), 576 (3), 575 (2), 520 (2), 472 (53), 342 (43), 186 (87), 120 (*100*). Anal. Calcd for $C_{24}H_{26}N_2O_8Pd$: C, 49.97; H, 4.54; N, 4.86. Found: C, 50.22; H, 4.66; N, 4.92.

(Nitrato){3-methoxy-2-(methoxycarbonyl)-1,1-bis(methoxycarbonyl)-1-[[9-[4-methoxy-3-(methoxycarbonyl)-2,2-bis(methoxycarbonyl)-4-oxobutyl][1,10-phenanthroline]-2-yl]methyl]-3-oxopropyl-*C,N,N*'}palladium (7). To a stirred solution of **6** (50 mg, 0.06 mmol) in CH_3CN (25 mL) was added $AgNO_3$ (2.0 equiv) at 25 °C. The immediate formation of a white precipitate was observed (AgCl)! After 1 h the mixture was filtered and the filtrate concentrated in vacuo to give a yellow solid. No further purification was attempted due to the instability of the complex: 10%; ^{1}H NMR δ 3.68 (s, CH_3, 6 H), 3.75 (s, CH_3, 6 H), 3.81 (s, CH_3, 6 H), 3.82 (s, CH_3, 6 H), 4.10 (s, phenCH_2, 2 H), 4.24 (s, phenCH_2, 2 H), 4.39 [s, $CH(CO_2Me)_2$, 1 H], 7.57 (d, 8-phen*H*, 8.4 Hz, 1 H), 7.81 (s, 5,6-phen*H*, 2 H), 7.88 (d, 3-phen*H*, J = 8.4 Hz, 1 H), 8.26 (d, 7-phen*H*, J = 8.4 Hz, 1 H), 8.34 (d, 4-phen*H*, J = 8.4 Hz, 1 H).

{2,2'-Carbonylbis[pyridine]-6,6'-diylbis[1,1-bis(ethoxycarbonyl)-2,1-ethanediyl]-*C,C',N,N*'}palladium (22). Freshly prepared NaOEt (0.7 mmol) in EtOH (1.0 mL) was added to a stirred, anhydrous THF solution (25 mL) of $PdCl_2(C_6H_5CN)_2$ (110 mg, 0.29 mmol) and tetraester **21** (158 mg, 0.30 mmol) under nitrogen atmosphere at 25 °C. After 12 h, the solvent was removed and the residue concentrated in vacuo followed by chromatography (ThLC) on silica gel eluting with EtOAc/EtOH (10:1). The desired complex was isolated as orange-yellow microcrystals: 15 mg (8%); mp 92–94 °C dec, R_f 0.26; ^{1}H NMR δ 1.14 (t, CH_2CH_3, J = 7.1 Hz, 12 H), 3.64 (s, pyCH_2, 4 H), 4.08 (m, CH_2CH_3, 8 H), 7.77 (d, 5-py*H*, J = 7.8 Hz, 2 H), 8.03 (t, 4-py*H*, J = 7.8 Hz, 2 H), 8.14 (d, 3-py*H*, J = 7.8 Hz, 2 H); IR ($CHCl_3$) 1728 (C=O), 1674 (C=O) cm^{-1}. Anal. Calcd for $C_{27}H_{30}N_2O_9Pd$: C, 51.24; H, 4.78; N, 4.43. Found: C, 51.66; H, 5.02; N, 4.65.

Acknowledgment. We wish to thank the National Science Foundation and the LSU Center for Energy Studies for partial support of this work.

Supplementary Material Available: Tables of bond distances and angles, coordinates for H atoms, anisotropic thermal parameters, and structure factors for complexes **6** and **17** (38 pages). pages). Ordering information is given on any current masthead page.

α-Diazomethyl and Bis(α-diazomethyl) Palladium Complexes. Preparation, Crystal and Molecular Structures, and Reactions

Shun-Ichi Murahashi,*[1a] Yasuo Kitani,[1a] Toru Uno,[1a] Takahiro Hosokawa,[1a] Kunio Miki,[1b] Tadashi Yonezawa,[1b] and Nobutami Kasai[1b]

Department of Chemistry, Faculty of Engineering Science, Osaka University, Toyonaka, Machikaneyama, Osaka, Japan 560, and the Department of Applied Chemistry, Faculty of Engineering, Osaka University, Yamadaoka, Suita, Osaka, Japan 565

Received May 28, 1985

α-Diazomethyl palladium complexes, $(PR^1_3)_2XPd[C(N_2)R]$ (**4**), where R = CO_2Et and C(O)Me, X = Cl, Br, and I, and R^1 = Et and Ph, have been prepared by the reaction of $(PR^1_3)_2PdX_2$ with $Hg[C(N_2)R]_2$, and complexes of the formula $(PR^1_3)_2Pd[C(N_2)R]_2$ (**5**), where R = CO_2Et, C(O)Me, Ph, *p*-$CH_3C_6H_4$, *i*-Pr, and *t*-Bu, R^1 = Et, Ph, and Bu, have been prepared by treatment of $(PR^1_3)_2PdX_2$ with $LiC(N_2)R$. These complexes, **4** and **5**, were characterized by ^1H and ^{13}C NMR and IR spectra. Complete X-ray analyses have been carried out for $(PPh_3)_2ClPd[C(N_2)CO_2Et]$ (**4a**) and $(PBu_3)_2Pd[C(N_2)CO_2Et]_2$ (**5d**). The crystal data are as follows. **4a**: a = 11.973 (**2**) Å, b = 29.719 (**6**) Å, c = 10.310 (**2**) Å, β = 94.71 (**2**), Z = 4, space group $P2_1/c$. **5d**: a = 11.946 (**3**) Å, b = 12.071 (**2**) Å, c = 15.174 (**3**) Å, β = 107.54 (**2**)°, Z = 2, space group $P2_1/n$. In each complex, the geometry around the Pd atom is trans square planar. The planes of α-diazomethyl group are almost perpendicular to the coordination plane of Pd. Their C(1)–N(1)–N(2) angles are almost linear, and the N(1)–N(2) bond lengths [1.160 (**15**) Å and 1.130 (**10**) Å] are longer in comparison with those of the general noncoordinated diazo groups. The temperature-dependent ^{13}C NMR spectra of $(PEt_3)_2Pd[C(N_2)Ph]_2$ (**5e**) showed restricted rotation about the Pd–C bond. The "in-beam" electron-impact (EI) mass spectrum of $(PEt_3)_2Pd[C(N_2)CO_2Et]_2$ (**5c**) indicated the presence of the carbene palladium complex $(PEt_3)_2Pd(CCO_2Et)_2$, while the corresponding spectrum of **5e** showed fragments corresponding to diphenylacetylene. Pyrolysis and photolysis of **5e** gave diphenylacetylene exclusively, indicating the intermediacy of the carbene complex $(PEt_3)_2Pd(CPh)_2$.

Diazoalkanes can be attached to metals to form three types of metal complexes:[2] the α-diazomethyl complex **1** and the complexes with a ligand bonded via terminal N atom (**2**)[3] or via a π-function of N≡N (**3**).[4] Complexes

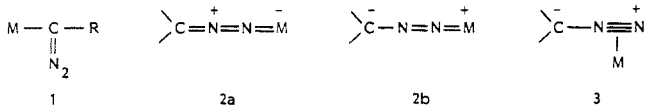

1 **2a** **2b** **3**

2 and **3** and related complexes have been extensively studied in view of the fixation of nitrogen or the mechanistic aspects of the catalytic decomposition of diazoalkenes. The α-metalated diazoalkanes **1** would be precursors of α-carbene[5] or carbyne metal complexes[6] and intermediates in the synthesis of substituted diazo compounds.[7]

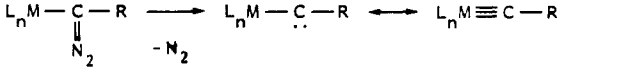

However, the diazo complexes **1**[8] reported are quite few and limited to those of non-transition metals[9,10] and group 1B[11] (11^{55}) and 2B[12] (12^{55}) transition metals. This paper reports the preparation of two types of α-diazomethyl palladium complexes **4** and **5**, which are the first complexes of the group 8 ($8–10^{55}$) transition metals,[13] and their

(1) (a) Department of Chemistry. (b) Department of Applied Chemistry.

(2) (a) Albini, A.; Kisch, H. *Top. Curr. Chem.* **1976**, *65*, 105. (b) Herrmann, W. A. *Angew. Chem., Int. Ed. Engl.* **1978**, *17*, 800.

(3) (a) **Typical examples for 2a.** $MX(N_2CR_2)(diphos)_2^+$ and $MX_2(N_2CR_2)(PMe_2Ph)_3$ (M = Mo, W). Hidai, M.; Mizobe, Y.; Uchida, Y. *J. Am. Chem. Soc.* **1976**, *98*, 7824. Ben-Shoshan, R.; Chatt, J.; Leigh, G. J.; Hussain, W. *J. Chem. Soc., Dalton Trans.* **1980**, 771. $WBr(N_2CMe_2)(diphos)_2^+$. Hidai, M.; Mizobe, Y.; Sato, M.; Kodama, T.; Uchida, Y. *J. Am. Chem. Soc.* **1978**, *100*, 5740. (b) **Typical examples for 2b.** $(C_5H_5)(CO)_3MM(C_5H_5)(CO)_2(N_2CHC(O)C_6H_5)$ (M = Mo, W). Herrmann, W. A.; Biersack, H. *Chem. Ber.* **1977**, *110*, 896. $(C_5H_5)Mn(CO)_2[N_2C(CO_2C_2H_5)_2]$. Herrmann, W. A.; Kriechbaum, G.; Ziegler, M. L.; Wulknitz, P. *Chem. Ber.* **1981**, *114*, 276. $IrCl(N_2CR_2)(PPh_3)_2$. Schramm, K. D.; Ibers, J. A. *Inorg. Chem.* **1980**, *19*, 1231, 2441, 2435. $(C_5H_5)_2Ti[N_2C(CO_2R)_2]_2$. Gambarotta, S.; Floriani, C.; Chiesi Villa, A.; Guastini, C. *J. Am. Chem. Soc.* **1982**, *104* 1918. (c) **Others.** Hillhouse, G. L.; Haymore, B. L. *J. Am. Chem. Soc.* **1982**, *104*, 1537 and references cited therein. (h) Messerle, L.; Curtis, M. D. *Ibid.* **1980**, *102*, 7789.

(4) (a) **Typical examples for complex 3.** $Ni(CN\text{-}t\text{-}Bu)_2$(diazofluorene). Nakamura, A.; Yoshida, T.; Cowie, M.; Otsuka, S.; Ibers, J. A. *J. Am. Chem. Soc.* **1977**, *99*, 2108. $Ru(CO)_2(N_2C_5Cl_4)(PPh_3)_2$. Schramm, K. D.; Ibers, J. A. *Ibid.* **1978**, *100*, 2932. $Cp(OC)_3MoMo(CR_2)(N_2CR_2)Cp$. Messerle, L.; Curtis, M. D. *Ibid.* **1982**, *104*, 889.

(5) **For transition-metal carbene complexes.** Review. (a) Fischer, E. O. *Adv. Organomet. Chem.* **1976**, *14*, 1. (b) Casey, C. P. *Chemtech* **1979**, 373. (c) Schrock, R. R. *Acc. Chem. Res.* **1979**, *12*, 98. (d) Brown, F. J. *Prog. Inorg. Chem.* **1980**, *27*, 1. (e) Herrmann, W. A. *Adv. Organomet. Chem.* **1982**, *20*, 159. (f) Dötz, K. H. *Angew. Chem., Int. Ed. Engl.* **1984**, *23*, 587. (g) Recent papers. Theopold, K. H.; Bergman, R. G. *J. Am. Chem. Soc.* **1983**, *105*, 464. Hill, A. F.; Roper, W. R.; Waters, J. M.; Wright, A. H. *Ibid.* **1983**, *105*, 5939. Casey, C. P.; Vollendorf, N. W.; Haller, K. J. *Ibid.* **1984**, *106*, 3754 and references cited therein.

(6) **For transition-metal carbyne complexes.** W and Cr. (a) Fischer, E. O.; Shubert, U.; Fischer, H. *Pure Appl. Chem.* **1978**, *50*, 857. (b) Holmes, S. J.; Clark, D. N.; Turner, H. W.; Schrock, R. R. *J. Am. Chem. Soc.* **1982**, *104*, 6322. Mayr, A.; McDermott, G. A.; Dorries, A. M. *Ibid.* **1985**, *4*, 606. (c) Mn. Herrmann, W. A. *J. Organomet. Chem.* **1975**, *97*, 1. (d) Co. Nicholas, K. M.; Nestle, M. O.; Seyferth, D. In "Transition Metal Organometallics in Organic Synthesis"; Alper H. Ed.; Academic Press: New York, 1978; Vol. 2, p 1. Fritch J. R.; Vollhardt, K. P. C. *Angew. Chem., Int. Ed. Engl.* **1980**, *7*, 559. (e) Mo. McCullough, L. G.; Schrock, R. R. *J. Am. Chem. Soc.* **1984**, *106*, 4067. (f) Ta and Nb. Reference 5c.

(7) Hermann, W. A. *Angew. Chem., Int. Ed. Engl.* **1978**, *17*, 800 and references therein.

(8) (a) Lappert, M. F.; Poland, J. S. *Adv. Organomet. Chem.* **1970**, *9*, 397. (b) Regitz, M. "Diazoalkane"; Thieme Verlag: Stuttgart, 1977. (c) Schöllkopf, U.; Banhidai, B.; Scholz, H.-U. *Justus Liebigs Ann. Chem.* **1972**, *761*, 137.

(9) **Si complexes.** (a) Ando, W.; Sekiguchi, A.; Hagiwara, T.; Migita, T.; Chowdhry, V.; Westheimer, F. H.; Kammula, S. L.; Green, M.; Jones, M., Jr. *J. Am. Chem. Soc.* **1979**, *101*, 6393 and references cited therein. (b) Ando, W.; Sekiguchi, A.; Sato, T. *Ibid.* **1981**, *103*, 5573. (c) Glidewell, C.; Sheldrick, G. M. *J. Chem. Soc., Dalton Trans.* **1972**, 2409.

(10) **Sn complexes.** (a) Fadini, A.; Glozbach, E.; Krommes, P.; Lorberth, J. *J. Organomet. Chem.* **1978**, *149*, 297 and references cited therein. (b) Gruning, R.; Krommes, P.; Lorberth, J. *Ibid.* **1977**, *128*, 167. (c) Lappert, M. F.; Lorberth. J.; Poland, J. S. *J. Chem. Soc. A* **1970**, 2954. See also ref 8c.

(11) **Hg complexes.** (a) Strausz, O. P.; Kennepohl, G. J. A.; Garneau, F. X.; DoMinh, T.; Kim. B.; Valenty, S.; Skell, P. S. *J. Am. Chem. Soc.* **1974**, *96*, 5723. (b) Herrmann, W. A.; Ziegler, M. L.; Serhadli, O. *Organometallics* **1983**, *2*, 958. (c) Herrmann, W. A. *Angew. Chem., Int. Ed. Engl.* **1974**, *13*, 812.

(12) **Ag complexes.** Schöllkopf, U.; Rieber, N. *Chem. Ber.* **1969**, *102*, 488.

(13) Preliminary commucication has appeared: Murahashi, S.-I.; Kitani, Y.; Hosokawa, T.; Miki, K.; Kasai, N. *J. Chem. Soc., Chem. Commun.* **1979**, 450.

0276-7333/86/2305-0356$01.50/0

Table I. α-Diazomethyl Palladium Complexes $L_2XPd[C(N_2)R]$ and $L_2Pd[C(N_2)R]_2$

complexes	method[a]	yield,[b] %	mp,[c] °C	color	$\nu(CN_2)$, cm^{-1}	$\nu(CO)$, cm^{-1}	$\lambda_{max}(CHCl_3)$, nm (ϵ)
4a	A	39	146–148	pink	2035	1645	532 (460)
4b	A	22	142	red	2010	1584, 1568	528 (370)
4c	A	28	oil	orange	2030	1645	
4d	A	17	oil	red	2030	1655	500 (460)
4e	A	10	148–149	brown	2035	1650	
4f	A	7	137–138	brown	2030	1640	
5a	C	21	138–139	yellow	2025	1640	448 (1290)
5b	C	27	137–138	yellow	2005	1587, 1577 1566	444 (1130)
5c	B	73	125–127	yellow	2025	1630	437 (810)
5d	B	61	92–94	yellow	2020	1640	438 (890)
5e	B	58	110–111	violet	1975, 1966		552 (493)
5f	B	25	91–92	violet	1980, 1970		
5g	B	38	81–83	violet	1965, 1953		
5h	B	10	93–97	violet	1960–1950		

[a] Method A, $(PR^1_3)PdX_2$ + $Hg[C(N_2)R]_2$; method B, $(PEt_3)PdCl_2$ + $LiC(N_2)R$; method C, $Pd(PPh_3)_4$ + $Hg[C(N_2)R]_2$. [b] Analytically pure sample. [c] With decomposition. Measured in a tube sealed under argon.

spectral studies, X-ray analyses, and their reactions. Recently, $OsCl(NO)(CN_2CO_2Et)[HgC(N_2)CO_2Et](PPh_3)_2$ has been prepared by using a similar method.[14]

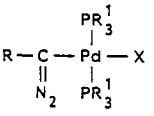

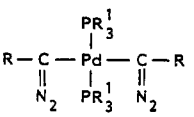

4a, R=CO_2Et, X=Cl, R^1=Ph
4b, R=C(O)Me, X=Cl, R^1=Ph
4c, R=CO_2Et, X=Cl, R^1=Et
4d, R=CO_2Et, X=Cl, R^1=Bu
4e, R=CO_2Et, X=Br, R^1=Ph
4f, R=CO_2Et, X=I, R^1=Ph

5a, R=CO_2Et, R^1=Ph
5b, R=C(O)Me, R^1=Ph
5c, R=CO_2Et, R^1=Et
5d, R=CO_2Et, R^1=Bu
5e, R=Ph, R^1=Et
5f, R=C_6H_4-p-Me, R^1=Et
5g, R=i-Pr, R^1=Et
5h, R=t-Bu, R^1=Et

Results and Discussion

A. Preparation. The reaction of $(PR^1_3)_2PdX_2$ (**6**) with $Hg[C(N_2)R]_2$ (**7**) in the dark (method A) gives mono α-diazomethyl palladium complexes **4**, which are air stable in the solid but decompose slowly in solution. The representative results of the formation of pure complexes **4** are summarized in Table I. The other palladium com-

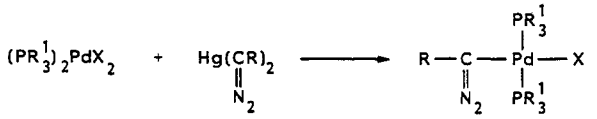

6 **7** **4**

pounds, such as $Pd(OAc)_2$, (η-COD)$PdCl_2$, and [(η^3-methallyl)$PdCl]_2$, induced decomposition of diazo Hg compounds. Phosphine ligands, particularly PPh_3, retard the decomposition efficiently, and $(PPh_3)_2PdCl_2$ gave higher yields of **4** in comparison with $(PBu_3)_2PdCl_2$ and $(PEt_3)_2PdCl_2$. The reaction of diphosphine complexes such as (diphos)$PdCl_2$ do not give the corresponding complex. The reactivity of $(PPh_3)_2PdX_2$ toward $Hg[C(N_2)R]_2$ is in the order X = Cl < Br < I, although the stability of complexes **4** is Cl > Br > I. Complexes **4** thus obtained gave satisfactory spectral data and elemental analyses. As shown in Table I, all of the complexes show a strong N≡N stretch absorption around 2010–2035 cm^{-1} and a Pd–Cl stretch around 335 cm^{-1}. The nitrogen atoms of the diazo compounds are not coordinated to palladium, because the N≡N stretch should shift to 1600 cm^{-1} if the nitrogen were to do so.[4] The N≡N stretch observed is shifted by ca. 80 cm^{-1} to a longer wavelength, compared with that of the parent diazo compounds (Table I), indicating a decrease in the triple-bond character of the nitrogen–nitrogen bond. The trans configuration of **4** was determined by ^1H and ^{13}C NMR spectral data. The methyl proton resonance of **4b** appears as quartet (J = 8 Hz).[15] As shown in Table II, the ^{13}C absorptions of the carbon attached to the phosphine (C_1) and the ortho and meta carbons (C_o and C_m) of triphenylphosphine of **4a** split to triplet[16] and that of the diazo carbon appears as a triplet (J = 8.8 Hz, AX_2, A = ^{13}C, X = ^{31}P).

Bis(α-diazomethyl) palladium complexes (**5**) have been prepared by adding a solution of $LiN(i\text{-}Pr)_2$ to a mixture of $(PR^1_3)_2PdCl_2$ and $HC(N_2)R$ in ether at −78 °C (method B). α-Lithiodiazo compounds $LiC(N_2)CO_2Et$,[17] $LiC(N_2)Ph$, and $LiC(N_2)C_6H_4$-p-CH_3 are unstable even at −78 °C, and the preparation of the corresponding complexes **5** was carried out upon treatment of the parent diazo compounds with $LiN(i\text{-}Pr)_2$ in the presence of $PdCl_2(PR^1_3)_2$ at −78 °C. Since diazo compounds $N_2CHPr\text{-}i$ and $N_2CHBu\text{-}t$ do not undergo lithiation with $LiN(i\text{-}Pr)_2$, $LiC(N_2)\text{-}i\text{-}Pr$ and $LiC(N_2)\text{-}t\text{-}Bu$ were prepared upon treatment of the parent diazo compounds with BuLi at −100 °C. Subsequent displacement of $(PR_3)_2PdCl_2$ with these lithium compounds at −100 °C gave complexes **5g** and **5h**. Noticeably, the second step of these displacements was extremely slow when compared with that for the formation of **5a** because of the steric environment around the palladium atom.

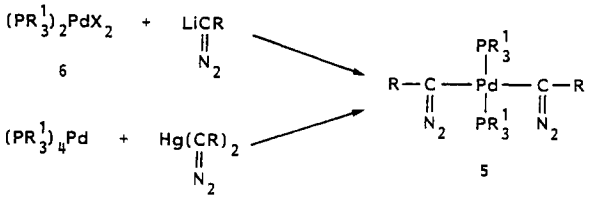

6 **5**

Bis(α-diazomethyl) palladium complexes alternatively can be prepared by the oxidative addition of bis(α-diazomethyl)mercury to $Pd(PPh_3)_4$, followed by reductive elimination of Hg (method C). Thus, treatment of $Hg[C(N_2)R]_2$ with $Pd(PPh_3)_4$ at room temperature under argon gave complexes **5a** and **5b**. Since transition-metal complexes are usually highly effective catalysts for the de-

(14) Gallop, M. A.; Jones, T. C.; Richard, E. F.; Roper, W. R. *J. Chem. Soc., Chem. Commun.* **1984**, 1002.

(15) Clark, H. C.; Tsang, W. S. *J. Am. Chem. Soc.* **1967**, *89*, 533.
(16) (a) Verstuyft, A. W.; Cary, L. H.; Nelson, J. H. *Inorg. Chem.* **1975**, *14*, 1495. (b) Pregosin, P. S.; Kunz, R. *Helv. Chim. Acta* **1975**, *58*, 423.
(17) Schöllkopf, U.; Banhidai, B.; Fransnelli, H.; Meyer, R.; Beckhaus, H. *Justus Liebigs Ann. Chem.* **1974**, 1767.

Table II. ^{13}C NMR Chemical Shifts of Complexes 4 and 5[a]

	temp, °C	δ[$^{13}C(N_2)$]	Pd–R signal[b,c] R in $C(N_2)R$	δ(others)	PR_3 signal[d]
4a	0	37.63 (t, 8.8)	171.67 (s)	14.56 (s, CH_3)	128.52 (t, 8.8, C_m)
				60.00 (s, CH_2)	130.63 (t, 47.1, P–C)
					130.92 (s, C_p)
					134.74 (t, 11.8, C_o)
5a	10	36.64 (t, 11.8)	173.25 (s)	14.62 (s, CH_3)	128.52 (t, 8.8, C_m)
				59.83 (s, CH_2)	130.69 (s, C_p)
					131.28 (t, 47.1, P–C)
					134.33 (t, 11.8, C_o)
5c	0	32.82 (t, 11.8)	174.96 (s)	14.85 (s, CH_3)	8.10 (s, CH_3)
				60.12 (s, CH_3)	15.26 (t, 25.5, CH_3)
5d	−15[e]	33.00 (t, 11.8)	175.19	14.74 (s, CH_3)	25.95 (s)
				60.01 (s, CH_2)	24.42 (t, 14.7)
					22.54 (t, 26.5)
					13.91 (s)
5e	27	37.05 (t, 11.8)	121.77 (s, C_p)		8.10 (s, CH_3)
			124.11 (s, C_o or C_m)		15.62 (t, 26.5, CH_2)
			128.58 (s, C_m)		
			142.96 (s, P–C)		
	0	37.05 (t, 11.8)	121.70 (s, C_p)		8.04 (s, CH_3)
	0	37.28 (t, 11.8)[f]	123.94 (s, C_o or C_p)		8.16 (s, CH_3)[f]
			128.52 (s, C_m or C_o)		15.32 (s, 26.5, CH_2)
			142.72 (s, P–C)		
5g	−30	35.24 (t, 12.7)		23.12 [s, $CH(CH_3)_2$]	8.15 (s, CH_3)
				29.94 [s, $CH(CH_3)_2$]	15.71 (t, 25.4, CH_2)
5h[g]	−30	35.50 (t, 13.2)		29.81 [s, $C(CH_3)_3$]	8.08 (s, CH_3)
				34.27 [s, $C(CH_3)_3$]	15.89 (t, 26.5, CH_2)

[a] Measured in CD_2Cl_2 unless otherwise noted. Downfield from Me_4Si in ppm. [b] Figures in parentheses are $^2J_{P-C}$ in Hz. Multiplicity abbreviations are as follows: s, singlet; t, triplet. [c] C_p, para position of Ph; C_o, ortho position; C_m, meta position. [d] Figures in parentheses are $[^nJ_{P-C} + {}^{n+2}J_{P-C}]$ in Hz. [e] A $CDCl_3$ solution. [f] Peaks due to the isomer. [g] Corrected chemical shifts using the signal of CD_2Cl_2 (δ 53.87).

Table III. Crystal Data for $(PPh_3)ClPd[C(N_2)CO_2Et]$ (4a) and $(PBu_3)_2Pd[C(N_2)CO_2Et]_2$ (5d)

	4a	5d
formula	$C_{40}H_{35}O_2N_2ClP_2Pd$	$C_{32}H_{64}O_4N_4P_2Pd$
fw	779.5	737.2
$F(000)$	1592	784
cryst system	monoclinic	monoclinic
space group	$P2_1/c$	$P2_1/n$
a, Å	11.973 (2)	11.946 (3)
b, Å	29.719 (6)	12.071 (2)
c, Å	10.310 (2)	15.174 (3)
β, deg	94.71 (2)	107.54 (2)
U, Å^3	3656.3 (10)	2086.4 (6)
Z	4	2
D(calcd), g cm^{-3}	1.416	1.173
D(measd), g cm^{-3}		1.16[a]
μ(Mo Kα), cm^{-1}	6.98	5.50

[a] By flotation in potassium tartrate aqueous solution.

composition of diazo compounds,[18] the diazo complexes formed should be isolated carefully under argon. At the early stage of the reaction, a red intermediate which seems to be $RC(N_2)HgPd(PR^1_3)_2C(N_2)R$ was observed, although its attempted isolation failed.

The structure of $(PR_3)_2Pd[C(N_2)R]_2$ (**5**) was determined as follows. The elemental analyses gave satisfactory results. The methyl proton resonances of triethylphosphine in **5c**, **5e**, **5f**, **5g**, and **5h** appeared as a quintet, the characteristic splitting pattern of trans bis(triethylphosphine). The ^{13}C NMR spectra **5c**, **5e**, and **5g** (Table II) show the methylene and methyl carbon resonances as a triplet and a singlet, respectively. The C_1 and C_3 carbon resonances of tributylphosphine of **5d** appear as a triplet and those of the C_2 and C_4 carbons as a triplet and singlet, respectively. The ^{13}C absorptions of C_1, C_o, and C_m carbons of **5a** appear as a triplet and those of the C_2 and C_4 carbons as a triplet and singlet, respectively. These results also support the trans bis(phosphine) structure. The diazo carbon resonances [C(ipso)] appear as a triplet, indicating that the diazo carbons locate equally from the two phosphines and bond to palladium directly. The IR spectra of **5** showed the absorption bands of diazo groups at 1950–2025 cm^{-1}, which are shifted to a ca. 90 cm^{-1} longer wavelength in comparison with those of the parent diazo compounds. Treatment of complex **5a** with hydrogen chloride led to the formation of $(PPh_3)_2PdCl_2$ and $ClCH_2CO_2Et$.

B. Description of Structure. Crystal structures of diazo complexes **4** and **5d** are shown in Figure 1. No abnormally short intermolecular atomic contacts are observed in both crystals, the shortest interatomic distances between non-hydrogen atoms being 3.23 (2) Å [O(1) (x, y, z)···C(14) ($-x$, $-y$, $1-z$)] for **4a** and 3.454 (9) Å [O(1) (x, y, z)···C(21) ($^1/_2 - x$, $-{}^1/_2 + y$, $^1/_2 - z$)] for **5d**.

The molecular structures are represented in Figure 2. In each complex, the geometry around the Pd atom is square-planar. The α-diazomethyl group is approximately planar except for the C(4) atom in each complex. The equations of these least-squares planes are listed in Table IV (supplementary material). The planes of α-diazomethyl group are almost perpendicular to the coordination planes of the Pd, the dihedral angles between these two planes being 81.6° for **4a** and 84.2° for **5d**, respectively. Two trialkylphosphine groups take a staggered conformation for the P–Pd–P axis in both complexes. Among the three butyl groups of the PBu_3 ligand in **5d**, two of them take on a trans structure and the other a cis structure, which can be understood considering the packing diagram of molecules. As shown in Figure 1, two butyl groups lie on the plane approximately parallel to the ac plane, while the other is located up or down toward the b axis.

Selected bond lengths and bond angles are listed in Tables VI and VII, respectively. The distances between

(18) (a) Yoshimura, N.; Murahashi, S.-I.; Moritani, I. *J. Organomet. Chem.* **1973**, *52*, C58. (b) Anciaux, A. J.; Hubert, A. J.; Noels, A. F.; Petiniot, N.; Teyssie, P. *J. Org. Chem.* **1980**, *45*, 695. (c) Doyle, M. P.; Tamblyn, W. H.; Bagheri, V. *Ibid.* **1981**, *46*, 5094. (d) Taber, D. F.; Raman, K. *J. Am. Chem. Soc.* **1983**, *105*, 5935. (e) D'Errico, J. J.; Curtis, M. D. *Ibid.* **1983**, *105*, 4479.

Table IV. Final Atomic Parameters for Non-Hydrogen Atoms in $(PPh_3)_2ClPd[C(N_2)CO_2Et]$ (4a)[a]

atom	x	y	z	B_{eq}/Å^2
Pd	0.20066 (6)	0.12728 (3)	0.13229 (7)	3.3
Cl	0.1901 (3)	0.18388 (10)	−0.0268 (3)	4.6
P(1)	0.0067 (3)	0.12040 (10)	0.1126 (3)	3.6
P(2)	0.3941 (3)	0.13515 (9)	0.1490 (3)	3.2
O(1)	0.2454 (8)	0.0675 (4)	0.5049 (8)	7.1
O(2)	0.2254 (8)	0.1386 (3)	0.4320 (8)	6.1
N(1)	0.2110 (8)	0.0403 (4)	0.2593 (9)	4.7
N(2)	0.2096 (10)	0.0021 (4)	0.2357 (13)	7.6
C(1)	0.2138 (8)	0.0826 (4)	0.2798 (10)	3.5
C(2)	0.2288 (9)	0.0942 (5)	0.4158 (10)	4.6
C(3)	0.2398 (15)	0.1547 (7)	0.5673 (13)	9.6
C(4)	0.1631 (16)	0.1914 (6)	0.5797 (15)	9.2
C(11)	−0.0568 (8)	0.0688 (4)	0.1705 (11)	4.0
C(12)	−0.1122 (10)	0.0391 (4)	0.0855 (12)	5.2
C(13)	−0.1652 (11)	0.0020 (5)	0.1348 (14)	6.5
C(14)	−0.1605 (12)	−0.0058 (5)	0.2651 (16)	7.3
C(15)	−0.1062 (10)	0.0236 (5)	0.3507 (13)	6.1
C(16)	−0.0531 (10)	0.0609 (5)	0.3050 (12)	5.3
C(21)	−0.0585 (9)	0.1641 (4)	0.2033 (10)	3.8
C(22)	−0.1624 (9)	0.1591 (4)	0.2514 (13)	5.2
C(23)	−0.2057 (11)	0.1932 (5)	0.3228 (15)	7.1
C(24)	−0.1483 (12)	0.2305 (5)	0.3535 (18)	8.1
C(25)	−0.0450 (12)	0.2368 (5)	0.3067 (16)	7.8
C(26)	0.0020 (10)	0.2044 (5)	0.2300 (13)	5.3
C(31)	−0.0504 (9)	0.1249 (4)	−0.0556 (10)	4.1
C(32)	−0.1455 (10)	0.1490 (5)	−0.0958 (13)	5.9
C(33)	−0.1843 (12)	0.1501 (5)	−0.2284 (15)	7.5
C(34)	−0.1288 (13)	0.1269 (6)	−0.3148 (13)	7.5
C(35)	−0.0371 (13)	0.1027 (6)	−0.2769 (14)	7.4
C(36)	0.0038 (10)	0.1032 (5)	−0.1498 (12)	5.8
C(41)	0.4388 (8)	0.1933 (4)	0.1661 (9)	3.7
C(42)	0.3834 (9)	0.2206 (4)	0.2488 (11)	4.7
C(43)	0.4180 (10)	0.2647 (5)	0.2714 (12)	5.6
C(44)	0.5050 (11)	0.2816 (5)	0.2107 (14)	6.2
C(45)	0.5621 (11)	0.2562 (5)	0.1286 (13)	6.2
C(46)	0.5262 (10)	0.2115 (4)	0.1063 (11)	4.7
C(51)	0.4539 (8)	0.1116 (4)	0.0091 (10)	3.7
C(52)	0.5658 (9)	0.0990 (5)	0.0150 (11)	4.9
C(53)	0.6120 (10)	0.0781 (5)	−0.0883 (12)	5.9
C(54)	0.5437 (11)	0.0689 (5)	−0.1995 (11)	5.6
C(55)	0.4357 (10)	0.0820 (4)	−0.2084 (10)	4.7
C(56)	0.3909 (9)	0.1028 (4)	−0.1066 (10)	4.1
C(61)	0.4741 (8)	0.1064 (4)	0.2828 (9)	3.3
C(62)	0.5246 (9)	0.1303 (4)	0.3886 (10)	4.4
C(63)	0.5922 (10)	0.1073 (5)	0.4819 (11)	5.3
C(64)	0.6120 (10)	0.0626 (5)	0.4730 (11)	5.8
C(65)	0.5603 (11)	0.0386 (5)	0.3723 (13)	6.0
C(66)	0.4924 (9)	0.0604 (4)	0.2779 (11)	4.6

[a] In this table and those subsequent established deviation in the least significant figure are given in parentheses. The B_{eq} values for non-hydrogen atoms are equivalent isotropic temperature factors calculated from anisotropic factors (Hamilton, W. C. *Acta Crystallogr.* **1959**, *12*, 609).

the Pd and terminal Cl atoms hitherto have been reported in the range of 2.24–2.45 Å, which the Pd–Cl bond length of **4a** [2.345 (3) Å] falls in. The Pd–P bond lengths in both complexes also fall in the range between 2.31 and 2.35 Å, which corresponds to those observed in the Pd complexes containing two mutually trans phosphine ligands.[19] The Pd–C(1) bond length in **4a** [2.015 (10) Å] is shorter than that in **5d** [2.078 (6) Å], which may be due to the weaker trans influence of the Cl atom in comparison with the C atoms, although they are as expected for a Pd(II)–C(sp^2) bond.

The C(1)–N(1)–N(2) angles of the α-diazomethyl group are almost linear in both complexes [177.2 (12) and 176.3 (8)°]. The N(1)–N(2) bond lengths [1.160 (15) and 1.130 (10) Å] are slightly longer and the C(1)–N(1) bond lengths

(19) Miki, K.; Kai, Y.; Yasuoka, N.; Kasai, N. *J. Organomet. Chem.* **1979**, *165*, 79.

Table V. Final Atomic Parameters for Non-Hydrogen Atoms in $(PBu_3)_2Pd[C(N_2)CO_2Et]_2$ (5d)

atom	x	y	z	B_{eq}/Å^2
Pd	0	0	0	3.8
P(1)	0.09888 (13)	0.12753 (12)	0.11016 (10)	4.1
O(1)	0.2821 (6)	−0.2381 (6)	0.0867 (4)	9.2
O(2)	0.2378 (5)	−0.1081 (5)	−0.0234 (4)	7.2
N(1)	0.0964 (5)	−0.1752 (4)	0.1348 (4)	5.3
N(2)	0.0706 (7)	−0.2240 (6)	0.1893 (5)	7.9
C(1)	0.1186 (5)	−0.1195 (5)	0.0704 (4)	4.4
C(2)	0.2193 (6)	−0.1634 (6)	0.0495 (5)	5.8
C(3)	0.3383 (10)	−0.1511 (11)	−0.0526 (9)	12.1
C(4)	0.3386 (12)	−0.1097 (14)	−0.1343 (9)	13.3
C(11)	0.2440 (6)	0.1561 (7)	0.0964 (5)	6.0
C(12)	0.2282 (7)	0.1956 (8)	−0.0044 (6)	7.6
C(13)	0.3459 (9)	0.2073 (10)	−0.0215 (9)	10.5
C(14)	0.3314 (12)	0.2405 (12)	−0.1212 (9)	12.8
C(21)	0.1331 (6)	0.0796 (6)	0.2296 (4)	5.1
C(22)	0.0208 (7)	0.0500 (7)	0.2552 (5)	6.2
C(23)	0.0495 (13)	−0.059 (8)	0.3481 (8)	9.0
C(24)	−0.0620 (12)	−0.0487 (13)	0.3720 (10)	12.1
C(31)	0.0252 (6)	0.2631 (5)	0.1071 (5)	5.6
C(32)	0.0984 (8)	0.3475 (6)	0.1782 (6)	8.2
C(33)	0.0285 (12)	0.4585 (11)	0.1689 (12)	14.3
C(34)	−0.0691 (19)	0.4759 (15)	0.1475 (18)	18.7

Table VI. Selected Bond Lengths (Å) for Non-Hydrogen Atoms in Complexes 4a and 5d

	4a	5d
Pd–C(1)	2.015 (10)	2.078 (6)
Pd–Cl	2.345 (3)	
Pd–P(1)	2.324 (3)	2.317 (2)
Pd–P(2)	2.321 (3)	
C(1)–N(1)	1.275 (13)	1.279 (8)
N(1)–N(2)	1.160 (15)	1.130 (10)
C(1)–C(2)	1.442 (15)	1.434 (9)
C(2)–O(1)	1.219 (16)	1.200 (9)
C(2)–O(2)	1.329 (15)	1.366 (9)
O(2)–C(3)	1.47 (3)	1.493 (14)
C(3)–C(4)	1.44 (3)	1.34 (3)
P(1)–C(11)	1.833 (11)	1.841 (7)
P(1)–C(21)	1.814 (10)	1.828 (7)
P(1)–C(31)	1.816 (11)	1.852 (7)
P(2)–C(41)	1.812 (11)	
P(2)–C(51)	1.802 (11)	
P(2)–C(61)	1.825 (10)	

Table VII. Selected Bond Angles (deg) for Complexes 4a and 5d

	4a	5d
C(1)–Pd–P(1)	91.4 (3)	88.30 (16)
C(1)–Pd–P(2)	89.7 (3)	90.70 (16)
P(1)–Pd–Cl	90.34 (10)	
P(2)–Pd–Cl	88.62 (10)	
C(1)–Pd–Cl	175.3 (3)	
P(1)–Pd–P(2)	178.95 (10)	180.0
Pd–C(1)–N(1)	121.7 (8)	119.5 (5)
Pd–C(1)–C(2)	124.9 (8)	129.1 (5)
N(1)–C(1)–C(2)	113.4 (10)	110.8 (6)
C(1)–N(1)–N(2)	177.2 (12)	176.3 (8)
C(1)–C(2)–O(1)	125.2 (12)	128.4 (7)
C(1)–C(2)–O(2)	110.9 (10)	110.4 (6)
O(1)–C(2)–O(2)	123.9 (12)	121.1 (7)
C(2)–O(2)–C(3)	116.1 (11)	114.3 (7)
O(2)–C(3)–C(4)	107.8 (15)	111.9 (12)
Pd–P(1)–C(11)	118.9 (4)	109.6 (3)
Pd–P(1)–C(21)	111.2 (4)	114.7 (3)
Pd–P(1)–C(31)	111.8 (4)	115.7 (3)
C(11)–P(1)–C(21)	102.9 (5)	103.6 (4)
C(11)–P(1)–C(31)	103.9 (5)	106.8 (4)
C(21)–P(1)–C(31)	107.2 (5)	105.5 (4)
Pd–P(2)–C(41)	112.8 (4)	
Pd–P(2)–C(51)	111.1 (4)	
Pd–P(2)–C(61)	117.9 (4)	
C(41)–P(2)–C(51)	108.3 (5)	
C(41)–P(2)–C(61)	103.9 (5)	
C(51)–P(2)–C(61)	101.9 (5)	

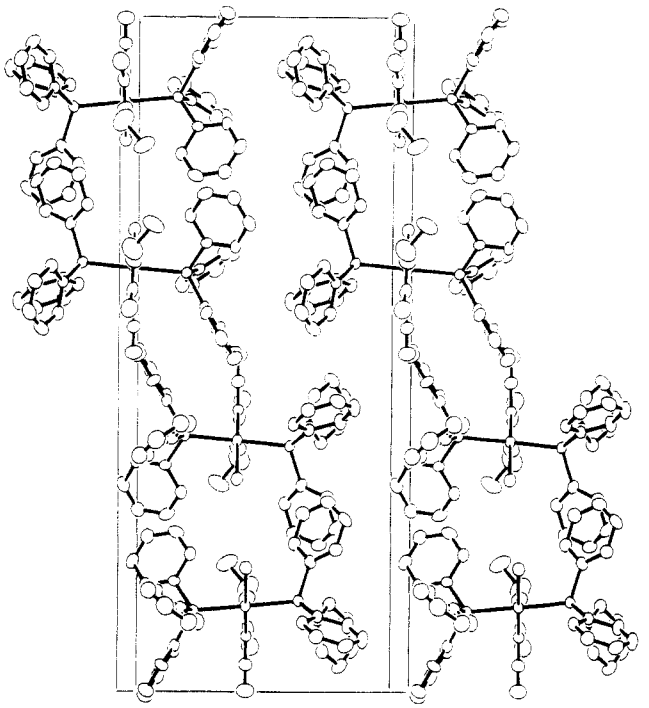

4a

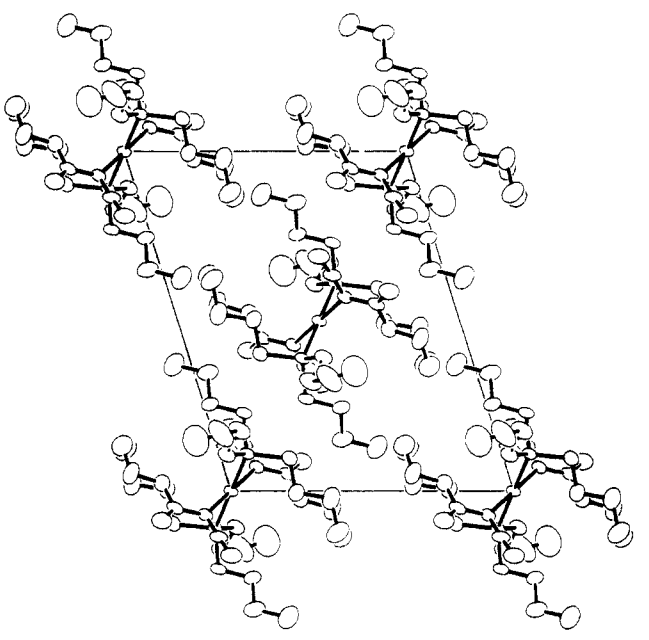

5d

Figure 1. Packing diagrams for **4a** and **5d** as viewed along with the c^* axis (for **4a**) and the b axis (for **5d**). Atoms are represented by thermal ellipsoids at 30% probability levels.

[1.275 (13) and 1.279 (8) Å] are shorter in both complexes, especially in **4a**, than the corresponding N–N and C–N bond lengths of the non-metalated diazomethane (N–N = 1.12 Å; C–N = 1.32 Å)[20] and related diazo compounds as shown (**6**–**8**).[21-23] These results, which are compatible

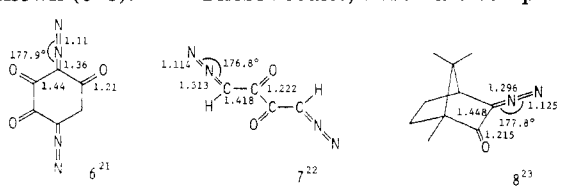

6[21] 7[22] 8[23]

(20) Cox, A. P.; Thomas, L. F.; Sheridan, J. *Nature (London)* **1958**, *181*, 1000.

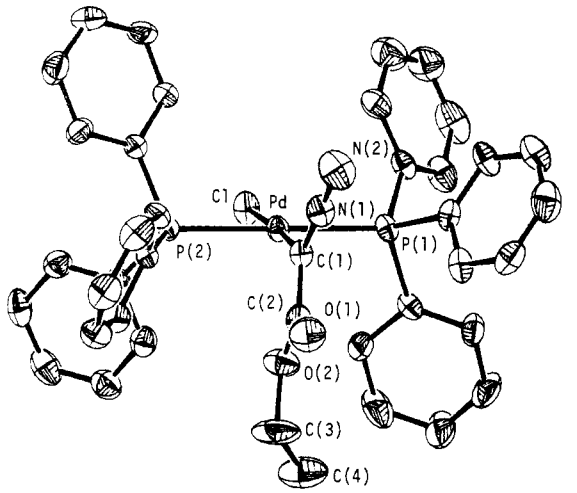

4a

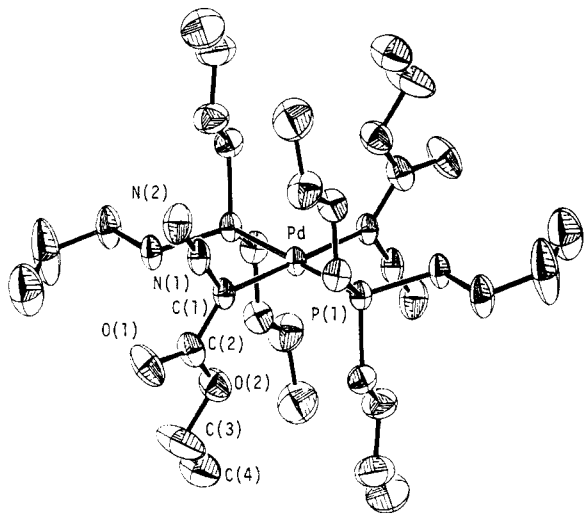

5d

Figure 2. Perspective views of the molecular structures of **4a** and **5d** along with the atomic numbering system. Atoms are represented by thermal ellipsoids at 30% probability levels. Hydrogen atoms and the numbering system for carbon atoms of the trialkylphosphine groups are omitted for clarity. The six carbon atoms of the phenyl group of PPh_3 in **4a** are numbered as C(n1)–C(n6) where n = 1–6, while the four C atoms of the butyl group in PBu_3 in **5d** as C(n1)–C(n4), where n = 1–3. The C(11), C(21), and C(31) atoms are attached to the P(1) atom, while C(41), C(51), and C(61) are attached to P(2).

with the results with IR spectral data as mentioned before, imply that the resonance structure **a** plays an important contribution in the present complexes.

(a) (b)

The ^{13}C NMR studies of diazo compounds have received much attention because of the peculiarly high-field resonances of diazomethyl carbon [C(ipso) carbon].[24] The chemical shift of this carbon in organometallic diazoalkanes of main-group elements tends to be further shifted to high

(21) Ansell, G. B. *J. Chem. Soc. B* **1969**, 729.
(22) Hope, H.; Black, K. T. *Acta Crystallogr., Sect. B: Struct. Crystallogr. Cryst. Chem.* **1972**, *28*, 3632.
(23) Cameron, A. F.; Hair, N. J.; Morris, D. G. *J. Chem. Soc., Perkin Trans. 2* **1972**, 1331.
(24) (a) Firl, J.; Runge, W.; Hartmann, W. *Angew. Chem., Int. Ed. Engl.* **1974**, *13*, 270. (b) Duthaler, R.; Forster, H. G.; Roberts, J. D. *J. Am. Chem. Soc.* **1978**, *100*, 4974.

field compared with the parent organic derivatives.[25] Such a tendency is also seen in the palladium complexes; the ^{13}C chemical shifts of the C(ipso) carbons of **5c** and **5e** appear at δ 32.8 and 37.0, which are at higher fields compared to δ 46.7 and 47.2 for $HC(N_2)COOEt$ and $HC(N_2)Ph$,[24] respectively, as shown in Table II. Regardless of the difference in substituents and ligands, no significant difference in the chemical shift of C(ipso) carbons is observed. In a series of bis(diazo) compounds bearing PEt_3 as a common ligand (**5c**, **5e**, **5g**, and **5h**) no meaningful shifts are observed.

Another interesting feature is the restricted rotation about the Pd–C bond of complex **5e**, which has been observed in the temperature-dependent ^{13}C NMR spectra (Table II). Restricted rotation about the bond axis between metal and organic ligands has not been well documented. Recently a high rotational barrier about the Pd–N bond has been reported in *trans*-$PdCl_2(R_1R_2C{=}NNR_3R_4)_2$ as the first example of isomerism in *trans*-$[MX_2L_2]$ complexes.[26] The unambiguous example of restricted rotation about the Pd–C bond in organopalladium σ-complexes was observed in $(PEt_3)_2Pd[C(N_2)Ph]_2$ (**5e**). The ^{13}C NMR spectrum of **5e** at 27 °C shows the diazo carbon resonance at δ 37.05 as a triplet ($^2J_{P-C}$ = 11.8 Hz) and the methylene and methyl carbon resonances of triethylphosphine at δ 15.62 (t, $^1J_{P-C} + {}^3J_{P-C}$ = 26.5 Hz) and 8.10 (s), respectively. At 0 °C, the triplet of the diazo carbon resonance and the singlet of the methyl carbon resonance split into two sets of signals [δ 37.05 (t, $^2J_{P-C}$ = 11.8 Hz) and 37.28 (t, $^2J_{P-C}$ = 11.8 Hz) and δ 8.08 (s) and 8.16 (s)], respectively, and the splitting occurs reversibly with temperature. In complex **5e**, there are two conformational isomers, i.e., syn and anti isomers with respect to the two diazo groups. The splitting pattern observed

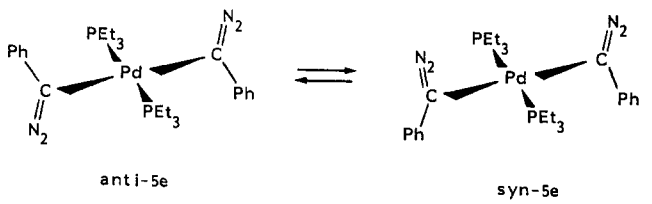

is in accord with the syn–anti isomerism arising from hindered rotation about the C–Pd bond. The trans–cis isomerism in the square-planar palladium complexes can be excluded because no spectral change was observed over the temperature range −30 to 50 °C in the triplet[27] of the methylene carbon of triethylphosphine. Further, the phenyl carbon resonances δ 142.96 (P–C), 128.58 (C_o or C_m), 124.11 (C_o or C_m), and 121.77 (C_p) also remained unchanged as sharp singlets. Over the temperature, slow decomposition of the diazo group took place. The free energy of the activation for the rotational barrier of the Pd–C bond in **5e** was calculated from the coalescence temperature (T_c = 13 °C) of the methyl carbon resonances of PEt_3 to be $\Delta G^{\ddagger}$ = 65 kJ/mol, which is similar to the values ($\Delta G^{\ddagger}$ = ~59 kJ/mol) for the Pd–N bond in *trans*-dichloro(dihydrazone)palladium complexes.[26] Complexes **5g** and **5h** bearing more bulky *i*-Pr and *t*-Bu groups show no splitting in their carbon resonances over the temp. range −30 to 27 °C. The high rotational barrier seems to give a single conformational isomer in solution.

C. Reactions. The mass spectra of $(PEt_3)_2Pd[C(N_2)CO_2Et]_2$ (**5c**) and $(PEt_3)_2Pd[C(N_2)Ph]_2$ (**5e**) were measured on an "in-beam" electron-impact (EI) mass spectrometry. There have been reported a few mass spectra of palladium complexes which exhibit palladium-containing fragments.[28] No metal-containing peak was observed in palladium complexes bearing phosphine ligands such as $Pd(PPh_3)_4$ by the conventional EI technique.[29] The "in-beam" technique, which has been successfully applied to obtain several mass spectra of thermally unstable compounds,[30] was thus adopted for the measurment of **5c** and **5e**.

The spectrum of **5c** gave no molecular ion peak [M or (M + 1)], but the fragment peaks due to $[(PEt_3)_2Pd(CCOOEt)_2]^{+\cdot}$ (*m/e* 512), which is formed by loss of $2N_2$ group, was detected with the intensity of 19% of the base peak (*m/e* 314) (see Experimental Section). This peak seems to correspond to α-palladiocarbene or -carbyne of a hitherto unknown species. By contrast, no palladium-containing fragment was observed in the mass spectrum of **5e**, where fragments corresponding to diphenylacetylene (*m/e* 178) were detected as the base peak. This observation seems to be compatible with the result of the thermal decomposition of **5e**.

Pyrolysis and photolysis of bis(α-diazomethyl) palladium complexes are of particular interest in view of the formation of carbenes from diazo compounds.[31] Recently, the coupling of two methylenes on a single metal center to ethylene and that of two carbynes to acetylene have been postulated by using Walsh correlation diagram.[32] There are a few reports of the carbene–carbene couplings on bis(carbene) complexes.[6b,33] Schrock reported that $W(CCMe_3)(CCMe_3)(CH_2CMe_3)$(dmpe) (dmpe = $Me_2PCH_2CH_2PMe_2$) reacts with dmpe to give 2,2,5,5-tetramethyl-*trans*-3-hexene and $W(CCMe_3)(dmpe)_2(H)$.[33] There is no report on the carbyne–carbyne coupling on bis(carbyne) complexes,[32b,34] and related work is the unique coupling of two $(CO)_4W{\equiv}CCH_3$ fragments to binuclear acetylene complexes.[35]

The thermolysis of a violet solution of $(PEt_3)_2Pd[C(N_2)Ph_2]_2$ (**5e**) in toluene at 120 °C gave diphenylacetylene in 67% yield in addition to stilbenes (cis/trans = 77/23;

(25) (a) Krommes, P.; Lorberth, J. *J. Organomet. Chem.* **1975**, *93*, 339. (b) Gruning, R.; Krommes, P.; Loberth, J. *J. Organomet. Chem.* **1977**, *128*, 167.

(26) (a) Natile, G.; Cattalini, L.; Gasparrini, F.; Caglioti, L. *J. Am. Chem. Soc.* **1979**, *101*, 498. (b) Natile, G.; Cattalini, L.; Gasparrini, F.; Caglioti, L.; Galli, B.; Misiti, D. *J. Chem. Soc., Dalton Trans.* **1979**, 1262.

(27) No splitting was observed in the triplet methylene carbon of PEt_3, probably because the resonances of two isomers were incidentically in the same chemical shift.

(28) (a) Cais, M.; Lupin, M. S. *Adv. Organomet. Chem.* **1970**, *8*, 211. (b) Grotyahn, L.; Kruger, P. *Org. Mass Spectrom.* **1977**, *20*, 27.

(29) Becconsall, L. K.; Job, B. E; O'Brien, S. *J. Chem. Soc. A* **1967**, 423.

(30) (a) Ohashi, M.; Tsujimoto, K.; Yasuda, A. *Chem. Lett.* **1976**, 439. (b) Ohashi, M. Nakayama, N.; Kudo, H.; Yamada, S. *Shitsuryo Bunseki* **1976**, *24*, 265.

(31) (a) Moss, R. A.; Jones, M., Jr. "Carbenes"; Wiley: New York, 1975; Vol. 1, 2. (b) Kirmse, W. "Carbene Chemistry", 2nd ed.; Academic Press: New York, 1971. (c) Murahashi, S.-I.; Okumura, K.; Naota, T.; Nagase, S. *J. Am. Chem. Soc.* **1982**, *104*, 2466 and references cited therein.

(32) (a) Hoffmann, R.; Wilker, C. N.; Eisenstein, O. *J. Am. Chem. Soc.* **1982**, *104*, 632. (b) Hoffmann, R.; Wilker, C. N.; Lippard, S. J.; Templeton, J. L.; Brower, D. C. *Ibid.* **1983**, *105*, 146.

(33) (a) Fischer-type bis(carbene) Cr, Mo, and W complexes. Lappert, M. F.: Pye, P. L.; McLaughlin, G. M.; *J. Chem. Soc., Dalton Trans.* **1977**, 1272. Lappert, M. F.; Pye, P. L.; Rogers, A. J. McLaughlin, G. M. *Ibid.* **1981**, 701. Hitchcock, P. B.; Lappert, M. F.; Terreros, P.; Winwright, K. P. *J. Chem. Soc., Chem. Commun.* **1980**, 1180. Rieke, R. D.; Kojima, H.; Öfele, K. *Angew. Chem., Int. Ed. Engl.* **1980**, *19*, 538. (b) Schrock-type bis(carbene) complexes Ta and Nb complexes, ref 6e, and W complexes, ref. 6b.

(34) The coupling of two isocyanides to a diaminoacetylene on a seven-coordinate Mo(II) complex has been reported. Lam, C. T.; Corfield, P. W. R.; Lippard, S. J. *J. Am. Chem. Soc.* **1977**, *99*, 617 and ref 32b.

(35) Fisher, E. O.; Ruhs, A.; Friedrich, P.; Huttner, G. *Angew. Chem., Int. Ed. Engl.* **1977**, *16*, 465.

(36) Beevor, R. G.; Freeman, M.; Green, M.; Morton, C. E.; Orpen, A. G. *J. Chem. Soc., Chem. Commun.* **1985**, 68.

(37) (a) Murahashi, S.-I.; Yoshimura, N.; Yamamoto, Y.; Moritani, I. *Tetrahedron* **1972**, *28*, 1485. (b) Teki, Y.; Takui, T.; Itoh, K.; Iwamura, H.; Kobayashi, K. *J. Am. Chem. Soc.* **1983**, *105*, 3722.

17%) (eq 1). Similar pyrolysis of $(PEt_3)_2Pd[C(N_2)C_6H_5$-p-$CH_3]_2$ (**5f**) gave bis(4-methylphenyl)acetylene and 1,2-bis(p-methylphenyl)ethylene in 65% and 13% yields, respectively. The following crossover reaction clearly shows that the acetylenes are not formed intermoleculary but intramolecularly. The pyrolysis of a 1:1 mixture of complex **5e** and complex **5f** gave diphenylacetylene and bis(4-methylphenyl)acetylene in 60% and 60% yields, respectively, in addition to stilbenes, and (4-methylphenyl)phenylacetylene could not be detected among the products. The acetylene formation can be rationalized by assuming initial extrusion of nitrogen to give carbene complex **9a**, which undergoes subsequent linking

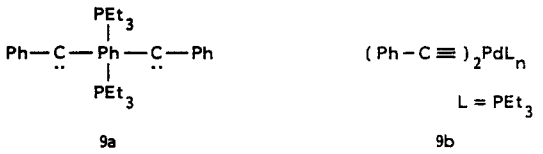

9a **9b**

to give diphenylacetylene. An alternative mechanism which involves the coupling of two carbyne ligands on palladium (**9b**) to an acetylene will not be excluded. The intermediacy of a metal–carbyne complex in the decomposition of α-diazoalkyl complexes has been suggested for the formation of the metal-bridging carbyne complexes via $(CO)_4Mn{\equiv}CCO_2R$[11b] and the intramolecular insertion reaction of $[OsCl(NO)(\equiv CCO_2R)(PPh_3)_2]I$.[14] The 1,1-reductive elimination of **5e** to give 1,2-bis(diazo)-1,2-diphenylethane, a precursor of diphenylacetylene, seems unlikely because the 1,1-reductive elimination of bis(phosphine)dialkylpalladium complexes proceeds only from the cis isomer.[38] The NMR spectral analysis shows that *trans*-**5e** does not undergo isomerization to the cis isomer under the reaction conditions. It is noteworthy that ketazines, which are generally formed by nucleophilic attack of diazo groups on divalent carbons, could not be detected. The formation of stilbene may be rationalized by assuming that the carbene complex **9** undergoes hydrogen abstraction from the PEt_3 ligand rather than the solvent. The deuterium incorporation into stilbene was not observed upon the thermolysis of **5e** in toluene-d_8. The present result seems to be closely related to the intramolecular photochemical hydrogen abstraction of $CpMo(PR_3)_2{\equiv}CCH$-t-Bu_2.[36]

Irradiation of $(PEt_3)_2Pd[C(N_2)Ph]_2$ (**5e**) in toluene using a high-pressure mercury lamp with a filter (>520 nm) at room temperature under argon produced diphenylacetylene in 61% yield. Apparently, the initial step is the extrusion of nitrogen to give a carbene complex. Although sequential extrusion of nitrogen cannot be excluded completely,[36] the one-photon photolysis of bis(diazo) compounds occurs readily.[37]

Equation 1 also indicates the generation of zerovalent bis(triethylphosphine)palladium, which is a typical palladium(0) catalyst.[39] Indeed, the catalytic alkylation of allyl acetate proceeds efficiently. Thus, the treatment of allyl acetate with sodium malonate in toluene in the presence of the palladium catalyst, which was derived from the pyrolysis of 3 mol % of complex **5e** in toluene at 120 °C, gave allylmalonate in 83% yield. Similar alkylations of allyl acetate with palladium catalysts, which are derived from diazo complexes **5a** and **5c**, proceed to give diethyl allylmalonate in 77% and 83% yields, respectively.

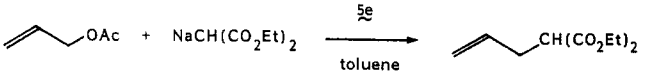

Experimental Section

^1H and ^{13}C NMR spectra were obtained by using JNM-MH 60 JNM-4H-100 JNM-4-100 (^1H), and JNM FX-100(^{13}C, ^1H) spectrometers. Infrared spectra were obtained by using 215 Hitachi Grating or Hitachi Perkin-Elmer 225 grating infrared spectrometers. UV spectra were obtained in $CHCl_3$ by using a Shimazu double-beam UV 200 spectrometer. Abbreviations: d = doublet, t = triplet, q = quartet, m = multiplet, s = strong. Melting points were measured in a tube which was sealed at 5 mmHg. All reactions were carried out in an argon atmosphere and in the dark covered with aluminum foil. All the solvents were dried and distilled under argon atmosphere. The following reagents were prepared according to the known methods: $(PR_3)_2PdX_2$,[40] $(PPh_3)_4Pd$,[41] $(PEt_3)_4Pd$,[42] $HC(N_2)CO_2Et$,[43] $HC(N_2)COMe$,[44] $HC(N_2)Ph$,[45] $HC(N_2)$-i-Pr,[46] $HC(N_2)$-t-Bu,[46] $Hg[C(N_2)CO_2Et]_2$,[47] $Hg[C(N_2)COMe]_2$,[47] $LiC(N_2)CO_2Et$.[17,48]

$(PPh_3)_2ClPdC(N_2)CO_2Et$ (4a). A suspension of $(PPh_3)_2PdCl_2$ (1.40 g, 2.00 mmol) and $Hg[C(N_2)CO_2Et]_2$ (1.28 g, 3.00 mmol) in dry benzene was stirred under argon at 20 °C for 48 h. The reaction was monitored by the IR absorption of $Hg[C(N_2)CO_2Et]_2$ at 2080 cm^{-1}. Addition of hexane (20 mL) followed by filtration of the yellow-brown precipitate gave a red solution. After concentration in vacuo, the residual red oil was dissolved in CH_2Cl_2 and subjected to Florisil column chromatography. Elution with CH_2Cl_2 under argon pressure, evaporation, trituration with ether, filtration, and washing with ether gave **4a** (1.02 g, 65%). Recrystallization from CH_2Cl_2–ether gave analytically pure red crystalline complex (0.61 g, 39%): mp 146–148 °C dec; ^1H NMR (δ, $CDCl_3$) 6.9–7.9 (br, 30 H, Ph), 3.38 (q, 2 H, J = 6.9 Hz, CH_2), 0.83 (t, 3 H, CH_3); IR (Nujol) 2035 (vs), 1645 (s), 1432 (s), 1275 (s), 1177 (s), 1090 (s), 700 (s), 687 (s), 515 (s), 508 (s), 488 cm^{-1} (s); UV ($CHCl_3$) 532 nm (ϵ 460), 324 (18 000), 290 (sh), 273 (sh), 245 (25 400). Anal. Calcd for $C_{40}H_{35}O_2N_2ClP_2Pd$: C, 61.63; H, 4.53; N, 3.59; Cl, 4.55. Found: C, 61.41; H, 4.51; N, 3.71; Cl; 4.50.

$(PPh_3)ClPdC(N_2)COMe$ (4b). A suspension of $(PH_3)_2PdCl_2$ (0.696 g, 0.99 mmol) and $Hg[C(N_2)COMe]_2$ (0.357 g, 0.97 mmol) was reacted at 20 °C for 20 h. Similar treatment gave pure red crystalline **4b** (0.158 g, 22%): mp 142 °C dec; ^1H NMR (δ, $CDCl_3$) 7.1–8.1 (br, 30 H, Ph), 0.95 (s, 3 H, Me); IR (Nujol) 2010, 1584, 1432, 1302, 1093, 745, 704, 688, 516 cm^{-1}; UV ($CHCl_3$) 528 nm (ϵ 370), 323 (19 000), 285 (sh), 278 (sh), 248 (25 700). Anal. Calcd for $C_{39}H_{33}ON_2ClP_2Pd$: C, 62.49; H, 4.44; N, 3.74; Cl, 4.73. Found: C, 62.67; H, 4.42; N, 3.74; Cl, 4.62.

$(PEt_3)_2ClPdC(N_2)CO_2Et$ (4c). A suspension of $(PEt_3)_2PdCl_2$ (0.414 g, 1.00 mmol) and $Hg[C(N_2)CO_2Et]_2$ (0.230 g, 0.54 mmol) in benzene (20 mL) was stirred at 20 °C for 2 days under argon. The solvent was removed in vacuo. The residue was washed with petroleum ether (bp 55 °C) (10 mL) three times. The petroleum ether solution was concentrated and subjected to silica gel chromatography. Elution with benzene gave $(PEt_3)_2PdCl_2$ (0.174 mg), and further elution with ether gave an unstable red-yellow

(38) (a) Loar, M. K.; Stille, J. K. *J. Am. Chem. Soc.* **1981**, *103*, 4174. (b) Moravskiy, A.; Stille, J. K. *Ibid.* **1981**, *103*, 4182. (c) Ozawa, F.; Ito, T.; Nakamura, Y.; Yamamoto, A. *Bull. Chem. Soc. Jpn.* **1981**, *54*, 1868.

(39) (a) Trost, B. M. *Tetrahedron* **1977**, *33*, 2615; *Acc. Chem. Res.* **1980**, *13*, 385. (b) Tsuji, J. "Organic Synthesis with Palladium Compounds"; Springer Verlag: Heidelberg, 1981.

(40) Jenkins, J. M.; Shaw, B. L. *J. Chem. Soc. A* **1966**, 770.

(41) Malatesta, L.; Angoletta, M. *J. Chem. Soc.* **1957**, 1186.

(42) Kuran, W.; Musco, A. *Inorg. Chim. Acta* **1975**, *12*, 187.

(43) Womack, E. B.; Nelson, A. B. *Org. Synth.* **1955**, *III*, 392.

(44) Arndt, F.; Amende, J. *Chem. Ber.* **1928**, *61*, 1124.

(45) Closs, G. L.; Moss, R. A. *J. Am. Chem. Soc.* **1964**, *86*, 4042.

(46) Kaufman, G. M.; Smith, J. A.; Stouw, G. G. V.; Shechter, H. *J. Am. Chem. Soc.* **1965**, *87*, 935.

(47) DoMinh, T.; Strausz, O. P.; Gunning, H. E. *Tetrahedron Lett.* **1968**, 5237.

(48) Pellicciare, R.; Frinquelli, R.; Ceccherelli, P.; Sisani, E. *J. Chem. Soc., Chem. Commun.* **1979**, 959.

oil (41 mg, 8%); ^{1}H NMR (δ, $CDCl_3$) 1.12 (q, $PCCH_3$), 1.20 (t, J = 7.2 Hz, $OCCH_3$), 1.78 (m PCH_2), 4.10 (q, OCH_2); IR (Nujol) 2030, 1645, 1270, 1180, 1040, 765, 725 cm^{-1}.

$(PBu_3)_2ClPdC(N_2)CO_2Et$ (4d). A solution of $(PBu_3)_2PdCl_2$ (1.164 g, 2.00 mmol) and $Hg[C(N_2)CO_2Et]_2$ (0.887 g, 208 mmol) in ether (100 mL) was allowed to react at room temperature for 100 h. Ether was removed in vacuo, and the residue was washed with petroleum ether (3 × 20 mL). The petroleum ether solution was concentrated and subjected to chromatography (Florisil). Elution with petroleum ether gave yellow $(PBu_3)_2PdCl_2$ (0.657 g, 1.13 mmol), and then elution with petroleum ether–ether (30:1) gave a red-orange complex. Further purification of the complex by similar chromatography gave pure **4d** (0.218 g, 17%): ^{1}H NMR (δ, $CDCl_3$) 0.98 (m, 18 H, $PCCH_3$), 1.28 (t, 3 H, J = 7.5 Hz, $OCCH_3$), 1.62 (m, 36 H, $P(CH_2)_3$), 4.21 (q, 2 H, J = 7.5 Hz, OCH_2); IR (Nujol) 2030, 1655, 1260, 1165, 1045 cm^{-1}; UV ($CHCl_3$) 500 nm (ϵ 460), 320 (sh), 290 (18 700), 247 (10 000). Anal. Calcd for $C_{28}H_{59}O_2N_2ClP_2Pd$: C, 50.98; H, 9.02; N, 4.23; Cl, 5.37. Found: C, 50.94; H, 9.02; N, 4.23; Cl, 5.33.

$(PPh_3)_2BrPdC(N_2)CO_2Et$ (4e). A suspension of $(PPh_3)_2PdBr_2$ (0.760 g, 0.96 mmol) and $Hg[C(N_2)CO_2Et]_2$ (0.464 g, 1.09 mmol) in benzene (15 mL) was stirred under argon for 15 h. The benzene solution was concentrated in vacuo and subjected to chromatography (Florisil). Elution with petroleum ether–ether (10:1) gave a red complex. Recrstallization from CH_2Cl_2–petroleum ether gave red, crystalline **4e** (70 mg, 9%): mp 148–149 °C dec; ^{1}H NMR (δ, $CDCl_3$) 0.86 (t, 3 H, J = 6.8 Hz, $OCCH_3$), 3.42 (q, 2 H, J = 6.8 Hz, OCH_2), 6.9–8.1 (m, 30 H, Ph); IR (Nujol) 2035, 1650, 1490, 1440, 1280, 1180, 1100, 740, 705, 695 cm^{-1}. Anal. Calcd for $C_{40}H_{35}O_2N_2BrP_2Pd$: C, 58.40; H, 4.28, N, 3.39; Br, 9.70. Found: C, 57.23; H, 4.22; N, 2.89; Br, 9.00.

$(PPh_3)_2IPdC(N_2)CO_2Et]_2$ (4f). A suspension of $(PPh_3)_2PdI_2$ (0.750 g, 0.85 mmol) and $Hg[C(N_2)CO_2Et]_2$ (0.560 g, 1.31 mmol) in benzene (15 mL) was stirred for 4 h. Filtration, concentration, and chromatographic separation (Florisil benzene–ether (10:1)) gave a brown complex, which was washed with ether–hexane (1:1). Concentration of the filtrate gave red-brown crystalline **4f** (50 mg, 7%): mp 137–138 °C dec; ^{1}H NMR (δ, $CDCl_3$) 0.87 (t, 3 H, J = 7.2 Hz, CH_3), 3.45 (q, 2 H, CH_2), 7.0–7.9 (m, 30 H, Ph); IR (Nujol) 2030, 1640, 1432, 1280, 1187, 1090, 700, 690 cm^{-1}. Anal. Calcd $C_{40}H_{35}O_2N_2IP_2Pd$: C, 55.16; H, 4.05; I, 14.51. Found: C, 54.09; H, 3.98; I, 14.57.

$(PPh_3)_2Pd[C(N_2)CO_2Et]_2$ (5a). To a suspension of $(PPh_3)_4Pd$ (1.76 g, 1.52 mmol) in dry benzene (30 mL) was added a solution of $Hg[C(N_2)CO_2Et]_2$ (0.640 g, 1.50 mmol) in dry benzene (40 mL) under argon. The mixture was stirred at 20 °C for 48 h. The pale yellow-green color of the solution changed to red and then brown. After filtration of mercury under argon, the filtrate was concentrated and subjected to chromatography (silica gel) under argon pressure. Elution with benzene gave triphenylphosphine; further elution with benzene–ether (10:1) gave a red oil. The oil was washed with ether to remove a red compound. Recrystallization of the orange residue from benzene–petroleum ether gave **5a** (182 mg, 21%): mp 138–139 °C dec; ^{1}H NMR (δ, $CDCl_3$) 0.87 (t, 6 H, J = 6.9 Hz, CH_3), 3.38 (q, 4 H, CH_2), 6.9–7.9 (m, 30 H, Ph); IR (Nujol) 2025, 1640, 1432, 1273, 1172, 1091, 1051, 741, 703, 691, 515, 504, 496 cm^{-1}; UV ($CHCl_3$) 490 nm (sh), 448 (ϵ 1290), 420 (sh), 330 (sh), 289 (28 000), 248 (31 700). Anal. Calcd for $C_{44}H_{40}O_4N_4P_2Pd$: C, 61.65; H, 4.70; N, 6.54. Found: C, 61.12; H, 4.58; N, 6.34.

$(PPh_3)_2Pd[(N_2)COMe]_2$ (5b). A mixture of $(PPh_3)_4Pd$ (1.164 g, 1.01 mmol) and $Hg[C(N_2)COMe]_2$ (0.384 g, 1.05 mmol) in dry benzene (30 mL) was stirred at 20 °C for 24 h under argon. An orange complex and mercury was precipitated. The upper red solution was removed under argon, and benzene (70 mL) was added. The mixture was heated at 50 °C and filtered by using a transfer tube packed with asbestos under argon. Evaporation of the solvent under reduced pressure gave orange **5b**, which was then washed with petroleum ether and ether (215 mg, 27%): mp 137–138 °C dec; ^{1}H NMR (δ, $CDCl_3$) 2.15 (s, 6 H, CH_3), 6.60–8.06 (m, 30 H, Ph); IR (Nujol) 2005, 1587, 1577, 1566, 1432, 1290, 750, 700, 690, 512 cm^{-1}; UV ($CHCl_3$) 490 nm (sh), 444 (ϵ 1130), 326 (sh), 288 (23 100), 249 (27 800). Anal. Calcd for $C_{42}H_{36}O_2N_4P_2Pd$: C, 63.29; H, 4.55; N, 7.03. Found: C, 63.34; H, 4.40; N, 6.94.

$(PEt_3)_2Pd[C(N_2)CO_2Et]_2$ (5c). To a solution of $HC(N_2)CO_2Et$ (0.406 g, 3.72 mmol) in ether (10 mL) was added slowly a solution of BuLi (3.69 mmol) in hexane with stirring at −100 °C. The orange solution obtained was then added to the solution of $(PEt_3)_2PdCl_2$ (0.310 g, 0.75 mmol) in ether (10 mL) at −100 °C. After the mixture was stirred at −100 °C for 30 min, the mixture was raised to 0 °C. After the addition of cold water (10 mL), the organic layer was separated, washed with water (3 × 10 mL) and saturated NaCl solution (2 × 10 mL), and dried. Removal of the solvent gave a brown residue, which was subjected to chromatography (Florisil). Elution with hexane–ether (10:1) gave an orange compound. Recrystallization from CH_2Cl_2–hexane gave pure **5c** (0.313 g, 73%). This compound was also prepared by a method similar to that described for the preparation of **5d**: mp 126–127 °C dec; ^{1}H NMR (δ, $CDCl_3$), 1.09 (q, 18 H, CH_3), 1.79 (m, 12 H, CH_2), 1.19 (t, 6 H, J = 7.3 Hz, CH_3), 4.06 (q, 4 H, J = 7.3 Hz, CH_2); IR (Nujol) 2025, 1630, 1270, 1155, 1033, 762, 722 cm^{-1}; UV ($CHCl_3$) 470 nm (sh), 437 (ϵ 810), 294 (18 800), 250 (22 300). Anal. Calcd for $C_{20}H_{40}O_4N_4P_2Pd$: C, 42.22, H, 7.08; N, 9.89. Found: C, 42.16; H, 7.05; N, 9.88.

$(PBu_3)_2Pd[C(N_2)CO_2Et]_2$ (5d). To a solution of $(i\text{-}Pr)_2NH$ (1.56 g, 15.4 mmol) in THF (23 mL) was added a solution of BuLi in hexane (13.6 mmol) at −78 °C. To the solution of $(i\text{-}Pr)_2NLi$ was added a solution of $(PBu_3)_2PdCl_2$ (3.16 g, 5.44 mmol) in THF (15 mL) at −78 °C, and immediately $HC(N_2)CO_2Et$ was added (1.54 g, 13.5 mmol) slowly. (The inverse addition of $(i\text{-}Pr)_2NLi$ to a mixture of $(PBu_3)_2PdCl_2$ and $HC(N_2)CO_2Et$ at −78 °C gave a similar result.) The mixture was stirred at −78 °C for 30 min and at 0 °C for 30 min. Water (30 mL) precooled to 0 °C was added. The organic layer was separated, washed with water and saturated NaCl solution, and dried over Na_2SO_4. Removal of the solvent gave a red-brown solid, which was then dissolved in small amount of ether and subjected to chromatography (Florisil). Elution with hexane–ether (10:1) gave orange complex. Further chromatography gave pure **5d** (2.41 g, 60%): mp 92–94 °C; ^{1}H NMR (δ, $CDCl_3$) 0.93 (m, 18 H, CH_3), 1.24 (t, 6 H, J = 7.1 Hz, CH_3), 1.52 (m, 36 H, CH_2), 4.10 (q, 4 H, CH_2); IR (Nujol) 2020, 1640, 1270, 1160, 1040, 900, 800, 775, 735, 720 cm^{-1}; UV ($CHCl_3$) 480 nm (sh), 438 (ϵ 890), 290 (20 400), 248 (25 400). Anal. Calcd for $C_{32}H_{64}N_4O_4P_2Pd$: C, 52.14; H, 8.75; N, 7.60. Found: C, 52.19; H, 8.73; N, 7.50.

$(PEt_3)_2Pd[C(N_2)Ph]_2$ (5e). Phenyldiazomethane was prepared upon treatment of benzaldehyde hydrazone (3.70 g, 32 mmol) with Ag_2O (7.3 g, 32 mmol) in the presence of anhydrous $MgSO_4$ (6.0 g) in dry ether (120 mL) according to the literature procedure.[49] The ether solution was separated and concentrated to half volume and cooled to −78 °C. A solution of $(PEt_3)_2PdCl_2$ (1.27 g, 3.08 mmol) in THF (20 mL) was added dropwise with stirring. Then, a solution of $(i\text{-}Pr)_2NLi$ (33 mmol) was added slowly at −78 °C. After the addition was completed, the dark violet solution was stirred at −78 °C for 10 min and then at 0 °C for 30 min. Addition of water (100 mL), which was deoxygenated by bubbling argon, was added. The organic layer was separated, washed with water (8 × 50 mL) and saturated NH_4Cl solution (2 × 50 mL), and dried over Na_2SO_4. Removal of the solvent in vacuo gave violet residue, which was washed with ether (5 × 20 mL). Recrystallization from THF–petroleum ether gave violet **5e** (1.02 g, 58%): mp 110–111 °C dec; ^{1}H NMR δ 1.00 (q, 18 H, CH_3), 1.62 (m, 12 H, CH_2), 6.72–7.71 (m, 10 H, Ph); IR (Nujol) 1975, 1966, 1590, 1484, 1308, 1300, 766, 750, 745, 725 cm^{-1}; UV ($CHCl_3$) 590 nm (sh), 522 (ϵ 490), 336 (26 000), 244 (249 000). Anal. Calcd for $C_{26}H_{40}N_4P_2Pd$: C, 54.12 H, 6.99; N, 9.71. Found: C, 54.03; H, 7.06; N, 9.62.

$(PEt_3)_2Pd[C(N_2)C_6H_5\text{-}p\text{-}CH_3]_2$ (5f). To a solution of *p*-tolualdehyde tosylhydrazone (2.1 g, 7.3 mmol) in dry triethylene glycol (12 mL) was added sodium methoxide (0.70 g, 13 mmol) under nitrogen, and the mixture was stirred for a few minutes. After removal of the methanol which had been generated under vacuum at 0 °C, the mixture was stirred at 62 °C for 45 min and poured into cold water. Extraction with pentane (10 mL × 5) and removal of the solvent at 0 °C gave (4-methylphenyl)diazomethane. To a mixture of the diazo compound obtained above in THF (1 mL) and $(PEt_3)_2PdCl_2$ (0.33 g, 0.80 mmol) in dry THF (2 mL) was added a solution of $LiN(i\text{-}Pr)_2$ (2.5 mmol) at −78 °C under argon. The mixture was stirred at −78 °C for 30 min and then at room temperature for 1 h. The mixture was poured into

(49) Mohrbacher, R. J.; Cromwell, N. H. *J. Am. Chem. Soc.* **1957**, *79*, 401.

ice–water. The ether extracts were washed with water (0 °C) and saturated NaCl solution. Removal of the solvent gave a residue, which was washed with ether and recrystallized from THF–hexane. Violet crystalline **5f** was obtained in 53% yield: mp 91–92 °C dec; ^{1}H NMR (δ, $CDCl_3$), 0.70–2.10 (m, 30 H), 2.28 (s, 6 H, Me), 6.8–7.5 (m, 8 H); IR (KBr) 2930, 2870, 1970, 1510, 1300, 1135, 810, 765, 725 cm^{-1}. Anal. Calcd for $C_{28}H_{44}N_4P_2Pd$: C, 55.58; H, 7.33; N, 9.26. Found: C, 55.30; H, 7.44; N, 9.05.

$(PPh_3)_2Pd[C(N_2)$-*i*-Pr$]_2$ (5g). The lithium salt, which was prepared from acetone tosylhydrazone (6.0 g, 25 mmol) and BuLi (25 mmol), was pyrolyzed at 80–130 °C under reduced pressure (0.3–0.1 mmHg). Isopropyldiazomethane was trapped in a 100-mL three-necked flask at −100 °C. THF (20 mL) was added at −78 °C, and a solution of BuLi (12 mmol) was added with stirring at −100 to −80 °C for 30 min, and then a solution of $(PEt_3)_2PdCl_2$ (1.23 g, 2.98 mmol) in THF (15 mL) was added dropwise at −100 °C. After further stirring at −100 to −80 °C for 30 min, methanol (5 mL) was added. The solvent was removed under reduced pressure (0.2 mmHg). After addition of ether (50 mL) at 0 °C and water (10 mL), the organic layer was separated by the syringe technique. The aqueous layer was extracted with ether (2 × 30 mL). The combined ether extracts were dried over Na_2SO_4. Evaporation of the solvent in vacuo (0.2 mmHg) at 0 °C followed. The violet residue was washed with pentane at 0 °C and dissolved in ether (40 mL). The ether was concentrated to about 10 mL and cooled to −100 °C, giving a precipitate. Recrystallization from ether–pentane gave **5f** (0.57 g, 38%): mp 81–83 °C dec; ^{1}H NMR (δ, $CDCl_3$) 1.03 (q, 18 H, CH_3), 1.03 (d, J = 6.7 Hz, CH_3), 1.80 (m, 12 H, CH_2), 2.36 (h, J = 6.7 Hz, CH); IR (Nujol) 1965, 1953, 1426, 1410, 1354, 1282, 1030, 760, 716 cm^{-1}. Anal. Calcd for $C_{20}H_{44}N_4P_2Pd$: C, 47.20; H, 8.71; N, 11.01. Found: C, 47.37; H, 8.81; N, 10.29.

$(PEt_3)_2Pd[C(N_2)$-*t*-Bu$]_2$ (5h). The sodium salt, which was prepared from trimethylacetaldehyde tosylhydrazone (8.0 g, 32 mmol), and BuLi (35 mmol), was pyrolyzed at 80–130 °C under reduced pressure (0.1–0.3 mmHg). *tert*-Butyldiazomethane was collected in a 100-mL three-necked flask at 100 °C. Addition of THF (25 mL) and BuLi solution in hexane (14 mmol) was followed by stirring at −100 to −80 °C for 1 h. The reaction mixture was cooled to −100 °C. A solution of $(PEt_3)_2PdCl_2$ (0.414 g, 0.1 mmol) in THF (20 mL) was added at −100 to −80 °C and the mixture was stirred for 1 h. At 0 °C, water (20 mL) was added. The organic layer was separated, washed with brine (2 × 20 mL), and dried (Na_2SO_4). Evaporation of the solvent, followed by recrystallization (−40 °C), gave violet complex **5g** (50 mg, 9%) (during the evaporation partial decomposition took place giving a green oil): mp 93–97 °C dec); ^{1}H NMR (δ, $CDCl_3$) 1.11 (q, 18 H, CH_3), 1.11 (s, 18 H, CH_3), 1.90 (m, 12 H, CH_2); IR (Nujol) 1960, 1949, 1276, 1034, 765, 718 cm^{-1}. Anal. Calcd for $C_{22}H_{48}N_4P_2Pd$: C, 49.02; H, 9.02; N, 10.47. Found: C, 48.26; H, 9.16; N, 9.53.

Thermolyses of $(PEt_3)_2Pd[C(N_2)Ph]_2$ (5e) and $(PEt_3)_2Pd$-$[C(N_2)C_6H_4$-*p*-$CH_3]_2$ (5f). A solution of **5e** (57.7 mg, 0.1 mmol) in dry toluene (1 mL) was heated at 120 °C for 1 min under argon. GC analysis (10% PEG on 80–100 mesh Celite column, 1 m × 4 mm, 100–220 °C) of the reaction mixture shows peaks attributable to triethylphosphine oxide, *trans*-stilbene, diphenylacetylene, and *cis*-stilbene at 8.5, 9.5, 10.3, and 11.4 min, respectively. Isolation of the products by Al_2O_3 column chromatography (Al_2O_3, 5 g) gave diphenylacetylene (12.0 mg, 67%) and stilbenes (cis/trans = 77/23; 3.1 mg, 17%). The thermal stability of complex **5a** is dependent on the solvent used. Complex **5a** in toluene decomposed completely at 50 °C for ca. 2 h, while in chloroform, it takes more than 20 h.

The same reaction of **5f** (60.5 mg, 0.1 mmol) gave bis(*p*-methylphenyl)acetylene (13.3 mg, 65%) and 1,2-bis(*p*-methylphenyl)ethylene (2.7 mg, 13%). The cis/trans ratio of the latter compound could not be determined due to overlapping of the GLC peak area.

Complex **5e** (19.2 mg, 0.33 mmol) was decomposed in toluene-d_8 (0.3 mL) by the same manner as above. Isolation of the products by Al_2O_3 column chromatography gave a mixture (5.7 mg) of diphenylacetylene and stilbene. The mass spectrum of stilbene obtained showed no deuterium incorporation.

Thermolysis of a Mixture of $(PEt_3)_2Pd[C(N_2)Ph]_2$ (5e) and $(PEt_3)_2Pd[C(N_2)C_6H_4$-*p*-$CH_3]_2$ (5f). A mixture of **5e** (58 mg, 0.1 mmol) and **5f** (61 mg, 0.1 mmol) in dry toluene (2 mL) was heated at 120 °C for 1 min under argon. Removal of the solvent followed by Al_2O_3 column chromatography (Al_2O_3, 10 g; hexane, 300 mL) gave a mixture of diphenylacetylene (60%), bis(*p*-methylphenyl)acetylene (60%), stilbene (15%), and bis(*p*-methylphenyl)ethylene (8%). The cis/trans ratio of the latter two compounds could not be determined due to overlapping of the GLC peak areas. The product yields were estimated by NMR analysis of the mixture.

Photolysis of $(PEt_3)_2Pd[C(N_2)Ph]_2$ (5e). A solution of $(PEt_3)_2Pd[C(N_2Ph]_2$ (57.7 mg, 0.1 mmol) in dry toluene (20 mL) was irradiated at room temperature by using a high-pressure mercury lamp with a Toshiba light filter, which cuts the light shorter than 520 nm. After 50 min, the violet color of the solution faded. Removal of the solvent followed by Al_2O_3 column chromatography gave diphenylacetylene (61%) and a trace amount of stilbene.

Palladium-Catalyzed Reaction of Allyl Acetates. To a solution of diazo complex **5e** (0.03 mmol) in dry toluene (0.7 mL) was added allyl acetate (1 mmol) and an internal standard (tridecane) under argon, and the mixture was heated at 120 °C for 10 min. A solution of sodium diethyl malonate in THF (2 mmol, 7 mL) was added dropwise. The reaction products were monitored by GLC. After 1 h, the reaction mixture was quenched by adding water, and the usual workup gave diethyl allylmalonate exclusively. The yields of the allylmalonate were as follows: for complex **5e**, the yields were 75% (after 10 min) and 83% (60 min); for **5c**, the yields were 76% (10 min) and 83% (60 min); for **5a**, the yields were 68% (10 min) and 77% (60 min).

X-ray Crystallographic Data Collection. Crystals of **4a** and **5d** are dark violet plates and orange prisms, respectively. Preliminary oscillation and Weissenberg photographs taken with Cu Kα radiation showed both the crystals belong to the monoclinic system. Systematic absences of reflections determined the space groups as $P2_1/c$ and $P2_1/n$ (both C_{2h}^5, no. 14) for **4a** and **5d**, respectively. Accurate unit-cell dimensions were determined by a least-squares fit of 2θ values of 25 strong reflections measured on a Rigaku automated, four-circle diffractometer. Crystal data are summarized in Table III. Well-shaped crystals with approximate dimensions of 0.45 × 0.25 × 0.15 mm for **4a** and 0.40 × 0.35 × 0.25 mm for **5d** were mounted on the diffractometer. Intensity data were collected by the θ–2θ scan technique using Zr-filtered (for **4a**) and graphite-monochromatized (for **5d**) Mo Kα radiation (λ = 0.71069 Å). The scan range and scan speed employed were $\Delta 2\theta = (2.0 + 0.70 \tan\theta)°$ and 4 min^{-1}, respectively. Background intensities were measured for 5.0 (for **4a**) and 7.5 s (for **5d**) at both ends of a scan. Four standard reflections (0,16,0, 563, 025, and 02$\bar{5}$ for **4a** and 400, 060, 008, and 343 for **5d**) measured at regular intervals to monitor the crystal stability and orientation showed no significant intensity decrease in each crystal. Usual Lp corrections were made, while no absorption corrections were carried out [max(μR) = 0.19 for **4a** and 0.16 for **5d**]. Totals of 6673 and 4834 reflections were collected with $(\sin\theta)/\lambda$ less than 0.60 and 0.65 for **4a** and **5d**, respectively.

Structure Solution and Refinement. Both structures were solved by the heavy-atom method. Three-dimensional Patterson syntheses revealed the position of the Pd atom for **4a** and those of the Pd and P atoms for **5d**. For **5d**, it was expected that the Pd atom occupies the center of symmetry (0,0,0) considering the crystallographic information. All the non-hydrogen atoms in both complexes were located from the subsequent Fourier maps based on these atomic positions. Refinements of both structures were carried out by the block-diagonal least-squares procedure using the HBLS-V program.[50] The function minimized is $\sum w(|F_o| - |F_c|)^2$. For the refinements, 3977 and 3867 reflections ($|F_o| > 3\sigma(|F_o|)$) were used for **4a** and **5d**, respectively. At the early stages of refinements, unit weights were employed. Several cycles of the isotropic refinements reduced the R values to 0.121 and 0.166 for **4a** and **5d**, where $R = \sum||F_o| - |F_c||/\sum|F_o|$. Subsequent anisotropic refinements converged with R = 0.084 (for **4a**) and 0.070 (for **5d**). Hydrogen atoms were reasonably located only for the phenyl hydrogens in **4a** from the difference Fourier maps calculated at these stages. Further refinements were carried out anisotropically

(50) Ashida, T. "The Universal Crystallorgraphic Computing System-Osaka", 2nd Ed.; The Computation Center: Osaka University, Osaka, Japan, 1979; p. 53.

for non-hydrogen atoms and isotropically for hydrogen atoms using the weighting scheme $w = (\sigma_{cs}^2 + a|F_o| + b|F_o|^2)^{-1}$, where σ_{cs} is the standard deviation obtained from counting statistics and a and b are constants adjusted in each step of the refinement. The final R indices are 0.076 for **4a** and 0.070 for **5d**. The final weighted R indices ($R_w = [\sum w(|F_o| - |F_c|)^2/\sum w|F_o|^2]^{1/2}$) are 0.087 and 0.104, and the weighting parameters a and b used in the final refinements are −0.0007 and 0.0021 for **4a** and 0.0213 and 0.0034 for **5d**, respectively. Atomic scattering factors used were taken from ref 51 for non-hydrogen atoms and from Stewart et al.[52] for hydrogen atoms. Final atomic parameters for non-hydrogen atoms are listed in Tables IV and V, respectively, and those for hydrogen atoms in **4a** is listed in Table VIII. All the bond lengths and bond angles are tabulated in Tables X–XII. Anisotropic temperature factors are given in Table XIII and XIV. Tables VIII–XIV and listings of observed and calculated structure factors are available as supplementary material.

Computation. All computations were done on an ACOS 800 computer at the Computation Center, Osaka University, and on an ACOS 700 computer at the Crystallographic Research Center, Institute for Protein Research, Osaka University. Figures 1 and 2 were drawn by the ORTEP program.[53]

Mass Spectra. In-beam EI mass spectra were obtained with a Hitachi RMU-6M single focusing mass spectrometer modified with an in-beam direct-inlet source.[30] To obtain in-beam EI spectra the sample was placed onto the end of the quartz of the modified direct inlet probe and inserted gently until the distance between the sample and the electron beam was less than 3 mm. The operating condition were as follows: ionizing voltage, 20 eV; ionizing current, 80 μA; chamber temperature, 195 °C; the source temperature, 200 °C. The major peaks of $(PEt_3)_2Pd[C(N_2)CO_2Et]_2$ (**5c**) over the range of the mass number 300, together with their intensities[54] and the corresponding ions proposed in brackets, are as follows; 512 [19%, $(PEt_3)_2Pd(CCO_2Et)^{+\cdot}$], 484 (48), 455 [58, $(PEt_3)_2Pd[C(N_2)CO_2Et]^+$], 427 [44, $(PEt_3)_2Pd(CCO_2Et)^+$], 399 (24), 394 [38, $(PEt_3)Pd(CO_2Et)_2^{+\cdot}$], 366 (37), 342 [52, $(PEt_3)_2Pd^+$], 337 (59), 314 (63), and 309 [40, $(PEt_3)Pd(CCO_2Et)^+$]. The mass spectrum of $(PEt_3)_2Pd[C(N_2)CO_2Et]_2$ (**5e**) shows the following peaks: 178 (100%, $PhC{\equiv}CPh^+$), 152 (10), 118 (14, $PEt_3^{+\cdot}$), 103 (6), 90 (17), and 62 (33).

Acknowledgment. We thank Yukio Fujisawa and Miho Ishikura for experimental works and Profs. Kazuo Tsujimoto and Mamoru Ohashi (University of Electro-Communication) for measurements of in-beam electron-impact mass spectra. We thank the Ministry of Education of financial support by Grant-in Aid for Scientific Research.

Supplementary Material Available: Tables of atomic parameters of hydrogen atoms, equations of least-squares planes, bond lengths and bond angles, and anisotropic temperature factors and listings of observed and calculated structure factors for complexes **4a** and **5d** (25 pages). Ordering information is given on any current masthead page.

(51) "International Tables for X-ray Crystallography"; Kynoch Press: Birmingham, 1974; Vol. IV, p 71.

(52) Stewart, R. F.; Davidson, E. R.; Simpson, W. T. *J. Chem. Phys.* **1965**, *42*, 309.

(53) Johnson, C. K. ORTEP-II, Report ORNL-5138; Oak Ridge National Laboratory; Oak Ridge, TN, 1976.

(54) The highest peak (313 over the range of the mass number 300 was selected as the base peak.

(55) In this paper the periodic group notation in parentheses is in accord with recent actions by IUPAC and ACS nomenclature committees. A and B notation is eliminated because of wide confusion. Groups IA and IIA become groups 1 and 2. The d-transition elements comprise groups 3 through 12, and the p-block elements comprise groups 13 through 18. (Note that the former Roman number designation is preserved in the last digit of the new numbering: e.g., III→3 and 13.)

Insertion Reactions of *N*-Sulfinyl Sulfonamides and Sulfur Bis(sulfonylimide)s into Transition-Metal–Carbon σ Bonds

Tak Wai Leung, Gary G. Christoph, Judith Gallucci, and Andrew Wojcicki*

Department of Chemistry, The Ohio State University, Columbus, Ohio 43210

Received June 20, 1985

Insertion reactions have been investigated of the *N*-sulfinyl sulfonamides $R'S(O)_2NSO$ (R' = Me, *p*-ClC_6H_4) and the sulfur bis(sulfonylimide) $[MeS(O)_2N]_2S$ into the metal–carbon σ bonds of $CpFe(CO)(L)Me$ (L = PPh_3, $P(OPh)_3$), $CpM(CO)_2(L)Me$ (M = Mo, W; L = PMe_2Ph, PPh_3), $CpM(CO)_3R$ (M = Mo, W; R = Me, $CH_2C_6H_4Cl$-*p*), $Mn(CO)_4(L)Me$ (L = CO, PPh_3), and $CpCr(NO)_2Me$. The complexes $CpFe(CO)(L)Me$ and $CpM(CO)_2(L)Me$ react with $R'S(O)_2NSO$ initially to yield insertion products containing the N-bonded $N[S(O)_2R']S(O)Me$ ligand; these complexes rearrange upon warming or column chromatography to isolable S-bonded $S[NS(O)_2R'](O)Me$ linkage isomers. Reaction between $CpCr(NO)_2Me$ and $MeS(O)_2NSO$ affords $CpCr(NO)_2\{N[S(O)_2Me]S(O)Me\}$, which could not be converted to its S-bonded isomer. The complexes $CpM(CO)_3R$ react with $MeS(O)_2NSO$ to give the N- and O-bonded species $CpM(CO)_3\{N[S(O)_2Me]S(O)R\}$ and $CpM(CO)_3\{OS[NS(O)_2Me]R\}$, respectively, in solution at −25 °C; these compounds decompose upon warming to intractable materials. Treatment of $Mn(CO)_5Me$ with $MeS(O)_2NSO$ affords $Mn(CO)_5\{N[S(O)_2Me]S(O)Me\}$ at −25 °C in solution. Insertion reactions of $[MeS(O)_2N]_2S$ with the aforementioned metal–Me complexes proceed to the appropriate compounds containing the $N[S(O)_2Me]S(Me)NS(O)_2Me$ ligand. These complexes were generally isolated as end products; however, with $Mn(CO)_4(L)Me$, further reaction occurred to yield isolable $(CO)_3(L)Mn\{N[S(O)_2Me]S(Me)NS(O)_2Me\}$ containing a bidentate insertion ligand. Reactions with $HPF_6{\cdot}OEt_2$ and Et_3OPF_6 of $CpFe(CO)_2\{N[S(O)_2Me]S(O)Me\}$ (**1**), $CpFe(CO)_2\{N[S(O)_2Me]S(Me)NS(O)_2Me\}$ (**2**), and $CpFe(CO)_2\{S[NS(O)_2Me](O)Me\}$ (**3**) lead to protonation at nitrogen in **1**, **2** (uncoordinated N), and **3** and alkylation at the sulfinyl oxygen in **1** and **3**. The structure of $CpFe(CO)_2\{S[NS(O)_2Me](O)CH_2Ph\}{\cdot}{}^1/_2CH_2Cl_2$ was determined by a single-crystal X-ray diffraction analysis. The crystals are triclinic of space group $P\bar{1}$ with a = 8.517 (7) Å, b = 10.624 (5) Å, c = 12.092 (9) Å, α = 109.58 (5)°, β = 90.05 (6)°, γ = 108.06 (5)°, and Z = 2. The structure was solved and refined to R = 0.040 and R_w = 0.040 by using 2178 independent reflections. The Fe–S bond distance is 2.212 (1) Å, suggesting some double-bond character in this linkage.

Introduction

It was shown in this laboratory that *N*-sulfinyl sulfonamides ($R'S(O)_2NSO$) and sulfur bis(sulfonylimide)s ($[R'S(O)_2N]_2S$), two classes of electronic and structural analogues of SO_2, readily insert into the Fe–C σ bonds of $CpFe(CO)_2R$.[1] The products of these reactions are $CpFe(CO)_2\{N[S(O)_2R']S(O)R\}$ (**1**) and $CpFe(CO)_2\{N[S(O)_2R']S(R)NS(O)_2R'\}$ (**2**), respectively. Complexes **1** isomerize upon heating to $CpFe(CO)_2\{S[NS(O)_2R'](O)R\}$ (**3**). Both insertion reactions, like that of SO_2,[2] proceed with inversion of configuration at the α-carbon atom of R.

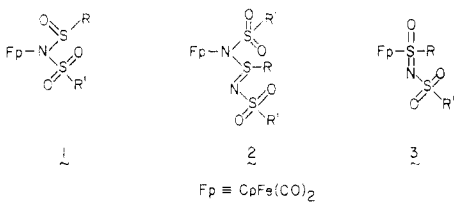

1 **2** **3**

To ascertain the generality and scope of the foregoing insertions, we have now examined reactions of $R'S(O)_2NSO$ and $[R'S(O)_2N]_2S$ with several other types of transition-metal–alkyl complexes. Reported here are the results of this investigation. Since initially complexes **3** could not be characterized as convincingly as complexes **1** and **2** by spectroscopic techniques,[1] we undertook a single-crystal X-ray diffraction study of one member of **3**, viz., $CpFe(CO)_2\{S[NS(O)_2Me](O)CH_2Ph\}$ (**3a**). We first consider a description of the molecular structure of this complex.

Results and Discussion

Crystal and Molecular Structure of $CpFe(CO)_2\{S[NS(O)_2Me](O)CH_2Ph\}{\cdot}{}^1/_2CH_2Cl_2$ (3a·$^1/_2CH_2Cl_2$). The crystal structure of **3a**·$^1/_2CH_2Cl_2$ consists of discrete molecules of $CpFe(CO)_2\{S[NS(O)_2Me](O)CH_2Ph\}$ (**3a**) and disordered CH_2Cl_2 solvent, with no unusually close contacts. The molecular structure of **3a** is shown in Figure 1. Selected bond lengths and angles are listed in Tables I and II, respectively.

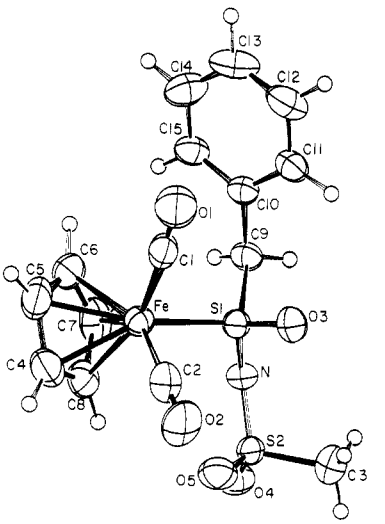

Figure 1. ORTEP drawing of **3a**, showing atom numbering scheme. Non-hydrogen atoms are drawn at the 50% probability level, and the hydrogen atoms are drawn artificially small.

The structure of **3a** is that inferred by us from spectroscopic data.[1] The molecule resulted from the addition of the $CpFe(CO)_2$ and CH_2Ph groups to the sulfinyl sulfur atom of the inserting $MeS(O)_2NSO$ species. Thus, the resulting $S[NS(O)_2Me](O)CH_2Ph$ ligand is a close structural analogue of the *S*-sulfinate ligands $S(O)_2R$.

All bond distances and angles within the $CpFe(CO)_2$ fragment appear normal.[3-5] The Fe–S(1) bond length of

(1) Severson, R. G.; Leung, T. W.; Wojcicki, A. *Inorg. Chem.* **1980**, *19*, 915.
(2) Wojcicki, A. *Adv. Organomet. Chem.* **1974**, *12*, 31.

0276-7333/86/2305-0366$01.50/0

Table I. Selected Bond Distances (Å) for 3a•$^1/_2CH_2Cl_2$, with Estimated Standard Deviations in Parentheses

Fe–S(1)	2.212 (1)	C(6)–C(7)	1.385 (7)
Fe–C(1)	1.777 (5)	C(7)–C(8)	1.402 (6)
Fe–C(2)	1.792 (5)	C(8)–C(4)	1.398 (6)
Fe–C(4)	2.095 (5)	S(1)–O(3)	1.480 (3)
Fe–C(5)	2.098 (5)	S(1)–C(9)	1.816 (4)
Fe–C(6)	2.093 (4)	S(1)–N	1.607 (3)
Fe–C(7)	2.104 (4)	S(2)–N	1.592 (3)
Fe–C(8)	2.079 (4)	S(2)–O(4)	1.432 (3)
C(1)–O(1)	1.146 (5)	S(2)–O(5)	1.436 (3)
C(2)–O(2)	1.140 (5)	S(2)–C(3)	1.746 (5)
C(4)–C(5)	1.411 (7)	C(9)–C(10)	1.501 (6)
C(5)–C(6)	1.422 (7)		

Table II. Selected Bond Angles (deg) for 3a•$^1/_2CH_2Cl_2$, with Estimated Standard Deviations in Parentheses

S(1)–Fe–C(1)	91.5 (2)	Fe–C(4)–C(5)	70.5 (3)
S(1)–Fe–C(2)	91.1 (2)	Fe–C(4)–C(8)	69.8 (3)
S(1)–Fe–C(4)	141.9 (2)	Fe–C(5)–C(6)	70.0 (3)
S(1)–Fe–C(5)	154.6 (2)	Fe–C(5)–C(4)	70.2 (3)
S(1)–Fe–C(6)	115.1 (2)	Fe–C(6)–C(7)	71.2 (3)
S(1)–Fe–C(7)	91.6 (1)	Fe–C(6)–C(5)	70.4 (3)
S(1)–Fe–C(8)	104.2 (2)	Fe–C(7)–C(8)	69.5 (3)
C(1)–Fe–C(2)	91.3 (2)	Fe–C(7)–C(6)	70.3 (3)
C(1)–Fe–C(4)	126.6 (2)	Fe–C(8)–C(4)	71.0 (3)
C(1)–Fe–C(5)	94.7 (2)	Fe–C(8)–C(7)	71.4 (3)
C(1)–Fe–C(6)	97.0 (2)	C(8)–C(4)–C(5)	108.1 (5)
C(1)–Fe–C(7)	130.0 (2)	C(4)–C(5)–C(6)	106.8 (5)
C(1)–Fe–C(8)	160.1 (6)	C(5)–C(6)–C(7)	108.6 (5)
C(2)–Fe–C(4)	88.0 (2)	C(6)–C(7)–C(8)	108.1 (4)
C(2)–Fe–C(5)	113.3 (2)	C(7)–C(8)–C(4)	108.4 (5)
C(2)–Fe–C(6)	152.1 (2)	Fe–S(1)–O(3)	111.3 (1)
C(2)–Fe–C(7)	138.5 (2)	Fe–S(1)–N	114.9 (1)
C(2)–Fe–C(8)	100.4 (2)	Fe–S(1)–C(9)	112.2 (2)
C(4)–Fe–C(5)	39.3 (2)	O(3)–S(1)–N	114.5 (2)
C(4)–Fe–C(6)	65.8 (2)	O(3)–S(1)–C(9)	107.1 (2)
C(4)–Fe–C(7)	65.5 (2)	N–S(1)–C(9)	95.6 (2)
C(4)–Fe–C(8)	39.1 (2)	S(1)–N–S(2)	121.3 (2)
C(5)–Fe–C(6)	39.7 (2)	N–S(2)–O(4)	106.0 (2)
C(5)–Fe–C(7)	65.7 (2)	N–S(2)–O(5)	113.7 (2)
C(5)–Fe–C(8)	66.0 (2)	N–S(2)–C(3)	106.8 (2)
C(6)–Fe–C(7)	38.6 (2)	O(4)–S(2)–O(5)	116.6 (2)
C(6)–Fe–C(8)	65.5 (2)	O(4)–S(2)–C(3)	107.5 (2)
C(7)–Fe–C(8)	39.2 (2)	O(5)–S(2)–C(3)	105.8 (2)
Fe–C(1)–O(1)	175.2 (4)	S(1)–C(9)–C(10)	114.5 (3)
Fe–C(2)–O(2)	175.0 (4)		

2.212 (1) Å is comparable to the distances of 2.201 (6) and 2.218 (2) Å in the *S*-sulfinato complexes CpFe(CO)$_2$[S(O)$_2$C$_6$F$_5$][5] and (η^5-C$_5$Me$_5$)Fe(CO)$_2$[S(O)$_2$CH$_2$CH=CHPh],[6] respectively. It is, like the latter two, appreciably shorter than the sum of the appropriate covalent radii (2.38 Å[6]), suggesting some double-bond character in this linkage as well.

The sulfinyl sulfur (S(1)) has a chiral tetrahedral environment which deviates somewhat from regularity (see Table II). (It is to be noted that the crystal is not chiral, as it contains both enantiomers.) The largest S(1) bond angles are Fe–S(1)–N and O(3)–S(1)–N (114.9 (1) and 114.5 (2)°, respectively), and the smallest is N–S(1)–C(9) (95.6 (2)°). The two sulfur–nitrogen bonds S(1)–N and S(2)–N measure 1.607 (3) and 1.592 (3) Å, respectively. Thus, they are significantly shorter than a single S—N bond (1.775 (2) Å) but longer than a double S=N bond (1.508 (5) Å).[7] Comparable S–N bond distances have been observed in other compounds containing four-coordinate sulfur and two-coordinate nitrogen.[8,9] The S(1)–N–S(2) bond angle of 121.3 (2)° is similar to the angle S(Me)–N–S(O)$_2$CF$_3$ of 116.1 (4)° in F$_3$CS(O)$_2$N[Sn(Me)]S(Me)NS(O)$_2$CF$_3$.[8] All S–O distances are close to accepted values.[10]

Insertion Reactions of Metal–Alkyl Complexes. (i) CpFe(CO)(L)Me. Solutions of CpFe(CO)(PPh$_3$)Me in CH_2Cl_2 rapidly change color from red to green upon treatment with 1 equiv of *p*-ClC$_6$H$_4$S(O)$_2$NSO or MeS(O)$_2$NSO. During column chromatography the green solutions gradually turn red, and from the red effluents complexes **5a** and, presumably, **5b** are obtained. Both are considerably less stable than **3**, and **5b** could not be satisfactorily characterized because of its instability.

The S-bonded structure of **5a** is inferred from the IR absorption bands at 1270 and 1148 cm^{-1} (ν(SO$_2$)) and at 1085 and 1020–980 cm^{-1} (ν(S=N) and ν(S=O), possibly in that same order).[11] Absorptions at similar frequencies were observed[1] for complexes **3** and, with the present elucidation of the molecular structure of **3a**, provide strong evidence for the assignments made in this study. The corresponding N-bonded linkage isomers **1** display no strong IR bands in the region ca. 1080–980 cm^{-1}.[1] The ^{1}H NMR spectrum of **5a** shows two Me signals of approximately equal intensity at δ 3.32 and 2.62. Since two chiral centers are present in the molecule—the metal and the sulfinyl sulfur—the spectrum likely reflects the presence of two diastereomers in roughly equal amounts.

The ^{1}H NMR spectrum at −25 °C of a green solution of equimolar amounts of CpFe(CO)(PPh$_3$)Me and *p*-ClC$_6$H$_4$S(O)$_2$NSO in CDCl$_3$ shows two Me signals at δ 1.70 and 1.44 (relative intensities ca. 2:1) and a broad unsymmetrical Cp resonance at δ 4.74. Upon warming the solution to room temperature, these signals disappear and are replaced by those observed for the isolated **5a**.

The foregoing observations may be readily accommodated by the consecutive reactions in eq 1. The green

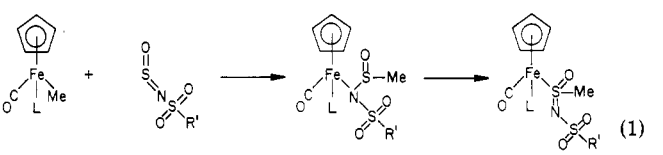

(1)

4a-c 5a-c

a L = PPh$_3$, R' = p-ClC$_6$H$_4$
b L = PPh$_3$, R' = Me
c L = P(OPh)$_3$, R' = Me

species is in all probability **4a**, which would also exist as a pair of diastereomers. The Me resonances of **4a** occur at higher fields than those of the isomeric **5a**, as do the corresponding resonances of **1** compared with **3**.[1]

When CpFe(CO)[P(OPh)$_3$]Me and MeS(O)$_2$NSO were allowed to react in CH_2Cl_2 at 25 °C, the original yellow solution gradually turned orange. An examination by ^{1}H NMR spectroscopy of the solid isolated after 15 min revealed the presence of more than one kind of product. However, longer reaction times or higher temperatures result in a complete conversion of this mixture to what appears to be a single product. This species was isolated as a stable yellow solid which was characterized as **5c** by elemental analysis and spectroscopic methods. Thus, the IR spectrum in the 1300–950-cm^{-1} region strongly resembles that of **5a**, and the ^{1}H NMR spectrum shows reso-

(3) Churchill, M. R. *Perspect. Struct. Chem.* **1970**, *3*, 157.
(4) Churchill, M. R.; Wormald, J. *J. Am. Chem. Soc.* **1971**, *93*, 354.
(5) Redhouse, A. D. *J. Chem. Soc., Dalton Trans.* **1974**, 1106.
(6) Churchill, M. R.; Wormald, J. *Inorg. Chem.* **1971**, *10*, 572.
(7) Bats, J. W.; Coppens, P.; Koetzle, T. F. *Acta Crystallogr., Sect. B: Struct. Crystallogr. Cryst. Chem.* **1971**, *27B*, 586.
(8) Bats, J. W.; Fuess, H.; Diehl, M.; Roesky, H. W. *Inorg. Chem.* **1978**, *17*, 3031.
(9) Gieren, A.; Hahn, C.; Dederer, B.; Roesky, H. W.; Amin, N. *Z. Anorg. Allg. Chem.* **1978**, *447*, 179.
(10) Abrahams, S. C. *Q. Rev., Chem. Soc.* **1956**, 407.
(11) Meij, R.; Oskam, A.; Stufkens, D. J. *J. Mol. Struct.* **1979**, *51*, 37.

nances at δ 4.68 (Cp) and 3.52 (OSMe) and at δ 4.59 (Cp) and 3.63 (OSMe), again indicative of the presence of two diastereomers, in the approximate ratio 3:2. The other product, which was observed in the reaction mixture after short reaction times and which undergoes conversion to **5c**, is almost certainly the N-bonded isomer **4c**. **4c** also appears to be present as a mixture of diastereomers, since additional Me proton resonances appear at δ 2.87, 2.66, 2.19, and 2.02.

The aforementioned behavior of $CpFe(CO)(L)Me$ toward $R'S(O)_2NSO$ is qualitatively similar to that of $CpFe(CO)_2R$. The latter complexes initially afford the N-bonded **1**, which isomerize on prolonged heating to the S-bonded **3**.[1] The results of this study indicate that the propensity of $CpFe(CO)(L)\{N[S(O)_2R']S(O)R\}$ to undergo such a linkage isomerization increases with an increasing basicity of the ligand L, i.e., $L = CO < P(OPh)_3 < PPh_3$. This order may result from an increasing stabilization of the transition state leading to the S-bonded complex through a delocalization of negative charge on the metal by Fe-to-S π bonding.

Reactions between $CpFe(CO)(L)Me$ ($L = PPh_3$, $P(OPh)_3$) and $[MeS(O)_2N]_2S$ proceed to **6** as depicted in eq 2. **6b** is stable as a solid at 25 °C, whereas **6a** decomposes

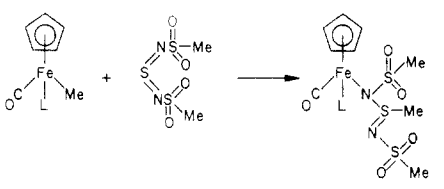

(2)

6a,b

a L = PPh_3
b L = $P(OPh)_3$

readily under these conditions. The IR spectrum of **6b** in the 1350–950-cm^{-1} region closely resembles the spectra of the dicarbonyl analogues **2**.[1] The ^1H NMR spectrum of **6a** shows three Me signals of equal intensity at δ 3.10, 2.95, and 1.90 and reveals no evidence of the presence of diastereomers. The same signals were observed in the spectrum of a solution of equimolar amounts of $CpFe(CO)(PPh_3)Me$ and $[MeS(O)_2N]_2S$ in $CDCl_3$ at −25 °C. By contrast, **6b** exhibits strong Me resonances at δ 3.13, 2.97, and 2.58 and weak ones at δ 3.20 and 2.91 (and presumably at δ 2.58). The intensities of these signals are consistent with the existence of two diastereomers in the approximate ratio 5:1.

(ii) $CpM(CO)_2(L)Me$ (M = Mo, W). Reactions of $CpM(CO)_2(L)Me$ (M = Mo, W; $L = PPh_3$, PMe_2Ph) with $MeS(O)_2NSO$ and $[MeS(O)_2N]_2S$ are similar to those of $CpFe(CO)(L)Me$. Thus, interaction of $CpMo(CO)_2(L)Me$ with $MeS(O)_2NSO$ in CH_2Cl_2 leads in each case to the formation of two products, with the red product undergoing complete conversion to the yellow one upon column chromatography. The isolated yellow solids, which are stable to air, were characterized as the S-bonded **7a** and **7b** by elemental analysis and IR and ^1H NMR spectroscopy. Their ^1H NMR spectra show the Cp and PMe_2 signals as doublets, thus indicating a trans geometry.[12]

When reaction of $CpMo(CO)_2(PMe_2Ph)Me$ with $MeS(O)_2NSO$ in $CDCl_3$ at −25 °C was examined by ^1H NMR spectroscopy, signals appeared which corresponded to those observed for **7a** but which occurred at somewhat different fields. Upon warming the solution to room temperature, these signals gradually disappeared and were replaced by those of **7a**. The position of the initial resonances, as well as the clean nature of the conversion, points to the intermediate species being the N-bonded **8a**.

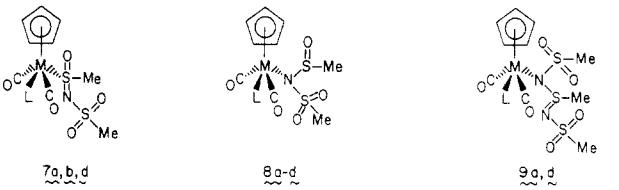

7a,b,d **8a-d** **9a,d**

a M = Mo, L = PMe_2Ph
b M = Mo, L = PPh_3
c M = W, L = PMe_2Ph
d M = W, L = PPh_3

Complexes **8** exhibit higher stability with respect to isomerization to **7** when M = W compared with M = Mo and can be isolated and characterized. Accordingly, addition of pentane to stirred solutions of equimolar amounts of $CpW(CO)_2(L)Me$ ($L = PMe_2Ph$, PPh_3) and $MeS(O)_2NSO$ in CH_2Cl_2 at 25 °C leads to the precipitation of red solids. The IR spectra in the 1350–980-cm^{-1} region of these products are very similar to those of the complexes **1**, showing no strong absorptions below 1080 cm^{-1}. The ^1H NMR spectra, given in Experimental Section, are entirely consistent with the trans N-bonded structures **8c** and **8d**. Upon thermolysis in CH_2Cl_2 at reflux, **8d** affords a yellow solid, the chemical analysis and IR and ^1H NMR spectra of which agree with its formulation as **7d**.

Room-temperature interaction between $CpMo(CO)_2(PMe_2Ph)Me$ or $CpW(CO)_2(PPh_3)Me$ and $[MeS(O)_2N]_2S$ yields a red, relatively unstable solid in each case. These solids are formulated as **9a** and **9d**, respectively, on the basis of similarity of their IR and ^1H NMR spectra to those of related complexes, e.g., **2** and **6**.

All of the aforementioned Mo and W dicarbonyl complexes were obtained exclusively as the trans isomers. The corresponding cis species, which would be expected to exist as diastereomers owing to the presence of two chiral centers, were not observed. It is relevant that all of the precursor metal–alkyl complexes were also the trans isomers.

(iii) $CpM(CO)_3R$ (M = Mo, W). A solution of $CpMo(CO)_3Me$ in CH_2Cl_2 at room temperature immediately changed color from yellow to red upon treatment with $MeS(O)_2NSO$. However, the red product decomposed during attempts at isolation. Similarly, reaction of $CpW(CO)_3Me$ with $MeS(O)_2NSO$ at 25 °C only led to decomposition.

Reaction between equimolar amounts of $CpMo(CO)_3Me$ and $MeS(O)_2NSO$ in $CDCl_3$ was then followed by ^1H NMR spectroscopy at −25 °C. The first spectrum, taken a few minutes after preparation of the solution, revealed two sets of signals: at δ 5.79 (Cp), 3.05 (Me), and 2.56 (Me) and at δ 5.90 (Cp), 2.95 (Me), and 2.37 (Me). The intensity ratio of the two sets was ca. 3:1. No change in this spectrum was observed when the temperature was lowered to −50 °C. However, when the temperature was allowed to rise, decomposition began at ca. 10 °C as the signals broadened and disappeared within a few minutes.

A parallel behavior was noted for each of $CpMo(CO)_3CH_2C_6H_4Cl$-*p* and $CpW(CO)_3Me$ reacting with $MeS(O)_2NSO$ in $CDCl_3$, also at −25 °C. Again, two species with similar resonances were observed by ^1H NMR spectroscopy, and both decomposed upon warming the solutions to room temperature.

The IR spectra in the ν(CO) region of solutions of $CpMo(CO)_3R$ (R = Me, $CH_2C_6H_4Cl$-*p*) and $MeS(O)_2NSO$ in CH_2Cl_2 or $CHCl_3$ at ca. 0 °C indicate that the products are tricarbonyl complexes. Thus, two strong absorptions

(12) Barnett, K. W; Slocum, D. W. *J. Organomet. Chem.* **1972**, *44*, 1.

occur at 2055 and 1970 cm^{-1}, the latter being broad and somewhat more intense.

One of the products of each of the aforementioned reactions is likely to be the N-bonded **10**, i.e., **10a**, **10b**, and **10c**, as the observed proton resonances compare well with those predicted from the spectra of analogous complexes **1**[1] and **8**. However, the other product does not appear to be the S-bonded linkage isomer of **10** analogous to **3** and **7**. Such an S-bonded species would be expected to show CH_2 and Me proton signals at considerably lower fields than those observed here. For example, $CpFe(CO)_2\{S[NS(O)_2Me](O)Me\}$ exhibits Me resonances at δ 3.40 and 3.00, whereas $CpFe(CO)_2\{S[NS(O)_2Me](O)CH_2Ph\}$ shows its CH_2 and Me resonances at δ 4.67 and 3.01, respectively.[1] Furthermore, the last-mentioned complex, as well as all other reported related $MS(X)(Y)CH_2Ph$ (X = O; Y = OBF_3, $OSbF_5$, $NS(O)_2R$) species containing chiral sulfur, unexpectedly shows the CH_2 resonance as a singlet instead of an AB quartet.[1,13] The appearance of this resonance as an AB quartet (δ 3.99, 3.71, $J_{H_AH_B}$ = 13 Hz; δ 4.17, 3.89, $J_{H_AH_B}$ = 13 Hz) for both products derived from $CpMo(CO)_3CH_2C_6H_4Cl$-*p* and $MeS(O)_2NSO$ in solution suggests that Mo–S bonded complexes are not present.

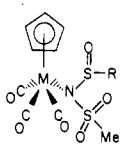

10a-c

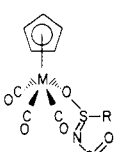

11a-c

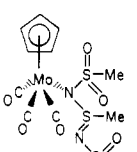

12a

a M = Mo, R = Me
b M = Mo, R = $CH_2C_6H_4Cl$-p
c M = W, R = Me

We believe that the most reasonable assignment to second products of these reactions is **11**. Related O-bonded complexes have been detected spectroscopically, but not isolated, in reactions of various metal carbonyl alkyl complexes with SO_2.[14] Since bonding properties of the ligands derived by insertion of $MeS(O)_2NSO$ into M–R in **10** and **11** are not expected to be significantly different, the positions of the IR ν(CO) bands of **10** and **11** should be similar, as indeed they are. Furthermore, one would reasonably predict the corresponding proton resonances of **10** and **11** to occur at comparable fields and, where appropriate, with comparable splitting patterns and to be similar to those reported for related *O*-sulfinates, $CpM(CO)_3[OS(O)R]$; again, this is borne out here.

The insertion of $MeS(O)_2NSO$ into the Mo–Me bond of $CpMo(CO)_3Me$ proceeds appreciably faster than that into the W–Me bond of $CpW(CO)_3Me$. This relative reactivity of M–Me thus parallels that toward a related inserting molecule, SO_2.[15] Other reactants also cleave Mo–R bonds more readily than the corresponding W–R bonds.[16]

Room-temperature reaction between $CpMo(CO)_3Me$ and $[MeS(O)_2N]_2S$ affords a red product of low thermal stability at 25 °C. The IR and ^1H NMR spectra of this solid match those recorded on a freshly prepared solution of equimolar amounts of the two reactants at −25 °C. The Me signals compare well with those reported earlier[1] for $CpFe(CO)_2\{N[S(O)_2Me]S(Me)NS(O)_2Me\}$, thus providing support for structure **12a**.

Reaction of $CpW(CO)_3Me$ with $[MeS(O)_2N]_2S$ at 25 °C resulted in the formation of a red, non-carbonyl decomposition material. No study was made of this reaction at low temperature.

(iv) $Mn(CO)_4(L)Me$. A solution of equimolar amounts of $Mn(CO)_5Me$ and $MeS(O)_2NSO$ in $CDCl_3$ at −25 °C showed the appearance and growth of equal-intensity ^1H NMR signals at δ 3.02 and 2.56 as the signals of the reactants gradually disappeared. The reaction was essentially complete in 30 min. The above resonances compare very well with those observed for the products of reactions of $CpFe(CO)_2Me$ and $CpM(CO)_3Me$ (M = Mo, W) with $MeS(O)_2NSO$, viz., **1** (R = R′ = Me),[1] **10a**, and **10c**, respectively. An analogous formulation, **13a**, is suggested on this basis. Attempts at isolation of **13a** at room temperature resulted in decomposition.

Since substitution of L = PR_3 for a CO group results in the formation of stable $MeS(O)_2NSO$ insertion products for $CpM(CO)_2(L)Me$ (M = Mo, W), reaction of *cis*-$Mn(CO)_4(PPh_3)Me$ with $MeS(O)_2NSO$ was conducted in an attempt to isolate an analogous complex. However, this reaction surprisingly afforded **15b**, which was synthesized independently from *cis*-$Mn(CO)_4(PPh_3)Me$ and $[MeS(O)_2N]_2S$ (vide infra). This unexpected product likely arises from the disproportionation of $MeS(O)_2NSO$ to SO_2 and $[MeS(O)_2N]_2S$ followed by insertion of the latter into the Mn–Me bond. Such a disproportionation, noted previously in reactions of $R'S(O)_2NSO$ with $CpFe(CO)_2R$,[1] is known to be catalyzed by bases.[16]

When equimolar amounts of $Mn(CO)_5Me$ and $[MeS(O)_2N]_2S$ in $CDCl_3$ were allowed to react in an NMR tube at −25 °C, new proton resonances of equal intensity grew in at δ 3.19, 3.02, and 2.87. The reaction reached completion in ca. 1 h as evidenced by the disappearance of the Me signals of the reactants. The temperature was then allowed to rise, and, at 10 °C, the three signals of the product started to decrease in intensity while two new signals at δ 3.20 and 3.04 of relative intensity 1:2 appeared and grew. When the temperature reached 25 °C, only the latter two resonances were observable. Lowering the temperature had no effect on the final spectrum.

Reaction at room temperature between $Mn(CO)_5Me$ and $[MeS(O)_2N]_2S$ in CH_2Cl_2 led to the isolation of a moderately stable yellow solid whose ^1H NMR spectrum is identical with that observed by monitoring a solution of the two reactants at 25 °C. The IR spectrum in the ν(CO) region of the isolated product shows absorption bands at 2145 (w), 2045 (s), 1950 (s), and 1930 (s) cm^{-1}, consistent with the presence of a cis tetracarbonyl species. The combined ^1H NMR–IR data point to structure **15a**, which arises first by insertion of $[MeS(O)_2N]_2S$ into the Mn–Me bond to yield **14a**, followed by chelation with loss of a CO ligand. The observation of only two $\nu(SO_2)$ bands in the IR spectrum of **15a** suggests that the $S(O)_2Me$ groups are equivalent and lends further support to the proposed structure.

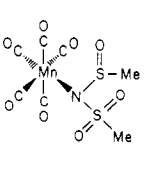

13a

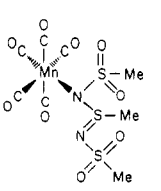

14a

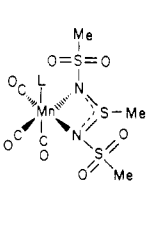

15a-c

a L = CO
b L = PPh_3
c L = C_5H_5N

(13) Severson, R. G.; Wojcicki, A. *J. Am. Chem. Soc.* **1979**, *101*, 877.
(14) Kroll, J. O.; Wojcicki, A. *J. Organomet. Chem.* **1974**, *66*, 95.
(15) Wojcicki, A. *Adv. Organomet. Chem.* **1973**, *11*, 87.
(16) Wucherpfennig, W.; Kresze, G. *Tetrahedron Lett.* **1966**, 1671.

Reactions of **15a** with PPh_3 and C_5H_5N result in the formation of stable yellow tricarbonyl derivatives **15b** and **15c**, respectively. The *fac* isomeric formulation is supported by the appearance of three strong IR ν(CO) absorption bands and of two Me ^{1}H NMR signals of relative intensity 1:2. **15b** also forms by reaction of *cis*-$Mn(CO)_4(PPh_3)Me$ with $[MeS(O)_2N]_2S$.

As stated above, the insertion of $MeS(O)_2NSO$ and $[MeS(O)_2N]_2S$ into the Mn–Me bond of $Mn(CO)_5Me$ at −25 °C requires ca. 0.5 and 1 h, respectively, for completion. Thus, these reactions are appreciably slower than the corresponding insertion reactions of $CpFe(CO)_2Me$[1] and $CpMo(CO)_3Me$, which under similar conditions are over within a few minutes. For comparison, the rates of SO_2 insertion at −65 to −18 °C follow the order $CpFe(CO)_2Me$ > $Mn(CO)_5Me$ > $CpMo(CO)_3Me$.[2]

(v) $CpCr(NO)_2Me$. Both $MeS(O)_2NSO$ and $[MeS(O)_2N]_2S$ readily insert into the Cr–Me bond of $CpCr(NO)_2Me$ in CH_2Cl_2 at ambient temperature to afford stable green oils which could not be induced to crystallize. These products were characterized by use of aforementioned IR and ^{1}H NMR spectroscopic criteria as the N-bonded **16** and **17**, respectively, and their formulations as 1:1 adducts of the appropriate reactants are supported by mass spectral data (Experimental Section). Attempts at thermal conversion of **16** to its S-bonded linkage isomer in CH_2Cl_2 at reflux for 10 h resulted in some decomposition and recovery of unreacted **16**.

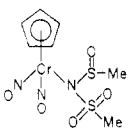

16

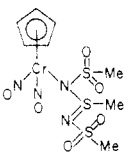

17

Protonation and Alkylation Reactions of 1, 2, and 3. A preliminary study was conducted of protonation and alkylation reactions of complexes derived by insertion of $R'S(O)_2NSO$ and $[R'S(O)_2N]_2S$ into M–R bonds. This study focused on complexes **1**, **2**, and **3** (R = R′ = Me) and the electrophilic reagents $HPF_6{\cdot}OEt_2$ and Et_3OPF_6.

Treatment of **1** (R = R′ = Me) with $HPF_6{\cdot}OEt_2$ in CH_2Cl_2 affords a deep red, air-stable precipitate which analytically corresponds to a 1:1 adduct of **1** and HPF_6 and which is a 1:1 electrolyte in $MeNO_2$. The IR spectrum of this product exhibits a medium-intensity ν(NH) band at 3250 cm^{-1}, two ν(CO) absorptions at 2060 and 2000 cm^{-1}, indicative of a cationic dicarbonyl species, and a ν(S=O) band at 1020 cm^{-1}. The lowering of the ν(S=O) from 1080 cm^{-1} in free **1**[1] to 1020 cm^{-1} in the product is strongly suggestive of structure **18** rather than that of the immediate precursor in eq 3.

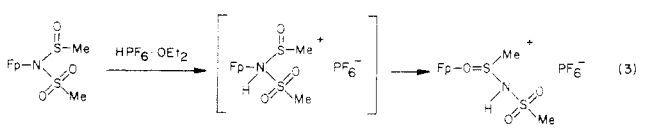

(3)

18

Solutions of **18** in acetone-d_6 undergo a rapid chemical transformation, which was examined by ^{1}H NMR spectroscopy. Thus, freshly prepared solutions (ca. 1 min) show intense signals at δ 5.50 (Cp), 3.30 (Me), and 3.02 (Me), in addition to weak signals at δ 5.67 (Cp), 3.11 (Me), and 2.97 (Me). After about 5 min, the former set of resonances disappears, the latter one increases in intensity, and a new, weaker set appears at δ 5.90 (Cp), 4.07 (Me), and 3.35 (Me). The more intense set of resonances is assigned to the products of reaction of **18** with $(CD_3)_2CO$ (eq 4), whereas the weaker set corresponds to the signals observed for **20** (vide infra). The assignment of the δ 5.67 resonance to the Cp group of $CpFe(CO)_2[OC(CD_3)_2]^+$ was confirmed on an authentic sample of this species.[17]

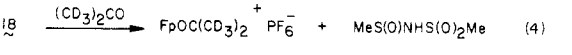

(4)

Alkylation of **1** (R = R′ = Me) with Et_3OPF_6 in CH_2Cl_2 affords an air-stable orange-red solid, which is formulated as **19** on the basis of chemical analysis, electrical conductivity, and IR and ^{1}H NMR data. Thus, the position of the ν(CO) absorptions indicates a cationic dicarbonyl species, and the absence of a ν(S=O) absorption suggests that alkylation occurred at the sulfinyl oxygen. The appearance of the CH_2 resonance as a quartet at δ 4.36 supports the presence of an OEt moiety. **19** is more stable than **18** in acetone-d_6; however, prolonged storage (24 h) leads to the appearance in the ^{1}H NMR spectrum of the resonance characteristic of $CpFe(CO)_2[OC(CD_3)_2]^+$ (δ 5.67).

The previously mentioned complex **20** arises upon protonation of **3** (R = R′ = Me) with $HPF_6{\cdot}OEt_2$. This yellow product is stable in the solid and in solutions of polar organic solvents. Its IR spectrum reveals a ν(NH) band at 3255 cm^{-1} and $\nu(SO_2)$ and ν(S=O) bands at 1370, 1180, and 1165 cm^{-1}. The appearance of a ν(S=O) absorption at 1180 or 1165 cm^{-1} further points to the presence of an NH rather than an SOH moiety. Complexes $\{CpFe(CO)(L)[S(O)(OEt)Me]\}PF_6$ (L = CO, PPh_3) show an IR ν(S=O) absorption at 1190–1188 cm^{-1}.[18]

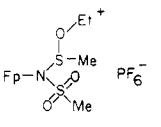

19

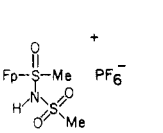

20

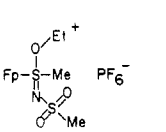

21

Reaction of **3** (R = R′ = Me) with Et_3OPF_6 leads to the isolation of a yellow solid which could not be completely characterized owing to low stability. Nonetheless, the appearance of the IR ν(CO) bands at 2080 and 2045 cm^{-1}, the absence of a ν(S=O) absorption, and the appearance of the CH_2 proton resonance as a quartet at δ 5.07 collectively suggest that alkylation occurred at the sulfinyl oxygen to yield complex **21**.

Complex **2** (R = R′ = Me) does not react with an equimolar amount of Et_3OPF_6 in CH_2Cl_2 at room temperature in 24 h. However, it does react readily under comparable conditions with $HPF_6{\cdot}OEt_2$ to yield **22** as a stable red solid. This formulation is based on chemical analysis, electrical conductivity, and spectroscopic data. The IR spectrum reveals the presence of an NH bond (ν(NH) 3240 cm^{-1}) and two inequivalent SO_2 groups ($\nu(SO_2)$ 1370, 1310, 1175, 1145 cm^{-1}) in a cationic dicarbonyl complex (ν(CO) 2060, 2005 cm^{-1}). The absence of a ν(S=N) absorption at 1100–900 cm^{-1} points to protonation at the uncoordinated rather than the Fe-bonded nitrogen. A fresh solution of **22** in acetone-d_6 shows the expected ^{1}H NMR signals at δ 5.62 (Cp), 3.64 (Me), 3.40 (Me), and 3.17 (Me). However, after 15 min, new signals are discernible at δ 5.67 (Cp), 3.29 (Me), and 3.13 (2 Me), suggestive of the reaction in eq 5. The two $S(O)_2Me$ groups in $MeS(O)_2NSNHS(O)_2Me$ would be rendered equivalent by rapid proton transfer between the nitrogen atoms.

(17) Foxman, B. M.; Klemarczyk, P. T.; Liptrop, R. E.; Rosenblum, M. *J. Organomet. Chem.* **1980**, *187*, 253.
(18) Poffenberger, C. A.; Wojcicki, A. *Inorg. Chem.* **1980**, *19*, 3795.

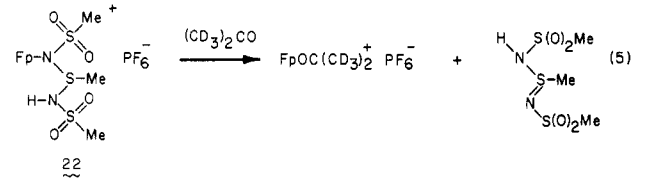

22

The foregoing protonation and alkylation reactions of **1**, **2**, and **3** reflect an interesting selectivity. Protonation proceeds to products containing an N–H bond, whereas alkylation occurs at the sulfinyl oxygen to yield S–O–R. Consistent with this pattern, complex **3**, which lacks an S=O group, is not alkylated by Et_3OPF_6. The selectivity in point may be a consequence of the relative hardness (or softness) of the H^+ and Et^+ acids and the N-donor and O-donor bases.

Conclusions

The behavior of *N*-sulfinyl sulfonamides and sulfur bis(sulfonylimide)s toward 18-electron transition-metal carbonyl and nitrosyl alkyl complexes parallels in many respects that of sulfur dioxide. Nonetheless, several important differences are apparent.

Thus, R'S(O)$_2$NSO insert into M'–R bonds generally to yield the N-bonded M'{N[S(O)$_2$R']S(O)R}, analogous to the M'[OS(O)R] from the SO_2 insertion. However, compared to the O-bonded sulfinates, these products are much more stable with respect to arrangement to their S-bonded linkage isomers. Several M'{N[S(O)$_2$R']S(O)R} complexes were readily isolated and characterized, and for CpCr(NO)$_2${N[S(O)$_2$Me]S(O)Me} linkage isomerization could not be effected even upon prolonged heating. Reactions of CpM(CO)$_3$R (M = Mo, W) with MeS(O)$_2$NSO yielded, in addition to the presumed CpM(CO)$_3${N[S(O)$_2$Me]S(O)R}, another product, possibly O-bonded CpM(CO)$_3${OS[NS(O)$_2$Me]R}. Both species are stable only at low temperature and decompose upon warming to intractable materials. Reaction between Mn(CO)$_5$Me and MeS(O)$_2$NSO also afforded an insertion product stable only at low temperature and assumed to contain an Mn{N[S(O)$_2$Me]S(O)Me} fragment.

Insertion of [R'S(O)$_2$N]$_2$S into M'–R bonds almost invariably yields M'{N[S(O)$_2$R']S(R)NS(O)$_2$R'} products. Unlike M'[OS(O)R] and M'{N[S(O)$_2$R']S(O)R}, these complexes display no tendency to undergo linkage rearrangement to the corresponding S-bonded isomers upon heating. However, Mn(CO)$_4$(L){N[S(O)$_2$Me]S(Me)NS(O)$_2$Me} (L = CO, PPh_3) convert at room temperature to the chelates (CO)$_3$(L)Mn{N[S(O)$_2$Me]S(Me)NS(O)$_2$Me}, probably owing to the lability of ligated CO.

Experimental Section

General Procedures. Irradiation experiments were carried out in Pyrex tubes with 350-nm lamps in a Rayonet Model RPR-100 photochemical reactor. Melting points were measured on a Thomas-Hoover capillary melting point apparatus and are uncorrected. Elemental analysis was done by Galbraith Laboratories, Inc., Knoxville, TN.

Physical Measurements. IR spectra were recorded on a Perkin-Elmer Model 337 spectrophotometer and were calibrated with polystyrene. Ambient temperature ^{1}H NMR spectra were measured on a Varian Associates EM-360L or EM-390 spectrometer with use of Me_4Si as an internal reference. Low-temperature ^{1}H NMR spectra were recorded on a Varian Associates EM-390 or HA-100 spectrometer. Mass spectra were obtained at 70 eV on an AEI Model MS-9 spectrometer by Mr. C. R. Weisenberger. Molar conductance was measured on ca. 10^{-3} M solutions by using a Lab-Line No. 11200 beaker-type conductivity cell in conjunction with an Industrial Instruments, Inc., Model RC 16B2 conductivity bridge.

Table III. Crystallographic Details for 3a·$^1/_2CH_2Cl_2$

mol formula	$C_{15}H_{15}FeNO_5S_2 \cdot {}^1/_2CH_2Cl_2$
mol wt	451.73
space group	$P\bar{1}$
a, Å	8.517 (7)
b, Å	10.624 (5)
c, Å	12.092 (9)
α, deg	109.58 (5)
β, deg	90.05 (6)
γ, deg	108.06 (5)
V, Å^3	973
Z	2
ρ_{calcd}, g cm^{-3}	1.541
radiatn	graphite-monochromated Mo Kα (λ(Kα_1) = 0.709 26 Å)
linear abs coeff, cm^{-1}	11.41
temp, °C	20 (1)
2θ limits	$4° \le 2\theta \le 50°$
scan speed	6°/min in 2θ
background time/scan time	0.5
scan range	1.0° below Kα_1 to 1.0° above Kα_2
data collected	$^+h,^\pm k,^\pm l$
unique data	3408
unique data, with $F_o^2 > 3\sigma(F_o^2)$	2178
final no. of variables	235
$R(F)^a$	0.040
$R_w(F)^b$	0.040
error in observn of unit weight, e	2.13

$^a R(F) = \sum||F_o| - |F_c||/\sum|F_o|$. $^b R_w(F) = [\sum w(|F_o| - |F_c|)^2/\sum wF_o^2]^{1/2}$ with $w = {}^1/\sigma^2(F_o)$.

Materials. All solvents were reagent grade quality and were purified further by the methods described by Jolly[19] prior to use. Commercially procured reagents were used as received. Literature procedures were employed to synthesize MeS(O)$_2$NSO,[20] *p*-ClC$_6$H$_4$S(O)$_2$NSO,[20] and [MeS(O)$_2$N]$_2$S.[16]

The following metal complexes were prepared by established methods: CpFe(CO)(PPh$_3$)Me,[21] CpFe(CO)[P(OPh)$_3$]Me,[22] CpMo(CO)$_3$Me,[23] CpMo(CO)$_2$(PPh$_3$)Me,[24] CpMo(CO)$_2$(PMe$_2$Ph)Me,[25] CpW(CO)$_3$Me,[23] CpW(CO)$_2$(PPh$_3$)Me,[26] CpCr(NO)$_2$Me,[23] Mn(CO)$_5$Me,[27] *cis*-Mn(CO)$_4$(PPh$_3$)Me,[28] CpFe(CO)$_2${N[S(O)$_2$Me]S(O)Me},[1] CpFe(CO)$_2${S[NS(O)$_2$Me](O)Me},[1] and CpFe(CO)$_2${N[S(O)$_2$Me]S(Me)NS(O)$_2$Me}.[1] CpW(CO)$_2$(PMe$_2$Ph)Me was prepared by irradiation of CpW(CO)$_3$Me and PMe$_2$Ph according to a general photochemical route to CpW(CO)$_2$(L)Me,[26,29] whereas CpMo(CO)$_3$CH$_2$C$_6$H$_4$Cl-*p* was synthesized by reaction of Na[CpMo(CO)$_3$] with ClCH$_2$C$_6$H$_4$Cl-*p* in a manner similar to that for CpMo(CO)$_3$Me.[23]

Crystallographic Analysis of CpFe(CO)$_2${S[NS(O)$_2$Me](O)CH$_2$Ph}·$^1/_2$CH$_2$Cl$_2$ (3a·$^1/_2$CH$_2$Cl$_2$). Crystals for X-ray diffraction of the previously prepared[1] title complex were grown from a 1:4 CH_2Cl_2–pentane solution at room temperature. An irregularly shaped crystal was used for data collection. The crystal system is triclinic with space group *P*1 or $P\bar{1}$. Cell parameters were determined by the least-squares fit of diffractometer setting angles for 13 reflections using Mo Kα radiation.

Intensity data were collected by the θ–2θ scan technique on a Syntex P$\bar{1}$ diffractometer. Ten standard reflections were

(19) Jolly, W. L. "The Synthesis and Characterization of Inorganic Compounds"; Prentice-Hall: New York, 1970.
(20) Kresze, G.; Maschke, A.; Albrecht, R.; Bederke, K.; Patzschke, H. P.; Smalla, H.; Trede, A. *Angew. Chem., Int. Ed. Engl.* **1962**, *1*, 89.
(21) Treichel, P. M.; Shubkin, R. L.; Barnett, K. W.; Reichard, D. *Inorg. Chem.* **1966**, *5*, 1177.
(22) Su, S. R.; Wojcicki, A. *J. Organomet. Chem.* **1971**, *27*, 231.
(23) Piper, T. S.; Wilkinson, G. *J. Inorg. Nucl. Chem.* **1956**, *3*, 104.
(24) Barnett, K. W.; Treichel, P. M. *Inorg. Chem.* **1967**, *6*, 294.
(25) Barnett, K. W.; Pollman, T. G. *J. Organomet. Chem.* **1974**, *69*, 413.
(26) Severson, R. G.; Wojcicki, A. *Ibid.* **1978**, *157*, 173.
(27) Closson, R. D.; Kozikowski, J.; Coffield, T. H. *J. Org. Chem.* **1957**, *22*, 598.
(28) Kraihanzel, C. S.; Maples, P. K. *J. Am. Chem. Soc.* **1965**, *87*, 5267.
(29) Alt, H. G. *J. Organomet. Chem.* **1977**, *124*, 167.

Table IV. Positional Parameters of Non-Hydrogen Atoms of 3a•$^1/_2CH_2Cl_2$, with Estimated Standard Deviations in Parentheses

atom	x	y	z
Fe	0.98424 (7)	0.13375 (6)	0.29118 (5)
S(1)	0.77689 (13)	0.21805 (11)	0.33926 (9)
S(2)	0.76603 (14)	0.25908 (12)	0.57890 (10)
O(1)	0.83535 (44)	−0.02349 (38)	0.04631 (30)
O(2)	0.82122 (43)	−0.11946 (34)	0.34838 (33)
O(3)	0.61400 (33)	0.10444 (28)	0.29735 (25)
O(4)	0.84171 (43)	0.37662 (32)	0.68525 (26)
O(5)	0.81400 (41)	0.13569 (32)	0.55839 (28)
N	0.79553 (43)	0.32047 (33)	0.47448 (29)
C(1)	0.89158 (58)	0.04289 (49)	0.14223 (46)
C(2)	0.88092 (54)	−0.01781 (48)	0.32973 (40)
C(3)	0.55193 (61)	0.20428 (59)	0.58618 (48)
C(4)	1.20857 (56)	0.13475 (52)	0.36323 (48)
C(5)	1.22707 (56)	0.14682 (57)	0.25090 (47)
C(6)	1.19658 (57)	0.27310 (57)	0.25721 (50)
C(7)	1.16158 (55)	0.33617 (48)	0.37034 (52)
C(8)	1.16564 (57)	0.24986 (53)	0.43547 (43)
C(9)	0.77830 (57)	0.35082 (43)	0.27570 (36)
C(10)	0.76942 (55)	0.30065 (42)	0.14341 (36)
C(11)	0.62322 (60)	0.20528 (49)	0.07176 (43)
C(12)	0.61737 (69)	0.16090 (51)	−0.04898 (45)
C(13)	0.75392 (75)	0.21092 (50)	−0.10062 (41)
C(14)	0.89881 (71)	0.30569 (51)	−0.03171 (44)
C(15)	0.90566 (61)	0.35016 (44)	0.08943 (39)
Cl(1)	0.3722 (13)	0.3919 (11)	0.8912 (11)
Cl(2)	0.4308 (18)	0.5086 (12)	1.1065 (11)
Cl(3)	0.3436 (14)	0.3878 (11)	0.9777 (13)
Cl(4)	0.5606 (20)	0.5575 (13)	1.1417 (12)
C(16)	0.5	0.5	1.0

measured after every 150 reflections and indicated a small rate of crystal decay. The data were corrected for the slight decay and put on an absolute scale using a Wilson plot.[30] No correction for absorption was made; it is estimated that lack of this correction introduces a maximum systematic error of 8.7%. Crystallographic details appear in Table III.

Intensity statistics indicated a centric space group. The structure was solved in $P\bar{1}$ by the Patterson method. The whole molecule was located by several cycles of structure factor and Fourier calculations. The structure was refined by the full-matrix least-squares procedure of the SHELX76 package[31] with the function minimized: $\sum w(|F_o| - |F_c|)^2$ where $w = 1/\sigma^2(F_o)$. After one cycle of anisotropic refinement of the non-hydrogen atoms, most of the hydrogen atoms were located in a difference electron density map. The hydrogen atoms were added as fixed contributions to the model with C–H = 1.00 Å and $B_H = B_C + 1.0$ Å^2. Also very prominent in this map was the appearance of a disordered CH_2Cl_2 solvent molecule with the carbon atom located at an inversion center. Two CH_2Cl_2 molecules were added to the model. Both molecules were located at an inversion center, had the carbon atom in common, and have slightly different orientations. The hydrogen atoms of the CH_2Cl_2 were not included in the model. The occupancy factors for the two CH_2Cl_2 molecules converged to values of 0.24 (1) and 0.26 (1), so that the orientations are present in approximately equal amounts. The final cycle of least-squares refinement converged to the R and R_w values listed in Table III (anisotropic refinement of the non-hydrogen atoms, isotropic refinement of the solvent molecules, and the hydrogen atoms held fixed). The final difference electron density map has a maximum peak height of 0.37 e Å^{-3}, which is in the vicinity of the disordered solvent molecule. The geometry of the CH_2Cl_2 molecule is poor, and the thermal parameter for the carbon atom is high. These are probably the result of treating the disorder with a single carbon atom and should have very little effect on the geometry of the molecule of interest.

(30) Programs used for data reduction are from the CRYM crystallographic computing package: Duchamp, D. J., American Crystallographic Association Meeting, Bozeman, MT, 1964, B14, and modified by G. G. Christoph at The Ohio State University.

(31) Sheldrick, G. M. "SHELX76 Program for Crystal Structure Determination"; University Chemical Laboratory: Cambridge, England, 1976.

Positional parameters of the non-hydrogen atoms are given in Table IV. Listings of temperature factors, hydrogen atom coordinates, and structure factors are available as supplementary material.[32]

Reactions of Metal–Alkyl Complexes with *N*-Sulfinyl Sulfonamides and Sulfur Bis(sulfonylimides)s. General Procedures. Reactions were conducted under an atmosphere of dry nitrogen and, unless otherwise indicated, at room temperature. Sample preparation and various manipulations of air- and/or moisture-sensitive materials were performed in a drybox filled with argon or on a vacuum line. Chromatography was done on columns packed with 60–100 mesh Florisil.

Reactions of CpFe(CO)(PPh$_3$)Me with R′S(O)$_2$NSO (R′ = *p*-ClC$_6$H$_4$, Me). A solution containing 1.2 g (3.0 mmol) of the title complex in 25 mL of CH_2Cl_2 was treated with 0.70 g (3.0 mmol) of *p*-$ClC_6H_4S(O)_2NSO$. Immediately the color changed from red to green. The solution was stirred for 10 min, concentrated to 10 mL, and chromatographed on a 20 × 1 cm column. A green band was developed which gradually changed color to red on elution with acetone. The red effluent was evaporated to dryness, and the glasslike residue was dissolved in 10 mL of CH_2Cl_2. Addition of 30 mL of pentane with stirring afforded 0.75 g (40% yield) of a red solid, **5a**: mp 60 °C dec; ^{1}H NMR ($CDCl_3$) δ 7.8–7.3 (m, 3Ph, C_6H_4), 4.66, 4.64 (s × 2, Cp), 3.32, 2.62 (s × 2, Me); IR ($CHCl_3$) ν(CO) 1970 (vs) cm^{-1}.

A similar reaction was conducted at 0 °C between the title complex and $MeS(O)_2NSO$ to yield an unstable red solid. The product decomposed within ca. 15 min when stored at room temperature.

Reaction of CpFe(CO)(PPh$_3$)Me with [MeS(O)$_2$N]$_2$S. A solution containing 1.0 g (2.3 mmol) of the title complex in 30 mL of CH_2Cl_2 at 0 °C was treated with 0.50 g (2.3 mmol) of $[MeS(O)_2N]_2S$. Immediately the color changed from red to green. The reaction mixture was stirred at 0 °C for 5 min and then chromatographed on a 20 × 1 cm column which was maintained at ca. 5 °C by means of a water-cooled jacket. A green band developed and was eluted with acetone. The effluent was evaporated to dryness to afford a green glasslike material, **6a**, which showed noticeable decomposition above 10 °C: ^{1}H NMR ($CDCl_3$) δ 8.0–7.0 (m, 3Ph), 5.00 (s, Cp), 3.10 (s, O_2SMe), 2.95 (s, O_2SMe), 1.90 (br, SMe); IR (Nujol) ν(CO) 1970 (vs) cm^{-1}.

Reaction of CpFe(CO)[P(OPh)$_3$]Me with MeS(O)$_2$NSO. To 1.5 g (3.2 mmol) of the title complex dissolved in 20 mL of CH_2Cl_2 was added 0.45 g (3.2 mmol) of $MeS(O)_2NSO$, and the resulting solution was stirred for 15 min, during which time it changed from yellow to orange. The solution was then chromatographed; the orange band with a trailing yellow edge was eluted with acetone, and the effluent was evaporated to dryness. The residue was redissolved in 50 mL of CH_2Cl_2, and the orange solution was kept at reflux for 6 h as its color changed to yellow. After being cooled to room temperature, the solution was concentrated and chromatography was repeated. The yellow effluent was evaporated to dryness, and the residue was crystallized from 10 mL of CH_2Cl_2 and 40 mL of pentane to afford 0.70 g (47% yield) of a yellow solid, **5c**: mp 140 °C dec; ^{1}H NMR ($CDCl_3$) δ 7.6–7.0 (m, 3Ph), 4.68, 4.59 (s × 2, Cp), 3.52, 3.63 (s × 2, OSMe), 3.04 (s, O_2SMe); IR ($CHCl_3$) ν(CO) 2000 (vs) cm^{-1}, (Nujol) ν(SO_2) 1270 (s), 1190 (s), ν(S=O), ν(S=N) 1130 (s), 1020 (s) cm^{-1}. Anal. Calcd for $C_{26}H_{26}FeNO_7PS_2$: C, 50.74; H, 4.26. Found: C, 50.57; H, 4.27.

Reaction of CpFe(CO)[P[OPh)$_3$]Me with [MeS(O)$_2$N]$_2$S. To 1.0 g (2.1 mmol) of the title complex dissolved in 30 mL of CH_2Cl_2 was added 0.50 g (2.3 mmol) of $[MeS(O)_2N]_2S$, and the reaction mixture was stirred for 30 min, during which time it gradually changed color from yellow to red. The solution was then chromatographed, and a red band was eluted with acetone. Evaporation of the effluent to dryness gave a glasslike material, which upon dissolution in 5 mL of CH_2Cl_2 and addition of 30 mL of pentane afforded a red precipitate. This solid **6b** was washed several times with 5-mL portions of Et_2O and then twice with 5-mL portions of pentane: ^{1}H NMR ($CDCl_3$) δ 7.5–7.0 (m, 3Ph), 4.80 (s, Cp), 3.20, 3.13 (s × 2, O_2SMe), 2.91, 2.97 (s × 2, O_2SMe), 2.58 (br, SMe); IR (Nujol) ν(CO) 1990 (vs), ν(SO_2) 1310 (s), 1285

(32) See paragraph at end of paper regarding supplementary material.

(s), 1205 (s), 1175 (s), 1145 (s), ν(S=N) 1020 (s) cm^{-1}.

Reactions of $CpMo(CO)_2(L)Me$ (L = PMe_2Ph, PPh_3) with $MeS(O)_2NSO$. A solution of 0.70 g (2.0 mmol) of $CpMo(CO)_2(PMe_2Ph)Me$ in 25 mL of CH_2Cl_2 was treated with 0.30 g (2.1 mmol) of $MeS(O)_2NSO$, stirred for 10 min, concentrated to 5 mL, and chromatographed. A red and a yellow band developed. Upon elution with 1:1 CH_2Cl_2–acetone the red band gradually turned yellow resulting in the appearance of a single broad band. This broad yellow band was removed with acetone, and the collected solution was evaporated to dryness. The product was recrystallized from 10 mL of CH_2Cl_2 and 30 mL of pentane. The yield of a yellow crystalline solid, **7a**, mp 145 °C dec, was 0.80 g (73%): ^1H NMR ($CDCl_3$) δ 7.8–7.5 (m, Ph), 5.31 (d, J_{PH} = 2 Hz, Cp), 3.61 (s, OSMe), 3.08 (s, O_2SMe), 2.01 (d, J_{PH} = 9 Hz, PMe_2); IR ($CHCl_3$) ν(CO) 1985 (m), 1905 (vs) cm^{-1}, (Nujol) $\nu(SO_2)$ 1260 (s), 1130 (s), ν(S=O), ν(S=N) 1110 (s), 1000 (s) cm^{-1}. Anal. Calcd for $C_{17}H_{22}MoNO_5PS_2$: C, 39.93; H, 4.34. Found: C, 39.71; H, 4.31.

A similar reaction between $CpMo(CO)_2(PPh_3)Me$ and $MeS(O)_2NSO$ afforded a yellow crystalline product, **7b**, mp 140 °C dec, in 76% yield: ^1H NMR ($CDCl_3$) δ 7.6–7.3 (m, 3Ph), 5.30 (br, Cp), 3.62 (s, OSMe), 3.05 (s, O_2SMe); IR ($CHCl_3$) ν(CO) 1990 (m), 1895 (vs) cm^{-1}, (Nujol) $\nu(SO_2)$ 1280 (s), 1140 (s), ν(S=O), ν(S=N) 1110 (s), 1005 (s) cm^{-1}.

Reaction of $CpMo(CO)_2(PMe_2Ph)Me$ with $[MeS(O)_2N]_2S$. To a solution containing 2.0 g (5.4 mmol) of $CpMo(CO)_2(PMe_2Ph)Me$ in 30 mL of CH_2Cl_2 was added 1.2 g (5.5 mmol) of $[MeS(O)_2N]_2S$. The resulting mixture changed color from yellow to red within a few minutes as stirring was continued for 20 min. Concentration of the reaction solution to 10 mL and addition of 40 mL of pentane resulted in the formation of a yellow precipitate which has collected by filtration. The yield of **9a** was 1.8 g (56%): ^1H NMR ($CDCl_3$) δ 7.7–7.4 (m, Ph), 5.19 (d, J_{PH} = 2.5 Hz, Cp), 3.24 (s, O_2SMe), 2.91 (s, Me), 2.85 (s, Me), 1.97 (d, J_{PH} = 9 Hz, PMe_2); IR (Nujol) ν(CO) 1965 (m), 1865 (vs), $\nu(SO_2)$ 1320 (s), 1300 (s), 1130 (s), ν(S=N) 1000 (s) cm^{-1}. The product decomposed within 48 h at room temperature.

Reaction of $CpW(CO)_2(PMe_2Ph)Me$ with $MeS(O)_2NSO$. To a solution of 1.0 g (2.1 mmol) of $CpW(CO)_2(PMe_2Ph)Me$ in 25 mL of CH_2Cl_2 was added 0.30 g (2.1 mmol) of $MeS(O)_2NSO$. The resulting solution was stirred for 30 min, concentrated to 5 mL, and treated with 30 mL of pentane to precipitate a red solid, **8c**. The yield was 0.80 g (64%). **8c**: ^1H NMR ($CDCl_3$) δ 7.7–7.3 (m, Ph), 5.19 (d, J_{PH} = 2.5 Hz, Cp), 3.08 (s, O_2SMe), 2.71 (s, OSMe), 2.05 (d, J_{PH} = 9 Hz, PMe_2); IR (Nujol) ν(CO) 1950 (m), 1850 (vs), $\nu(SO_2)$ 1300 (s), 1140 (s), ν(S=O) 1080 (s) cm^{-1}. The complex gradually decomposed at room temperature.

Reaction of $CpW(CO)_2(PPh_3)Me$ with $MeS(O)_2NSO$. A solution of 1.0 g (1.7 mmol) of $CpW(CO)_2(PPh_3)Me$ and 0.25 g (1.7 mmol) of $MeS(O)_2NSO$ in 30 mL of CH_2Cl_2 was stirred for 15 min and then treated with 100 mL of pentane to induce the precipitation of a red solid. The solid **8d** was recrystallized from 10 mL of CH_2Cl_2 and 30 mL of pentane. The yield was 0.50 g (40%). **8d**: ^1H NMR ($CDCl_3$) δ 7.6–7.1 (m, 3Ph), 5.21 (d, J_{PH} = 2.5 Hz, Cp), 3.10 (s, O_2SMe), 2.61 (s, OSMe); IR (Nujol) ν(CO) 1960 (m), 1850 (vs), $\nu(SO_2)$ 1310 (s), 1145 (s), ν(S=O) 1090 (s) cm^{-1}.

Thermolysis of $CpW(CO)_2(PPh_3)\{N[S(O)_2Me]S(O)Me\}$ (8d). The title complex (0.5 g) was dissolved in 50 mL of CH_2Cl_2, and the resulting solution was maintained at reflux for 10 h. After being cooled to 25 °C, the solution was concentrated and chromatographed. A yellow band was eluted with acetone, the solvent was evaporated, and the residue was recrystallized from 5 mL of CH_2Cl_2 and 20 mL of pentane. The yield of yellow crystals of **7d**, mp 147 °C dec, was 0.3 g (60%): ^1H NMR ($CDCl_3$) δ 7.6–7.3 (m, 3Ph), 5.41 (d, J_{PH} = 1.5 Hz, Cp), 3.80 (s, OSMe), 3.04 (s, O_2SMe); IR ($CHCl_3$) ν(CO) 1980 (m), 1895 (vs) cm^{-1}, (Nujol) $\nu(SO_2)$ 1270 (s), 1130 (s), ν(S=O), ν(S=N) 1100 (s), 1000 (s) cm^{-1}.

Reaction of $CpW(CO)_2(PPh_3)Me$ with $[MeS(O)_2N]_2S$. To a solution of 1.5 g (2.6 mmol) of $CpW(CO)_2(PPh_3)Me$ in 35 mL of CH_2Cl_2 was added 0.55 g (2.6 mmol) of $[MeS(O)_2N]_2S$. After being stirred for 30 min, the solution was concentrated to 10 mL and treated with 50 mL of pentane to precipitate a red solid, **9d**. The yield was 1.2 g (58%). **9d**: ^1H NMR ($CDCl_3$) δ 7.7–7.0 (m, 3Ph), 5.22 (d, J_{PH} = 2.5 Hz, Cp), 3.25 (s, O_2SMe), 2.86 (s, Me), 2.82 (s, Me); IR (Nujol) ν(CO) 1965 (m), 1865 (vs), $\nu(SO_2)$ 1310 (s), 1160 (s), 1140 (s), 1100 (s), ν(S=N) 1010 (s) cm^{-1}. The product gradually decomposed at room temperature.

Reaction of $CpMo(CO)_3Me$ with $[MeS(O)_2N]_2S$. A solution of 0.36 g (1.4 mmol) of $CpMo(CO)_3Me$ in 30 mL of CH_2Cl_2 at 0 °C was treated with 0.30 g (1.4 mmol) of $[MeS(O)_2N]_2S$ and then stirred at 0 °C for 30 min. Chromatography at ca. 5 °C afforded two bands. The yellow band was eluted with CH_2Cl_2 and, upon evaporation of the solvent, gave 0.1 g of unreacted $CpMo(CO)_3Me$. The red band was eluted with acetone and afforded an unstable glasslike material upon evaporation to dryness: ^1H NMR ($CDCl_3$) δ 5.87 (s, Cp), 3.14 (s, O_2SMe), 2.95 (s, O_2SMe), 2.53 (s, SMe); IR ($CHCl_3$) ν(CO) 2050 (s), 1980 (vs), 1960 (vs) cm^{-1}.

Reaction of $Mn(CO)_5Me$ with $[MeS(O)_2N]_2S$. A solution of 0.85 g (4.0 mmol) of $Mn(CO)_5Me$ in 25 mL of CH_2Cl_2 was treated with 0.87 g (4.0 mmol) of $[MeS(O)_2N]_2S$, and the resulting mixture was stirred for 2 h. To this solution was added 60 mL of pentane to precipitate a yellow solid, **15a**, which was collected by filtration and washed first several times with 5-mL portions of Et_2O and then twice with 5-mL portions of pentane, mp 80 °C dec. The yield was 1.1 g (65%). **15a**: ^1H NMR ($CDCl_3$) δ 3.20 (s, SMe), 3.04 (s, $2O_2SMe$); IR ($CHCl_3$) ν(CO) 2145 (w), 2045 (s), 1950 (s), 1930 (s) cm^{-1}, (Nujol) $\nu(SO_2)$ 1320 (s), 1140 (s), ν(S=N) 960 (m), 920 (m) cm^{-1}. The product gradually decomposed at room temperature.

Reaction of *cis*-$Mn(CO)_4(PPh_3)Me$ with $[MeS(O)_2N]_2S$. To 1.0 g (2.2 mmol) of the title complex dissolved in 30 mL of CH_2Cl_2 was added with stirring 0.50 g (2.3 mmol) of $[MeS(O)_2N]_2S$. Stirring was continued for 2 h, and then the deep yellow solution was treated with 60 mL of pentane to precipitate a yellow solid. The product **15b** was recrystallized from 10 mL of CH_2Cl_2 and 40 mL of cyclohexane, mp 125 °C dec. The yield was 1.2 g (80%). **15b**: ^1H NMR ($CDCl_3$) δ 7.9–7.3 (m, 3Ph), 3.19 (s, $2O_2SMe$), 1.99 (s, SMe); IR ($CHCl_3$) ν(CO) 2035 (vs), 1950 (vs), 1930 (vs) cm^{-1}, (Nujol) $\nu(SO_2)$ 1320 (s), 1300 (s), 1140 (s), ν(S=N) 920 (s), 900 (s) cm^{-1}. Anal. Calcd for $C_{24}H_{24}MnN_2O_7PS_3$: C, 45.43; H, 3.81. Found: C, 45.29; H, 3.88.

Reactions of $(CO)_4\overline{Mn\{N[S(O)_2Me]S(Me)NS(O)_2Me\}}$ with L (L = C_5H_5N, PPh_3). Freshly prepared title complex (1.0 g, 2.6 mmol) and C_5H_5N (0.50 g, 6.3 mmol) were allowed to react in 30 mL of CH_2Cl_2 for ca. 4 h. Pentane (60 mL) was then added to precipitate the product which was collected by filtration and washed with Et_2O and pentane. The yield of a yellow solid, **15c**, mp 120 °C dec, was 0.25 g (21%): ^1H NMR ($CDCl_3$) δ 9.20 (d, J = 6 Hz, 2,6 H of C_5H_5N), 8.2–7.3 (m, 3,4,5 H of C_5H_5N), 3.28 (s, $2O_2SMe$), 2.25 (s, SMe); IR ($CHCl_3$) ν(CO) 2040 (vs), 1925 (vs), 1900 (vs) cm^{-1}, (Nujol) $\nu(SO_2)$ 1300 (s), 1135 (s), ν(S=N) 960 (m), 925 (m) cm^{-1}. Anal. Calcd for $C_{11}H_{14}MnN_3O_7S_3$: C, 29.27; H, 3.13. Found: C, 29.17; H, 3.25.

A similar reaction between the title complex (1.0 g, 2.6 mmol) and PPh_3 (0.70 g, 2.7 mmol) afforded 0.40 g (23%) of **15b**.

Reaction of $CpCr(NO)_2Me$ with $MeS(O)_2NSO$. Addition of 0.40 g (2.8 mmol) of $MeS(O)_2NSO$ to 0.50 g (2.6 mmol) of $CpCr(NO)_2Me$ in 25 mL of CH_2Cl_2 resulted in the formation of a deep green solution. This solution was stirred for 30 min, concentrated to 10 mL, and chromatographed. A green band that developed was eluted with acetone. Removal of the solvent afforded a green oil, **16**, which could not be induced to crystallize. The yield was 0.70 g (77%). **16**: ^1H NMR ($CDCl_3$) δ 5.79 (s, Cp), 3.00 (s, O_2SMe), 2.60 (s, SMe); IR ($CHCl_3$) ν(NO) 1815 (vs), 1700 (vs) cm^{-1}, (neat) $\nu(SO_2)$ 1300 (s), 1140 (s), ν(S=O) 1090 (s) cm^{-1}; mass spectrum, m/e 303 $(P - NO)^+$ (weak), 273 $(P - 2NO)^+$ (strong), 258 $(P - 2NO - Me)^+$ (strong).

Reaction of $CpCr(NO)_2Me$ with $[MeS(O)_2N]_2S$. To a solution of 0.50 g (2.6 mmol) of $CpCr(NO)_2Me$ in 25 mL of CH_2Cl_2 was added 0.60 g (2.7 mmol) of $[MeS(O)_2N]_2S$, and the resulting mixture was stirred for 15 min. The solution was then concentrated to 10 mL and chromatographed. Acetone eluted a green band which, upon evaporation of the solvent, yielded 0.80 g (73%) of a dark green oil, **17**. The oil could not be induced to crystallize: ^1H NMR ($CDCl_3$) δ 5.84 (s, Cp), 3.11 (s, O_2SMe), 2.92 (s, O_2SMe), 2.81 (s, SMe); IR ($CHCl_3$) ν(NO) 1820 (vs), 1710 (vs) cm^{-1}, (neat) $\nu(SO_2)$ 1308 (s), 1285 (s), 1130 (s), ν(S=N) 1015 (s) cm^{-1}; mass spectrum, m/e 350 $(P - 2NO)^+$ (strong).

Reaction of $CpFe(CO)_2\{N[S(O)_2Me]S(O)Me\}$ (1) with $HPF_6{\cdot}OEt_2$. To 0.2 g (0.6 mmol) of the title complex in 15 mL

of CH_2Cl_2 was added 0.2 g (0.9 mmol) of $HPF_6{\cdot}OEt_2$, and the resulting solution was stirred for 15 min. A deep red solid that precipitated was filtered off and washed first with 10 mL of CH_2Cl_2 and then with 10 mL of pentane. The yield of this air-stable product **18**, mp 108 °C dec, was almost quantitative (0.3 g): Λ_m $(MeNO_2)$[33] 108 $\Omega^{-1}cm^2$ mol^{-1}. Anal. Calcd for $C_9H_{12}F_6FeNO_5PS_2$: C, 22.56; H, 2.52. Found: C, 22.68; H, 2.77.

Reaction of $CpFe(CO)_2\{N[S(O)_2Me]S(O)Me\}$ (1) with Et_3OPF_6. The title complex (1.0 g, 3.0 mmol) in 40 mL of CH_2Cl_2 was treated with 0.92 g (3.0 mmol) of Et_3OPF_6, and the resulting solution was stirred for ca. 45 min. A fine orange-red precipitate that appeared was filtered off and washed consecutively with CH_2Cl_2, Et_2O, and pentane; mp 137 °C dec. The yield of **19** was essentially quantitative: ^1H NMR (acetone-d_6) δ 5.70 (s, Cp), 4.26 (q, J = 7 Hz, CH_2), 3.56 (s, SMe), 3.17 (s, O_2SMe), 1.39 (t, J = 7.0 Hz, CMe); IR (Nujol) ν(CO) 2050 (vs), 2010 (vs), $\nu(SO_2)$ 1340 (s), 1160 (s) cm^{-1}; Λ_m $(MeNO_2)$[33] 103 Ω^{-1} cm^2 mol^{-1}. Anal. Calcd for $C_{11}H_{16}F_6FeNO_5PS_2$: C, 26.05; H, 3.18. Found: C, 25.89; H, 3.06.

Reaction of $CpFe(CO)_2\{S[NS(O)_2Me](O)Me\}$ (3) with $HPF_6{\cdot}OEt_2$. The title complex (0.2 g, 0.6 mmol) in 15 mL of CH_2Cl_2 was treated with 0.2 g (0.9 mmol) of $HPF_6{\cdot}OEt_2$, and the resulting solution was stirred for 15 min. A yellow precipitate that formed was filtered off and washed first with 10 mL of CH_2Cl_2 and then with 10 mL of pentane; mp 123 °C dec. The yield of **20** was essentially quantitative: ^1H NMR (acetone-d_6) δ 8.9–8.6 (br, NH), 5.90 (s, Cp), 4.07 (s, OSMe), 3.35 (s, O_2SMe); IR (Nujol) ν(CO) 2080 (vs), 2050 (vs) cm^{-1}; Λ_m $(MeNO_2)$[33] 105 Ω^{-1} cm^2 mol^{-1}. Anal. Calcd for $C_9H_{12}F_6FeNO_5PS_2$: C, 22.56; H, 2.52; N, 2.92. Found: C, 22.38; H, 2.57; N, 2.82.

Reaction of $CpFe(CO)_2\{S[NS(O)_2Me](O)Me\}$ (3) with Et_3OPF_6. To 0.50 g (1.5 mmol) of the title complex in 20 mL of CH_2Cl_2 was added 0.37 g (1.5 mmol) of Et_3OPF_6, and the resulting solution was stirred for 8 h. The reaction mixture was then filtered to separate a trace amount of brown decomposition material from a yellow filtrate. The filtrate was evaporated to a yellow glass, **21**: IR (Nujol) ν(CO) 2080 (vs), 2045 (vs), $\nu(SO_2)$ 1325 (s), 1175 (s), ν(S=N) 980 (m) cm^{-1}. The product decomposed during attempts at crystallization from CH_2Cl_2–pentane or MeCN–Et_2O.

Reaction of $CpFe(CO)_2\{N[S(O)_2Me]S(Me)NS(O)_2Me\}$ (2) with $HPF_6{\cdot}OEt_2$. The title complex (1.0 g, 2.4 mmol) in 20 mL of CH_2Cl_2 was treated with 0.53 g (2.4 mmol) of $HPF_6{\cdot}OEt_2$, and the resulting solution was stirred for 10 min. A red precipitate that formed was filtered off and washed consecutively with Et_2O, CH_2Cl_2, and pentane; mp 140 °C dec. The yield of **22** was quantitative: Λ_m $(MeNO_2)$[33] 108 Ω^{-1} cm^2 mol^{-1}. Anal. Calcd for $C_{10}H_{15}F_6FeN_2O_6PS_3$: C, 21.59; H, 2.72. Found: C, 21.31; H, 2.96.

Acknowledgment. We are grateful to the National Science Foundation for support of this research through Grant CHE-7911882.

Registry No. 1, 66973-81-7; **2**, 66973-87-3; **3**, 66868-27-7; **3a**, 66868-29-9; **3a**·$^1/_2CH_2Cl_2$, 99475-93-1; **5a**, 99475-72-6; **5c**, 99475-74-8; **6a**, 99475-73-7; **6b**, 99475-75-9; **7a**, 99475-76-0; **7b**, 99475-77-1; **7d**, 99475-80-6; **8c**, 99475-78-2; **8d**, 99475-79-3; **9a**, 99494-40-3; **9d**, 99475-81-7; **12a**, 99475-82-8; **15a**, 99475-83-9; **15b**, 99475-84-0; **15c**, 99475-85-1; **16**, 99475-86-2; **17**, 99475-87-3; **18**, 99475-89-5; **19**, 99475-91-9; **20**, 99494-42-5; **21**, 99494-44-7; **22**, 99494-46-9; $CpFe(CO)(PPh_3)Me$, 12100-51-5; $CpFe(CO)[P(OPh)_3]Me$, 12290-98-1; p-$ClC_6H_4S(O)_2NSO$, 52867-26-2; $MeS(O)_2NSO$, 40866-96-4; $[MeS(O)_2N]_2S$, 5636-09-9; *trans*-$CpMo(CO)_2(PMe_2Ph)Me$, 99529-37-0; *trans*-$CpMo(CO)_2(PPh_3)Me$, 32007-82-2; *trans*-$CpW(CO)_2(PMe_2Ph)Me$, 57194-80-6; *trans*-$CpW(CO)_2(PPh_3)Me$, 57236-51-8; $CpMo(CO)_3Me$, 12082-25-6; $Mn(CO)_5Me$, 13601-24-6; *cis*-$Mn(CO)_4(PPh_3)Me$, 14054-69-4; $CpCr(NO)_2Me$, 53522-59-1; $CpFe(CO)_2[OC(CD_3)_2]^+$, 99475-92-0.

Supplementary Material Available: Listings of temperature factors, hydrogen atom coordinates, and structure factors for complex **3a**·$^1/_2CH_2Cl_2$ (12 pages). Ordering information is given on any current masthead page.

(33) For typical values of 1:1 electrolytes in $MeNO_2$ see: Geary, W. J. *Coord. Chem. Rev.* **1971**, *7*, 81.

Revised MNDO parameters for silicon

Michael J. S. Dewar, Eamonn F. Healy, James J. P. Stewart, James. Friedheim, and Gilbert. Grady

Organometallics, **1986**, 5 (2), 375-379• DOI: 10.1021/om00133a029 • Publication Date (Web): 01 May 2002

Revised MNDO Parameters for Silicon

Michael J. S. Dewar,* James Friedheim, Gilbert Grady, Eamonn F. Healy, and James J. P. Stewart

Department of Chemistry, The University of Texas at Austin, Austin, Texas 78712

Received May 24, 1985

MNDO has been reparametrized for silicon. The results for a wide variety of silicon-containing compounds are in much better agreement with experiment. Enthalpies of reaction and activation are compared with results from recent high level ab initio calculations.

Introduction

While MNDO calculations, using the original[1] parameters for silicon, have given satisfactory results in many cases,[2] recent extensive calculations, here and elsewhere,[3] have revealed certain inadequacies. In particular, calculations with the previous parameters showed an undue preference for divalent silicon. One manifestation of this was to be seen in reactions involving SiR_2 species. Reactions involving the formation of such silylenes were invariably predicted to be much too exothermic (see Table II). The original MNDO version also performed badly for compounds containing multiply bonded silicon, greatly underestimating the strengths of the multiple bonds. For example, silaethylene and silacetylene were predicted to have bond orders of 1 and 2, respectively (Table VII). Large errors also occurred in calculations for compounds of silicon with other heteroatoms, most notably oxygen.

We have now reoptimized the parameters for silicon, taking advantage of a new and much more efficient algorithm for parametrization. The increased speed of the new procedure allowed far more reference functions to be included in the basis set. In addition the β_s and β_p parameters as well as the orbital exponents ζ_s and ζ_p were uncoupled and allowed to optimize independently.

Procedure

The sum of squares of the differences between the calculated values for the properties and the reference values was used to define the error function SSQ. These properties included heats of formation, ionization energies, dipole moments, and geometries. The first derivatives of the heat of formation and ionization energies with respect to the various parameters were calculated analytically. The derivatives of the dipole moments were evaluated by finite difference, and the derivative of the energy with respect to geometry was used as a measure of the deviation of the calculated geometry from the experimental. A knowledge of these derivatives allowed the calculation of the derivative of the SSQ with respect to the various parameters.

If the surface were purely parabolic and the exact Hessian, or second derivative, matrix was known, then the optimum set of parameters (P') could be evaluated in one step from the current set (P) using the relationship

$$P' = P - GH^{-1}$$

where G is the first derivative matrix and H^{-1} is the inverse Hessian. However, because of the more complex nature of the surface and the advisability of choosing small step sizes, a more conservative approach was adopted. From a knowledge of the derivatives of the SSQ for two slightly different sets of parameters an approximate Hessian was constructed. A line search along the search direction yielded the optimum step size, and this information was

Table I. Revised MNDO Parameters for Silicon

optimized parameters	value	derived parameters	value
U_{ss}/eV	-37.037 533 0	E_{heat}(298 K)/kcal mol^{-1}	108.39
U_{pp}/eV	-27.769 678 0	E_{el}/eV	-82.839 422 0
ζ_s/au	1.315 986 0	D_1/au	1.258 034 9
ζ_p/au	1.709 943 0	D_2/au	0.978 582 4
β_s/eV	-9.086 804 0	ρ_1/au	0.360 896 7
β_p/eV	-1.075 827 0	ρ_2/au	0.366 424 4
α/Å^{-1}	2.205 316 0	ρ_3/au	0.450 674 0
g_{ss}/eV	9.820 000 0		
g_{pp}/eV	7.310 000 0		
g_{sp}/eV	8.360 000 0		
g_{p2}/eV	6.540 000 0		
h_{sp}/eV	1.320 000 0		

Table II. Heats of Formation for a Variety of Substituted Silylenes and Silanes Using the Original Silicon Parameters

	MNDO	obsd	error
SiH	70.30	86.40[a]	-16.10
SiH_2	26.31	58.60[b]	-32.29
SiF_2	-216.48	-147.90[a]	-68.48
$SiCl_2$	-105.63	-39.60[a]	-66.04
$SiBr_2$	-51.64	-12.20[c]	-38.44
SiH_4	1.20	7.30[a]	-6.10
$SiH_3(CH_3)$	-15.53	-7.77[d]	-7.76
$SiH_2(CH_3)_2$	-41.54	-19.98[d]	-21.56
$SiH(CH_3)_3$	-66.46	-37.43[d]	-29.03
$Si(CH_3)_4$	-90.10	-57.10[a]	-31.50
$SiH_2(C_2H_5)_2$	-56.61	-43.62[e]	-12.99
$SiH(C_2H_5)_3$	-85.49	-48.00[e]	-37.69
$Si(C_2H_5)_4$	-111.03	-64.40[e]	-47.60
Si_2H_6	11.5	7.30[a]	4.20
Si_3H_8	32.5	29.90[a]	2.60

[a] Wagman, D. D.; Evans, W. H.; Parker, V. B.; Schumm, R. H.; Halow, I.; Bailey, S. M.; Churney, K. L.; Nuttall, R. L. *J. Phys. Chem. Ref. Data, Suppl.* **1982**, *11*, 2. [b] Vanderwielen, A. J.; Ring, M. A.; O'Neal, H. E. *J. Am. Chem. Soc.* **1975**, *97*, 993. [c] Schafer, H.; Braderreck, H.; Morcher, B. *Z. Anorg. Allg. Chem.* **1967**, *352*, 122. [d] Pedley, J. B.; Iseard, B. S. "CATCH Tables for Silicon Compounds"; University of Sussex, 1972. [e] Pedley, J. B.; Rylance, J. Sussex-N.P.L. Computer Analysed Thermochemical Data, University of Sussex, 1977.

(1) Dewar, M. J. S.; Rzepa, H. S.; McKee, M. L. *J. Am. Chem. Soc.* **1978**, *100*, 3607.
(2) Dewar, M. J. S.; Healy, E. F. *Organometallics* **1982**, *1*, 1705.
(3) Verwoerd, W. S. *J. Comput. Chem.* **1982**, *3*, 445.

0276-7333/86/2305-0375$01.50/0

Table III. Calculated Heats of Formation, Ionization Potentials, and Dipole Moments for Molecules Containing Silicon

compound	ΔH_f/kcal·mol^{-1}		IP/eV		dipole moment/D[a]	
	calcd	obsd	calcd	obsd	calcd	obsd
SiH	90.2	86.4[b]	5.97		0.69	
SiH_2	64.3	58.6[c]	7.34		0.13	
*SiH_4	1.2	7.3[d]	11.93	12.36[e]		
$(CH_3)SiH_3$	−14.0	−7.8[f]	11.53		0.14	0.74[g]
*$(C_2H_5)SiH_3$	−21.6		11.14		0.10	0.81
$(CH_3)_2SiH_2$	−28.8	−20.0[f]	11.40		0.18	0.75
$(C_2H_5)_2SiH_2$	−44.0	−43.6[h]	11.09		0.23	
$(CH_3)_3SiH$	−44.3	−37.4[f]	11.40		0.17	0.525
$(C_2H_5)_3SiH$	−64.0	−48.0[h]	11.05		0.21	
*$(CH_3)_4Si$	−59.1	−57.1[b]	11.33	10.29[i]		
$(C_2H_5)_4Si$	−82.0	−64.4[h]	10.90		0.07	
*$H_2C{=}CHSiH_3$	6.3	−1.9[b]	10.23	10.40[j]	0.56	0.66
silylacetylene	34.7		10.90		1.07	0.316[g]
SiBr	57.8	50.0[b]	6.83		3.38	
H_3SiBr	−18.0		11.22		3.44	1.31
*$(CH_3)_3SiBr$	−62.3	−70.0[k]	11.19		3.24	
$SiBr_2$	11.2	12.2[h]	9.43		4.04	
*$SiBr_4$	−50.4	−99.3[b]	12.62	10.90[l]		
SiCl	29.7	45.3[b]	6.65		2.95	
H_3SiCl	−43.9	−75.9[b]	12.03	11.61[m]	3.31	1.31
$(CH_3)_2HSiCl$	−73.0	−69.9[h]	11.80		3.28	
$(CH_3)_3SiCl$	−87.4	−84.6[k]	11.74		3.24	
*$SiCl_2$	−46.3	−39.6[b]	9.83		3.82	
H_2SiCl_2	−83.5		12.52	11.70[n]	3.42	1.17
$(CH_3)SiCl_2H$	−97.4	−96.0[k]	12.33		3.59	
$(CH_3)_2SiCl_2$	−111.2	−107.1[k]	12.22		3.69	
$HSiCl_3$	−117.9	−122.6[b]	13.15	11.94[n]	2.70	0.86
*$SiCl_4$	−147.6	−157.0[b]	13.81	12.03[l]		
$(CH_3)SiCl_3$	−131.2	−136.7[h]	12.87		3.15	
SiF	−28.8	1.7[b]	6.02		0.36	
*SiF_2	−164.9	−147.9[b]	9.94		1.24	1.23
H_3SiF	−96.4		11.98		1.32	1.27
H_2SiF_2	−192.6	−194.0[d]	12.22	12.85[n]	2.12	1.55
$HSiF_3$	−285.1	−283.0[d]	14.00		2.70	1.27
*SiF_4	−370.4	−385.9[b]	15.83	16.45[o]		
$(CH_3)SiH_2F$	−110.3		11.63		1.43	1.71
$(CH_3)SiHF_2$	−205.5		11.90		2.28	2.11
SiI	92.1		7.16		3.03	
SiO	−22.6		10.70		2.31	3.10[g]
$(SiH_3)SO$	−112.5					0.24[g]
$(CH_3)_3SiI$	−34.5		10.35		2.70	
*$(CH_3)_3SiOH$	−121.9	−119.4[k]	10.92		1.34	
1,1-dimethylsilacyclobutane	−33.7	−33.0[h]	10.70		0.80	
*$HN(Si(CH_3)_3)_2$	−123.2	−113.9[h]	9.69		0.29	0.41
*Si_2H_6	22.4	19.2[b]	9.62			
*$Si_2(CH_3)_6$	−73.7	−86.8[h]	9.71			
Si_3H_8	31.8	29.9[b]	9.48		0.45	

[a] Except where noted all experimental dipole moments were obtained from: Nelson, R. D.; Lide, D. R.; Maryott, A. A. *Natl. Stand. Ref. Data Ser. (U.S., Natl. Bur. Stand.)* **1967**, *NSRDS-NBS 10*. [b] Wagman, D. D.; Evans, W. H.; Parker, V. B.; Schumm, R. H.; Halow, I.; Bailey, S. M.; Churney, K. L.; Nuttall, R. L. *J. Phys. Chem. Ref. Data, Suppl.* **1982**, *11*, 2. [c] Vanderwielen, A. J.; Ring, M. A.; O'Neal, H. E. *J. Am. Chem. Soc.* **1975**, *97*, 993. [d] Stull, D. R.; Prophet, H. *Natl. Stand. Ref. Data Ser. (U.S., Natl. Bur. Stand.)* **1971**, NSRDS-NBS 37. [e] Pullen, B. P.; Carlson, T. A.; Moddeman, W. E.; Schweitzer, G. K.; Bull, W. E.; Grimm, F. A. *J. Chem. Phys.* **1970**, *53*, 768. [f] Pedley, J. B.; Iseard, B. S. "CATCH Tables for Silicon Compounds"; University of Sussex, 1972. [g] McClellan, A. L. "Tables of Experimental Dipole Moments"; W. H. Freeman: San Francisco, 1963. [h] Pedley, J. B.; Rylance, J. Sussex-N.P.L. Computer Analysed Thermochemical Data, University of Sussex, 1977. [i] Jonas, A. E.; Schweitzer, G. K.; Grimm, F. A.; Carlson, T. A. *J. Electron Spectrosc.* **1972**, *1*, 29. [j] Weidner, U.; Schweig, A. *J. Organomet. Chem.* **1972**, *39*, 261. [k] Cox, J. D.; Pilcher, G. "Thermochemistry of Organic and Organometallic Compounds"; Academic Press: New York, 1970. [l] Green, J. C.; Green, M. L. H.; Joachim, P. J.; Orchard, A. F.; Turner, D. W. *Philos. Trans. R. Soc. London, Ser. A* **1970**, *A268*, 111. [m] Cradock, S.; Whiteford, R. A. *Trans. Faraday. Soc.* **1971**, *67*, 3425. [n] Frost, D. C.; Herring, F. G.; Katrib, A.; McLean, R. A. N.; Drake, J. E.; Westwood, N. P. C. *Can. J. Chem.* **1971**, *49*, 4033. [o] Bassett, P. J.; Lloyd, D. R. *J. Chem. Soc. A.* **1971**, 641.

Table IV. Calculated Charge Distributions

molecule	atom (charge, e)	molecule	atom (charge, e)
SiH	Si (+0.417), H (−0.417)	SiH_3Br	Si (+1.562), H (−0.353), Br (−0.505)
SiH_2	Si (+0.947), H (−0.473)	SiH_3Cl	Si (+1.610), H (−0.358), Cl (−0.537)
SiH_4	Si (+1.603), H (−0.401)	SiH_3F	Si (+1.665), H (−0.381), F (−0.527)
$(CH_3)SiH_3$	Si (+1.481), C (−0.367), H (−0.375)	SiH_3I	Si (+1.383), H (−0.341), I (−0.359)
silylacetylene	Si (+1.626), C (−0.530, −0.076), H (−0.389, +0.146)	Br_3SiF	Si (+1.459), F (−0.446), Br (−0.338)
Si_2H_6	Si (+1.007), H (−0.336)	Cl_3SiF	Si (+1.633), F (−0.458), Cl (−0.392)
$Si_2(CH_3)_6$	Si (+0.721), C (−0.238)	SiO	Si (+0.746), O (−0.746)
Si_3H_8	Si (+1.534, −0.522), H (−0.385, −0.104)	$(SiH_3)_2O$	Si (+1.706), H (−0.404), O (−0.987)

used to update the Hessian matrix. By repeating this procedure an optimum set of parameters was obtained. The algorithm used was a modification of the Davidon–Fletcher–Powell (DFP) procedure.[4]

Table V. Calculated (Observed) Geometrical Parameters

molecule	bond lengths (Å)	calcd	(obsd)	bond angles (deg)	calcd	(obsd)	ref
SiH	SiH	1.374	(1.520)				*a*
SiH_2	SiH	1.380	(1.516)	HSiH	97.3	(92.1)	*b*
SiH_4	SiH	1.376	(1.481)				*c*
$(CH_3)SiH_3$	SiC	1.801	(1.869)	HCH	106.9	(107.7)	*d*
				HSiH	109.0	(108.2)	
$H_2C{=}CHSiH_2$	SiC	1.772	(1.853)	SiCC	128.4	(122.9)	*e*
	SiH	1.380	(1.475)	HSiH	110.4	(108.7)	
$BrSiH_3$	SiBr	2.228	(2.210)	HSiBr	106.9	(107.9)	*f*
$BrSiF_3$	SiBr	2.219	(2.153)	FSiF	106.6	(108.5)	*g*
	SiF	1.585	(1.560)				
Br_3SiH	SiBr	2.197	(2.170)	BrSiBr	108.9	(111.6)	*h*
	SiH	1.366	(1.494)				
Br_3SiF	SiBr	2.210	(2.171)	BrSiBr	108.7	(111.6)	*h*
	SiH	1.368	(1.481)				
ClSiH	SiH	1.369	(1.561)	HSiCl	99.0	(102.8)	*i*
	SiCl	2.103	(2.064)				
$ClSiH_3$	SiH	1.369	(1.485)	HSiCl	106.9	(108.7)	*f*
	SiCl	2.112	(2.049)				
Cl_2SiH_2	SiH	1.365	(1.480)	ClSiCl	108.6	(109.7)	*j*
	SiCl	2.097	(2.033)				
$Cl_2HSi(CH_3)$	SiC	1.791	(1.850)	CSiH	115.2	(110.9)	*k*
	SiH	1.370	(1.467)	CSiCl	109.8	(109.8)	
	SiCl	2.101	(2.040)	ClSiCl	107.0	(108.8)	
Cl_3SiH	SiCl	2.087	(2.019)	ClSiCl	108.5	(110.6)	*l*
	SiH	1.367	(1.465)	HSiCl	110.5	(108.3)	
Cl_3SiF	SiCl	2.094	(2.019)	ClSiCl	109.1	(109.4)	*l*
	SiF	1.572	(1.520)	FSiCl	109.9	(109.5)	
$Cl_3Si(CH_3)$	SiC	1.793	(1.876)				*m*
	SiCl	2.090	(2.021)				
$FSiH_3$	SiF	1.595	(1.596)	HSiF	108.4	(108.4)	*n*
	SiH	1.379	(1.480)				
F_2Si	SiF	1.578	(1.590)	FSiF	96.9	(100.8)	*o*
F_3SiH	SiH	1.375	(1.447)	FSiF	105.1	(108.3)	*p*
	SiF	1.593	(1.562)				
$F_3Si(CH_3)$	SiF	1.594	(1.574)	HCSi	112.0	(110.0)	*q*
	SiC	1.803	(1.812)				
ISiH	SiI	2.395	(2.451)	HSiI	101.0	(102.7)	*r*
$ISiH_3$	SiH	1.370	(1.487)	HSiI	108.4	(108.4)	*f*
	SiI	2.386	(2.437)				
$ISiF_3$	SiI	2.406	(2.387)				*s*
Si_2H_6	SiSi	2.173	(2.327)	HSiH	107.7	(107.8)	*t*
$(SiH_3)_2O$	SiH	1.385	(1.486)	SiOSi	177.4	(144.1)	*u*
	SiO	1.615	(1.634)	OSiH	108.9	(109.9)	
				HSiH	109.7	(109.1)	

[a] Rosen, B. "Spectroscopic Data Relative to Diatomic Molecules"; Pergamon Press: New York, 1970. [b] Dubois, I. *Can. J. Phys.* **1968**, *46*, 2485. [c] Dang-Nhu, M.; Pierre, G.; Saint-Loup, R. *Mol. Phys.* **1974**, *28*, 447. [d] Kilb, R. W.; Pierce, L. *J. Chem. Phys.* **1957**, *27*, 108. [e] O'Reilly, J. M.; Pierce, L. *J. Chem. Phys.* **1961**, *34*, 1176. [f] Kawley, R.; McKinney, P. M.; Robiette, A. G. *J. Mol. Spectrosc.* **1970**, *34*, 390. [g] Sheridan, J.; Gordy, W. *J. Chem. Phys.* **1951**, *19*, 965. [h] Holm, R.; Mitzloff, M.; Hartmann, H. *Z. Naturforsch., A*: **1968**, *23A*, 1819. [i] Herzberg, G.; Verma, R. D. *Can. J. Phys.* **1964**, *42*, 395. [j] Davis, R. W.; Gerry, M. C. L. *J. Mol. Spectrosc.* **1976**, *60*, 117. [k] Endo, K.; Takeo, H.; Matsumura, C. *Bull. Chem. Soc. Jpn.* **1977**, *50*, 626. [l] Holm, R.; Mitzloff, M.; Hartmann, H. *Z. Naturforsch., A* **1967**, *22A*, 1287. [m] Mockler, R. C.; Bailey, J. H.; Gordy, W. *J. Chem. Phys.* **1953**, *21*, 1710. [n] Georghiou, C.; Baker, J. G.; Jones, S. R. *J. Mol. Spectrosc.* **1976**, *63*, 89. [o] Shoji, H.; Tanaka, T.; Hirota, E. *J. Mol. Spectrosc.* **1973**, *47*, 268. [p] Hoy, A. R.; Bertram, M.; Mills, I. M. *J. Mol. Spectrosc.* **1973**, *46*, 429. [q] Durig, J. R.; Li, Y. S.; Tong, C. C. *J. Mol. Struct.* **1972**, *14*, 255. [r] Billingsley, J. *Can. J. Phys.* **1972**, *50*, 531. [s] Sams, L. C.; Jache, A. W. *J. Chem. Phys.* **1967**, *47*, 1314. [t] Shotton, K. C.; Lee, A. G.; Jones, W. J. *J. Raman Spectrosc.* **1973**, *1*, 243. [u] Almenningen, A.; Bastiansen, O.; Ewing, V.; Hedberg, K.; Traetteberg, M. *Acta Chem. Scand.* **1963**, *17*, 2455.

Table VI. Vibrational Frequencies

compd	assignt	descriptn	MNDO, cm^{-1}	exptl, cm^{-1}	ref	compd	assignt	descriptn	MNDO, cm^{-1}	exptl, cm^{-1}	ref
$SiHD_3$		Si–H stretch	2360	2187.2	*a*	$CH_3C{\equiv}C$-SiH_3	A	Si–H stretch	2374	2182	*d*
$SiHF_3$		Si–H stretch	2404	2316.8	*a*		E	Si–H stretch	2338	2182	
$SiHCl_3$		Si–H stretch	2364	2260.3	*a*		A	Si–H deformation	1011	943	
Si_2HD_5		Si–H stretch	2349	2162.5	*a*						
SiH_4	A	symmetric stretch	2399	2185	*b*		E	Si–H deformation	960	937	
	T	asymmetric stretch	2347	2189							
	E	asymmetric bend	929	972			E	SiH_3 rock	749	697	
	T	asymmetric bend	991	913			A	Si–C stretch	610	523	
CH_3SiH_3	A1	SiH_3 stretch	2382	2169	*c*		E	Si–C–C bend	189	132	
	E	SiH_3 stretch	2345	2166		HSiOH-(trans)	a′	O–H stretch	4144	3650	*e*
	E	SiH_3 bend	1004, 958	946			a′	Si–H stretch	2287	1872	
							a′	H–Si–O bend	975	937	
	A1	SiH_3 deformation	958	946			a′	Si–O stretch	1002	851	
							a′	Si–O–H bend	839	723	
	A1	Si–C stretch	803	701			a″	torsion	564	659	
	E	SiH_3 rock	634	545		cyclopropyl-$SiHD_2$		Si–Ha stretch	2354	2162.7	*f*
								Si–Hs stretch	2356	2157.8	

[a] McKean, D. C.; Torto, I.; Morrisson, A. R. *J. Phys. Chem.* **1982**, *86*, 307. [b] Kattenberg, H. W.; Oskam, A. *J. Mol. Spectrosc.* **1974**, *49*, 52. [c] Wilde, R. E. *J. Mol. Spectrosc.* **1962**, *8*, 427. [d] Cradock, S.; Koprowski, J.; Rankin, D. W. H. *J. Mol. Struct.* **1981**, *77*, 113. [e] Ismail, Z. K.; Hauge, R. H.; Fredin, L.; Kauffman, J. W.; Margrave, J. L. *J. Chem. Phys.* **1982**, *77*, 1617. [f] McKean, D. C.; Morrisson, A. R.; Dakkouri, M. *Spectrochim. Acta, Part A* **1984**, *40A*, 771.

Table VII

	original MNDO		revised MNDO			
	ΔH_f[b]	d(Si–Si)[c]	ΔH_f[b]	d(Si–Si)[c]	ab initio d(Si–Si)[c]	ref
H_3SiSiH_3	22.9	2.284	22.4	2.173	2.352	a
$H_2Si{=}SiH_2$	48.4	2.670	74.9	1.967	2.083	a
$HSi{\equiv}SiH$	126.5	2.10	127.0	1.806		

[a] Glidwell, C. *J. Organomet. Chem.* **1981**, *217*, 11. [b] In kcal/mol. [c] In Å.

Results and Discussion

Table I shows the final set of parameters obtained for silicon in the usual notation. One unexpected result was the relative ordering of the ζ_s and ζ_p parameters, the value for the latter being larger. However, this is compensated for by the fact that the value for β_s is much more negative than that for β_p, these parameters being coupled in their contribution to the one electron matrix. The one-center, two-electron parameters (g and h) were kept constant at their previous values.[1]

Table II gives the errors in the calculated heats of formation (ΔH_f) for selected silicon compounds using the original parameters. The emphasis here is on those molecules for which the original parameters performed badly, but other compounds are also included to facilitate comparison with the present work. In addition to the previously stated large negative errors for Si^{II} compounds, it can also be seen that progressive methyl and ethyl substitution in silane (SiH_4) resulted in increasing negative errors in the heats of formation. This problem has been rectified with the new parameterization. The remaining tables, unless otherwise stated, all contain results obtained with the revised set of parameters.

Table III shows the heats of formation (ΔH_f), first ionization potentials derived by using Koopmans' theorem (I_1), and dipole moments (μ) for a broad range of silicon-containing compounds. The molecules included in the basis set are indicated by asterisks. Where possible, experimental values are included for comparison.

The errors in the calculated heats of formation, while predictably larger than those for the organic elements (CHON),[5] represent a big improvement over those given by the previous set of parameters (see Table II). Errors greater than 20 kcal/mol now occur only in one or two exceptional cases.

The errors in the calculated ionization energies are large, varying from 0.17 to 1.78 eV. Similar errors have also been found for the other third-period elements[6,7] and, in the case of large negative errors, have been attributed to use of the core approximation in MNDO. In any case, all attempts to rectify this problem in the case of silicon resulted in an impairment of the results for other properties.

The errors in the calculated dipole moments are comparable with those reported for S[6] and Cl.[7] They show no trend.

The calculated charge distributions (Table IV) give formal charges much greater than what would be expected from the standard electronegativity values and are also greater than those predicted by the original MNDO parameters. This latter fact is attributable to the value for the U_{ss} parameter, which is 3.5 eV more positive than the original value. Though unsatisfactory, this failing was considered less important than the dramatic improvements in the calculated heats of formation (Tables II and III).

Table VIII. Calculated Reaction Energies

reactn	MNDO, kcal/mol	ab initio	ref
$H_2C{=}SiH_2 \rightarrow H_3CSiH$	+9.2	−0.4	a
$HC{\equiv}SiH \rightarrow H_2C{=}Si$	−20.0	−49.1	b
$H_2Si{=}SiH_2 \rightarrow H_3SiSiH$	+15.3	−8.1	a
$H_2C{=}Si + H_2 \rightarrow H_2C{=}SiH_2$	−43.3	−31.0	c
$H_2C{=}SiH_2 + H_2 \rightarrow H_3CSiH_3$	−52.1	−56.9	c
$HC{\equiv}SiH + H_2 \rightarrow H_2C{=}SiH_2$	−63.3	−71.7	c
$H_2 + SiO \rightarrow H_2Si{=}O$	−2.9	2.5	d
$H_2Si{=}O \rightarrow HSiOH$(trans)	−9.6	−3.7	d
$H_2O + H_2Si{=}O \rightarrow H_2Si(OH)_2$	−73.1	−72.6	d

[a] Yoshioka, Y.; Goddard, J. D.; Schaefer III, H. F. *J. Am. Chem. Soc.* **1981**, *103*, 2452. [b] Hoffmann, M. R.; Yoshioka, Y.; Schaefer III, H. F. *J. Am. Chem. Soc.* **1983**, *105*, 1084. [c] Gordon, M. S.; Pople, J. A. *J. Am. Chem. Soc.* **1981**, *103*, 2945. [d] Kudo, T.; Nagase, S. *J. Phys. Chem.* **1984**, *88*, 2833.

Table IX. Calculated Enthalpies of Activation

reactn	MNDO, kcal/mol	ab initio	ref
$H_2Si{=}O \rightarrow HSiOH$(trans)	79.2	60.8	a
HSiOH(trans) → HSiOH(cis)	5.4	9.3	a
$H_2Si{=}CH_2 \rightarrow HSiCH_3$	59.1	41.0	b

[a] Kudo, T.; Nagase, S. *J. Phys. Chem.* **1984**, *88*, 2833. [b] Yoshioka, Y.; Goddard, J. D.; Schaefer III, H. F. *J. Am. Chem. Soc.* **1980**, *102*, 7644.

Table V compares the calculated geometries with experiment. The errors in the bond lengths are slightly greater than those found with the previous set of parameters, while those for the bond angles are similar (1.8°). Si–C and Si–H bonds are consistently predicted to be too short, the average errors being 0.06 and 0.125 Å, respectively. While much greater than the corresponding errors for the organic elements (CHNO), these discrepancies in Si–C and Si–H bonds are systematic. The errors in lengths of bonds between silicon and halogens are comparable with those given by MNDO for compounds of other third-period elements.

Table VI compares the calculated and observed vibrational frequencies for a number of silicon-containing compounds. As in other cases,[8] the calculated values are systematically (only one vibrational mode out of the 29 reported is predicted too low in frequency) too high, by ≃9%.

Table VII gives the heats of formation (ΔH_f) and bond lengths for Si–Si multiply bonded species and compares these with the results obtained from the previous set of parameters and with ab initio results. A more thorough MNDO investigation of disilenes and related molecules will be the subject of a future paper; however, it should be noted here that the revised MNDO bond lengths show the expected decrease with the increase in bond order. This was not the case with the original parameters.

Tables VIII and IX involve comparisons of our calculated values, not with experiment, but with recent ab initio results. Table VIII compares heats of reaction for a number of rearrangements of silicon compounds and for

(4) Fletcher, R.; Powell, M. J. D. *Comput. J.* **1963**, *6*, 163. Davidon, W. C. *Ibid.* **1968**, *10*, 406.
(5) Dewar, M. J. S.; Thiel, W. *J. Am. Chem. Soc.* **1977**, *99*, 4899, 4907.
(6) Dewar, M. J. S.; McKee, M. L. *J. Comput. Chem.* **1983**, *4*, 84.
(7) Dewar, M. J. S.; Rzepa, H. S. *J. Comput. Chem.* **1983**, *4*, 158.
(8) Dewar, M. J. S.; Ford, G. P. *J. Am. Chem. Soc.* **1977**, *99*, 1685.

some additional reactions. The agreement is highly satisfactory, especially in view of the fact that most of the ab initio calculations were carried out at a very high level. The calculated enthalpies of activation reaction also show good agreement, except for reactions involving hydrogen migration. MNDO is well-known to give values that are much too large in such cases.

Acknowledgment. This work was supported by the Air Force Office of Scientific Research (Contract No. F49620-83-C-0024) and The Robert A. Welch Foundation (Grant F-126), The National Science Foundation (Grant CHE82-17948), and the Tektronix Foundation. The calculations were carried out by using a DEC VAX 11/780 computer purchased with funds provided by the National Science Foundation and The University of Texas at Austin.

Registry No. SiH, 13774-94-2; SiH_2, 13825-90-6; Si, 7440-21-3; SiF_2, 13966-66-0; $SiCl_2$, 13569-32-9; $SiBr_2$, 14877-32-8; SiH_4, 7803-62-5; $SiH_3(CH_3)$, 992-94-9; $SiH_2(CH_3)_2$, 1111-74-6; $SiH(CH_3)_3$, 993-07-7; $Si(CH_3)_4$, 75-76-3; $SiH_2(C_2H_5)_2$, 542-91-6; $SiH(C_2H_5)_3$, 617-86-7; $Si(C_2H_5)_4$, 631-36-7; Si_2H_6, 1590-87-0; Si_3H_8, 7783-26-8; $(C_2H_5)SiH_3$, 2814-79-1; $H_2C{=}CHSiH_3$, 7291-09-0; HC≡CSi, 1066-27-9; SiBr, 12350-21-9; H_3SiBr, 13465-73-1; $(CH_3)_3SiBr$, 2857-97-8; $SiBr_4$, 7789-66-4; SiCl, 13966-57-9; H_3SiCl, 13465-78-6; $(CH_3)_2HSiCl$, 1066-35-9; $(CH_3)_3SiCl$, 75-77-4; H_2SiCl_2, 4109-96-0; $(CH_3)SiCl_2H$, 75-54-7; $(CH_3)_2SiCl_2$, 75-78-5; $HSiCl_3$, 10025-78-2; $SiCl_4$, 10026-04-7; $(CH_3)SiCl_3$, 75-79-6; SiF, 11128-24-8; H_3SiF, 13537-33-2; H_2SiF_2, 13824-36-7; $HSiF_3$, 13465-71-9; SiP_4, 7783-61-1; $(CH_3)SiH_2F$, 753-44-6; $(CH_3)SiHF_2$, 420-34-8; SiI, 13841-19-5; SiO, 10097-28-6; $(SiH_3)SO$, 99583-30-9; $(CH_3)_3SiI$, 16029-98-4; $(CH_3)_3SiOH$, 1066-40-6; $HN(Si(CH_3)3)_2$, 999-97-3; $Si_2(CH_3)_6$, 1450-14-2; $(SiH_3)_2O$, 13597-73-4; ISiH, 36098-67-6; $ISiH_3$, 13598-42-0; $ISiF_3$, 16865-60-4; $SiHD_3$, 13537-02-5; Si_2HD_5, 77815-94-2; HSiOH (trans), 83892-34-6; cyclopropyl-$SiHO_2$, 92917-37-8; $H_2Si{=}SiH_2$, 15435-77-5; HSi<<tbdSiH, 36835-58-2; 1,1-dipethylsilacyclobutane, 2295-12-7.

Communications

Synthesis of $[(\mu\text{-H})Fe_4(CO)_{12}BH]^-$ from $[(\mu\text{-H})Fe_3(CO)_9BH_3]^-$ via Cluster Expansion Involving H_2 Elimination

Catherine E. Housecroft and Thomas P. Fehlner*

Department of Chemistry, University of Notre Dame Notre Dame, Indiana 46556

Received August 29, 1985

Summary: A rational and high yield cluster expansion reaction with clean stoichiometry to form the butterfly anionic cluster $[(\mu\text{-H})Fe_4(CO)_{12}BH]^-$ (III) is reported. An important driving force for the reaction is the elimination of H_2. $Fe(CO)_5$ rather than CO is the other product. This particular cluster transformation represents a synthetic realization of our recent bonding analysis of $(\mu\text{-H})Fe_4(CO)_{12}CH$ (II) which is isoelectronic with III.

The "butterfly" cluster $(\mu\text{-H})Fe_4(CO)_{12}BH_2$ (I) was isolated as a serendipidous product of the reaction of $Fe_2(CO)_6B_2H_6$ and $Fe_2(CO)_9$.[1] Although this reaction constitutes a cluster expansion, its mechanism and stoichiometry are complex, a feature often associated with cluster expansions.[2] We report here the high yield transformation of $[(\mu\text{-H})Fe_3(CO)_9BH_3]^-$[3] (IV) to $[(\mu\text{-H})Fe_4(CO)_{12}BH]^-$ (III) which is the anion of I.

In a typical reaction, a solution of 0.02 mmol of the PPN (PPN = bis(triphenylphosphine)nitrogen(1+) ion) salt of IV in 1.5 mL of toluene: dichloromethane (13:2) was added to 0.04 mmol of $Fe_2(CO)_9$. On stirring at room temperature for 40 min, the solution changed from a deep orange-red to an intense brown color and all the $Fe_2(CO)_9$ was consumed. The final solution contained a single ferraborane

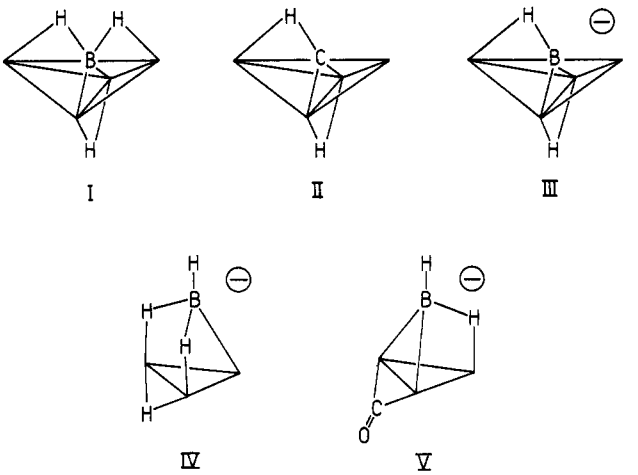

anion, III (obtained in ≥90% by NMR), which is identified as follows: protonation in toluene by CF_3COOH gives I quantitatively by NMR; the 96.3-MHz ^{11}B NMR of III ($CD_3C(O)CD_3$, −25 °C) exhibits a broad singlet (fwhm 180 Hz) at 150.0 ppm that narrows on proton decoupling (fwhm 100 Hz) indicating $J_{BH} \approx 80$ Hz; the 300-MHz ^1H NMR ($CD_3C(O)CD_3$, −30 °C) shows resonances at δ 7.77–7.58 (m, 30 H) due to PPN, δ −8.5 (br, 1 H) due to one Fe–H–B proton, and δ −24.9 (s, 1 H) due to one Fe–H–Fe proton;[4] the infrared spectrum (acetone, cm^{-1}) shows ν_{CO} 2060 (w), 2040 (w), 2003 (vs), 1983 (vs), 1955 (m), and 1932 (m) (about 50 cm^{-1} below those of I) and a distinctive band, not due to PPN, at 808 (w) cm^{-1} (similar bands have been denoted as characteristic of interstitial atoms[5]). This is consistent with the large change in ^{11}B NMR shift from 6.2 ppm in IV to 150.0 ppm in III. Such a shift indicates a significant perturbation in the environment of the boron, viz., the transformation of an apical boron with terminal

(1) Wong, K. S.; Scheidt, W. R.; Fehlner, T. P. *J. Am. Chem. Soc.* **1982**, *104*, 1111. Fehlner, T. P.; Housecroft, C. E.; Scheidt, W. R.; Wong, K. S. *Organometallics* **1983**, *2*, 825.

(2) Vahrenkamp, H. *Adv. Organomet. Chem.* **1983**, *22*, 169. P. Chini, *J. Organomet. Chem.* **1980**, *200*, 37.

(3) Vites, J. C.; Housecroft, C. E.; Jacobsen, G. B.; Fehlner, T. P. *Organometallics* **1984**, *3*, 1591.

(4) The integral for the metal hydride signal actually integrates as 0.2 H; low MH integrals are not uncommon: Crabtree, R. H.; Segmuller, B.; Uriarte, R. J. *Inorg. Chem.* **1985**, *24*, 1949.

(5) Johnson, B. F. G.; Lewis, J.; Nelson, W. J. H.; Nicholls, J. N.; Vargas, M. D. *J. Organomet. Chem.* **1983**, *249*, 255.

0276-7333/86/2305-0379$01.50/0

Synthesis of [(.mu.-H)Fe4(CO)12BH]- from [(.mu.-H)Fe3(CO)9BH3]- via cluster expansion involving hydrogen elimination

Catherine E. Housecroft, and Thomas P. Fehlner

Organometallics, **1986**, 5 (2), 379-380• DOI: 10.1021/om00133a030 • Publication Date (Web): 01 May 2002

some additional reactions. The agreement is highly satisfactory, especially in view of the fact that most of the ab initio calculations were carried out at a very high level. The calculated enthalpies of activation reaction also show good agreement, except for reactions involving hydrogen migration. MNDO is well-known to give values that are much too large in such cases.

Acknowledgment. This work was supported by the Air Force Office of Scientific Research (Contract No. F49620-83-C-0024) and The Robert A. Welch Foundation (Grant F-126), The National Science Foundation (Grant CHE82-17948), and the Tektronix Foundation. The calculations were carried out by using a DEC VAX 11/780 computer purchased with funds provided by the National Science Foundation and The University of Texas at Austin.

Registry No. SiH, 13774-94-2; SiH_2, 13825-90-6; Si, 7440-21-3; SiF_2, 13966-66-0; $SiCl_2$, 13569-32-9; $SiBr_2$, 14877-32-8; SiH_4, 7803-62-5; $SiH_3(CH_3)$, 992-94-9; $SiH_2(CH_3)_2$, 1111-74-6; $SiH(CH_3)_3$, 993-07-7; $Si(CH_3)_4$, 75-76-3; $SiH_2(C_2H_5)_2$, 542-91-6; $SiH(C_2H_5)_3$, 617-86-7; $Si(C_2H_5)_4$, 631-36-7; Si_2H_6, 1590-87-0; Si_3H_8, 7783-26-8; $(C_2H_5)SiH_3$, 2814-79-1; $H_2C{=}CHSiH_3$, 7291-09-0; HC≡CSi, 1066-27-9; SiBr, 12350-21-9; H_3SiBr, 13465-73-1; $(CH_3)_3SiBr$, 2857-97-8; $SiBr_4$, 7789-66-4; SiCl, 13966-57-9; H_3SiCl, 13465-78-6; $(CH_3)_2HSiCl$, 1066-35-9; $(CH_3)_3SiCl$, 75-77-4; H_2SiCl_2, 4109-96-0; $(CH_3)SiCl_2H$, 75-54-7; $(CH_3)_2SiCl_2$, 75-78-5; $HSiCl_3$, 10025-78-2; $SiCl_4$, 10026-04-7; $(CH_3)SiCl_3$, 75-79-6; SiF, 11128-24-8; H_3SiF, 13537-33-2; H_2SiF_2, 13824-36-7; $HSiF_3$, 13465-71-9; SiP_4, 7783-61-1; $(CH_3)SiH_2F$, 753-44-6; $(CH_3)SiHF_2$, 420-34-8; SiI, 13841-19-5; SiO, 10097-28-6; $(SiH_3)SO$, 99583-30-9; $(CH_3)_3SiI$, 16029-98-4; $(CH_3)_3SiOH$, 1066-40-6; $HN(Si(CH_3)3)_2$, 999-97-3; $Si_2(CH_3)_6$, 1450-14-2; $(SiH_3)_2O$, 13597-73-4; ISiH, 36098-67-6; $ISiH_3$, 13598-42-0; $ISiF_3$, 16865-60-4; $SiHD_3$, 13537-02-5; Si_2HD_5, 77815-94-2; HSiOH (trans), 83892-34-6; cyclopropyl-$SiHO_2$, 92917-37-8; $H_2Si{=}SiH_2$, 15435-77-5; HSi<<tbdSiH, 36835-58-2; 1,1-dipethylsilacyclobutane, 2295-12-7.

Communications

Synthesis of $[(\mu\text{-H})Fe_4(CO)_{12}BH]^-$ from $[(\mu\text{-H})Fe_3(CO)_9BH_3]^-$ via Cluster Expansion Involving H_2 Elimination

Catherine E. Housecroft and Thomas P. Fehlner*

Department of Chemistry, University of Notre Dame Notre Dame, Indiana 46556

Received August 29, 1985

Summary: A rational and high yield cluster expansion reaction with clean stoichiometry to form the butterfly anionic cluster $[(\mu\text{-H})Fe_4(CO)_{12}BH]^-$ (III) is reported. An important driving force for the reaction is the elimination of H_2. $Fe(CO)_5$ rather than CO is the other product. This particular cluster transformation represents a synthetic realization of our recent bonding analysis of $(\mu\text{-H})Fe_4(CO)_{12}CH$ (II) which is isoelectronic with III.

The "butterfly" cluster $(\mu\text{-H})Fe_4(CO)_{12}BH_2$ (I) was isolated as a serendipidous product of the reaction of $Fe_2(CO)_6B_2H_6$ and $Fe_2(CO)_9$.[1] Although this reaction constitutes a cluster expansion, its mechanism and stoichiometry are complex, a feature often associated with cluster expansions.[2] We report here the high yield transformation of $[(\mu\text{-H})Fe_3(CO)_9BH_3]^-$[3] (IV) to $[(\mu\text{-H})Fe_4(CO)_{12}BH]^-$ (III) which is the anion of I.

In a typical reaction, a solution of 0.02 mmol of the PPN (PPN = bis(triphenylphosphine)nitrogen(1+) ion) salt of IV in 1.5 mL of toluene: dichloromethane (13:2) was added to 0.04 mmol of $Fe_2(CO)_9$. On stirring at room temperature for 40 min, the solution changed from a deep orange-red to an intense brown color and all the $Fe_2(CO)_9$ was consumed. The final solution contained a single ferraborane

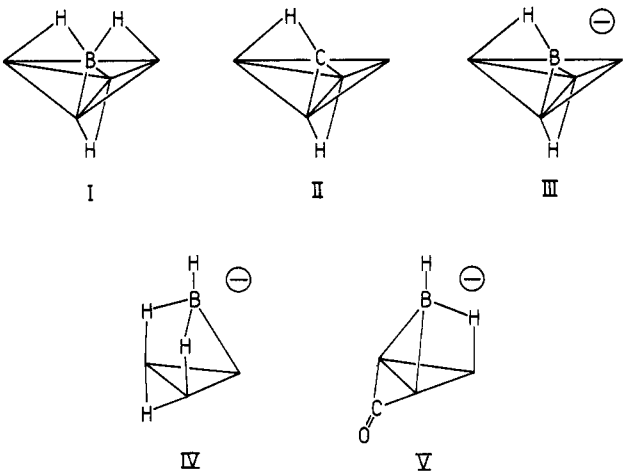

anion, III (obtained in ≥90% by NMR), which is identified as follows: protonation in toluene by CF_3COOH gives I quantitatively by NMR; the 96.3-MHz ^{11}B NMR of III ($CD_3C(O)CD_3$, −25 °C) exhibits a broad singlet (fwhm 180 Hz) at 150.0 ppm that narrows on proton decoupling (fwhm 100 Hz) indicating $J_{BH} \approx 80$ Hz; the 300-MHz ^1H NMR ($CD_3C(O)CD_3$, −30 °C) shows resonances at δ 7.77–7.58 (m, 30 H) due to PPN, δ −8.5 (br, 1 H) due to one Fe–H–B proton, and δ −24.9 (s, 1 H) due to one Fe–H–Fe proton;[4] the infrared spectrum (acetone, cm^{-1}) shows ν_{CO} 2060 (w), 2040 (w), 2003 (vs), 1983 (vs), 1955 (m), and 1932 (m) (about 50 cm^{-1} below those of I) and a distinctive band, not due to PPN, at 808 (w) cm^{-1} (similar bands have been denoted as characteristic of interstitial atoms[5]). This is consistent with the large change in ^{11}B NMR shift from 6.2 ppm in IV to 150.0 ppm in III. Such a shift indicates a significant perturbation in the environment of the boron, viz., the transformation of an apical boron with terminal

(1) Wong, K. S.; Scheidt, W. R.; Fehlner, T. P. *J. Am. Chem. Soc.* **1982**, *104*, 1111. Fehlner, T. P.; Housecroft, C. E.; Scheidt, W. R.; Wong, K. S. *Organometallics* **1983**, *2*, 825.

(2) Vahrenkamp, H. *Adv. Organomet. Chem.* **1983**, *22*, 169. P. Chini, *J. Organomet. Chem.* **1980**, *200*, 37.

(3) Vites, J. C.; Housecroft, C. E.; Jacobsen, G. B.; Fehlner, T. P. *Organometallics* **1984**, *3*, 1591.

(4) The integral for the metal hydride signal actually integrates as 0.2 H; low MH integrals are not uncommon: Crabtree, R. H.; Segmuller, B.; Uriarte, R. J. *Inorg. Chem.* **1985**, *24*, 1949.

(5) Johnson, B. F. G.; Lewis, J.; Nelson, W. J. H.; Nicholls, J. N.; Vargas, M. D. *J. Organomet. Chem.* **1983**, *249*, 255.

0276-7333/86/2305-0379$01.50/0

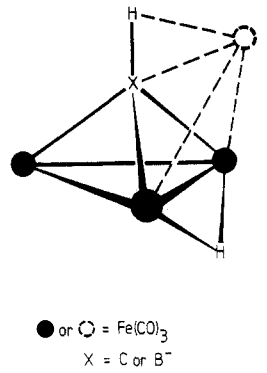

Figure 1. Schematic representation of II or III seen in terms of an $(\mu\text{-H})M_3XH$ core interacting with a fourth metal fragment; note that the originally terminal H is nicely placed to readily become X–H–M bridging.

hydrogen to an environment in which the boron has no terminal hydrogen and is surrounded by four iron atoms.[6] This unusual downfield shift also suggests that III has a structure similar to those of I and II; i.e., the ^{11}B chemical shift of I is 116 ppm[1] and II exhibits a large downfield ^{13}C shift (δ 335) for the cluster carbon.[7] Hence III is the conjugate Brønsted base of I in which the missing proton comes from an Fe–H–B interaction.[8]

In contrast to many cluster expansions, the reaction studied here has a clean stoichiometry that we have fully defined. The conversion of IV to III proceeds via the elimination of 1.0 ± 0.1 mol of H_2/mol of IV.[9] No other gaseous product was detected by gas–liquid chromatography with stoichiometric amounts of $Fe_2(CO)_9$ or during the first 40 min of reaction with excess $Fe_2(CO)_9$. The only iron-containing product other than III under stoichiometric conditions was $Fe(CO)_5$, and quantitative infrared spectroscopy showed that 3.0 ± 0.2 mol of $Fe(CO)_5$ were produced per mole of IV.[10] Finally, measuring the maximum NMR yield of III/mol of IV as a function of moles of $Fe_2(CO)_9$ showed the requirement for 2 mol of $Fe_2(CO)_9$/mol of IV. Hence, the stoichiometry, expressed by eq 1, has been fully established. In the presence of a large

$$[(\mu\text{-H})Fe_3(CO)_9BH_3]^- + 2Fe_2(CO)_9 \rightarrow [(\mu\text{-H})Fe_4(CO)_{12}BH]^- + H_2 + 3Fe(CO)_5 \quad (1)$$

excess of $Fe_2(CO)_9$, and at reaction times greater than 1 h, the yield of III was reduced. Under these conditions CO and $Fe_3(CO)_{12}$ were observed but no other product containing boron was evident by NMR. This further emphasizes the sensitivity of cluster building reactions to conditions.[11]

An important characteristic of the conversion of IV to III is the elimination of H_2. The ferraborane V, $[Fe_3(CO)_9(\mu\text{-CO})BH_2]^-$, which is related to IV by the replacement of two hydrogens by CO[3] does *not* react with $Fe_2(CO)_9$ under the conditions specified above. Thus, it is reasonable to consider the elimination of the endo hydrogens from IV to be a driving force for the reaction.[12] As H_2 elimination is a form of oxidation this reaction might be considered a type of redox condensation.[2]

In a strictly formal sense, removing H_2 from IV generates the cluster fragment $[(\mu\text{-H})Fe_3(CO)_9BH]^-$ that can be viewed as a building block of III (Figure 1); i.e., the Fe–H–B of III can be envisaged as originating from the terminal BH hydrogen of IV interacting with the new metal fragment. This parallels the geometrical description and molecular orbital fragment analysis of II that we recently presented.[13] Hence, our experimental approach to the synthesis of III has apparently brought about a synthetic, if not mechanistic, realization of our earlier theoretical analysis.

In conclusion, the transformation of IV to III is an example of a clean and rational cluster building synthesis that is assisted by the elimination of H_2. This suggests that hydrogen-rich clusters may constitute important cluster building materials in the future.

Acknowledgment. We gratefully acknowledge the support of the National Science Foundation (CHE81-09503 and CHE84-08251).

Registry No. I, 80572-82-3; III, 99582-34-0; IV, 92055-46-4; $Fe_2(CO)_9$, 15321-51-4.

(6) The X-ray crystal structure of I shows that the boron lies only 0.03 Å above a line joining the two "wingtip" Fe atoms: ref 1.
(7) Tachikawa, M.; Muetterties, E. L. *J. Am. Chem. Soc.* **1980**, *102*, 4541.
(8) The skeletal protons in II exchange, however, the FeHB and FeH-Fe protons in III undergo a more facile fluxional process. Hence, the replacement of C by B^- lowers the activation barrier to skeletal proton migration.
(9) The volume of gas evolved was measured using a gas microvolumeter: Davis, D. D.; Stevenson, K. L. *J. Chem. Educ.* **1977**, *54*, 394.
(10) Consideration of the heats of formation of $Fe(CO)_5$, $Fe_2(CO)_9$ and $Fe_3(CO)_{12}$ suggests that the formation of $Fe(CO)_5$ is energetically favored over $Fe_3(CO)_{12}$ in this instance.
(11) The sensitivity of cluster building reactions to conditions has recently been pointed out: Fjare, D. E.; Gladfelter, W. E. *J. Am. Chem. Soc.* **1984**, *106*, 4799.
(12) The elimination of H_2 is a factor in other known cluster building reactions, e.g., metallacarborane chemistry (see, for example: Grimes, R. N. In "Organometallic Reactions"; Becker, E. I., Tsutsui, M.; Eds.: Plenum Press: New York, 1977; Vol. 6 p 63) and is an important factor in borane cage interconversions (see, for example: DeKock, R. L.; Fehlner, T. P.; Housecroft, C. E.; Lubben, T. V.; Wade, K. *Inorg. Chem.* **1982**, *21*, 25).
(13) Fehlner, T. P.; Housecroft, C. E. *Organometallics* **1984**, *3*, 764.

Synthesis and Structure of a Metallophosphenium–Borane(3) Complex Containing a Bridging BH_3 Group

William F. McNamara, Eileen N. Duesler, Robert T. Paine,* and J. V. Ortiz
Department of Chemistry, University of New Mexico Albuquerque, New Mexico 87131

Peter Kölle and Heinrich Nöth
Institute für Anorganische Chemie, Universität München D-8000 München 2, FRG

Received September 11, 1985

Summary: Combination of $Na(C_5H_5)Mo(CO)_3$ with $(C_6H_5)P(Cl)\{N[Si(CH_3)_3]_2\}$ in THF results in the generation of a metallophosphenium compound, $(C_5H_5)Mo(CO)_2\{P(Ph)\{N[Si(CH_3)_3]_2\}\}$, which in the presence of B_2H_6 or H_3B·THF forms a borane(3) complex, $(C_5H_5)Mo(CO)_2\{P(BH_3)(Ph)\{N[Si(CH_3)_3]_2\}\}$. The solid-state structure of the complex has been determined by X-ray diffration techniques and found to contain the borane group B-bonded to the phosphorus atom and μ-H-bonded to the Mo atom, thereby providing an unusual four-membered ring, Mo–P–$B(H_2)$–(μ-H). Insights into the bonding are provided by qualitative MO analysis.

Nucleophilic group 6 metal carbonylates $Na(C_5H_5)M(CO)_3$ (M = Cr, Mo, W) when allowed to react with several classes of monochlorophosphanes P(X)(Y)(Cl) usually form

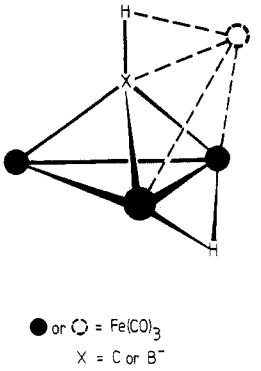

Figure 1. Schematic representation of II or III seen in terms of an $(\mu\text{-H})M_3XH$ core interacting with a fourth metal fragment; note that the originally terminal H is nicely placed to readily become X–H–M bridging.

hydrogen to an environment in which the boron has no terminal hydrogen and is surrounded by four iron atoms.[6] This unusual downfield shift also suggests that III has a structure similar to those of I and II; i.e., the ^{11}B chemical shift of I is 116 ppm[1] and II exhibits a large downfield ^{13}C shift (δ 335) for the cluster carbon.[7] Hence III is the conjugate Brønsted base of I in which the missing proton comes from an Fe–H–B interaction.[8]

In contrast to many cluster expansions, the reaction studied here has a clean stoichiometry that we have fully defined. The conversion of IV to III proceeds via the elimination of 1.0 ± 0.1 mol of H_2/mol of IV.[9] No other gaseous product was detected by gas–liquid chromatography with stoichiometric amounts of $Fe_2(CO)_9$ or during the first 40 min of reaction with excess $Fe_2(CO)_9$. The only iron-containing product other than III under stoichiometric conditions was $Fe(CO)_5$, and quantitative infrared spectroscopy showed that 3.0 ± 0.2 mol of $Fe(CO)_5$ were produced per mole of IV.[10] Finally, measuring the maximum NMR yield of III/mol of IV as a function of moles of $Fe_2(CO)_9$ showed the requirement for 2 mol of $Fe_2(CO)_9$/mol of IV. Hence, the stoichiometry, expressed by eq 1, has been fully established. In the presence of a large

$$[(\mu\text{-H})Fe_3(CO)_9BH_3]^- + 2Fe_2(CO)_9 \rightarrow [(\mu\text{-H})Fe_4(CO)_{12}BH]^- + H_2 + 3Fe(CO)_5 \quad (1)$$

excess of $Fe_2(CO)_9$, and at reaction times greater than 1 h, the yield of III was reduced. Under these conditions CO and $Fe_3(CO)_{12}$ were observed but no other product containing boron was evident by NMR. This further emphasizes the sensitivity of cluster building reactions to conditions.[11]

An important characteristic of the conversion of IV to III is the elimination of H_2. The ferraborane V, $[Fe_3(CO)_9(\mu\text{-CO})BH_2]^-$, which is related to IV by the replacement of two hydrogens by CO[3] does *not* react with $Fe_2(CO)_9$ under the conditions specified above. Thus, it is reasonable to consider the elimination of the endo hydrogens from IV to be a driving force for the reaction.[12] As H_2 elimination is a form of oxidation this reaction might be considered a type of redox condensation.[2]

In a strictly formal sense, removing H_2 from IV generates the cluster fragment $[(\mu\text{-H})Fe_3(CO)_9BH]^-$ that can be viewed as a building block of III (Figure 1); i.e., the Fe–H–B of III can be envisaged as originating from the terminal BH hydrogen of IV interacting with the new metal fragment. This parallels the geometrical description and molecular orbital fragment analysis of II that we recently presented.[13] Hence, our experimental approach to the synthesis of III has apparently brought about a synthetic, if not mechanistic, realization of our earlier theoretical analysis.

In conclusion, the transformation of IV to III is an example of a clean and rational cluster building synthesis that is assisted by the elimination of H_2. This suggests that hydrogen-rich clusters may constitute important cluster building materials in the future.

Acknowledgment. We gratefully acknowledge the support of the National Science Foundation (CHE81-09503 and CHE84-08251).

Registry No. I, 80572-82-3; III, 99582-34-0; IV, 92055-46-4; $Fe_2(CO)_9$, 15321-51-4.

(6) The X-ray crystal structure of I shows that the boron lies only 0.03 Å above a line joining the two "wingtip" Fe atoms: ref 1.

(7) Tachikawa, M.; Muetterties, E. L. *J. Am. Chem. Soc.* **1980**, *102*, 4541.

(8) The skeletal protons in II exchange, however, the FeHB and FeH-Fe protons in III undergo a more facile fluxional process. Hence, the replacement of C by B^- lowers the activation barrier to skeletal proton migration.

(9) The volume of gas evolved was measured using a gas microvolumeter: Davis, D. D.; Stevenson, K. L. *J. Chem. Educ.* **1977**, *54*, 394.

(10) Consideration of the heats of formation of $Fe(CO)_5$, $Fe_2(CO)_9$ and $Fe_3(CO)_{12}$ suggests that the formation of $Fe(CO)_5$ is energetically favored over $Fe_3(CO)_{12}$ in this instance.

(11) The sensitivity of cluster building reactions to conditions has recently been pointed out: Fjare, D. E.; Gladfelter, W. E. *J. Am. Chem. Soc.* **1984**, *106*, 4799.

(12) The elimination of H_2 is a factor in other known cluster building reactions, e.g., metallacarborane chemistry (see, for example: Grimes, R. N. In "Organometallic Reactions"; Becker, E. I., Tsutsui, M.; Eds.: Plenum Press: New York, 1977; Vol. 6 p 63) and is an important factor in borane cage interconversions (see, for example: DeKock, R. L.; Fehlner, T. P.; Housecroft, C. E.; Lubben, T. V.; Wade, K. *Inorg. Chem.* **1982**, *21*, 25).

(13) Fehlner, T. P.; Housecroft, C. E. *Organometallics* **1984**, *3*, 764.

Synthesis and Structure of a Metallophosphenium–Borane(3) Complex Containing a Bridging BH_3 Group

William F. McNamara, Eileen N. Duesler, Robert T. Paine,* and J. V. Ortiz

Department of Chemistry, University of New Mexico Albuquerque, New Mexico 87131

Peter Kölle and Heinrich Nöth

Institute für Anorganische Chemie, Universität München D-8000 München 2, FRG

Received September 11, 1985

Summary: Combination of $Na(C_5H_5)Mo(CO)_3$ with $(C_6H_5)P(Cl)\{N[Si(CH_3)_3]_2\}$ in THF results in the generation of a metallophosphenium compound, $(C_5H_5)Mo(CO)_2\{P(Ph)\{N[Si(CH_3)_3]_2\}\}$, which in the presence of B_2H_6 or H_3B·THF forms a borane(3) complex, $(C_5H_5)Mo(CO)_2\{P(BH_3)(Ph)\{N[Si(CH_3)_3]_2\}\}$. The solid-state structure of the complex has been determined by X-ray diffration techniques and found to contain the borane group B-bonded to the phosphorus atom and μ-H-bonded to the Mo atom, thereby providing an unusual four-membered ring, Mo–P–$B(H_2)$–(μ-H). Insights into the bonding are provided by qualitative MO analysis.

Nucleophilic group 6 metal carbonylates $Na(C_5H_5)M(CO)_3$ (M = Cr, Mo, W) when allowed to react with several classes of monochlorophosphanes P(X)(Y)(Cl) usually form

0276-7333/86/2305-0380$01.50/0

either metallophosphanes $(C_5H_5)M(CO)_3[P(X)(Y)]$ (A),

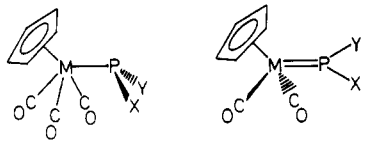

A B

which possess a pyramidal phosphorus atom and an active lone pair,[1,2] or metallophosphenium complexes[3] $(C_5H_5)M(CO)_2[P(X)(Y)]$ (B), which contain a formal M=P multiple bond, planar phosphorus atom geometry, and coordinated phosphorus lone pair.[4,5] The subtle factors that control the formation and isolation of A and B complexes as well as their reaction chemistry are of interest in several laboratories. Evolving studies by Malisch and co-workers[6] primarily on pyramidal metallophosphanes show that much of the chemistry of the A-type species is dominated by reactivity of the uncommitted phosphorus lone pair. Electrophilic attack at the phosphorus atom in B complexes, on the other hand, might not be expected since the lone-pair electron density is anticipated to be involved in the M=P bond. Molecular orbital analysis[4c] for $(C_5H_5)Mo(CO)_2[PN(CH_3)CH_2CH_2NCH_3]$ (1) suggests that electrophilic reactivity should instead be found in addition reactions at the metal center or at ancillary ligands and in degradation processes of the M-P-X unit.[7] In fact, little chemistry of B complexes has been explored.[6b,8] We report here on the formation of a type B metallophosphenium complex, $(C_5H_5)Mo(CO)_2\{P(Ph)\{N[Si(CH_3)_3]_2\}\}$ (2) and its unanticipated electrophilic addition of BH_3.

Reaction of $Na(C_5H_5)Mo(CO)_3$[9] with $(C_6H_5)P(Cl)\{N[Si(CH_3)_3]_2\}$ in equimolar amounts in tetrahydrofuran at 25 °C (6 h) followed by reflux (24 h) resulted in a purple solution containing a crude product, $(C_5H_5)Mo(CO)_2\{P(Ph)\{N[Si(CH_3)_3]_2\}\}$ (2). Ninety-five percent of the expected carbon monoxide was collected and measured with a Toepler pump. The THF solution[10] was vacuum evaporated, the purple residue extracted with benzene, the solution filtered to remove NaCl, the benzene filtrate evaporated to dryness, and microcrystalline 2 collected in 90–95% yield. Analytically pure samples of 2 were obtained by recrystallization from THF at 5 °C.[11]

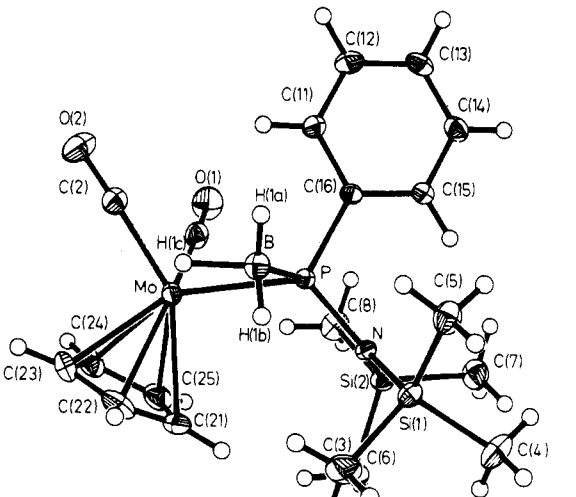

Figure 1. Molecular geometry and atom labeling scheme for $CpMo(CO)_2\{P(Ph)\{N[Si(CH_3)_3]\}(\mu\text{-H-}BH_2)$. Selected bond distances (Å) and angles (deg) include Mo–C(1) = 1.961 (4), Mo–C(2) = 1.965 (4), Mo–P = 2.464 (1), C(1)–O(1) = 1.151 (5), C(2)–O(2) = 1.153 (5), P–B = 1.897 (4), P–N = 1.700 (3), P–C(16) = 1.816 (3), N–Si(1) = 1.779 (3), and N–Si(2) = 1.775 (3) and C(1)–Mo–C(2) = 78.5 (2), C(1)–Mo–P = 82.0 (1), C(2)–Mo–P = 112.8 (1), Mo–C(1)–O(1) = 176.9 (3), Mo–C(2)–O(2) = 178.0 (4), Mo–P–B = 72.6 (1), Mo–P–N = 123.0 (1), Mo–P–C(16) = 121.1 (1), B–P–N = 118.1 (2), N–P–C(16) = 107.1 (1), B–P–C(16) = 110.6 (2), P–N–Si(1) = 117.2 (1), and P–N–Si(2) = 120.7 (1).

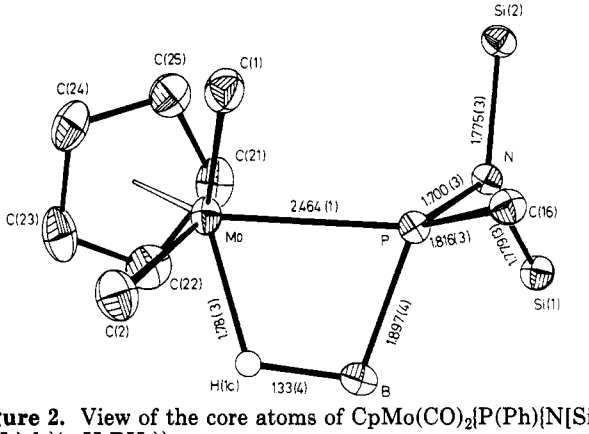

Figure 2. View of the core atoms of $CpMo(CO)_2\{P(Ph)\{N[Si(CH_3)_3]_2\}(\mu\text{-H-}BH_2)\}$.

Infrared spectra[11] reveal two bands, 1948 and 1876 cm^{-1}, in the terminal carbonyl stretching region which are shifted upfrequency from the corresponding bands in $(C_5H_5)Mo(CO)_2[PN(CH_3)CH_2CH_2NCH_3]$ (1), 1894 and 1815 cm^{-1}.[4] This suggests that the phosphenium fragment in 2 acts as a better π-acceptor than the fragment in 1. The $^{31}P\{^1H\}$ spectrum shows a single resonance, 316 ppm, which is

(1) Cooke, M.; Green, M.; Kirkpatrick, D. *J. Chem. Soc. A* **1968**, 1507.
(2) Malisch, W.; Kuhn, M. *J. Organomet. Chem.* **1974**, *73*, C1. Malisch, W.; Maisch, R.; Colquhoun, I. J.; McFarlane, W. *Ibid.* **1981**, *220*, C1. Maisch, R.; Barth, M.; Malisch. W. *Ibid.* **1984**, *260*, C35.
(3) The following nomenclature is employed here to distinguish between the two classes of complexes A and B: $(C_5H_5)M(CO)_3[P(X)(Y)]$ is designated as a pyramidal metallophosphane and $(C_5H_5)M(CO)_2[P(X)(Y)]$ is designated as a planar metallophosphenium complex.
(4) (a) Light, R. W.; Paine, R. T. *J. Am. Chem. Soc.* **1978**, *100*, 2230. (b) Light, R. W.; Paine, R. T. *Inorg. Chem.* **1978**, *18*, 2345. (c) Hutchins, L. D.; Campana, C. F.; Paine, R. T. *J. Am. Chem. Soc.* **1980**, *102*, 4521. (d) Hutchins, L. D.; Duesler, E. N.; Paine, R. T. *Organometallics* **1982**, *1*, 1254. (e) Dubois, D. A.; Duesler, E. N.; Paine, R. T. *Ibid.* **1983**, *2*, 1903.
(5) Cowley, A. H.; Norman, N. C.; Quaskie, S. *J. Am. Chem. Soc.* **1984**, *106*, 5007.
(6) (a) Maisch, R.; Ott, E.; Buchner, W.; Malisch, W.; Colquhoun, I. J.; McFarlane, W. *J. Organomet. Chem.* **1985**, *286*, C31. (b) Gross, E.; Jörg, K.; Fiederling, K.; Göttlein, A.; Malisch, W.; Boese, R. *Angew. Chem., Int. Ed. Ed.* **1984**, *23*, 738. (c) Some related chemistry of arsane and stibane analogues has appeared: Mahmoud, K. A.; Rest, A. J.; Luksza, M.; Jörg, K.; Malisch, W. *Organometallics* **1984**, *3*, 501 and references therein.
(7) The Mo=P double bond in 1 is comprised of phosphenium ion in-plane lone pair ($8a_1$) σ donation to the empty $CpMo(CO)_2^-$ LUMO (3a', z^2) and $CpMo(CO)_2^-$ fragment back-donation from the occupied π pseudosymmetry orbital (HOMO, 1a'', xz) to the empty phosphenium ion π^* LUMO ($4b_1$). The resulting HOMO in 1 is neither of these orbitals but instead is a nonbonding metal d orbital. The LUMO in the complex is the antibonding complement to the π fragment MO mixing described above ($1a''$–$4b_1$).[4c]
(8) Malisch, W.; Jörg, K.; Wekel, E. "Abstracts of Papers", 189th National Meeting of the American Chemical Society, Miami Beach, 1985; American Chemical Society: Washington, D.C., 1985; INOR 250.
(9) $NaCpMo(CO)_3$ was prepared from $[CpMo(CO)_3]_2$ and Na/Hg in THF: King, R. B.; Iqbal, M. Z.; King, A. D. *J. Organomet. Chem.* **1979**, *171*, 53. The phosphane was prepared from $PhPCl_2$ and $NaN(SiMe_3)_2$ in Et_2O by a procedure similar to that described for related phosphanes: Zeiss, W.; Feldt, C.; Weis, J.; Dunkel, G. *Chem. Ber.* **1978**, *111*, 1180.
(10) Abbreviations used in the text include THF = tetrahydrofuran, Cp = cyclopentadienide, and Me = methyl.
(11) Compound 2 was isolated under inert-atmosphere conditions. Characterization: mp 119–122 °C dec; MS (70 eV), m/e 485 (M^+), 427 ($M - 2CO$)$^+$; IR (carbonyl region, cyclohexane) 1948 (vs), 1876 (vs) cm^{-1}; ^1H NMR (25 °C) (CH_2Cl_2/CD_2Cl_2) δ 7.5 (m, phenyl), 5.6 (Cp), 0.32 ($SiMe_3$); $^{13}C\{^1H\}$ NMR (CH_2Cl_2/CD_2Cl_2) δ 131–128 (m, phenyl), 93.1 (d, $^2J_{CP}$ = 1.7 Hz, Cp), 3.3 (d, $^3J_{CP}$ = 2.7 Hz, $SiMe_3$); $^{31}P\{^1H\}$ NMR (THF, H_3PO_4 standard) δ 316. Anal. Calcd for $MoPSi_2O_2NC_{19}H_{28}$: Mo, 19.8; P, 6.4; Si, 11.6; O, 6.6; N, 2.9; C, 47.0; H, 5.8. Found: Mo, 19.4; P, 6.3; Si, 11.3; O, 6.0; N, 2.9; C, 47.8; H, 6.0.

shifted considerably downfield from the phosphane precursor P(Ph)(Cl){N[Si(CH$_3$)$_3$]$_2$}, 143 ppm, and the position is within a wide range of low-field shifts found in other metallophosphenium complexes.[4,12] Analytical and spectroscopic data, therefore, are consistent with the assignment of **2** as a member of the B-type complexes, and its ready isolation as a solid complex make its application for investigations of reaction chemistry favorable.

Unexpectedly, **2** combined rapidly at 25 °C with either B_2H_6 or H_3B·THF in methylcyclohexane solution as indicated by a solution color change from purple to yellow green, and a pale, yellow-green solid, (C$_5$H$_5$)Mo(CO)$_2${P(BH$_3$)(Ph){N[Si(CH$_3$)$_3$]$_2$} (**3**), was isolated in greater than 95% yield. Single crystals of **3** were obtained from a concentrated THF solution. Infrared spectra[13] for **3** show two carbonyl stretching frequencies, 1973 and 1905 cm^{-1}, which are shifted significantly upfrequency from the corresponding pair of carbonyl bands in **2**. This shift is consistent with decreased Mo→CO back-bonding in **3** relative to **2**, which implies enhanced Mo→P back-bonding in **3**. The latter effect would be expected if some of the phosphane electron density originally localized in the Mo=P bond were transferred to a P→B donor–acceptor interaction. Absorptions at 2497 and 2428 cm^{-1} are assigned to B–H stretching modes.[14] The ^{31}P{^{1}H} NMR spectrum (25 °C) of **3** shows a relatively broad resonance at 49.5 ppm with no evidence for P–B coupling; however, the ^{11}B NMR spectrum displays a doublet centered at −55.6 ppm (J_{BP} = 52 Hz).[15]

Although the formation of **3** was unexpected, the analytical and most of the spectroscopic data appear to be consistent with the formation of a simple phosphane–borane complex. The ^{1}H, ^{31}P, and ^{11}B NMR data,[16] however, suggest that some unusual static or dynamic structural features might be operating in **3**. Consequently, an X-ray crystallographic analysis was undertaken.[17]

The structure determination verifies the composition of **3**, and it reveals an unanticipated structural feature. A view of the entire molecule is displayed in Figure 1, and a view of the central core is shown in Figure 2. The structure contains a piano-stool CpMo(CO)$_2$ fragment bonded to the phosphorus fragment P(Ph){N[Si(CH$_3$)$_3$]$_2$} with the borane boron atom bonded to the phosphorus atom. Instead of adopting a simple donor–acceptor P→BH$_3$ structure with three terminal B–H bonds as is normally found for phosphane–borane complexes, the phosphorus atom bonds to the borane group leaving two terminal B–H bonds and a bridging B–H–Mo interaction. The phosphorus atom is four-coordinate, and its geometry is only slightly distorted from trigonal planar toward tetrahedral.[18] The Mo–P distance, 2.464 (1) Å, is relatively elongated in **3** compared to the related distance in the metallophosphenium complex **1**, 2.213 (1) Å. This is consistent with loss of a large degree of the Mo=P multiple-bond character. The Mo–P bond distance in **3** is also slightly longer than the average Mo–P distance, 2.422 Å, in the compound Mo$_2$Cp$_2$(CO)$_4$(μ-H)(μ-PMe$_2$) (**4**).[19] The P–N bond distance, 1.700 (3) Å, is long compared to the average P–N distance in **1**, 1.645 Å. This elongation probably results more from the relatively small degree of P–N π bonding in the phosphenium fragment due to the competing Si–N π interaction and less from the effect of borane coordination. On the other hand, the P–B bond distance, 1.897 (4) Å, is typical of distances found in a number of phosphane–boranes and cyclic phosphinoboranes, 1.84–1.96 Å.[20]

The terminal B–H bond distances, B–H(1a) = 0.94 (4) Å and B–H(1b) = 1.02 (4) Å, are shorter than expected since they do not fall within three standard deviations of the normal range of B–H(t) distances, 1.21–1.24 Å, found in phosphane–boranes.[20] Furthermore, the bridging B–H(1c) distance, 1.33 (4) Å, is clearly longer than the B–H(t) distances. There is, of course, strong precedent for the appearance of B–H(t) distances shorter than B–H(br)–B distances in neutral boranes [e.g., 1.196 (8) Å, B–H(t), and 1.339 (6) Å, B–H(br), in B_2H_6[21]] although an interesting exception to this rule is found in Cu(PPh$_2$Me)$_3$(BH$_4$) [B–H(t) = 1.185 (5), 1.182 (6), and 1.330 (6) Å and B–H–Cu(br) = 1.170 (5)° [22]]. It is interesting to compare B–H(1c) with the Mo–H–B bridge distance in Mo(CO)$_4$(BH$_4$)$^-$, 1.20 (10) Å.[23] It is also interesting to note that the Mo···B sepa-

(12) Cowley, A. H.; Kemp, R. A. *Chem. Rev.*, in press.

(13) Compound **3** was prepared by vacuum transfer of 0.5 equiv of B_2H_6 to 1 equiv of **2** or by addition of 1 equiv of H_3B·THF by syringe techniques to 1 equiv of **2**. Characterization: mp 119–122 °C; MS (70 eV), *m/e* 499 (M$^+$), 485 (M − BH$_3$)$^+$, 471 (M − CO)$^+$, 429 (M − BH$_3$ − 2CO)$^+$; IR (methyl cyclohexane) 2497 (w, ν_{BH}), 2428 (w, ν_{BH}), 2028 (w), 1973 (vs, ν_{CO}), 1905 (vs, ν_{CO}), 1483 (w), 1425 (w), 1268 (sh), 1256 (m, ν_{Si-C}), 1107 (w), 957 (w), 920 (s, ν_{PN}), 870 (s); ^{1}H NMR (25 °C, CD$_2$Cl$_2$) δ 7.3–7.0 (m, phenyl), 5.3 (Cp), 0.35 (SiMe$_3$), 0.24 (SiMe$_3$), −8.6 (μ-BH); ^{13}C{^{1}H} NMR (CH$_2$Cl$_2$/CD$_2$Cl$_2$) δ 140 (d, J_{CP} = 4 Hz, ipso C, phenyl), 130–125 (m, phenyl), 92.5 (Cp), 5.3 (SiMe$_3$), 4.4 (SiMe$_3$); ^{31}P{^{1}H} NMR (THF) δ 49.5; ^{11}B NMR (CD$_2$Cl$_2$) δ −55.6 (d, J_{BP} = 52 Hz). The ^{1}H and ^{13}C NMR data suggest that there are inequivalent SiMe$_3$ groups on the amide nitrogen atom.

(14) Dolphin, D.; Wick, A. "Tabulation of Infrared Spectral Data"; Wiley: New York, 1977. Verkade, J. G. *Coord. Chem. Rev.* **1972/1973**, *9*, 2.

(15) Under experimental conditions explored to date the ^{31}P{^{1}H} and ^{31}P NMR spectra at 25 °C show no evidence for P–B coupling; however, the line width of the resonance ($W_{1/2} \approx 200$ Hz) would make observation of a small coupling constant unlikely. The ^{11}B NMR spectrum, on the other hand, displays a doublet structure, J_{PB} = 52 Hz, but the B–H coupling has not yet been detected. Variable-temperature NMR analyses are planned in order to attempt to resolve all of the expected coupling interactions.

(16) The ^{1}H NMR spectrum shows a single resonance at −8.6 ppm in an area ratio of ~1:5 compared to the Cp hydrogen atoms. There are also several broad resonances which appear around the base of the silyl methyl resonance centered at 0.3 ppm. The high-field resonance offers some evidence to support an assignment of a bridge B–H–Mo unit, found in the crystal structure, for the solution state species. Variable-temperature ^{1}H NMR studies which should resolve this question are in progress.

(17) Compound **3** crystallizes in the orthorhombic space group $P2_12_12_1$ with lattice constants a = 10.171 (2), b = 12.537 (2), c = 18.837 (3), β = 90.0°, V = 2401.8 (7) Å,^{3} Z = 4, and ρ_{calcd} = 1.38 g cm^{-3}. Diffraction data were collected on a Syntex P3/F diffractometer by using Mo Kα radiation at 20 °C. The structure was solved by direct methods on 6013 unique reflections with $F \geq 3\sigma(F)$. The structure was refined anisotropically on all non-hydrogen atoms (isotropic on all hydrogen atoms), and the final discrepancy indices were R_F = 0.042 and R_{wF} = 0.038.

(18) The sum of bond angles Mo–P–N, Mo–P–C(16), and N–P–C(16) is 351.2°. This indicates that the original trigonal-planar geometry about the phosphorus atom in **2** has not been grossly distorted toward tetrahedral in **3**. The bond angles involving the P–B bond vector, and the MoPNC(16) unit are Mo–P–B = 72.6°, B–P–C(16) = 110.6°, and B–P–N = 118.1°. These angles indicate that the B atom is slightly displaced toward the Mo atom as would be expected for a Mo–H–B bridge interaction.

(19) Petersen, J. L.; Dahl, L. F.; Williams, J. M. *J. Am. Chem. Soc.* **1974**, *96*, 6610.

(20) Corbridge, D. E. C. "The Structural Chemistry of Phosphorus"; Elsevier: Amsterdam, 1974; pp 391–392 and references therein. Kuczkowski, R. L.; Lide, D. R. *J. Chem. Phys.* **1967**, *46*, 357. Durig, J. R.; Li, Y. S.; Carreira, L. A.; Odom, J. D. *J. Am. Chem. Soc.* **1973**, *95*, 2491. Pasinski, J. P.; Kuczkowski, R. L. *J. Chem. Phys.* **1971**, *54*, 1903. Bryan, P. S.; Kuczkowski, R. L. *Inorg. Chem.* **1972**, *11*, 553. Black, D. L.; Taylor, R. C. *Acta Crystallogr. Sect. B: Struct. Crystallogr. Cryst. Chem.* **1975** *B31*, 1116. Caution, of course, must be exercised in comparing B–H or Mo–H bond distances between molecules since relatively large standard deviations in the distances are inherent. We have employed a conservative 3σ test in all comparisons. Differences in bond distances within 3σ are assumed to indicate equal bond distances.

(21) Bartell, L. S.; Carroll, B. L. *J. Chem. Phys.* **1965**, *42*, 1135.

(22) Takusagawa, F.; Fumagalli, A.; Koetzle, T. F.; Shore, S. G.; Schmitkons, T.; Fratini, A. V.; Morse, K. W.; Wei, C.-Y.; Bau, R. *J. Am. Chem. Soc.* **1981**, *103*, 5165.

(23) Kirtley, S. W.; Andrews, M. A.; Bau, R.; Grynkewich, G. W.; Marks, T. J.; Tipton, D. L.; Whittlesey, B. R. *J. Am. Chem. Soc.* **1977**, *99*, 7154.

ration in **3** is 2.622 (4) Å which is considerably longer than the Mo···B separation in $Mo(CO)_4(BH_4)^-$, 2.41 (2) Å, and longer than the sum of the estimated covalent radii, 2.44–2.49 Å. Lastly, the Mo–H(1c) distance, 1.78 (3) Å, is slightly shorter but within three standard deviations of a range of Mo–H–Mo bridge distances, 1.85–1.89 Å,[24] and significantly shorter than the average Mo–(H–B) bridging distance in $Mo(CO)_4(BH_4)^-$, 2.02 Å.

As a final structural point it is noted that the bridging hydride occupies a coordination position on the Mo atom; therefore, the $CpMo(CO)_2(H)[P(X)(Y)]$ fragment should be considered as a four-legged piano stool. The average M–CO distance, 1.963 Å, and OC–Mo–CO angle, 78.5 (2°), compare favorably with the respective parameters in other $CpMo(CO)_2L_2$ complexes.[25]

The bonding in **3** has been examined with extended Hückel calculations[26] which reveal two principal interactions between the simplified fragments $CpMo(CO)_2PH_2$ and BH_3. One high-lying occupied MO and the LUMO of the $CpMo(CO)_2PH_2$ fragment are chiefly bonding and antibonding combinations of a d orbital on the Mo atom and the p orbital on the P atom that is perpendicular to the PH_2 plane. While the bulk of the electron density in the bonding orbital is on the phosphorus atom, the LUMO is primarily localized on the Mo atom.[27] The high-lying occupied MO of $CpMo(CO)_2PH_2$ donates electron density into the BH_3 fragment LUMO, the p orbital on the B atom perpendicular to the BH_3 plane, resulting in a B–P interaction. The $CpMo(CO)_2PH_2$ LUMO also accepts electron density from one of the degenerate HOMO's of the BH_3 group which lies in the BH_3 plane and is a bonding combination of a B atom p orbital with the s orbital of the bridging hydrogen atom.[28] (The other two H atom s orbitals also mix constructively with the other lobe of the B atom p orbital.) Mo–H_b bonding is enhanced and B–H_b bonding is diminished (relative to the separated fragments) by this mixing of fragment MO's. Such appropriations of electron density are well-known for C–H bonds where a wealth of structures has illuminated the preliminary stages of C–H bond activation.[29] Furthermore, it is intriguing to note that the structure of **3** might be considered to represent a trapped intermediate in the addition of a B-H bond across the formal Mo=P bond.

The formation and solid-state structure of **3** can be rationalized and understood with the bonding picture described above. It remains to be demonstrated that the same structure prevails in solution. Detailed IR and NMR studies of solutions of **3** are in progress, and additional studies of the reactions of electrophilic reagents with **2** are underway.

Acknowledgment. R.T.P. and J.V.O. wish to acknowledge the donors of the Petroleum Research Fund, administered by the American Chemical Society for the support of this research. R.T.P. and H.N. recognize support for collaborative studies on borophane ligands provided by a NATO travel grant.

Registry No. **2**, 99641-85-7; **3**, 99641-86-8; $NaN(SiMe_3)_2$, 1070-89-9; $(C_6H_5)P(Cl)\{N[Si(CH_3)_3]_2\}$, 84174-75-4; $Na(C_5H_5)Mo(CO)_3$, 12107-35-6; B_2H_6, 19287-45-7; $H_3B{\cdot}THF$, 14044-65-6; $PhPCl_2$, 644-97-3.

Supplementary Material Available: Listings of observed and calculated structure factors, positional parameters, anisotropic thermal parameters, and bond distances and angles (21 pages). Ordering information is given on any current masthead page.

(24) Love, R. A.; Chin, H. B.; Koetzle, T. F.; Kirtley, S. W.; Whittlesey, B. R.; Bau, R. *J. Am. Chem. Soc.* **1976**, *98*, 4491.
(25) Curtis, M. D.; Han, K. R. *Inorg. Chem.* **1985**, *24*, 378.
(26) (a) Hoffmann, R. *J. Chem. Phys.* **1963**, *39*, 1397. (b) Hoffmann, R.; Lipscomb, W. N. *Ibid.* **1962**, *36*, 2179; **1962**, *37*, 2872. (c) Ammeter, J. H.; Burgi, H. B.; Thibeault, J. C.; Hoffmann, R. *J. Am. Chem. Soc.* **1978**, *100*, 3686. (d) Parameters: Summerville, R. H.; Hoffmann, R. *J. Am. Chem. Soc.* **1976**, *98*, 7240. (e) Both D_{3h} BH_3 and BH_3 with observed bond lengths were used. Some averaging of experimental bond lengths and bond angles was necessary to impose C_s symmetry. (f) Calculations performed with the interactive program EHT, by J. V. Ortiz.
(27) The π Mo–P interaction is much less covalent in $CpMo(CO)_2PH_2$ than in **1**, where the p orbital on the phosphorus atom is destabilized by the NR_2 groups.
(28) The same qualitative picture emerges whether the observed BH_3 geometry or an idealized D_{3h} BH_3 geometry is employed in the calculations.
(29) C–H–transition-metal bonds are reviewed in: Brookhart, M.; Green, M. L. H. *J. Organomet. Chem.* **1983**, *250*, 395. An extensive theoretical analysis is presented in: Saillard, J. Y.; Hoffmann, R. *J. Am. Chem. Soc.* **1984**, *106*, 2006.

On the Metal Coordination in Base-Free Tris(cyclopentadienyl) Complexes of the Lanthanoids. 2.[1] The X-ray Structure of $(C_5L_5)_3La^{III}$: A Notably Stable Polymer Displaying More Than Three Different La···C Interactions

Stefan H. Eggers, Jürgen Kopf, and R. Dieter Fischer*
Institut für Anorganische and Angewandte Chemie Universität Hamburg, D-2000 Hamburg 13, F.R.G.

Received July 30, 1985

Summary: Crystalline base-free Cp_3La (Cp = C_5H_5; monoclinic *P*, space group $P2_1$; a = 8.427 (5) Å, b = 9.848 (5) Å, c = 8.456 (6) Å, β = 115.80 (6)°; Z = 2; R = 0.077) forms polymeric zig-zag chains of distinct $(C_5H_5)_2La(\mu\text{-}\eta^5\text{:}\eta^2\text{-}C_5H_5)$ units involving two nonequivalent terminal Cp ligands. The individual La···C distances cluster predominantly around 2.6, 2.8, 2.9, and 3.0 Å within the unexpectedly wide range 2.560–3.034 Å.

While the synthesis of base-free $(C_5H_5)_3M$ complexes (including the first well-defined organo-rare-earth compounds;[2] M = Sc, Y, La, Ce, Pr, Nd, Sm, Gd, Dy, Er, and Yb)[3] dates back to 1954, the elucidation of the crystal and molecular structures of representatives of this fundamental class of compounds has turned out considerably more difficult than for the majority of their derivatives.[2,4] In 1969, a first report based on a crystallographic X-ray analysis suggested for Cp_3Sm a rather complex situation involving two different polymeric chains along with strongly disordered Cp rings.[5,6] While crystalline $(C_5H_5)_3Sc$ involves chains of well-defined $(\eta^5\text{-}C_5H_5)_2Sc(\mu\text{-}\eta^1\text{:}\eta^1\text{-}C_5H_5)$ units,[7] the likewise polymeric compound $(C_5H_5)_3Pr$ (**1**) is built up of zig-zag chains of distinct $(\eta^5\text{-}C_5H_5)_2Pr(\mu\text{-}\eta^x\text{:}\eta^5\text{-}C_5H_5)$ units with $1 < x < 2$.[1] Our continuing interest in the structures of Cp_3Ln systems (Ln =

(1) Part 1: Hinrichs, W.; Melzer, D.; Rehwoldt, M.; Jahn, W.; Fischer, R. D. *J. Organomet. Chem.* **1983**, *251*, 299.
(2) For the most recent reviews on organolanthanoid chemistry, see: (a) Schumann, H. *Angew. Chem., Int. Ed. Engl.* **1984**, *23*, 474. (b) Schumann, H.; Genthe, W. In "Handbook on the Physics and Chemistry of Rare Earths", Gschneidner, K. A., Ed.; Elsevier: Amsterdam, 1984; Vol. 6, p 445. (c) Schumann, H. In "Fundamental and Technological Aspects of Organo-f-Element Chemistry"; Marks, T. J., Fragalà, I. L., Eds.; D. Reidel Publishing Company, Dordrecht, Holland, 1985; p 1.
(3) Wilkinson, G.; Birmingham, J. M. *J. Am. Chem. Soc.* **1954**, *76*, 6210, for further literature see ref 2.
(4) For a review on organolanthanoid structures, see: Palenik, G. J. In "Systematics and the Properties of the Lanthanides"; Sinha, S. P., Ed.; D. Reidel Publishing Company: Dordrecht, Holland, 1983; p 153.
(5) Wong, C.; Lee, T.; Lee, Y. *Acta Crystallogr., Sect. B: Struct. Crystallogr. Cryst. Chem.* **1969**, *B25*, 2580.
(6) Most recently, a reinvestigation of the frequently questioned (see ref 1) structure of Cp_3Sm[5] has been attempted and turned out extremely difficult: Eggers, S.; Kopf, J.; Fischer, R. D., unpublished results.
(7) Atwood, J. L.; Smith, K. D. *J. Am. Chem. Soc.* **1973**, *95*, 1488.

0276-7333/86/2305-0383$01.50/0

ration in **3** is 2.622 (4) Å which is considerably longer than the Mo···B separation in $Mo(CO)_4(BH_4)^-$, 2.41 (2) Å, and longer than the sum of the estimated covalent radii, 2.44–2.49 Å. Lastly, the Mo–H(1c) distance, 1.78 (3) Å, is slightly shorter but within three standard deviations of a range of Mo–H–Mo bridge distances, 1.85–1.89 Å,[24] and significantly shorter than the average Mo–(H–B) bridging distance in $Mo(CO)_4(BH_4)^-$, 2.02 Å.

As a final structural point it is noted that the bridging hydride occupies a coordination position on the Mo atom; therefore, the $CpMo(CO)_2(H)[P(X)(Y)]$ fragment should be considered as a four-legged piano stool. The average M–CO distance, 1.963 Å, and OC–Mo–CO angle, 78.5 (2°), compare favorably with the respective parameters in other $CpMo(CO)_2L_2$ complexes.[25]

The bonding in **3** has been examined with extended Hückel calculations[26] which reveal two principal interactions between the simplified fragments $CpMo(CO)_2PH_2$ and BH_3. One high-lying occupied MO and the LUMO of the $CpMo(CO)_2PH_2$ fragment are chiefly bonding and antibonding combinations of a d orbital on the Mo atom and the p orbital on the P atom that is perpendicular to the PH_2 plane. While the bulk of the electron density in the bonding orbital is on the phosphorus atom, the LUMO is primarily localized on the Mo atom.[27] The high-lying occupied MO of $CpMo(CO)_2PH_2$ donates electron density into the BH_3 fragment LUMO, the p orbital on the B atom perpendicular to the BH_3 plane, resulting in a B–P interaction. The $CpMo(CO)_2PH_2$ LUMO also accepts electron density from one of the degenerate HOMO's of the BH_3 group which lies in the BH_3 plane and is a bonding combination of a B atom p orbital with the s orbital of the bridging hydrogen atom.[28] (The other two H atom s orbitals also mix constructively with the other lobe of the B atom p orbital.) Mo–H_b bonding is enhanced and B–H_b bonding is diminished (relative to the separated fragments) by this mixing of fragment MO's. Such appropriations of electron density are well-known for C–H bonds where a wealth of structures has illuminated the preliminary stages of C–H bond activation.[29] Furthermore, it is intriguing to note that the structure of **3** might be considered to represent a trapped intermediate in the addition of a B-H bond across the formal Mo=P bond.

The formation and solid-state structure of **3** can be rationalized and understood with the bonding picture described above. It remains to be demonstrated that the same structure prevails in solution. Detailed IR and NMR studies of solutions of **3** are in progress, and additional studies of the reactions of electrophilic reagents with **2** are underway.

Acknowledgment. R.T.P. and J.V.O. wish to acknowledge the donors of the Petroleum Research Fund, administered by the American Chemical Society for the support of this research. R.T.P. and H.N. recognize support for collaborative studies on borophane ligands provided by a NATO travel grant.

Registry No. **2**, 99641-85-7; **3**, 99641-86-8; $NaN(SiMe_3)_2$, 1070-89-9; $(C_6H_5)P(Cl)\{N[Si(CH_3)_3]_2\}$, 84174-75-4; $Na(C_5H_5)Mo(CO)_3$, 12107-35-6; B_2H_6, 19287-45-7; $H_3B{\cdot}THF$, 14044-65-6; $PhPCl_2$, 644-97-3.

Supplementary Material Available: Listings of observed and calculated structure factors, positional parameters, anisotropic thermal parameters, and bond distances and angles (21 pages). Ordering information is given on any current masthead page.

(24) Love, R. A.; Chin, H. B.; Koetzle, T. F.; Kirtley, S. W.; Whittlesey, B. R.; Bau, R. *J. Am. Chem. Soc.* **1976**, *98*, 4491.
(25) Curtis, M. D.; Han, K. R. *Inorg. Chem.* **1985**, *24*, 378.
(26) (a) Hoffmann, R. *J. Chem. Phys.* **1963**, *39*, 1397. (b) Hoffmann, R.; Lipscomb, W. N. *Ibid.* **1962**, *36*, 2179; **1962**, *37*, 2872. (c) Ammeter, J. H.; Burgi, H. B.; Thibeault, J. C.; Hoffmann, R. *J. Am. Chem. Soc.* **1978**, *100*, 3686. (d) Parameters: Summerville, R. H.; Hoffmann, R. *J. Am. Chem. Soc.* **1976**, *98*, 7240. (e) Both D_{3h} BH_3 and BH_3 with observed bond lengths were used. Some averaging of experimental bond lengths and bond angles was necessary to impose C_s symmetry. (f) Calculations performed with the interactive program EHT, by J. V. Ortiz.
(27) The π Mo–P interaction is much less covalent in $CpMo(CO)_2PH_2$ than in **1**, where the p orbital on the phosphorus atom is destabilized by the NR_2 groups.
(28) The same qualitative picture emerges whether the observed BH_3 geometry or an idealized D_{3h} BH_3 geometry is employed in the calculations.
(29) C–H–transition-metal bonds are reviewed in: Brookhart, M.; Green, M. L. H. *J. Organomet. Chem.* **1983**, *250*, 395. An extensive theoretical analysis is presented in: Saillard, J. Y.; Hoffmann, R. *J. Am. Chem. Soc.* **1984**, *106*, 2006.

On the Metal Coordination in Base-Free Tris(cyclopentadienyl) Complexes of the Lanthanoids. 2.[1] The X-ray Structure of $(C_5L_5)_3La^{III}$: A Notably Stable Polymer Displaying More Than Three Different La···C Interactions

Stefan H. Eggers, Jürgen Kopf, and R. Dieter Fischer*
Institut für Anorganische and Angewandte Chemie Universität Hamburg, D-2000 Hamburg 13, F.R.G.

Received July 30, 1985

Summary: Crystalline base-free Cp_3La (Cp = C_5H_5; monoclinic *P*, space group $P2_1$; a = 8.427 (5) Å, b = 9.848 (5) Å, c = 8.456 (6) Å, β = 115.80 (6)°; Z = 2; R = 0.077) forms polymeric zig-zag chains of distinct $(C_5H_5)_2La(\mu\text{-}\eta^5\text{:}\eta^2\text{-}C_5H_5)$ units involving two nonequivalent terminal Cp ligands. The individual La···C distances cluster predominantly around 2.6, 2.8, 2.9, and 3.0 Å within the unexpectedly wide range 2.560–3.034 Å.

While the synthesis of base-free $(C_5H_5)_3M$ complexes (including the first well-defined organo-rare-earth compounds;[2] M = Sc, Y, La, Ce, Pr, Nd, Sm, Gd, Dy, Er, and Yb)[3] dates back to 1954, the elucidation of the crystal and molecular structures of representatives of this fundamental class of compounds has turned out considerably more difficult than for the majority of their derivatives.[2,4] In 1969, a first report based on a crystallographic X-ray analysis suggested for Cp_3Sm a rather complex situation involving two different polymeric chains along with strongly disordered Cp rings.[5,6] While crystalline $(C_5H_5)_3Sc$ involves chains of well-defined $(\eta^5\text{-}C_5H_5)_2Sc(\mu\text{-}\eta^1\text{:}\eta^1\text{-}C_5H_5)$ units,[7] the likewise polymeric compound $(C_5H_5)_3Pr$ (**1**) is built up of zig-zag chains of distinct $(\eta^5\text{-}C_5H_5)_2Pr(\mu\text{-}\eta^x\text{:}\eta^5\text{-}C_5H_5)$ units with $1 < x < 2$.[1] Our continuing interest in the structures of Cp_3Ln systems (Ln =

(1) Part 1: Hinrichs, W.; Melzer, D.; Rehwoldt, M.; Jahn, W.; Fischer, R. D. *J. Organomet. Chem.* **1983**, *251*, 299.
(2) For the most recent reviews on organolanthanoid chemistry, see: (a) Schumann, H. *Angew. Chem., Int. Ed. Engl.* **1984**, *23*, 474. (b) Schumann, H.; Genthe, W. In "Handbook on the Physics and Chemistry of Rare Earths", Gschneidner, K. A., Ed.; Elsevier: Amsterdam, 1984; Vol. 6, p 445. (c) Schumann, H. In "Fundamental and Technological Aspects of Organo-f-Element Chemistry"; Marks, T. J., Fragalà, I. L., Eds.; D. Reidel Publishing Company, Dordrecht, Holland, 1985; p 1.
(3) Wilkinson, G.; Birmingham, J. M. *J. Am. Chem. Soc.* **1954**, *76*, 6210, for further literature see ref 2.
(4) For a review on organolanthanoid structures, see: Palenik, G. J. In "Systematics and the Properties of the Lanthanides"; Sinha, S. P., Ed.; D. Reidel Publishing Company: Dordrecht, Holland, 1983; p 153.
(5) Wong, C.; Lee, T.; Lee, Y. *Acta Crystallogr., Sect. B: Struct. Crystallogr. Cryst. Chem.* **1969**, *B25*, 2580.
(6) Most recently, a reinvestigation of the frequently questioned (see ref 1) structure of Cp_3Sm[5] has been attempted and turned out extremely difficult: Eggers, S.; Kopf, J.; Fischer, R. D., unpublished results.
(7) Atwood, J. L.; Smith, K. D. *J. Am. Chem. Soc.* **1973**, *95*, 1488.

0276-7333/86/2305-0383$01.50/0

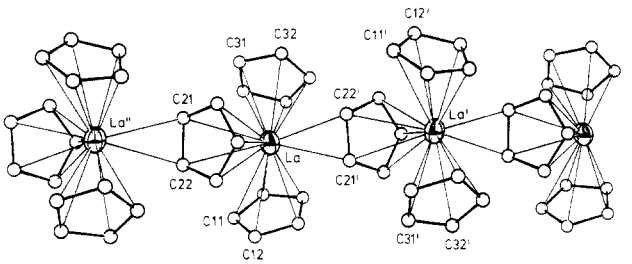

Figure 1. ORTEP plot of $[(C_5H_5)_3La]_\infty$. Selected bond lengths (in Å) and angles (deg): La–C11 2.999 (6); La–C12, 2.949 (6); La–C13, 2.680 (6); La–C14, 2.560 (6); La–C15, 2.774 (5); La–C23, 2.947 (6); La–C24, 2.912 (5); La–C31, 2.897 (6); La–C32, 2.858 (6); La–C34, 2.730 (5); La''–C21, 3.034 (6); La''–C22, 3.032 (6); La''–C23 to La''–C25 ≥ 3.713; Cent1–La–Cent2, 111.5 (2); Cent1–La–Cent3, 114.9 (2); Cent2–La–Cent3, 116.5 (2); La'–La–La'', 114.8.

La–Lu) has primarily[8] been focused on the La complex $(C_5H_5)_3La$ (**2**), mainly for three reasons. (a) Owing to the maximal ionic radius in case of Ln(III) = La(III),[9] notable differences even between the structures of **1** and **2** might be envisioned. (b) While the literature is still devoid of any detailed description of the chemistry of **2**, this compound belongs to the few commercially available organolanthanoids[10] and has been claimed to be advantageous in arriving, e.g., at some prostaglandine precursors.[11] (c) The only X-ray studies of organo La complexes so far reported are those of the two base adducts of **2**, $Cp_3La{\cdot}THF$[12] (**3**) and $Cp_3La(NCMe)_2$[13] (**4**).

Following the original procedure,[3] sublimed **2** was prepared in yields up to 89%.[14] In contrast to an earlier attempt,[12] single crystals suitable for an X-ray study were obtained aside major portions of amorphous material both during the stepwise high-vacuum sublimation of crude **2** (250–300 °C) and by resublimation (ca. 235 °C). The structure of **2**[15] resembles that of **1**[1] in view of a number of features, including the crystal system and the space group. Thus, **2** forms uniform nonlinear polymeric chains, carrying again adversely disordered Cp rings, but, in contrast to **1**, **2** consists of well-defined $(\eta^5\text{-}C_5H_5)_2La(\mu\text{-}\eta^2{:}\eta^5\text{-}C_5H_5)$ units (Figure 1). The bridging Cp ring lies notably more remote from its η^5-bonded Ln atom than the two terminal η^5-Cp ligands: **2**, Cent(Cp)–Ln = 2.705 (5) ($(La-C)_{av}$ = 2.955), 2.555 (6), 2.532 (6) Å; **1**,[1] 2.602 ($(Pr-C)_{av}$ = 2.875), 2.526, 2.488 Å. The lengths of the two μ-C···La′ contacts of **2**, 3.034 (6) and 3.032 (6) Å (**1**,[1] 2.940 and 3.130 Å), appear, after correction for the appropriate radius of Ln(III),[9] comparable with those of the short intramolecular Ln···C contacts of two recently examined $(C_5H_5)_2$-Ln···$(CH_3)Si(CH_3)_2CHSi(CH_3)_3$ systems.[16]

While distinct M–C(methyl) bonds may be ruled out in the latter case and although the sublimation enthalpy of **2** does not notably exceed that of **1** (nor the values of other Cp_3Ln systems),[17] there is increasing experimental evidence of a more pronounced tendency of **2** (relative to **1**) to form the sparingly soluble polymer, or to oligomerize in solution, rather than to add one Lewis base molecule, L. Thus, in CH_2Cl_2 which cleaves Cp_3Ln aggregates more readily than C_6H_6[18] the solubility of **1** (11.4 mg/mL) exceeds that of **2** (0.6 mg/mL) by more than 1 order of magnitude. Actually, the ^1H NMR spectrum of **2** in CD_2Cl_2 displays two Cp proton resonances even at room temperature (δ 6.25 and 6.09; I_{rel} = ca. 2 and 3) whereas **1** gives rise to one singlet down to −40 °C (δ 21.1).[18] Hence, at least one $(Cp_3La)_n$ species might be sufficiently long-lived on the ^1H NMR time scale, while the reverse seems to hold for the new adduct $Cp_3La{\cdot}NHEt_2$,[19] the CH_2 resonance of which is, unlike that of its Pr homologue,[20] devoid of any diastereotopic splitting down to −70 °C. It has, moreover, been impossible to isolate adducts of **2** with Et_2O[21] and Et_3N.[19]

While the crystalline Lewis base adducts of **1** and **2** like, e.g., **3**[12] and **4**[13] usually involve three equivalent terminal η^5-Cp ligands with rather close-lying individual Ln–C distances,[22] one terminal Cp ligand of **2**, and to a lesser extent of **1**, too, shows a pronounced, and hitherto unprecedented,[23] alternance of its Ln–C distances: e.g., **2**, $(La-C)_{min}$ = 2.560 (6), $(La-C)_{max}$ = 2.999 (6), and $(La-C)_{av}$ = 2.805 Å; **1**,[1] $(Pr-C)_{min}$ = 2.590 (8), $(Pr-C)_{max}$ = 2.910 (10), $(Pr-C)_{av}$ = 2.784 Å.[24] While the strikingly small value of $(La-C)_{min}$ approaches the shortest individual Ln–C(Cp) distances so far reported[25] and would also correlate with those expected for genuine La–C σ-bonds,[26] $(La-C)_{max}$

(8) A systematic survey of the mostly nonuniform structures of base-free Cp_3Ln systems with Ln = La, Pr, Nd, Er, Tm, and Lu is going to be published in due course.

(9) $r(La)-r(Pr)$ = 0.06 Å; see: Shannon, R. D. *Acta Crystallogr. Sect. A: Cryst. Phys., Diffr., Theor. Gen. Crystallogr.* **1976**, *A32*, 751.

(10) Together with Cp_3Sm; Strem Chemicals Inc., No. 57-3000 and 62-3500.

(11) Thus, unlike MCp (e.g., M = Li, Na, Tl), **2** reacts, e.g., with alkylsulfonates to give exclusively the 5-alkylcyclopentadienes: French Patents 2 221 424 (1973) and 2 259 089 (1974).

(12) Rogers, R. D.; Atwood, J. L.; Emad, A.; Sikoric, P. J.; Rausch, M. D. *J. Organomet. Chem.* **1981**, *216*, 383.

(13) Li, X.-F.; Eggers, S.; Kopf, J.; Jahn, W.; Fischer, R. D.; Apostolidis, C.; Kanellakopulos, B.; Benetollo, F.; Polo, A.; Bombieri, G. *Inorg. Chim. Acta* **1985**, *100*, 183.

(14) Reaction of 5.35 g (21.8 mmol) of $LaCl_3$ with 6.2 g (70.4 mmol) of NaCp over 8 h; the crude product was dried at 130 °C for 5 h; high vacuum sublimation (in Schlenk tube of 25-cm length and 3.5-cm diameter): 8 h, up to 220 °C; 8 h, up to 260 °C; 8 h, up to 300 °C. Color of sublimed **2**: yellowish. Total yield: 6.5 g (19.4 mmol = 89%) of $(C_5H_5)_3La$ (maximal yield according to ref 3, 25%).

(15) Crystal data (25 °C): monoclinic P, $P2_1$, a = 8.427 (5) Å, b = 9.848 (5) Å, c = 8.456 (6) Å, β = 115.80 (6)°, Z = 2, ρ = 1.757 g·cm^{-3}, Syntex $P2_1$, Mo K_α, graphite monochromator, $4.5° < 2\theta < 50°$; full-matrix least-squares refinement (treating the ring C atoms exactly as described in ref 1) based on 1721 observed reflections ($I > 3\sigma(I)$) led after numerical absorption corrections to a final R (unweighted) of 0.0771 (anisotropic temperature factor, positions of H atoms calculated).

(16) (a) Ln = Nd: Nd···C = 2.895 (7) Å, Nd–C(σ-bond) = 2.517 (7) Å. Mauermann, H.; Swepston, P. N.; Marks, T. J. *Organometallics* **1985**, *4*, 200. (b) Ln = Y: Y···C = 2.85 Å, Y–C (σ-bond) = 2.43 Å. Teuben, J. H. In "Fundamental and Technological Aspects of Organo-f-Element Chemistry"; Marks, T. J., Fragalà, I. L., Eds.; D. Reidel Publishing Company: Dordrecht, Holland, 1985; p 195.

(17) Exception: Ln = Lu: (a) Devyatykh, G. G.; Borisov, G. K.; Krasnova, S. G. *Dokl. Akad. Nauk SSSR* **1972**, *203*, 110. (b) Devyatykh, G. G.; Borisov, G. K.; Zyuzina, L. F.; Krasnova, S. G. *Dokl. Akad. Nauk SSSR* **1973**, *212*, 127.

(18) Jahn, W. Ph. D. Thesis, Universität Hamburg, 1983.

(19) Eggers, S. H.; Fischer, R. D., unpublished results.

(20) Jahn, W.; Yünlü, K.; Oroschin, W.; Amberger, H.-D.; Fischer, R. D. *Inorg. Chim. Acta* **1984**, *95*, 85.

(21) Completely white (in contrast to sublimed **2**) and analytically very pure **2** could readily be isolated from suspensions of **2** in OEt_2.

(22) For the structure of $Cp_3Pr(NCMe)_2$, see ref 13. For the structure of $Cp_3Pr{\cdot}THF$, see: Fan, Y.; Lü, P.; Jin, Zh.; Chen, W. *Sci. Sin., Ser. B (Engl. Transl.)* **1984**, *27*, 993.

(23) For comparison, for the sterically rather congested complex Ta$(\eta^5\text{-Cp})(\eta^2\text{-}C_2H_4)(PMe_2Ph)_2Cl_2$ was found: $(Ta-C)_{min}$ = 2.37 (1) Å, $(Ta-C)_{max}$ = 2.62 (3) Å; here $(Ta-C)_{min}$ does not turn out drastically smaller than $(Ta-C)_{min}$ of less perturbed Cp_nTa^{III} systems (n = 1 or 2). See: Atwood, J. L.; Honan, M. B.; Rogers, R. D. *J. Cryst. Spectrosc. Res.* **1982**, *12*, 205 and references therein. (b) The relative scattering of La–C in **2** also exceeds that of Th–C in the complex $Me_2Si(C_5Me_4)_2Th(CH_2SiMe_3)_2$ where a rather pronounced dispersion about the average ring C-C distance has been observed too: Fendrick, C. M.; Mintz, E. A.; Schertz, L. D.; Marks, T. J.; Day, V. W. *Organometallics* **1984**, *3*, 819.

(24) For the other terminal Cp ligand of **2** were found: $(La-C)_{min}$ = 2.730 (5) Å, $(La-C)_{max}$ = 2.897 (6) Å, $(La-C)_{av}$ = 2.818 Å.

(25) $(Ln-C)_{min}$ is, e.g., 2.582 (7) Å in $[Cp_2Sm(SiMe_3)_2]^-$ (Schumann, H.; Nickel, S.; Hahn, E.; Heeg, M. J. *Organometallics* **1985**, *4*, 800) and 2.48 (5) Å in Cp_2LuCl-THF (Ni, Ch.-Zh.; Zhang, Zh.-M.; Deng, D.-L.; Qian, Ch.-T. *J. Organomet. Chem.*, in press. Qian, Ch.-T., personal communication).

(26) See, for comparison, Nd–C(HSi_2) of $(C_5Me_5)_2NdCH(SiMe_3)_2$;[16a] however, $(La-C)_{min}$ of **2** is smaller than Pr–C(N) of $Cp_3PrCN\text{-}c\text{-}C_6H_{11}$ (2.68 Å): Burns, J. H.; Baldwin, W. H. *J. Organomet. Chem.* **1976**, *120*, 361.

equals the comparatively long bridging contact La′···μ-C(Cp).

In summary, the coordination of La(III)) in **2** is, probably due to optimal intra- and interchain packing, so irregular that any description in terms of either a common coordination polyhedron or a formal coordination number (in terms of integer electron pairs) appears inappropriate. Including all La···C contacts up to 3.035 Å, the same total ligand hapticity of 17 as for **4**[13] would result.

Acknowledgment. We gratefully appreciate grants (for S.E.) by the Allgemeiner Forschungspool der Universität Hamburg and by the Deutscher Akademischer Austauschdienst (DAAD), Bonn. Dipl.-Chem. Holger Schultze kindly contributed a fraction of carefully sublimed **2**.

Registry No. **2**, 1272-23-7.

Supplementary Material Available: Tables of crystal data, atomic parameters and temperature factors, most important bond distances and angles, anisotropic thermal parameters, calculated hydrogen atomic parameters, and observed and calculated structure factors (15 pages). Ordering information is given any current masthead page.

On the Mechanism of the Hydrogenation/Dehydrogenation of a C_2 Fragment on a Triiron Cluster Site

T. K. Dutta, J. C. Vites, and T. P. Fehlner*

Department of Chemistry, University of Notre Dame Notre Dame, Indiana 46556

Received September 6, 1985

Summary: Deuterium tracer studies show that the proton-induced hydrogenation/dehydrogenation of a triiron vinylidene anion/triiron ethylidyne proceeds via a mechanism in which protonation/deprotonation takes place on the organic fragment while hydrogenation/dehydrogenation occurs on the triiron fragment. Evidence is presented for the formation of an unsaturated intermediate in the protonation step.

Reactions on ligands bound to metal cluster systems are of great interest as they can serve as realistic models for reactions occurring in heterogeneous phases.[1] Presently, however, concepts of cluster reactivity are based extensively on the isolation and characterization of reasonably stable systems. Although the structure and bonding of such species provide a necessary foundation for an understanding of reactivity, they are no substitute for true mechanistic investigations.[2] Recently we reported[3] that the deprotonation of $(\mu\text{-H})_3Fe_3(CO)_9(\mu_3\text{-}CCH_3)$(I) results in the loss of H_2 and the formation of the vinylidene anion[4]

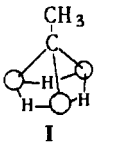

I

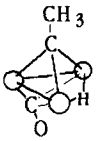

III

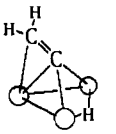

II

$[(\mu\text{-H})Fe_3(CO)_9C{=}CH_2^-]$ (II) (eq 1). This reaction is quantitative at 25 °C. The reverse reaction takes place

$$H_3Fe_3(CO)_9CCH_3 + NR_3 \underset{-1}{\overset{1}{\rightleftharpoons}} HFe_3(CO)_9C{=}CH_2^- + HNR_3^+ + H_2 \quad (1)$$

at 25 °C under 1 atm of H_2 in 70% yield. As these two reactions constitute the formal dehydrogenation and hydrogenation of a C_2 fragment on a metal cluster framework under mild conditions and as the cluster system is a relatively simple one in terms of structure, we are investigating some aspects of the mechanism of the reaction. An obvious question raised by reaction 1 concerns the hydrogens removed as H^+ and H_2, viz, where do they come from in the forward reaction and where do they go in the reverse reaction ? On many clusters the protonation of metal–metal bonds is thermodynamically favored,[5] however, this is not a mechanistic requirement. Indeed, examples of kinetically controlled protonation are known.[6] A direct way of answering this question is by isotopic labeling provided hydrogen scrambling in the products is slow relative to product characterization. As there was no evidence from ^1H NMR that the two types of hydrogen in I exchanged at room temperature, the conversion of II to I in the presence of H^+ was investigated first.

Treating a 1.0-mmol sample of $K[HFe_3(CO)_9C{=}CH_2]$ with H_2 in the presence of D^+ yielded 0.7 mmol of I which, when analyzed by ^1H and ^2H NMR, was shown to contain 85% of the D in the methyl group of the capping carbon. As demonstrated by the spectra in Figure 1, treating a similar sample of II with D_2 in the presence of H^+ yields selectively labeled I, i.e., $HD_2Fe_3(CO)_9CCH_3$. The first labeling experiment suggests that the proton attacks the vinylidene fragment of II in preference to the iron base. This would produce an unsaturated intermediate, one possible representation of which is shown in Scheme I. Protonation at this position would weaken the coordination of the vinylidene double bond to the third iron, thereby opening a coordination site for H_2 at the unique iron. This provides a route for the incoming H's of H_2 to go directly to basal Fe–H–Fe positions to form I as we observe. If the unsaturated intermediate has a finite lifetime, it should be easily trapped by Lewis bases. Thus, we can rationalize the formation $(\mu\text{-H})Fe_3(CO)_9(\mu\text{-CO})(\mu_3\text{-}CCH_3)$, III,[7,8] which is produced on protonation in the presence of CO and which always constitutes the major byproduct of reaction −1. In the latter case, III is attributed to reaction of the intermediate with adventitious CO.

(1) Muetterties, E. L.; Rhodin, T. N.; Band, E.; Brucker, C. F.; Pretzer, W. R. *Chem. Rev.* **1979**, *79*, 91.
(2) A recent report illustrates the danger of basing mechanistic ideas on stable, reasonable structures: Stoutland, P. O.; Bergman, R. G. *J. Am. Chem. Soc.* **1985**, *107*, 4581.
(3) Vites, J. C.; Jacobsen, G.; Dutta, T. K.; Fehlner, T. P. *J. Am. Chem. Soc.* **1985**, *107*, 5563.
(4) Lourdichi, M., Jr.; Mathieu, R. *Nouv. J.* de Chim. **1982**, *6*, 231.
(5) Deeming, A. J. "Transition Metal Clusters"; Johnson, B. F. G., Ed.; Wiley: New York, 1980.
(6) Stevens, R. E.; Gladfelter, W. L. *J. Am. Chem. Soc.* **1982**, *104*, 6454.
(7) Kolis, J. W.; Holt, E. M.; Shriver, D. F. *J. Am. Chem. Soc.* **1983**, *105*, 7307.
(8) Vites, J. C.; Housecroft, C. E.; Jacobsen, G. B.; Fehlner, T. P. *Organometallics* **1984**, *3*, 1591.

0276-7333/86/2305-0385$01.50/0

equals the comparatively long bridging contact La′···μ-C(Cp).

In summary, the coordination of La(III)) in **2** is, probably due to optimal intra- and interchain packing, so irregular that any description in terms of either a common coordination polyhedron or a formal coordination number (in terms of integer electron pairs) appears inappropriate. Including all La···C contacts up to 3.035 Å, the same total ligand hapticity of 17 as for **4**[13] would result.

Acknowledgment. We gratefully appreciate grants (for S.E.) by the Allgemeiner Forschungspool der Universität Hamburg and by the Deutscher Akademischer Austauschdienst (DAAD), Bonn. Dipl.-Chem. Holger Schultze kindly contributed a fraction of carefully sublimed **2**.

Registry No. **2**, 1272-23-7.

Supplementary Material Available: Tables of crystal data, atomic parameters and temperature factors, most important bond distances and angles, anisotropic thermal parameters, calculated hydrogen atomic parameters, and observed and calculated structure factors (15 pages). Ordering information is given any current masthead page.

On the Mechanism of the Hydrogenation/Dehydrogenation of a C_2 Fragment on a Triiron Cluster Site

T. K. Dutta, J. C. Vites, and T. P. Fehlner*

Department of Chemistry, University of Notre Dame Notre Dame, Indiana 46556

Received September 6, 1985

Summary: Deuterium tracer studies show that the proton-induced hydrogenation/dehydrogenation of a triiron vinylidene anion/triiron ethylidyne proceeds via a mechanism in which protonation/deprotonation takes place on the organic fragment while hydrogenation/dehydrogenation occurs on the triiron fragment. Evidence is presented for the formation of an unsaturated intermediate in the protonation step.

Reactions on ligands bound to metal cluster systems are of great interest as they can serve as realistic models for reactions occurring in heterogeneous phases.[1] Presently, however, concepts of cluster reactivity are based extensively on the isolation and characterization of reasonably stable systems. Although the structure and bonding of such species provide a necessary foundation for an understanding of reactivity, they are no substitute for true mechanistic investigations.[2] Recently we reported[3] that the deprotonation of $(\mu\text{-H})_3Fe_3(CO)_9(\mu_3\text{-}CCH_3)$(I) results in the loss of H_2 and the formation of the vinylidene anion[4]

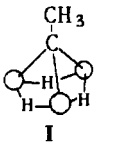

I

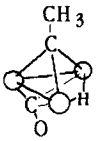

III

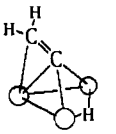

II

$[(\mu\text{-H})Fe_3(CO)_9C{=}CH_2^-]$ (II) (eq 1). This reaction is quantitative at 25 °C. The reverse reaction takes place

$$H_3Fe_3(CO)_9CCH_3 + NR_3 \underset{-1}{\overset{1}{\rightleftharpoons}} HFe_3(CO)_9C{=}CH_2^- + HNR_3^+ + H_2 \quad (1)$$

at 25 °C under 1 atm of H_2 in 70% yield. As these two reactions constitute the formal dehydrogenation and hydrogenation of a C_2 fragment on a metal cluster framework under mild conditions and as the cluster system is a relatively simple one in terms of structure, we are investigating some aspects of the mechanism of the reaction. An obvious question raised by reaction 1 concerns the hydrogens removed as H^+ and H_2, viz, where do they come from in the forward reaction and where do they go in the reverse reaction ? On many clusters the protonation of metal–metal bonds is thermodynamically favored,[5] however, this is not a mechanistic requirement. Indeed, examples of kinetically controlled protonation are known.[6] A direct way of answering this question is by isotopic labeling provided hydrogen scrambling in the products is slow relative to product characterization. As there was no evidence from ^1H NMR that the two types of hydrogen in I exchanged at room temperature, the conversion of II to I in the presence of H^+ was investigated first.

Treating a 1.0-mmol sample of $K[HFe_3(CO)_9C{=}CH_2]$ with H_2 in the presence of D^+ yielded 0.7 mmol of I which, when analyzed by ^1H and ^2H NMR, was shown to contain 85% of the D in the methyl group of the capping carbon. As demonstrated by the spectra in Figure 1, treating a similar sample of II with D_2 in the presence of H^+ yields selectively labeled I, i.e., $HD_2Fe_3(CO)_9CCH_3$. The first labeling experiment suggests that the proton attacks the vinylidene fragment of II in preference to the iron base. This would produce an unsaturated intermediate, one possible representation of which is shown in Scheme I. Protonation at this position would weaken the coordination of the vinylidene double bond to the third iron, thereby opening a coordination site for H_2 at the unique iron. This provides a route for the incoming H's of H_2 to go directly to basal Fe–H–Fe positions to form I as we observe. If the unsaturated intermediate has a finite lifetime, it should be easily trapped by Lewis bases. Thus, we can rationalize the formation $(\mu\text{-H})Fe_3(CO)_9(\mu\text{-CO})(\mu_3\text{-}CCH_3)$, III,[7,8] which is produced on protonation in the presence of CO and which always constitutes the major byproduct of reaction −1. In the latter case, III is attributed to reaction of the intermediate with adventitious CO.

(1) Muetterties, E. L.; Rhodin, T. N.; Band, E.; Brucker, C. F.; Pretzer, W. R. *Chem. Rev.* **1979**, *79*, 91.
(2) A recent report illustrates the danger of basing mechanistic ideas on stable, reasonable structures: Stoutland, P. O.; Bergman, R. G. *J. Am. Chem. Soc.* **1985**, *107*, 4581.
(3) Vites, J. C.; Jacobsen, G.; Dutta, T. K.; Fehlner, T. P. *J. Am. Chem. Soc.* **1985**, *107*, 5563.
(4) Lourdichi, M., Jr.; Mathieu, R. *Nouv. J.* de Chim. **1982**, *6*, 231.
(5) Deeming, A. J. "Transition Metal Clusters"; Johnson, B. F. G., Ed.; Wiley: New York, 1980.
(6) Stevens, R. E.; Gladfelter, W. L. *J. Am. Chem. Soc.* **1982**, *104*, 6454.
(7) Kolis, J. W.; Holt, E. M.; Shriver, D. F. *J. Am. Chem. Soc.* **1983**, *105*, 7307.
(8) Vites, J. C.; Housecroft, C. E.; Jacobsen, G. B.; Fehlner, T. P. *Organometallics* **1984**, *3*, 1591.

0276-7333/86/2305-0385$01.50/0

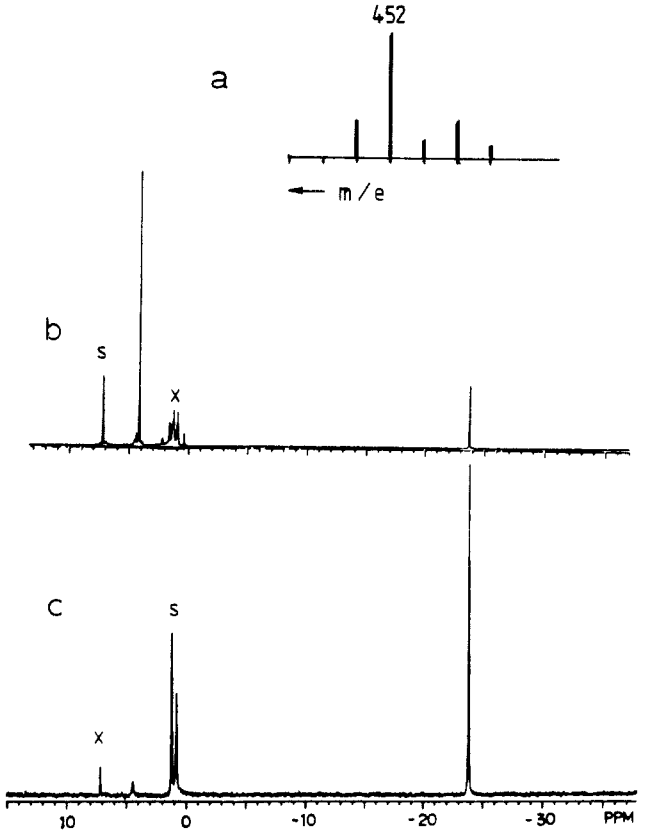

Figure 1. (a) Mass spectrometric relative intensity distribution in the parent ion region for $HD_2Fe_3(CO)_9CCH_3$: 451.819 (obsd); 452.8186 (calcd). (b) ^1H NMR of $HD_2Fe_3(CO)_9CCH_3$ in C_6D_6 (S); X indicates impurities. (c) ^2H NMR of $HD_2Fe_3(CO)_9CCH_3$ in hexanes (S) with C_6D_6 impurity.

Scheme I

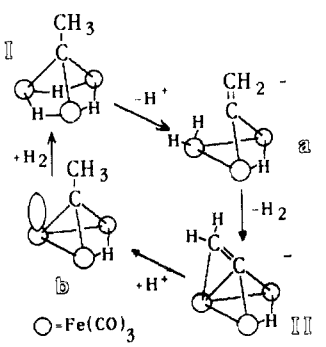

The existence of I, selectively labeled with two deuterium atoms in basal positions, allows the mechanism of reaction 1 to be probed. In the dehydrogenation reaction carried out with $HD_2Fe_3(CO)_9CCH_3$, $[HN(C_2H_5)_3^+]$ is observed,[9] suggesting that the proton lost comes from the CCH_3 fragment. Analysis by mass spectrometry of the hydrogen produced on deprotonation of $HD_2Fe_3(CO)_9CCH_3$ shows D_2:HD:H_2 to be 53:37:10. Qualitatively this demonstrates that the H_2 released from I also comes predominantly from the metal positions and not from the hydrocarbon fragment. Hence, as indicated in Scheme I, these two results suggest that deprotonation of I at the CCH_3 position yields an intermediate which undergoes rapid H_2 elimination from the iron base.

The ratio of D_2 to HD produced on the deprotonation of $HD_2Fe_3(CO)_9CCH_3$ is considerably higher than the 1:2 statistical ratio expected for exclusive, random elimination from the basal positions. The only way to explain the observed ratio is to invoke an overall inverse kinetic isotope effect of 2.9. One way to account for part of the observed effect is to postulate that hydrogen elimination from deprotonated I occurs via an intermediate (a) that has two terminal hydrogens. As the zero-point energy is lower for Fe–H–Fe vs. Fe–H, the lighter isotope will prefer the bridging position, thereby enhancing D_2 elimination relative to HD.[10]

We have already noted the effect of protonation–deprotonation on both the mobility and most stable arrangements of protons on hydrocarbon metal clusters[3] as well as the isoelectronic ferraborane,[8] and the above shows that the role of the H^+ ion is a dramatic one here as well. This is emphasized by the fact that heating I in the presence of CO at 60 °C only slowly forms III from I.[11,12] Also in the absence of a methyl substituent in I, deprotonation results in the loss of a proton and causes no loss of H_2.[3] This suggests, then, that the production of the double bond on deprotonation of the CCH_3 fragment of I is important to the loss of H_2; i.e., there may be an intramolecular displacement of H_2 by the CC double bond on (a) as shown in Scheme I.

Recently, Keister and co-workers have published some elegant mechanistic studies on the dehydrogenation of $H_3Ru_3(CO)_9COCH_3$ to $HRu_3(CO)_{10}COCH_3$ and the reverse reaction.[13] They provided evidence that this reaction proceeds through an unsaturated metal intermediate and, most recently,[14] suggest a structure similar to that of intermediate (b) in Scheme I. They reason from their kinetic studies that the addition of H_2 to a single metal site followed by rate-determining insertion of 2H into the metal–metal bonds is the probable detailed pathway for the hydrogenation reaction. As seen above, our work on the related iron systems both supports and complements their conclusions.

This study also demonstrates a potentially general route to reactive intermediates not requiring ligand dissociation and its associated activation process that can impose short lifetimes on intermediates. For example, the thermal activation of III[11] in the presence of D_2 leads to I but the deuterium is found in both positions; i.e., at this temperature the reaction proceeds via a pathway that permits the scrambling of the hydrogens. Thus, proton-induced ligand dissociation/association constitutes a gentle method for entering a reaction surface at a high-energy intermediate.

Acknowledgment. The support of the National Science Foundation under Grant CHE 8408251 is gratefully acknowledged as is the aid of Dr. C. E. Housecroft with the ^2H NMR. We thank Dr. J. B. Keister for giving us a preprint of his work.

(9) On the basis of NMR analysis, the ammonium salt observed contained 90 ± 10% H in the NH position.

(10) Calvert, R. B.; Shapley, J. R. *J. Am. Chem. Soc.* **1978**, *100*, 7726.
(11) Vites, J. C.; Fehlner, T. P. *Organometallics* **1984**, *3*, 491.
(12) The differences in rates for loss of H_2 via deprotonation vs. thermolysis is at least 10^4.
(13) Bavaro, L. M.; Montangero, P.; Keister, J. B. *J. Am. Chem. Soc.* **1983**, *105*, 4977.
(14) Dalton, D. M.; Barnett, D. J.; Duggan, T. P.; Keister, J. B.; Malik, P. T.; Modi, S. P.; Shaffer, M. R.; Smesko, S. A. *Organometallics* **1985**, *4*, 1854.

Formation of Adducts of Molecular Hydrogen and Dicarbonyl(η^5-cyclopentadienyl)hydridomolybdenum in Low-Temperature Matrices

Ray L. Sweany

Department of Chemistry, University of New Orleans
New Orleans, Louisiana 70148

Received June 7, 1985

Summary: Dihydrogen reacts with photolytically generated $HMoCp(CO)_2$ to form cis and trans dihydrogen adducts in argon matrices. In addition to adduct formation, hydrogen exchanges for deuterium during photolysis in the parent molecule, presumably via the intermediency of the D_2 adduct.

Hydrogen has shown a remarkable reactivity toward coordinatively unsaturated transition-metal complexes in inert-gas matrices. Several complexes have oxidatively added hydrogen[1,2] whereas others give complexes of dihydrogen with the H–H bond intact.[3] This novel mode of attachment is fairly resilient; pentacarbonyl(dihydrogen)chromium, is stable at temperatures as high as 238 K in liquid Xe[4] and the hydrogen adduct of bis(phosphine)tricarbonyltungsten is stable at room temperature in hydrogen atmospheres and has been characterized by X-ray and neutron diffraction methods.[5] Recently, even a stable iridium(III) complex of dihydrogen has been detected by NMR.[6] Presuming that a more electron-rich group 6 metal center might oxidatively add hydrogen, $HMoCp(CO)_3$ was photolyzed in hydrogen-containing matrices. Here, I report the formation of cis and trans dihydrogen adducts of $HMoCp(CO)_2$, formed by the photolysis of $HMoCp(CO)_3$ in hydrogen-containing matrices. Prolonged photolysis of these complexes gives evidence for exchange of the hydride ligand with one of the hydrogen atoms of the H_2 moiety.

The photochemistry of $HMoCp(CO)_3$ has been ably described by Rest and co-workers.[7] In matrices which have been doped with up to 20 mol% hydrogen, new bands appear upon ultraviolet irradiation along with the bands due to $HMoCp(CO)_2$. (See Figure 1.) When the matrix is exposed to the visible light of the glower the new bands gain additional intensity as the bands due to $HMoCp(CO)_2$ become attenuated. The new bands belong to two sets of two. The first set includes bands at 2000 and 1930 cm^{-1}. The second set include bands at 1987 and 1920 cm^{-1}. The position of the lower energy band of either set is shifted 2 cm^{-1} to longer wavelengths when D_2 is substituted for H_2 in the matrix. The bands of the two sets can be differentiated by their behavior in response to irradiation by a medium-pressure mercury lamp filtered by cobalt glass. The bands of set II become attenuated whereas the bands of set I are barely affected. The bands of set I are assigned

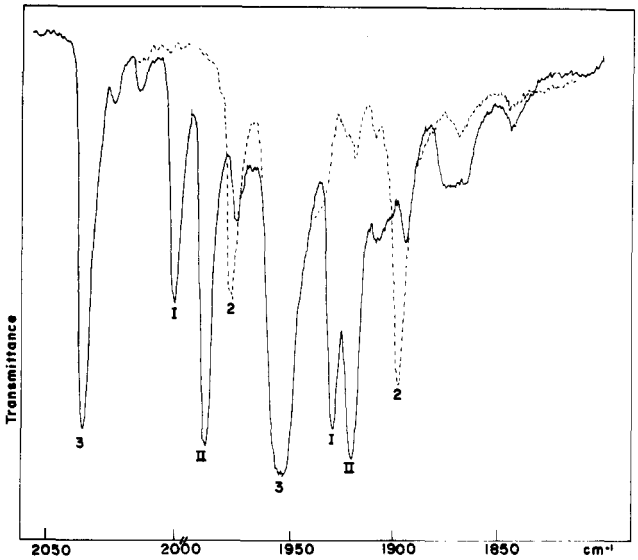

Figure 1. Spectrum of $HMoCp(CO)_3$ which has been photolyzed for 2.5 h with a low-pressure mercury lamp in the presence of 15 mol % D_2. Bands which are marked by Arabic numbers refer to the number of carbonyls on a complex which does not contain D_2. Thus, 3 refers to $HMoCp(CO)_3$. Bands marked by I are assigned to *trans*-$HMoCp(CO)_2(D_2)$ while bands marked by II are due to the cis isomer. The spectrum which has been traced by a dashed line is that of photolyzed $HMoCp(CO)_3$ in argon. The abscissa scale of the original spectra changes at 1990 cm^{-1} from 20 cm^{-1}/in to 25 cm^{-1}/in.

to *trans*-$HMoCp(CO)_2(H_2)$ and the bands of set II are assigned to the cis isomer.

There are several reasons for claiming that both sets of bands are due to species that have reacted with one molecule of hydrogen. The new bands grow in as the bands due to $HMoCp(CO)_2$ become attenuated, yet they do not appear at all in the absence of dihydrogen. In the presence of 7 mol % CO, both sets of bands appear in the same ratio of intensity as they are found in the absence of extra CO. This is not the expected behavior if the loss of more than one CO was required to form one of the species. In the presence of 13 mol % CO, no significant intensity is observed for either set. The simplest explanation is to assume that $HMoCp(CO)_2$ reacts with H_2 or CO, the choice of which is determined by the availability of the incoming ligand to the vacant coordination site, as well as by the stability of the resulting adduct under photolytic conditions. If the hydrogen simply substitutes for CO in a complex that retains the gross structure of the parent, two isomers are expected, cis and trans. The relative intensity of the two bands within the set will be most nearly equal for the cis isomer.[7] It is unlikely that the hydrogen has

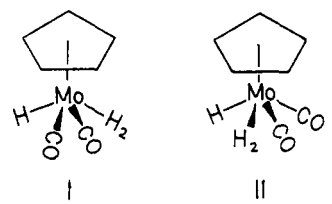

reacted with the cyclopentadienyl ligand. If hydrogen were being oxidatively added to the metal and then transferred to the ring, or if the ring were being reduced directly, the presence of CO in the matrix would produce a variety of new compounds with absorptions at higher energy than what are observed because four or possibly more carbonyls would be competing for the same π-electron density.

The mode of the interaction of hydrogen with the metal can be deduced from the comparison of the frequency of

(1) Sweany, R. L. *J. Am. Chem. Soc.* **1981**, *103*, 2410.
(2) Sweany, R. L. *J. Am. Chem. Soc.* **1982**, *104*, 3739. Hydrogen has also oxidatively added to naked metal atoms: Ozin, G. A.; Mitchell, S. A.; Prieto-Garcia, J. *Angew. Chem., Int. Ed. Engl.* **1982**, *21*, 380. Ozin, G. A.; Gracie, C. *J. Phys. Chem.* **1984**, *88*, 643. Ozin, G. A.; McCaffrey, M. G. *Ibid.* **1984**, *88*, 645.
(3) Sweany, R. L. *J. Am. Chem. Soc.* **1985**, *107*, 2374.
(4) Upmacis, R. K.; Gadd, G. E.; Poliakoff, M.; Simpson, M. B.; Turner, J. J.; Whyman, R.; Simpson, A. F. *J. Chem. Soc., Chem. Commun.* **1985**, 27.
(5) Kubas, G. J.; Ryan, R. R.; Swanson, B. I.; Vergamini, P. J.; Wasserman, H. J. *J. Am. Chem. Soc.* **1984**, *106*, 451.
(6) Crabtree, R. H.; Lavin, M. *J. Chem. Soc., Chem. Commun.* **1985**, 794.
(7) Mahmoud, K. A.; Rest, A. J.; Alt, H. G. *J. Chem. Soc., Dalton Trans.* **1984**, 187.

0276-7333/86/2305-0387$01.50/0

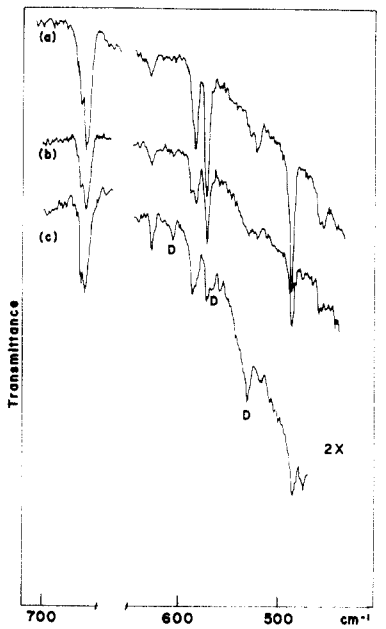

Figure 2. Spectra obtained during the photolysis of $HMoCp(CO)_3$ in a matrix composed of 20 mol % D_2 and 7 mol % CO in argon. Tracing a is of the unphotolyzed matrix. Tracing b was of a spectrum taken after 60 of irridation by a low-pressure mercury lamp. Tracing c was made of a spectrum taken after 75 additional minutes of photolysis, using a medium pressure mercury lamp. The spectrum was recorded with a 2× ordinate expansion. Bands marked by D show the positions of absorptions which are assignable to $DMoCp(CO)_3$. The shoulder on the high energy side of the band at 655 cm^{-1} is due to CO_2. The species to which the band at 630 cm^{-1} belongs is unknown.

carbonyl stretching vibrations of the hydrogen-containing moiety with those of $HMoCp(CO)_2$. If the hydrogen had oxidatively added, it is reasonable to expect a fairly dramatic blue shift of the carbonyl modes. For example, the oxidative addition of H_2 to $Fe(CO)_4$ results in a 42 cm^{-1} shift in the totally symmetric breathing mode.[1] This behavior has been rationalized by presuming hydride ligands are negatively charged and processes which involve the formation of the hydride from hydrogen atoms result in electron density being withdrawn from the metal.[8,9] The dependability of this group property is the basis for the reliability of the force constant calculations by Timney.[10] The symmetric stretching vibrations of the cis isomer is shifted by 13 cm^{-1} to shorter wavelengths than the similar mode of $HMoCp(CO)_2$: short of the shift observed for $Fe(CO)_4$ and considerably larger than the 3 cm^{-1} shift observed for $Cr(CO)_5$.[3] Taken at face value, these comparisons suggest an interaction which comes closer to being described as oxidative addition than what is exhibited by $H_2CrCO)_5$.

A full vibrational characterization of these species has not been possible because the new species are themselves photolyzed by the radiation which is used to create them. Thus, adequate infrared intensity has only been achieved for the carbonyl modes; the largest optical density of any of the adduct modes that has been achieved thus far is 1.3 o.d. With so little adduct formed in these experiments, other modes which are important for the characterization of the molecules have not been detected.[11] The regions of the spectrum between 700 and 400 cm^{-1} of the parent molecule, $HMoCp(CO)_3$, contain many of the M–CO stretching and deformation modes, and they are quite sensitive to the isotope of hydrogen. When $HMoCp(CO)_3$ is photolyzed in D_2-containing matrices, the spectrum gives evidence of slow isotope exchange in the parent molecule as shown in Figure 2. The bands of the deuterium isotopomer that are marked by D are, in two instances, quite well resolved from the correlated bands of $HMoCp(CO)_3$, and over periods of several hours of photolysis there is clear evidence of the formation of $DMoCp(CO)_3$, especially in the presence of 7 mol % CO. The extra CO increases the probability that $HMoCp(CO)_2$ will react with CO to give back starting material but is not so concentrated that no adduct forms. In the presence of 13 mol % CO no significant quantities of adduct forms and no H–D exchange is noted. This precludes the possibility that the exchange is due to reactions of hydrogen atoms.[7,12]

Registry No. $HMoCp(CO)_2$, 85150-17-0; $HMoCp(CO)_3$, 12176-06-6; $DMoCp(CO)_3$, 79359-05-0.

(8) Sweany, R. L.; Owens, J. W. *J. Organomet. Chem.* **1983**, *255*, 327.
(9) Photolyses of $HWCp(CO)_3$ in hydrogen-containing matrices lead to the growth of bands which correlate to those reported herein. In addition, bands grow in which are at or to higher energy of 2060 cm^{-1}. Work is proceeding to identify the species which are responsible for these bands. Consistent with this line of reasoning would be a claim that these species had resulted from the oxidative addition of hydrogen.
(10) Timney, J. A. *Inorg. Chem.* **1979**, *18*, 2502.
(11) Unfortunately, both the M–H stretching and deformation modes of $HMoCp(CO)_3$ are weak. Although the M–H stretching frequency has been observed, there have been no studies which have assigned the M–H deformation mode for this molecule or the analogous $HWCp(CO)_3$. Davison, A.; McCleverty, J. A.; Wilkinson, G. *J. Chem. Soc.* **1963**, 1133. Davidson, G.; Duce, D. A. *J. Organomet. Chem.* **1976**, *120*, 229.
(12) The photolysis of $HMoCp(CO)_3$ gives evidence of the homolytic cleavage of the Mo–H bond in CO[7] and H_2-containing matrices. In solid deuterium, hot hydrogen atoms have been shown to abstract deuterium, although the reaction gives a 40% yield, at best. The reaction is the function of the excess energy of the hydrogen atom and, in this study, the probability of the hydrogen atom colliding with a deuterium molecule before it is thermalized. Miyazaki, T.; Tsuruta, H.; Fueki, K. *J. Phys. Chem.* **1983**, *87*, 1611.

Pentacoordinated Silicon Hydrides: Very High Affinity of the Si–H Bond for the Equatorial Position

Claire Brelière, Francis Carré, Robert J. P. Corriu,* Monique Poirier, and Gérard Royo
Institut de Chimie Fine—Hétérochimie et amino-acides—UA 1097
Université des Sciences et Techniques du Languedoc
34060 Montpellier Cédex, France

Received July 16, 1985

Summary: An X-ray investigation of two pentacoordinated silicon hydrides shows that the Si–H bonds occupy equatorial positions in the trigonal-bipyramidal structures.

It is well-known that nucleophilic substitution at silicon takes place with either retention or inversion of configuration according to the nature of the leaving group.[1] In a previous paper, we have reported a scale of apicophilicity deduced from the study of pentacoordinate silicon compounds such as 1 in which the *o*-$Me_2NCH_2C_6H_4$ ligand is intramolecularly bonded to the silicon atom.[2]

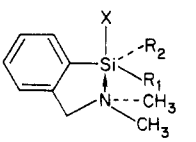

1

(1) Corriu, R. J. P.; Guerin, C.; Moreau, J. J. E. *Top. Stereochem.* **1984**, *15*, 43 and references therein.

0276-7333/86/2305-0388$01.50/0

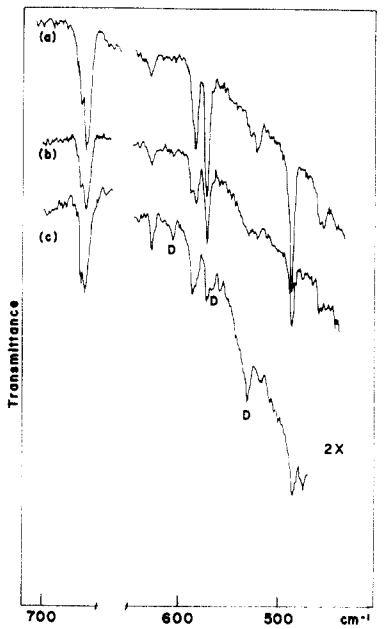

Figure 2. Spectra obtained during the photolysis of $HMoCp(CO)_3$ in a matrix composed of 20 mol % D_2 and 7 mol % CO in argon. Tracing a is of the unphotolyzed matrix. Tracing b was of a spectrum taken after 60 of irridation by a low-pressure mercury lamp. Tracing c was made of a spectrum taken after 75 additional minutes of photolysis, using a medium pressure mercury lamp. The spectrum was recorded with a 2× ordinate expansion. Bands marked by D show the positions of absorptions which are assignable to $DMoCp(CO)_3$. The shoulder on the high energy side of the band at 655 cm^{-1} is due to CO_2. The species to which the band at 630 cm^{-1} belongs is unknown.

carbonyl stretching vibrations of the hydrogen-containing moiety with those of $HMoCp(CO)_2$. If the hydrogen had oxidatively added, it is reasonable to expect a fairly dramatic blue shift of the carbonyl modes. For example, the oxidative addition of H_2 to $Fe(CO)_4$ results in a 42 cm^{-1} shift in the totally symmetric breathing mode.[1] This behavior has been rationalized by presuming hydride ligands are negatively charged and processes which involve the formation of the hydride from hydrogen atoms result in electron density being withdrawn from the metal.[8,9] The dependability of this group property is the basis for the reliability of the force constant calculations by Timney.[10] The symmetric stretching vibrations of the cis isomer is shifted by 13 cm^{-1} to shorter wavelengths than the similar mode of $HMoCp(CO)_2$: short of the shift observed for $Fe(CO)_4$ and considerably larger than the 3 cm^{-1} shift observed for $Cr(CO)_5$.[3] Taken at face value, these comparisons suggest an interaction which comes closer to being described as oxidative addition than what is exhibited by $H_2CrCO)_5$.

A full vibrational characterization of these species has not been possible because the new species are themselves photolyzed by the radiation which is used to create them. Thus, adequate infrared intensity has only been achieved for the carbonyl modes; the largest optical density of any of the adduct modes that has been achieved thus far is 1.3 o.d. With so little adduct formed in these experiments, other modes which are important for the characterization of the molecules have not been detected.[11] The regions of the spectrum between 700 and 400 cm^{-1} of the parent molecule, $HMoCp(CO)_3$, contain many of the M–CO stretching and deformation modes, and they are quite sensitive to the isotope of hydrogen. When $HMoCp(CO)_3$ is photolyzed in D_2-containing matrices, the spectrum gives evidence of slow isotope exchange in the parent molecule as shown in Figure 2. The bands of the deuterium isotopomer that are marked by D are, in two instances, quite well resolved from the correlated bands of $HMoCp(CO)_3$, and over periods of several hours of photolysis there is clear evidence of the formation of $DMoCp(CO)_3$, especially in the presence of 7 mol % CO. The extra CO increases the probability that $HMoCp(CO)_2$ will react with CO to give back starting material but is not so concentrated that no adduct forms. In the presence of 13 mol % CO no significant quantities of adduct forms and no H–D exchange is noted. This precludes the possibility that the exchange is due to reactions of hydrogen atoms.[7,12]

Registry No. $HMoCp(CO)_2$, 85150-17-0; $HMoCp(CO)_3$, 12176-06-6; $DMoCp(CO)_3$, 79359-05-0.

(8) Sweany, R. L.; Owens, J. W. *J. Organomet. Chem.* **1983**, *255*, 327.
(9) Photolyses of $HWCp(CO)_3$ in hydrogen-containing matrices lead to the growth of bands which correlate to those reported herein. In addition, bands grow in which are at or to higher energy of 2060 cm^{-1}. Work is proceeding to identify the species which are responsible for these bands. Consistent with this line of reasoning would be a claim that these species had resulted from the oxidative addition of hydrogen.
(10) Timney, J. A. *Inorg. Chem.* **1979**, *18*, 2502.
(11) Unfortunately, both the M–H stretching and deformation modes of $HMoCp(CO)_3$ are weak. Although the M–H stretching frequency has been observed, there have been no studies which have assigned the M–H deformation mode for this molecule or the analogous $HWCp(CO)_3$. Davison, A.; McCleverty, J. A.; Wilkinson, G. *J. Chem. Soc.* **1963**, 1133. Davidson, G.; Duce, D. A. *J. Organomet. Chem.* **1976**, *120*, 229.
(12) The photolysis of $HMoCp(CO)_3$ gives evidence of the homolytic cleavage of the Mo–H bond in CO[7] and H_2-containing matrices. In solid deuterium, hot hydrogen atoms have been shown to abstract deuterium, although the reaction gives a 40% yield, at best. The reaction is the function of the excess energy of the hydrogen atom and, in this study, the probability of the hydrogen atom colliding with a deuterium molecule before it is thermalized. Miyazaki, T.; Tsuruta, H.; Fueki, K. *J. Phys. Chem.* **1983**, *87*, 1611.

Pentacoordinated Silicon Hydrides: Very High Affinity of the Si–H Bond for the Equatorial Position

Claire Brelière, Francis Carré, Robert J. P. Corriu,* Monique Poirier, and Gérard Royo
Institut de Chimie Fine—Hétérochimie et amino-acides—UA 1097
Université des Sciences et Techniques du Languedoc
34060 Montpellier Cédex, France

Received July 16, 1985

Summary: An X-ray investigation of two pentacoordinated silicon hydrides shows that the Si–H bonds occupy equatorial positions in the trigonal-bipyramidal structures.

It is well-known that nucleophilic substitution at silicon takes place with either retention or inversion of configuration according to the nature of the leaving group.[1] In a previous paper, we have reported a scale of apicophilicity deduced from the study of pentacoordinate silicon compounds such as 1 in which the *o*-$Me_2NCH_2C_6H_4$ ligand is intramolecularly bonded to the silicon atom.[2]

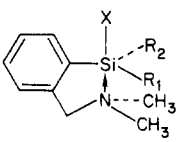

1

(1) Corriu, R. J. P.; Guerin, C.; Moreau, J. J. E. *Top. Stereochem.* **1984**, *15*, 43 and references therein.

0276-7333/86/2305-0388$01.50/0

We have observed that the apicophilicity of X is related to the polarizability or, in other words, to the ability of the Si–X bond to be stretched. This order is parallel to the ability of the X group to be displaced with inversion of configuration.

pentacoordination ability: $\xrightarrow{X=H,\ OR<F,\ SR<OAc,\ Cl,\ Br}$

stereochemistry: retention $\longrightarrow$ inversion

In the case of silicon bonded to alkoxy, hydride, and alkyl groups, no diastereotopy could be observed in the NMe_2 group by ^1H NMR down to −90 °C.[2] However, ^{29}Si NMR brings new evidence for intramolecular pentacoordination.

When silicon is bonded to alkyl or alkoxy groups, we do not observe an upfield chemical shift corresponding to pentacoordination.[3] The ^{29}Si NMR shows a significant upfield shift in the range of pentacoordinated structures for silicon hydrides. For instance, in the case of *o*-$NMe_2CH_2C_6H_4Si(\alpha\text{-}C_{10}H_7)H_2$, although we do not observe the diastereotopism of NMe_2 groups, the ^{29}Si chemical shift is displaced 11.6 ppm upfield (at 30 °C) indicating the formation of a Si←N coordinative bond.[3] This apparent anomalous behavior can be explained if the two hydrogen atoms occupy equatorial positions, resulting in a plane of symmetry.

It is interesting to consider the structure of the adducts formed by N→Si coordination in systems similar to **1** since these are good models for the intermediates involved in nucleophilic substitution at silicon. The Si–H bond is always displaced with retention of configuration, and several pathways have been proposed.[1]

In this paper, we report the structure of two silicon hydrides **2** and **3** in which there is an intramolecular Si←N bond.

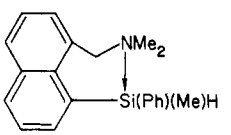

2

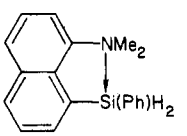

3

The important aspect of the present work is the equatorial position of the Si–H bond, the apical position in both cases being occupied by the phenyl group (Figure 1).

These results show the great aptitude of the Si–H bond for pentacoordinated structures and its ability to be in the equatorial position.[5,6] It is now interesting to discuss this

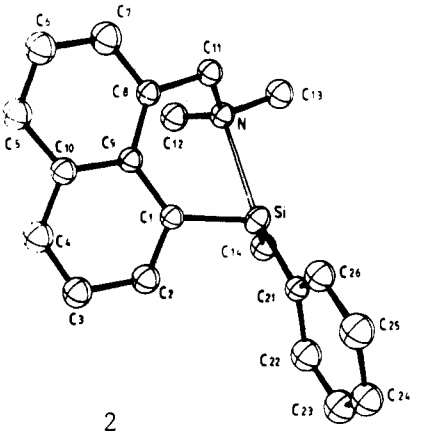

2

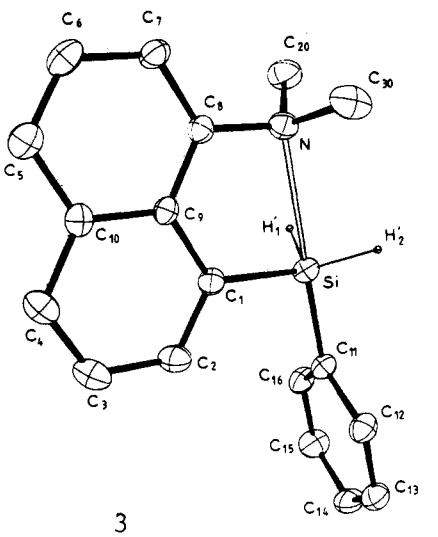

3

Figure 1. Perspective views of the silanes **2** and **3**. Main features for compound **2** are $Si–C_1$ = 1.88 (1), $Si–C_{14}$ = 1.90 (2), $Si–C_{21}$ = 1.91 (1), and Si←N = 2.66 (1) Å and $N–Si–C_{21}$ = 166.8 (6), $N–Si–C_1$ = 80.8 (5), and $C_1–Si–C_{21}$ = 104.3 (6)°. Bond lengths (Å) and angles (deg) for compound **3**: $Si–C_1$ = 1.881 (4), Si–H = 1.44 (2), $Si–C_{11}$ = 1.893 (4), Si←N = 2.584 (3); $N–Si–C_{11}$ = 178.7 (1), $N–Si–C_1$ = 76.0 (1), $C_1–Si–C_{11}$ = 105.2 (2), mean H–Si–N = 75.3, mean $H–Si–C_{11}$ = 104.7°. The hydrogen atoms were not determined for silane **2**.[4]

observation in connection with the retention of configuration in nucleophilic substitution at silicon. In the preceding papers devoted to this problem, we have shown that electrophilic assistance is not the driving force for retention of configuration at silicon.[1] We proposed an equatorial attack of the nucleophile to explain the frontal displacement.[1]

The results reported here show that equatorial attack certainly is not the most favorable process. The nucleophilic displacement of the Si–H bond with retention of configuration certainly takes place by apical attack of the nucleophile, the Si–H bond being in the equatorial position as suggested recently by the results obtained by Deiters and Holmes.[7]

Furthermore, these results provide further evidence that electrophilic assistance does not control the process of retention as proposed in S_Ni-Si process:[8] even in the ab-

(2) Corriu, R. J. P.; Royo, G.; de Saxce, A. *J. Chem. Soc., Chem. Commun.* **1980**, 892.

(3) (a) Helmer, B. J.; West, R.; Corriu, R. J. P.; Poirier, M.; Royo, G.; de Saxce, A. *J. Organomet. Chem.* **1983**, *251*, 295. (b) In the case of compounds **2**, and **3**, the ^{29}Si chemical shifts observed are −25.84 and −44.16 ppm upfield than −19.81 ppm measured for $1\text{-}C_{10}H_7(C_6H_5)Si(Me)H$ and −35.62 ppm for $1\text{-}C_{10}H_7(C_6H_5)SiH_2$.

(4) Crystallographic information: Silane **2**: $C_{20}H_{23}NSi$; a = 11.857 (3) Å, b = 13.078 (4) Å, c = 11.087 (3) Å; space group $P2_12_12_1$; Z = 4; Mo Kα radiation; R = 0.078 for 739 unique observed reflections. The space group indicates that the crystal grown for the structure determination was the result of a *spontaneous resolution* of the compound from the racemic solution. The absolute configuration displayed in Figure 1 was determined via the Hamilton test (Hamilton W. C. *Acta Crystallogr.* **1965**, *18*, 502), comparing the present structure, with x, y, z coordinates, with a molecule having $-x$, y, z coordinates. The R_w factors were 0.086 and 0.087, respectively. In the final refinement only the Si atom had an anisotropic temperature factor. Silane **3**: $C_{18}H_{19}NSi$; a = 12.341 (3) Å, b = 8.187 (2) Å, c = 15.667 (4) Å, β = 91.43 (1)°, space group $P2_1/n$; Z = 4, Cu Kα radiation; R = 0.056 for 1784 unique reflections. The hydrogen atoms were located by difference Fourier synthesis, and their coordinates were kept fixed during the last least-squares refinement cycles, where all non-hydrogen atoms had adjustable anisotropic temperature factors. Full details of these structures are available as supplementary material.

(5) Cook, D. I.; Fields, R.; Green, M.; Haszeldine, R. N.; Iles, B. R.; Jones, A.; Newlands, M. J. *J. Chem. Soc. A* **1966**, 887.

(6) Ebsworth, E. A. V., private communication.

(7) Deiters, J. A.; Holmes, R. P. "Oral Presentation in Organosilicon Symposium", Baton Rouge, LA, April 1985.

(8) Sommer, L. H. In "Stereochemistry, Mechanism and Silicon"; McGraw-Hill: New York, 1965; p 177.

sence of any interaction, we observe frontal attack; the N–Si–H angle measured here for the compound **3** is as small as 75.3°, whereas in the case of pentacoordinated silicon chlorides as previously reported, the coordination of the nitrogen atom takes place opposite to the leaving group, in good agreement with the geometry of the inversion of configuration.[1]

These results are a good demonstration of the fact that the attack of nucleophile (frontal or back side) at silicon is mainly controlled by the nature of the leaving group. A further important problem which we have to consider now is to determine whether the hydrogen atom departs directly from the equatorial position or whether a pseudorotation process occurs, resulting in departure of hydrogen atom from an apical position.

Finally these results provide a good model for the nucleophilic activation of Si–H bonds in reductions performed by silicon hydrides activated by the fluoride ion.

Acknowledgment. We wish to acknowledge T. Stout for help in preparing the English version of this manuscript. F.C. thanks Pr. J. Lapasset, Groupe de Dynamique des Phases Condensées, L.A. au CNRS no. 233, Université des Sciences et Techniques du Languedoc, for accurate collecting of a data set with compound **3**, on a CAD-3 diffractometer.

Registry No. 2, 99642-64-5; 3, 99642-65-6.

Supplementary Material Available: Tables I and II, lists of structure factors amplitudes for compounds **2** and **3**, Table III, summary of crystal data, intensity measurements, and refinement, Table IV, atomic coordinates and thermal parameters for compound **2**, Tables V and VI, bond lengths and bond angles for **2**, Tables VII–XI, fractional coordinates for the Si, N, and C atoms, anisotropic temperature factors for these atoms, fractional coordinates and isotropic temperature factors for the H atoms, bond lengths, and selected bond angles for compound **3**, respectively (24 pages). Ordering information is given on any current masthead page.

(9) (a) Corriu, R. J. P.; Perz, R.; Réyé, C. *Tetrahedron* **1983**, *39*, 999 and references therein. (b) Sharma, R. K.; Fry, J. L. *J. Org. Chem.* **1983**, *48*, 2112.

Decomposition of Iridium Alkoxide Complexes *trans*-ROIr(CO)(PPh_3)$_2$ (R = Me, *n*-Pr, and *i*-Pr): Evidence for β-Elimination

Karen A. Bernard, Wayne M. Rees, and Jim D. Atwood*†

Department of Chemistry
University at Buffalo, State University of New York
Buffalo, New York 14214

Received May 15, 1985

Summary: Decomposition of *trans*-ROIr(CO)(PPh_3)$_2$ in the presence of PPh_3 leads to HIr(CO)(PPh_3)$_3$ for R = Me, *n*-Pr, and *i*-Pr. For R = H, *t*-Bu, or Ph, this decomposition is not observed. For R = *i*-Pr similar quantities of acetone and 2-propanol are observed with total yield of 90% based on starting iridium complex. Propanal is formed for R = *n*-Pr. The reaction between *trans*-*i*-PrOIr(CO)(PPh_3)$_2$ and HIr(CO)(PPh_3)$_3$ readily yields 2-propanol. Thus a β-hydrogen abstraction to yield organic carbonyl and HIr(CO)(PPh_3)$_3$ is indicated with 2-propanol possibly formed by a binuclear reaction between *trans*-*i*-PrOIr(CO)(PPh_3)$_2$ and HIr(CO)(PPh_3)$_3$.

Alkoxide complexes have considerable utility in organic synthesis, especially for reactions catalyzed by copper.[1-8] The synthesis and structures of a number of alkoxides have been reported,[1,2,9-14] although several simple reactions of alkoxide complexes are only now being examined.[15-23] Our high yield syntheses of *trans*-ROIr(CO)(PPh_3)$_2$ allow the study of simple reactions utilizing the coordination site available on iridium. We have previously reported on carbonylation reactions;[15,16] we now report on the decomposition which leads to iridium hydride through a mechanism of β-elimination.

The decomposition of alkyl complexes by β-elimination is well established for a number of complexes.[24-27] Although such a step may be important in synthetic applications of transition-metal alkoxide complexes,[28] only one study of the decomposition of transition-metal alkoxide complexes has been reported.[1] This study of the decomposition of "CuOR" near 100 °C led to Cu(0), alcohol, and ketone or aldehyde for secondary and primary alkoxides, respectively (eq 1). The results indicated competing mechanisms of β-elimination of aldehyde (ketone) and homolytic scission of the Cu–O bond producing alkoxy radicals.[1]

† Alfred P. Sloan Foundation Fellow.

(1) Whitesides, G. M.; Sadowski, J. S.; Lilburn, J. *J. Am. Chem. Soc.* **1974**, *96*, 2829.
(2) Milstein, D.; Huckaby, J. L. *J. Am. Chem. Soc.* **1982**, *104*, 6150.
(3) Wasserman, H. H.; Robinson, R. P.; Carter, C. G. *J. Am. Chem. Soc.* **1983**, *105*, 1697.
(4) Cornforth, J.; Sierakowski, A. F.; Wallace, T. W. *J. Chem. Soc., Perkin Trans 1* **1982**, 2299.
(5) Huche, M.; Berlan, J.; Pourcelat, G.; Cresson, P. *Tetrahedron Lett.* **1981**, *22*, 1329.
(6) Leoni, P.; Pasquali, M. *J. Organomet. Chem.* **1983**, *255*, C31.
(7) Cornforth, J.; Sierakowski, A. F.; Wallace, T. W. *J. Chem. Soc., Chem. Commun.* **1979**, 294.
(8) Chan, T. H.; Harrod, J. F.; van Gheluwe, P. *Tetrahedron Lett.* **1974**, 4409.
(9) Bradley, D. C. *Prog. Inorg. Chem.* **1960**, *2*, 303.
(10) Bradley, D. C. *Adv. Inorg. Chem. Radiochem.* **1972**, *15*, 259.
(11) Mehrota, R. C. *Inorg. Chim. Acta Rev.* **1967**, *1*, 99.
(12) Ku, R. V.; San Filippo, J., Jr. *Organometallics* **1983**, *2*, 1360.
(13) Bochmann, M.; Wilkinson, G.; Young, G. B.; Hursthouse, M. B.; Malik, K. M. A. *J. Chem. Soc., Dalton Trans.* **1980**, 1863.
(14) Pasquali, M.; Fiaschi, P.; Floriani, C.; Gaetani-Manfredotti, A. *J. Chem. Soc., Chem. Commun.* **1983**, 197.
(15) Rees, W. M.; Atwood, J. D. *Organometallics* **1985**, *4*, 402.
(16) Rees, W. M.; Fettinger, J. C.; Churchill, M. R.; Atwood, J. D. *Organometallics* **1985**, *4*, 2179.
(17) Banditelli, G.; Bonati, F.; Minghetti, G. *Synth. Inorg. Met.-Org. Chem.* **1973**, *3*, 415.
(18) Bryndza, H. E., "The 11th International Conference on Organometallic Chemistry", Callaway Gardens, GA, Oct 1983.
(19) Bryndza, H. E. *Organometallics* **1985**, *4*, 406.
(20) Chisholm, M. H.; Cotton, F. A. *Acc. Chem. Res.* **1978**, *11*, 356 and references therein.
(21) Eller, P. G.; Kubas, G. J. *J. Am. Chem. Soc.* **1977**, *99*, 4346.
(22) Tsuda, T.; Watanabe, K.; Miyata, K.; Yamamoto, H.; Saegusa, T. *Inorg. Chem.* **1981**, *20*, 2728.
(23) Tsuda, T.; Sanada, S.-I.; Ueda, K.; Saegusa, T. *Inorg. Chem.* **1976**, *15*, 2329.
(24) Atwood, J. D. "Inorganic and Organometallic Reaction Mechanisms"; Brooks/Cole Publishing Company: Monterey, CA, 1985.
(25) Whitesides, G. M.; Stedronsky, E. R.; Casey, C. P.; Fillippo, J. S., Jr. *J. Am. Chem. Soc.* **1970**, *92*, 1426.
(26) Whitesides, G. M.; Gaasch, J. F.; Stedronsky, E. R. *J. Am. Chem. Soc.* **1972**, *94*, 5258.
(27) Evans, J.; Schwartz, J.; Urquhart, P. W. *J. Organomet. Chem.* **1974**, *81*, C37.
(28) Kaesz, H. D.; Saillant, R. *Chem. Rev.* **1972**, *72*, 231.

0276-7333/86/2305-0390$01.50/0

sence of any interaction, we observe frontal attack; the N–Si–H angle measured here for the compound **3** is as small as 75.3°, whereas in the case of pentacoordinated silicon chlorides as previously reported, the coordination of the nitrogen atom takes place opposite to the leaving group, in good agreement with the geometry of the inversion of configuration.[1]

These results are a good demonstration of the fact that the attack of nucleophile (frontal or back side) at silicon is mainly controlled by the nature of the leaving group. A further important problem which we have to consider now is to determine whether the hydrogen atom departs directly from the equatorial position or whether a pseudorotation process occurs, resulting in departure of hydrogen atom from an apical position.

Finally these results provide a good model for the nucleophilic activation of Si–H bonds in reductions performed by silicon hydrides activated by the fluoride ion.

Acknowledgment. We wish to acknowledge T. Stout for help in preparing the English version of this manuscript. F.C. thanks Pr. J. Lapasset, Groupe de Dynamique des Phases Condensées, L.A. au CNRS no. 233, Université des Sciences et Techniques du Languedoc, for accurate collecting of a data set with compound **3**, on a CAD-3 diffractometer.

Registry No. 2, 99642-64-5; 3, 99642-65-6.

Supplementary Material Available: Tables I and II, lists of structure factors amplitudes for compounds **2** and **3**, Table III, summary of crystal data, intensity measurements, and refinement, Table IV, atomic coordinates and thermal parameters for compound **2**, Tables V and VI, bond lengths and bond angles for **2**, Tables VII–XI, fractional coordinates for the Si, N, and C atoms, anisotropic temperature factors for these atoms, fractional coordinates and isotropic temperature factors for the H atoms, bond lengths, and selected bond angles for compound **3**, respectively (24 pages). Ordering information is given on any current masthead page.

(9) (a) Corriu, R. J. P.; Perz, R.; Réyé, C. *Tetrahedron* **1983**, *39*, 999 and references therein. (b) Sharma, R. K.; Fry, J. L. *J. Org. Chem.* **1983**, *48*, 2112.

Decomposition of Iridium Alkoxide Complexes *trans*-ROIr(CO)(PPh_3)$_2$ (R = Me, *n*-Pr, and *i*-Pr): Evidence for β-Elimination

Karen A. Bernard, Wayne M. Rees, and Jim D. Atwood*†

Department of Chemistry
University at Buffalo, State University of New York
Buffalo, New York 14214

Received May 15, 1985

Summary: Decomposition of *trans*-ROIr(CO)(PPh_3)$_2$ in the presence of PPh_3 leads to HIr(CO)(PPh_3)$_3$ for R = Me, *n*-Pr, and *i*-Pr. For R = H, *t*-Bu, or Ph, this decomposition is not observed. For R = *i*-Pr similar quantities of acetone and 2-propanol are observed with total yield of 90% based on starting iridium complex. Propanal is formed for R = *n*-Pr. The reaction between *trans*-*i*-PrOIr(CO)(PPh_3)$_2$ and HIr(CO)(PPh_3)$_3$ readily yields 2-propanol. Thus a β-hydrogen abstraction to yield organic carbonyl and HIr(CO)(PPh_3)$_3$ is indicated with 2-propanol possibly formed by a binuclear reaction between *trans*-*i*-PrOIr(CO)(PPh_3)$_2$ and HIr(CO)(PPh_3)$_3$.

Alkoxide complexes have considerable utility in organic synthesis, especially for reactions catalyzed by copper.[1-8] The synthesis and structures of a number of alkoxides have been reported,[1,2,9-14] although several simple reactions of alkoxide complexes are only now being examined.[15-23] Our high yield syntheses of *trans*-ROIr(CO)(PPh_3)$_2$ allow the study of simple reactions utilizing the coordination site available on iridium. We have previously reported on carbonylation reactions;[15,16] we now report on the decomposition which leads to iridium hydride through a mechanism of β-elimination.

The decomposition of alkyl complexes by β-elimination is well established for a number of complexes.[24-27] Although such a step may be important in synthetic applications of transition-metal alkoxide complexes,[28] only one study of the decomposition of transition-metal alkoxide complexes has been reported.[1] This study of the decomposition of "CuOR" near 100 °C led to Cu(0), alcohol, and ketone or aldehyde for secondary and primary alkoxides, respectively (eq 1). The results indicated competing mechanisms of β-elimination of aldehyde (ketone) and homolytic scission of the Cu–O bond producing alkoxy radicals.[1]

† Alfred P. Sloan Foundation Fellow.

(1) Whitesides, G. M.; Sadowski, J. S.; Lilburn, J. *J. Am. Chem. Soc.* **1974**, *96*, 2829.
(2) Milstein, D.; Huckaby, J. L. *J. Am. Chem. Soc.* **1982**, *104*, 6150.
(3) Wasserman, H. H.; Robinson, R. P.; Carter, C. G. *J. Am. Chem. Soc.* **1983**, *105*, 1697.
(4) Cornforth, J.; Sierakowski, A. F.; Wallace, T. W. *J. Chem. Soc., Perkin Trans 1* **1982**, 2299.
(5) Huche, M.; Berlan, J.; Pourcelat, G.; Cresson, P. *Tetrahedron Lett.* **1981**, *22*, 1329.
(6) Leoni, P.; Pasquali, M. *J. Organomet. Chem.* **1983**, *255*, C31.
(7) Cornforth, J.; Sierakowski, A. F.; Wallace, T. W. *J. Chem. Soc., Chem. Commun.* **1979**, 294.
(8) Chan, T. H.; Harrod, J. F.; van Gheluwe, P. *Tetrahedron Lett.* **1974**, 4409.
(9) Bradley, D. C. *Prog. Inorg. Chem.* **1960**, *2*, 303.
(10) Bradley, D. C. *Adv. Inorg. Chem. Radiochem.* **1972**, *15*, 259.
(11) Mehrota, R. C. *Inorg. Chim. Acta Rev.* **1967**, *1*, 99.
(12) Ku, R. V.; San Filippo, J., Jr. *Organometallics* **1983**, *2*, 1360.
(13) Bochmann, M.; Wilkinson, G.; Young, G. B.; Hursthouse, M. B.; Malik, K. M. A. *J. Chem. Soc., Dalton Trans.* **1980**, 1863.
(14) Pasquali, M.; Fiaschi, P.; Floriani, C.; Gaetani-Manfredotti, A. *J. Chem. Soc., Chem. Commun.* **1983**, 197.
(15) Rees, W. M.; Atwood, J. D. *Organometallics* **1985**, *4*, 402.
(16) Rees, W. M.; Fettinger, J. C.; Churchill, M. R.; Atwood, J. D. *Organometallics* **1985**, *4*, 2179.
(17) Banditelli, G.; Bonati, F.; Minghetti, G. *Synth. Inorg. Met.-Org. Chem.* **1973**, *3*, 415.
(18) Bryndza, H. E., "The 11th International Conference on Organometallic Chemistry", Callaway Gardens, GA, Oct 1983.
(19) Bryndza, H. E. *Organometallics* **1985**, *4*, 406.
(20) Chisholm, M. H.; Cotton, F. A. *Acc. Chem. Res.* **1978**, *11*, 356 and references therein.
(21) Eller, P. G.; Kubas, G. J. *J. Am. Chem. Soc.* **1977**, *99*, 4346.
(22) Tsuda, T.; Watanabe, K.; Miyata, K.; Yamamoto, H.; Saegusa, T. *Inorg. Chem.* **1981**, *20*, 2728.
(23) Tsuda, T.; Sanada, S.-I.; Ueda, K.; Saegusa, T. *Inorg. Chem.* **1976**, *15*, 2329.
(24) Atwood, J. D. "Inorganic and Organometallic Reaction Mechanisms"; Brooks/Cole Publishing Company: Monterey, CA, 1985.
(25) Whitesides, G. M.; Stedronsky, E. R.; Casey, C. P.; Fillippo, J. S., Jr. *J. Am. Chem. Soc.* **1970**, *92*, 1426.
(26) Whitesides, G. M.; Gaasch, J. F.; Stedronsky, E. R. *J. Am. Chem. Soc.* **1972**, *94*, 5258.
(27) Evans, J.; Schwartz, J.; Urquhart, P. W. *J. Organomet. Chem.* **1974**, *81*, C37.
(28) Kaesz, H. D.; Saillant, R. *Chem. Rev.* **1972**, *72*, 231.

0276-7333/86/2305-0390$01.50/0

$$\text{"}RCH_2OCu\text{"} \rightarrow Cu(0) + RCH_2OH + RCH(O) \quad (1)$$

The alkoxides were prepared by reactions similar to those previously reported.[15,16] The spectroscopic parameters are consistent with the formulation *trans*-$ROIr(CO)(PPh_3)_2$.[29] Decomposition reactions of the alkoxides are carried out as follows: a solution of 0.10 g of the iridium alkoxide complex and 0.08 g of PPh_3 (~2–3 equiv) in 20 mL of cyclohexane are placed in a pressure tube fitted with a Teflon stopcock and allowed to stir at 70 °C for several hours. To detect the organic products by gas chromatography (Varian 2440 FID, 12 ft Carbowax, 60 °C), the reaction is carried out in 10 mL of HPLC grade toluene (Aldrich) which was dried over CaH_2 and distilled directly onto the alkoxy complex.

The alkoxides which contain β-hydrogens *trans*-$ROIr(CO)(PPh_3)_2$ (R = Me, *i*-Pr, and *n*-Pr) decompose at moderate rates at 70 °C; in the presence of PPh_3 the iridium product is $HIr(CO)(PPh_3)_3$ identified by comparison to independently prepared samples.[30] Similar reactions are not observed for R = H, Ph, or *t*-Bu. For *trans*-*i*-$PrOIr(CO)(PPh_3)_2$ the decomposition leads to acetone and 2-propanol (eq 2). The acetone and 2-propanol were

$$\textit{trans-i-}PrOIr(CO)(PPh_3)_2 + PPh_3 \rightarrow HIr(CO)(PPh_3)_3 + CH_3C(O)CH_3 + CH_3CHOHCH_3 \quad (2)$$

formed in comparable amounts (total yield of the two is 90% as an average of three decompositions). Similar decomposition of *trans*-*n*-$PrOIr(CO)(PPh_3)_2$ leads to propanal (92%). We have been unable to detect formaldehyde during decomposition of *trans*-$MeOIr(CO)(PPh_3)_2$.[31] The observation of ketone and alcohol for R = *i*-Pr indicates that decomposition of these alkoxides may be similar to copper(I) alkoxides where both products were also observed.[1] As suggested previously the alcohol may arise from fission of the metal–alkoxide bond with hydrogen abstraction or from a binuclear reaction between the formed hydride and remaining alkoxide.

To check the latter possibility, we have examined the reaction between $HIr(CO)(PPh_3)_3$ and *trans*-*i*-$PrOIr(CO)(PPh_3)_2$.

$$\textit{trans-i-}PrOIr(CO)(PPh_3)_2 + HIr(CO)(PPh_3)_3 \rightarrow i\text{-}PrOH + ? \quad (3)$$

Reaction 3 proceeds readily at room temperature to give a good yield of 2-propanol and an unidentified air-sensitive iridium compound. No trace of acetone was observed in this binuclear elimination. This binuclear elimination of alcohol from a metal hydride and a metal alkoxy could arise from a hydrogen bridging (as a hydride) between the two iridium atoms or a hydrogen bond interaction (as a proton) between the HIr and the oxygen of the alkoxy. Further experiments are in progress to delineate the mechanism of the binuclear elimination. Use of *trans*-$CD_3OIr(CO)(PPh_3)_2$ or *trans*-$(CD_3)_2CDOIr(CO)(PPh_3)_2$ in C_6H_{12} leads to $DIr(CO)(PPh_3)_3$ identified by comparison to an independently prepared sample and previous report.[33,34]

Three pieces of evidence strongly implicate a β-elimination in the decomposition of *trans*-$ROIr(CO)(PPh_3)_2$, R = Me, *n*-Pr, or *i*-Pr. (1) The decomposition only occurs for alkoxides which contain β-hydrogens. (2) The decomposition produces an iridium hydride, $HIr(CO)(PPh_3)_3$, the expected complex from a β-hydrogen elimination. (3) For the *n*-propoxy and *i*sopropoxy complexes the expected organic products (propanal and acetone, respectively) are observed in high yield. The alcohol product that is also observed may result from a binuclear elimination between the alkoxide complex and the formed hydride.

Acknowledgment. We acknowledge the donors of the Petroleum Research Fund, administered by the American Chemical Society, and the Alfred P. Sloan Foundation for partial support of this research. A loan of $IrCl_3 \cdot XH_2O$ was generously provided by Johnson Matthey Corp.

(29) The carbonyl stretching frequency (C_6H_{12}) and NMR spectra (in benzene-d_6—each spectra has a multiplet at ~7 ppm): *trans*-$CH_3OIr(CO)(PPh_3)_2$, 1951 cm^{-1}, 3.4 (s) ppm; *trans*-*n*-$PrOIr(CO)(PPh_3)_2$, 1951 cm^{-1}, 3.65 (t), 1.16 (m), 0.60 (t) ppm; *trans*-*t*-$BuOIr(CO)(PPh_3)_2$, 1951 cm^{-1}, 0.89 (s) ppm; *trans*-$PhOIr(CO)(PPh_3)_2$, 1958 cm^{-1}; *trans*-*i*-$PrOIr(CO)(PPh_3)_2$, 1945 cm^{-1}, 0.72 (d), 4.0 (septet) ppm; *trans*-$HOIr(CO)(PPh_3)_2$, 1923 cm^{-1}; $HIr(CO)(PPh_3)_3$, 2070 (IR–H), 1933 cm^{-1} (C–O).

(30) Wilkinson, G. *Inorg. Synth.* **1972**, *13*, 127.

(31) Formaldehyde undergoes reactions with many of the iridium complexes through an apparent initial oxidative addition.[32]

(32) Bernard, K. A.; Atwood, J. D., manuscript in preparation.

(33) Vaska, L. *J. Am. Chem. Soc.* **1966**, *88*, 4100.

(34) Based on the absence of the Ir–H stretch at 2070 cm^{-1}, we estimate the amount of $HIr(CO)(PPh_3)_3$ at less than 10%.

An Unusual Solvent Effect in the Reaction of Ethylmagnesium Bromide with Triethylborane in Ethyl Ether or Tetrahydrofuran. A Simple Direct Route to Tetraorganylborate Complexes

Herbert C. Brown* and Uday S. Racherla

Richard B. Wetherill Laboratory, Purdue University
West Lafayette, Indiana 47907

Received September 10, 1985

Summary: The reaction of organic halides, magnesium turnings, and boron trifluoride etherate yields triorganylboranes quantitatively in anhydrous ethyl ether (modified organometallic method) but leads to quantitative formation of tetraorganylborate complexes in tetrahydrofuran. A detailed study of the reaction of ethylmagnesium bromide with triethylborane revealed that essentially no reaction occurs in ethyl ether, EtMgBr + BEt_3, but complete combination occurs in tetrahydrofuran, Et_4BMgBr. This development provides a simple, convenient route for the synthesis of tetraorganylborate complexes.

Recently we described a general quantitative synthesis of triorganylboranes via a modified organometallic method[1] (eq 1).

$$3RX + 3Mg + BF_3 \cdot OEt_2 \rightarrow \underset{90\text{–}99\%}{R_3B} + 3MgFX \quad (1)$$

During this study, we discovered an unusual solvent effect. ^{11}B NMR examination of the reaction mixture revealed that the reaction of ethyl bromide, magnesium turnings, and boron trifluoride etherate (taken in 3.5:3.5:1 molar ratio) in ethyl ether forms triethylborane (100%), but in tetrahydrofuran, the reaction leads to the exclusive formation of the bromomagnesium tetraethylborate–THF complex[2] (eq 2).

$$3.5EtBr + 3.5Mg + BF_3 \cdot OEt_2 \xrightarrow[2\text{ h}]{\text{Et}_2\text{O}} \underset{100\%}{Et_3B} + 3MgFBr\downarrow + 0.5\,EtMgBr$$
$$\xrightarrow[2\text{ h}]{\text{THF}} \underset{87.5\%}{\tfrac{7}{8}\,Et_4BMgBr \cdot n\text{THF}} + \underset{12.5\%}{\tfrac{1}{8}\,BF_3 \cdot \text{THF}} + \tfrac{21}{8}\,MgFBr \quad (2)$$

(1) Brown, H. C.; Racherla, U. S. *J. Org. Chem.*, in press.

(2) Both reactions were performed at 0.25 M concentration. By ^{11}B NMR, all of the species formed, namely, triethylborane (δ 86.6), $BF_3 \cdot OEt_2$ (δ 0), and the ate complex (δ −16.6), could be readily distinguished.

0276-7333/86/2305-0391$01.50/0

$$\text{"}RCH_2OCu\text{"} \rightarrow Cu(0) + RCH_2OH + RCH(O) \quad (1)$$

The alkoxides were prepared by reactions similar to those previously reported.[15,16] The spectroscopic parameters are consistent with the formulation *trans*-$ROIr(CO)(PPh_3)_2$.[29] Decomposition reactions of the alkoxides are carried out as follows: a solution of 0.10 g of the iridium alkoxide complex and 0.08 g of PPh_3 (~2–3 equiv) in 20 mL of cyclohexane are placed in a pressure tube fitted with a Teflon stopcock and allowed to stir at 70 °C for several hours. To detect the organic products by gas chromatography (Varian 2440 FID, 12 ft Carbowax, 60 °C), the reaction is carried out in 10 mL of HPLC grade toluene (Aldrich) which was dried over CaH_2 and distilled directly onto the alkoxy complex.

The alkoxides which contain β-hydrogens *trans*-$ROIr(CO)(PPh_3)_2$ (R = Me, *i*-Pr, and *n*-Pr) decompose at moderate rates at 70 °C; in the presence of PPh_3 the iridium product is $HIr(CO)(PPh_3)_3$ identified by comparison to independently prepared samples.[30] Similar reactions are not observed for R = H, Ph, or *t*-Bu. For *trans*-*i*-$PrOIr(CO)(PPh_3)_2$ the decomposition leads to acetone and 2-propanol (eq 2). The acetone and 2-propanol were

$$\textit{trans-i-}PrOIr(CO)(PPh_3)_2 + PPh_3 \rightarrow HIr(CO)(PPh_3)_3 + CH_3C(O)CH_3 + CH_3CHOHCH_3 \quad (2)$$

formed in comparable amounts (total yield of the two is 90% as an average of three decompositions). Similar decomposition of *trans*-*n*-$PrOIr(CO)(PPh_3)_2$ leads to propanal (92%). We have been unable to detect formaldehyde during decomposition of *trans*-$MeOIr(CO)(PPh_3)_2$.[31] The observation of ketone and alcohol for R = *i*-Pr indicates that decomposition of these alkoxides may be similar to copper(I) alkoxides where both products were also observed.[1] As suggested previously the alcohol may arise from fission of the metal–alkoxide bond with hydrogen abstraction or from a binuclear reaction between the formed hydride and remaining alkoxide.

To check the latter possibility, we have examined the reaction between $HIr(CO)(PPh_3)_3$ and *trans*-*i*-$PrOIr(CO)(PPh_3)_2$.

$$\textit{trans-i-}PrOIr(CO)(PPh_3)_2 + HIr(CO)(PPh_3)_3 \rightarrow i\text{-}PrOH + ? \quad (3)$$

Reaction 3 proceeds readily at room temperature to give a good yield of 2-propanol and an unidentified air-sensitive iridium compound. No trace of acetone was observed in this binuclear elimination. This binuclear elimination of alcohol from a metal hydride and a metal alkoxy could arise from a hydrogen bridging (as a hydride) between the two iridium atoms or a hydrogen bond interaction (as a proton) between the HIr and the oxygen of the alkoxy. Further experiments are in progress to delineate the mechanism of the binuclear elimination. Use of *trans*-$CD_3OIr(CO)(PPh_3)_2$ or *trans*-$(CD_3)_2CDOIr(CO)(PPh_3)_2$ in C_6H_{12} leads to $DIr(CO)(PPh_3)_3$ identified by comparison to an independently prepared sample and previous report.[33,34]

Three pieces of evidence strongly implicate a β-elimination in the decomposition of *trans*-$ROIr(CO)(PPh_3)_2$, R = Me, *n*-Pr, or *i*-Pr. (1) The decomposition only occurs for alkoxides which contain β-hydrogens. (2) The decomposition produces an iridium hydride, $HIr(CO)(PPh_3)_3$, the expected complex from a β-hydrogen elimination. (3) For the *n*-propoxy and *i*sopropoxy complexes the expected organic products (propanal and acetone, respectively) are observed in high yield. The alcohol product that is also observed may result from a binuclear elimination between the alkoxide complex and the formed hydride.

Acknowledgment. We acknowledge the donors of the Petroleum Research Fund, administered by the American Chemical Society, and the Alfred P. Sloan Foundation for partial support of this research. A loan of $IrCl_3 \cdot XH_2O$ was generously provided by Johnson Matthey Corp.

(29) The carbonyl stretching frequency (C_6H_{12}) and NMR spectra (in benzene-d_6—each spectra has a multiplet at ~7 ppm): *trans*-$CH_3OIr(CO)(PPh_3)_2$, 1951 cm^{-1}, 3.4 (s) ppm; *trans*-*n*-$PrOIr(CO)(PPh_3)_2$, 1951 cm^{-1}, 3.65 (t), 1.16 (m), 0.60 (t) ppm; *trans*-*t*-$BuOIr(CO)(PPh_3)_2$, 1951 cm^{-1}, 0.89 (s) ppm; *trans*-$PhOIr(CO)(PPh_3)_2$, 1958 cm^{-1}; *trans*-*i*-$PrOIr(CO)(PPh_3)_2$, 1945 cm^{-1}, 0.72 (d), 4.0 (septet) ppm; *trans*-$HOIr(CO)(PPh_3)_2$, 1923 cm^{-1}; $HIr(CO)(PPh_3)_3$, 2070 (IR–H), 1933 cm^{-1} (C–O).

(30) Wilkinson, G. *Inorg. Synth.* **1972**, *13*, 127.

(31) Formaldehyde undergoes reactions with many of the iridium complexes through an apparent initial oxidative addition.[32]

(32) Bernard, K. A.; Atwood, J. D., manuscript in preparation.

(33) Vaska, L. *J. Am. Chem. Soc.* **1966**, *88*, 4100.

(34) Based on the absence of the Ir–H stretch at 2070 cm^{-1}, we estimate the amount of $HIr(CO)(PPh_3)_3$ at less than 10%.

An Unusual Solvent Effect in the Reaction of Ethylmagnesium Bromide with Triethylborane in Ethyl Ether or Tetrahydrofuran. A Simple Direct Route to Tetraorganylborate Complexes

Herbert C. Brown* and Uday S. Racherla

Richard B. Wetherill Laboratory, Purdue University
West Lafayette, Indiana 47907

Received September 10, 1985

Summary: The reaction of organic halides, magnesium turnings, and boron trifluoride etherate yields triorganylboranes quantitatively in anhydrous ethyl ether (modified organometallic method) but leads to quantitative formation of tetraorganylborate complexes in tetrahydrofuran. A detailed study of the reaction of ethylmagnesium bromide with triethylborane revealed that essentially no reaction occurs in ethyl ether, EtMgBr + BEt_3, but complete combination occurs in tetrahydrofuran, Et_4BMgBr. This development provides a simple, convenient route for the synthesis of tetraorganylborate complexes.

Recently we described a general quantitative synthesis of triorganylboranes via a modified organometallic method[1] (eq 1).

$$3RX + 3Mg + BF_3 \cdot OEt_2 \rightarrow \underset{90\text{–}99\%}{R_3B} + 3MgFX \quad (1)$$

During this study, we discovered an unusual solvent effect. ^{11}B NMR examination of the reaction mixture revealed that the reaction of ethyl bromide, magnesium turnings, and boron trifluoride etherate (taken in 3.5:3.5:1 molar ratio) in ethyl ether forms triethylborane (100%), but in tetrahydrofuran, the reaction leads to the exclusive formation of the bromomagnesium tetraethylborate–THF complex[2] (eq 2).

$$3.5EtBr + 3.5Mg + BF_3 \cdot OEt_2 \xrightarrow[2\text{ h}]{\text{Et}_2\text{O}} \underset{100\%}{Et_3B} + 3MgFBr\downarrow + 0.5\,EtMgBr$$
$$\xrightarrow[2\text{ h}]{\text{THF}} \underset{87.5\%}{\tfrac{7}{8}\,Et_4BMgBr \cdot n\text{THF}} + \underset{12.5\%}{\tfrac{1}{8}\,BF_3 \cdot \text{THF}} + \tfrac{21}{8}\,MgFBr \quad (2)$$

(1) Brown, H. C.; Racherla, U. S. *J. Org. Chem.*, in press.

(2) Both reactions were performed at 0.25 M concentration. By ^{11}B NMR, all of the species formed, namely, triethylborane (δ 86.6), $BF_3 \cdot OEt_2$ (δ 0), and the ate complex (δ −16.6), could be readily distinguished.

0276-7333/86/2305-0391$01.50/0

Further, the use of 4 equiv each of ethyl bromide and magnesium turnings in the above method results in complete conversion to tetraethylborate complex (eq 3).

$$4EtBr + 4Mg + BF_3{\cdot}OEt_2 \xrightarrow[2\ h]{THF,\ 25\ ^\circ C} Et_4BMgBr{\cdot}nTHF + 3MgFBr{\cdot}nTHF \quad (3)$$

We decided to study the reaction of ethylmagnesium bromide (EtMgBr) with triethylboron (Et_3B) in ethyl ether (EE) and in tetrahydrofuran (THF). ^{11}B NMR readily distinguishes between Et_3B and Et_4BMgBr. Both Et_3B and Et_4BMgBr are stable to water at 25 °C. Consequently, the ethane evolved on addition of water provides a quantitative measure of the free EtMgBr in the presence of Et_3B and Et_4BMgBr.

The reaction of EtMgBr[3] (1.0 mL, 3.0 M, 3 mmol) with triethylborane (0.29 g, 3 mmol) in ether (10.6 mL) produced a clear upper layer and a much smaller viscous gray-colored lower layer. There was no observable change over 6 h. ^{11}B NMR analysis of the upper layer showed Et_3B (δ 86.6) exclusively, with not even a trace of the ate complex, whereas analysis of the small lower layer showed only the $Et_4MgBr{\cdot}nOEt_2$ complex (δ −16.6). In a duplicate experiment, water (5 mL) was added to the reaction mixture and the resulting ethane evolved determined to be 2.9 mmol.[4] This experiment establishes that $Et_4BMgBr{\cdot}nOEt_2$ is completely insoluble in ether, and the amount formed is only 0.1 mmol or approximately 4%[5] (eq 4).

$$\underset{96\%}{Et_3B} + \underset{96\%}{EtMgBr} \xrightleftharpoons{EE,\ 6\ h} \underset{4\%}{Et_4BMgBr{\cdot}nOEt_2} \quad (4)$$

Under the same conditions, the reaction of EtMgBr[3] (1.0 mL, 3.0 M, 3 mmol) with Et_3B (0.29 g, 3 mmol) in THF (10.6 mL) afforded in 6 h a heterogeneous reaction mixture, a clear upper layer and a white crystalline solid. ^{11}B NMR analysis of the upper layer showed exclusively the $Et_4BMgBr{\cdot}nTHF$ complex (δ −16.5). The solid was next isolated and characterized by ^1H NMR and microanalysis to be the complex $EtBMgBr{\cdot}4THF$.[5] Once again, in a duplicate experiment, water was added to the reaction mixture. The ethane evolved was 0.1 mmol, corresponding to the formation of 2.9 mmol of Et_4BMgBr, a conversion of 96% (eq 5).

$$\underset{4\%}{Et_3B} + \underset{4\%}{EtMgBr} \xrightleftharpoons[25\ ^\circ C]{THF,\ 6\ h} \underset{96\%}{Et_4BMgBr{\cdot}4THF} \quad (5)$$

At this stage it was clear that the formation of Et_4BMgBr from Et_3B and EtMgBr is highly unfavorable in ether but highly favorable in THF. It appeared that the better coordinating properties of THF[6] might be responsible. To test this conclusion, the following experiments were run.

The addition of EtMgBr in ether (1.0 mL, 3.0 M, 3 mmol) to Et_3B (0.29 g, 3 mmol) in a mixture of ether (9.6 mL) and THF (0.87 g, 1.0 mL, 12 mmol) at 25 °C afforded in 6 h 89% of the $Et_4BMgBr{\cdot}4THF$ complex (eq 6).

$$\underset{11\%}{Et_3B} + \underset{11\%}{EtMgBr} \xrightleftharpoons[25\ ^\circ C,\ 6\ h]{EE\text{–}THF} \underset{89\%}{Et_4BMgBr{\cdot}4THF} \quad (6)$$

Moreover, when the Et_4BMgBr-4THF (1.56 g, 3 mmol), taken into ether (12 mL), was stirred at 25 °C for 6 h in ether (12 mL), the Et_3B measured by NMR and the EtMgBr found by hydrolysis are both 20% (±5%) (eq 7).

$$\underset{80\%}{Et_4BMgBr{\cdot}4THF} \xrightleftharpoons[25\ ^\circ C,\ 6\ h]{EE} \underset{20\%}{Et_3B} + \underset{20\%}{EtMgBr} \quad (7)$$

On the basis of these data, it appears that the formation of $Et_4BMgBr{\cdot}nOEt_2$ from a mixture of Et_3B and EtMgBr in anhydrous ether (0.25 M) at 25 °C represents a highly unfavorable equilibrium. However, this still does not fully explain why absolutely no ate complex formation was indicated[7] in our original triorganylborane synthesis in ethyl ether[1] (0.25 M, eq 2 and 8). A major difference between

$$3.5\,EtBr + 3.5Mg + BF_3{\cdot}OEt_2 \xrightarrow{EE,\ 2h} \begin{matrix} Et_3B \\ 99\% \\ + \\ 3MgFBr \end{matrix} + \begin{matrix} Et_4BMgBr{\cdot}nOEt_2 \\ 0\% \\ + \\ 0.5\,EtMgBr \end{matrix} \quad (8)$$

the two reactions described by eq 4 and 8 is the presence of solid magnesium halide, assumed to be MgFBr, in the latter experiment. It was thought possible that the EtMgBr was extracted by this solid. This possibility was tested by the following experiment.

EtMgBr in ethyl ether (3.0 mL, 3.0 M, 9 mmol) was slowly added to $BF_3{\cdot}OEt_2$ (0.43 g, 3 mmol) in ether (7.6 mL) at a rate such that the ether refluxed gently. The reaction mixture was then stirred for 2 h, and an additional quantity of EtMgBr (1.0 mL, 3.0 M, 3 mmol) in ether was added. Stirring was continued for 2 h, and then the reaction mixture (0.25 M) was allowed to settle. The ether phase was separated. The solid was washed thoroughly with ether (12 mL). The combined ether phase and washings and the solid were separately treated with water. There was obtained 2.7 mmol of ethane from the solid and only 0.4 mmol of ethane from the ether solution. Thus, in the above experiment, approximately 90% of the excess EtMgBr (2.7 mmol) was extracted from the ether solution by the solid (presumably MgFBr). This observation accounts for the failure to observe any formation of $Et_4BMgBr{\cdot}nOEt_2$ in the original triorganylborane synthesis[1] (eq 2 and 8).

In our original study of the synthesis of triorganylboranes by the "modified organometallic route",[1] we observed the same phenomena for 11 different organic halides (alkyl, alicyclic, aryl, and allylic). Consequently, this difference between the behavior of ether and THF on the formation of tetraorganylborate complexes appears to be quite general. This should not be taken to mean that the formation of tetraorganylborate complexes cannot ever occur in ether. Indeed, Kondo and Murahashi[8] used such formation of spiro ate complexes to achieve a valuable conversion of organoboranes into the corresponding Grignard reagents (eq 9).

$$R_3B + 2BrMg(CH_2)_5MgBr \xrightarrow{Et_2O} 3RMgBr + (CH_2)_5\overset{-}{B}(CH_2)_5\overset{+}{M}gBr \quad (9)$$

We earlier attempted to achieve such interconversion.[9] Unfortunately, much of our work utilized THF solutions and the undetected formation of "ate" complexes com-

(3) For the nature of the Grignard reagent in ether solvents, see: (a) Ashby, E. C. *Q. Rev., Chem. Soc.* **1967**, *21*, 259. (b) *Pure Appl. Chem.* **1980**, *52*, 545. For simplicity, ethylmagnesium bromide is represented throughout this paper as EtMgBr, although this may not always be the reactive species in solution.

(4) Brown, H. C.; Kramer, G. W.; Levy, A. B.; Midland, M. M. "Organic Syntheses via Boranes"; Wiley-Interscience: New York, 1975.

(5) ^1H NMR spectrum was consistent with the structure $Et_4BMgBr{\cdot}4THF$: δ 0.85–1.65 (m, 20 H), 1.8–2.05 (m, 16 H), 3.75–4.05 (m, 16 H). The results of microanalysis also matched with this structure. Calcd for [$Et_4BMgBr{\cdot}4THF$]: C, 55.47; H, 10.08; Br, 15.38; Mg, 4.68. Found: C, 54.14; H, 10.23; Br, 15.07; Mg 4.38.

(6) Coates, G. E.; Green, M. L. H.; Powell, P.; Wade, K. "Principles of Organometallic Chemistry"; Methuen and Company: London, 1969.

(7) ^{11}B NMR analysis of the residual solid showed in tetrahydrofuran no boron species.

(8) Kondo, K.; Murahashi, S.-I. *Tetrahedron Lett.* **1979**, 1237.

(9) Buhler, J. D. Ph.D. Thesis, Purdue University, 1973.

plicated the interconversion.

Now that this phenomenon is understood, it is evident that it provides the basis for an exceptionally simple synthesis of tetraorganylborates, as well as the basis for achieving a very simple conversion of organoboranes into Grignard reagents (eq 10).

$$R_3B + 3R'MgX \rightarrow 3RMgX + R'_3B \qquad (10)$$

Acknowledgment. We wish to thank the National Science Foundation (Grant CHE-8414171) for financial support of this research.

Stabilization of a Large Arsenic–Oxygen Heterocycle via Metal Coordination. The Synthesis and X-ray Crystal Structure of $[Mo(CO)_3]_2[cyclo\text{-}(CH_3AsO)_6]$

Arnold L. Rheingold* and Anthony-J. DiMaio

Department of Chemistry, University of Delaware Newark, Delaware 19716

Received November 5, 1985

Summary: In the presence of molecular oxygen, $Mo(CO)_6$, and *cyclo*-$(CH_3As)_5$ form the first example of a metal-coordinated alkylarsaoxane, $[Mo(CO)_3]_2[cyclo\text{-}(CH_3AsO)_6]$ (**1**), containing a 12-membered alternating As–O ring coordinated to two $Mo(CO)_3$ groups. The As–O ring exists as a flattened, trans bimetal-capped cubocta-hedron with two planes of three arsenic atoms positioned for coordination and a central plane of six oxygen atoms. Crystals of **1** are orthorhombic of space group *Cmca*, with a = 13.424 (2), Å, b = 16.909 (3) Å, c = 11.818 (2) Å, Z = 4, and V = 2682.6 (7) Å^3.

Alkylarsaoxanes, $(RAsO)_n$, are thought to exist as cyclotrimers, cyclotetramers, and other more highly associated, interchangeable ring and chain forms,[1] but none of the proposed structures has been isolated or confirmed crystallographically.[2,3] The potential for arsaoxanes to serve as multidentate ligands offers a means for the isolation of discrete species. We now report the synthesis and characterization of a dimolybdenum hexacarbonyl complex of *cyclo*-$(CH_3AsO)_6$ containing a 12-membered As–O heterocycle bridging $Mo(CO)_3$ groups, $\{[Mo(CO)_3]_2[cyclo\text{-}(CH_3AsO)_6]\}$ (**1**).

Complex **1** is prepared from toluene solutions of $Mo(CO)_6$ and *cyclo*-$(AsCH_3)_5$ in which various quantities of dioxygen are dissolved and heated in Carius tubes at 150 °C for 48 h. Upon slow cooling, pale yellow crystals of **1**[4] along with $[Mo(CO)_3]_2[cyclo\text{-}(AsCH_3)_{10}]$ (**2**)[5] are obtained.

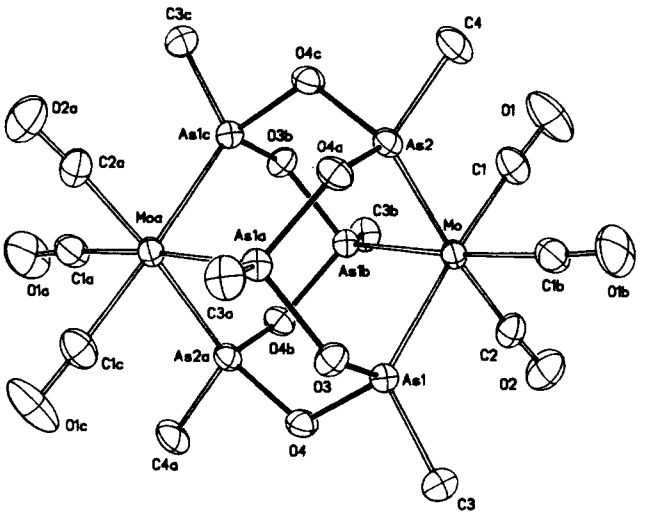

Figure 1. Thermal ellipsoid diagram for $\{(CH_3AsO)_6[Mo(CO)_3]_2\}$ (**1**) and atom labeling scheme with hydrogen atoms deleted. Bond distances (Å): Mo-As(1), 2.556 (1); Mo–As(1b), 2.557 (1); MoAs(2), 2.535 (1); As(1)–O(3), 1.793 (2); As(1)–O(4), 1.794 (3); As(2)–O(4a), 1.787(3). Bond angles (deg): As(1)–Mo–As(2), 92.8 (0); As(1)–Mo–As(1b), 93.7 (0); As(2)–Mo–As(1b), 92.8 (0); Mo–As(1)–O(3), 116.9 (1); Mo–As(1)–O(4), 116.4 (1); Mo–As(2)–O(4a), 118.4 (1); Mo–As(2)–O(4c), 118.4; As(1)–O(3)–As(1a), 119.7 (2); As(1)–O(4)–As(2a), 118.1 (2); O(3)–As(1)–O(4), 100.9 (1); O(4a)–As(2)–O(4c), 101.2 (2).

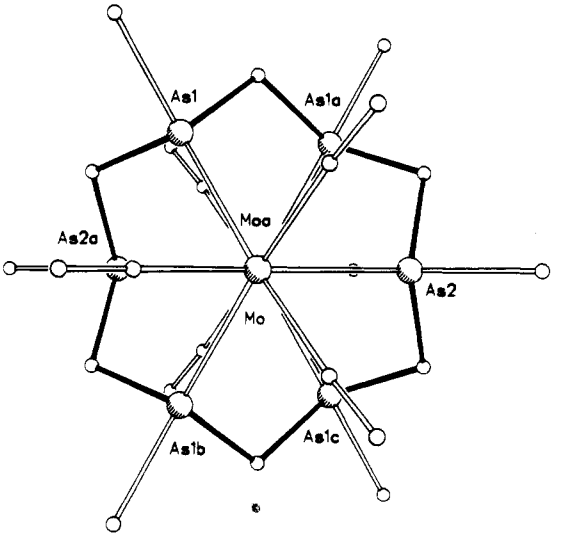

Figure 2. A projection of the structure of **1** viewed down the Mo···Mo′ vector.

1 was separated from the much less soluble **2** in boiling CH_2Cl_2. The product ratio of **1** to **2** varies with the initial oxygen concentration; at the extremes, only **1** is isolated in 77% yield (based on $(CH_3As)_5$) with addition of stoichiometric quantities of O_2 (eq 1) while only **2** is isolated in rigorously degassed systems (eq 2).

$$Mo(CO)_6 + cyclo\text{-}(AsMe)_5 \xrightarrow[\text{toluene, 150 °C}]{O_2} \underset{\mathbf{1}}{\{[Mo(CO)_3]_2(CH_3AsO)_6\}} \quad (1)$$

$$Mo(CO)_6 + cyclo\text{-}(AsMe)_5 \xrightarrow[\text{toluene, 150 °C}]{\text{degassed}} \underset{\mathbf{2}}{\{[Mo(CO)_3]_2(CH_3As)_{10}\}} \quad (2)$$

Compound **1** crystallizes as discrete molecules (Figures 1 and 2) without significant intermolecular contacts.[6] The

(1) Durand, M.; Laurent, J.-P. *J. Organomet. Chem.* **1974**, *77*, 225. Marsmann, H. C.; Van Wazer, J. R. *J. Am. Chem. Soc.* **1970**, *92*, 3969.

(2) The literature abounds with names for compounds of formula RAsO: alkylarsaoxane, arsenosoalkane, alkylarsine oxide, and alkylarsenious oxide are the most commonly encountered.

(3) Arsaoxanes are among the oldest known organometallic compounds. $[(CH_3)_2AsOAs(CH_3)_2]$: Cadet de Gassincourt, L. C. *Mem. Math. Phys. Savants Étrangers.* **1760**, *3*, 363. CH_3AsO: von Baeyer, A. *Justus Liebigs Ann. Chem.* **1858**, *107*, 279.

(4) (**1**) ^{1}H NMR ($CDCl_3$): δ 1.91; IR ν_{CO} 1980 s, 1906 s, 1875 m; decomp. temp, 300 °C. Anal. Calcd: C, 14.47; H, 1.81; As, 45.16. Found: C, 14.48; H, 1.88; As, 45.36.

(5) (**2**) ^{1}H NMR (benzene-d_6): δ 1.61 sh, 1.57 s; IR ν_{CO} 1926 s, 1868 m, 1843 m; decomp temp, 255 °C. Anal. Calcd: C, 15.25; H, 2.38. Found: C, 15.27; H, 2.59.

0276-7333/86/2305-0393$01.50/0

plicated the interconversion.

Now that this phenomenon is understood, it is evident that it provides the basis for an exceptionally simple synthesis of tetraorganylborates, as well as the basis for achieving a very simple conversion of organoboranes into Grignard reagents (eq 10).

$$R_3B + 3R'MgX \rightarrow 3RMgX + R'_3B \qquad (10)$$

Acknowledgment. We wish to thank the National Science Foundation (Grant CHE-8414171) for financial support of this research.

Stabilization of a Large Arsenic–Oxygen Heterocycle via Metal Coordination. The Synthesis and X-ray Crystal Structure of $[Mo(CO)_3]_2[cyclo\text{-}(CH_3AsO)_6]$

Arnold L. Rheingold* and Anthony-J. DiMaio

Department of Chemistry, University of Delaware Newark, Delaware 19716

Received November 5, 1985

Summary: In the presence of molecular oxygen, $Mo(CO)_6$, and *cyclo*-$(CH_3As)_5$ form the first example of a metal-coordinated alkylarsaoxane, $[Mo(CO)_3]_2[cyclo\text{-}(CH_3AsO)_6]$ (**1**), containing a 12-membered alternating As–O ring coordinated to two $Mo(CO)_3$ groups. The As–O ring exists as a flattened, trans bimetal-capped cubocta-hedron with two planes of three arsenic atoms positioned for coordination and a central plane of six oxygen atoms. Crystals of **1** are orthorhombic of space group *Cmca*, with a = 13.424 (2), Å, b = 16.909 (3) Å, c = 11.818 (2) Å, Z = 4, and V = 2682.6 (7) Å^3.

Alkylarsaoxanes, $(RAsO)_n$, are thought to exist as cyclotrimers, cyclotetramers, and other more highly associated, interchangeable ring and chain forms,[1] but none of the proposed structures has been isolated or confirmed crystallographically.[2,3] The potential for arsaoxanes to serve as multidentate ligands offers a means for the isolation of discrete species. We now report the synthesis and characterization of a dimolybdenum hexacarbonyl complex of *cyclo*-$(CH_3AsO)_6$ containing a 12-membered As–O heterocycle bridging $Mo(CO)_3$ groups, $\{[Mo(CO)_3]_2[cyclo\text{-}(CH_3AsO)_6]\}$ (**1**).

Complex **1** is prepared from toluene solutions of $Mo(CO)_6$ and *cyclo*-$(AsCH_3)_5$ in which various quantities of dioxygen are dissolved and heated in Carius tubes at 150 °C for 48 h. Upon slow cooling, pale yellow crystals of **1**[4] along with $[Mo(CO)_3]_2[cyclo\text{-}(AsCH_3)_{10}]$ (**2**)[5] are obtained.

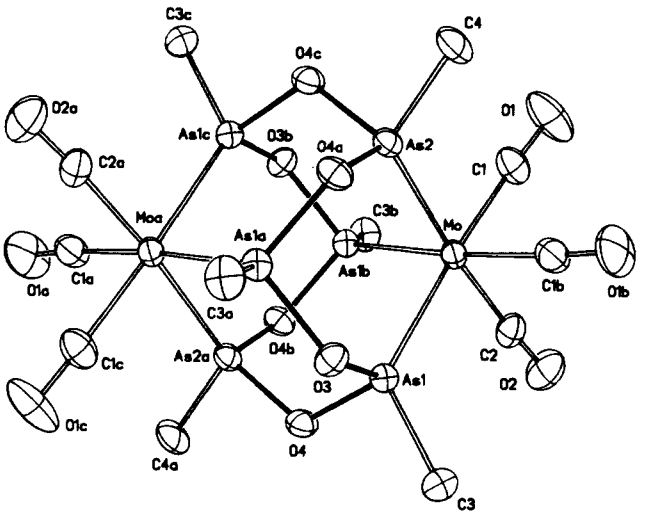

Figure 1. Thermal ellipsoid diagram for $\{(CH_3AsO)_6[Mo(CO)_3]_2\}$ (**1**) and atom labeling scheme with hydrogen atoms deleted. Bond distances (Å): Mo-As(1), 2.556 (1); Mo–As(1b), 2.557 (1); MoAs(2), 2.535 (1); As(1)–O(3), 1.793 (2); As(1)–O(4), 1.794 (3); As(2)–O(4a), 1.787(3). Bond angles (deg): As(1)–Mo–As(2), 92.8 (0); As(1)–Mo–As(1b), 93.7 (0); As(2)–Mo–As(1b), 92.8 (0); Mo–As(1)–O(3), 116.9 (1); Mo–As(1)–O(4), 116.4 (1); Mo–As(2)–O(4a), 118.4 (1); Mo–As(2)–O(4c), 118.4; As(1)–O(3)–As(1a), 119.7 (2); As(1)–O(4)–As(2a), 118.1 (2); O(3)–As(1)–O(4), 100.9 (1); O(4a)–As(2)–O(4c), 101.2 (2).

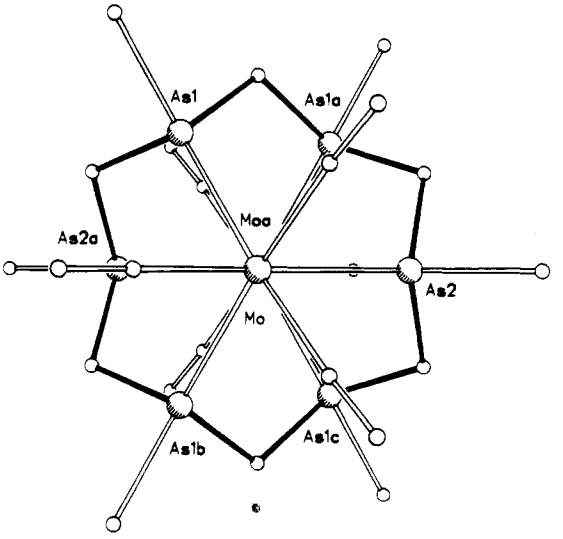

Figure 2. A projection of the structure of **1** viewed down the Mo···Mo′ vector.

1 was separated from the much less soluble **2** in boiling CH_2Cl_2. The product ratio of **1** to **2** varies with the initial oxygen concentration; at the extremes, only **1** is isolated in 77% yield (based on $(CH_3As)_5$) with addition of stoichiometric quantities of O_2 (eq 1) while only **2** is isolated in rigorously degassed systems (eq 2).

$$Mo(CO)_6 + cyclo\text{-}(AsMe)_5 \xrightarrow[\text{toluene, 150 °C}]{O_2} \underset{\mathbf{1}}{\{[Mo(CO)_3]_2(CH_3AsO)_6\}} \quad (1)$$

$$Mo(CO)_6 + cyclo\text{-}(AsMe)_5 \xrightarrow[\text{toluene, 150 °C}]{\text{degassed}} \underset{\mathbf{2}}{\{[Mo(CO)_3]_2(CH_3As)_{10}\}} \quad (2)$$

Compound **1** crystallizes as discrete molecules (Figures 1 and 2) without significant intermolecular contacts.[6] The

(1) Durand, M.; Laurent, J.-P. *J. Organomet. Chem.* **1974**, *77*, 225. Marsmann, H. C.; Van Wazer, J. R. *J. Am. Chem. Soc.* **1970**, *92*, 3969.

(2) The literature abounds with names for compounds of formula RAsO: alkylarsaoxane, arsenosoalkane, alkylarsine oxide, and alkylarsenious oxide are the most commonly encountered.

(3) Arsaoxanes are among the oldest known organometallic compounds. $[(CH_3)_2AsOAs(CH_3)_2]$: Cadet de Gassincourt, L. C. *Mem. Math. Phys. Savants Étrangers.* **1760**, *3*, 363. CH_3AsO: von Baeyer, A. *Justus Liebigs Ann. Chem.* **1858**, *107*, 279.

(4) (**1**) ^{1}H NMR ($CDCl_3$): δ 1.91; IR ν_{CO} 1980 s, 1906 s, 1875 m; decomp. temp, 300 °C. Anal. Calcd: C, 14.47; H, 1.81; As, 45.16. Found: C, 14.48; H, 1.88; As, 45.36.

(5) (**2**) ^{1}H NMR (benzene-d_6): δ 1.61 sh, 1.57 s; IR ν_{CO} 1926 s, 1868 m, 1843 m; decomp temp, 255 °C. Anal. Calcd: C, 15.25; H, 2.38. Found: C, 15.27; H, 2.59.

0276-7333/86/2305-0393$01.50/0

crystallographic site symmetry is $2/m$; O(3) and O(3b) define the two fold rotational axis and O(2), C(2), Mo, As(2), and C(4) define the mirror plane. The structure of **1** contains a 12-membered ring of alternating CH_3As groups and oxygen atoms; these 12 atoms form a flattened cuboctahedron which is trans bicapped by $Mo(CO)_3$ groups. The As–O ring configuration and the crystallographic symmetry require a coplanar arrangement for the six oxygen atoms which is sandwiched between two planes of three As atoms each. These exterior planes or arsenic atoms are positioned to form *fac*-$Mo(CO)_3L_3$ coordination environments at the metal center. The average of the three Mo–As distances, 2.55(1) Å, compares closely to those found in known structures.[7] The average As–O distance, 1.791 (3) Å, is very similar to that found in other caged As(III)–O structures: As_4O_6 (**3**), 1.80 Å;[8] $As_4O_4(CH_2)_2$ (**4**), ⟨av⟩ 1.795(7);[9] and $As_3O_3[(CH_2)_3CCH_3]$ (**5**) ⟨av⟩ 1.77 (1) Å.[10] The As–Mo–As angles are slightly obtuse, ⟨av⟩ 93.1°, and consistent with octahedral Mo geometry, while the C–Mo–C angles are slightly acute, ⟨av⟩ 87.2 (3)°. Whereas the O–As–O angles, ⟨av⟩ 101.0 (1)°, are very similar to As_4O_6, 100°, to **3**, 101.8 (4)°, and to **5**, 100.5°, the As–O–As angles in **1**, 118.1 (2) and 119.7 (2)°, are considerably smaller than in **3**, **4**, or **5**, which are in the range 126–129°. This decrease in the As–O–As angles has the effect of flattening the cubooctahedron and better positioning the six As atoms for metal coordination. Complex **1** is electron precise with a clearly definable 18e count at each metal center; each As(III) atom serves as a conventional 2e donor.

Our results suggest that the formation and stability of the *cyclo*-hexaarsaoxane ligand requires the presence of a stabilizing superstructure. The homoatomic cyclopentaarsine precursor to **1** reacts vigorously with dioxygen to form species of empirical formula CH_3AsO, but the route to **1** undoubtedly involves considerable metal-centered assistance in the organization of a 12-membered ring. Ellermann et al.[11] have recently reported a novel cryptand $[N(CH_2CH_2)_3]_8(As_4O_4)_6$ (**6**) containing an eight-membered alternating As–O ring in which each As atom is joined to two other As_4O_4 rings via $N(CH_2CH_2-)_3$ tripod bridge networks. The As–O bond distance (average 1.79 (5) Å and the As–O–As (average 118 (2)°) and O–As–O (average 101 (1)°) angles compare closely to those found in **1**. To date the known structures containing organoarsaoxane ring systems are either caged by organic linkages, **4**–**6**, or by metal carbonyl coordination, **1**, suggesting that such rings may prove to be very difficult to isolate without a superstructure. In fact, NMR studies[1] clearly indicate the cyclotrimers and tetramers of $(CH_3AsO)_n$ are involved in dynamic reorganization equilibria with higher cyclic and possibly linear species.

A complete discussion of the homocyclic decaarsine complex **2** will appear elsewhere.[12]

Acknowledgment. The National Science Foundation provided assistance in the purchase of the diffractometer. The Center for Catalytic Science and Technology at the University of Delaware provided support for the research.

Registry No. **1**, 99686-49-4; **2**, 99686-50-7; $Mo(CO)_6$, 13939-06-5; *cyclo*-$(AsCH_3)_5$, 20550-47-4.

Supplementary Material Available: Tables of atomic coordinates, a complete listing of bond distances and angles, anisotropic temperature factors, hydrogen atom coordinates, and observed and calculated structure factors (13 pages). Ordering information is given on any current masthead page.

(6) Crystal data for **1**, $C_{12}H_{18}As_6Mo_2O_{12}$: M_r = 995.7, orthorhombic, space group *Cmca*; a = 13.424 (2) Å, b = 16.909 (3) Å, c = 11.818 (2) Å, V = 2682.6 (7) Å, Z = 4, D_{calcd} = 2.47 g cm^{-3}, $F(000)$ = 1872, μ(Mo Kα) = 80.6 cm^{-1}. A pale yellow crystal (0.33 × 0.34 × 0.35 mm) was grown from CH_2Cl_2. Data were collected at 23 °C on a Nicolet R3 diffractometer. The structure was solved by direct methods and difference Fourier techniques. The 1605 symmetry-allowed reflections collected ($+h$, $+k$, $+l$; $4° \le 2\theta \le 50°$) were corrected for absorption; of these, 1309 with $F_o \ge 4\sigma(F_o)$ were used in refinement with anisotropic parameters for all non-hydrogen atoms. Hydrogen atom contributions were idealized and updated. At convergence R_F = 2.68%, R_{wF} = 2.94%, and GOF = 1.337 with a 13.4 data to parameter ratio.

(7) Rheingold, A. L.; Foley, M. J.; Sullivan, P. J. *J. Am. Chem. Soc.* **1982**, *104*, 4727.

(8) Bozorth, R. M. *J. Am. Chem. Soc.* **1923**, *45*, 1621.

(9) Kopf, J.; Von Denten, K.; Klar, G. *Inorg. Chim. Acta* **1980**, *37*, 67.

(10) Mckerley, B. J.; Reinhardt, K.; Mills, J. L.; Reisner, G. M.; Korp, J. D.; Bernal, I. *Inorg. Chim. Acta* **1978**, *31*, L411.

(11) Ellermann, J.; Veit, A.; Lindner, E.; Hoehne, S. *J. Organomet. Chem.* **1983**, *252*, 153.

(12) Rheingold, A. L.; DiMaio, A.-J.; Fountain, M. E., manuscript in preparation.

Stepwise Assembly of a Trinuclear Bis(carbyne) Complex from Cyclopentadienylcobalt Units and Bis(trimethylsilyl)acetylene: Isolation and Conversion of $Cp_2M_2(RC{\equiv}CR)$ and $(CpM)_3(RC{\equiv}CR)$ [M = Co and R = $(CH_3)_3Si$]

Bruce Eaton, Joseph M. O'Connor, and K. Peter C. Vollhardt*

Department of Chemistry
University of California at Berkeley
and the Materials and Molecular Research Division
Lawrence Berkeley Laboratory
Berkeley, California 94720

Received August 26, 1985

Summary: Reaction of $(\eta^5\text{-}C_5H_5)Co(C_2H_4)_2$ (**7**) with bis(trimethylsilyl)acetylene (btmsa) in THF at 23 °C gives $(\eta^5\text{-}C_5H_5)_2Co_2$(btmsa) (**9**). The structure of **9** was determined by X-ray crystallography, revealing the presence of a Co–Co double bond: 2.18 Å, to our knowledge the shortest cobalt–cobalt bond in existence. Complex **9** reacts further with **7** at 55 °C to produce $(\eta^5\text{-}C_5H_5)_3Co_3$(btmsa) (**10**). Complex **10** adds carbon monoxide to give $(\eta^5\text{-}C_5H_5)_3Co_3$(btmsa)(CO) (**11**). Both **10** and **11** are converted to $(\eta^5\text{-}C_5H_5)_3Co_3[\mu_3\text{-}\eta^1\text{-}CSi(CH_3)_3]_2$ (**6**) in boiling *m*-xylene or hot methylcyclohexane. A crossover experiment involving $(\eta^5\text{-}CH_3C_5H_4)_2Co_2$(btmsa) and **10** establishes the intramolecular nature of the rearrangement to **6**.

Mononuclear transition-metal complexes of the cobalt triad **1** react with alkynes to give trinuclear bis(carbyne) clusters **2** (Scheme I).[1-3] Among the alkyne substrates which have been examined in these reactions, bis(trimethylsilyl)acetylene (btmsa) exhibits anomalous behavior. Sakurai and Hayashi have reported that **1** (M = Co) converts to **3** in 93% yield in the presence of 2 equiv of btmsa in boiling xylene.[4] More recently, we reported that **1** (M

(1) (a) Fritch, J. R.; Vollhardt, K. P. C.; Thompson, M. R.; Day, V. W. *J. Am. Chem. Soc.* **1979**, *101*, 2768. (b) Fritch, J. R.; Vollhardt, K. P. C. *Angew. Chem., Int. Ed. Engl.* **1980**, *19*, 559. (c) Fritch, J. R.; Vollhardt, K. P. C. *Isr. J. Chem.*, in press and the references therein.

(2) Yamazaki, H.; Wakatsuki, Y.; Aoki, K. *Chem. Lett.* **1979**, 1041.

(3) Gardner, S. A.; Andrews, P. S.; Rausch, M. D. *Inorg. Chem.* **1973**, *12*, 2396. Toan, T.; Broach, R. W.; Gardner, S. A.; Rausch, M. D.; Dahl, L. F. *Inorg. Chem.* **1977**, *16*, 279.

(4) Sakurai, H.; Hayashi, J. *J. Organomet. Chem.* **1972**, *39*, 365; **1974**, *70*, 85.

0276-7333/86/2305-0394$01.50/0

crystallographic site symmetry is $2/m$; O(3) and O(3b) define the two fold rotational axis and O(2), C(2), Mo, As(2), and C(4) define the mirror plane. The structure of **1** contains a 12-membered ring of alternating CH_3As groups and oxygen atoms; these 12 atoms form a flattened cuboctahedron which is trans bicapped by $Mo(CO)_3$ groups. The As–O ring configuration and the crystallographic symmetry require a coplanar arrangement for the six oxygen atoms which is sandwiched between two planes of three As atoms each. These exterior planes or arsenic atoms are positioned to form *fac*-$Mo(CO)_3L_3$ coordination environments at the metal center. The average of the three Mo–As distances, 2.55(1) Å, compares closely to those found in known structures.[7] The average As–O distance, 1.791 (3) Å, is very similar to that found in other caged As(III)–O structures: As_4O_6 (**3**), 1.80 Å;[8] $As_4O_4(CH_2)_2$ (**4**), ⟨av⟩ 1.795(7);[9] and $As_3O_3[(CH_2)_3CCH_3]$ (**5**) ⟨av⟩ 1.77 (1) Å.[10] The As–Mo–As angles are slightly obtuse, ⟨av⟩ 93.1°, and consistent with octahedral Mo geometry, while the C–Mo–C angles are slightly acute, ⟨av⟩ 87.2 (3)°. Whereas the O–As–O angles, ⟨av⟩ 101.0 (1)°, are very similar to As_4O_6, 100°, to **3**, 101.8 (4)°, and to **5**, 100.5°, the As–O–As angles in **1**, 118.1 (2) and 119.7 (2)°, are considerably smaller than in **3**, **4**, or **5**, which are in the range 126–129°. This decrease in the As–O–As angles has the effect of flattening the cubooctahedron and better positioning the six As atoms for metal coordination. Complex **1** is electron precise with a clearly definable 18e count at each metal center; each As(III) atom serves as a conventional 2e donor.

Our results suggest that the formation and stability of the *cyclo*-hexaarsaoxane ligand requires the presence of a stabilizing superstructure. The homoatomic cyclopentaarsine precursor to **1** reacts vigorously with dioxygen to form species of empirical formula CH_3AsO, but the route to **1** undoubtedly involves considerable metal-centered assistance in the organization of a 12-membered ring. Ellermann et al.[11] have recently reported a novel cryptand $[N(CH_2CH_2)_3]_8(As_4O_4)_6$ (**6**) containing an eight-membered alternating As–O ring in which each As atom is joined to two other As_4O_4 rings via $N(CH_2CH_2-)_3$ tripod bridge networks. The As–O bond distance (average 1.79 (5) Å and the As–O–As (average 118 (2)°) and O–As–O (average 101 (1)°) angles compare closely to those found in **1**. To date the known structures containing organoarsaoxane ring systems are either caged by organic linkages, **4**–**6**, or by metal carbonyl coordination, **1**, suggesting that such rings may prove to be very difficult to isolate without a superstructure. In fact, NMR studies[1] clearly indicate the cyclotrimers and tetramers of $(CH_3AsO)_n$ are involved in dynamic reorganization equilibria with higher cyclic and possibly linear species.

A complete discussion of the homocyclic decaarsine complex **2** will appear elsewhere.[12]

Acknowledgment. The National Science Foundation provided assistance in the purchase of the diffractometer. The Center for Catalytic Science and Technology at the University of Delaware provided support for the research.

Registry No. **1**, 99686-49-4; **2**, 99686-50-7; $Mo(CO)_6$, 13939-06-5; *cyclo*-$(AsCH_3)_5$, 20550-47-4.

Supplementary Material Available: Tables of atomic coordinates, a complete listing of bond distances and angles, anisotropic temperature factors, hydrogen atom coordinates, and observed and calculated structure factors (13 pages). Ordering information is given on any current masthead page.

(6) Crystal data for **1**, $C_{12}H_{18}As_6Mo_2O_{12}$: M_r = 995.7, orthorhombic, space group *Cmca*; a = 13.424 (2) Å, b = 16.909 (3) Å, c = 11.818 (2) Å, V = 2682.6 (7) Å, Z = 4, D_{calcd} = 2.47 g cm^{-3}, $F(000)$ = 1872, μ(Mo Kα) = 80.6 cm^{-1}. A pale yellow crystal (0.33 × 0.34 × 0.35 mm) was grown from CH_2Cl_2. Data were collected at 23 °C on a Nicolet R3 diffractometer. The structure was solved by direct methods and difference Fourier techniques. The 1605 symmetry-allowed reflections collected ($+h$, $+k$, $+l$; $4° \le 2\theta \le 50°$) were corrected for absorption; of these, 1309 with $F_o \ge 4\sigma(F_o)$ were used in refinement with anisotropic parameters for all non-hydrogen atoms. Hydrogen atom contributions were idealized and updated. At convergence R_F = 2.68%, R_{wF} = 2.94%, and GOF = 1.337 with a 13.4 data to parameter ratio.

(7) Rheingold, A. L.; Foley, M. J.; Sullivan, P. J. *J. Am. Chem. Soc.* **1982**, *104*, 4727.

(8) Bozorth, R. M. *J. Am. Chem. Soc.* **1923**, *45*, 1621.

(9) Kopf, J.; Von Denten, K.; Klar, G. *Inorg. Chim. Acta* **1980**, *37*, 67.

(10) Mckerley, B. J.; Reinhardt, K.; Mills, J. L.; Reisner, G. M.; Korp, J. D.; Bernal, I. *Inorg. Chim. Acta* **1978**, *31*, L411.

(11) Ellermann, J.; Veit, A.; Lindner, E.; Hoehne, S. *J. Organomet. Chem.* **1983**, *252*, 153.

(12) Rheingold, A. L.; DiMaio, A.-J.; Fountain, M. E., manuscript in preparation.

Stepwise Assembly of a Trinuclear Bis(carbyne) Complex from Cyclopentadienylcobalt Units and Bis(trimethylsilyl)acetylene: Isolation and Conversion of $Cp_2M_2(RC{\equiv}CR)$ and $(CpM)_3(RC{\equiv}CR)$ [M = Co and R = $(CH_3)_3Si$]

Bruce Eaton, Joseph M. O'Connor, and K. Peter C. Vollhardt*

Department of Chemistry
University of California at Berkeley
and the Materials and Molecular Research Division
Lawrence Berkeley Laboratory
Berkeley, California 94720

Received August 26, 1985

Summary: Reaction of $(\eta^5\text{-}C_5H_5)Co(C_2H_4)_2$ (**7**) with bis(trimethylsilyl)acetylene (btmsa) in THF at 23 °C gives $(\eta^5\text{-}C_5H_5)_2Co_2$(btmsa) (**9**). The structure of **9** was determined by X-ray crystallography, revealing the presence of a Co–Co double bond: 2.18 Å, to our knowledge the shortest cobalt–cobalt bond in existence. Complex **9** reacts further with **7** at 55 °C to produce $(\eta^5\text{-}C_5H_5)_3Co_3$(btmsa) (**10**). Complex **10** adds carbon monoxide to give $(\eta^5\text{-}C_5H_5)_3Co_3$(btmsa)(CO) (**11**). Both **10** and **11** are converted to $(\eta^5\text{-}C_5H_5)_3Co_3[\mu_3\text{-}\eta^1\text{-}CSi(CH_3)_3]_2$ (**6**) in boiling *m*-xylene or hot methylcyclohexane. A crossover experiment involving $(\eta^5\text{-}CH_3C_5H_4)_2Co_2$(btmsa) and **10** establishes the intramolecular nature of the rearrangement to **6**.

Mononuclear transition-metal complexes of the cobalt triad **1** react with alkynes to give trinuclear bis(carbyne) clusters **2** (Scheme I).[1-3] Among the alkyne substrates which have been examined in these reactions, bis(trimethylsilyl)acetylene (btmsa) exhibits anomalous behavior. Sakurai and Hayashi have reported that **1** (M = Co) converts to **3** in 93% yield in the presence of 2 equiv of btmsa in boiling xylene.[4] More recently, we reported that **1** (M

(1) (a) Fritch, J. R.; Vollhardt, K. P. C.; Thompson, M. R.; Day, V. W. *J. Am. Chem. Soc.* **1979**, *101*, 2768. (b) Fritch, J. R.; Vollhardt, K. P. C. *Angew. Chem., Int. Ed. Engl.* **1980**, *19*, 559. (c) Fritch, J. R.; Vollhardt, K. P. C. *Isr. J. Chem.*, in press and the references therein.

(2) Yamazaki, H.; Wakatsuki, Y.; Aoki, K. *Chem. Lett.* **1979**, 1041.

(3) Gardner, S. A.; Andrews, P. S.; Rausch, M. D. *Inorg. Chem.* **1973**, *12*, 2396. Toan, T.; Broach, R. W.; Gardner, S. A.; Rausch, M. D.; Dahl, L. F. *Inorg. Chem.* **1977**, *16*, 279.

(4) Sakurai, H.; Hayashi, J. *J. Organomet. Chem.* **1972**, *39*, 365; **1974**, *70*, 85.

0276-7333/86/2305-0394$01.50/0

Scheme I

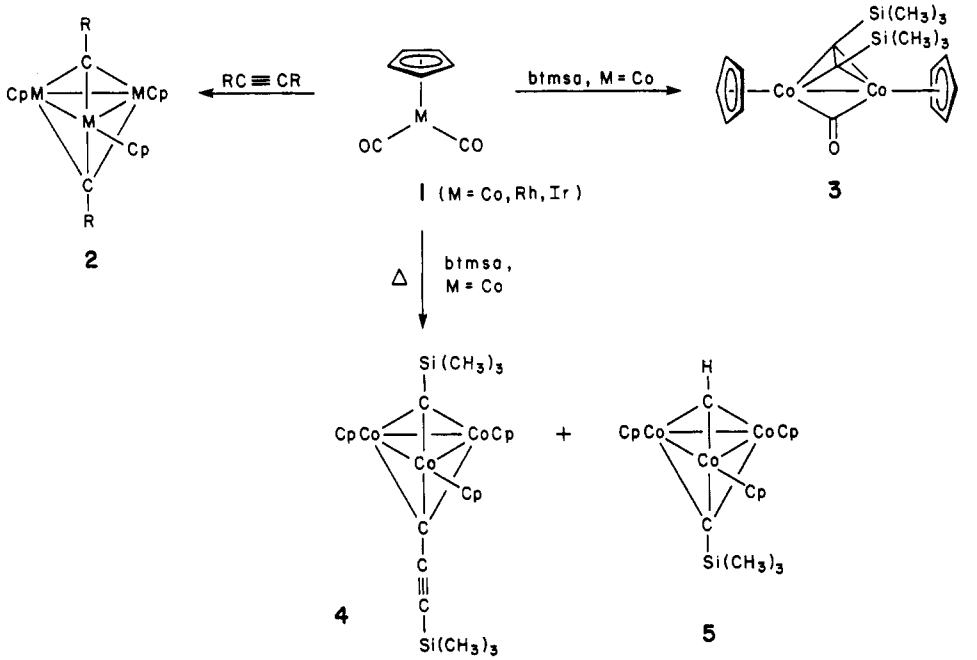

= Co) transforms in refluxing btmsa to produce very low yields of the bis(carbyne) clusters **4** and **5**, in addition to a number of mononuclear cobalt complexes and tetrakis(trimethylsilyl)butatriene.[3a,c] Significantly, none of the hitherto elusive bis[(trimethylsilyl)(carbyne]complex **6** was observed in these reactions.

Concerning the mechanism of bis(carbyne) cluster formation (**1** → **2**), a number of fundamental questions remain as to how the trinuclear core assembles and what the structural requirements are for alkyne bond cleavage.[5] Here we report the *stepwise* formation of a bis[(trimethylsilyl)carbyne] cluster, **6**, from the reaction of $(\eta^5\text{-}C_5H_5)Co(C_2H_4)_2$ (**7**) and btmsa. We further demonstrate that the presence of an additional ligand in cyclopentadienyl alkyne clusters of the cobalt triad is not a requirement for bis(carbyne) cluster generation. The presence of a carbonyl ligand in related systems has recently been suggested to reduce the barrier to alkyne cleavage.[5]

When $(\eta^5\text{-}C_5H_5)Co(C_2H_4)_2$[6] (**7**; 44 mg, 0.244 mmol, 0.39 M), and excess btmsa (0.73 mmol, 1.18 M) are dissolved in THF-d_8 and the solution freeze–pump–thaw–degassed five times, the ^{1}H NMR spectrum indicates a 1:5 ratio of **7** to a new compound (**8**, Scheme II) with chemical shifts at δ 4.59 (s, 5 H), 2.40 (half of an AA′BB′ pattern, 2 H), and 0.36 (s, 18 H).[7] A $^{13}C\{^1H\}$ NMR spectrum of the sample has resonances assigned to **8** at δ 98.46 [$C_2(Si(CH_3)_3]_2$], 84.16 (C_5H_5), 34.79 (C_2H_4), and 1.39 [$Si(CH_3)_3$].[8] On the basis of the NMR data, we formulate the structure of **8** as $(\eta^5\text{-}C_5H_5)Co(C_2H_4)[C_2(Si(CH_3)_3)_2]$. Attempts to isolate **8** by evaporation of the solvent (10^{-3} mmHg, 12 h) result in formation of an air-sensitive maroon solid, **9**. The mass spectrum and elemental analysis of **9** indicate a bimetallic formulation of composition $(C_5H_5)_2Co_2[C_2Si(CH_3)_3)_2]$.[9] A highly symmetrical structure for **9** is required by the ^{1}H NMR (benzene-d_6) spectrum, which has singlets at δ 4.22 (10 H) and 0.19 (18 H). An indication of the nature of its structure is provided by the extremely

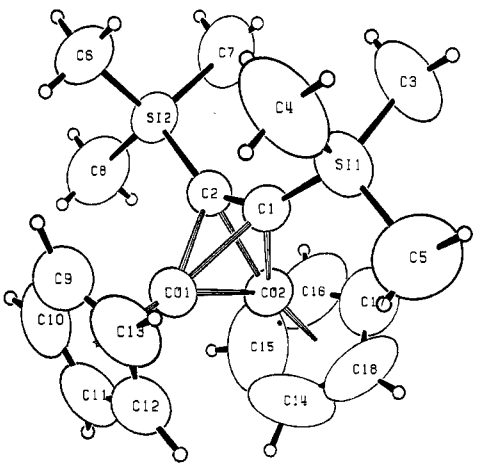

Figure 1. ORTEP drawing of **9**. Ellipsoids are scaled to represent the 50% probability surface.

(5) Clauss, A. D.; Shapley, J. R.; Wilker, C. N.; Hoffmann, R. *Organometallics* **1984**, *3*, 619. See also: Chi, Y.; Shapley, J. R. *Organometallics* **1985**, *4*, 1900.

(6) **7**: ^{1}H NMR (THF-d_8) δ 4.66 (s, 5 H), 2.56, 0.51 (AA′BB′, 8 H); ^{1}H NMR (benzene-d_6) δ 4.28 (s, 5 H), 2.53, 0.65 (AA′BB′, 8 H). Jonas, K.; Deffense, E.; Habermann, D. *Angew. Chem., Int. Ed. Engl.* **1983**, *22*, 716. *Angew. Chem. Suppl.* **1983**, 1005.

(7) The other half of the AA′BB′ pattern is presumably obscured by the large resonances for btmsa at δ 0.36 and 0.14. In addition to the resonances for **7** and **8**, a singlet is observed at δ 5.37 for uncomplexed ethene.

(8) Additional signals at δ 85.7 and 37.8 are assigned to **7**, signals at δ 114.0 and 0.19 to uncomplexed btmsa, and a signal at δ 123.5 is attributed to uncomplexed ethene.

(9) (a) **9**: mp (sealed capillary) 184–190 °C dec; ^{1}H NMR (benzene-d_6) δ 4.22 (s, 10 H), 0.19 (s, 18 H); $^{13}C\{^1H\}$ NMR (THF-d_8, −30 °C) δ 172.8, 84.9, 0.02; IR (THF) 1578 (s), 1244 (s) cm^{-1}; HRMS calcd for $C_{18}H_{28}Co_2Si_2$ 418.0394, found 418.0385. Compound **9** is best purified by sublimation (75% yield). (b) While this work was in progress, the reaction of **7** with btmsa to give $(\eta^5\text{-}C_5H_5)_2Co_2$(btmsa) of unspecified structure was briefly mentioned in a review article: Jonas, K. *Angew Chem., Int. Ed. Engl.* **1985**, *24*, 295. (c) All new isolated compounds gave satisfactory analytical and spectroscopic data.

(10) Crystal data: crystal size 0.23 × 0.30 × 0.30 mm, space group $P2_1/c$, a = 15.2917 (16) Å, b = 9.0636 (8) Å, c = 15.9110 (11) Å, V = 2190.8 (6) Å^3, μ_{calcd} = 16.2 cm^{-1}, d_{calcd} = 1.27 g cm^{-3}, Enraf-Nonius CAD-4 diffractometer, radiation Mo Kα (λ = 0.71073 Å), scan range 3° ≤ 2θ ≤ 45°, reflections collected 3195, unique 2179 with $F^2 > 3\sigma(F^2)$, R = 0.029, R_w = 0.0385. Inspection of the azimuthal scan data showed a variation I_{min}/I_{max} = 0.93 for the average curve. An empirical correction for absorption, based on the azimuthal scan data, was applied to the intensities.

Scheme II

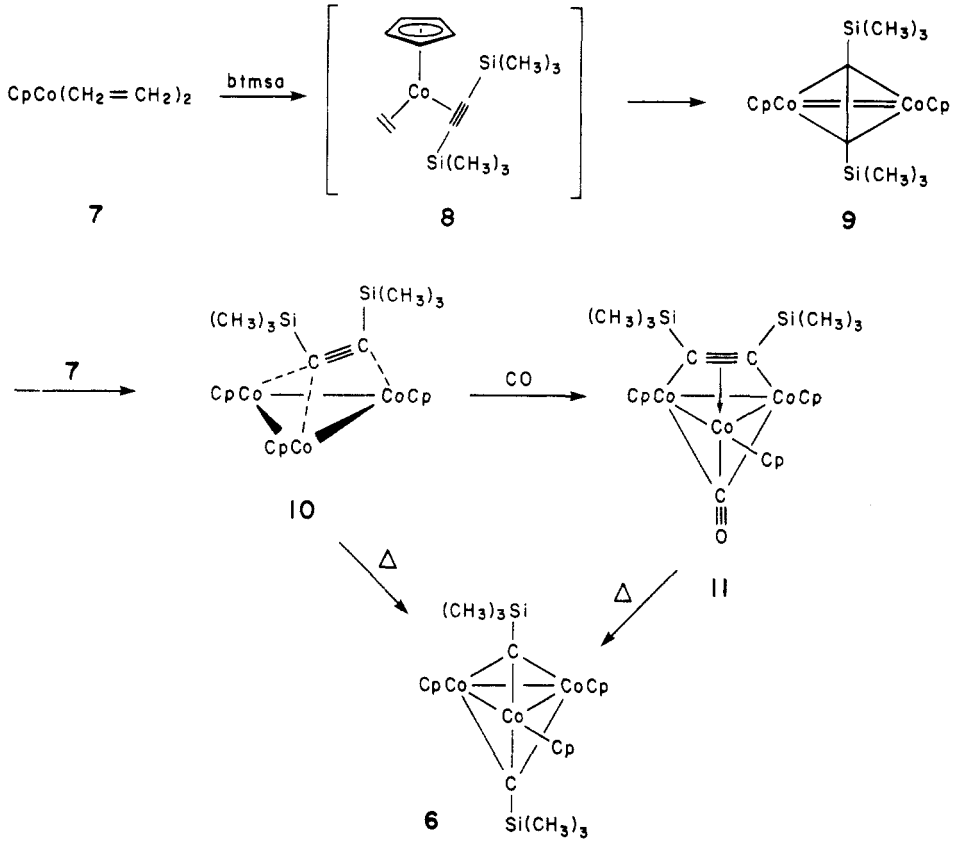

facile CO uptake (23 °C) to give **3**.[4]

In order to unambiguously determine the geometry of the btmsa ligand with respect to the cobalt–cobalt bond and because of the unusual features of this compound, an X-ray diffraction study was performed (Figure 1).[10] The structure consists of a bridging btmsa unit oriented perpendicular[11] to the cobalt–cobalt axis. The Co–Co bond length of 2.185 Å is consistent with the presence of a cobalt–cobalt double bond and is, to our knowledge, the shortest cobalt–cobalt distance hitherto measured.[12] The C1–C2 bond length (1.336 Å) is typical of a double bond.

When a diethyl ether solution of **9** (135 mg, 0.32 mmol, 0.16 M) and **7** (0.46 mmol, 0.02 M) is sealed in a vial under vacuum at −77 °C and heated at 55 °C for 33 h, a new trinuclear btmsa cluster, **10**,[9c,13] is formed in 70% isolated yield (chromatography, alumina II, 10% diethyl ether–hexane). The ^{1}H NMR (benzene-d_6) spectrum at 20 °C consists of a singlet at δ 4.18 (15 H), assigned to the protons of three equivalent C_5H_5 ligands, and a broad resonance at 0.27 (18 H), assigned to the protons of a fluxional btmsa. At 80 °C, these resonances are sharpened and shift to δ 2.99 (s, 15 H) and 0.02 (s, 18 H). The ^{1}H NMR (THF-d_8) spectrum of **10** at −90 °C consists of singlets at δ 5.20 (5 H) and 4.83 (10 H), which are assigned to the protons of a unique and two equivalent C_5H_5 ligands, respectively. Singlets are also observed at δ 1.03 (3 H), 0.62 (6 H), and −0.08 (9 H) and are attributed to the protons of two unique trimethylsilyl groups, *one of which exhibits hindered rotation about the sp-carbon–silicon bond.* To our knowledge, such behavior is unprecedented for a complexed (trimethylsilyl)alkyne and may have its cause in the coordinatively unsaturated nature of the cluster. The observation of nonequivalent trimethylsilyl units suggests an assignment of the btmsa ligand as perpendicular to one cobalt–cobalt bond in the frozen conformation. A crystal structure determination has been reported by Dahl for the isoelectronic alkyne cluster $Fe_3(CO)_9(Ph_2C_2)$.[14]

Exposure of THF solutions of **10** to carbon monoxide (1 atm) at 23 °C results in formation of a second btmsa cluster **11**[9c,15] (40% yield). Hexane solutions of **11** have a strong, sharp band in the IR spectrum at 1700 cm^{-1}, indicative of a triply bridging carbonyl ligand.[16] The ^{1}H NMR (acetone-d_6) spectrum has resonances at δ 4.02 (s, 15 H, C_5H_5) and 0.54 [s, 18 H, $Si(CH_3)_3$], which remain

(11) Hoffman, D. M.; Hoffman, R. *J. Chem. Soc., Dalton Trans.* **1982**, 1471.

(12) Compare the metal–metal bond lengths in $Co_2(CO)_6(C_2$-*t*-$Bu_2)$, 2.46 Å, $[\eta^5$-$C_5(CH_3)_5]_2Co_2(CO)_2$, 2.34 Å, $(\eta^5$-$C_5H_5)_2Fe_2(\mu$-$NO)_2$, 2.326 Å, and $Fe_2(CO)_6(C_2$*t*-$Bu_2)$, 2.316 Å. Cotton, F. A.; Jamerson, J. D.; Stults, B. R. *J. Am. Chem. Soc.* **1976**, *98*, 1774. Ginsburg, R. E.; Cirjak, L. M.; Dahl, L. F. *J. Chem. Soc., Chem. Commun.* **1979**, 468. Bailey, W. I.; Collins, D. M.; Cotton F. A.; Baldwin, J. C.; Kaska, W. C. *J. Organomet. Chem.* **1979**, *165*, 373. For related diiron compounds with two perpendicular bridging alkyne ligands (Fe–Fe ≈ 2.22 Å) see: Nicholas, K.; Bray, L. S.; Davis, R. E.; Pettit, R. *J. Chem. Soc., Chem. Commun.* **1971**, 608. Schmitt, H.-J.; Ziegler, M. L. *Z. Naturforsch., B: Anorg. Chem., Org. Chem.* **1973**, *28B*, 508.

(13) **10**: mp (sealed capillary) 212–215 °C; ^{1}H NMR (benzene-d_6, 20 °C) δ 4.18 (s, 15 H), 0.27 (br s, 18 H); ^{1}H NMR (benzene-d_6, 80 °C) δ 2.99 (s, 15 H), 0.02 (s, 18 H); ^{1}H NMR (THF-d_8, −100 °C) δ 5.20 (s, 5 H), 4.83 (s, 10 H), 1.03 (s, 3 H), 0.62 (s, 6 H), −0.08 (s, 9 H); ^{13}C{^{1}H} NMR (THF-d_8, −60 °C) δ 212.39, 80.49, 77.26, 5.76, 5.08, 3.86 (*only one of the sp carbons* was observed); ^{13}C{^{1}H} NMR (THF-d_8, 21 °C) δ 84.8, 4.25 (the sp carbons were not observed); IR (THF) 1242 cm^{-1}; HRMS calcd for $C_{23}H_{33}Co_3Si_2$ 542.0117, found 542.0103.

(14) Blount, J. F.; Dahl, L. F.; Hoogzand, C.; Hübel, W. *J. Am. Chem. Soc.* **1966**, *88*, 292.

(15) **11**: mp (sealed capillary) 295 °C dec; ^{1}H NMR(acetone-d_6) δ 4.02 (s, 15 H), 0.54 (s, 18 H); IR (hexane) 1700 cm^{-1}; HRMS calcd for $Co_3Si_2C_{24}H_{33}O$ 570.0066, found 570.0071.

(16) For comparison $(\eta^5$-$C_5H_5)_3Rh_3(CO)(Ph_2C_2)$ has bands at 1693 (sh) and 1678 (s) cm^{-1},[5] $(\eta^5$-$C_5H_5)_3Ir_3(CO)(Ph_2C_2)$ at 1736 (s) cm^{-1},[5] and $(\eta^5$-$C_5H_5)_3Co_3(CO)(C_2(CF_3)_2)$ at 1698 cm^{-1}.[17]

(17) Freeman, M. B.; Hall, L. W.; Sneddon, L. G. *Inorg. Chem.* **1980**, *19*, 1132.

(18) **6**: mp 246–248 °C; ^{1}H NMR (benzene-d_6) δ 4.44 (s, 15 H), 0.79 (s, 18 H); ^{13}C{^{1}H}NMR (THF-d_8, −60 °C) δ 363.2, 83.2, 4.25; mp 246–248 °C; HRMS calcd for $C_{23}H_{33}Co_3Si_2$ 542.0177, found 542.0103.

sharp even at −88 °C. Thus, the addition of a triply bridging carbonyl ligand to **10** greatly reduces the barrier to alkyne rotation on the face of the trinuclear core.

When a *m*-xylene solution of **10** is heated under nitrogen for 36 h, followed by evaporation of the volatiles and chromatography of the residue, a pink, air-stable, crystalline solid **6** is isolated in 69% yield.[9c,18] The ^{1}H NMR (acetone-d_6) spectrum has singlets at δ 4.56 (15 H, C_5H_5) and 0.82 [18 H, $Si(CH_3)_3$], and the $^{13}C\{^1H\}$ NMR (THF-d_8, −60 °C) spectrum has a resonance at δ 363 assigned to the carbyne carbon.[1] Similarly, when **11** is heated in *m*-xylene at reflux for 36 h and the volatiles are evaporated, a ^{1}H NMR (benzene-d_6) spectrum of the residue indicates a 2:1 ratio of **3** to **6** (35% isolated yield of **6**).

The reactions of **10** and **11** to give **6** are particularly interesting in light of a recent report that $(\eta^5\text{-}C_5H_5)_3M_3(CO)(C_2Ph_2)$ [M = Rh, Ir] are converted to $(\eta^5\text{-}C_5H_5)_3M_3(CPh)_2$ with no evidence for an unsaturated $Cp_3M_3(C_2Ph_2)$ species.[5] On the basis of the experimental data and a theoretical analysis for the corresponding reaction of $(\eta^5\text{-}C_5H_5)_3M_3(C_2H_2)(CO)$, an unsaturated alkyne intermediate, $(\eta^5\text{-}C_5H_5)_3M_3(C_2R_2)$, was discounted. The proposed mechanism invoked an edge-bonded alkyne which underwent a carbonyl shift (μ_3 to terminal) concerted with alkyne cleavage.

In order to rule out the intervention of an arene complex in facilitating the conversion of **10** to **6**, the same reaction was carried out in methylcyclohexane, providing the product at the *same* rate. To provide proof for the intramolecularity of this transformation and to rule out reversible dissociation of $\eta^5\text{-}C_5H_5Co$ from **10**, formation $(\eta^5\text{-}C_5H_5)_2Co_2(\mu\text{-}CR)_2$ and reassociation to furnish **6** (as suggested by a reviewer) a crossover experiment was performed. Thus, heating **10** in the presence of $(\eta^5\text{-}CH_3C_5H_4)_2Co_2(btmsa)$[9c,19] gave **6** and the unchanged labeled dinuclear cluster without any sign of crossover.

In conclusion, we now have evidence for the sequential conversion of a mononuclear cobalt precursor **7** to mononuclear **8**, dinuclear **9**, and trinuclear alkyne **10** complexes, with ultimate formation of a trinuclear bis(carbyne), **6**. The entire process represents the first well-characterized case of alkyne-mediated assembly of a trinuclear bis(carbyne). In addition, we have demonstrated that the presence of an additional ligand in trinuclear cyclopentadienylcobalt is not a requirement for alkyne scission.

Acknowledgment. The crystal structure analysis was carried out by Dr. F. J. Hollander, staff crystallographer at the U.C. Berkeley, Department of Chemistry X-ray facility (CHEXRAY). This work was supported by NSF-CHE 8504987. K. Peter C. Vollhardt is a Miller Professor in Residence (1985–1986).

Supplementary Material Available: A listing of positional and thermal parameters and tables of bond lengths, bond angles, and structure factors of **9** (22 pages). Ordering information is given on any current masthead page.

(19) Made in a manner analogous to **9** via $(\eta^5\text{-}CH_3C_5H_4)Co(C_2H_4)_2$ [^{1}H NMR (benzene-d_6) δ 4.56 (dd, J = 1.9, 1.8 Hz, 2 H), 4.11 (dd, J = 1.8, 1.6 Hz, 2 H), 2.42, 0.79 (AA'BB', 8 H), 1.26 (s, 3 H); ^{13}C NMR (benzene-d_6) δ 96.40, 86.13, 84.56, 39.21, 11.88] by treatment with btmsa to give $(\eta^5\text{-}CH_3C_5H_4)_2Co_2$ (btmsa) [^{1}H NMR (THF-d_8) δ 4.58 (dd, J = 1.9, 1.8 Hz, 4 H), 3.89 (dd, J = 1.8, 1.7 Hz, 4 H), 1.84 (s, 6 H), 0.27 (s, 18 H)].

Metathesis-Like Reaction of a Tungsten Alkylidyne Complex with Cyclohexyl Isocyanate[1]

Karin Weiss,*† Ulrich Schubert,‡ and Richard R. Schrock§

Laboratorium für Anorganische Chemie der Universität Bayreuth, Postfach 3008 8580 Bayreuth, West Germany, Institut für Anorganische Chemie der Universität Würzburg, Am Hubland 8700 Würzburg, West Germany, and Department of Chemistry, Room 6-331 Massachusetts Institute of Technology Cambridge, Massachusetts 02139

Received August 5, 1985

Summary: The reaction between W(C-*t*-Bu)(1,2-dimethoxyethane)Cl_3 and cyclohexyl isocyanate is proposed to yield an intermediate containing a cyclohexylimido and a ketenyl ligand. A second cyclohexyl isocyanate then inserts into the tungsten–carbon single bond of the ketenyl ligand to form an oxazetin tungstenacycle. Crystals of the final product are monoclinic with a = 9.311 (9) Å, b = 16.60 (2) Å, c = 14.91 (1) Å, β = 100.26 (7)°, V = 2268.1 Å^3, space group $P2_1/c$, Z = 4, and d(calcd) = 1.79 g/cm^3.

Reactions between carbyne or alkylidyne complexes and organic compounds containing a double bond are rare. Two examples are addition reactions of heterocumulenes like SO_2[2] to carbyne complexes prepared by Roper and addition of CO_2[3] to Fischer-type carbyne complexes. We report here a metathesis-like reaction between cyclohexyl isocyanate and W(C-*t*-Bu)(dme)Cl_3 (dme = 1,2-dimethoxyethane). This reaction is one example of what is likely to be a class of reactions whose crucial feature is a metathesis-like or Wittig-like[4] reaction of the alkylidyne ligand.

Addition of 2 equiv of cyclohexyl isocyanate in dichloromethane at 0 °C to 224 mg of W(C-*t*-Bu)(dme)Cl_3[5] yields a deep red reaction mixture from which red crystals can be obtained (260 mg, 85% yield) upon addition of pentane.[6] An X-ray structural study[7] shows the product to be the molecule W(NCy)[N(Cy)C(O)C(CO) (*t*-Bu)]Cl_3 (**1**; Figure 1) containing three meridional chloride ligands, a cyclohexylimido ligand, and a bidentate, ketenyl-sub-

*Universität Bayreuth.
‡Universität Würzburg.
§Massachusetts Institute of Technology.

(1) Investigations of Polymerizations and Metathesis Reactions. 6. For Part 5 see: Weiss, K.; Krauss, H. L. *J. Catal.* **1984**, *88*, 424.
(2) Wright, A. H. Ph.D. Thesis, University of Auckland, 1983.
(3) Fischer, E. O.; Filippou, A. C.; Alt, H. G.; Thewalt, U. *Angew. Chem.* **1985**, *97*, 215; *Angew. Chem. Int. Ed. Engl.* **1985**, *24*, 203.
(4) See: Freudenberger, J. H.; Schrock, R. R.; following paper in this issue.
(5) Schrock, R. R.; Clark, D. N.; Sancho, J.; Wengrovius, J. H.; Rocklage, S. M.; Pedersen, S. F. *Organometallics* **1982**, *1*, 1645.
(6) Partial ^{13}C NMR: δ 184.8 and 183.5 (C=C=O and NC=*O*), 73.3 (=NCH), 61.4 (-N-CH), 50.5 (*C*=C=O). IR (cm^{-1}): 2110 (vs, C=C=O), 1605 (m, NCO), 1620 (m, NCO). Mass spectrum parent ion observed in the region m/e 610 with appropriate isotopic pattern.
(7) Crystals were grown from $CDCl_3$. A total of 2577 independent reflections ($2° \le 2\theta \le 48°$, Mo Kα radiation, Syntex $P2_1$ diffractometer) were used to solve the structure by the Patterson method (Syntex XTL). Empirical absorption, Lorentz, and polarization corrections were applied. Hydrogen positions were found by difference Fourier methods or were calculated according to ideal geometry. Full-matrix least-squares refinement with anisotropic thermal parameters for all non-hydrogen atoms (hydrogen parameters were not refined) led to R = 0.083 and R_w = 0.087 ($1/w = \sigma^2$), all structure factors included.

0276-7333/86/2305-0397$01.50/0

sharp even at −88 °C. Thus, the addition of a triply bridging carbonyl ligand to **10** greatly reduces the barrier to alkyne rotation on the face of the trinuclear core.

When a *m*-xylene solution of **10** is heated under nitrogen for 36 h, followed by evaporation of the volatiles and chromatography of the residue, a pink, air-stable, crystalline solid **6** is isolated in 69% yield.[9c,18] The ^{1}H NMR (acetone-d_6) spectrum has singlets at δ 4.56 (15 H, C_5H_5) and 0.82 [18 H, $Si(CH_3)_3$], and the $^{13}C\{^1H\}$ NMR (THF-d_8, −60 °C) spectrum has a resonance at δ 363 assigned to the carbyne carbon.[1] Similarly, when **11** is heated in *m*-xylene at reflux for 36 h and the volatiles are evaporated, a ^{1}H NMR (benzene-d_6) spectrum of the residue indicates a 2:1 ratio of **3** to **6** (35% isolated yield of **6**).

The reactions of **10** and **11** to give **6** are particularly interesting in light of a recent report that $(\eta^5\text{-}C_5H_5)_3M_3(CO)(C_2Ph_2)$ [M = Rh, Ir] are converted to $(\eta^5\text{-}C_5H_5)_3M_3(CPh)_2$ with no evidence for an unsaturated $Cp_3M_3(C_2Ph_2)$ species.[5] On the basis of the experimental data and a theoretical analysis for the corresponding reaction of $(\eta^5\text{-}C_5H_5)_3M_3(C_2H_2)(CO)$, an unsaturated alkyne intermediate, $(\eta^5\text{-}C_5H_5)_3M_3(C_2R_2)$, was discounted. The proposed mechanism invoked an edge-bonded alkyne which underwent a carbonyl shift (μ_3 to terminal) concerted with alkyne cleavage.

In order to rule out the intervention of an arene complex in facilitating the conversion of **10** to **6**, the same reaction was carried out in methylcyclohexane, providing the product at the *same* rate. To provide proof for the intramolecularity of this transformation and to rule out reversible dissociation of $\eta^5\text{-}C_5H_5Co$ from **10**, formation $(\eta^5\text{-}C_5H_5)_2Co_2(\mu\text{-}CR)_2$ and reassociation to furnish **6** (as suggested by a reviewer) a crossover experiment was performed. Thus, heating **10** in the presence of $(\eta^5\text{-}CH_3C_5H_4)_2Co_2(btmsa)$[9c,19] gave **6** and the unchanged labeled dinuclear cluster without any sign of crossover.

In conclusion, we now have evidence for the sequential conversion of a mononuclear cobalt precursor **7** to mononuclear **8**, dinuclear **9**, and trinuclear alkyne **10** complexes, with ultimate formation of a trinuclear bis(carbyne), **6**. The entire process represents the first well-characterized case of alkyne-mediated assembly of a trinuclear bis(carbyne). In addition, we have demonstrated that the presence of an additional ligand in trinuclear cyclopentadienylcobalt is not a requirement for alkyne scission.

Acknowledgment. The crystal structure analysis was carried out by Dr. F. J. Hollander, staff crystallographer at the U.C. Berkeley, Department of Chemistry X-ray facility (CHEXRAY). This work was supported by NSF-CHE 8504987. K. Peter C. Vollhardt is a Miller Professor in Residence (1985–1986).

Supplementary Material Available: A listing of positional and thermal parameters and tables of bond lengths, bond angles, and structure factors of **9** (22 pages). Ordering information is given on any current masthead page.

(19) Made in a manner analogous to **9** via $(\eta^5\text{-}CH_3C_5H_4)Co(C_2H_4)_2$ [^{1}H NMR (benzene-d_6) δ 4.56 (dd, J = 1.9, 1.8 Hz, 2 H), 4.11 (dd, J = 1.8, 1.6 Hz, 2 H), 2.42, 0.79 (AA'BB', 8 H), 1.26 (s, 3 H); ^{13}C NMR (benzene-d_6) δ 96.40, 86.13, 84.56, 39.21, 11.88] by treatment with btmsa to give $(\eta^5\text{-}CH_3C_5H_4)_2Co_2$ (btmsa) [^{1}H NMR (THF-d_8) δ 4.58 (dd, J = 1.9, 1.8 Hz, 4 H), 3.89 (dd, J = 1.8, 1.7 Hz, 4 H), 1.84 (s, 6 H), 0.27 (s, 18 H)].

Metathesis-Like Reaction of a Tungsten Alkylidyne Complex with Cyclohexyl Isocyanate[1]

Karin Weiss,*† Ulrich Schubert,‡ and Richard R. Schrock§

Laboratorium für Anorganische Chemie der Universität Bayreuth, Postfach 3008 8580 Bayreuth, West Germany, Institut für Anorganische Chemie der Universität Würzburg, Am Hubland 8700 Würzburg, West Germany, and Department of Chemistry, Room 6-331 Massachusetts Institute of Technology Cambridge, Massachusetts 02139

Received August 5, 1985

Summary: The reaction between W(C-*t*-Bu)(1,2-dimethoxyethane)Cl_3 and cyclohexyl isocyanate is proposed to yield an intermediate containing a cyclohexylimido and a ketenyl ligand. A second cyclohexyl isocyanate then inserts into the tungsten–carbon single bond of the ketenyl ligand to form an oxazetin tungstenacycle. Crystals of the final product are monoclinic with a = 9.311 (9) Å, b = 16.60 (2) Å, c = 14.91 (1) Å, β = 100.26 (7)°, V = 2268.1 Å^3, space group $P2_1/c$, Z = 4, and d(calcd) = 1.79 g/cm^3.

Reactions between carbyne or alkylidyne complexes and organic compounds containing a double bond are rare. Two examples are addition reactions of heterocumulenes like SO_2[2] to carbyne complexes prepared by Roper and addition of CO_2[3] to Fischer-type carbyne complexes. We report here a metathesis-like reaction between cyclohexyl isocyanate and W(C-*t*-Bu)(dme)Cl_3 (dme = 1,2-dimethoxyethane). This reaction is one example of what is likely to be a class of reactions whose crucial feature is a metathesis-like or Wittig-like[4] reaction of the alkylidyne ligand.

Addition of 2 equiv of cyclohexyl isocyanate in dichloromethane at 0 °C to 224 mg of W(C-*t*-Bu)(dme)Cl_3[5] yields a deep red reaction mixture from which red crystals can be obtained (260 mg, 85% yield) upon addition of pentane.[6] An X-ray structural study[7] shows the product to be the molecule W(NCy)[N(Cy)C(O)C(CO) (*t*-Bu)]Cl_3 (**1**; Figure 1) containing three meridional chloride ligands, a cyclohexylimido ligand, and a bidentate, ketenyl-sub-

*Universität Bayreuth.
‡Universität Würzburg.
§Massachusetts Institute of Technology.

(1) Investigations of Polymerizations and Metathesis Reactions. 6. For Part 5 see: Weiss, K.; Krauss, H. L. *J. Catal.* **1984**, *88*, 424.
(2) Wright, A. H. Ph.D. Thesis, University of Auckland, 1983.
(3) Fischer, E. O.; Filippou, A. C.; Alt, H. G.; Thewalt, U. *Angew. Chem.* **1985**, *97*, 215; *Angew. Chem. Int. Ed. Engl.* **1985**, *24*, 203.
(4) See: Freudenberger, J. H.; Schrock, R. R.; following paper in this issue.
(5) Schrock, R. R.; Clark, D. N.; Sancho, J.; Wengrovius, J. H.; Rocklage, S. M.; Pedersen, S. F. *Organometallics* **1982**, *1*, 1645.
(6) Partial ^{13}C NMR: δ 184.8 and 183.5 (C=C=O and NC=*O*), 73.3 (=NCH), 61.4 (-N-CH), 50.5 (*C*=C=O). IR (cm^{-1}): 2110 (vs, C=C=O), 1605 (m, NCO), 1620 (m, NCO). Mass spectrum parent ion observed in the region m/e 610 with appropriate isotopic pattern.
(7) Crystals were grown from $CDCl_3$. A total of 2577 independent reflections ($2° \le 2\theta \le 48°$, Mo Kα radiation, Syntex $P2_1$ diffractometer) were used to solve the structure by the Patterson method (Syntex XTL). Empirical absorption, Lorentz, and polarization corrections were applied. Hydrogen positions were found by difference Fourier methods or were calculated according to ideal geometry. Full-matrix least-squares refinement with anisotropic thermal parameters for all non-hydrogen atoms (hydrogen parameters were not refined) led to R = 0.083 and R_w = 0.087 ($1/w = \sigma^2$), all structure factors included.

0276-7333/86/2305-0397$01.50/0

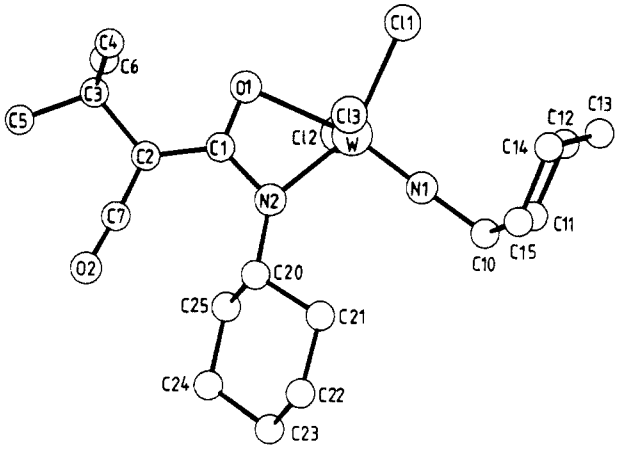

Figure 1. An ORTEP drawing of 1. Ellipsoid option and hydrogen atoms have been omitted for clarity.

Table I. Selected Bond Lengths (Å) and Angles (deg) for 1

	Bond Lengths (Å)		
W-C(11)	2.345 (4)	C(1)-O(1)	1.25 (2)
W-C(12)	2.330 (5)	C(1)-N(2)	1.37 (2)
W-C(13)	2.360 (5)	C(1)-C(2)	1.45 (2)
W-N(1)	1.667 (11)	C(2)-C(7)	1.32 (2)
W-N(2)	2.005 (13)	C(7)-O(2)	1.15 (2)
W-O(1)	2.237 (11)	N(1)-C(10)	1.50 (2)
		N(2)-C(20)	1.45 (2)
	Bond Angles		
C(11)-W-C(12)	88.2 (2)	N(2)-W-O(1)	62.0 (5)
C(11)-W-C(13)	86.0 (2)	N(2)-W-C(11)	152.4 (4)
C(12)-W-C(13)	167.6 (2)	W-N(1)-C(10)	177.6 (11)
N(1)-W-C(11)	102.4 (4)	W-O(1)-C(1)	88.7 (9)
N(1)-W-C(12)	96.7 (4)	W-N(2)-C(1)	95.6 (9)
N(1)-W-C(13)	95.3 (4)	W-N(2)-C(20)	139.6 (10)
N(1)-W-N(2)	104.9 (5)	N(2)-C(1)-O(1)	113.7 (13)
N(1)-W-O(1)	166.9 (5)	N(2)-C(1)-C(2)	127.2 (13)
O(1)-W-C(11)	90.6 (3)	C(2)-C(7)-O(2)	175.7 (19)
		C(1)-C(2)-C(7)	123.0 (15)

stituted acylamido ligand. The C(1), O(1), N(2), C(2), C(3), and C(7) atoms of the acylamido ligand lie in a plane, but the tungsten atom lies 0.373 (6) Å out of this plane. The W-N(1) distance (Table I) is comparable to that in other imido complexes.[8] The W-O(1) bond is distinctly longer than the W-N(2) bond, and the C(1)-O(1) bond significantly shorter than the C(1)-N(2) bond, suggesting that mesomeric form A is a better description than B.

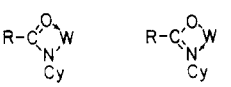

A B

Treatment of 1 with methanol at room temperature yields the malonic ester shown in eq 1, according to NMR, IR, and mass spectral characterization.[9]

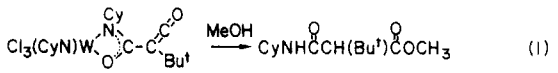

(1)

We propose that the first step in the reaction between W(C-*t*-Bu)(dme)Cl_3 and cyclohexyl isocyanate is that shown in eq 2. Metallacycles similar to the proposed tungsten azetin intermediate are formed in the reactions of SO_2[2] and CO_2[3] noted earlier. A second equivalent of cyclohexyl isocyanate then inserts into the tungsten-

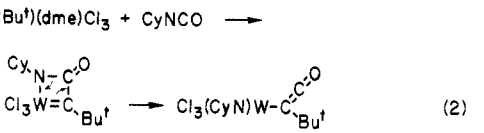

(2)

ketenyl bond to give the bidentate acylamido ligand. This type of insertion of isocyanates into metal-carbon bonds has been documented in reactions involving MMe_xCl_{5-x} (M = Nb, Ta; x = 1, 2[10]) and $TiCp_2$(alkyl)[11] species.

The reaction shown in eq 2 is likely to be one of a general class of reactions between high oxidation state alkylidyne complexes and heteroatomic double bonds. For example, preliminary results suggest that carbodiimides[12] react with W(C-*t*-Bu)(dme)Cl_3 in a manner analogous to that described here for cyclohexyl isocyanate. The results reported here should be compared with those involving reactions between W(VI) alkylidyne or tungstenacyclobutadiene complexes and the carbonyl functionality.[4]

Registry No. 1, 99605-36-4; W(C-*t*-Bu)(dMe)Cl_3, 83416-70-0; CyNHC(O)CH(*t*-Bu)C(o)OCH_3, 99605-37-5; CyNCO, 3173-53-3.

Supplementary Material Available: Listings of the final atomic parameters, observed and calculated structure factors, and anisotropic thermal parameters (17 pages). Ordering information is given on any current masthead page.

(8) (a) Weiher, U.; Dehnicke, K.; Fenske, D. *Z. Anorg. Allg. Chem.* **1979**, *457*, 105. (b) Nielson, A. J.; Waters, J. M. *Polyhedron* **1982**, *1*, 561.

(9) Partial ^{13}C NMR ($CDCl_3$): δ 173.1 and 169.8 (NC=O, OC=O), 63.2 (NCH), 507 (OCH_3). IR (cm^{-1}): 3290 (s, NH), 1745 (vs, OC=O), 1640 and 1545 (vs, HNC=O). Mass spectrum: m/e 255.

(10) Wilkins, J. D. *J. Organomet. Chem.* **1974**, *67*, 269.

(11) Klei, E.; Telgen, J. H.; Teuben, J. H. *J. Organomet. Chem.* **1981**, *209*, 297.

(12) Weiss, K.; unpublished results.

Wittig-Like Reactions of Tungsten Alkylidyne Complexes[1]

John H. Freudenberger and Richard R. Schrock*

Department of Chemistry, Room 6-331
Massachusetts Institute of Technology
Cambridge, Massachusetts 02139

Received September 6, 1985

Summary: W(C-*t*-Bu)(DIPP)$_3$ (DIPP = 2,6-diisopropylphenoxide) reacts rapidly with acetonitrile to give [W(N)(DIPP)$_3$]$_x$ and *t*-BuC≡CMe. It reacts with acetone, benzaldehyde, paraformaldehyde, ethyl formate, and *N*,*N*-dimethylformamide to give oxo vinyl complexes of the type W(O)(*t*-BuC=CR_1R_2)(DIPP)$_3$. The tungstenacyclobutadiene complex W(C_3Et_3)(DIPP)$_3$ reacts similarly with acetone, benzaldehyde, ethyl formate and *N*,*N*-dimethylformamide to give complexes of the type W(O)(EtC=CR_1R_2)(DIPP)$_3$. The oxo vinyl complexes can be hydrolyzed by base to yield the expected olefinic product in good to excellent yield. The olefin product is mainly the cis isomer in most cases.

Tantalum and niobium neopentylidene complexes[2] and an incipient titanium methylene complex[3] are known to react with the carbonyl function in a Wittig-like manner, not only with aldehydes and ketones but also with esters and amides. Recently, similar reactions with various zir-

(1) Multiple Metal-Carbon Bonds. 41. For part 40 see: Strutz, H.; Dewan, J. C.; Schrock, R. R. *J. Am. Chem. Soc.* **1985**, *107*, 5999.

(2) Schrock, R. R. *J. Am. Chem. Soc.* **1976**, *98*, 5399.

(3) (a) Tebbe, F. N.; Parshall, G. W.; Reddy, G. S. *J. Am. Chem. Soc.* **1977**, *100*, 3611. (b) Pine, S. H.; Zahler, R.; Evans, D. A.; Grubbs, R. H. *Ibid.* **1980**, *102*, 3270.

0276-7333/86/2305-0398$01.50/0

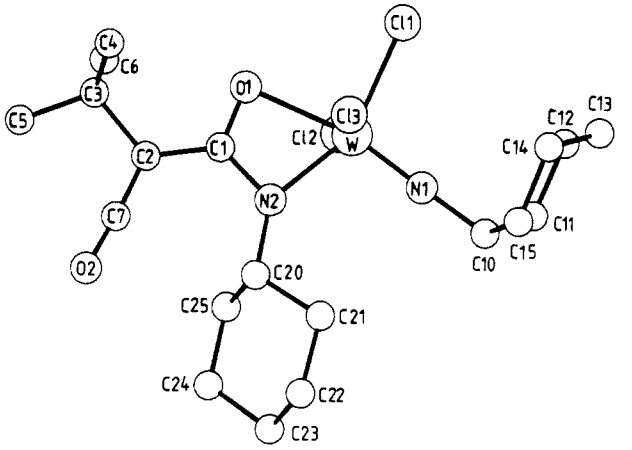

Figure 1. An ORTEP drawing of 1. Ellipsoid option and hydrogen atoms have been omitted for clarity.

Table I. Selected Bond Lengths (Å) and Angles (deg) for 1

	Bond Lengths (Å)		
W-C(11)	2.345 (4)	C(1)-O(1)	1.25 (2)
W-C(12)	2.330 (5)	C(1)-N(2)	1.37 (2)
W-C(13)	2.360 (5)	C(1)-C(2)	1.45 (2)
W-N(1)	1.667 (11)	C(2)-C(7)	1.32 (2)
W-N(2)	2.005 (13)	C(7)-O(2)	1.15 (2)
W-O(1)	2.237 (11)	N(1)-C(10)	1.50 (2)
		N(2)-C(20)	1.45 (2)
	Bond Angles		
C(11)-W-C(12)	88.2 (2)	N(2)-W-O(1)	62.0 (5)
C(11)-W-C(13)	86.0 (2)	N(2)-W-C(11)	152.4 (4)
C(12)-W-C(13)	167.6 (2)	W-N(1)-C(10)	177.6 (11)
N(1)-W-C(11)	102.4 (4)	W-O(1)-C(1)	88.7 (9)
N(1)-W-C(12)	96.7 (4)	W-N(2)-C(1)	95.6 (9)
N(1)-W-C(13)	95.3 (4)	W-N(2)-C(20)	139.6 (10)
N(1)-W-N(2)	104.9 (5)	N(2)-C(1)-O(1)	113.7 (13)
N(1)-W-O(1)	166.9 (5)	N(2)-C(1)-C(2)	127.2 (13)
O(1)-W-C(11)	90.6 (3)	C(2)-C(7)-O(2)	175.7 (19)
		C(1)-C(2)-C(7)	123.0 (15)

stituted acylamido ligand. The C(1), O(1), N(2), C(2), C(3), and C(7) atoms of the acylamido ligand lie in a plane, but the tungsten atom lies 0.373 (6) Å out of this plane. The W-N(1) distance (Table I) is comparable to that in other imido complexes.[8] The W-O(1) bond is distinctly longer than the W-N(2) bond, and the C(1)-O(1) bond significantly shorter than the C(1)-N(2) bond, suggesting that mesomeric form A is a better description than B.

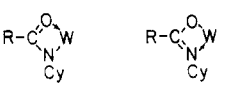

A B

Treatment of 1 with methanol at room temperature yields the malonic ester shown in eq 1, according to NMR, IR, and mass spectral characterization.[9]

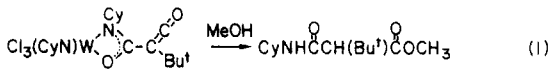

(1)

We propose that the first step in the reaction between W(C-*t*-Bu)(dme)Cl_3 and cyclohexyl isocyanate is that shown in eq 2. Metallacycles similar to the proposed tungsten azetin intermediate are formed in the reactions of SO_2[2] and CO_2[3] noted earlier. A second equivalent of cyclohexyl isocyanate then inserts into the tungsten-

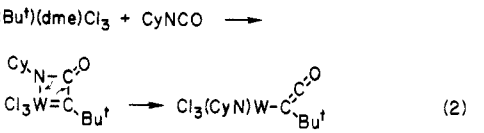

(2)

ketenyl bond to give the bidentate acylamido ligand. This type of insertion of isocyanates into metal-carbon bonds has been documented in reactions involving MMe_xCl_{5-x} (M = Nb, Ta; x = 1, 2[10]) and $TiCp_2$(alkyl)[11] species.

The reaction shown in eq 2 is likely to be one of a general class of reactions between high oxidation state alkylidyne complexes and heteroatomic double bonds. For example, preliminary results suggest that carbodiimides[12] react with W(C-*t*-Bu)(dme)Cl_3 in a manner analogous to that described here for cyclohexyl isocyanate. The results reported here should be compared with those involving reactions between W(VI) alkylidyne or tungstenacyclobutadiene complexes and the carbonyl functionality.[4]

Registry No. 1, 99605-36-4; W(C-*t*-Bu)(dMe)Cl_3, 83416-70-0; CyNHC(O)CH(*t*-Bu)C(o)OCH_3, 99605-37-5; CyNCO, 3173-53-3.

Supplementary Material Available: Listings of the final atomic parameters, observed and calculated structure factors, and anisotropic thermal parameters (17 pages). Ordering information is given on any current masthead page.

(8) (a) Weiher, U.; Dehnicke, K.; Fenske, D. *Z. Anorg. Allg. Chem.* **1979**, *457*, 105. (b) Nielson, A. J.; Waters, J. M. *Polyhedron* **1982**, *1*, 561.

(9) Partial ^{13}C NMR ($CDCl_3$): δ 173.1 and 169.8 (NC=O, OC=O), 63.2 (NCH), 507 (OCH_3). IR (cm^{-1}): 3290 (s, NH), 1745 (vs, OC=O), 1640 and 1545 (vs, HNC=O). Mass spectrum: m/e 255.

(10) Wilkins, J. D. *J. Organomet. Chem.* **1974**, *67*, 269.

(11) Klei, E.; Telgen, J. H.; Teuben, J. H. *J. Organomet. Chem.* **1981**, *209*, 297.

(12) Weiss, K.; unpublished results.

Wittig-Like Reactions of Tungsten Alkylidyne Complexes[1]

John H. Freudenberger and Richard R. Schrock*

Department of Chemistry, Room 6-331
Massachusetts Institute of Technology
Cambridge, Massachusetts 02139

Received September 6, 1985

Summary: W(C-*t*-Bu)(DIPP)$_3$ (DIPP = 2,6-diisopropylphenoxide) reacts rapidly with acetonitrile to give [W(N)(DIPP)$_3$]$_x$ and *t*-BuC≡CMe. It reacts with acetone, benzaldehyde, paraformaldehyde, ethyl formate, and *N*,*N*-dimethylformamide to give oxo vinyl complexes of the type W(O)(*t*-BuC=CR_1R_2)(DIPP)$_3$. The tungstenacyclobutadiene complex W(C_3Et_3)(DIPP)$_3$ reacts similarly with acetone, benzaldehyde, ethyl formate and *N*,*N*-dimethylformamide to give complexes of the type W(O)(EtC=CR_1R_2)(DIPP)$_3$. The oxo vinyl complexes can be hydrolyzed by base to yield the expected olefinic product in good to excellent yield. The olefin product is mainly the cis isomer in most cases.

Tantalum and niobium neopentylidene complexes[2] and an incipient titanium methylene complex[3] are known to react with the carbonyl function in a Wittig-like manner, not only with aldehydes and ketones but also with esters and amides. Recently, similar reactions with various zir-

(1) Multiple Metal-Carbon Bonds. 41. For part 40 see: Strutz, H.; Dewan, J. C.; Schrock, R. R. *J. Am. Chem. Soc.* **1985**, *107*, 5999.

(2) Schrock, R. R. *J. Am. Chem. Soc.* **1976**, *98*, 5399.

(3) (a) Tebbe, F. N.; Parshall, G. W.; Reddy, G. S. *J. Am. Chem. Soc.* **1977**, *100*, 3611. (b) Pine, S. H.; Zahler, R.; Evans, D. A.; Grubbs, R. H. *Ibid.* **1980**, *102*, 3270.

0276-7333/86/2305-0398$01.50/0

Table I. Preparation and Hydrolysis of Oxo Vinyl Complexes W(O)(vinyl)(O-2,6-C_6H_3-*i*-Pr_2)$_3$

R in W(CR)(DIPP)$_3$	carbonyl	isol yield,[a] %	isomers[b]	hydrolysis products[c]	yield, %
t-Bu	Me_2CO	81	3:1 (rot)	Me_2C=CH-*t*-Bu (i)	99[d]
t-Bu	CH_2O	77	none	H_2C=CH-*t*-Bu (i)	85[d]
t-Bu	PhCHO		1:4 (cis:trans)	PhHC=CH-*t*-Bu (c) (1:4; cis:trans)	95[d]
t-Bu	EtOCHO	82	none	*cis*-(EtO)HC=CH-*t*-Bu (i or c)	60[e,g]
t-Bu	Me_2NCHO	78	3:2[f]	Me_2NHC=CH-*t*-Bu (i or c)	60[e,h]
Et	Me_2CO	78	2:1 (−45°; rot)	Me_2C=CHEt (i)	97[d]
Et	PhCHO	80	none	*cis*-PhHC=CHEt (i or c)	82[d]
Et	EtOCHO	~40	none	*cis*-(EtO)HC=CHEt (i)	~30[e,i]
Et	Me_2NCHO	77	none	Me_2NHC=CH-*t*-Bu (i or c)	75[e,h]

[a] C and H analyses for the eight isolated products are satisfactory. [b] Ratio of rotomers (rot) or geometric (cis, trans) isomers at 25 °C, unless otherwise noted. "None" implies that there are no geometric isomers and that any rotomers interconvert rapidly on NMR time scale at 25 °C. [c] Hydrolysis of isolated (i) or crude (c) samples was effected by shaking samples dissolved in ether, toluene, or C_6D_6 with ~1 N aqueous KOH until the sample was essentially colorless (5–15 min). Stereochemistries were assigned according to ^{1}H NMR spectra. [d] By GLC vs. internal standard. [e] By ^{1}H NMR integration vs. DIPPH (assuming 3.0 equiv). [f] It is unknown at present whether these are rotational or geometric isomers. [g] Hydrolysis of crude product in C_6D_6 yields 67% (EtO)HC=CH-*t*-Bu as a 14:1 mixture of cis and trans isomers along with a 19% yield of *t*-BuCH_2CHO, presumably the result of hydrolysis of (EtO)HC=CH-*t*-Bu during workup. Yields using isolated, crystalline product are 60% pure *cis*-(EtO)HC=CH-*t*-Bu and 33% *t*-BuCH_2CHO. [h] Stereochemistry could not be assigned due to formation of the iminium ion in the presence of DIPPH. [i] The products consist of 30% pure *cis*-(EtO)HC=CHEt and 41% PrCHO.

conium complexes have been successful.[4] For some time we have been looking for Wittig-like reactions of d^0 alkylidyne complexes, since the metal–carbon triple bond in such species is also thought to be polarized M^+C^-.[5] We report several such reactions here for tungsten complexes containing the 2,6-diisopropylphenoxide (DIPP) ligand.

W(C-*t*-Bu)(DIPP)$_3$[6] in ether or toluene reacts immediately with acetonitrile to give *t*-BuC≡CMe quantitatively and a red, insoluble, air-stable complex that analyzes as W(N)(DIPP)$_3$. We propose that it is a polymer with linear W≡N→W chains analogous to [W(N)(O-*t*-Bu)$_3$]$_x$.[7] By analogy with tungstenacyclobutadiene intermediates in acetylene metathesis,[6] we believe the intermediate in the reaction to be an azatungstenacyclobutadiene complex (eq 1). The reaction between W(C-*t*-Bu)(DIPP)$_3$ and *t*-

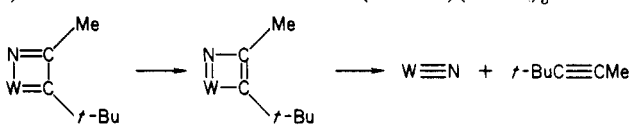

(1)

$BuCH_2CN$ produces a monoadduct that can be crystallized from pentane at −40 °C and that decomposes over a period of several hours at 25 °C to give large, well-formed crystals of [W(N)(DIPP)$_3$]$_x$.

W(C-*t*-Bu)(DIPP)$_3$ in ether reacts immediately with acetone to give an orange-red crystalline product in high yield. IR, ^{1}H NMR, and ^{13}C NMR data are all consistent with the product being an oxo vinyl species, i.e., W(O)(*t*-BuC=CMe_2)(DIPP)$_3$.[8a] Two isomers are observed at 25 °C in a ratio of ~3:1. We propose that the structure of W(O)(*t*-BuC=CMe_2)(DIPP)$_3$ is either a trigonal bipyramid with the oxo and vinyl ligands in the equatorial plane or a related square pyramid with the oxo ligand in the apical position. (The structure of W(C_3Et_3)(DIPP)$_3$ is actually somewhere between TBP and SP.[6]) The vinyl ligand probably lies in the same plane as the W=O bond, perhaps primarily for steric rather than electronic reasons (see below), and the isomers therefore arise due to restricted rotation about the W–C bond (eq 2). W(O)(*t*-BuC=CMe_2)(DIPP)$_3$ can be hydrolyzed with aqueous 1 N KOH in 15 min to give *t*-BuHC=CMe_2 in high yield along with free DIPPH (Table I).

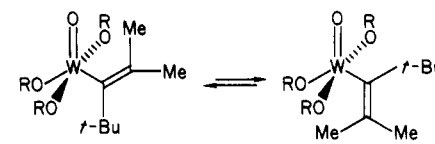

(2)

W(C-*t*-Bu)(DIPP)$_3$ reacts with benzaldehyde, paraformaldehyde, ethyl formate, and *N,N*-dimethylformamide to give analogous oxo vinyl species in high yield.[8b] The slowest reaction is with DMF. In fact, an adduct is first observed[9] which upon being heated in toluene to 50 °C overnight yields dark red prisms of the oxo vinyl product. Geometric isomers of the oxo vinyl product of the reaction with benzaldehyde are observed; hydrolysis yields a mixture consisting largely of the trans olefin product.

The tungstenacyclobutadiene complex W(C_3Et_3)(DIPP)$_3$ also reacts with acetone, benzaldehyde, ethyl formate, and DMF to give complexes of the type W(O)(vinyl)(DIPP)$_3$. The rate of the reaction is limited in this case by the apparently required loss of 3-hexyne from the tungstenacyclobutadiene ring[6] to give intermediate W(CEt)(DIPP)$_3$ ($k \simeq 4 \times 10^{-4}$ s^{-1}; $t_{1/2} \simeq 30$ min). For example, the reaction with 1 equiv of acetone requires ~3 h to go to completion at 25 °C. The reaction between W(C_3Et_3)(DIPP)$_3$ and paraformaldehyde fails at 25 °C, probably because the concentration of formaldehyde is too low to compete with 3-hexyne for incipient W(CEt)(DIPP)$_3$. Ten equivalents of ethyl formate are required for the reaction to be com-

(4) (a) Clift, S. M.; Schwartz, J. *J. Am. Chem. Soc.* **1984**, *106*, 8300. (b) Hartner, F. W., Jr.; Schwartz, J.; Clift, S. M. *Ibid.* **1983**, *105*, 640.
(5) Listemann, M. L.; Schrock, R. R. *Organometallics* **1985**, *4*, 74.
(6) Churchill, M. R.; Ziller, J. W.; Freudenberger, J. H.; Schrock, R. R. *Organometallics* **1984**, *3*, 1554.
(7) Chisholm, M. H.; Hoffman, D. M.; Huffman, J. C. *Inorg. Chem.* **1983**, *22*, 2903.
(8) (a) $\nu_{WO} \simeq 975$ cm^{-1} (Nujol). Two, presumably C_α, vinylic carbon atom signals in the two isomers are found at 208.2 and 207.2 ppm in a ratio of ~1:3. (b) All oxo vinyl compounds exhibit a ν_{WO} band at 975–945 cm^{-1} and C_α resonances in the range of ~180–220 ppm. C_β resonances were found only for vinyl complexes containing an H_β in the range 114–129 ppm (J_{CH} = 159–153 Hz) for those containing alkyl groups and 140–170 ppm ($J_{CH} \simeq$ 160–178 Hz) for O- or N-substituted derivatives. The ^{1}H and ^{13}C NMR spectra of W(O)(C-*t*-Bu=CH_2)(DIPP)$_3$ will illustrate: ^{1}H NMR (C_6D_6) δ 7.02 (d, 6, ^3J = 7.5 Hz, H_m), 6.84 (t, 3, ^3J = 7.5 Hz, H_p), 6.65 (d, 1, ^2J = 3.1 Hz, C-*t*-Bu=C$H_A$$H_B$), 6.14 (d, 1, ^2J = 3.1 Hz, C-*t*-Bu=CH$_A$$H_B$), 3.73 (m, 6, C$HMe_2$), 1.20 (s, 9, C-*t*-Bu=CH$_A$H$_B$), 1.22, 1.17, and 1.12 (all d, 12, ^3J = 6.8 Hz, CHMe_2); ^{13}C NMR (C_6D_6) δ 213.4 (s, C_α), 158.4 (C_{ipso}), 158.1 (s, C_{ipso}), 140.3 (s, C_o), 137.9 (s, C_o), 124.9, 123.9, 123.5 (all d, J_{CH} = 156–160 Hz, C_m and C_p), 114.0 (dd, J_{CH} = 153 and 159 Hz, C_β), 41.0 (s, CMe_3), 30.8 (q, J_{CH} = 126 Hz, CMe_3), 27.4, 27.2 (both d, J_{CH} = 128 Hz, $CHMe_2$), 24.5, 24.2, and 23.5 (all q, J_{CH} = 124–126 Hz, CHMe_2).

(9) W(CCMe$_3$)(DIPP)$_3$(DMF): ^{1}H NMR (C_6D_6) δ 7.60 (s, 1, Me_2NCHO), 7.16 (d, 6, H_m), 6.92 (t, 3, H_p), 4.09 (hept, 6, J = 6.8 Hz, $CHMe_2$), 1.55 (s, 3, Me_AMe_BNCHO), 1.43 (s, 3, Me_AMe_BNCHO), 1.36 (d, 36, J = 6.8 Hz, CHMe_2), 1.00 (s, 9, CMe_3); ^{13}C NMR (C_6D_6) δ 292.4 (s, C_α), 168.7 (d, J_{CH} = 198 Hz, Me_2NCHO), 160 (br, s, C_{ipso}), 138.2 (s, C_o), 123.0 (d, J_{CH} = 155 Hz, C_m), 121.3 (d, J_{CH} = 160 Hz, C_p), 51.0 (s, CMe_3), 36.6 (q, J_{CH} = 140 Hz, $MeMe'NCHO$), 34.1 (q, CMe_3), 31.5 (q, J_{CH} = 140 Hz, $MeMe'NCHO$), 26.8 (d, J_{CH} = 129 Hz, $CHMe_2$), 24.0 (q, CHMe_2); IR (Nujol) ν_{CO} 1650 cm^{-1}.

plete in ~5 h, and the oxo vinyl complex is isolated in only poor yield (~40%) from pentane at -40 °C. The oxo vinyl complexes of the type W(O)(EtC=CRR')(DIPP)$_3$ differ from those of the type W(O)(*t*-BuC=CRR')(DIPP)$_3$ in that no rotational isomers are observed at 25 °C. Note also that in this case only one geometric isomer of the oxo vinyl product of the reaction with benzaldehyde is observed, and only the cis hydrolysis product is observed.

Reactions of W(CR)(DIPP)$_3$ (R = *t*-Bu or Et) with the carbonyl function are believed to involved nucleophilic attack on the Lewis acid activated carbonyl carbon atom by the alkylidyne carbon atom to give an oxytungstenacyclobutene intermediate which then rearranges to the oxo vinyl product (eq 3). The ring opening becomes stereoselective when R is not *tert*-butyl as a result of the larger of R_1 or R_2 being forced away from the crowded coordination sphere of the metal.

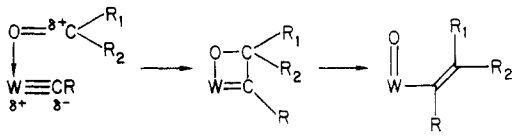

It is interesting to note that analogous reactions involving W(CR)(O-*t*-Bu)$_3$ either are considerably slower[10] or do not yield analogous oxo vinyl species at all.[11] We also know that acetyl chloride reacts with W(C-*t*-Bu)(DIPP)$_3$ to give an ~85% yield of *t*-BuC≡CMe and what appears to be a mixture of W(O)(DIPP)$_3$Cl and a small amount of W(O)(DIPP)$_4$. Further experiments will be required in order to establish the scope, generality, and selectivity of Wittig-like reactions involving complexes of the type W(CR)(OR')$_3$.

Acknowledgment. R.R.S. thanks the National Science Foundation for support (Grant CHE 84-02892).

Registry No. W(C-*t*-Bu)(DIPP)$_3$, 91229-76-4; *t*-BuC≡CMe, 999-78-0; W(N)(DIPP)$_3$, 99594-92-0; *t*-BuCH$_2$CN, 3302-16-7; W(O)(*t*-BuC=CMe$_2$)(DIPP)$_3$, 99594-93-1; W(O)(*t*-BuC=CH$_2$)(DIPP)$_3$, 99594-94-2; W(O)(*t*-BuC=CHPh)(DIPP)$_3$, 99594-95-3; W(O)(*t*-BuC=CHOEt)(DIPP)$_3$, 99594-96-4; W(O)(*t*-BuC=CH(NMe$_2$))(DIPP)$_3$, 99594-97-5; W(C$_3$Et$_3$)(DIPP)$_3$, 91229-77-5; W(O)(EtC=CMe$_2$)(DIPP)$_3$, 99594-98-6; W(O)(EtC=CHPh)(DIPP)$_3$, 99594-99-7; W(O)(EtC=CHOEt)(DIPP)$_3$, 99595-00-3; W(O)(EtC=CH(NMe$_2$))(DIPP)$_3$, 99595-01-4.

(10) W(C-*t*-Bu)(O-*t*-Bu)$_3$ does not react readily with acetonitrile at 25 °C, although W(CEt)(O-*t*-Bu)$_3$ will react with excess acetonitrile over a period of several minutes.

(11) The reaction between W(C-*t*-Bu)(O-*t*-Bu)$_3$ and acetone is sluggish. The reaction is complete after 16 h at 60 °C, but several products are observed.

A High-Resolution Solid-State ^{13}C NMR Study of Fe(C$_5$H$_5$)(CO)$_2$CH$_3$/Alumina Surface Chemistry

Paul J. Toscano and Tobin J. Marks*

Department of Chemistry, Northwestern University Evanston, Illinois 60201

Received September 17, 1985

Summary: ^{13}C CPMAS NMR spectroscopy has been employed to characterize surface reaction pathways involving the complexes CpFe(CO)$_2$CH$_3$, CpFe(^{13}CO)$_2$CH$_3$, CpFe(CO)$_2$(^{13}CH$_3$) (Cp = η^5-C$_5$H$_5$), and dehydroxylated (DA) or partially dehydroxylated (PDA) γ-alumina. A number of possible reaction modes can be ruled out, and surface-induced migratory CO insertion to yield a carbene-like acyl complex is identified as the predominant if not exclusive pathway.

Elucidating the structure(s) of adsorbates arising from the chemisorption of organometallic molecules on high surface area metal oxides (e.g., γ-alumina, silica)[1] is a challenging problem of considerable significance in catalysis.[1,2] Proposed surface reaction pathways include protonolysis of hydrocarbyl ligands by surface OH groups,[1,3] transfer of hydrocarbyl ligands to exposed Lewis acid sites,[4] substitution of carbonyl or other ligands by surface oxide (O^{2-}) or OH groups,[1a,c,5] coordination of carbonyl ligands by surface Lewis acid sites,[1a] nucleophilic addition of surface O^{2-} or OH groups to carbonyl ligands,[1a,c] oxidative addition of OH groups to metal-metal bonds,[1a,6] and a host of others.[1] These reaction pathways and the structures of the resulting organometallic molecule–surface complexes have largely been inferred from the nature of products evolved during the chemisorption process and/or, with varying degrees of definition, from surface spectroscopies (principally vibrational, but also Mössbauer, XPS, EPR, etc.). In many cases, these structural assignments are qualitative in nature and could be greatly strengthened by additional information.

In this communication, we illustrate the efficacy in such structural studies of high-resolution solid-state ^{13}C NMR spectroscopy, utilizing cross polarization (CP), high-power ^{1}H decoupling, and magic-angle spinning (MAS),[7,8] by characterizing for the first time the reaction pathways of a transition-metal carbonyl alkyl complex (selected isotopomers of CpFe(CO)$_2$CH$_3$, Cp = η^5-C$_5$H$_5$) with γ-alumina surfaces. This particular compound is of interest since it offers a multiplicity of potential surface transformations (vide supra), including surface-induced migratory CO insertion (A, inferred as a contributing pathway largely on

(1) (a) Basset, J. M.; Chaplin, A. *J. Mol. Catal.* **1983**, *21*, 95 and references therein. (b) Yermakov, Yu. I. *J. Mol. Catal.* **1983**, *21*, 35 and references therein. (c) Iwamoto, M.; Kusano, H.; Kagawa, S. *Inorg. Chem.* **1983**, *22*, 3365 and references therein. (d) Yermakov, Yu. I.; Kuznetsov, B. N.; Zakharov. V. A. "Catalysis by Supported Complexes"; Elsevier: Amsterdam, 1981. (e) Bailey, D. C.; Langer, S. H. *Chem. Rev.* **1981**, *81*, 109. (f) Ballard, D. G. H. *J. Polym. Sci., Polym. Chem. Ed.* **1975**, *13*, 2191-2212.

(2) (a) Firment, L. E. *J. Catal.* **1983**, *82*, 196-212 and references therein. (b) Gavens, P. D.; Bottrill, M.; Kelland, J. W.; McMeeking, J. In "Comprehensive Organometallic Chemistry"; Wilkinson, G., Stone, F. G. A., Abel, E. W., Eds.; Pergamon Press: Oxford, 1982; Chapter 22.5. (c) Galli, P.; Luciani, L.; Checchini, G. *Angew. Makromol. Chem.* **1981**, *94*, 63. (d) Karol, F. J.; Wu, C.; Reichle, W. T.; Maraschin, N. J. *J. Catal.* **1979**, *60*, 68.

(3) He, M.-Y.; Xiong, G.; Toscano, P. J.; Burwell, R. L., Jr.; Marks, T. J. *J. Am. Chem. Soc.* **1985**, *107*, 641-652.

(4) Toscano, P. J.; Marks, T. J. *J. Am. Chem. Soc.* **1985**, *107*, 653-659.

(5) (a) Bowman, R. G.; Burwell, R. L., Jr. *J. Catal.* **1980**, *63*, 463-475 and references therein. (b) Bowser, W. M.; Weinberg, W. H. *J. Am. Chem. Soc.* **1981**, *103*, 1453-1458.

(6) Li, X.-J.; Gates, B. C.; Knözinger, H.; Delgado, E. A. *J. Catal.* **1984**, *88*, 355-361 and references therein.

(7) For authoritative reviews of the subject, see: (a) Fyfe, C. A. "Solid State NMR for Chemists"; CRC Press: Guelph, 1983. (b) Maciel, G. E. *Science (Washington, D.C.)* **1984**, *26*, 282-288. (c) Mehring, M. "Principles of High Resolution NMR in Solids"; Springer-Verlag: New York, 1983; Chapters 2 and 4. (d) Yannoni, C. S. *Acc. Chem. Res.* **1982**, *15*, 201-208.

(8) For other recent applications of ^{13}C CPMAS NMR to organometallic surface chemistry, see: (a) Hanson, B. E.; Wagner, G. W.; Davis, R. J.; Motell, E. *Inorg. Chem.* **1984**, *23*, 1635-1636 and references therein (Mo(CO)$_6$/alumina). (b) Liu, D. K.; Wrighton, M. S.; McKay, D. R.; Maciel, G. E. *Inorg. Chem.* **1984**, *23*, 212-220 (silica "anchored" ruthenium carbonyls). (c) McKenna, W. P.; Eyring, E. M. *J. Mol. Catal.* **1985**, *29*, 363-369 (Mo$_2$(C$_3$H$_5$)$_4$/silica and alumina). (d) Reference 4 (organoactinide alkyls on alumina).

0276-7333/86/2305-0400$01.50/0

plete in ~5 h, and the oxo vinyl complex is isolated in only poor yield (~40%) from pentane at -40 °C. The oxo vinyl complexes of the type W(O)(EtC=CRR')(DIPP)$_3$ differ from those of the type W(O)(*t*-BuC=CRR')(DIPP)$_3$ in that no rotational isomers are observed at 25 °C. Note also that in this case only one geometric isomer of the oxo vinyl product of the reaction with benzaldehyde is observed, and only the cis hydrolysis product is observed.

Reactions of W(CR)(DIPP)$_3$ (R = *t*-Bu or Et) with the carbonyl function are believed to involved nucleophilic attack on the Lewis acid activated carbonyl carbon atom by the alkylidyne carbon atom to give an oxytungstenacyclobutene intermediate which then rearranges to the oxo vinyl product (eq 3). The ring opening becomes stereoselective when R is not *tert*-butyl as a result of the larger of R_1 or R_2 being forced away from the crowded coordination sphere of the metal.

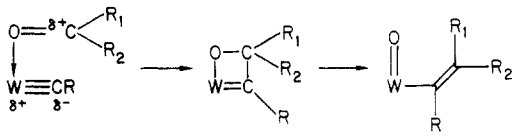

It is interesting to note that analogous reactions involving W(CR)(O-*t*-Bu)$_3$ either are considerably slower[10] or do not yield analogous oxo vinyl species at all.[11] We also know that acetyl chloride reacts with W(C-*t*-Bu)(DIPP)$_3$ to give an ~85% yield of *t*-BuC≡CMe and what appears to be a mixture of W(O)(DIPP)$_3$Cl and a small amount of W(O)(DIPP)$_4$. Further experiments will be required in order to establish the scope, generality, and selectivity of Wittig-like reactions involving complexes of the type W(CR)(OR')$_3$.

Acknowledgment. R.R.S. thanks the National Science Foundation for support (Grant CHE 84-02892).

Registry No. W(C-*t*-Bu)(DIPP)$_3$, 91229-76-4; *t*-BuC≡CMe, 999-78-0; W(N)(DIPP)$_3$, 99594-92-0; *t*-BuCH$_2$CN, 3302-16-7; W(O)(*t*-BuC=CMe$_2$)(DIPP)$_3$, 99594-93-1; W(O)(*t*-BuC=CH$_2$)(DIPP)$_3$, 99594-94-2; W(O)(*t*-BuC=CHPh)(DIPP)$_3$, 99594-95-3; W(O)(*t*-BuC=CHOEt)(DIPP)$_3$, 99594-96-4; W(O)(*t*-BuC=CH(NMe$_2$))(DIPP)$_3$, 99594-97-5; W(C$_3$Et$_3$)(DIPP)$_3$, 91229-77-5; W(O)(EtC=CMe$_2$)(DIPP)$_3$, 99594-98-6; W(O)(EtC=CHPh)(DIPP)$_3$, 99594-99-7; W(O)(EtC=CHOEt)(DIPP)$_3$, 99595-00-3; W(O)(EtC=CH(NMe$_2$))(DIPP)$_3$, 99595-01-4.

(10) W(C-*t*-Bu)(O-*t*-Bu)$_3$ does not react readily with acetonitrile at 25 °C, although W(CEt)(O-*t*-Bu)$_3$ will react with excess acetonitrile over a period of several minutes.

(11) The reaction between W(C-*t*-Bu)(O-*t*-Bu)$_3$ and acetone is sluggish. The reaction is complete after 16 h at 60 °C, but several products are observed.

A High-Resolution Solid-State ^{13}C NMR Study of Fe(C$_5$H$_5$)(CO)$_2$CH$_3$/Alumina Surface Chemistry

Paul J. Toscano and Tobin J. Marks*

Department of Chemistry, Northwestern University Evanston, Illinois 60201

Received September 17, 1985

Summary: ^{13}C CPMAS NMR spectroscopy has been employed to characterize surface reaction pathways involving the complexes CpFe(CO)$_2$CH$_3$, CpFe(^{13}CO)$_2$CH$_3$, CpFe(CO)$_2$(^{13}CH$_3$) (Cp = η^5-C$_5$H$_5$), and dehydroxylated (DA) or partially dehydroxylated (PDA) γ-alumina. A number of possible reaction modes can be ruled out, and surface-induced migratory CO insertion to yield a carbene-like acyl complex is identified as the predominant if not exclusive pathway.

Elucidating the structure(s) of adsorbates arising from the chemisorption of organometallic molecules on high surface area metal oxides (e.g., γ-alumina, silica)[1] is a challenging problem of considerable significance in catalysis.[1,2] Proposed surface reaction pathways include protonolysis of hydrocarbyl ligands by surface OH groups,[1,3] transfer of hydrocarbyl ligands to exposed Lewis acid sites,[4] substitution of carbonyl or other ligands by surface oxide (O^{2-}) or OH groups,[1a,c,5] coordination of carbonyl ligands by surface Lewis acid sites,[1a] nucleophilic addition of surface O^{2-} or OH groups to carbonyl ligands,[1a,c] oxidative addition of OH groups to metal-metal bonds,[1a,6] and a host of others.[1] These reaction pathways and the structures of the resulting organometallic molecule–surface complexes have largely been inferred from the nature of products evolved during the chemisorption process and/or, with varying degrees of definition, from surface spectroscopies (principally vibrational, but also Mössbauer, XPS, EPR, etc.). In many cases, these structural assignments are qualitative in nature and could be greatly strengthened by additional information.

In this communication, we illustrate the efficacy in such structural studies of high-resolution solid-state ^{13}C NMR spectroscopy, utilizing cross polarization (CP), high-power ^{1}H decoupling, and magic-angle spinning (MAS),[7,8] by characterizing for the first time the reaction pathways of a transition-metal carbonyl alkyl complex (selected isotopomers of CpFe(CO)$_2$CH$_3$, Cp = η^5-C$_5$H$_5$) with γ-alumina surfaces. This particular compound is of interest since it offers a multiplicity of potential surface transformations (vide supra), including surface-induced migratory CO insertion (A, inferred as a contributing pathway largely on

(1) (a) Basset, J. M.; Chaplin, A. *J. Mol. Catal.* **1983**, *21*, 95 and references therein. (b) Yermakov, Yu. I. *J. Mol. Catal.* **1983**, *21*, 35 and references therein. (c) Iwamoto, M.; Kusano, H.; Kagawa, S. *Inorg. Chem.* **1983**, *22*, 3365 and references therein. (d) Yermakov, Yu. I.; Kuznetsov, B. N.; Zakharov. V. A. "Catalysis by Supported Complexes"; Elsevier: Amsterdam, 1981. (e) Bailey, D. C.; Langer, S. H. *Chem. Rev.* **1981**, *81*, 109. (f) Ballard, D. G. H. *J. Polym. Sci., Polym. Chem. Ed.* **1975**, *13*, 2191-2212.

(2) (a) Firment, L. E. *J. Catal.* **1983**, *82*, 196-212 and references therein. (b) Gavens, P. D.; Bottrill, M.; Kelland, J. W.; McMeeking, J. In "Comprehensive Organometallic Chemistry"; Wilkinson, G., Stone, F. G. A., Abel, E. W., Eds.; Pergamon Press: Oxford, 1982; Chapter 22.5. (c) Galli, P.; Luciani, L.; Checchini, G. *Angew. Makromol. Chem.* **1981**, *94*, 63. (d) Karol, F. J.; Wu, C.; Reichle, W. T.; Maraschin, N. J. *J. Catal.* **1979**, *60*, 68.

(3) He, M.-Y.; Xiong, G.; Toscano, P. J.; Burwell, R. L., Jr.; Marks, T. J. *J. Am. Chem. Soc.* **1985**, *107*, 641-652.

(4) Toscano, P. J.; Marks, T. J. *J. Am. Chem. Soc.* **1985**, *107*, 653-659.

(5) (a) Bowman, R. G.; Burwell, R. L., Jr. *J. Catal.* **1980**, *63*, 463-475 and references therein. (b) Bowser, W. M.; Weinberg, W. H. *J. Am. Chem. Soc.* **1981**, *103*, 1453-1458.

(6) Li, X.-J.; Gates, B. C.; Knözinger, H.; Delgado, E. A. *J. Catal.* **1984**, *88*, 355-361 and references therein.

(7) For authoritative reviews of the subject, see: (a) Fyfe, C. A. "Solid State NMR for Chemists"; CRC Press: Guelph, 1983. (b) Maciel, G. E. *Science (Washington, D.C.)* **1984**, *26*, 282-288. (c) Mehring, M. "Principles of High Resolution NMR in Solids"; Springer-Verlag: New York, 1983; Chapters 2 and 4. (d) Yannoni, C. S. *Acc. Chem. Res.* **1982**, *15*, 201-208.

(8) For other recent applications of ^{13}C CPMAS NMR to organometallic surface chemistry, see: (a) Hanson, B. E.; Wagner, G. W.; Davis, R. J.; Motell, E. *Inorg. Chem.* **1984**, *23*, 1635-1636 and references therein (Mo(CO)$_6$/alumina). (b) Liu, D. K.; Wrighton, M. S.; McKay, D. R.; Maciel, G. E. *Inorg. Chem.* **1984**, *23*, 212-220 (silica "anchored" ruthenium carbonyls). (c) McKenna, W. P.; Eyring, E. M. *J. Mol. Catal.* **1985**, *29*, 363-369 (Mo$_2$(C$_3$H$_5$)$_4$/silica and alumina). (d) Reference 4 (organoactinide alkyls on alumina).

0276-7333/86/2305-0400$01.50/0

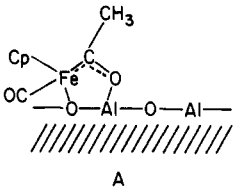

A

the basis of ν_{CO} surface infrared spectroscopy[9]). We assess here the relative importance of this and several other plausible reaction modes as well as describe the electronic structure of the surface acyl as expressed by ^{13}C NMR parameters.

^{13}C CPMAS NMR spectra were recorded on a JEOL FX-60QS spectrometer with Chemagnetics solid-state accessories operating at 15.0 MHz (^{13}C). High-power ^{1}H decoupling, magic-angle spinning (2.5–2.7 kHz), and standard cross polarization techniques were employed.[4] The magic angle was set and the spinning rate measured with internal KBr.[4] A contact time (T_{cp}) of 3 ms was found to yield optimum overall signal-to-noise ratios; however, times as long as 20 ms were employed in cases involving unprotonated sites (vide infra). A pulse delay of 4–6 s was found to be optimum. A broadening function of 25–50 Hz was routinely employed in weighting the FID's. ^{13}C NMR spectra were referenced to $(CH_3)_4Si$ as previously described.[4] All sample preparations and manipulations were performed in Schlenk-type glassware interfaced to a high-vacuum (10^{-4}–10^{-5} torr) line or in a nitrogen-filled Vacuum Atmospheres glovebox equipped with an efficient, recirculating atmosphere purification system. Argon (Matheson, prepurified) and nitrogen (Matheson, prepurified) were purified further by passage through a supported MnO oxygen removal column and a Davison 4-Å molecular sieve column. Pentane (H_2SO_4 washed; distilled from Na/K/benzophenone) was condensed and stored in vacuo in a bulb on the vacuum line.

Dehydroxylated (DA) and partially dehydroxylated alumina (PDA) were prepared as previously reported.[3,4] DA has ca. 0.12 surface OH groups/100 Å^2, while PDA has ca. 4/100 Å^2.[3] $CpFe(CO)_2(^{13}CH_3)$ in which the methyl group is enriched to 99% in ^{13}C was prepared from K-[$CpFe(CO)_2$][10] and $^{13}CH_3I$ (99% ^{13}C, Cambridge Isotopes). $CpFe(^{13}CO)_2CH_3$ in which the carbonyl groups are enriched to ca. 20% in ^{13}C (by IR spectroscopy of a pentane solution) was prepared from K[$CpFe(^{13}CO)_2$] and CH_3I. K-[$CpFe(^{13}CO)_2$] was prepared from [$CpFe(^{13}CO)_2]_2$ (enriched by stirring a THF solution of [$CpFe(CO)_2]_2$ over a catalytic amount of 10% Pd/charcoal under 600 mm of 99% ^{13}CO (Cambridge Isotopes)) and K[$B(C_2H_5)_3H$].[10] The samples for ^{13}C NMR were prepared on a high-vacuum line by pouring a pentane (8–10 mL) solution containing ca. 0.16 mmol of the appropriately labeled $CpFe(CO)_2CH_3$ complex onto 0.50 g of DA or PDA. The orange-yellow solution was rapidly decolorized and the alumina became tan. The pentane slurry was stirred under Ar for 1 h at ambient temperature. At the end of this time, the suspension was filtered and the impregnated alumina was washed with fresh pentane until the filtrate was colorless. If thorough washing is not carried out, considerable amounts of unreacted starting complex are detected in the CPMAS spectrum. The impregnated alumina was then dried in vacuo at room temperature (8 h) and brought into the glovebox. It was loaded into a Kel-F NMR rotor which was subsequently sealed with high-vacuum grease as previously described.[4]

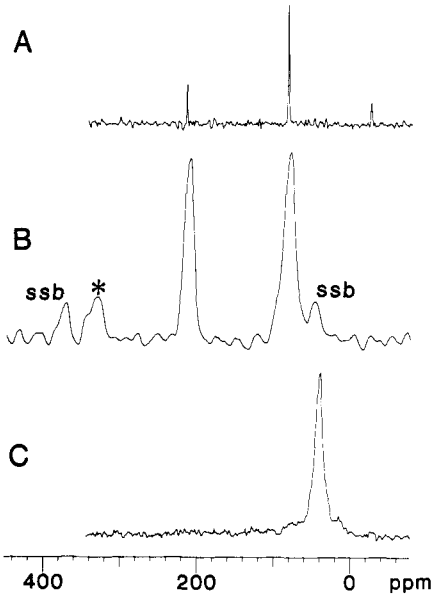

Figure 1. ^{13}C CPMAS NMR spectra (15.0 MHz) of (A) neat $CpFe(CO)_2CH_3$ (35 000 scans, 4-s repetition, 3-ms contact time), (B) $CpFe(^{13}CO)_2CH_3$/DA (20% ^{13}C, 100 000 scans, 6-s repetition, 20-ms contact time; ssb indicates spinning sideband and the asterisk the acyl carbonyl resonance (see text)), and (C) $CpFe(CO)_2(^{13}CH_3)$/DA (99% ^{13}C, 12 000 scans, 4-s repetition, 3-ms contact time).

The ^{13}C CPMAS NMR spectrum of neat $CpFe(CO)_2CH_3$ is shown in Figure 1A. On the basis of solution ^{13}C data[11] and CPMAS parameters for related (unadsorbed) complexes,[12] the signal at δ 218.0 can be straightforwardly assigned to the terminal CO ligands,[13] that at δ 86.1 to the C_5H_5 group, and that at δ −21.8 to the Fe–CH_3 functionality. The CPMAS spectrum of $CpFe(^{13}CO)_2CH_3$ (20% ^{13}C) adsorbed on DA is shown in Figure 1B and that of $CpFe(CO)_2(^{13}CH_3)$ (99% ^{13}C) on DA in Figure 1C. Some broadening of the adsorbate resonances is apparent which may reflect the heterogeneity of surface environments and is normally observed in such studies.[4,8] The surface spectra indicate that the starting complex has been completely consumed and that a new species has been formed with a low-field carbonyl-derived resonance at δ 333.9 (Figure 1B; this feature is reproducibly observed in $CpFe(^{13}CO)_2CH_3$/DA spectra but not observed in $CpFe(CO)_2CH_3$/DA or $CpFe(CO)_2(^{13}CH_3)$/DA spectra), a new $^{13}CH_3$-derived resonance at δ 45.2 (Figure 1C), and virtually unshifted C_5H_5 (δ 82.9, Figure 1B) and terminal ^{13}CO (δ 213.9, Figure 1B) signals. None of these features are observed in spectra of pure DA. Clearly the $CpFe(^{13}CO)$ unit has remained intact upon adsorption. In these results, there is no evidence for significant methyl transfer[4] to a surface aluminum site (B, $\delta(^{13}CH_3)$ would be expected at ca. −20) nor for significant nucleophilic addition to a carbonyl ligand (C, $\delta(Fe^{13}CO_2Al)$ would be expected at ca. 170–210[14]) nor for significant protonolysis (D, a $^{13}CH_3$ signal would not be observed). Rather, the CPMAS spectra can be readily interpreted in terms of the sur-

(9) Correa, F.; Nakamura, R.; Stimson, R. E.; Burwell, R. L., Jr.; Shriver, D. F. *J. Am. Chem. Soc.* **1980**, *102*, 5112–5114.
(10) Gladysz, J. A.; Williams, G. M.; Tam, W.; Johnson, D. L.; Parker, D. W.; Selover, J. C. *Inorg. Chem.* **1979**, *18*, 553–558.
(11) Gansow, O. A.; Schexnayder, D. A.; Kimura, B. Y. *J. Am. Chem. Soc.* **1972**, *94*, 3406–3408.
(12) Dorn, H. C.; Hanson, B. E.; Motell, E. *J. Organomet. Chem.* **1982**, *224*, 181–187.
(13) Pregosin, P. S. *Annu. Rep. NMR Spectrosc.* **1981**, *11A*, 227–271.
(14) (a) Gibson, D. H.; Ong, T.-S. *Organometallics* **1984**, *3*, 1911–1913. (b) Gibson, D. H.; Owens, K.; Ong, T.-S. *J. Am. Chem. Soc.* **1984**, *106*, 1125–1127. (c) Catellani, M.; Halpern, J. *Inorg. Chem.* **1980**, *19*, 566–568.

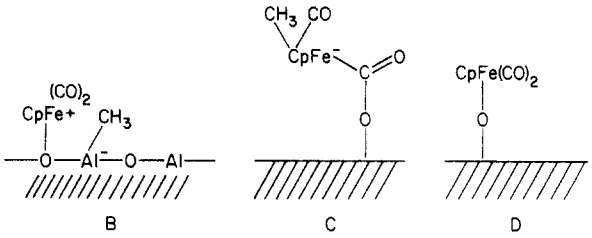

face-induced migratory CO insertion pathway, with species A being the major if not exclusive product. In understanding the CPMAS spectra, it should be recognized that electrophilic addition to metal acyl complexes is a common route to metal carbene complexes (eq 1)[15] and that the acyl

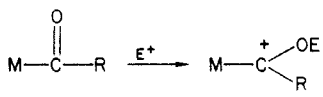

(1)

carbon atom in A may be anticipated to have considerable "carbenoid" character. Indeed, the observed chemical shift is downfield of that for typical $CpFe(CO)(L)COCH_3$ acyl complexes (δ ~250–280)[16] and in the region of $CpFe(CO)(L)C(H)R^+$ carbene complexes (δ ~340).[17] The shape of the δ 333.9 ^{13}CO signal in Figure 1B most likely reflects a heterogeneity in surface aluminum centers,[4,8] inefficient cross polarization (this carbon atom has no directly bound protons[18]), and/or residual dipolar coupling arising from spatial proximity to the ^{27}Al quadrupole[4,19,20] ($I = {}^5/_2$, $Q = 0.149\ e \times 10^{-24}\ cm^2$). The presently observed value of $\delta(^{13}CH_3)$ agrees well with $\delta(^{13}CH_3)$ data reported for $CpFe(CO)(L)COCH_3$ (δ ~50)[16] and methylcarbene ($M(CO)_5C(OCH_3)CH_3$, δ ~50) complexes.[21] In accord with our structural assignment, major displacements of the $CpFe(CO)_2CH_3$, $Fe(C_5H_5)$, and $Fe^{13}CO$ resonance positions are not observed on going to CpFe(CO) acyl[16] and carbene[17] complexes.

Several experiments were also carried out by using PDA as a support. Despite the greater surface hydroxyl coverage, essentially identical CPMAS results were obtained and indicate that surface-induced migratory CO insertion is the major reaction pathway.

In conclusion, this study of $CpFe(CO)_2CH_3/\gamma$-alumina chemistry further illustrates the power of ^{13}C CPMAS NMR spectroscopy for characterizing organometallic molecule–metal oxide surface interactions. Several reactivity modes can be readily discounted, and a surface-induced migratory insertion process to produce a carbene-like acyl has been shown to be the major pathway on both dehydroxylated and partially dehydroxylated supports.

Acknowledgment. We are grateful to the Department of Energy for support of this research under Contract DEAC 02-81ER10980. We thank Profs. R. L. Burwell, Jr., and D. F. Shriver for helpful information.

Registry No. $CpFe(CO)_2CH_3$, 12080-06-7; $CpFe(^{13}CO)_2CH_3$, 80409-88-7; $CpFe(CO)_2(^{13}CH_3)$, 99643-69-3; $K[CpFe(^{13}CO)_2]$, 99655-38-6; CH_3I, 74-88-4; $K[CpFe(CO)_2]$, 60039-75-0; $^{13}CH_3I$, 4227-95-6; $[CpFe(^{13}CO)_2]_2$, 99643-70-6; $K[B(C_2H_5)_3H]$, 22560-21-0; $[CpFe(CO)_2]_2$, 12154-95-9.

(15) (a) Fischer, H.; Kreissl, F. R.; Hofmann, P.; Dötz, K.-H.; Weiss, K. "Transition Metal Carbene Complexes"; Verlag Chemie: Weinheim, 1983. (b) Brown, T. J. *Prog. Inorg. Chem.* **1980**, *27*, 1-122. (c) Casey, C. P. In "Reactive Intermediates"; Jones, M., Jr., Moss, R. A., Eds.; Wiley: New York, 1981; Vol. 2, pp 135–174.

(16) Kuhlmann, E. J.; Alexander, J. J. *Inorg. Chim. Acta* **1979**, *34*, L193–L195.

(17) Brookhart, M.; Nelson, G. O. *J. Am. Chem. Soc.* **1977**, *99*, 6099–6101.

(18) (a) As would be expected,[7,18b] the ^{13}CO-derived signals increased in relative intensity on incrementally increasing T_{cp} from 3 to 20 ms. Little improvement was noted for T_{cp} greater than 20 ms, and this spectrum is the one presented in Figure 1B. (b) Alemany, L. B.; Grant, D. M.; Alger, T. D.; Pugmire, R. J. *J. Am. Chem. Soc.* **1983**, *105*, 6697–6704.

(19) Broadening and/or splitting of ^{13}C resonances in spatial proximity to quadrupolar nuclei arises when the energy of the quadrupolar interaction is comparable in magnitude to that of the Zeeman interaction. In such cases, the quadrupolar interaction tilts the axis of quantization of the quadrupolar nucleus away from the static field direction, so that residual dipolar coupling to the ^{13}C nucleus is not removed by the MAS. We have previously shown[4] that directly bonded ^{13}C–^{27}Al(alumina) interactions can be extremely large (≳750 Hz at 15 MHz). Since this interaction has a r_{C-Al}^{-3} dependence, the relatively small effect observed in Figure 1B is not surprising.

(20) For other examples of this phenomenon, see: (a) Naito, A.; Ganapathy, S.; McDowell, C. A. *J. Magn. Reson.* **1982**, *48*, 367–381. (b) Naito, A.; Ganapathy, S.; McDowell, C. A. *J. Chem. Phys.* **1981**, *74*, 5393–5397. (c) Hexam, J. G.; Frey, M. H.; Opella, S. J. *J. Am. Chem. Soc.* **1981**, *103*, 224–226.

(21) Kreiter, C. G.; Formacek, V. *Angew. Chem., Int. Ed. Engl.* **1972**, *11*, 141–142.

(η^4-Butadiene)bis(pentamethylcyclopentadienyl)-thorium

Gerhard Erker,* Thomas Mühlenbernd, Reinhard Benn, and Anna Rufińska

Max-Planck-Institut für Kohlenforschung
Kaiser-Wilhelm-Platz 1
D-4330 Mülheim a.d. Ruhr, Germany

Received November 26, 1985

Summary: Cp^*_2Th(butadiene) (**2**) was obtained in 80% isolated yield from the reaction of $Cp^*_2ThCl_2$ (Cp^* = pentamethylcyclopentadienyl) with (butadiene)magnesium. The (diene)thorium complex exhibits dynamic NMR spectra which point to a rapidly proceeding (diene)metallocene topomerization ($\Delta G^{\ddagger}_{23°C}$ = 15.5 kcal/mol). **2** was characterized by several chemical reactions. It adds stereoselectively to the NCα bond of pyridine to yield the (η^3-allyl)thorium complex **4**. Similarly, coupling of the diene moiety of **2** with a CO ligand of chromium hexacarbonyl produces the thorium oxy carbene chromium complex **6** in high yield.

The organometallic chemistry of the actinide element thorium and the oxygenophilic 4B (4^{13}) transition metals, especially zirconium and hafnium, shows some remarkable similarities.[1] In view of the extraordinary features exhibited by the group 4 metallocene (diene) complexes[2] it

(1) This is especially true for the reactions of the respective metal hydrocarbyls with carbon monoxide (a) but can be extended to other structural and chemical features as well (b). For leading references see: (a) Marks, T. J.; Fagan, P. J.; Manriquez, J. M.; Day, C. S.; Day, V. W. *J. Am. Chem. Soc.* **1978**, *100*, 7112. Sonnenberger, D. C.; Mintz, E. A.; Marks, T. J. *Ibid.* **1984**, *106*, 3484. Moloy, K. G.; Marks, T. J. *Ibid.* **1984**, *106*, 7051. Erker, G. *Acc. Chem. Res.* **1984**, *17*, 103. Bercaw, J. E.; Wolczanski, P. T. *Ibid.* **1980**, *13*, 121. (b) Streitwieser, A., Jr.; Luke, W. D.; *J. Am. Chem. Soc.* **1981**, *103*, 3241. Erker, G.; Mühlenbernd, T.; Benn, R.; Rufińska, A.; Tsay, Y.-H.; Krüger, C. *Angew. Chem.* **1985**, *97*, 336.

(2) (a) Erker, G.; Wicher, J.; Engel, K.; Rosenfeldt, F.; Dietrich, W.; Krüger, C. *J. Am. Chem. Soc.* **1980**, *102*, 6344. Erker, G.; Wicher, J.; Engel, K.; Chiang, A.-P.; Krüger, C. *Chem. Ber.* **1982**, *115*, 3300. (b) Erker, G.; Engel, K.; Müller, G.; Krüger, C. *Organometallics* **1984**, *3*, 128. (c) Erker, G.; Krüger, C.; Müller, G. *Adv. Organomet. Chem.* **1985**, *24*, 1.

0276-7333/86/2305-0402$01.50/0

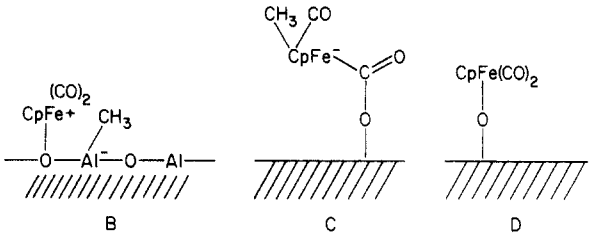

face-induced migratory CO insertion pathway, with species A being the major if not exclusive product. In understanding the CPMAS spectra, it should be recognized that electrophilic addition to metal acyl complexes is a common route to metal carbene complexes (eq 1)[15] and that the acyl

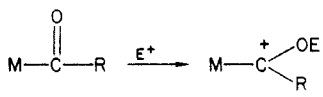

(1)

carbon atom in A may be anticipated to have considerable "carbenoid" character. Indeed, the observed chemical shift is downfield of that for typical $CpFe(CO)(L)COCH_3$ acyl complexes (δ ~250–280)[16] and in the region of $CpFe(CO)(L)C(H)R^+$ carbene complexes (δ ~340).[17] The shape of the δ 333.9 ^{13}CO signal in Figure 1B most likely reflects a heterogeneity in surface aluminum centers,[4,8] inefficient cross polarization (this carbon atom has no directly bound protons[18]), and/or residual dipolar coupling arising from spatial proximity to the ^{27}Al quadrupole[4,19,20] ($I = {}^5/_2$, $Q = 0.149\ e \times 10^{-24}\ cm^2$). The presently observed value of $\delta(^{13}CH_3)$ agrees well with $\delta(^{13}CH_3)$ data reported for $CpFe(CO)(L)COCH_3$ (δ ~50)[16] and methylcarbene ($M(CO)_5C(OCH_3)CH_3$, δ ~50) complexes.[21] In accord with our structural assignment, major displacements of the $CpFe(CO)_2CH_3$, $Fe(C_5H_5)$, and $Fe^{13}CO$ resonance positions are not observed on going to CpFe(CO) acyl[16] and carbene[17] complexes.

Several experiments were also carried out by using PDA as a support. Despite the greater surface hydroxyl coverage, essentially identical CPMAS results were obtained and indicate that surface-induced migratory CO insertion is the major reaction pathway.

In conclusion, this study of $CpFe(CO)_2CH_3/\gamma$-alumina chemistry further illustrates the power of ^{13}C CPMAS NMR spectroscopy for characterizing organometallic molecule–metal oxide surface interactions. Several reactivity modes can be readily discounted, and a surface-induced migratory insertion process to produce a carbene-like acyl has been shown to be the major pathway on both dehydroxylated and partially dehydroxylated supports.

Acknowledgment. We are grateful to the Department of Energy for support of this research under Contract DEAC 02-81ER10980. We thank Profs. R. L. Burwell, Jr., and D. F. Shriver for helpful information.

Registry No. $CpFe(CO)_2CH_3$, 12080-06-7; $CpFe(^{13}CO)_2CH_3$, 80409-88-7; $CpFe(CO)_2(^{13}CH_3)$, 99643-69-3; $K[CpFe(^{13}CO)_2]$, 99655-38-6; CH_3I, 74-88-4; $K[CpFe(CO)_2]$, 60039-75-0; $^{13}CH_3I$, 4227-95-6; $[CpFe(^{13}CO)_2]_2$, 99643-70-6; $K[B(C_2H_5)_3H]$, 22560-21-0; $[CpFe(CO)_2]_2$, 12154-95-9.

(15) (a) Fischer, H.; Kreissl, F. R.; Hofmann, P.; Dötz, K.-H.; Weiss, K. "Transition Metal Carbene Complexes"; Verlag Chemie: Weinheim, 1983. (b) Brown, T. J. *Prog. Inorg. Chem.* **1980**, *27*, 1-122. (c) Casey, C. P. In "Reactive Intermediates"; Jones, M., Jr., Moss, R. A., Eds.; Wiley: New York, 1981; Vol. 2, pp 135–174.

(16) Kuhlmann, E. J.; Alexander, J. J. *Inorg. Chim. Acta* **1979**, *34*, L193–L195.

(17) Brookhart, M.; Nelson, G. O. *J. Am. Chem. Soc.* **1977**, *99*, 6099–6101.

(18) (a) As would be expected,[7,18b] the ^{13}CO-derived signals increased in relative intensity on incrementally increasing T_{cp} from 3 to 20 ms. Little improvement was noted for T_{cp} greater than 20 ms, and this spectrum is the one presented in Figure 1B. (b) Alemany, L. B.; Grant, D. M.; Alger, T. D.; Pugmire, R. J. *J. Am. Chem. Soc.* **1983**, *105*, 6697–6704.

(19) Broadening and/or splitting of ^{13}C resonances in spatial proximity to quadrupolar nuclei arises when the energy of the quadrupolar interaction is comparable in magnitude to that of the Zeeman interaction. In such cases, the quadrupolar interaction tilts the axis of quantization of the quadrupolar nucleus away from the static field direction, so that residual dipolar coupling to the ^{13}C nucleus is not removed by the MAS. We have previously shown[4] that directly bonded ^{13}C–^{27}Al(alumina) interactions can be extremely large (≳750 Hz at 15 MHz). Since this interaction has a r_{C-Al}^{-3} dependence, the relatively small effect observed in Figure 1B is not surprising.

(20) For other examples of this phenomenon, see: (a) Naito, A.; Ganapathy, S.; McDowell, C. A. *J. Magn. Reson.* **1982**, *48*, 367–381. (b) Naito, A.; Ganapathy, S.; McDowell, C. A. *J. Chem. Phys.* **1981**, *74*, 5393–5397. (c) Hexam, J. G.; Frey, M. H.; Opella, S. J. *J. Am. Chem. Soc.* **1981**, *103*, 224–226.

(21) Kreiter, C. G.; Formacek, V. *Angew. Chem., Int. Ed. Engl.* **1972**, *11*, 141–142.

(η^4-Butadiene)bis(pentamethylcyclopentadienyl)-thorium

Gerhard Erker,* Thomas Mühlenbernd, Reinhard Benn, and Anna Rufińska

Max-Planck-Institut für Kohlenforschung
Kaiser-Wilhelm-Platz 1
D-4330 Mülheim a.d. Ruhr, Germany

Received November 26, 1985

Summary: Cp^*_2Th(butadiene) (**2**) was obtained in 80% isolated yield from the reaction of $Cp^*_2ThCl_2$ (Cp^* = pentamethylcyclopentadienyl) with (butadiene)magnesium. The (diene)thorium complex exhibits dynamic NMR spectra which point to a rapidly proceeding (diene)metallocene topomerization ($\Delta G^{\ddagger}_{23°C}$ = 15.5 kcal/mol). **2** was characterized by several chemical reactions. It adds stereoselectively to the NCα bond of pyridine to yield the (η^3-allyl)thorium complex **4**. Similarly, coupling of the diene moiety of **2** with a CO ligand of chromium hexacarbonyl produces the thorium oxy carbene chromium complex **6** in high yield.

The organometallic chemistry of the actinide element thorium and the oxygenophilic 4B (4^{13}) transition metals, especially zirconium and hafnium, shows some remarkable similarities.[1] In view of the extraordinary features exhibited by the group 4 metallocene (diene) complexes[2] it

(1) This is especially true for the reactions of the respective metal hydrocarbyls with carbon monoxide (a) but can be extended to other structural and chemical features as well (b). For leading references see: (a) Marks, T. J.; Fagan, P. J.; Manriquez, J. M.; Day, C. S.; Day, V. W. *J. Am. Chem. Soc.* **1978**, *100*, 7112. Sonnenberger, D. C.; Mintz, E. A.; Marks, T. J. *Ibid.* **1984**, *106*, 3484. Moloy, K. G.; Marks, T. J. *Ibid.* **1984**, *106*, 7051. Erker, G. *Acc. Chem. Res.* **1984**, *17*, 103. Bercaw, J. E.; Wolczanski, P. T. *Ibid.* **1980**, *13*, 121. (b) Streitwieser, A., Jr.; Luke, W. D.; *J. Am. Chem. Soc.* **1981**, *103*, 3241. Erker, G.; Mühlenbernd, T.; Benn, R.; Rufińska, A.; Tsay, Y.-H.; Krüger, C. *Angew. Chem.* **1985**, *97*, 336.

(2) (a) Erker, G.; Wicher, J.; Engel, K.; Rosenfeldt, F.; Dietrich, W.; Krüger, C. *J. Am. Chem. Soc.* **1980**, *102*, 6344. Erker, G.; Wicher, J.; Engel, K.; Chiang, A.-P.; Krüger, C. *Chem. Ber.* **1982**, *115*, 3300. (b) Erker, G.; Engel, K.; Müller, G.; Krüger, C. *Organometallics* **1984**, *3*, 128. (c) Erker, G.; Krüger, C.; Müller, G. *Adv. Organomet. Chem.* **1985**, *24*, 1.

0276-7333/86/2305-0402$01.50/0

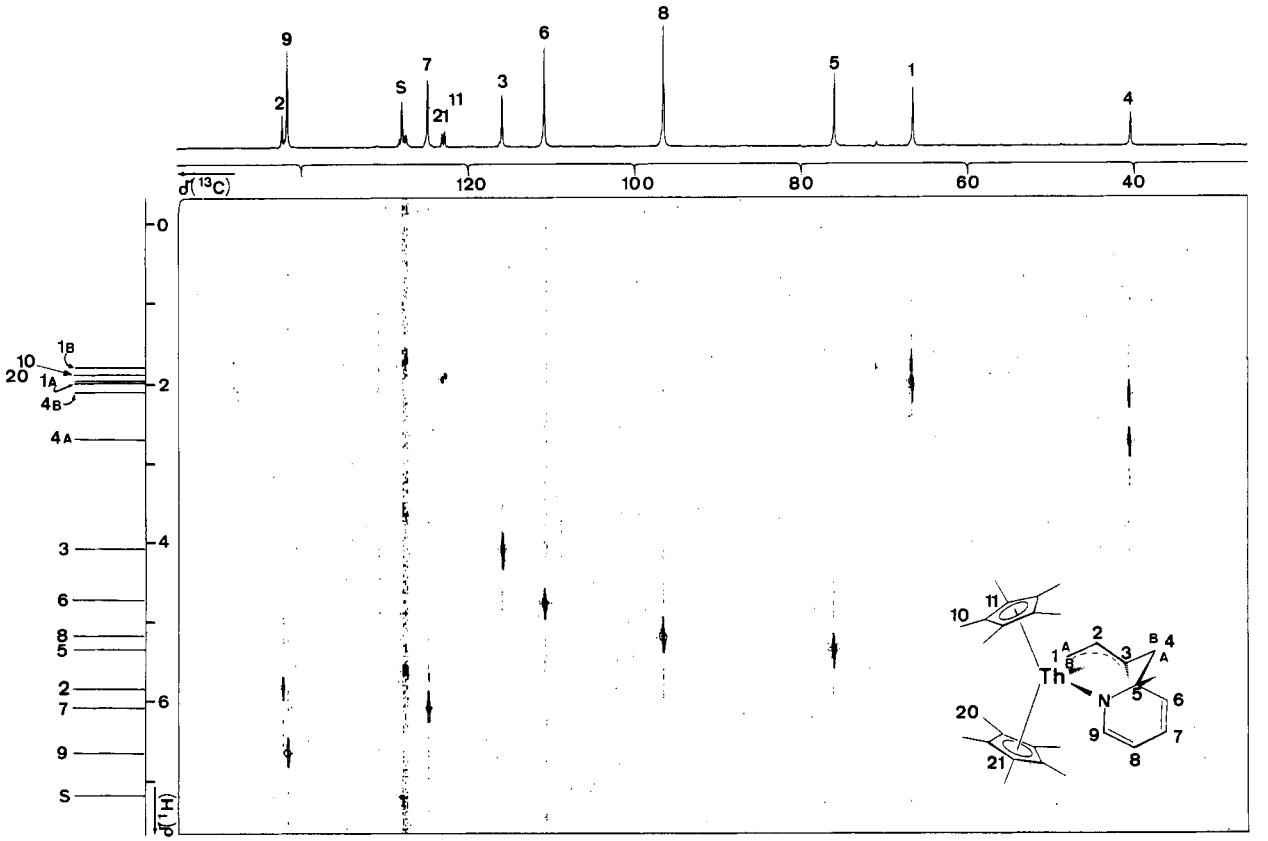

Figure 1. Contour plot of the ^{13}C, ^{1}H correlated 2-D NMR spectrum of *cis*-4 at 9.4 T and 310 K. Stereospecific assignment of the Cp* resonances was not attempted. The stereochemical assignment was confirmed by strong NOE effects of H2 with H4B and of H5 with H3 (H3 with H5).

was tempting to prepare analogous conjugated diene actinide complexes and compare their chemistry. Zirconocene and hafnocene form unique mononuclear (*s-trans*-η^4-butadiene)metallocene complexes,[2a] which equilibrate with their σ^2,π-type structured (*s-cis*-diene)-MCp_2 isomers.[2b] The butadiene ligand in these complexes undergoes CC coupling reactions with olefins, alkynes, conjugated dienes, nitriles, ketones, aldehydes, or Schiff bases to form metallacyclic allylmetallocene complexes.[3] Coupling of the butadiene moiety with a metal carbonyl, e.g., at the zirconium center, leads to metallacyclic Fischer-type zirconium oxy carbene complexes.[3c]

We have prepared (η^4-butadiene)bis(pentamethylcyclopentadienyl)thorium (**2**) starting from the readily available $Cp^*_2ThCl_2$ (**1**).[4] Reaction of **1** with a slight excess of the oligomeric butadiene dianion equivalent (butene-1,4-diyl)magnesium ("butadiene magnesium")[5] in ether at low temperature proceeds smoothly to give **2** (yellow-orange microcrystalline solid, 80% isolated yield from benzene after workup at ambient temperature). **2** is a stable compound at room temperature, albeit extremely sensitive to air and moisture. The NMR spectra indicate that (butadiene)$ThCp^*_2$ thus obtained contains only a single isomer.[6] The conjugated diene ligand is oriented in the *s-cis* conformation. The (butadiene)thorium moiety exhibits

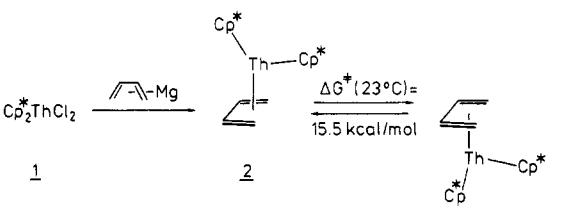

a substantial metal alkyl character (^1H NMR (toluene-d_8, −20 °C) δ −0.52 (H1a), 3.46 (H1s), 4.96 (H2), coupling constants $^3J_{HH}$ = 10.1 (H1s, H2), 12.3 (H1a, H2), 11.4 Hz (H2, H2'), $^2J_{HH}$ = 9.3 Hz (H1s, H1a); ^{13}C NMR, (toluene-d_8, −80 °C) δ 68.4 (dd, $^1J_{CH}$ = 127, 151 Hz, C1), 119.6 (d, 155 Hz, C2). **2** exhibits dynamic NMR spectra, leading to equilibration of both the H1s/H1a and the Cp* resonances at high temperature. In contrast, two sets of pentamethylcyclopentadienyl signals are observed in the low-temperature limiting spectra: δ 1.80, 1.96 (^1H, −20 °C); δ 11.05, 11.93 (q), 122.7, 123.9 (s) (^{13}C, −80 °C, both in toluene-d_8). We interpret this behavior as resulting from a rapid topomerization (i.e., ring inversion)[7] of the metallacyclic σ^2,π-type structured (*s-cis*-butadiene)$ThCp^*_2$ framework ($\Delta G^{\ddagger}_{+23°C}$ = 15.5 ± 0.3 kcal/mol).[8]

2 is a very reactive metal–diene complex. It rather violently reacts with organic carbonyl compounds to form

(3) (a) Erker, G.; Engel, K.; Dorf, U.; Atwood, J. L.; Hunter, W. E. *Angew. Chem.* **1982**, *94*, 915. (b) Erker, G.; Engel, K.; Atwood, J. L.; Hunter, W. E. *Ibid.* **1983**, *95*, 506. Erker, G.; Dorf, U. *Ibid.* **1983**, *95*, 800. (c) Erker, G.; Dorf, U.; Benn, R.; Reinhardt, R.-D.; Petersen, J. L. *J. Am. Chem. Soc.* **1984**, *106*, 7649. Erker, G.; Dorf, U.; Mynott, R.; Tsay, Y.-H.; Krüger, C. *Angew. Chem.* **1985**, *97*, 572. (d) Erker, G.; Engel, K.; Frömberg, W., unpublished results.

(4) Fagan, P. J.; Manriquez, J. M.; Maatta, E. A.; Seyam, A. M.; Marks, T. J. *J. Am. Chem. Soc.* **1981**, *103*, 6650.

(5) (a) Ramsden, H. E. U.S. Patent 3 388 179, 1968. (b) Yasuda, H.; Fujita, K.; Ohnuma, Y.; Tani, H. *J. Organomet. Chem.* **1976**, *113*, 201.

(6) Cp^*_2Th(butadiene) (**2**): mp 167 °C dec; MS (70 MeV) *m/e* 556 (M^+), 502 (Cp^*_2Th), 500 (100%, $Cp^*_2Th - H_2$); IR (KBr) ν 2960, 2895, 2850, 1500, 1480, 1435, 1375, 1030, 770 cm^{-1}. Anal. Calcd for $C_{24}H_{36}Th$ (556.6): C, 51.79; H, 6.52. Found: C, 52.13; H, 5.89.

(7) Kessler, H. *Angew. Chem.* **1970**, *82*, 237. Sandström, J. "Dynamic NMR Spectroscopy"; Academic Press: London, New York, 1982. Kaplan, J. I.; Fraenkel, G. "NMR of Chemically Exchanging Systems"; Academic Press: New York, 1980.

(8) Obtained from the coalescence of the ^1H NMR methyl resonances: $T_{coal.}$ = +23 °C; $\delta\nu$ = 10 Hz (−60 °C) at 1.41 T. Günther, H. "NMR Spectroscopy"; Wiley: Chichester, 1980.

Scheme I

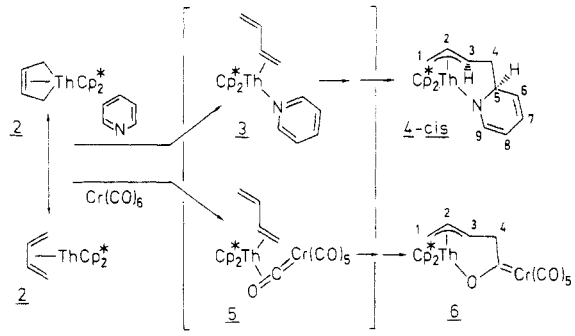

as yet unidentified product mixtures. In contrast to the group 4 metallocene–butadiene complexes,[3] **2** even reacts with pyridine. At room temperature CC coupling at the pyridine α-position occurs with the conjugated diene ligand. The stable bicyclic (π-allyl)thorium complex **4** is obtained,[9] which does not contain the aromatic π-electron system any more. The metallacyclic CC coupling reaction proceeds with a remarkable stereospecificity. Of the two possible diastereoisomers (characterized, e.g., by a respectively cis,trans arrangement of the hydrogen atoms at C3 and C5) formation of only one could be detected within the accuracy of the NMR analysis. As a result of an extensive NMR investigation (complete identification of all carbon and hydrogen resonances was achieved by 2-D NMR techniques and selective decoupling experiments; see Figure 1) we assign this product the *cis*-**4** structure (see Scheme I) [vicinal coupling constants (in Hz) $^3J_{HH}$ = 2.9 (H3, H4A), 11.0 (H3, H4B), 4.9 (H4A,H5), 11.7 (H4B, H5)].

Recently we had presented evidence that the reaction of the (butadiene)zirconocene and -hafnocene systems with a metal carbonyl might represent a novel one-step synthesis of the important class of Fischer-type carbene complexes.[3c,10] Starting from the $Cp^*_2Th(\eta^4$-butadiene) complex (**2**) the analogous CC coupling of the diene ligand with coordinated carbon monoxide of chromium hexacarbonyl proceeds equally facile. **2** is consumed almost completely in a period of 5 h at room temperature when stirred with a suspension of excess $Cr(CO)_6$ in ether. After recrystallization from hexane we have obtained an 85% yield of the metallacyclic (π-allyl)metal oxy chromium carbene complex **6** (Scheme I).[11]

These few examples of chemical features of the novel (butadiene)thorium complex **2** indeed seem to confirm the expected similarities between group 4 and actinide metal conjugated diene chemistry. However, our observations also indicate sufficient substantial differences to expect a rapid and important development of the already rich (conjugated diene)metallocene chemistry on going from the d-block transition metals to the actinide elements.[12]

Acknowledgment. Financial aid from the Minister für Wissenschaft und Forschung des Landes Nordrhein-Westfalen, the Fritz Thyssen Stiftung, and Fonds der Chemischen Industrie is gratefully acknowledged.

Registry No. **1**, 67506-88-1; **2**, 99668-63-0; **4**, 99705-82-5; **6**, 99668-64-1; (butadiene-1,4-diyl)magnesium, 70809-00-6; pyridine, 110-86-1; chromium hexacarbonyl, 13007-92-6.

(9) (a) **4** was prepared by reacting 0.83 g (1.5 mmol) of **2** with 0.12 mL (1.5 mmol) of pyridine in 50 mL of diethyl ether at −78 °C. After the mixture was warmed to room temperature, the solvent was removed in vacuo. Recrystallization from benzene at +10 °C gave 0.76 g (1.2 mmol, 80% yield) of **4**: mp 164 °C dec; IR (KBr) ν 2965, 2905, 2860, 1605 (C=C), 1510 (π-allyl), 1435, 1375, 1225, 1040, 835, 800, 750 cm^{-1}. For NMR data see Figure 1. Anal. Calcd for $C_{29}H_{44}NTh$ (635.7): C, 54.79; H, 6.50. Found: C, 54.74; H, 6.39. (b) The ^{13}C, ^1H shift-correlated 2-D NMR spectrum of **4** was recorded with the standard pulse sequence. For a recent review, cf.: Benn, R.; Günther, H. *Angew. Chem.* **1983**, *95*, 381. NMR data of **4** (C_6D_6, +37 °C): ^1H NMR (coupling constants in Hz) δ 2.00 (H1A), 1.80 (H1B, $^2J_{1A,B}$ = 4.5), 5.80 (H2, $^3J_{1A,2}$ = 8.2, $^3J_{1B,2}$ = 14.2, $^3J_{2,3}$ = 15.7), 4.07 (H3, $^3J_{3,4A}$ = 2.9, $^3J_{3,4B}$ = 11.0), 2.73 (H4A), 2.16 (H4B), 5.30 (H5, $^3J_{4A,5}$ = 4.9, $^3J_{4B,5}$ = 11.7, $^3J_{5,6}$ = 2.0), 4.73 (H6, $^3J_{6,7}$ = 8.9), 6.06 (H7, $^3J_{7,8}$ = 5.3), 5.14 (H8, $^3J_{8,9}$ = 6.5), 6.63 (H9), 1.94 and 1.88 (H10 and H20); ^{13}C NMR (coupling constants $^1J_{CH}$ in Hz) δ 66.9 (C1, dd, $J_{C,H1B}$ = 154, $J_{C,H1A}$ = 138), 142.7 (C2, d, 147), 116.3 (C3, d, 142), 40.7 (C4, t, 129), 76.3 (C5, d, 137), 111.1 (C6, d, 161), 125.2 (C7, d, 157), 96.9 (C8, d, 164), 142.1 (C9, d, 155), 123.4 and 123.1 (Cp, s), 12.1 and 11.6 (Me_5Cp, q, 125).

(10) Fischer, E. O.; Dötz, K. H. "Transition Metal Carbene Complexes"; Verlag Chemie: Weinheim 1983. For a different type of a "one-step" carbonyl to carbene ligand conversion see: (a) Petz, W. *J. Organomet. Chem.* **1974**, *72*, 369. (b) Bercaw, J. E.; Wolczanski, P. T.; Threlkel, R. S. *J. Am. Chem. Soc.* **1979**, *101*, 218.

(11) **6**: mp 179 °C dec; IR (C_6D_6) ν(CO) 2048, 1980, 1925 cm^{-1}. Assignment of the ^1H and ^{13}C resonances by ^{13}C,^1H shift-correlated 2-D NMR ($C_6D_5CD_3$, +37 °C): ^1H NMR (coupling constants $J_{H,H}$ in Hz) δ 1.78 and 1.80 (Cp*), 1.84 (H1B), 1.95 (H1A, $^2J_{1B,1A}$ = −18.6, $^3J_{1A,2}$ = 8.2, $^3J_{1B,2}$ = 14.2), 5.24 (H2, $^3J_{2,3}$ = 16.1), 3.86 (H3), 4.52 (H4A), 3.17 (H4B, $^3J_{3,4A}$ = 4.2, $^3J_{3,4B}$ = 10.0); ^{13}C NMR (coupling constants $^1J_{C,H}$ in Hz): δ 11.1 and 11.3 (Me_5Cp, q, 127.0), 124.9 and 125.5 (Cp*, s), 72.2 (C1, dd, $J_{C,H1B}$ = 155, $J_{C,H1A}$ = 137.5), 146.5 (C2, d, 146), 114.2 (C3, d, 143), 69.5 (C4, dd, $J_{C,H4A}$ = 125.0, $J_{C,H4B}$ = 132.0), 378.0 (carbene-C), 219.1 (CO, cis), 224.5 (CO, trans). Anal. Calcd for $C_{30}H_{36}O_6CrTh$ (776.6): C, 46.40; H, 4.67. Found: C, 46.30; H, 4.96.

(12) For a theoretical treatment of the bonding situation of bent metallocene complexes of actinides (a) and transition metals (b) see: (a) Tatsumi, K.; Nakamura, A. *J. Organomet. Chem.* **1984**, *272*, 141. Tatsumi, K.; Hoffmann, R. *Inorg. Chem.* **1984**, *23*, 1633. Tatsumi, K.; Nakamura, A.; Hofmann, P.; Stauffert, P.; Hoffmann, R. *Organometallics* **1985**, *4*, 404 and personal communication. (b) Lauher, J. W.; Hoffmann, R. *J. Am. Chem. Soc.* **1976**, *98*, 1729.

(13) In this paper the periodic group notation is in accord with recent actions by IUPAC and ACS nomenclature committees. A and B notation is eliminated because of wide confusion. Groups IA and IIA become groups 1 and 2. The d-transition elements comprise groups 3 through 12, and the p-block elements comprise groups 13 through 18. (Note that the former Roman number designation is preserved in the last digit of the new numbering: e.g., III→3 and 13.)

under standard reaction conditions. However, at room temperature the ligation of one pyrazolyl ring may be replaced with a $P(OCH_3)_3$ or a CO ligand to form novel compounds in which the pyrazolylborate ligand binds in a bidentate manner. At room temperature the CO adducts $[CpRuHB(3,5\text{-}Me_2pz)_3(CO)]$ and $[CpRuBpz_4(CO)]$ exhibit conformational isomerism on the IR time scale that is averaged on the NMR time scale. The reaction of $[CpRuBpz_4(CO)]$ and $[CpRu(CH_3CN)_2CO]PF_6$ allowed the isolation of a new binuclear ruthenium complex, $[Cp_2Ru_2(CO)_2Bpz_4]PF_6$.

Acknowledgment. We wish to thank Professor J. D. Britton for his expert assistance in the X-ray structure determination. A.M.M. acknowledges a Louise T. Dosdall Fellowship in science. The X-ray diffractometer was purchased in part through funds provided by the National Science Foundation Grant CHE 77-28505. We thank the Engelhard Minerals and Chemicals Corp. for a generous loan of $RuCl_3 \cdot 3H_2O$. This work was supported by the Department of Energy Grant DOE/DE-ACO2-83ER13103.

Supplementary Material Available: Listings of thermal parameters, hydrogen atom positions, and observed and calculated structure factors (12 pages). Ordering information is given on any current masthead page.

Oxidative Addition Mechanisms of a Four-Coordinate Rhodium(I) Macrocycle

James P. Collman,* John I. Brauman, and Alex M. Madonik

Department of Chemistry, Stanford University, Stanford, California 94305

Received February 13, 1985

Oxidative addition of a wide range of alkyl halides (RX) to the four-coordinate Rh(I) macrocyclic complex **5b** yields six-coordinate Rh(III)–alkyl adducts. The reactions exhibit second-order kinetics (first order in substrate and Rh(I) complex) for all substrates except hindered alkyl iodides, and the reactivity trends (X = I > Br > OTs > Cl; R = methyl > primary > secondary > tertiary [no reaction]) are consistent with a nucleophilic, S_N2-like mechanism. The observed activation parameters and rate variation with solvent polarity also support this interpretation. Complex **5b** is the most reactive neutral nucleophile which has been isolated (k = 2000 M^{-1} s^{-1} for iodomethane at 25 °C in tetrahydrofuran); it exhibits unusually high sensitivity to steric hindrance and leaving-group polarizability, characteristics it shares with other metal-centered nucleophiles. The shift to a one-electron mechanism in reactions with hindered iodides (2,2-dimethyl-1-iodopropane, 3,3-dimethyl-1-iodobutane, and 2-iodopropane) is signaled by their departure from second-order kinetics and by their unexpectedly high rates; even 1-iodoadamantane forms an adduct. Furthermore, scrambling of stereochemistry is observed in the addition of *erythro*-3,3-dimethyl-1-iodobutane-*1,2-d*$_2$. While a radical chain mechanism is implicated by these kinetic results, any free radical intermediates must be very short-lived, as no rearrangement was detected in the reaction of 6-iodo-1-heptene. It seems likely that electron transfer from the Rh(I) reagent leads to the formation of radical pairs, most of which collapse to product without escaping the solvent cage.

Introduction

The oxidative addition of alkyl halides to low-valent transition-metal centers has been intensively studied,[1] particularly as it is the most general method of forming metal–carbon σ bonds. Nonetheless, fundamental questions remain about the detailed mechanism of the reactions. Early work distinguished between the one-electron change observed at odd-electron centers such as the pentacyanocobalt(II) anion[2] and the apparent two-electron process involved in additions to even-electron centers, such as Vaska's iridium(I) complex.[3] Chock and Halpern[3a] proposed a nucleophilic mechanism for the addition of methyl iodide to Vaska's complex, with attack by the metal center at carbon leading to an S_N2-like transition state. They contrasted this behavior to that of dioxygen and dihydrogen, which form cis adducts with Vaska's complex by a concerted, three-center process.

The rate laws and activation parameters for the addition of methyl iodide to Vaska's complex[3a,4] and a variety of other d^8 metal complexes[5-7] were shown to support the proposed nucleophilic mechanism. The relative rates of addition for other alkyl halides were found to reflect the expected influences of steric hindrance and leaving-group reactivity.[7] More basic phosphines were found to enhance to nucleophilicity of a metal center,[8-10] although increasing steric bulk in the ligands can mask these effects.[7a,9]

Attempts to demonstrate the expected inversion of configuration at carbon resulting from these oxidative additions led to conflicting reports[11-13] and ultimately to the recognition of a competing, radical-chain mechanism

(1) Stille, J. K.; Lau, K. S. Y. *Acc. Chem. Res.* **1977**, *10*, 434.
(2) (a) Halpern, J.; Maher, J. P. *J. Am. Chem. Soc.* **1965**, *87*, 5361. (b) Chock, P. B.; Halpern, J. *J. Am. Chem. Soc.* **1969**, *91*, 582.
(3) (a) Chock, P. B.; Halpern, J. *J. Am. Chem. Soc.* **1966**, *88*, 3511. (b) Vaska, L. *Acc. Chem. Res.* **1976**, *9*, 175.
(4) Stieger, H.; Kelm, H. *J. Phys. Chem.* **1973**, *77*, 290.
(5) Douek, I. C.; Wilkinson, G. *J. Chem. Soc. A* **1969**, 2604.
(6) Uguagliati, P.; Palazzi, A.; Deganello, G.; Belluco, U. *Inorg. Chem.* **1970**, *9*, 724.
(7) (a) Hart-Davis, A. J.; Graham, W. A. G. *Inorg. Chem.* **1970**, *9*, 2658. (b) Hart-Davis, A. J.; Graham, W. A. G. *Inorg. Chem.* **1971**, *10*, 1653.
(8) Ugo, R.; Pasini, A.; Fusi, A.; Cenini, S. *J. Am. Chem. Soc.* **1972**, *94*, 7364.
(9) Kubota, M.; Kiefer, G. W.; Ishikawa, R. M.; Bencala, K. E. *Inorg. Chim. Acta* **1973**, *7*, 195.
(10) Thompson, W. H.; Sears, C. T., Jr. *Inorg. Chem.* **1977**, *16*, 769.
(11) Pearson, R. G.; Muir, W. R. *J. Am. Chem. Soc.* **1970**, *92*, 5519.
(12) Labinger, J. A.; Braus, R. J.; Dolphin, D.; Osborn, J. A. *J. Chem. Soc., Chem. Commun.* **1970**, 612.
(13) Jensen, F. R.; Knickel, B. *J. Am. Chem. Soc.* **1971**, *93*, 6339.

0276-7333/86/2305-0310$01.50/0

which predominates in the reactions of secondary halides with iridium(I) complexes.[14] Clear-cut inversion of stereochemistry was observed for oxidative additions to a number of anionic metal centers.[15-18] The term "supernucleophile" was coined to describe these complexes because of their high reactivity.[19] Kinetic data have substantiated the S_N2-like nature of their reactions with alkyl halides.[18,19] However, even with the "supernucleophiles", proper choice of substrate can tip the balance toward radical pathways.[20]

In our laboratory, low-valent macrocyclic complexes have been examined both as potential building blocks for metal–metal bonded oligomers and as convenient systems for mechanistic studies. Our attention early focused on the monoanionic chelate BPDOH,[21] the cobalt complexes of which had been introduced by Costa's group[22] as models for vitamin B_{12}. At first these workers could only generate the nucleophilic cobalt(I) species in situ via borohydride reduction of a cobalt(III) precursor, but later various five-coordinate adducts such as carbonyl complex **1a** were isolated.[23a] The related complex **1b** was prepared in this laboratory.[23b] These complexes are moderately reactive toward alkyl halides.

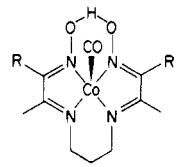

1a R = Me
b R = Et

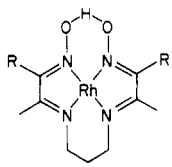

2

It was of obvious interest to study rhodium and iridium complexes of this ligand. While attempts in this laboratory to insert iridium into the macrocycle were unsuccessful,[24] a suitable synthesis of its rhodium derivatives was soon found.[25] A rhodium(I) species of exceptional reactivity could be isolated, which proved to be the coordinatively unsaturated complex **2**.[26] This rhodium-containing macrocycle and certain of its derivatives have proven to be ideal reagents for a detailed mechanistic study of oxidative addition reactions with alkyl halides. We have delineated both one- and two-electron mechanisms for these reactions and show in this paper how the choice of pathway is influenced by the reagent's sensitivity to the structure of the alkyl group and to the nature of the leaving group. Some aspects of this work have been reported in earlier communications.[27]

Scheme I

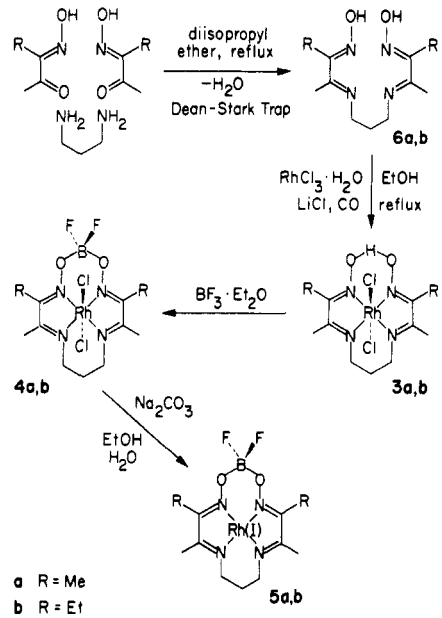

Results

Synthesis.[28] The preparation of Rh(I) complex **2** begins with metal insertion into the BPDOH ligand[22] to give the Rh(III) dichloride derivative **3a**. This Rh(III) complex can be reduced in basic aqueous ethanol to give the Rh(I) complex **2**, which precipitates as golden oxygen-sensitive microcrystals. It is highly reactive toward electrophiles.[27a] However, some of these reagents attack the oxime bridge of the ligand as well as the metal center. To circumvent this difficulty, the bridging proton was replaced with the less reactive boron difluoride ion through treatment of the Rh(III) dichloride **3a** with boron trifluoride etherate prior to the reduction step. Reduction of **4a** to the Rh(I) complex **5a** is accomplished as before, using the mild base sodium carbonate to avoid cleavage of the BF_2 bridge. Unfortunately, the BF_2 bridge lowers the already poor solubility of these complexes still further, so the ligand synthesis was modified to incorporate an ethyl substituent (Scheme I).[27b] Rhodium complexes of this new ligand, PPDOH,[29] were prepared as before.

The BF_2-bridged Rh(I) complexes are isolated as air-sensitive green microcrystals and like the H-bridged compounds give deep purple solutions which are highly oxygen sensitive. Compound **5b** is characterized by absorption maxima at 560 and 522 nm (ϵ 21 500 and 11 050). Its ^1H and ^{13}C NMR spectra show the expected features for the planar macrocyclic system. The IR spectrum is less revealing, although BO and BF stretching bands at 1155 and 990 cm^{-1}, respectively, confirm the presence of the BF_2 bridge.

Despite its coordinative unsaturation, $Rh^I(PPDOBF_2)$ is surprisingly reluctant to add axial ligands to form

(14) (a) Bradley, J. S.; Connor, D. E.; Dolphin, D.; Labinger, J. A.; Osborn, J. A. *J. Am. Chem. Soc.* **1972**, *94*, 4043. (b) Labinger, J. A.; Kramer, A. V.; Osborn, J. A. *J. Am. Chem. Soc.* **1973**, *95*, 7908.

(15) Johnson, R. W.; Pearson, R. G. *J. Chem. Soc., Chem. Commun.* **1970**, 986.

(16) Jensen, F. R.; Madan, V.; Buchanan, D. H. *J. Am. Chem. Soc.* **1970**, *92*, 1414.

(17) (a) Whitesides, G. M.; Boschetto, D. J. *J. Am. Chem. Soc.* **1969**, *91*, 4313. Whitesides, G. M.; Boschetto, D. J. *J.* Am. *Chem. Soc.* **1971**, *93*, 1529. (b) Bock, P. L.; Boschetto, D. J.; Rasmussen, J. R.; Demers, J.P.; Whitesides, G. M. *J. Am. Chem. Soc.* **1974**, *96*, 2814.

(18) (a) Collman, J. P. *Acc. Chem. Res.* **1975**, *8*, 342. (b) Collman, J. P.; Finke, R. G.; Cawse, J. N.; Brauman, J. I. *J. Am. Chem. Soc.* **1977**, *99*, 2515.

(19) Schrauzer, G. N.; Deutsch, E. *J. Am. Chem. Soc.* **1969**, *91*, 3341.

(20) (a) Breslow, R.; Khanna, P. L. *J. Am. Chem. Soc.* **1976**, *98*, 1297. (b) Krusic, P. J.; Fagan, P. J.; San Fillippo, J., Jr. *J. Am. Chem. Soc.* **1977**, *99*, 250.

(21) 2,2-[1,3-propanediylbis(nitrilo)]bis[3-butanone oximato], here abbreviated BPDOH; also known as $C_1(DO)(DOH)_{pn}$.

(22) Costa, G.; Mestroni, G.; de Savorgnani, E. *Inorg. Chim. Acta* **1969**, *3*, 323.

(23) (a) Costa, G.; Mestroni, G.; Tauzher, G. *J. Chem. Soc., Dalton Trans.* **1972**, 450. (b) Finke, R. G.; Smith, B. L.; McKenna, W. A.; Christian, P. A *Inorg. Chem.* **1981**, *20*, 687.

(24) MacLaury, M. R. Ph.D. Thesis, Stanford University, 1974.

(25) Collman, J. P.; Gagné, R. R., unpublished results.

(26) The structure of **2** was confirmed by X-ray crystallography: Murphy, D. W. Ph.D. Thesis, Stanford University, 1973.

(27) (a) Collman, J. P.; Murphy, D. W.; Dolcetti, G. *J. Am. Chem. Soc.* **1973**, *95*, 2687. (b) Collman, J. P.; MacLaury, M. R. *J. Am. Chem. Soc.* **1974**, *96*, 3019.

(28) Abbreviations: DME = 1,2-dimethoxyethane; DMF = dimethylformamide; Et_2O = diethyl ether; EtOH = ethanol; MeCN = acetonitrile; MeOH = methanol; THF = tetrahydrofuran.

(29) 2,2′-[1,3-propanediylbis(nitrilo)]bis[3-pentanone oximato], PPDOH also known in the literature as $C_2(DO)(DOH)_{pn}$); the BF_2-bridged ligand will be denoted $PPDOBF_2$.

Table I. Kinetics of Reactions with Alkyl Bromides[a]

substr	concn, mM	**5b**, mM	no. of runs	k, M^{-1} s^{-1}
benzyl bromide	0.4	0.02	4	255 ± 8
benzyl bromide	1.0	0.1	4	153 ± 1
benzyl bromide	2.0	0.1	4	206 ± 2
				av 205 ± 50
1-bromobutane[b,d]	107	0.5	4	(1.66 ± 0.04) × 10^{-2}
1-bromobutane[b,d]	52	0.5	2	(1.75 ± 0.10) × 10^{-2}
1-bromobutane[b,d]	52	0.5	4	(1.63 ± 0.02) × 10^{-2}
				av (1.67 ± 0.05) × 10^{-2}
2-bromopropane[c]	535	1.3	2	3.4 × 10^{-5}
bromocyclohexane[b]	1000	1.0	2	(1.48 ± 0.15) × 10^{-5}
bromocyclohexane[b]	2000	1.0	1	(0.96 ± 0.01) × 10^{-5}
				av (1.25 ± 0.25) × 10^{-5}
1-bromoadamantane[c]				no reaction

[a] Reactions at 25 ± 2 °C in THF; errors are one standard deviation (see text). [b] Determined at 30.5 ± 2 °C. [c] Values obtained by Collman and MacLaury.[27b] [d] Rate unaffected by the presence of 50 mM duroquinone.

Table II. Kinetics of Alkyl Chlorides, Tosylates, and Thiocyanates[a]

substr	concn, mM	**5b**, mM	no. of runs	k, M^{-1} s^{-1}
1-chlorobutane[b]	2000	1.0	3	(2.20 ± 0.30) × 10^{-6}
n-butyl tosylate[b]	250	1.0	4	(1.41 ± 0.04) × 10^{-3}
n-butyl tosylate[b]	500	1.0	4	(1.46 ± 0.04) × 10^{-3}
n-butyl tosylate[b]	1000	1.0	4	(1.35 ± 0.01) × 10^{-3}
				av (1.41 ± 0.04) × 10^{-3}
benzyl chloride	20	0.1	4	0.115 ± 0.001
benzyl chloride	50	0.1	4	0.121 ± 0.001
				av 0.118 ± 0.003
benzyl thiocyanate	2	0.1	4	1.32 ± 0.01
benzyl thiocyanate	10	0.1	4	1.53 ± 0.02
benzyl thiocyanate	20	0.1	4	1.64 ± 0.02
				av 1.50 ± 0.15

[a] Reactions at 25 ± 2 °C in THF; error are one standard deviation (see text). [b] Determined at 30.5 ± 2 °C.

five-coordinate derivatives. There is no change in its absorption spectrum in the presence of various nitrogen bases, but triphenylphosphine does bind effectively.[24] Complex **5b** also has remarkably low affinity for carbon monoxide, in contrast to Co(I) analogue **1b**. A blue CO adduct does form in solution (λ_{max} 660, 340 nm in THF; ν(CO) 1995 cm^{-1} in MeCN solution), but the equilibrium is readily reversed by bubbling nitrogen through the solution. The CO stretching frequency (compare compound **1b**, ν(CO) 1955 cm^{-1}) implies a lower degree of π-bonding in this adduct.

$Rh^{I}(PPDOBF_2)$ readily adds a wide variety of alkyl halides and sulfonates to form Rh(III)-alkyl derivatives with the halide or sulfonate anion coordinated in the trans position (eq 1).

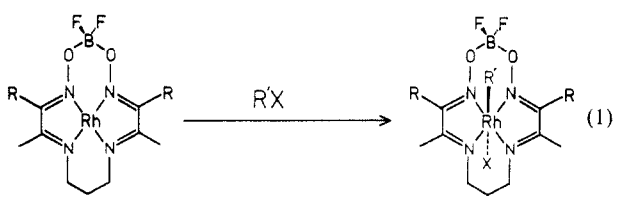

(1)

5a) R = Me
b) R = Et

Some of these derivatives had been prepared previously,[24,27b] and the crystallograhically determined structure of the methyl iodide adduct has been published.[30] Except where noted, all the adducts discussed below were isolated as crystalline solids and fully characterized by IR and NMR spectroscopy and elemental analysis. Most of these complexes show good stability, reflecting the inaccessibility of typical decomposition pathways such as β-elimination in the presence of the macrocyclic ligand. Secondary alkyl derivatives are noticeably light sensitive, but heating solutions of the isopropyl iodide or cyclohexyl bromide adduct in the dark, under nitrogen, in refluxing CD_3CN for 4 h resulted in only minor decomposition, according to NMR analysis.

A variety of Rh–acyl complexes could also be prepared via the oxidative addition of acid chlorides to **5b** (see also ref 24). These adducts have the expected acyl carbonyl absorption in their infrared spectra.

Kinetics: Oxidative Additions Exhibiting Second-Order Behavior. Kinetics of these oxidative additions were studied in THF solution with a large excess of alkyl halide, by monitoring the disappearance of the Rh(I) absorption at 560 nm, where the yellow Rh(III) products have virtually no absorption. The rate of Rh(I) disappearance showed good pseudo-first-order behavior[31] for the reactions of alkyl chlorides, bromides, tosylates, thiocyanates, and unhindered primary iodides. Agreement among three to four duplicate runs using the same solutions was generally excellent, and the average value of the rate constant together with its standard deviation is reported for each set of runs. The concentration of substrate was varied in separate experiments over a factor of two- to tenfold without changing the derived second-order rate constants significantly, except in reactions involving a few highly reactive substrates. Where necessary, larger errors are quoted for the overall average values of the rate constants,

(30) Collman, J. P.; Christian, P. A.; Current, S.; Denisevich, P.; Halbert, T. R.; Schmittou, E. R.; Hodgson, K. O. *Inorg. Chem.* **1976**, *15*, 223.

(31) The absorption data were fit to the equation $\ln (A_0/A) = k_{obsd}t$; the second-order rate constant $k = k_{obsd}/[S]$ (S = substrate).

Table III. Kinetics of Unhindered Alkyl Iodides[a]

substr	concn, mM	5b, mM	no. of runs	k, M^{-1} s^{-1}
iodomethane	0.2	0.02	4	2600 ± 50
iodomethane	0.4	0.02	4	1800 ± 50
iodomethane	0.5	0.02	3	2100 ± 50
iodomethane	0.5	0.02	3	2850 ± 80
				av 2300 ± 500
1-iodobutane	12.5	0.1	3	1.47 ± 0.03
1-iodobutane	12.5	0.1	4	1.45 ± 0.03
				av 1.46 ± 0.03
1-iodobutane[b]	1.8	0.06	3	1.37 ± 0.03
1-iodobutane[c]	1.8	0.06	3	2.70 ± 0.20
1-iodobutane[d]	1.8	0.06	3	0.54 ± 0.01
iodomethylcyclopropane	12.5	0.1	4	2.46 ± 0.03
iodomethylcyclopropane	25.0	0.1	4	2.45 ± 0.03
				av 2.45 ± 0.03

[a] Reactions at 25 ± 2 °C in THF; errors are one standard deviation (see text). [b] Value obtained by MacLaury[24] at 25.5 ± 0.5 °C. [c] At 46.6 ± 0.5 °C. [d] At 11.9 ± 0.5 °C.

to reflect the greater scatter between independent sets of kinetic runs. The reactions of acid chlorides with **5b** were too fast to measure by our techniques, even at high dilution. See Tables I–III for a compilation of second-order rate constants. The wide range of calculated rate constants reflects the marked sensitivity of the Rh(I) reagent to substrate structure (R = benzyl > methyl ≫ *n*-butyl ≫ iso-propyl ≫ 1-adamantyl [no reaction with the bromide]) and to the nature of the X group (I ≫ Br ≫ OTs ≫ Cl). These orderings are suggestive of a nucleophilic mechanism, as will be discussed further below.

The effect of solvent polarity on the rates of these reactions was assessed by measuring the rate for the addition of *n*-butyl bromide in benzene and acetone as well as THF. The rate was greater in more polar solvents, with an overall fourfold enhancement in going from benzene to acetone (see Table IV).

Cationic Rh(III) Intermediates. An essential feature of a nucleophilic mechanism for the addition of alkyl halides to $Rh^{I}(PPDOBF_2)$ would be rate-limiting displacement of a leaving group from carbon, thus forming a cationic Rh(III)–alkyl intermediate. Trans addition about the metal would seem to require such an intermediate, and trapping this intermediate with a second anionic species would provide direct evidence for its existence (eq 2). Such evidence has been sought unsuccessfully in the

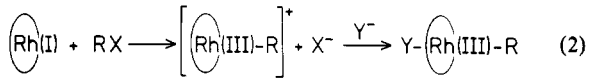

(2)

reactions of other d^8 metal centers.[32] Unfortunately, this trapping experiment cannot be realized in the case of **5b** because of the demonstrable lability of coordinated halides in the Rh(III) products. Thus, mixing two Rh(III)–alkyl halide adducts differing as to the identity of both the alkyl and halide groups gives rise to four species in solution, resulting from scrambling of the coordinated halides. Experiments with the two NMR-distinguishable macrocyclic ligands (i.e., $PPDOBF_2$ and $BPDOBF_2$) proved that no alkyl group transfer accompanies this rapid halide exchange (eq 3). Halide exchange also occurs readily in the presence of tetraethylammonium halides.

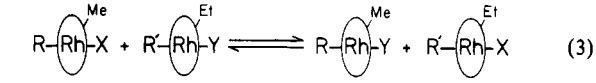

(3)

Coordinated thiocyanate anion proved to be labile as well; the replacement of coordinated thiocyanate (ν(SCN) 2085 cm^{-1}) by a halide anion is readily apparent by IR spectroscopy, since free thiocyanate in acetonitrile solution exhibits ν(SCN) at 2045 cm^{-1}. Conversely, the addition of sodium thiocyanate to a solution of a Rh(III)–alkyl halide complex results in the appearance of coordinated thiocyanate and precipitation of sodium halide.

In light of these observations, we reexamined the trapping experiment reported by Collman and MacLaury,[27b] who claimed to intercept the cationic intermediate when *n*-butyl bromide was added to $Rh^{I}(PPDOBF_2)$ in the presence of lithium chloride. We observed no incorporation of chloride into the Rh(III)–alkyl products. Indeed, halide exchange with the products appears to be limited by the poor solubility of LiCl in the ethereal solvents (THF, DME) which were used. If LiCl is handled in air, on the other hand, it becomes visibly wet and is then able to promote halide exchange even in ethereal solvents. Thus, the earlier report of halide incorporation into the oxidative addition products may have resulted from the use of incompletely dried LiCl.

The lability of halides coordinated to the Rh(III) complexes implies the transient existence of five-coordinate species. We prepared such a cationic complex according to eq 4. As isolated, cationic complex **8b** did not contain coordinated acetonitrile, according to its NMR and IR spectra and its elemental analysis.

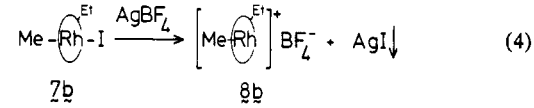

7b 8b (4)

Stereochemistry at Carbon. The demonstration of inversion of configuration constitutes a traditional proof of nucleophilic substitution at carbon. Experiments involving the addition of various secondary bromides (*cis*- and *trans*-4-bromo-1-methylcyclohexane or optically active 2-bromooctane) to Rh(I) complex **5b** led invariably to stereochemically scrambled products.[24] While Rh(I)–Rh(III) alkyl transfers might produce scrambling of stereochemistry through successive inversions at carbon in the Rh(III)–alkyl products (eq 5, R = methyl, benzyl), we have

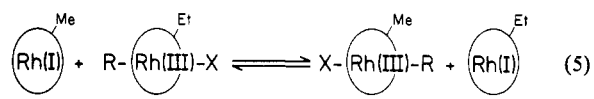

5a 5b (5)

found that these exchanges do not operate with the bulky groups in question.[34] There remains the possibility that these products are configurationally unstable under the vigorous conditions (several hours at reflux) required to complete reactions with such poor substrates. Careful examination of the products derived from cyclohexyl bromide revealed a 22% yield of the Rh(III) dibromide accompanying the expected Rh(III)–cyclohexyl derivative, which was isolated in 76% yield following chromatographic separation of the products. Decomposition of the secondary alkyl adducts under the reaction conditions could lead to scramling of stereochemistry as well as the observed byproduct formation.

(32) (a) Chock, P. B.; Halpern, J. *Proc. Int. Conf. Coord. Chem., 10th* **1967**, 135. (b) Pearson, R. G.; Muir, W. R. *J. Am. Chem. Soc.* **1970**, *92*, 5519.

(33) The four species may be detected by TLC (silica, 30% MeCN/CH_2Cl_2) or NMR analysis. The various methyl halide adducts are particularly easy to differentiate by NMR, but benzyl and isopropyl complexes with differing coordinated halides are also distinguishable. Scrambling is equally facile in dry THF, acetone, or MeCN.

(34) Collman, J. P.; Brauman, J. I.; Madonik, A. M. *Organometallics*, in press.

Table IV. Effect of Solvent Polarity on Kinetics[a]

solv	substr, mM	**5b**, mM	no. of runs	k, M^{-1} s^{-1}
benzene	174.5	0.35	4	$(9.40 \pm 0.10) \times 10^{-3}$
benzene	337	0.35	4	$(9.64 \pm 0.10) \times 10^{-3}$
benzene	667	0.35	4	$(9.09 \pm 0.10) \times 10^{-3}$
				av $(9.40 \pm 0.20) \times 10^{-3}$
tetrahydrofuran[b]				av $(1.67 \pm 0.05) \times 10^{-2}$
acetone	105	1.0	4	$(3.83 \pm 0.20) \times 10^{-2}$
acetone	106	1.0	4	$(3.69 \pm 0.60) \times 10^{-2}$
acetone	247	1.0	4	$(3.80 \pm 0.04) \times 10^{-2}$
				av $(3.77 \pm 0.07) \times 10^{-2}$

[a] Addition of 1-bromobutane to **5b** at 30.5 ± 2 °C; errors are one standard deviation (see text). [b] See Table I.

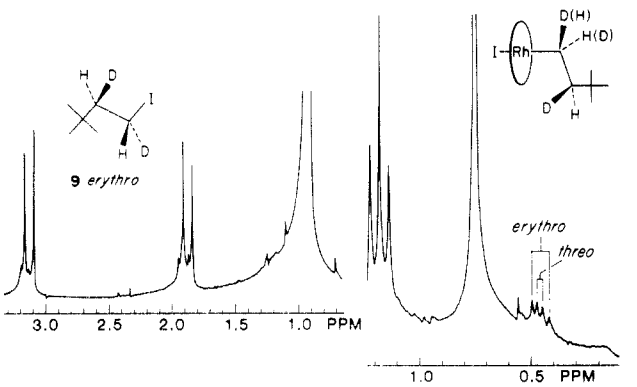

Figure 1. Broad-band deuterium-decoupled ^1H NMR spectra of erythro iodide **9** and its $Rh^I(PPDOBF_2)$ adduct.

It was evident that a convincing test of the stereochemistry at carbon in $Rh^I(PPDOBF_2)$ oxidative additions would require a more reactive substrate. Optically active secondary iodides were ruled out, owing to their non-second-order kinetic behavior in reactions with Rh(I) (see below). The stereospecifically deuterated primary iodide **9** (Figure 1) was selected as a suitable candidate. Its preparation will be described elsewhere;[34] substrates of this type were introduced by Whitesides and his collaborators[17] and have been widely applied to problems of stereochemistry in organometallic systems.

$Rh^I(PPDOBF_2)$ adds **9** cleanly, the expected Rh(III)–alkyl iodide being the only product detected by TLC. However, this adduct is an equal mixture of threo and erythro diastereomers, according to its deuterium-decoupled NMR spectrum (Figure 1). Thus, oxidative addition of **9** to Rh(I) proceeds with racemization at carbon. In this case the reaction conditions (less than 1 h at ambient temperature) are not expected to cause homolysis of Rh–C bonds in the products. This expectation is supported both by the lack of side products and by the observation that the Rh(III)–cyclopropylcarbinyl derivative **10** showed minimal rearrangement or decomposition after 14 h at 75 °C in CD_3CN solution (demonstrated by the absence of olefinic resonances in the NMR spectrum (eq 6).

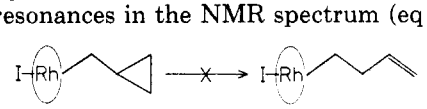

(6)

10

At this point, kinetic results for the addition of neohexyl iodide to **5b** made it clear that this substrate (and its deuterated analogue **9**) belongs to the class of hindered iodides, which may be reacting via a radical pathway. The scrambling of stereochemistry during the addition of **9** confirms this suspicion.

Kinetics: Deviation from Second Order with Hindered Iodides. Deviations from second-order kinetics were observed in reactions with sterically hindered alkyl iodides, including the secondary substrate isopropyl iodide and the primary substrates neopentyl and neohexyl (3,3-dimethyl-1-butyl) iodide. In the presence of excess isopropyl iodide, the behavior of Rh(I) disappearance was non-first order with respect to the Rh(I) concentration, the order varying from 0.6 to 1.2. With neopentyl iodide as substrate, the reaction order with respect to [Rh(I)] varied from 0.3 to 0.8. Kinetic data for these two substrates could also be described by assuming that two parallel reactions were occurring with zero- and first-order dependence on the Rh(I) concentration, respectively (eq 7).[35]

$$-d[Rh(I)]/dt = k_0 + k_1[Rh(I)] \quad (7)$$

Passable agreement was obtained within a given set of kinetic runs using the same Rh(I) and substrate solutions. However, the derived rate constants varied by more than tenfold between independent sets of kinetic runs. Rate constants derived in this manner are listed in Table V (k_0 was always very small and is not reported). The largest variations arose from the use of different batches of the Rh(I) reagent. Analytically pure $Rh^I(PPDOBF_2)$ gave one of the highest rates for the reaction with isopropyl iodide (entry 9 in Table V). Even more striking is the tenfold increase in the derived rate constant when the initial Rh(I) concentration was raised fivefold (entry 10).

Kinetics for the addition of neohexyl iodide to Rh(I) were also determined with a large excess of substrate present (50 mM vs. Rh(I) at 0.1 mM). The apparent order of the reaction with respect to [Rh(I)] varied from 1.3 to 1.6 in consecutive kinetic runs using the same substrate and Rh(I) solutions. Data from the last third of the reaction were well fit at first order, yielding an average rate constant of 0.09 ± 0.01 M^{-1} s^{-1}.

These peculiar and irreproducible results led us to suspect the intervention of a radical chain mechanism in the reactions with hindered iodides. Addition of duroquinone had no effect on the rate of reaction with neopentyl iodide (entry 14 in Table V). Galvanoxyl was found to react slowly with the Rh(I) reagent, so its use as a radical scavenger was precluded. It was thought that light might be an initiator of these reactions (although preparative reactions were routinely shielded from light). However, varying the amount of light passing through the kinetic cell (by adjusting the slit width of the spectrophotometer) did not appreciably alter the rate of Rh(I) disappearance in the reaction with isopropyl iodide.

The progress of these reactions could also be monitored by NMR spectroscopy. No CIDNP effects were seen during the reaction of $Rh^I(PPDOBF_2)$ with isopropyl or

(35) The integrated form of this equation is $\ln((([Rh(I)]_0 + k_0/k_1)/([Rh(I)] + k_0/k_1)) = k_1t$. Thus, k_0/k_1 is a term added to all the concentration data to obtain a first-order fit. Concentration data were derived from absorption $A(t)$ and the infinity absorption, $A_{infinity}$, according to the Beer–Lambert law: $A(t) - A_{infinity} = \epsilon cl$ (ϵ = the molar extinction coefficient, c = the Rh(I) concentration, and l = the cell path, cm).

Table V. Kinetics of Hindered Iodides[a]

entry	substr	(mM)[b]	5b, mM[b]	order[c]	k,[d] M^{-1} s^{-1}
1	2-iodopropane[e]	(25)	0.1	0.5	$(8.8 \pm 1.0) \times 10^{-2}$
2	2-iodopropane[e]	(50)	0.1	0.6	$(6.8 \pm 0.4) \times 10^{-2}$
3	2-iodopropane[e]	(50)	0.1	0.6	$(1.4 \pm 0.1) \times 10^{-1}$
4	2-iodopropane[e]	(50)	0.1	0.6	$(1.7 \pm 0.1) \times 10^{-1}$
5	2-iodopropane[e]	(50)	0.1	1.1	$(2.7 \pm 0.1) \times 10^{-1}$
6	2-iodopropane[e]	(50)	0.1	1.2	$(2.5 \pm 0.3) \times 10^{-1}$
7	2-iodopropane[e]	(50)	0.1	1.1–1.3	$(4.2 \pm 0.7) \times 10^{-1}$
8[f]	2-iodopropane[e]	(50)	0.1	0.7–1.0	$(5.1 \pm 2.0) \times 10^{-1}$
9[g]	2-iodopropane[e]	(50)	0.1	0.6–0.8	$(1.4 \pm 0.5) \times 10^{-1}$
10[g]	2-iodopropane[e]	(50)	0.5	1.4–1.6	(2.0 ± 0.5)
11	2,2-dimethyl-1-iodopropane[h]	(245)	0.5	0.8–1.0	$(1.0 \pm 0.1) \times 10^{-2}$
12	2,2-dimethyl-1-iodopropane[h]	(489)	0.5	0.7–1.0	$(1.4 \pm 0.1) \times 10^{-2}$
13	2,2-dimethyl-1-iodopropane[h]	(123)	0.5	0.7–0.8	$(7.3 \pm 0.5) \times 10^{-3}$
14[i]	2,2-dimethyl-1-iodopropane[h]	(245)	0.5	0.9–1.1	$(1.4 \pm 0.1) \times 10^{-2}$
15	2,2-dimethyl-1-iodopropane[h]	(250)	1.0	0.5–0.6	$(2.5 \pm 0.1) \times 10^{-3}$
16	2,2-dimethyl-1-iodopropane[h]	500	1.0	0.3–0.5	$(1.3 \pm 0.1) \times 10^{-3}$

[a] THF solvent. [b] Initial concentration after mixing equal portions of Rh(I) and substrate solutions. [c] Apparent order of Rh(I) disappearance with respect to its concentration (range for a given set of runs). [d] Rate from best pseudo-first-order fit to the data (see text). Each value is the average over a set of 3–4 runs (errors are one standard deviation). [e] Reactions at 25 ± 2 °C. [f] Substrate was diluted with THF containing 0.2 mM **5b**. [g] Analytically pure **5b** was used. [h] Reactions at 30.5 ± 2 °C. [i] Substrate solution contained 50 mM duroquinone.

Table VI. Effect of Alkyl Structure on Substitution at RX[a]

reagent	X	R_1 = Me R_2 = 1-Bu	R_1 = 1-Bu R_2 = 2-Pr	R_1 = 2-Pr R_2 = neo-Pen
$Rh^I(PPDOBF_2)$	Br		500	
	I	1600	10	100
organic nucleophile[b]	av	75	16	2400
$Co^{II}(CN)_5^{3-}$	I	0.2	0.04	

[a] Values are the rate ratios $k(R_1X)/k(R_2X)$ for substitution by the reagent specified. [b] Average values quoted from ref 42a. [c] See ref 2b.

neopentyl iodide in CD_3CN solution. The kinetics of neopentyl iodide addition were determined by NMR under second-order conditions, and most of the runs gave passable fits at second order.[36] The average rate constant was $(6.0 \pm 0.8) \times 10^{-3}$ M^{-1} s^{-1} (in CD_3CN solution at 28.5 °C, reactant concentrations 20 mM). This value falls in the range of second-order rate constants extracted from the data for this reaction under conditions of excess substrate (see above).

The apparent rate of Rh(I) addition to neopentyl iodide is less than 100-fold slower than the reaction with isopropyl iodide, which in turn is less than 10-fold slower than the reaction with the comparatively unhindered substrate *n*-butyl iodide. These rates for hindered substrates appear to be inconsistent with a nucleophilic mechanism (see below). Conclusive proof that another mechanism can operate is provided by the reaction of **5b** with 1-iodoadamantane, which proceeds at least as fast as that with neopentyl iodide. The 1-adamantyl–Rh(III) adduct was obtained in greater than 50% yield. In this case, backside attack at carbon is clearly impossible. The behavior of the iodide constrasts strikingly with that of the bromide, which fails to react with Rh(I) even under forcing conditions.

Radical Intermediates. A versatile probe for the intermediacy of radicals is the use of substrates which can give rise to rearranged products if free radicals are generated.[37] Collman et al.[27a] had already examined the addition of 6-bromo-1-hexene to **RhI**$(PPDOBF_2)$, obtaining the unrearranged adduct in good yield, accompanied by no more than traces of cyclized products. We have found that cyclopropylcarbinyl iodide (**11**) likewise gives an unrearranged adduct (**10**, eq 6) with only traces of olefinic products detectable in the reaction solutions by NMR. Kinetic data for this substrate (Table III) indicate a normal second-order reaction with Rh(I).

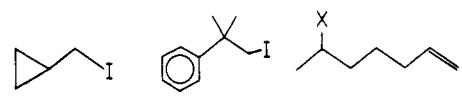

11 12 13a) X = Br
b) X = I

Several other substrates were selected as probes for the role of radical intermediates in the reactions of secondary and hindered alkyl iodides. Neophyl iodide (1-iodo-2-methyl-2-phenyl-propane, **12**) is an analogue of neopentyl iodide. While the neopentyl radical is stable, the neophyl radical has long been known to rearrange, although the rate is modest (762 s^{-1}).[37] However, addition of neophyl iodide to Rh(I) gives only the unrearranged adduct.

Examples of a secondary system analogous to 6-bromo-1-hexene are compounds **13a** and **13b**, 6-bromo- and 6-iodo-1-heptene.[38] The rate of cyclization for the 6-hepten-2-yl radical (1.3×10^5 s^{-1}) has recently been ascertained to be slightly greater than that for 5-hexen-1-yl.[37] Reaction of **13a** or **13b** with Rh(I) complex **5b** led to normal adducts with the olefinic unit intact, only one product being detected by NMR or TLC. Thus, any radical intermediates are trapped at least 10 times faster than they can cyclize. Given a cyclization rate of 10^5 s^{-1}, and assuming that the intercepting species is Rh(I) at 20 mM, the second-order rate constant for the trapping reaction must be greater than 5×10^7 M^{-1} s^{-1}. The adduct of **13b** was a labile oil that darkened on heating or exposure to light, and it was never obtained in crystalline form.

Discussion

Reactivity of $Rh^I(PPDOBF_2)$. The extraordinary reactivity of **5b** can be assessed by comparison with other

(36) For the reaction Rh(I) + S → P (rate constant k_2), assuming ordinary second-order kinetics ($-d[Rh(I)]/dt = k_2[Rh(I)][S]$), the integrated equation is $(\ln([Rh(I)]_0/[S]_0) - \ln([Rh(I)]/([Rh(I)] + [S]_0 - [Rh(I)]_0)))/([S]_0 - [Rh(I)]_0) = k_2t$. Since the NMR data yield product/reactant ratios ($Q = P/S$), these must be converted to concentration data according to the following formulas: with Rh(I) in excess, $[Rh(I)] = [Rh(I)]_0 - [S]_0Q/(Q + 1)$; with substrate in excess, $[Rh(I)] = [S]_0/(Q + 1)$. The initial values $[Rh(I)]_0$ or $[S]_0$ can be recalculated from $Q_{infinity}$: with Rh(I) in excess, $Q_{infinity} = [S]_0/([Rh(I)]_0 - [S]_0)$; with substrate in excess, $Q_{infinity} = [Rh(I)]_0/([S]_0 - [Rh(I)]_0)$.

(37) For a review of the use of free radical arrangements as mechanistic probes, see: Griller, D.; Ingold, K. U. *Acc. Chem. Res.* **1980**, *13*, 317. Revised rate for the neophyl rearrangement: Lindsay, D. A.; Lusztyk, J.; Ingold, K. U. *J. Am. Chem. Soc.* **1984**, *106*, 7087.

(38) Place, P.; Roumestant, M. L.; Gore, J. *Bull. Soc. Chim. Fr.* **1976**, *43*, 169.

neutral d^8 complexes. It adds methyl iodide some 5×10^4 times faster than Vaska's Ir(I) complex,[3a] making it the most reactive neutral nucleophile yet isolated.[39] This complex undoubtedly owes its reactivity in part to coordinative unsaturation, since its five-coordinate adduct with triphenylphosphine is 20-fold less reactive.[24] Complex **5b** differs from the more reactive anionic center $Fe(CO)_4^{2-}$ in that it does not induce elimination from secondary halides via proton abstraction[18] and from the highly reactive neutral system Cp_2ZrL_2[39a,b] in that halogen atom abstraction does not appear to dominate its interaction with alkyl halides.

Evidence for a Nucleophilic Mechanism. For transition-metal centers with even d electron counts, four potential mechanisms for the oxidative addition of alkyl halides have been cited in the literature: (1) nucleophilic, S_N2-like attack at carbon,[3a,5-7,9,10,15-19] (2) a concerted, three-center attack on the carbon–halogen bond,[1,8,11] (3) halogen atom abstraction in a radical chain mechanism,[14,39a,40] and (4) halogen atom abstraction in a radical pair mechanism.[39a,40b,41] In reactions of $Rh^I(PPDOBF_2)$ with alkyl chlorides, bromides, sulfonates, and unhindered iodides, the kinetic data in Tables I–IV combined with other evidence allow a clear choice in favor of the nucleophilic mechanism.

Concerted, three-center attack on the carbon–halogen bond can be ruled out immediately as being geometrically unrealistic for trans addition to a planar, macrocyclic complex.

A radical chain mechanism would be unlikely to give the highly reproducible kinetic results obtained with these substrates. The unrearranged adduct **10** is obtained from cyclopropylcarbinyl iodide, **11**, which virtually rules out the possibility of a free radical intermediate in this case, as the rate at which the cyclopropylcarbinyl radical would have to be trapped by Rh(I) (to prevent ring opening) would exceed normal diffusion-controlled rates.

The nucleophilic mechanism predicts second-order kinetics, first order in metal complex and substrate, as is observed for all the reactions listed in Tables I–IV. Furthermore, the dependence of Rh(I) reactivity on the leaving group and on the structure of the alkylating agent can be compared to a wealth of information on reactions of traditional organic nucleophiles. The rates of alkyl halide addition to **5b** are extremely sensitive to the structure of the alkyl group, as illustrated by the relative rates shown in Table VI. This ordering is characteristic of a nucleophilic mechanism, while reactions which generate radical intermediates have exactly the opposite order of substrate preference.[2b,43] The unreactivity of 1-bromoadamantane (where backside attack at carbon is impossible) may be contrasted to its reportedly high rate of addition to a Cr(II) macrocycle by a halogen atom abstraction mechanism.[44]

Table VII. Effect of Leaving Group on Substitution at RX[a]

reagent	R	X_1 = I X_2 = Br	X_1 = Br X_2 = Cl	X_1 = Br X_2 = OTs
$Rh^I(PPDOBF_2)$	1-butyl	100	7000	10
organic nucleophile[b]	av	3	50	0.16
$CpRh(CO)PPh_3$[c]	benzyl	16	500	
$Na_2Fe(CO)_4$[d]	1-decyl	50	450	2
$Co^I(DMG)_2L^-$[e]	methyl	10	250	

[a] Figures are the rate ratios $k(RX_1)/k(RX_2)$ for the reagent specified. [b] Average values quoted from ref 42b. [c] Data from ref 7b. [d] Data from ref 18. [e] Data from ref 19 (DMG = dimethylglyoximato).

While the Rh(I) complex **5b** shows the usual nucleophilic preference for unhindered substrates, the actual rate differences between methyl and *n*-butyl iodide or *n*-butyl and isopropyl bromide are about 25 times greater than those typically exhibited by organic S_N2 reactions (Table VI). H. C. Brown and his co-workers[45] have demonstrated that bulky organic nucleophiles display exaggerated sensitivity to steric hindrance in alkyl halides. Unusually large rate differences have also been noted for addition of methyl vs. ethyl iodide to the d^8 centers $CpM^I(CO)PPh_3$ (M = Co, Rh, Ir).[7] Thus, there is excellent precedent for viewing systems such as **5b** as sterically hindered nucleophiles, whose reactivity toward alkyl halides will vary enormously with the structure of the alkyl group.[46]

The preference of $Rh^I(PPDOBF_2)$ for various leaving groups is exemplified by the relative rates for reactions with the *n*-butyl derivatives in THF at 25 °C (Table VII). The ordering is typical of a conventional nucleophilic reaction, except for the low position of the tosylate group. Most metal-centered nucleophiles share this sluggish reactivity toward tosylates.[47] In general, their reactions exhibit unusually strong dependence on the nature of the leaving group (compared to organic nucleophiles, see Table VII), although complex **5b** appears to be an extreme case.

Conventional organic nucleophiles also vary widely in their sensitivity to leaving groups,[48a] and this variation has been analyzed in terms of the "hard–soft" acid–base relationships between the reactants.[48b] Thus, reactions in which nucleophile and leaving group are of similar "hardness" (i.e., polarizability) will be favored. As a result, "hard" nucleophiles such as chloride or ethoxide exhibit relatively low selectivity among halide leaving groups and react fastest with tosylates, which are relatively "hard" Lewis bases. "Softer" nucleophiles such as iodide show a much greater preference for the larger, more polarizable halide leaving groups and disfavor tosylates. Evidently, transition-metal-centered nucleophiles are softer still, as contrasts among the halide leaving groups are even higher, and tosylates fall below bromides in reactivity.

Our data for the solvent dependence and activation parameters for alkyl halide addition to **5b** also support a nucleophilic mechanism. The presumed intervention of a five-coordinate cationic intermediate (eq 2) implies a polar transition state. The fourfold rate increase noted in going from benzene to acetone as solvent can be at-

(39) Schwartz and co-workers[39a,b] have reported the oxidative addition of alkyl halides to Cp_2ZrL_2 complexes (L = tertiary phosphine); this system appears to be 3 to 4 orders of magnitude more reactive than **5b**, depending on the identity of the halide. However, their kinetic data indicate that the reactive species is Cp_2ZrL, while the only isolable compounds in this series are Cp_2ZrL_2' (L_2' = chelating phosphine). By contrast, coordinatively unsaturated **5b** is directly isolable, and its reactions are uncomplicated by ligand dissociation processes. (a) Williams, G. M.; Gell, K. I.; Schwartz, J. *J. Am. Chem. Soc.* **1980**, *102*, 3660. (b) Gell, K. I.; Schwartz, J. *J. Am. Chem. Soc.* **1981**, *103*, 2687.

(40) (a) Kramer, A. V.; Labinger, J. A.; Bradley, J. S.; Osborn, J. A. *J. Am. Chem. Soc.* **1974**, *96*, 7145. (b) Williams, G. M.; Schwartz, J. *J. Am. Chem. Soc.* **1982**, *104*, 1122.

(41) Kramer, A. V.; Osborn, J. A. *J. Am. Chem. Soc.* **1974**, *96*, 7832.

(42) (a) Streitweiser, A., Jr. "Solvolytic Displacement Reactions"; McGraw-Hill: New York, 1962; p 13. (b) Streitweiser, A., Jr. "Solvolytic Displacement Reactions"; McGraw-Hill: New York, 1962; p 30. (c) Streitweiser, A., Jr. "Solvolytic Displacement Reactions"; McGraw-Hill: New York, 1962; p 17.

(43) Kochi, J. K.; Powers, J. W. *J. Am. Chem. Soc.* **1970**, *92*, 137.

(44) Samuels, G. J.; Espenson, J. H. *Inorg. Chem.* **1979**, *18*, 2587.

(45) (a) Brown, H. C.; Cahn, A. *J. Am. Chem. Soc.* **1955**, *77*, 1715. (b) Brown, H. C.; Eldred, N. R. *J. Am. Chem. Soc.* **1949**, *71*, 445.

(46) Curiously, the Co(I) derivatives of vitamin B_{12} and synthetic macrocycles studied by Schrauzer and Deutsch[19] do not exhibit exaggerted sensitivity to steric hindrance in alkylating agents. This reactivity pattern is, however, comparable to that of other supernucleophiles (see, for example, ref 18).

(47) Pearson, R. G.; Figdore, P. E. *J. Am. Chem.Soc.* **1980**, *102*, 1541.

(48) (a) Bunnett, J. F. *J. Am. Chem. Soc.* **1957**, *79*, 5969. (b) Pearson, R. G.; Songstad, J. *J. Am. Chem. Soc.* **1967**, *89*, 1827.

tributed to stabilization of the transition state by the more polar solvent. This effect is comparable to that observed in the Menschutkin reaction (quaternization of tertiary amines by reaction with alkyl halides) and in the reactions of Vaska's complex.[3a] The lability of coordinated halides in Rh(III)–alkyl adducts, as well as the isolation of cationic complex **8b**, confirms the feasibility of cationic intermediates.

Activation parameters for the addition of *n*-butyl iodide to **5b** were determined in THF: $\Delta H^{\ddagger} = 7.9 \pm 2.2$ kcal mol^{-1}, $\Delta S^{\ddagger} = 32 \pm 6$ cal mol^{-1} K^{-1} (see Table III). The large negative entropy of activation is suggestive of a highly ordered transition state. The parameters fall in the same range as those for the Menschutkin reaction and for the oxidative addition of methyl iodide to a variety of d^8 complexes.[3a,5-8]

Recent analyses of nucleophilic substitution, both in the gas phase[49a,b] and in solution[49c,d] have identified "intrinsic" barriers which determine the contribution a given nucleophile or leaving group makes to the activation energy of the reaction. These "intrinsic" barriers may be equated with the activation energy for the self-displacement reaction, in which the nucleophile and leaving group are identical.[49e,f] Knowledge of these "intrinsic" barriers, combined with the value of $\Delta G°$ for the reaction under consideration, allows prediction of the reaction rate. Deviations from the predicted rates may be ascribed to such special interactions as hard–soft acid–base effects or exceptional steric interference between nucleophile and leaving group.[49a] Unfortunately, $\Delta G°$ values are rarely available for organometallic reactions (but see ref 50 for a study of Ir(I) oxidative additions). In the case of Rh(I) complexes **5a,b**, the self-displacement reaction can be observed (eq 5, R = methyl, benzyl),[34] but we have not determined its activation parameters. It is clear, however, that one of the major factors associated with great intrinsic nucleophilicity[49b] is in these systems, viz., the energy for $CH_3Rh^{III+} \rightarrow CH_3^+ + Rh^I$ is fairly low. Further work in these areas will be important for a more complete understanding of transition-metal nucleophiles.

A Competing Radical Mechanism for Reaction with Hindered Iodides. Experiments with stereochemical probe **9** revealed scrambling of stereochemistry during addition of hindered alkyl iodides to **5b**. This result, in conjunction with the non-second-order kinetics observed with these substrates, is highly suggestive of a mechanism involving free radical intermediates. The reaction rates for these substrates are surprisingly fast (Tables V and VI), and adduct formation with 1-iodoadamantane is incompatible with a nucleophilic mechanism.

The ultimate measure of a nucleophile's polarizability (which is reflected in its sensitivity to the "hardness" or "softness" of leaving groups, see above) may be its tendency to react by single electron transfer. Indeed, one extreme view of the S_N2 process is "single electron transfer taking place synchronously with bond reorganization".[51] The choice of a one-or two-electron pathway for a given metal center is modulated by the accessibility of the necessary oxidative states. Eberson[52] has shown (using Marcus theory) that the range of rates observed for the oxidative addition of alkyl halides to Co(I) supernucleophiles is consistent with an initial electron-transfer step. While kinetic data for these systems generally support a nucleophilic mechanism, the fact that they react with tertiary halides[19,53] indicates that another mechanism must operate as well. In at least one case, an electrogenerated Co(I) macrocycle appears to react with even methyl iodide via iodine atom abstraction.[54] That Co(I) macrocycles[20a] and other transition-metal nucleophiles[20b] can shift from two- to one-electron pathways for reactions involving iodide as the leaving group is well documented. We believe that $Rh^I(PPDOBF_2)$ favors a one-electron mechanism in reactions with hindered alkyl iodides.

Preliminary electrochemical measurements indicate that an initial electron-transfer step is feasible. It is well-known that alkyl iodides are more susceptible than other alkyl halides to one-electron reduction/halogen atom abstraction.[55] Indeed, only hindered iodides exhibit unusual kinetic behavior in their reactions with Rh(I) reagent **5b**, while other hindered halides react very slowly (as expected for a nucleophilic mechanism) and 1-bromoadamantane fails to add even under forcing conditions.

For the hindered iodides, the obvious mechanistic possibilities are a radical chain process involving halogen atom abstraction by Rh(II) or, on the other hand, halogen atom abstraction by Rh(I) leading to a (Rh(II), R·) radical pair. Obtaining evidence to corroborate the suspected role of radical intermediates has proven difficult. The peculiar and irreproducible kinetic results offer no clue to the reaction mechanism, although only a chain process should deviate noticably from second-order behavior. The radical scavenger duroquinone does not inhibit the reaction with neopentyl iodide. These reactions are not photochemically initiated, since changing the light flux or excluding light entirely has no significant effect on the observed rates.

The use of molecular rearrangements as probes for radical intermediates also gave negative results. The absence of rearranged products from neophyl iodide is not surprising, as even $Co^{II}(CN)_5^{3-}$ gives an unrearranged adduct with this substrate.[56] That an uncyclized (if labile) adduct is obtained from 6-iodo-1-heptene imposes much more stringent limitations on the lifetimes of possible radical intermediates. Trapping of the 6-hepten-2-yl radical by Rh(I) would have to occur at a remarkably high rate ($>10^8$ M^{-1} s^{-1}). The activation barrier for trapping would have to be very low. By comparison, the rates of radical capture by Cr(II)[43,44] or a V(I) hydride[57] are 2 orders of magnitude lower.

Rapid capture of radical intermediates would be more plausible if they were generated as part of a radical pair. In this case, their capture could easily compete with rearrangement, while still allowing loss of stereospecificity as seen with the labeled iodide **9**. This mechanism also accounts for the high yields of oxidative addition products,

(49) (a) Pellerite, M. J.; Brauman, J. I. *J. Am. Chem. Soc.* **1980**, *102*, 5993. (b) Pellerite, M. J.; Brauman, J. I. *J. Am. Chem. Soc.* **1983**, *105*, 2672. (c) Albery, W. J.; Kreevoy, M. M. *Adv. Phys. Org. Chem.* **1978**, *16*, 87. (d) Lewis, E. S.; Kukes, S.; Slater, C. D. *J. Am. Chem. Soc.* **1980**, *102*, 1619. (e) Murdoch, J. R. *J. Am. Chem. Soc.* **1972**, *94*, 4410. (f) Murdoch, J. R.; Magnoli, D. E. *J. Am. Chem. Soc.* **1982**, *104*, 3792.

(50) Yoneda, G.; Blake, D. M. *Inorg. Chem.* **1981**, *20*, 67. Mondal, J. U.; Blake, D. M. *Coord. Chem. Rev.* **1982**, *47*, 205.

(51) Shaik, S. S.; Pross, A. *J. Am. Chem. Soc.* **1982**, *104*, 2708.

(52) Eberson, L. *Adv. Phys. Org. Chem.* **1981**, *19*, 79. Eberson, L. *Acta Chem. Scand., Ser. B* **1982**, *B36*, 533–543.

(53) Puxeddu, A.; Costa, G.; Marsich, N. *J. Chem. Soc. Dalton Trans.* **1980**, 1489.

(54) Rillema, D. P.; Endicott, J. F.; Papaconstantinou, E. *Inorg. Chem.* **1971**, *10*, 1739.

(55) See ref 2b and 43. Rh(I) complex **5b** was examined by cyclic voltammetry in acetonitrile (using a PAR potentiostat, SCE reference electrode, platinum working electrodes, and 0.1 M *n*-$Bu_4N^+PF_6^-$ electrolyte), and it exhibits two partly reversible waves at −1.36 and −1.23 V (peak separations of slightly over 100 mV; under the same conditions ferrocene is reversibly oxidized at +0.40 V). Thus, the Rh(I) complex is at least as strong a reducing agent as the corresponding cobalt macrocycles (ref 52 and: Elliot, C. M.; Hershenhart, E.; Finke, R. G.; Smith, B. L. *J. Am. Chem. Soc.* **1981**, *103*, 5558–5566).

(56) Kwiatek, J.; Seyler, J. K. *Adv. Chem. Ser.* **1968**, *No. 70*, 207.

(57) Kinney, R. J.; Jones, W. D.; Bergman, R. G. *J. Am. Chem. Soc.* **1978**, *100*, 7902.

as opposed to products derived from radical coupling. However, some of the radical pairs must separate and initiate chain reactions in order to account for the peculiar kinetic results. Such a partitioning of radical pairs could give rise to CIDNP effects,[39a,40a] but their absence is not decisive. Odd-electron metal species have been directly observed by ESR in the case of Cp_2ZrL_2 oxidative additions[40b] (which appear to proceed by a mixed radical pair, radical chain mechanism), but reacting solutions of Rh(I) reagent **5b** are ESR silent. Unfortunately, the lower reactivity of the Rh(I) complex virtually guarantees that the steady-state concentration of radical intermediates will be too low for detection.

In summary, our results are most consistent with a radical pair mechanism for addition of hindered iodides, combined with some reaction via radical chains of short duration. Thus, the lifetime of any radical intermediates is brief and their steady-state concentration low.

Summary

$Rh^I(PPDOBF_2)$ is the most reactive neutral nucleophile which has yet been isolated. Its reactivity trends illustrate the importance of steric constraints and polarizability of the metal center in determining its reactivity toward alkyl halides. For this Rh(I) reagent, the shift from a two-electron to a one-electron mechanism occurs in reactions with hindered alkyl iodides. Knowledge of these reactivity patterns should be of use in interpreting the behavior of synthetically valuable Rh–alkyl intermediates.

Experimental Section

Physical and Spectroscopic Measurements. NMR spectra were recorded on either a Varian T-60 instrument (used for organic samples) or a Varian XL-100 instrument equipped with a Nicolet Technology pulse generator and data system (used for spectra of metal complexes, including ^{13}C spectra; probe temperature 28.5 °C).[58a] Deuterium broad-band-decoupled ^1H NMR spectra were recorded at the Department of Chemistry, University of California (Berkeley), on a custom-built 180-MHz superconducting instrument with a Nicolet Technology pulse generator and data system. The assistance of Dr. Rudi Nunlist in acquiring these spectra is gratefully acknowledged.

UV–visible spectra were recorded on a Cary 219 spectrometer using 1- and 10-mm quartz flow cells supplied by Hellma Cells (these cells were airtight when capped with rubber septa). IR spectra were recorded on a Beckman Acculab 3 spectrometer. Gas chromatographic analyses were conducted on a Hewlett-Packard Model 5750B or 5880A instrument equipped with flame ionization detectors. The principal analytical column was a 2 m × $^1/_8$ in. aluminum column packed with 10% OV-101 on Chromosorb W (AW DMCS, supplied by Supelco, Inc.). Melting points were determined in glass capillaries using a Mel-Temp apparatus and are uncorrected.

Elemental analyses were performed by the Stanford Microanalytical Laboratory at the Department of Chemistry; all samples were weighed in air.

Kinetic Methods. All manipulations of the Rh(I) complexes **5a,b** were carried out under an atmosphere of purified nitrogen, as previously described.[58b]

Oxidative addition reactions of $Rh^I(PPDOBF_2)$ were conveniently studied by monitoring the disappearance of the strong Rh(I) absorption band at 560 nm. The yellow-orange Rh(III) products have negligible absorption at this wavelength. These reactions were carried out under pseudo-first-order conditions, with at least a 20-fold excess of substrate (for a few highly reactive substrates, a 10-fold excess was used). Reactions were followed to at least 95% completion, and 20–30 points from all parts of the absorption decay curve were used to calculate the rate constants.[31] Correlation coefficients for the first-order fits were almost always greater than 0.999, corresponding to relative standard deviations of less than 1% in the slope of the first-order plot. Three to four duplicate runs were averaged for each substrate concentration used.

Since solutions of the Rh(I) reagent are highly air sensitive, all kinetic solutions were prepared in the glovebox. A stock of 2 mM solution of Rh(I) was prepared by dissolving 42 mg (0.1 mmol) in 50 mL of THF. Substrate solutions were prepared in separate volumetric flasks. Two techniques were used for mixing the Rh(I) and substrate solutions. For relatively slow reactions (second-order rate constants less than 0.1 M^{-1} s^{-1}) it was possible to mix equal portions of the two solutions in the glovebox and subsequently fill and cap a 1-mm flow cell which could be transferred to the spectrophotometer in time to observe most of the course of the reaction. For these experiments, the cell holder was maintained at 30.5 ± 0.5 °C, which was close to the actual temperature of the glovebox. The septa-capped cells excluded air sufficiently well to allow only 10% oxidation of the stock Rh(I) solution over several hours. For reactions requiring longer times, the septa-capped cell was returned to the glovebox and only removed for periodic checks on the reaction's progress.

For more rapid reactions, a dual syringe mixing device was used.[24] This device allowed rapid mixing of two thermostated solutions directly into a flow cell mounted in the spectrophotometer. The two gas-tight syringes were charged with Rh(I) and substrate solutions in the glovebox and connected to the mixing valve, and the flow cell before the apparatus was removed for installation on the spectrophotometer. The syringes contained 10 mL of solution, sufficient for several duplicate runs. The outflow of the cell was run through a syringe needle into a waste flask; this flask was capped with a septum and vented with a second needle, so as to reduce back-diffusion of oxygen. Rh(I) solutions in the flow cell remained unoxidized for at least an hour, ample time for completion of all the reactions studied in this manner. It was economical to dilute the stock Rh(I) solution 9:1 and use a 10-mm path flow cell for most of these rapid mixing studies. For these experiments, the cell holder was maintained at 25.0 ± 0.5 °C, but the Rh(I) and substrate solutions were not actually thermostated in most cases. Assuming similar activation parameters (i.e., those determined for the addition of *n*-butyl iodide to $Rh^I(PPDOBF_2)$), rate constants measured at 30.5 °C should be reduced by 30% for comparison with data obtained at 25 °C. NMR kinetic experiments were run at 28 °C, so rate constants derived from them are approximately 12% higher than would be expected at 25 °C.

Solvents and Reagents. All solvents used in the glovebox were distilled under nitrogen prior to being taken into the box and were further deaerated by drawing the box atmosphere through them for 20 min via a fritted glass tube before use. THF, DME, ether, benzene, and cyclohexane were distilled from sodium/benzophenone. MeCN was predried by stirring over two successive portions of boric anhydride (5% w/v) followed by distillation from P_2O_5, discarding the first and last 10% of the distillate, and finally distilled from anhydrous K_2CO_3. Acetone was stirred over these successive portions of B_2O_3 (5% w/v), decanted, and distilled.

Solvents for use in air were of reagent grade and were stored over activated Linde 3A molecular sieves. Although molecular sieves induce aldol condensation of acetone,[59] acetone not so treated could not be used for chromatography of Rh(III)–alkyl complexes without concomitant hydrolysis of the BF_2 bridge in the macrocycle. Diisopropyl ether was distilled from sodium/benzophenone to remove peroxidic impurities.

Column chromatography was carried out using 60–200 mesh, type 62 grade silica gel supplied by W. R. Grace, which was activated by storage at 80 °C. Thin-layer chromatography plates (Silica GF) were purchased from Analtech; for use in the glovebox they were predried at 100 °C and left under vacuum in the glovebox antechamber overnight.

Commercial triethylamine was distilled successively from phthalic anhydride and metallic sodium. Pyridine was distilled from NaOH pellets and stored over 3A molecular sieves. Meth-

(58) (a) Chemical shifts are reported relative to internal Me_4Si and were calculated relative to the residual solvent peaks. ^1H NMR spectra: CD_3CN, δ 1.93; CD_3COCD_3, δ 2.04; CD_2Cl_2, δ 5.27; $CDCl_3$, δ 7.25. ^{13}C spectra: CD_3CN, δ 1.94. (b) Collman, J. P.; Rothrock, R. K.; Finke, R. G.; Moore, E. J.; Rose-Munch, F. *Inorg. Chem.* **1982**, *21*, 146.

(59) Burfield, D. R.; Smithers, R. N. *J. Org. Chem.* **1978**, *43*, 3966.

anesulfonyl chloride was distilled from P_2O_5 under reduced pressure. Toluenesulfonyl chloride was used as received from Aldrich. Boron trifluoride etherate was treated with a small excess of anhydrous ether, distilled from CaH_2, and then stored under nitrogen.

LiCl (Alfa) and LiBr (MCB) were dried under vacuum using the times and temperatures recommended[60] and were transferred to the glovebox under vacuum. NaSCN (Baker) was recrystallized from hot MeOH, washed with anhydrous ether, and dried under vacuum at 130 °C.

Tetraethylammonium bromide (MCB) was recrystallized from hot MeOH/acetone by cooling.[60] Tetraethylammonium chloride[61] and tetraethylammonium iodide were prepared by neutralization of tetraethylammonium hydroxide (Eastman, 10% aqueous solution) with concentrated hydrochloric and hydroiodic acids, respectively, followed by recrystallization. These three salts were dried under vacuum over P_2O_5.

NMR solvents were purchased from Aldrich (acetone-d_6, $CDCl_3$), MSD (CD_2Cl_2, CD_3CN), and Stohler Isotopic Chemicals (CD_3CN). CD_3CN used in mechanistic studies was purified in the same manner as the normal solvent and stored in the glovebox.

Substrates for Oxidative Addition. Alkyl halides were repurified by passage through activity I neutral alumina (Woelm) and stored in dark bottles over copper turnings. All substrates were degassed by three cycles of freeze–pump–thawing and transferred to the glovebox under nitrogen.

Benzyl chloride, benzyl bromide, benzyl thiocyanate, acetyl chloride, 2-bromopropane, 2-iodopropane, bromocyclohexane, and 1,2-dibromoethane were purchased commercially and purified according to the recommendations of Perrin, Armarego, Perrin.[60] Tipson's procedure[62] was employed for the synthesis of *n*-butyl tosylate, which was distilled.

Neopentyl iodide was prepared by treatment of the mesylate (obtained from neopentyl alcohol (Aldrich) by the Crossland and Servis procedure[63]) with NaI in diethyl acetamide at 110 °C[64] followed by distillation [bp 56.5–57.5 °C (57 torr) (lit.[65] 70 °C (100 torr))]. Preparation of 1-iodoadamantane from commercially available 1-bromoadamantane (Eastman)) was accomplished as described by Schleyer and Nicholas,[66a] and the product had the reported spectral properties:[66b] mp 72.5–73.5 °C (lit.[66a] 75.3–76.4 °C).

Conversion of (chloromethyl)cyclopropane (Aldrich) to the corresponding iodide 11 was carried out by heating the chloride with NaI in acetone at reflux overnight[67] [bp 68 °C (70 torr) (lit.[67] 53–54 °C (53 torr))]. The method of Place et al.[38] was used to prepare 6-bromo- and 6-iodo-1-heptene (**13a,b**) from the corresponding tosylate (obtained from the alcohol[68] by the Tipson procedure[62]). The 6-haloheptenes were purified by column chromatography on silica, eluting with CH_2Cl_2. Their purity by GC analysis was greater than 95%, and their spectral properties agreed with those previously reported.[38]

1-Iodo-2-methyl-2-phenylpropane (12). A preparation of neophyl iodide has been described,[56] but no physical properties were given. For this work 2-methyl-2-phenyl-1-propanol (Chemical Samples Co.) was converted to the tosylate by the Tipson procedure:[62] mp 73.5–74.5 °C (lit.[69] 74–75 °C). The tosylate (30 mmol, 9.13 g) and NaI (40.9 mmol, 6.13 g) were combined in diethylacetamide (20 mL) and heated to 110 °C overnight, according to the procedure of Whitesides and Sowinski.[64] Following their workup, distillation afforded 1.95 g (25%) of a product boiling at 98–98.5 °C (3.5 torr): ^1H NMR ($CDCl_3$) δ 1.50 (s, 6 H), 3.43 (s, 2 H), 7.32 (m, 5 H).

1-Bromo-3,3-dimethylbutane. The mesylate ester of 3,3-dimethyl-1-butanol (Aldrich) was prepared in the usual manner[63] and converted directly to the bromide through the action of $MgBr_2$ in ether.[38] After the literature workup, the product was distilled at 53.5 °C (50 torr) (lit.[70] 58.5–59.0 °C (51 torr)). The bromide was greater than 99% pure by GC analysis (10% OV-101, 120 °C).

3,3-Dimethyl-1-iodobutane. The corresponding mesylate ester (prepared as in the previous synthesis) was converted directly to the iodide by treatment with a twofold excess of MgI_2 in ether at room temperature for 1 h.[38] Workup and distillation gave a 62% yield of the desired compound (based on the crude mesylate) which boiled at 64–65 °C (29 torr) (lit.[70] 71 °C (38 torr)) and was 98% pure by GC analysis (10% OV-101, 100 °C).

Rhodium Complexes. Syntheses of the BPDOH[22] and PPDOH[23b] ligands have been described. All complexes analyzed correctly for the elements indicated (within ±0.4% of the calculated values) except where otherwise noted.

***trans*-Dichloro[2,2′-[1,3-propanediylbis(nitrilo)]bis[3-pentanone oximato]]rhodium(III), *trans*-(Cl_2)Rh(PPDOH) (3b).** A three-neck flask equipped with a magnetic stirring bar, a reflux condenser connected to a mineral oil bubbler, and a fritted glass inlet tube was charged with a suspension of LiCl (3.4 g, 80 mmol) and $RhCl_3 \cdot 3H_2O$ (Englehard, 3.00 g, 40.0% Rh, 11.7 mmol) in 300 mL of absolute alcohol. Carbon monoxide [*caution: toxic gas*; use a well-ventilated fume hood] was passed through the solution, and the mixture was heated under reflux for 2–3 h until the color had changed from deep burgandy to light orange. The free PPDOH ligand (5.40 g, 20.2 mmol) was introduced cautiously while the CO purge was maintained. A dense orange precipitate appeared almost immediately. The mixture was heated an additional 2–3 h while the flow of CO was continued. After the solution was cooled, the precipitate was collected on a glass frit and then extracted with four 40-mL portions of hot CH_2Cl_2. To these extracts was added 500 mL of absolute alcohol, and the solution was stored at 6 °C overnight to induce crystallization. The resulting mass of orange needles was collected on a glass frit and washed with EtOH. Additional crops could be obtained by reducing the volume of the filtrate from the recrystallization and also from the original reaction mixture by reducing its volume. These crops were recrystallized from CH_2Cl_2/EtOH to give the pure compound. The yield varied from 65 to 70% based on Rh: IR (KBr pellet) ν(CN) 1595 (m), ν(OHO) 1130 (s) cm^{-1}; ^1H NMR ($CDCl_3$) δ 1.08 (t, J = 7 Hz, 6 H), 2.37 (s, 6 H), 2.80 (q on m, J = 7 Hz, 4 H + 2 H), 4.00 (br t, J = 5 Hz, 4 H), oxime proton not observed. Anal. ($C_{13}H_{23}Cl_2N_4O_2Rh$) C, H, N, Cl, Rh.

***trans*-Dichloro[difluoro[2,2′-[1,3-propanediylbis(nitrilo)]bis[3-pentanone oximato]]borato]rhodium(III), *trans*-(Cl_2)Rh(PPDOBF$_2$) (4b).** In a Schlenk reaction vessel, *trans*-(Cl_2)Rh(PPDOH) (**3b**) (2.25 g, 5.1 mmol) in 30 mL of anhydrous ether was treated with 7.5 mL of $BF_3 \cdot Et_2O$ [*caution: toxic vapor and liquid*], which was introduced via syringe. The reaction mixture was stirred overnight under nitrogen, and the resulting yellow powder collected on a Schlenk frit and washed with copious amounts of anhydrous ether. The yield (after drying under vacuum) was 24.7 g (99%): IR (KBr pellet) ν(CN) 1620 (m), 1550 (m), ν(BO) 1190 (s), 815 (s), ν(NO) 1130 (s), ν(BF) 1010 (s) cm^{-1}; ^1H NMR ($CDCl_3$) δ 1.22 (t, J = 7.5 Hz, 6 H), 2.51 (s, 6 H), 2.64 (br p, J = 5 Hz, 2 H), 2.87 (q, J = 7.5 Hz, 4 H), δ 4.10 (br m, 4 H). Anal. ($C_{13}H_{22}BCl_2F_2N_4O_2Rh$) C, H, N, Cl.

Rh^I(PPDOBF$_2$) (5b). A two-necked Schlenk vessel[23b] was equipped with a magnetic stirring bar and charged with *trans*-(Cl_2)Rh(PPDOBF$_2$) (**4b**, 3.00 g, 6.15 mmol) as a slurry in 30 mL of water and 15 mL of EtOH. An L-shaped addition tube was charged with 2.40 g of anhydrous Na_2CO_3. The slurry was degassed with three cycles of freeze–pump–thawing, and the Na_2CO_3 was added to the stirred slurry under nitrogen. As the slurry warmed to room temperature it rapidly changed in color from light orange to red, purple, and finally to deep green. After the solution was stirred for 2.5 h, the green microcrystalline product was collected on a Schlenk frit and then washed with three 30-mL portions of carefully deoxygenated water, followed by two 10-mL portions of 50% aqueous alcohol, and finally with four 30-mL portions of anhydrous ether. The product was dried under vacuum

(60) Perrin, D. D.; Armarego, W. L. F.; Perrin, D. R. "Purification of Laboratory Compounds"; Pergamon Press: New York, Oxford, 1966.
(61) Coppens, G.; Kevill, D. N.; Cromwell, N. H. *J. Org. Chem.* **1962**, *27*, 3299.
(62) Tipson, R. S. *J. Org. Chem.* **1944**, *9*,235.
(63) Crossland, R. K.; Servis, K. L. *J. Org. Chem.* **1970**, *35*, 3195.
(64) Sowinski, A. F.; Whitesides, G. M. *J. Org. Chem.* **1979**, *44*, 2369.
(65) Beringer, F. M.; Schultz, H. S. *J. Am. Chem. Soc.* **1955**, *77*, 5533.
(66) (a) Schleyer, P. v. R.; Nicholas, R. D. *J. Am. Chem. Soc.* **1961**, *83*, 2700. (b) Fort, R. C., Jr.; Schleyer, P. v. R. *J. Org. Chem.* **1965**, *30*, 789.
(67) Meek, J. S.; Rowe, J. W. *J. Am. Chem. Soc.* **1955**, *77*, 6675.
(68) Peterson, P. E.; Kamat, R. J. *J. Am. Chem. Soc.* **1969**, *91*, 4521.
(69) Winstein, S.; Morse, B. K.; Grunwald, E.; Schreiber, K. C.; Corse, J. *J. Am. Chem. Soc.* **1952**, *74*, 1113.
(70) Whitesides, G. M.; Sevenair, J. P.; Goetz, R. W. *J. Am. Chem. Soc.* **1967**, *89*, 1135.

Table VIII. Rhodium(III)-Alkyl Halide Adducts

	X	equiv used	solv	reaction time	reaction temp	yield, %	spectral data[a]	formula	anal.[b]	no.
					Adducts Derived from $Rh^I(BPDOBF_2)$					
Me	I	excess	MeCN	<1 min	RT[g]	86	δ 0.40 (t, J = 2.3 Hz, 3 H)	$C_{12}H_{21}BF_2IN_4O_2Rh$	C, H, N, I[c]	
$(CH_3)_2CH$	Br	large excess	THF	3.5 h	reflux	71	δ 0.41 (d of d, J = 7 Hz, J = 2.7 Hz, 6 H), 1.11 (m, J = 7 Hz, 1 H)	$C_{14}H_{25}BBrF_2N_4O_2Rh$	C, H, N, Br	*d*
					Adducts Derived from $Rh^I(PPDOBF_2)$					
Me	I	excess	MeCN	<1 min	RT	85	δ 0.40 (t, J = 2.4 Hz, 3 H)	$C_{14}H_{25}BF_2IN_4O_2Rh$	C, H, N, I	
Me	Br	excess	THF	<1 min	RT	82	δ 0.25 (t, J = 2.5 Hz, 3 H)	$C_{14}H_{25}BBrF_2N_4O_2Rh$	C, H, N, Br	*e*
Me	Cl	excess	THF	0.5 h	RT		δ 0.18 (t, J = 2.4 Hz, 3 H)	$C_{14}H_{27}BCl_3F_2N_4O_2Rh$	C, H, N[f]	*c, d*
n-C_4H_9	I	2×	THF	<5 min	RT	77	δ 0.74 (t, J = 6.4 Hz, 3 H) on m (2 H), 1.08 (m, 2 H), 1.2–1.4 (m, 2 H)	$C_{17}H_{31}BF_2IN_4O_2Rh$	C, H, N, I	
n-C_4H_9	Br	2×	THF	1 h	reflux	85	δ 0.74 (t, J = 6.3 Hz, 3 H) on m (2 H), 1.09 (m, 4 H)	$C_{17}H_{31}BBrF_2N_4O_2Rh$	C, H, N, Br	*h*
n-C_4H_9	Cl	large excess	THF	10 h	reflux	87	δ 0.77 (t, J = 6 Hz, 3 H) on m (2 H), 1.17 (m, 4 H)	$C_{17}H_{31}BClF_2N_4O_2Rh$	C, H, N, Cl	*i, j*
n-C_4H_9	OTs	5×	THF	2 h	reflux	64	δ 0.74 (t, J = 6 Hz, 3 H), 1.12 (m, 6 H), 2.32 (s, 3 H), 7.13 + 7.57 (d, J = 8.1 Hz, 4 H tot)	$C_{24}H_{38}BF_2N_4O_5RhS$	C, H, N, S	*k*
$(CH_3)_2CH$	I	5×	MeCN	5 min	RT	86	δ 0.34 (d of d, J = 6.8 Hz, J = 1.1 Hz, 6 H), 1.09 (m, 1 H)	$C_{16}H_{29}BF_2IN_4O_2RH$	C,[l] H, N, I[l]	*m*
$(CH_3)_2CH$	Br	large excess	THF	2 h	reflux	50	δ 0.43 (d of d, J = 6.9 Hz, J = 1.3 Hz, 6 H), 1.3 (m, 1 H)	$C_{16}H_{29}BBrF_2N_4O_2Rh$	C, H, N, Br	*d*
Bz	Br	1.5×	THF	<1 min	RT	57	δ 2.63 (d, J = 3.2 Hz, 2 H), 6.8–7.1 (m, 5 H)	$C_{20}H_{29}BBrF_2N_4O_2Rh$	C, H, N, Br[n]	*o*
Bz	Cl	1.5×	THF	45 min	RT	60	δ 2.51 (d, J = 3.4 Hz, 2 H), 6.8–7.2 (m, 5 H)	$C_{20}H_{29}BClF_2N_4O_2Rh$	C, H, N, Cl	
c-$(C_3H_5)CH_2$	I	2×	THF	10 min	RT	75	δ −0.25 (m, 2 H), 0.10 (m, 2 H), 0.35 (m, 1 H), 1.1–1.3 (m, 2 H)	$C_{17}H_{29}BF_2IN_4O_2Rh$	C, H, N, I	
$(CH_3)_3CCH_2$	I	1.5×	THF	1 h	reflux	91	δ 0.69 (s, 9 H), 1.27 (m, 2 H)	$C_{18}H_{33}BF_2IN_4O_2Rh$	C, H, N, I[p]	*o*
1-adamantyl	I	2×	MeCN	2 h	reflux	52	δ 1.42 (d, J = 2.6 Hz, 6 H), 1.54 (m, 6 H), 1.74 (br m, 3 H)	$C_{23}H_{37}BF_2IN_4O_2Rh$	C, H, N, I	*q*
$(CH_3)_3C(CH_2)_2$	I	2×	MeCN	0.5 h	RT	81	δ 0.44 (d, J = 18 Hz, on 1:1:1 t, J = 2.5 Hz, 2 H), 0.71 (s, 9 H), 1.3 (m, 2 H)	$C_{19}H_{35}BF_2IN_4O_2Rh$	C, H, N, I	*i*
$(CH_3)_3C(CH_2)_2$	Br	2×	THF	16 h	reflux	84	δ 0.54 (d, J = 17.8 Hz, on 1:1:1 t, J = 2.5 Hz, 2 H), 0.72 (s, 9 H), 1.2 (m, 2 H)	$C_{19}H_{35}BBrF_2N_4O_2Rh$	C, H, N, Br	
MeCO	Cl	2×	THF	<1 min	RT	96	ν(CO) 1690 (s) cm^{-1}; δ 1.83 (d, J = 1.2 Hz, 3 H)	$C_{15}H_{25}BClF_2N_4O_3Rh$	C, H, N, Cl	
Bz	SCN	2×	THF	<5 min	RT	87	ν(SCN) 2090 (s) cm^{-1}; δ 2.67 (d, J = 3 Hz, 2 H), 6.8, 7.1, 7.3 (br m, ratio 2:2:1, 5 H tot)	$C_{21}H_{29}BF_2N_5O_2RhS$	C, H, N, S	

[a] NMR spectra were recorded by using CD_3CN solvent unless otherwise noted; IR spectra were taken for the samples in KBr pellets. [b] All analyses were within ±0.4% of the calculated values unless otherwise noted. [c] I: calcd, 23.86; found, 22.80. [d] NMR spectrum in acetone-d_6. [e] Prepared by P. A. Christian (Stanford University). [f] N: calcd, 10.12; found, 10.67. [g] Isolated as 1:1 solvate with CH_2Cl_2. [h] UV–vis (acetone): λ_{max} 368 nm (ε 5530). [i] NMR spectrum in CD_2Cl_2. [j] UV–vis (acetone) λ_{max} 380 nm (ε 6260). [k] Recrystallization from CH_2Cl_2 by addition of a 1:1 mixture of THF and cyclohexane. [l] Anal. Calcd: C, 32.68; I, 21.58. Found: C, 31.96; I. 22.32. [m] Purified by column chromatography on silica gel, eluting with 30% $MeCN/CH_2Cl_2$. [n] Br: calcd, 13.56; found, 14.43. [o] NMR spectraum in $CDCl_3$. [p] I: calcd, 20.60; found, 19.38. [q] The first band obtained by chromatography contained *trans*-$(I_2)Rh^{III}(PPDOBF_2)$, which was recrystallized from THF/cyclohexane and characterized by its NMR spectrum (CD_3CN): δ 1.06 (t, J = 7.6 Hz), 2.40 (s), 2.60 (m), 2.79 (q, J = 7.6 Hz), 4.06 (br 1:1:1 t, J = 4.4 Hz). [r] Recrystallization from CH_2Cl_2/cyclohexane. [s] RT = room temperature.

and collected off the frit in the glovebox. The averate yield was 80%. This microcrystalline product was sufficiently pure for most synthetic and mechanistic studies, but analysis showed that it contained a small amount of oxidized material (analysis for carbon was about 1% low). Recrystallization in the glovebox from acetone/cyclohexane followed by drying under vacuum at 100 °C overnight gave an analytically pure sample: ^{1}H NMR (CD_3CN) δ 1.02 (t, J = 7.5 Hz, 6 H), 1.96 (s, overlapping residual solvent peak), 2.21 (m, 2 H), 2.48 (q, J = 7.5 Hz, 4 H), 3.65 (m, 4 H); ^{13}C NMR (CD_3CN) δ 10.4 (q), 16.4 (t), 20.7 (t), 32.8 (t), 53.1 (t), 157.8 (s), 165.5 (s); IR (KBr pellet) ν(CN) 1620 (m), 1560 (m), ν(BO) 1155 (s), ν(NO) 1100 (s), ν(BF) 990 (s) cm^{-1}; UV-vis (THF) λ_{max} 560 nm (ϵ 21 500), 519 (ϵ 11 050), in acetone, λ_{max} 554 nm (ϵ 23 700), 519 (ϵ 12 050), in benzene; λ_{max} 562.5 nm (ϵ 21 000), 525.5 (ϵ 12 000). Anal. ($C_{13}H_{22}BF_2N_4O_2Rh$) C, H, N, F, Rh; calcd 24.6, found 25.3.

***trans*-Dichloro[2,2′-[1,3-propanediylbis(nitrilo)]bis[3-butanone oximato]]rhodium(III), *trans*-(Cl$_2$)Rh(BPDOH) (3a).**[71] Insertion of Rh into the (BPDOH) ligand was carried out exactly as described in the preparation of **3b**, above: IR (KBr pellet) ν(CN) 1620 (m), 1525 (m), ν(NO) 1140 (s) cm^{-1}; ^{1}H NMR (CD_2Cl_2) δ 2.35 (s), 2.45 (s) on m (14 H total), 4.05 (m, 4 H), oxime proton not observed. Anal. ($C_{11}H_{19}Cl_2N_4O_2Rh$) C, H, N, Cl.

***trans*-Dichloro[difluoro[2,2′-[1,3-propanediylbis(nitrilo)]bis[3-butanone oximato]]borato]rhodium(III), *trans*-(Cl$_2$)Rh(BPDOBF$_2$) (4a).** This compound was prepared in exactly the same fashion as *trans*-(Cl$_2$)Rh(PPDOBF$_2$), starting with *trans*-(Cl$_2$)Rh(BPDOH) (**3a**): ^{1}H NMR ($CDCl_3$) δ 2.41 and 2.44 (s, total 12 H), 2.60 (m, 2 H), 4.04 (m, 4 H). Anal. Calcd for $C_{11}H_{18}BCL_2F_2N_4O_2Rh$: C, 28.67; H, 3.94; N, 12.16. Found: C, 27.98; H, 3.96; N, 11.74.

Rh^I(BPDOBF$_2$) (5a). The reduction of *trans*-(Cl$_2$)Rh(BPDOBF$_2$) (**4a**) to give this compound as a green microcrystalline solid was carried out in the same manner as the preparation of Rh^I(PPDOBF$_2$): ^{1}H NMR (CD_3CN) very broad and indistinct, peaks at δ 2.1 and 3.4.

Oxidative Addition Products. Typical synthetic reactions used 0.25–0.50 mmol of the Rh(I) reagent and an excess of alkylating agent. Light was routinely excluded from these reactions. When necessary the reactions were heated under reflux until the characteristic purple color of the Rh(I) complex had disappeared. After a purity check by TLC (eluting with acetone or 30% $MeCN/CH_2Cl_2$) the adducts were usually recrystallized from CH_2Cl_2/EtOH. All adducts were characterized by IR and ^{1}H NMR spectroscopy and by analysis. Their IR spectra consistently exhibited bands assigned to ligand stretching modes (KBr pellet): ν(CN) 1605 (m), 1530 (m), ν(BO) 1170 (s), 820 (s), ν(BF) 1000 (s), ν(NO) 1120 (s) cm^{-1}. The macrocyclic ligands also exhibited a relatively unvarying set of NMR signals, confirming their planar geometry (and hence trans addition of the substrate) throughout this series of compounds. For complexes of PPDOBF$_2$ these peaks occur at δ 1.08 (t, J = 7.6 Hz, 6 H), 2.15 (m, 2 H), 2.30 (t, J = 1.2 Hz, 6 H), 2.76 and 2.78 (q, J = 7.6 Hz, 4 H total), and 3.7–4.3 (br m, 4 H), while peaks are observed at δ 2.25 and 2.28 (s, 12 H total), 2.75 (m, 2 H), and 3.7 and 4.2 (br d of d, J_{vic} = 8 Hz, J_{gem} = 15 Hz, 4 H) for complexes of the BPDOBF$_2$) ligand (CD_3CN solution). See Table VIII for specific reaction conditions and further characterization of the adducts.

[(Me)Rh(PPDOBF$_2$)]$^+$BF$_4^-$ (8b). The methyl iodide adduct **7b** of Rh^I(PPDOBF$_2$) (0.10 mmol, 56 mg) in 8 mL of MeCN was treated with a slight excess of $AgBF_4$ (Alfa, 20 mg) in the glovebox. A white precipitate formed instantly. The solvent was evaporated and the residue extracted with THF. The product was recrystallized from CH_2Cl_2/diisopropyl ether. The yield was 31 mg (60%): ^{1}H NMR (CD_3CN) δ 0.19 (d, J = 2.5 Hz, 3 H), 1.12 (t, J = 7.6 Hz, 6 H), 2.40 (t, J = 1.3 Hz, 6 H), 2.5–3.0 (m, 4 H + 2 H), 3.97 (br m, 4 H); ^{1}H NMR in CD_2Cl_2 showed no evidence of MeCN solvate in the product. Anal. Calcd for $C_{14}H_{25}B_2F_6N_4O_2Rh$: C, 32.35; H, 4.85; N, 10.78. Found: C, 31.07; H, 4.97; N, 10.16.

***trans*-(c-C$_6$H$_{11}$)(Br)Rh(PPDOBF$_2$) and *trans*-(Br$_2$)Rh(PPDOBF$_2$) (16).** The Rh(I) reagent (**5b**, 200 mg, 0.48 mmol) was treated with a large excess of cyclohexyl bromide (1–2 mL) in 10 mL of MeCN at reflux for 3 h. The reaction mixture was separated on a silica column, eluting with 30% $MeCN/CH_2Cl_2$. Two bands were collected and recrystallized separately from CH_2Cl_2/EtOH. The leading band afforded the dibromide in 22% yield (62 mg), while the slower moving species proved to be the expected alkyl bromide adduct (213 mg, 76%). For the dibromide: ^{1}H NMR (CD_2Cl_2) δ 1.18 (t, J = 7.7 Hz, 6 H), 2.52 (s, 6 H), 2.67 (m, 2 H), 2.92 (q, J = 7.5 Hz, 4 H), 4.1 (br m, 4 H). Anal. ($C_{13}H_{22}BBr_2F_2N_4O_2Rh$) C, H, N, Br. For the cyclohexyl bromide adduct: ^{1}H NMR (CD_2Cl_2) δ 1.16 (t, J = 7.6 Hz, 6 H) on (m, 6 H), 1.53 (br m, 4 H), 2.35 (s, 6 H), 2.7–3.0 (m 4 H), 3.7–4.3 (br m, 4 H). Anal. ($C_{19}H_{33}BBrF_2N_4O_2Rh$) C, H, N, Br.

***trans*-(Ph(CH$_3$)$_2$CCH$_2$)(I)Rh(PPDOH).** A solution of Rh^I(PPDOBF$_2$) (100 mg, 0.24 mmol) in 5 mL of MeCN was treated with a twofold excess of neophyl iodide (**12**, 0.48 mmol, 135 mg) and stirred and heated under reflux for 40 min. After removal of the solvent the product was recrystallized from CH_2Cl_2 by addition of a mixture of THF and cyclohexane and the crystals were washed with ether. The BF_2 bridge suffered hydrolysis during recrystallization, leading to isolation of the proton-bridged complex (123 mg, 81%): IR (KBR pellet) ν(CN) 600 (m), ν(OHO) 1455 (s), ν(NO) 1135 (s) cm^{-1}; ^{1}H NMR (CD_3CN) δ 0.93 (t, J = 7.6 Hz, 6 H), 1.09 (s, 6 H), 1.50 (d, J = 2.9 Hz, 2 H), 1.94 (s, overlapping residual solvent peak), 2.1–2.9 (m, J = 7.6 Hz, 4 H), 3.6–4.1 (m, 4 H), 7.14 (m, 5 H). Anal. ($C_{23}H_{36}IN_4O_2Rh$) C, H, N, I.

***trans*-((CH$_3$)$_3$CCHDCHD)(I)Rh(PPDOBF$_2$).** The reaction of **5b** and *erythro*-3,3-dimethyl-1-iodobutane-*1,2-d*$_2$[34] was carried out exactly as in the case of the undeuterated substrate (see Table VIII). The yield was 87%. Deuterium-decoupled ^{1}H NMR revealed that the complex was a mixture of diastereomers (note the two doublets at δ 0.43; cf. Figure 1): IR (KBr pellet) ν(CD) 2160 (w) cm^{-1}; ^{1}H NMR (180-MHz deuterium decoupled, CD_2Cl_2) δ 0.43 (d, J = 13.4 Hz, on d, J = 4.1 Hz, 1 H total), 0.71 (s, 9 H), 1.13 (t, J = 7.5 Hz, 6 H), 1.3 (m, 1 H), 2.30 (s, 6 H), 2.77 and 2.80 (q, J = 7.5 Hz, 4 H total), 3.77 and 4.29 (ABX pattern, J_{gem} = 15.5 Hz, J_{vic} = 7.9 Hz, 4 H total). Anal. ($C_{19}H_{33}D_2BF_2IN_4O_2Rh$) C, H, N, I.

NMR Studies of Rh(I) Oxidative Additions. 6-Bromo-1-heptene (13a). The stock Rh(I) solution (0.5 mL, 0.01 mmol) was treated with 1 equiv of this substrate (2.0 μL). The ensuing reaction was quite slow, but after several weeks at room temperature most of the substrate had been consumed. The only methyl doublet in the ^{1}H NMR spectrum was at δ 0.33, and it was further split by coupling to ^{103}Rh, exactly as observed in the isopropyl bromide adduct. The olefinic resonance at δ 4.8–5.3 appeared to be undiminished in intensity.

6-Iodo-1-heptene (13b). A ^{1}H NMR experiment with this substrate (2.0 μL) was conducted exactly as described above for the bromide. The reaction was complete within one half-hour. The uncyclized adduct was formed cleanly (one spot by TLC), and it exhibited the following ^{1}H NMR spectrum: δ 0.24 (d of d, J = 6.9 Hz, J = 1.3 Hz, 3 H), 0.4–0.7 (m, 2 H), 1.09 (t, J = 7.6 Hz, on m, 6 H), 1.3–1.7 (m, 2 H), 2.29 (s, 6 H) on 2.2–2.5 (m, 2 H), 2.75 (q, J = 7.6 Hz, on m, 4 H + 2 H), 3.7–3.9 (m, 2 H), 4.1–4.3 (m, 2 H), 4.8–5.1 (m, 2 H), 5.6–5.9 (m, 1 H). The same product was obtained from a preparative scale reaction. It was nearly pure according to TLC analysis. However, it proved to be labile, darkening readily when warmed or exposed to light. A sample purified by preparative TLC (eluting with 30% $MeCN/CH_2Cl_2$) had a ^{1}H NMR spectrum indistinquishable from the one just presented, but attempts to crystallize it were unsuccessful.

Acknowledgment. We are grateful to Professor Richard Finke (the University of Oregon) for many helpful discussions. We also thank Dr. Paul Christian and Dr. Richard Rothrock for experimental advice and for providing samples of several rhodium complexes. This work was funded by the National Science Foundation through Grant NSF CHE78-09443 and the Stanford NMR Center Grants NSF GP23633 and NIH RR00711. Alex M. Madonik was the recipient of an NSF Predoctoral Fellowship.

Registry No. **3a**, 41707-61-3; **3b**, 99355-02-9; **4a**, 99355-03-0; **4b**, 61129-11-1; **5a**, 41707-60-2; **5b**, 53335-25-4; **6a**, 7223-54-3; **6b**, 75961-81-8; **7b**, 57255-98-8; **8b**, 99355-24-5; **9**, 99343-40-5; **12**, 19479-63-1; **13a**, 38334-98-4; **13b**, 13389-36-1; **16**, 99355-26-7;

(71) Prepared by R. A. Stark: Stark, R. A. Ph.D. Thesis, Stanford University, 1974.

(Me)(I)Rh(BPDOBF$_2$), 99355-04-1; ((CH$_3$)$_2$CH)(Br)Rh(BPDOBF$_2$), 99355-05-2; (Me)(Br)Rh(PPDOBF$_2$), 99355-06-3; (Me)(Cl)Rh(PPDOBF$_2$), 99355-07-4; (*t*-C$_4$H$_9$)(I)Rh(PPDOBF$_2$), 99355-08-5; (*t*-C$_4$H$_9$)(Br)Rh(PPDOBF$_2$), 99355-09-6; (*t*-C$_4$H$_9$)(Cl)Rh(PPDOBF$_2$), 99355-10-9; (*t*-C$_4$H$_9$)(OTs)Rh(PPDOBF$_2$), 99355-11-0; ((CH$_3$)$_2$CH)(I)Rh(PPDOBF$_2$), 99355-12-1; ((CH$_3$)$_2$CH)(Br)Rh(PPDOBF$_2$), 99355-13-2; (Bz)(Br)Rh(PPDOBF$_2$), 99355-14-3; (Bz)(Cl)Rh(PPDOBF$_2$), 99355-15-4; (*c*-(C$_3$H$_5$)CH$_2$)(I)Rh(PPDOBF$_2$), 99355-16-5; ((CH$_3$)$_3$CCH$_2$)(I)Rh(PPDOBF$_2$), 99355-17-6; (B)(I)Rh(PPDOBF$_2$) (B = 1-adamantyl), 99355-18-7; ((CH$_3$)$_3$C(CH$_2$)$_2$)(I)Rh(PPDOBF$_2$), 99355-19-8; ((CH$_3$)$_3$C(CH$_2$)$_2$)(Br)Rh(PPDOBF$_2$), 99355-20-1; (MeCO)(Cl)Rh(PPDOBF$_2$), 99355-21-2; (Bz)(SCN)Rh(PPDOBF$_2$), 99355-22-3; (*c*-C$_6$H$_{11}$)(Br)Rh(PPDOBF$_2$), 99355-25-6; (Br$_2$)Rh(PPDOBF$_2$), 99355-27-8; ((CH$_3$)$_3$CCHDCHD)(I)Rh(PPDOBF$_2$), 99355-28-9; RhCl$_3$, 10049-07-7; MeI, 74-88-4; (CH$_3$)$_2$CHBr, 75-26-3; MeBr, 74-83-9; MeCl, 74-87-3; *t*-C$_4$H$_9$I, 558-17-8; *t*-C$_4$H$_9$Br, 507-19-7; *t*-C$_4$H$_9$Cl, 507-20-0; *t*-C$_4$H$_9$OTS, 4664-57-7; (CH$_3$)$_2$CHI, 75-30-9; BzBr, 100-39-0; BzCl, 100-44-7; *c*-(C$_3$H$_5$)CH$_2$I, 33574-02-6; (CH$_3$)$_3$CCH$_2$I, 15501-33-4; BI (B = 1-adamantyl), 768-93-4; (CH$_3$)$_3$C(CH$_2$)$_2$I, 15672-88-5; (CH$_3$)$_3$C(CH$_2$)$_2$Br, 1647-23-0; MeCOCl, 75-36-5; BzSCN, 3012-37-1; 1-bromobutane, 109-65-9; bromocyclohexane, 108-85-0; 1-bromoadamantane, 768-90-1; 1-chlorobutane, 109-69-3; 2-methyl-2-phenyl-1-propanol, 100-86-7; 2-methyl-2-phenyl-1-propanol tosylate, 21816-03-5; 1-iodobutane, 542-69-8; *n*-butyl tosylate, 778-28-9.

Supplementary Material Available: A table of analytical data (5 pages). Ordering information is given an any current masthead page.

Arylnickel(III) Species Containing NO_3, NO_2, and NCS Ligands. ESR Data and the X-ray Crystal Structure of Hexacoordinate (Pyridine)bis(isothiocyanato)-[*o*,*o*′-bis{(dimethylamino)methyl}phenyl]nickel(III)

David M. Grove, Gerard van Koten,* Wilhelmus P. Mul, Adolphus A. H. van der Zeijden, and Jos Terheijden

Anorganisch Chemisch Laboratorium, University of Amsterdam, Nieuwe Achtergracht 166, 1018 WV Amsterdam, The Netherlands

Martin C. Zoutberg and Casper H. Stam

Laboratorium voor Kristallografie, University of Amsterdam, Nieuwe Achtergracht 166, 1018 WV Amsterdam, The Netherlands

Received March 20, 1985

A method for the interconversion of the five-coordinated Ni(III) species [Ni{C$_6$H$_3$(CH$_2$NMe$_2$)$_2$-*o*,*o*′}X$_2$] (X = Cl, Br, I) and its application to the synthesis of the new species with X = NO_3 and NO_2 are described. For X = NCS the same route leads to the formation of species in which the Ni(III) center is hexacoordinate and ESR data are reported. For one derivative, [Ni{C$_6$H$_3$(CH$_2$NMe$_2$)$_2$-*o*,*o*′}(NCS)$_2$(C$_5$H$_5$N)] (**5b**), the molecular geometry has been established by X-ray crystallographic methods. Crystals of **5b**, C$_{19}$H$_{24}$NiN$_5$S$_2$, are orthorhombic with a = 13.146 (2), b = 16.101 (4) Å, c = 10.064 (1) Å, V = 2122 (1) Å^3, and Z = 4. Refinement included 1308 reflections leading to a final R value of 0.058. The structure of **5b** consists of a hexacoordinate Ni(III) center which is directly σ-bonded to the phenyl carbon of the C$_6$H$_3$(CH$_2$NMe$_2$)$_2$-*o*,*o*′ ligand (Ni(III)–C = 1.900 (9) Å). The Ni center is further bonded to five nitrogen donor ligands: to two mutually trans N-bonded NCS ligands (1.965 (6) Å), to two trans NMe$_2$ ligands (2.207 (6) Å), and to the pyridine N atom which is trans to the C donor site (2.057 (8) Å). On the basis of these structural data and in combination with the ESR data with $g_\parallel > g_\perp$, it is concluded that the unpaired electron resides in the $d_{x^2-y^2}$ orbital.

Introduction

In the last few years it has become increasingly apparent that nickel plays an important role in certain biological systems, e.g., the hydrogenases,[1] and this has emphasized the relevance of studies concerning the range and stabilty of the less common Ni(I) and Ni(III) oxidation states.[2] Those inorganic coordination complexes of trivalent (d^7) nickel are paramagnetic, and in the majority of examples known stabilization of this oxidation state is accomplished by the use of N donor ligands of a polydentate or macrocyclic nature.[3-5]

Recently, with use of the terdentate anionic N,N′,C ligand C$_6$H$_3$(CH$_2$NMe$_2$)$_2$-*o*,*o*′ we prepared the novel square-pyramidal arylnickel(III) species [Ni{C$_6$H$_3$(CH$_2$NMe$_2$)$_2$-*o*,*o*′}X$_2$] (X = Cl, Br, I) (**1a–c**), which were the first reported true Ni(III) organometallics.[6] The presence of a C–Ni(III) σ-bond makes these compounds also interesting models for the arylnickel(III) intermediates postulated to be key intermediates in the nickel-catalyzed cross-coupling reactions of alkyl Grignards with aryl halides.[7]

(1) (a) Thompson, A. J. *Nature (London)* **1982**, *298*, 602 and references therein. (b) Albracht, S. P. J.; van der Zwaan, J. W.; Fontijn, R. D. *Biochim. Biophys. Acta* **1984**, *766*, 245–258 and references therein.
(2) (a) Nag, K.; Chakravorty, A. *Coord. Chem. Rev.* **1980**, *33*, 87–147. (b) Haines, R. I.; McAuley, A. *Coord. Chem. Rev.* **1981**, *39*, 77–119.
(3) Jacobs, S. A.; Magerum, D. W. *Inorg. Chem.* **1984**, *23*, 1195–1201.
(4) Lati, J.; Koresh, J.; Meijerstein, D. *Chem. Phys. Lett.* **1975**, *33*, 286–288.
(5) Bencini, A.; Fabrizzi, L.; Poggi, A. *Inorg. Chem.* **1981**, *20*, 2544–2549.
(6) Grove, D. M.; van Koten, G.; Zoet, R.; Murrall, N. W.; Welch, A. J. *J. Am. Chem. Soc.* **1983**, *105*, 1379–1380.
(7) Smith, G.; Kochi, J. K. *J. Organomet. Chem.* **1980**, *198*, 199–214. Negishi, E. *Acc. Chem. Res.* **1982**, *15*, 340–348.

0276-7333/86/2305-0322$01.50/0